AD A032141

AFML-TR-76-54

16

CONFERENCE ON AEROSPACE TRANSPARENT MATERIALS AND ENCLOSURES

18–21 NOVEMBER 1975
ATLANTA, GEORGIA

MATERIALS ENGINEERING BRANCH
SYSTEMS SUPPORT DIVISION

APRIL 1976

TECHNICAL REPORT AFML-TR-76-54

Approved for public release; distribution unlimited

DDC
RECEIVED
NOV 17 1976
B

AIR FORCE MATERIALS LABORATORY
AIR FORCE WRIGHT AERONAUTICAL LABORATORIES
AIR FORCE SYSTEMS COMMAND
WRIGHT-PATTERSON AIR FORCE BASE, OHIO 45433

NOTICE

When Government drawings, specifications, or other data are used for any purpose other than in connection with a definitely related Government procurement operation, the United States Government thereby incurs no responsibility nor any obligation whatsoever; and the fact that the Government may have formulated, furnished, or in any way supplied the said drawings, specifications, or other data, is not to be regarded by implication or otherwise as in any manner licensing the holder or any other person or corporation, or conveying any rights or permission to manufacture, use, or sell any patented invention that may in any way be related thereto.

This report has been reviewed by the Information Office (IO) and is releasable to the National Technical Information Service (NTIS). At NTIS, it will be available to the general public, including foreign nations.

This technical report has been reviewed and is approved for publication.

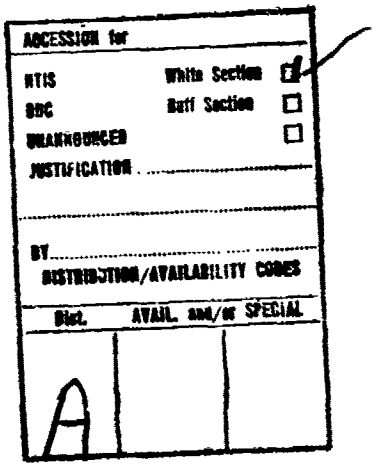
Samuel A Marolo

SAMUEL A. MAROLO
Project Engineer

FOR THE COMMANDER

Albert Olevitch

ALBERT OLEVITCH
Chief, Materials Engineering Branch
Systems Support Division



Copies of this report should not be returned unless return is required by security considerations, contractual obligations, or notice on a specific document.

AIR FORCE - 24 SEPTEMBER 76 - 425

Unclassified

SECURITY CLASSIFICATION OF THIS PAGE (When Data Entered)

REPORT DOCUMENTATION PAGE	READ INSTRUCTIONS BEFORE COMPLETING FORM
1 REPORT NUMBER: AFML-TR-76-54	2 GOVT ACCESSION NO. / 3 RECIPIENT'S CATALOG NUMBER
4 TITLE (and Subtitle): CONFERENCE ON AEROSPACE TRANSPARENT MATERIALS AND ENCLOSURES, 18-21 November 1975, Atlanta, Georgia.	5 TYPE OF REPORT & PERIOD COVERED: Conference Report, 18-21 November 1975 / 6 PERFORMING ORG. REPORT NUMBER
7 AUTHOR(s): Compiled by Samuel A. Marolo	8 CONTRACT OR GRANT NUMBER(s): F33615-72-C-2193, Task 76
9 PERFORMING ORGANIZATION NAME AND ADDRESS: AFFDL/AFML, Wright-Patterson Air Force Base, Ohio 45433	10 PROGRAM ELEMENT, PROJECT, TASK AREA & WORK UNIT NUMBERS: Project 2202, Project 7381, Task 738106
11 CONTROLLING OFFICE NAME AND ADDRESS: AFFDL/FEW, Wright-Patterson Air Force Base, OH 45433	12 REPORT DATE: April 1976 / 13 NUMBER OF PAGES: 906
14 MONITORING AGENCY NAME & ADDRESS (if different from Controlling Office) 914p.	15 SECURITY CLASS. (of this report): Unclassified / 15a DECLASSIFICATION DOWNGRADING SCHEDULE

16 DISTRIBUTION STATEMENT (of this Report)

Distribution Statement A
Approved for Public Release; distribution unlimited

2202, 7381 (17) 06

17 DISTRIBUTION STATEMENT (of the abstract entered in Block 20, if different from Report)

18 SUPPLEMENTARY NOTES

19 KEY WORDS (Continue on reverse side if necessary and identify by block number) Polycarbonate, Interlayers, Aircraft Transparencies, Windshields, Canopies, Acrylic, Bird Impact, Coating, Optical Requirements, Transparent Materials, Environment Resistance

20 ABSTRACT (Continue on reverse side if necessary and identify by block number)

The purpose of this report is to make available the technical papers presented at the Eleventh Conference on "Aerospace Transparent Materials and Enclosures." Thirty-nine technical papers are presented in seven sessions that address transparency design and performance, characterization, materials and processes, and bird impact resistance.

The papers contained herein have been reproduced directly from the original manuscripts.

DD FORM 1 JAN 73 1473 EDITION OF 1 NOV 65 IS OBSOLETE

Unclassified

SECURITY CLASSIFICATION OF THIS PAGE (When Data Entered)

012320

FOREWORD

This report was prepared by the Materials Engineering Branch under Project 2202, "Improved Windshield Protection" and Project 7381, "Materials Application," Task 738106, "Materials Engineering and Design Data for Air Force Weapons Systems." It was administered under the direction of the Air Force Materials Laboratory, Air Force Systems Command. Mr. S. A. Marolo (AFML/MXE) served as Project Engineer.

The technical papers contained in this report were presented at the Air Force Materials Laboratory/Air Force Flight Dynamics Laboratory Conference on "Aerospace Transparent Materials and Enclosures," which was held at the Atlanta Internationale Hotel, Atlanta, Georgia, on 18-21 November 1975.

Gratitude and appreciation is expressed to Mr. Robert E. Wittman, AFFDL/FEW, and Mr. Joseph Militello and Mrs. Audrey Sachs, University of Dayton for the excellent job accomplished as Conference Technical Coordinator, Conference Administrator, and Conference Secretary, respectively. Gratitude is also expressed to Mr. George Peterson, Director, Air Force Materials Laboratory and Colonel Albert Preyss, Director, Air Force Flight Dynamics Laboratory for their introductory remarks and most importantly for their support of the Conference and their expressed concern and support of this technical area.

The report was submitted by the author on 10 March 1976.

Publication of this report does not constitute Air Force approval of the findings or conclusions presented. It is published only for the exchange and stimulation of ideas.

TABLE OF CONTENTS

	Page
SESSION 1 - DESIGN AND PERFORMANCE (PART I)	1
Operational Aspects and Performance of Transparencies Fitted to Current and Future Generation Civil Aircraft B. D. Gibbs, British Airways	3
Design Guidelines for Subsonic Transport Windshields P. H. Bain, Boeing	23
High Strength Glass in Service - A Status Report R. W. Wright Triplex	39
General Aviation Business Aircraft Transparencies - An Update H. U. Reppermund and W. W. Hornsey, PPG	67
SESSION 2 - DESIGN AND PERFORMANCE (PART II)	79
B-1 Windshield Overview B. R. Emrich, Air Force Materials Laboratory, B-1 SPO and D. L. Russell, Aeronautical Systems Division, B-1 SPO	81
Development of the Windshield for the B-1 Aircraft R. C. Shelton, Swedlow	111
Glass/Plastic Transparent Armor for Helicopters W. C. McDonald, Goodyear Aerospace and G. R. Parsons, Army Materials and Mechanics Research Center	147
Stress-Solvent Crazing of Cast Acrylic J. H. Large, Brunel University and K. B. Armstrong, British Airways	165
Evaluation of Scratch and Spall Resistant Windshields J. R. Plumer, Army Materials and Mechanics Research Center and W. C. McDonald, Goodyear Aerospace	195
Design and Development of Helicopter Transparent Enclosures J. H. McGarvey, Army Air Mobility Research and Development Laboratory and B. F. Kay, Sikorsky Aircraft	243

TABLE OF CONTENTS (CONT'D)

	Page
SESSION 3 - MATERIALS CHARACTERIZATION (PART I)	265
Report on Progress of the ASTMF7.08 Subcommittee on Aerospace Transparent Enclosures and Materials R. A. Morozowicz, Northrop	267
Rain Erosion Behavior of Transparent Plastics and Protective Coatings T. L. Peterson, Air Force Materials Laboratory	277
Non-Destructive Inspection Techniques for Acrylic Canopies G. F. Thomas and S. I. Shelton, LTV	305
Fracture Toughness of Stretched Acrylic Plastic S. A. Sutton, Naval Research Laboratory	335
The Effect of Thermal History on the Mechanical Properties and Crystallinity of Polycarbonate R. J. Morgan and J. E. O'Neal, McDonnell Douglas	349
Prevention of Fracture in BPA-Polycarbonate Structures D. W. Caird, General Electric	367
SESSION 4 - MATERIALS CHARACTERIZATION (PART II)	379
Environmental Resistance of Coated and Laminated Polycarbonate Transparencies G. E. Wintermute and R. A. Huyett, Goodyear Aerospace and S. A. Marolo, Air Force Materials Laboratory	381
Stability of Transparent Materials Under Worldwide Climatic Conditions J. M. Kolyer, Rockwell International	405
At Last, A Meaningful Windshield Life Test J. B. Olson, Sierracin/Sylmar	433
Current Aspects of Optical Requirements for Aircraft Transparencies N. S. Corney and W. Shaw, Ministry of Defence	469

TABLE OF CONTENTS (CONT'D)

	Page
SESSION 5 - MATERIALS AND PROCESSES (PART I)	483
Progress in the Development of New Transparent Plastics and Interlayer Materials T. J. Reinhart, Jr. and E. A. Arvay, Air Force Materials Laboratory	485
Tough, Transparent, Heat- and Flame-Resistant Thermoplastics via Silicone Block-Modified Bisphenol Fluorenone Polycarbonate R. P. Kambour, J. E. Corn, S. Miller, and G. E. Niznik General Electric	507
Design, Synthesis, and Development of New Transparent Polymers for Military Applications R. Fish, J. Parker, and G. Fohlen, NASA/Ames	541
Fabrication of Fire Resistant Transparencies S. S. Schwartz, Hughes Aircraft and D. Kourtides and R. Fish, NASA/Ames	567
The Use of Laminated Acrylic Transparencies on High-Performance Aircraft R. C. Shelton, Swedlow	581
The Challenge of Coating and Assembling Space Shuttle Windows J. K. Murphy, Optical Coating Laboratory	603
SESSION 6 - MATERIALS AND PROCESSES (PART II)	639
An Elastomeric, Thermoplastic, Polycarbonate-Compatible Aircraft Interlayer Useful from -65 to 350°F G. L. Ball III, D. W. Werkmeister, and I. O. Salyer Monsanto	641
Heat Resistant Sheet Interlayer J. E. Mahaffey, PPG	657
Advanced Adhesives for Transparent Armor R. E. Sacher and J. R. Plumer, Army Materials and Mechanics Research Center	671

TABLE OF CONTENTS (CONT'D)

	Page
Thin Film Coatings on Plastic Substrates J. D. Rancourt, Optical Coating Laboratory	687
Polycarbonate Protection D. L. Voss, Sierracin/Sylmar	709
SESSION 7 - BIRD IMPACT RESISTANCE	761
Birdstrikes and the United States Air Force Major A. T. Driscott, Directorate of Aerospace Safety	763
Radar Ornithology and Bird/Aircraft Collisions S. A. Gauthreaux, Jr., Clemson University	777
Bird Impact Forces in Aircraft Windshield Design R. L. Peterson, Air Force Flight Dynamics Laboratory and J. P. Barber, University of Dayton	791
Bird Strike Capabilities of Aircraft Transparency Materials A. O. Ingelse and G. E. Wintermute, Goodyear Aerospace	831
Bird Impact Test Program for Windshields of Small, Light Aircraft J. B. R. Heath and A. J. Bosik, National Research Council	851
Bird Resistant Transparencies in High Performance Aircraft - An Update H. E. Littell, Jr., PPG	887

SESSION 1

DESIGN AND PERFORMANCE (PART I)

OPERATIONAL ASPECTS AND PERFORMANCE OF TRANSPARENCIES FITTED TO CURRENT AND FUTURE GENERATION CIVIL AIRCRAFT

B. D. Gibbs
British Airways
European Division
Hounslow, Middlesex, England

PRECEDING PAGE BLANK-NOT FILMED

ABSTRACT

Transparency defects experienced on civil aircraft can be listed under two main headings: Electrical and Structural. Following the Boston and Paris accidents involving crew incapacitation due to smoke/fumes entering the flight deck, it is hardly surprising that some pilots considered it necessary to submit flight safety reports after experiencing transparency electrical defects that had generated smoke/fumes in the flight deck.

The majority of electrical defects are associated with a breakdown of the heating film. In at least one case this has been brought about by a "run away" condition of a temperature controller.

With one noticeable exception involving a small executive aircraft there have been no significant structural failures of transparencies fitted to civil aircraft, but the introduction of chemically toughened glass has increased the probability of damage following hail encounter.

Bird impact is an ever present problem particularly in those regions lacking suitable bird dispersal equipment and data on migratory movements.

A recent impact on a Trident aircraft resulted in bird debris entering the flight deck via the rear edge of the port direct vision panel.

With respect to financial considerations, the introduction of more sophisticated transparencies has imposed a heavy burden on the civil operator.

Experience to date shows that the level of reliability on some transparencies falls considerably short of that required by the airlines.

On future aircraft the civil operator would like to see even greater emphasis placed on the question of reliability. This may involve a radical deviation from current development programmes, particularly if the use of new materials is to be considered.

The civil operator is ready and able to provide industry with a 'platform' for evaluating the performance of new transparency designs under service conditions.

Introduction

The first part of this paper set out to review some of the in service problems associated with the unserviceability of civil aircraft Transparencies particularly those which have featured in flight safety reports.

The second part is devoted to general operational aspects and also includes data appertaining to performance, reliability and operating costs.

The final section of the paper is concerned with the requirements of Transparencies fitted to future aircraft, and advocates that more effort should be given to the consideration of alternative materials.

1. Operational Problems

1.1. Windshield Panel Outer Glass Failure

Over the past two years this particular defect has been experienced on B.747, L.1011 and BAC.1-11 aircraft. In some cases the vision loss was such that it was only possible for one pilot to land the aircraft satisfactorily. In the case of the B.747/L.1011, failure of the outer Chemcor layer has been caused by hail impact. The solution proposed by the manufacturer is an increase in the thickness of the outer layer, but it is too early to establish whether further changes will be necessary to completely eliminate this problem.

Experience to date suggests that this chemically toughened glass is particularly sensitive to hail impact, and it would be interesting to know if tests have been carried out to establish how conventional toughened glass compares in this respect.

In the case of the L.1011/B.747 it is however possible to remove the cracked outer glass in flight using the windshield washer system. However a recent experience on an L.1011 resulting in reduced visibility following glass shed, has questioned whether aircraft should be retained in service without first removing the thin outer PVB layer.

Whilst on the subject of hail it is perhaps worthwhile noting the extent to which even a relatively slow speed aircraft can become damaged if it encounters a particularly severe hail storm. Fig. 1 illustrates the results of such an encounter on a Viscount several years ago before weather rader became mandatory. It is interesting to note that although the fuselage was substantially damaged by the hail, the flight deck Transparencies escaped with just a single crack in the outer glass of the centre windshield panel.

1.2. Windshield Panel Electrical Defects

1.2.1. BAC.1-11 Windshield Panels

The failures of BAC.1-11 windshield panels have mainly been caused by high stresses set up in the outer glass layer following electrical breakdown of a bus bar. Modifications carried out to the panels have not been wholly successful in eliminating this very troublesome defect. It is hoped that panels now being obtained from an alternative supplier will eventually provide a solution.

1.2.2. Trident Windshield Panels

Following the Boeing 707 incidents at Paris and Boston, flight crews have become increasingly aware of the potential danger associated with smoke or fumes in the flight deck.

Two recent flight safety reports have been raised on Trident aircraft following the detection of smoke in the flight deck. After some difficulty the source of smoke was eventually traced to a faulty electrical connection on one of the windshield panels.

The manufacturer has introduced improvements to the panel to prevent further trouble, but the incidents have clearly illustrated that because of the proximity of Transparencies to the flight crew, every effort should be made to prevent defects that could interfere with the normal operation of the aircraft.

1.3. Side Windshield Defects

A large portion of the outer ply of a B.747 No.3 windshield panel recently became detached in flight (Fig. 2). The cause of the failure is not yet known but as there has been evidence of edge splitting on other panels of the same type, it is suspected that this particular defect may have been a contributary factor. The outer PVB layer was ruptured at a point adjacent to the panel control thermostat permitting a small air leak to take place through the inner panel around the periphery of the thermostat.

Another incident involving an L.1011 No.6 windshield panel highlights the importance of using reliable windshield heating equipment. A defect in the No.6 panel temperature controller caused a massive overheat of sufficient magnitude

1.3. Side Windshield Defects (Contd)

to cause thermal relaxation of the outer stretched acrylic main ply. Controllers must be designed to prevent a single failure causing Transparency damage.

1.4. Bird Strikes

Although bird strikes are recorded frequently on civil aircraft they rarely cause significant damage.

There have only been two noteworthy bird strikes involving Transparencies on British Airways aircraft. The first of these occurred some 7 years ago when a seagull hit the centre windshield panel of a Viscount just after take off. The panel was substantially damaged, and although penetration did not occur the co-pilot was slightly injured by glass debris.

The second incident involved a Trident aircraft and once again occurred just after take off. The strike took place on the pt. d.v. window and bird debris entered the flight deck through the rear edge of the panel frame (Fig. 3). None of the crew was injured and there was no evidence of damage to the d.v. window frame or the surrounding structure.

It is perhaps worthwhile also recording another significant bird strike that occurred on a Trident aircraft. Although this did not involve the Transparencies, the force of the impact was such that the unfortunate bird passed through the nose radome and front pressure bulkhead and terminated its' life deposited over the Captain's legs.

1.5. Lightning Strikes and Static Discharges

Although some 40% of lightning strikes and static discharges on aircraft occur in the area of the nose, it is rare for the flight deck Transparencies to become damaged. In fact over the past 10 years within British Airways there have only been two windshield panel changes brought about by the effects of lightning.

In both cases the aircraft type concerned (a Trident) was struck just forward of the windshield assembly causing spots of molten metal from the fuselage skin to precipitate onto the outer surface of the pt. windshield panel. The metal deposits were eventually polished out and the subject panels have since been re-fitted to other aircraft.

1.5. Lightning Strikes and Static Discharges (Contd)

The accummulation of static on flight deck Transparencies has in some cases caused operators considerable trouble. In extreme cases electrical equipment used in the heating system has been irreparably damaged. (1). The problem only appears to affect certain types of aircraft.

Flight crews have occasionally observed static discharges on the external surfaces of flight deck windshield panels.

This phenomenon normally has no detrimental effect on the aircraft or its equipment, and usually provides the crew with some light relief on long sectors.

However on one occasion the crew of a Vanguard aircraft observed static discharge taking place between one of the internal electrical contacts of a d.v. window and the adjacent aircraft structure.

At the time of the incident the aircraft was flying in the vicinity of an electrical storm. To confirm that the discharge was not caused by the aircraft's electrical supply, the crew removed the supply fuses. The discharge continued.

The discharge was eventually stopped by the crew selecting the d.v. window locking handle open. The handle operates microswitches that isolate the window from its electrical supply. The terminal block of the affected window was subsequently found to be burnt.

1.6. Deicing/Demisting Performance

The heating intensities and control temperatures used on civil aircraft flight deck Transparencies appear to be adequate for the majority of flight conditions.

To illustrate the point a Vanguard aircraft flying over Spain some years ago encountered some extremely severe icing conditions (estimated to be 6 times greater than the maximum continuous design case). Although some of the side panels iced up, forward vision through the front windshield panels was maintained throughout the encounter without selecting HIGH heat.

1.7. Cabin Windows

1.7.1. Outer Panel Failures

Crazing of Perspex (PPMA) cabin windows is still an all too frequent cause of removal and in some cases has resulted in total failure of the outer panel.

In the case of one incident involving a Vanguard cabin window virtually the complete outer panel became detached in flight after it had cracked (Fig. 4).

The window comprised two $\frac{3}{8}$" thick Perspex panels bonded to a spruce edge member.

On initial investigation the failure was somewhat difficult to understand as the outer panel normally carries no pressure load. The failure was eventually attributed to the combined effects of crazing and an excessive pressure load acting on the panel caused by a kinked air drier hose.

The outer panel of the Trident cabin window shown in Fig. 5 cracked vertically down the centre when the aircraft was flying at 24,000' at max. cabin pressure. The window comprised a $\frac{3}{8}$" thick Perspex outer panel and a $\frac{1}{8}$" inner panel of the same material.

The two pieces of the panel were retained in position by the edge seal despite the reduced level of support available, and although considerably thinner than the outer panel, the inner panel withstood the pressurisation load without further incident. The cause of the failure was attributed to crazing.

1.7.2. Interspace Contamination

Some time ago a rather unusual 'defect' became apparent on a number of cabin windows fitted to Vanguard aircraft. (Fig. 6).

The 'defect' consisted of a number of 'spider' shaped deposits on the interspace surface of the inner panel and the immediate reaction was to assume that they were either a rare species of fungii or the results of a chemical change in the panel.

1.7.2. Interspace Contamination (Contd)

Investigation subsequently revealed that the deposits were quite harmless and were caused by the evaporation of small water droplets (containing harmless impurities in solution) impinging on the surface of the inner panel. The interspace is vented to ambient through a silica gel crystal air drier which under certain flight conditions can become overloaded permitting water droplets to pass into the interspace. The 'spider' shaped patterns were almost certainly caused by vibration.

2. General Operational Aspects

2.1. Windshield Panel Heating

Operators, particularly those flying aircraft fitted with thick PVB windshield panels are naturally concerned that the aircraft should be capable of withstanding a bird strike under all operational conditions.

This concern is more apparent where operators extend their services into regions where knowledge of bird movements and the means to minimise the risk of a bird strike by the use of suitable dispersal equipment is likely to be minimal.

In the early 1960s tests were carried out to establish that below ambient temperatures of 0°C the majority of thick PVB windshield panels took up to 40 mins. to reach the required bird impact temperature. Where electrical supplies are not available prior to start up this obviously imposes an unacceptable limitation. There ore it is common practice after long turn rounds to observe the unheated windshield limiting airspeed below 10,000' if the ambient temperature is less than 0°C. It is interesting to note that the "warm up time" for a thick PVB windshield panel is mainly determined by the thickness of the PVB layer and not by the heating intensity.

It should also be remembered that the operator may have to use an aircraft for a considerable time without full windshield heating. Under these conditions a severe speed restriction would clearly be an embarrassment.

2.2. Emergency Procedures

Certain windshield defects do not require immediate action on the part of the flight crew, and indeed in some cases rectification can be deferred for several days.

In order to provide flight crews with adequate data on the subject in a concise form British Airways has drawn up a special emergency drill. An example of this for Trident aircraft is shown in Fig. 7 and it can be seen that an illustration of the various types of glass failure has been included to help crews select the appropriate drill.

2.3. Combination of Glass and Acrylic Windshield Panels

Because of the obvious weight advantage and other factors, several operators are replacing glass windshield panels on their aircraft with equivalent panels manufactured in acrylic.

However where the heating configuration employs a "shared" temperature controller facility (i.e. a controller determining the temperature of more than one panel), the combination of glass and acrylic panels on an aircraft must be carried out with extreme caution to prevent the possibility of either a severe overheat condition or a degradation in deice/demist performance.

2.4. Maintenance Standards

The satisfactory condition of aircraft Transparencies can only be ensured if the operator carries out the necessary maintenance and takes appropriate steps in the event of a defect arising.

Although the majority of operators take adequate care, there has been at least one flight incident involving a small executive aircraft where following failure of a flight deck window outer panel, the inner (standby) panel became detached giving rise to a rapid decompression.

The aircraft and crew survived the incident, and subsequent investigation revealed that the subject window had not been maintained in accordance with the manufacturer's recommendations.

In this particular instance no loss of life occurred as the crew were strapped in. The consequences of a similar failure on a cabin window requires no clarification.

2.5. Rain Repellent Systems

In flight rain repellent systems are fitted to a wide range of civil aircraft including L.1011, B.747, Trident and BAC.1-11 aircraft. Other aircraft employ pre-flight applied rain repellents.

In general the benefits of rain repellents will only really become apparent in heavy rain, and on some aircraft it is difficult to ensure that adequate repellent is being applied to the windshield panels.

2.6. Transparency Maintenance Costs

Following the purchase of wide bodied aircraft the civil operator has been confronted with a significant increase in the cost of maintaining his Transparencies.

With some of the newer Transparencies now costing upwards of 17,000 dollars the burden on the operator is likely to increase still further unless a significant improvement in reliability can be achieved.

Even when account is taken of the greater revenue earning ability of wide bodied aircraft, the relative cost of maintaining the Transparencies* on for example L.1011 aircraft (expressed as cost per unit flying hour per lb. pay load) is still some 30% greater than that of the Trident.

At the last Transparency Symposium it was stated that an MTBR of 10,000 hrs. for wide bodied aircraft Transparencies was a realistic goal. Although there is no reason why this goal should not be realised, current experience within British Airways indicates that it will only be achieved as a result of continued development by the manufacturer.

* Flight deck Transparencies only.

3. Future Requirements

With maintenance costs imposing an ever increasing financial burden on the civil operator it is essential that a major effort should be made to improve the reliability of Transparencies fitted to future civil aircraft.

3.1. Flight Deck Transparencies

Flight deck windshield panels constitute the major proportion of the civil operators total expenditure on Transparencies and it is therefore potentially in this area that continued development and new thinking is likely to have the maximum benefit.

Although the incorporation of "edge heating" has considerably improved the performance of thick PVB Transparencies there is now sufficient evidence to show that provided the current problems with glass facing plies can be resolved, in the long term a multilaminate Transparency design is more likely to achieve the level of reliability sought by the operator.

With few exceptions the current problems with large stretched acrylic multilaminate Transparencies have been associated with the outer glass ply.

As the prime function of the glass is to provide a surface resistant to the abrasive effects of windshield wipers why is it not possible to consider an alternative method of rain removal, e.g. an air blast system. This would enable the designer to replace the outer glass with an acrylic ply treated with a hard coating to give some degree of protection against dust erosion.

APUs are now fitted to virtually all new civil aircraft and as such should overcome one of the main problems associated with an air blast rain dispersal system, namely lack of sufficient bleed air on the approach because of the low power setting of the main engines.

The imminent introduction of the SST will demand a new level of reliability on all components particularly those likely to affect dispatchability.

As Transparencies core within this category every effort must be made to ensure that in the event of a defect there is sufficient redundancy in the design to avoid expensive service delays.

3.1. Flight Deck Transparencies (Contd)

Most of the larger operators are setting up extensive overhaul and repair facilities in order that a greater percentage of component servicing can be accomplished "in house".

To date operators have not seriously considered extending their facilities to include the repair of windshield panels (mainly replacement of the heated glass assembly), but it is possible that moves in this direction will be made in the near future.

It is therefore suggested that where possible the possibility of "in house" repair be taken into account in the design of new Transparencies.

3.2. Cabin Windows

The introduction of the SST has forced the aircraft designer to reduce the size of cabin windows and because of the high surface temperatures encountered in flight has dictated that outer panels be manufactured in glass.

No doubt the aircraft designer will eventually come up with a strong economic case for eliminating cabin windows altogether. Such a move however will be strongly resisted by the operator because for a variety of psychological and practical reasons passengers derive considerable satisfaction from visual contact with the external environment.

Accepting that cabin windows will always be required what then is the optimum design that will minimise maintenance costs.

There is considerable service experience with the two basic types of cabin window design (either the inner or outer panel carrying the pressure load), and it is suggested that the optimum design will comprise a stretched acrylic inner panel (taking the pressure load) and a thermally or chemically toughened glass outer panel capable of withstanding the pressure load if the inner panel failed.

This design will probably be heavier and initially more expensive than a conventional cabin window, but provided care is taken in the design, the life of the outer panel should be virtually unlimited, and with the inner panel protected from

3.2. Cabin Windows (Contd)

external contamination and to a certain extent from ultra violet radiation, it should in the long term prove to be the optimum configuration.

3.3. New Materials

The possibility of using new materials e.g. ceramics and their effect on the design of new Transparencies has been discussed at previous Symposiums.

From the civil operators view point however there has been little evidence of new materials on both Transparencies currently in service and those proposed for new aircraft.

Experience to date suggests that in order to make further advances in reliability the possibility of using new materials must be given greater priority. The ultimate goal must be the discovery of a transparent metal.

3.4. Service Evaluation of New Designs

The time scale for establishing the performance of new Transparency designs is by necessity several years, therefore it is imperative that new ideas for future aircraft should where possible be evaluated on current aircraft.

Provided sufficient ground tests have been carried out to satisfy the approval authorities, the civil operator is willing and able to offer industry a "platform" for the evaluation of new Transparency designs.

If the future level of reliability cannot be improved over that currently being achieved, the operator will be faced with the prospect of spending large sums of money each year on replacement Transparencies.

REFERENCES

1. Static Electrification of Windscreens and Canopies

P.J. SHARP
Lucas Aerospace Co.
Luton. England.

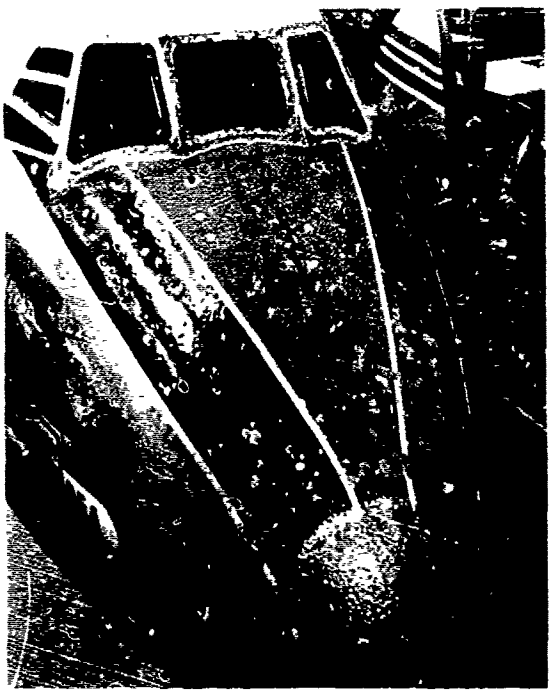


Fig. 1 Hail Damage



Fig. 2 B747 No.3 Windshield Panel Outer Ply Failure.

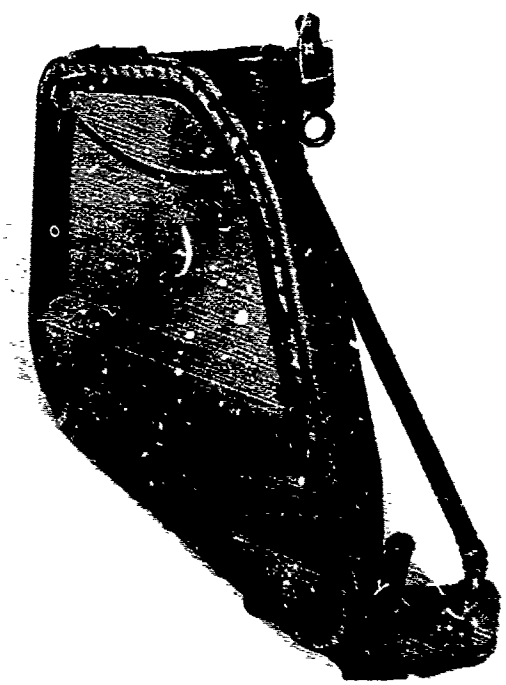


Fig. 3 Bird Strike Trident D.V. Window

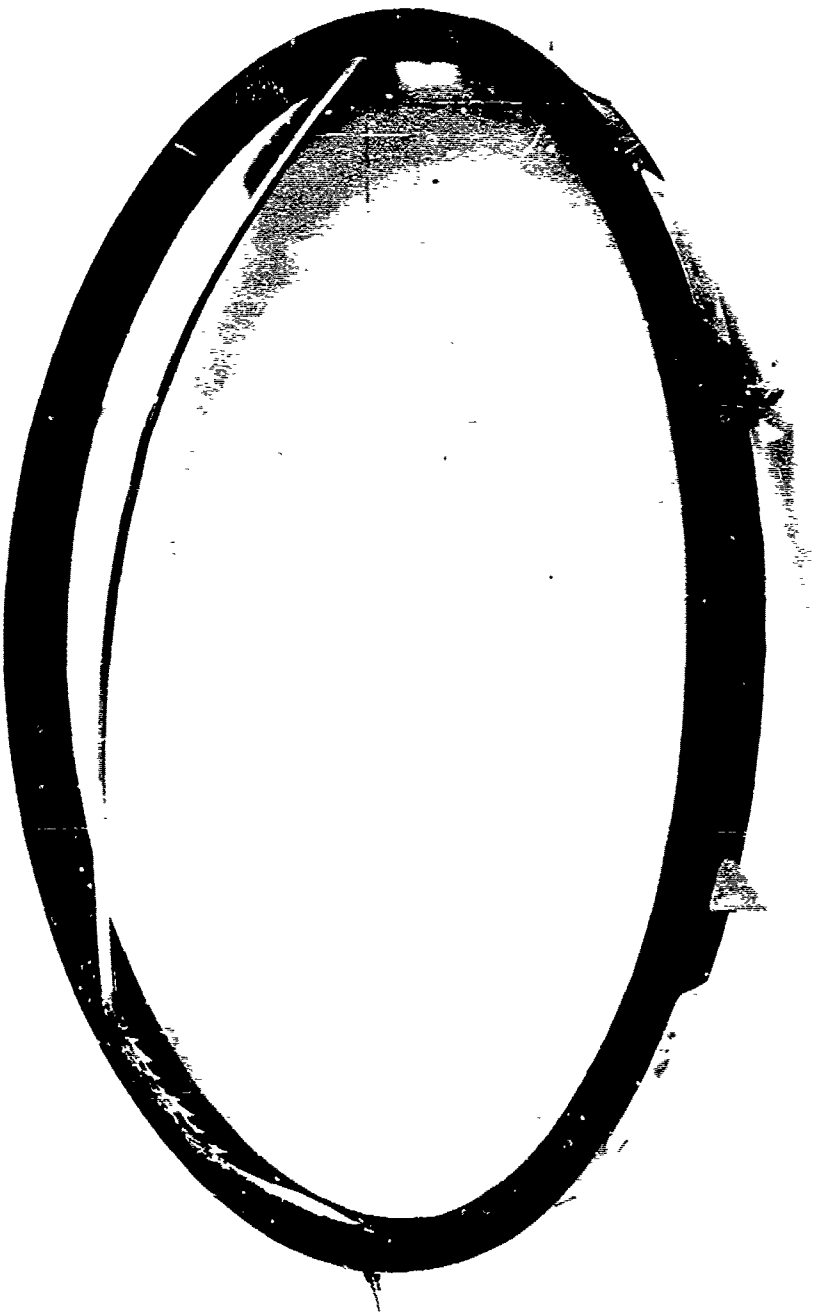


Fig. 4 Vanguard Cabin Window Outer Panel Failure



Fig. 5 Trident Cabin Window
Outer Panel Failure

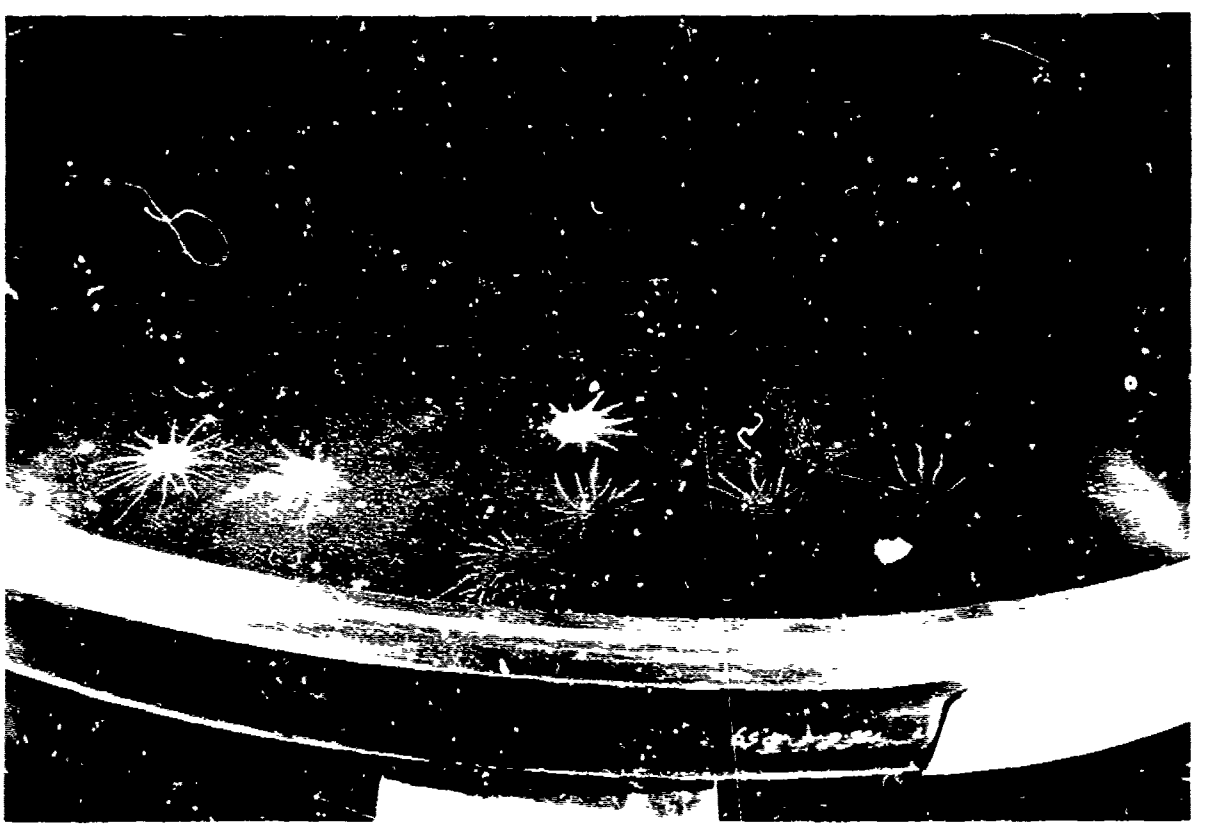


Fig. 6 Vanguard Cabin Window 'Spider' Deposits

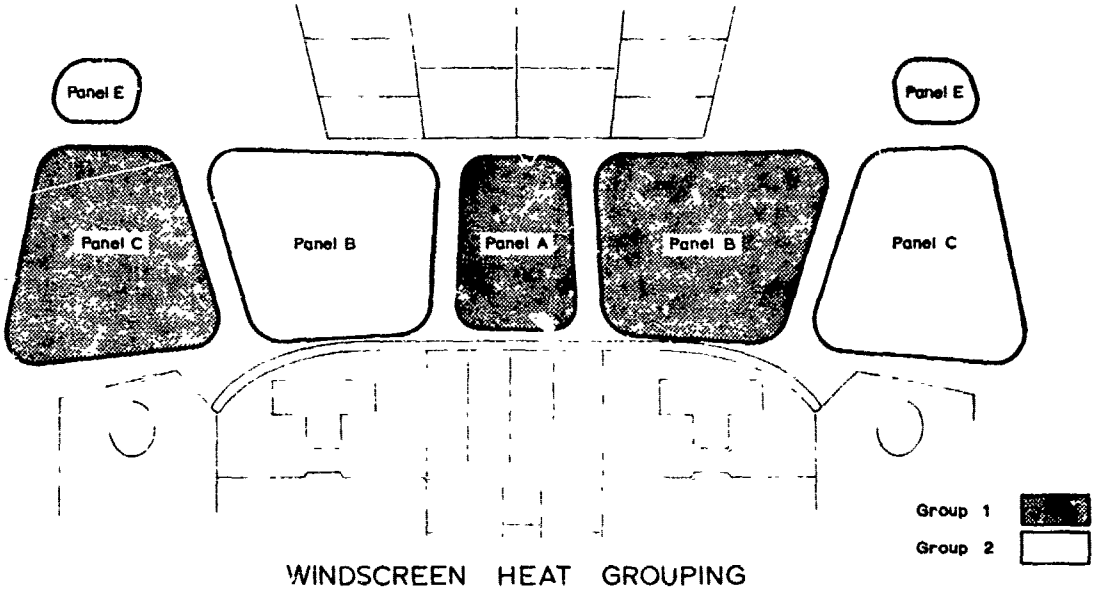
WINDSCREEN/W/S HEATING/WINDOW FAILURES

SYMPTOMS	ACTION SEQUENCE				
	Windscreen	DV Window	Eyebrow Window	Rear (Teardrop) Window	Passenger Cabin Window
A Shattering of intermediate glass laminate (complete loss of vision)	4:7	4:9	-	-	-
B Cracking of outer glass laminate (partial loss of vision)	7:10	8:10	-	-	-
C Cracking of inner glass laminate (partial loss of vision)	8:10	8:10	-	-	-
D Delamination of the glass and vinyl in excess of one third of the panel area	8:10	8:10	8:10	-	-
E Rapid increase in any delamination of the glass and vinyl	4:9	4:9	4:9	-	-
F Shattering of inner glass laminate	-	-	4:9	-	-
G Shattering of outer glass laminate	-	-	8:10	-	-
H Cracking or excessive crazing/ scratching of inner or outer panel	-	-	-	1:4:11	2:3:4:11
J Burning, arcing fumes	5:7:10	5:10	5:10	-	-
K Windscreen Overheat MI cycling	12	-	-	-	-
L Windscreen Overheat MI steady orange and black	6:7	-	-	-	-

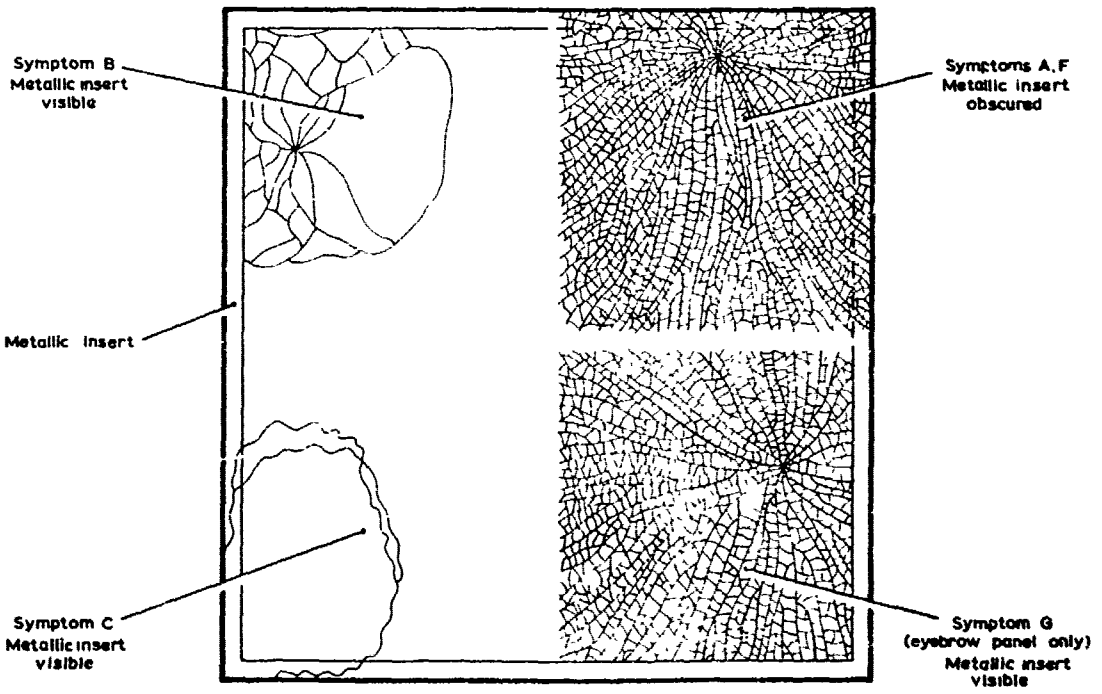
Action List (the items to be actioned in each particular case are indicated in the table).

1. Seat harness - On.
2. Cabin notices - On.
3. Evacuate area within 6 ft of window, if possible.
4. Descend and depressurise as soon as practicable.
5. Identify affected Group (diagram opposite). Appropriate Windscreen Heat Master switch off. If identification not possible, select both Windscreen Heat Master switches off.
6. Check CB's of affected Group.
   Group 1, CB's BA-G1A, 1B, 1C
   Group 2, CB's BA-G-2A, 2B, 2C
7. Observe Unheated Windscreen Limiting Speeds.
8. No immediate action.
9. Further unpressurised flights are permissible provided any vision loss is accepted.
10. Further pressurised flights are permissible provided any vision loss is accepted.
11. Further unpressurised flights are permissible provided the outer panel is complete.
12. Accept overheat at circuit control.

Fig. 7 Transparency Failure Emergency Drill (Part 1)



WINDSCREEN HEAT GROUPING



WINDSCREEN FAILURE SYMPTOMS

Fig. 7 Transparency Failure Emergency Drill (Part 2)

DESIGN GUIDELINES FOR SUBSONIC TRANSPORT WINDSHIELDS

P. H. Bain
The Boeing Commercial Airplane Company
Seattle, Washington

DESIGN GUIDELINES FOR SUBSONIC TRANSPORT WINDSHIELDS

by Peter Bain

The Boeing Commercial Airplane Company
Seattle, Washington

Presented at the Conference on
Aerospace Transparent Materials
and Enclosures
November 18–21, 1975
Atlanta, Georgia

ABSTRACT

The Boeing Company has recently completed a comprehensive Windshield Design Guide which provides data to assist in the design of windshields for subsonic transport airplanes.

This paper examines the need for such a document, and gives a brief look at its overall contents. One particular section, Performance and Durability, is discussed in greater detail, and qualitatively compares the performance of the windshields of the new generation of wide-body jets, with that of their predecessors.

A review of some of the major causes of delamination is presented together with a report on The Boeing Company's related test programs. The results of such test work, which has been conducted with a view toward increasing durability, will form, together with data from commercial experience, a base for future recommendations in this windshield design guide.

DESIGN GUIDELINES FOR SUBSONIC TRANSPORT WINDSHIELDS

During the last few years, The Commercial Airplane Division of The Boeing Company, has begun to identify various specialized components and sysems that require rather more than a standard textbook type analysis. These will form the subject of comprehensive and detailed design guides. The basic purpose of these guides is to concisely present as much relevant data to the designer as is possible. It is not intended to provide a set of hard and fast rules. Such an approach would signal the end of logical thought and progression. By the consideration of criteria, the presentation of materials, a review of earlier and current technology, including mistakes as well as successes, and an assessment of future developments, a good understanding of all aspects of the design problem will be obtained. With this knowledge, the best solution may be more readily derived.

In view of its considerable complexity and sophistication of design, it is of no surprise to find that the windshield was an early contender for this course of action. Very few other airplane components have such widely varied design possibilities. Figure 1 compares the detail design of the windshields of the DC-10, the L-1011 and the three versions of the Boeing 747.

These windshields are all designed to similar requirements, they are all bird-resistant and fail-safe. They are designed to give optimum vision characteristics, yet their configurations are widely dissimilar. And they all have logical reasons for their particular design. Some of us here may have strong views regarding the performance of glass versus acrylic, or the assets of a particular interlayer or coating Yet many differing materials and processes have found a place in current windshield design, and are probably performing with similar results. If different opinions occur within the ranks of experienced designers, how then does a new windshield designer make up his mind? Structural engineers on the whole have a profound suspicion of glass or plastic when it is used in a load carrying capacity. Their understanding of optics, electrical heating and bonding systems is often limited, yet it is usually from their ranks that windshield designers are drawn. Here, indeed, is a real need for the concise and orderly presentation of all the salient factors pertaining to windshield design,to assist a new designer in making the correct decisions.

Where, then, does one find this information? Windshield related documentation completed under Air Force or NASA contracts, or published directly by various departments of Air Force Systems Command form an excellent base. Windshield suppliers themselves publish a great deal of data and many technical papers and, indeed, are expected to lead in such research. A search of Boeing's documented records produced many hundreds of reports associated with windshield design, many of which are based upon our considerable fleet experience.

All this information must then be classified into sections for formulation into a comprehensive document.

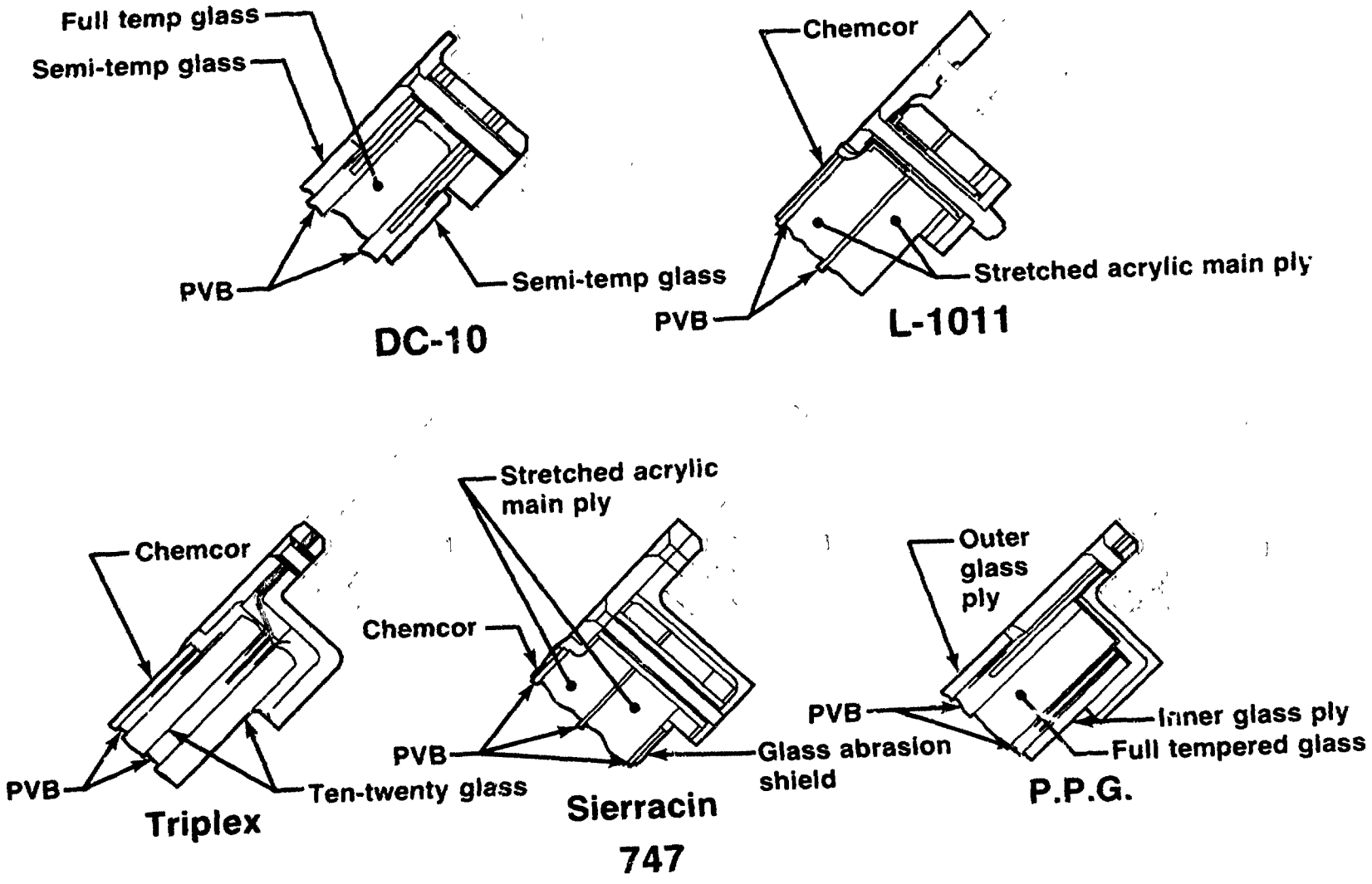


Figure 1.–Windshield Comparison

Figure 2 summarizes the contents of the recently completed Boeing Windshield Design Guide.

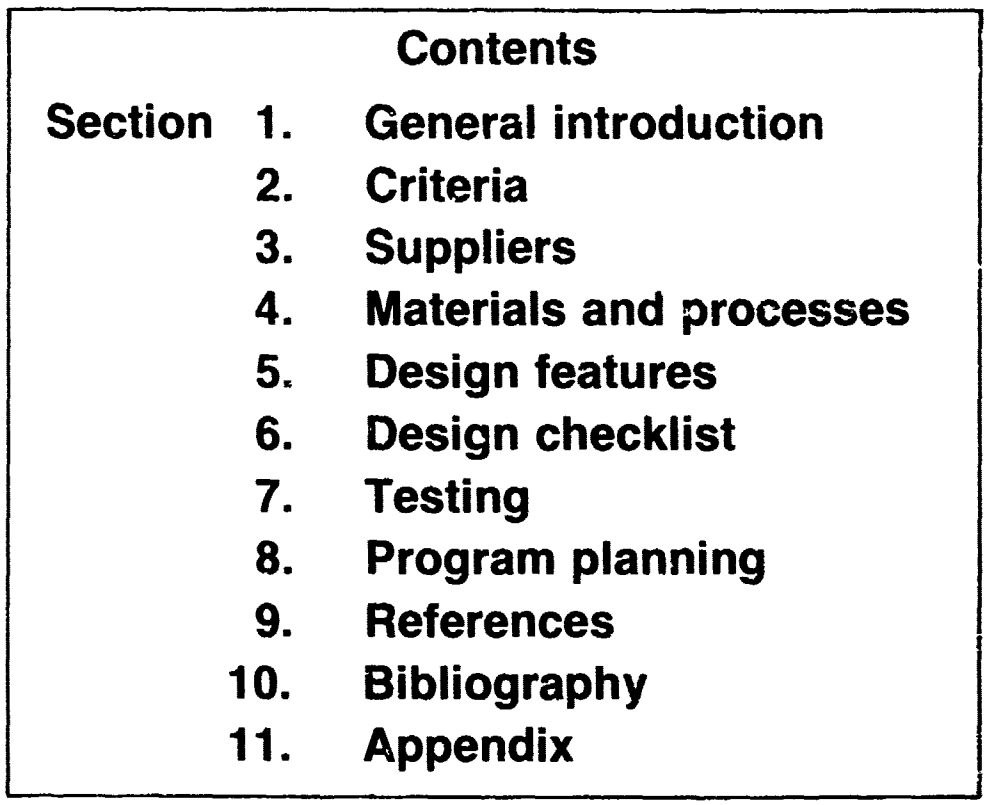


Figure 2.–The Boeing Company Windshield Design Guide

Time does not permit discussion of all these sections, much of which is elementary, but a brief synopsis is presented of the more important. The contents of Sections 1 and 2 are obvious from their title. Section 3 presents a brief description of supplier and subcontractor history and capability. The companies concerned were invited to supply their own comments for this section, to which was added our own assessment of their performance in research, development and production. Materials, including glass, monolithic plastics, and interlayers are described in Section 4. Details of tempering, forming, thermal characteristics and specialized coatings are also discussed here. Section 5 is entitled "Design Features" and contains information on the variable aspects of windshield design. Geometry, field of vision, optics, heating systems, main structural panes, outer panes, interlayers, windshield mounting and sealing are typical subjects which are discussed in great detail. Recommendations included in each of these sections are of a general form and do not inhibit the choice of the designer.

Following the design features section is a design checklist, a short section on testing, and one on program planning, together with the reference, bibliography and appendix which complete the first edition of the guide.

Figure 3 presents the proposed contents of a new section currently being planned, which is to be concerned with performance and durability.

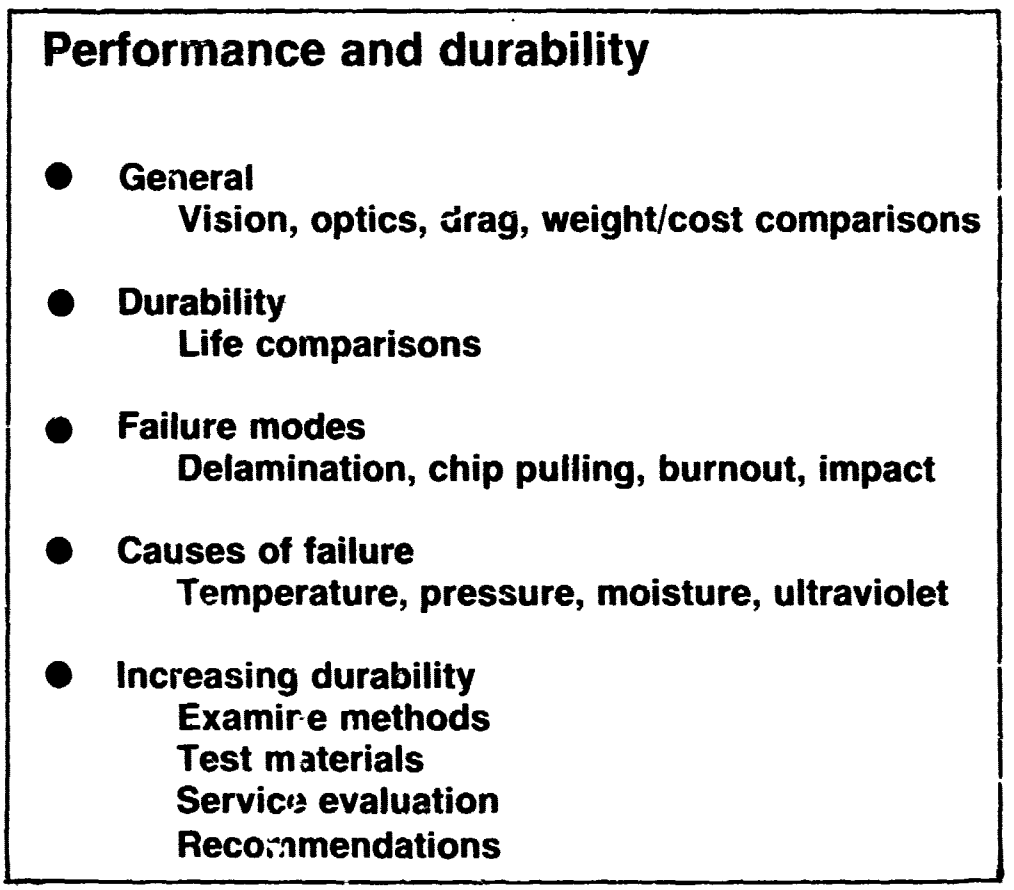


Figure 3.–Proposed New Section–Windshield Design Guide

It is the content of this section which will be explored more fully.

The problems of windshield design have been compounded with the advent of wide body commercial jets. Flight decks have become wider and their transparencies larger, in order to provide sufficient vision. To obviate large flat areas in the important nose lines, with their detrimental effects on drag and noise, curved windshield panels have been introduced on some models. This in itself was a "first" for large commercial bird-resistant windshields. New design concepts have been introduced and bird "bouncing" rather than bird "bagging" has become the rule.

How, then, does the performance of these new windshields compare with that of their forerunners? The prime objective of the windshield together with its associated side windows, is to provide a sufficiently extensive field of vision to ensure the safe operation of the airplane. It is universally agreed that a great improvement of vision field has been obtained, and without the necessity of additional crown windows. Additionally, these windshields and windows, in spite of their greatly increased size and more complex geometry, have retained their extremely high optical quality. In the service experience so far obtained, their bird strike resistance and fail-safe capability has been demonstrated several times. However, throughout the whole family of windshields there is not the marked improvement of service life that had been hoped for. The same old modes of failure still occur. Delamination and its associates of coating disruption and burnout, chip pulling and vinyl cracking are still the principal reasons for windshield replacement. In some cases, modifications and improvements to the original design have resulted in some service life extension, but no dramatically increased durability appears to be forthcoming.

The mechanics of delamination and their causes have been researched and discussed many times in the past, and it is generally agreed that there is not just one predominant cause. Figure 4 suggests a few mechanical and environmental conditions which may promote delamination.

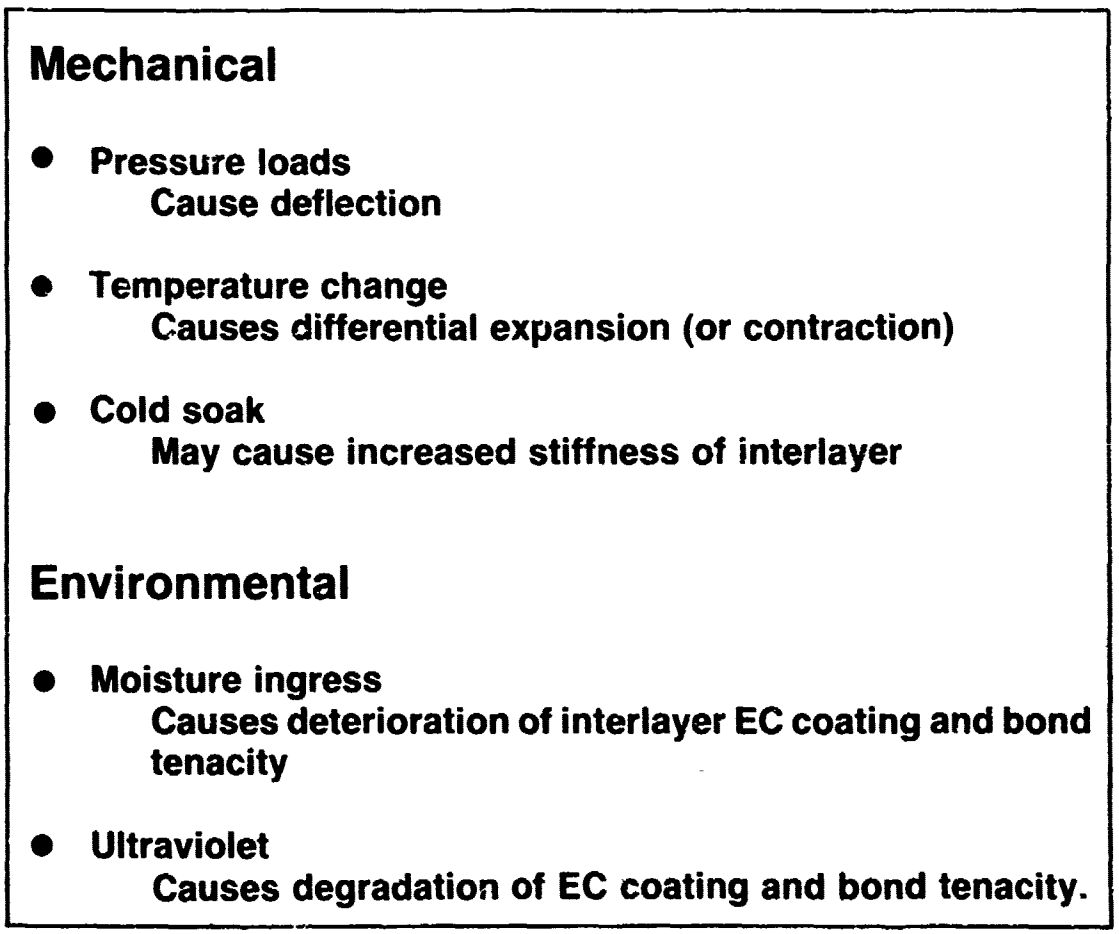


Figure 4.–Causes of Delamination

Cabin pressure causes deflection of the pane which induces some delaminating force; temperature excursions cause differential thermal expansion or contraction between the various laminates, which creates additional delaminating forces; cold soaking has the effect of shrinking and stiffening certain interlayer materials, thus increasing delaminating loads and possibly locking in these bondline stresses. Environmental conditions also tend to promote delamination by deterioration of the interlayer material, the coating or the tenacity of bond. Moisture ingress and possibly ultraviolet are the main environmental causes of such deterioration, and of the two, moisture ingress is the only one that we can presently take steps to preclude.

Figure 5 suggests three approaches to provide increased durability.

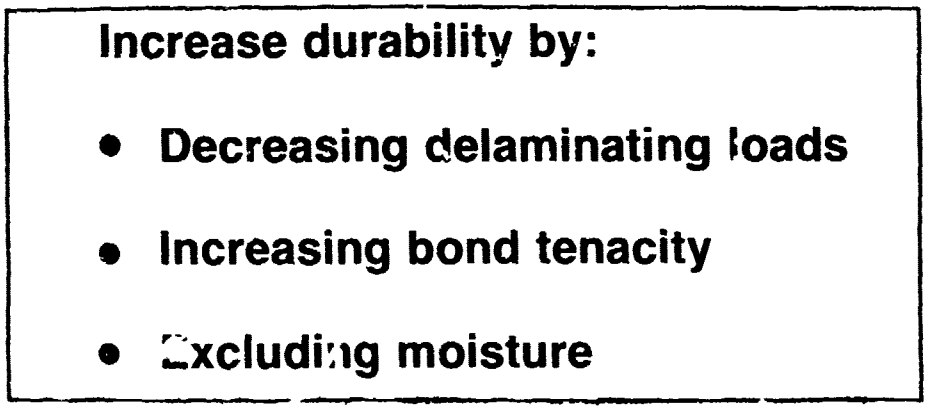


Figure 5.–Durability Increase

1. Decrease delaminating loads by decreasing the stiffness of the interlayer. A less rigid interlayer will reduce shear load at the bondline.

2. Increase bond tenacity by the evaluation of interlayer materials and consideration of the characteristics of any coating.

3. Exclude moisture by an efficient sealing system.

The Design Development Group of The Boeing Company has been working for some time on the problems of windshield durability. As The Boeing Company purchases all its transparencies from specialist suppliers and is not in the transparency business, per se, its ability to fabricate specimens is limited. However, with the excellent cooperation of many leading transparency fabricators, both in this country and abroad, Boeing has been able to set up a variety of test programs to evaluate available materials at the same time and under the same conditions. Although we have signed proprietary protection agreements with these participating companies, and cannot divulge specific results or even identify participants, a brief description of the test programs themselves, with a general overview of results is of considerable interest.

In an effort to provide information related to reducing delaminating loads, some test work was directed toward the variation of interlayer stiffness, particularly with regard to changing temperatures. To make a consistent practical comparison of stiffness between the temperature range of 130° F and -90° F, a small test beam specimen and test fixture was devised which could be entirely contained within a variable temperature test chamber, as shown diagramatically in Figure 6.

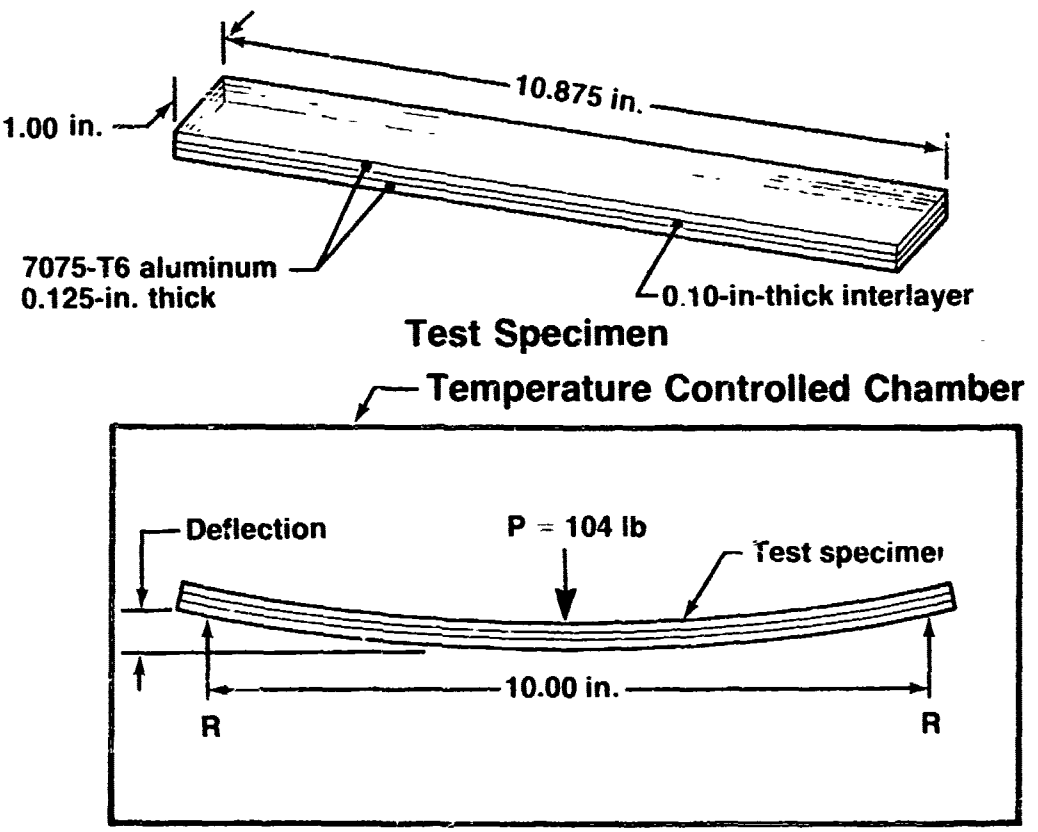


Figure 6.–Test Fixture Interlayer Stiffness–Diagramatic

The specimens used a variety of 0.10-inch thick interlayers, each bonded between two strips of 0.125-inch thick 7075-T6 Aluminum Alloy. This alloy has the same elastic modulus as glass, and was used for convenience. It is also a better thermal match for the interlayers, having a higher coefficient of thermal expansion than glass. Since stiffness of the aluminum alloy caps is essentially independent of temperature, the measured deflection variations reflect the contribution of the interlayer to beam stiffness through the temperature range tested.

In practice the test beam was installed in the fixture and brought to test temperature. A constant load of 104 pounds was then applied at the beam center, and deflection readings taken, until creep was negligible. After each run the beam was removed and exposed to room temperature, and in some cases water at 100° F, until the interlayer relaxed and returned to its undeflected shape. The beam was then reinstalled and the test sequence repeated for the next temperature.

Time/deflection curves were plotted for temperatures between 130° F and -90° F. Maximum deflection was reached after ten minutes on all specimens at nearly all temperatures. Figure 7 shows the general pattern of deflections for a variety of interlayer materials throughout the temperature range after ten minutes exposure to load.

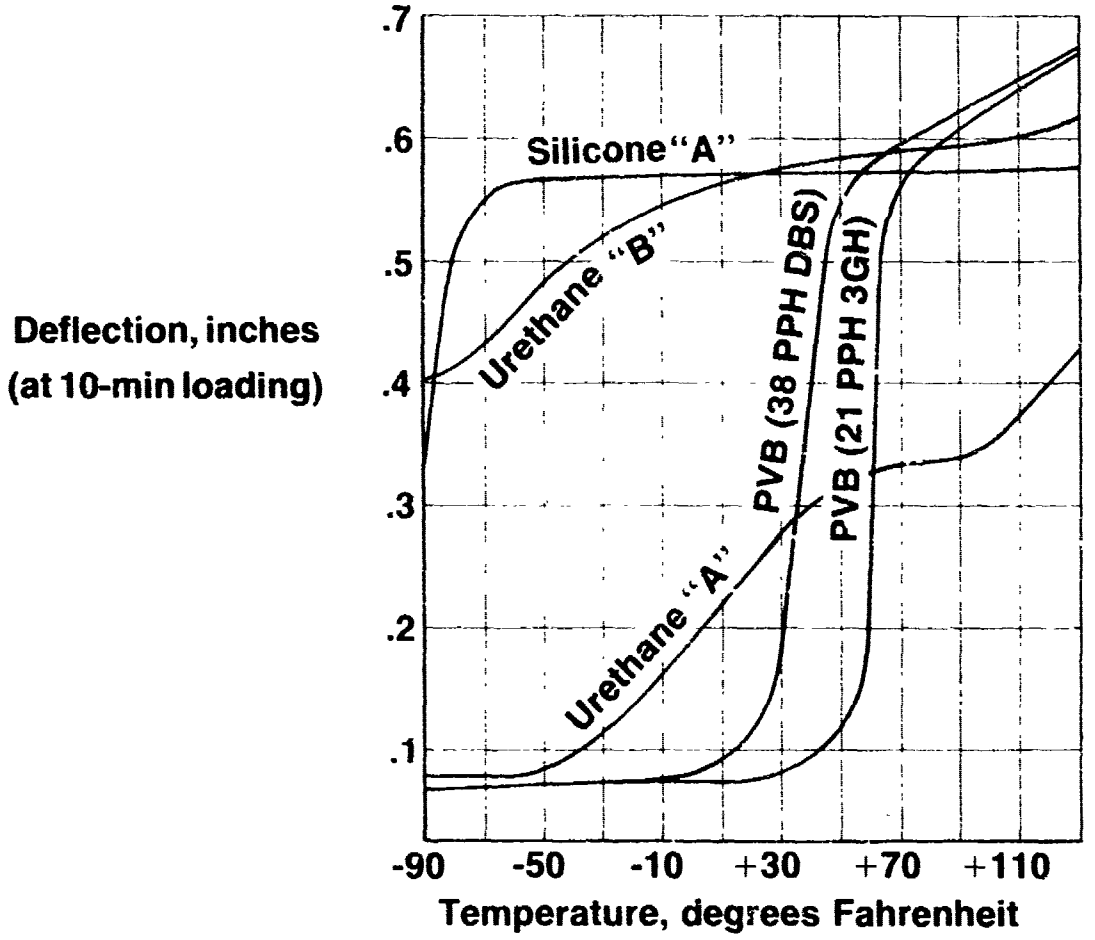


Figure 7.–Interlayer Stiffness Tests–Temperature/Deflection

From this diagram we may assume the curves depict practical temperature/stiffness relationship and we see a dramatic stiffness change of PVB as compared to the other samples. If this increase of stiffness is seen as a decreasing ability to relieve bondline shear stress caused by differential thermal shrinkage, it would indicate the marked increase of such stress after the temperature drops below approximately 30° F or 50° F when either of the PVBs are used as an interlayer. We know that operating temperatures in certain windshield cold spots are quite likely to be as cold as -20° F, and even less all over the windshield when parked overnight in certain geographical areas.

The next group of tests was intended to compare the bond tenacity of different interlayers. Test specimens, 12 inches square with two glass plies, or one ply each of glass and acrylic and bonded together with an appropriate interlayer, were subjected to cold shock cycles. The interlayer was monitored with thermocouple and recorder. Each specimen was imersed in the cold bath until the desired temperature was reached, then withdrawn and allowed to return to room temperature. The procedure was repeated for ten cycles to -90° F or until failure.

Figure 8 shows the results obtained with glass on glass specimens.

Part	Interlayer	Temperature and cycles	Type of failure
1a	0.38 PVB (21% 3GH) (w/slip plane)	10 -10 -30 -50 -70 -90	Delam
1b		-25 -40 -60 -70 -70 -70 -85 -90 -90	None
1c		-45 -52 -72 -75 -75 -74 -85 -90 -90 -90	Chips
2a	0.38 PVB (21% 3GH)	30 10 -10 -30 -50	Delam
2b		-35 -47 -45	Delam and chips
2c		-53 -55 -70 -72 -72 -72 -75 -75 -74 -75 -90 -90	Shattered
3a	0.10 PVB (21% 3GH) (w/slip plane)	10 -10 -30 -70 -90 ← → -90	None
3b		-90 ← → -90	None
4a	0.03 PBV (21% 3GH) (w/slip plane)	-90 ← → -90	None
4b		-90 ← → -90	None
5a	0.38 Urethane "A"	10 -10 -30 -50 -70 -90 ← → -90	None
5b		-30 ← → -90	None
6a	0.10 Urethane "A"	10 -10 -30 -70 -90 ← → -90	None
6b		-90 ← → -90	None
7a	0.03 Urethane "A"	0 ← → -90	None
7b		-90 ← → -90	None

[-90] 1 cycle at -90° F Target is 10 cycles at -90° F

Figure 8.–Cold Shock Test–Glass-on-Glass Specimens

A comparison between types one and two clearly confirms the advantages of slip planes with relatively thick PVB. and also illustrates the intensity of the bondline stress.

Specimens three and four support the assumption that thin interlayers between glass plies feel less stress than thick when subjected to temperature variations. Specimens five, six and seven are differing thicknesses of urethane, and demonstrate its greater bond tenacity. Urethane has a greater coefficient of thermal expansion than PVB but as we have seen earlier, it is not subject to a similar degree of stiffening at low temperatures. In the 0.38-inch thick, and also in the thinner specimens, no failure was induced after ten cycles at -90° F.

Before considering the results of the glass and acrylic specimens, it is well to analyze the probable effect of the test. It is expected the main effect will be from the acrylic moving shearwise past the glass due to its greater thermal expansion coefficient. The interlayer must either transmit this motion into bondline shear stress, or to absorb it by interlayer shear deflection, or a combination of both. In this case, it is expected that the thicker interlayers will have the better performance. The results, shown in Figure 9 indicate that two out of three thin PVB specimens did in fact, delaminate on the first cycle.

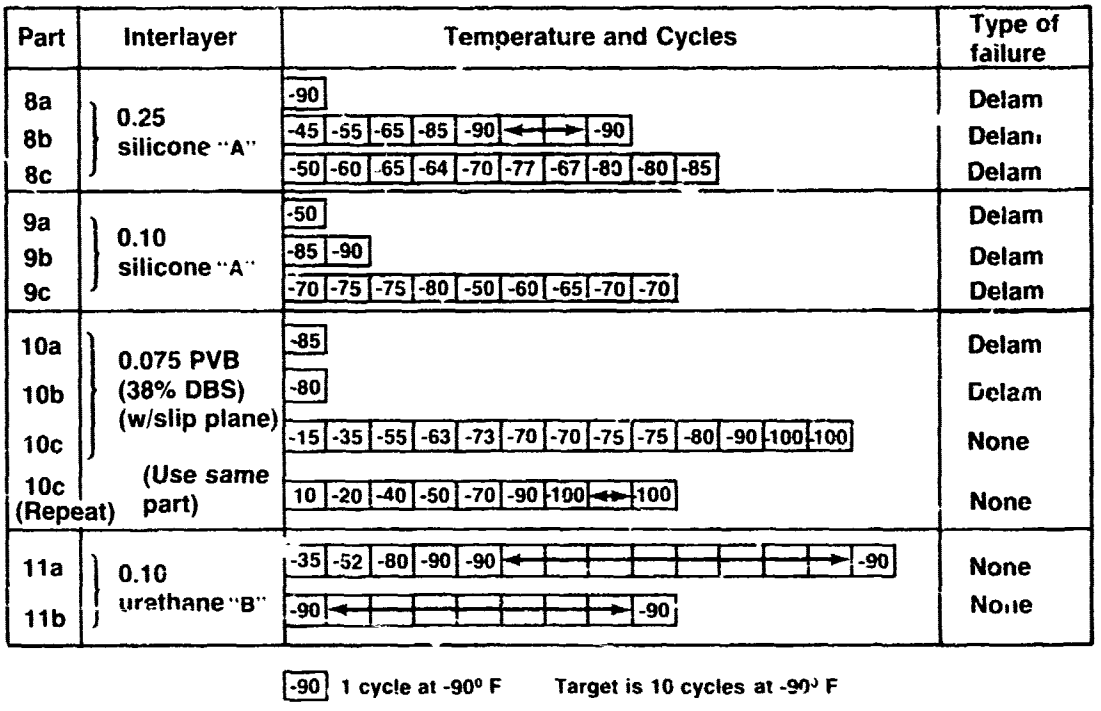


Figure 9.–Cold Shock Test–Glass-on-Acrylic Specimens

Of the silicone specimens, those with the thicker interlayer faired better than the thin, although, to be fair to this material all delaminations were at the gold coat interface with the glass. The urethane, as with the all glass specimens, showed an excellent performance.

Our latest test program directed toward the delamination problem is still in progress. It consists of a series of flatwise tension and shear creep tests being performed on a range of typical windshield laminates, of which the general configuration is shown in Figure 10.

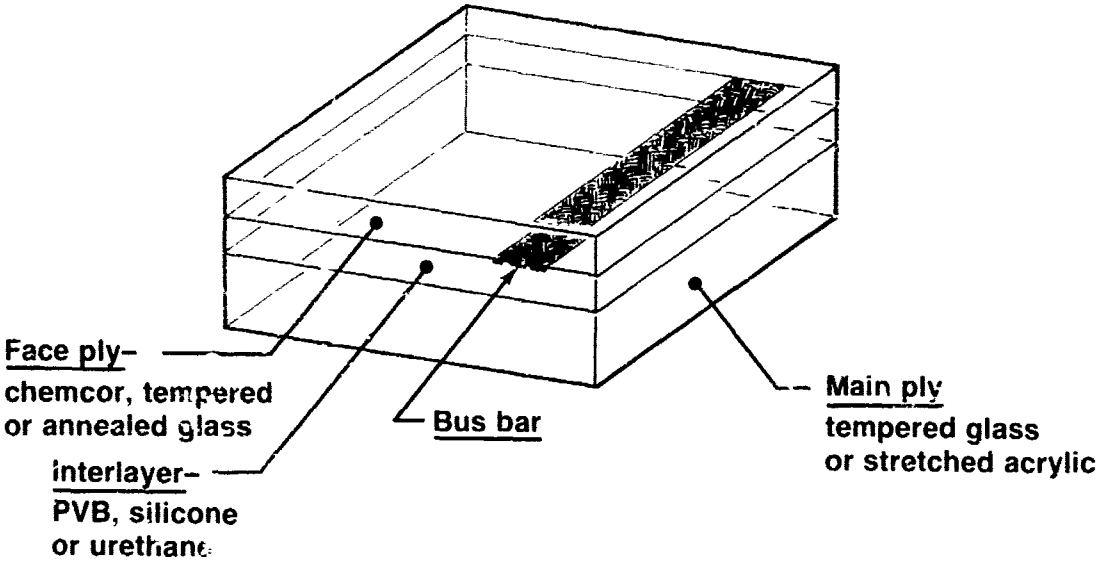


Figure 10.–Two-Inch-Square Specimen for Creep Testing

The 2-inch-square specimens have a relatively thin face ply, of either chemcor, tempered or annealed glass. The interlayer is of PVB, silicone or urethane in their recommended thicknesses, and the rear main ply is of tempered glass or stretched acrylic approximately 1/2-inch thick. Representative electrically conductive (EC) coatings, both with and without bus bar, were supplied on some of the specimens.

Initially, ultimate tests in flatwise tension and also in shear, were performed. Percentage values of these ultimate loads were then estimated that would produce failures in approximately 1, 10, and 150 hours. These loads were applied continuously to the specimens and times to failure noted. Some tests were also carried out using a load estimated for 1000-hour life. Presently only the results of the flatwise tensile tests at 120° F are available and these are shown in Figure 11.

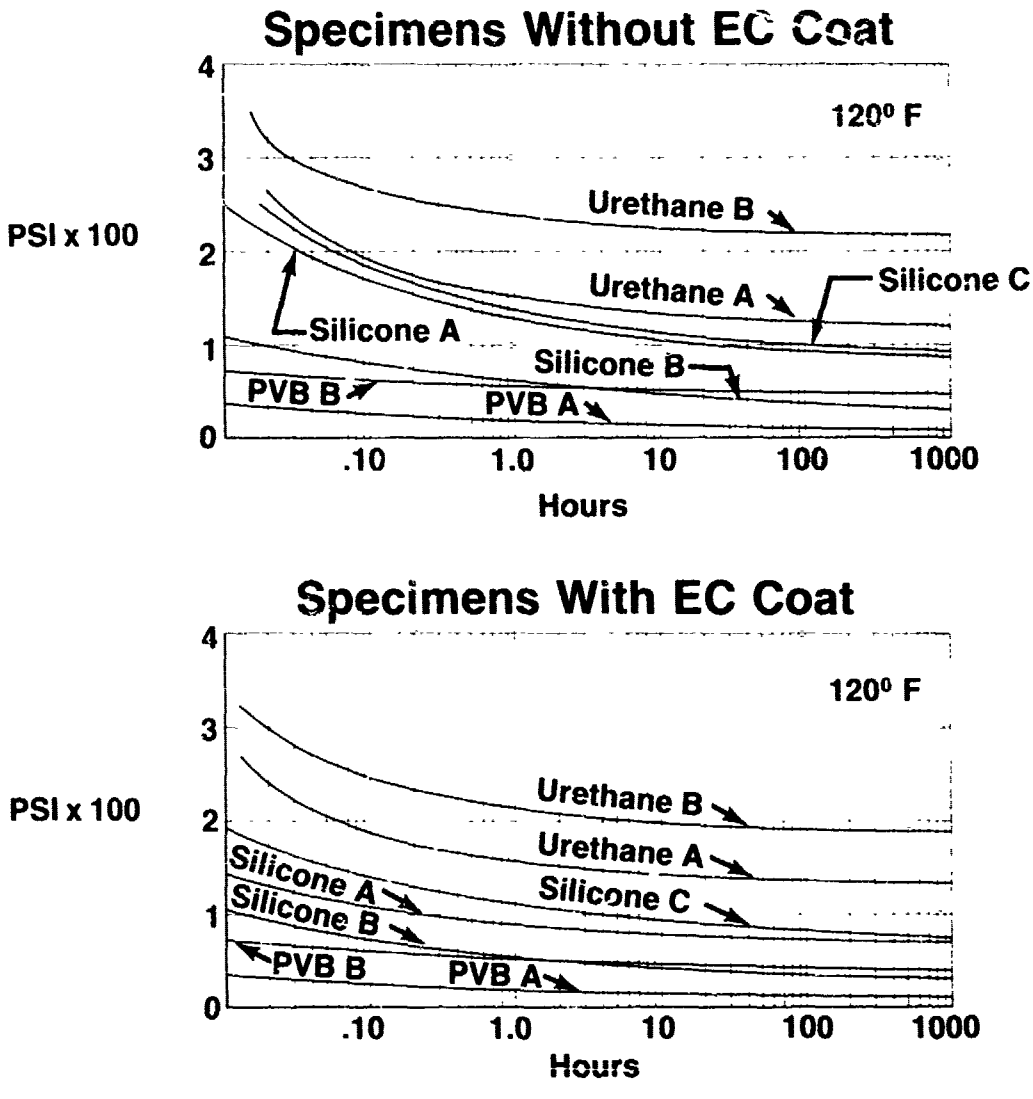


Figure 11.–Tensile Creep

Time-to-failure is shown along the base to a logarithmic scale and stress appears in a linear scale to the side.

All the interlayers tested exhibited similar creep characteristics but again the urethanes demonstrated superior tenacity. Curves for both coated and uncoated specimens show similar relationships of the various interlayers. The results so far obtained from the shear tests follow a similar pattern to that which is shown here.

In order to gain flight experience of urethane, some Boeing 707 series crown windows are to be fitted with an additional thin lamination of this material between the PVB interlayer and main glass ply. These special windows will soon be placed in commercial service for evaluation. Also, there is one production Boeing 747 windshield in service with an additional thin urethane lamination. It is understood that similar evaluation is also taking place on DC-9 and DC-10 aircraft. Such service experience is invaluable in evaluation of any material, for no meaningful conclusions may be drawn without it. We, at The Boeing Company, will continue to test and evaluate any material or process that shows promise, particularly with regard to windshield durability. As new data becomes available, recommendations will be presented in future editions or revisions of the Windshield Design Guide, to ensure a continuing awareness of materials and processes which will result in improved windshield design and performance.

HIGH STRENGTH GLASS IN SERVICE - A STATUS REPORT

R. W. Wright
Triplex Safety Glass Co. Ltd.
Birmingham, England

PAGE BLANK-NOT FILMED

HIGH STRENGTH GLASS IN SERVICE

- A STATUS REPORT

By

R. W. Wright

Triplex Safety Glass Co. Ltd.
Birmingham, England.

ABSTRACT

The design and testing of windshields for the A300B and the Boeing 747, using Triplex high strength glass "TEN-TWENTY", was reported at the 1973 Conference and considerable flight experience is now accumulating since the introduction of these windshields into service. Details are given of subsequent developments, particularly of thin curved high strength glasses optimised for use as a facing ply on the Boeing 747 windshields. Other technically advanced airplanes using "TEN-TWENTY" for light-weight, high optical quality and reliability include the AV8A Harrier, the DHC-7, and the Concorde.

Concorde, with a total of 16 different cockpit glazing panels, has unique transparency requirements coupling stringent airline standards of reliability with sustained supersonic flight at very high altitude. These requirements have been met by a combination of glass technologies using some novel design concepts including electro-conductive coating on monolithic glazings.

1. INTRODUCTION

Since the first introduction of "TEN-TWENTY" high strength glass into military and airline service several years ago, its range of applications has progressively increased. "TEN-TWENTY" glass is now being produced in a variety of shapes, sizes, thicknesses and strengths and its basic versatility will be discussed together with details of some of its more interesting applications. The progress and development of windshields embodying "TEN-TWENTY" glass, over the last two years or so, is also described.

Although this paper is essentially a status report on "TEN-TWENTY" high strength glass, this aspect is not treated in isolation and associated aspects, such as design, interlayers and coatings are briefly reported.

Some other glasses, falling into the category of high strength, having particularly interesting applications, are also discussed.

2. DISCUSSION

2.1 The Versatility of "TEN-TWENTY" High Strength Glass

The summary in Figure 1 presents the features now available for the family of "TEN-TWENTY" glasses. One of the significant features of this glass is that its range of properties has been developed in the last two years, providing a very versatile material for the windshield designer.

Although initially launched as a flat glass, available in a limited range of thicknesses, having a Modulus of Rupture of 45,000 lb/sq. inch for use as a main structural element, continued development has enlarged the range to almost any thickness of glass available between $\frac{1}{8}$ inch (3 mm) and $\frac{1}{2}$ inch (12 mm). At the same time an M.O.R. can be accurately selected between the extremes 25,000 to 45,000 lb/sq. inch. From the weight saving point of view, it is practical to produce a windshield of comparable weight to stretched acrylic constructions. Coupled with the ability to form the glass to cylindrical and conical curves, we can provide a choice of fracture pattern ranging from mild cracking to a full crystalline pattern. We are now producing "TEN-TWENTY" glasses for not only main structural plies but for thin outer facing plies. Typical applications are described.

2.2 Present Uses of "TEN-TWENTY" Glass

Boeing 747 Front Windshield (Figure 2)

It is not intended to describe the design philosophy being used on this windshield since this has been adequately covered at a previous conference. (Reference 1) It is however useful to review the first two years experience and to highlight weaknesses revealed.

The longest serving windshields have exceeded 24 months service, and the high time "TEN-TWENTY" windshield has flown for 7950 hours. Although some removals have occurred to date, the statistics indicate a very good service life as likely to evolve. These windshields are now operational with about 15 airlines on a world-wide basis.

Some of the problems encountered, and their solutions, are worthy of note and these are summarised in Figure 3. Rain erosion of the external weather seal initially proved to be significant and examination of windshields showed that some corrective action was necessary. As may be seen in Figure 4, a re-profiling of this weather seal, and the addition of a polyurethane protective layer substantially strengthened the seal. To date, no further problems have been reported.

Hail impact failures of the exterior chemically toughened 0.05 inch glass have also been noted, prior to the introduction of an alternative $\frac{1}{8}$ inch (3 mm) "TEN-TWENTY" facing ply. The glass has a far greater resistance to hail impact, whilst giving a high level of residual vision. At the same time the overall optical quality of the windshield is not jeopardised. Trials using full scale hail impact tests led to the selection of a glass with an M.O.R. of about 27,000 lb/sq. in. This gives a significant improvement in the hail impact failure speed and still provides excellent residual vision. This eliminates the need for front ply stripping procedures, and could permit short term flight continuation. Typical residual vision after a hail impact failure is shown in Figure 5.

Development of this glass to the required optical standard was not without its difficulties and by very careful control of the bending process of the $\frac{1}{8}$ inch (3 mm) facing plies to match the $\frac{1}{2}$ inch (12 mm) main plies, optical requirements were met.

The final significant mode of failure on early windshields was delamination and some of the delaminating stresses are considered to be associated with the 'cold draping' of the thin chemically toughened outer glasses. The introduction of the new $\frac{1}{8}$ inch (3 mm) "TEN-TWENTY" outer glass significantly lowers these stresses and process improvements have been introduced to further improve adhesion levels. These primarily affect the interlayer bond to the Triplex "HYVIZ" electro-conductive coating and the strength and stability of this coating provides compatibility with high levels of adhesion.

Hawker Siddeley AV8A (Harrier) Front Windshield

The general role of this V.T.O. fighter is well known and it is in service in large numbers with both the U.S. Marine Corps and the Royal Air Force. (Figure 6)

With any attack aircraft operating at low level and high speeds, the need for a rugged windshield is vital. With the AV8A Harrier, component reliability is essential when based at forward battle zones. Its main structural design case is that of low level-high speed bird impact and the windshield has a multi-laminate, clamped-in, "TEN-TWENTY" construction, as shown in Figure 7.

Three $\frac{1}{4}$ inch (6 mm) "TEN-TWENTY" plies provide the main laminated structural element and this is faced with a conventionally tempered outer glass.

Because of power limitations the windshield is not heated and fogging is prevented by having an inner airspace, closed with a further thin tempered glass.

Because of the high M.O.R. used for the structural "TEN-TWENTY" glasses a very light-weight windshield has resulted, matching closely the weight of a stretched acrylic design fitted on early Harriers.

A very high optical standard is demanded since the gun sight system functions through the windshield. The airspace glass has therefore to be matched to the structural elements to achieve the desired standard.

Having inherently simple design, the windshield has proved to be very reliable and removals since service introduction 4 years ago have been minimal.

Possible developments of this windshield on future Harriers, assuming available power, could be the addition of a heating film, eliminating the airspace.

Airbus Industrie A300B Front Windshield (Figure 8)

This windshield, embodying two 0.4 inch (10 mm) "TEN-TWENTY" main glasses having an M.O.R. of 45,000 lb/sq. inch, was described in considerable detail at the 1973 Conference. (Reference 1)

The aircraft is entering service with increasing numbers of airlines and windshield hours are building up rapidly. The multi-laminate, "TEN-TWENTY", clamped-in concept, together with other design features aimed at maximum reliability is proving well able to combat the cyclic thermal and pressure stresses generated. Triplex's cyclic 'Life Test' rig has subjected sample windshields to a 10,000 flying hour simulation, which is a meaningful indication of the windshield's potential service life.

Like the Harrier, the A300B also requires a high optical quality and as an example, its primary vision area requires absolute and binocular deviation limits of 5 minutes of arc. This puts great demands on the process control necessary to both the "TEN-TWENTY" glass manufacture and its assembly.

De Havilland Canada DHC-7 Front Windshield (Figure 9)

Together with Triplex "HYVIZ" coatings, "TEN-TWENTY" glass is now flying in the DHC-7 prototypes. Here again a very simple construction embodying a $\frac{1}{4}$ inch (6 mm) and a 5/16 inch (8 mm) high strength glass ply is used in a clamped-in construction, very similar to that used on the A300B.

In common with all "TEN-TWENTY" multi-laminate constructions, bird impact is met using the "bird bounce" philosophy, in that the structural plies are undamaged by a bird impact at the design speed. Invariably, facing plies survive unscathed since they are predominantly compressively stressed at the moment of impact. A sequence taken from a high speed film of the DHC-7 qualification test is shown in Figure 10.

Concorde SST (Figure 11)

Now that Concordes are shortly to enter service with British Airways and Air France, it is relevant to discuss the complexities of the flightdeck transparencies. To meet the severe design parameters (Figure 12) and at the same time accommodate both high speed and low speed configurations, a total of 16 panels are involved. These embody a range of technologies, including "TEN-TWENTY", Corning Chemcor and conventionally tempered glasses, Gold Film and "HYVIZ" coatings, Polyvinyl Butyral and cast-in-place silicone interlayers.

Apart from the harsh environment, airline standards of reliability and high utilisation rates are needed.

In the supersonic cruise configuration the main brunt of the kinetic heating effect is met by the Visors, with the front windshields exposed only when the Visors are retracted for the approach. Figures 13 and 14 show the Visor structure in the raised and lowered attitudes. At the sides of the flightdeck, the D.V. and Side panels are exposed to the kinetic heating effect, building up to nearly 250°F (120°C). Each of these panels have two individual panes. The outer is a heatshield, separated by an airspace from the inner pressure bearing assembly.

The view from the flightdeck is not restrictive, as might be supposed, and some pilots prefer to taxy and take off with the Visor in the 'up' position. A general pilot's eye view is shown in Figure 15.

The development of each of the transparencies was a major task and for simplicity I have grouped these into three main types:

A. Front Windshields

B. Side and D.V. Panels

C. Visors

Typical cross sectional views of these are shown in Figure 16.

The Front Windshield incorporates both "TEN-TWENTY" glass and a "HYVIZ" heating film and has seen continuing development up to the present design (Figure 17). The original windshields were designed as far back as 1962 and were of the familiar extended edge type with a metal insert within a thick Polyvinyl Butyral interlayer. Two 0.6 inch (15 mm) air tempered plies were necessary to meet a double 'fail safe' requirement. The next phase introduced a clamped-in-place multi-laminate windshield. This had three air tempered 0.4 inch (10 mm) plies to provide the double fail safe feature and gave about a 12% weight saving. Finally, the arrival of "TEN-TWENTY" permitted the substitution of 0.3 inch (8 mm) glasses as the main plies, giving a further 19% weight saving. This design is now in series production. The 4 lb. bird impact case at 512 m.p.h. is the main structural parameter and is particularly stringent since the windshield has a severe bird impact angle. The size of the panel is also considerable, as may be seen in Figure 18.

The D.V. and Side panels have also seen several changes, the emphasis being on the outer heatshields. Early heatshields had two glass plies laminated together with specially processed Polyvinyl Butyral. A gold film heating system was also employed. At the time, tests had shown this concept to be capable of meeting the kinetic heating effect although the margin was small. In the early flight phases it became evident that a superior solution was required and a monolithic flush fitting "TEN-TWENTY" design proved possible (Figure 19). Although having an installed angle of less than 30^{0} to the line of flight there was nevertheless a bird impact requirement which was satisfactorily met. Heating is achieved with an exposed "HYVIZ" film on the rear surface of the monolith, within the airspace. This was made possible by the inherent robustness and stability of the "HYVIZ" coating.

As far as we know, this concept of a heated, bevel edged, monolithic glass is unique.

The Visors, lastly, presented some novel problems. The retractable Visor structure incorporates six separate transparencies, two curved, four flat, as shown in Figure 20. The curved Visors are two-ply laminates of normal tempered glass whilst the flat items use Corning Chemcor chemically tempered glasses. The four longer Visors are over 6 feet long and because of their very shallow installed angle, the achievement of a high optical standard required extensive development, particularly in the case of the curved glasses. Careful matching of accurately formed glasses is essential.

Although early Visors used a specially processed Polyvinyl Butyral interlayer, production items now incorporate Swedlow SS5272Y (HT) high temperature silicone interlayer. This cast-in-place material was selected specifically for its ability to withstand sustained temperatures well in excess of the operational requirement.

As can be seen the complexity of Concorde's glazing has called upon a range of high strength glass applications, both "TEN-TWENTY" and conventionally tempered.

3. CONCLUSION

To sum up therefore, it has been shown that "TEN-TWENTY" high strength glass is well past its development phase as a versatile material with a great range of applications. It is in regular military and airline service on a number of aircraft on a worldwide basis.

References

1. "The design, development and testing of flat and curved all glass windshields for wide bodied aircraft using the latest developments in high strength glass and electro-conductive coatings."
- Paper by W. G. Roberts at the 1973 Las Vegas Conference on Aerospace Transparencies and Enclosures.

The versatility of Triplex Ten Twenty high strength glass

Thickness	inches	0·12	0·16	0·24	0·32	0·39	0·47
	(mm)	(3)	(4)	(6)	(8)	(10)	(12)
Strength (modulus of rupture)	lbs/sq.inch	25,000	35,000	40,000	50,000		
Size		0·02 sq ft to 10 sq ft					
Forms		Flat, conically or cylindrically curved					
Fracture Pattern		Large or small particle size					

Figure 1

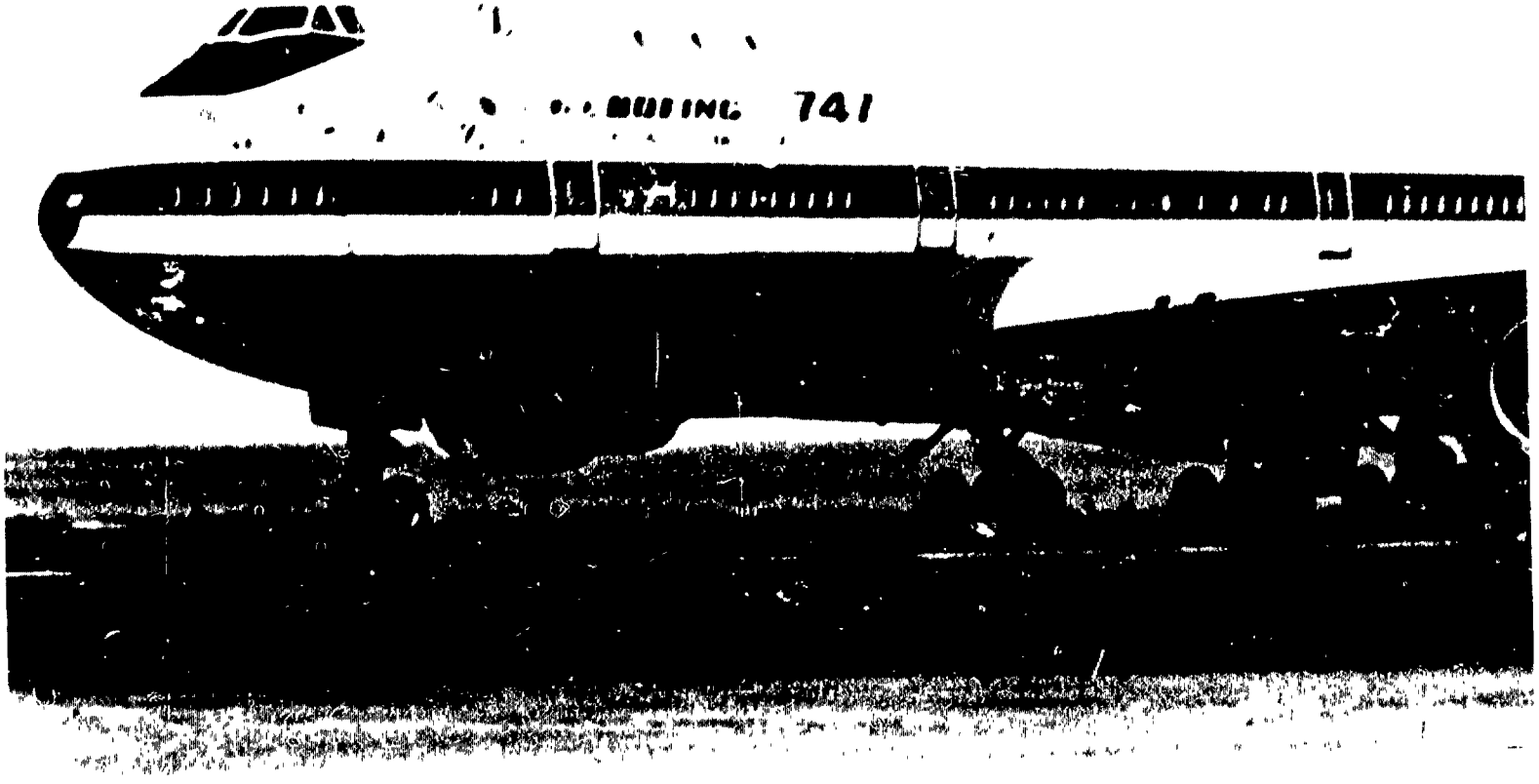


Figure 2

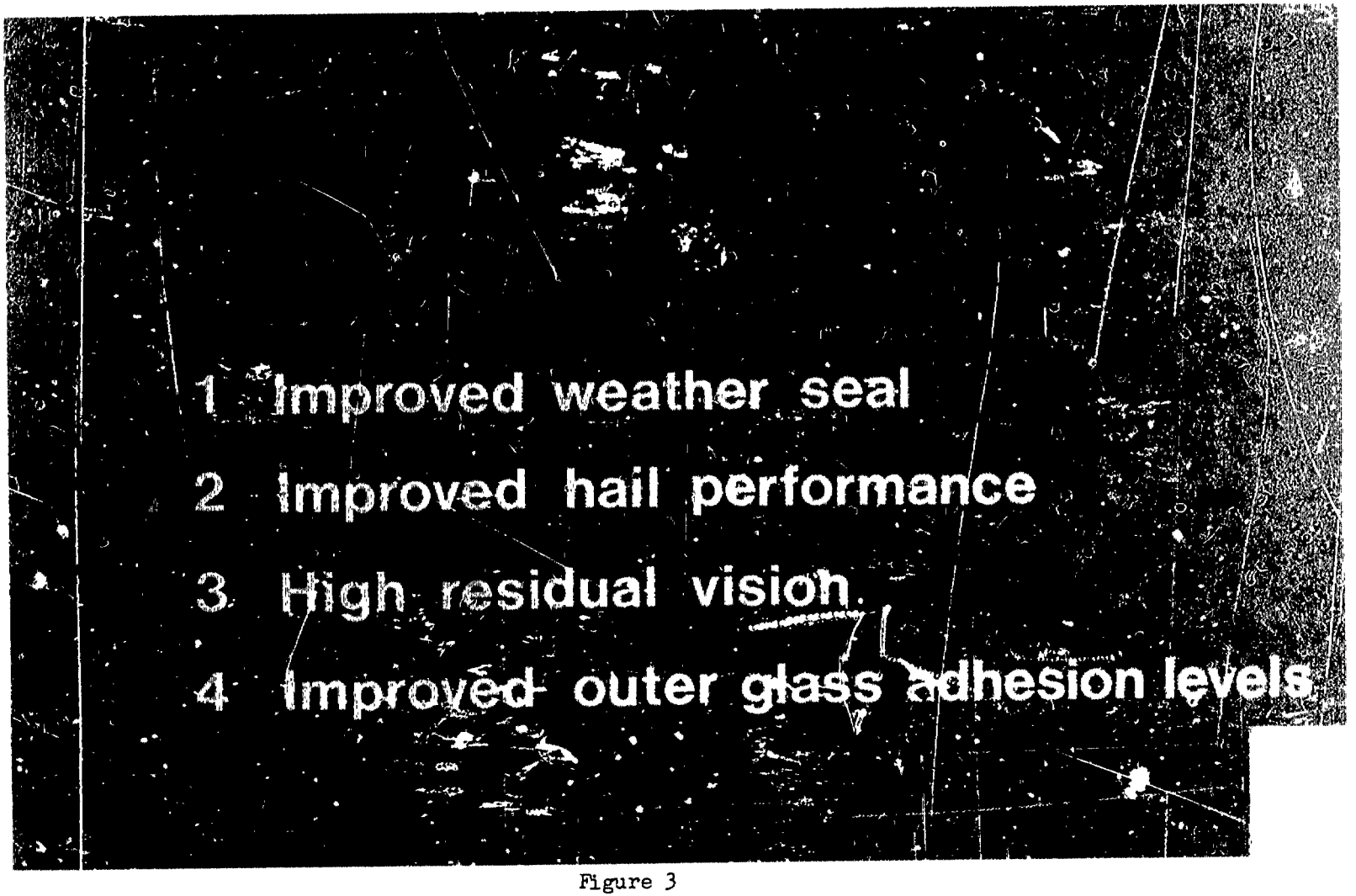

1 Improved weather seal
2 Improved hail performance
3 High residual vision
4 Improved outer glass adhesion levels

Figure 3

Boeing 747 weather seal improvement

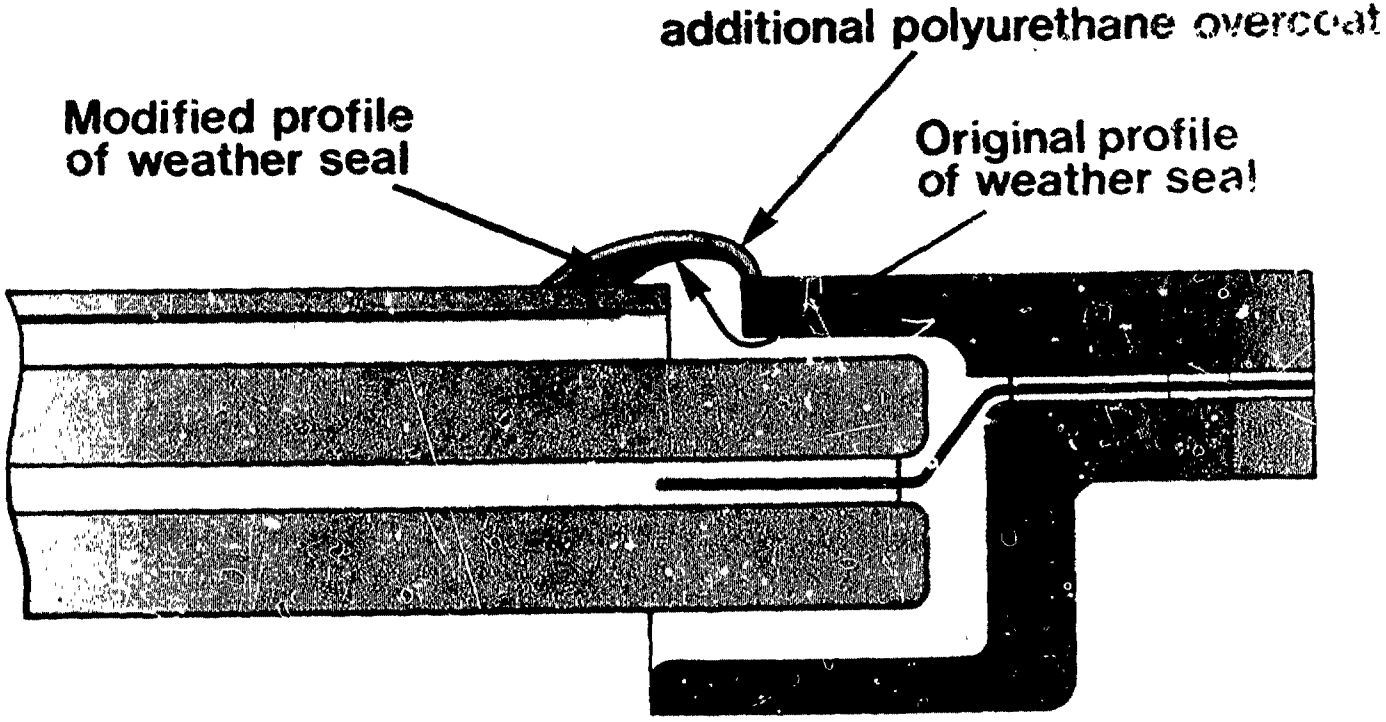


Figure 4

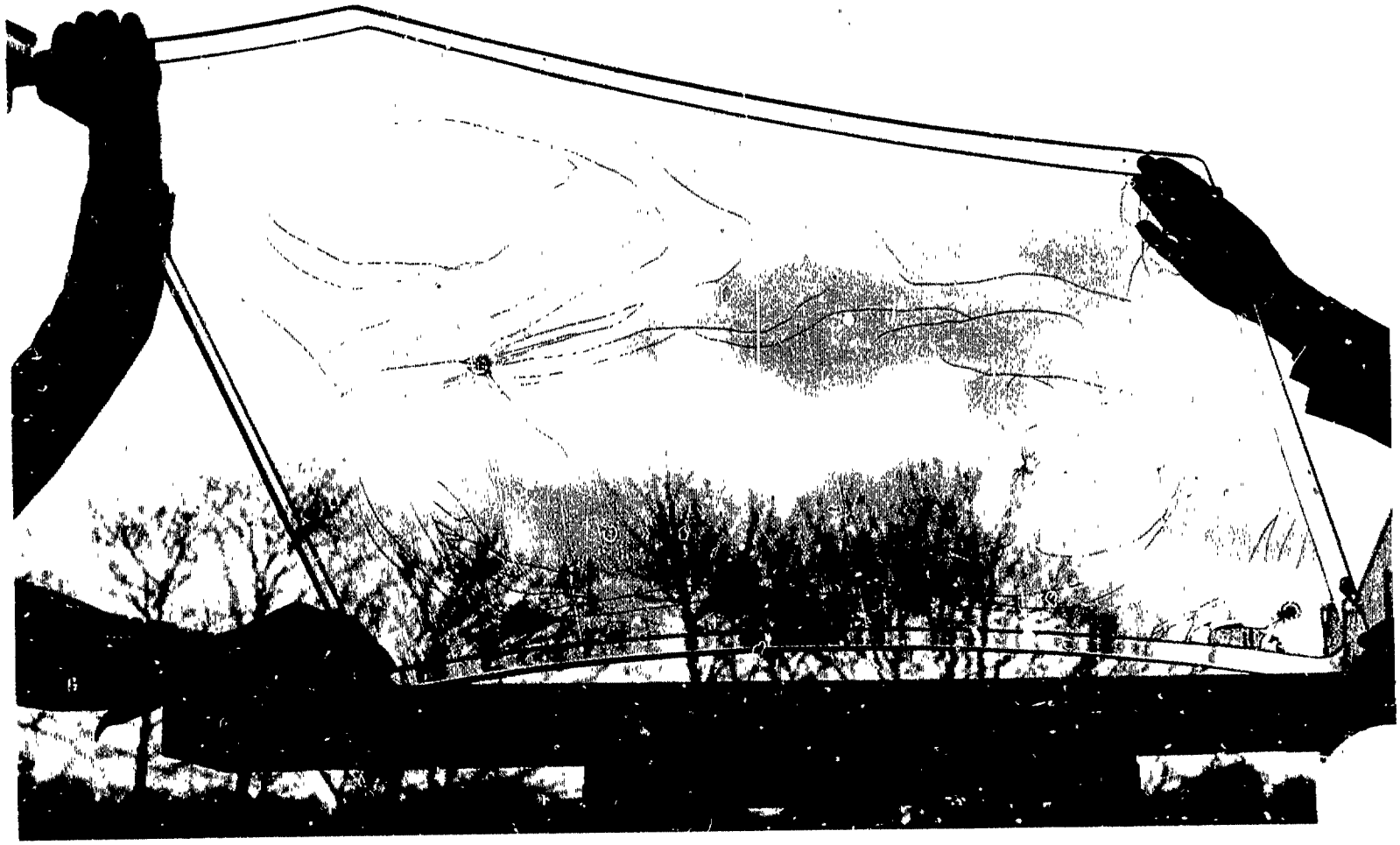


Figure 5

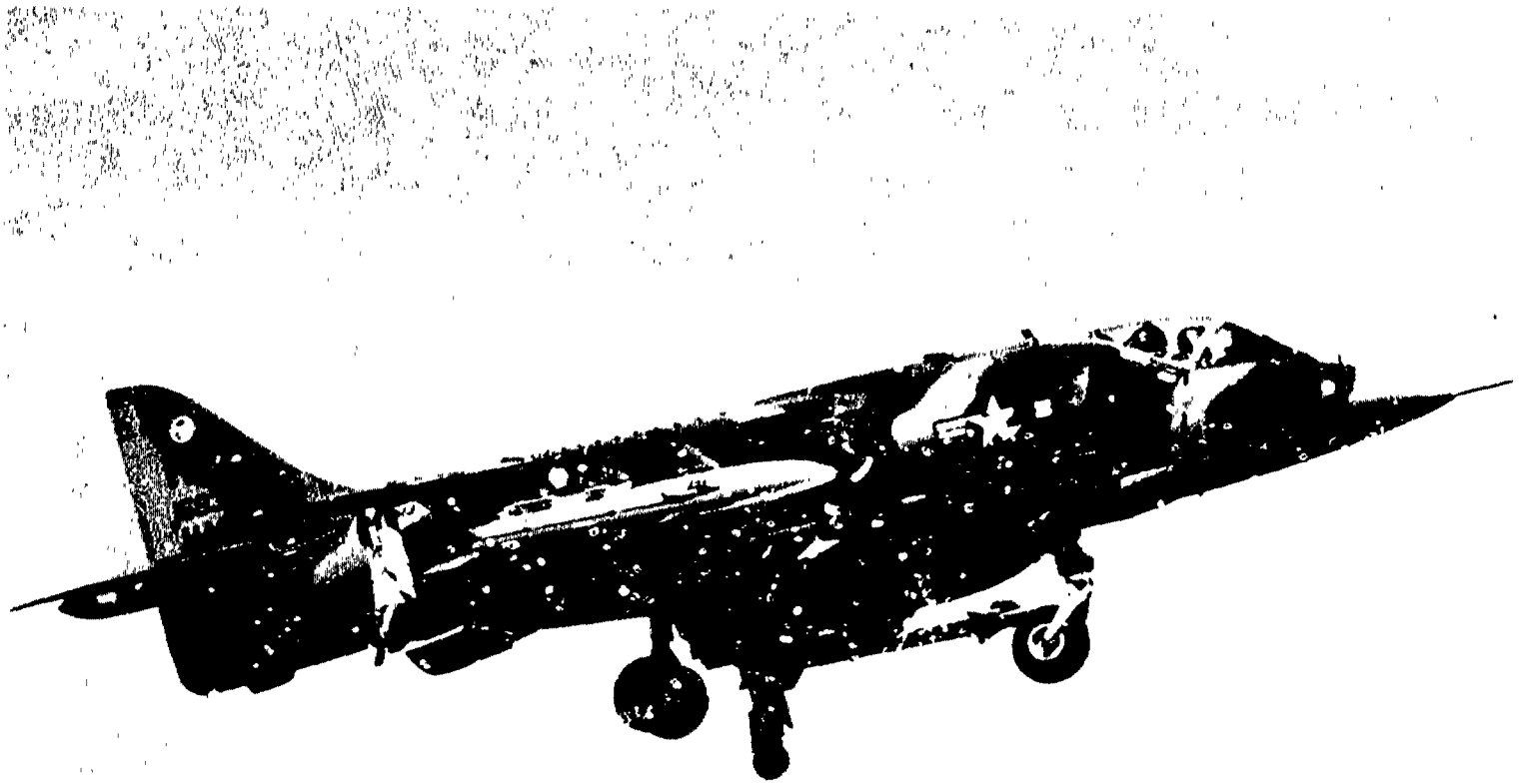


Figure 6

AV8A(Harrier)front windshield

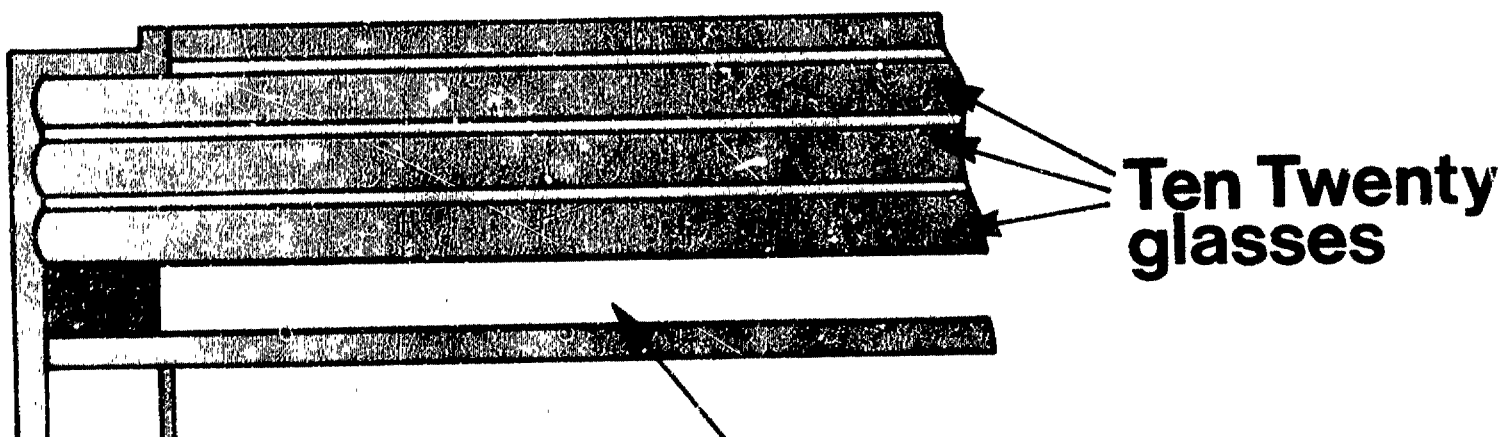


Figure 7



Figure 8



Figure 9

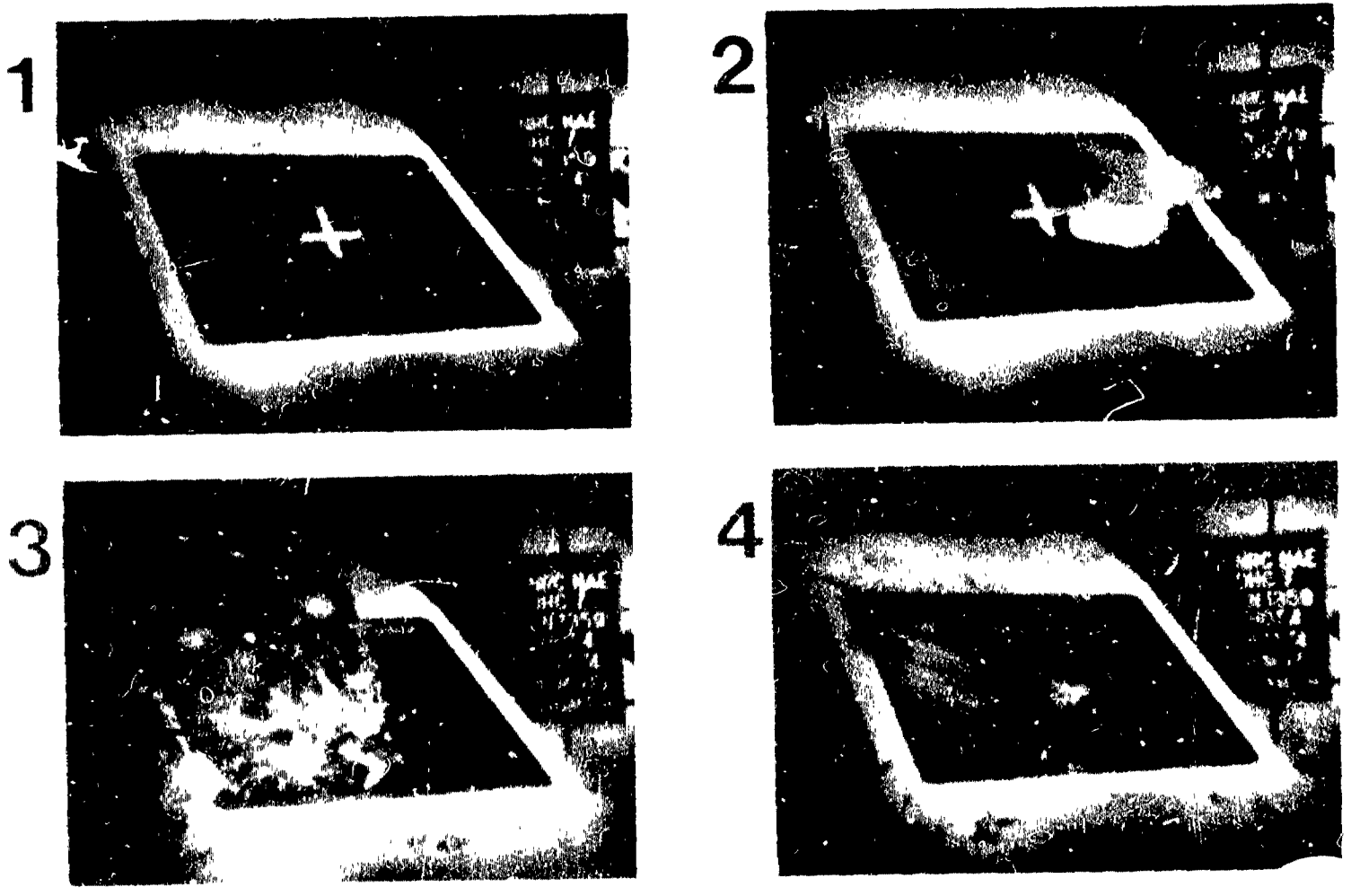


Figure 10

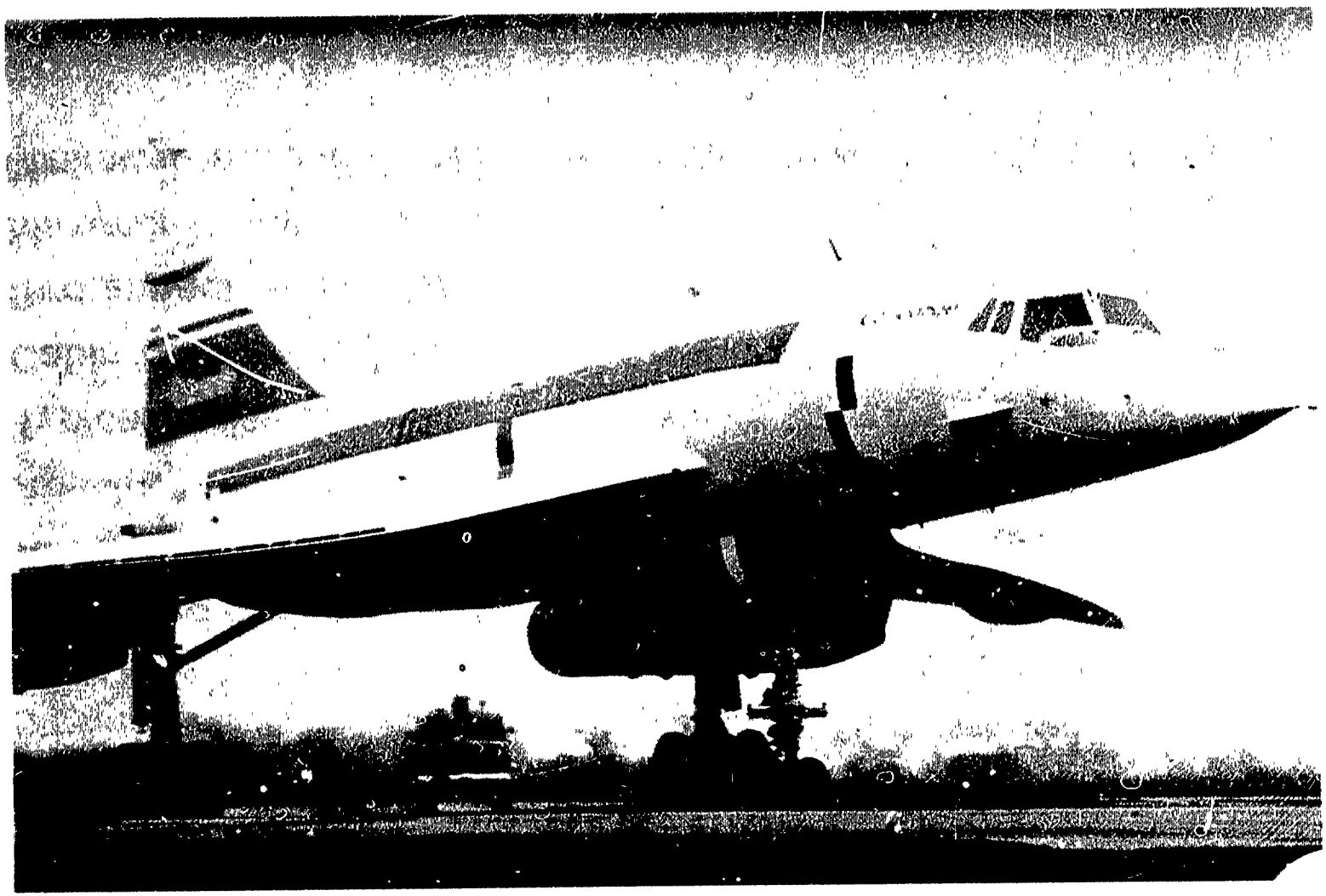


Figure 11

BAC/Aerospatiale Concorde

Performance and environment, relative to flight deck transparencies

Sustained cruise speed	Mach 2.2
Altitude	60,000 feet
Absolute pressure	1 lb/sq. in.
Typical cruise duration	2½ hours
Cabin differential pressure	11¾ lb/sq. in.
Bird impact requirement	4 lb bird at 512 mph
Maximum temperature with kinetic heating	120°C (250°F)
Minimum environmental design temperature	-70°C (-95°F)

Figure 12



Figure 13



Figure 14

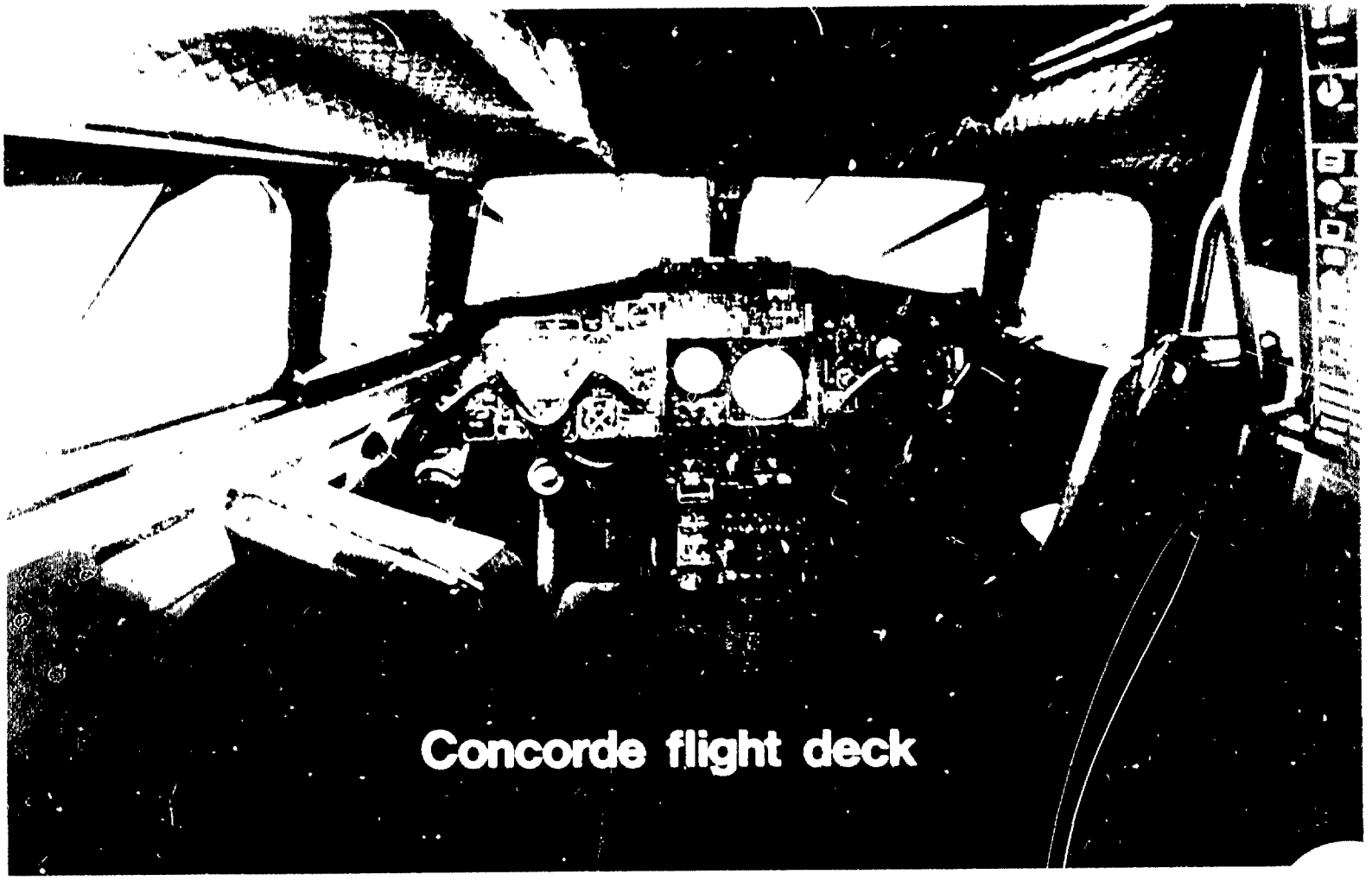
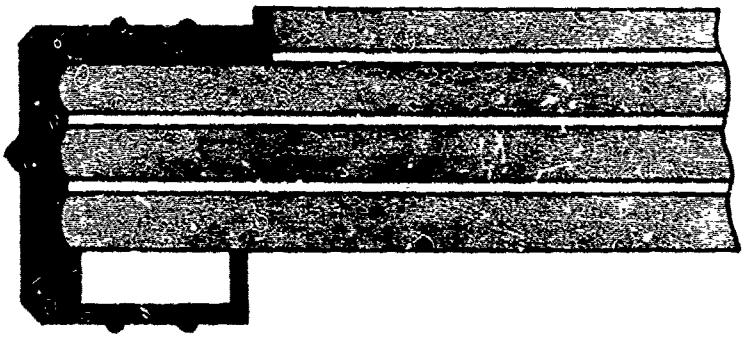
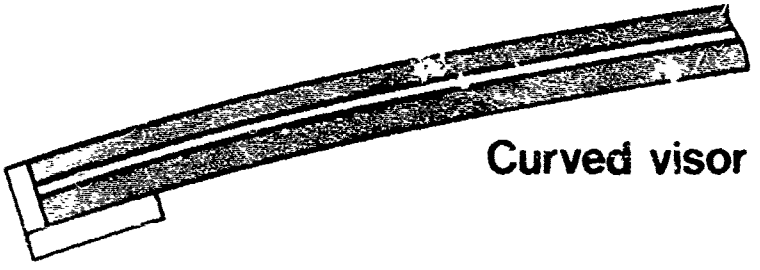


Figure 15

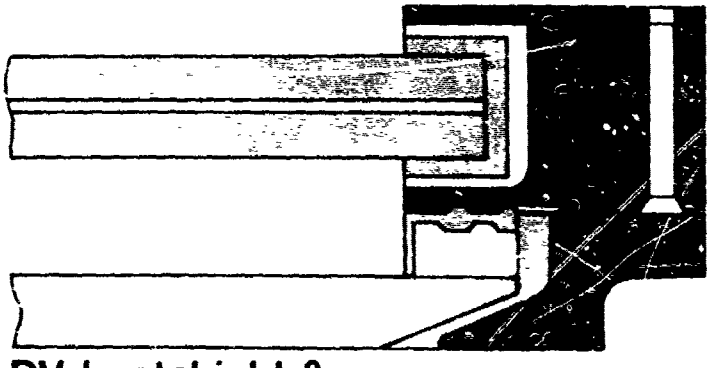
Concorde flight deck transparencies



Main front windshield



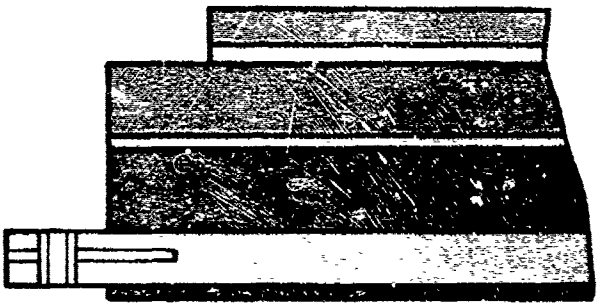
Curved visor



DV heatshield & pressure pane assembly

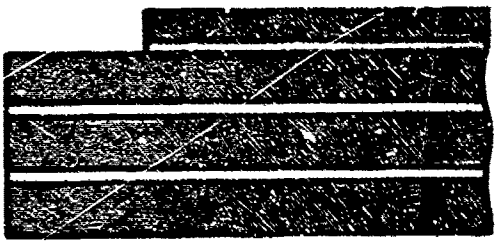
Figure 16

Concorde front screen designs to meet 4 lb. bird impact at 512 mph



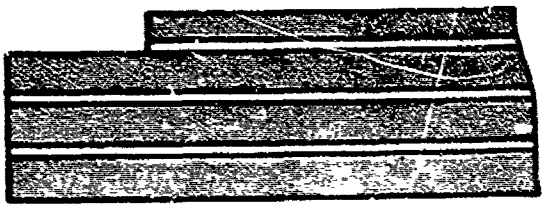
2·15 ins

Prototype (159 lbs)



1·55 ins

Preproduction (139 lbs)



1·32 ins

C Ten Twenty Production (113 lbs)

Figure 17

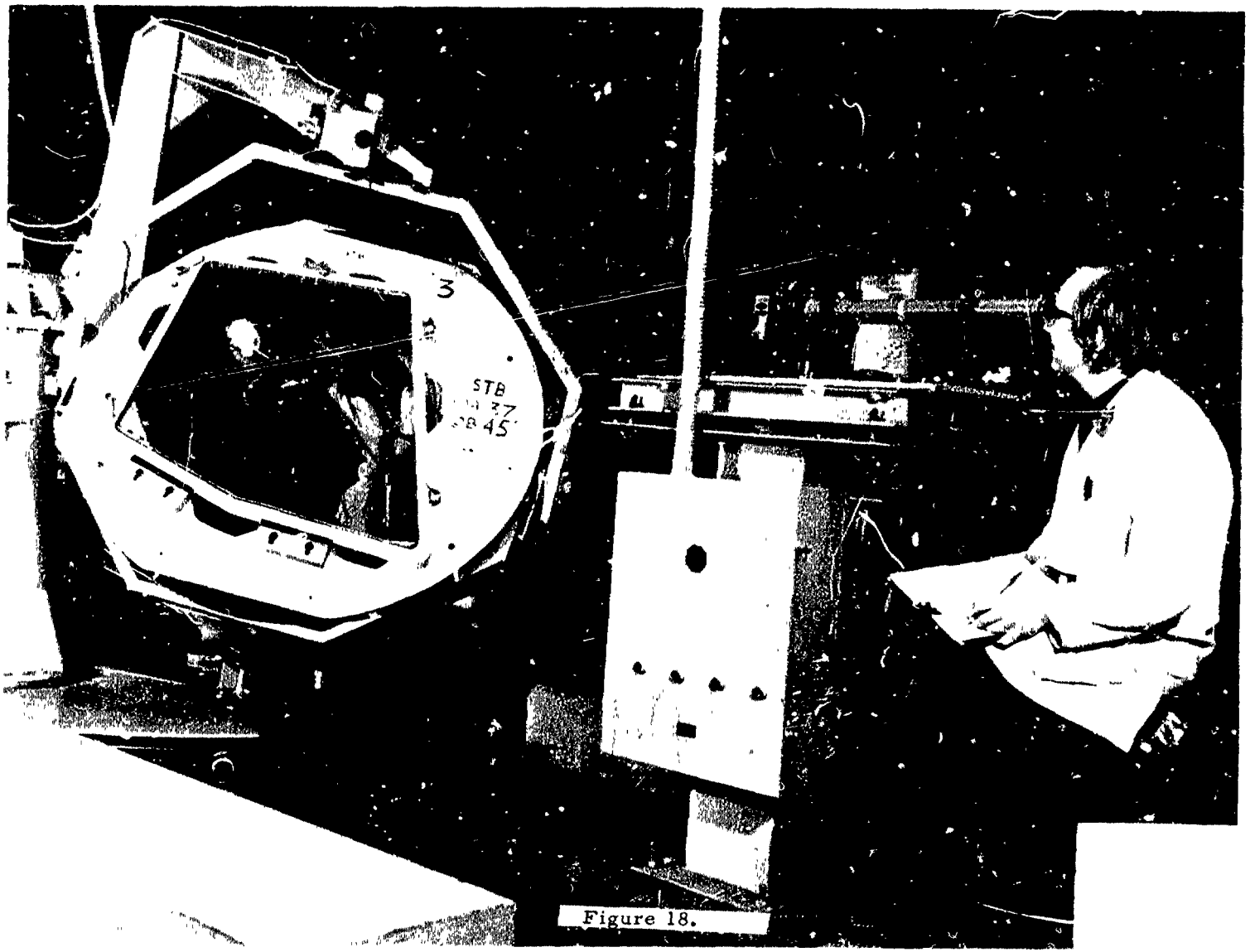
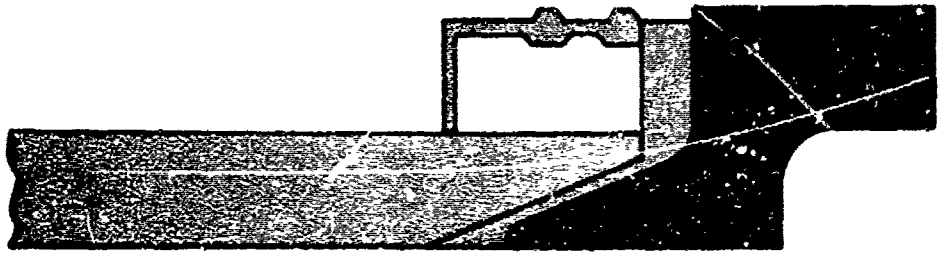


Figure 18.

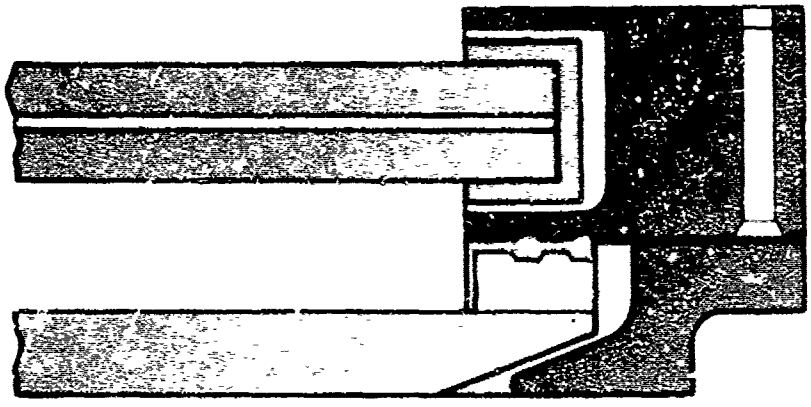
Concorde DV window



8mm Ten Twenty heatshield glass edge profile



Heatshield sub assembly



Final assembly of heatshield and pressure pane

Figure 19

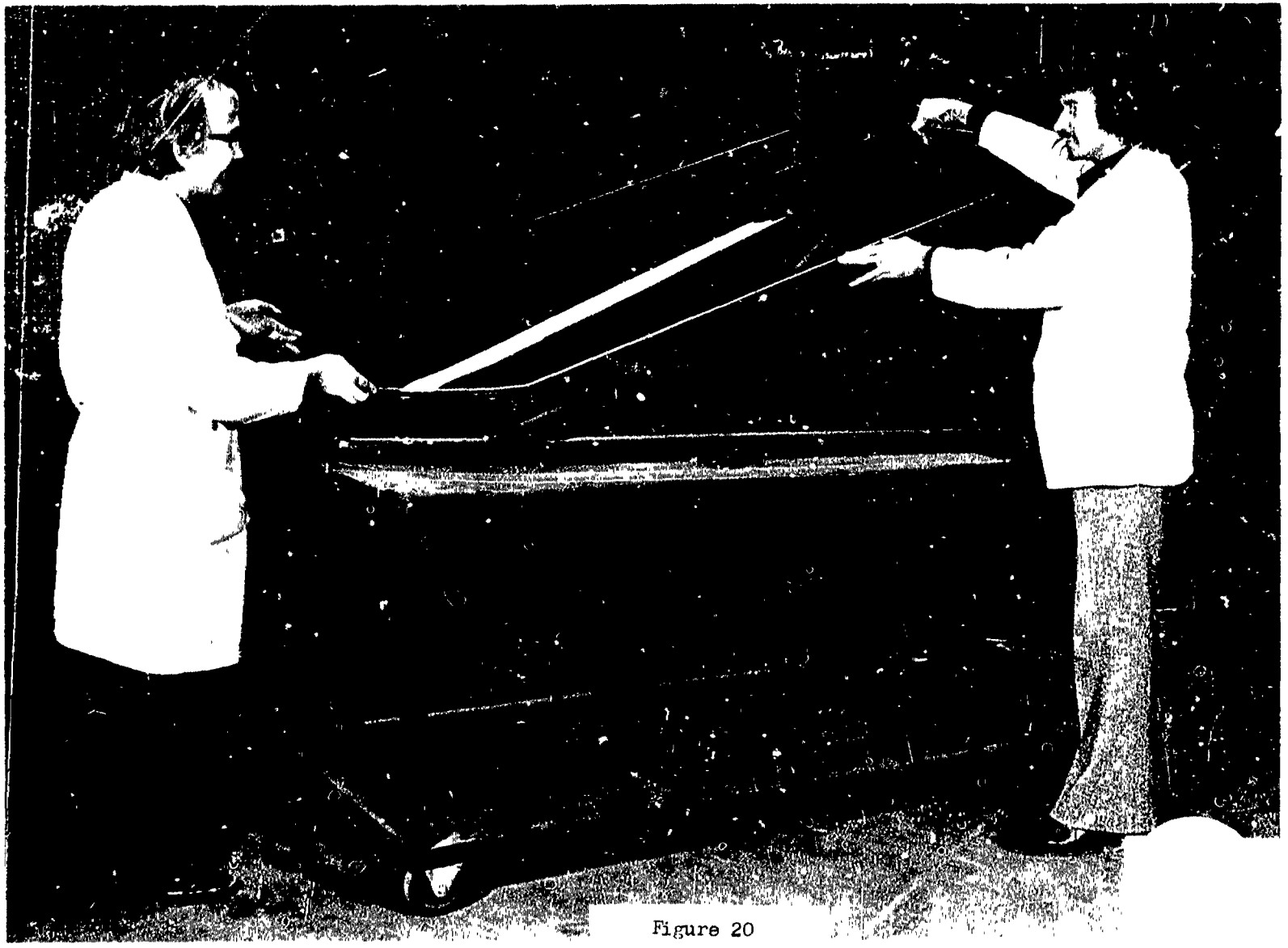


Figure 20

GENERAL AVIATION BUSINESS AIRCRAFT TRANSPARENCIES - AN UPDATE

H. U. Reppermund and W. W. Hornsey
PPG Industries, Inc.
Huntsville, Alabama

GENERAL AVIATION BUSINESS AIRCRAFT TRANSPARENCIES - AN UPDATE

H. U. Reppermund
W. W. Hornsey

PPG Industries, Inc.

Abstract

The transparency requirements of the general aviation industry vary considerably, depending on the aircraft mission and FAR certification category. Typical windshield requirements can include compound curvature, minimum weight, anti-ice/fog, capability to react pressurization stresses, and bird resistance. PPG currently supplies a full range of products for this multi-faceted industry including unheated laminated stretched acrylic through electrically heated multi-ply glass laminates.

This paper discusses how progress has been made to meet the challenging requirements of the general aviation industry. Solutions to design and service problems have been made possible by many new component material discoveries and design innovations. These solutions have been implemented on several designs and have accrued many successful flight hours. This paper will examine these improvements and will discuss several cross-sections which are in actual use today.

These improvements include:

a) New applications of fiber glass reinforced plastics and other materials for edge attachments.

b) An interlayer material that has demonstrated bird impacts up to 400 knots with excellent low temperature characteristics.

c) Thin tempered glass for pressurization loading via hoop tension.

d) Two-stage electrical heating systems for 28 volt DC power.

e) Improved sealants.

In PPG's 40 year history of aircraft transparencies, there has not been any time span as demanding as the last three years in the General Aviation Market. The challenges faced in windshield design and materials were many, but the technical achievements were even greater. These achievements required new and improved materials and inventiveness from the designer.

Within the past three years, design demands of the general aviation business type aircraft windshields have been extensive. These demands have included:

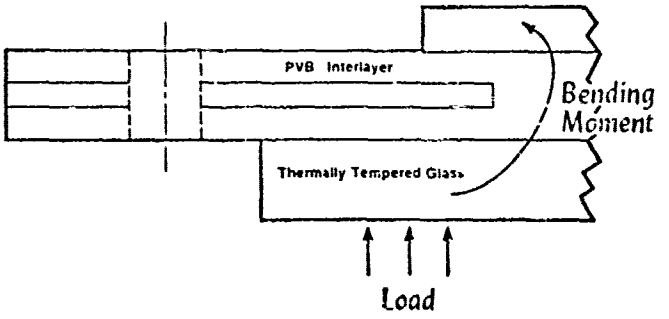
Increased Bird Protection
Better De-icing Ability
Lighter Weight Windshields
Compound Curvature Windshields
Reduced Delamination
Improved Edge Attachments
Improved Sealants
Improved Service Life

Each of these demands will be addressed under the following sections:

I. A New Windshield Design
II. A New Edge Attachment
III. A New Interlayer
IV. De-icing Capability
V. Improved Weather Sealant

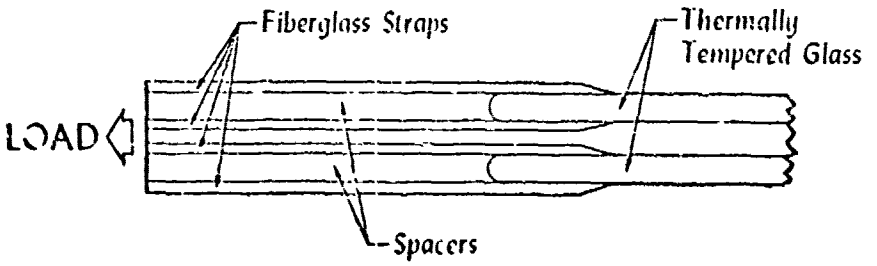
A NEW WINDSHIELD DESIGN

Older general aviation glass windshields and the airframe mounting surfaces were designed to accept plug loading. In these windshields the glass thickness had to be substantial enough to withstand a large bending moment caused by this type of loading.



Although these windshields perform well, the demand for lighter weight transparencies was great.

Recently, through inventiveness and the use of new materials, glass windshields have been designed and fabricated that can be loaded primarily in hoop tension. These curved windshields are designed so that the glass plies are attached to the airframe in such a manner to permit direct transfer of the tensile load into the airframe.



The bending moments which contributed to delamination and sometimes early failure have been drastically reduced or virtually eliminated.

The advantages of this type of design are many. Of major significance is the reduction in weight that is achieved. In the hoop tension loaded windshields, the glass is subject to a tensile load along the axis of the plies resulting in reduced stresses. With the same margin of safety, hoop tension loaded windshields can now be designed with much thinner glass plies. Part of the reason for this is that each ply is loaded equally resulting in a windshield that acts as one piece of glass rather than a laminate.

Introduction of the new windshield also allowed for more exotic compound shapes to be fabricated. This is true mainly due to the fact that glass plies of equal thickness could now be used in design. Along with these new shapes came a remarkable improvement in the optics of such windshields. Again, this achievement is mainly attributable to the use of glass plies of the same thickness.

The main contribution to the design and use of hoop tension loaded windshields was the development of a new edge attachment. This achievement has been of such major importance that it deserves individual attention.

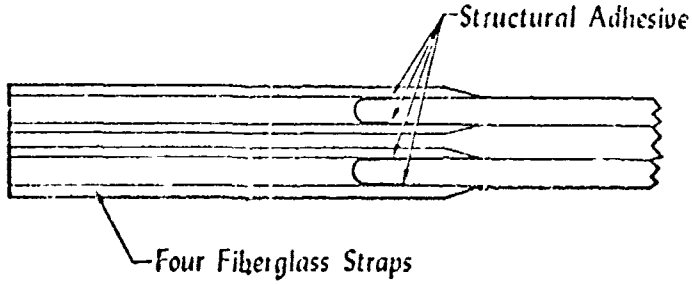
A NEW EDGE ATTACHMENT

The challenge in this area was to design a method for attaching the glass plies to the airframe so that the stress would be uniformly distributed. Additionally, the materials and design would have to perform this function throughout the temperature range of -65°F to +180°F. A third parameter desired was the use of a material which could be molded into exact curvature Finally, the structural properties had to be capable of withstanding the tensile loads created by hoop tension. It was felt that each of these requirements must be met for success of the new windshield design.

The great temperature range dictated that the material chosen have expansion properties which closely match the properties of glass. This decision led to the selection of fiberglass as a prime candidate for bonding to the glass and attachment to the airframe. Further studies into fiberglass properties showed that the tensile strength was greater than 35,000 psi. This value was determined to be more than adequate for the application desired. The fact that fiberglass was a material capable of being molded into almost any configuration only added to the success expected from its use.

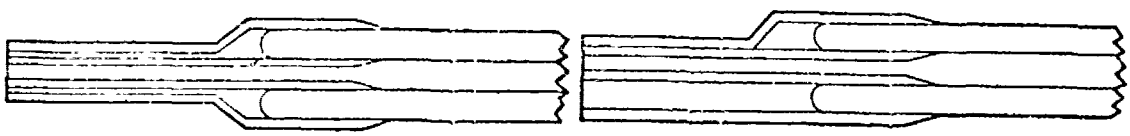
With the selection of material made, the remaining decision involved the method to be used to attach it to the glass edge. Through many test samples, a bonding system was developed which meets all of the

desired criteria.



The use of straps on both sides of each glass ply insured that the stress in the glass would be transmitted uniformly to the airframe. Furthermore, the structural adhesive in combination with the fiberglass straps was capable of withstanding hoop tension loads in the range of 1,000 lbs./lineal inch throughout the desired temperature range.

To date, many windshields emplpying the above design have been manufactured and are successfully operated in General Aviation aircraft. Variations in edge thickness and edge width are sometimes necessary to accommodate the airframe installation.



Double Offset *Single Offset*

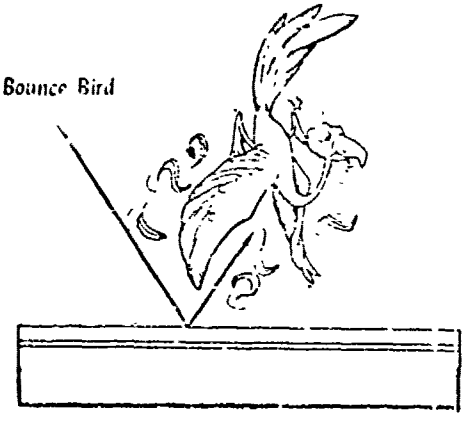
The success of any such new concept is determined through actual use, and results of in-flight service have proven this design to be excellent. Long life and dependable service are now realities with

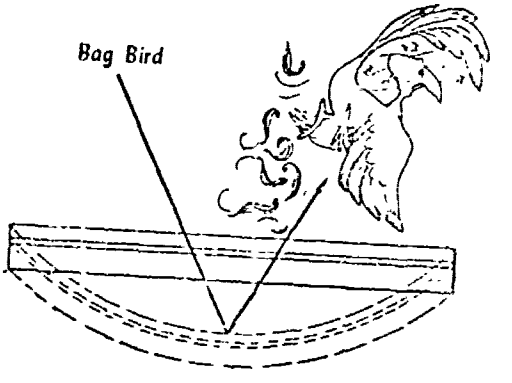
the hoop tension windshield using the new edge attachment.

A NEW INTERLAYER

A new sheet interlayer (termed PPG 112 which is described in detail by Jim Mahaffey in another paper) has recently been developed which promises to add a whole new dimension to General Aviation transparencies. In comparison with conventional interlayers, it has much greater tensile strength over a wide temperature range, excellent elongation properties at low temperatures, and adhesion to glass superior to that obtained with PVB interlayer.

The high tensile strength, elongation properties, and resistance to tearing has made it possible to design lightweight, bird resistant windshields using the interlayer to "bag" the bird.





Upon impact, the window deflects until the glass breaks and the interlayer absorbs most of the kinetic energy.

Recent bird impact tests conducted at the National Research Council in Ottawa, Canada, have shown the following results.

Glass Thickness (In.)	Interlayer Thickness (In.)	Impact Speed (Knots)	Bird Wt. (Lb.)	Temp. °F
2 Plies 3/16	.330	280	4	+1
2 Plies 1/8	.330	404	4	68°F
1 Ply 3/16	.330	299	4	68°F
2 Plies 3/32	.330	353	4	71°F

Results

No Penetration

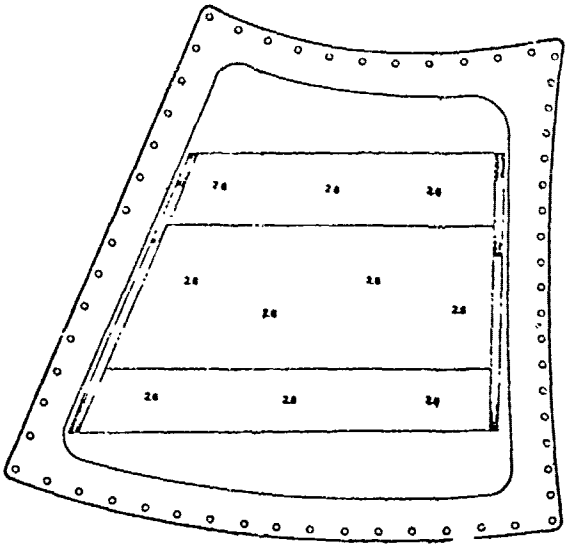
These results illustrate the superior performance of this new interlayer at low and room temperatures. The advantages are obvious; increased bird protection at a significantly reduced weight.

A common cause of failure in aircraft windshields has been delamination or adhesion chips. One of the major advantages of the new interlayer is that its superior adhesion to glass, its unequaled cold temperature strength, and good elongation properties greatly reduce this problem.

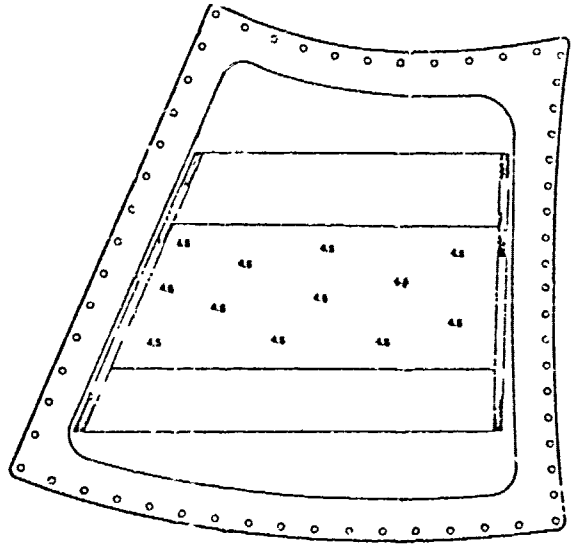
The technical advances made possible by this new interlayer are achievements unsurpassed in the aircraft transparency field. The increased bird protection and the reduced delamination qualities are two areas which have long needed a technological breakthrough.

DE-ICING CAPABILITIES

Uniform heat distribution, 4.5 watts/in.^{2} heat dissipation, good optics, and a deiced area large enough to suit any pilot can now be achieved with a two (2) stage Aircon® heating system. This system of fine wires is made up of two separate circuits. The main circuit is composed of a large area designed for approximately 2.6 watts/in.^{2} and is used under normal flight condition.



For maximum de-icing ability, there is a smaller area within the fully heated area that can be switched on from the instrument panel. This area is normally designed to distribute 4.5 watts/in.^{2} nominal.



Reliable systems of this nature are now in use which draw up to 70 amps current on high power. Hence, there is virtually no limit to the size of the heated area except for the available aircraft power. This achievement in windshield heating systems has given the windshield designer and aircraft pilot the advance needed for better flight safety and performance.

IMPROVED WEATHER SEALANT

The development and use of heat vulcanized (HV) silicone is a step forward toward improving the service life of the general aviation windshield. This sealant exhibits properties that prevent wind and rain erosion and moisture degradation. When combined with good adhesion to glass, metal, and interlayer, the moisture ingress that can cause delamination is effectively prevented. HV silicone has been employed on many existing designs on today's aircraft, and all field reports are extremely encouraging.

CONCLUSION

The continuing development of new materials and innovative ways to provide product improvement are requirements in serving the general aviation industry. Technology is the key, and the challenge exists for engineers to design the windshields to meet the performance requirements and to provide an excellent service life for the product. The future requirements of this industry will include even greater strength to weight ratios, greater reliability, more viewing area, and additional sophistication in bird proofing and deicing capability. Furthermore, the apparent continuing fast growth of the general aviation industry must be supported by improved products. The windshield designers and fabricators will have interesting and challenging tasks as this industry continues to expand.

SESSION 2

DESIGN AND PERFORMANCE (PART II)

B-1 WINDSHIELD OVERVIEW

B. R. Emrich
Air Force Materials Laboratory, B-1 SPO
Wright-Patterson Air Force Base, Ohio

and

D. L. Russell
Aeronautical Systems Division, B-1 SPO
Wright-Patterson Air Force Base, Ohio

PRECEDING PAGE BLANK-NOT FILMED

INTRODUCTION

The B-1 Windshield Development Program is best brought into perspective by taking a quick look at the history of the program as shown in Figure 1. This summarizes the windshields key decision points and configuration changes as related to the B-1's critical milestone events. In June 1970, Rockwell International (RI) was awarded a research, development, test and evaluation (RDT&E) contract to build three flight tests aircraft. Early windshield trade-off studies (Ref. 1) made between August 1970 and September 1970, plus windshield and windshield design development tests (Ref. 2,3), were instrumental in selecting the B-1's initial windshield design configuration. The RI-designed windshield was subcontracted to Swedlow, Inc., by fall of 1971 and also to Sierracin in mid-1973 for manufacturing and double source capabilities. In mid-1973 the B-1's critical design review effort established firm B-1 windshield primary design features and systems requirements. From this point it became a matter of manufacturing windshields suitable for flight worthiness, fine tuning the design configuration to meet desired performance parameters and conducting design verification testing to qualify a production windshield configuration. This paper will review the major development activities and considerations involved during the June 1970 through November 1975 time period in prompting windshield material configuration changes (Figure 1) and discuss the reasons and constraints which dictated the selection of the existing production design.

The B-1 windshield scenario portrayed in this paper will explain why modifications were made on the windshield material configuration to meet requirements or performance needs. Overall the B-1 windshield configuration varied in total thickness form 1.488 to 1.440 inches, acrylic or glass outer ply, polycarbonate or acrylic spall plate and a P-Static coating on the glass outer ply only. The constant factors related to the materials configuration were the silicone cast in place (CIP) interlayer and the .875 polycarbonate structural ply. The B-1 windshield basically consist of five laminated transparencies (outer ply, two interlayer plies, structural ply, spall plate) plus three coatings (P-Static, electroconductive, abrasion), for a total of eight layers, and six different materials, and six paralled faces. Producing this combination of materials into a large size, curved windshield to satisfy structural, aerodynamic, optical, human factor, anti-ice/de-fog and environmental requirements becomes the unique B-1 development program.

REQUIREMENTS

Figure 2 shows an example of the B-1's mission profiles and relates windshield requirements associated with meeting desired aircraft performance to mission needs. Problems encountered in existing aircraft windshields directed the B-1 to include many, sometimes conflicting design requirements, into the Prime Item Development Specification (PIDS) in an attempt to avoid past inadequacies. Previous aircraft windshield considerations or goals were established as B-1 contractural requirements with the intention of providing a optimized windshield design for best B-1 performance. A review

of the B-1 windshield requirements and how these requirements influence design by constraints created in the state-of-the-art of windshield technology and aircraft basic design features will be discussed later. The basic B-1 mission is low altitude penetration with long distances and high subsonic speeds. The B-1 manned bomber is being designed as a technologically-updated replacement for the B-52. Among the major advantages of the B-1 over the B-52 are: 50 percent greater low-level penetration speed, as well as being nearly three times faster at altitude. Since the low altitude penetration is the primary mission the major design parameters were categorized as follows: configuration constraints were aerodynamics and visibility; structural constraints were bird impact plus internal pressure, high external temperatures; visibility constraints were optical distortion and light transmission; environmental constraints were temperature, anti-ice, radar reflectivity, and P-static and corona discharge. The low-altitute mission has imposed severe design requirements on the windshield system which must be met with acceptable cost, reliability and maintainability. We will now take a look at how each of these requirements played a role in the sequence of events to selecting a optimized windshield configuration.

CONFIGURATION CONSTRAINTS (FIGURE 3)

The windshield shape (radius of curvature) and slope (angle of incidence) were dictated by aerodynamics (drag); bird impact data was also a key factor in establishing windshield slope. The interior crew compartment arrangement determined the pilots eye position, which when combined with the MIL-STD-850B visibility requirements were the major contributors to determining the size. During the early phase of the B-1 program weight played a critical part in the design of the windshield structure since it was an integral part of the escape (ejectable) crew module. It was a delicate balance of aerodynamics, visibility and weight factors which provided the basic for the windshield features. The results of these configuration constraints were the following: a unique shape, a five sided polygon, making it difficult to heat uniformally; 2. the largest single piece (approx. 15 sq. ft), flat or curved (59 inch radius) aircraft windshield ever to be produced, (Figure 4) new manufacturing technology was required plus additional handling problems during installation were experienced; 3. slope angle of 65 degrees, conflicted with desirable optics. The escape module (Figure 5) was extremely weight critical due to ejection considerations. Keeping weight to a minimum the windshield became a primary structural component of the escape module making up a sizeable portion of the module surface area.

STRUCTURAL REQUIREMENTS (FIGURE 6)

The baseline configuration having been established the structural requirements were then adrressed. These constraints played the major role in material selection, material configuration and thickness. The B-1 windshield, being a primary structural component, is capable of carrying pressurization and aerodynamic loads. In addition the edge attachment (Ref. 5) was designed to give the windshield capability to carry not only hoop tension, but also frame shear and bending loads. The windshield cross-section was designed to maximize the bending stiffness consistent with weight optimizatior and bird resistance by increasing shear coupling of structural plies. The initial trade-off and development studies as mentioned on Figure 1 were mainly

involved in materials selection (Ref. 1), edge attachment design development, edge attachment design verification testing, availability, technical risk, past experience, cost, weight, data from literature and material property tests, where existing property data could not be directly correlated to the B-1 requirements. These initial efforts were covered during the previous conference on transparencies (Ref. 4) and thus are not repeated in this paper. It will suffice to mention that the following materials were candidate materials for the B-1 windshield: Acrylic (MIL-P-8184), stretched acrylic (MIL-P-25690), polycarbonate (MIL-P-83310), Glass (MIL-P-25662) plus silicone and polyurethane interlayers. Stretched acrylic, polycarbonate and glass were selected for further consideration as structural plies. As cast acrylic and chemically tempered glass were selected as potential outer ply materials. Silicone was chosen as the interlayer material because of the thermal environment of the B-1 (excess of 250°F). The conclusion of these initial trade-off studies (Ref. 5) resulted in selection of a 5 ply glass stretched acrylic windshield (Figure 7).

At this point in time, 1970-71, the bird strike requirement began to play the major role in the windshield design, along with considerations to creep and flexure. Windshield design studies, design development testing (DDT) and a materials evaluation study (Ref. 6,7,8) were performed to arrive at the most acceptable material configuration.

The windshield was required to withstand a four pound bird at 650 mph, which is considerably higher than any previous windshield design. The bird impact design development tests were conducted on a simplified test fixture which simulated the stiffness of the windshield backup structure, the 59 inches radius of curvature and a 65 degree angle of incidence (Figure 8). The summary of test results demonstrating the two parameters considered critical in the design, weight and penetration, as related to material configuration are shown in Figure 9. All the 3 ft. by 3 ft. panels, except the multilayer acrylic configuration were impacted at 650 mph plus or minus 10 mph using a 4 pound chicken. The acrylic panel was impacted at 454 mph. No penetration occured on the five ply polycarbonate/acrylic and the five ply all glass configurations.

Since the weight of the all glass configuration (Figure 9) was more than double the weight of the five ply polycarbonate/acrylic configuration and costlier to procure, the polycarbonate laminate was chosen for the preliminary design concept. To further substantiate this selection creep and flexure design development tests demonstrated the polycarbondate superior to acrylic. A center post attachment creep DDT demonstrated the acrylic design was not capable of withstanding the sustained temperature and loads required for the B-1 supersonic mission.

ENVIRONMENTAL CONSTRAINTS (FIGURE 10)

It was decided by optimization studies that gold electrically conductive coating on the inside surface of the acrylic outer ply was the best and most practical way to anti-ice the windshield. This coating will also serve to reduce the radar cross section of the air vehicle, but was expected to reduce light transmission 17 to 25%. A internal air blast system

was used for defogging purposes after consideration of another electrically conductive coating on the inside surface of the polycarbonate spall shield. Static charge build up due to frictional interation between the environment and a nonconducting windshield can produce external surface charges sufficiently large to ARC through to subsurface conductive coatings used in de-icing. Radio frequency interference, electronic failures and burn through of the de-icing may result; thus the need for a antistatic coating was imperative.

The state of the art in 1971-72 for antistatic windshield coatings on plastic constructions consisted of a colloidal graphite which produced a 10% decrease in light transmission and had poor durability. However, it was expected from development efforts that a durable antistatic coating was forthcoming or would be made available as a result of the B-1 requirement. Unfortunately, this was not the case as will be shown later.

Rain is removed from the windshield by a Rainbow Type III fluid system. As an emergency backup system, hot air vents are used for rain removal.

As Figure 1 shows after preliminary design decisions were made and study investigations completed it became necessary to initiate fabrication of full scale windshields to assure availability for flight testing. In the fall of 1971 Swedlow was awarded the subcontract to build research, development, test and evaluation (RDT&E) B-1 windshields. The windshield configuration at initial procurement time is shown in Figure 11.

The coatings to reduce reflectivity and dissipate static charge buildup remained in consideration. The as cast acrylic and 0.160 inch silicone interlayer was used as a thermal barrier to protect the structural integrity of the polycarbonate and degradation to the de-ice coating. The 0.875 thick polycarbondate structural ply and inner spall shield thicknesses was determined largely from bird impact resistance testing as shown earlier.

OPTICAL CONSTRAINTS (FIGURE 12)

Optics were a prime consideration during all phases of the windshield development effect. A quantitative measure of optical properties could not be realized until a full-scale article was manufactured. It was made clear at this point that the state-of-the-art of windshield technology was lacking in fulfilling desired performance characteristics. Although it is true that certain aspects of the design and materials taken one at a time had been achieved in other designs, the B-1 windshield is unique by its complexity of simultaneous requirements and resultant features. During the next 12 months (1972-73) minor modifications were made to the windshield configuration to reduce distortion which occured in the initial fabrication of the windshield. The first change was to substitute a .150 inch stretched acrylic for the .150 inch polycarbondate inner layer material (Figure 13). The rationale was to fine tune the optics by providing a surface more suitable to

polishing procedures (Ref. 9). It was realized that bird impact resistance would be reduced to some extent. Having accomplished very little improvement by this modification it was decided, in addition to the stretched acrylic inner ply, to double the thickness of the ASCAST acrylic outer ply thus providing two surfaces capable of fine polishing (Figure 14). This made a noticeable improvement in optics but not significant enough to warrant sacrificing bird impact resistance.

It became apparent that windshield optical requirements would have to be defined in more realistic terms. The system contractor (Rockwell International), fabricator subcontractors and the Air Force decided the windshield surface area should be divided into various distortion level zones, in addition to reducing haze and light transmission requirements (Figure 15).

Another major fabrication difficulty related to the material configuration was delamination caused by poor adherence between the electrical conductivity coating and the outer acrylic ply. This anomally was not resolved in time for the delivery schedule of aircraft No. 1. Therefore the E.C. coating was not applied on the aircraft No. 1 windshield panels. Without the E.C. Coating, optics were slightly improved on the modified configuration, but only a minimal hot air de-icing capability was available for the windshield.

Details concerning the manufacturing process briefly mentioned will be discussed in the next paper by R. C. Shelton of Swedlow (Ref. 9).

In order to improve optics, reduce or eliminate delaminations, improve heating uniformity in the de-icing pattern, obtain a P-Static capability without sacrificing other requirements, the material configuration was modified as shown in Figure 16. The Chemcor glass outer ply with a P-Static Coating procured from Corning glass replaced the as-cast acrylic outer ply primarily too resolve concerns relative to environmented requirements and improved the capability of fabricators to produce satisfactory windshields having a electrical conductive coating. The polycarbonate inner ply was restored to assure maximum bird impact resistance. A titanium retainer was added to protect the edge of the glass thus reducing the probability of early glass failure and aid in sealing the windshield from moisture ingress.

The glass outer ply windshield (Figure 16) was selected at the B-1 critical design review (June 1973) as the windshield for further development and evaluation (Figure 1). The availability of glass outer ply windshields for RDT&E aircraft became an immediate concern. In order to improve the availability situation an additional subcontractor (Sierracin, Sylmar, Calif) began in July 1973 to manufacture glass outer ply windshields.

Along with the procurement of the glass outer windshield a revised set of optical requirements were established (Figure 17). The critical area (Zone 1-Figure 15) was significantly enlarged which was indicative of improved manufacturing procedures and need for improved optics. To date five sets of glass outer ply windshields (Figure 16) have been delivered

and optically evaluated. Figure 18 summarizes and compares the optical properties of the plastic and glass outer windshields to the original and revised requirements. The glass outer ply windshield demonstrated improved optics relative to distortion and light transmission on a consistant basis.

During the 1972-1974 period continuous efforts by the contractor and various Air Force organizations were made to establish minimum optical requirements. A set of minimum optical requirements have been imposed on the two B-1 windshield manufactures. But it is recognized additional technology is needed to assure the accuracy of the established acceptance levels.

DESIGN VERIFICATION TESTING (REF. 10, 11)

The major full scale evaluation of the B-1 windshield began in December of 1974 with the first flight of air vehicle No. 1 using the Figure 14 (acrylic outer ply) configuration. The full scale verification test plan consists of two tests: a bird impact test (completed in July 1975) and the crew module elevated temperature and pressure cyclic test (now in progress). (The bird impact tests used windshield panels with an acrylic outer ply (see Figure 13). While the cyclic test is using glass outer ply panels (see Figure 16). The cyclic test was initiated in November 1975 and is scheduled for completion by March 1976. Since no test results have been completed to is date on the cyclic test, only the overall test plan is reviewed (Table 1).

The elevated temperature and pressure cyclic testing is being conducted at Rockwell International Los Angeles using a structurally representative prototype crew module. The elevated temperatures are being achieved using a heating blanket over the transparencies and cooling is accomplished by applying liquid nitrogen to test arrangement. The test consists of five blocks of spectrum A, an extended creep cycle, and ten blocks of spectrum B. The extended creep cycle test will be performed at the end of first block of spectrum A.

The bird resistance tests were conducted in the bird impact test unit of the Von Karman Gas Dynamics Facility at the Arnold Engineering Development Center (AEDC) during the period June 25 through July 29, 1975. The test article consisted of a structurally representative prototype B-1 crew module. The crew module was mounted in a support frame which was, in turn, bolted to the test area floor. The test article was mounted at zero-degree angle-of-attack aircraft attitude and all test were done at ambient temperature. The designated impact point for the individual shots is shown in Figure 19. First the right, then the left panel was impacted; then both panels were removed and new ones installed for the last shot. The right panel was impacted on the last shot.

A summary of the test conditions and results is presented in Figure 19. None of the windshields tested were damaged to any significant degree. The outer acrylic ply spalled and cracked on all shots but there did not appear.

TABLE 1: CREW MODULE ELEVATED TEMPERATURE & PRESSURE CYCLE TEST

SPECTRUM "A"

77 CREEP CYCLES

75^0 - 254^0
0 - 10.6 PSI } HOLD 18 MINUTES

123 R.T. CYCLES

75^0F CONSTANT
0 - 10.6 PSI } NO HOLD

TOTAL 200 CYCLES

1 BLOCK - 5 REQUIRED

EXTENDED CREEP CYCLE

1 CYCLE

75^0 - 254^0
0 - 10.6 SPI } HOLD 48 MINUTES

CYCLE REQUIRED AT END OF BLOCK I OF SPECTRUM "A"

SPECTRUM "B"

116 HOT CYCLES

254^0 CONSTANT
0 - 10.6 PSI } NO HOLD

184 R.T. CYCLES

75^0 CONSTANT
0 - 10.6 PSI } NO HOLD

TOTAL 300 CYCLES

1 BLOCK - 10 REQUIRED

TOTAL NUMBER OF CYCLES = 4001

to be any damage to the main polycarbonate structural ply. On shot No. 2 cracking of the polycarbonate spall plate occured. The primary cause of the cracking was later determined to be a flaw in an improperly drilled bolt hole. In shots No. 1 and No. 3 the spall plates were undamaged. On shot No. 3, structural damage occured to the eyebrow longeron on the right hand side immediately back of the impact area. A piece of the longeron torn off during impact and cracks were formed in the longeron web. The impaired area covered a width of approximately 21 inches. An insignificant amount of bird debris penetrated the interior of the module in this area. (Ref.11)

TECHNOLOGY NEEDS

It became very evident during the B-1 windshield development program that deficiencies exist in high performance aircraft transparency technology to reliably reproduce large size windshields having desired performance capabilities. These deficiencies can be reduced in part by more adequate design, through improve analytical models and agreed to requirements defined by the scientific, engineering community and users. The B-1 program reemphasized technology needs brought out continously during this conference; that is the need for new materials with higher optical quality, improved durability in erosive and normal weathering conditions, and reliable structural high impact resistant plastics. Improved thermal stability of plastics are desirable such that thermal treatment during service and repair does not significally impair structural integrity; improved film type interlayers to reduce fabrication difficulties associated with cast in place type interlayers. Improvements in the area of coatings on plastic substrates (anti-static, electrical comductivity, weather resistant) are needed. Good examples of such a need experienced on the B-1 was the inadequate adhesion of the silicone interlayer and acrylic outer ply to the electrical conductive coating; also the lack of durable P-static coatings on the outer surface panel of plastic substrates. Solutions to todays needs relative to durability, reliability, improved materials; optically and better sheet formable interlayers, improved bond integrity and increased resistance to environmental effect of conductive and abrasion resistant coatings are being investigated. There does not appear to be any short term answers which will provide capabilities to improve todays needs.

REFERENCES

1. TFD 70-945. B-1 Windshield Trade Study Program, 15 Dec. 1970. North American Rockwell.

2. Crew Module Test: CM-9, CM-1, CM-10, CM-13; North American Rockwell Feb 71 thru July 71.

3. TFD-73-627. Windshield Edge Joint Test CM-13. 18 Mar 73. North American Rockwell.

4. AFML-TR-73-126. Conference on Transparent Aircraft Enclosures; pp 173-195. "Material Evaluation B-1 Crew Module Windshield and Windows." Air Force Materials Laboratory.

5. TFD-71-195. Miscellaneous Windshield Design Data, 4 Feb. 1971. North American Rockwell.

6. TFD-70-678. B-1 Windshield Test Plan. 17 Sept 1970. North American Rockwell.

7. TFD-70-836. B-1 Windshield Materials Study. 2 Oct. 70. North American Rockwell.

8. TFD-71-1433. B-1 Windshield and Window Seal Study. 15 Oct. 71. North American Rockwell.

9. Conference on Aerospace Transparent Materials and Enclosures. 18-21 Nov. 75 paper by R.C. Shelton, Development of the Windshield for the B-1 Aircraft, Swedlow, Inc.

10. TFD-75-1105. Test Readiness review for the DVT-2 crew module transparencies temperature and pressure. 14 Oct. 75. Rockwell International.

11. AEDC-DR-75-87. Results of Qualification Testing of Bird Resistant Windshields for the B-1 Aircraft. September 1975. Arnold Air Force Station.

12. NA-75-67, VOL. 1. Technical Proposal For Windshield Technology Demonstrator Program.

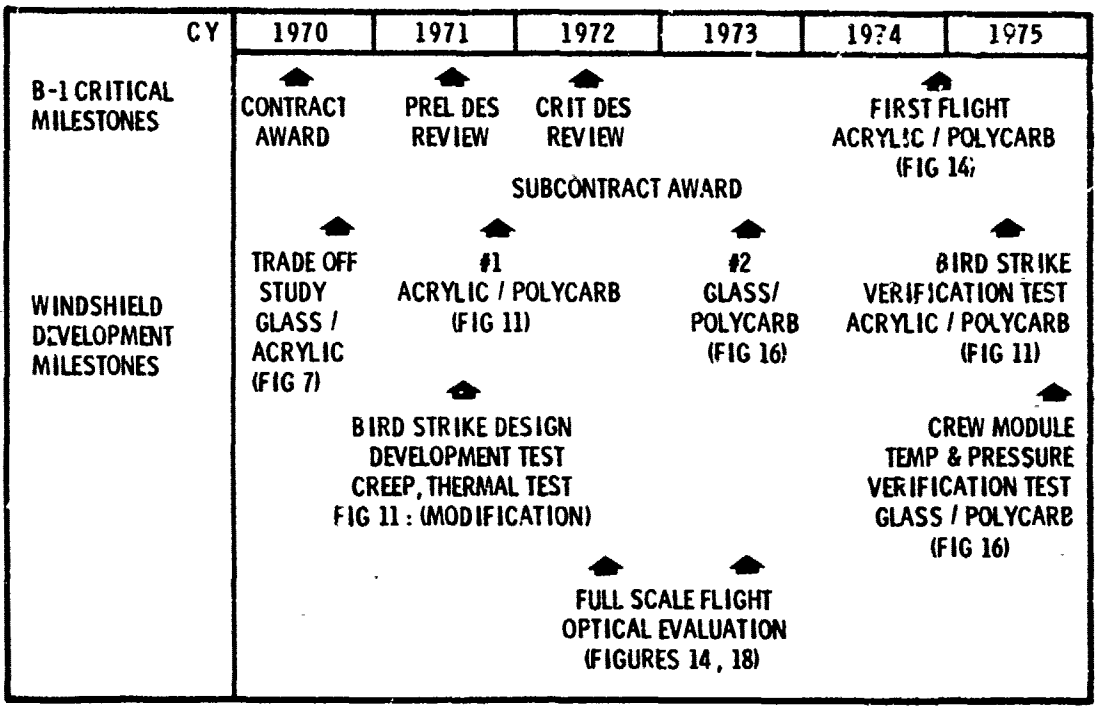


FIGURE 1: B-1 WINDSHIELD PROGRAM-KEY EVENTS AND CHANGES

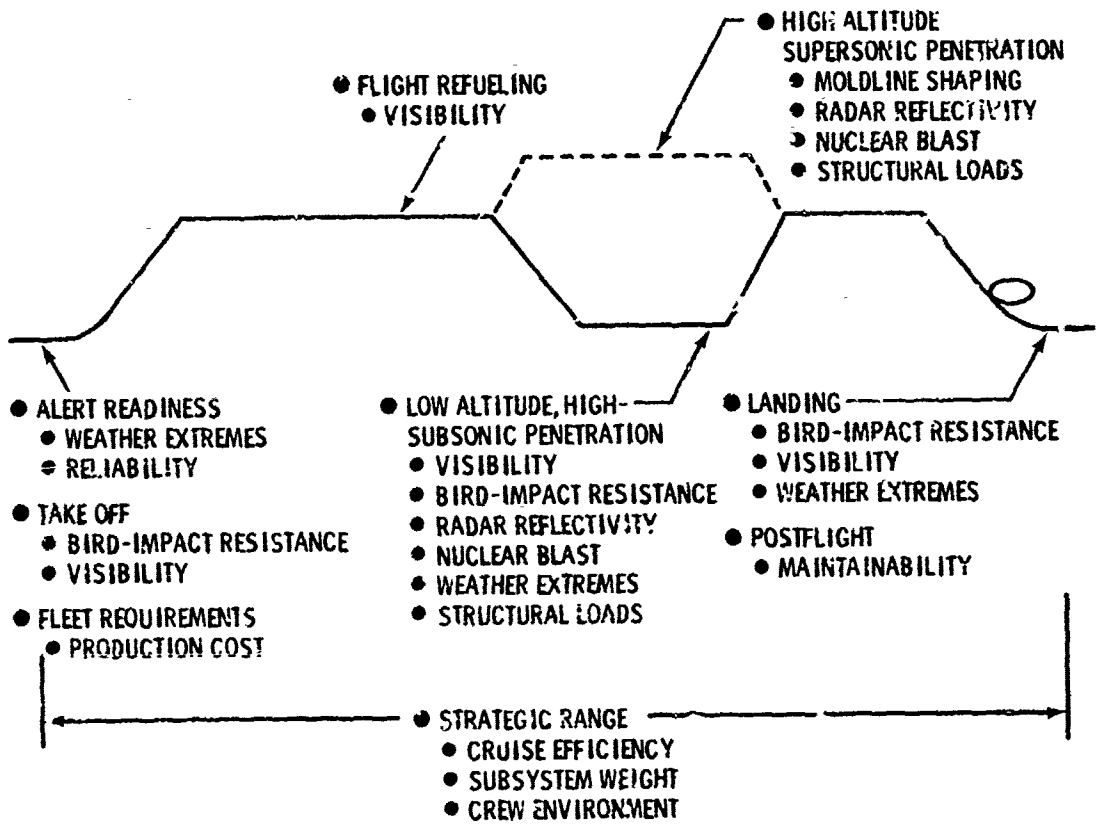
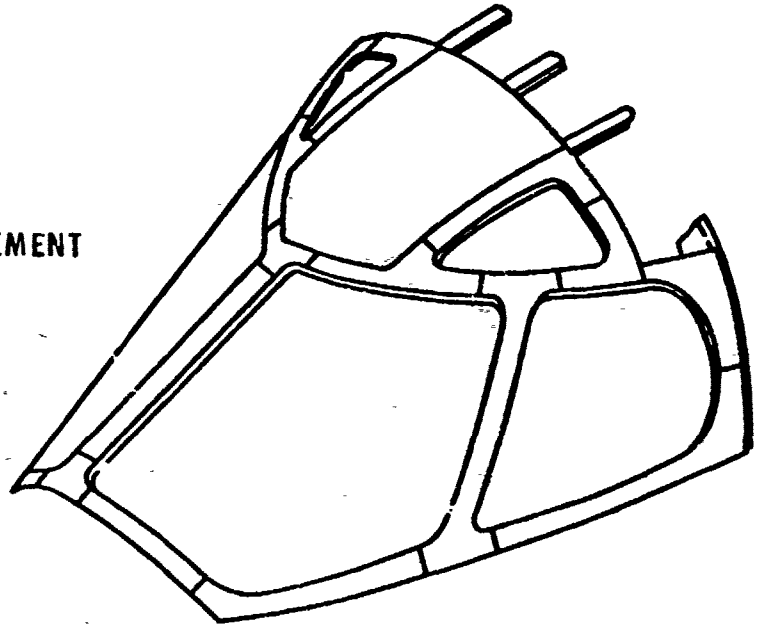


FIGURE 2: B-1 MISSION REQUIREMENTS FOR WINDSHIELD DESIGN (REF. 12)

- AERODYNAMICS
- INTERIOR ARRANGEMENT
- STRUCTURE
  - WEIGHT
- HUMAN FACTORS
  - VISION



RESULT:

- SIZE: 2495 square inches
- RADIUS: 59 inches
- ANGLE OF INCIDENCE: 65^{0}

FIGURE 3: CONFIGURATION BASELINE CONSTRAINTS AND IMPLICATIONS

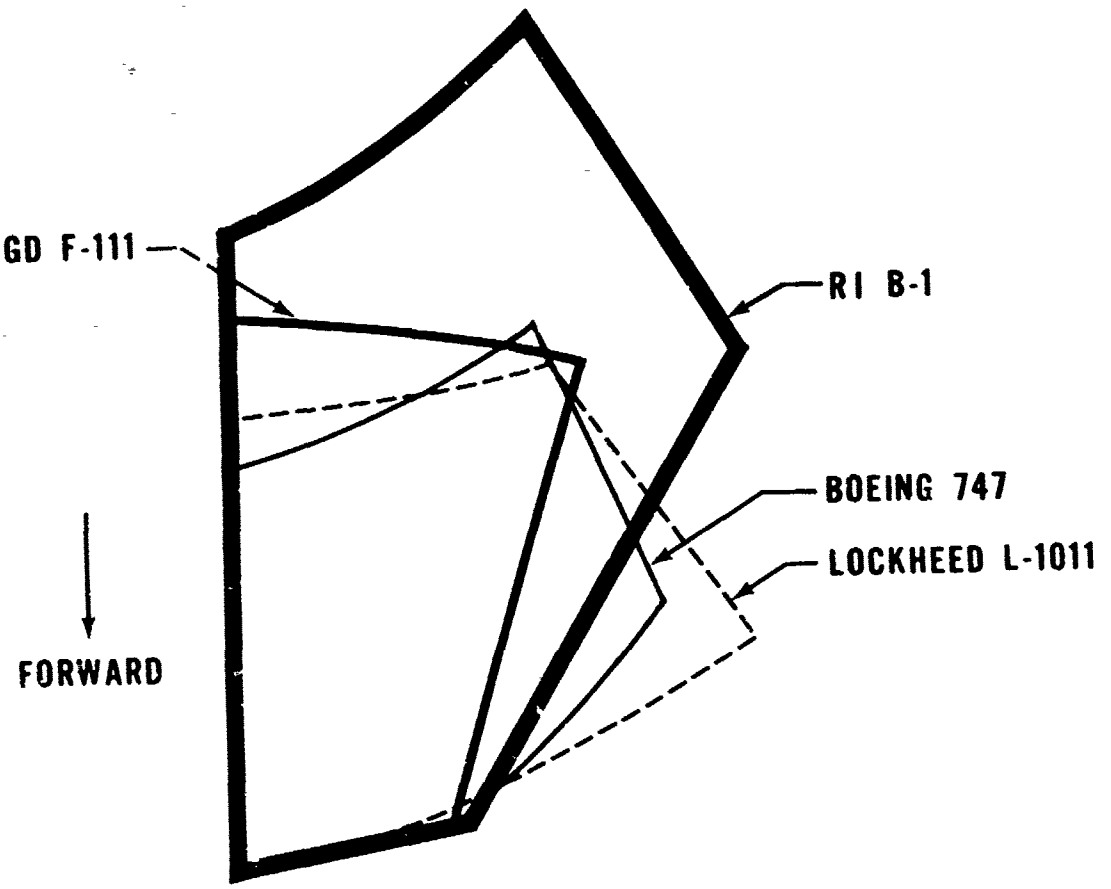


FIGURE 4: WINDSHIELD SIZE COMPARISONS

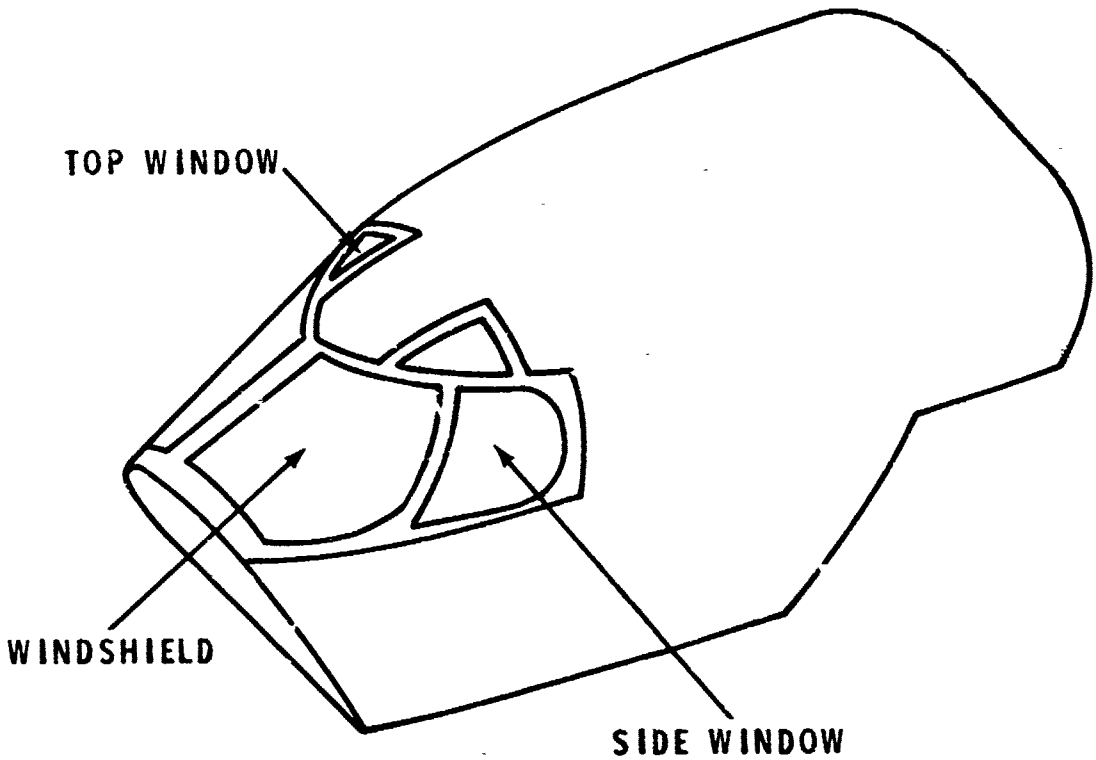


FIGURE 5: E-1 CREW MODULE TRANSPARENCIES

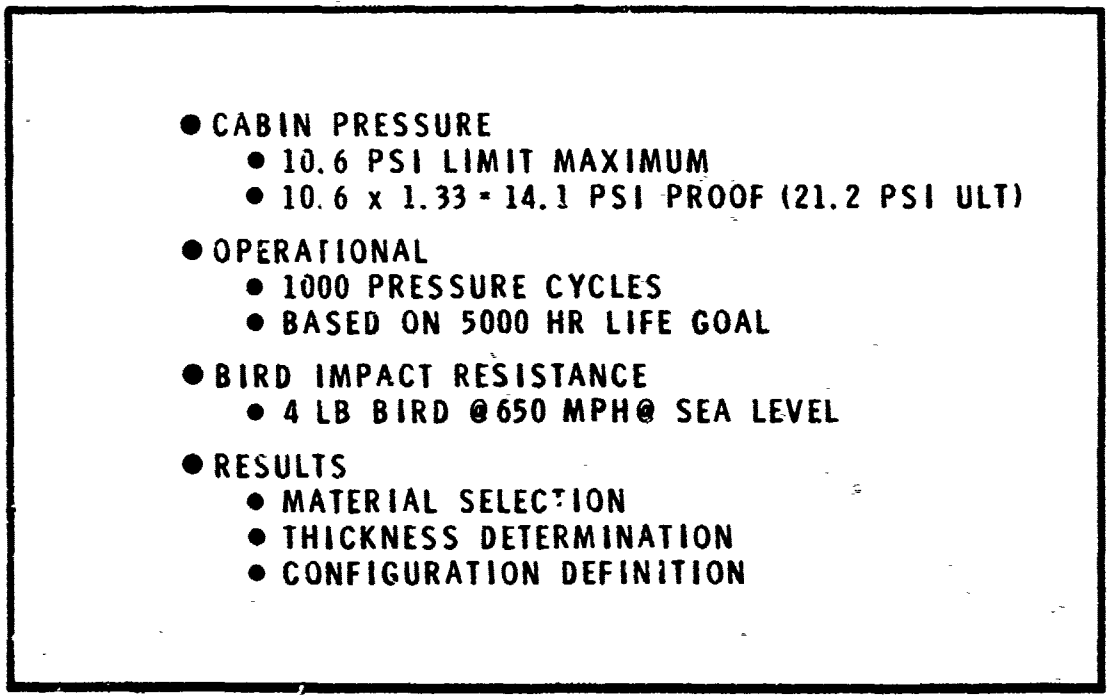


FIGURE 6: B-1 WINDSHIELD STRUCTURAL REQUIREMENTS AND IMPLICATIONS

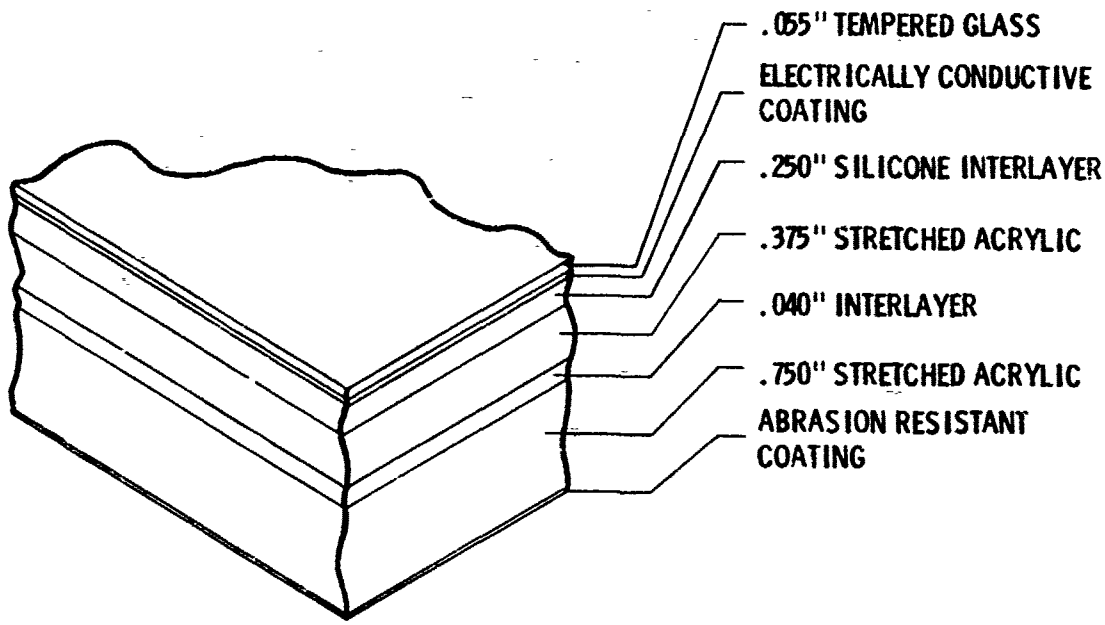


FIGURE 7: GLASS-STRETCHED ACRYLIC CONFIGURATION

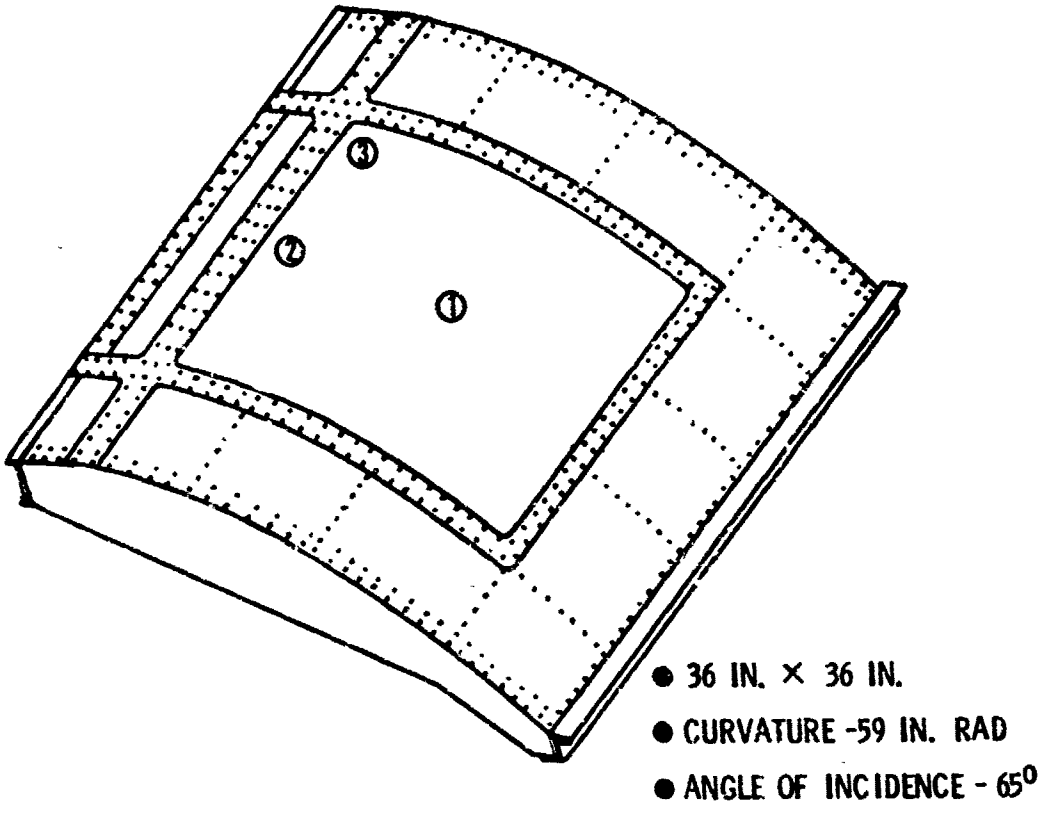


FIGURE 8: DESIGN DEVELOPMENT TEST PANEL DESCRIPTION FOR B-1 BIRDSTRIKE

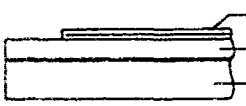
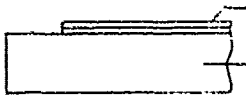
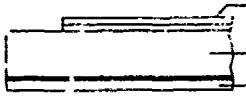
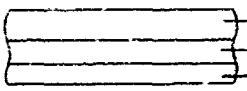
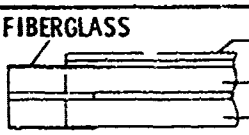
CONFIGURATION	LOCATION OF IMPACT	WEIGHT PER A/C (LBS)	RESULTS
	CENTER	255	PENETRATION
	CORNER	220	PENETRATION
	CENTER CORNER EDGE	232	NO PENETRATION
	CORNER	321	PENETRATION
	EDGE	513	NO PENETRATION

FIGURE 9: SUMMARY OF DESIGN DEVELOPMENT B-1 WINDSHIELD BIRD IMPACT TEST

● P-STATIC & CORONA DISCHARGE	ANTI-STATIC COATING REQUIRED ON WINDSHIELD PANELS
● RADAR REFLECTIVITY	MINIMUM CROSS SECTION
● NUCLEAR HARDENING	MAINTAIN STRUCTURAL CAPABILITY
● ANTI-ICING/DEFOG	GOLD COATING

FIGURE 10: ENVIRONMENTAL CONSTRAINTS AND ASSOCIATED IMPLICATIONS

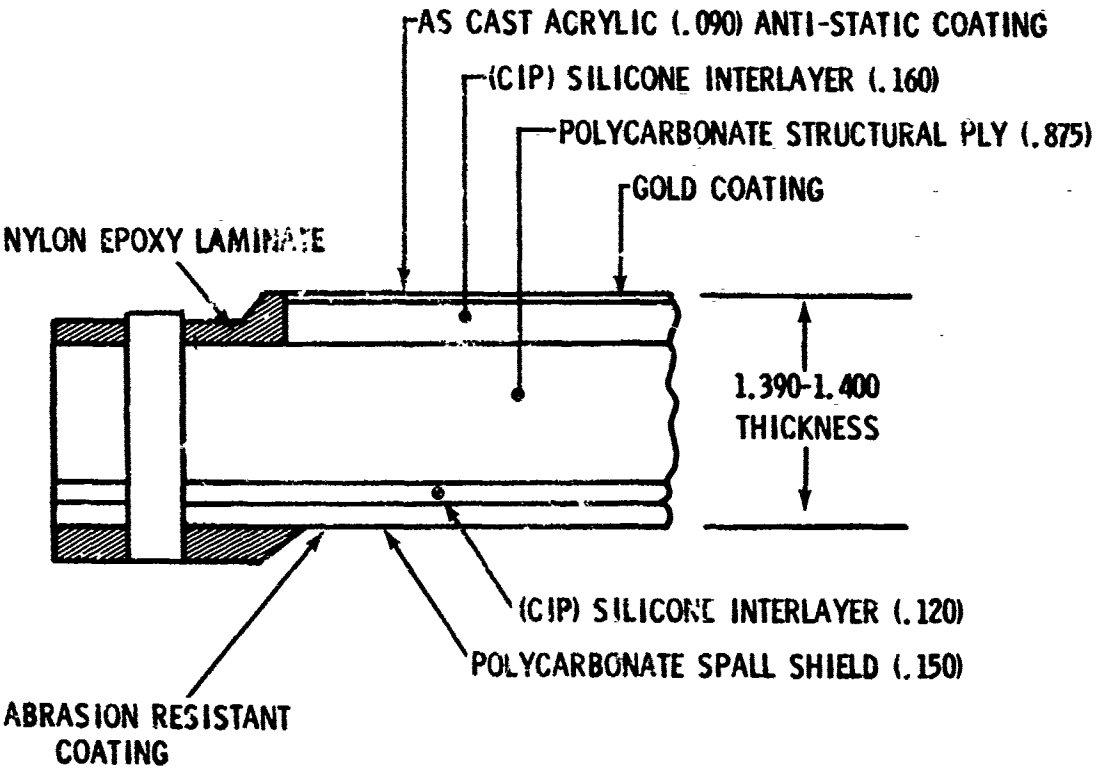


FIGURE 11: ROT & E B-1 WINDSHIELD PROCUREMENT CONFIGURATION

●LUMINOUS TRANSMITTANCE	85% MIN-MEASURED ALONG PILOTS HORIZONTAL LINE OF SIGHT
●HAZE	3% MAX
●ANGULAR DEVIATION	3 MIN OF ARC MAX IN 8^0 HALF ANGLE CONE AROUND PILOTS LINE OF SIGHT 4 MIN MAX IN REMAINING AREAS
●DISTORTION	1:10 MAX SLOPE OF GRID LINES

FIGURE 12: B-1 WINDSHIELD OPTICAL REQUIREMENTS

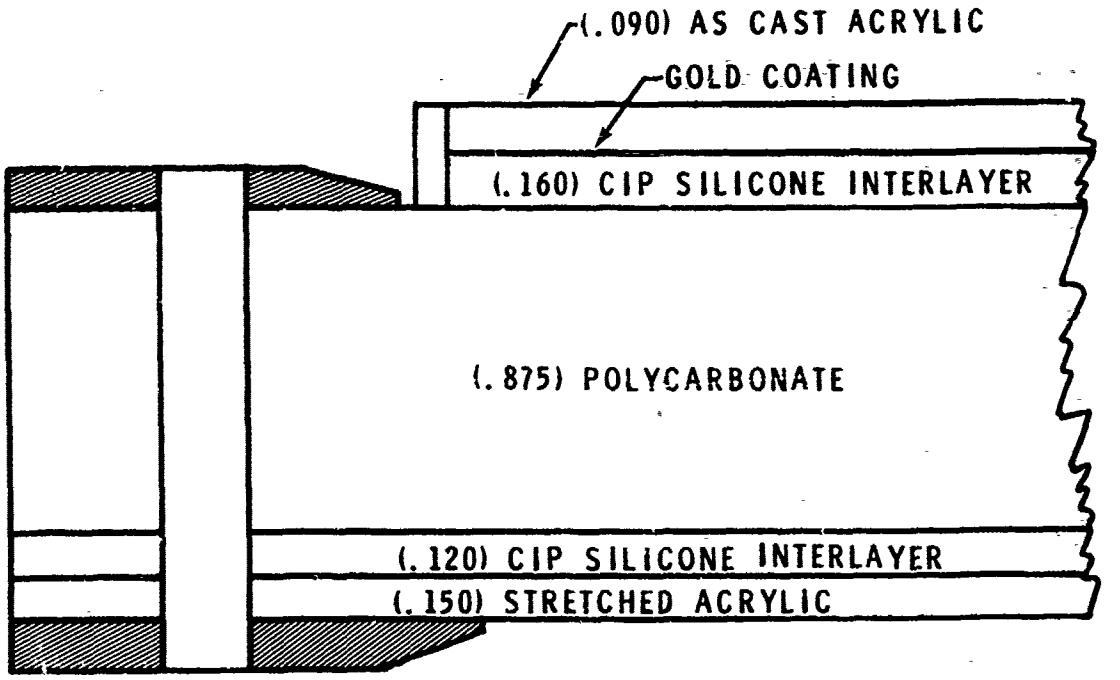


FIGURE 13: B-1 WINDSHIELD MODIFICATION NUMBER 1

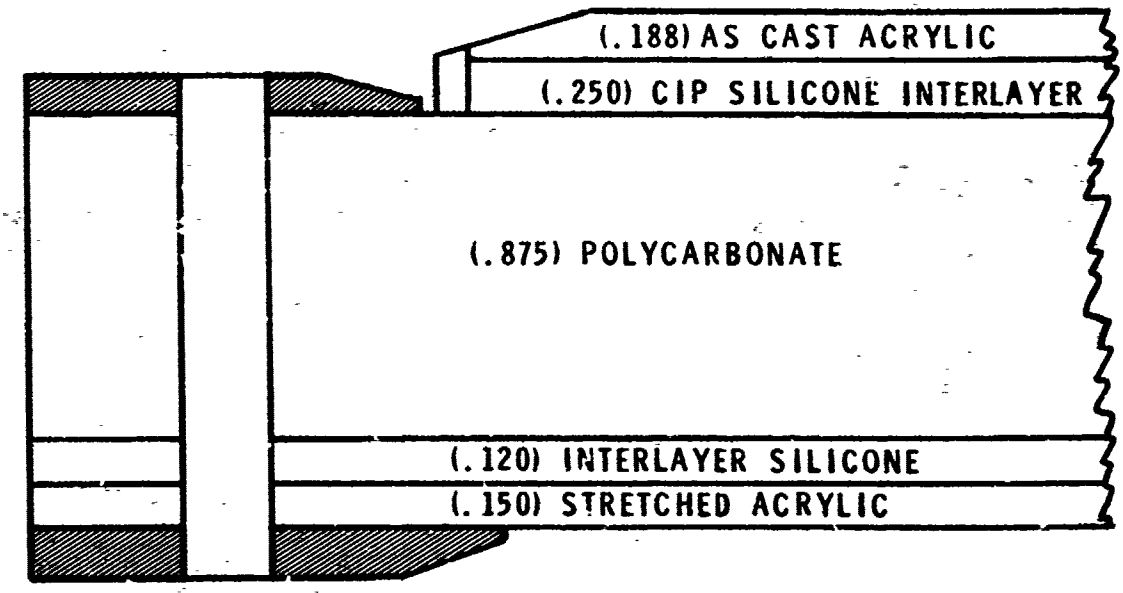
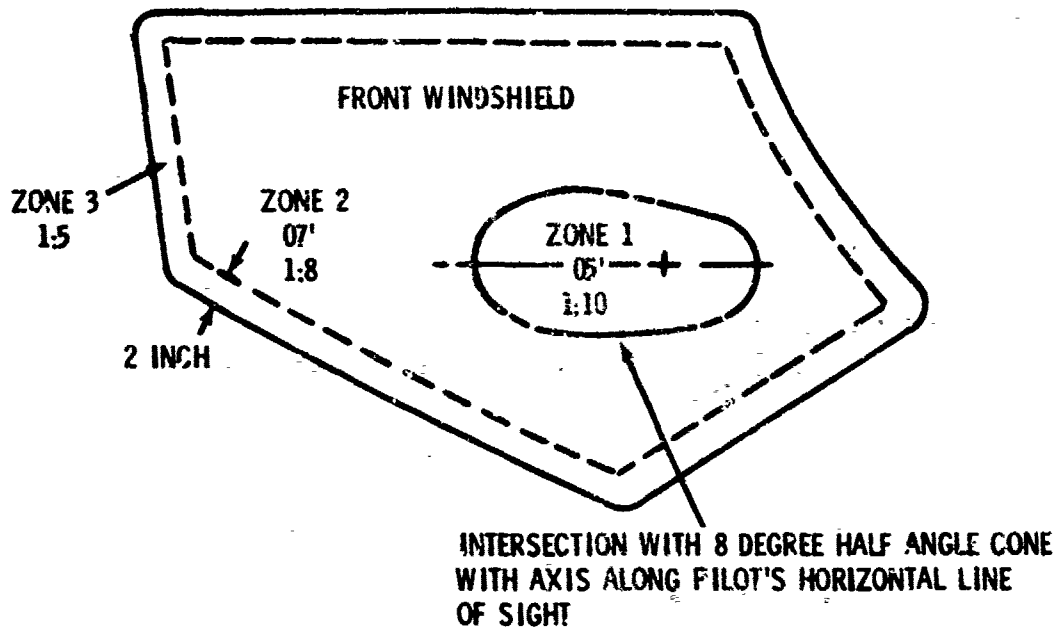


FIGURE 14: B-1 WINDSHIELD MODIFICATION NUMBER 2



LIGHT TRANS: 50% NORMAL

HAZE: 5%

1/2" DELETION LINE AREA OPTICS FREE

FIGURE 15: B-1 WINDSHIELD REVISED OPTICAL REQUIREMENTS

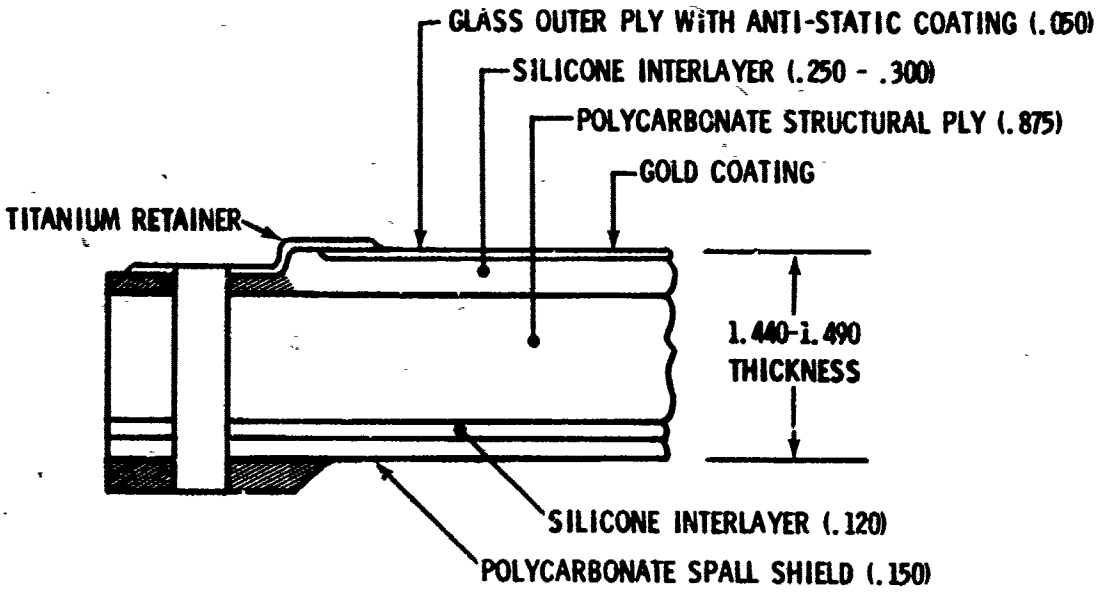


FIGURE 16: B-1 WINDSHIELD CONFIGURATION SELECTED FOR FLIGHT AND VERIFICATION TEST

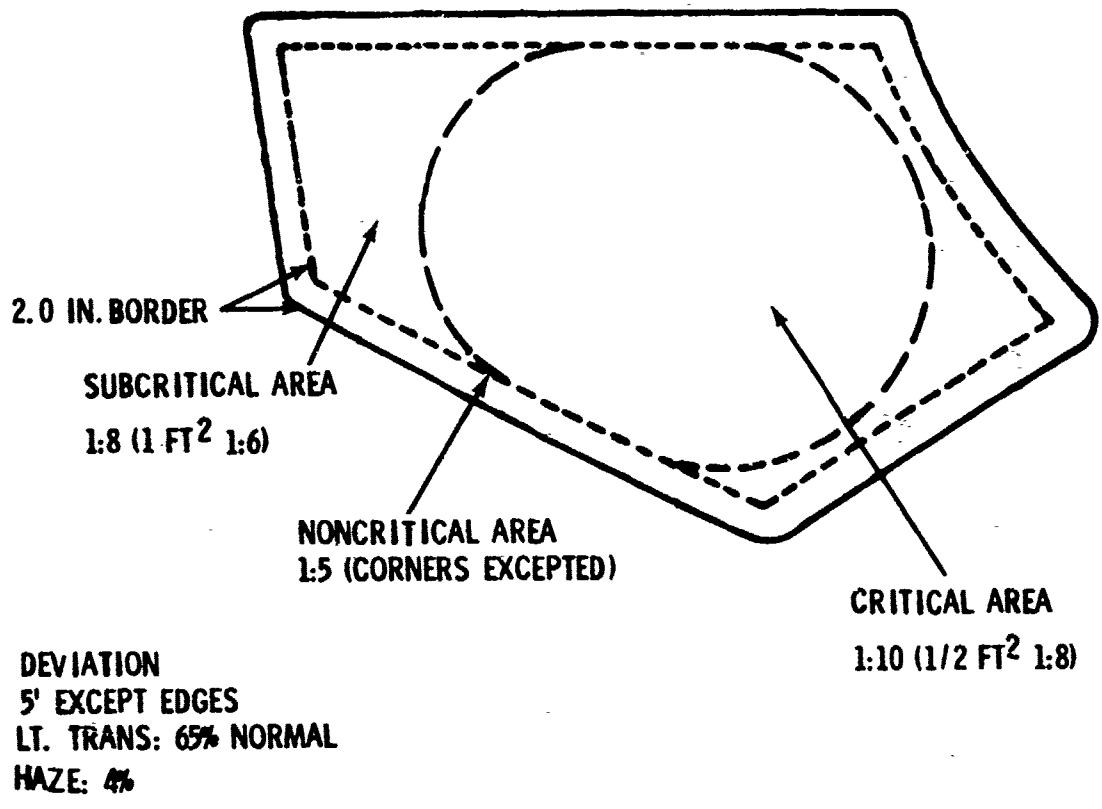
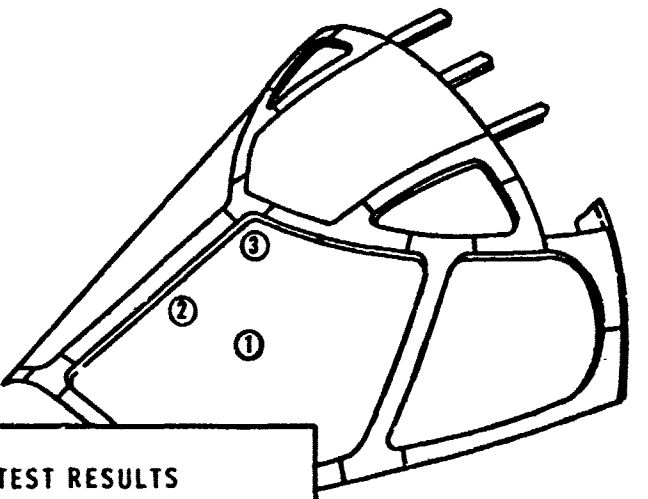


FIGURE 17: REVISED OPTICAL REQUIREMENTS FOR GLASS-POLYCARBONATE WINDSHIELD CONFIGURATION

REQUIREMENT	CONTRACT REQ	PLASTIC PLY		GLASS PLY RDT & E	MINIMUM ACCEPT.
		RDT & E	ACTUAL		
DISTORTION (LINE OF SIGHT) CRITICAL SUB-CRITICAL NON-CRITICAL EDGE / 1/2 INCH	 1 : 10 1 : 10 1 : 10	 1 : 10 1 : 10 1 : 10	 1 : 6 SOME AREAS	 1 : 10 1 : 8 1 : 5 NONE	 * 1 : 10 1 : 8 1 : 5 NONE
LIGHT TRANSMISSION	85 % LOS	70 % NORMAL	52 % NORMAL	65 % NORMAL	50 % NORMAL
HAZE	3 %	4 %	4-5 %	4 %	5 %
ANGULAR DEVIATION	3 - 4 FT LOS	3 - 4 FT NORMAL	3'CRITICAL AREAS 4' 95 % AREA 4-9' of 5 %	5 FT NORMAL	5 FT NORMAL

* SMALL ZONE (FIG. 15)

FIGURE 18: SUMMARY OF OPTICAL REQUIREMENTS, REVISIONS FOR VARIOUS WINDSHIELD CONFIGURATIONS



TEST NO.	BIRD WEIGHT (LBS)	BIRD VELOCITY (MPH)	TEST RESULTS
1	4.01	648.4	No penetration, structural ply and spall shield undamaged.
2	4.02	643.6	No penetration, structural ply undamaged spall shield cracked.
3	4.01	651.8	No penetration, structural ply and spall shield undamaged, some support structure damage.

FIGURE 19: BIRD STRIKE VERIFICATION TEST RESULTS AND BIRD IMPACT LOCATIONS

DEVELOPMENT OF THE WINDSHIELD FOR THE B-1 AIRCRAFT

R. C. Shelton
Swedlow, Inc.
Garden Grove, California

BEST AVAILABLE COPY

DEVELOPMENT OF THE WINDSHIELD

FOR THE B-1 AIRCRAFT

R. C. Shelton

SWEDLOW, INC.

ABSTRACT

The windshield for the B-1 aircraft, designed by Rockwell International Corporation and currently being fabricated by Swedlow, Inc., is the largest and most demanding transparency of which we are aware.

The B-1 windshield consists of an outer layer of thin chemically tempered glass, a structural member of thick ground and polished polycarbonate, a spall shield of thin ground and polished polycarbonate, laminated into a single composite with Swedlow's SS-5272Y(HT) high-temperature resistant cast-in-place silicone interlayer. The windshield also incorporates a transparent electrically conductive coating on the inboard surface of the outer glass layer for anti-ice and radar-reflection purposes. A transparent, electrically conductive coating is applied to the outboard surface of this outer glass layer for anti-static purposes. An abrasion resistant coating is applied to the inboard surface of the polycarbonate spall shield for protective purposes.

This paper will present the major development activities conducted by Swedlow, Inc. which led to the successful production of the B-1 windshield. Included will be the identification and discussion of certain technical problems that required resolution. Items such as grinding and polishing of polycarbonate to rigid dimensional and finish tolerances, conductive coating development, edge attachment materials and bonding procedures will be included.

Also to be included in this paper will be a discussion of the evolution of the windshield configuration from the original "development" model to the current "production" model.

The successful manufacture of this windshield has been the result of a tremendous advancement in the state-of-the-art of windshield fabrication technology.

1.0 INTRODUCTION

The B-1 aircraft, shown in Figure 1, designed to replace the aging B-52, incorporates a windshield which involves a configuration and material combination never before produced by Swedlow, Inc.

All of the components of the windshield were in existence at the time of design finalization by Rockwell. Although similar transparencies had been fabricated for Rockwell's bird-impact testing, (Reference 2), they were not as large and did not incorporate into one composite all of the requirements as specified for the B-1 windshield.

The B-1 windshield is the largest, most complex transparency with which we have been involved. The approximate size of the B-1 windshield is shown in Figures 2 and 3.

Upon entering the contract with Rockwell International Corp. to manufacture this windshield, Swedlow, Inc. recognized that there were certain requirements that would be achieved only through the application of development processes.

The purpose of this paper is to present a summary of the major activities conducted by Swedlow, Inc. which led to the successful fabrication of the windshield for the B-1 aircraft.

2.0 WINDSHIELD CONFIGURATION

2.1 Current

Figure 4 shows a cross-section view of the B-1 windshield configuration as it is now being produced. The windshield consists of an outer ply of chemically strengthened glass, a structural member of thick ground and polished polycarbonate, a spall shield of thin ground and polished polycarbonate, laminated into one composite with Swedlow's cast-in-place silicone interlayer. The windshield incorporates a transparent electrically conductive coating on the inboard surface of the glass ply for anti-ice and radar-reflection. A transparent electrically conductive coating is applied to the outboard surface of the outer glass ply for anti-static purposes. A protective coating is applied to the inside surface of the thin polycarbonate spall shield.

2.2 Evolution

Since there have been several cross-sectional configurations of the windshield during the history of the program, a brief review seems to be in order. (See Table 1)

The first configuration shows the windshield design as originally presented to Swedlow, Inc., and as originally manufactured. It

consisted of an outer ply of 0.090 inch maximum as-cast acrylic (MIL-P-8184) which carried an electrically conductive coating, an interlayer, a structural member of polycarbonate, another interlayer, a spall shield of polycarbonate and a protective coating.

The second configuration was a modification to the first in an effort to improve optical quality. In this configuration; the spall shield of polycarbonate was replaced with stretched acrylic. The objective was to provide a material that could be optically refinished after the part was laminated. (The first configuration had the protective coating applied to the polycarbonate in the flat state and thus precluded any refinishing after laminating.) This change improved optical quality but not to the extent desired by Rockwell.

The third configuration represents an additional modification where the outer 0.090 inch as-cast acrylic face was replaced with 0.188 inch as-cast acrylic. This modification greatly improved the optical quality and we were able to furnish windshields to Rockwell with optical quality acceptable for flight purposes. During the interlayer casting and curing operation, the outer 0.090 inch as-cast acrylic would become rippled. This rippling is substantially reduced through the use of the thicker, stiffer, as-cast acrylic.

None of the configurations discussed (1, 2, or 3) would meet the anti-static requirement and presented difficulty in maintaining the anti-ice coating temperature within acceptable limits.

The fourth configuration is the current production configuration previously discussed. The outer as-cast acrylic is replaced with 0.050 inch Chemcor (Corning Glass Works chemically tempered glass). The glass solves the anti-static problem and improves the function of the de-icing coating by minimizing the coating operating temperature. The use of the glass as the outer ply also helps to improve the optical quality since its higher modulus resists the rippling encountered with the 0.090 inch as-cast acrylic during interlayer cure. Another change occurred which is not as obvious. Processing was sufficiently developed to apply the protective coating to the polycarbonate spall shield, after the laminating process. This allowed us to optimize the inner surface of the polycarbonate prior to application of the coating.

3.0 MATERIALS AND PROCESS DEVELOPMENT

3.1 Polycarbonate

Many materials were evaluated by Rockwell International prior to their selection of polycarbonate as the windshield primary structural member (Reference 1 and 2).

Polycarbonate, being an extruded plastic material does not compare favorably with a cast material, such as acrylic, and is not optically acceptable for use in high performance aircraft windshields in its "as-extruded" condition. When used in aircraft transparencies, the "as-extruded" material must undergo additional processing to improve the optical quality. To further the problem, the B-1 windshield's overall size, thickness, and viewing angle are, to our knowledge, beyond that of any other aircraft currently utilizing polycarbonate transparencies.

3.1.1 Grinding and Polishing

Of normal concern when using the material is the ability to attain and maintain the high optical quality necessary for aircraft transparencies. To resolve these problems, Swedlow, Inc. has developed the ability to optically refinish the polycarbonate sheeting through grinding and polishing processing.

Swedlow has ground and polished acrylic sheeting for aircraft transparencies for many years. However, because of the softer surface of polycarbonate, machine grinding and polishing was considered impractical, and the technique which industry developed for optical refinishing of polycarbonate became hot pressing. The limits placed on quality attainable by this method are established from the surface finish of the pressing cauls. For aircraft which have windshield viewing incident angles which are high, as is the B-1, Swedlow considered this transferred quality to be unsatisfactory.

Swedlow believed that machine grinding and polishing was necessary to reduce optical distortion and angular deviation. The ability to grind and polish polycarbonate circumvents the imposed limitations placed on optical refinishing by pressing cauls and affords improvements in optical quality which Swedlow considered necessary.

Using its acrylic grinding and polishing techniques as a baseline, Swedlow was able to successfully develop the technique for the machine grinding and polishing of polycarbonate. As might be expected, the grinding and polishing of polycarbonate sheeting requires considerably more time than does acrylic. This is due primarily to the larger number of operations required. This is necessary to prevent the formation of deep scratches which are difficult to remove.

The grinding and polishing of polycarbonate sheeting, using the Swedlow developed technique, results in sheeting with superior optical quality when compared to "press polished" sheeting. To illustrate this superiority, refer to Figures 5, 6, 7 and 8. Figure 5 is a sheet of polycarbonate that has been fusion bonded and press polished. This was done by a firm other than Swedlow. Figure 6 is the same sheet after it was ground and polished by Swedlow, Inc. Because of the viewing angle (90°) the difference is not readily obvious. However, Figures 7 and 8 demonstrate the

improvement attained as a result of grinding and polishing. Figure 7 is the sheet before grinding and polishing, and Figure 8 is after grinding and polishing, when viewed at an angle to simulate the B-1 windshield (25°). This angle is based on the angle obtained at the aircraft centerline. Our calculations show the viewing angle from pilot's eye position, at the lower forward corner, to be about 9°. Table 2 shows the thickness of the sheet before and after the grinding operation.

Having demonstrated the ability to grind and polish polycarbonate to close dimensional and optical tolerances, as required for the structural member, it became necessary to adapt the process to the polycarbonate spall shield. The spall shield, which is only 0.150 inches thick, required the utilization of a different holding technique. Whereas the thick structural member could be held to the grinding table by means of vacuum, this was not feasible with the thin material, and alternate means of securing to the table was required.

Another benefit that may be a result of the grinding and polishing is the degree of surface stress introduced into the sheet. While no attempt has been made to measure the differences, it is felt, by Swedlow, they could be substantial. If this is true, press polished material could have the potential of earlier failure than ground and polished sheeting.

3.1.2 Fusion Bonding

The polycarbonate material utilized for optical applications is extruded to a maximum 0.375 inches thick and requires lamination of plies to the required thickness. For the B-1 structural member, three plies of nominal 0.315 inch thick extruded polycarbonate are "fusion bonded", and then ground and polished.

To insure that adequate adhesion is being obtained during the "fusion bonding" operation, the interlaminar shear strength was determined using the test procedure defined in MIL-P-25690 (Paragraph 4.6.9). The test specimen used is shown in Figure 9. The results obtained were consistently above 4000 PSI, and usually in the 6000 PSI range.

3.1.3 Forming and Drying

The forming of the polycarbonate sheet presented a serious problem, basically due to the size of the blank being formed. Past experience with polycarbonate was not usable for the B-1 Windshield because of its large size.

Because of subsequent operations, a blank size of 52" x 80" was selected for forming. A rectangular shape allows us considerable latitude as regards left or right hand, forward or aft panel placements.

Because of the size and weight of the blank required for the structural member, conventional handling and forming techniques were

found to be inadequate.

Several approaches to the forming of the structural member were investigated, all aimed at attempting to heat the sheet without touching the die surface to minimize any mark off.

As a result we developed a special forming technique for the large polycarbonate structural member that yielded excellent contour, retained the optical quality of the ground and polished sheet, both with a minimum of mark off. The thick ground and polished sheet is hung in an oven utilizing a proprietary method, since conventional techniques were unsuccessful.

It should be noted at this point that variations in the as-received polycarbonate material precludes establishing a standard set of processing conditions. The original lot of material required long drying cycles. Subsequent lots of material required substantially less drying time. Table 3 illustrates this effect. With each new lot of polycarbonate sheet received, evaluations are conducted to determine required drying times.

Normal forming temperatures are in the 340°F to 400°F range with the best results obtained at about 370°F. (Reference 3).

Table 4 shows the variation required in forming different lots of polycarbonate. To illustrate Lot "X" material could not be formed at Lot "Y" temperatures, whereas Lot "Y" material would bubble at Lot "X" temperature.

Figure 10 is a curve generated from data contained in AFML-TR-72-117 and shows the drying time - vs - thickness of polycarbonate at 260 ± 5°F. Although this is a general curve and can be utilized as a guide line, Swedlow, Inc. has found from our own experience that lot to lot evaluation is the best way to set the processing conditions.

3.1.4 Drilling and Reaming

A. Size

We have accomplished the art of drilling very close tolerance holes through polycarbonate. Rockwell International Corp.'s original tolerance on attaching holes was very tight (+.0005, -.001). This is the kind of tolerance you might expect in a metal component, but to our knowledge, it has never before been required in a plastic part. Rockwell determined, later in the program, that such tight tolerances were not required and changed them as shown in Table 5.

B. Finish

At the outset of the program, no special hole finish was

required. However, due to polycarbonate cracking at the holes, at first attributed entirely to surface finish condition, a change was made by Rockwell International Corp. calling for a 20 micro inch finish in the attaching holes. Further evaluations of the polycarbonate material showed the cracking was due to a combination of environmental exposure and hole finish. Overcoming the environmental exposure problem enabled a relaxation of the hole finish from 20 micro inches to 63 micro inches.

Swedlow's development of drilling and reaming technique was accomplished prior to the tolerance or finish change being made. As a result, Swedlow consistently produces a hole finish in polycarbonate of 10 micro inches, or better.

The development of the technique to provide the tight tolerance holes with a mirror finish became a major development activity on our part and was successfully accomplished.

Table 5 shows the changes that occurred in the attaching holes during the early development of the windshield.

3.2 Outer Ply

As noted in the introduction, the outer ply of the current windshield configuration is 0.050 inch chemically tempered glass, and the original callout was 0.090 inch maximum as-cast acrylic.

3.2.1 As-Cast Acrylic

To successfully fabricate acceptable windshields for flight, a means of achieving the best optical quality in the finished windshield is necessary. This requires high quality in each of the individual plies. This coupled with the fact that the as-cast acrylic carried the electrically conductive coating, Swedlow, Inc. attempted to develop the grinding technique for very thin as-cast acrylic. Not only would this provide the required optical quality in the individual sheet, but it would also provide a uniform thickness necessary for proper de-icing without hot spots. Although we spent considerable effort in attempting to develop the grinding and polishing technique for thin as-cast acrylic, we were only partly successful. We were able to obtain good thickness control, but unsuccessful in achieving an improvement in optical quality over that obtainable with high quality select sheeting. Therefore, we proceeded with as-cast sheeting selected for use on the B-1 windshield.

3.2.2 Glass

The outer ply of the windshield is now 0.050 inch thick Chemcor, chemically strengthened glass made by the Corning Glass Works. The change was made from as-cast acrylic to improve optics,

provide a durable anti-static coating and improve the anti-icing coating operation.

Because of the size of the glass member, special handling techniques had to be instituted.

3.3 Interlayer

The interlayer used for the B-1 windshield is Swedlow's SS-5272Y(HT) cast-in-place silicone interlayer. This interlayer has excellent low and high temperature capabilities as required to meet the demands of the B-1 environments. This interlayer will not discolor at high temperatures, has excellent optical qualities, clarity, adhesion to the face sheets and toughness. This interlayer is a low modulus material and is compatible with vacuum deposited metallic films as required for radar reflective or electrical conductive coatings. Figure 11 illustrates the retention of tensile strength and elongation at temperatures from -160°F to +300°F. This interlayer required no development since it has been in production use for many years. As far as evaluation for the B-1 program is concerned, this interlayer was previously tested by Rockwell International Corp. where its suitability was determined. (Reference 1).

3.4 Edge Attachment

3.4.1 Laminate

Originally, the Rockwell requirement for the edge laminate designated a MIL specification epoxy resin to be used to manufacture the nylon-epoxy edge attachment material. Rockwell also established the requirements for the laminate. During initial fabrication it was determined that the resin system so specified would not meet the specified requirements. Subsequent evaluation by Rockwell showed that Swedlow's X6N-225 epoxy-nylon laminate would meet the physical requirements specified by Rockwell, and was so utilized.

Figures 12 and 13 show the tensile strength and modulus of Swedlow's X6N-225 epoxy-nylon laminate versus temperature.

As a matter of fact, Swedlow's X6N-225 epoxy-nylon laminate is used on all transparencies for the B-1 aircraft, even though Swedlow manufactures only the windshield.

3.4.2 Bonding

The subject of development of the bonding of the epoxy-nylon edge laminate to the polycarbonate with RTV-630 adhesive will not be discussed here since the basic materials and procedures were previously discussed (Reference 1). There were considerable evaluations conducted between Swedlow and Rockwell to establish items such as primer, stand-off times, shelf-life and the like.

The adhesive shear strength requirement specified by Rockwell is 350 psi when tested at +220°F. The bond strength is determined using control specimens shown in Figure 14. This requirement is consistently met.

3.5 Protective Coating

The need to protect the polycarbonate surface from abrasion and solvent action is well known and will not be discussed here. To provide protection for the polycarbonate, Swedlow applies its SS-6432 protective coating. During the course of this program, we have developed the ability to (1) Flow coat and cure the protective coating on a flat sheet, then wrap the flat sheet as the inner member of the windshield; (2) Flow coat and cure the protective coating to the inside surface of the laminated windshield composite.

This latter development has enabled us to refinish the polycarbonate spall shield surface after laminating and prior to application of the protective coating.

3.6 Electrically Conductive Coating

3.6.1 History

The electrically conductive coating resistivity profile for the windshield presented problems at the inception of the B-1 program.

Originally, the windshield was to have, as an objective, a uniform coating over the entire windshield surface for anti-icing and radar-reflection. Figure 15 presents the evolution of the E-C coating pattern.

Configuration 1 was extensively investigated and found to be unacceptable, since the uniform coating could not be achieved.

Configuration 2 was the primary alternative to Configuration 1 but technically could not be achieved due to the inflected curvature of shape and the inability to achieve uniform power dissipation through resistivity grading of such a configuration.

Configuration 3 was investigated and was an attempt to bring the coated area into a rectangular form by heavily coating the areas adjacent to the actual bus-bars to form a new "effective" bus-bar termination line. This configuration was rejected due to the complete loss of light transmission in the heavily coated areas.

Configuration 4 was an attempt to change the configuration of the upper bus-bar to form a "Dog-Leg" and was rejected due to the impossibility of resistivity grading to achieve uniform power dissipation and the need to adhere to the principal of orthogonal current and voltage stream tubes.

Configuration 5 is known as the "Swing Pattern". This configuration was selected because of its ideal shape for a coating geometry and would yield a near uniform power dissipation throughout the coated area.

During the course of this development effort it was determined that the coating material originally selected for the windshield, (multi-layer stack) was incompatible with the B-1 windshield outer as-cast material and performance requirements. An alternate coating system was selected (monolithic gold) which resulted in an acceptable coating with some reduction of visible light transmission.

3.6.2 Swing Pattern Configuration

The need for undertaking this development was prompted by the concluded inability to achieve an anti-ice coating pattern which would cover the entire B-1 windshield vision area.

Figure 16 shows in more detail the geometry of the "swing pattern".

The heated area geometry is provided by vacuum deposition of a transparent conductive coating over the entire windshield surface. The heated area is bounded by constant radius deletion lines to provide uniform heating within this area. Bus-bars are deposited as radially positioned elements.

Within the heated area the conductive film is developed such that resistivity grading occurs in a radial direction in order to provide a constant power density.

3.6.3 Coating Type

The coating system originally selected for use with the as-cast acrylic outer ply was found to be incompatible with the as-cast acrylic.

As a result, a monolithic gold electrically conductive element was used as the anti-icing element on as-cast acrylic outer plies. The "swing pattern" coating development was successfully accomplished on the as-cast acrylic, using the monolithic gold coating.

When the change in the outer ply was made from as-cast acrylic to Chemcor glass, the coating type also changed. The coating utilized for as-cast acrylic is monolithic gold, whereas the coating utilized on glass is a multi-layer stack (metal oxides on either side of gold).

3.6.4 Vacuum Deposited Coating Design Process

The proprietary nature of the coating process limits what can be said with respect to the design and coating process. The design effort may, however, be described in a general sense and will be

done here in order to define the development activity which occurred.

The first step is to generate a resistivity profile which will meet the power and area requirements of the specification.

From the resistivity profile coating machinery is selected which is used in the vacuum chamber.

In addition there are other pieces of equipment which must be designed such as bus-bar and holding fixtures, deletion line apparatus, etc.

After this machinery is made, it is moved into the vacuum chamber and parts coated to refine the grading.

Prior to this activity, the electrically conductive film type is selected. Vacuum coatings which are used on transparencies for power dissipation are hinged around gold. Evolving from gold are coating stacks which incorporate metal oxide films on either side of the gold. These stacks act to modify the current conduction thus changing the resistivity limits. They also optically anti-reflect the gold, increasing light transmittance.

These conductive coatings are a portion of a thin film system. Base coats, top coats and primers are used in conjunction with the gold film. These additional film elements are required in order to enhance adhesion, to mask substrate surface scratches, and to offer processing protection to the conductive film. It is normally necessary to evaluate the film system's compatibility to processing and environmental factors.

Table 6 presents the final requirements established for the electrically conductive coating for the B-1 windshield swing pattern configuration.

Table 7 presents typical properties measured on full-sized parts.

The electrically conductive development effort resulted in the production of the necessary tooling, a process capable of producing coatings and the production of acceptable coatings.

4.0 SUMMARY

This paper has attempted to show the extensive development activity required to produce a windshield of the magnitude required for the B-1 Aircraft.

Some of the areas had to be touched on only briefly for proprietary reasons.

The development activities required have been successfully accomplished by Swedlow, Inc. and implemented to produce the B-1 windshield.

5.0 CONCLUSION

The successful production of highly complex, large multi-layer composite windshields has been demonstrated.

The first flight of the B-1 aircraft, made in December of 1974, was made using windshields fabricated by Swedlow, Inc. The initial windshields were of a back-up nature and incorporated the thick as-cast acrylic outer ply and a stretched acrylic spall shield.

Glass-faced windshields, which are considered the production configuration, have also been delivered.

The successful fabrication of these complex windshields has demonstrated an advancement in the state-of-the-art of windshield technology.

Swedlow, Inc. is extremely proud of our achievements in advancing the state-of-the-art of windshield technology. We know it has been attained primarily through our vigorous comprehensive company-funded research and development programs.

6.0 ACKNOWLEDGEMENTS

Swedlow, Inc. wishes to thank the Rockwell International Corp. for their cooperation during the development of the B-1 windshield. Also, the sponsoring agency for the B-1 windshield is:

Aeronautical Systems Division
Wright Patterson Air Force Base
Ohio (ASH)

7.0 REFERENCES

(1) J. E. Mahaffey, Rockwell International Corporation, "Material Evaluation B-1 Crew Module Windshield and Windows". Paper presented at the Conference on Transparent Aircraft Enclosures, Las Vegas, Nevada. February 5-8, 1973.

(2) F. T. McQuilken, Rockwell International Corporation, "The Design Development of a Birdproof Windshield for the B-1 Strategic Bomber". Paper presented at the Conference on Transparent Aircraft Enclosures, Las Vegas, Nevada. February 5-8, 1973.

(3) General Electric Company, "Lexan Polycarbonate Resin"

(4) Richard S. Hassard, "Design Criteria Transparent Polycarbonate Plastic Sheet". Technical Report: AFML-TR-72-117, Air Force Materials Laboratory, Air Force Systems Command, Wright Patterson Air Force Base, Ohio. August 1972.

TABLE 1

B-1 WINDSHIELD

CROSS-SECTIONAL CONFIGURATION EVOLUTION

OUTER PLY	.090" AS-CAST ACRYLIC	.090" AS-CAST ACRYLIC	.188" AS-CAST ACRYLIC	.050 GLASS
INTERLAYER	.160" CAST-IN-PLACE SILICONE, SS-5272Y (HT)	.160" CAST-IN-PLACE SILICONE, SS-5272Y (HT)	.160" CAST-IN PLACE SILICONE, SS-5272Y (HT)	.300" CAST-IN-PLACE SILICONE, SS-5272Y (HT)
STRUCTURAL MEMBER	.870" GROUND AND POLISHED POLYCARBONATE	SAME	SAME	SAME
INTERLAYER	.120" CAST-IN-PLACE SILICONE, SS-5272Y (HT)	SAME	SAME	SAME
SPALL SHIELD	.150" GROUND AND POLISHED POLYCARBONATE	.150" GROUND AND POLISHED STRETCHED ACRYLIC	.150" GROUND AND POLISHED STRETCHED ACRYLIC	.150" GROUND AND POLISHED POLYCARBONATE
PROTECTIVE COATING	YES	NO	NO	YES
OBJECTIVE	ORIGINAL	IMPROVE OPTICS	IMPROVE OPTICS (BACK-UP)	CURRENT

TABLE 2

POLYCARBONATE SHEET
GROUND AND POLISHED

POLYCARBONATE THICKNESS	
BEFORE GRINDING	AFTER GRINDING
0.502"	0.446"
0.500"	0.450"
0.498"	0.450"
0.500"	0.449"
0.495"	0.447"
0.505"	0.447"
0.503"	0.446"
0.507"	0.446"
0.505"	0.447
0.500"	0.446"
0.511"	0.445"
0.507"	0.450"
0.506"	0.450"
0.503"	0.449"
0.498"	0.447"
VARIATION: 0.495" to 0.511"	0.445" to 0.450"

TABLE 3

DRYING TIME VARIATIONS
BETWEEN TWO LOTS OF POLYCARBONATE

LOT	0.315" DRYING TIME/ TEMPERATURE	.870" DRYING TIME/ TEMPERATURE
"X"	36 to 168 Hrs. @ 260 ± 5°F	160 Hrs. @ 260 ± 5°F
"Y"	36 to 48 Hrs. @ 220 ± 5°F	48 Hrs. @ 220 ± 5°F

TABLE 4

POLYCARBONATE FORMING
TEMPERATURE VARIATIONS

LOT	.870" SHEET
"X"	370°F
"Y"	<340°F

TABLE 5

ATTACHING HOLES

	ORIGINAL	TRANSITION	FINAL
Size	0.4063	Same	0.4063
Tolerances	+0.0005, -0.001	Same	+0.0005, -0.0043
Finish (RMS)	None	20	63

TABLE 6

ELECTRICAL REQUIREMENTS - B-1
WINDSHIELD

PROPERTY	REQUIREMENT
Resistivity Limits	30Ω/□ Max.
Power Density	3 Watts/in^2 Min. 6 Watts/in^2 Max.
Voltage	374 to 411
Heated Area	1081 in^2
R_{bb}	21.31Ω Min. to 28.19Ω Max.
K_h	$\leq$ 1.33
K_m	$\geq$ 0.75
K_{s1}	1.0 ± 0.12
K_{s2}	1.0 ± 0.12
K_a	$\leq$ 1.1

TABLE 7

TYPICAL ELECTRICAL PROPERTIES -
B-1 WINDSHIELD

PROPERTY	TYPICAL MEASURED VALUE	
	BEFORE LAMINATION	AFTER LAMINATION
R_{bb}	28.33	27.9
K_h	1.07	1.08
K_m	0.72	0.79
K_{s1}	1.07	1.02
K_{s2}	1.07	1.02
K_a	0.77	0.76

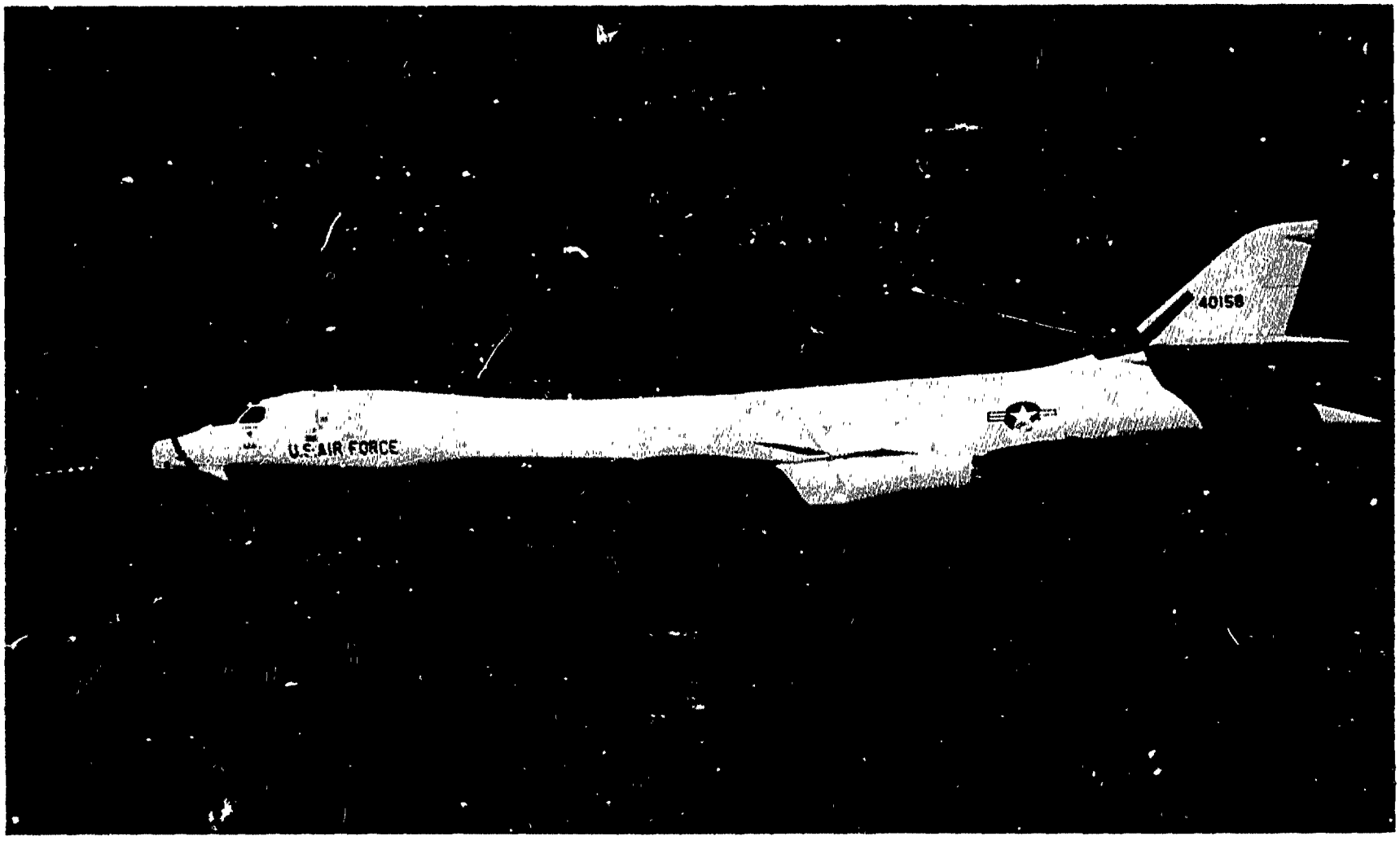


FIGURE 1 - ROCKWELL INTERNATIONAL CORP.,
B-1 BOMBER

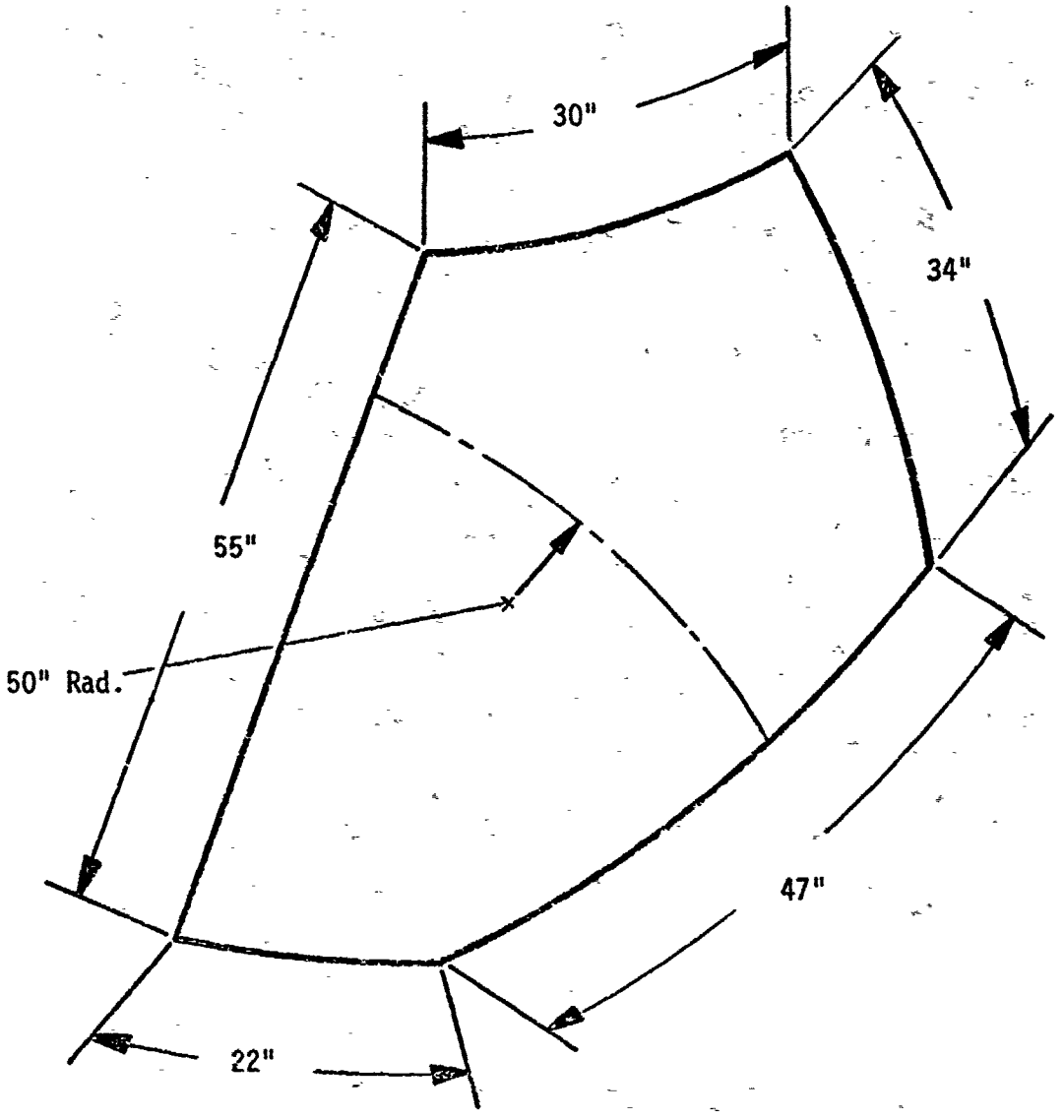


FIGURE 2 - B-1 WINDSHIELD, APPROXIMATE SIZE

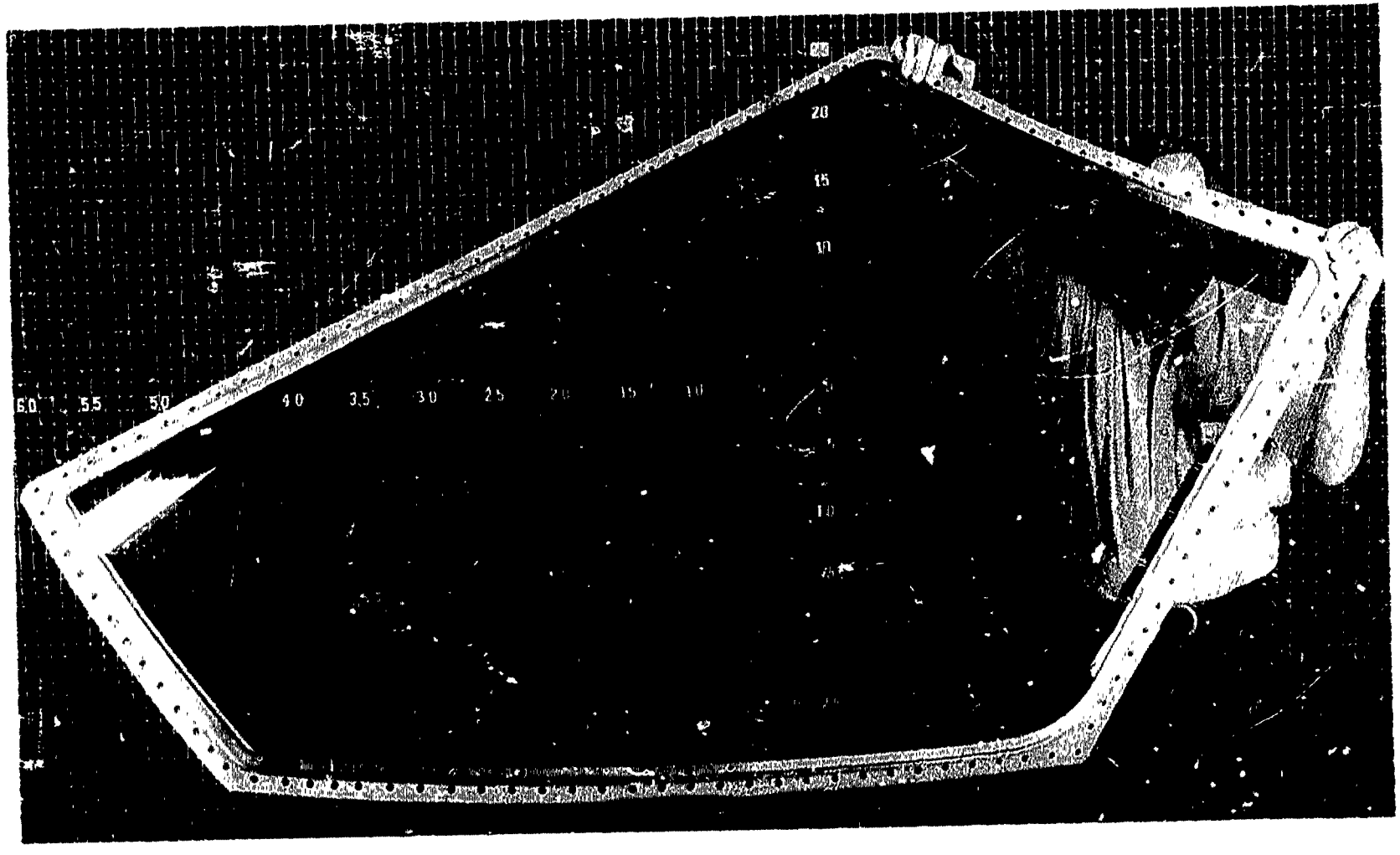
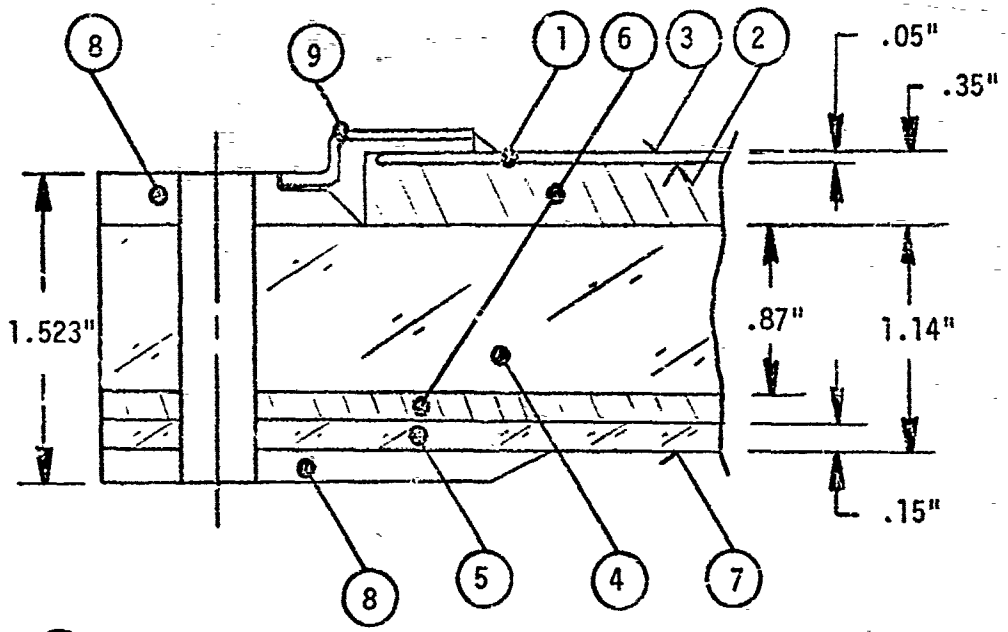


FIGURE 3 - B-1 WINDSHIELD



(1) Face ply : Chemically tempered glass.

(2) Anti-ice Coating : A transparent electrically conductive metallic coating.

(3) Anti-static Coating : A transparent, electrically conductive coating.

(4) Structural Member : Polycarbonate meeting the requirements of MIL-P-83310, fusion bonded to thickness; then ground and polished for optical quality.

(5) Spall Shield : Polycarbonate meeting the requirements of MIL-P-83310, ground and polished for optical quality.

(6) Interlayer : Swedlow's SS-5272Y(HT) cast-in-place silicone interlayer for mating the face ply to the structural member and the spall shield to the structural member.

(7) Swedlow's SS-6432 Protective Coating.

(8) Swedlow X6N-225 Epoxy-nylon Edge Reinforcement.

(9) Titanium Zee Strap

FIGURE 4 - CROSS-SECTION OF B-1 WINDSHIELD

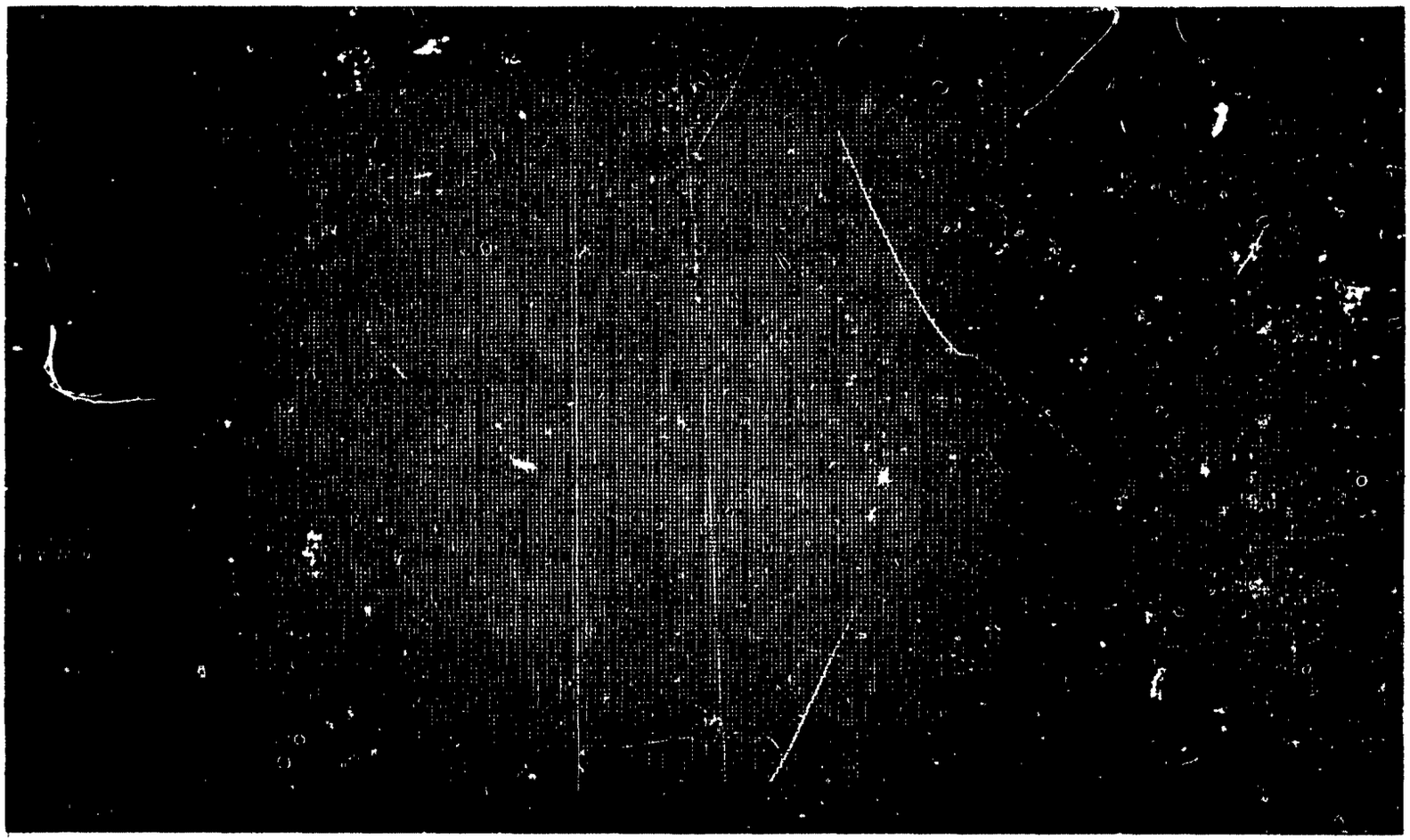


FIGURE 5 - POLYCARBONATE, PRESS POLISHED.
PRIOR TO GRINDING AND POLISHING (90°)

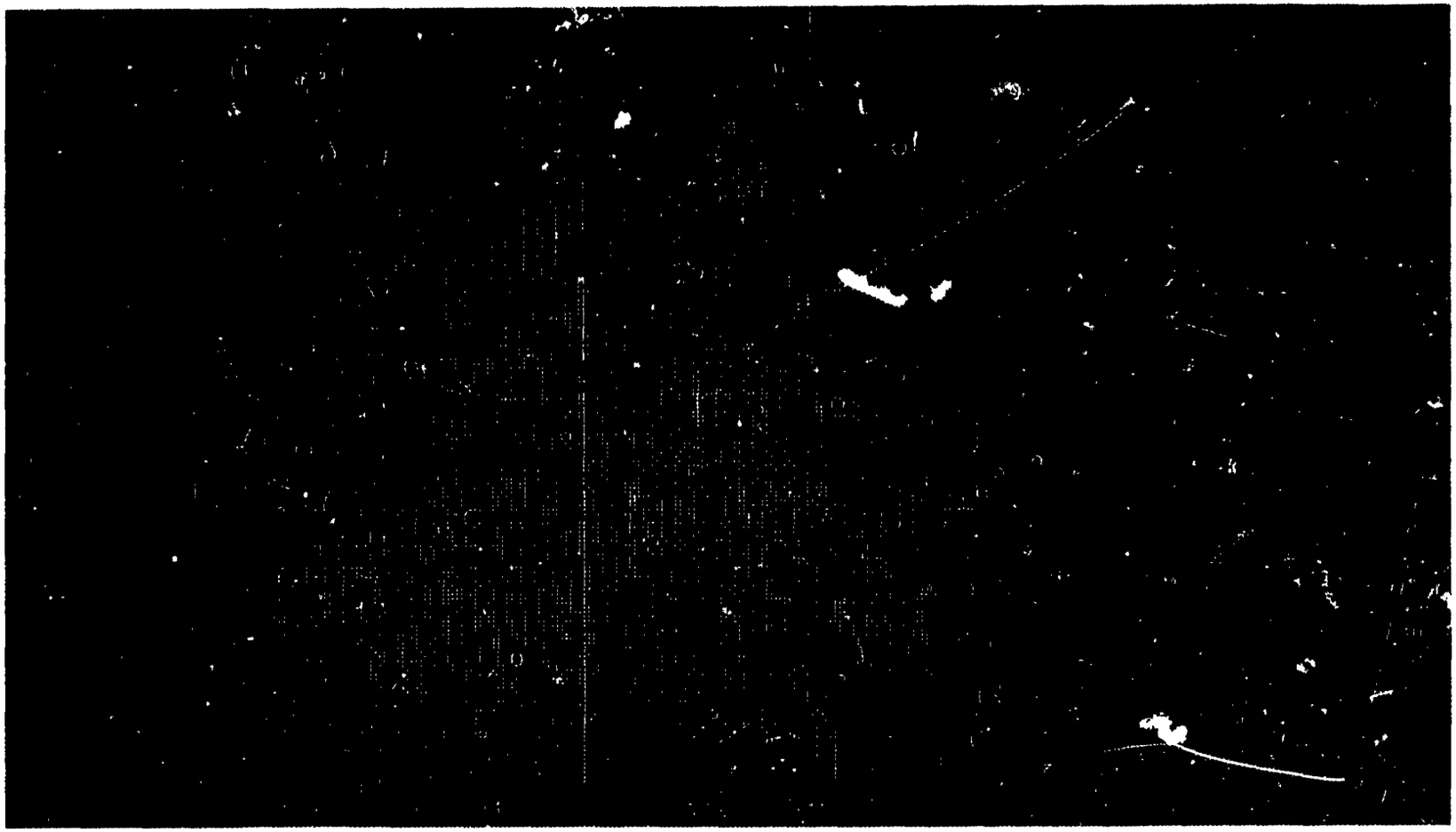


FIGURE 6 - POLYCARBONATE, PRESS POLISHED.
AFTER GRINDING AND POLISHING (90°)

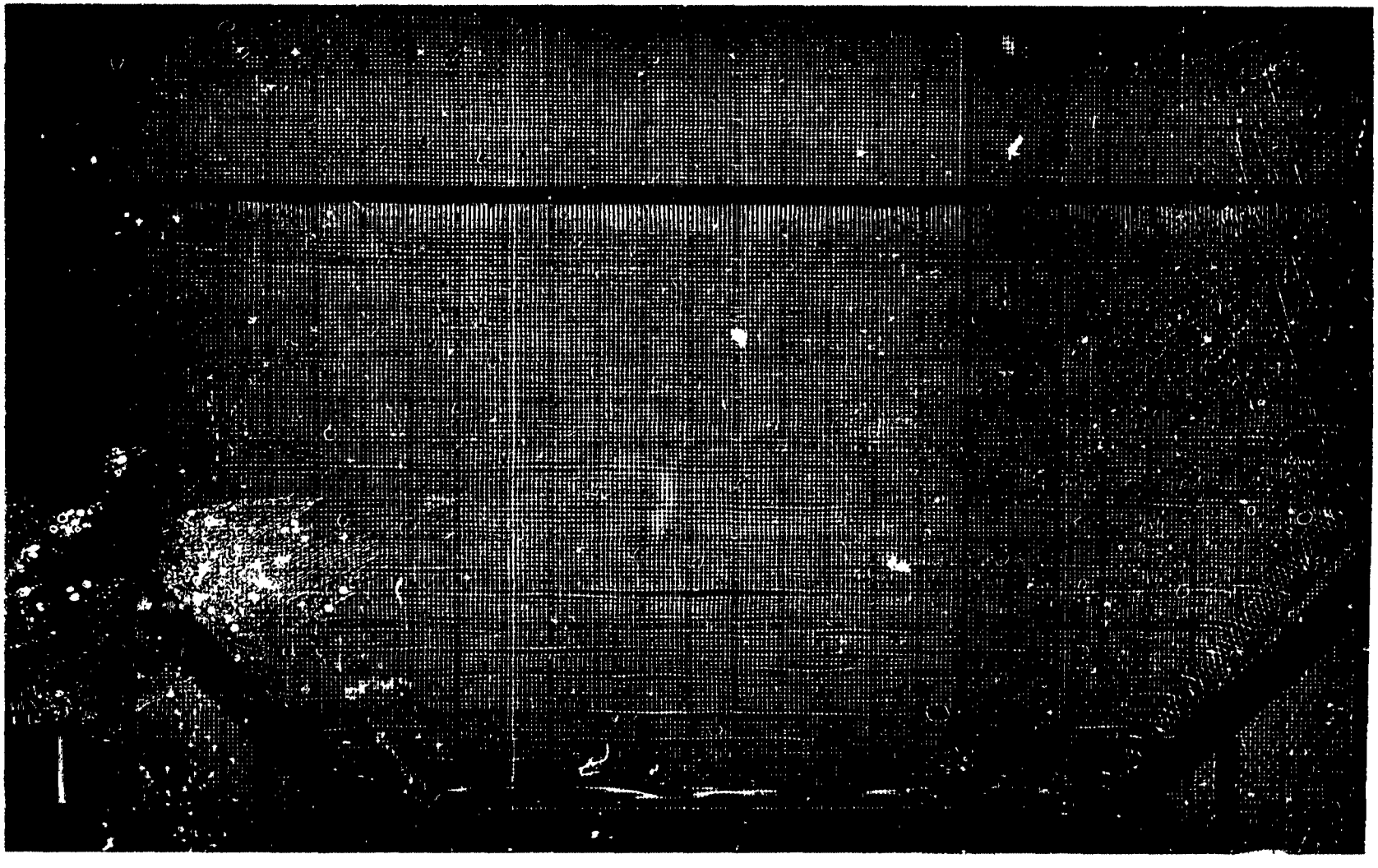


FIGURE 7 - POLYCARBONATE, PRESS POLISHED.
PRIOR TO GRINDING AND POLISHING (25°)

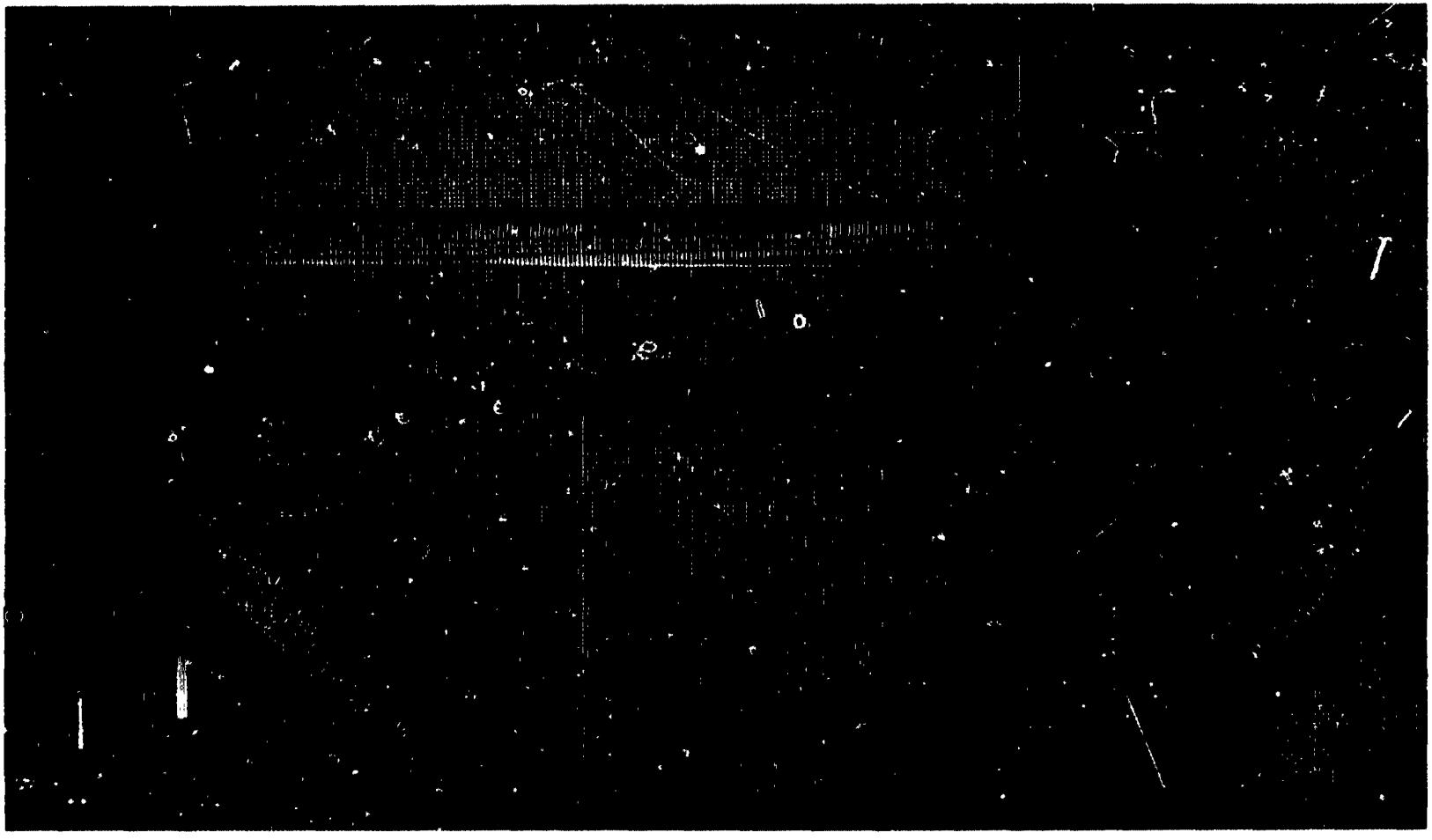


FIGURE 8 - POLYCARBONATE, PRESS POLISHED.
AFTER GRINDING AND POLISHING (25°)

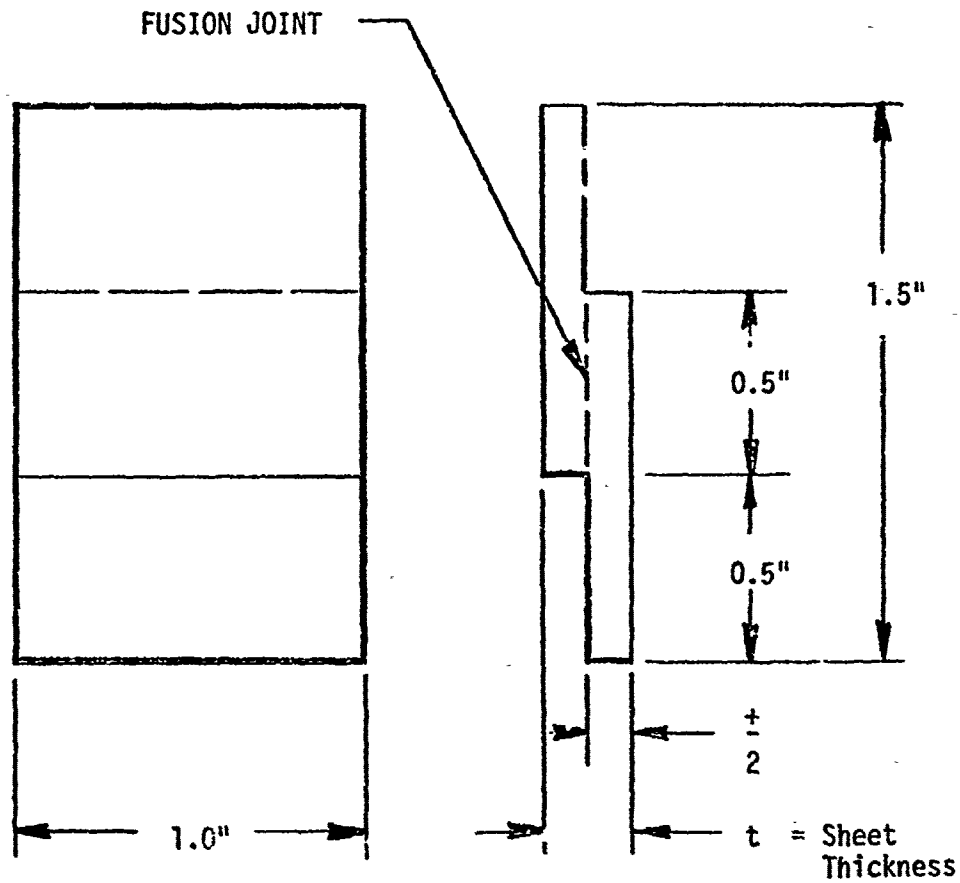


FIGURE 9 - FUSION BOND JOINT TEST SPECIMEN

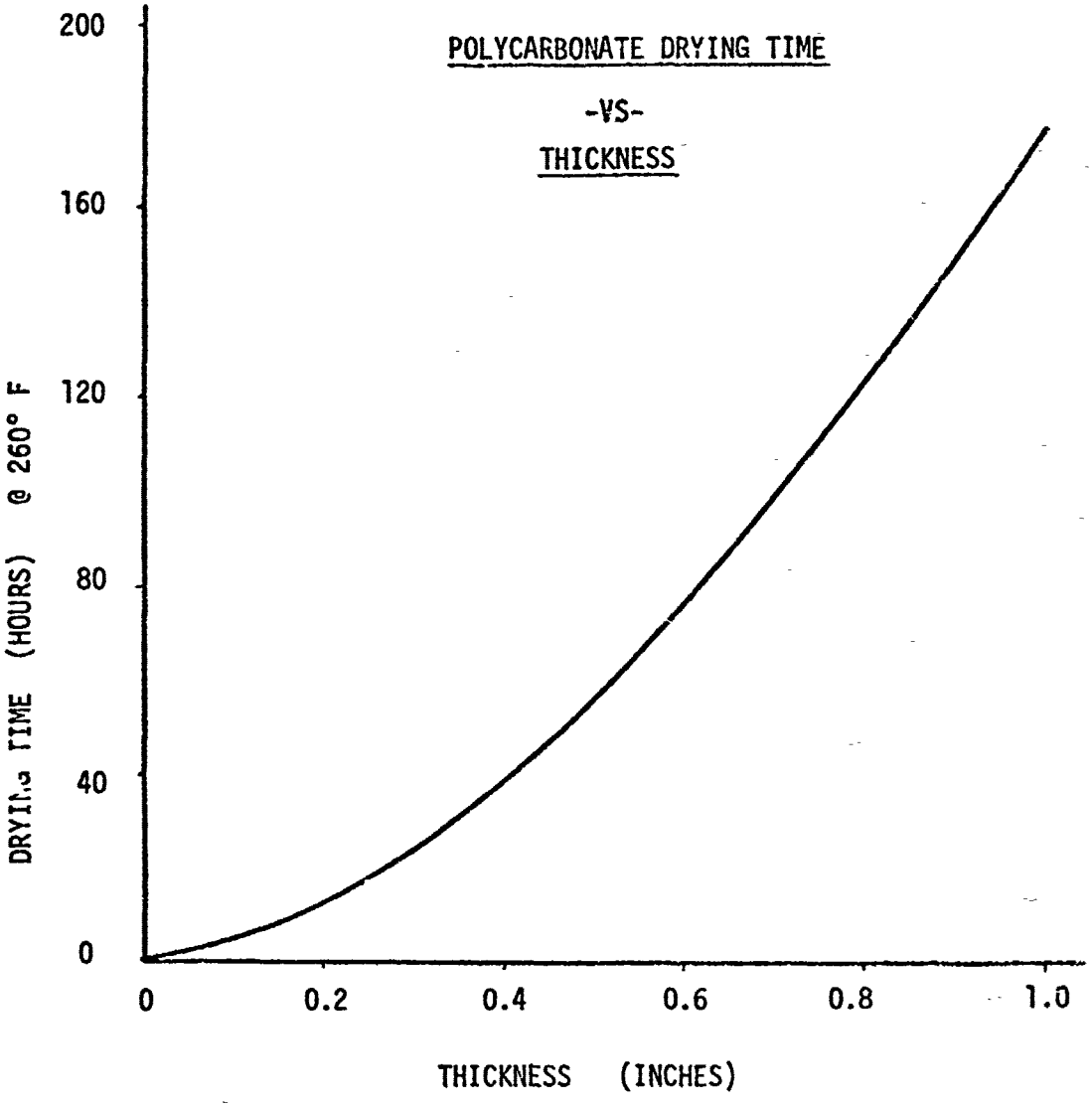


FIGURE 10 - POLYCARBONATE DRYING TIME

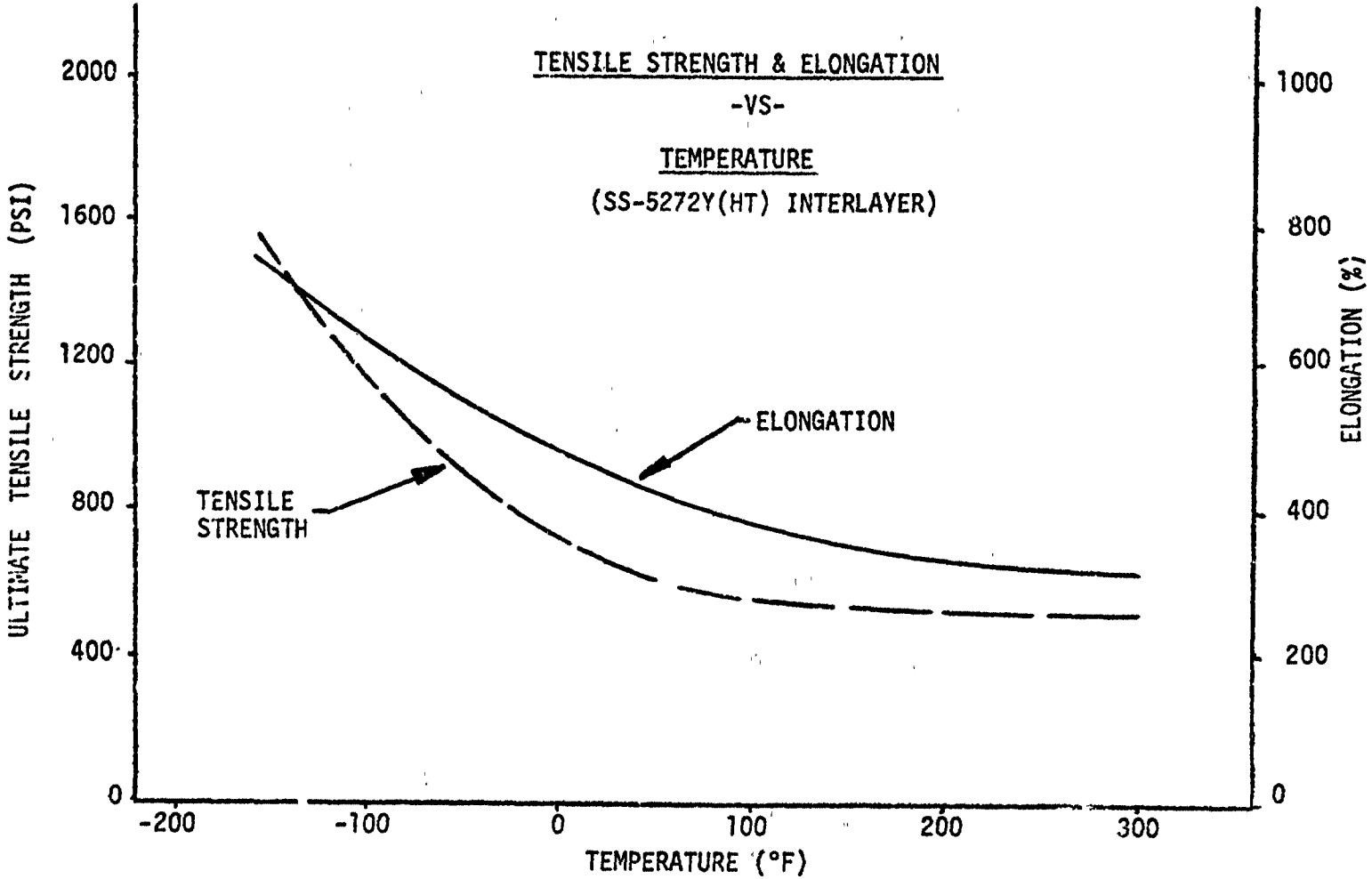


FIGURE 11 - TENSILE STRENGTH AND ELONGATION OF SS-5272Y(HT)

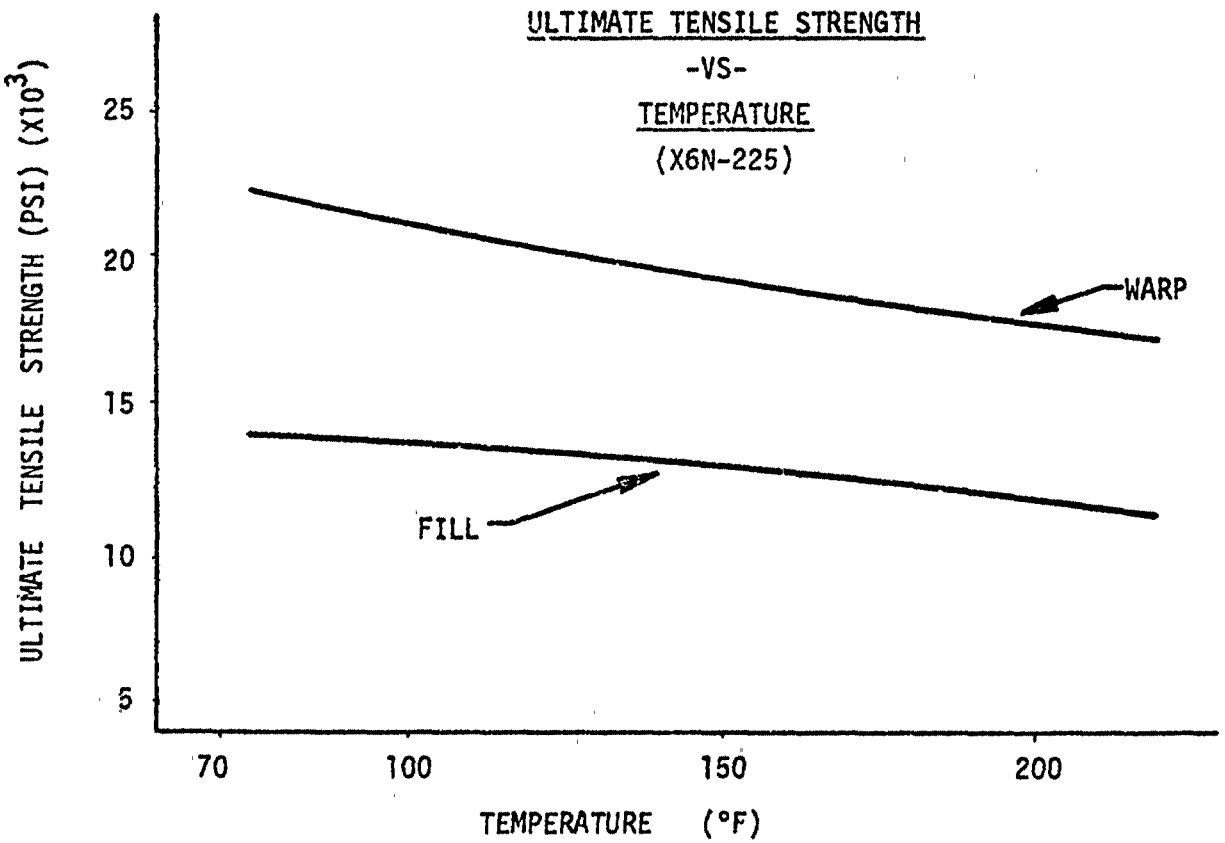


FIGURE 12 - ULTIMATE TENSILE STRENGTH OF X6N-225 EPOXY-NYLON LAMINATE

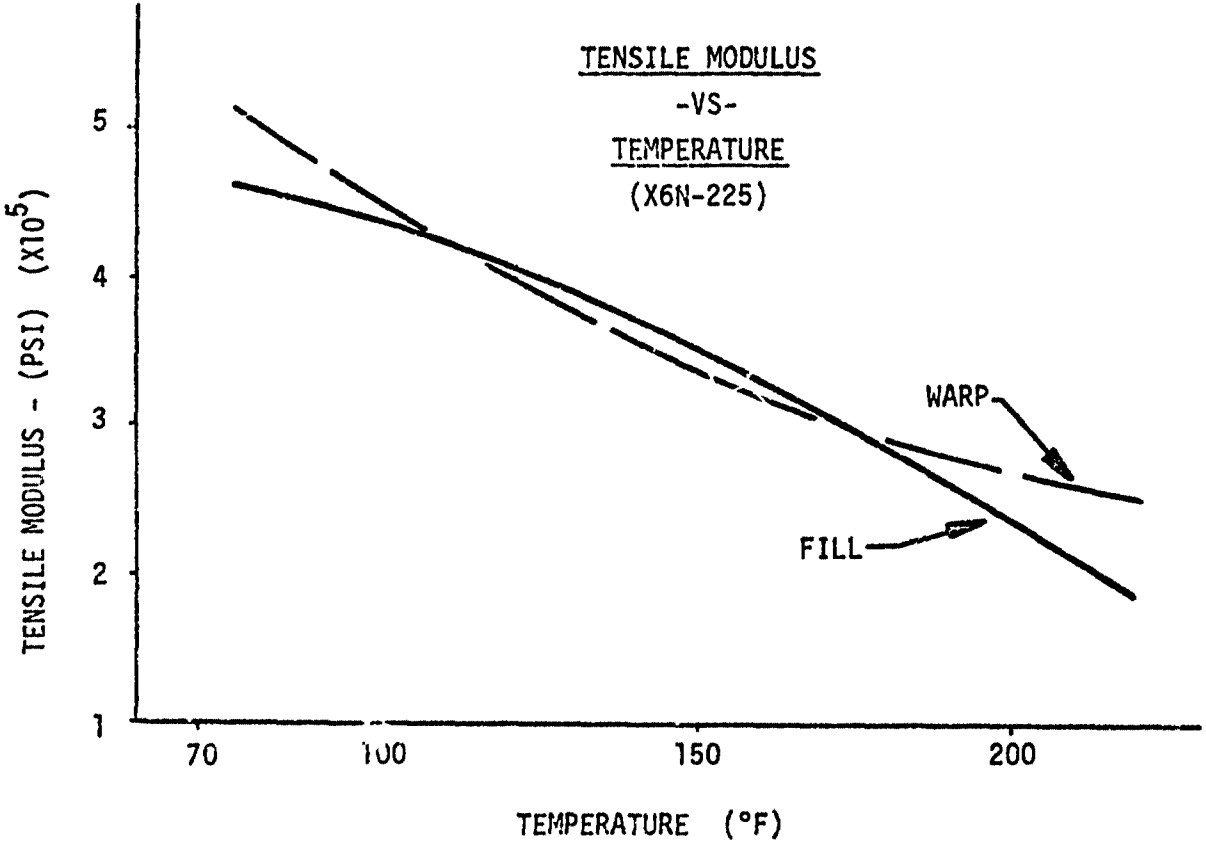


FIGURE 13 - TENSILE MODULUS OF X6N-225 EPOXY-NYLON LAMINATE

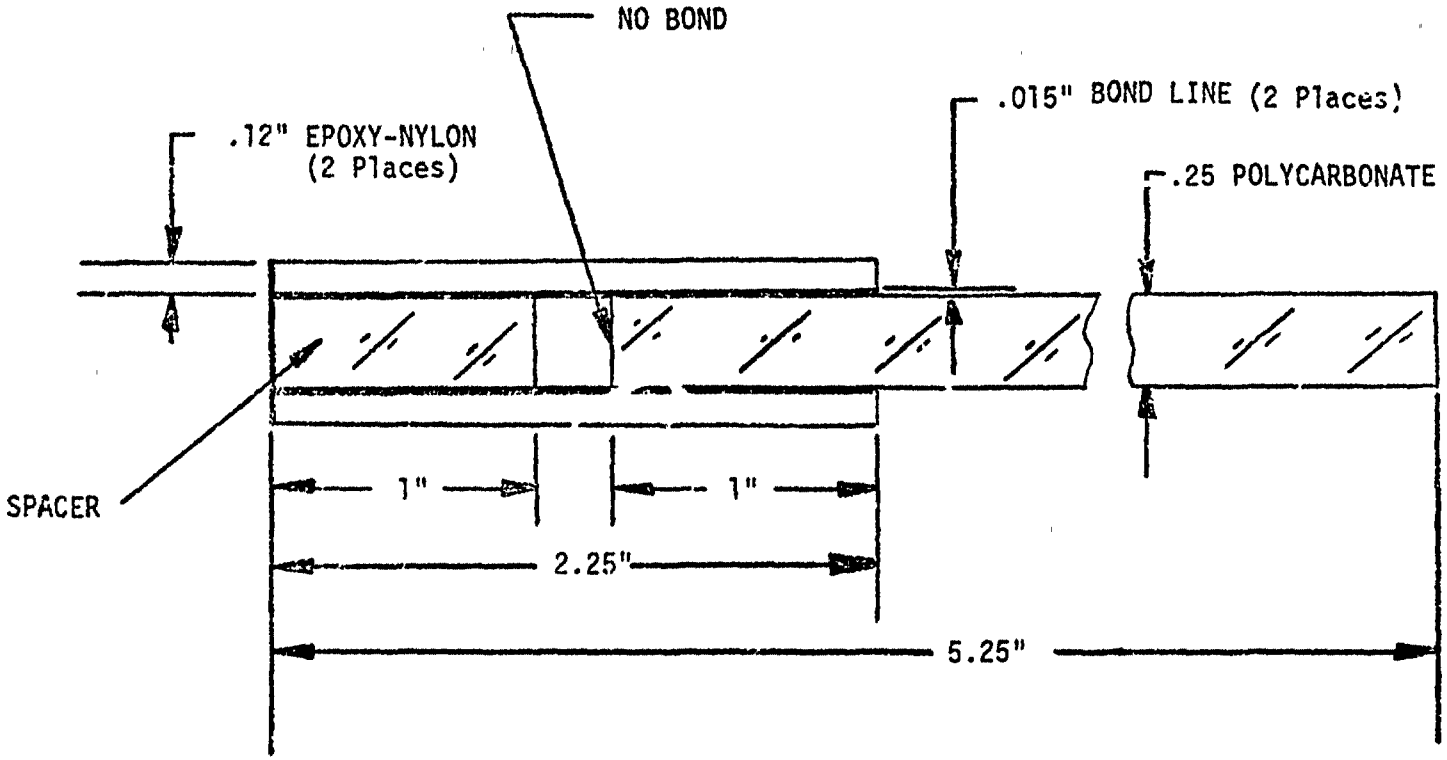


FIGURE 14 - ADHESIVE CONTROL TEST SPECIMEN

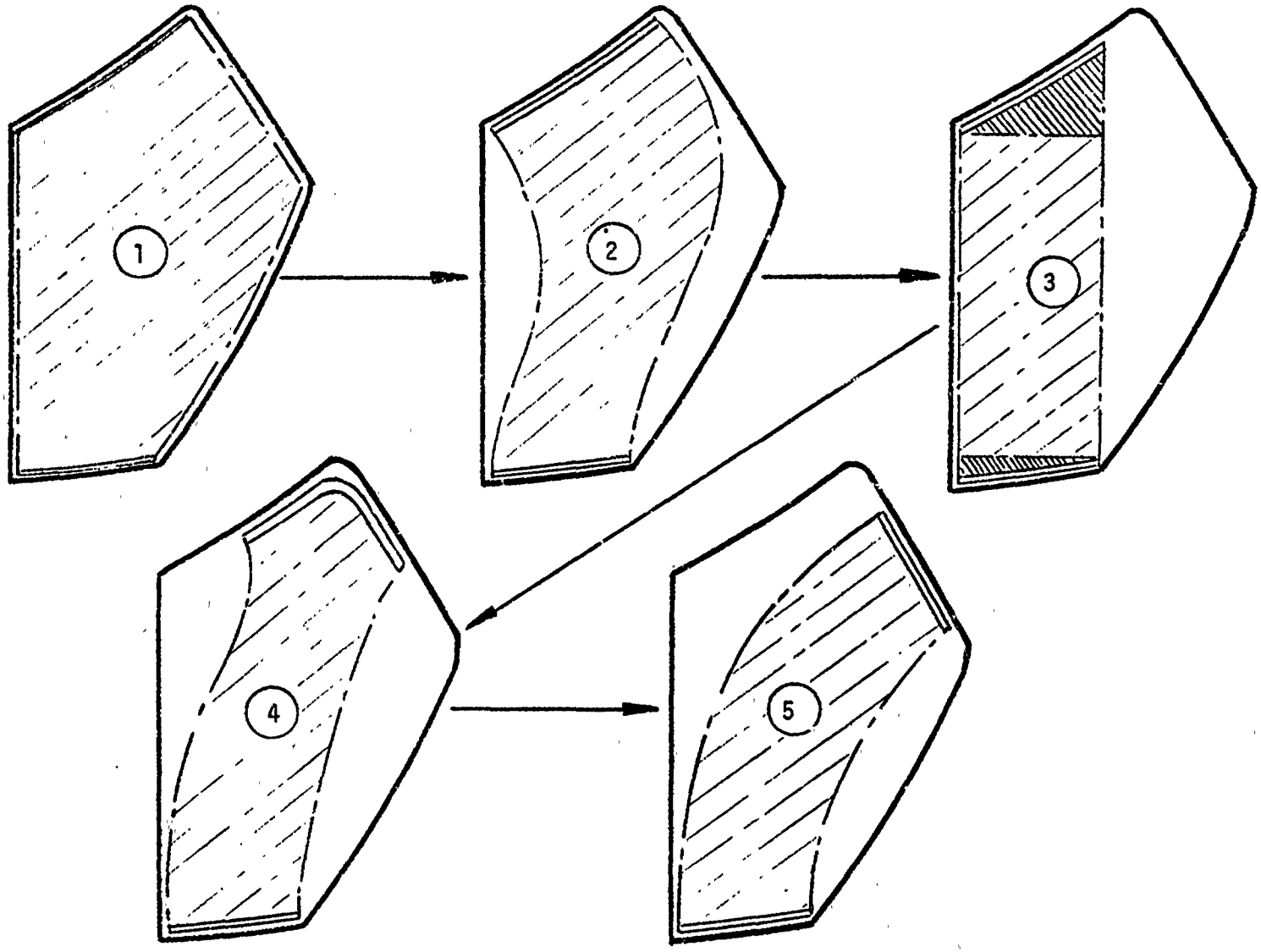


FIGURE 15 - ELECTRICAL CONDUCTIVE COATING CONFIGURATION EVOLUTION

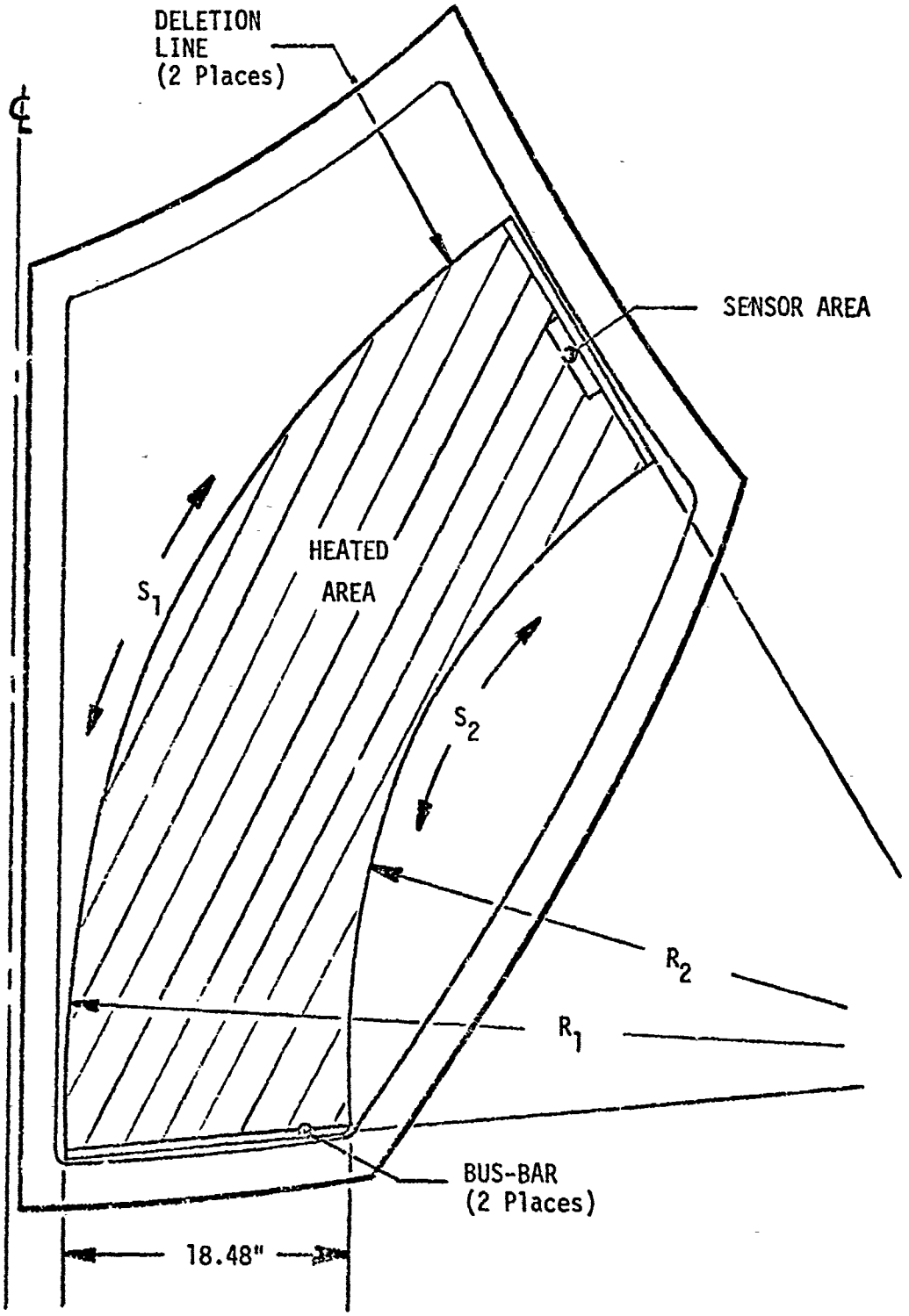


FIGURE 16 - SWING PATTERN COATING CONFIGURATION

GLASS/PLASTIC TRANSPARENT ARMOR FOR HELICOPTERS

W. C. McDonald
Goodyear Aerospace Corporation
Litchfield Park, Arizona

and

G. R. Parsons
Army Materials and Mechanics Research Center
Watertown, Massachusetts

GLASS/PLASTIC TRANSPARENT ARMOR FOR HELICOPTERS

by

Wilson C. McDonald, Goodyear Aerospace Corporation

Gordon R. Parsons, Army Materials and Mechanics Research Center

ABSTRACT

This paper covers a program for the development of scaleup technology to produce contoured transparent glass/plastic armored glazings for the UH-1D helicopter. This work incorporated recent advances in high-performance glass/plastic composite transparent armor technology. Primary emphasis was placed on the design and scaleup required to add a significant level of such protection to a current inventory aircraft. The design and fabrication of direct replacement armored windshields duplicating the UH-1 contour and trim represented a significant advancement in the state-of-the-art. The program achievements clearly represent a milestone in aircrew protection and aircraft survivability. Findings apply to present aircraft, and provide the basis for the most efficient incorporation of transparent armor in the next generation of aircraft.

The work was performed by Goodyear Aerospace for the Army Materials and Mechanics Research Center, Watertown, Massachusetts (contract number DAAG-46-73-C-0075).

I. INTRODUCTION

The helicopter is playing an increasingly important role in modern warfare. Expanded combat area mission requirements such as search, rescue, attack, and other close proximity missions have exposed the helicopter to greater levels of hostile fire than previously experienced. Although opaque armor has been added to protect some vital components and crew seat assemblies, very little has been done to offer protection in the sizable transparent glazings. The standard glazings currently used have virtually no ballistic defeat capability and when penetrated often generate varying levels of injurious spall.

The best solution to maintaining high levels of visibility, while reducing ballistic vulnerability, is the incorporation of transparent armor. Recent advances in the state-of-the-art have made this practical. High-performance glass/plastic composites have been developed which provide ballistic protection at an areal density and thickness significantly lower than prior state-of-the-art laminated glass armor. The glass/plastic composite also eliminates the backside spalling of injurious particles upon ballistic impact. Although the performance of such armor was well documented by laboratory testing, no attempt had been made to design and replace the glazings with armor in an inventory aircraft.

II. TECHNICAL APPROACH

1. GENERAL

Basically, this program was divided into three phases. Phase I included the design of the armor installation as well as ballistic and environmental testing to document performance. Manufacturing drawings and instructions for the armor installation were prepared. Phase II consisted of the fabrication of eight shipsets of the transparent armor and hardware in accordance with the drawings. Phase III effort included environmental testing of three shipsets of the full-scale parts produced during Phase II. One additional shipset of transparent armor was installed in a UH-1H helicopter to verify the design and installation procedures and to allow flight test evaluation. The remaining four shipsets of armor were delivered to the contracting agency, Army Materials and Mechanics Research Center (AMMRC), Watertown, Massachusetts.

2. PHASE I - TRANSPARENT ARMOR DESIGN AND EVALUATION

The Phase I effort included the fabrication of several sizes of flat armor composite test panels for verification of environmental and ballistic properties suited to the proposed usage.

The configuring of the armor installation and the structural analysis were conducted concurrently in Phase I.

A mockup of each armor panel was made and installed in one hand of a UH-1B helicopter fuselage to confirm the feasibility of the design, demonstrate functional features, and assess possible modifications required.

After incorporation of the necessary changes, manufacturing drawings were prepared for the complete UH-1D transparent armor installation.

a. Composite Verification

Flat panels of the armor were fabricated for testing to verify predicted ballistic and environmental performance levels. Ballistic performance is classified and is not discussed herein.

The composite makeup as specified by AMMRC is as follows:

Material	Thickness (in.)
Soda-lime annealed plate glass	0.250
Polyvinyl butyral (PVB) interlayer	0.060
Soda-lime annealed plate glass	0.125
Code F4X-1 cast-in-place (CIP) Goodyear Aerospace proprietary interlayer	0.100
Polycarbonate (ultraviolet stabilized) with Code 701 Goodyear Aerospace proprietary abrasion-resistant coating	0.125

A total of 30 flat 12-inch × 12-inch test panels were fabricated and delivered to AMMRC for ballistic evaluation. Ten flat 36-inch × 36-inch test panels were fabricated for environmental testing. Five flat test panels of reduced size (3 inches × 8 inches) were fabricated to permit ultraviolet stabilization testing in the standard test cabinet. Prior to the environmental tests, the optical properties of each 36-inch × 36-inch panel were measured; results are shown in Table I.

After 240 hours of accelerated ultraviolet testing in accordance with ASTM D1499-64 and G23 procedures, the haze had increased only one percent, while the luminous transmittance remain unchanged.

During the thermal testing, there was no visible change in optics. However, it was discovered that all glass edges had to be reasonably well ground to eliminate edge defects if thermal breakage was to be eliminated. Basically, all panels were cycled to +160 deg F and -65 deg F for 48 hours. For the exact military specification, refer to Table I.

The only test that presented any real problem was the humidity test. During this test, some opacity developed in the panels. Testing to MIL-STD-810B calls for 240 hours of exposure with up to 95-percent relative humidity and 160-deg F temperatures. This cycle is known to be very hard on many plastics and coatings. The polycarbonate backing on the armor panels is a hygroscopic material which permits the passage of moisture. This in turn can affect interlayers, primer coatings, and abrasion-resistant coatings.

When the panels were subjected to a constant 160 deg F and 35-percent relative humidity, it was found that the haze remained low (approximately 2 percent) and the luminous transmittance stayed in the 85-percent range. Field testing to date has not disclosed any serious problems.

b. Structural Criteria Study

The structural criteria study included defining potential structural attachment areas, maximum loadings imposed on armor attachments and the fuselage structure, structural adequacy of attachments and structure, and the effect of added armor weight on basic aircraft weight and balance.

In general, this investigation indicated that the armor attachments and fuselage structure were adequate for the intended use.

TABLE I - ENVIRONMENTAL TEST DATA, *UH-1D GLASS/PLASTIC*

36-INCH × 36-INCH FLAT COMPOSITE VERIFICATION PANELS

Panel no.	Test type	MIL-STD-810B		Luminous transmittance (percent average)		Haze (percent average)		Optical deviation (minutes)	
		Method no.	Procedure no.	Original	After test	Original	After test	Original	After test
1	Low temperature	502	1	81.9	82.0	1.00	0.90	1.02	0.90
2	Low temperature	502	1	82.1	82.1	1.06	0.90	0.60	0.60
5	High temperature	501	1	81.8	81.5	1.30	1.10	2.04	1.98
6	High temperature	501	1	81.2	81.9	1.13	0.90	1.32	1.74
7	Thermal shock	503	1	81.4	81.7	0.97	1.00	0.02	-
8	Thermal shock	503	1	81.9	81.9	0.98	1.00	0.01	-
9	Humidity	507	1	81.6	74.8[a]	1.03	42.50[a]	0.60	-
10	Humidity	507	1	81.7	76.3[b]	1.03	46.40[b]	1.02	-

[a]Values measured after drying 16 hours at 120 deg F were as follows: luminous transmittance, 81.8 percent; haze, 2.5 percent.

[b]Values measured after drying approximately 30 days at ambient temperature were as follows: luminous transmittance, 81.6 percent; haze, 2.4 percent.

Running concurrently with this effort was the design of armor panels configured to provide the maximum protection possible within the limitations of operational constraints, mission profile, and added weight.

The windshield and crew door armor protection was accomplished with composite panels of the same shape and size as the standard UH-1D glazings. The highly double-contoured shape of the standard lower cabin window does not lend itself to duplication with the laminated armor construction.

Several combinations of internally mounted flat and single curvature panels were evaluated to add protection in this area. The major considerations which influenced the fitting of armor panels in the lower cabin windows included:

1. Optics - Visibility through the lower cabin windows is particularly important during landing operations. To maintain the best possible optics, plane surfaces and low-angle-of-incidence viewing were sought for the armor panel installation. Minimization of distracting framing or attachments encroaching upon the viewing area was also important.

2. Every effort was made to maximize the use of flat armor panels and thus provide the lowest-cost armor installation possible.

3. Operational clearances - Provision had to be made for adequate clearance between the armor panels and the various aircraft components extending into the lower cabin window area. Specific components requiring attention were as follows:

    a. Lower cabin window glazing
    b. Rudder pedal assembly
    c. Foot rests
    d. Communicator
    e. Electrical cables
    f. Instrument air lines.

4. Operational maintenance - Several aspects of operational maintenance had to be considered when adding the armor installation in the lower cabin window area. One aspect related to the routine maintenance, adjustments, and replacement actions required on the

components of the unmodified UH-1D aircraft. Consideration was also required for similar functions applicable to the armor installation.

It became apparent that a removable armor panel would be needed on each of these left- and right-hand lower window installations. Access is necessary for periodic cleaning of the standard glazing interior surface and the transparent armor, as well as for routine maintenance of aircraft components located in the lower cabin window area. Access is likewise necessary to daily install and remove sensitive gear when operating in a combat area.

c. Fabrication of Mockup Windows

Upon completion of the initial design, a mockup of all armor panels and installation hardware was prepared for one hand of the aircraft. The mockup was used to confirm the feasibility of the armor addition, demonstrate functional features, and provide means for assessing possible modifications. Several changes were incorporated as a result of working with the mockup installation.

d. Ballistic Verification Tests

A series of physical tests was conducted on typical configurations with bonded armor attachments. The results of these tests using tension, peel, and torsional loading modes were used to support the analysis effort in the structural criteria study.

Ballistically induced loads imposed on the bonded attachments are complex and difficult to calculate. It was therefore necessary to verify the ballistic performance by test firing armor panels supported by typical bonded brackets and clips. A similar situation existed in the retention of the sliding crew door armor panel under ballistic impact. This panel is supported along both vertical edges by engagement of the outboard 1/4-inch-thick ply of glass in a U-channel structure.

The armor composite used in these panels duplicated the ply configuration of the UH-1D requirement. The bonded attachment ballistic test panels were mounted by bolting each attachment to rigid structure. The panels simulating the sliding crew door were mounted for test firing by full length engagement in a supported U-channel along both vertically oriented sides.

Each test panel was subjected to from one to four impacts of caliber .30 ball M2 projectiles. Maximum energy transfer was thus imparted to the test panels and attachments.

These tests indicate that both the bonded attachments and glass engagement of the U-channel on the sliding crew door armor panel should withstand ballistic impact loads at the design threat level. Projectile strikes within 1-3/4 inches of the center of bonded attachments did not disrupt the bond to the panel. The glass fracture resulted in a softening of the local support; however, the other three attachments were unaffected. Panel retention after withstanding such close-proximity hits at three of the four attachments remained secure.

Projectile strikes within two inches of the unsupported edges of the sliding crew door panels resulted in local fracture of the glass ply engaging the channel. The fractured glass was retained in place and continued to support the panel. Much of this glass was lost after the panel was removed from the support channels. Test panel number 4 withstood three impacts, one in the center and two near one edge, without leaving the support. The actual crew door sliding windows have 27.0 inches of vertical edge support. This is nearly twice that of the ballistic test articles and provides additional undamaged glass in the channels for support.

e. Drawings

After completion of the mockup review and incorporation of the design modifications, manufacturing drawings were prepared in accordance with MIL-D-1000, Category A.

f. Installation Instructions

Detailed instructions were written for the transparent armor installation. These instructions, when used in conjunction with the installation drawings, supplied the information needed to modify the UH-1D aircraft and to install the armor panels.

3. PHASE II - PROTOTYPE GLASS/PLASTIC LAMINATE FABRICATION

a. General

The Phase II effort encompassed the fabrication of eight shipsets of transparent armor for the UH-1D aircraft. The armor manufactured in accordance with the drawings prepared in Phase I was complete with all framing and attachments necessary for installation. One shipset of armor is shown in Figure 1.

Good tooling is required to form the plastic backing ply and support the glass and plastic components during the interlayer processing. Very little variance in glass contour can be accommodated by the forming and casting tools when flyable optics are required in the composite windshield. The degree of reproducibility attainable in the glass contour thus significantly affects the economic feasibility of quantity production by dictating the tooling requirements.

Dimensional variations in the windshield glass required the fabrication of special tools for each piece of glass to ensure that all components were properly matched.

With quantity production and improvement in the glass forming processing, good part-to-part contour control can be achieved.

The flat panels were processed in the usual manner without difficulty.

b. Mar Resistance

The glass/plastic composite armor used in the UH-1D program incorporates a polycarbonate plastic backing ply. The unique toughness and ductility exhibited by polycarbonate significantly contribute to the ballistic efficiency and nonspalling characteristics of the armor system.

Unfortunately, polycarbonate has a number of adverse characteristics, including low abrasion and chemical resistance. An abrasion-resistant coating was applied to the exposed backside surface of the material to protect the polycarbonate in the rigorous and potentially degrading environment of military helicopters.

4. PHASE III - ENVIRONMENTAL TESTING

During Phase III, one shipset of armor was installed in a UH-1H helicopter at the U.S. Army Proving Ground (YPG), Laguna Field, Yuma, Arizona. Environmental testing of full-scale armor panels was also repeated.

a. Windshield Installation

The standard windshields were removed intact and were suitable for reinstallation upon completion of the armor evaluation. Both the left- and right-hand armored windshields fit the structure contour well. No difficulty was encountered in marking,

drilling, or trimming the windshields. The installation went as planned, and the only modification required was relocation of the free air temperature gauge and slight modification of the windshield wiper arms (see Figure 2).

b. Crew Door Installation

The doors were modified and the transparent armor panels installed at the Goodyear Aerospace plant in accordance with the installation instructions. The armor added to each door included a flat sliding window and a flat triangular fixed window as shown in Figure 3.

The modified crew doors were then easily installed on the test aircraft.

c. Lower Forward Installation

The installation of the transparent armor in the lower forward cabin window includes three flat panels, two fixed and one removable, on each side. These panels are mounted internally within the confines of the standard glazing, which is retained. The armor was installed in accordance with the installation instructions. The outboard rudder pedals were slightly modified by grinding a small amount of metal off one edge to permit proper clearance when the pedals were in the fully extended position. It was observed that some appreciable dimensional variations from ship to ship and model to model do exist which can somewhat slow the installation (see Figure 4).

After completion of the armor installation, the test aircraft was weighed to determine the new basic weight and center of gravity. The effect of the transparent armor installation on the test aircraft was calculated in accordance with the Army Aviation Maintenance Engineering Manual, Weight and Balance, TM55-405-9.

It was determined that the installation had increased the basic aircraft weight by 193 pounds (5428 pounds to 5621 pounds). The center of gravity (CG) of the basic aircraft was moved forward from station 144 to station 141. Allowable CG limits for takeoff are 134 to 144 and 131 to 144 for landing.

d. Flight Test Evaluation

The set of transparent armor installed and flown at the U.S. Army Proving Ground, Yuma, Arizona, was tested from December 1974 through June 1975. To minimize

expense, the helicopter with the special glazings was used in support of other missions. The total flight time accumulated on the transparent armor was 44 hours, which included 5 hours of flight during inclement weather conditions at locations other than Yuma. Flights were made in light, medium, and heavy rain; and were made in daytime under instrument flight rules, including approaching through clouds to breakout. For each flight made, the pilot filled out an aircraft flight test and evaluation report on the glass/plastic armor. He was requested to comment on the glazings in level flight, hover, takeoff, and landing. Comments on operation of controls, aircraft flight characteristics, and maintainability were also made.

Since each pilot was requested to report critically on the armor installation, the comments varied considerably, as could be expected.

Nearly all agreed that the flight characteristics of the aircraft near the forward CG limit were undesirable. They suggested that the battery be moved aft to correct the problem. This is often done to compensate for other gear and did correct the nose-heavy effect.

Slight distortion around the outer edge of the windshield was commented on by most pilots but was not considered to be a serious problem in flight.

Some glare from the lower cabin panels during flight over water was reported.

The sliding window in the door broke once when the door was slammed shut. This problem was corrected by extending the window guides further down into the door.

Several pilots stated that when ice formed on the lower half of the windshield, the defrosters were not as effective as on the thinner acrylic windshield.

Nearly all pilots interviewed stated they would want the transparent armor on their aircraft in combat. The more each pilot flew the aircraft, the more complimentary he became.

III. SUMMARY

Glass/plastic transparent armor offers the unique combination of improved ballistic defeat characteristics and low areal density necessary for aircraft usage. The armor is capable of projectile or fragment defeat without backside spalling of injurious

particles and can be manufactured for numerous threat levels at an areal density which permits a significant amount of coverage within allowable weight limits. This performance can be offered in direct replacement panels or parasitic panels placed behind existing glazings. The program achievements demonstrate how aircrew protection and aircraft survivability can be substantially increased.

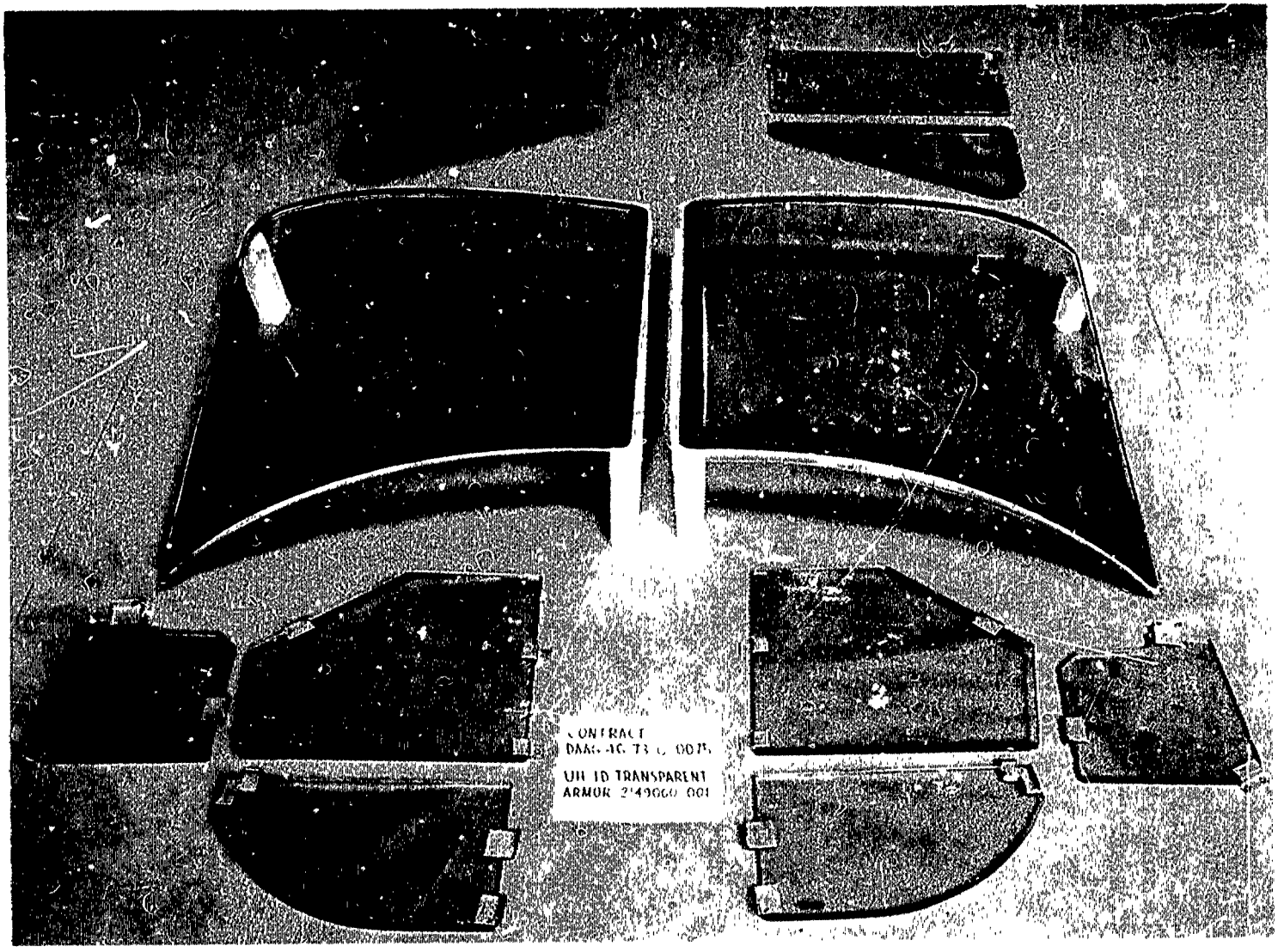


Figure 1 - Display of UH-1D Transparent Armor

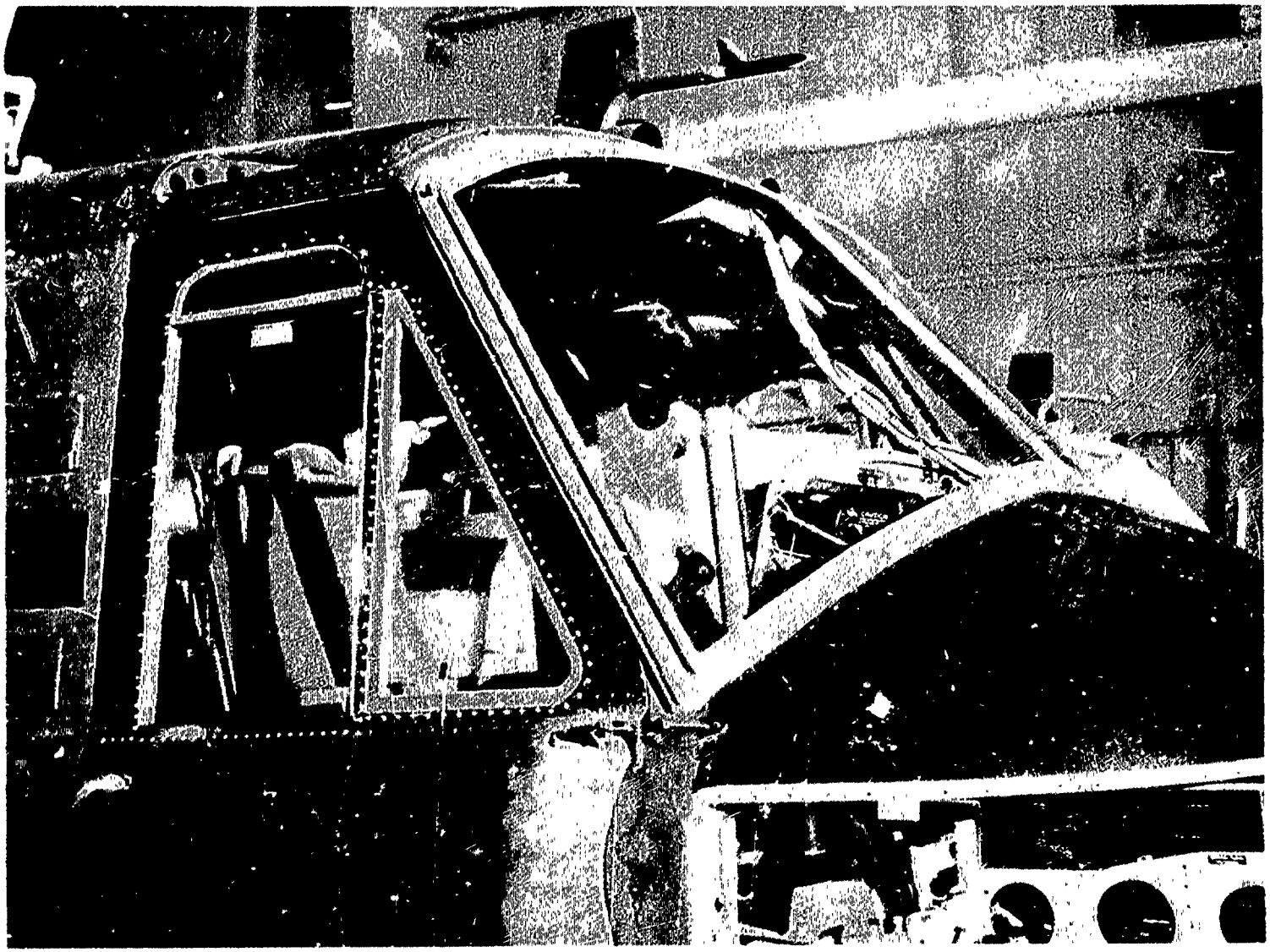


Figure 2 - UH-1D Windshield and Cabin Door



Figure 3 - UH-1D Cabin Door Transparent Armor

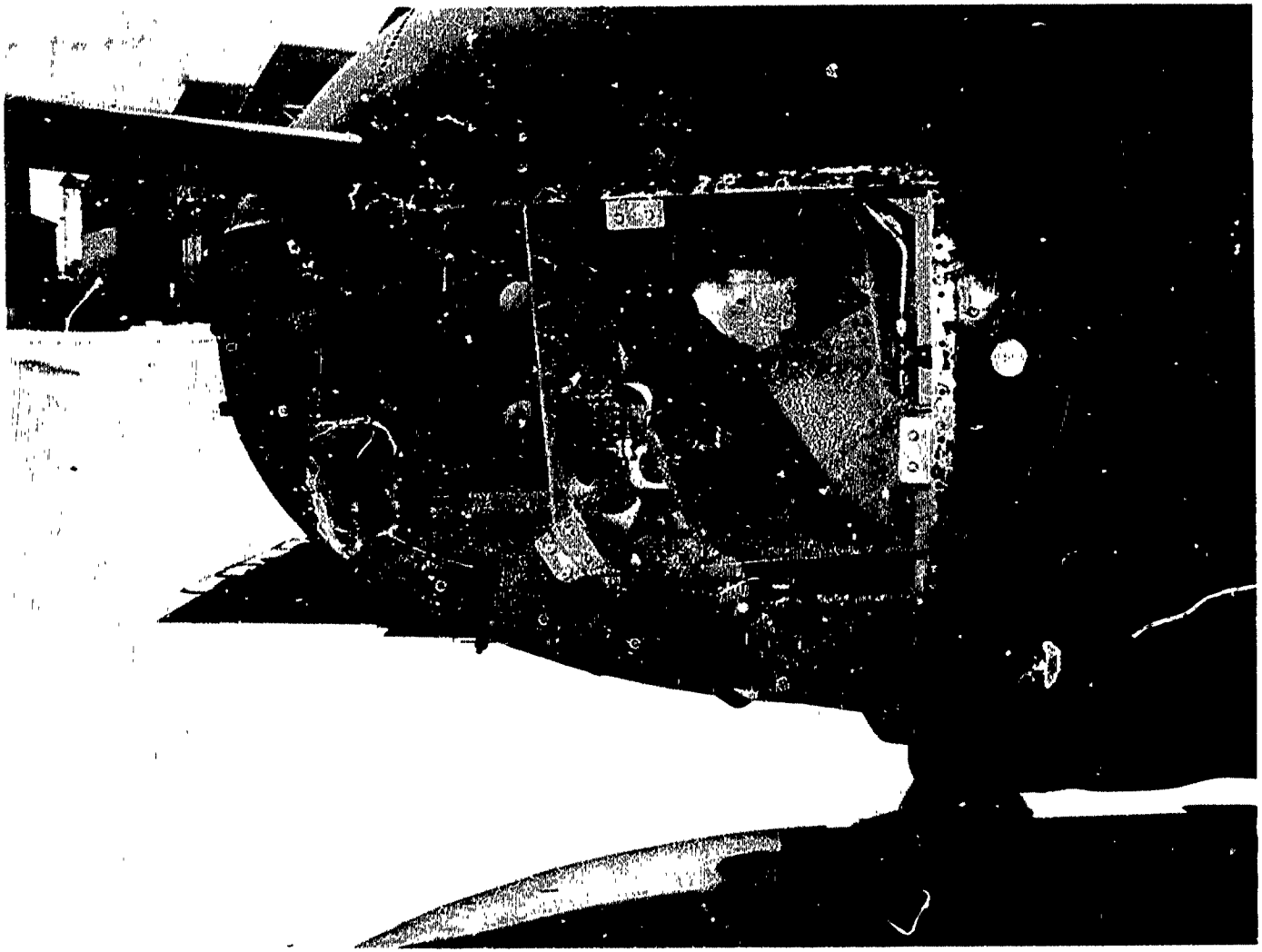


Figure 4 - UH-1D Lower Cabin Window

STRESS-SOLVENT CRAZING OF CAST ACRYLIC

J. H. Large
Brunel University
Department of Mechanical Engineering
Uxbridge, Middlesex, England

and

K. B. Armstrong
British Airways
Overseas Division
Hounslow, Middlesex, England

PRECEDING PAGE BLANK-NOT FILMED

Abstract

Crazing of stretched and cast acrylics used within airframe structures has been emphasized with the higher altitude operation of current aircraft. Premature failure of cabin window panes during service operation, especially of cast acrylics is associated with panes exhibiting advanced crazing.

A three-dimensional structural analysis of aircraft (BAC VC10) cabin inner window pane was completed with the use of an advanced finite element and membrane computer program. The successful operation of the program yielded a detailed structural analysis of the pane under consideration in terms of deflection, principal and shear stresses. It is concluded that the particular pane geometry performs in the manner expected for a hybrid membrane-plate structure.

Experimental investigation was able to relate the incidence of crazing of test coupons subjected to various levels of stress only and also of samples subjected to stress and contamination with commonly used solvents of acrylic. Threshold values of crazing are related to stress, solvent and temperature parameters, and a relationship between craze depth and stress level for various solvents and temperatures is indicated.

Review of Past Work

Recent experimental work on the structure and properties of crazes and the relation between craze formation and material failure is well documented[1], together with the characteristics of crazes in transparent, glassy, isotropic polymers, such as polymethyl methacrylates or acrylic, there is a wealth of knowledge[2]. Yet the understanding of the phenomena is far from complete and there exists considerable confusion in the identification of a single and isolated reason to account for the initial formation of crazing, subsequent craze propagation and the role of crazing in the deterioration of material properties.

Acrylic may fail either by crazing or cracking, in either case the mode of failure is brittle[3,4]. Crazing differs from cracking, not necessarily in geometric form but in that the craze void comprises a region infilled with micropores enclosed by drawn polymer in a fibrillar form[5]. Typically the craze voids consist of 50% micropores by volume[6], with the major micropore dimension of 200 to 300Å. In contrast, a crack represents a separation of the material, bringing two distinct planes across a void which is not bridged with polymer material.

John H. Large,
School of Engineering,
Department of Mechanical Engineering,
Brunel University,
Uxbridge, Middlesex,
England

K. B. Armstrong
Development Engineer,
British Airways,
Londong (Heathrow) Airport,
Hounslow,
Middlesex, England

Since the opposing walls of the craze are bridged by material the stress distribution of the area surrounding the craze will be markedly different from that of a crack. It cannot be assumed that the stress normal to the craze wall is zero as in the case of a free boundary crack, since the craze infill contains stress transmission paths across its thickness. In the generalized case of acrylic material partially severed by a craze palne, the proportion of load transmitted across the plane may lie between zero, as for a crack, and the value appropriate for the homogeneous solid if, for the latter the craze is fully load bearing.

Craze formation occurs in polymethyl methacrylate materials exposed to hostile atmospheres which are solvent laden, particularly with alcohol[7], and crazing rate, that is the time interval between exposure to solvents and the establishment of crazing, is promoted by additional environmental factors such as temperature and humidity. Fresh micropores form at the tip of the craze void after the material is solvated by solvent to its equilibrium swelling condition for a particular craze depth. It is suggested that cavitation at the craze tip promotes solvent flow into the craze[6] although, conversely, it may be argued that cavitation occurs after solvent penetration to the tip[8] which is rapid by stress-assisted sorption.

Whatever the mechanism of solvent penetration, the transmission of solvent to the craze tip is governed by fluid flow parameters of which viscosity is a significant factor. In laboratory trials craze formation may be considerably accelerated by addition of suitable viscosity reducing agents such as ethylene glycol which alone is a poor crazing agent of polymethyl methacrylate. The addition of such agents accelerates crazing but does not substantially modify the nature of the craze. Mixtures of ethylene glycol/methanol of varying strength, and similarly with ethyl alcohol, applied to coupons of cast acrylic suggest that methanol and alcohol respectively continue to act as the main crazing agent[9].

Acrylics will also craze when subjected to uniaxial tensile stress in atmospheres which are apparently free of harmful agents. Crazing thus formed has a similar geometry to cracks but contains the characteristic polymer infill and with the plane of the craze at right-angles to the uniaxial stress axis. Typically the length of the craze is very much greater than its thickness. Uniaxially stressed coupons of acrylic subjected to solvent contamination either by immersion, coating or by contact within a gaseous atmosphere, craze at an accelerated rate with the onset of crazing occuring at considerably reduced stress levels. For example, uncontaminated coupons were found to craze at the uniaxial stress threshold of 45.3 $10^6 N/M^2$ compared with similar but contaminated coupons at the lower thresholds of: methyl methacrylate monomer 4.5 $10^6 N/M^2$, iso-propyl alcohol 5.8 $10^6 N/M^2$, ethyl alcohol $5.10^6 N/M^2$, and n-hexane 15 $10^6 N/M^2$. Further, ambient temperature variation contributed significantly to both oneset and depth of crazing, particularly for alcohol[9] - similar results arise from variation of relative humidity which is consistent with previous experimental trial[7].

The elastic properties of uncrazed and crazed acrylic indicates a corresponding deterioration resulting from the presence of crazing. Solvent-free crazed acrylic exhibits a lower elastic modulus than that for uncrazed acrylic, and coupons crazed by stress-solvent action, at considerably lower stress threshold levels as outlined previously but of a comparable craze depth, perform at a markedly lower elastic modulus reducing by approximately 30% of the uncrazed modulus, compared with 11% reduction for stress-crazing alone[10]. Unfortunately the comparison between stress crazed and stress-solvent crazed acrylic is unreliable because of difficulties in the quantitative assessment of craze surface density and, to a lesser extent, depth of craze. However, distinction is made between the fracture modes for uncrazed acrylic and similar coupons of stress-solvent and stress-crazed acrylic. Stress-solvent fracture surfaces suggest a brittle failure mechanism and, in contrast, the fragmented and rough fracture surfaces of uncrazed coupons are not consistent with brittle failure[11].

In fracture mechanics there is little to differentiate between a craze and a crack. If a craze is capable of transmitting load its existence indicates a stress-field perturbation present at the tip. Accordingly there exists a localized stress maximum on the craze axis at the tip, otherwise the transformation of formerly homogeneous polymer material to a void bridged with craze micropores would not occur there. Therefore, there are similarities in the stress distribution in the vicinity of the tips of crazes and cracks. The elastic properties of the material occupying the craze void serves to reduce the stress concentration phenomena that occurs in a crack of similar geometry. The action of solvents is to establish the tip of the craze as a solvent plasticized region, although this does not necessarily imply that a crack is an essential prerequisite of a craze. More likely, crazes which have been infused with solvent but which have dried, with a subsequent deterioration of elastic properties, develop rapidly under further strain into a geometry more likened to a pre-boundary crack than a deeper craze.

Airframe Acrylic Transparencies - VC10 Cabin Enclosure

In reality the physical environment of service cast acrylic[14] transparencies suggests a complexity of craze promoting agents and conditions. Indeed, deterioration of the mechanical properties of acrylic transparencies, particularly those enclosures located within airframes, accompanied by areas of severe crazing is not uncommon. Failure of cast acrylic cabins inner window panes during service operation, although of low incidence, is both undesirable and unpredictable.

The inner window is subjected to uniform pressure loading, arising from service cabin differentials of up to 0.65 bar, which produce complex tensile stress distributions on the outer face. The void separating inner and outer window panes is continually evacuated during service by a desiccator system. Solvent contamination of the inner pane outer

face during service is improbable, although it is possible for solvents from the cabin tc be drawn into the window pane void at cruising altitudes. The solvent contamination that occurs most likely originates from routine inter-flight cleansing and programmed maintenance work. Solvents accumulating within the airframe during servicing are evacuated from the cabin and surrounds during the first take-off phase producing climatic conditions within the window vodid conductive to short-term condensation of air-borne solvents onto the outer face of the inner pane, which is subjected to increasing stress levels, and on the inner face of the outer pane, which is essentially unstressed.

Thus the origins of crazing of aircraft transparencies may be quite complex; there exists a variety of solvents in common use during operation maintenance, airframe overhaul and routine inter-flight cleaninsing[12], airframe temperatures may vary between stand-down in the tropics (37°C) to operational cruising at altitude (-48°C), although it is unlikely that the inner pane is subjected to the latter extreme; and the cabin pressure differential loading provides complex tensile stress distributions on the outer face of the inner window pane.

Nature of the Inner Pane Stress Distribution

The inner window pane acts, when subjected to the uniform cabin pressure differential of 0.65 bar (9.5LBf/in^2), as a hybrid plate/membrane structure. Simple plate analysis[16] yields unrealistic values of maximum bending stress σ and deflection z for a flat elliptical plate, both occuring at the plate centre,

$$\sigma = 560 \text{ bar } (8100 \text{ LBf/in}^2)$$
$$z = 48 \text{ mm } (1.89 \text{ in})$$

Analysis of a curved window pane, acting as part of an infintiely long cylinder[17], yields a maximum membrane stress

$$\sigma = 178 \text{ bar } (2580 \text{ LFf/in}^2)$$

which compares favorably with previous experimental trial

$$\sigma = 156 \text{ bar } (2293 \text{ LBf/in}^2)$$
$$z = 11.84 \text{ mm } (0.466 \text{ in})$$

For computer analysis one quarter of the symmetric inner pane was represented by a composite griddage of bending and membrane elements. Inner pane edge conditions, that is where the pane is uniformly pressure clamped against the reveal, is of the form of simple prop supports at each peripheral node. Nodes 4, 8 and 12 being rotationally restrained about the y axis; and nodes 15, 17 and 18 restrained about the x axis. Further rotational restraint applied to the major axis about the x axis and to the minor axis about the y axis, in order to maintain deflection symmetry.

Displacements of the peripheral nodes, that is sliding displacement in the plane of the pane, were prohibited by additional restraints acting in x, y and z axis, although rotation about these axis was unrestrained.

The refined computer simulation yields stress distribution data for the inner pane at each nodal point, with centrepoint stress and deflection data compatible with previous experimental trail

	Z = 11.84 mm (0.465in)	Ref. (13)
Centre point deflection	Z = 10.1 mm (0.397in)	Computed
Centre point stress	σ = 163 bar (2396 LBf/in^2)	Ref. (13)
	σ = 149 bar (2190 LBf/in^2)	Computed

Mode of Failure

The magnitude of the uniaxial stress field present in the inner pane is insufficient to promote failure of the pane as a pressure containing shell. Inner panes that have failed during service operations have been subjected to uniform pressure loading consistent with the analysis, and all have clearly exhibited crazing to a lesser or greater extent.

Experimental trials [10] indicated a marked difference in the deterioration of elastic modulus for acrylics with stress-solvent crazing and stress crazing alone. It is possible that cleansing, servicing and routine flight operations provide conditions which promote solvent infusion and subsequent drying, thereby producing the existence of the craze-crack geometry discussed previously. As a result coplanar crack and craze co-exist, with the craze matter some distance ahead of the craze tip. The stress distribution surrounding the crack-craze may be represented by an equivalent bullet-shaped crack[19] but with a proportion of uniaxial stress being transmitted by the craze matter but, also, accompanied by a sharp stress peturbation at the tip.

A typical stress concentration factor of between 4 and 5 acting at the tip could promote conditions of a structural failure local to the crack-craze perturbation and, certainly, further stress induced crazing would be likely to occur there.

In the complex service situation several mechanisms that may result in inner pane failure co-exist. The important phenomenon of fatigue and creep have been shown to be active[4]. For the VC10 aircraft operating on overseas Division routes 6000 flying hours approximately represents 4500 hours at full pressure load (maximum stress of 2396 LBf/in^2). This steady load condition may produce material creep resulting in

fine cracking of the acrylic surface. Three possible avenues to inner pane failure may follow:

i) the pane may fail simply by continued creep of acrylic material;

ii) the existence of fine cracks and associated stress perturbations at the locality of the tips may accelerate failure by fatigue, for example, a stress concentration factor of 4 would drastically advance failure by fatigue from what is normally expected, a pane life in excess of airframe life, to an expected life of less than 1000 cycles or 4000 flying hours in addition to the 6000 flying hours previously cited - coinciding with the data of Figure 7.

and or iii) solvent, from the sources previously discussed, may enter the fine cracks produced by creep. Thus the inner pane condition after some service may be conducive to stress-solvent crazing with the accompanying deterioration of acrylic properties, resulting in premature failure of the pane from either the mechanism outlined in ii) or by the simple reduction of the effective strength of the pane.

Conclusions

Crazing of cast acrylic window panes is promoted by combination of three factors: stress, solvent, temperature.

Absolute ethyl alcohol at normal ambient temperature is particularly active in the propagation of crazing.

In-flight service loads of 0.65 bar produce stress magnitudes within the pane that are acceptable for the cast acrylic material. However, attention is drawn to the cautious footnote of the early work of Ref. (2)

> 'The results (from accelerated crazing tests on Plexiglas*) recommend a maximum stress of 900/1000 LBf/in^2 (61/68 bar) if extended outdoor service is expected, since within this limit, Plexiglas retains its original transparency and strength indefinitely.'

The mechanisms of solvent infusion into the craze are diverse. Nevertheless, solvent infused into craze subsequently dries out, the craze develops into a craze-crack geometry with a characteristic high stress perturbation at the tip. Such higher local stress concentrations may promote structural failure of the inner pane and may also accelerate propagation of the craze.

However, the outer pane is not subjected to stress and yet crazing

*cast acrylic

occurs considerably in advance of its neighbouring inner pane. The outer pane crazes for reasons other than creep and or fatigue, and it is suggested that other factors such as ultra-violet light absorption and water/solvent solution take-up may contribute significantly to the oneset and propagation of crazing. Possible factors contributing to outer pane crazing are discussed in Appendix I

Appendix I

Little is known on the effect of absorption of ultra-violet and infra-red light frequencies on the physical properties of polymethyl methacrylate materials.

Although difficult to quanitatively verify, incidence of crazing is higher for aircraft flying long-haul Overseas Division routes (British Airways), at a correspondingly high altitude, than for similar aircraft operating on domestic and European routes at lower altitudes. Cast acrylic absorbs much of the higher UV spectrum [15] and the outer pane would act effectively as a filter, thereby protecting the inner pane from this source. Figure 7 gives the historical record of crazing for outer and inner panes of which the crazing rate for the outer panes, which are unstressed, is considerably advanced. Solvent contamination, attack by the atmosphere and other possible hostile contacts have been disregarded for this crude comparison.

Water absorption of the hygroscopic acrylic is well documented, [7] particularly if in solution with common solvents of the acrylic. Certain of the solvents of acrylic are water soluble but have thermal expansion coefficients in their liquid phase of 4 to 6 greater than that of water - Table I.

Water-solvent solutions may be absorbed by the outer pane whilst parked and during the climb phase. The take-up of water-solvent solutions may not be totally rejected during the cruise at high altitude, leaving a proportion of solution within the microstructure of the acrylic. Solution within the microstructure will produce an internal loading of the acrylic related to the relative vapor pressure, or swelling pressure, of the particular water-solvent solution. Thus a possible explanation for the crazing of the notionally unstressed outer panes may be that considerable stress loading is applied from within by the osmotic swelling pressure.

Although little data exists, it may be that UV absorption deteriorates the mechanical properties of the outer layers of the acrylic. If so, the material is less able to withstand osmotic loading and, perhaps, this results in the dense and relatively rapid crazing of the outer pane.

TABLE I Comparative Thermal Expansion Coefficients

LIQUID A	RATIO $^{A}/_{B}$	REMARKS
WATER	1	
ETHYL ALCOHOL	4.35-5.4	SEVERE CRAZING AGENT WS
BENZENE	6	CRAZING AGENT WI
METHYL ALCOHOL	5.8	CRAZING AGENT WS
CARBON TETRA.	6	CRAZING AGENT WI
CLYCOL	2.4	MILD CRAZING AGENT WS

B Thermal Expansion Coefficient for Water

A Thermal Expansion Coefficient for LIQUID A

WS Water Soluble

WI Water Insoluble

REFERENCES

1. Rabinowtiz, S. and Beardmore, P. Critical reviews in Macromolecular Sciences Vol. 1 No. 1 p.1.

2. Bevis, M. and Hull, D. J. Mot.Sc. 5,983 (1970).

3. Hahn, G.T., Hoagland, R. G., Kanninen, M.F., and Rosenfield A.R., Proc. of the INt.Conf. on Dynamic Crack Propagation Lehigh University, 1972.

4. Armstrong, K. BOAC Eng.Report EE-R-71-3(A) 1971.

5. Lambour R.P., and Holik, A.S.J. Polymer Sc. PtA-2, 1393 1969.

6. Marshall G.P., Culver L.E. and Williams J. G. Proc. Roy. Soc. PtA 319, 165, 1970.

7. Blythe, B. and Wright, V. Crazing Tests CHEM 1298 RAE 1957.

8. Andrews, E.H., and Bevan L. Polymer 13, 337 1972.

9. Newton, P. J. and Large J.H. Preliminary Investigations relating to the Crazing of Acrylic Panes. Int. Brunel University 1972.

10. Large J.H. Formation of Crazing in Polymethyl methacrylates int. Brunel University 1973.

11. Taverner, J.B. and Large J.H. Polymethyl Methacrylate Crazing int. Brunel University 1974.

12. B.A.C. Confidential Test Results for the VC10 Cabine Window Pane 1966.

13. B.A.C., VC10 Maintenance Manual 1975. 56-20-0 Cabin Maintenance Practices.

14. Design Recommendations on Organic Transparencies SBAC Tech. Spec. No. 63.

15. Armstrong K. National Physical Laboratories, Empirical Trial of UV Absorption for cast/stretched acrylic - internal, British Airways 1975.

16. Morley J. Strength of Materials, Longmans, 1941.

17. Turner C.E. Introd. to Plate and Shell Theory, Longmans 1968.

18. Murray J. and Hull. Polymer 10, 451 1969.

19. Andres, E.H. Bevan L. Levy G, and Willis J. Solvent and Stress Cracking and Crazing in Polymeric
PT I and II PD/42/022/DM QMC.

20. Hall H. and Russell E. W. Polymethyl Methacrylate (Perspex type) (London) 1973. Plastics Chem. 54 1949.

21. Malik Hussain. Effect of crazing on Physical Properties of Poly (methyl methacrylate) M.Sc. Thesis Loughborough 1972.

22. Menges G. and Schmidt H. Correlation of stress Crazing in Thermoplastics, Plastics and Polymers. Vol. 38 133 1970.

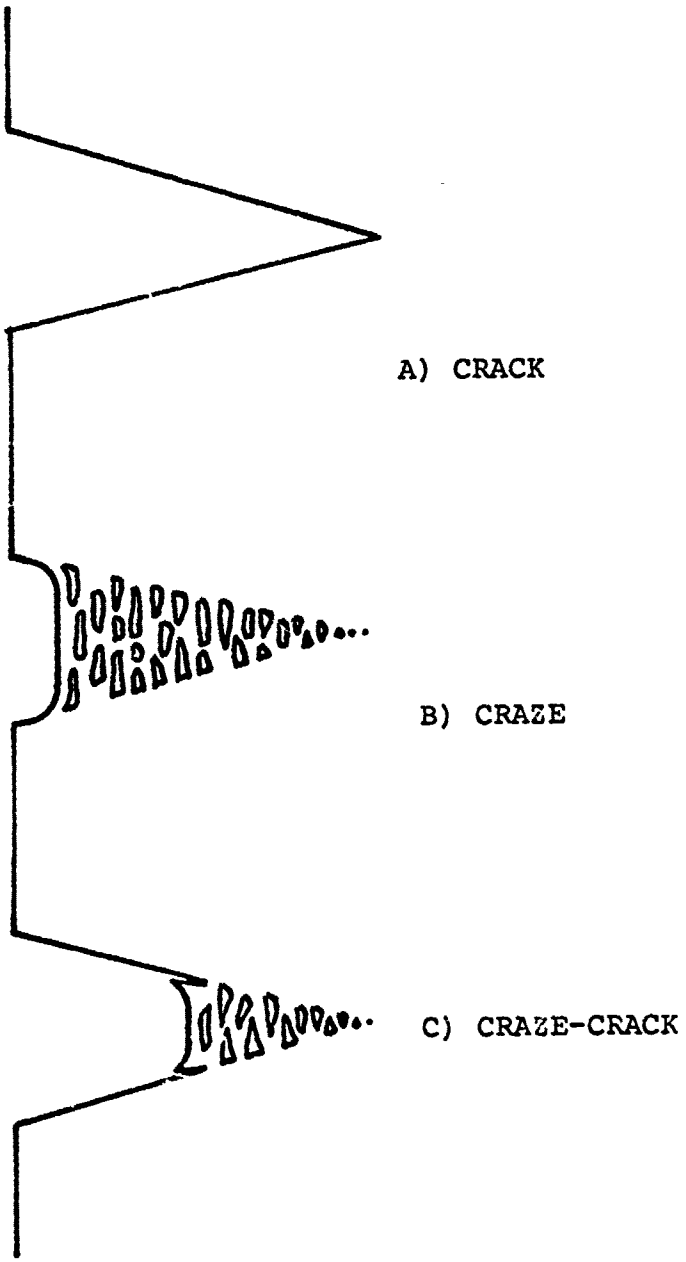


FIGURE 1. CRACK, CRAZE AND CRACK-CRAZE SCHEMATICS

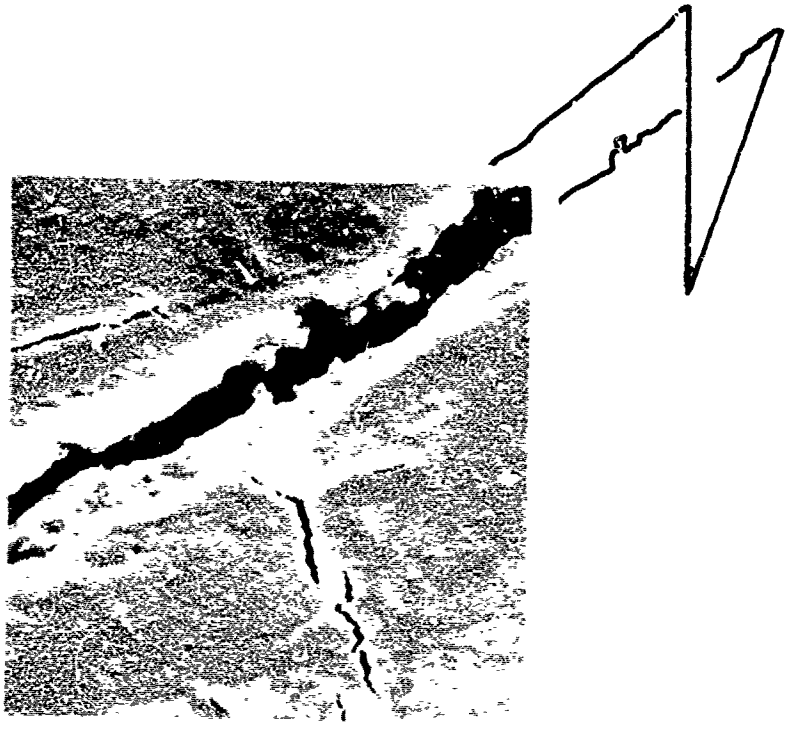
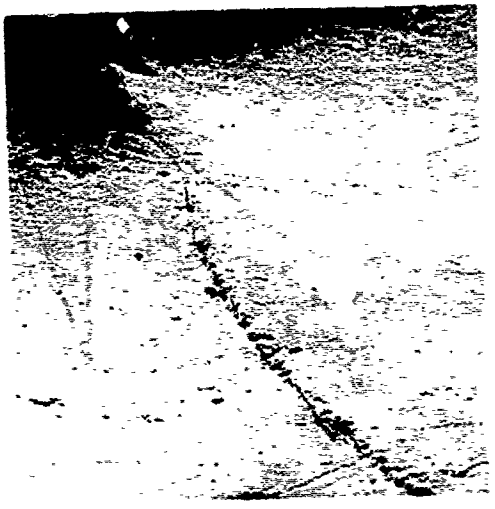
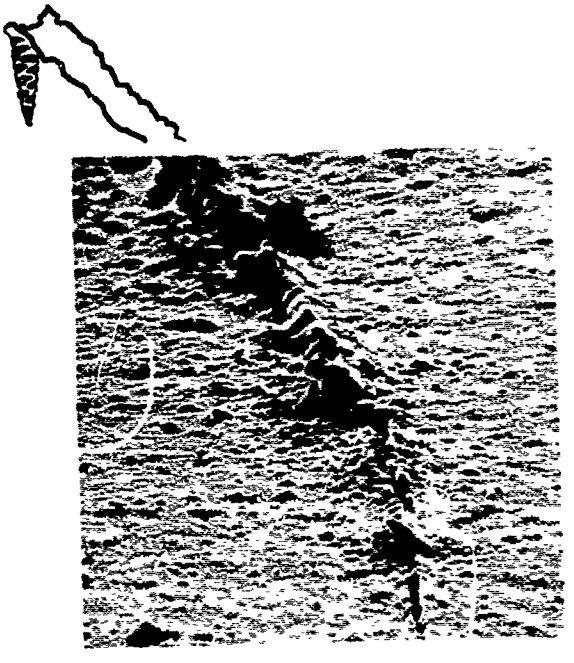


FIGURE 2. CRACK x 8.10^3

ELECTRON MICROGRAPH



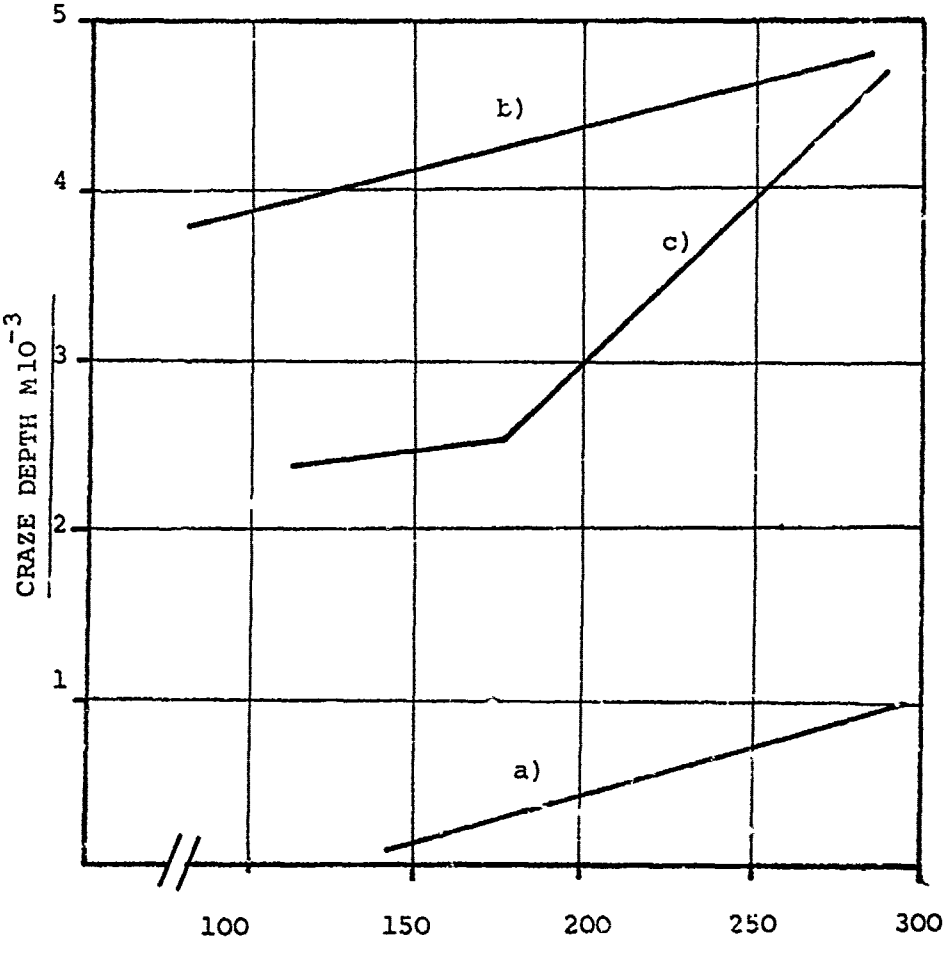
A) CRAZE x 10^3



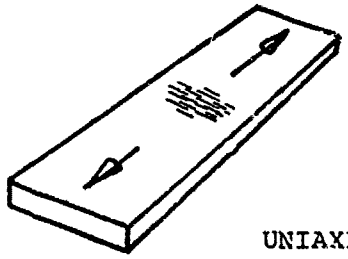
B) CRAZE 10.10^3

FIGURE 3. CRAZE

ELECTRON MICROGRAPH



a) 37°C
b) 20°C
c) -48°C



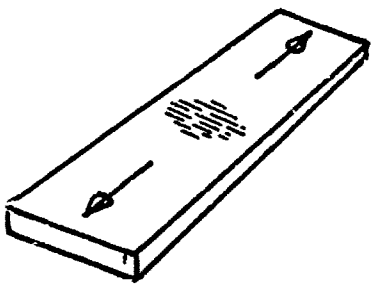
UNIAXIAL STRESS FIELD

FIGURE 4 TEMPERATURE - STRESS ALCOHOL CRAZING[9]

TABLE

$N/M^2 10^6$

SOLVENT	STRESS
UNCONTAMINATED	45.3
METHYL METHACRYLATE MONOMER	4.5
150 PROPYL ALCOHOL	5.8
ETHYL ALCOHOL	5
- HEXANE	15



UNIAXIAL THRESHOLD STRESS

FIGURE 5[9]

CRAZING THRESHOLD STRESS FOR VARIOUS SOLVENT AT 20°C

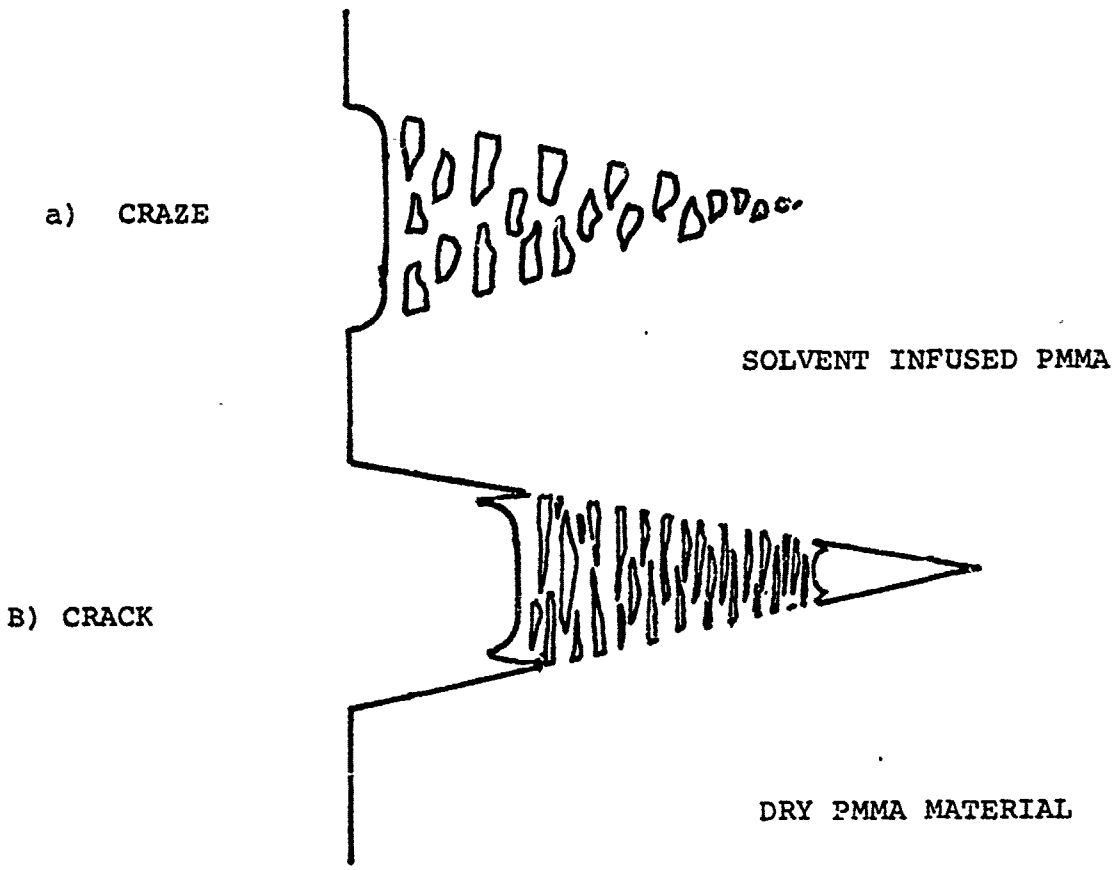


FIGURE 6 CRACK DEVELOPMENT FROM A CRAZE SCHEMATIC

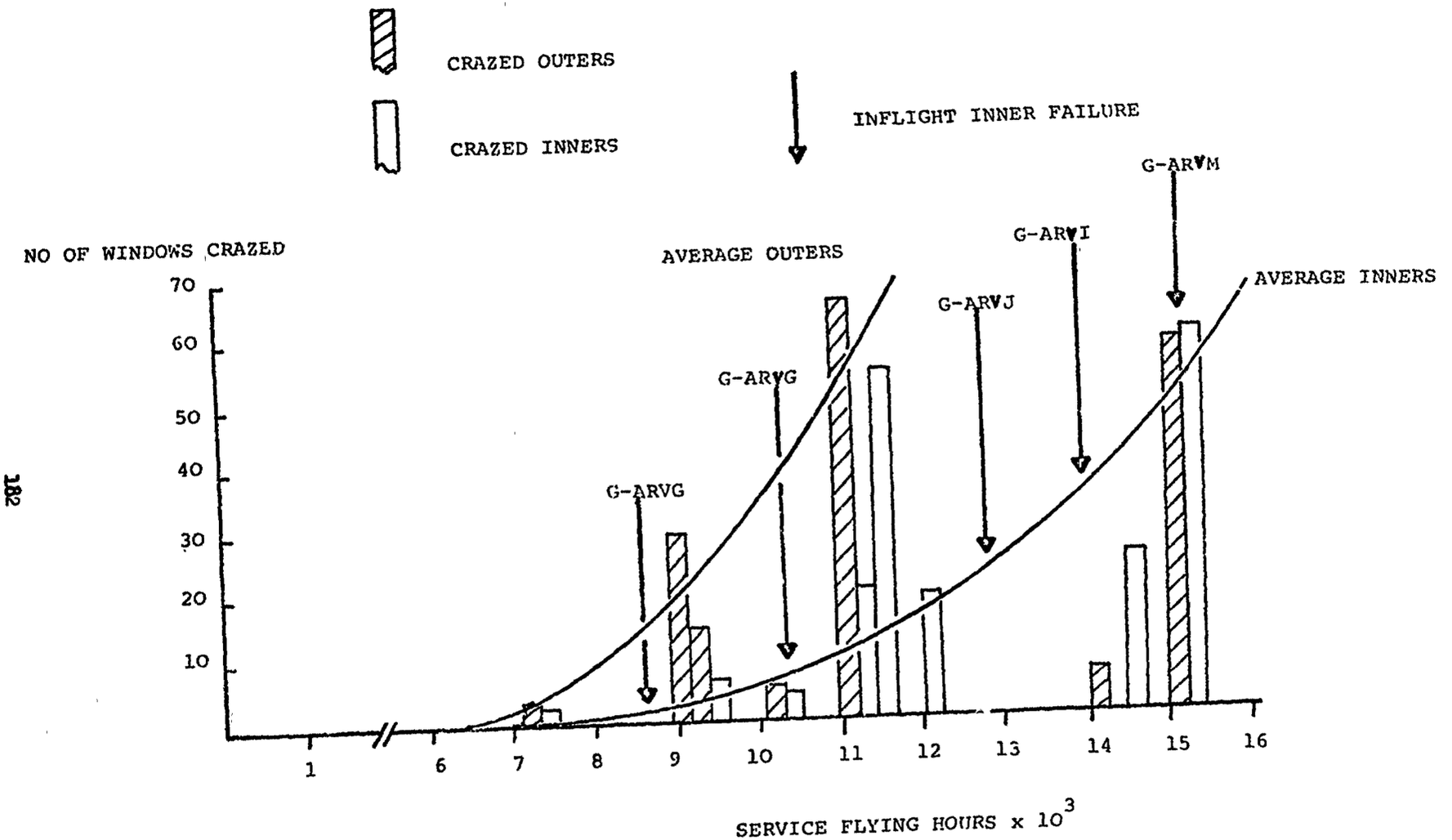


FIGURE 7 RATE OF CRAZING AND FAILURE FOR SERVICE V^{C10} WINDOWS

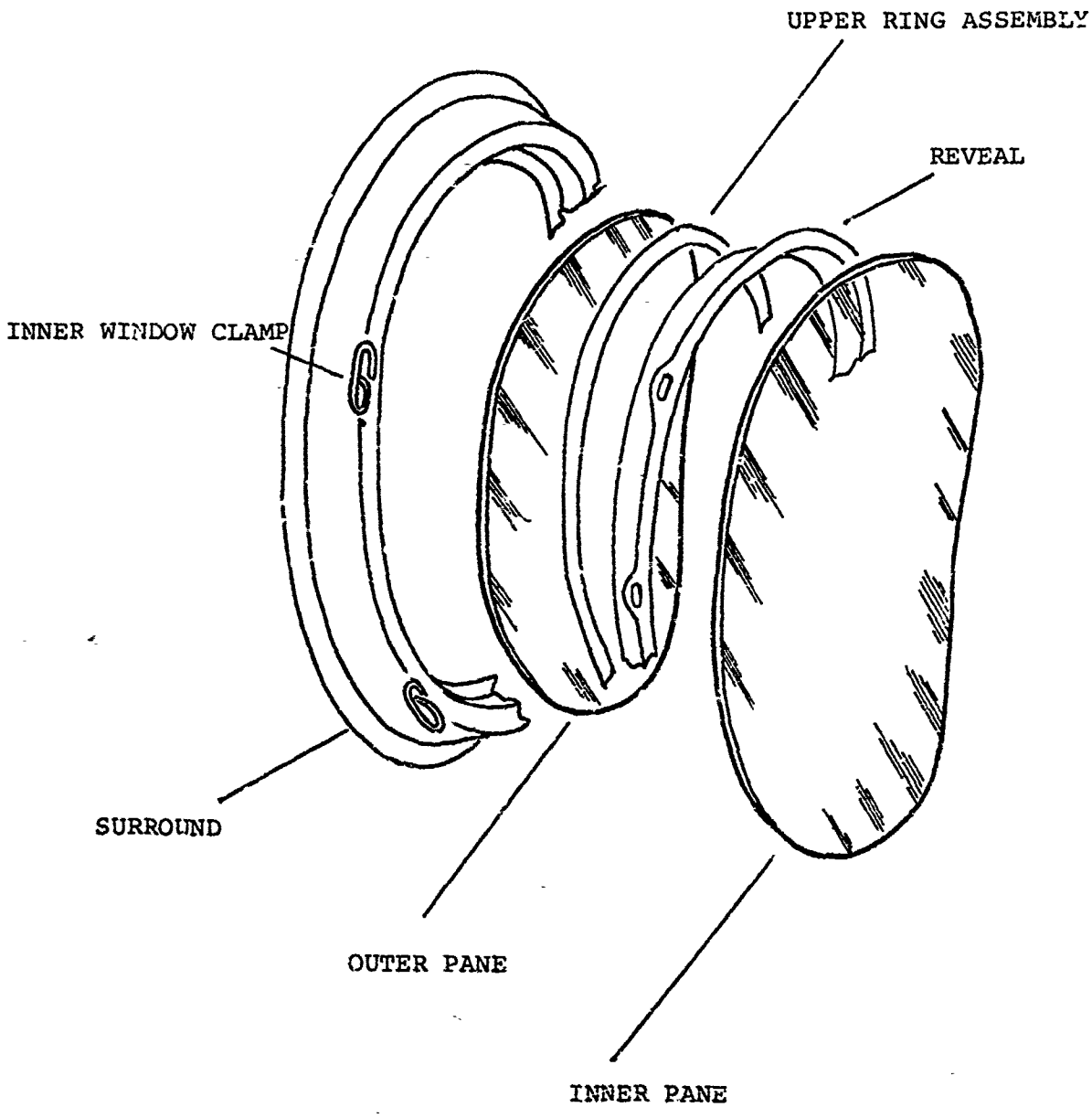


FIGURE 8 CABIN WINDOW PANE ASSEMBLY

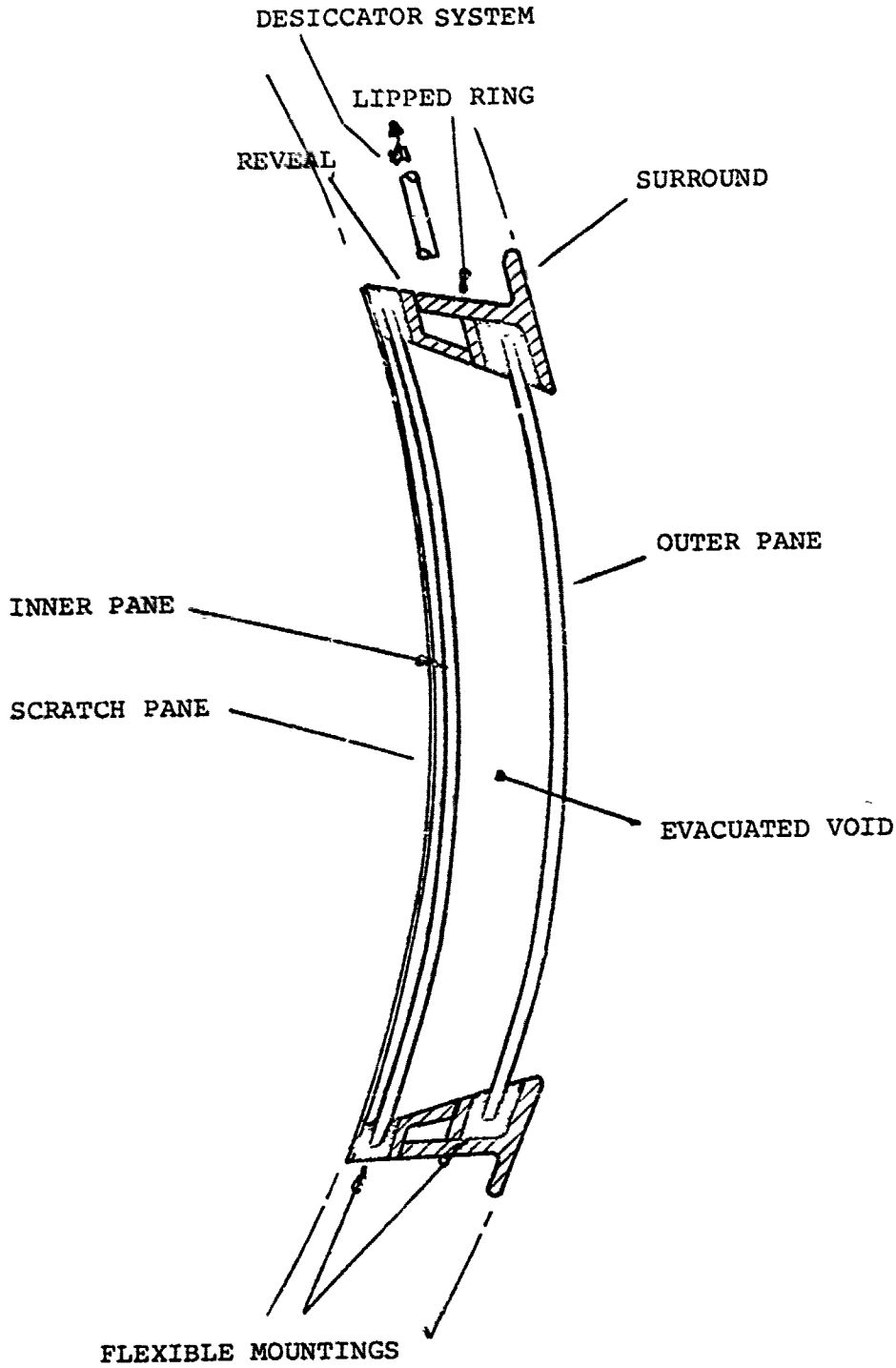


FIGURE 9 CABIN WINDOW PANE ASSEMBLY

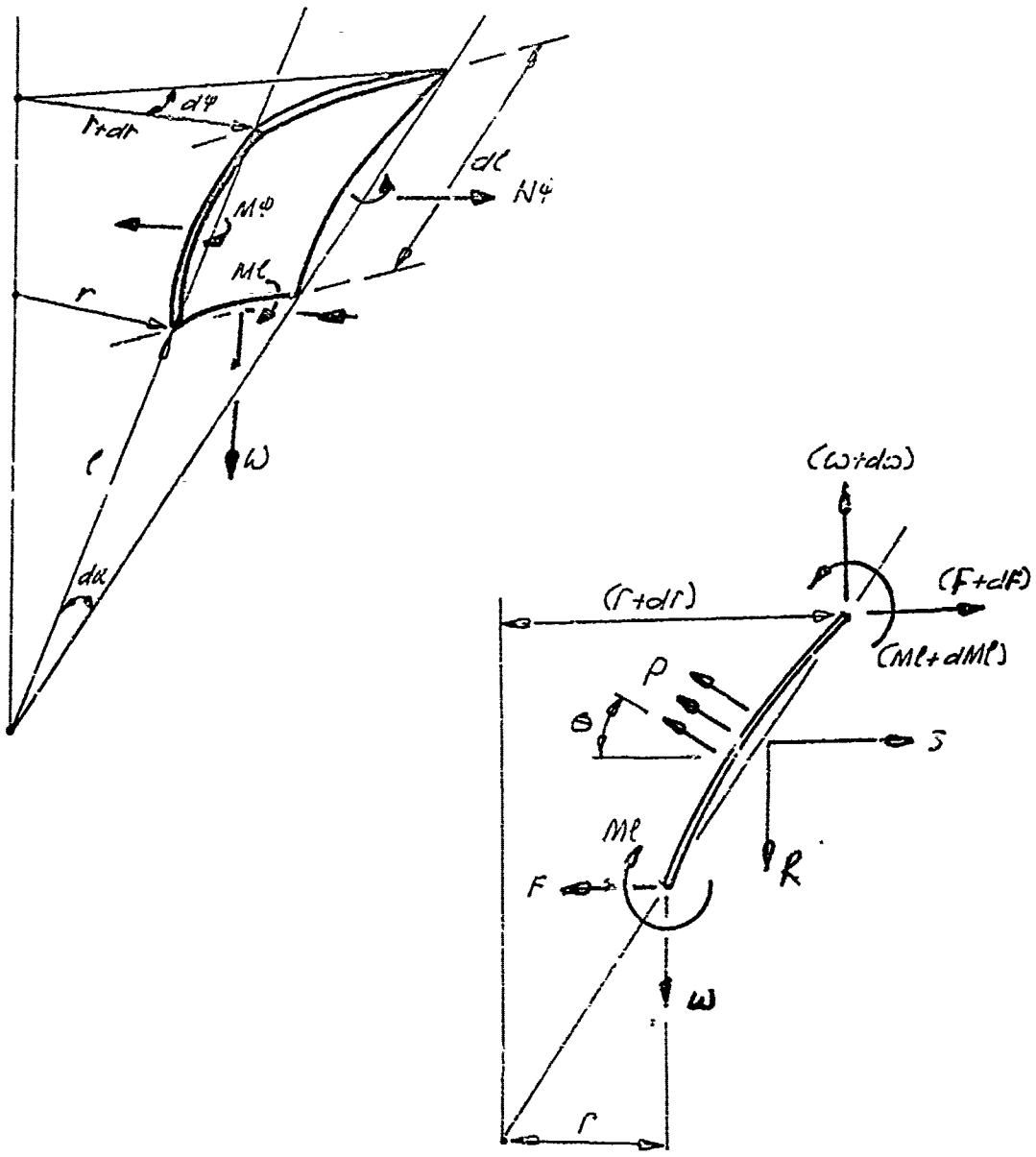
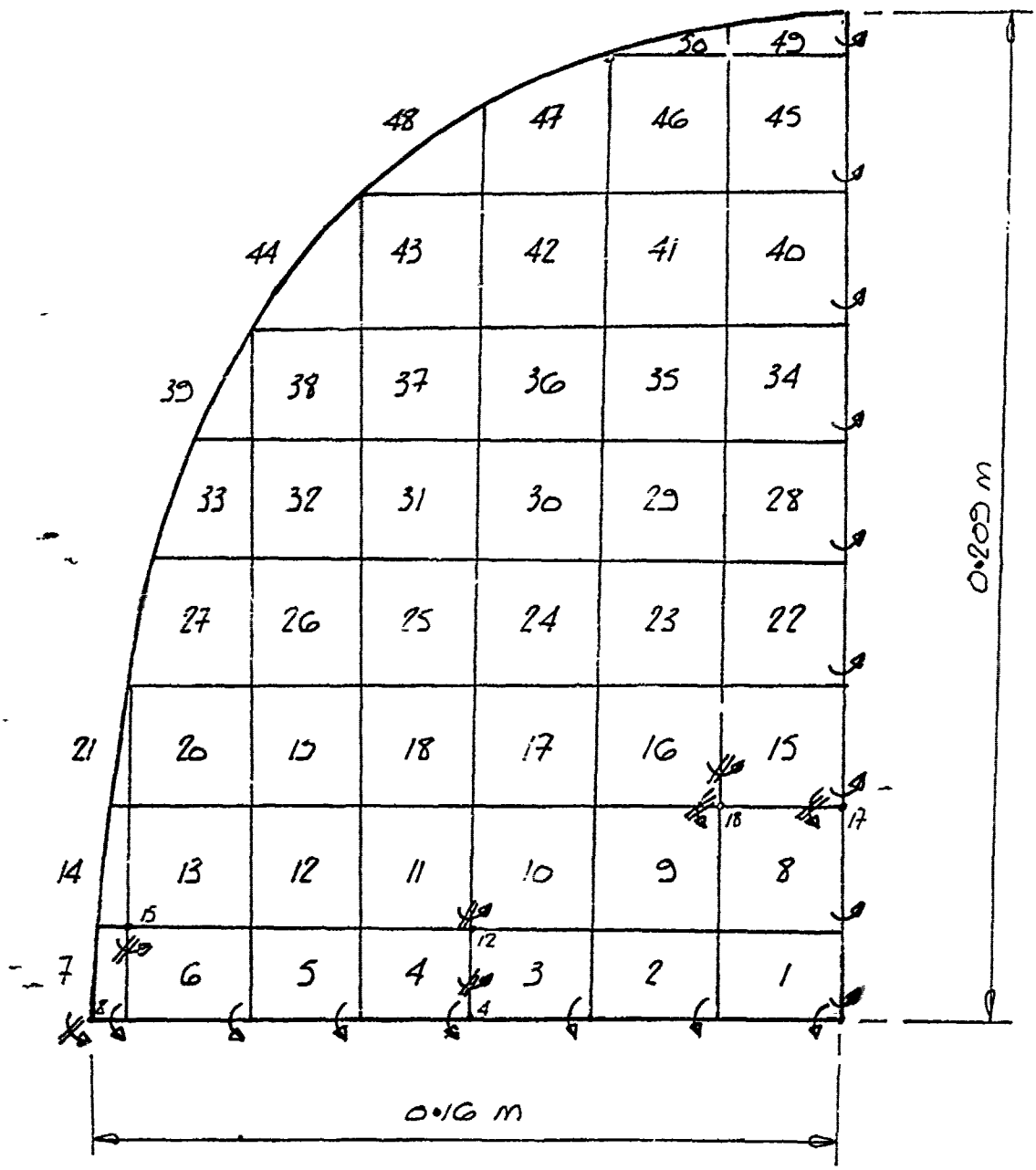


FIGURE 10 ELEMENT OF INNER PANE SHELL MID-SURFACE





RESTRAINED



UNRESTRAINED

FIGURE 11 REFINED MESH MODEL FOR QUARTER PANE

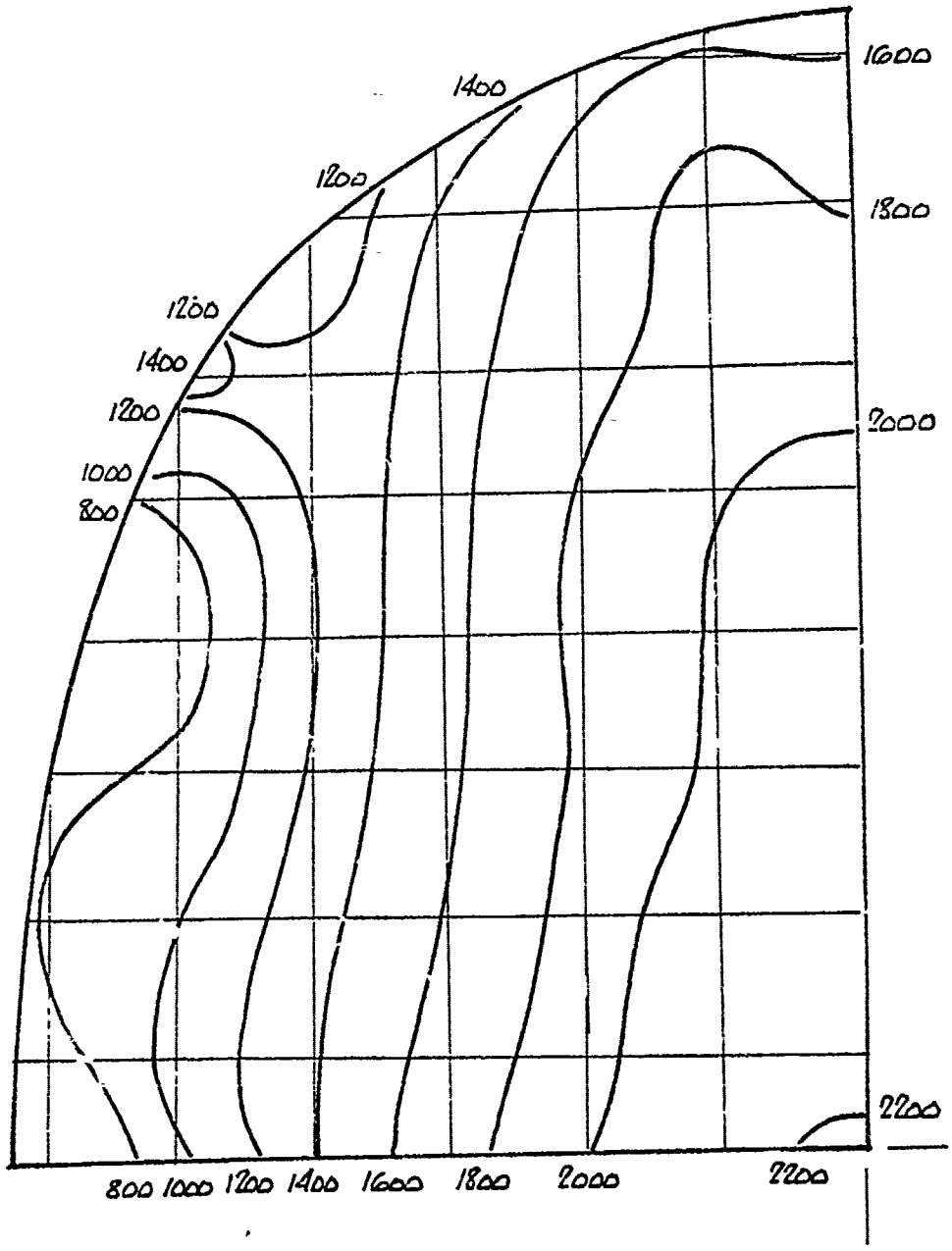


FIGURE 12 MAXIMUM PRINCIPAL MEMBRANE STRESS CONTOURS/INNER PANE OUTER FACE

PRESSURE LOAD 9.5 lbf/in^2 6.35 mm PANE

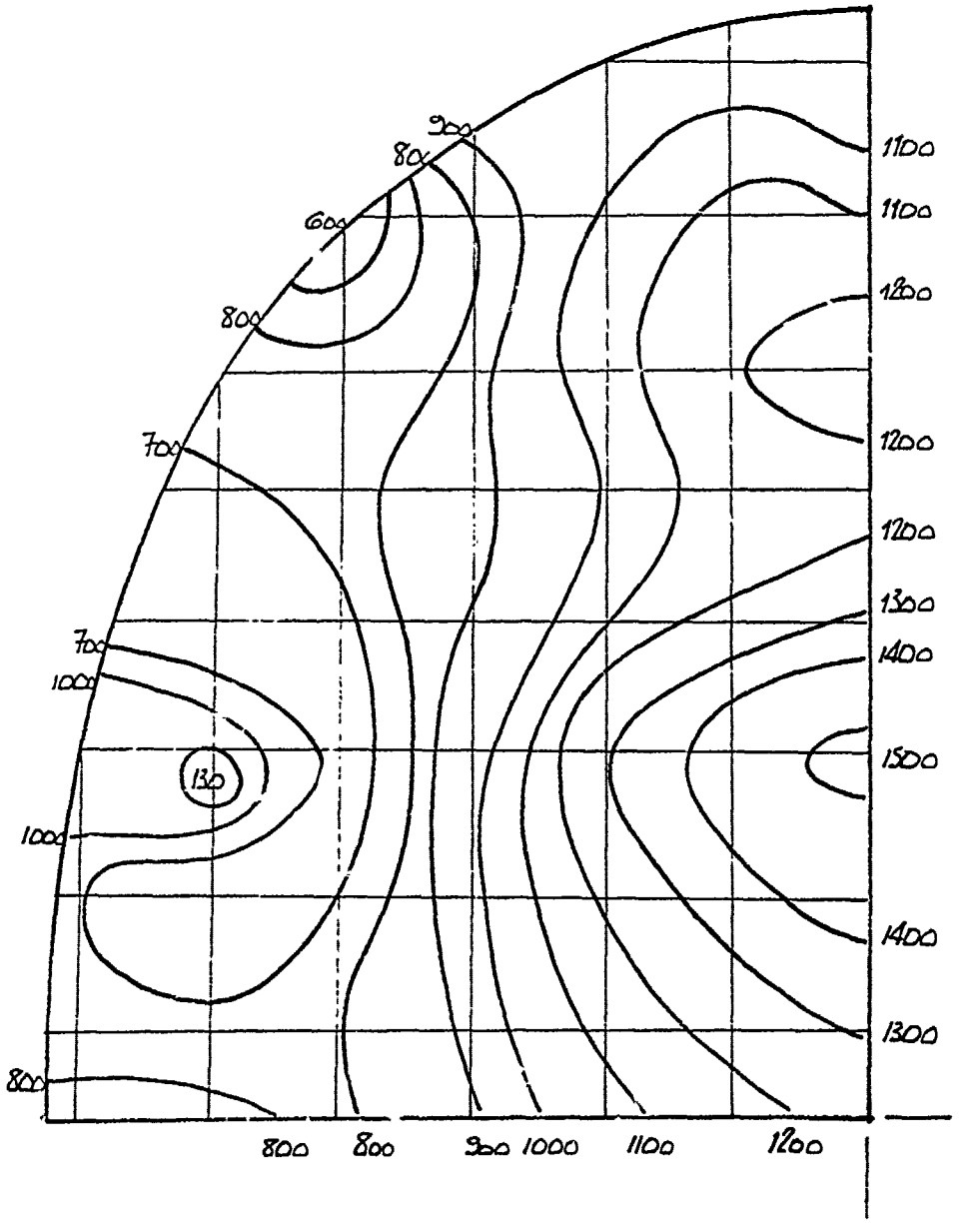


FIGURE 13 PRINCIPAL SHEAR STRESS CONTOURS - INNER PANE OUTER FACE

PRESSURE LOAD 9.5 lbf/in^2 6.35 mm PANE

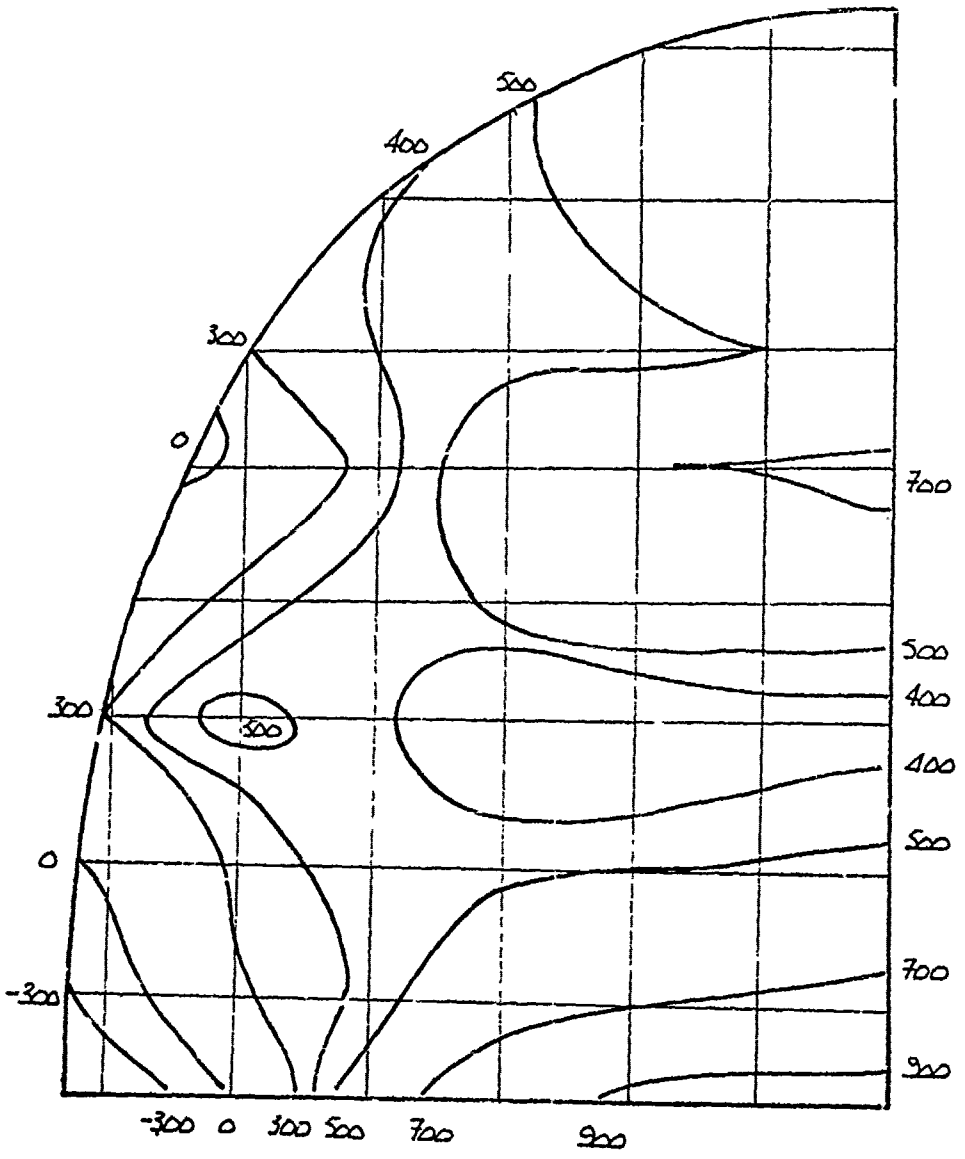
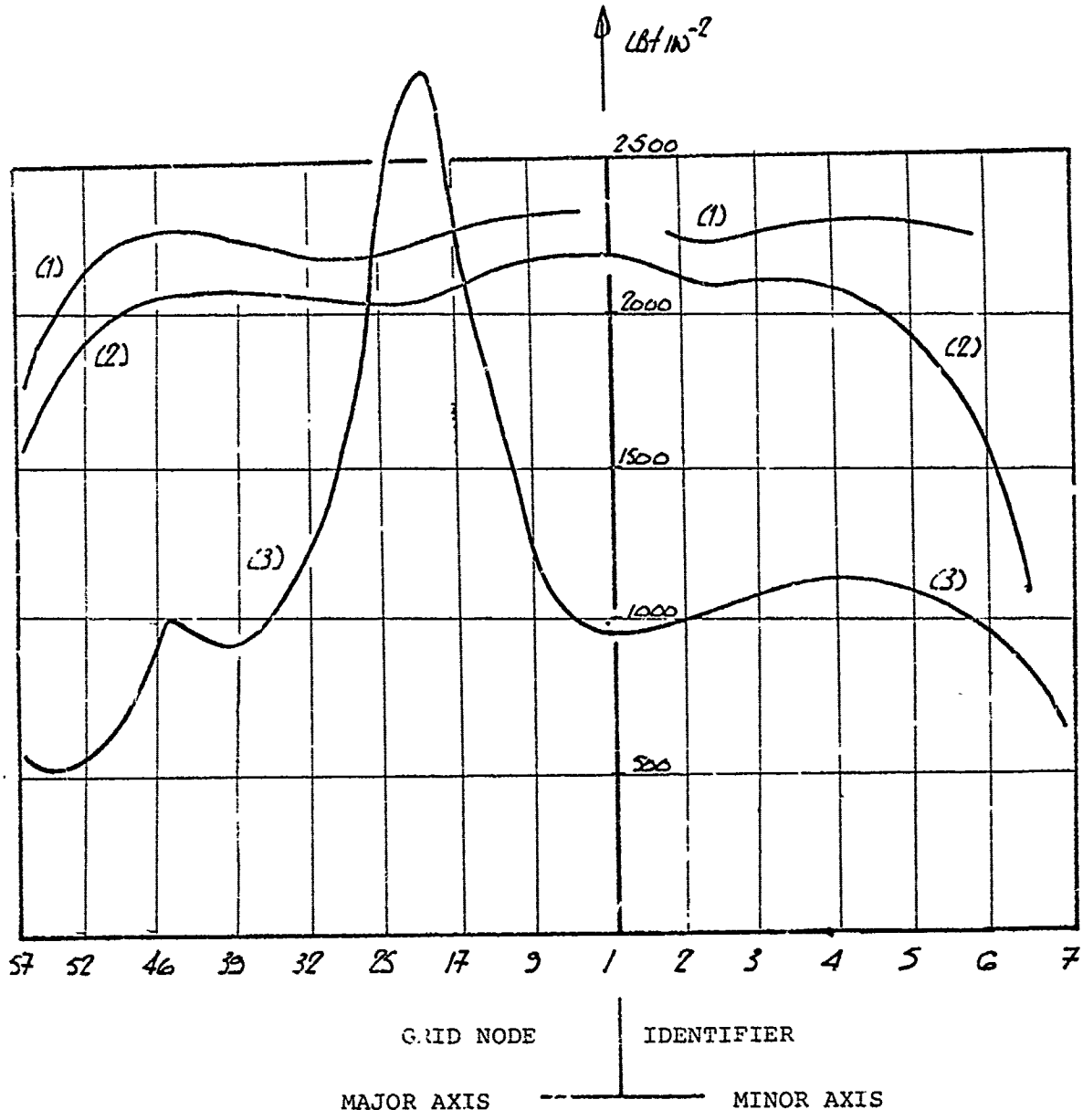


FIGURE 14 MINIMUM PRINCIPAL MEMBRANE STRESS CONTOUR - INNER PANE
OUTER FACE
PRESSURE LOAD 9.5 lbf/in^2 6.35 mm PANE



1. EMPIRCAL RESULTS FROM REF. 13.
2. MAXIMUM PRINCIPAL MEMBRANE STRESS - COMPUTED
3. MAXIMUM PRINCIPAL BENDING STRESS - COMPUTED

FIGURE 15 COMPUTED STRESS LEVELS FOR VC.10 INNER PANE/OUTER FACE PRESSURE LOAD 9.5 lbf/IN^2-635mm PANE

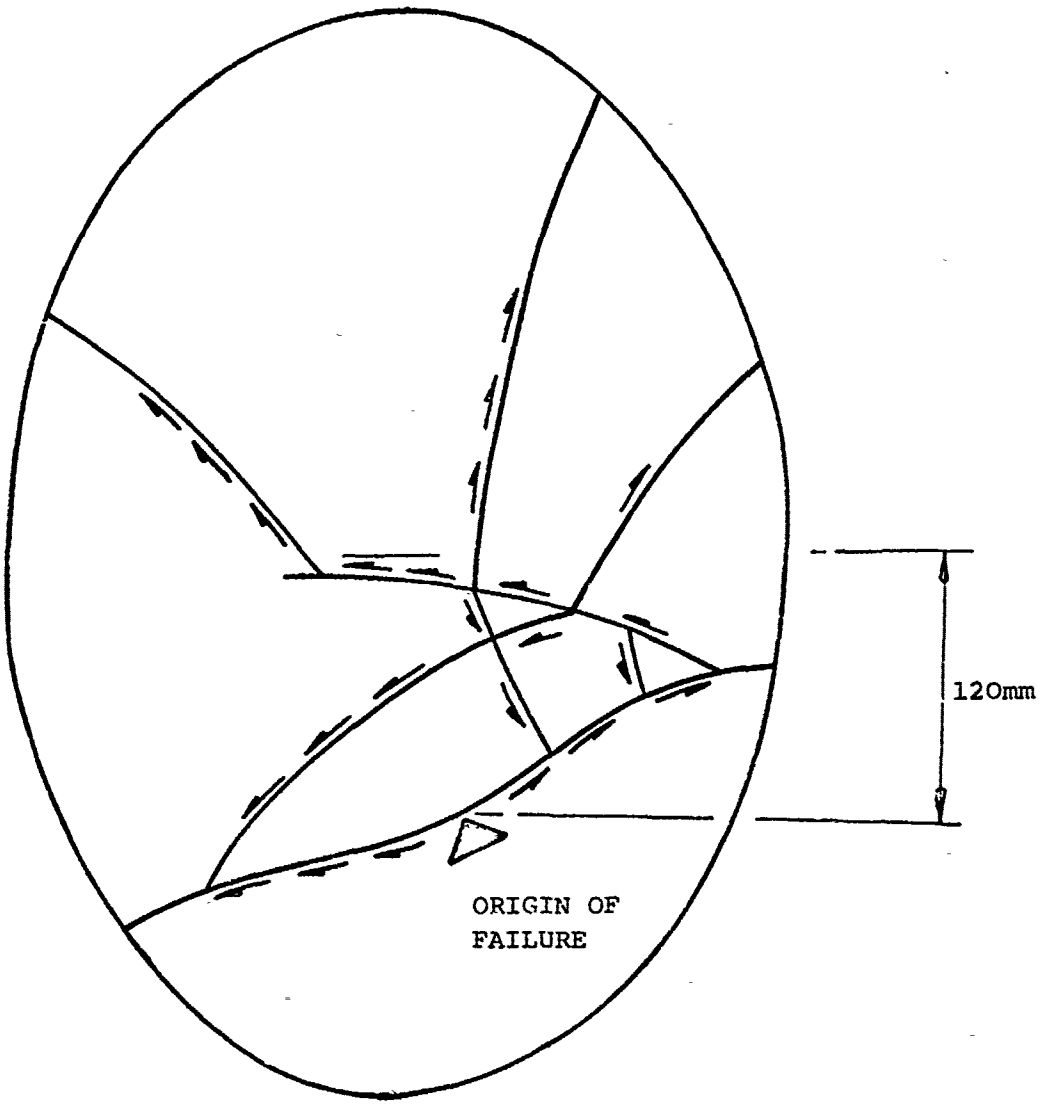


FIGURE 16 TYPICAL SERVICE FAILURE OF INNER PANE
VIEW ON INSIDE FACE



Figure 17

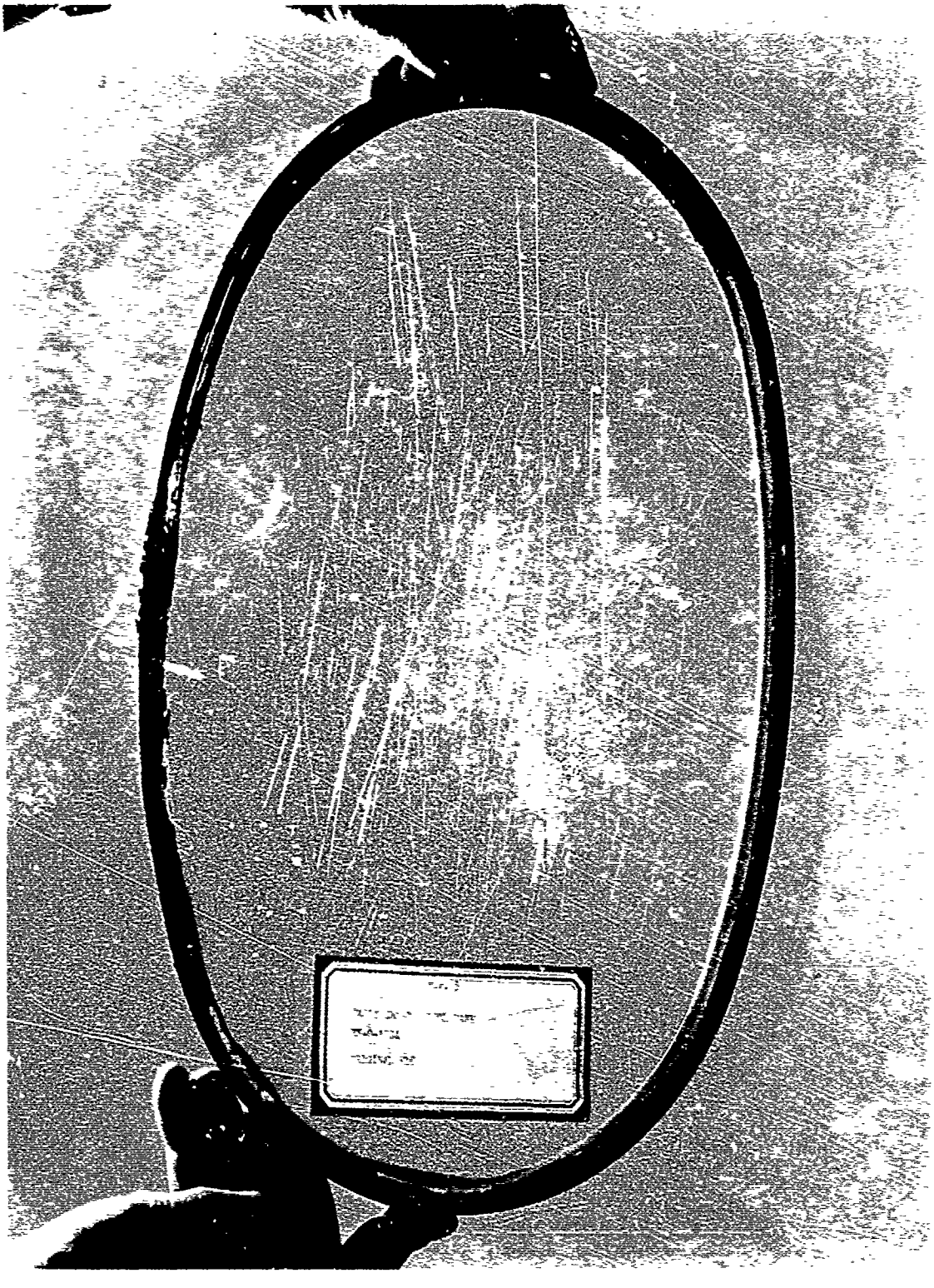


Figure 18

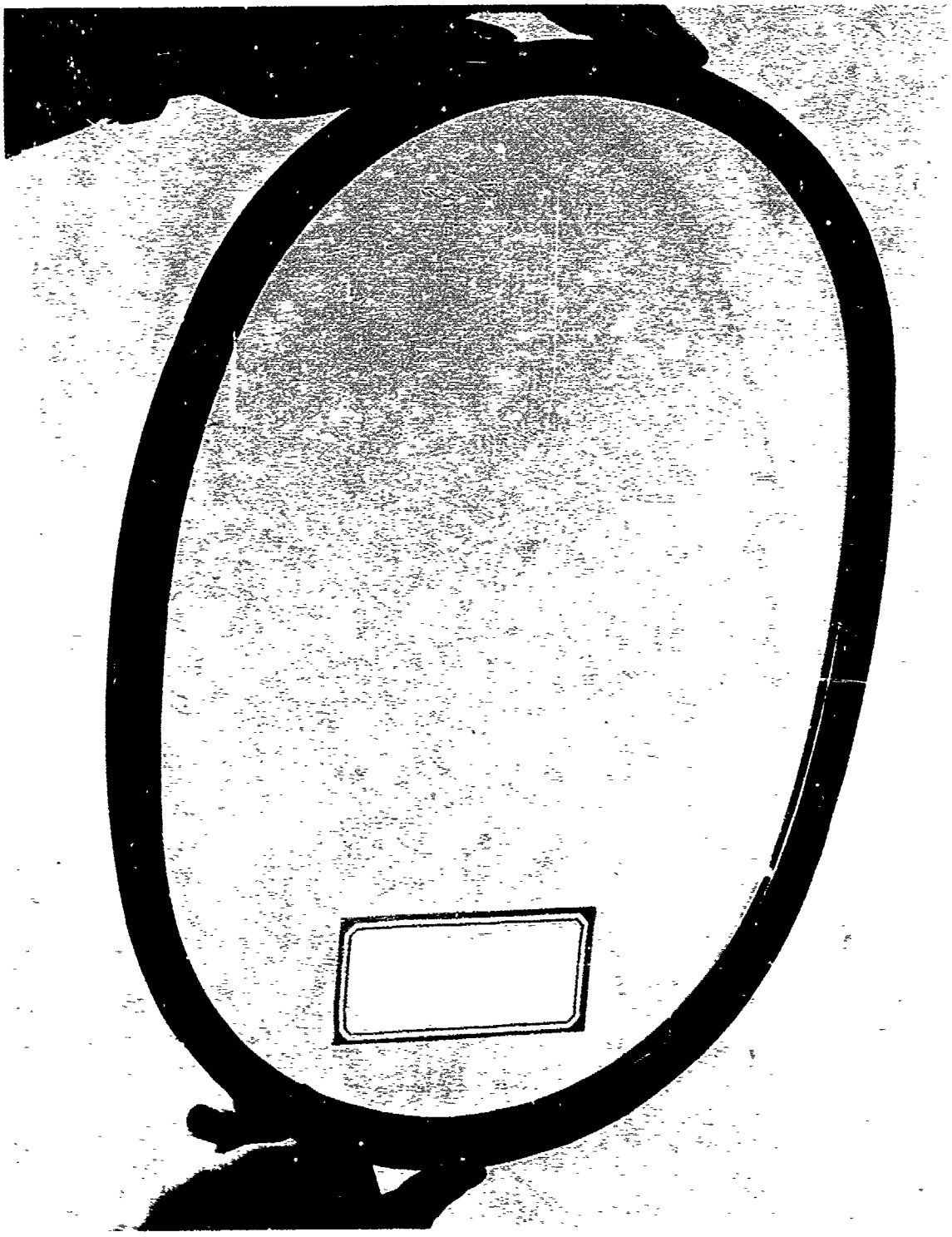


Figure 19

EVALUATION OF SCRATCH AND SPALL RESISTANT WINDSHIELDS

J. R. Plumer
U. S. Army Materials and Mechanics Research Center
Watertown, Massachusetts

and

W. C. McDonald
Goodyear Aerospace Corporation
Arizona Division
Litchfield Park, Arizona

ABSTRACT

EVALUATION OF SCRATCH AND SPALL RESISTANT WINDSHIELDS

BY

JOHN R. PLUMER
U. S. Army Materials and Mechanics Research Center
Watertown, Mass. 02172

WILSON C. MCDONALD
Goodyear Aerospace Corporation
Arizona Division
Litchfield Park, Arizona 85340

A program was conducted to develop and assess materials configurations offering a potential improvement to the scratching and spalling problems present in existing Army helicopter windshields.

Two prototype designs were fabricated for the UH-1 helicopter, flight tested at Ft. Rucker, Alabama, and subjected to ballistic and bird impact tests while under flight-simulated conditions. The designs tested included an acrylic windshield (used as the standard), a monolithic polycarbonate windshield with an abrasion resistant coating on both surfaces, and a glass-plastic composite using Chemcor(1) and polycarbonate materials.

Flight test results demonstrated that the coated polycarbonate design can provide aproximately 1200 service flight hours, or 4 times the average service life span of a typical acrylic windshield. Ballistic impact testing of the polycarbonate designs produced the best spall resistance, (essentially no spall) while the other configurations produced many dangerous fragments. Bird impact results graphically demonstrated that the polycarbonate prototype provided the superior resistance, i.e., resistance to bird strikes at speeds up to 120 knots while the standard acrylic windshield was incapable of defeating a bird strike at the UH-1 cruising speed of 90 knots.

In general, the superior mechanical properties, and the flight worthiness of the coated polycarbonate configuration have been demonstrated.

(1) TM, Corning Glass Works, Corning, NY.

INTRODUCTION

Recent combat experience has demonstrated that the frequent replacement of Army helicopter glazings is mainly necessitated by loss of transparency due to surface scratching, primarily caused by wiper blade action and prop-wash blown dust.

The acrylic glazing currently used in most Army aircraft, is insufficiently hard for the abrasive conditions encountered in the field, and produces potentially dangerous spall on foreign object impact, e.g., blown rocks or small arms fire.

Previous work in this development program resulted in the design and contract fabrication of prototype windshields for UH-1 Army helicopter in 2 basic configurations, each of which incorporates fabrication concepts to increase serviceability, provide for increased crew safety, and utilize readily available commercial materials, Reference 1.

The object of this effort is two-fold: (1) to determine the flight worthiness and the serviceability (resistance to abrasion) of the two prototype windshield concepts through actual flight testing of full-size windshield parts, and (2) to assess the relative improvement in spallation characteristics of these concepts through bird impact and ballistic impact of full size parts in a simulated flight regime.

This report summarizes the initial laboratory work contributing to the design and subsequent fabrication of the prototype parts. The flight testing of these prototype windshields has been evaluated to verify the considered improvements in the serviceability offered by both design concepts. Bird and ballistic impact studies were performed utilizing full size windshields parts and a simulated flight regime. This experience was examined to verify the results from laboratory impact studies conducted on subsize materials specimens. Recommendations of an optimal prototype windshield configuration, suitable for retrofit or existing aircraft, are made on a basis of the flight test performance and the bird and ballistic impact study damage.

DEVELOPMENT OF PROTOTYPE GLAZINGS

The problems of scratching and spalling encountered with acrylic plastic glazings were addressed by incorporation of coated polycarbonate as either a rear ply in a composite configuration, or as a monolithic sheet. One prototype glazing concept utilized a thin glass cladding for abrasion resistance, coupled with a polycarbonate backup ply to provide the required strength and spall resistance. A second prototype concept utilized a hard surface coating applied to inner and outer surfaces of a monolithic polycarbonate glazing to achieve improvements in abrasion resistance.

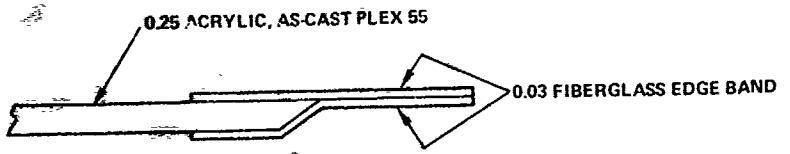
The laboratory ballistics studies were carried out (Reference 1) on test samples to determine improvements in spallation characteristics of these configurations as compared to the currently used acrylic plastic. The results showed monolithic polycarbonate produced 13 times less spall by weight than an acrylic UH-1 windshield. The glass/polycarbonate configuration produced 1/3 the spall of the current material.

A variety of commercially available protective coatings were evaluated by utilizing two test apparatus designed to simulate aircraft conditions. Abcite, a hard surface coating, provided the best coated scratch protection for the plastic component. Resistance to abrasion over current acrylic material was increased by a factor of 130. Cladding the plastic surface with glass provided abrasion resistance over 1000 times that of acrylic plastic.

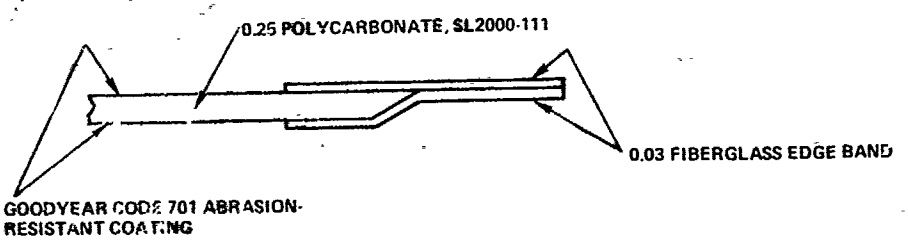
In-house laboratory ballistic and abrasion testing of sample materials and configurations indicated that two windshield designs, glass-clad polycarbonate and Abcite coated polycarbonate, should provide an effective increase in serviceability (abrasion resistance) and virtually eliminate the problems of spallation encountered with acrylic plastics. Laboratory data was insufficient (i.e., not representative of all parameters of actual flight conditions) to permit a selection of one configuration over another. Consequently, both designs were fabricated into full size, flightworthy prototype windshield parts for the UH-1 helicopter.

Evaluation of flight testing and tests simulating service impact conditions (bird and ballistic test study) carried out on these prototype windshields provided verification of the laboratory studies and permitted assessment of the potential of both designs.

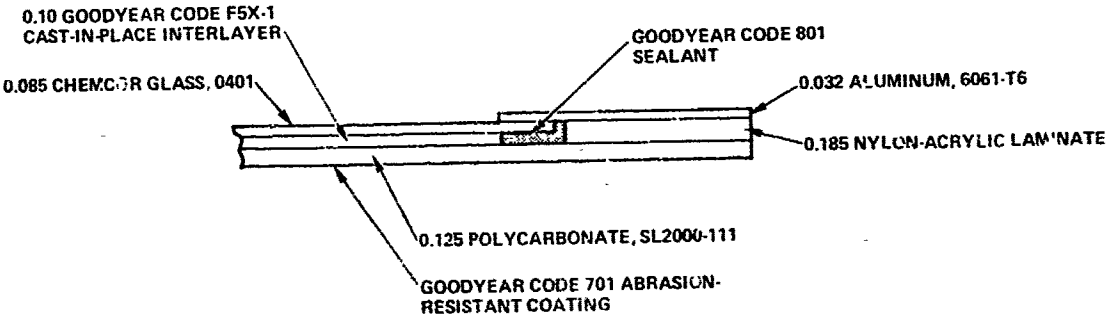
Prototype parts of both designs were fabricated for AMMRC by Goodyear Aerospace Corporation, Contract #DAAG 46-73-C-0079. The structural requirements for the UH-1 helicopter windshields were analyzed by the Contractor. Design requirements for the scratch and spall concepts were integrated with the structural requirements for the windshield parts, thus producing flight-worthy, full size prototype windshield glazings suitable for field and flight test evaluation. Configurations of the prototype windshield parts are shown in Figure 1. Typical properties of the windshield are shown in Table 1. These configurations, including edge attachment, conformed to Bell Helicopter drawing P/N 204-030-666-44, i.e., righthand (pilot) glazings. Three prototype parts in each configuration were fabricated during this phase of the program; work was begun in the spring of 1973.



STANDARD ACRYLIC WINDSHIELD



POLYCARBONATE WINDSHIELD



CHEMCOR-PLASTIC WINDSHIELD

Figure 1 - UH-1 Windshield Test Constructions

TABLE 1

WINDSHIELD TEST DATA

Windshield type	Total Weight (lb)	Luminous transmittance (percent)	Haze (percent)
Standard acrylic	12.7	91.5	1.0
Polycarbonate	13.8	89.0	1.0
Chemcor* - Plastic	24.2	90.0	0.5

*TM, Corning Glass Works, Corning, N. Y. 14830

FLIGHT TEST STUDY

Program Scope and Objectives:

The purpose of the flight test program was to verify anticipated improvements in abrasion resistant properties and consequently enhanced maintainability offered by both design concepts.

The specific objectives of the testing were as follows:

a. To determine if any deficiencies occur in the test windshields during flight testing.

b. To determine if any increase or decrease in wear and abrasion is evident when compared to standard windshields. Test pilots and maintenance personnel were instructed to be especially critical of optical characteristics in flight and the surface condition of the glazings after each flight.

Description of Prototype Parts:

UH-1 windshield parts submitted for flight testing and evaluation included the following:

a. Monolithic polycarbonate-Abcite coated, Serial Numbers SN-1 and SN-2.
b. Glass-polycarbonate composite type, Serial Numbers SN-5 and SN-6.
c. As-cast acrylic parts (2 each), copilot configuration.

Test Procedure:

A two year (maximum) flight test program (TECOM Project No. A1-171-001-001) was established with the U. S. Army Test and Evaluation Command through coordination by the Army Aviation Systems Command. Under TECOM direction the U. S. Army Aviation Test Board conducted this product improvement test in the vicinity of Fort Rucker, Alabama and Apalachicola, Florida during the period 27 July 1973 through February 1975. Four test windshields for the pilots position and two standard windshields for the co-pilot position were tested as follows: (a) the test and standard windshields were installed using standard maintenance procedures outlines in Reference 2. The windshields were inspected for stratches and distortion as outlined in Reference 3 and 4. The windshield wiper system was modified so that one switch controlled both wipers. Cleaning procedures utilizing water only were specified, instructions were stenciled on test and control parts. (b) Test windshield SN-1 was installed in the pilot's position and a new standard windshield in the copilot's position on JUH-1H helicopter SN 68-15380 on 27 July 1973. Both windshields were removed on 23 August 1974. (c) Test windshield SN-2 was installed in the pilot's position with a new standard windshield in the copilot's position in JUH-1H helicopter SN66-499 in 8 September 1973. On 23 August 1974, at 735.9 flight hours, both windshields were transferred in JUH-1H helicopter SN68-15380 and remained in test through 1 February 1975. (d) Test windshield SN-5 was installed in the pilot's position in JUH-1H helicopter SN68-16361 on 17 January 1974 and tested until 25 April 1974. Test windshield SN-6 was installed in the pilot's position in JUH-1H helicopter SN68-16361 on 25 April 1974 and tested until 1 May 1974. The installation of test windshields SN-5 and SN-6 was witnessed by representatives from the manufacturer and AMMRC.

Test Results

Flight hours logged by the four prototype parts are shown in Table 2.

Table 2

Prototype Parts	Flight Hours	Time in Months	Termination
SN-1 (coated polycarbonate)	1199.2	13	Loss of Coating
SN-2 (Coated polycarbonate)	967.0	11.5	Request by AMMRC
SN-5 (Glass/ polycarbonate)	389.7	3	Minor Distortion
SN-6 (Glass/ polycarbonate	73.3	1/4	Severe Distortion

Both Abcite coated polycarbonate parts (SN-1 and SN-2) showed a moderate loss of Abcite coating on the outer surfaces after approximately 900 flight hours, however visual properties were not severely affected. Deep scratches developed throughout the test period in both the SN-1 and SN-2 prototype and the standard acrylic control parts. This is due to sand-size particles being carried across the surface of the glazing during wiper blade action. Control and test parts both appeared to develop this type of scratching with equal ease. Shallow scratching (i.e., wear) within the wiper blade path developed more rapidly and to a greater extent on the acrylic parts. The coated polycarbonate parts maintained overall superior optics for a longer time throughout the test. This is demonstrated by the photograph in Figure 2 which shows the superior optics of windshield (SN-2) midway through the testing.

Flight testing of prototype windshield (SN-1) was terminated due to partial loss of the coating. Without this coating it was obvious wear would rapidly develop, Figure 3. The SN-2 windshield was removed at the request of AMMRC at approximately 1000 hours, to determine feasibility of recoating this part with Abcite. Partial loss of the coating was also experienced. At the conclusion of flight testing, both coated polycarbonate parts, aside from the scratching and partial loss of coating, appeared free of defects, (e.g., cracking, excessive haze, or microcrazing). Both control parts were also free of these defects. The SN-2 prototype and acrylic windshield at the conclusion of flight testing are shown by photographs in Figures 4 and 5. The glass clad polycarbonate prototypes (SN-5 and SN-6) exhibited virtually no scratching or surface wear, nor were other deficiencies revealed. The primary objection voiced on the flight characteristics of this prototype was the slight distortion present in each of the parts. This distortion may be detected in the photographs shown in Figures 6 and 7.

General comments by the flight test pilots of each of these windshields stated although the distortion was small and in a usually noncritical portion of the windshield (See Figure 6), it caused some eye strain and some orientation difficulties. Other pilots' comments noted the parallax error (due to differences in right hand and left hand windshield thicknesses) as a visual annoyance. This could not be resolved within the scope of the program as it would require glass/plastic windshields in both left and right hand configurations but would not be a problem in production windshields.

Discussion:

The flight test results of both configurations of prototypes verified the concepts for improving abrasion resistance. The polycarbonate coating did provide improved wear characteristics over plain acrylic, the superior resistance was maintained up until a time when an appreciable amount of a surface coating was lifted off (approximately 900 hours) as a result of environmental affects, primarily absorption of water within the polycarbonate

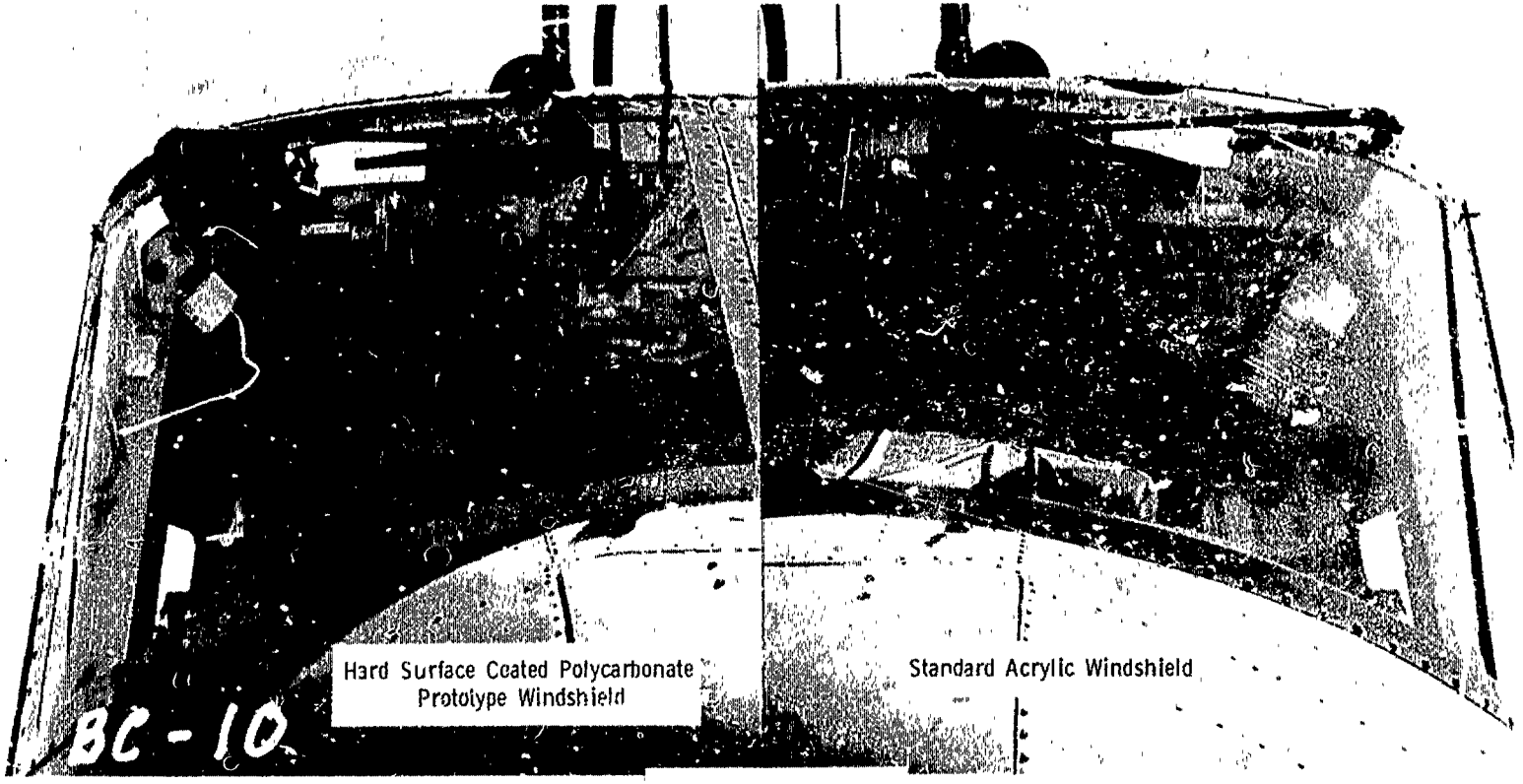


Figure 2 - Windshields During Flight
Testing 385 Flight Hours

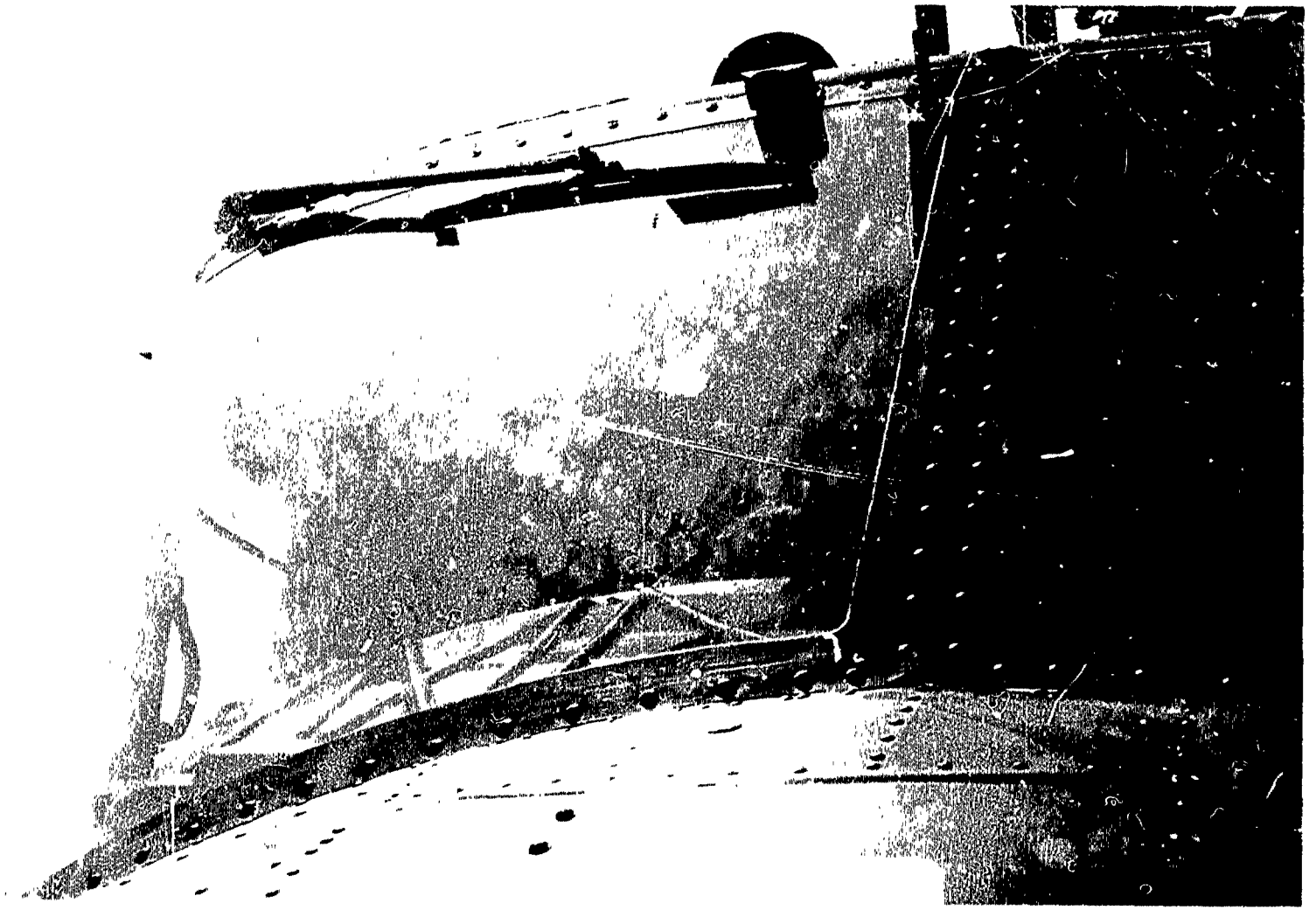


Figure 3 - SN-1 at 1190.2 Flight Hours

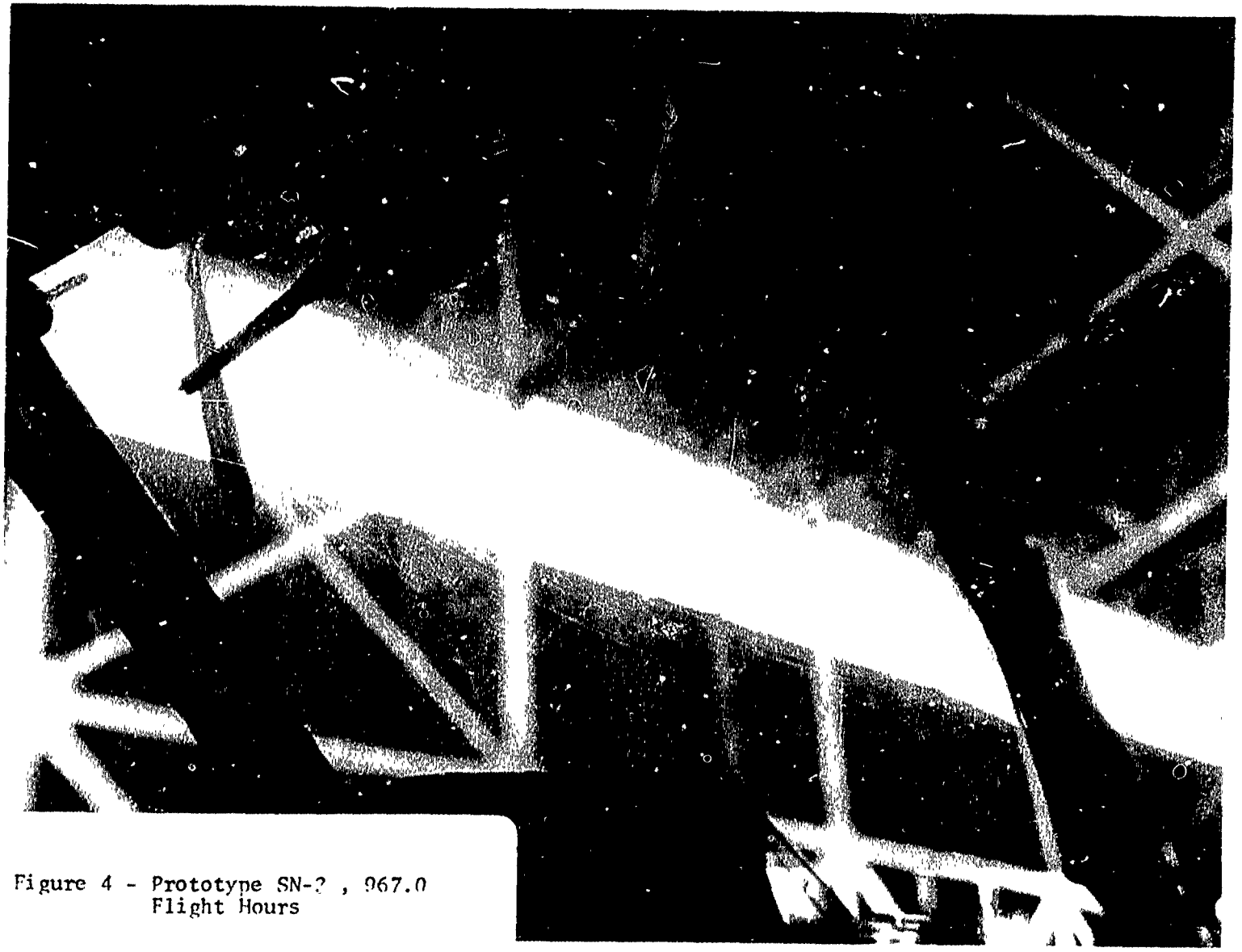


Figure 4 - Prototype SN-? , 967.0 Flight Hours

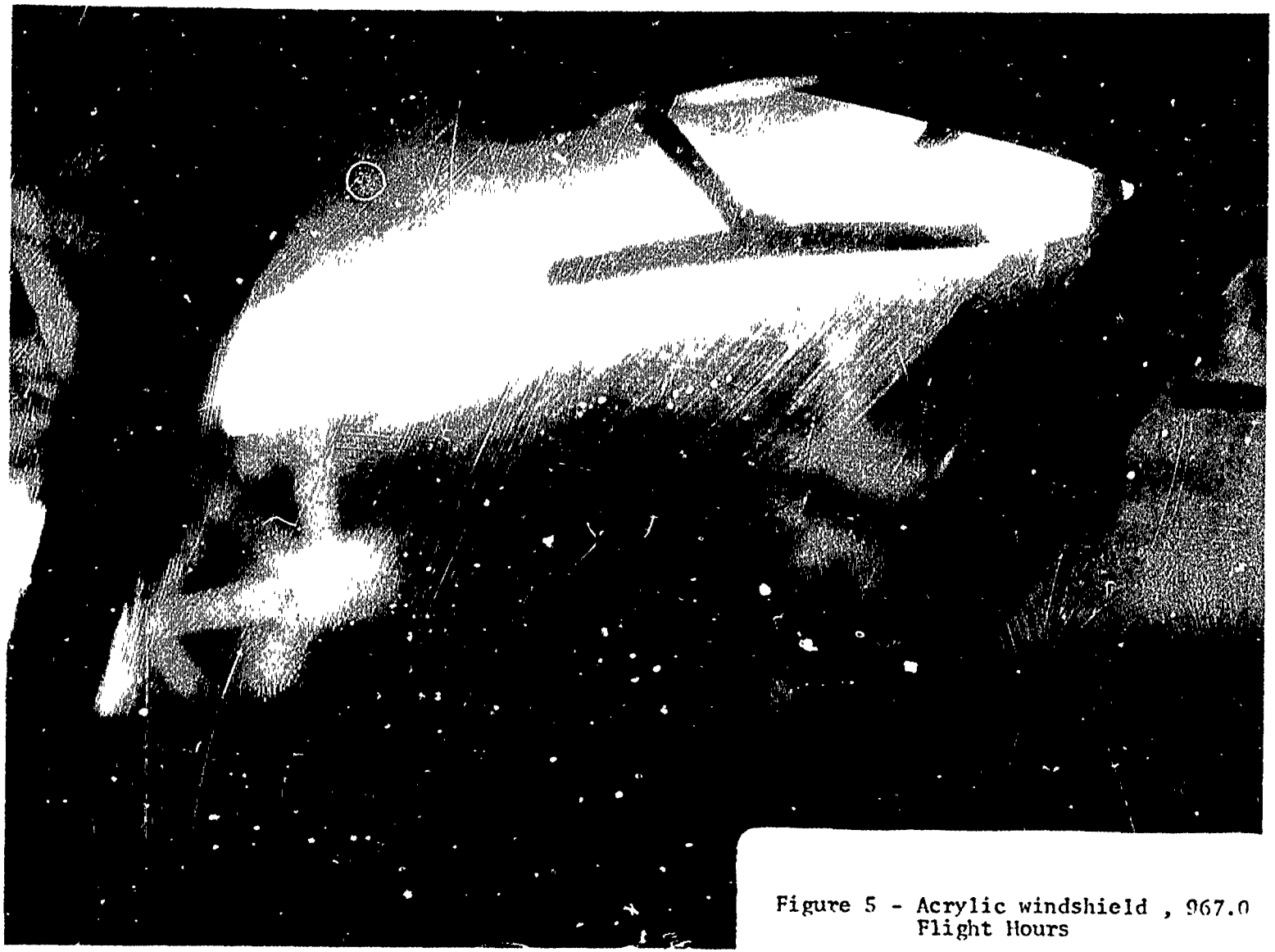


Figure 5 - Acrylic windshield , 967.0 Flight Hours

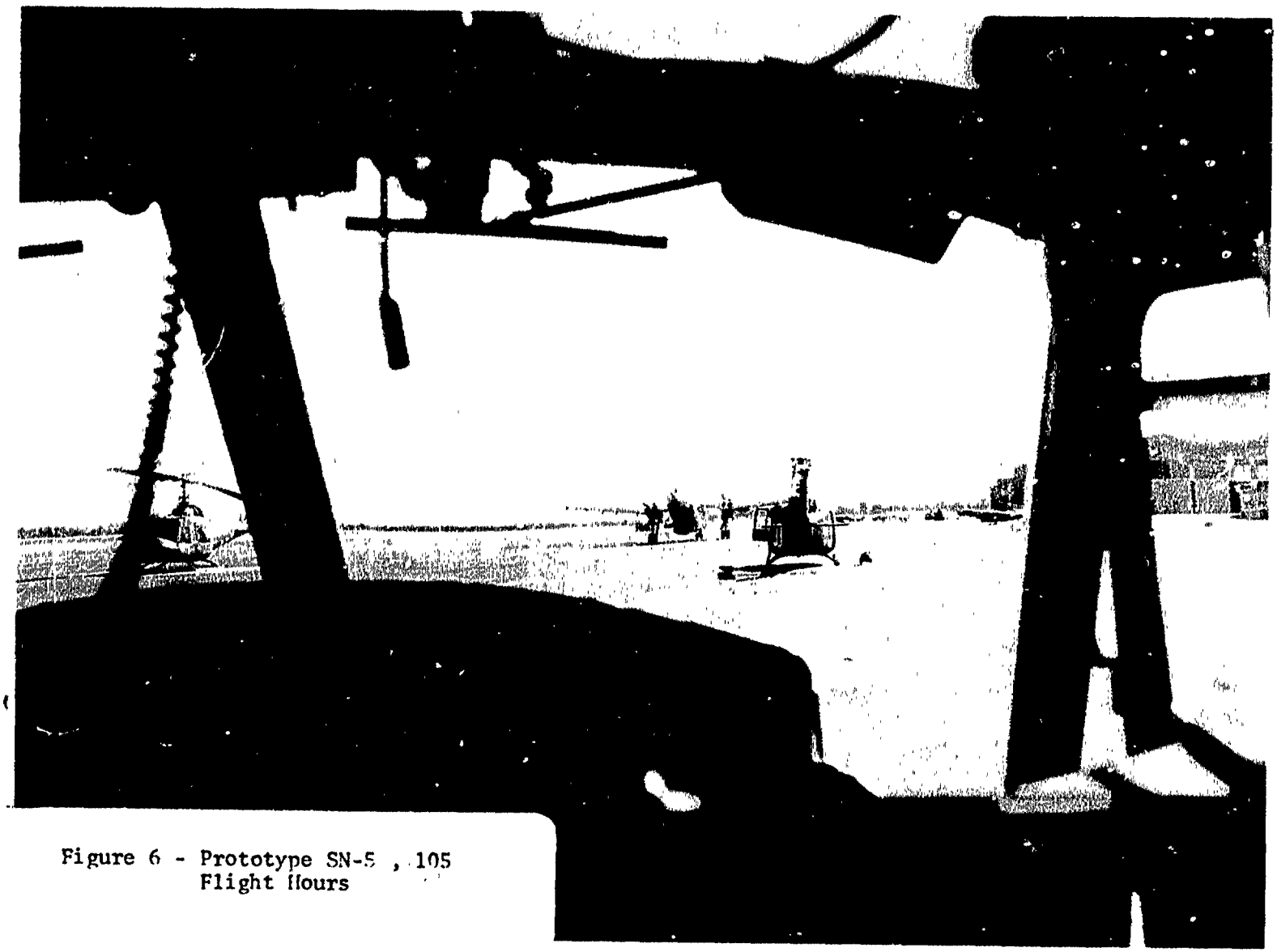


Figure 6 - Prototype SN-5 , 105 Flight Hours

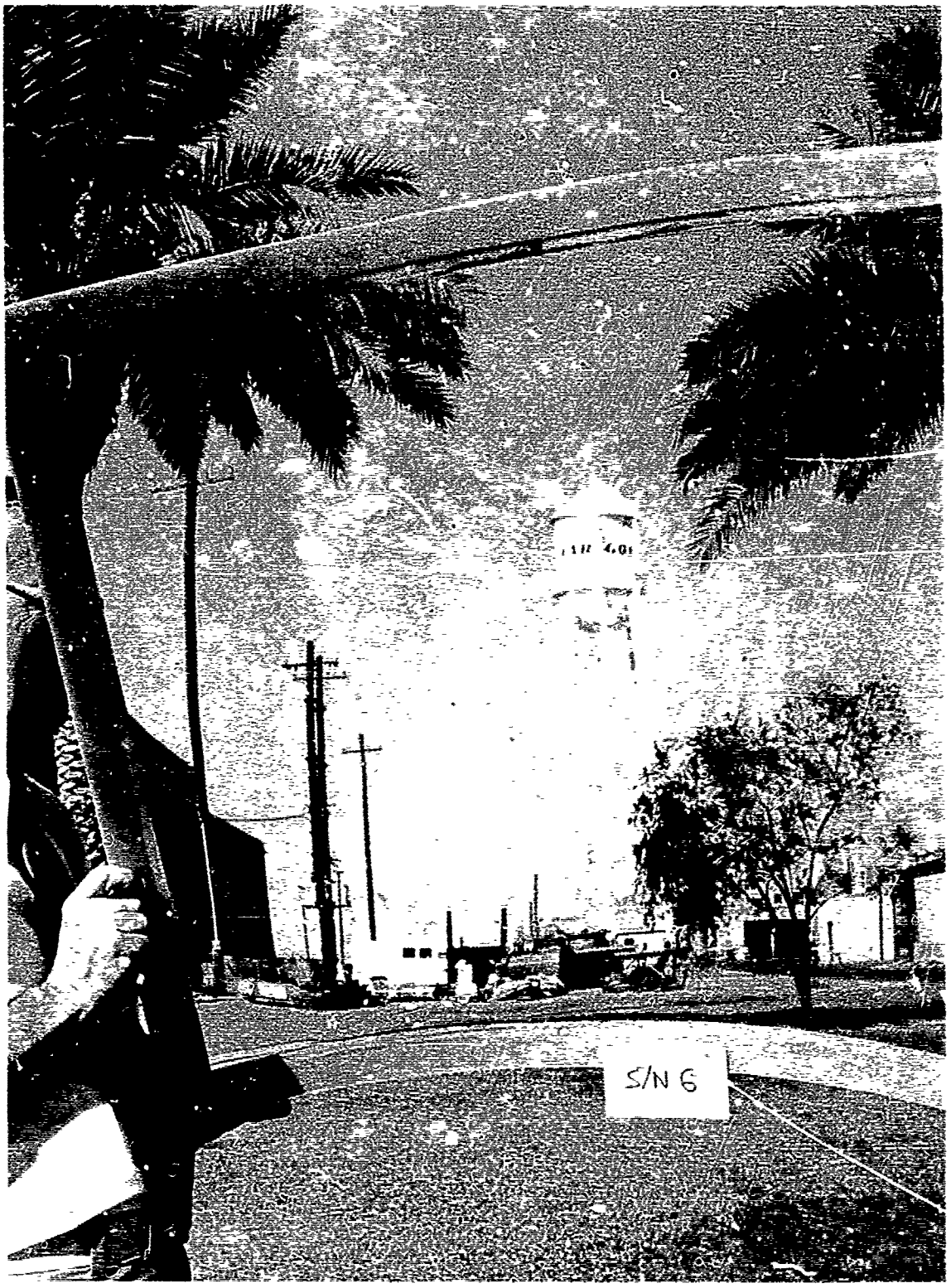


Figure 7 - Glass/Polycarbonate Prototype

material causing a debonding of the abcite coating. Previous studies (Reference 5) and observations made during the flight test phase of this program indicate that severe scratching and an appreciable amount of surface wear (haze) develops on acrylic UH-1 windshields by approximately 350 flight hours; in many cases this warrants replacement of the windshields. The glass faced prototype provided excellent abrasion resistance, exhibiting virtually no scratching or abrasion at the conclusion of the flight testing. The distortion present in the glass face polycarbonate parts primarily resulted from the difficulties of obtaining reproduceable glass contours during limited production of the glass components used in this configuration. It was felt by the Contractor that distortion could be greatly reduced by further development work with the glass suppliers.

BALLISTIC AND BIRD IMPACT STUDY

Program Scope and Objectives:

Contract DAAG46-75-C-0005 was issued with Goodyear Aerospace Corp. as a continuing effort to determine how these improved abrasion-resistant helicopter windshields would react under ballistic and bird impact. Good data have been lacking in these areas, and this contract was initiated to fill in some of the information gaps that existed on helicopter windshields.

The work effort was conducted at the Litchfield Park, Arizona, plant where both fabrication and test facilities are located. The program was broken down into the following efforts:

1. Monolithic polycarbonate windshields -

   Two 1/4-inch monolithic polycarbonate windshields were fabricated with an abrasion coating (Abcite)[a] on both the inner and outer surfaces. The windshield configurations, including edge attachment, conformed to Bell Helicopter drawing P/N 204-030-666-44. A third part previously fabricated by Goodyear Aerospace was supplied by the Army to provide the remaining part needed for the test program. The parts were fabricated using SL 2000-111 grade press-polished polycarbonate.

2. Glass-plastic windshields -

   Two composite glass-plastic windshields were fabricated to the standard UH-1 shape. The third unit previously built by Goodyear Aerospace was furnished by the Army for inclusion in the test program.

3. Standard acrylic windshields -

   The Army furnished for the program three standard as-cast acrylic UH-1 windshields (P/N 204-030-666-44) from inventory.

Details of the construction of these test articles are shown in Figure 1.

[a]TM, E. I. DuPont de Nemours, Inc., Wilmington, Delaware

BALLISTIC TESTING

General:

Ballistic testing was conducted on one each of the three windshield types being evaluated. Each windshield was subjected to three ballistic strikes using caliber .30 ball M2 projectiles at a velocity approximately 100-yard range. The strikes were well above the defeat threshold velocity for any of the three windshield constructions tested.

The tests were designed to measure the quantity and nature of back side spalling resulting from such penetrations. An assessment of post-hit structural integrity and visibility for each windshield construction was also sought.

Test Procedure:

Each windshield tested was mounted in the UH-1 structure in a manner approximating a normal installation for this article. A transparent plastic box was mounted directly behind the windshield. This box was utilized to apply a vacuum to the aft side of the windshield during test to simulate aerodynamic loading imposed at the aircraft redline speed of 120 knots (see Figure 8). The calculated loading for the windshield at 120 knots was 0.328 psi.

The quantity and nature of ballistic spall generated by the penetration of each windshield were recorded in two ways. A witness sheet of 0.020-inch-thick 2024 T3 aluminum alloy was used to record the dispersion pattern and relative lethality of the spall particles.

The witness sheet was positioned within the pressure box as a vertically oriented, peripherally supported diaphragm located at the pilot's nominal eye position (aircraft station 53.0). A spall particle having sufficient remaining energy to pierce the witness sheet material placed parallel to and six inches behind the target is normally expected to produce lethal damage or its equivalent from a variety of mass-velocity combinations (Reference 6).

The witness sheet positioned at station 53.0 was approximately 28 inches behind the impact area of each windshield. This location was selected since it approximated the pilot's position and provided visual access to the back side of the windshield for the high-speed cameras which provided the second source of spall documentation. Two high-speed cameras were used to record the overall windshield response and characteristics of any spall generated.

One high-speed camera operating at 3,000 frames per second was used to view the front side of the windshield. The back side of the windshield was monitored with a 11,000-frame-per-second camera during each test firing. One additional camera operating at a standard framing rate was used to document the test setup and individual firing sequences. A schematic

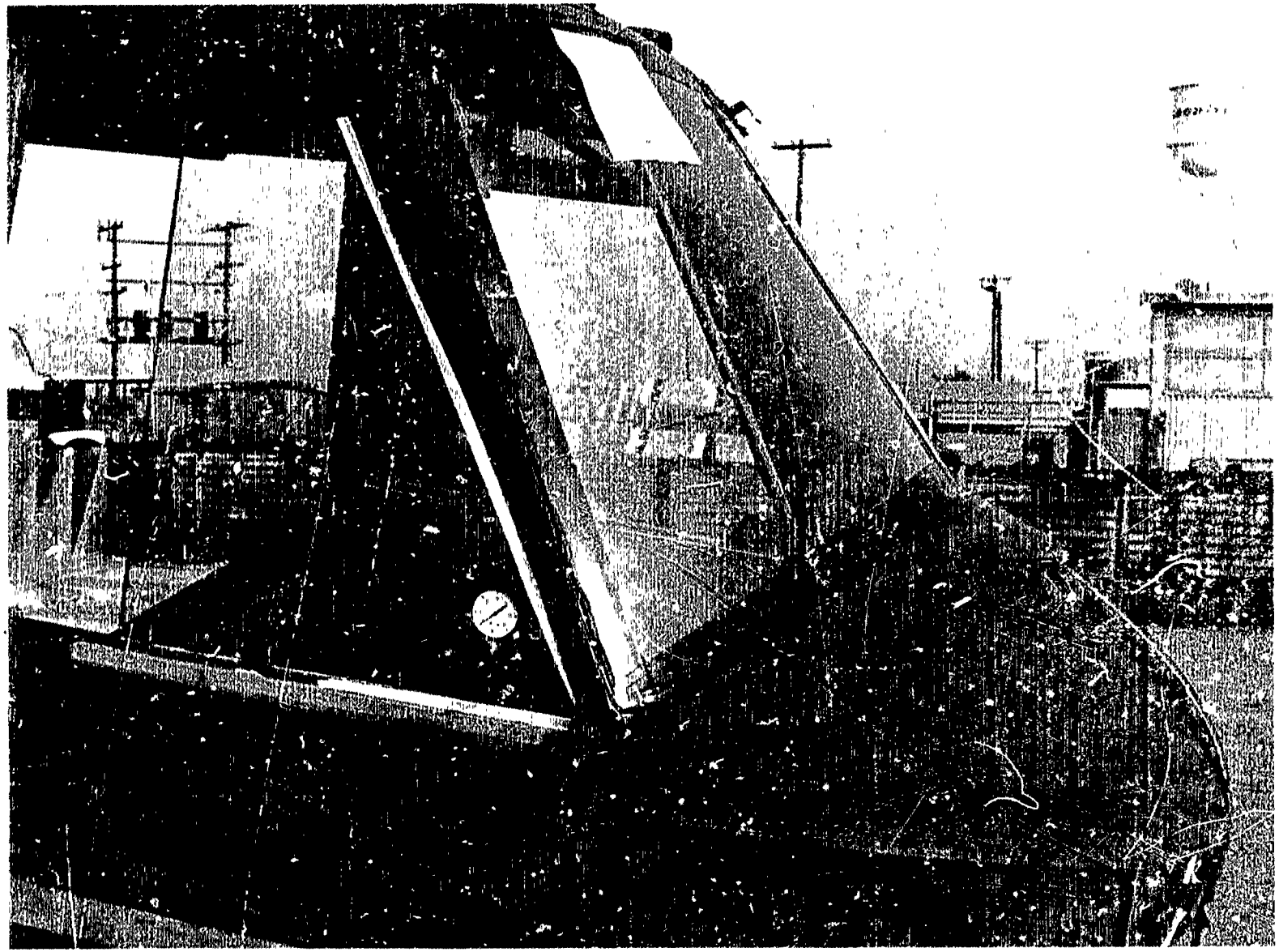


Figure 8 - UH-1 Windshield Ballistic Test Structure with Pressure Box

of the ballistic test setup used in this evaluation is shown in Figure 9. The actual test setup is illustrated in Figure 10.

Each windshield was impacted with a total of 3 caliber .30 ball M2 projectiles which had been reloaded to simulate the remaining velocity for this round at 100-yard range (2550 ft/s). A centrally located equilateral triangle shot placement pattern was used for all three windshields tested. Measurement of the post-test articles showed that the actual center-to-center shot spacings ranged from 6.75 to 9.00 inches.

Test Results:

The back side spalling characteristics of each type of windshield tested are summarized in Table 3. Photographs of the expended test articles, Figures 11, 12 and 13, illustrate the extent of overall damage resulting from the ballistic penetrations. Much of the overall glass fracture in the Chemcor-plastic windshield was incurred during post-test removal from the aircraft structure and subsequent handling. More accurate display of the post-hit visibility through this article is shown in the motion picture documentation. The extent of post-hit crack propagation which would occur in flight as a result of aircraft vibration and flight loads imposed is unknown.

Additional details of the comparative material behavior are shown in the front and back side closeup photographs, Figures 14 through 19. The witness sheets from each test are shown in Figures 20, 21 and 22. Spall data reported for each test excluded the single perforation of the witness sheet caused by the bulk of the projectile.

Analysis of Spall Characteristics:

Typical back side spall particles collected following one ballistic penetration of each type of windshield are illustrated in Figure 23. The particles from the Chemcor-plastic composite which perforated the witness sheet were not collected and therefore are not included in Figure 23.

After both the physical evidence and photographic data collected were reviewed, the following summary of performance was prepared:

1. Chemcor-plastic composite windshield -

   The ballistic penetration of this windshield generated many spall particles, a number of which had potentially lethal penetrating characteristics. These penetrating particles are probably both glass and bullet fragments.

   The glass outer layer acts to partially break up the projectile. The glass particles and bullet fragments, both having relatively high density, comprise the most hazardous spall. The ductility of the plastic backing ply restricts the dispersion of the spall.

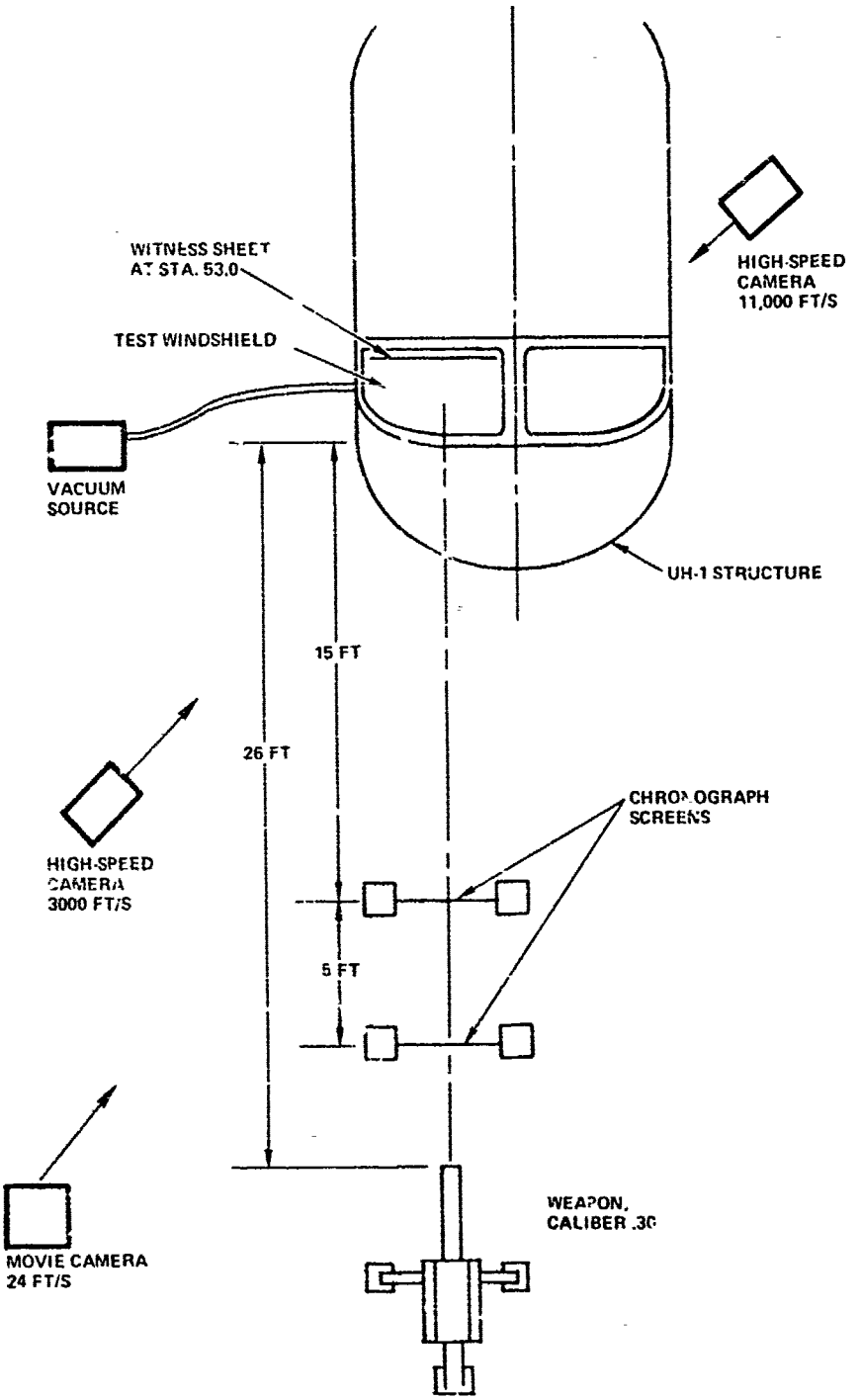


Figure 9- Ballistic Test Setup, Schematic Plan View



Figure 10 - Ballistic Test Setup, UH-1 Windshields

TABLE 3 - WINDSHIELD BACK SIDE SPALLING BALLISTIC TEST DATA

Test article	Round no.	Test temperature (deg F)	Velocity (ft/s)	Witness sheet perforations	Witness sheet marks	Maximum dispersion of spall (in.)
P/N 204-030-666-44	1	70	2579	0	6*	14.50
UH-1 standard acrylic	2	70	2526	0	2*	8.75
windshield	3	75	2540	0	2*	12.75
UH-1 prototype windshield	1	65	2566	6	36	10.75
Chemcor-plastic composite	2	65	2540	10	65	18.00
	3	65	2540	10	32	13.75
UH-1 prototype windshield	1	65	2632	0	0	-
Monolithic polycarbonate	2	75	2500	0	0	-
	3	75	2500	0	0	-

*Spall particles were very widely dispersed, and many did not strike the witness sheet.

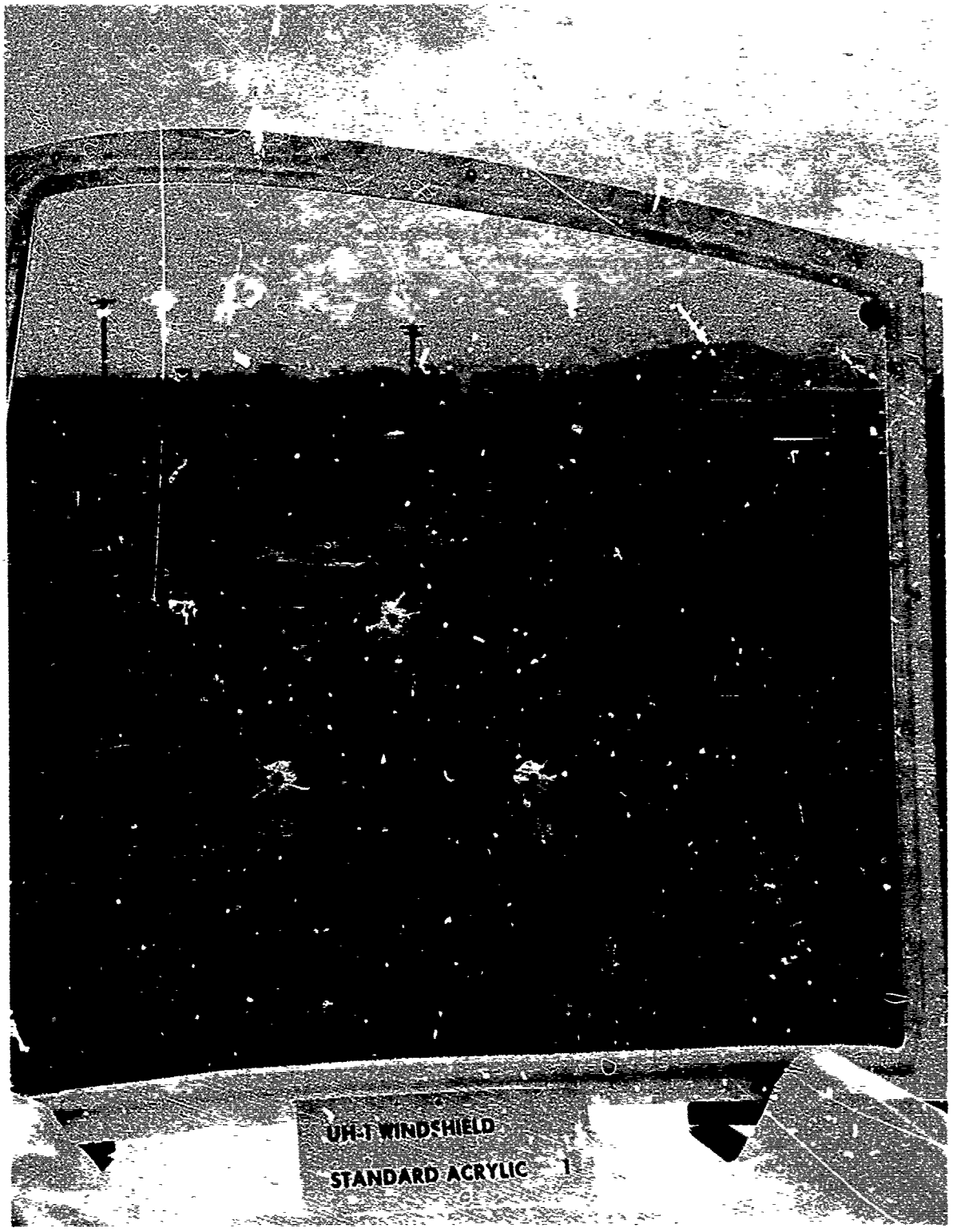


Figure 11 - UH-1 Standard Acrylic Windshield, Ballistic Test Article, Post-Test Display

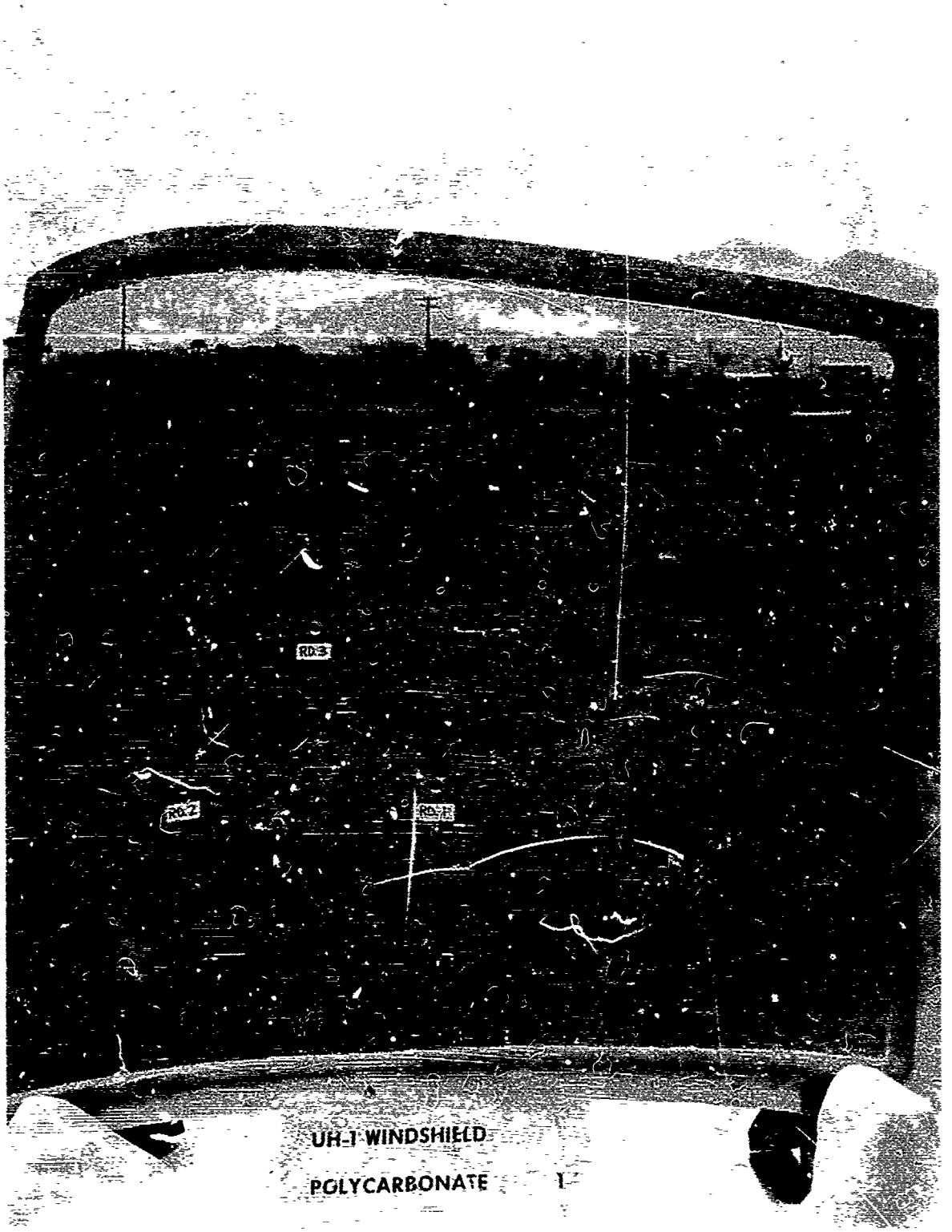


Figure 12 - UH-1 Polycarbonate Windshield, Ballistic Test Article, Post-Test Display

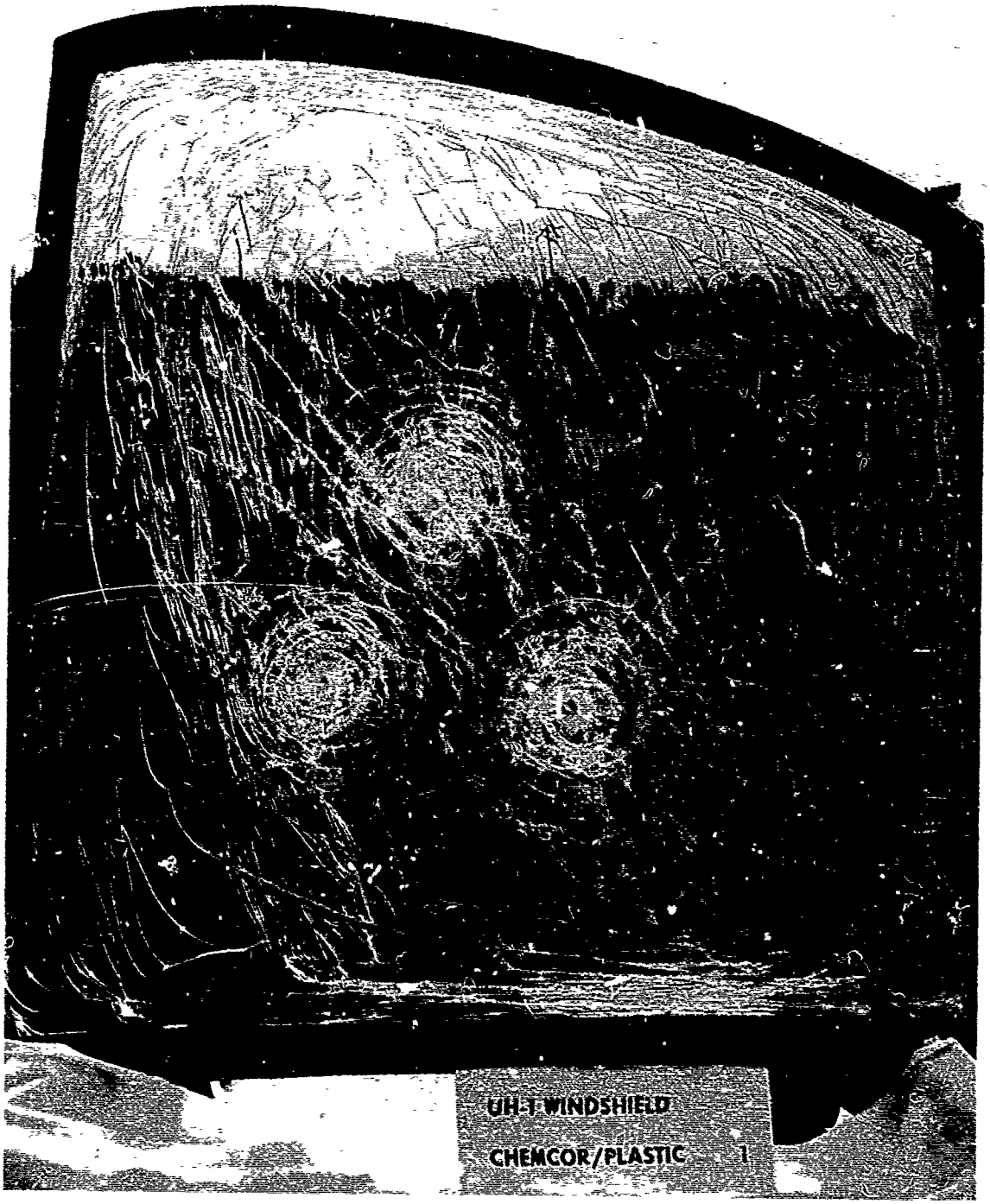


Figure 13 - UH-1 Chemcor-Plastic Windshield, Ballistic Test Article, Post-Test Display

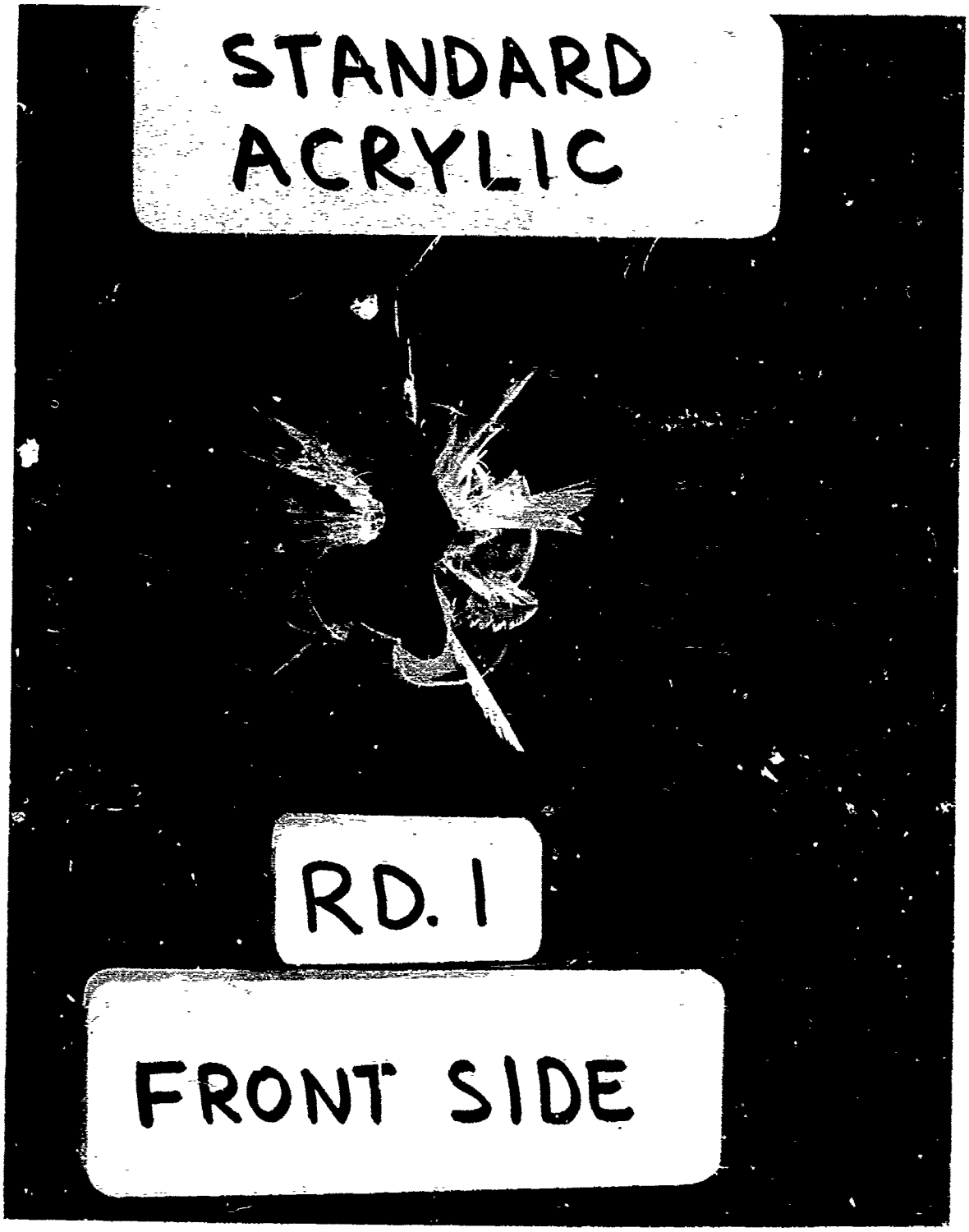


Figure 14 - UH-1 Standard Acrylic Windshield Ballistic Penetration, Front Side Detail

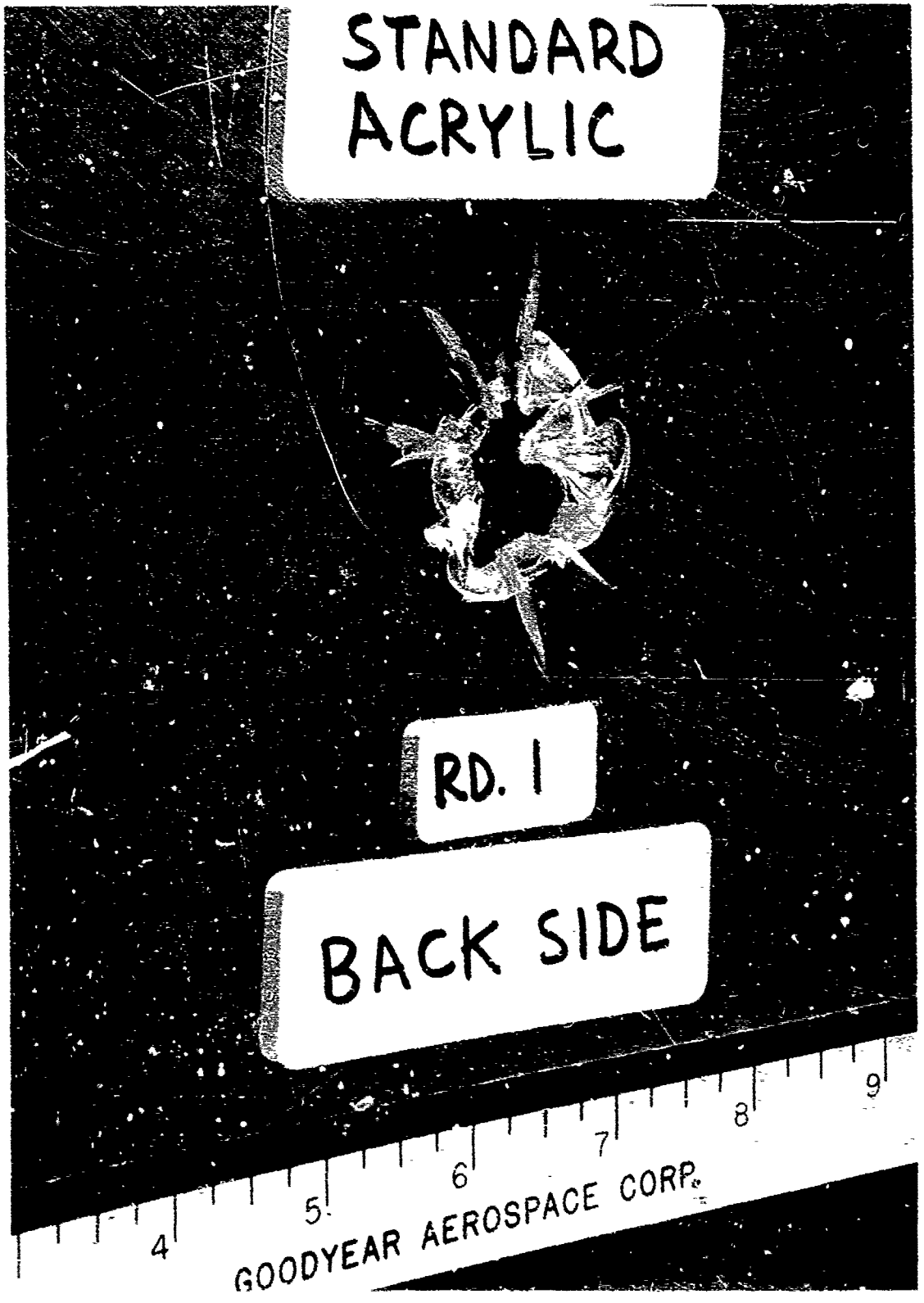


Figure 15 - UH-1 Standard Acrylic Windshield Ballistic Penetration Back Side Detail

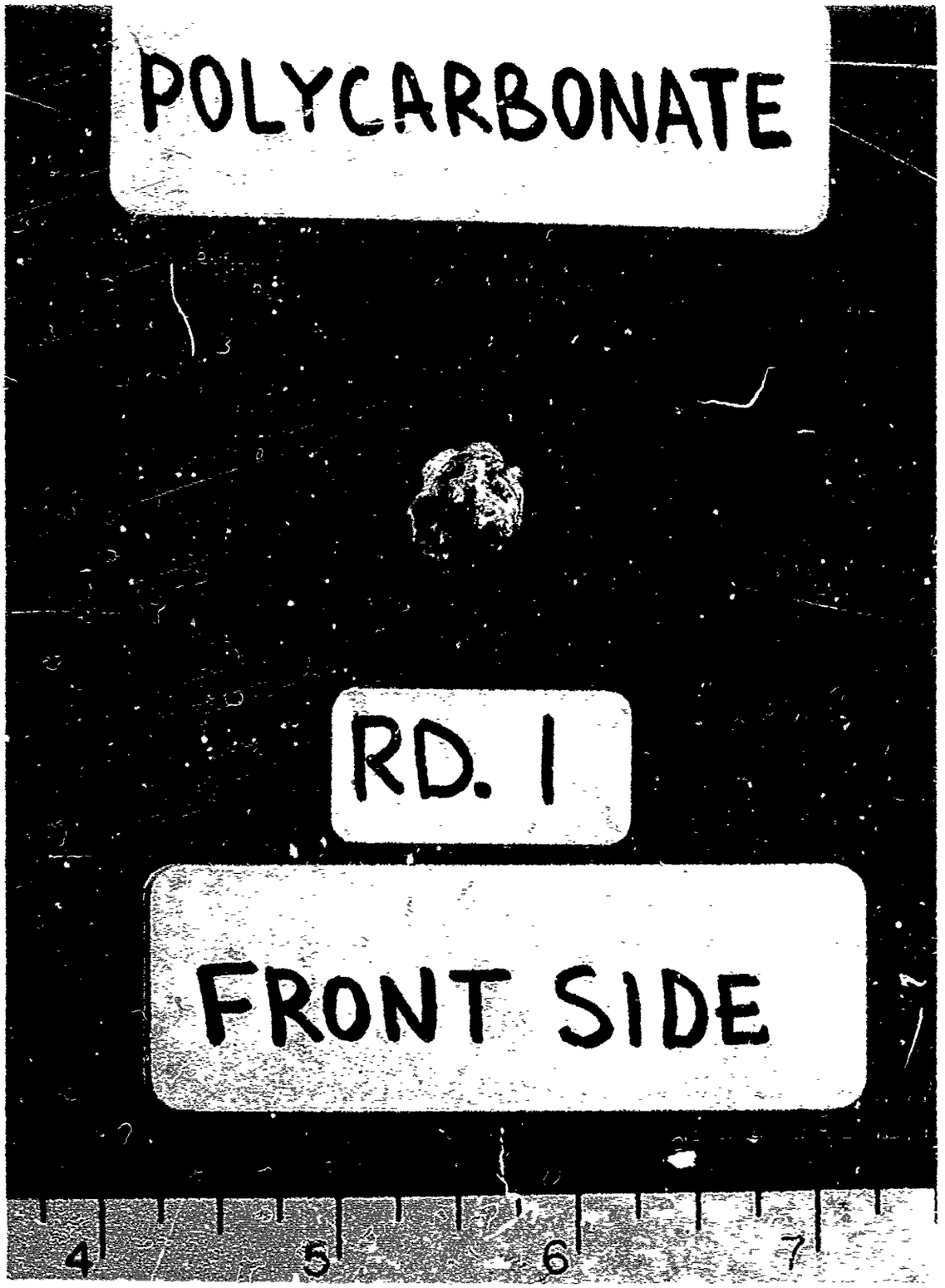


Figure 16 - UH-1 Polycarbonate Windshield Ballistic Penetration, Front Side Detail

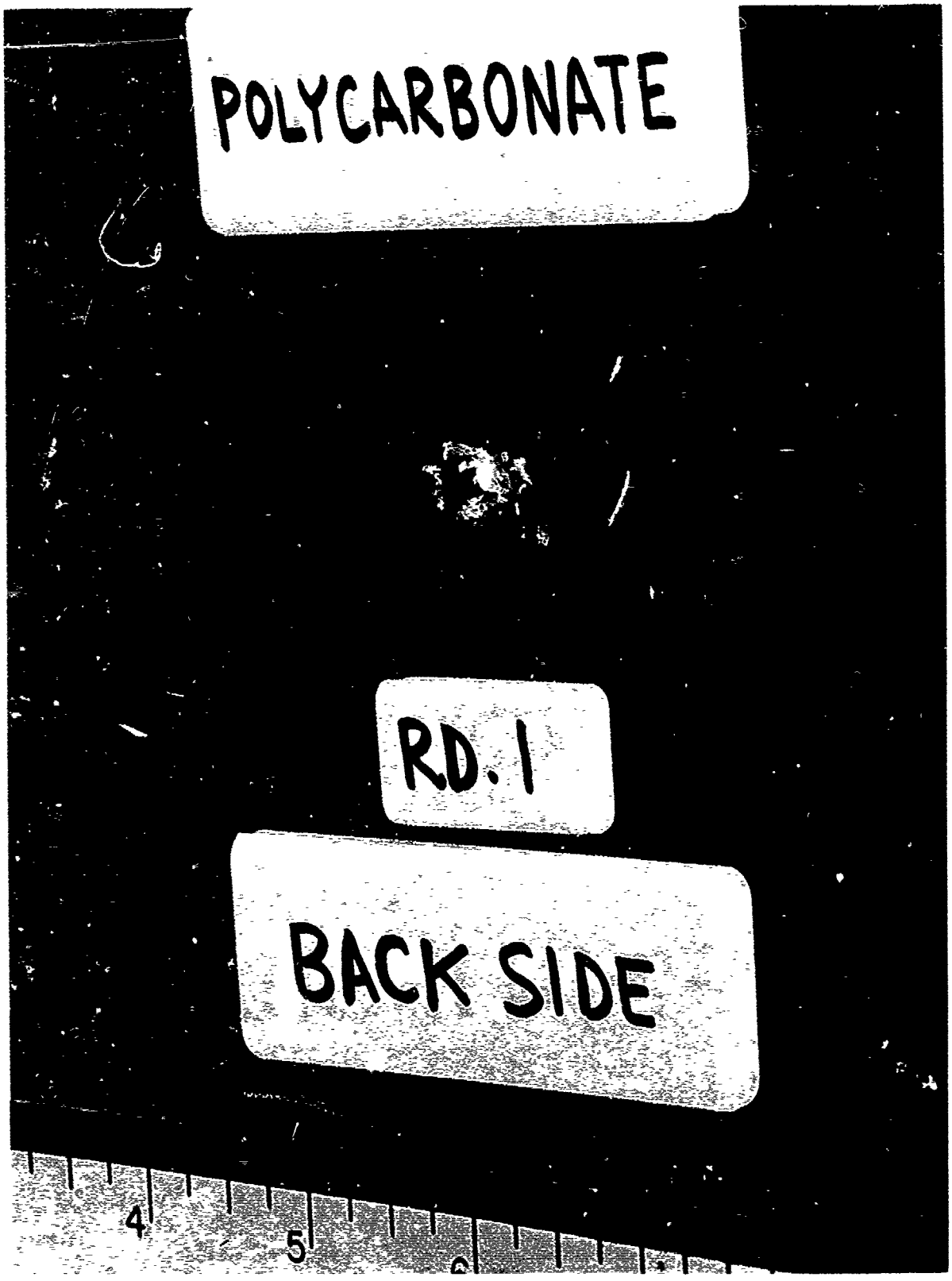


Figure 17 - UH-1 Polycarbonate Windshield Ballistic Penetration, Back Side Detail

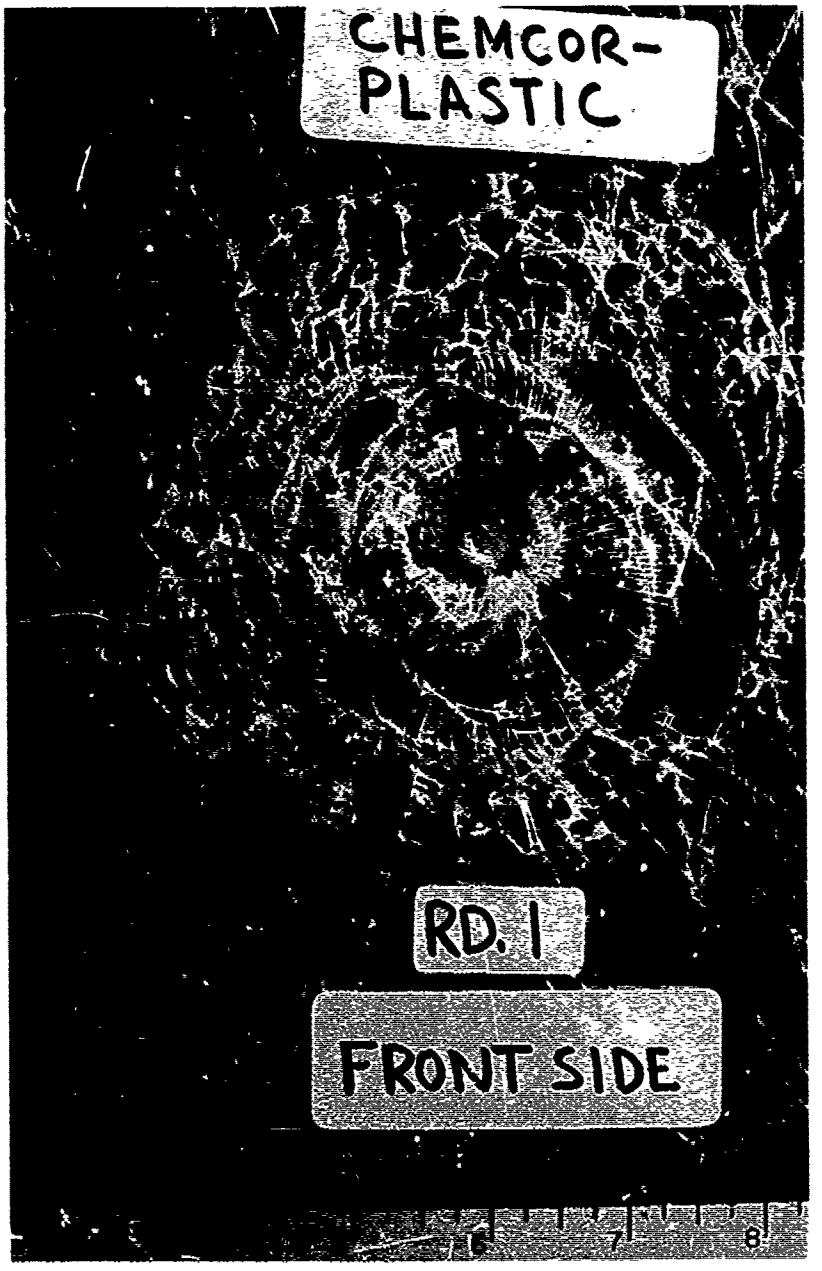


Figure 18 - UH-1 Chemcor-Plastic Windshield Ballistic Penetration, Front Side Detail

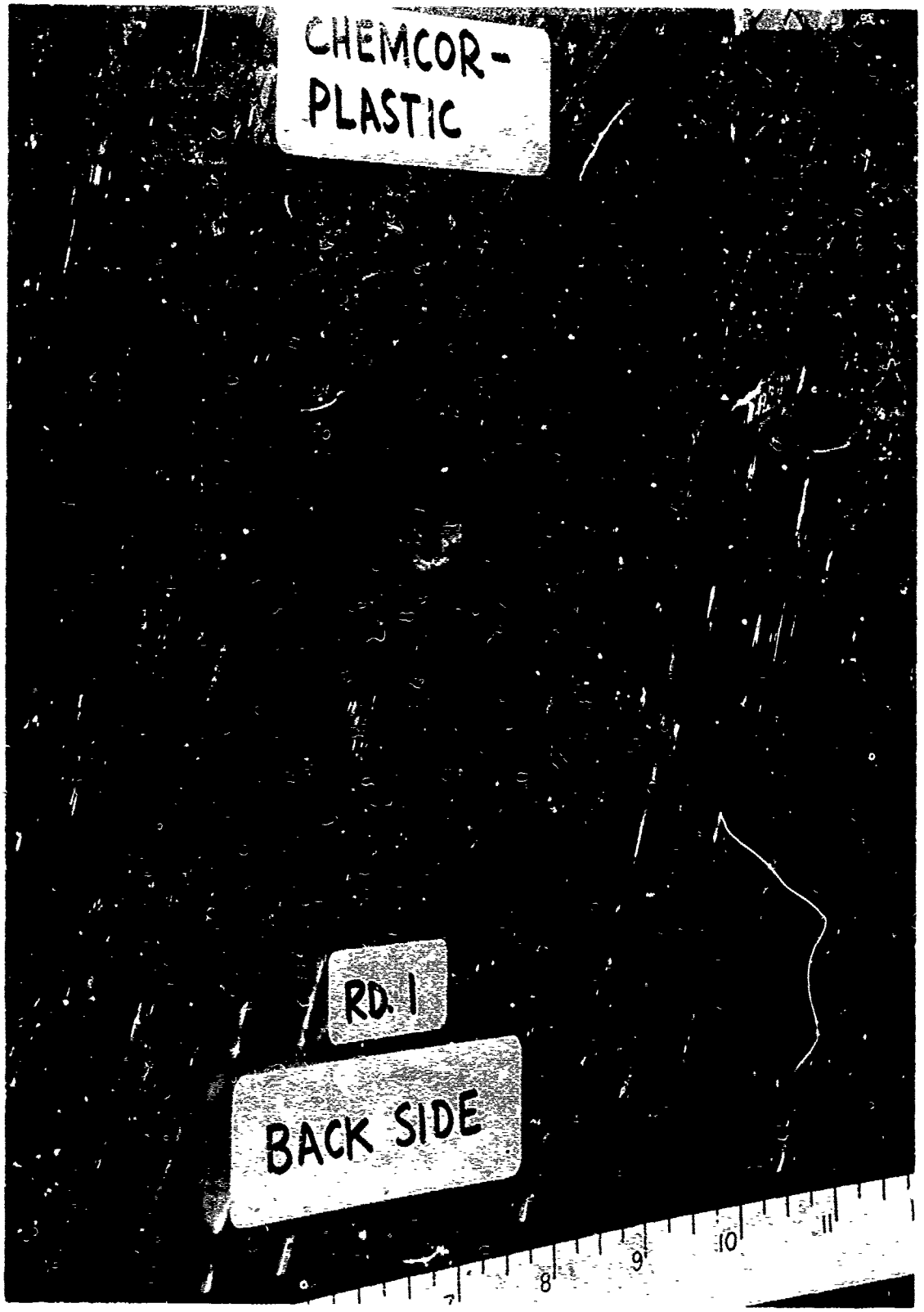


Figure 19 - UH-1 Chemcor-Plastic Windshield Ballistic Penetration, Back Side Detail

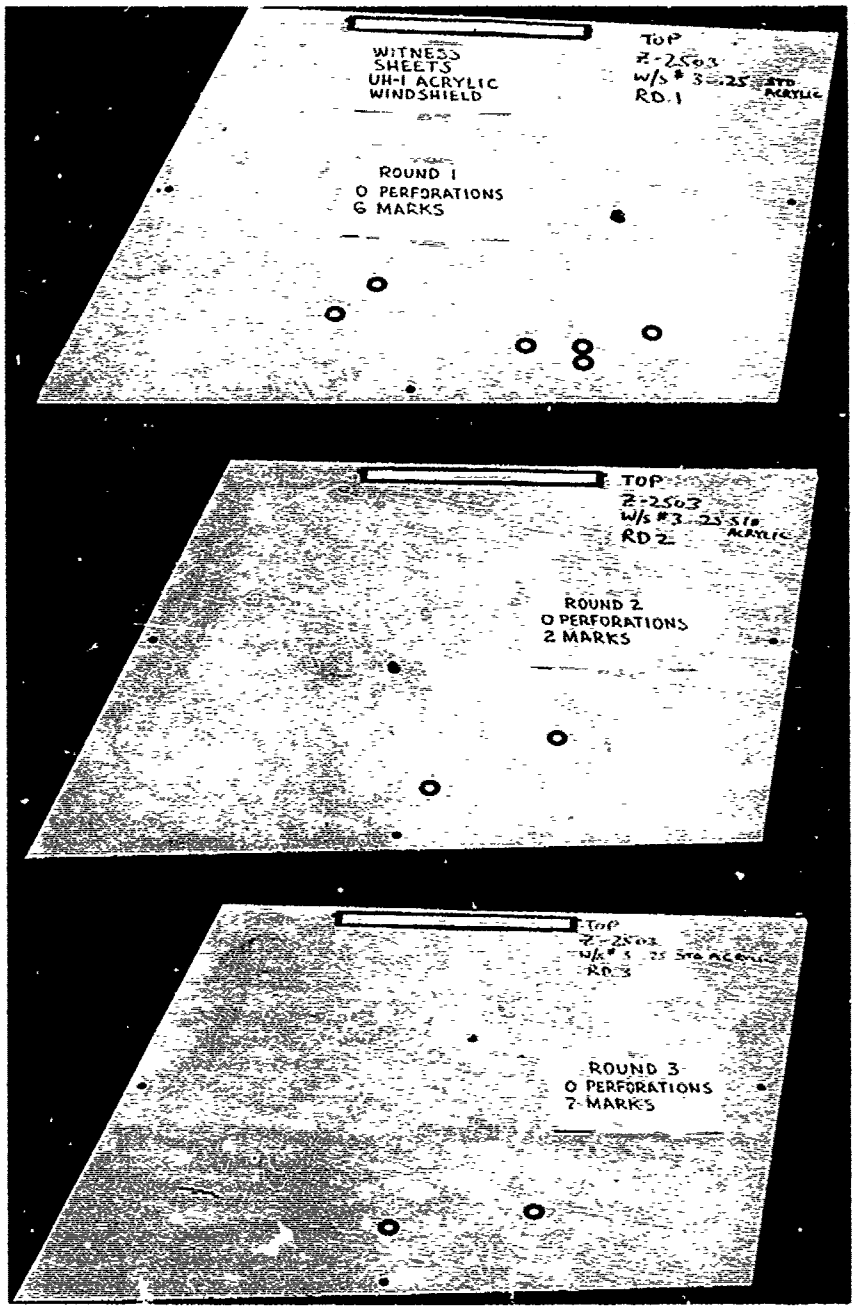


Figure 20 - UH-1 Standard Acrylic Windshield Ballistic Spall Witness Sheets, Post-Test Display

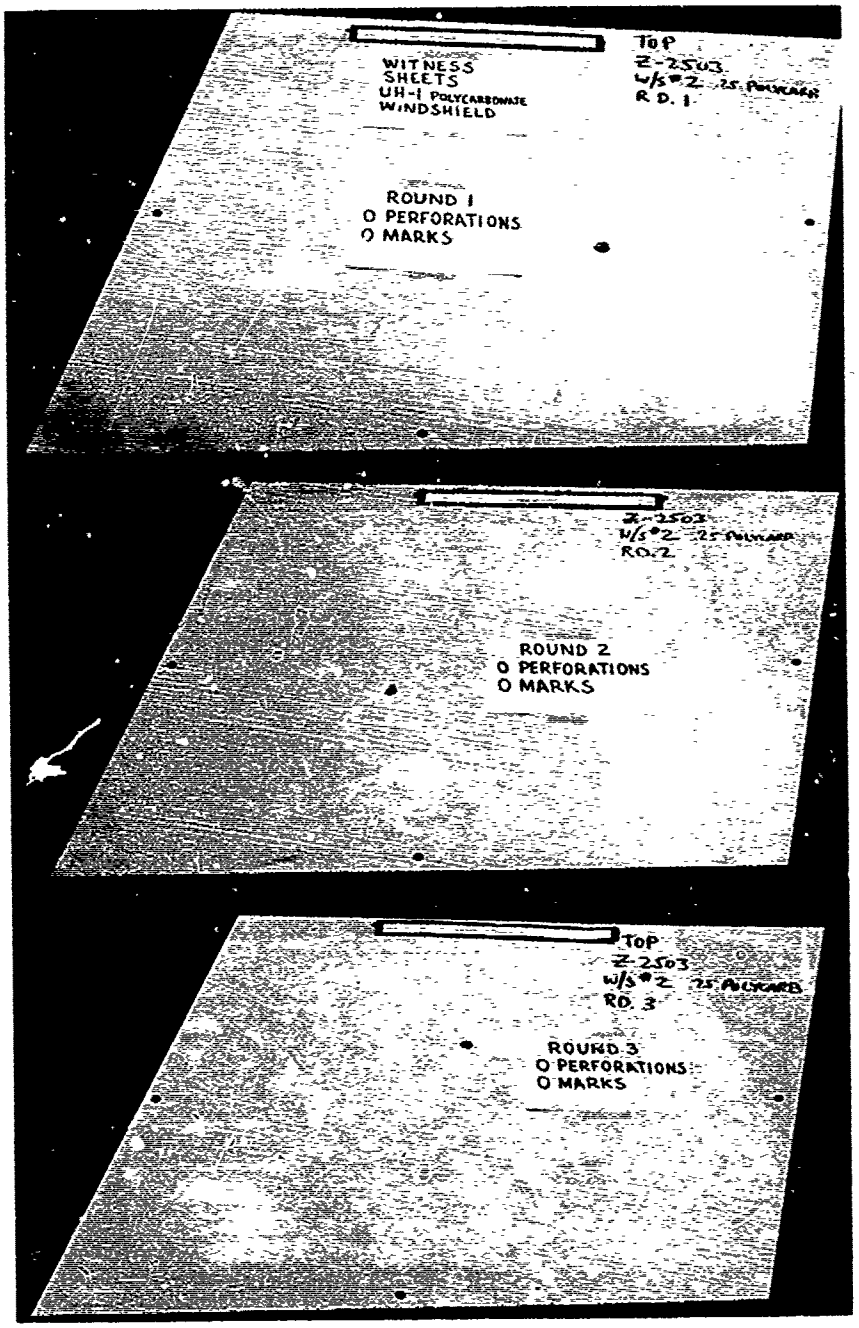


Figure 21 - UH-1 Polycarbonate Windshield Ballistic Spall Witness Sheets, Post-Test Display

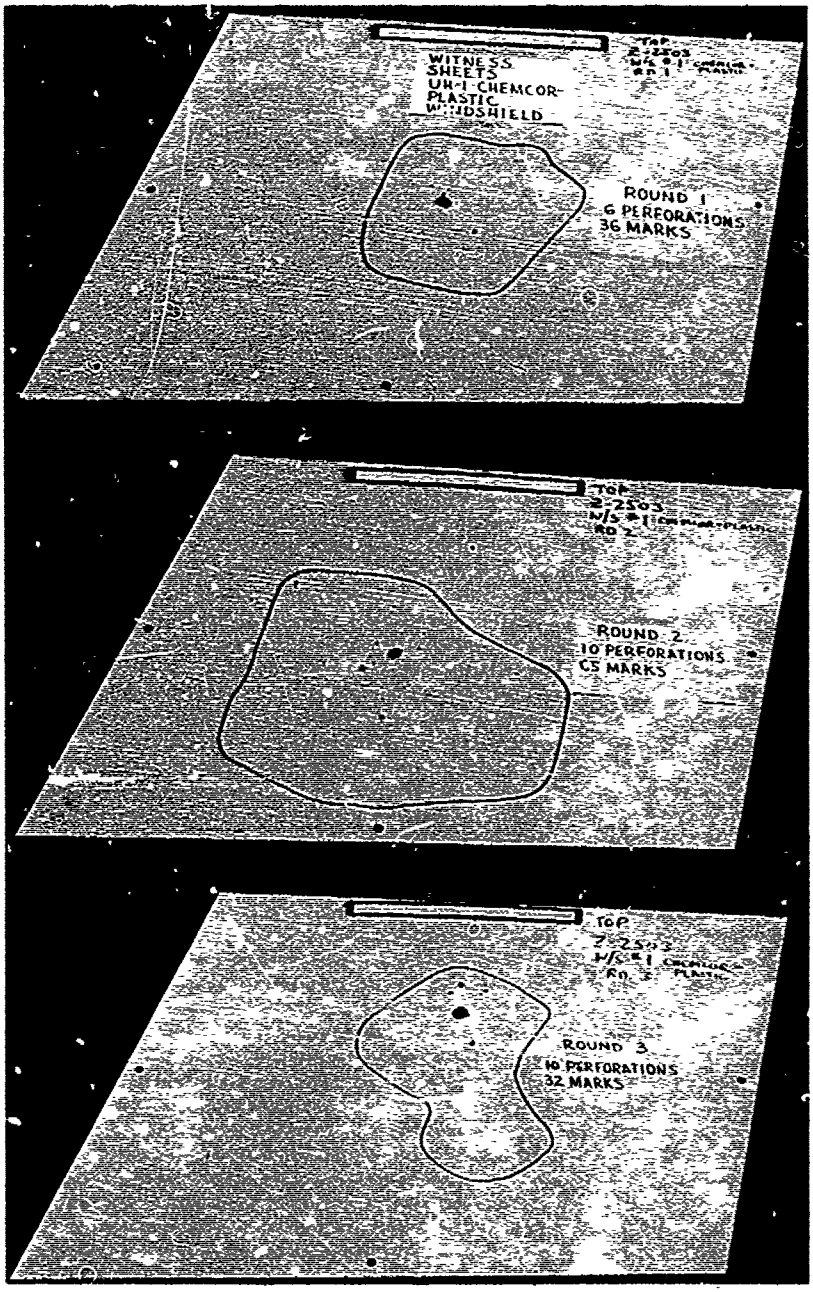


Figure 22 - UH-1 Chemcor-Plastic Windshield Ballistic Spall Witness Sheets, Post-Test Display

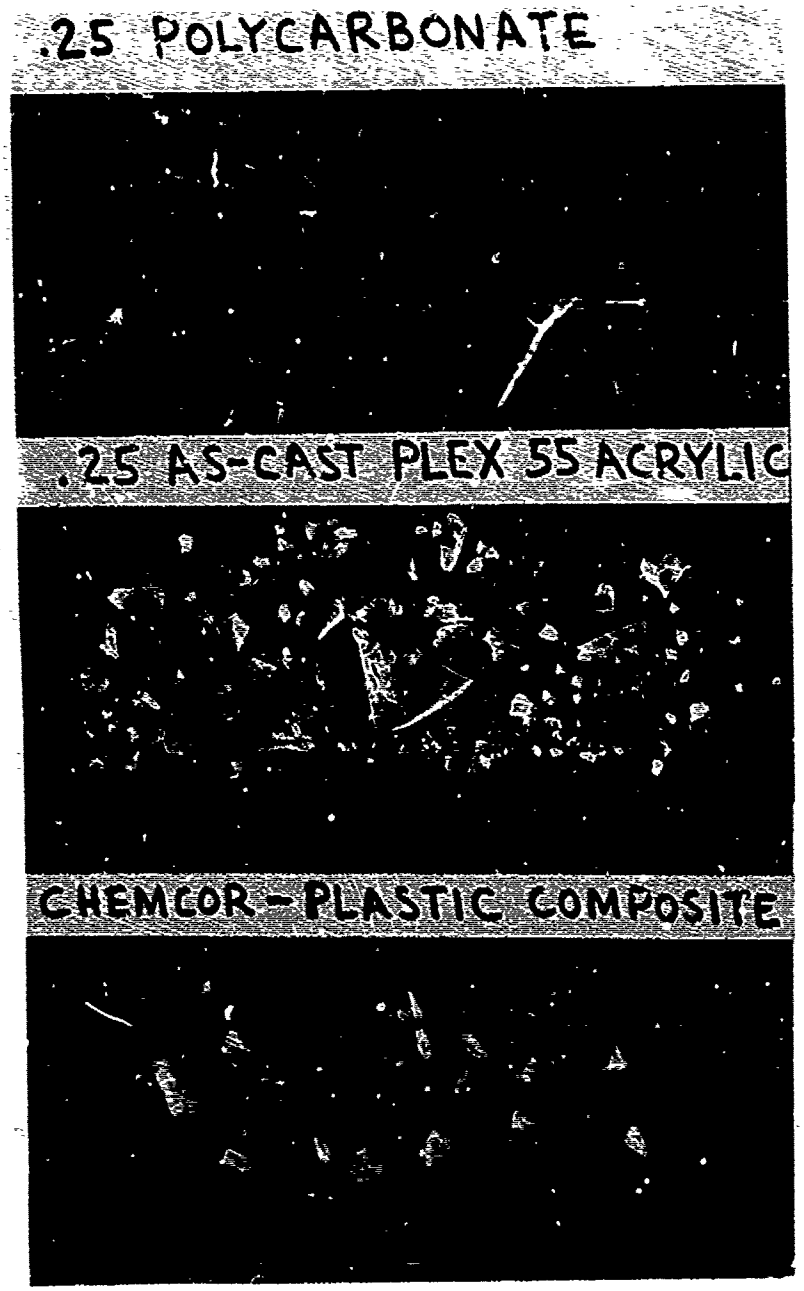


Figure 23 - Typical Ballistic Spall Particles, Single Penetration

The higher-density glass and bullet spall strike the witness sheet at nearly the same instant as the bullet.

This is followed by a cloud of slower, extremely fine particles consisting mostly of glass. The post-hit structural integrity and vision qualities of the windshield appear adequate.

2. Standard acrylic windshield -

The acrylic windshield fractures locally at the impact site. A wide variety of particle sizes is removed and widely dispersed. The acrylic particles are sharp edged and potentially dangerous. The extreme dispersion of the particles caused some of them to miss the witness sheet. None of the particles which struck the witness sheet resulted in a potentially lethal perforation.

The combined factors of quantity, dispersion, and cutting nature of the spall from the acrylic windshield are very unfavorable. The use of helmet visors by the aircrew would add significant eye protection against this type of spall. The disruptive effect on the aircrew flight control created by the spall would be considerable. The post-hit structural integrity and vision qualities for the standard acrylic windshield appear adequate.

3. Monolithic polycarbonate windshield -

The polycarbonate windshield withstood the three ballistic penetrations with a minimum amount of damage and spall.

Ductile penetration without cracking, and wound closure to approximately a 1/8-inch-diameter hole were typical. The back side spalling was limited to a very few small polycarbonate particles. None of these particles marked the witness sheets.

BIRD IMPACT TESTING

General:

The Goodyear Aerospace bird impact test facility was used to conduct all testing.

The compressed air gun used has a 60-foot-long launch tube with a 6-inch inside diameter barrel. A pressure tank assembly is attached to one end of the launch tube and has a working pressure of 250 psi. The pressure used can be controlled to obtain the bird velocity desired. The four-pound birds used for these tests were loaded in an aluminum sabot which carried them through the barrel. The aluminum container was stopped by a ring at the end of the barrel, while the bird continued to the target.

The velocity of the bird was measured by using counters to measure the time interval between breaking of "start" and "stop" wires. The stop wire is approximately six feet in front of the target window. A UH-1B fuselage was cut in two behind the front door bulkhead so as to maintain the same structural integrity as an unaltered aircraft. This fuselage section was then positioned and anchored in front of the gun where all tests were conducted (See Figure 24).

The same transparent pressure box employed in ballistic testing was used during each bird shot to simulate aerodynamic loading (See Figure 25).

High-speed motion picures were used to provide the coverage of each test. Cameras operating at 3000 frames per second were used to view the front and side of each windshield during test. The cameras were initiated automatically as a part of the firing sequence. Timed relays were used in the firing circuit to initiate the cameras prior to actuation of the gun.

Test Results:

The monolithic polycarbonate windshields were selected as the first test items.

Windshield No. 1 was impacted at 114.5 knots with a four-pound bird. This impact resulted in a diagonal crack running from the upper right-hand corner to the lower left-hand edge of the windshield when viewed from the front (See Figure 26). The bird bounced into the air, and there was no debris in back of the windshield.

Upon close examination of the part, it was noticed that the aircraft structure had bent directly above the spot where the crack terminated. The movies taken confirm the crack initiated in the center of the windshield. The fuselage was bent out into the proper position and readied for the next test.

Monolithic polycarbonate windshield No. 2 was then installed and impacted in the same manner. The impact velocity was 120.8 knots. This impact resulted in several cracks forming and the loss of two pieces of polycarbonate, one in each upper corner of the windshield. The two pieces fell outboard away from the fuselage. A break in the polycarbonate occurred along the upper edge attachment. This edge break permitted the remaining polycarbonate to flex inboard and allowed the bird to deflect upward into the pilot's compartment. The bird hit the top of the pressure box before falling to the floor. The center polycarbonate flexed back into position and was firmly held in place by the lower edge attachment (see Figure 27).

The fuselage again bent inward in the same upper inboard area, and the windshield cracks seemed to initiate from this area.

Standard acrylic windshield No. 1 was then mounted in the fuselage and was impacted with the four-pound bird traveling at 121.9 knots. The bird penetrated the windshield and hit the back of the vacuum chamber. The

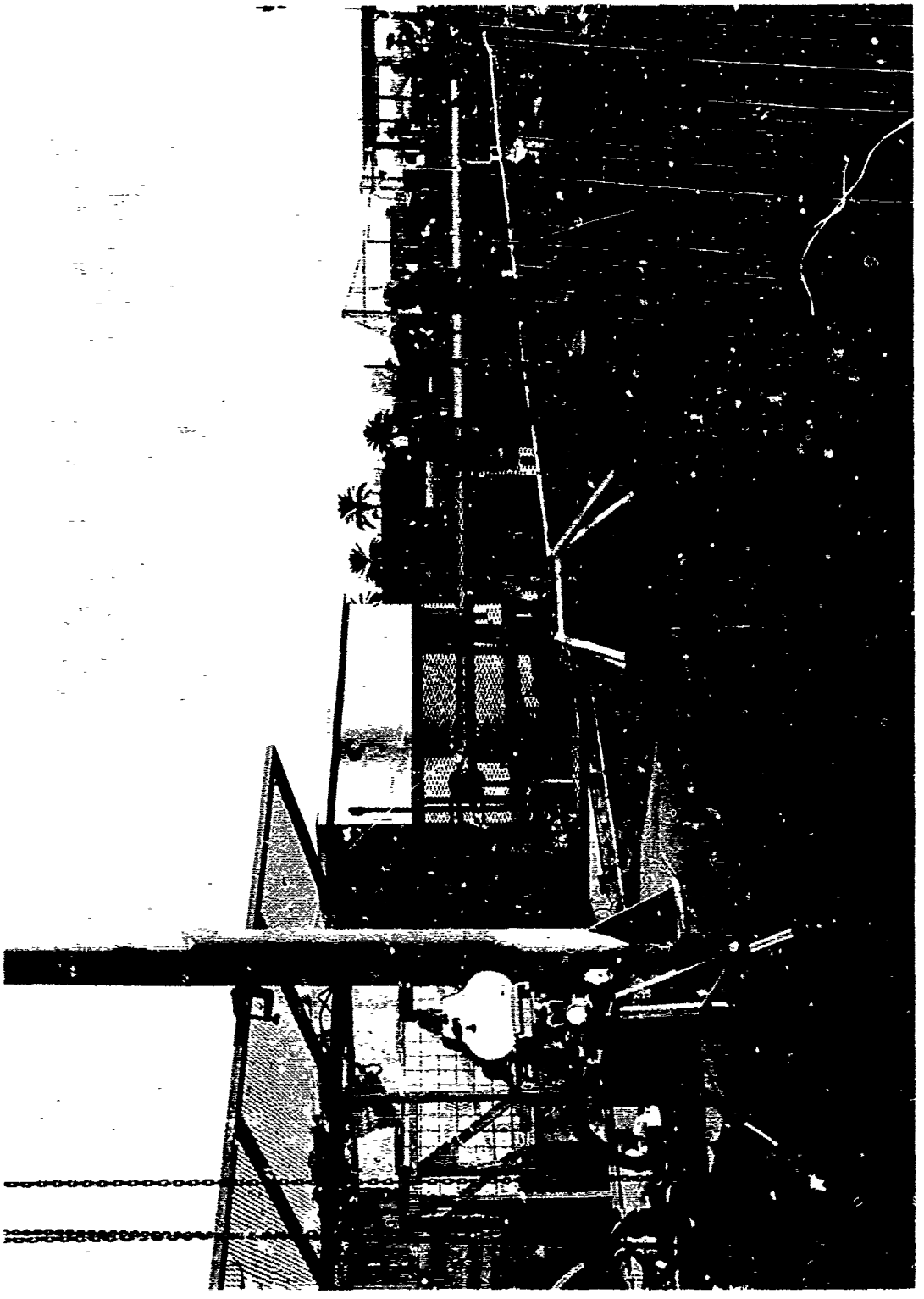


Figure 24 - Bird Impact Test Facility

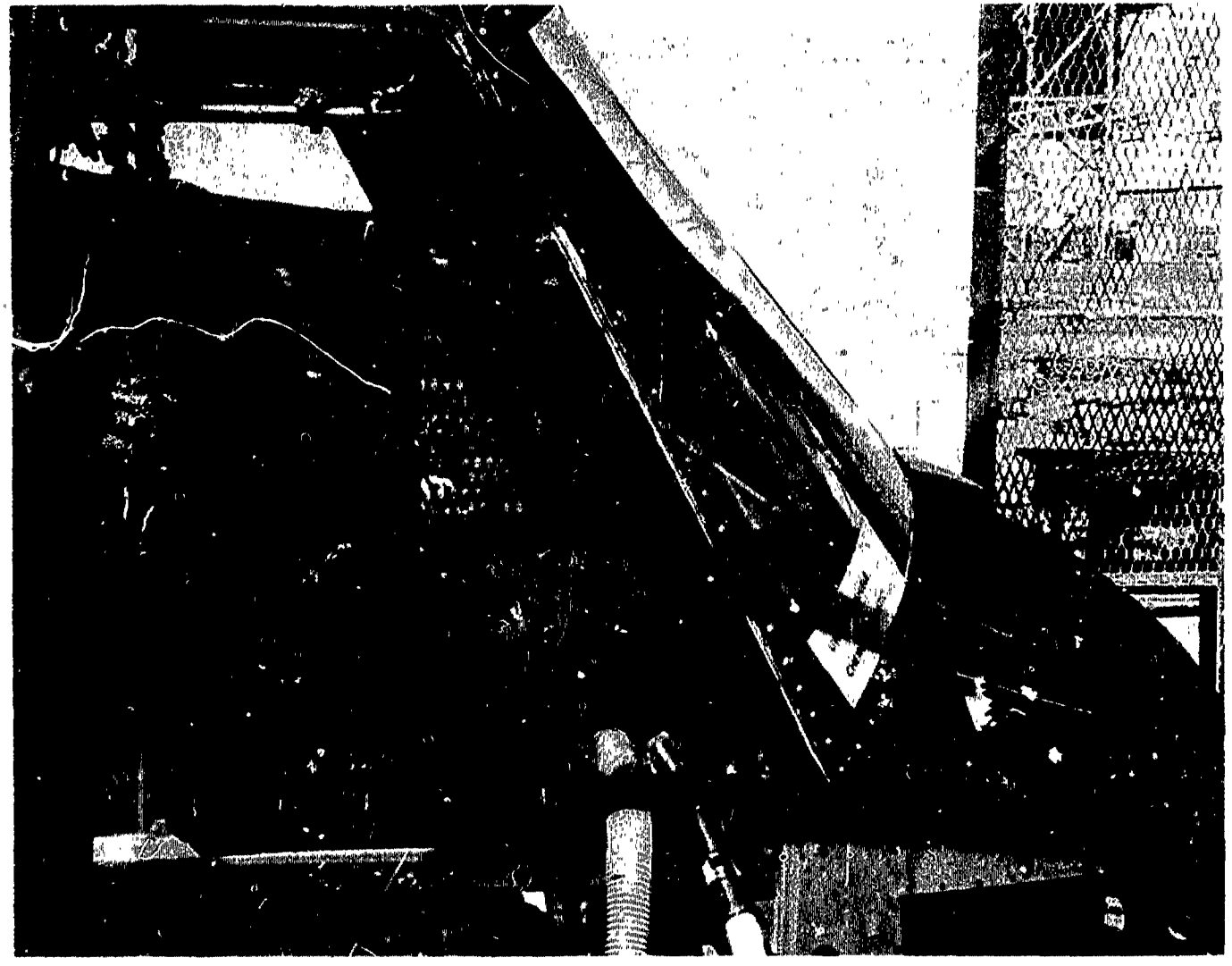


Figure 25 - Bird Impact Test Structural and Pressure Box Detail

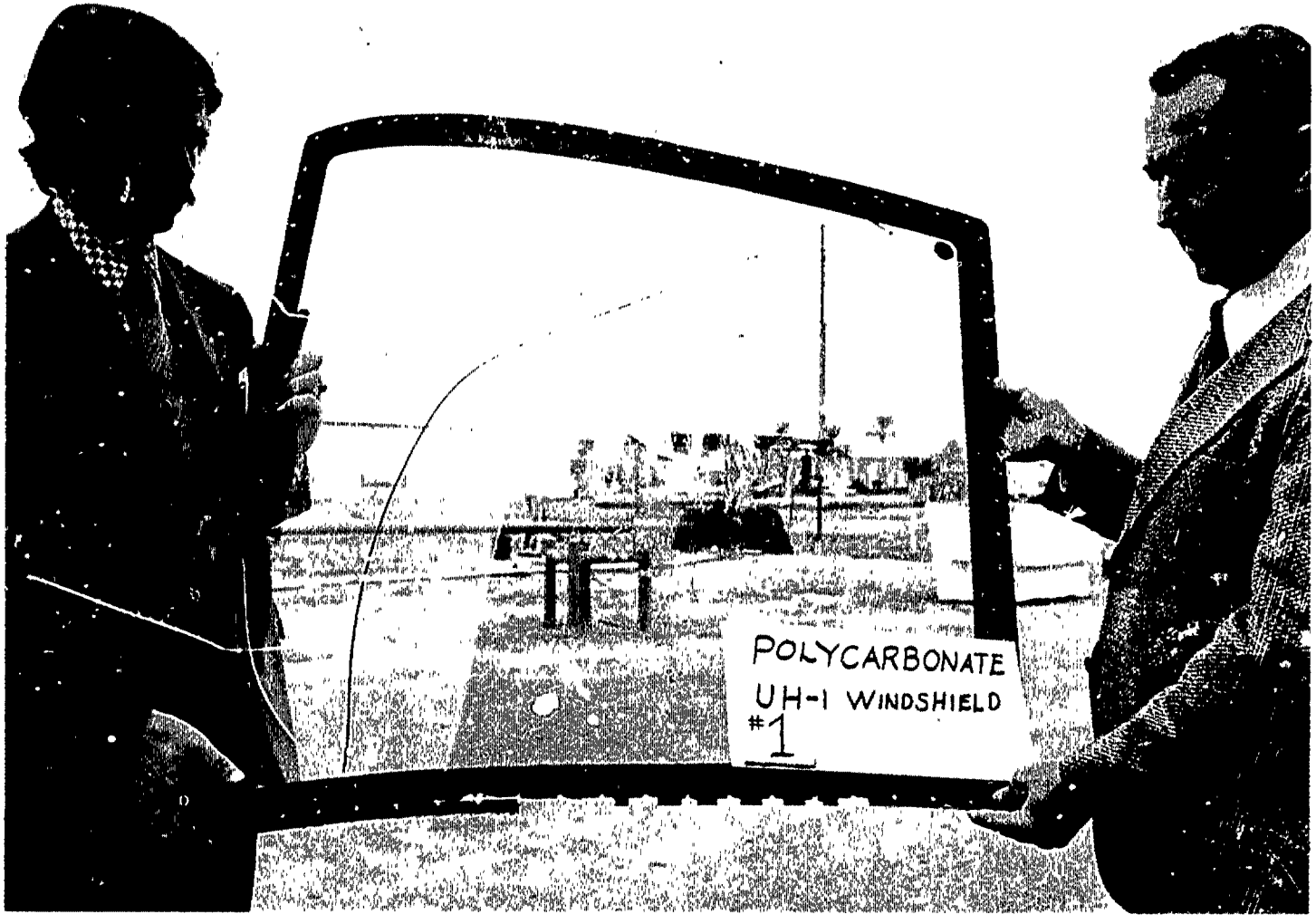


Figure 26 - Bird-Impacted UH-1 Polycarbonate Windshield Number 1



Figure 27 - Bird-Impacted UH-1 Polycarbonate Windshield Number 2

Plexiglas broke out of the frame with only a few jagged fragments remaining along the edge (See Figure 28).

The fuselage was not damaged by the impact.

Because of the catastrophic failure mode of the first standard acrylic windshield, the second standard part was fired at 85.6 knots, which is nearer the cruising speed of the UH-1 aircraft. The bird also penetrated this windshield, breaking out nearly 80 percent of the acrylic (see Figure 29).

The fifth windshield tested was the No. 1 Chemcor-plastic composite. The bird was fired at 115 knots and failed to penetrate the structure. The glass and plastic broke on the lower inboard corner at the edge attachment and bent inward sufficiently to permit small glass particles to enter the lower part of the vacuum chamber (See Figure 30). The bird bounced upward and fell about ten feet from the aircraft.

The second Chemcor-plastic windshield failed in a similar manner at 92.2 knots. No penetration of the bird occurred, but when the composite broke along the lower inboard edging, small spall particles entered the lower part of the vacuum box (See Figure 31). The bird bounced and fell approximately ten feet from the windshield.

CONCLUSIONS AND RECOMMENDATIONS

Conclusions:

Major conclusions from the test program are as follows:

1. Fabrication

   All three types of composites fabricated for this program can be manufactured with currently available materials and state-of-the-art fabrication procedures.

2. Abrasion Resistance

   Flight testing of the Abcite coated polycarbonate windshields demonstrated the feasibility of using a protective coating for enhancement of abrasion resistance and increase of serviceability.

   Glass cladding demonstrated superior abrasion resistance over either plain acrylic or Abcite coated polycarbonate.

3. Ballistic Performance

   a. Ballistic impact of the monolithic polycarbonate windshields shows that very little spall is released and that partial closure of the wound takes place. This construction proved superior in this respect to the other two types tested.

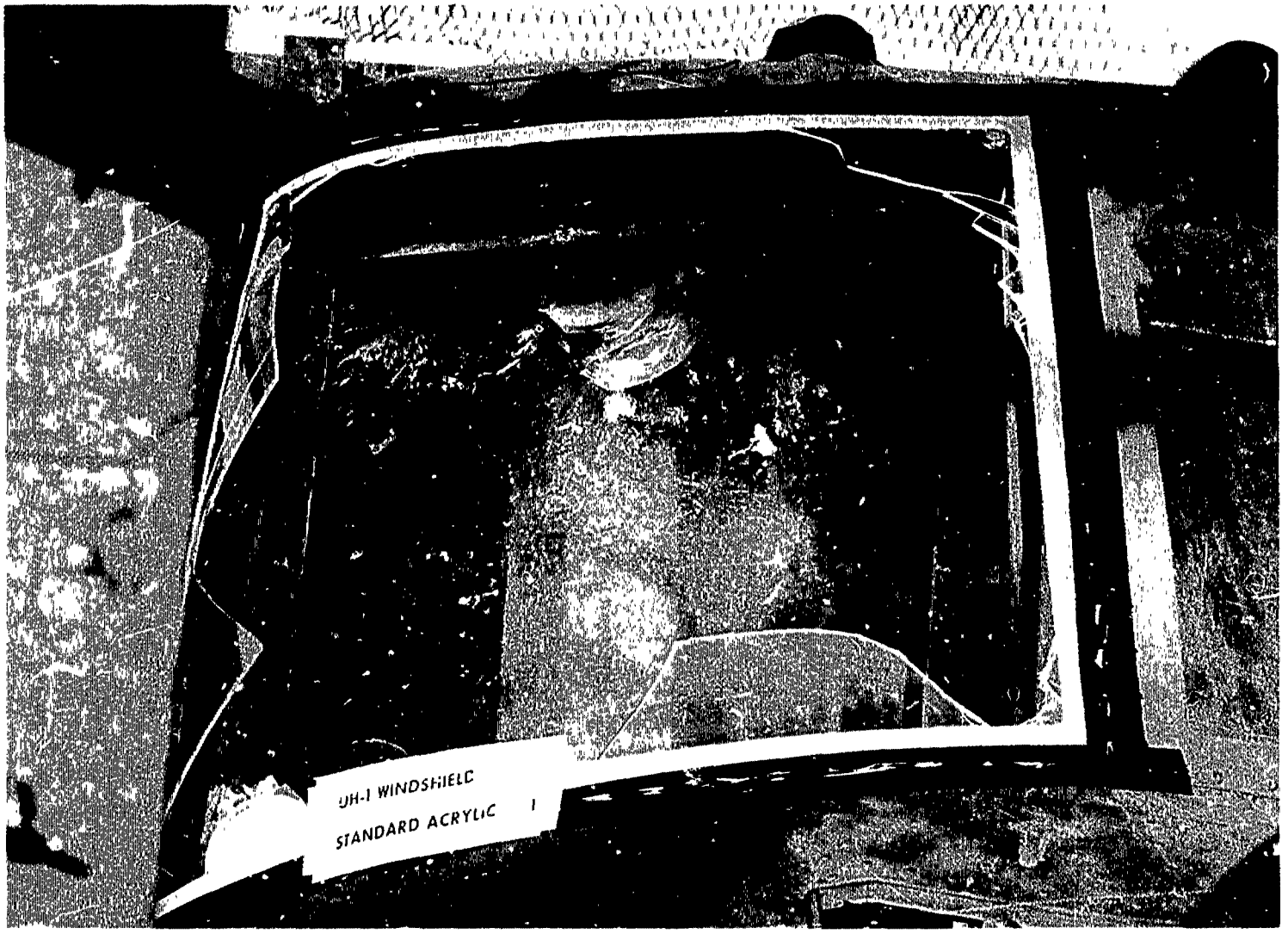


Figure 28 - Bird-Impacted UH-1 Standard Acrylic Windshield Number 1

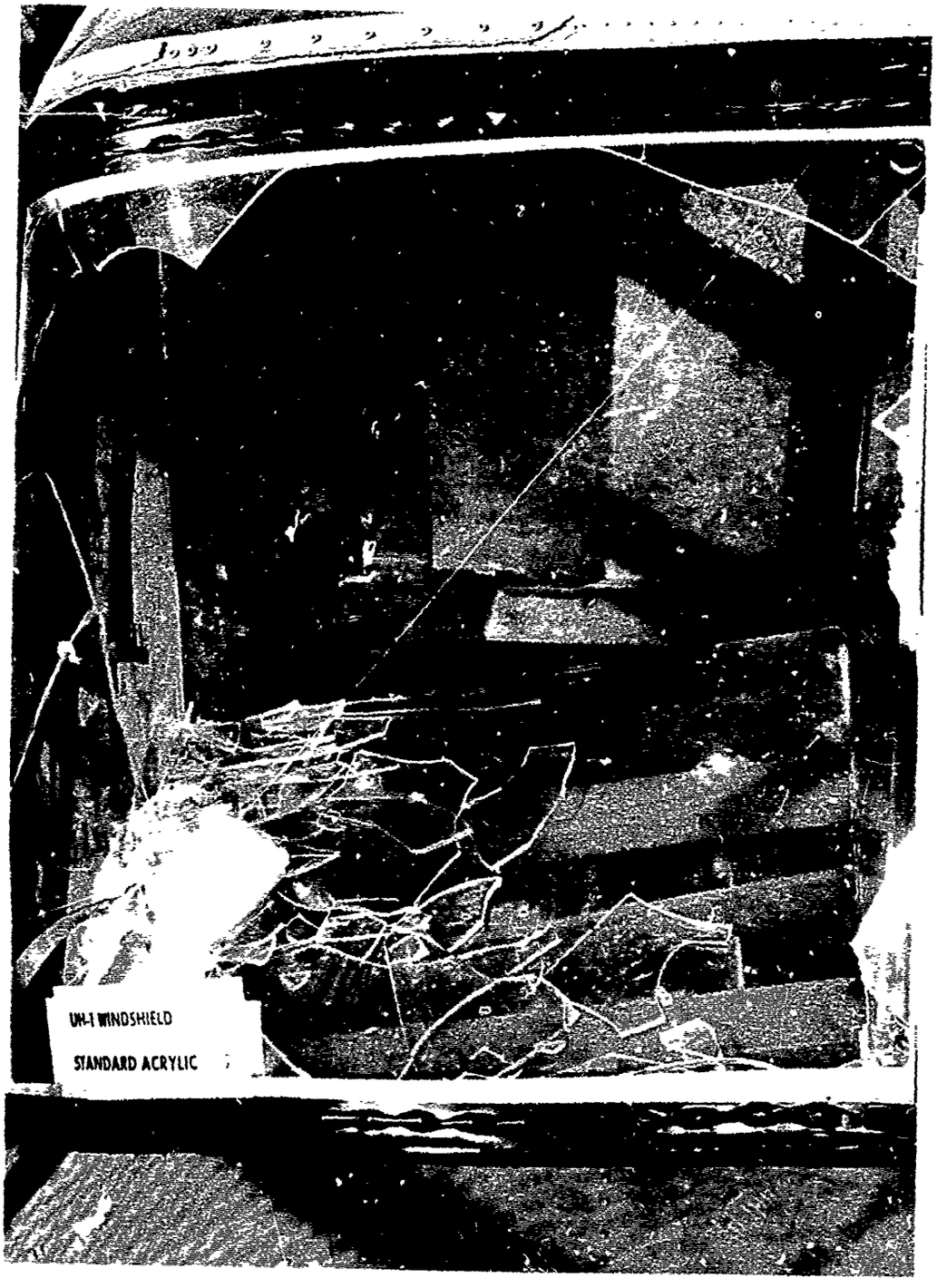


Figure 29 - Bird-Impacted UH-1 Standard Acrylic Windshield Number 2



Figure 30 - Bird-Impacted Chemcor-Plastic Windshield Number 1



Figure 31 - Bird-Impacted UH-1 Chemcor-Plastic Windshield Number 2

b. Spall from ballistic impact of the standard acrylic windshield results in many widely dispersed, sharp-edged fragments of considerably varying sizes. The spall particles generated did not appear to have potentially lethal pentrating capability.

The ballistic characteristics of this windshield rank second to those of the monolithic polycarbonate type.

c. The Chemcor-plastic windshields were the only articles tested which generated spall particles having potentially lethal penetrating characteristics. The plastic backing ply acts to restrict the dispersion of the spall, particularly the heavir particles passed. Many very fine glass particles follow the heavier particles in a more widely dispersed cloud. The overall spalling characteristics of the Chemcor-plastic windshields were the least acceptable of all windshields tested in this program.

4. Bird Impact Study

a. Both the monolithic polycarbonate with abrasion coating and the Chemcor-plastic composite construction offer far greater bird strike protection to UH-1 aircrews than the standard acrylic windshield.

b. The standard acrylic windshield at both the cruising speed (90 knots) and the maximum speed of the UH-1 is incapable of defeating a bird strike. The as-cast Plexiglas breaks into large, sharp-edged fragments which could cause serious injury to the aircrew.

c. The two monolithic polycarbonate windshields tested indicated they would provide considerable protection against bird strikes, even at redline speed (120 knots) of the UH-1 aircraft. Improved restraint by the edgeband appears necessary to improve bird strike performance.

d. Chemcor-plastic composite offers bird protection from cruising speed (90 knots) to maximum redline speed (120 knots) of the UH-1 aircraft. Some breakage occurred along the edgeband transition of both windshields in the lower inboard corner. The breakage allowed spall to enter the cabin area. A redesign of the edge attachment is needed to withstand the bird strike loading.

Recommendations:

The favorable abrasion resistance and excellent impact resistant properties demonstrated by the Abcite coated polycarbonate prototype design results in the recommendation that this configuration would be feasible and desirable as a retrofit item on aircraft operating in severe field or combat situations.

Based on this program the following recommendations are also made:

1. The bird strike information provided during this study offers designers of helicopter transparencies data which will be useful when bird defeat and spall resistance are factors which must be considered.

   However, since the bird strike data obtained on this program are based on very limited testing, it is recommended that additional parts be tested to define more exactly the threshold velocity of each of the monolithic polycarbonate and the Chemcor-plastic windshield designs.

2. It appears that the bird resistance of both the monolithic polycarbonate and the Chemcor-plastic windshield can be improved by a redesign of the edge attachments. The results of the testing to date have emphasized the importance of edge restraint materials and design in withstanding such loads. Additional bird strike tests should be employed during any redesign effort.

3. Additional bird strike tests should be conducted on the redesigned windshields to document the effect of the following parameters on performance:

   a. Temperature

   b. Outdoor weathering (accelerated exposure)

   c. Bird weight

   d. Effect of strike proximity to edgeband.

4. Test articles of the redesigned windshields should be installed on aircraft for flight testing. This will allow evaluation of the performance and maintainability of the articles in the service environment.

REFERENCES

1. PLUMER, J. R., *"Development of Scratch and Spall-Resistant Windshields,"* Army Materials and Mechanics Research Center, AMMRC TR 74-19, August 1974.

2. Technical Manual 55-1520-210-34, *"Direct Support and General Support Maintenance Manual,"* 10 September 1972, revised 16 August 1974.

3. Technical Manual 55-1520-210-20, *"Organizational Maintenance Manual,"* 10 September 1971, revised 9 October 1974.

4. a. Letter, AMSAV-EFT, Headquarters, U. S. Army Aviation Systems Command, 20 November 1972, Subject. *"Request for UH-1D/H Product Improvement Windshield Tests."*

5. James. H; Ingelse, A.O.; *"Design Test and Acceptance Criteria for Army Helicopter Transparent Structures,"* USAAMRDL, TR-73-19, Ft. Eustis, VA., May 1973.

6. Watertown Arsenal Laboratories Monograph Series Report WAL MS-12, *"Ballistic Concepts Employed in Testing Lightweight Armor,"* 5 October 1959.

DESIGN AND DEVELOPMENT OF HELICOPTER TRANSPARENT ENCLOSURES

J. H. McGarvey
U.S. Army Air Mobility Research and Development Laboratory
Fort Eustis, Virginia

and

B. F. Kay
Sikorsky Aircraft Division
United Technologies Corporation
Stratford, Connecticut

DESIGN AND DEVELOPMENT OF HELICOPTER TRANSPARENT ENCLOSURES

J. H. McGarvey - U. S. Army Air Mobility Research and Development Laboratory
B. F. Kay - Sikorsky Aircraft Division, United Technologies Corporation

ABSTRACT

Sikorsky Aircraft is currently engaged in a program sponsored by the U. S. Army Air Mobility Research and Development Laboratory to develop design, acceptance and test criteria for helicopter transparent enclosures. In addition, a comprehensive Helicopter Transparent Enclosures Design Handbook will be prepared. The effort is being accomplished in three major tasks:

* Establishment of Preliminary Criteria
* Verification of Criteria by Analysis and Test
* Preparation of Design Handbook

In general, criteria shall be substantiated using published data and historical acceptance. Where there is a lack of criteria, or where conflicting criteria exist, analysis and tests are being performed. Emphasis is placed on structural substantiation methods and the airframe/transparency interface.

Specific tasks that have been completed or are in progress include the following:

Windshield endurance tests are being performed in a manner intended to duplicate actual service conditions. The tests are being conducted with several types of structural loading applied to different windshield types, while subjected to various environmental conditions. Suitable instrumentation is used to determine critical loading combinations. The actual load spectrum used for these tests are based on typical utility helicopter mission profiles.

A NASTRAN (NASA STRuctural ANalysis) finite element analysis has been performed to determine the applicability of this type of analysis for helicopter cockpits. Finite element analyses can more accurately predict the internal stress distributions in complex structures, which can result in potential weight savings and improvements in component reliability. The analyses performed in this study showed that stresses induced in windshields from fuselage wracking can be significant.

As abrasion has been the number one cause for helicopter transparency replacements, a series of tests were conducted to enable simulation of the various forms of abrasion in the laboratory. The tests were conducted on glass, acrylic and polycarbonate, with the acrylic and polycarbonate materials with and without abrasion resistant hardcoats.

INTRODUCTION

Helicopter transparencies have a relatively poor service record and represent an exceptionally high percentage of airframe maintenance costs. Some of the more plausible reasons why are: (1) Helicopter transparency requirements have just recently become sophisticated and consequently, transparency expertise remains principally fixed-wing oriented; and (2) Because of their complexity, helicopter development is concentrated on dynamic systems, thereby limiting the scope and vigor of helicopter transparency R&D pursuits.

The Army, recognizing these deficiencies, funded two parallel studies conducted by PPG Industries and Goodyear Aerospace Corporation to document the scope of the problem, and recommend action in the form of design, test and acceptance criteria. Results of these studies, published in USAAMRDL Technical Reports TR 73-19[1] and TR 73-65[2], show that windshields are a major source of airframe damage - particularly heated windshields. Some heated windshields have a Mean Time Between Failure (MTBF) as low as 200-300 hours. Furthermore, many scratches, pits, scores, and overall optically degraded transparencies are "lived with" in the field. Thus, the reported time between removals is artificially higher than warranted. Some of these deficiencies persist well after the helicopter has been put into service. These studies also pointed out that for a given type or class of helicopter, there is no generally accepted method for ranking the relative importance of transparency characteristics leading to an effective trade-off of the many conflicting requirements. The necessity for a major effort to develop design, test and acceptance criteria for helicopter transparent enclosures is evident.

The Eustis Directorate, USAMMRDL awarded a contract in June of 1974 to Sikorsky Aircraft which is intended to establish validated design, acceptance and test criteria based upon additional research and extensive laboratory and analytical studies. Emphasis is being placed on structural substantiation methods and the airframe transparency interface. A comprehensive Design Handbook for Helicopter Transparent Enclosures will also be produced as a product of the work performed in this program. The effort is being accomplished in three major tasks:

* Establishment of Preliminary Criteria
* Verification of Criteria by Analysis and Test
* Preparation of Design Handbook

This paper is, in effect, an interim report on some of the noteworthy results achieved to date. The program final report and Design Handbook are scheduled for release during the latter part of 1976.

Some of the specific tasks that have been completed or are in progress are described in this paper.

Structural Endurance Tests

Existing structural qualification tests are not comprehensive enough to support high MTBF's. In order to formulate meaningful qualification tests for transparencies, the magnitude as well as frequency of occurrence for all loading conditions must be known This total loading environment for helicopters must include the effects of aerodynamic pressure, maneuvers and gust loads, temperature, humidity and vibration, all of which may be coupled to various degrees.

Helicopter operations are essentially conducted at low altitude where local geographic weather conditions prevail. This means that undue conservatism would result if extreme MIL-SPEC environments (-65°F or +160°F) were assumed to occur continuously and simultaneously with all structural loading conditions. To establish more realistic conditions, actual worldwide climatic variations[3] were reviewed and typical climates were analyzed.

From this analysis, two idealized climates were conservatively created to represent a hot climate and a cold climate for structural endurance testing. Tables I and II summarize this effort. High temperature (160°F) exposure is omitted from the hot-climate tabulation because it is not representative of flight conditions, but only ground or storage conditions.

TABLE I

Cold Climate Temperature Distribution

Temperature	Percent of Time
+40°F	45%
+25°F	25%
-25°F	25%
-65°F	5%

TABLE II

Hot Climate Temperature Distribution

Temperature	Percent of Time
100°F	95%
125°F	5%

Similarly, the ground - air-ground spectrum for helicopters cannot be based on maximum pressure loading alone as commonly accepted for fixed-wing aircraft because such conditions are encountered only during infrequent high-speed maneuvers. The utility helicopter mission profile was analyzed as a case study to determine what a typical helicopter usage spectrum might look like. The ground - air-ground (GAG) cycle was derived from criteria calling for four flights per hour, coupled conservatively with the 20,000 peak load occurrences per 5000 flight hours. Table III shows the results of this analysis.

TABLE III

Typical Utility Helicopter Usage Spectrum

Load Factor	Velocity	Vibration	Pressure	Percent Time
1.0 g	V max	0.8 g	1 psi	5%
2.25 g	1.1 V_{cruise}	0.6 g	0.75 psi	5%
1.5 g	1.1 V_{cruise}	0.4 g	0.62 psi	90%

The criteria developed for the utility helicopter is being used in instrumented structural/environmental tests designed to quantitatively show the effects and interaction of complex loading conditions that affect the life of a windshield. The basic hypothesis is that once the cause of failure can be isolated and studied under controlled conditions, improvements can be developed that will extend service life. Proof of this concept for fixed wing aircraft transparencies has been established in References 4 and 5.

NASTRAN Finite Element Analysis

The expansive transparent areas found on most helicopters offer potentially significant savings in weight when thicknesses are minimized. In order to achieve this objective, while maintaining structural integrity, the magnitude of the design operating stresses in the transparent enclosure must be reliably known. Conventional "hand" methods of rigid body stress analysis have significant deficiencies when applied to typical helicopter transparencies. A more accurate approach is to use a finite element analysis.

Also, in the past, canopies for helicopters have been considered secondary structure, and analyzed only for local airloads and inertia loads. Influence on overall cockpit bending was assumed negligible, and usually ignored during structural analysis. However, since canopies are rigidly fastened to the primary structure, secondary loads can be induced as a result of primary structure deflections from application of flight loads.

NASTRAN can be used to determine; (1) The amount of fuselage wracking that can occur during accelerating maneuvers; and (2) The effect on windshield stress.

Case Study

A Sikorsky YUH-60A UTTAS (Utility Tactical Transport Aircraft System) nose section was used as a model for a case study. UTTAS represents the newest generation of Army helicopters, has relatively large windshields supported by slender posts (Figure 1), and is subjected to high aerodynamic pressure and maneuver loads.



Figure 1. Sikorsky YUH-60A UTTAS Helicopter.

Specific factors investigated in the NASTRAN analysis were:

* Effect of fuselage deformation on windshield stress
* Interaction between membrane and bending stresses due to transparency curvature
* Effects of elastic supports on windshield stress
* Effects of large displacements on analytical accuracy

NASTRAN Model Description

Two NASTRAN models were constructed which varied in size and degree of refinement. The basic model contained the upper cockpit, windshields, lower cockpit and forward cabin. The windshield model was composed of 200 TRIA1 triangular plate bending elements having six degrees of freedom. TRIA1 is a triangular plate bending element which allows for independent specification of membrane and bending properties. The basic model is shown in Figure 2.

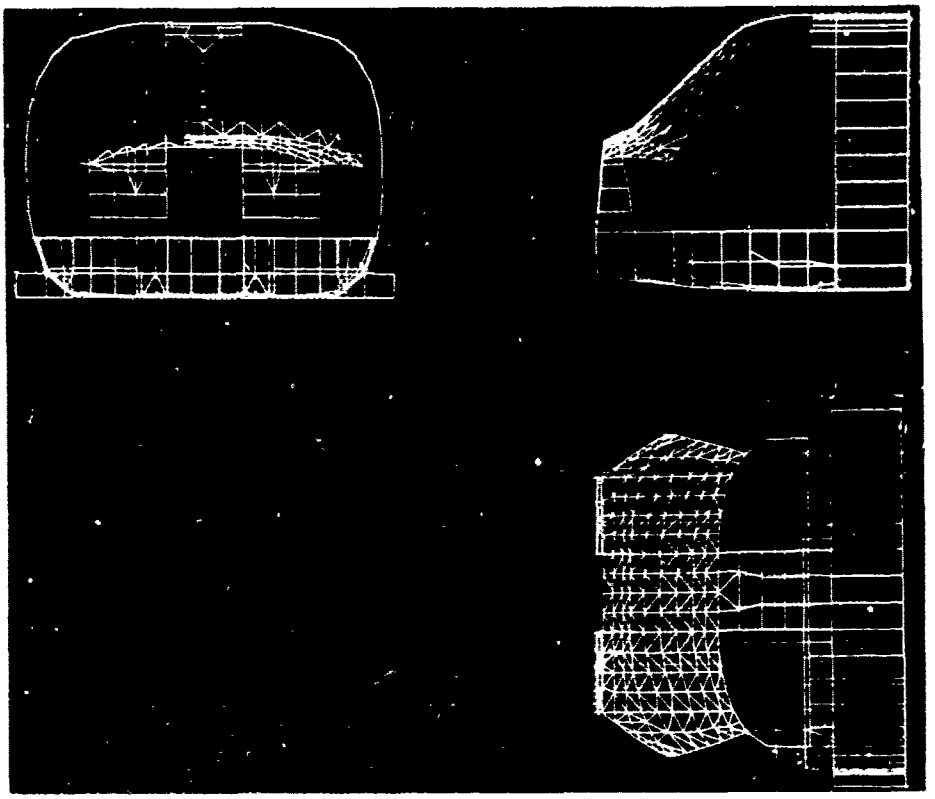


Figure 2. NASTRAN Model of YUH-60A Nose Section.

The second model, identical in all respects to the basic model except for omission of windshields, was constructed to obtain displacements of the windshield support structure from inertia loading.

Three different laminated windshields were modeled; glass/glass, glass/acrylic, and acrylic/polyester. All were idealized as monolithic structures.

DISCUSSION OF RESULTS

Effects of Fuselage Deformation on Windshield Stress

To evaluate the effects of fuselage deformation on windshield stress, an inertial loading condition representative of a symmetrical pullout maneuver was analyzed using the NASTRAN model, with and without the windshields installed. This condition produced critical down bending loads in the area of the cockpit.

First, the analysis was performed on the model without the windshields. The results of this analysis showed that the displacements that occur during maneuvers are significant. Figure 3 is a profile view of the center post deflected shape. Note that the post has a maximum camber of approximately 1/16 inch. Since the post is stiffer than the windshield, this camber will induce windshield stresses.

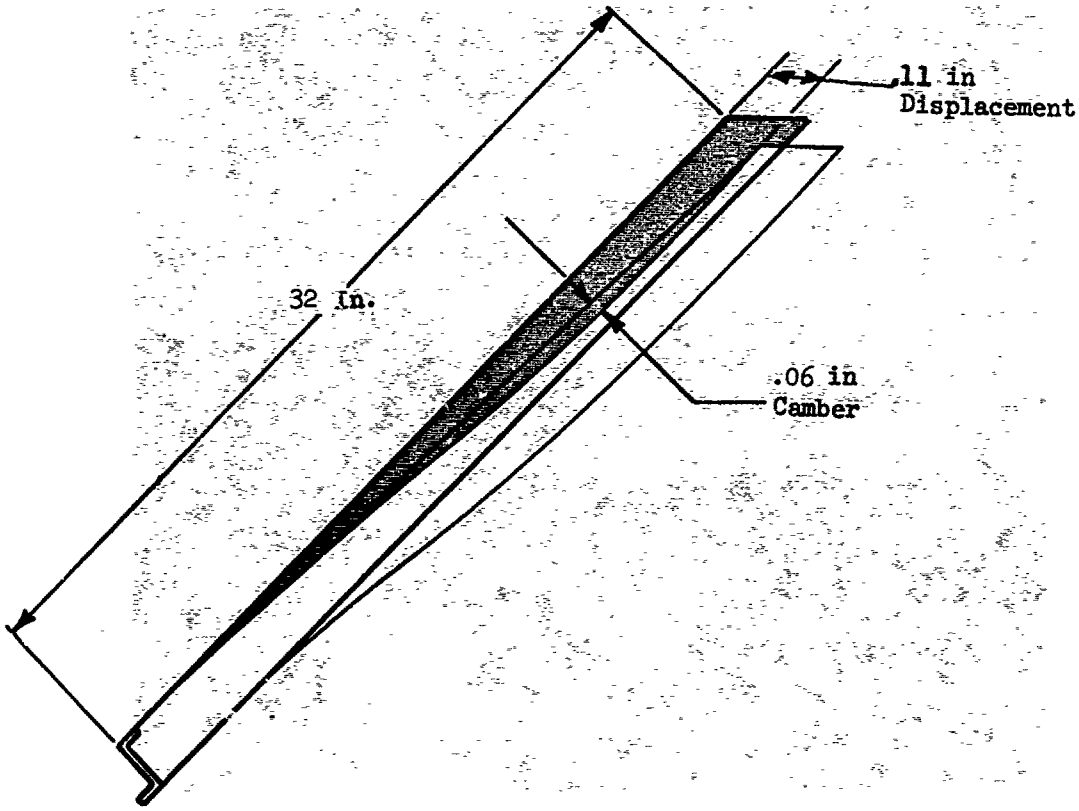


Figure 3. Deflection Mode for Windshield Post.

Figure 4 shows the deformed outboard windshield structure superimposed on the undeformed shape. This illustration shows graphically how fuselage wracking can warp and twist windshields. Most windshields are mounted with a certain degree of flexibility via oversized mounting holes and gaskets. However, for the conditions analyzed, the displacements were large, and would not be absorbed by normal edge attachment flexibility.

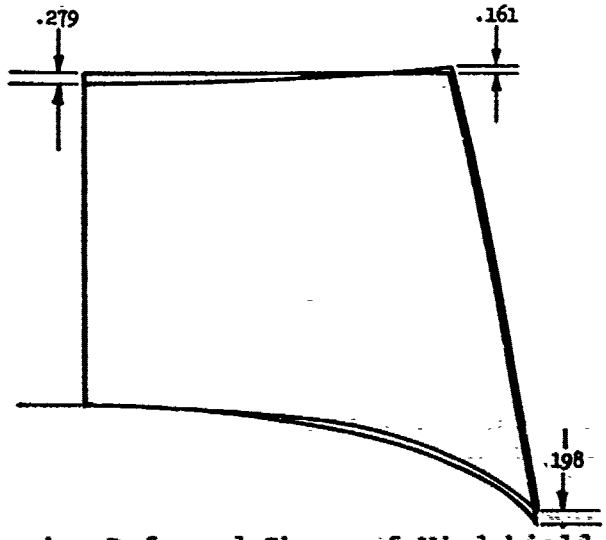


Figure 4. Deformed Shape of Windshield Cavity.

In the NASTRAN model which assumed the windshield installed maximum tensile stresses in the windshield were calculated to be approximately 2000 psi. The semi-tempered soda-lime glass commonly used in windshields has an abraded strength of approximately 6500 psi, therefore, stresses from fuselage wracking cannot be considered negligible.

The distribution of in-plane windshield forces normal to the center posts is plotted in Figure 5. This distribution is indicative of how cockpit deflections induced in-plane bending loads into the windshields.

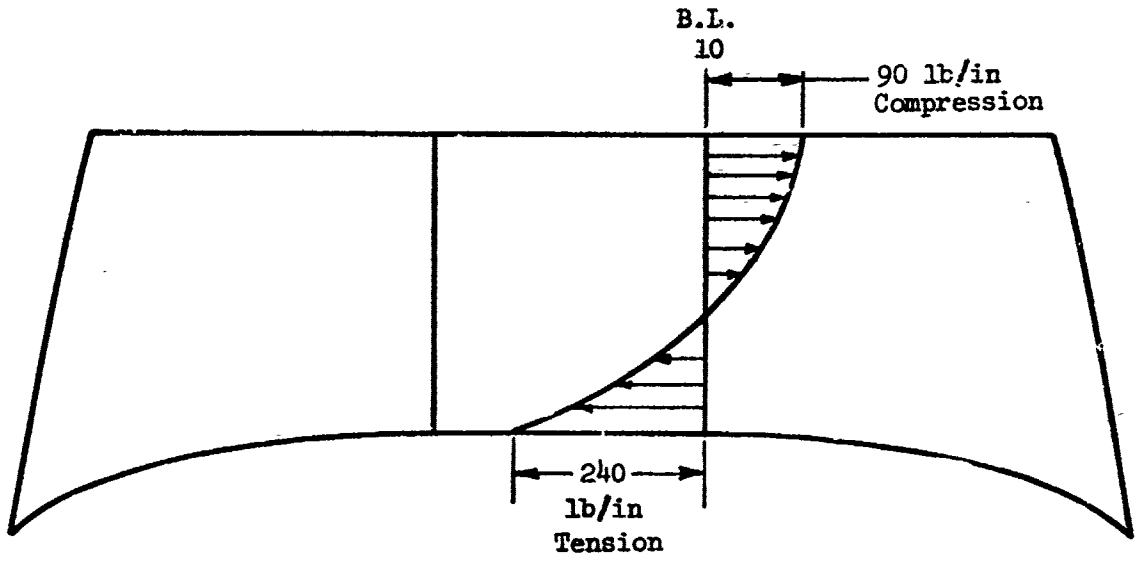


Figure 5. In-Plane Forces Normal to B.L. 10 Post Vertical Bending Condition.

Effects of Transparency Curvature on Windshield Stress

Many helicopter cockpit transparency shapes have second degree curvature, either compound or conic. When subjected to pressure loading, these structures support loads partially by membrane action, and partially by bending. Classical handbook equations do not apply to these shapes and unique analytical solutions are required to determine stress.

It was demonstrated that NASTRAN does have the capability to analyze conic shaped structures subjected to pressure loading. This was accomplished by analyzing a typical aerodynamic pressure loading condition. A .3 psi uniform pressure, representative of cruise speed loading was used for this case. The maximum calculated stress in the center windshield was 2435 psi while the maximum stress in the outboard curved windshields were only 942 psi, despite the outboard panels having approximately twice the area of the center panel. The stresses in the outboard panels were predominantly in-plane, while the stresses in the center panel were predominantly bending.

Effect of Elastic Supports on Stress

The effects of elastic supports on windshield stresses were evaluated by performing both linear and differential stiffness analyses for several load conditions. Differential stiffness considers first order changes in geometry that occur due to deflections, while the linear analysis does not.

Comparing the results of the two methods of analysis, differential stiffness showed only slight changes for the stresses in the outboard area of the structure, but significant changes of up to 100% in the center region. This occurred because the large displacements and stresses in the center region have a greater effect on altering geometry than the small loads and displacements in the outboard region.

A typical computer generated contour plot of the transverse displacements for the center windshield under uniform pressure loading is shown in Figure 6. The total deflection is divided into 14 equal increments with each increment represented by one line. It may be observed that the maximum displacement is not at the center of the windshield, but more towards the lower sill. This is due to the bottom sill having a lower stiffness than the upper sill.

Effect of Large Displacements on Analytical Accuracy

In order for the results of the NASTRAN analysis to be valid, it is necessary that the deflections satisfy the assumptions used in thin plate theory, that the deflections remain small in comparison with the thickness of the plate.

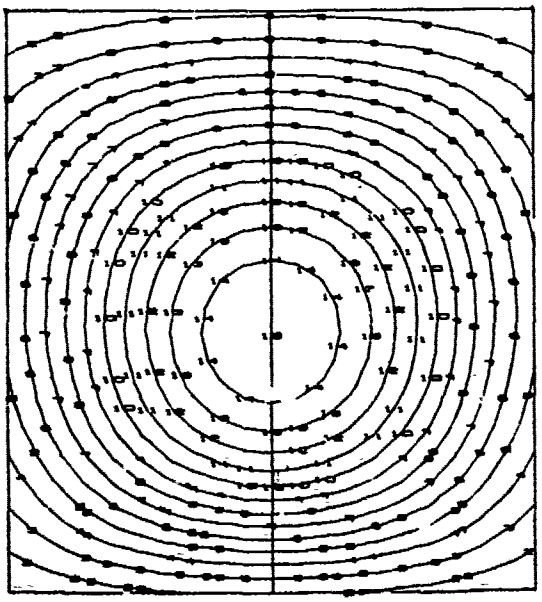


Figure 6. Computer Generated Displacement Plot for Center Windshield Under 1 PSI Loading.

To determine when the NASTRAN analysis would become invalid, three center flat windshield configurations (glass/acrylic, acrylic/polyester, glass/glass) were analyzed for a higher pressure loading of 1 psi. For the glass/acrylic and acrylic/polyester,windshields, the calculated deflection to thickness ratios were much greater than one (13), and the NASTRAN analysis must be considered invalid. These two flat windshield configurations support the pressure load by combined membrane-bending action which the NASTRAN program, as presently structured, cannot analyze.

For windshields where the transverse load is supported by membrane action, future work is planned to investigate the feasibility of developing a large displacement finite element program suitable for this type of structure.

The deflection to thickness ratio for the glass/glass design was 6.5, which is not unrealistic for this type of structure. The NASTRAN results are to be correlated with measured data obtained from instrumented tests performed on identical configurations.

Suitability

The NASTRAN finite element analysis was found to be suitable for the analysis of homogeneous transparencies of the following types:

1. Flat plates and curved shells where the transverse deflections are small in comparison to the thickness of the part.

2. Curved shells where the pressure loads are resisted by in-plane forces (similar to hoop tension or compressive arch).

It is not suitable for the analysis of transversely loaded flat plates where the load is carried partially or entirely by membrane effects. It is also not suitable for the analysis of unsymmetrically laminated windshields where the coupling effects from the interlayer are important, because as a practical matter, the windshields must be modeled as monolithic structures.

ABRASION TESTS

Existing field service has demonstrated that the most prevalent problem experienced with Army helicopter windshields are abrasion and resultant loss of transparency. Abrasion may be caused by windshield wiper action, impingement of sand or dust particles, and improper cleaning procedures. Figure 7 is an example of the type of damage caused by windshield wipers.

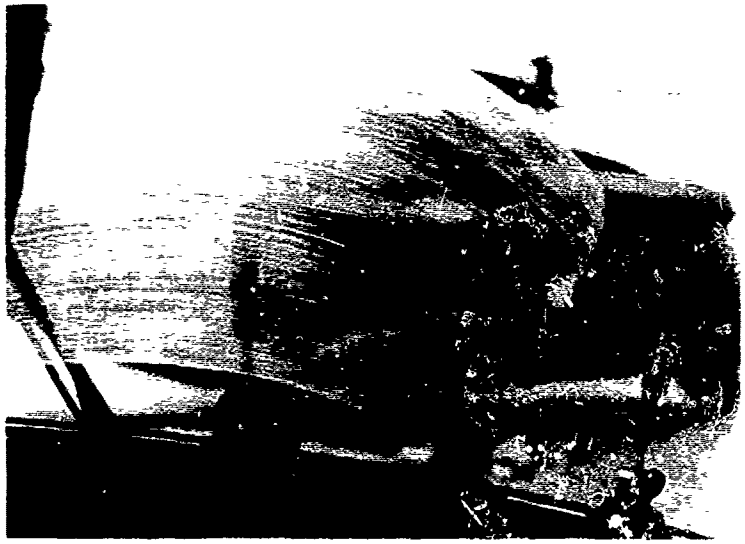


Figure 7. Windshield Wiper Abrasion.

Laboratory simulation of these conditions are required as part of component qualification so that service performance can be reasonably predicted prior to introduction to service. The series of tests described herein were conducted with this purpose in mind. Five generic materials were tested to evaluate their comparative performance. They were:

Acrylic
Hardcoated acrylic
Polycarbonate
Hardcoated polycarbonate
Glass

The pronounced effect of abrasion on transparent materials is to increase the surface haze. Haze is generally defined in terms of the percent of light scattered and therefore lost in passage through the material. To provide a frame of reference, a material with 30% haze would be considered translucent rather than transparent.

Periodic haze measurements were taken at intervals corresponding approximately to each 5% increase in haze.

The first series of tests was conducted by Swedlow, Inc., Garden Grove, California, in accordance with Sikorsky specifications. The hardcoat used was SS-6590, a proprietary abrasion resistant coating formulated by Swedlow, Inc. In addition to the five materials listed above, two sets of coated polycarbonate and acrylic specimens were also tested after artificial aging consisting of 250 hours exposure to 100% relative humidity at 160°F. Similar test conditions have shown that typical hardcoats may degrade significantly in respect to adhesion and abrasion resistance after this type environment exposure.

Apparatus and methods used to perform the dry rubbing abrasion and windshield wiper test were based on the test work conducted by Plumer, and described in Reference 6.

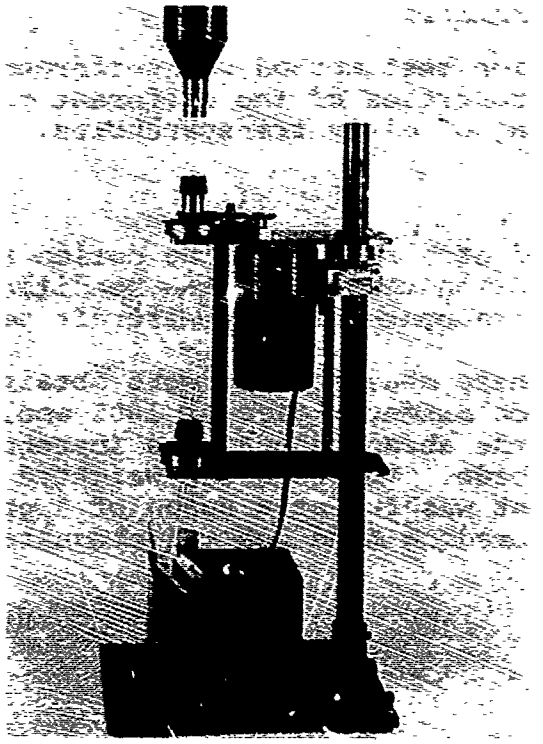


Figure 9. Apparatus for Falling Sand Test.

WINDSHIELD WIPER TEST

This test method was performed to simulate the effect of windshield wiper operation on the various transparency materials. The apparatus consisted of a specimen holding fixture mounted at approximately 45° with provisions to mount material specimens. A windshield wiper driver arm and Hycar rubber blade (30-40 Shore Hardness) attached to an aircraft type motor was also mounted to the test fixture as well as a system for regulating and discharging the abrasive slurry onto the 16 x 21 inch test specimen at 300 ml/minute rate (See Figure 10).

The slurry consisted of 1600 grams of AC Air Cleaner Test Dust (coarse) in 16 liters of water. A peristaltic pump was used to recirculate and apply the slurry, and vigorous stirring was required in the reservoir to prevent the settling out of the abrasive. Eight points were selected on each sample according to a mask previously made which sampled the haze on the periphery of the part as well as in the middle. The windshield wiper blades were adjusted to 0.5 pounds per linear inch of blade length and operated at 100 cycles per minute. Every 12,000 cycles the windshield wiper blades were changed and additional slurry was added as required.

DRY RUBBING ABRASION TEST

This type of abrasion test method was performed to evaluate the rubbing abrasion properties of the different materials from simulated dry wiping of dirty transparencies.

Procedure

Apparatus consisted of a reciprocating motion abrader designed to provide a wiping action that simulates conditions encountered by field cleaning of transparencies by aircraft personnel.

Prior to testing, haze measurements were obtained for all samples. A one-inch diameter disc of 100% wool felt, 1/8 inch thick cemented to the abrading head was impregnated with dry 400 grit boron carbide. The head was weighted with 500 grams of load and the test was run at a speed of approximately 50 cycles per minute. The abrading head was reimpregnated after each 25 cycle period.

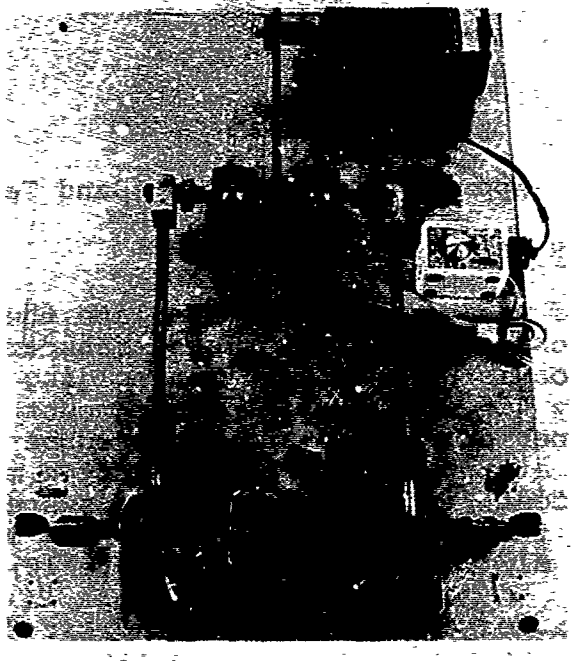


Figure 8. Apparatus for Dry Rubbing Abrasion Test.

FALLING SAND TEST

This type of abrasion test method was performed in compliance with ASTM D-670-70 (except that measurement of gloss was not required) to evaluate the effect of impingement by abrasive particles. The apparatus consists of a hopper and glass tube rotating at about 7 rpm that allows a free fall of abrasive at 200 to 250 grams/minute from the fixed height of 25 inches. The test specimen is 3 x 6 inches and is held at 45° position to the fall of abrasive particles (See Figure 9).

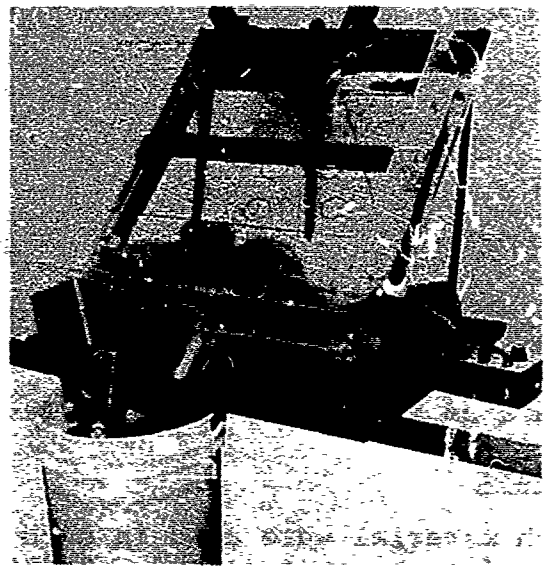


Figure 10. Windshield Wiper Test Apparatus.

The second series of tests was conducted by Gentex Corporation, Carbondale, Pennsylvania, in accordance with Sikorsky specifications. The hardcoat used was 5 microns of Abcite coating (Trademark E.I. DuPont DeNemours and Company). A blowing sand and dust test using MIL-STD-810B, Method 510, with airflow set at 3500 fpm, was attempted, but after 24 hours of testing, all specimens were unaffected and showed no change in initial haze measurements. Sand used for this test was too fine and powdery.

WET RUBBING ABRASION TEST

This test method was performed to simulate the effects of wiping dirty wet windshields, wherein the dirt contains abrasive particles. The specimens were mounted on a turntable and rotated at 10 rpm while continually applying a slurry of water and fine sand through a three-inch tube placed vertically over the specimen as shown in Figure 11.

One sample at a time was mounted in the center of the turntable. The center of the three-inch tube was offset 1-1/2 inches from the center of the specimen. This allowed full abrasion over the entire area of the specimen. A piece of foam rubber which was wrapped around and fastened to the bottom of the slurry tube rested on the specimen during the test. This simulated a wiping effect duplicating actual service conditions and also produced more consistent and uniform haze measurements. A one-pound per square inch constant pressure was obtained by using a 17-inch long tube and keeping the slurry above 15 inches.

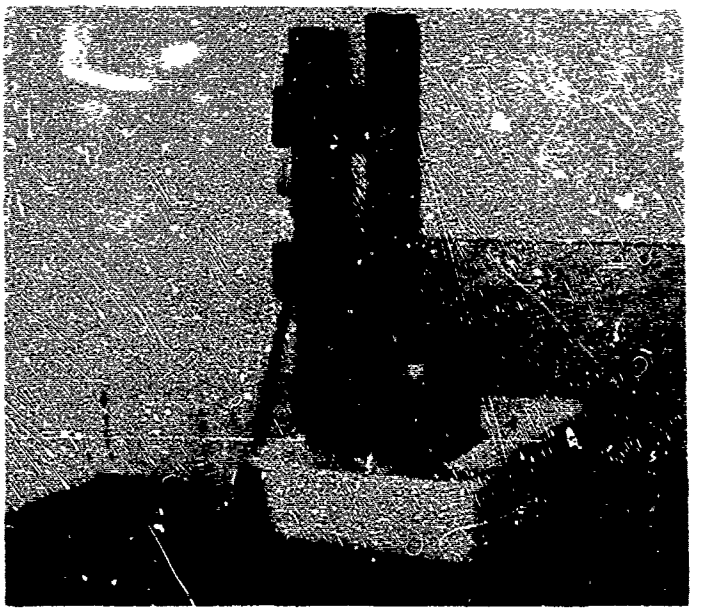


Figure 11. Apparatus for Slurry Abrasion Test.

Consistency of Test Data

Five specimens of each material were used in each test to evaluate consistency of results for the test method. Scatter of test measurements for the dry rubbing abrasion test and falling sand test was minimal, with deviation of no more than 3% haze from the average measured values. Consistency of measurements for the slurry rubbing abrasion test was not as good, and deviations greater than 11% haze were observed, with the average deviation being approximately 5% haze.

Considerable variation in measurements occurred during the windshield wiper test. Fluctuations in readings of over 10% haze were noted for measurements taken from the same specimen, and also from specimen to specimen. Some of the factors causing the variability are inherent to the type of abrasion, and others are related to the characteristics of the wiper blade, flatness of the test specimen, and wetting action of the abrasive slurry on different substrates.

RESULTS

The tests showed that the tolerance to abrasion of uncoated acrylic or polycarbonate material is very poor as measured by the falling sand, rubbing abrasion and windshield wiper tests that were conducted. The application of hard coats to acrylic and polycarbonate glazing material imparts a significant increase in the tolerance to abrasion as indicated by the test results. The effect of artificial aging, 250 hours exposure to 100% humidity at 160°F environment was found to severely degrade adhesion of the SS-6590 hardcoat to the polycarbonate substrate. Marginal

adhesion of unaged SS-6590 hardcoat to polycarbonate was also noted during the windshield wiper test. Glass material was found to be vastly superior to the hardcoated materials during the rubbing abrasion and windshield wiper tests, but not as good as the hardcoated materials when subjected to the falling sand impingement tests.

A summary of the results of all four abrasion tests is presented in Table IV. Windshield wiper test results are shown in Figure 12.

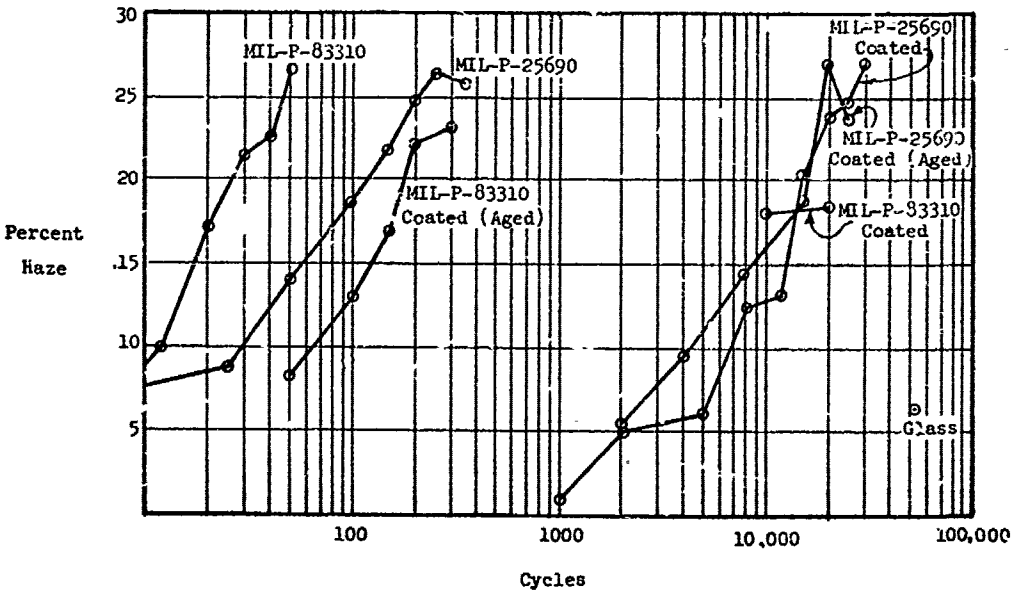


Figure 12. Windshield Wiper Test Results.

TABLE IV

Summary of Abrasion Test Results

Material	Test: Falling* Sand	Dry** Rubbing Abrasion	Slurry** Rubbing Abrasion (30% haze)	Wind-** shield Wiper
Polycarbonate	110 gm	15-27%	60	50-30%
Polycarbonate (Hardcoated)	5500	600-11%	750	50,000-25%
Aged Polycarbonate (Hardcoated)	7500	500-10%	---	500-30%
Acrylic	190	24-30%	70	350-30%
Acrylic (Hardcoated)	6500	1500-14%	200	25,000-25%
Aged Acrylic (Hardcoated)	7500	1500-11%	---	25,000-25%
Glass	1300	1500-1.5%	3600	50,000-5%

* Grams of sand required to produce 30% haze.
** Average number of test cycles or revolutions to produce the percent of haze listed.

It should be noted that the intent of this task was only to develop means to predict the performance of transparent materials when exposed to abrasive environments, and not to select materials for that purpose. Accordingly, complete qualification testing was not implemented for the hardcoats. Prior to production commitments for any hardcoated plastics, it is recommended that thorough qualification testing be performed. This would include, in addition to the tests described previously, rigorous environmental testing.

CORRELATION OF TEST RESULTS

A realistic correlation between the test methods for rubbing abrasion and windshield wiper abrasion can be made with actual service experience. For example, several cycles of windshield wiper operation on dry or dirty acrylic helicopter windshields will have immediate effect in producing objectionable haze. The windshield wiper test performed, duplicated this condition by increasing the original haze level in stretched acrylic by 5% after only 25 cycles of operation. Likewise, the dry rubbing abrasion tests produced an increase in haze of 8% after only 3 cycles and the slurry abrasion test produced 12% haze after 10 cycles on stretched acrylic, which is representative of the damage produced by wiping plastic transparencies with dirty rags.

Correlation of the falling sand test to actual service experience is a bit more difficult, because this failure mode is rare in comparison to the other forms of abrasion. However, some estimation of the severity of the test can be obtained by calculating the flux of the impinging sand particles and comparing it to Army specifications for density of blowing sand which is 0.1 gm/ft^3. Using this approach, 1 gm of falling sand can be roughly equated to 4 minutes exposure to blowing sand at 11 ft/sec or 7.5 mph.

An increase in haze of 10% was measured for the stretched acrylic material after exposure to 50 gm of falling sand, which might be likened to 3 hours exposure to dense blowing sand. When one considers that sand storms can induce higher impingement velocities, notwithstanding flight through the storm, the potential hazard from impinging sand can be fully appreciated. Note that the kinetic energy of the impinging particles is proportional to the square of their velocities. It is felt that the reason impingement abrasion damage to helicopter transparencies has not been documented as a serious problem is that there has been only minimal exposure to conducive environments.

DESIGN HANDBOOK

The Design Handbook being prepared at the conclusion of this program is intended to be a single source technical document covering the important aspects of helicopter transparency engineering. It will be easy to read for design engineers, specialists, and non-technical personnel, and will contain liberal use of tables, charts and illustrations.

The Design Handbook will include a General Specification that will consolidate and standardize design, acceptance and test criteria for all types of transparencies used on helicopters. A rationale for the specification will be included in the Design Handbook along with guidelines for performing tradeoffs.

While the handbook is intended to be comprehensive in subject matter, it is not intended to supersede unabridged references

such as MIL-HDBK-17A, "Plastics for Aerospace Vehicles, Part II, Transparent Glazing Materials," but instead will complement and make reference to such documents. Here the emphasis will be on design, rather than material properties.

Although a comprehensive literature survey has been conducted, any additional non-proprietary material from interested parties would still be welcome and considered for inclusion in the Design Handbook. All such material would be gratefully acknowledged. Material should be mailed to:

Sikorsky Aircraft Division
United Technologies Corporation
North Main Street
Stratford, Connecticut 06602
Attention: Bruce F. Kay,
Aircraft Design & Development

CONCLUSIONS

1. Stresses due to airframe deflections can be significant and must be accounted for in windshield design. Advanced analytical tools such as NASTRAN must be used to determine the magnitude of such stresses. In addition, the NASTRAN analysis can be used to analyze irregular shapes and transparencies mounted on elastic supports.

2. Meaningful abrasion tests have been developed which can be used to predict performance of transparent materials exposed to abrasive environments.

3. Realistic endurance test criteria has been developed which will lead to greatly improved service lives for helicopter heated windshields.

4. Final program output will provide:

   a. A uniform specification for design, acceptance and test criteria.
   b. Single source comprehensive design handbook for reference, planning, and design and development of future helicopters.

REFERENCES

1. James, H. C., et al, Goodyear Aerospace Corp., "Design, Test, and Acceptance Criteria for Army Helicopter Transparent Enclosures," USAAMRDL-TR-73-19, U. S. Army Air Mobility Research and Development Laboratory, Ft. Eustis, Virginia, May 1973.

2. Cook, L. M., et al, PPG Industries, "Development of Design, Test, and Acceptance Criteria for Army Helicopter Transparent Enclosures," USAAMRDL-TR-73-65, U. S. Army Air Mobility Research and Development Laboratory, Ft. Eustis, Virginia, September 1973.

3. Anon., "U. S. Naval Weather Service World Wide Airfield Summaries," Vol. I, VIII, IX.

4. Roberts, W. G., Triplex Safety Glass Company, Ltd., "The Design, Development and Testing of Flat and Curved All Glass Windshields for Wide Bodied Aircraft Using the Latest Developments in High Strength Glass and Electroconductive Coatings," AFML-TR-73-126, Air Force Materials Laboratory, Wright-Patterson Air Force Base, Ohio, June 1973.

5. Campbell, L.G. and Marshall, J.W., "Windshield Flight Environment Simulator," Presented to the Aircraft Air Conditioning Forum, April 11, 1974, Sierracin Corporation, Sylmar, California.

6. Plumer, J.R. "Development of Scratch and Spall Resistent Windshields," AMMRC-TR-74-19 Army Materials and Mechanics Research Center, Watertown, Massachusetts, 1974.

SESSION 3

MATERIALS CHARACTERIZATION (PART I)

PRECEDING PAGE BLANK-NOT FILMED

REPORT ON PROGRESS OF THE ASTM F7.08 SUBCOMMITTEE ON AEROSPACE TRANSPARENT ENCLOSURES AND MATERIALS

R. A. Merozowicz
Chairman, ASTM F7.08
Northrop Corporation
Aircraft Division
Hawthorne, California

REPORT ON PROGRESS OF THE ASTM F7.08 SUBCOMMITTEE ON AEROSPACE TRANSPARENT ENCLOSURES AND MATERIALS

BY RICHARD MOROZOWICZ
CHAIRMAN, ASTM F7.08

NORTHROP CORPORATION
AIRCRAFT DIVISION
HAWTHORNE, CALIFORNIA

ABSTRACT

Thirteen task force teams have been established within ASTM F7.08 subcommittee on aerospace transparent enclosures and materials. Each task force is evaluating test procedures to develop meaningful standard test methods. This paper presents a progress report on each of the 13 selected evaluative areas. The areas are abrasion, aging, bond integrity, chemical/moisture, distortion, electrostatics, bird impact, hail impact, interlayer, scratch, scratch versus structural integrity, thermal and toughness.

INTRODUCTION

In 1973, the many problem areas in testing transparent enclosures and materials caused a study group to recommend the establishment of an ASTM subcommittee. The ASTM F7.08 subcommittee on aerospace transparent enclosures and materials was created to:

a. develop new standards where inadequate procedures exist;

b. select and improve standards where conflicting test procedures lead to nonreproducible test data.

An organizational meeting identified 40 troublesome areas and 13 of the more serious ones were selected for resolution. Volunteer task forces were created and a chairman for each of the 13 task forces was named.

Many meetings and man-hours have gone into studies by the subcommittee. Significant progress is being made by the task forces. The status of each task force and its chairman is shown in Figure 1. Task force progress is as follows.

ABRASION TASK FORCE

Many of the test methods in use in industry for determining abrasion resistance are being evaluated. These methods all appear to be good indicators and require considerable analysis to determine the one that will be recommended by the task force for ASTM adoption.

AGING TASK FORCE

The first draft of the recommended test method for aging, also referred to as environmental resistance of aerospace transparent enclosures, was produced on 7 February 1975. This method is for the purpose of investigating the effect of exposure to thermal shock, condensing humidity and simulated weather on proposed aerospace transparent enclosure designs.

BOND INTEGRITY TASK FORCE

In May 1975 a preliminary test method draft, determined from literature search and technical experience, was produced. It incorporates the traditional tests which are the costly destructive methods for the measurement of bond line strength. The prime objective of the task force is to develop a nondestructive test method for determining the integrity of the bond in transparent composites. Discovery of a simple instrument that

FIGURE 1.

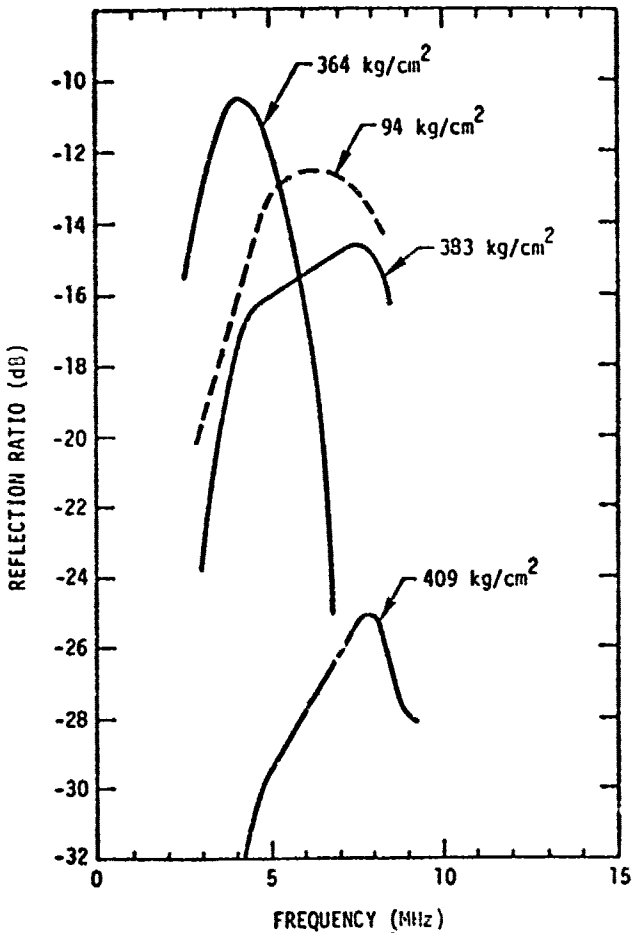
STATUS TEST METHODS AND STANDARDS ASTM F 7.08

TEST METHOD / TASK FORCE	CHAIRMAN	AFFILIATION	MAIL DRAFT TO F 7.08 DATE DUE	MAIL DRAFT TO F 7.08 DATE DONE	NEGATIVES NO. REC'V'D	NEGATIVES DATE ALL RESOLVED	MAIL DRAFT TO EDITORIAL DATE DUE	MAIL DRAFT TO EDITORIAL DATE DONE	RETURN DATE DUE	RETURN DATE DONE	MAIL DRAFT TO F 7 DATE DUE	MAIL DRAFT TO F 7 DATE DONE	NEGATIVES NO. REC'V'D	NEGATIVES DATE ALL RESOLVED	MAIL DRAFT TO ASTM HQ DATE DUE	MAIL DRAFT TO ASTM HQ DATE DONE	NEGATIVES NO. REC'V'D	NEGATIVES DATE ALL RESOLVED	PUBLISH IN VOLUME 25 DATE DUE	PUBLISH IN VOLUME 25 DATE DONE
ABRASION - RUB	O.MINNICH	DOUGLAS	1 DEC 75																	
IMPINGE			1 DEC 75																	
AGING	M.POLLOCK	BOEING		7 FEB 75	9		5 JAN 76													
BOND INTEGRITY	S.SCHWARTZ	HUGHES		14 MAY 75	9		19 DEC 75													
CHEMICAL/MOISTURE	G.BISCHOFF	NORTHROP																		
DISTORTION	J.FARGO	LOCKHEED	1 MAY 76																	
ELECTROSTATICS	K.MOORE	CONTI-NENTAL	15 NOV 75	13 NOV 75																
LIGHTNING																				
IMPACT, BIRD	J.LAWRENCE	DOUGLAS	19 JAN 76																	
IMPACT, HAIL	R.BRISTOW	BOEING		16 NOV 74	8		17 NOV 75													
INTERLAYER	J.MYLES	GRUMMAN	6 NOV 75	6 NOV 75																
SCRATCH - STANDARD (GLASS) TEST METHOD	F.NORRIS	LOCKHEED													26 MAY 75				AVAIL. OCT. 76	
				27 AUG 74	6	10 SEP 75	—	16 SEP 75	30 SEP 75	7 OCT 75	—	5 NOV 75								
SCRATCH - STANDARD (PLASTICS) TEST METHOD																				
SCRATCH (GLASS) VS. STRENGTH (PLASTICS)	R.SEAGO (ACTING)	BELL																		
THERMAL FLAW UNIFORMITY	R.PASELK	ROCKWELL		1 JUL 75	5		10 DEC 75													
TOUGHNESS	J.KOZMATA	DOUGLAS	1 OCT 76																	

could be applied to a laminated transparent windshield and provide an instant reading of bond line strength would be ideal. A search into the potential use of holography, laser, x-ray, thermography, sound attenuation and other methods are suggested for consideration.

Fokker and Harmonic nondestructive bond tests are used quite extensively on nontransparent assemblies, but they determine only the existence of voids in the bond line by a complex program of standards preparation and comparison of these standards. The latter nondestructive methods are not appropriate for this area of investigation.

Dr. George Alers of the Rockwell Science Center has performed some work in establishing the bond strength of a solvent cemented joint on two 1/2 inch blocks of acrylic compared to the reflection of ultrasonic energy. Graphs, Figure 2, in his report indicate the correlation of higher bond strength to higher reflection ratio. The dotted line is the reflection of a bonded area made with PS 30 cement. Dr. Alers findings and other new methods are being pursued.



Graphs of the frequency dependence of the ultrasonic energy reflected from adhesive bonds between Lucite blocks formed by placing an adhesive or solvent at the interface. These data were deduced from Fourier transforms of the RF signal reflected from the bond line.

FIGURE 2.

CHEMICAL/MOISTURE TASK FORCE

The assignment to produce a test method for chemical/moisture resistance of transparent materials is being pursued by evaluation of a number of existing methods and search for new methods. The most meaningful test method will be selected and submitted in a preliminary draft at a time as yet to be established.

DISTORTION TASK FORCE

The characteristic in a transparency that causes objects to wiggle and deform is called distortion. Investigation is in progress of the many methods that place measurable values on distortion. This is a difficult area and many different methods are being studied. Photographs with single exposures, double exposures and triple exposures are used; photographs with inner and outer lens masks provide other means of recording the wiggly images. A draft of an acceptable procedure is scheduled for issuance by 1 May 1976.

ELECTROSTATIC TASK FORCE

Three separate drafts of test methods have been prepared for surface resistivity and volume conductivity. The proposed recommended method has been submitted to F7.08 for review. Tests are continuing at both Boeing and Douglas. A unique method under consideration is the practice of spraying an electric charge onto the surface of a windshield by means of a high voltage probe. It is believed that it is important to incorporate surface charging in this test method because of experiences by commercial airlines where "arcing" from surface charges caused undesirable visual displays and induced interference currents into windshield heating circuits and aircraft wiring. There are examples, in military aircraft, of personnel injured from shocks as high as 50,000 volts. This area of investigation is most important to the understanding and control of electrostatic phenomenon.

BIRD IMPACT TASK FORCE

Two methods of bird impact simulation have been evaluated and submitted in a proposed procedure for task force review and comment. One method impacts a rocket-propelled, sled mounted transparency into a hanging bird carcass. The other uses a smooth bore gun to fire a packaged bird carcass into a stationary transparency. The gun fire test is being recommended as the least costly, more easily controlled and more accurate in resultant data. Final determination will be established upon completion of the procedure coordination.

HAIL IMPACT TASK FORCE

Due to the difficulty in simulating the interaction of an aerospace transparent surface with the many varied sizes of hailstones encountered in flight, it has not been possible to develop reproducible results that are meaningful for use by the designer. The dimensions of ice particles in the atmosphere range from microscopic up to 7 inches; at ground level from 1/4 inch to 2 inches. The task force is selecting an iceball size and composition that will be recommended for use as a standard. The various transparencies employed, their thickness and the recommended test procedure has been submitted to F7.08 for review and will be incorporated into ASTM standards

INTERLAYER TASK FORCE

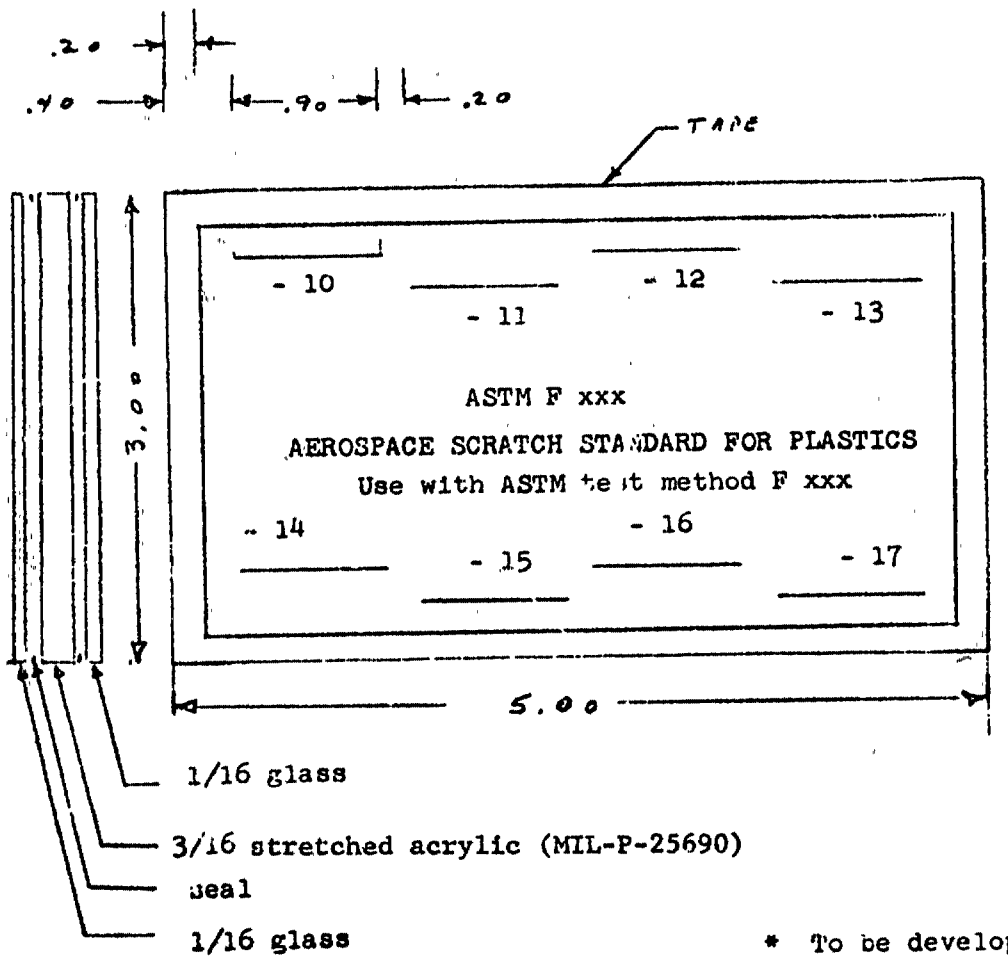
The process of laminating transparent materials for use in aerospace transparent enclosures requires the use of interlayer material in the form of sheet or as a mixture of substances that may be cast or poured between rigid transparent plies to cure into a rigid or semi-rigid material. It is the goal of the task force to establish test methods that will be employed by both the supplier and the user of the materials to assure compatibility of test results. A draft of 18 proposed test methods for the measurement of interlayer material properties has been submitted to F7.08 and is presently being evaluated.

GLASS SCRATCH TASK FORCE

The establishment of a method for determination of scratch intensity on glass has been the prime goal of this activity. As a result of continued evaluation of various methods, it was determined that a glass scratch standard was necessary to assure reproducible results in scratch evaluation. Robert Beal, an active member of this task force, developed a glass scratch standard that has been adopted as the standard recommended for use and is identified as ASTM Standard Number F428. A draft of the proposed test methods to be used in conjunction with the glass standard was submitted to ASTM and is in coordination.

PLASTICS SCRATCH TASK FORCE

Made up of the same members as the glass scratch task force, this activity is pursuing the same basic objectives as has been accomplished with glass. A uniform standard (Figure 3) is to be developed in conjunction with a test method procedure.



Scratch depth
(Tentative *)

- 10
- 11
- 12
- 13
- 14
- 15
- 16
- 17

FIGURE 3.

* To be developed by the inspection committee of the ASTM F 7.08 Scratch Task Force. Goal is to have, from scratch to scratch, uniform gradation in appearance to the naked eye.

SCRATCH VERSUS STRUCTURAL INTEGRITY TASK FORCE

This new activity will concentrate on standardization of a test method for the determination of scratch effect on the strength of glass, and another method for the same effect on plastics. Prior development of the glass scratch standard will allow scratch control in this area of study. Methods will be proposed as this study progresses.

THERMAL TASK FORCE

A draft of a proposed method for the detection of flaws in a heated windshield has been submitted to F7.08. This method employs a Polariscope. Two other methods for the determination of temperature uniformity throughout a heated windshield are in progress and will be forthcoming.

TOUGHNESS TASK FORCE

Search for an improved standard test method for toughness of plastics is progressing. The Naval Research Lab in Washington, D.C. is working with F7.08 and it is anticipated that an ASTM test method will be developed by this joint effort and possibly a new version of MIL-P-25690.

DISCUSSION

The ASTM F7.08 Subcommittee and the activities of the various task forces reflect the dedication of the membership. Each activity is striving to develop test methods that are the simplest, most practical and technically adequate and correct for application by all affected using activities: the designer, the manufacturer, the laboratory, and quality assurance functions. The process of examination and reexamination for constant upgrading of test methods is necessary to maintain pace with the state-of-the-art as well as to advance the transparent enclosures and materials technology. It is the subcommittee goal to continue in this effort and to encourage participation by others in this field.

RAIN EROSION BEHAVIOR OF TRANSPARENT PLASTICS AND PROTECTIVE COATINGS

T. L. Peterson
Air Force Materials Laboratory
Wright-Patterson Air Force Base, Ohio

RAIN EROSION BEHAVIOR OF TRANSPARENT PLASTICS AND PROTECTIVE COATINGS

Timothy L. Peterson
Air Force Materials Laboratory
Air Force Wright Aeronautical Laboratories (AFSC)
Wright-Patterson Air Force Base, Ohio 45433

ABSTRACT

This paper describes the erosion behavior of coated and uncoated transparent plastics as determined in the simulated subsonic rain erosion environment of the AFML rotating arm apparatus. The damage mechanisms for polycarbonate and acrylic are defined, and the resulting losses in transmission are described. Although these plastics are quite susceptible to rain erosion damage, little damage occurs at low subsonic velocities when the angle of drop impingement is low. However, thin film protective coatings are rapidly removed in the simulated rain environment, even at low velocities and low impingement angles. This lack of durability in an erosive environment of protective films is a serious problem when these coatings are used to improve the abrasion resistance of polycarbonate windshields. Rates of removal for these coatings in the simulated rain environment are presented, and the mechanisms of coating removal are illustrated in this paper. The rain erosion behavior of a ductile polyurethane cladding for the protection of polycarbonate is also described.

I. INTRODUCTION

The damaging effects of multiple rain droplet impacts on transparent materials are being investigated by the Air Force Materials Laboratory. In addition to various glasses and infrared window materials such as ZnS and GaAs, several transparent plastic materials have been investigated. These include polycarbonate (Lexan), acrylic (Plexiglas), stretched acrylic, polysulfone, and allyl diglycol carbonate (CR-39). Of these plastics, polycarbonate, acrylic, and stretched acrylic are most commonly used in aircraft transparencies, and the erosion behavior of these materials will be presented in this paper. Surface frosting or pitting occurs after subsonic exposure of these materials to rain causing a subsequent increase in haze and loss in transmission. This optical degradation generally becomes significantly large before the damage has progressed far enough to allow measurement of mass loss.

When polycarbonate is used in aircraft windshields and canopies, its surface must be protected from abrasion, solvent, and other aggressive environments. Thin protective coatings are preferred for this purpose because they are readily applied to transparencies of compound curvature, do not increase weight, and have a relatively low application cost. The durability of these protective coatings in an erosive environment is therefore an important consideration. Results presented in this paper show that thin film protective coatings generally are removed rapidly in the simulated rain environment. The results of these tests have been validated by in-service experience.

Because of the lack of durability of thin protective films, other methods of protecting polycarbonate are being investigated. The rain erosion behavior of ductile polyurethane claddings fusion bonded to polycarbonate (Reference 1) has been investigated. These materials, while not as erosion resistant as polycarbonate, are much more erosion resistant than thin protective coatings. Their use in the future will therefore depend upon their meeting other requirements such as abrasion resistance, thermal shock, and environmental stability.

The discussion of materials by brand name in this paper is in no way to be taken as an endorsement or criticism by the Air Force or the Government. These materials were selected as representative of a class of materials and their names are a convenient way of handling and discussing them. The Government incurs no liability or obligation to any supplier of materials from the information included in this paper.

II. EXPERIMENTAL PROCEDURE

The rain erosion investigations of these transparent plastic materials were conducted in the simulated environment of the Air Force Materials Laboratory rotating arm apparatus (see Figure 1). This equipment includes an eight foot diameter propeller blade mounted horizontally and powered by a 400 horsepower electric motor. Variable speeds up to 600 mph at the blade tip where the specimens are inserted can be attained during erosion testing.

The water system used to simulate the rain environment is mounted above the blade. A 8 foot diameter, 1 inch aluminum pipe ring is equipped with 96 equally spaced hypodermic needles to yield a rainfall simulation of 1 inch per hour. The water system enables a stream of undistorted water droplets of 1.5mm to 2.0mm diameter, as determined photographically, to impinge on the specimens.

Results obtained on the rotating arm apparatus are used extensively because of correlation between them and actual flight test results. These tests and other in-service observations verify that the rankings of erosion resistance of materials and modes of failure obtained on the rotating arm are confirmed in actual flight experience.

All specimens used in these investigations were flat and were 1/8 inch thick. They were mounted in holders which allowed rain impingement at angles of 30°, 60°, and 90° with respect to the specimen surface. The dimensions of the 30° specimens were 15/16 inch x 1 inch, the 60° specimens were 17/32 inch x 1 inch, and the 90° specimens were 1/2 inch x 1 inch. The range of impact velocities used in these investigations included a minimum of 345mph and a maximum of 600mph.

The effect of erosion damage on the transmission of light through these materials was measured using a Beckman DK-2A recording spectrophotometer. Transmission measurements were made before rain exposure and after various exposure times. During these measurements the specimens were placed approximately 6 inches from the entrance port of the integrating sphere. Thus all of the scattered light which was transmitted through the eroded specimens did not enter the sphere. Transmission losses measured in this manner more accurately correlate with vision impairment and increases in haze than do measurements of losses in total transmission through the specimens. The removal of protective coatings was evaluated by visual and by microscopic inspection.

III. RESULTS AND DISCUSSION

A. Uncoated Transparent Plastics

The nature of the erosion damage for polycarbonate and acrylic after exposure to the standard rain field (1 inch/hour, 1.8mm diameter drops) at normal impact and a velocity of 500mph is shown in Figures 2 and 3. Acrylic is obviously significantly less resistant to rain erosion than polycaronate. After 25 minutes exposure, scattered pitting of the polycarbonate surface occurs while the surface of acrylic is completely frosted after 5 minutes exposure.

The initial damage to polycarbonate exposed at 500mph or 600mph is in the form of very shallow ripple patterns distributed randomly over the surface. Although these ripple formations sometimes occur as circular arcs, complete ring patterns are not observed. A micrograph of one of these ripple formations is shown in Figure 4.

The condition of the surface of polycarbonate after 25 minutes exposure at 500mph and 90° impact is shown in Figure 5. In addition to the areas of plastic deformation on the surface, shallow erosion pits have formed. Although some pitting does occur along surface scratches, in general, pit formation is not dependent on existing surface scratches. It is believed that localized cracking within the highly deformed areas serves as a nucleation site for pit formation.

The micrograph in Figure 6 shows the condition of polycarbonate impacted by rain droplets at a 30° angle for 30 minutes at 600mph. The ductile response of the material is illustrated by permanent deformation at the rims of the pits. Transmission through polycarbonate at this stage of the erosion process has been reduced to about 86% of the initial transmission.

In contrast to polycarbonate, acrylic behaves in a completely brittle manner when impacted by water droplets at subsonic velocities. Initial damage to acrylic is in the form of multiple ring fractures which are shown in Figure 7. The outer diameter of these ring fractures varies but is typically on the order of two-thirds the diameter of the impacting drops (1.8mm). Based upon calculations of the number of impacts which have occurred and the number of ring fractures observed in the micrograph, it is believed that the majority of the drop impacts during the first minute of exposure at 500mph result in the formation of ring fractures. The formation of these ring fractures which overlap but are fairly uniformly distributed over the surface result in a transmission loss of approximately 5 percent of the initial transmission.

The photomicrographs in Figure 8 show the erosion damage in acrylic after 10 minutes at 400mph. In addition to the formation of several overlapping ring fractures, pre-existing surface scratches have also grown as a result of exposure to the rain environment.

Although the ring fractures are quite shallow, fine particle removal occurs in a brittle manner at points of intersection between the multiple rings. However, much of the pitting shown in Figure 8 has nucleated as a result of the interaction of the ring fractures with pre-existing surface scratches. Fine particles are continually removed from points of intersection of ring fractures with scratches and other ring fractures as the exposure time to rain increases. As can be seen in Figure 9, the surface layer of the acrylic is removed as the regions where pits have nucleated expand laterally.

The surface of stretched acrylic after 30 minutes at 500mph and 30° impingement angle is shown in Figure 10. Ring cracking is not evident although ring cracks are observed on cast acrylic exposed to the same environment. However, much more surface pitting is observed in the stretched acrylic than is observed in the cast acrylic. This pitting occurs in a brittle manner and generally initiates at fine scratches on the surface.

The effect of subsonic rain exposure on the transmission of acrylic and polycarbonate is shown in Figures 11 through 14 for various exposure conditions. Each data point represents the average of transmission measurements at .55 micron on at least two specimens. Transmission, expressed as a percentage of the initial transmission prior to exposure, is plotted versus exposure time to show transmission loss as a function of velocity for 30° and 90° impact angles. Curves of increase in haze versus exposure time show similar trends.

Three general observations can be made concerning the rain erosion behavior of acrylic and polycarbonate as illustrated by these transmission loss curves.

(1) Polycarbonate is much more resistant to subsonic rain erosion damage and subsequent transmission loss than is acrylic. Based upon the erosion mechanism studies, the ductility of polycarbonate is probably the property most responsible for its erosion resistance. Typical values of elongation at break are 110% for polycarbonate and 5% for acrylic. Polycarbonate also has a much higher notch impact strength than does acrylic. However, the erosion resistance of plastic materials cannot always be correlated with impact strength (References 2 and 3). When discussing possible correlations of erosion resistance with mechanical properties, it must be remembered that the rain erosion problem presents a unique loading condition which is not closely allied with the usual mechanical property evaluations.

(2) Erosion damage is highly dependent upon impact velocity. Transmission loss as a function of impact velocity for both acrylic and polycarbonate at 30° and 90° impact angles is illustrated by the figures.

Previous investigations have demonstrated that subsonic rain erosion damage as measured by weight loss is a function of the normal component of velocity to approximately the fifth power. The effect of velocity is also observed in the micrographs of the eroded surfaces. The ripple patterns observed on surfaces of polycarbonate specimens after normal drop impacts at 500mph are not observed after normal impacts at 400mph. In addition, while each drop impact at 500mph results in the formation of ring cracks in acrylic exposed at 90°, ring cracks are not observed for each individual impact at 400mph.

(3) Erosion damage and subsequent transmission loss are significantly lowered by reducing the impact angle. In fact, both materials are essentially undamaged by relatively long exposures to the standard rain field at 30° impact angle and 345mph.

Polycarbonate and acrylic can therefore be used in aircraft windshield applications where rain is encountered at low impingement angles and low subsonic velocities with no rain erosion problems. However, in applications such as missile domes which are hemispherical and have 90° or near 90° incidence angles, the use of polycarbonate, and acrylic to an even greater extent, is limited by rain erosion considerations.

B. Protective Coatings and Claddings

Several thin film protective coatings on both polycarbonate and acrylic have been investigated in the simulated subsonic rain erosion environment. These thin films are removed quite rapidly in this erosive environment. Data for the removal of Abcite, Texstar 212, Sierracote 230, and Texstar 254 from polycarbonate specimens impacted by rain at 30° is presented in Table 1. Many other coatings have been investigated, but these four coatings are representative of erosion behavior, and they have been or are being used on polycarbonate aircraft enclosures.

The percentages given in Table 1 represent the percentage of the surface area from which the coating has been removed as determined by visual inspection. Because of the nature of the removal process, there can be some variance in these percentages, especially at 345 mph and a 30° impact angle. The percentages in Table 1 must therefore be considered as typical values.

Abcite and Texstar 212 are representative of hard protective coatings. Abcite coated acrylic has also been investigated. When Abcite is applied to acrylic, it is slightly more durable in a rain erosive environment at the 30° impact angle than when it is applied to polycarbonate. This is most likely due to better adhesion of the coating to acrylic which makes the coating more resistant to removal by the flow of water over the surface.

At higher impact angles, the removal rates are the same for both substrates.

Sierracote 233 and Texstar 254 are more ductile coatings than Abcite or Texstar 212. As indicated by Table 1, coatings with some ductility are generally more durable in rain than are the more brittle, harder coatings. The Texstar 254 coating is as durable in the rain erosion environment as any coating evaluated to date.

Two features of rain drop impacts are responsible for removal of the protective coatings. The stresses which result from the high impact pressures cause damage in the form of crack initiation and propagation or growth of surface scratches. The second source of damage from the drop impact is the radial outward flow of water away from the impact site. This flow of water over the surface is responsible for lifting and tearing away of the coating at imperfections such as cracks, scratches or at exposed edges of the coating.

Figure 15 illustrates a removal mechanism for Abcite on polycarbonate. Multiple ring cracks are formed as a result of drop impacts. High velocity radial outward flow of water is then responsible for coating removal. In Figure 15 the darker areas are those areas where the Abcite coating remains. Since the angle of impact for the specimens in this figure is 30°, the velocity of water flow is highest toward the right of the micrograph and results in much greater coating removal in this direction. Flow of water along the surface due to subsequent drop impacts attacks the edge of the coating where it has previously broken off and removes more of the coating.

Another mechanism of coating removal is illustrated by the micrograph in Figure 16. Ring cracks are not formed in the Texstar 254 coating, but surface scratches grow and become more pronounced as a result of drop impacts. This is also a 30° specimen and coating removal occurs predominantly in one direction. This coating is more resistant to coating removal by the flow of water over the surface after small areas of coating removal have been initiated. This is believed to be due to improved adhesion to the polycarbonate substrate.

Thin protective coatings do not improve the erosion resistance of the plastic substrates. In some cases, the mechanism of erosion damage in the plastic substrate is altered by the presence of the coating. Figure 17 shows part of a ring crack formation in polycarbonate observed after removal of the Abcite coating in 1 minute at 500mph and 90° impact. In this case the ring fractures initiate in the Abcite coating and propagate a short distance into the substrate. After removal of the coating, the polycarbonate behaves in a ductile manner and these ring cracks do not propagate nor do new cracks initiate.

Eventually these ring cracks are obscurred by the normal damage mechanisms in polycarbonate and their overall effect on transmission loss is negligible.

Not only do thin coatings not improve the erosion resistance of plastics, but the erosion resistance can be degraded significantly if the properties of the plastic surface are altered by application of the coating. Figure 18 illustrates the poor erosion resistance of polycarbonate to which a polymeric coating to prevent fogging and improve abrasion resistance had been chemically bonded. Cracks not only propagate from the brittle coating into the polycarbonate, but the polycarbonate continues to erode in a brittle manner after removal of the coating. The degradation in erosion resistance caused by embrittlement of the polycarbonate surface is indicated by a comparison of the frosted appearance of the surface in Figure 18 after 5 minutes at 500mph to the isolated pitting in uncoated polycarbonate after 25 minutes at 500mph in Figure 2.

Because of the lack of durability of thin protective films in service environments, other methods of protecting polycarbonate must be investigated. Other methods for protecting polycarbonate include laminating or fusion bonding of an abrasion resistant outer cladding material to the polycarbonate. Specimens with an outer layer of acrylic fusion bonded to polycarbonate have been investigated in the rain environment. The rain erosion behavior of the acrylic cladding is comparable to that of the acrylic specimens described earlier.

Preliminary investigations of the erosion behavior of a transparent ductile polyurethane cladding fusion bonded to polycarbonate have been conducted. This concept is being developed by Sierracin and additional information may be found in Reference 1.

The polyurethane claddings, which are approximately .01 inch thick, are much more resistant to rain erosion than are the thin protective coatings. The ductility of the polyurethanes allows them to resist erosion damage at 345mph and 30° impact angle. The higher impact pressures at higher impact velocities cause pitting of the surface similar to that seen in polycarbonate. The surface of one of the polyurethane claddings (Sierraclad 4) after exposure for 30 minutes at 600mph and 30° impact angle is shown in Figure 19. Some evidence of permanent deformation at the rims of pits is seen.

The effect of rain exposure on Sierraclad 4 at a 30° impact angle is shown in Figure 20. The erosion resistance of Sierraclad 4 is between that of polycarbonate and acrylic at the lower velocities and approaches that of acrylic at 600mph (see Figure 21). Sierraclad 4 is therefore acceptable for applications in current aircraft windshields in terms of meeting rain erosion requirements.

Other requirements, of course, must be met but they will not be discussed here.

IV. SUMMARY

Although both are susceptible to subsonic rain erosion damage, polycarbonate is superior to acrylic in retention of transmission after exposure. Polycarbonate and acrylic have limited application for enclosures where rain exposures at normal or near normal impingement angles are involved. However, they have been successfully used in aircraft windshields where rain impingement occurs at low angles.

Thin film protective coatings are rapidly removed in a rain environment, even at low velocities and low impingement angles. Ductile protective coatings generally are more durable than hard, brittle coatings but as the impact angles and velocities are increased, the differences in removal rates among the various coatings diminish. Thin protective coatings have generally not performed acceptably in service.

Erosion and abrasion resistant claddings are approaches which may successfully provide protection for polycarbonate windshields and canopies.

REFERENCES

1. D. L. Voss, "Polycarbonate Protection", presented at Conference on Aerospace Transparent Materials and Enclosures, Atlanta, Georgia, November 1975.

2. H. Oberst, Rain Erosion and Molecular Properties of Synthetic Materials, Royal Aircraft Establishment Library Translation No. 1335, December 1968.

3. W. F. Adler, private communication.

TABLE 1

Removal of Protective Coatings from Polycarbonate in 1 inch/hour Simulated Rainfall at 30° Impact Angle

VELOCITY MPH	EXPOSURE TIME (MIN)	PERCENTAGE OF COATING REMOVAL			
		ABCITE	TEXSTAR 212	SIERRACOTE 233	TEXSTAR 254
345	5	---	3%	0	----
	15	---	100%	20%	----
	30	---		75%	----
	120	---			30%
400	5	40%	----	50%	----
	10	80%	----	100%	----
	30	100%	----		
500	1	60%	----	5%	----
	5	100%	----	100%	15 %
	10		----		50%
	15		----		75%

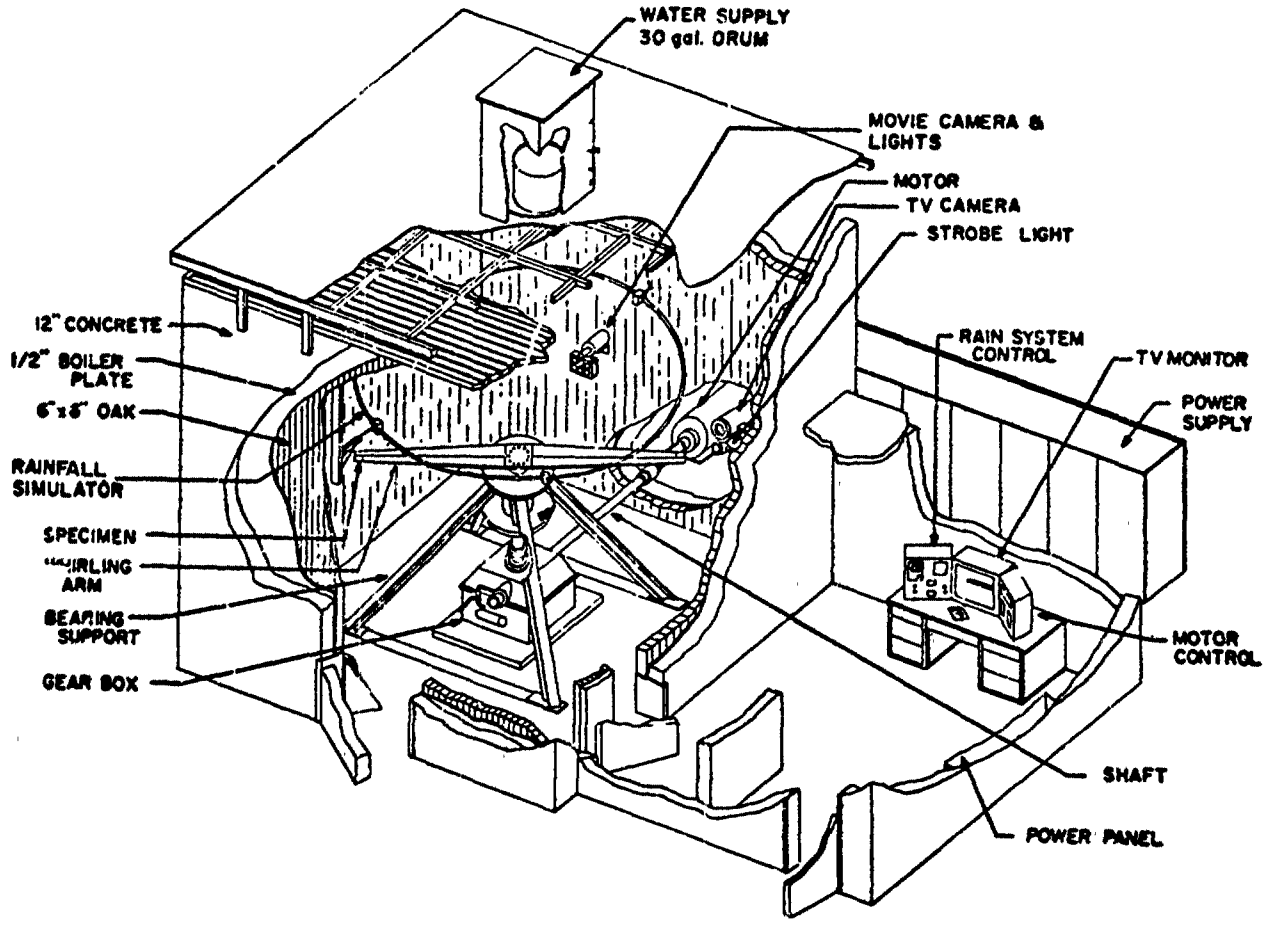


Figure 1. AFML Rotating Arm Apparatus

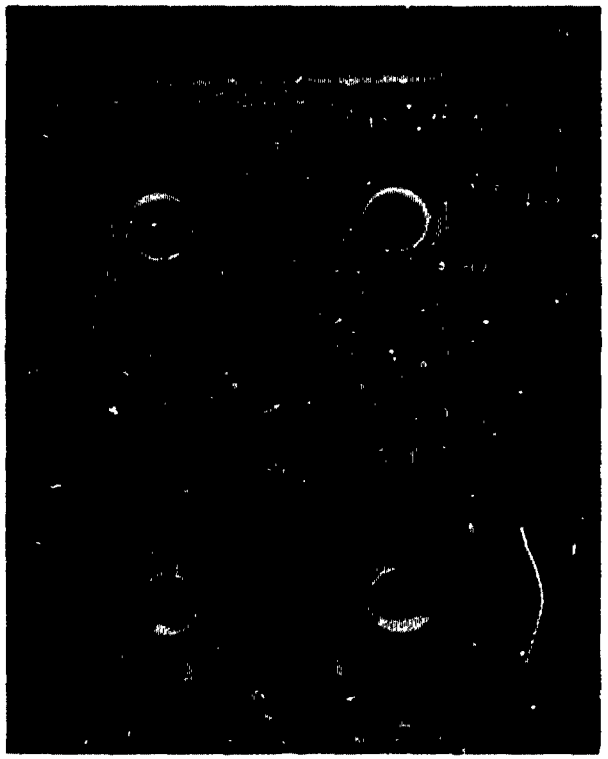


Figure 2. Eroded polycarbonate after 25 minutes exposure to rain at 500 mph and 90° impact angle.

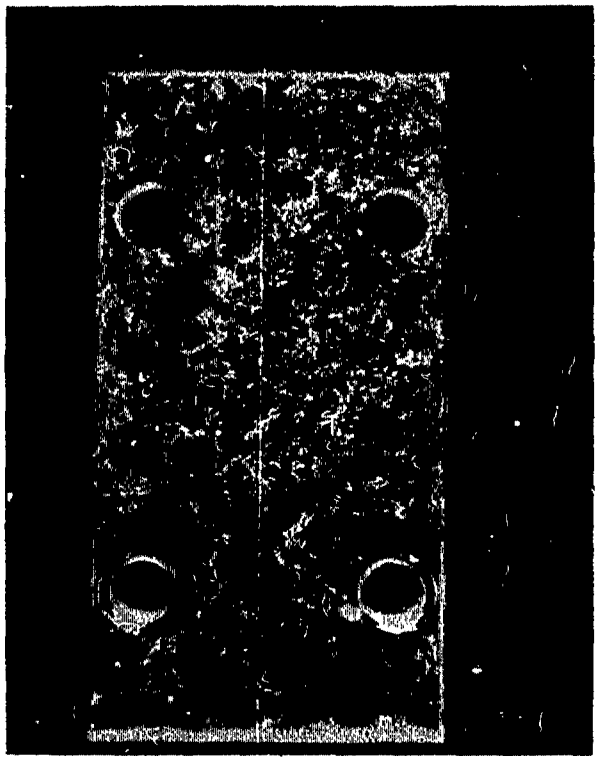


Figure 3. Eroded acrylic after 5 minutes exposure to rain at 500 mph and 90° impact angle.

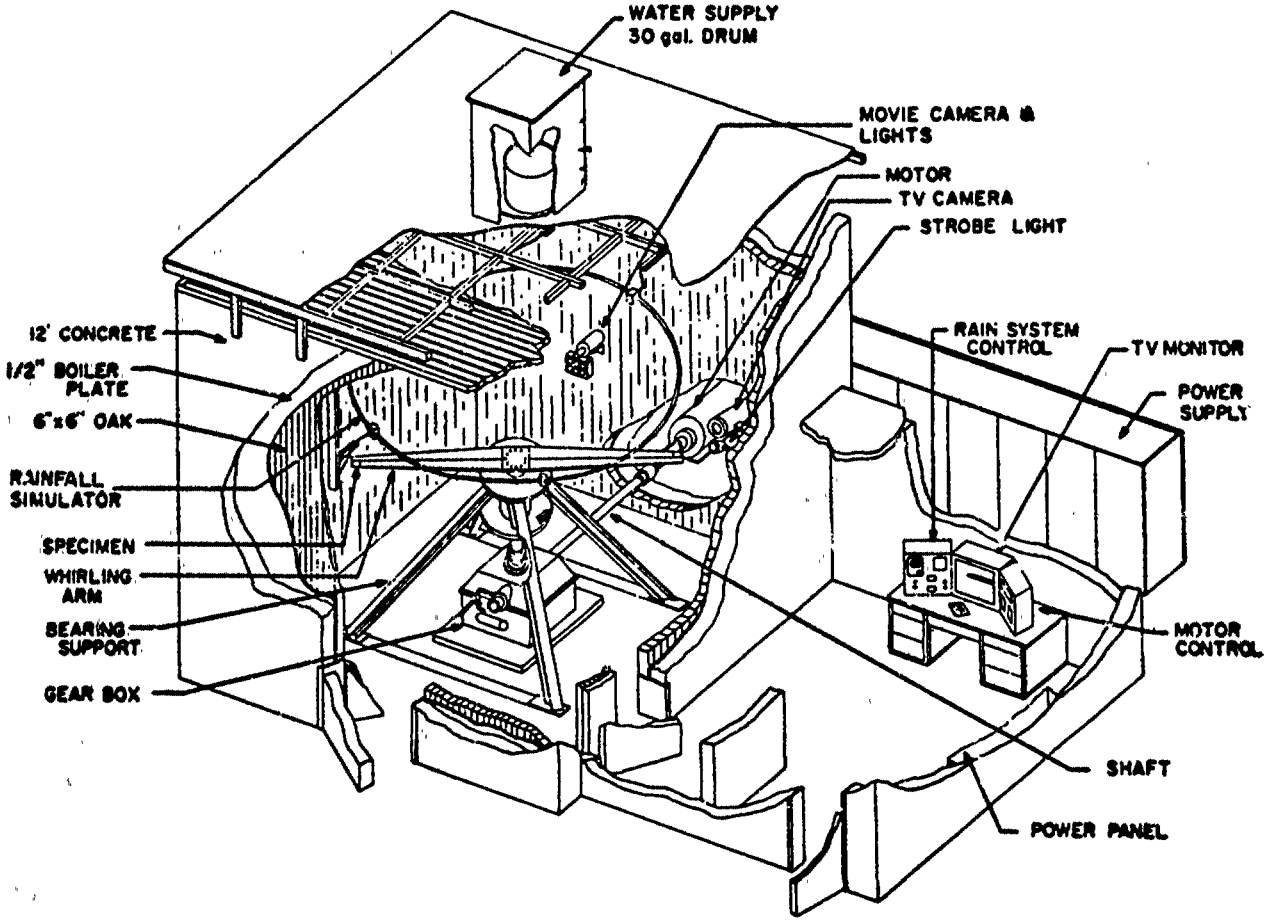


Figure 1. AFML Rotating Arm Apparatus

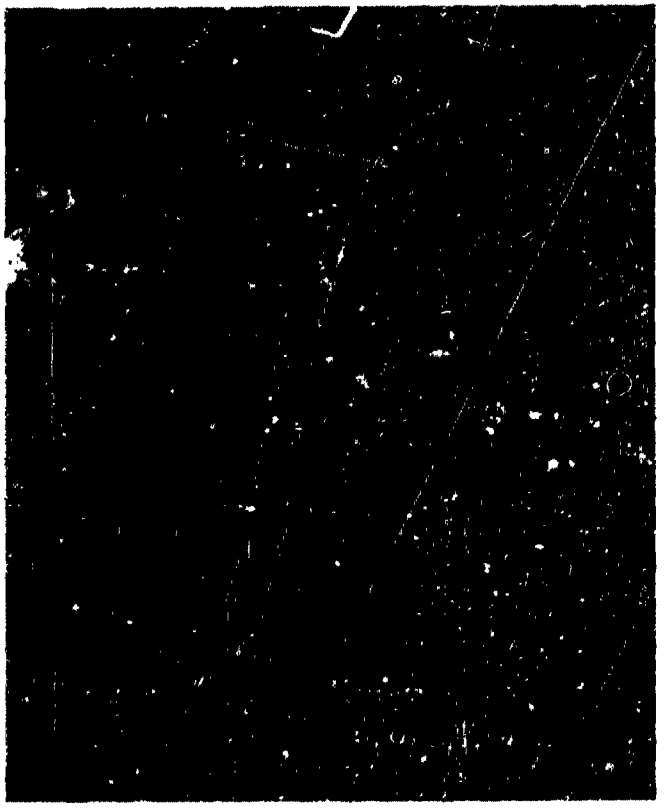


Figure 4. Deformation of polycarbonate surface due to initial drop impacts at 500 mph. 175x

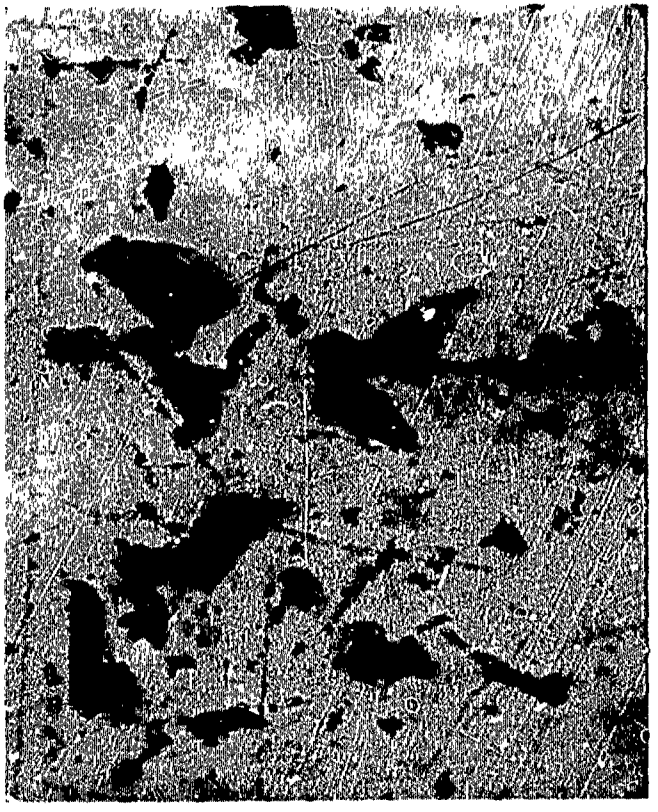


Figure 5. Pitting of polycarbonate after 25 minutes exposure at 500 mph and 90° impact angle. 44x

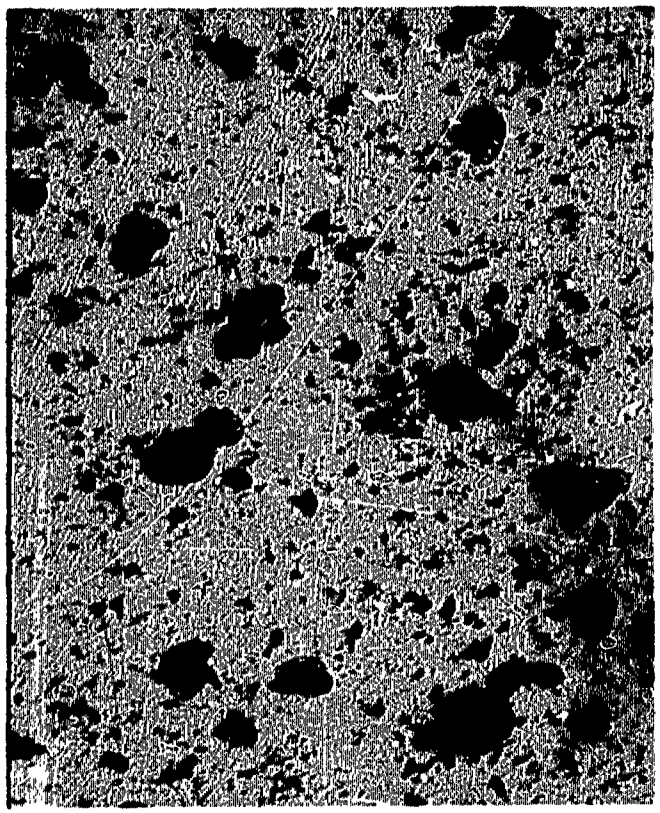
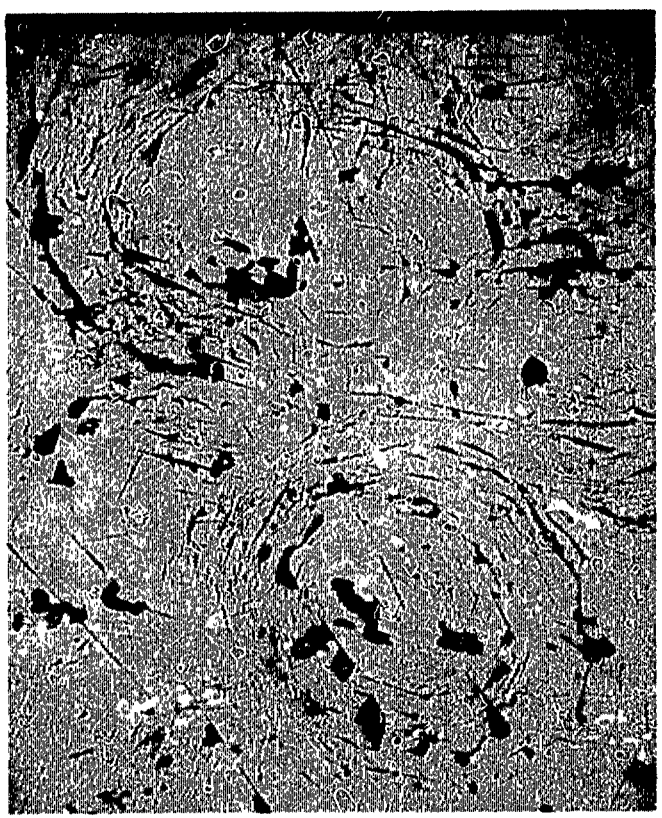


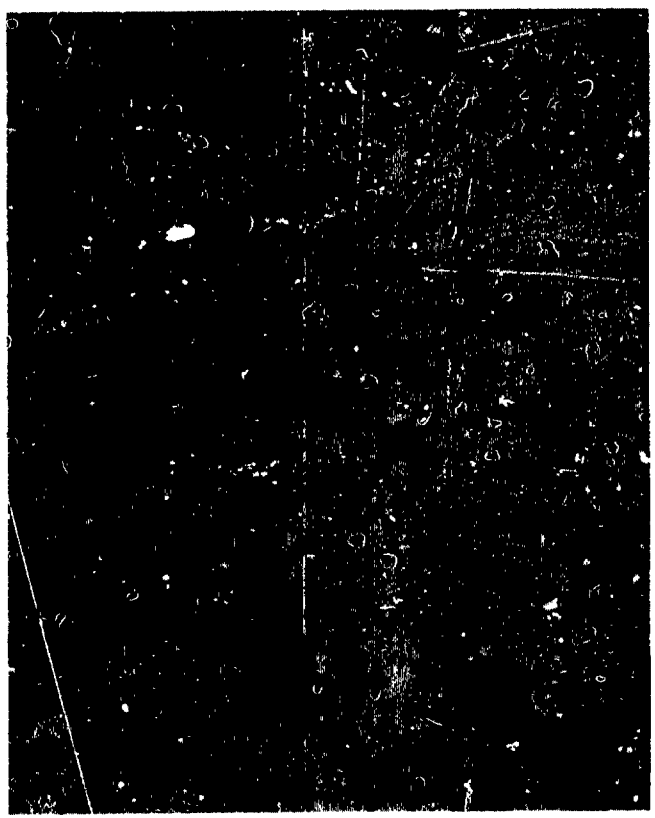
Figure 6. Pitting of polycarbonate after 30 minutes exposure at 500 mph and 30° impact angle. 44x



Figure 7. Initial rain erosion damage to acrylic after 1 minute at 500 mph. 44x



44x



175x

Figure 8. Eroded acrylic after 10 minutes exposure at 400 mph and 90° impact angle.

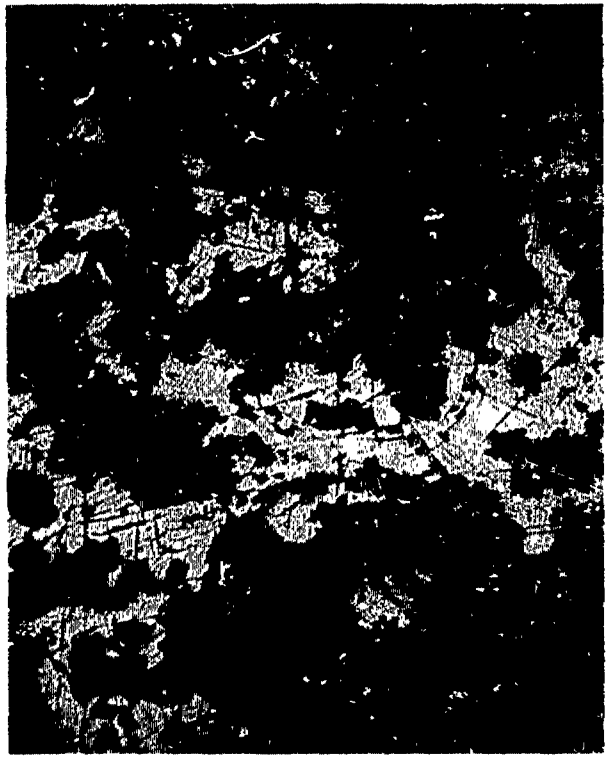


Figure 9. Eroded acrylic after 30 minutes exposure at 400 mph and 90° impact angle. 44x

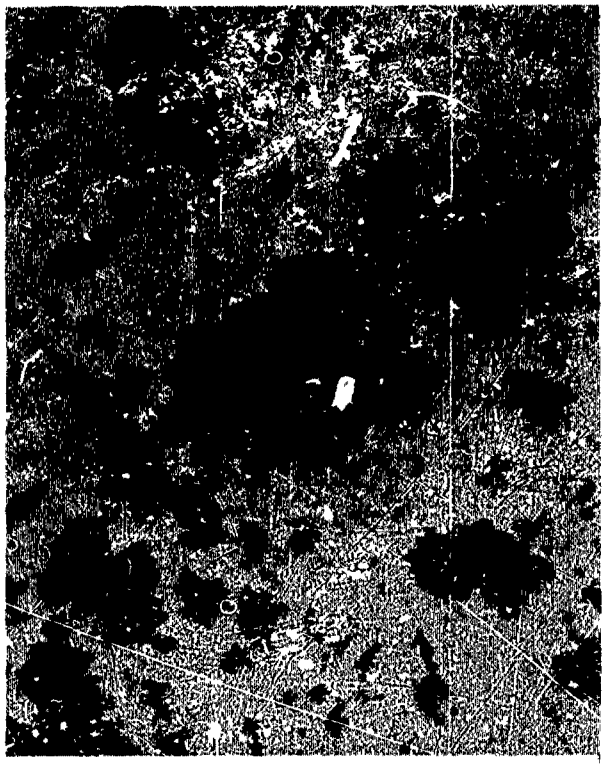


Figure 10. Pitting of stretched acrylic after 30 minutes exposure at 500 mph and 30° impact angle. 50x

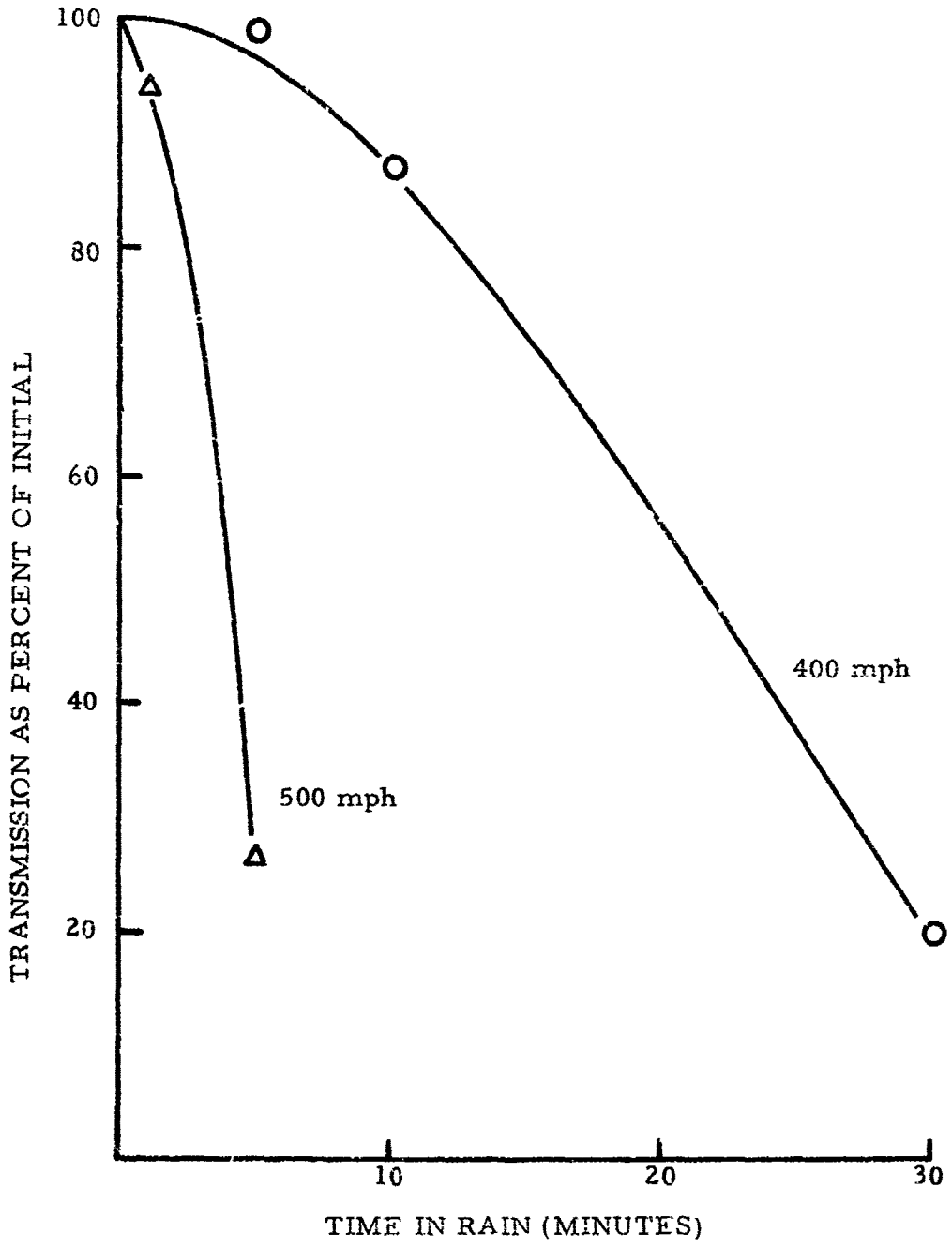


Figure 11. Transmission for acrylic after rain erosion at a 90° impact angle as a function of velocity.

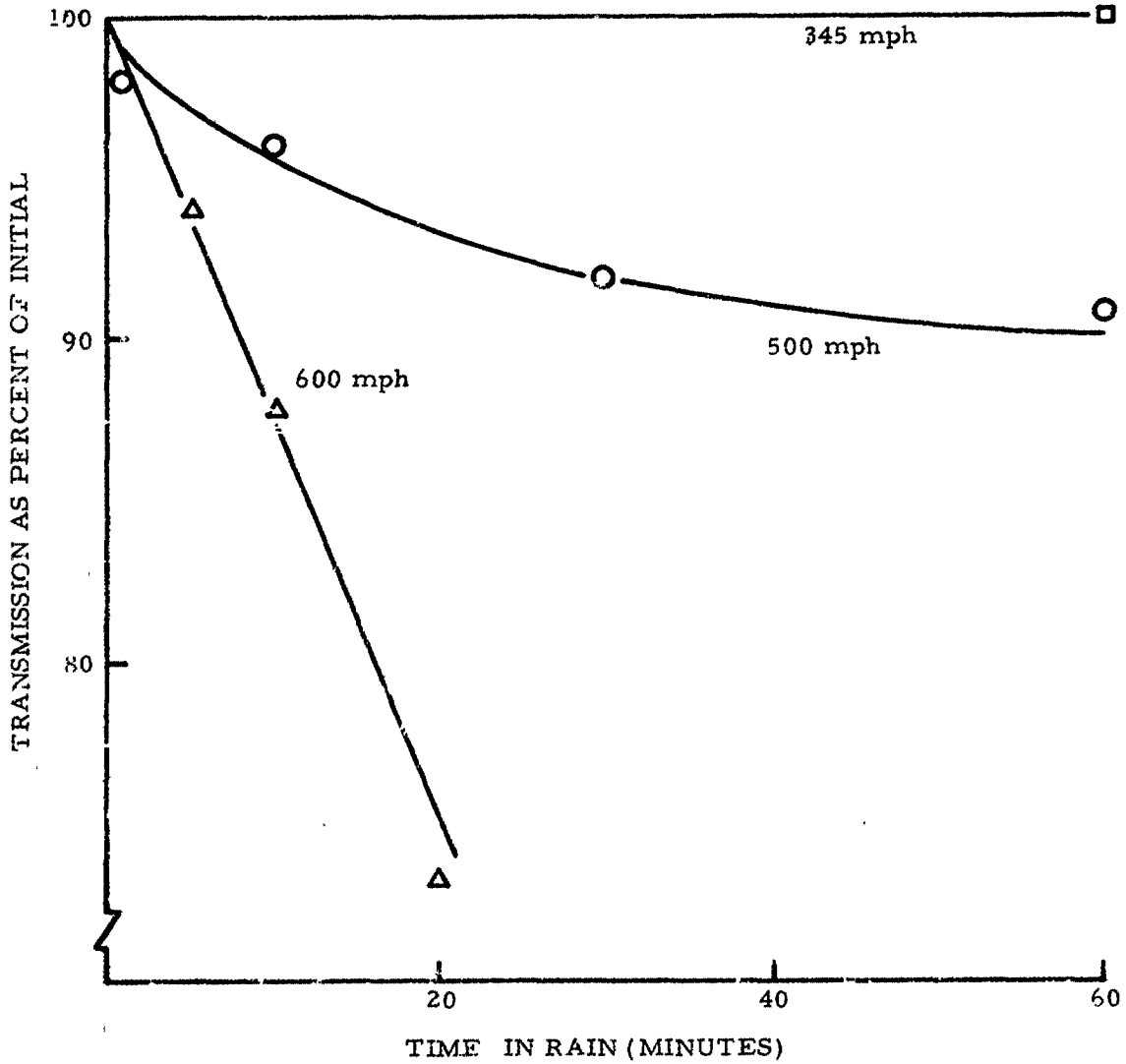


Figure 12. Transmission for acrylic after rain erosion at a 30° impact angle as a function of velocity.

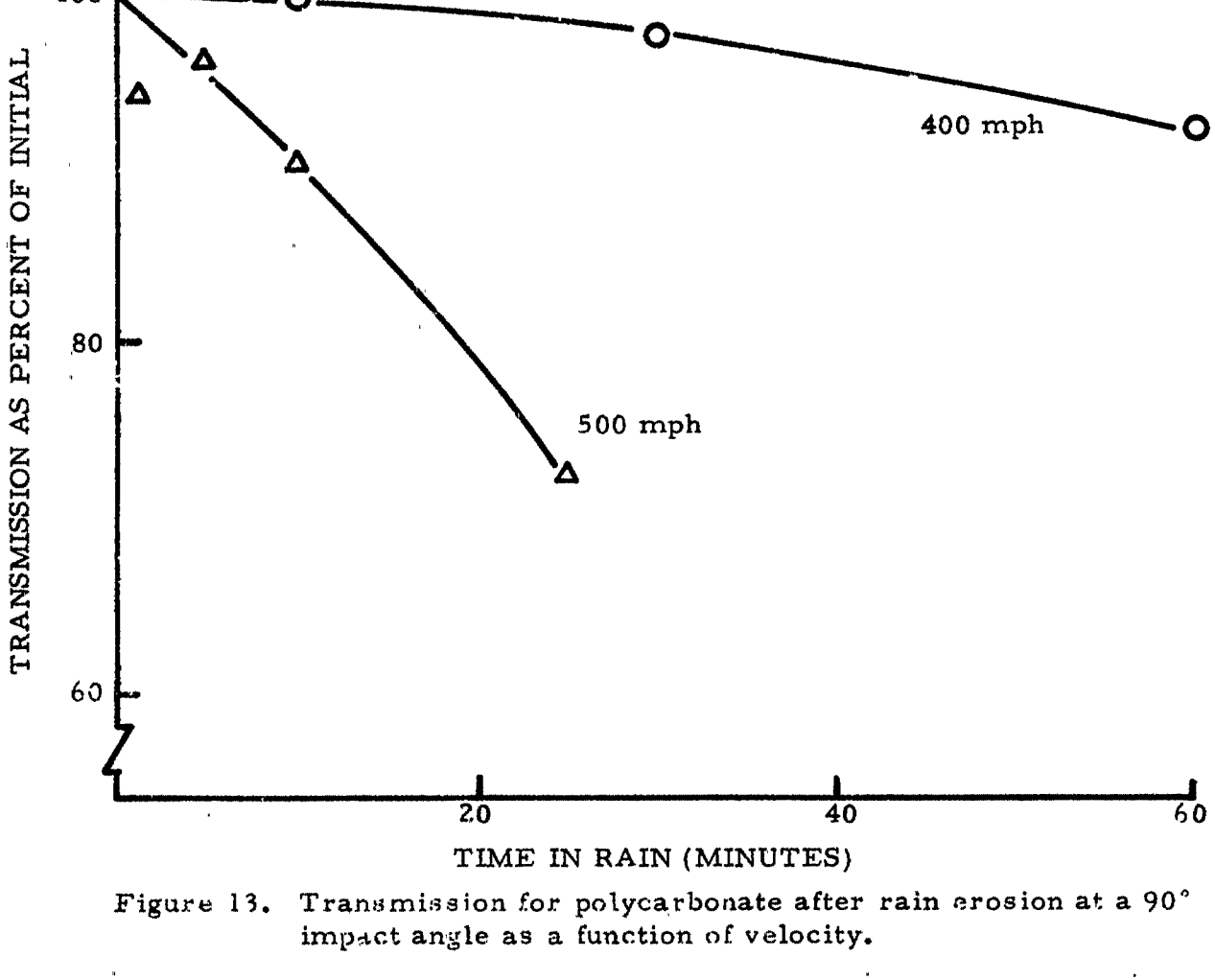


Figure 13. Transmission for polycarbonate after rain erosion at a 90° impact angle as a function of velocity.

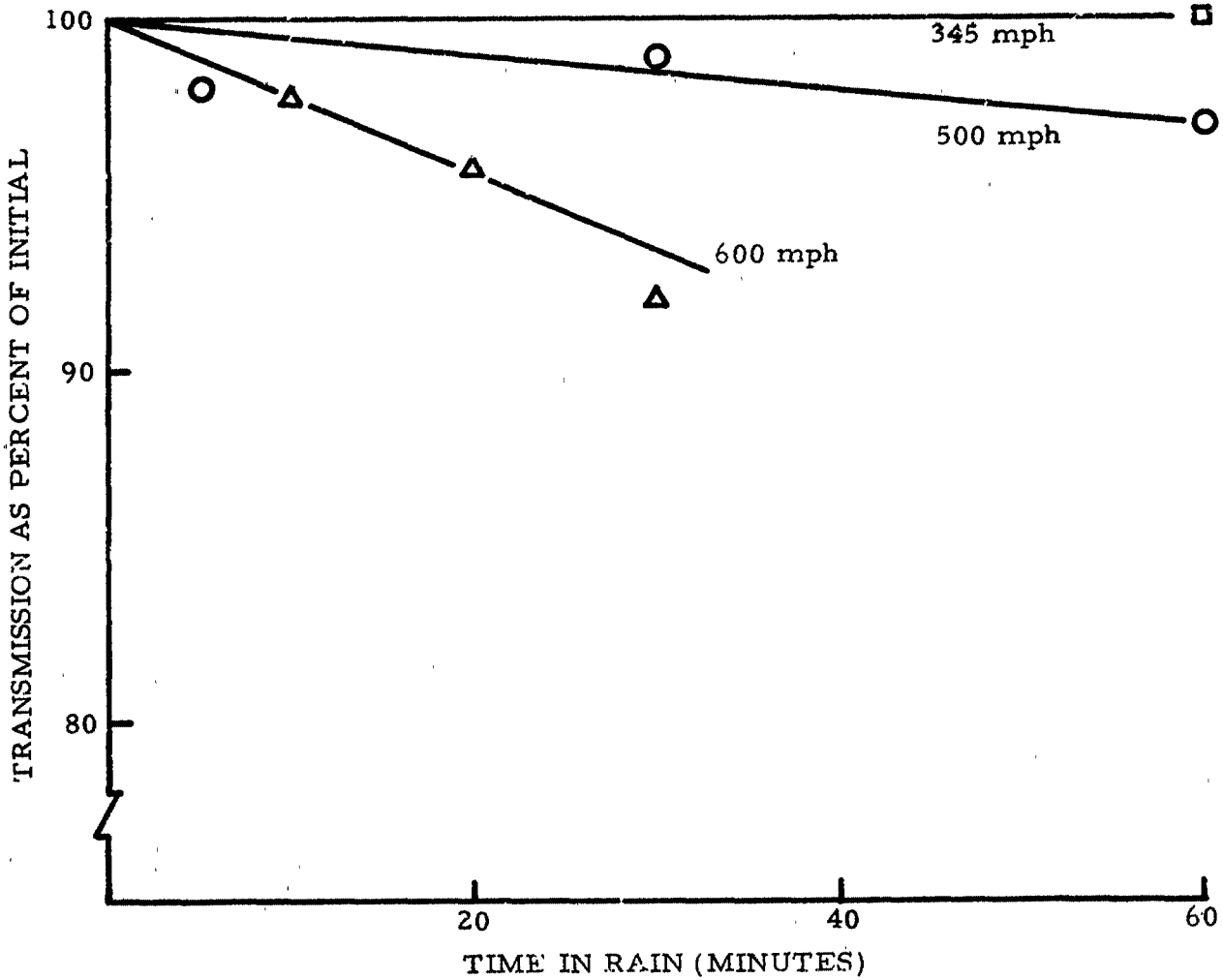


Figure 14. Transmission for polycarbonate after rain erosion at a 30° impact angle as a function of velocity.

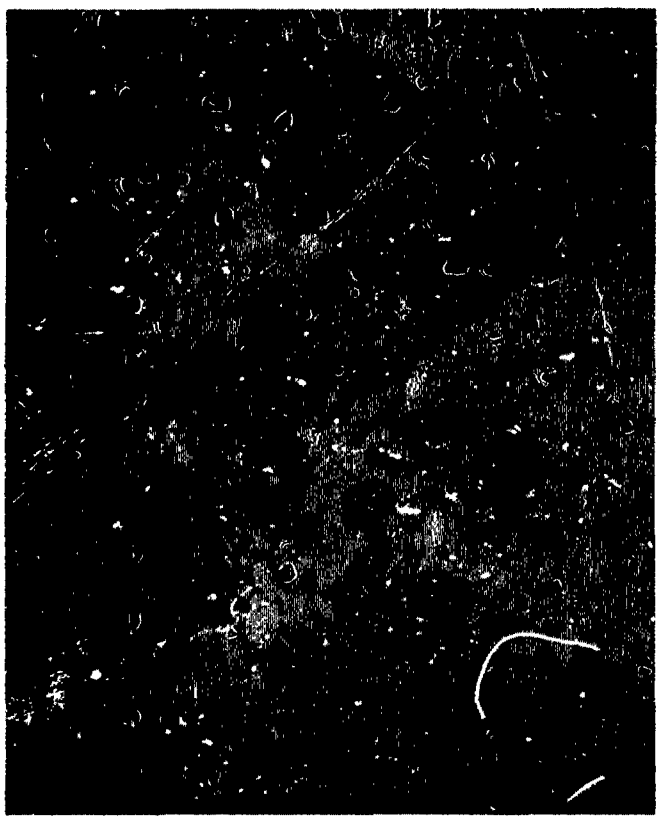


Figure 15. Removal of Abcite from polycarbonate. 44x

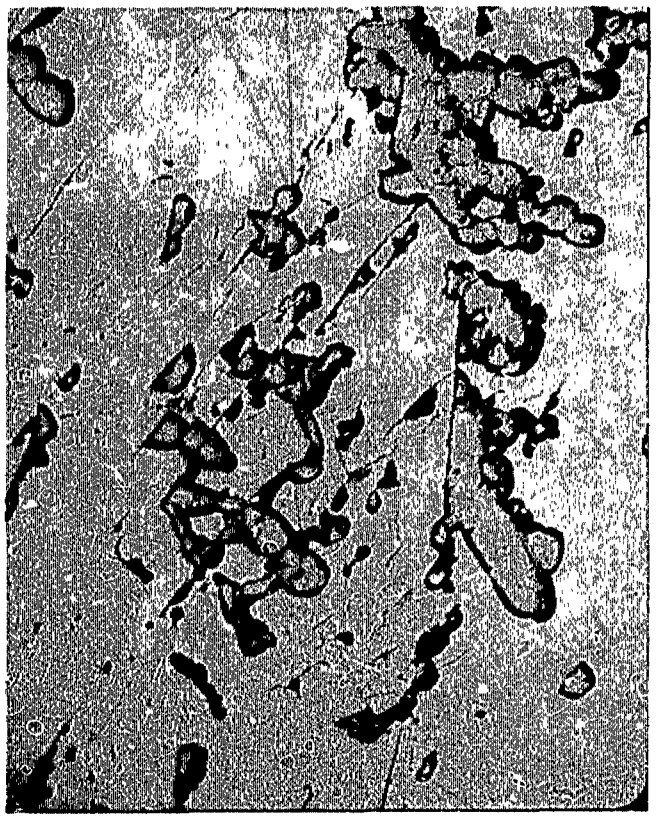


Figure 16. Removal of Texstar 254 from polycarbonate. 44x

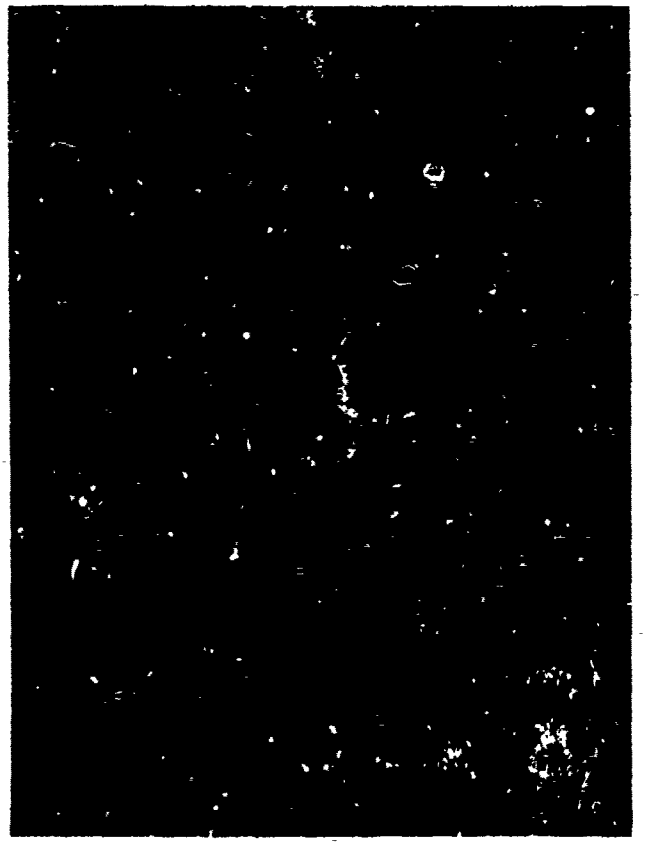
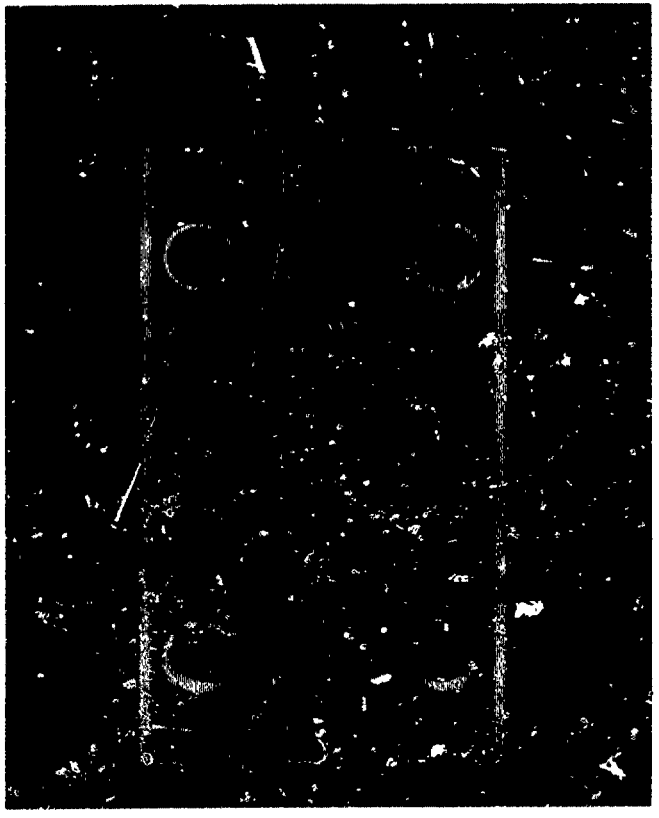


Figure 17. Ring cracks in polycarbonate after removal of Abcite coating in 1 minute at 500 mph. 175x



(a) Brittle damage mechanisms. 44x



(b) Surface frosting after 5 minutes at 500 mph.

Figure 18. Degradation of erosion resistance of polycarbonate after coating.

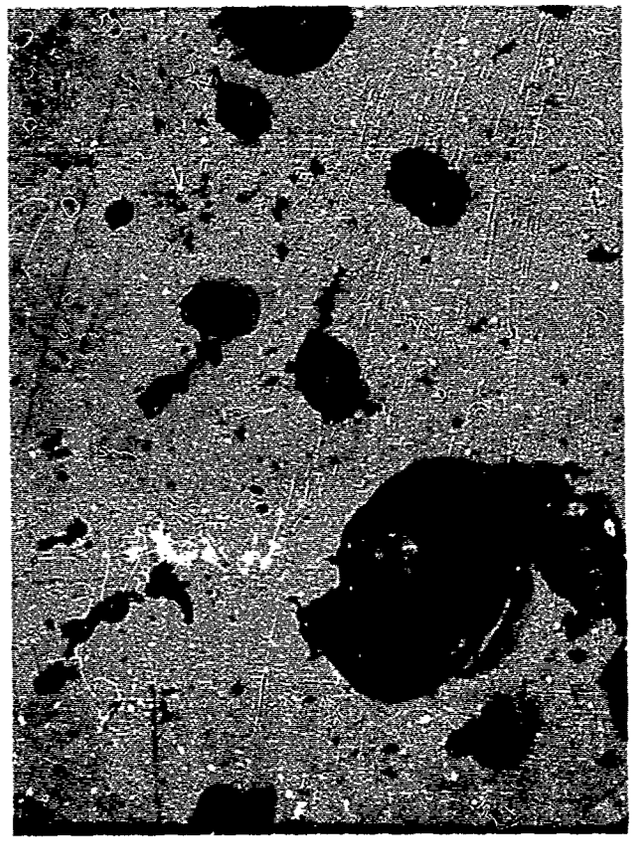


Figure 19. Pitting of Sierraclad 4 after 30 minutes exposure at 600 mph and 30° impact angle. 175x

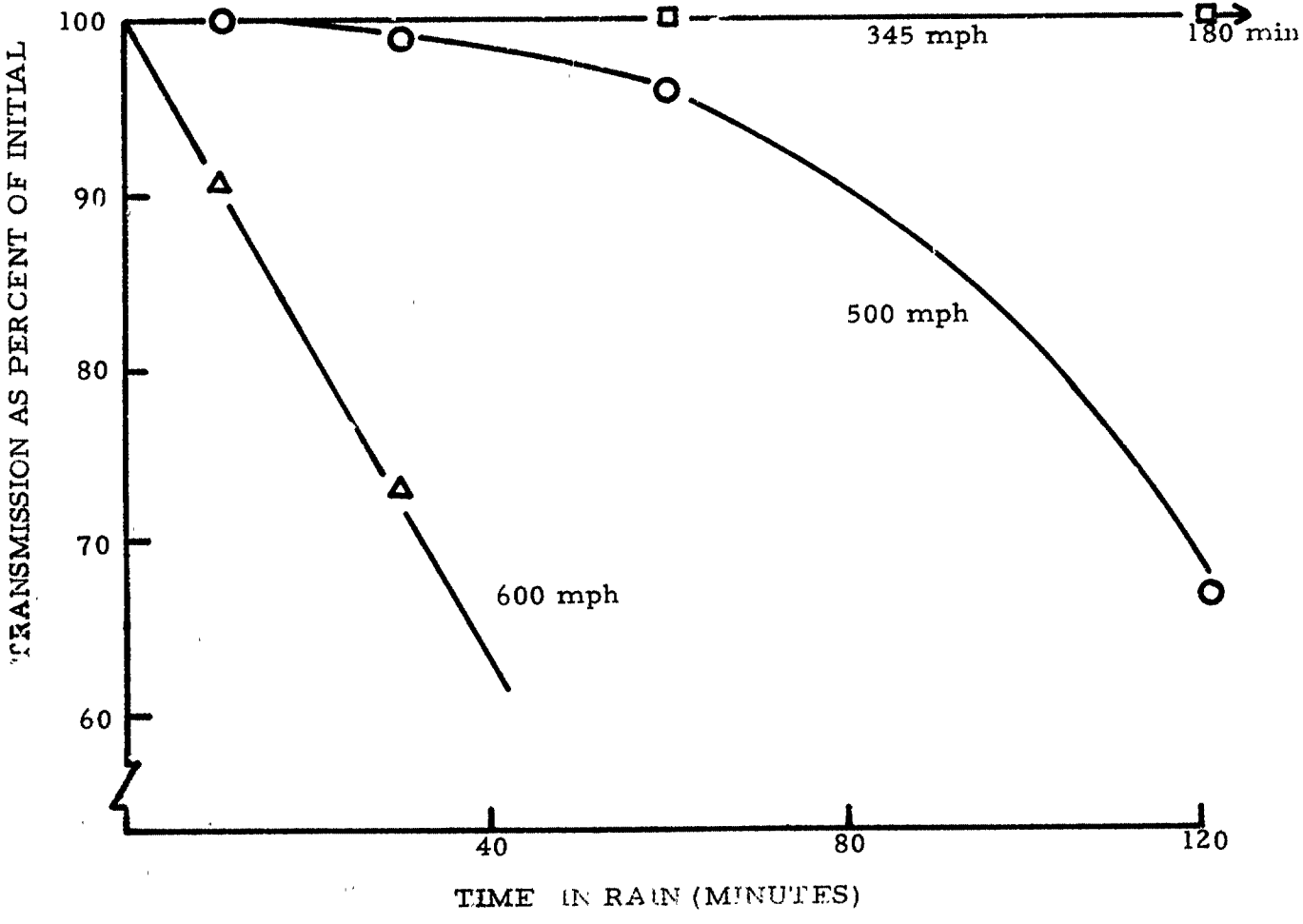


Figure 20. Transmission for Sierraclad 4 after rain erosion at a 30° impact angle as a function of velocity.

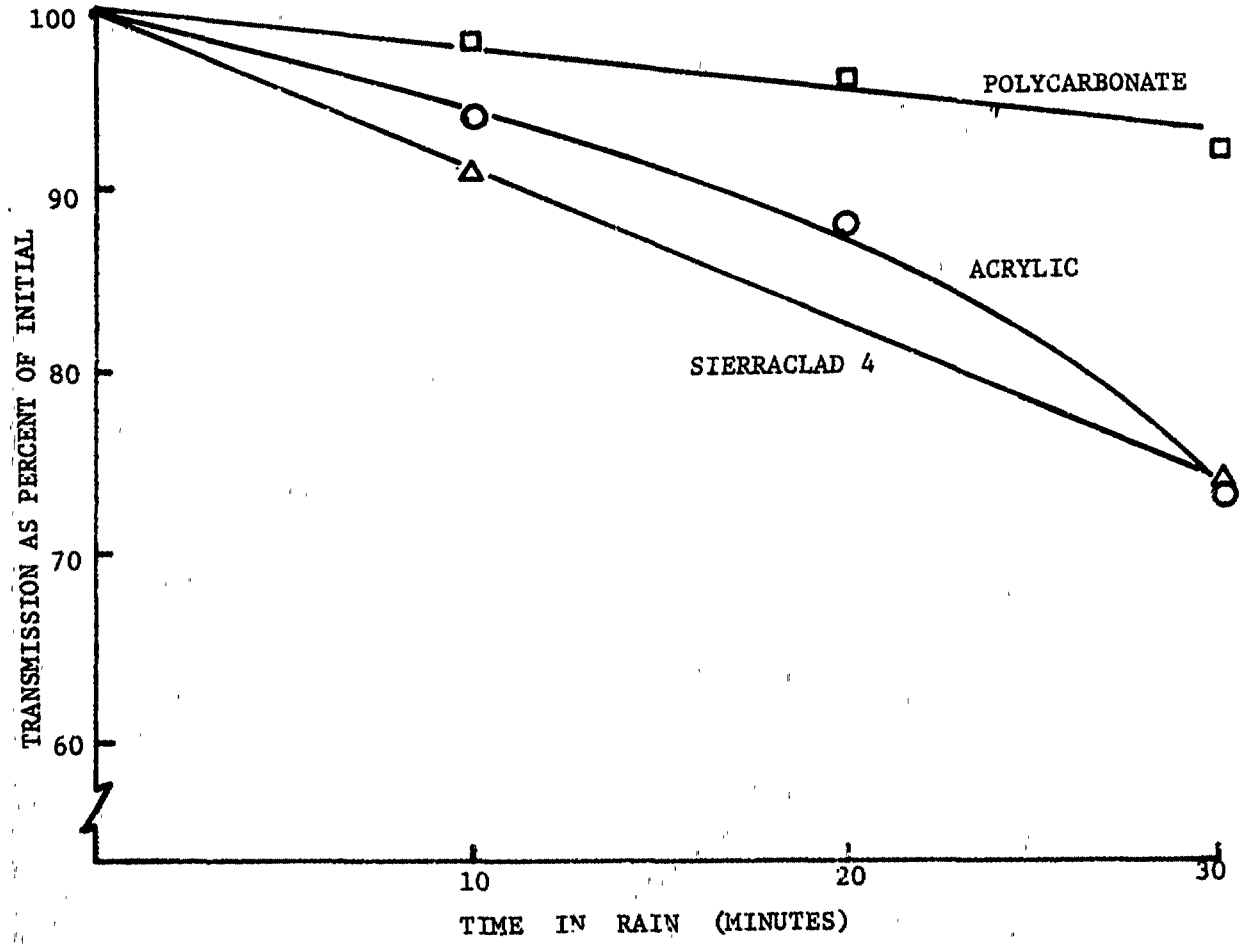


Figure 21. Transmission for polycarbonate, acrylic, and Sierraclad 4 after rain erosion at 600 mph and a 30° impact angle.

NON-DESTRUCTIVE INSPECTION TECHNIQUES FOR ACRYLIC CANOPIES

G. F. Thomas and S. I. Shelton
LTV Aerospace Corporation
Vought Systems Division
Dallas, Texas

NON-DESTRUCTIVE INSPECTION TECHNIQUES FOR ACRYLIC CANOPIES

G. F. Thomas and S. I. Shelton

LTV Aerospace Corporation
Vought Systems Division

ABSTRACT

The advantages and necessities of non-destructive inspection (NDI) of aircraft structural components have gained wide recognition in the Aerospace industry. This extends to evaluation of transparent enclosure materials in which the structural adequacy and integrity of the component must be determined. This paper describes the task required in the development and application of an ultrasonic NDI method for detection of defects and determination of variations in material characteristics in aircraft canopies.

Selection and development of applicable NDI techniques sensitive for measurement or detection of three test conditions is discussed. Three different techniques were required. These include: (1) a pulse-echo technique for detection of debond condition at the inner surface of the nylon and canopy glass, (2) a delta technique for detection of subcritical cracks in canopy glass, and (3)an angle beam technique for determination of the distance between the canopy glass and attach holes. A brief theoretical approach to each technique is presented in terms of wave propagation and response characteristics relative to location, size, type, and orientation of defects or variations in required material properties.

Transducer evaluation and reference standard development is described as well as the development of various fixturing devices and inspection aids. Inspection capabilities, limitations, and test results are discussed. Information is presented concerning the application of the techniques for each test condition in terms of procedures, equipment requirements, and personnel training.

INTRODUCTION

It is desirable to be able to insure that acrylic canopies are free of defects or variations in materials characteristics which could affect their structural adequacy. Non-destructive inspection (NDI) provides a means of monitoring several areas of concern, enabling detection of adverse characteristics before propagation beyond allowable limits occurs. The inspection techniques include a method of determining bond integrity for canopies with bonded edge attachments, a method of detection of subcritical cracks in stretched acrylic canopies and a method of monitoring the precise relationship of the glazing within the bonded edge attachment.

It is not suggested that these techniques are universally applicable to all designs without modification. These techniques are presented here to demonstrate a basic approach from which alternate techniques applicable to specific designs may be developed.

Ideally the NDI method selected should be applicable to both production inspection and in-service inspection of installed canopies.

NDI is a system based primarily on the use of various energy fields, each of which can be applied to the component to be inspected by various methods and techniques utilizing detailed test procedures. The traditional NDI approach is to:

- Look for defects or variations in design tolerances.
- Characterize these defects or variations in terms of required properties.
- Select an inspection method/technique(s) sensitive to these conditions.
- Set up (develop) and verify inspection procedures.

Ultrasonic was selected as the NDI method for the task described in this paper because of its reliability and also because of its versatility, adaptability, and applicability.

Visual inspection of installed acrylic canopies is limited in reliability. Small cracks which are readily visible on test specimens are considerably more difficult to detect visually on a canopy installed on an aircraft. This is due, in part, to the light-pipe effect where light enters the end of the test specimen and is reflected off the crack interface. Furthermore, the size of the specimen allows rapid reorientation to provide a favorable eye-to-specimen angle and specimen-to-illumination angle. On an installed canopy such a procedure is time consuming at best and may be physically impossible. Similar problems are encountered in visual inspection of bondlines of edge attachment member. Visual inspection cannot assess the relative location of the glazing within the edge member.

The ultrasonic techniques presented in this paper have no such limitations. A primary criterion in their development was that they be usable on

installed canopies. Suitable crew stands or other access to the canopy are all that is required for the inspection in addition to the ultrasonic apparatus.

The flaws utilized in proving these techniques were generated by artificial means, i.e. overstressing or overaging specimens constructed in canopy configuration. However, application to actual canopies is straightforward.

ULTRASONIC METHOD

Most ultrasonic testing employs pulsed energy in which a piezoelectric transducer converts high-frequency electrical signals or impulses into mechanical vibrations. The mechanical waves from the transducer are coupled to the material under test and serve as the probing sound energy medium. The coupling medium is usually oil or water.

Inspection is performed by an analysis of the ultrasonic waves received by the transmitter/receiver transducer, as in pulse-echo or shear wave techniques, or by a second transducer (receiver), as in the delta technique. Regardless of which ultrasonic technique is used, the received mechanical ultrasonic waves are converted back into electrical signals by the piezoelectric transducer and amplified and displayed on a cathode ray tube (CRT) for interpretation. The amount of energy received may be directly related to the defect orientation and cross-sectional area or to material variations, all with respect to the incident beam. Three main modes of vibration are commonly used in ultrasonic inspection: longitudinal, shear, and surface waves. For the types of conditions under evaluation in this paper, primary emphasis is directed to the longitudinal and shear modes of energy.

The more commonly employed techniques of testing with ultrasonic energy are best explained with emphasis on wave propagation. An oscillatory pulse of energy traveling in an unbounded elastic solid may have two distinct components, viz, longitudinal (compressional) and shear (transverse) waves. Longitudinal waves usually are generated at normal incidence in which the sound energy enters perpendicular to the material under test. Shear waves will be generated provided mode conversion occurs.

As a result of mode conversion within the material, longitudinal waves may become shear waves, and conversely. This conversion occurs when a sound beam strikes an interface between materials of different acoustic velocity or impedance properties, at other than normal incidence. In addition, sound energy may be converted to other modes of vibration during reflection or refraction. Within the material each mode of energy, longitudinal waves or shear waves, will propagate at their characteristic velocities for that material. Shear waves have a velocity of approximately one-half that of longitudinal waves. Longitudinal waves exist when the motion of particles of a medium is parallel to the direction of propagation. In shear waves, the particle motion of the material is perpendicular to the direction of wave propagation. The relationship of particle motion and wave propagation is depicted in Figure 1.

TECHNIQUES

General

Many important factors were considered in the development of the three techniques described herein. These factors dictated to a large extent the selection of a particular technique. A primary consideration was the capability of the techniques to be applied on installed as well as uninstalled canopies. Another major concern was the accessibility of the area of inspection relative to transducer placement or position. Finally, it was desired to provide technique applications and signal analysis which would be straightforward and readily interpretable by qualified personnel.

The three techniques were developed using a Sperry UM721 Reflectoscope, 105 db pulser/receiver, fast transigate, and off-the-shelf transducers. Preliminary laboratory evaluations were conducted in an immersion ultrasonic tank as shown in Figure 2 which provided controlled X, Y, and Z axes angular movement. A transducer manipulator device was also used in the development of the delta technique. Specially designed fixturing devices and inspection aids were developed and utilized. After tests had established the values of parameters for optimum operation, transducer wedges or holding devices with fixed dimensions and simpler design were made for routine inspection.

Transducer evaluation primarily consisted of experimentally selecting the transducer or combination of transducers which would provide sufficient ultrasonic energy within the inspection zone to detect the condition under evaluation. This was accomplished by optimizing transducer parameters such as frequencies, compositions, damping characteristics, shapes, and physical arrangements to provide maximum detection capability with minimum presentation of extraneous signals on the CRT screen.

Reference standards representative of the condition to be inspected were developed for each technique. The purpose of standards is to (1) establish inspection procedures, (2) determine sensitivity levels, and (3) standardize equipment. Repeatability of an inspection is of prime importance.

It was noted in development of all techniques that variations in temperature affect signal response. At canopy temperatures above approximately 90°F, increased attentuation may cause significant signal reduction. Therefore, it is required to reduce canopy temperatures to an allowable inspection level.

Pulse-Echo Technique for Detection of Debond Condition at the Inner Surface of the Nylon and Canopy Glass

In the case of determination of debond condition, the relationship between materials of different acoustic impedance is an important consideration. Generally, the greater the impedance mismatch between two adjacent materials, the greater the percentage of reflected sound energy. Conversely, the closer the impendance match between two adjacent materials, the greater the percentage of transmitted sound energy.

The expressions relating to sound energy interaction at normal (perpendicular) incidence to interfaces between two media is given as follows:

$$R = \left(\frac{Z_2 - Z_1}{Z_2 + Z_1} \right)^2$$

$$T = \frac{4Z_2 Z_1}{(Z_2 + Z_1)^2}$$

$$Z = PV$$

$$R + T = 1$$

where,

R = Coefficient of reflection

T = Coefficient of transmission

Z = Impedance (Z_1 and Z_2 = Acoustic impedance of respective media)

P = Density (material)

V = Velocity (sound)

Approximate acoustic impedance values for Nylon = 2.9, Acrylic = 3.1, and Air = .0004. It can be seen that a larger percentage of sound energy will be reflected from an acrylic/air boundary (debond) than from an acrylic/nylon boundary (bond).

The limited access to the area of inspection required construction of a special scanning device as depicted in Figure 3. The conical truncated collimator permits entry of the sound into the selected area without producing excessive spurious indications.

A 5.0 MHz, 0.187 inch diameter straight beam medium damped transducer connected by a coupling fixture to the collimator scanning device was used. Other size, type, and frequency transducers were evaluated but proved unacceptable for this application.

A reference standard was developed and is shown in Figure 4. The instrumentation was standardized by coupling the transducer holder to the standard with lightweight oil. Test sensitivity was adjusted to produce a response from the reference flaw of approximately 80% of the vertical scale on the CRT screen. This signal is electronically gated with an alarm level set to trigger at approximately 40% of the vertical scale. A typical CRT screen presentation of a bonded and non-bonded area is presented in Figure 5.

After standardization of equipment, the entire edge area was inspected as shown in Figure 6. The transducer holder is coupled by lightweight oil to the canopy. Scanning is accomplished by slowly sliding the transducer holder

along the canopy glass and observing the CRT screen and gate alarm level for any indication in the gate corresponding to the response from the reference flaw of the standard. When scanning, it is necessary to insure adequate couplant between transducer holder and canopy and that any response in the gated area on the CRT screen is caused by a debond condition and not from the canopy glass back surface in non-nylon backed areas.

All indications that equal or exceed the alarm level are marked for additional evaluation. By using the sensitivity settings noted above, debond conditions as small as 0.125 inch diameter have been detected and verified by additional testing.

Delta Technique for Detection of Subcritical Cracks in Canopy Glass

The detection of subcritical cracks posed a different problem than that presented by a debond condition. The position or orientation of a crack was such that standard pulse-echo or shear wave conceivably could not detect this condition as depicted in Figure 7. Also, accessibility to the area of inspection was of major concern. Therefore, a delta technique was used for detection of cracks.

The delta technique was named for the triangular positions or "delta" pattern of the search units (transducers) used in the ultrasonic test (see Figure 8). All forms of delta employ two or more transducers; one being a receiver that is positioned normal (perpendicular) to the surface being inspected, the other transducer is a transmitter that is angulated to introduce sound energy into the material at an angle that provides best energy partition. The axis of sound propagation of the receiver and transmitter transducers must lie in a common plane. The sound energy travels until it strikes an interface, is reflected from the interface, and is detected by the receiving search unit (Figure 9). An interface is anything that has an acoustic impedance different from the parent material and results in an interruption of the propagation pattern of the sound beam.

As previously noted, when sound energy is propagated through one medium into another medium with different acoustical characteristics at an angle other than normal incidence, the sound energy is refracted. Two primary modes of energy are produced through refraction, longitudinal and shear waves. The angle of refraction depends on the ratio of velocities within the media and the angle of incidence of the transmitting search unit in relation to the boundaries of the media. The angle of refraction can be determined by Snell's Law as defined by

$$\frac{\text{Sin}\,\alpha}{Vc} = \frac{\text{Sin}\,\phi}{Vs} = \frac{\text{Sin}\,\beta}{V_L}$$

where,

Sin = Sine of angle
Vc = Velocity of sound energy in coupling medium
Vs = Velocity of shear energy
V_L = Velocity of longitudinal energy

The delta configuration used in this technique was first established using a laboratory fixturing device which permitted coupling through immersion of the test part and transducers and provided angulation and movement of transducer in the X, Y, and Z axes (Figure 10). The arrangement of transducers used in a delta head normally can be simple in that the distance between the transmitter and receiver transducers is a fixed distance and the angle of incidence of the transmitter is constant.

However, in order to obtain this relationship between the transducers and the material to be inspected a "trial and error" period must be experienced. A close approximation of the delta head design can be obtained through the application of simple mathematics and the use of the physical characteristics of the material under evaluation.

Optimizing the configuration consisted of determining the best combination of transducer composition, frequency, position, and angle of incidence. The optimum energy pattern produced is depicted in Figure 11. It can be seen that both longitudinal and shear wave energy is produced but the predominant energy pattern is longitudinal. Basically, the energy distribution was such that the area under inspection was flooded with energy uniformly distributed throughout the cross-section.

It was determined that using miniature 5.0 MHz, 0.250 inch diameter focused beam transducers composed of lead zirconate would produce optimum results. The configuration was used to design a plastic transducer holder (Figure 12) in which the coupling medium is lightweight oil.

A reference standard was developed and is shown in Figure 13. Artificial defects 0.125 x 0.062 inch (half circle) at an angle of 25° to 55° from the horizontal have readily been detected in test standards. The instrumentation was standardized on the reference standard as depicted in Figure 14. The response from the reference flaw is maximized and electronically gated. The signal height is adjusted to approximately 80% on the CRT screen. The alarm level was set to trigger the gate at a signal height of approximately 50% of the vertical scale.

After standardization of equipment inspection is performed as depicted in Figure 15. Scanning consists of slightly twisting the transducer holder while moving back and forth and to the right and left in relation to the area of interest and indexing approximately 0.050 inch increments along the canopy edge. During scanning, it is necessary to insure adequate couplant between the transducer holder and canopy, and within the transducer holder. Care must also be taken to assure removal of air bubbles within the holder.

All indications that equal or exceed the alarm level are marked for additional evaluation. Subcritical fatigue cracks in the order of 0.100 x 0.060 inch and approximately 30° - 40° from the horizontal have been detected in test parts. Detection of flaws smaller than 0.100 x 0.060 inch would increase the signal-to-noise ratio and increase spurious indications making interpretation of the response difficult.

Angle Beam Technique for Determination of the Distance Between the Canopy Glass and Attach Holes

The location of the edge of the canopy glass presented a problem unlike either of the foregoing techniques. An accurate determination is necessary to measure the distance between the edge of the canopy glass and the attach holes which are drilled into the nylon bonded to the glass. In the unassembled condition, although the nylon is translucent, an accurate visual measurement cannot be obtained. Also, after canopy installation with sealant and fasteners, no visual measurement is possible. Only the centerline of the fastener through the attach holes can be determined. The relation of the edge of the glass to these holes must be made ultrasonically.

Inspection of the area of interest required angulating the transmitter/receiver transducer. In this case longitudinal wave energy is primarily produced and propagates through the point of entry to the edge of the glass. The acoustic impedance mismatch between the nylon and glass causes significant reflection of the transmitted energy. Some energy is transferred into the nylon, but the major portion of energy is reflected back in the direction of the transducer.

The configuration of the edge of the glass causes the return path of the energy to assume divergent paths because of the dimensional variations and energy mode conversion. This presented a prime consideration in regard to required angulation of the transducer. It was necessary to select an angle which would provide a return path in which a significant portion of the energy would be detected by the transmitter/receiver transducer.

Establishing the technique was first conducted in an immersion research tank using water as the coupling medium. After test parameters were determined, a plastic transducer holder was fabricated (Figure 16) in which the transmitter is coupled to the holder. Experiments determined that 70° provided the optimum angle of incidence.

A 2.25 MHz, 0.500 inch diameter straight beam lightly damped lead zirconate transducer connected by a coupling device to the holder was used. Several other size, type, and frequency transducers were evaluated but were unsuccessful.

A reference standard was developed and is as described in Figure 17. The instrumentation was standardized on this standard as depicted in Figure 18. The response from the end of the standard is maximized at approximately 80% height and positioned at approximately 50% of the horizontal scale on the CRT screen. Using either the instrument markers or a grease pencil, the position of the leading edge of the response from the end of the standard was marked on the CRT. The pointer was positioned such that it is exactly in line with the end of the standard.

After standardization of equipment, inspection is performed as shown in Figure 19. The inspection procedure consists of scanning in the direction toward the end of the part and observing the CRT screen for the indication corresponding to the edge of the canopy glass. The transducer holder is positioned along the scan direction such that the leading edge of the response

appears at 50% of horizontal scale on the CRT as previously established. Holding the transducer holder in position, a mark is placed on the aluminum strip (or nylon) in line with the pointer. By establishing several marks and connecting them with a pencil, the edge of the acrylic glass is determined. Visual assessment can be made between the distance of the centerline of the fastener and the edge of the hole. Very close (±0.005 inch) approximation between the edge of the canopy and the attach holes has been determined by this technique.

CONCLUSIONS

The ultrasonic equipment specified herein or equivalent equipment provides improved reliability of inspection of acrylic canopies. The inspection system is portable and lends itself to on-line field inspection. Suitable crew stands or other access to the canopy are all that is required for the inspection in addition to the ultrasonic apparatus.

The techniques are performed on the exterior surface of the canopy. No removal of the canopy from aircraft is required since each inspection can be done either in the installed or uninstalled condition.

The inspection task can be performed by trained, qualified, and certified service inspection personnel utilizing detailed procedures. The procedures developed and prepared for each technique define equipment, material, reference standard, and inspection requirements. Special transducer holders (wedges) and reference standards must be fabricated.

The time required to accomplish the inspection is approximately one hour for the debond technique and two hours each for the other two techniques.

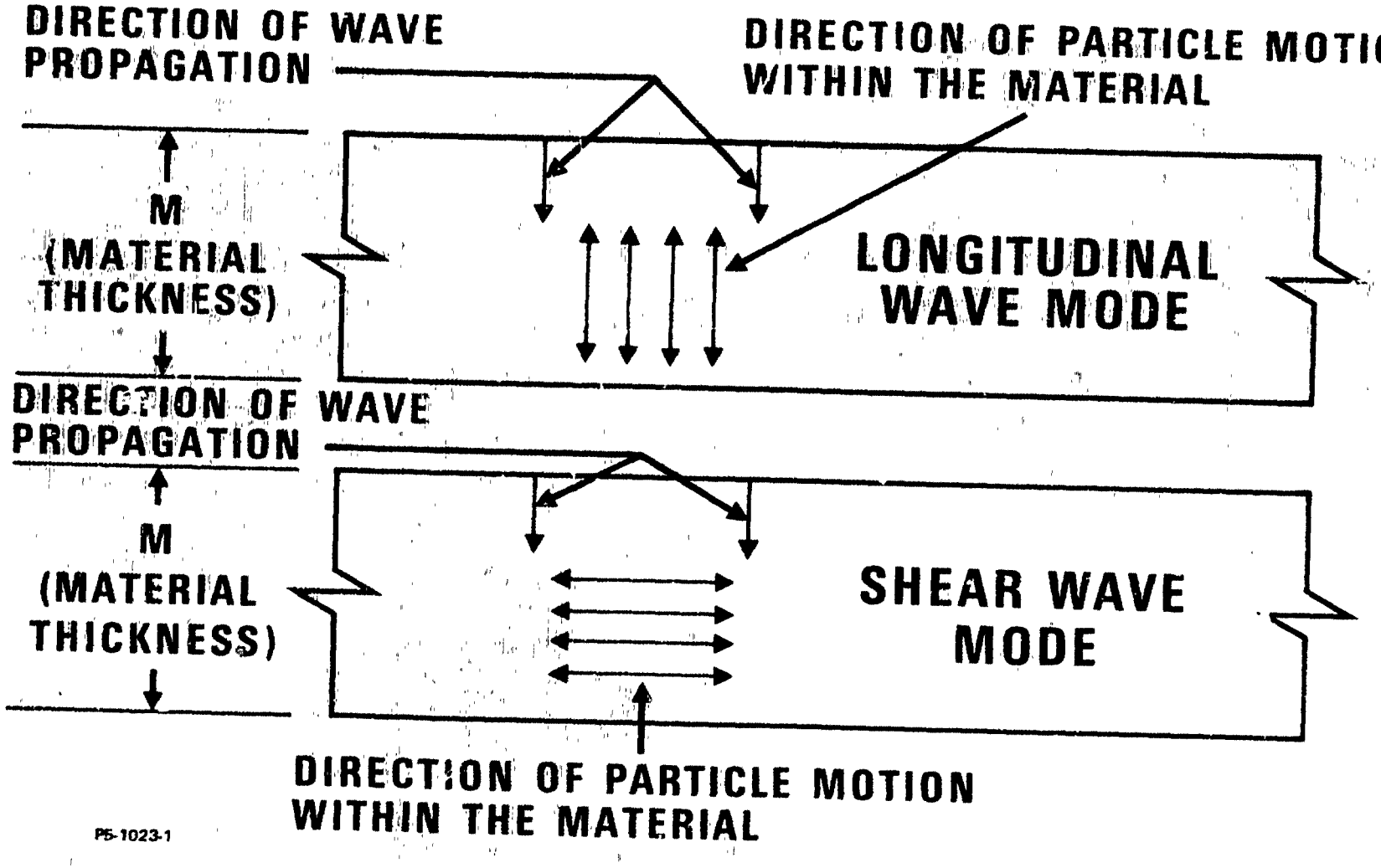


Figure 1. RELATIONSHIP OF PARTICLE MOTION AND WAVE PROPAGATION

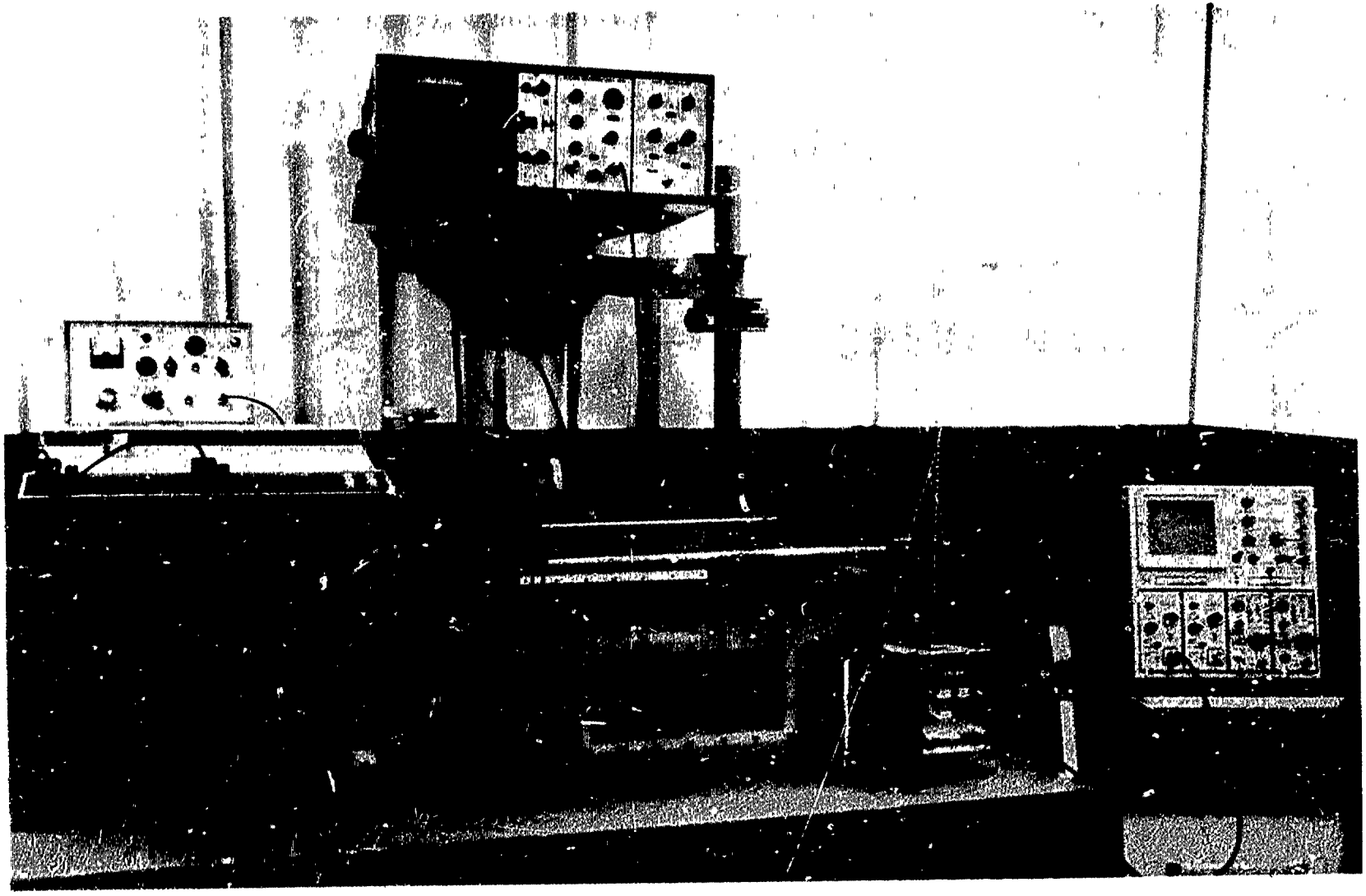


Figure 2. LABORATORY – ULTRASONIC TEST SYSTEM

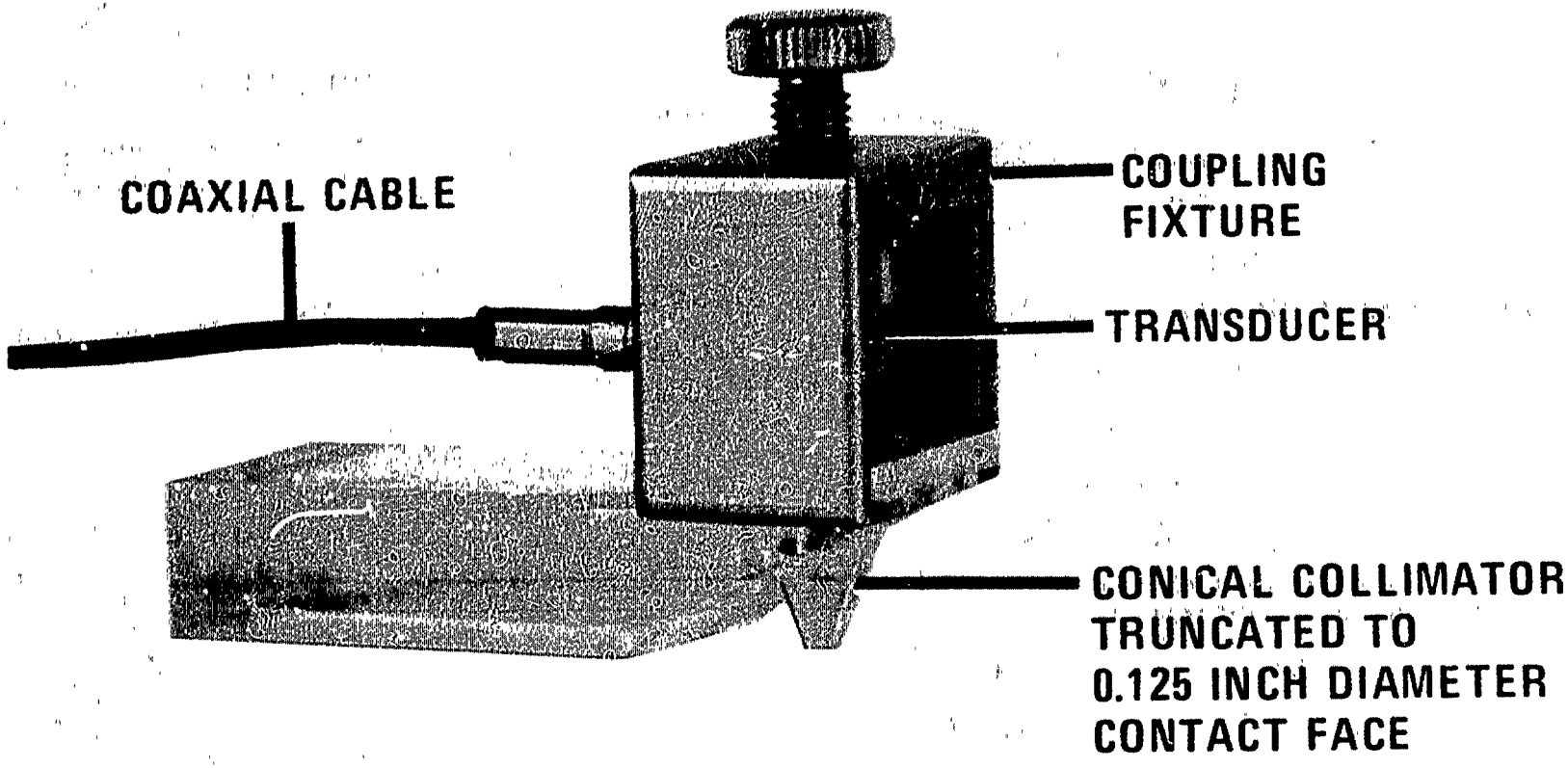


Figure 3. TRANSDUCER HOLDER – PULSE ECHO TECHNIQUE

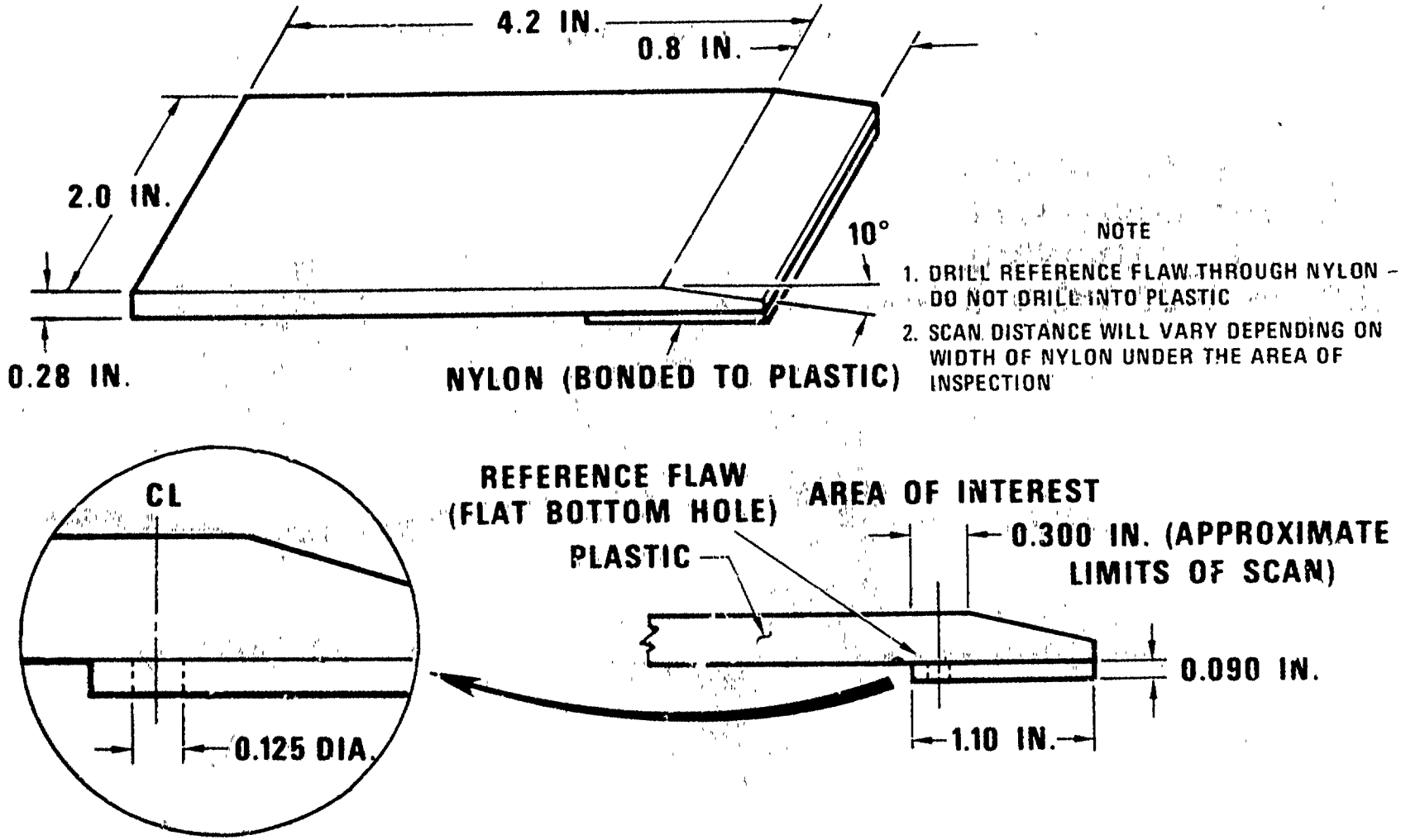


Figure 4. REFERENCE STANDARD – PULSE ECHO TECHNIQUE

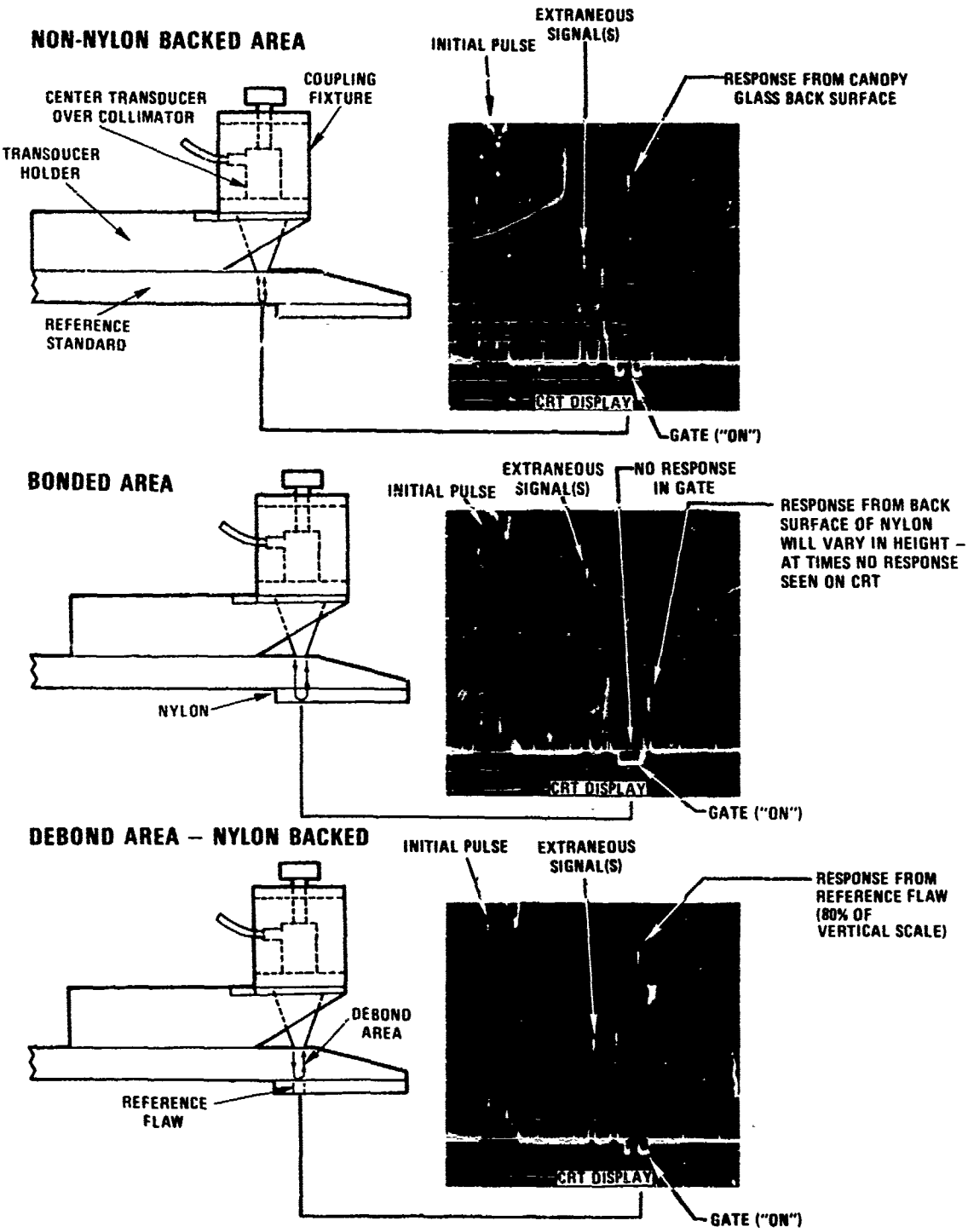


Figure 5. TYPICAL CRT SCREEN PRESENTATION – PULSE ECHO TECHNIQUE

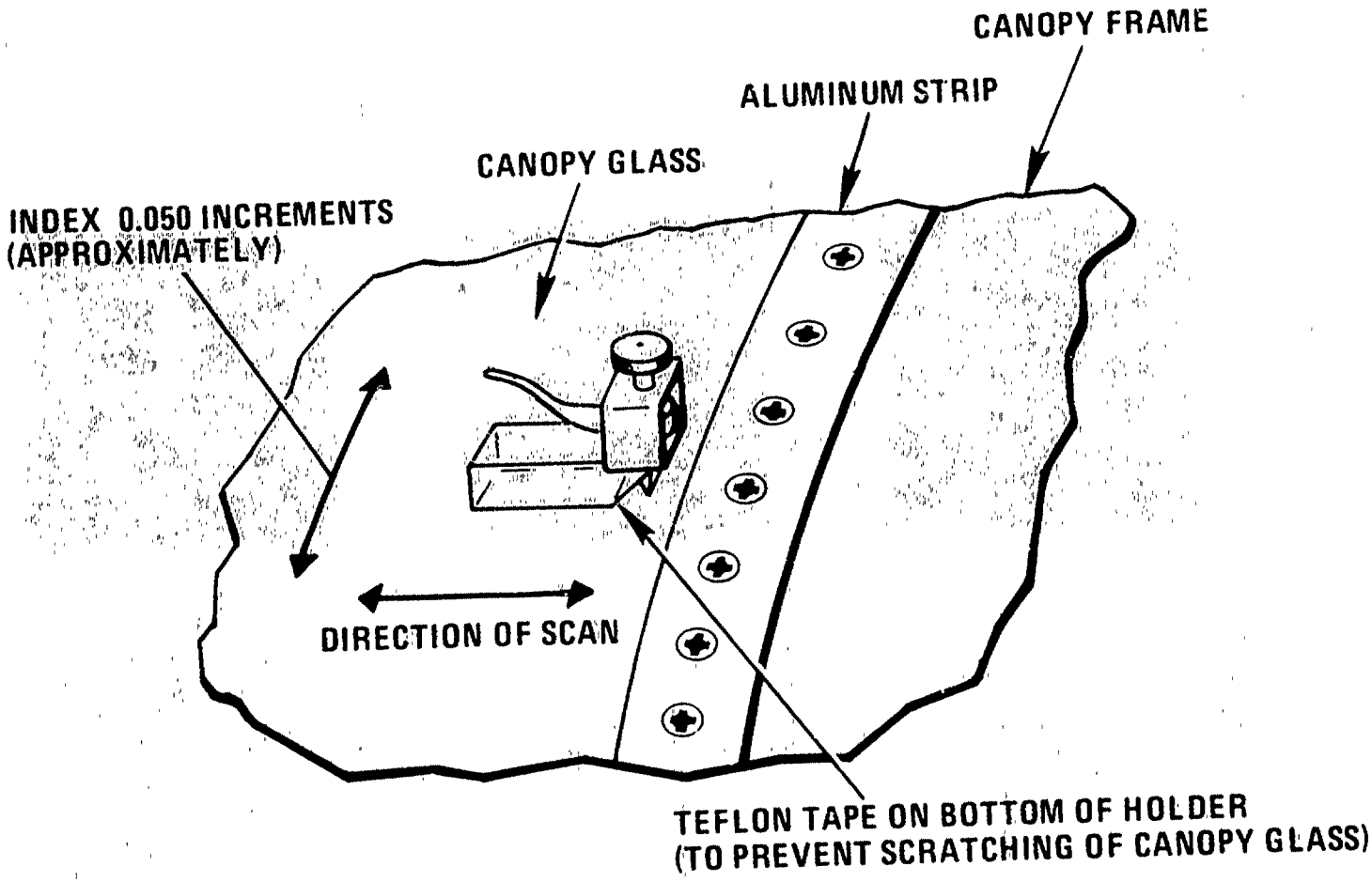
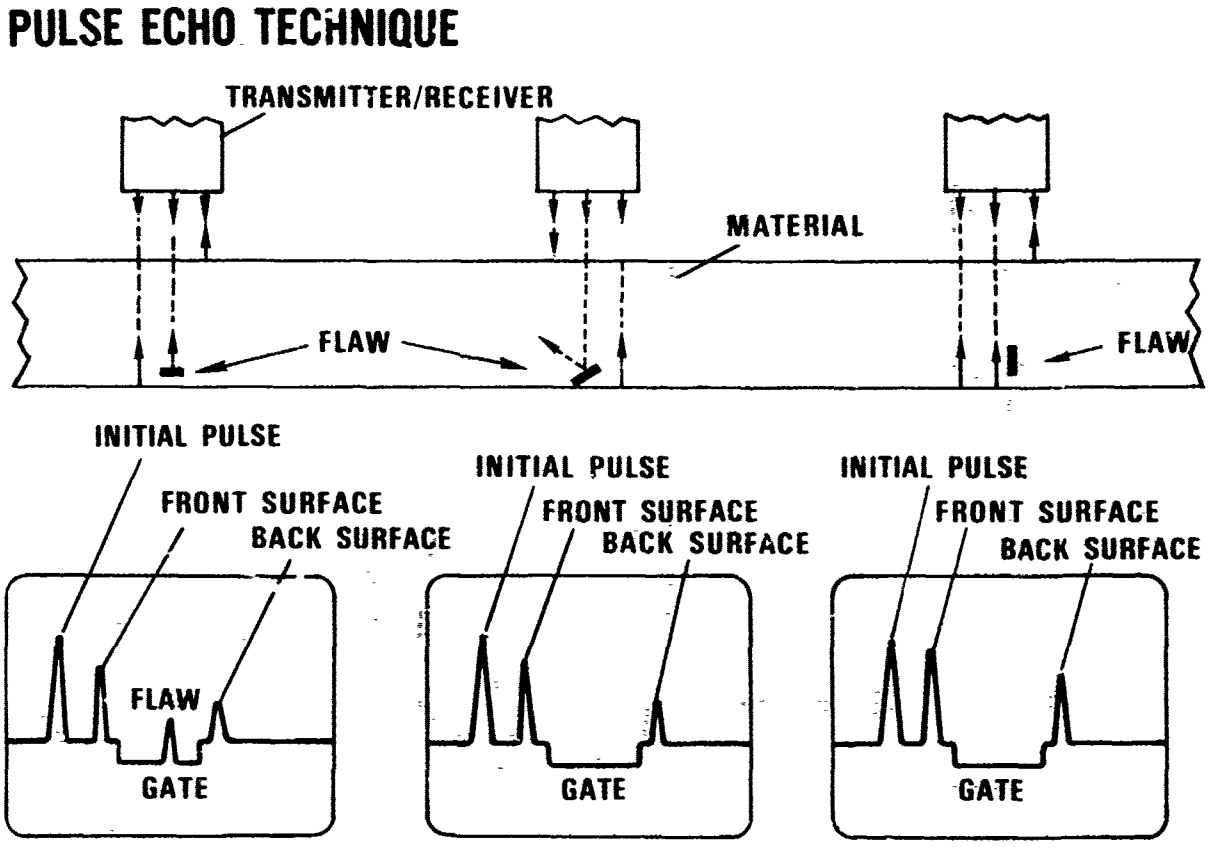


Figure 6. TYPICAL PLACEMENT OF TRANSDUCER HOLDER ON AREA OF INSPECTION – PULSE ECHO TECHNIQUE



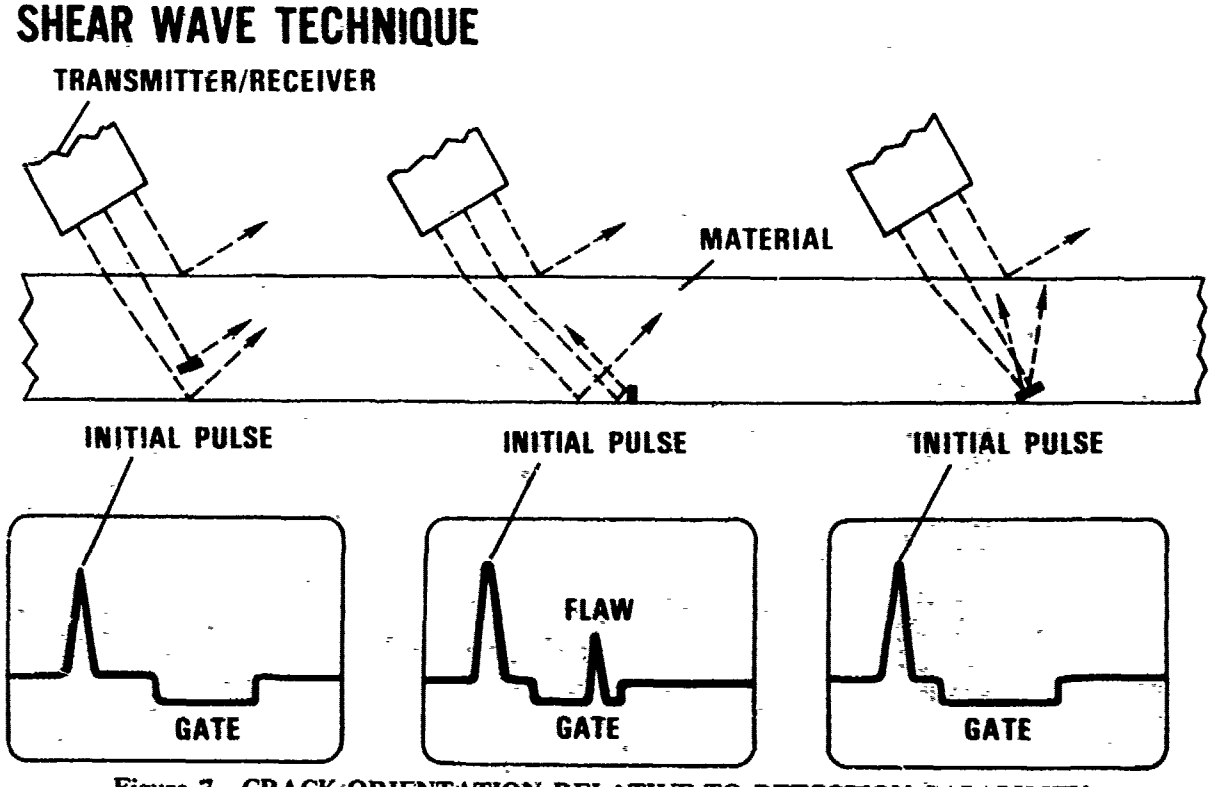


Figure 7. CRACK ORIENTATION RELATIVE TO DETECTION CAPABILITY

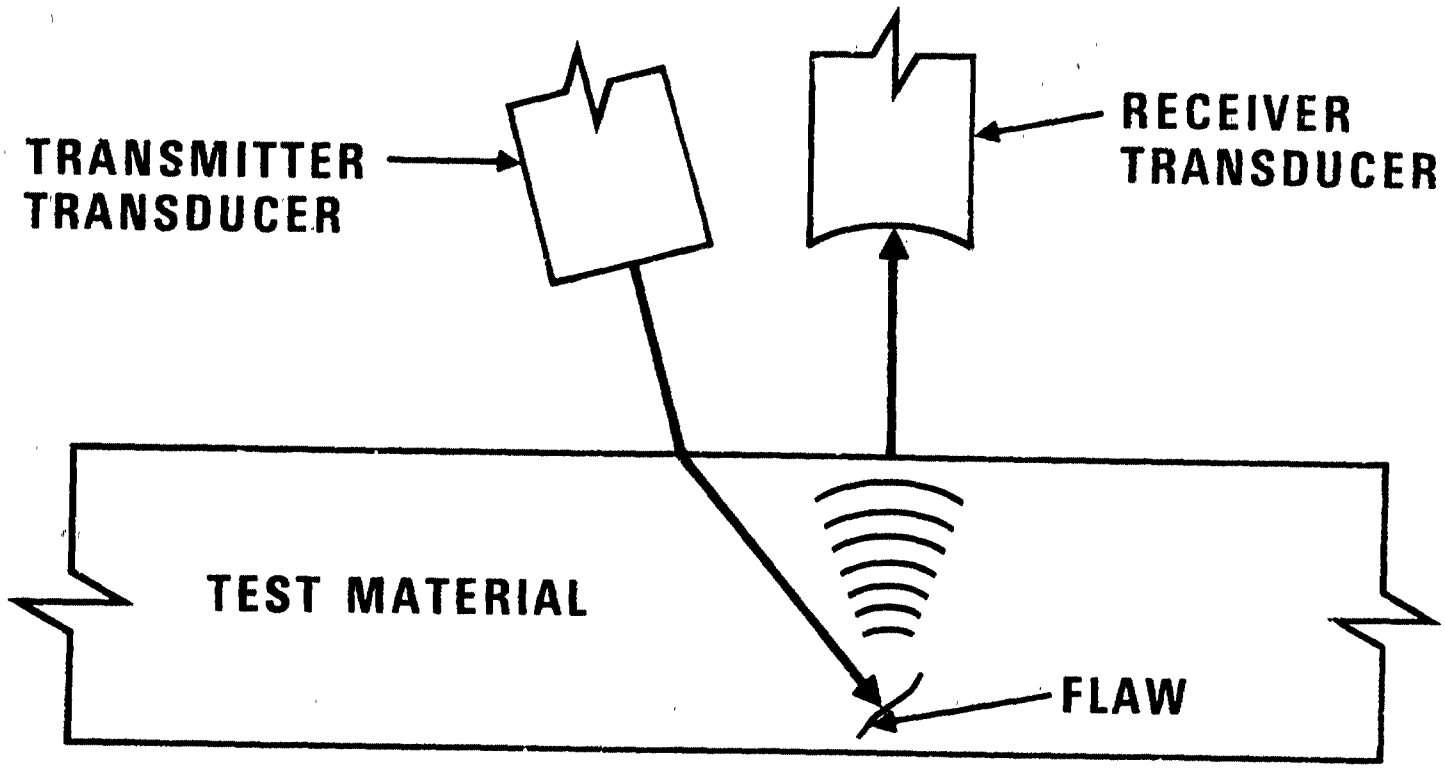


Figure 8. TYPICAL DELTA CONFIGURATION

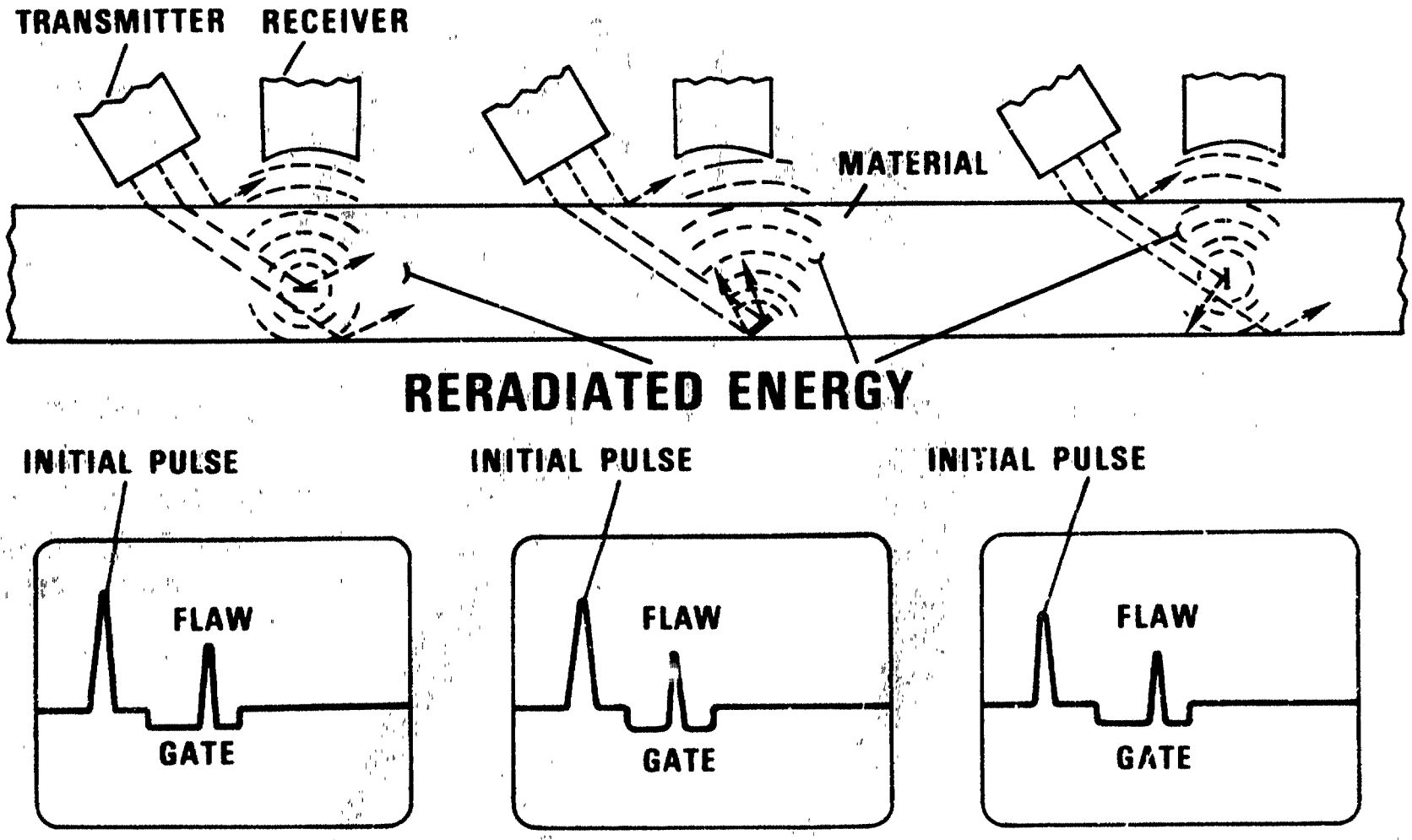


Figure 9. DELTA CRACK DETECTION CONCEPT

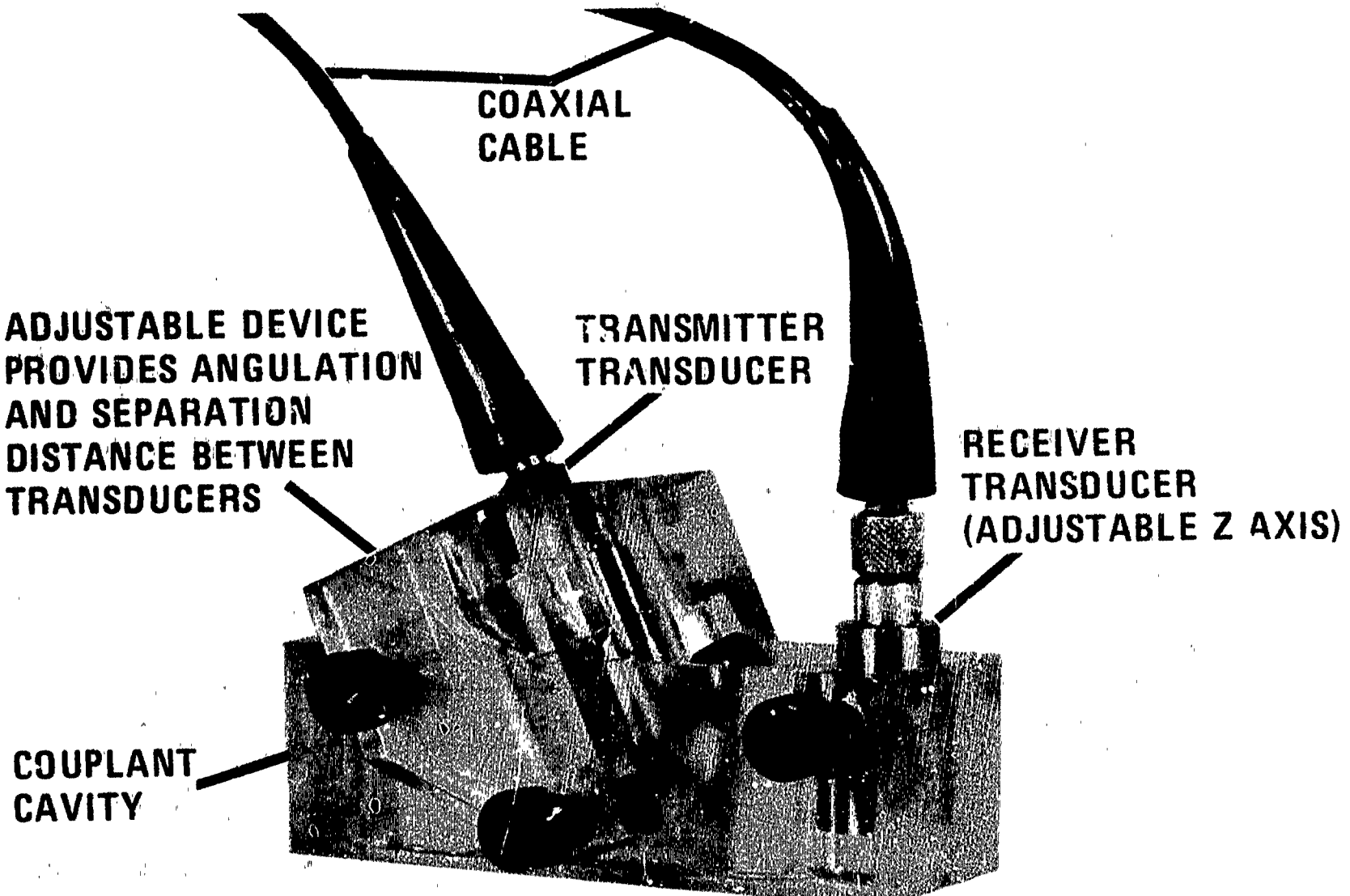
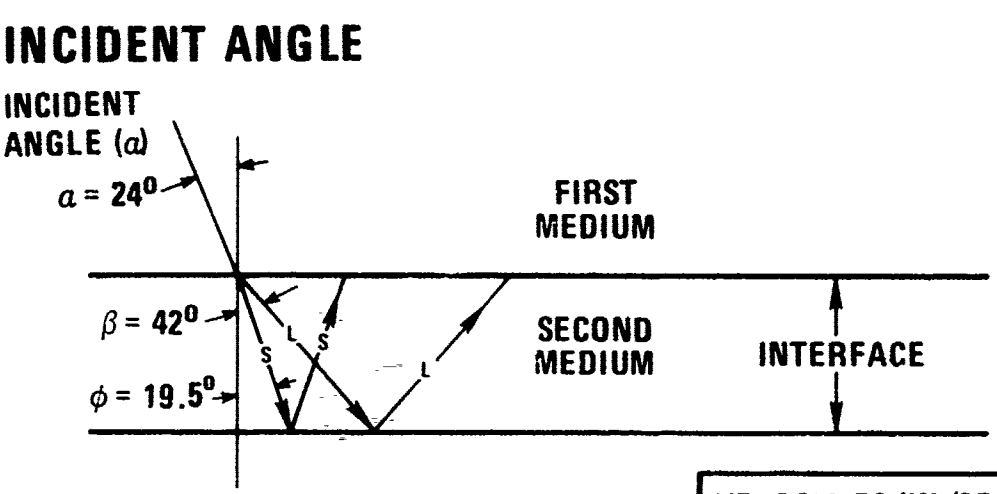


Figure 10. LABORATORY FIXTURING DEVICE – DELTA TECHNIQUE

INCIDENT ANGLE



APPLYING SNELL'S LAW OF REFRACTION:

$$\frac{\sin a}{V_C} = \frac{\sin \phi}{V_S} = \frac{\sin \beta}{V_L}$$

RESULTS IN REFRACTED ANGLE

(L) = 42° LONGITUDINAL MODE

(S) = 19.5° SHEAR MODE

VELOCITIES (IN./SEC x 10^5):

ACRYLIC (STRETCHED)

V_L = 1.05

V_S = 0.441

ACRYLIC (CAST)

V_L = 1.09

V_S = 0.560

COUPLANT (OIL)

V_L = 0.685

SOUND ENERGY PATTERN

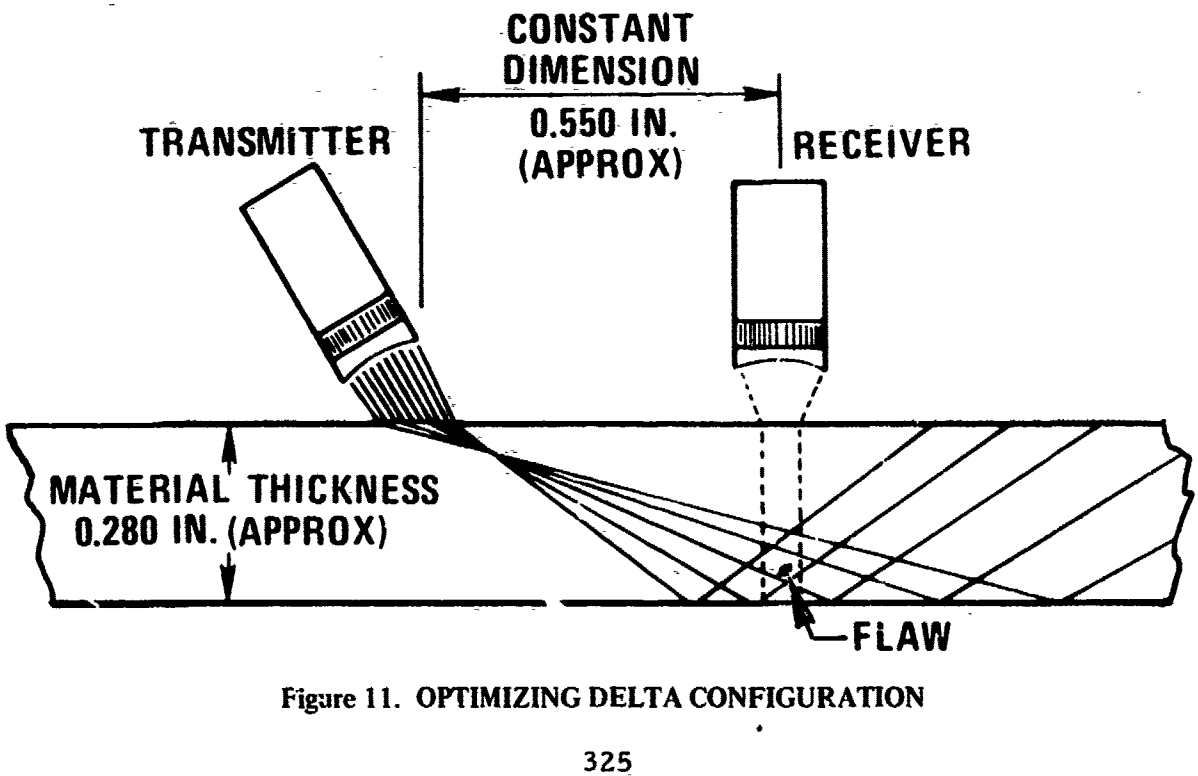


Figure 11. OPTIMIZING DELTA CONFIGURATION

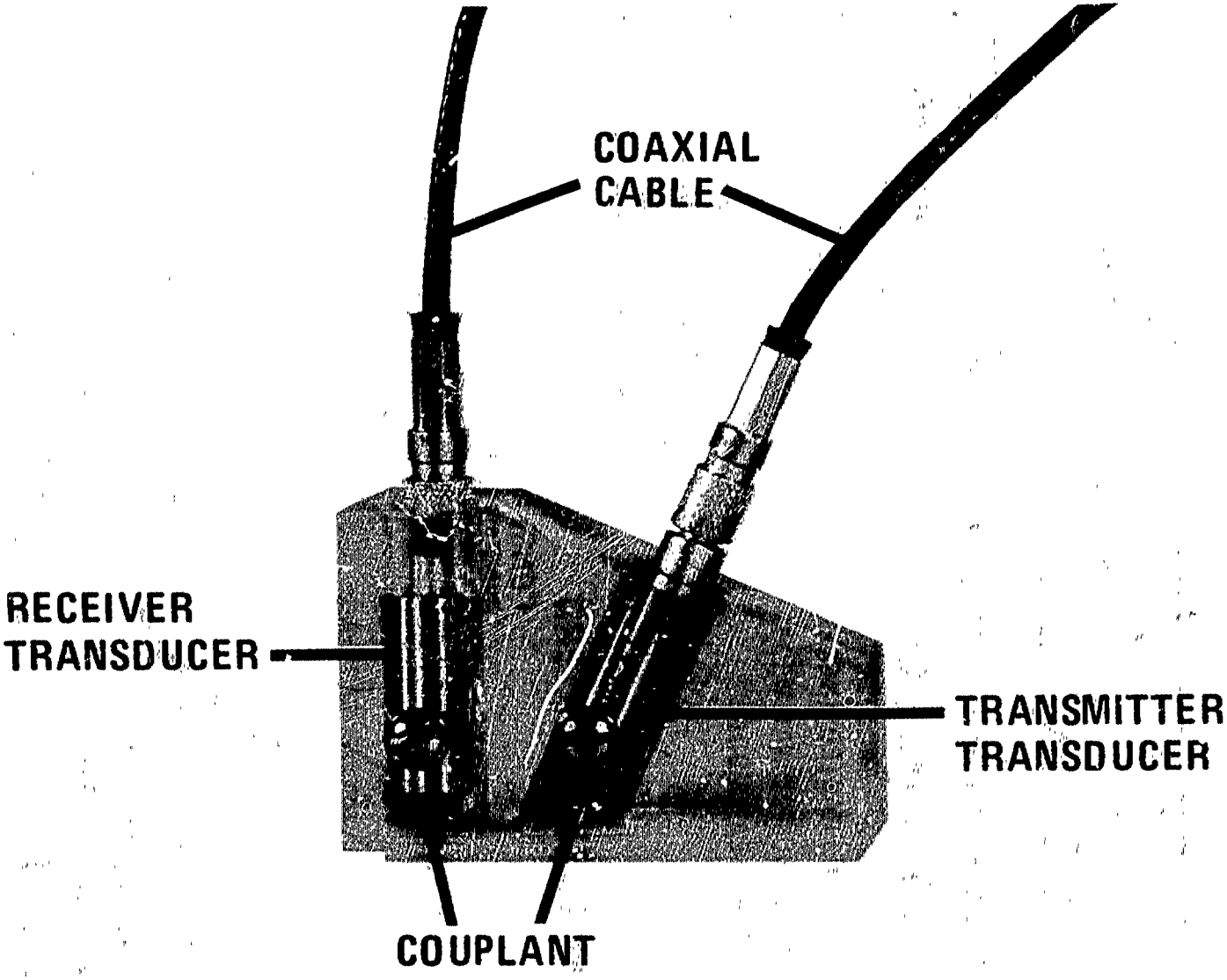


Figure 12. TRANSDUCER HOLDER – DELTA TECHNIQUE

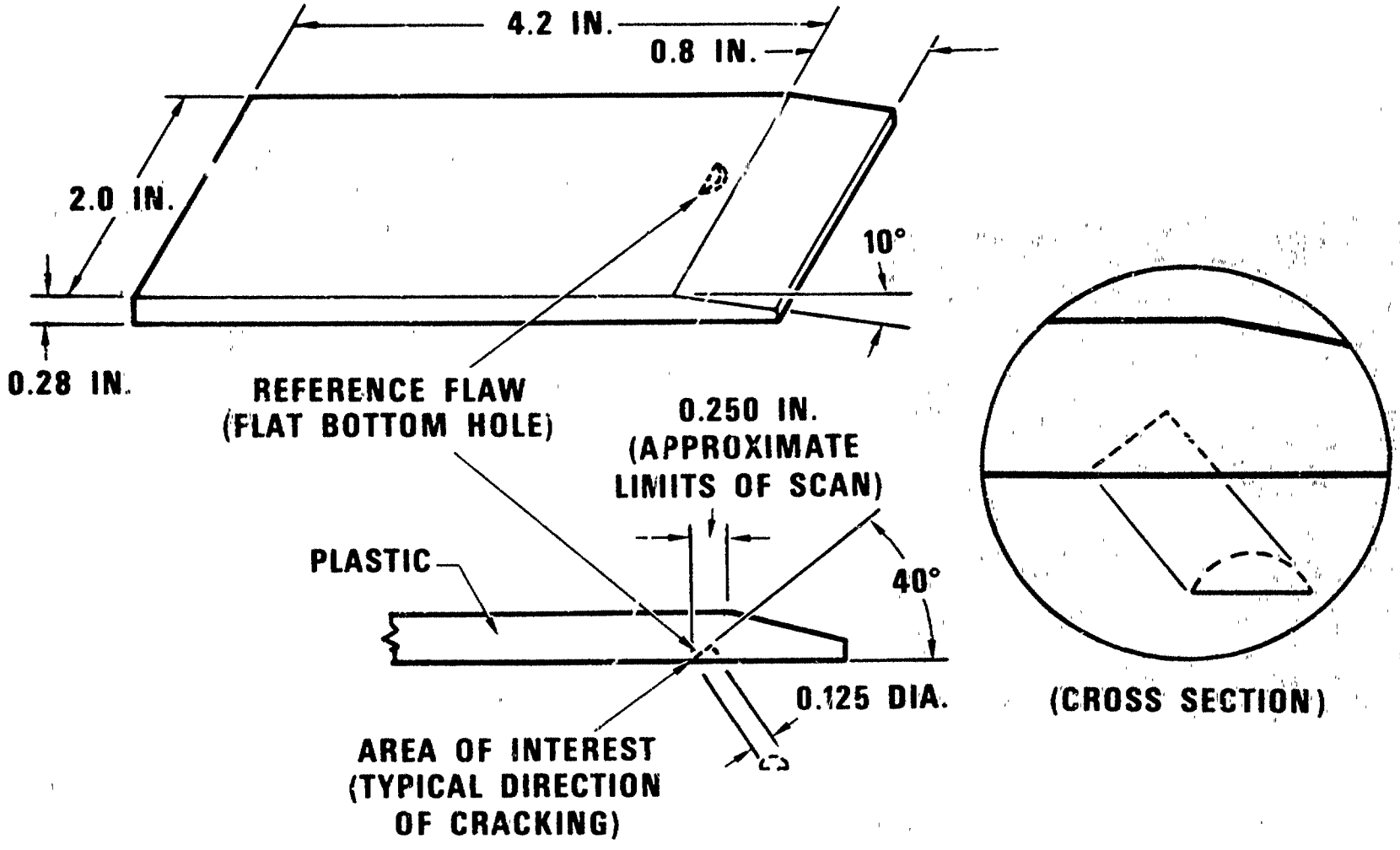


Figure 13. REFERENCE STANDARD – DELTA TECHNIQUF

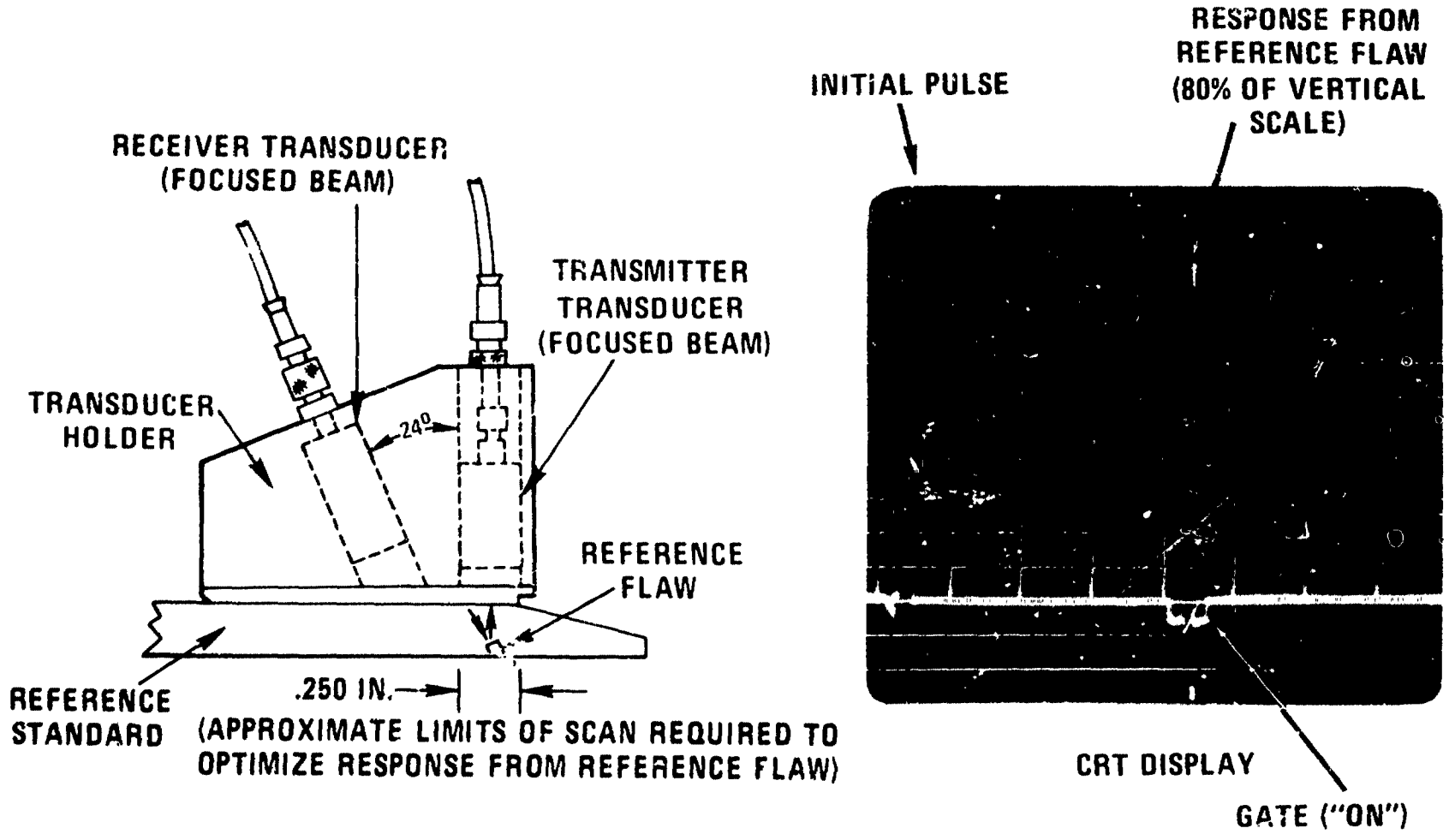


Figure 14. TYPICAL CRT SCREEN PRESENTATION – STANDARDIZING DELTA TECHNIQUE

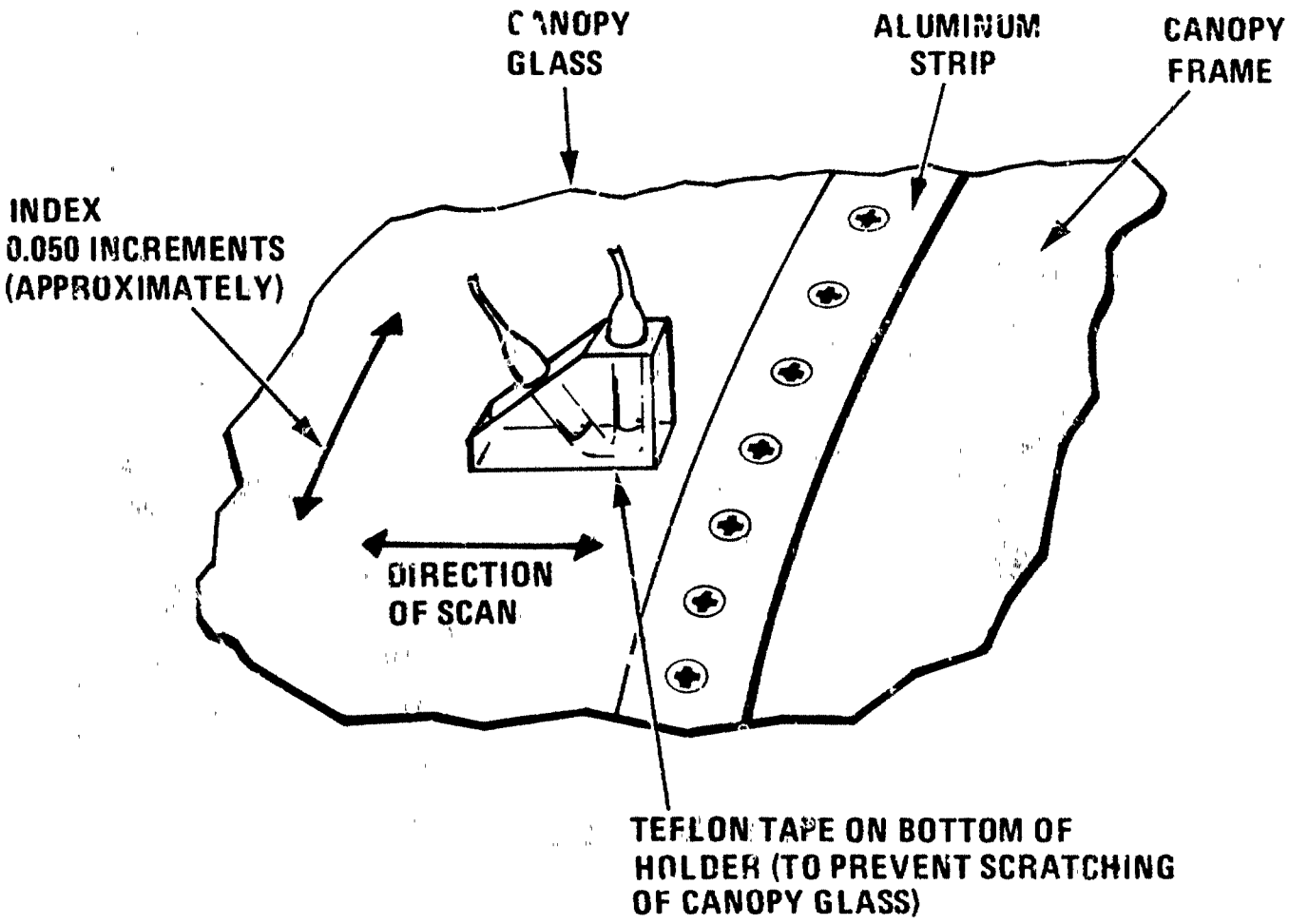


Figure 15. TYPICAL PLACEMENT OF TRANSDUCER HOLDER ON AREA OF INSPECTION – DELTA TECHNIQUE

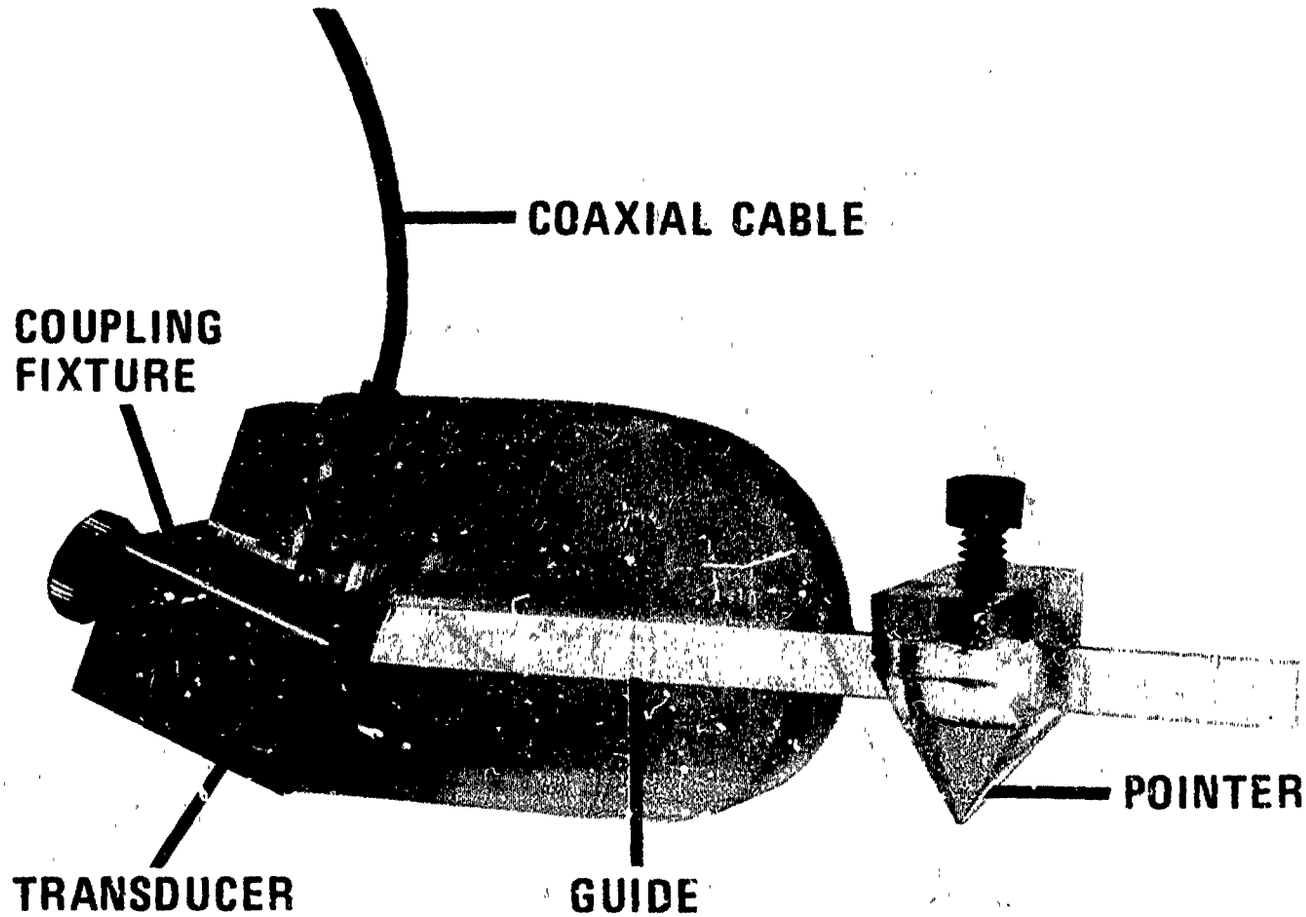


Figure 16. TRANSDUCER HOLDER – ANGLE BEAM TECHNIQUE

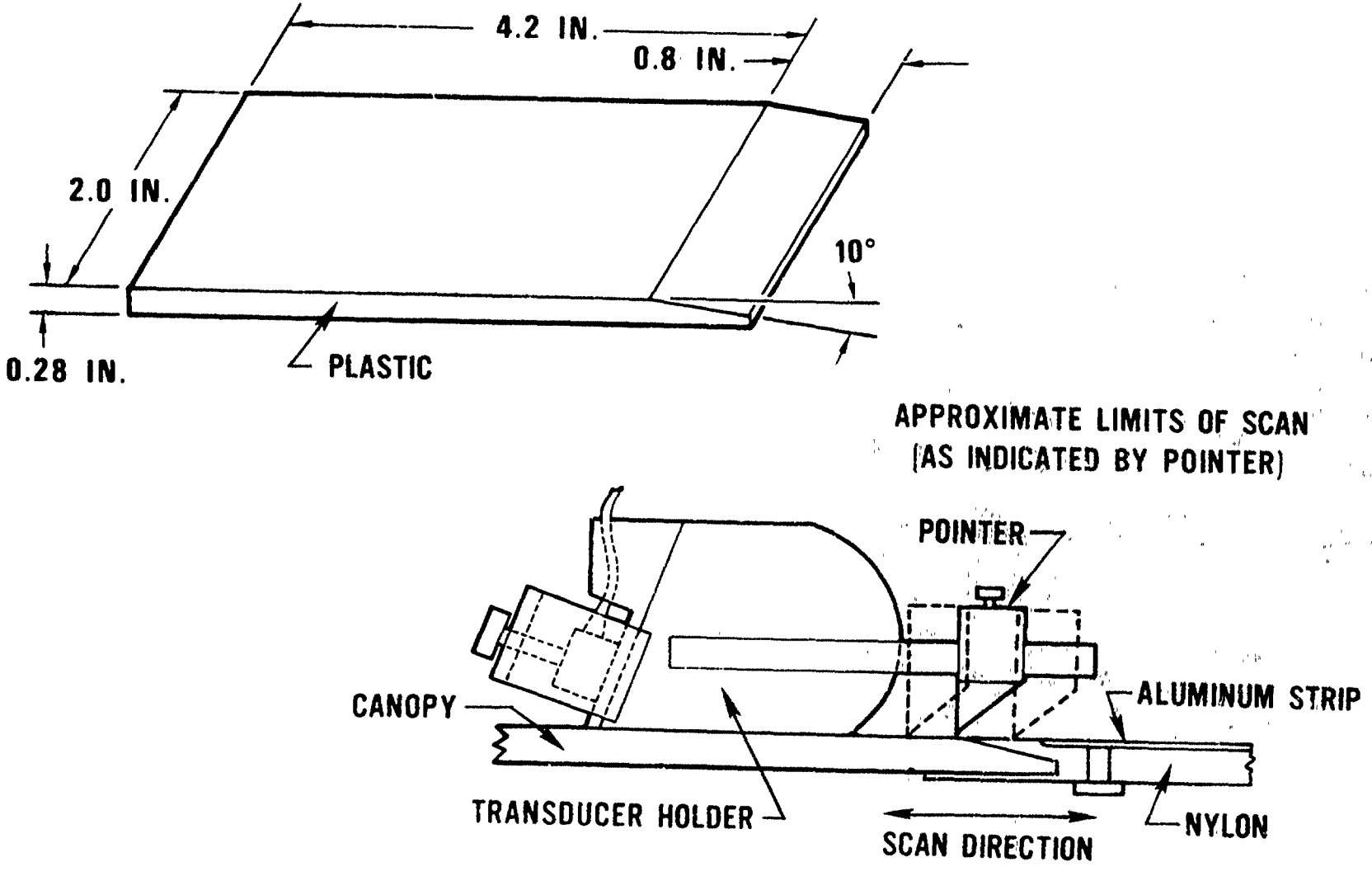


Figure 17. REFERENCE STANDARD – ANGLE BEAM TECHNIQUE

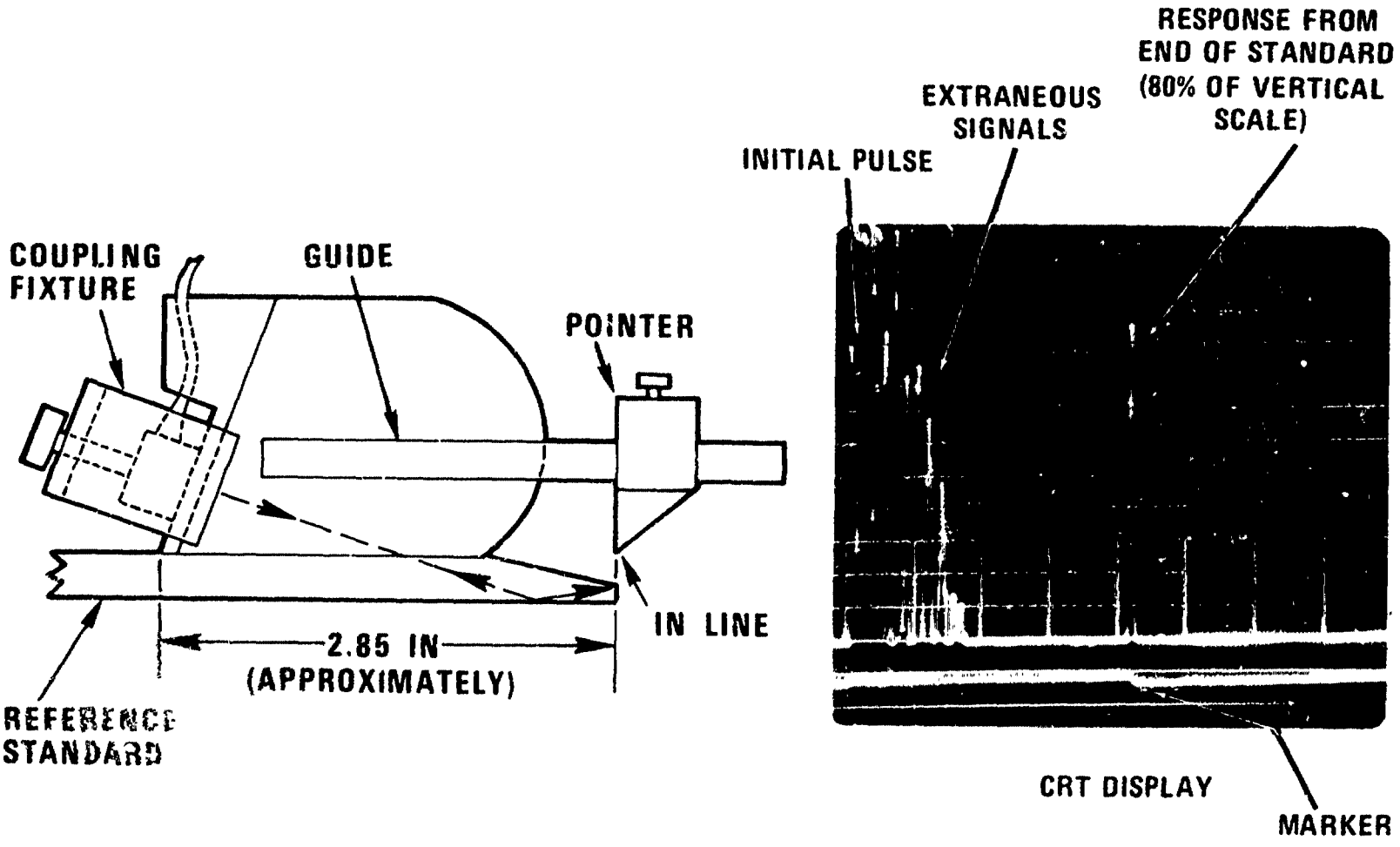


Figure 18. TYPICAL CRT SCREEN PRESENTATION – ANGLE BEAM TECHNIQUE

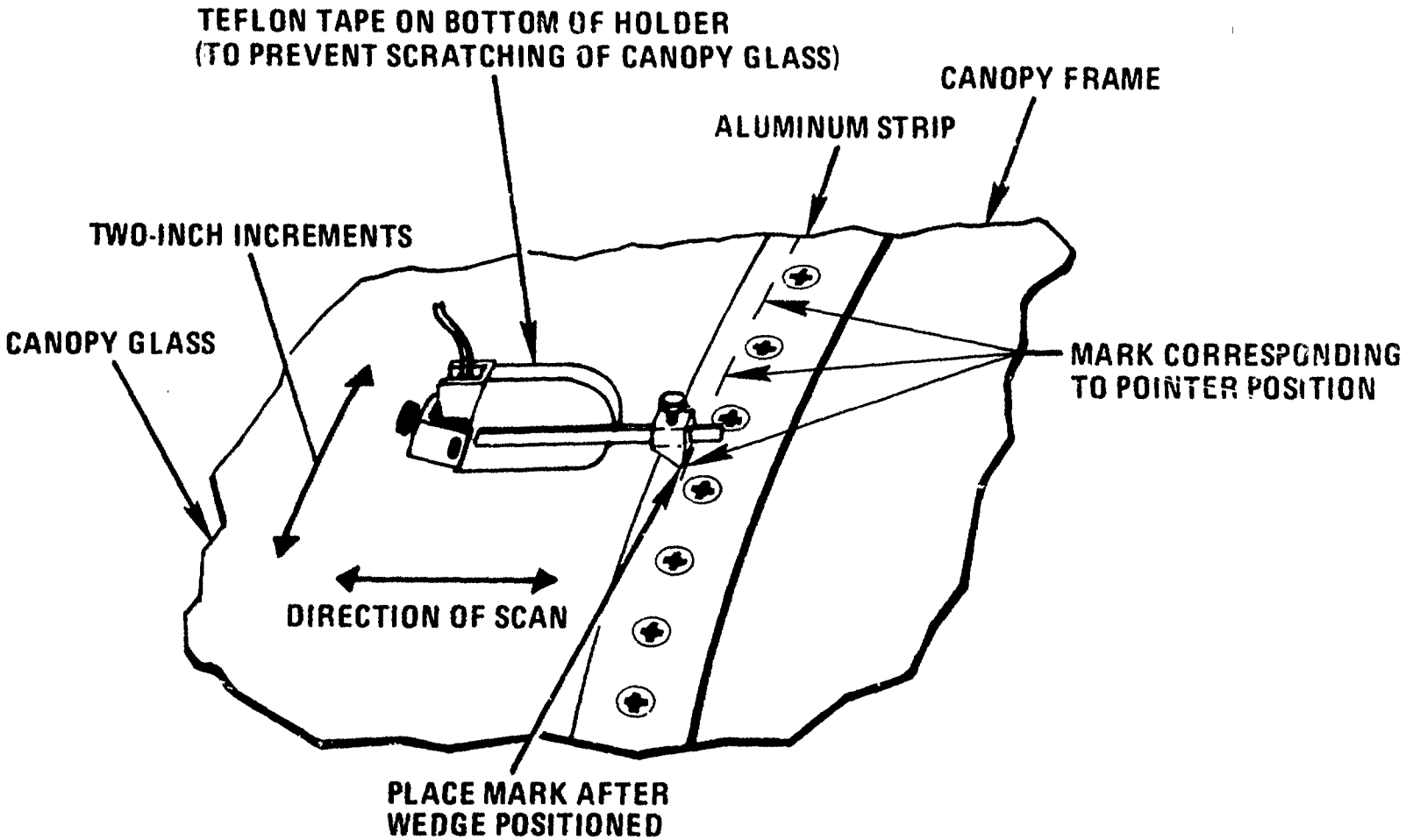


Figure 19. TYPICAL PLACEMENT OF TRANSDUCER HOLDER ON AREA OF INSPECTION – ANGLE BEAM TECHNIQUE

FRACTURE TOUGHNESS OF STRETCHED ACRYLIC PLASTIC

S. A. Sutton
Ocean Technology Division
Naval Research Laboratory
Washington, D. C.

FRACTURE TOUGHNESS OF STRETCHED ACRYLIC PLASTIC

by

Stephen A. Sutton
Ocean Technology Division
Naval Research Laboratory
Washington, D. C. 20375

ABSTRACT

This paper presents the method and result of a parametric study of instability toughness, as measured by the critical stress intensity factor, K_c, of a multiaxially stretched acrylic plastic. A large number of computer controlled tests were conducted on the compact tension specimen under high compliance loading/load control. These tests reveal the significant effects upon K_c of a wide range of loading rates and specimen thickness, and specimen geometry. A direct and immediate application of the results is the recommendation of a new fracture toughness acceptance test for these materials.

INTRODUCTION AND BACKGROUND

Since the emergence of stretched acrylic about 20 years ago it has beome a dominant material in aircraft transparency applications. The multiaxial or biaxial hot-stretching process produces a material with a much higher resistance to thru-crack propagation. The fracture mechanics characterization of this toughness has unfortunately not been used to any extent in design of these structures, but is a widely used and vital determinant of material quality which can vary appreciably due to the many variables involved in the stretching process.

The technique currently used for determining the fracture toughness of stretched acrylic is described in the military specification MIL-P-25690 A (1). The test method was established during the relatively early stages of development of fracture mechanics stemming from a set of pioneering papers in the field by Kies, et al (2,3). The method has not been modified to reflect the progress that has been made in this rapidly advancing field.

The testing method involved using a displacement controlled (primarily screw type) testing machine to pull a center cracked specimen (CCS) to failure (Fig. 1). The critical stress intensity factor K_c, was calculated from the load and crack length at instability using a relation from early calibration results (2,3). This relation agrees well with later analytical stress analyses of the CCS geometry (4). The range of loading rates allowed is broad and thickness effects were not considered.

This paper describes a fundamental application of fracture mechanics to develop an improved technique for characterizing the instability fracture toughness of this material. Points of prime interest and concern include specimen geometry, size, thickness, type of loading and loading rate, and convenience of the technique for toughness characterization of plastic materials.

MATERIAL AND SPECIMENS

The compact tension specimen (CTS) shown in Figure 3 was selected for the characterization program. This geometry is widely accepted and has been analyzed by Srawley and Gross (5). The CTS offers several advantages over the currently used CCS specimen including smaller size, lower loads to failure, simplified pin loading and alignment and ease of pre-cracking. In addition the presence of two crack tips in the CCS geometry leads to a low estimate of toughness since the weaker of the two crack tips determines failure. The CTS has no such problem.

The choice of half-height to width ratio (H/W) for the CTS is somewhat arbitrary but the accepted ASTM value of 0.6 was chosen. The specimens had a length (L) of 2 in (5 cm) and 2.4 in (6 cm) and ranged in nominal thickness from 1/8 inch (.32 cm) to 7/8 inch (2.2 cm) which encompass the more widely used thickness.

A V-tipped notch was machined in the specimen and a natural crack initiated at the notch using the procedure outlines in the current specification (1). This technique produced a sharp, natural crack extending .1 inch (2 mm) or more beyond the machined notch. This depth was found adequate to remove the crack tip from the effects of the machined notch which include stress field irregularities and change in material structure induced by the machining heat.

The material used was a commercially prepared bi-axially stretched acrylic conforming to MIL-P-25690 A.

LOADING PARAMETERS.

The loading parameters can play a very important role in the crack propagation behavior particularly in polymeric materials where viscoelastic effects are significant. In essence, the method for performing the test or loading machine type and compliance can affect the results. Precautions must be taken to separate material behavior from such effects.

The most fundamental loading parameter in these fracture toughness tests is the stress intensity factor, K, since it characterizes the stress state in the fracture process zone at the crack tip (within the constraints of linear elastic fracture mechanics). If there is little stable crack growth during the course of loading, K is proportional to the applied load so that using load control effectively controls the stress intensity factor. The use of load control has the advantage of accentuating instability as opposed to displacement control which tends to foster stable crack growth. From a statics point of view, there is no load relaxation with increasing crack length as in the displacement control (quasi-fixed grip) and from an energy point of view there is a large reservoir of readily available energy for crack propagation when a high-response load control is used.

Since one of the purposes of this research is a toughness characterization technique that is easy to implement, a means of accomplishing load control on a displacement (screw type) testing machine was developed and used in all tests. The loading scheme is to place a highly compliant member in series with the specimen as shown in Figure 2. Since the compliance of the member is much greater than that of the specimen, the load transmitted by the member is very nearly proportional to the crosshead displacement. A constant crosshead rate therefore produces a proportionally constant rate of force application, which produces a proportionally constant rate of increase in the stress intensity factor. In addition, the compliance of the testing machine (grips, crosshead, and frame) is rendered insignificant as that the use of the compliant member tends to isolate the specimer from the testing machine. Load control can also be used in conjunction with the compliant member where the effect of the member is to standardize the dynamic response characteristics of the system. The

compliant member used in these tests was a fiberglass laminated beam configuration chosen for its strength, light weight, and reasonably high stiffness. Pulling was accomplished using a displacement controlled hydraulic actuator.

EXPERIMENTAL CONTROL

The tests and data evaluation were conducted using a computer based system for experimental control and data acquisition, and data analysis which includes processing, associative storage and retrieval, data base searching, and display. The system is shown schematically in Figure 4 and will be described in detail in a forthcoming report (6). Basically, a computer program inputs the test parameters, i.e., loading rate expressed as K-rate, initial crack length, and specimen geometry and size. The program conducts the test measuring appropriate information then processes and stores the data. Force, displacement, and time (see Figure 2) are monitored during the test and the crack length at failure was determined visually after failure. From these values the critically stress intensity factor K_{Ic} is computed using the Srawley and Gross relationship (5), and the actual loading rate K-rate is determined. The principle advantage of the computer based system is the ease and speed for running the nearly 300 tests and evaluating their results.

RESULTS AND DISCUSSION

The results can be considered to accomplish two basic purposes. The first is to show the effects on toughness of the various experimental parameters, and the second is to demonstrate whether linearly elastic fracture mechanics (K_{Ic}) is applicable to these materials. A total of nearly 300 tests were conducted and the parameters of greatest interest are the loading rate (K-rate), thickness, specimen size, and initial crack length. In all tests a small amount of stable crack growth preceeded instability ranging up to approximately .04 in (1 mm) for the low loading rates in thin specimens. This growth is considered beneficial in that it moves the fracture process zone in which the instability initiates away from the initial precrack tending to smooth any precrack irregularities.

The fracture surfaces observed were typical of those for stretched acrylic. A zone of pre-instability crack growth displays much tearing which reflects the energy dissipation mechanisms. The fracture surfaces indicate no large scale plastic yielding which enhances the use of linearly elastic fracture mechanics (K_{Ic}) as a fracture criterion.

Figure 5 is a master graph showing the results of nearly 300 tests and reveals the effects of loading rate and thickness on K_{Ic}. The graph shows the measured values of K_{Ic} for loading rates (K-rate) ranging from 22 psi$\sqrt{\text{in}}$/sec (25 N/cm$^{3/2}$-sec, failure occurs in approximately 3 minutes) to 450 psi$\sqrt{\text{in}}$/sec

(500 $N/cm^{3/2}$-sec, failure in 5 seconds). Trend curves derived from averaging appropriate groups of data are shown in Figure 6. The most striking observation is the rapid decrease in toughness with increase in rate of loading. The increase is expected, however, and is typically the case in viscoelastic or rate sensitive materials. The lower loading rates allow more plastic flow which leads to the higher toughness values. At the lower rates the thinner specimens are tougher than the thicker whic is again expected since the thinner tend toward a state of plane stress. At the higher rates, all values tend to converge. The probable cause is that the higher rate allows less plastic deformation and the specimens tend more toward the plane strain condition so that the toughness values converge for the different thickness.

The two specimen sizes tested (H/W = .6) had widths (W) of 2 inches (5 cm) and 2.5 inches (6.2 cm). There appears to be no significant effect of size on K_c, although the size difference is not great. Different crack lengths, widths, and H/W ratios, within certain bounds, are of course accounted for in the linear elastic stress analysis. The analysis would be expected to apply unless the plastic zone size becomes large with respect to the dimensions of the specimen which is not the case in the current tests and the linearly elastic fracture mechanics approach is applicable. However, the stress analysis assumes plane strain conditions so will not be perfectly accurate for the plane strain tended toward the thin specimens at low loading rates. The error so induced in the K calculation is related to the Poisson ratio for the material and will be no greater than approximately 10%.

A striking feature in all tests is the large amount of scatter in the K_{Ic} values. Toughness testing, especially in the stretched acrylics, have always exhibited wide scatter due primarily to the unstable nature of the phenomenon. The two immediate suspected causes of the scatter are variations in crack geometry, and material variability. Careful comparison of the failed fracture surfaces revealed no correlation between crack tip geometry and toughness (for example, one might expect an eccentric crack front to produce a low toughness value). One does observe a larger slow growth region in specimens with higher toughness. This is expected since the high toughness reflects the greater energy dissipation which produces a large pre-instability damage zone. It appears that the most likely cause of the observed scatter is variability of the material (on the microscale) which is amplified by the unstable nature of the phenomenon.

RECOMMENDATIONS

A primary purpose of this investigation is to recommend an improved technique for characterizing toughness of stretched acrylic material. On the basis of the tests described above, the following recommendations seem justified:

1. The compact tension specimen (CTS) with standard H/W ratio of 0.6 (see Figure 3) is a convenient specimen for all thicknesses examined (1/8 inch to 7/8 inch). A standard size (e.g., W = 2 in) should be specified. A standard but non-critical crack length (e.g., a/W = 0.5) should be chosen and current pre-cracking techniques continued.

2. Loading rate should be specified as a constant K-rate. The use of load control and/or displacement control with a compliant member greatly simplifies the K-rate control. The compliant member also serves to isolate the test from the testing machine and to accentuate instability.

3. It may be desirable to specify a much higher loading rate (K-rate) than the current specification (e.g., 200 psi $\sqrt{in}$/sec). The data (Figures 5 and 6) indicate that K_{Ic} is less dependent on thickness at this higher loading rate. In addition, the higher rates more closely indicate behavior under impact conditions which is a very important consideration in many applications.

The above recommendations and conclusions are intended to update and strengthen the fracture toughness acceptance test as well as render the test easier and less costly to run. In addition, the data described herein will hopefully provide insight into the fundamental fracture and failure behavior of these aircraft glazing materials.

REFERENCES

1. Military Specification - Plastic, Sheets and Parts, Modified Acrylic Base, Monolithic, Crack Propagation Resistance, MIL-P-25690 (USAF).

2. Kies, J. A., "Aircraft Glazing Materials - A Method for Evaluating the Shatter Resistance of Aircraft Canopy Materials," NRL Memorandum Report 237, Naval Research Laboratory, Washington, D. C. November 1953.

3. Kies, J. A. and Smith, H. L., "Aircraft Glazing Materials - Resistance to Crack Propagation - Glazing Materials," NRL Memorandum Report No. 372, Naval Research Laboratory, Washington, D. C. October 1954.

4. Brown W. F. and Srawley, J. E. "Plane Strain Crack Toughness of High Strength Metallic Materials," ASTM STP 410, 1966, p. 11.

5. Srawley, J. E. and Gross, B., "Stress Intensity for Bend and Compact Specimens," Engineering Fracture Mechanics, Vol. 4, September 1972, p. 587.

6. Sutton, S. A., "A Model for Computer-Based Data Acquisition and Control," to be published.

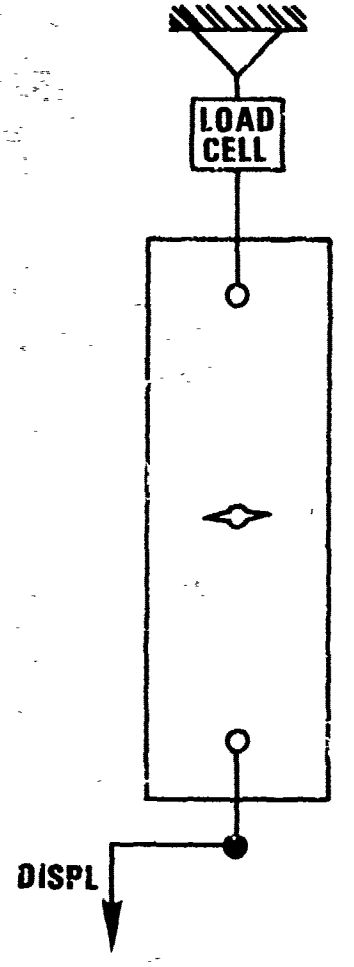


Figure 1. Center Crack Specimen Loading Scheme per Mil-P-25690.

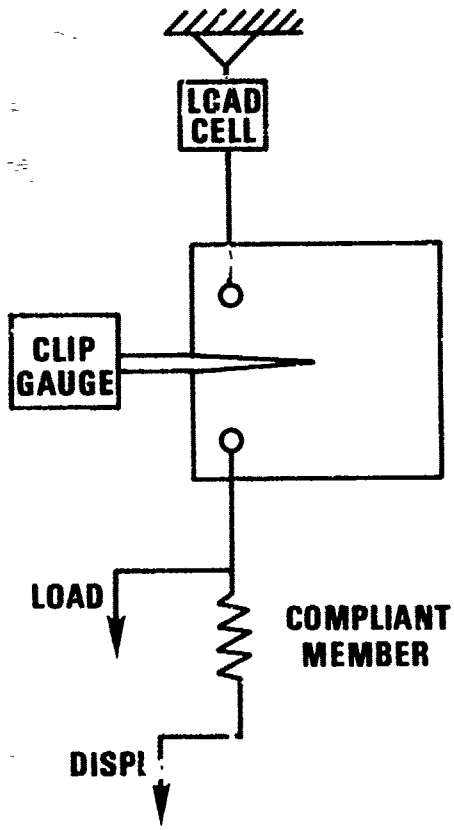


Figure 2. Compact Tension Specimen Loading Scheme.

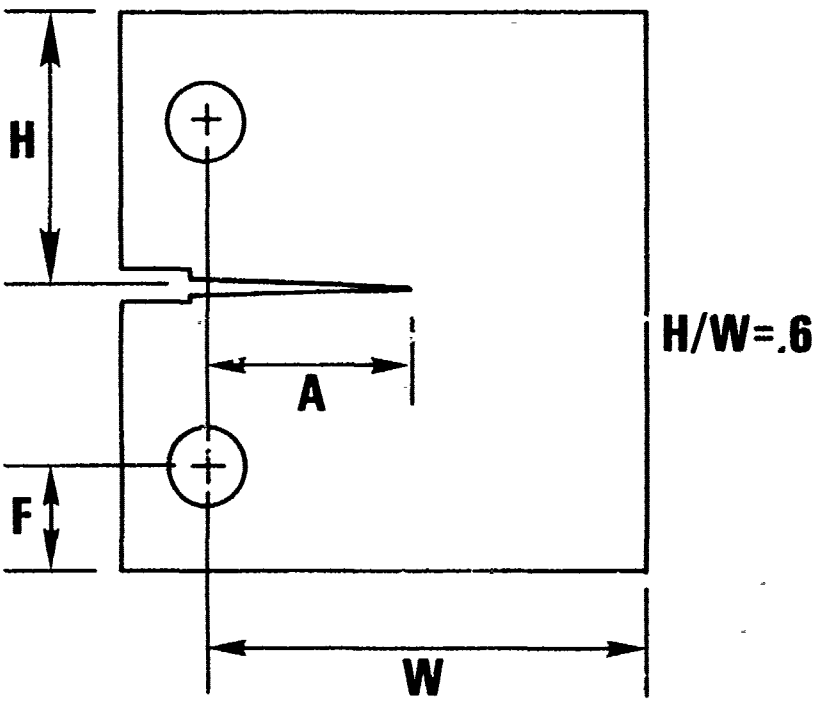


Figure 3. Compact Tension Specimen.

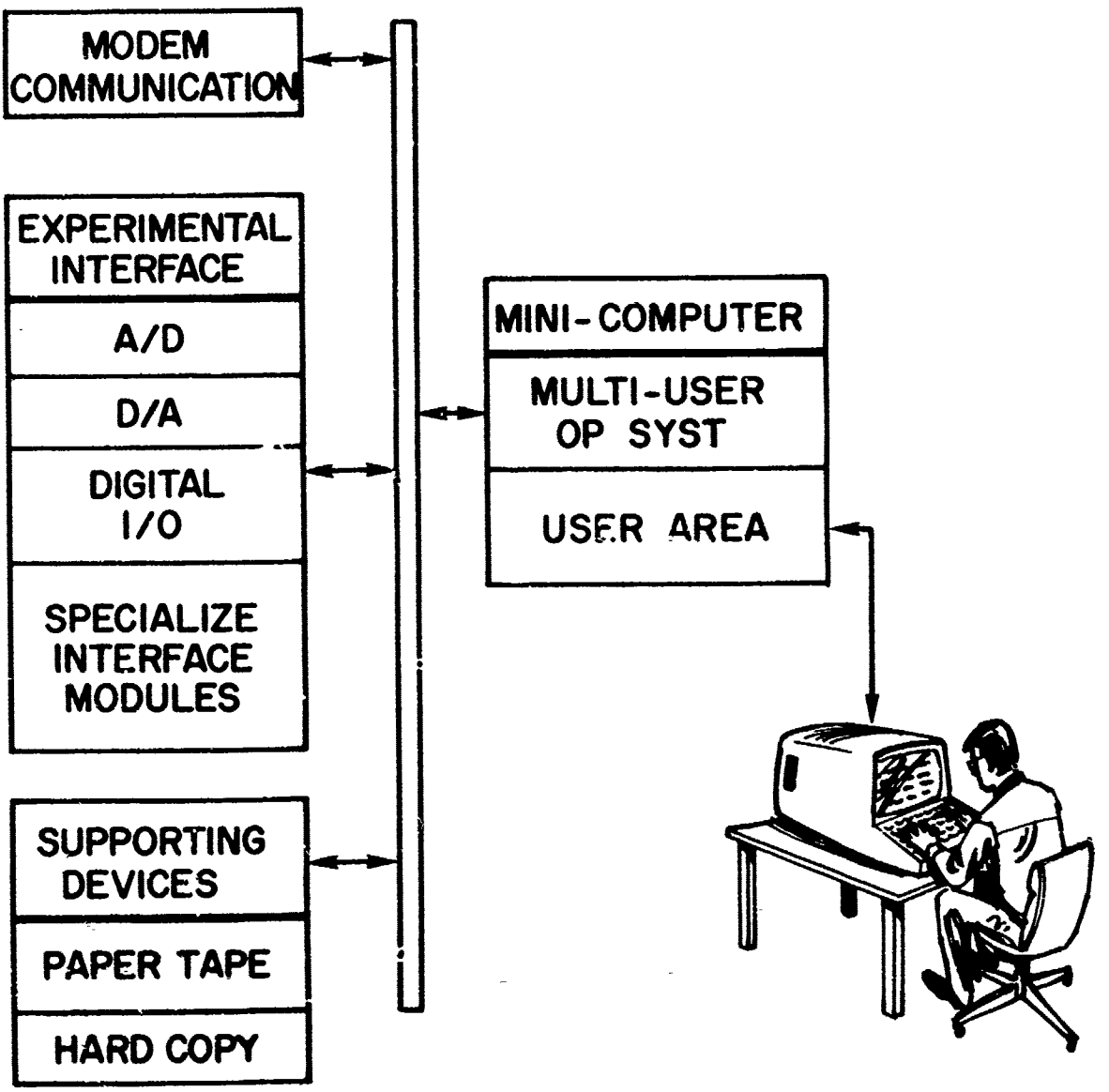


Figure 4. Computer Based Data Acquisition and Evaluation System

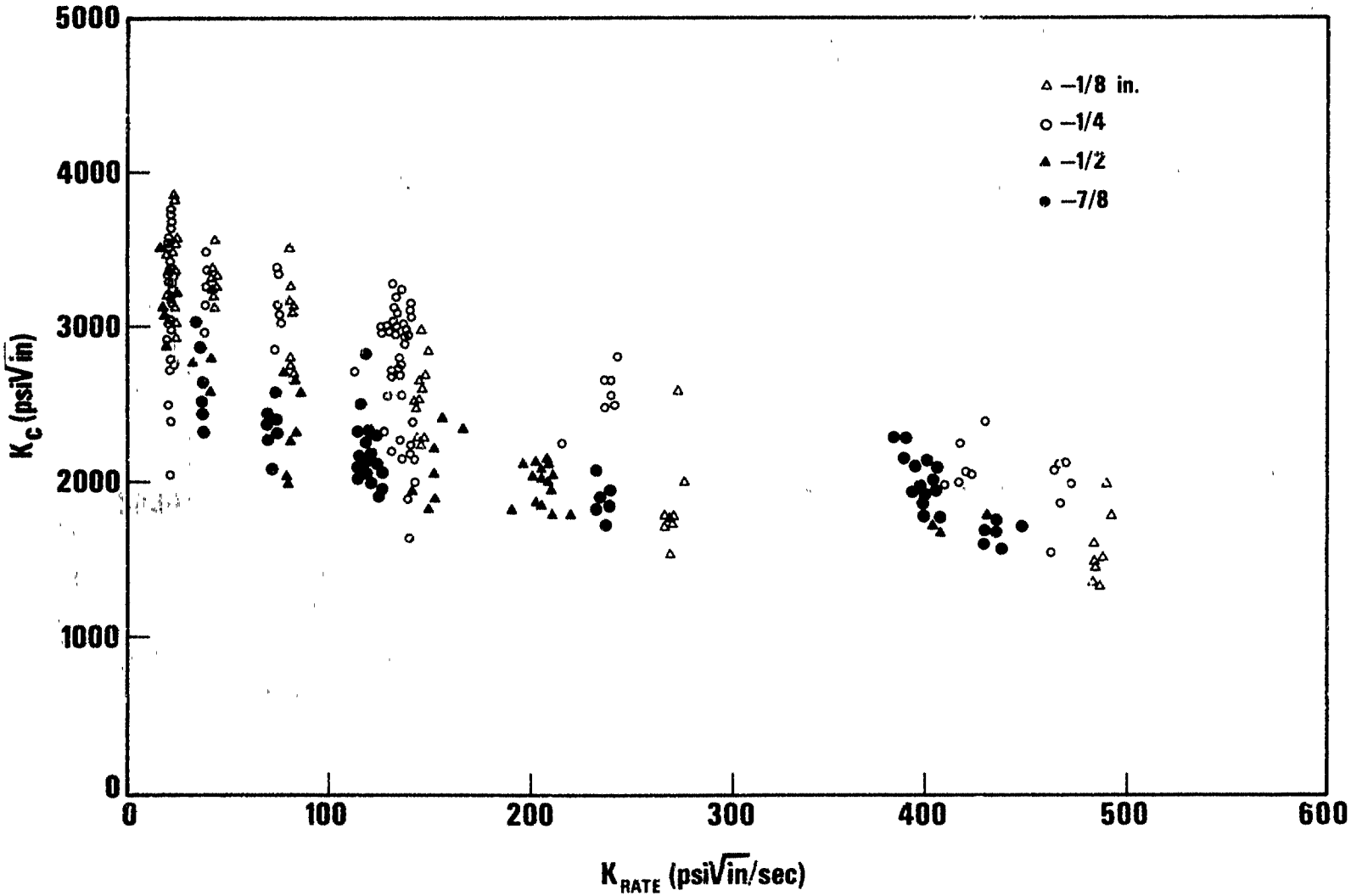


Figure 5. Fracture Toughness (K_{Ic}) for Varying Loading Rates (K_{rate}) and Thickness.

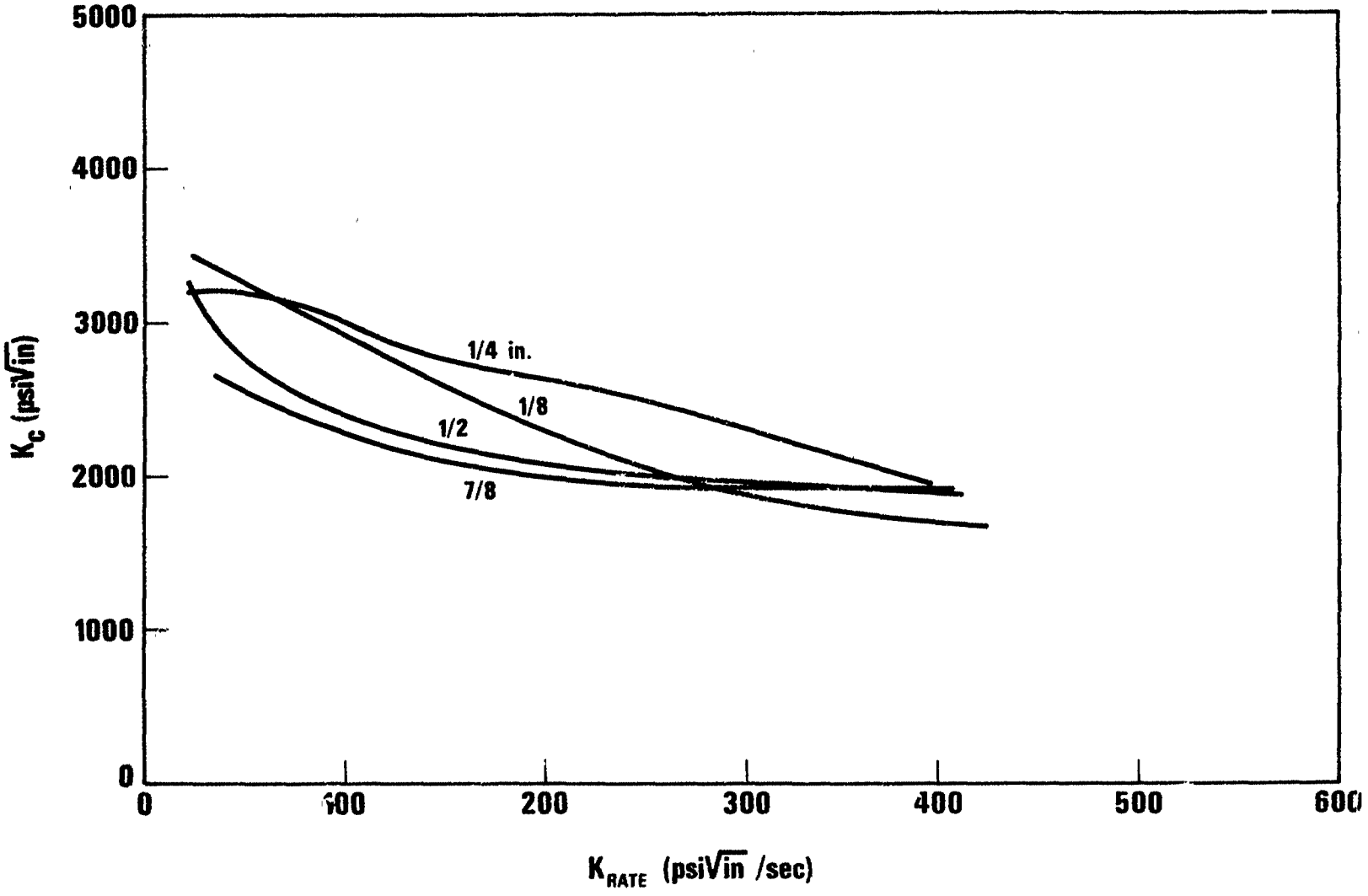


Figure 6. Fracture Toughness (K_{Ic}) for Varying Loading Rates (K_{rate}) and Thickness Trend Curves.

THE EFFECT OF THERMAL HISTORY ON THE MECHANICAL PROPERTIES AND CRYSTALLINITY OF POLYCARBONATE

R. J. Morgan and J. E. O'Neal
McDonnell Douglas Research Laboratories
McDonnell Douglas Corp.
St. Louis, Missouri

The Effect of Thermal History on the Mechanical Properties and Crystallinity of Polycarbonate*

Roger J. Morgan and James E. O'Neal
McDonnell Douglas Research Laboratories
McDonnell Douglas Corp., St. Louis, Mo. 63166

Abstract

The use of polycarbonate in aerospace transparency applications requires a detailed knowledge of the effect of thermal history on optical clarity and mechanical properties, particularly in the impact strain-rate range. The room-temperature tensile mechanical properties and fracture topographies of polycarbonate are reported as a function of strain rate, sample preparation, and thermal history above and below T_g. The bulk physical structural changes produced by various thermal treatments were monitored by density, yield stress, and differential scanning calorimetry observations. Ordered regions do not form in bulk polycarbonate at or below 145°C. The deterioration in the mechanical properties of polycarbonate on glassy-state annealing above 80°C, relative to a quenched or 145°C equilibrium-state glass, are caused by liquid-like packing changes in free volume. In room-temperature tensile tests, the 125°C equilibrium-state glass exhibits transitional behavior from shear yielding to a crazing failure mode in the 10^2/min strain-rate region. For glasses of greater free volume, such as quenched and 145°C equilibrium-state glasses, this transition occurs at higher strain rates. It is concluded that exposure to temperatures above 80°C results in accumulative deterioration in the impact properties of polycarbonate because of a decrease in free volume. Embrittlement results in the cessation of shear yielding and reversion to a crazing failure mode with a correspond - ing decrease in molecular flow and energy to failure. Density measurements indicate that ordered regions do start to grow immediately above T_g ($T_g \simeq 150$°C) in bulk polycarbonate, with a corresponding serious loss in the optical clarity of this material.

This research was conducted under the McDonnell Douglas Independent Research and Development Program.

Introduction

The use of polycarbonate in aerospace transparency applications requires a detailed knowledge of the effect of fabrication procedures and service environment on optical clarity and mechanical properties. To achieve this goal, it is necessary to determine the basic structural parameters controlling the mechanical properties and optical clarity and how such parameters are modified by fabrication procedures and environmental factors.

The mechanical properties of a polymer glass primarily depend on the amount of flow occurring during the failure process, either microscopically via crazing or shear banding or macroscopically via necking. This flow absorbs energy during the failure process and enhances the toughness of the polymer glass. Any phenomenon that inhibits flow will embrittle the glass and seriously limit its use. The flow processes involve both the movement of polymer chain segments, consisting of 10-50 monomer units, and ordered regions when present.

The free volume is the primary physical parameter affecting the mechanical response of a polymeric glass. The free volume distribution, however, and the role of such a distribution in the mechanical properties are subjects of considerable controversy. Ordered regions have been reported in polymer glasses, primarily by Geil[1] and Yeh[2], from electron microscope studies of surface replicas of both thick (> 500 Å) and thin (< 500 Å) films and from both dark- and bright-field contrast microscopy of unshadowed thin films. These workers have also monitored the alignment of such ordered regions during deformation and during growth and interconnection after annealing. A number of structural models for the "amorphous" state of polymers have been proposed to explain these observations [1, 3-5].

The evidence against the presence of ordered regions in amorphous polymers is based on both theoretical studies and experimental observations. Flory[6], on the basis of statistical mechanical models of polymer chains, contends that a polymer chain should assume random configurations unbiased by neighboring chains. His calculations are consistent with experimental evidence from rubber elasticity, cyclization equilibria, and the thermodynamics of polymer solutions. Other workers [7] claim that amorphous polymers consist of a homogeneous mass of randomly coiled chains, on the basis of small-angle x-ray and small-angle neutron scattering observations.

Hence, at present, it is uncertain whether ordered regions observed in thin films and on surfaces exist within the bulk of amorphous polymers. If ordered regions exist in amorphous polymers, it is uncertain what effect they have on the failure processes of polymer glasses. Certainly the size and concentration of any ordered regions and the strength of their interactions could have a significant effect on the flow processes that occur during failure.

Polycarbonate embrittles when exposed to temperatures between 80° and 130°C ($T_g \simeq 150$°C) which results in decreases in impact strength, fracture energy, and extension to break and increases in the tensile and flexural yield strengths [8-14]. This embrittlement is accompanied by a density increase of 0.1 to 0.2% [10,11,14]. LeGrand[11] reports that the original properties can be restored by annealing the embrittled specimens above T_g. Flexural yield-stress data by Golden et al.[10], however, indicate that the mechanism causing restoration of the original properties begins in the glassy state at $\sim$130°C. X-ray diffraction studies show no detectable increase in short-range order of embrittled specimens [10,11,15]. Ordered nodules and nodular aggregates (several hundred angstroms) that enlarge on annealing below T_g and partially break up above T_g, have been observed on the surfaces of thin films and etched thick specimens of polycarbonate [16-19]. Prespherulitic and spherulitic structures also have been grown on the surfaces of thin films annealed below T_g [17-19]. More recently, Neki and Geil [20] have attempted to correlate the morphological changes observed in the etched surfaces of thick films with the tensile mechanical, thermal, dielectric, and dynamic mechanical properties of polycarbonate annealed above and below T_g

In this paper we report the effect of thermal history and sample preparation on the physical structure, optical clarity, and mechanical properties of polycarbonate. The purpose of this work was to determine (1) the structural changes responsible for the reported deterioration in the mechanical properties, (2) the temperature at which crystalline regions start to grow in the bulk, and (3) how these observations, together with fabrication procedures, affect the long-term useful life of polycarbonate in aerospace applications. The room-temperature tensile mechanical properties of polycarbonate are reported as a function of (1) thermal history, above and below T_g, (2) sample preparation, and (3) strain rate. Scanning electron microscopy was used to monitor the fracture topographies. The physical structure and the changes induced by thermal history were monitored by (1) density, (2) differential scanning claorimetry, (3) bright-field transmission electron microscopy of thin films (< 500 Å), and (4) transmission electron microscopy of carbon-platinum surface replicas of NaOH-etched thick films, similar to those used for the mechanical studies.

Experimental

Materials

The bisphenol A polycarbonate (poly-4,4 '-dioxydiphenyl 2,2-propane carbonate) (Lexan, General Electric) had a viscosity-average molecular weight of 30,000 and contained no additives. The polymer was in the powdered form and prior to any sample preparation was preheated at 125°C overnight in vacuum to remove moisture.

Experiment

Solution cast films and compression-molded specimens were prepared for mechanical property studies. Films ($\sim$ 0.1 mm thick) were cast from methylene chloride containing 20 wt % polymer, and dogbone-shaped specimens were punched from the films by suitably shaped dies. Compression-molded sheets ($\sim$ 1 mm thick) of polycarbonate were prepared by molding the dry powder at 180°C for 15 min at 34 NM/m^2 (5000 psi) and then cooling under pressure. Dogbone-shaped specimens were machined from the sheets, and the edges were polished along the gage length. All specimens were vacuum annealed at 160°C for 1 h, which removed molding stresses. The tensile stress-strain properties were determined on an Instron (TM-S-1130) in the crosshead speed range of 0.05-100 cm/min.

For density measurements, 1 cm^3 specimens were cut from compression-molded plugs and were subsequently polished with 600 A-grade sandpaper. The room-temperature density measurements were performed by hydrostatic weighing, utilizing the high-precision technique of Bowman et al.[21].

Thin films of polycarbonate ($\sim$ 500 Å thick) suitable for bright-field transmission electron microscopy were prepared by spreading a few drops of a 1% methylene chloride solution onto a glass slide. The films were exposed to vacuum for 12 h at room temperature, and any remaining solvent was evolved at 160°C for 30 min under vacuum. The morphology of thick polycarbonate films ($\sim$ 0.1 mm thick) was investigated from carbon-platinum, first-stage replicas of NaOH-etched surfaces. Fracture surfaces for scanning electron microscopy studies were coated with gold while the sample was rotated in vacuum. An electron microscope (JEOL model JEM-100B) was used for the transmission and scanning electron microscope studies.

Differential scanning calorimetry (DSC) analysis was performed with a differential scanning calorimeter (Rigaku model M8075) using a heating rate of 5°C/min.

Results

Mechanical Properties and Fracture Topographies

Table 1 shows the effect of consecutive, glassy-state annealing cycles between 145° and 125°C on the room-temperature yield stress of solution-cast (series A) and compression-molded (series B) polycarbonate at a strain rate of 6.7×10^{-2}/min. Prior to testing, the samples in the series A-1 to A-8 and B-1 to B-7 were exposed to the same thermal history as all preceding samples within each series. The yield stresses shown in Table 1 are an average of five specimens for each thermal history. All specimens exhibited necking and cold drawing prior to fracture, which generally occurred at ∿ 12% extension, with the exception of a few specimens which neck ruptured because of inherent flaws at the growing neck. In series B, the yield stress attained following 3 h annealing at 145°C remained unchanged after 4 days further annealing at this temperature. This constant yield stress indicates that the glass essentially attained an equilibrium state within 3 h annealing at 145°C. In both series A and B, the yield stress attained after annealing at 145°C increased on annealing at 125°C and then reverted to its original value on subsequently annealing at 145°C. The yield stress changes were reversible for two consecutive annealing cycles between 145° and 125°C for series A and for one annealing cycle for series B. The data in series A show that the yield stress approaches a constant value after ∿ 6 days at 125°C Quenching from 160°C, just above T_g, lowers the yield stress relative to that for samples annealed in the glassy state. The originai, unannealed, slow-cooled, solution-cast specimen (A-1) exhibits a yield stress that is intermediate between the 125° and 145°C annealed specimens.

Table 1 Effect of consecutive annealing cycles on the yield stress of (A) solution-cast films and (B) compression-molded specimens of polycarbonate

	Thermal history	Yield stress (kg/cm^2)
A-1	Solution-cast; 60°C, 24 h; 160°C, 1 h; cooled 2°C/min to room temperature	615 ± 10
A-2	145°C, 4 days	596
A-3	125°C, 1 day	621
A-4	145°C, 2 days	593
A-5	125°C, 2 days	627
A-6	125°C, 1 day	635
A-7	125°C, 3 days	643
A-8	145°C, 4 days	601
A-9	Quenched in ice water from 162°C after 10 min	456
B-1	Compression-molded; 180°C, 15 min; cooled 2°C/min to room temperature; 160°C, 1 h; quenched in ice water	611 ± 10
B-2	145°C, 3 h	686
B-3	145°C, 6 h	687
B-4	145°C, 1 day	678
B-5	145°C, 4 days	682
B-6	125°C, 1 day	727
B-7	145°C, 4 days	688

The thicker compression-molded specimens all exhibited greater yield stresses than the solution-cast films. For materials that deform plastically, the crack-growth mechanism depends on specimen thickness [22]. Plastic deformation at essentially constant volume can readily be accommodated in thin specimens by lateral contraction. In thicker specimens, lateral contraction becomes more difficult, and plane stress conditions, ahead of the crack, change to plane strain conditions, which cause a transition from ductile to brittle fracture. The ductile-brittle transition for the notched impact strength of polycarbonate has been shown to depend on the specimen thickness [9,23]. A similar phenomenon may explain the greater yield stresses observed for our thicker specimens.

The effect of strain rate on the room-temperature yield stress of compression-molded polycarbonates of different thermal histories (i.e., quenched in ice water from 290°C; annealed for 4 days at 145°C; or annealed for 6 days at 125°C) were investigated. The 145° and 125°C annealed glasses both attained their respective equilibrium states within experimental error (c.f., Table 1 and Fig. 1). Our objective was to determine the effect of strain rate on the yield stress and mode of failure of these glasses. All glasses exhibited a definite macroscopic yield point and underwent cold drawing up to strain rates of $\sim 10^1$/min, which was the limit of the response of the tensile tester to record the yield stress accurately. A plot of the log (strain rate) versus yield stress is shown for the three types of glasses in Fig. 1. The tensile yield stress for these glasses is a linear logarithmic function of strain rate, as has been reported by previous workers for polycarbonate [24-27]. The 125°C equilibrium-state glass exhibits the least strain rate dependence, with the 145°C equilibrium-state and the quenched glasses exhibiting progressively lower yield stresses and ~ 11% and ~ 40% greater strain rate dependencies respectively. Specimens were fractured in tension in the $10^1 - 1.5 \times 10^2$/min strain rate range, and the fracture topographies were investigated. In this range, the quenched and 145°C equilibrium-state glasses underwent cold drawing prior to fracture. A typical fracture surface for a 145°C equilibrium-state glass for which fracture occurred in the cold-drawn region, is shown in the scanning electron micrograph in Fig. 2. The 125°C equilibrium-state glasses at strain rates of $\sim > 10^2$/min ceased to cold

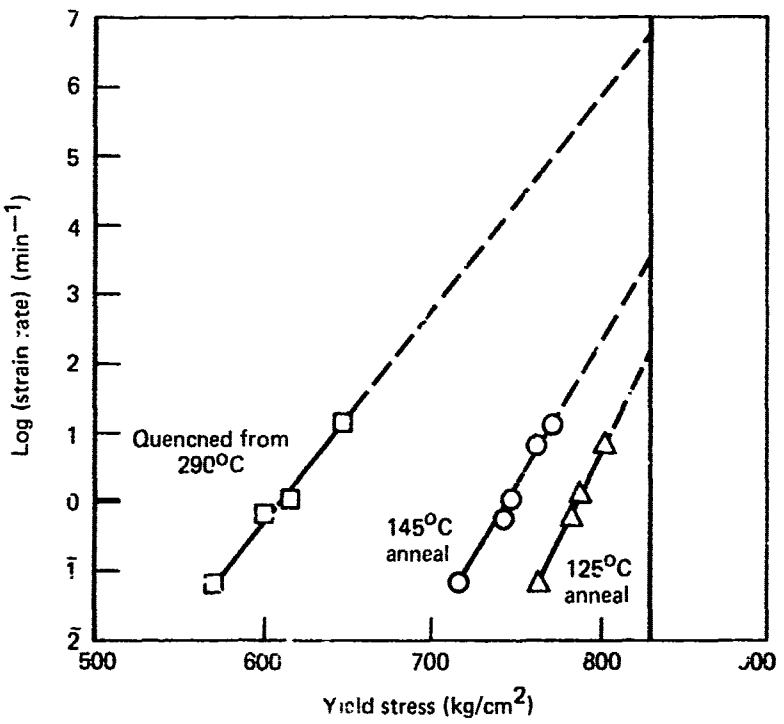


Figure 1. Log (strain rate) versus room-temperature tensile yield stress for compression-molded polycarbonate (a) quenched from 290°C, (b) annealed at 145°C for 4 days and (c) annealed at 125° for 6 days.

draw and failed by either neck rupturing or crazing. Figure 3 shows a scanning electron micrograph of a typical neck-rupture fracture surface for a 125°C equilibrium-state glass, when tested at strain rate of 1.33 x 10^2/min. The fracture surface shows that failure occurred prior to neck formation but after macroscopic shear zones had propagated to approximately the center of the specimen. Figure 4 shows the fracture topography of a 125°C equilibrium-state glass that failed via crazing at a strain rate of 1.33 x 10^2/min. The initiation region shown in the top left of Fig. 4 is large and extends to ∿ 500 μm from the edge of the sample. This region consists of a porous structure containing 500-1000 Å diam broken fibrils. A patch pattern is observed (Fig. 4) in the faster crack-growth region, which is caused by cracks propagating along the boundary between the crazed and uncrazed material and jumping irregularly from one boundary to the other [28-30]. Concentric circles, also evident in this region, can be attributed to shock waves producing superimposed oscillatory stresses which interact with the propagating crack [30].

Hence, in the 10^2/min strain rate region, the 125°C equilibrium-state glass ceased to cold draw and exhibited mixed failure modes characteristic of a transition from ductile to brittle behavior. Such a transition presumably occurs at higher strain rates for the quenched and 145°C equilibrium-state glasses.

Density Measurements

The room-temperature density of compression-molded polycarbonate as a function of thermal history is shown in the series designated A to E in Table 2. In series A to D, one sample for each series was exposed to the consecutive annealing conditions shown in Table 2. [It should be noted that freshly molded specimens exhibited greater densities (i.e., 1.1992 ± 0.002 g/cm^3) than annealed specimens in series A to D, because of the presence of molding stresses. These stresses were removed by annealing at 160°C for 1 h.] In series E, a different sample, prepared under the same conditions with the exception of the 12 h anneal temperature, was used for each of the E-1 to E-4 measurements.



Figure 2. Scanning electron micrograph of fracture surface of 145°C equilibrium-state polycarbonate, tested at a strain rate of 1.33 x 10^2/min.



Figure 3. Scanning electron micrograph of neck-rupture fracture surface of 125°C equilibrium-state polycarbonate, tested at a strain rate of 1.33×10^{2}/min.



Figure 4. Scanning electron micrograph of fracture surface of 125°C equilibrium-state polycarbonate that failed via crazing at a strain rate of 1.33×10^{2}/min.

Table 2 Room-temperature density of compression-molded polycarbonate as a function of thermal history

	Thermal history	Room temperature density (g/cm^3)
A-1	Compression-molded; 180°C, 15 min; cooled, 2°C/min to room temperature; 160°C, 1 h; 145°C, 3 h	1.1971 ± 0.0002
A-2	145°C, 6 h	1 1975
A-3	145°C, 4 days	1.1972
B-1	Compression-molded 270°C, 0.5 h; quenched in ice water; 160°C, 1 h; 145°C, 3 h	1.1975
B-2	145°C, 24 h	1.1972
C-1	Compression-molded; 180°C, 15 min; cooled, 2°C/min to room temperature; 160°C, 1 h; 145°C, 4 days	1.1972
C-2	125°C, 1 day	1.1982
C-3	145°C 3 days	1.1973
C-4	125°C, 2.5 days	1.1986
C-5	125°C, 3.5 days	1.1988
D-1	Compression-molded; 180°C, 15 min; cooled, 2°C/min to room temperature; 160°C, 1 h; 125°C, 1 day	1.1981
D-2	145°C, 4 days	1.1974
	Compression-molded; 180°C, 15 min; cooled, 2°C/min to room temperature; 160°C, 1 h	
E-1	152°C, 12 h	1.1974
E-2	160°C, 12 h	1.1975
E-3	165°C, 12 h	1.1988
E-4	172°C, 12 h	1.2024

In series A and B, polycarbonate attained a density of 1.1973 ± 0.0002 g/cm^3 within 3 h annealing at 145°C. No further density changes occurred, within experimental error, after 4 days further annealing at 145°C. The constant 145°C equilibrium-state density was attained within 3 h, irrespective of whether the original sample was compression molded from 180°C for 15 min (series A) or quenched from above the crystalline melting point (i.e., from 270°C) (series B). This observation indicates that the 180°C, 15 min compression-molded sample did not contain any significant crystalline or pre-crystalline regions within the ± 0.0002 g/cm^3 experimental error. In series C and D, the changes in density on thermal cycling between 145° and 125°C were reversible within experimental error. The density approaches a constant value within ∼ 6 days at 125°C, which indicates that the glass essentially attained its equilibrium state at 125°C within this time period. The density change between the 145° and 125°C equilibrium-state samples is equivalent to a volume coefficient of expansion of ∼ 6 x 10^{-5}/°C, which is of the same magnitude as that normally associated with a polymer in the liquid state. The densities of specimens in series E increased progressively with temperature above 160°C after 12 h annealing at each temperature. Specimen F-4 annealed at 172°C for 12 h, exhibited a distinct opaqueness. These observations indicate that crystallization starts to occur above 160°C. The density remains constant within the annealing temperature range 145° to 160°C. A plot of the density versus annealing temperature is shown in Fig. 5.

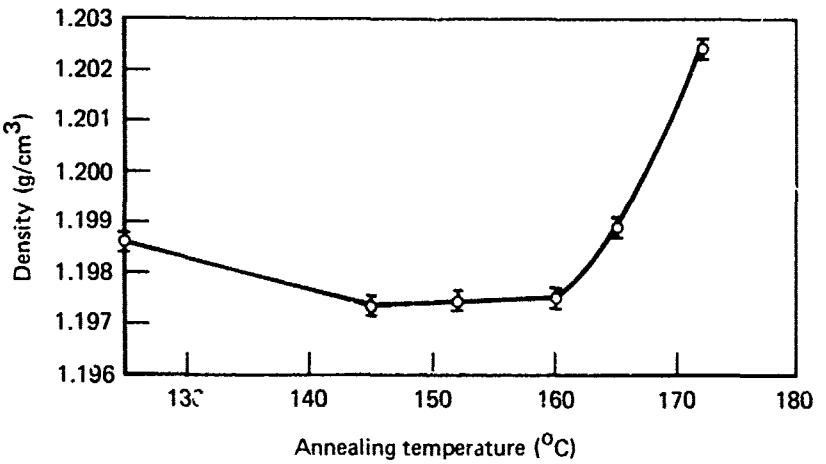


Figure 5. Density of compression-molded polycarbonate versus annealing temperature.

Electron Microscopy

Bright-Field Transmission Electron Microscopy of Thin Films – Bright-field transmission electron micrographs of polycarbonate thin films revealed a nodular network structure. In Fig. 6, 50-60 Å nodules (dark regions) appear to be interconnected by ∼ 30-40 Å internodular cross-links.

Carbon-Platinum Surface Replicas of Etched, Thick Films – The surface replicas of 125° and 145°C equilibrium-state, thick polycarbonate films etched with either 1% or 5% aqueous NaOH, exhibited similar structural features. A typical surface, shown in Fig. 7, consisted of poorly defined 150-300 Å nodules with isolated regions of more pronounced nodules and prespherulitic structures.

Differential Scanning Calorimetry

Differential scanning calorimetry plots for polycarbonate as a function of various thermal histories are shown in Fig. 8 The 125°C annealed glass exhibits a considerably larger enthalpy change at T_g than the 145°C annealed glass. This enthalpy difference is reversible on consecutively annealing between 145° and 125°C. Both of the annealed glasses exhibit a low endotherm in the 200-250°C range, which was not observed for a glass rapidly cooled from 290°C. The 125° and 145°C annealed glasses exhibited a similar endothermic crystalline melting point at 236°C, after 1.5 days annealing at 172°C. These semi-crystalline specimens also exhibited a small endotherm at 204°C.

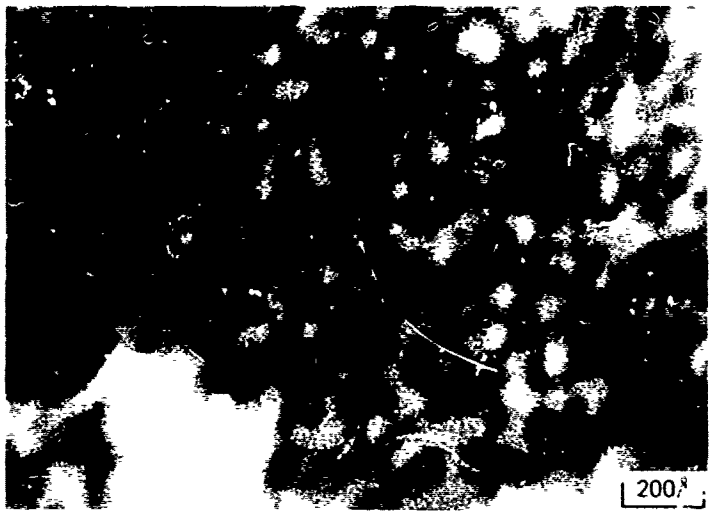


Figure 6. Bright-field transmission electron micrograph of the nodular network structure in polycarbonate thin film annealed at 105°C for 7 days.

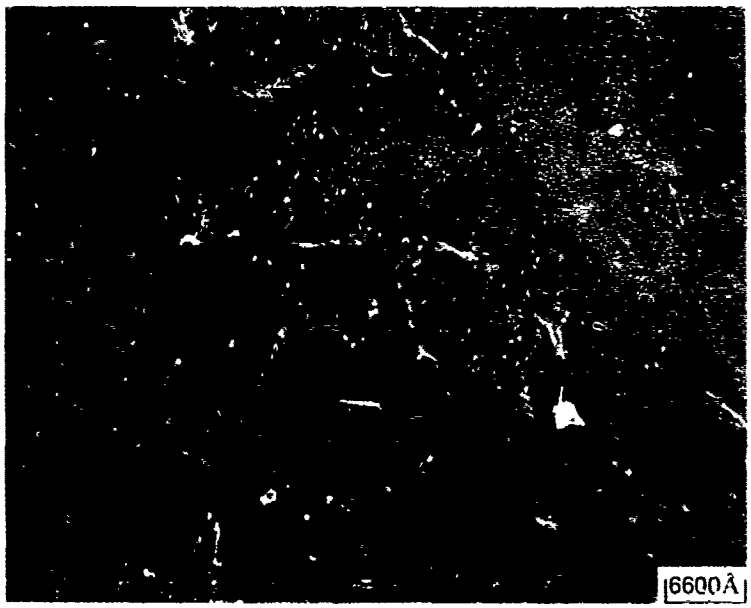


Figure 7. Carbon-platinum surface replica of NaOH-etched 145°C equilibrium-state polycarbonate.

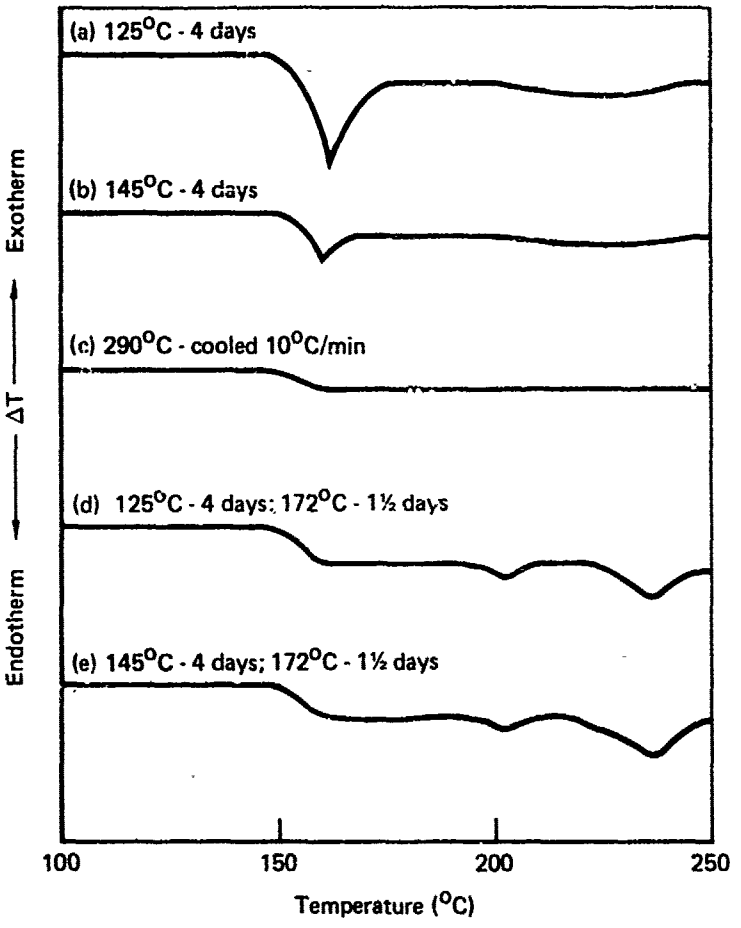


Figure 8. DSC curves for polycarbonate with various thermal histories.

Discussion

Effect of Thermal History on Mechanical Properties

The room-temperature yield stress (strain rate $\sim 10^{-2}$/min) and density data of 180°C, compression-molded polycarbonate specimens indicate that the 145°C equilibrium state is attained within 3 h annealing at 145°C. No further changes in the room-temperature yield stress and density occurred in these glasses after prolonged annealing times (i.e., > 4 days) in the glassy state. These glasses exhibit a increase in the room-temperature yield stress and density when annealed at 125°C. The 125°C equilibrium state is attained within 6 days annealing at 125°C. The following evidence suggests that this increase in yield stress and density results from liquid-like packing changes in free volume and not from the permanent growth of ordered regions: (1) Consecutive glassy-state annealing cycles between 145° and 125°C produce reversible changes in the room-temperature yield stress and density. (2) The volume coefficient of expansion calculated from the reversible density changes is of the same magnitude as that normally associated with free-volume changes (i.e., $\sim 6 \times 10^{-5}$/°C). (3) The 125°C annealed glasses exhibit a greater enthalpy change at T_g than the 145°C annealed glasses.

The changes in free volume, or local order, in the glassy state are a result of an extension to temperatures below T_g of packing changes associated with the liquid state. The volume-temperature plot schematically shows in Fig. 9 the extension of the liquid volume-temperature plot below T_g. This extrapolated plot represents the equilibrium state of the glass. The time necessary to achieve the equilibrium state at a given temperature below T_g will depend on the glassy-state mobility. Below a certain temperature, the glassy-state mobility is too small to allow any changes in free volume. The free volume and associated mechanical properties of the glass will depend on the previous thermal history of the polymer above and below T_g.

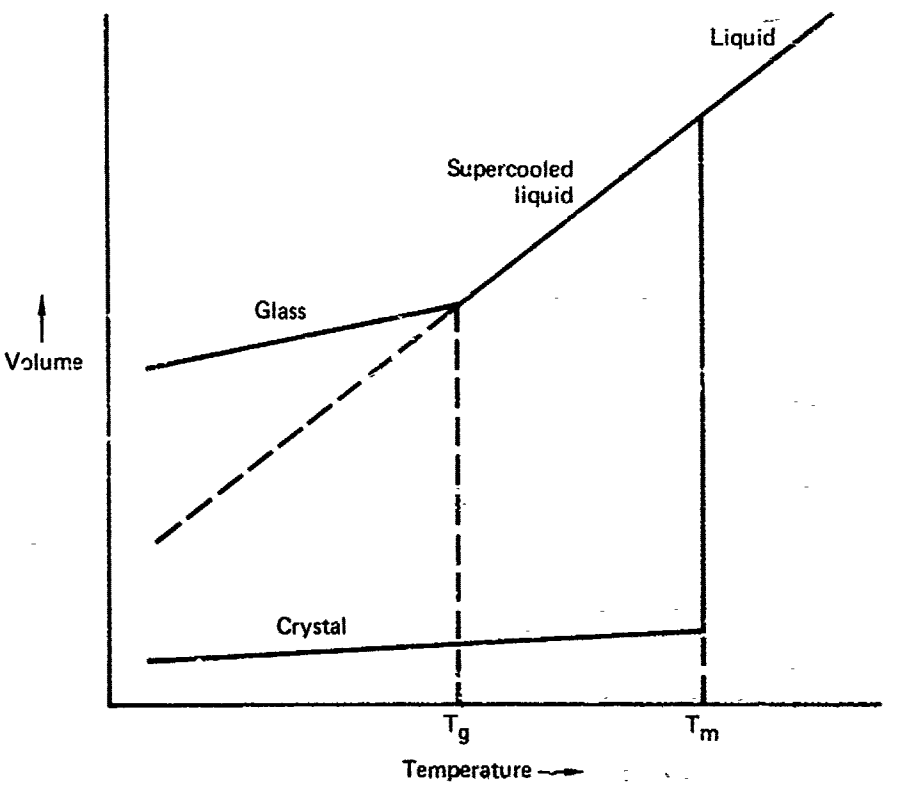


Figure 9. Schematic volume-temperature plot for polycarbonate.

The free volume changes produce only a small difference in the yield stress of the 125° and 145°C equilibrium-state glasses at low strain rates. However, at higher strain rates in the impact range ($\sim 10^4$/min), free-volume differences significantly affect the failure modes and energy-to-failure of polycarbonate. The room-temperature tensile data and fracture topography studies of polycarbonate at strain rates of $\sim 10^2$/min show that the quenched and 145°C equilibrium-state glasses still deform by shear yielding and macroscopic cold drawing. The 125°C equilibrium-state glass, however, exhibits transitional behavior from shear yielding to crazing in the 10^2/min strain rate region. LeGrand [11] has reported that annealing at 125°C causes polycarbonate to embrittle and fail via crazing in room-temperature, notched impact tests at strain rates of $\sim 10^4$/min. In LeGrand's work [11], the unannealed glasses, whose previous thermal history was not defined, failed in a ductile manner without crazing. Hull and Owen [30], from fracture topography studies of notched impact specimens of polycarbonate tested from −196° to 130°C, also concluded that only brittle specimens failed by crazing. Hence, we can conclude that the 125°C equilibrium-state glass starts to embrittle in a tensile test at a strain rate of $\sim 10^2$/min by the cessation of shear yielding and reversion to a crazing failure mode with a corresponding decrease in molecular flow and energy-to-failure.

Embrittlement occurs approximately at the strain rate where the shear yield stress equals the crazing stress (i.e., at the position where the shear yield stress-strain rate plot intersects the crazing stress-strain rate plot). For such a transition to occur, the strain-rate dependence of shear yielding must be greater than that of the crazing stress; otherwise the two strain-rate plots would not intersect at higher strain rates. [The temperature dependence of shear yielding, which will follow the same trend as the strain-rate dependence, has been reported to be greater than that of the crazing-stress dependence for other polymer glasses [31,32]]. At present, the magnitude and strain-rate dependence of the crazing stress of polycarbonate as a function of thermal history and free volume of the glass are unknown. Hence, for the quenched and 145°C equilibrium-state glasses, it is not possible to predict the onset of the tensile ductile-brittle transition from extrapolation of the log (strain rate) - yield stress plots and the strain rate and stress level at which this transition occurs for the 125°C equilibrium-state glass. [If we assume that the crazing stress for polycarbonate is essentially independent of strain rate and thermal history, the ductile-brittle transition should occur at the same stress level (i.e., $\sim$ 830 kg/cm^2) for all glasses (Fig. 1). Such a stress would not be attained until the strain rate is $\sim 10^4$/min and $\sim 10^6$/min for the 145°C equilibrium-state glass and the quenched glass respectively.]

Hence, the reported embrittlement of polycarbonate above 80°C in the impact strain rate range is a result of liquid-like packing changes in free volume. The notched Izod impact strength of polycarbonate has been reported to decrease by a factor of eight on annealing quenched glasses above 80°C in the glassy state [10,11,14]. The deterioration in the impact properties of polycarbonate will be cumulative for each exposure about 80°C. Therefore, the desirable high-impact properties of polycarbonate cannot be fully utilized for aircraft windshield applications that are intermittently exposed to temperatures above 80°C. The impact strength of embrittled polycarbonate, however, is still $\sim$ 4 times larger than that of polystyrene and polymethyl methacrylate [33].

Crystallization and Optical Clarity

The growth of crystalline regions in polycarbonate will deteriorate the optical clarity. However, density measurements show that precrystalline and/or crystalline regions do not form in the bulk until above T_g. Ordered regions do not form when a 145°C equilibrium-state glass is subsequently annealed at 125°C. Consecutive glassy-state annealing cycles between 145° and 125°C produced reversible changes in density and yield stress, which can only be explained in terms of liquid-like packing changes in free volume. Solution-cast and 180°C compression-molded glasses attain a constant yield stress and density within 3 h annealing at 145°C, with no further changes occurring after prolonged annealing at 145°C (i.e., > 4 days). Furthermore, a glass quenched from 270°C attains the 145°C equilibrium-state density within 3 h annealing at 145°C. The latter observation discounts the possibility that any significant ordered regions are formed by solution casting or are present in the original commercial powder and not destroyed on molding at 180°C.

Above 145°C, certain regions of polycarbonate become more ordered in relation to the 145°C equilibrium state. In the 145° to 160°C range, for a 12 h annealing period, the density remains constant within experimental error relative to the 145°C equilibrium-state density and does not decrease with increasing temperature. (The regions separating such ordered regions, however, exhibit a greater free volume at 160°C than for the 145°C equilibrium state as indicated by a lower room-temperature yield stress.) Above 160°C, the rate of growth of

ordered crystalline regions increases as evidenced by a progressive increase in density and opaqueness with temperature. In addition, DSC endotherms characteristic of crystalline melting points were observed for a sample annealed at 172° for 36 h. It is evident from these observations that polycarbonate is capable of crystallizing just above T_g over a period of 12 h, but crystallization is inhibited by mobility restrictions as the glassy state is appraoched.

If normal free-volume changes alone occurred in the 145° to 175°C range, the density would linearly decrease with temperature, corresponding to a volume coefficient of expansion of $\sim 6 \times 10^{-5}$/°C. In Fig. 10, the percentage density increase caused by the growth of ordered regions relative to the density calculated assuming normal free-volume changes is plotted versus temperature in the 145° to 175°C range. Extrapolation of this plot to 145°C reveals that the percent density increase at this temperature associated with the growth of ordered regions is in the 0 to 0.08% range. This conclusion is consistent with the constant density exhibited by the 145°C equilibrium-state polycarbonate, within a 0.034% experimental error, over a 4-day anneal period at 145°C. This observation indicates that the percent density increase as a result of the growth of any ordered regions over a 12 h anneal period at 145°C must be $< 0.004\%$, for a linear growth of such regions with time. Hence, it is reasonable to conclude that ordered regions do not grow in bulk polycarbonate below T_g. Their growth is apparently inhibited by the mobility restrictions of the glassy state. The optical clarity of polycarbonate will not therefore deteriorate as a result of crystallization, on exposure to temperatures below 145°C.

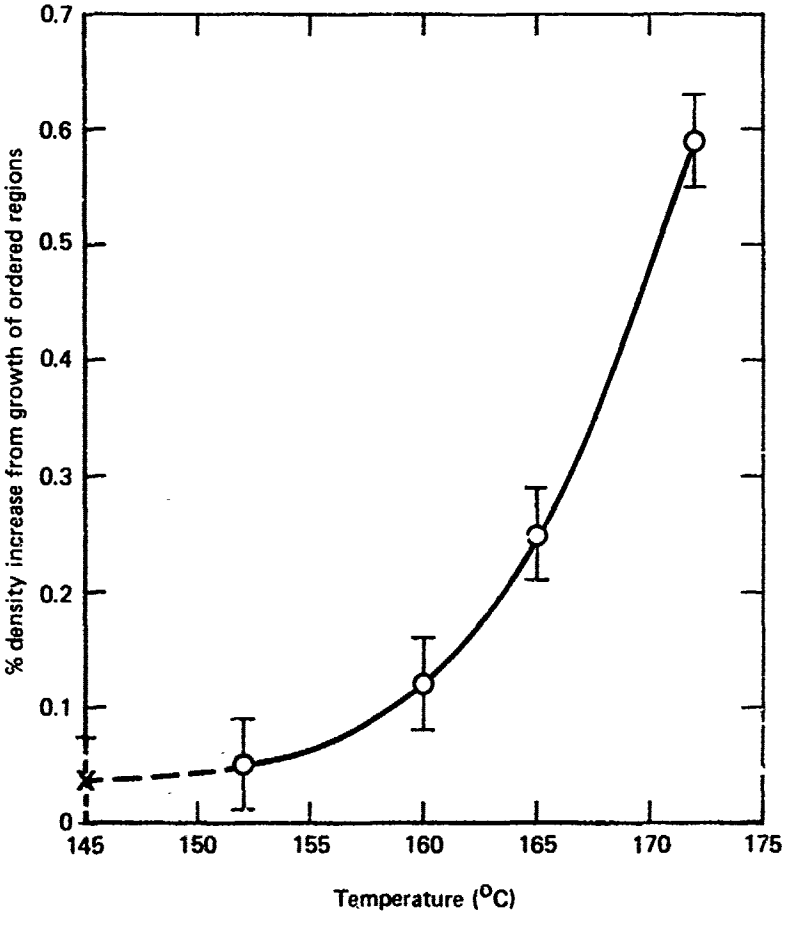


Figure 10. Percent density increase in bulk polycarbonate, caused by the growth of ordered regions, vs temperature in the 145 - 175°C range.

At or immediately above T_g, however, ordered regions do start to form in the bulk. Whether such regions are isolated spherulites or are smaller precrystalline nodular structures is uncertain at present. The ability of polycarbonate to crystallize at or immediately above T_g allows precrystalline and/or crystalline entities to grow below the bulk T_g in thin films and on the free surfaces of thick films where molecular mobility restrictions are less severe than in the bulk. The observation of these structures has led to the fallacious assumption that such structures grow in the bulk below T_g and control the mechanical properties.

Relaxation of Fabrication Stresses

The fabrication procedures of aircraft windshields is generally held proprietary by the manufacturer. Any cold forming (deformation below T_g) in fabrication will result in the tendency of the deformed glass to revert to its original shape when sufficient glassy-state mobility is available. Cold-drawn polycarbonate will start to exhibit dimensional recovery above 80°C [12,34-36]. For example, 10% dimensional recovery occurs within 24 h at 100°C, and up to ∿ 30% dimensional recovery can occur below T_g [36]. Hence, exposure of polycarbonate windshields to in-flight temperatures above 80°C could result in partial dimensional recovery of the windshield to its original shape if it was fabricated below T_g. This phenomen could result in the development of stresses and possible separation of the polycarbonate from any coating or adhesive utilized in the windshield configuration.

Summary

The mechanical properties of polycarbonate are controlled by the free volume of the glass. Above 80°C, the molecular mobility is sufficient to allow the free volume to decrease and any cold-formed fabrication stresses to relax. The free-volume decrease causes embrittlement in the impact strain rate range. Embrittlement results in the cessation of shear yielding and reversion to a crazing failure mode with a corresponding decrease in molecular flow and energy-to-failure. Precrystalline and/or crystalline regions do not form in the bulk glassy-state and, therefore, the optical clarity of polycarbonate will not deteriorate below T_g as a result of the growth of such regions.

Hence, the intermittent exposure of polycarbonate aircraft windshields to temperatures above 80°C, could cause a cumulative loss in impact properties and the development of stresses from relaxation of any cold-drawn material formed during fabrication. These phenomena will depend on fabrication procedures and the thermal history utilized by the manufacturer.

References

1. P. H. Geil, Polymer Preprints 15, (No. 2), 336 (1974).
2. G. S. Y. Yeh, Crit. Rev. Macromol. Sci. 1, 173 (1972).
3. G. S. Y. Yeh, J. Macromol. Sci. - Phys. B6, 465 (1972).
4. S. M. Aharoni, J. Macromol. Sci. - Phys. B7, 73 (1973).
5. S. M. Aharoni, J. Appl. Polym. Sci. 17, 1507 (1973).
6. P. J. Flory, Polymer Preprints 15, (No. 2), 2 (1974).
7. Symposium on Physical Structure of the Amorphous State, Polymer Preprints 15, (No. 2) (1974).
8. G. Peilstocker, Kunststoffe 51, 509 (1961).
9. G. Peilstocker, Brit. Plastics 35, 365 (1962).
10. J. H. Golden, B. L. Hammant and E. A. Hazell, J. Appl. Polym. Sci. 11, 1571 (1967)
11. D. G. LeGrand, J. Appl. Polym. Sci. 13, 2129 (1969).
12. D. G. LeGrand, J. Appl. Polym. Sci. 16, 1367 (1972).
13. R. E. Robertson and C. W. Joynson, J. Appl. Polym. Sci. 16, 733 (1972).
14. G. Allen, D C. W. Morley and T. Williams, J. Mater. Sci. 8, 1449 (1973).
15. G. D. Wignall and G. W. Longman, J. Mater. Sci. 8, 1439 (1973).
16. W. Frank, H. Goddar and H. A. Stuart, J. Polym. Sci. B5, 711 (1967).
17. S. H. Carr, P. H. Geil and E. Baer, J. Macromol. Sci. - Phys. B2 (1), 13 (1968).
18. A. Seigmann and P. H. Geil, J. Macromol. Sci. - Phys. B4(2), 239 (1970).
19. A. Seigmann and P. H. Geil, J. Macromol. Sci. - Phys. B4(2), 273 (1970).
20. K. Neki and P. H. Geil, J. Macromol. Sci. - Phys. B8(1-2), 295 (1973).
21. H. A. Bowman, R. M. Schoonover and M. W. Jones, J. Res. Natl. Bur. Std. (U.S.) 71C, 179 (1967).
22. G. R. Irwin, J. A. Kies and H. L. Smith, Proc. ASTM 58, 640 (1958).
23. T. L. Smith, Molecular Order - Molecular Motion, H. H. Kausch, Ed., (Interscience, New York, 1971) p. 269.
24. R. E. Robertson, J. Appl. Polym. Sci. 7, 433 (1963).
25. C. Bauwens - Crowet. J. C. Bauwens and G. Homes, J. Polym. Sci. A-2, 7, 735 (1969).
26. P. Zitek, and J. Zelinger, J. Appl. Polym. Sci. 14, 1243 (1970).
27. T. E. Brady and G. S. Y. Yeh, J. Appl. Phys. 42, 4622 (1971).
28. J. Murray and D. Hull, Polymer 10, 451 (1969).
29. J. Murray and D. Hull, J. Polym. Sci. A-2, 8, 583 (1970).
30. D. Hull and T. W. Owen, J. Polym. Sci. (Phys. Ed.) 11, 2039 (1973).
31. S. S. Sternstein and L. Ongchin, Polym. Preprints 10, 1117 (1969).

32. R. N. Haward, B. M. Murphy and E. F. T. White, J. Polym. Sci. A-2 9, 801 (1971).

33. L. E. Nielsen, Mechanical Properties of Polymers, (Van Nostrand Reinhold Co., 1962).

34. I. V. Yannas and A. C. Lunn, J. Polym. Sci. B9, 611 (1971).

35. A. C. Lunn and I. V. Yannas, J. Polym. Sci. (Phys. Ed.) 10, 2189 (1972).

36. T. E. Brady and G. S. Y. Yeh, Polym. Letters 10, 731 (1972).

PREVENTION OF FRACTURE IN BPA-POLYCARBONATE STRUCTURES

D. W. Caird
General Electric Company
Plastics Business Division
Pittsfield, Massachusetts

ABSTRACT

This paper identifies the requirements and means for translating the normal toughness properties of BPA-polycarbonate resins into structures which will sustain impact stresses without crazing, cracking or fracturing during use. The controlling factors are flaw geometry plus notch sensitivity of the material - with flaw geometry and size - being of dominant importance. It is shown that within the range of typical notch sensitivity variations of these polycarbonate resins, toughness and ductile response to high stress rates are retained where surface or internal flaws of critical geometries are avoided in manufacture or design, and are prevented from generating in use.

I. INTRODUCTION

At the present state of commercial reality, BPA-polycarbonates uniquely possess the combined properties of clarity, optics, thermal dimensional stability and toughness required for applications of transparent plastics for glazing in areas where maximum assurance of fracture resistance coupled with desirable, or in some cases even acceptable strength to weight ratios are needed. Examples include motor vehicle, railcar and security glazings where protection of personnel and material against the whole gamut of vandal attacks is critical. And high performance aircraft add the severe requirements of fracture resistance to high magnitude, high velocity bird impacts - possibly 300 to 800 mph on a structure that may be only 1/2 to 1 inch thick - together with dimensional stability in thermal environments generated at supersonic speeds. The translation of the established toughness properties of these present resins into structures which will sustain such major impact and associated stresses without catastrophic fracture is a necessary condition for successful application in these areas. It is the objective of this paper to establish some guidelines toward this goal based on our present knowledge of the fracture behavior of LEXAN® PC resins of the grades now used in producing transparent extruded sheet. This discussion includes concepts presented in an earlier paper "Maximizing LEXAN Performance"(1) which have been sustained in principle and practice. It extends this data to include our present understanding of the intrinsic resistance of these resins to fracture, and to stress-crazing or cracking as such. It identifies effective means of inhibiting these phenomena by attention to preventing contamination from incompatible environments whose INTERACTION with material stresses is an apparent prerequisite to the development of environmental-stress flaws. It emphasizes that such flaws frequently play the critical role in fracture.

® Trademark of The General Electric Company

II. INTRINSIC TOUGHNESS OF BPA-POLYCARBONATES

BPA-polycarbonates do not fit the classical picture[2] of plastics and inorganic glasses where unnotched specimens exhibit definable ductile-brittle transitions as temperature is lowered below the glass transition, T_g, into the use range; or as rate of straining is increased to impact velocities. Specifically:

- There is no identifiable temperature, at least down to liquid nitrogen range (-195C/-320F) where normal PC resins, of the grades used in extruded sheet exhibit an intrinsic ductile-brittle transition in the absence of detectable flaws, generally of macroscopic dimensions.

- Similarly, at least in impact tests at normal ambients, planar specimens have shown no evidence of brittle fracture or spalling - again in the absence of initiating flaws - up to ballistics velocities.

For example, TABLE I summarizes drop dart results on 1/8 inch thick specimens cut from randomly selected sheet. Specimens were supported on a solid base over a 2 inch diameter hole immediately after removal from liquid nitrogen. Five and 10 lb darts having 1/2 inch radius tips were used in guided free fall tests up to eight foot heights to impose the nominal impact levels.

TABLE I
Low Temperature Dart Impact (-195°C - nominal)

Test Series	No. of Specimens	Nom. Impact (ft-lbs)	Ductile Response (%)	(Plastic flow)
1a	20	40	95	surface crater
b	10	80	70	dent
2	24	40	65	surface crater
3	24	40	23	surface crater
4a	10	20	40	slight crater
b	10	20	40	slight crater

These data are far from extensive and, at this time differences in % ductile response are attributed to variations in minor internal or surface flaws which are not "critical" at higher temperatures where ductile response is normal up to elongations where tear rupture begins. The significant fact is that ductile response due to intrinsic plastic deformation exists at these temperatures. The problem becomes - how to retain it at any temperature!

In this regard, it is of further interest to observe that these low temperature dart impact tests did not distinguish ductility differences between as-extruded and annealed (20 hrs/125°C) specimens where these were taken from the same sheet, although a significant increase in tensile yield strength[1][3] together with a measurable increase in density [3] do occur on annealing. This is understandable since increase in yield stress on annealing is relatively small compared to the yield stress increase and concomittant increase in notch sensititity of PC resins at -195°C. The magnitude of yield stress at liquid nitrogen temperature has not been measured directly, but can be roughly estimated as 16,000 - 20,000 psi or higher by extrapolation of available yield vs. temperature data.

The foregoing should not be construed to imply that increases in "notch-sensitivity" of these PC resins due to thermal annealing effects may not have some substantial contribution to determing critical flaw geometries at any given set of conditions. We will discuss such interactions later. It is, however, the ability of BPA based polycarbonate resins to tolerate flaws normally present in current commercial products that sets these resins apart from inherently brittle materials. In the latter, microstructural flaws - possibly even at the molecular structure level - must be classified as 'critical' below defined ductile-brittle transitions. Also, it must be evident from the foregoing discussion that the statement that BPA based polycarbonate resins are <u>intrinsically</u> ductile does not mean that they cannot be fractured when subjected to a variety of stress conditions. It does, however, suggest that if we know how to avoid 'critical flaw' conditions, we can make substantial strides in eliminating fracture failures. The considerations are; What do we need to know?; and, What do we do?

III. NOTCH SENSITIVITY AND CRITICAL FLAW CONSIDERATIONS

Qualitatively, we can define two interacting factors which determine whether ductile deformation or catastropic fracture will occur in BPA polycarbonate structures under sufficiently high stress-magnitude and stress-rate loadings to result in one or the other effect; viz:

- <u>Notch-sensitivity</u> of the resin. This is a material property dependent on the thermal history of the structure, and

- <u>Criticality of the geometry of surface or internal flaws</u> in the regions affected by the stresses. Such flaws are NOT intrinsic material properties. They

are created by secondary operations or effects.

Notch-Sensitivity Considerations

Notch-sensitivity relates to those material characteristics which determine, (a) the degree to which imposed tensile stresses are stored elastically within the material: this implies a modulus contribution, (b) the rate and magnitude at which such stored stress is transferred through the material and concentrated at any given localized notch or flaw tip area: this implies a strain to yield contribution, and (c) the manner and extent to which these stresses either further concentrate to initiate a 'critical' flaw and to propagate it as a travelling crack or are relieved by ductile yielding during the period of stressing: this implies a yield stress contribution.

It is known that thermal history (annealing) -- together with specimen thickness and temperature -- affects the notch-sensitivity of intentionally flawed or notched PC specimens of the Izod type; and it is instructive, therefore, to examine the effects of thermal annealing on the modulus, yield stress, and yield strain properties of unnotched specimens to see what correlations may exist. Table II summarizes studies by the author and by D.G. LeGrand reported in greater detail elsewhere[1,3]. The data were obtained on PC resins of similar mol. wgt. in the range used in extruded sheet, but on specimens of widely different thicknesses and fabrication. Both yield strength and annealing effects are remarkably consistent.

TABLE II
Effects of Annealing on Tensile Properties

Anneal (Hrs/125C)	Tensile Properties (Avg)* Yield Stress (PSI)	(%Δ)	Yield Strain (%)	(%Δ)	Yield Ratio Stress/Strain (PSI)
Tests on extruded films (1)					
0	8200	----	8.0	----	102000
1	8900	8.5	6.2	-22	144000
400	9650	18	5.4	-32	176000
*Modulus values did not alter with annealing.					
Tests on molded tensile bars (3)					
0	8200	----			
10	9700	18			
100	9800	19.5			

These values show significant increase in stress and decrease in

strain to yield which we postulate to relate to the intrinsic notch sensitivity of these resins. In Table II the combined effects of yield stress increase and strain decrease are expressed as yield ratios which I propose as empirical expressions of intrinsic notch-sensitivity of these resins. In the case of lower mol. wgt. resins than those in Table II, the rate of increase and the maximum increase in yield stress and in yield ratio on annealing is greater than the values shown; and in the case of higher mol. wgt., it is lower. The latter is, of course, to be preferred but is limited by current extrusion technology in sheet manufacture.

To put these values into perspective, the minimum yield ratio shown in Table II may be considered an approximation of the least notch-sensitive or most ductile state for this resin, approaching the condition which results with rapid cooling from the glass transition temperature. The highest yield ratio is an approximation of the most notch-sensitive state produced at annealing temperatures. These changes occur quite rapidly at temperatures in the 120°C-135°C range as is evident in Table II and discussed in greater detail in my previous paper. However, on heating to T_g (150°C) or above, these yield stress/strain changes reverse and on recooling the resins revert to the least notch-sensitive condition. The phenomenon of increase in notch-sensitivity may occur at usual drying temperatures. The phenomenon of reversibility with recovery of maximum ductility normally occurs at thermoforming temperatures which are usually above T_g.

At this time, I emphasize the fact that even in their most notch-sensitive states, these resins are ductile in the absence of 'critical' notches or flaws which we will now discuss.

Critical Flaw Considerations

To most design engineers in the plastics field the concept of a distinct ductile-brittle transition temperature characteristic of a given plastic is accepted as almost axiomatic. Insofar as PC resins are concerned, however, this is a misconcept; and when the question of such a transition comes up -- as it often does -- the only answer is; it depends: For experience with BPA polycarbonate shows that ductile-brittle transitions can occur at any temperature extending even to those well above room ambient; and that ductility can be retained at very low temperatures as we have discussed. Fracture behavior depends on what the flaw geometry may be in any given test specimen or much more importantly in any given structure under a variety of stress

conditions. For an example of this principle, notched Izod impact strength -- which is improperly often considered almost a material property -- is known to result in largely brittle fracture at room temperature on PC resins in their most ductile state if the specimen thickness exceeds about 3/16", but to give ductile yield with the absorption of 16 to 18 ft-lb. of energy if the specimen thickness is 1/8". Also, published data show a ductile-brittle temperature for these particular 1/8" thick notched Izod specimens at about 0°C, and the question is frequently raised, "How do you use this transition temperature data?" The answer is -- you don't; for structures in the real world are not composed of notched Izod geometries. If they were, the transition temperature would increase to room ambient if intrinsic notch-sensitivity is sufficiently increased by thermal annealing as we have discussed. Moreover, where this occurs, ductile response can be restored without changing the notch-sensitivity parameter by simply reducing the specimen thickness to about 1/10"; which effectively changes the notch or flaw-geometry. This example is intended to illustrate the fact that brittle behavior, at least in PC resins, results from the interaction of notch-sensitivity and flaw-geometry factors. This phenomenon, which may be obscured in typically brittle glasses becomes evident in these PC resins where we see evidence -- as discussed earlier -- that they are remarkably tolerant of normal micro-structural flaws. All available evidence indicates very strongly that flaw geometry in a PC structure is the dominant and controlling factor in fracture phenomena with a contribution from notch-sensitivity where flaws approaching critical dimensions for any given set of stress conditions exist. In this context, flaw geometry is intended to include, especially, the degree of sharpness (or radius) existing at the flaw tip; with the criticality of other size parameters such as crack or flaw width and depth varying in relation to this radius.

Relatively large radius flaws are likely to be created by improper design as, for example, too little radius at bends or at abrupt, stress raising changes in dimensions. This is the type, also, which is frequently encountered in improper machining operations where excess-roughness or even incipient tears sometimes occur. Such flaws may usually be readily detected and corrected.

It is the very small radius flaw geometry that is most troublesome since overall 'critical' sizes which may result in impact propagation and fracture failure can be quite small, (although under most conditions they are of macroscopic dimensions). Among the structural defects which have been identified as producing such extremely sharp radius flaws may be listed the condition that may exist at the interface of a fusion or solvent bonded joint. Also, highly 'critical' flaw geometries have been produced by brittle overlays such as brittle, adherent adhesives, coatings, and claddings which themselves fracture and generate crack flaws at the PC interface which can then continue to propagate through the stressed structure. Environmental-stress and the related environmental-fatigue cracks fall into this category with tip radii probably approaching those at a propagating crack, and with the added complication that their initiation and growth is usually time dependent. Conditions which produce flaws of these types can be very subtle, but they can generally be detected - or, better, anticipated - and corrected where we understand, first their importance and second, how to look for them.

The "impact" of this part of my discussion is:

- CHERCHEZ LA FLAW: find it and identify what caused it; and eliminate it!

- This is the secret to inhibiting and eventually eliminating fracture failures.

IV. INHIBITION OF ENVIRONMENTAL-STRESS CRACKING

At this point, I want to focus attention on understanding the nature of environmental-stress interactions of BPA-polycarbonate resins: this is mandatory for their successful application where structures may be subjected to significant elastic tensile stresses from any of a variety of causes. As examples:

- Fabrication stresses due to thermoforming, machining, or assembly operations -- and especially where these may involve possible exposures to incompatible contaminants.

- Thermal stresses from sudden ambient differentials in use, and

- Externally imposed mechanical stresses from bending, vibration, etc.

It is obviously important to minimize such stresses by special attention to appropriate fabrication and design principles. Less obviously, and more often overlooked: it is equally important to recognize that significant residual or transient stresses may always be present, and that these stresses may attain 'critical' levels for a variety of environmental-stress exposures which can generate time dependent craze-crack initiation and growth into extremely critical flaw geometries; AND that it is possible to inhibit these effects by preventing or minimizing <u>environmental</u> presence or penetration!

I use the designation ENVIRONMENTAL-STRESS very deliberately to emphasize the INTERACTION of environments and stresses where environments are identifiable entities or agents at least in the case of these PC resins. In this regard I exclude temperature from being a direct stress-cracking environment, and postulate that it contributes, rather, to producing stress transients, to affecting the degree of notch-sensitivity of the resin, and to activating potentially incompatible environments. This is a concept which I have not previously found stated explicitly in the literature where a distinction generally appears to be made between stress-cracking (e.g. versus time in a given thermal ambient but where probable contaminants are overlooked or assumed negligible), and environmental-stress-effects.

In the case of PC resins, laboratory studies have demonstrated that where these resins have uncontaminated surfaces they are intrinsically resistant to stress-crazing or cracking at stresses up to the yield strength of the resin and at temperatures from normal ambients up to annealing temperatures where stresses are relieved by uniform material creep. Applications applying this principle are proving successful.

The phenomenon of inherent resistance of these resins to thermal-stress-cracking in the absence of an incompatible contaminant is illustrated in Table III.

TABLE III.

Environmental-Stress-Cracking of PC Resins

Surface Condition of Test Piece.	Test Condition:* Outer Fiber @ 130°C		Craze/Crack Effects
	Strain (%)	Stress (psi)	
Misc.contam.due to long-term exposure	0.45 to 0.7	1500 to 2400	Pos.; Variable
Handled - (hand-wiped)	0.45	1500	Pos.
	2.0	6800	Pos.-Severe!
Clean - (uncontaminated or decontaminated)	>2.0	>6800	Neg.
Decontaminated & protected by a compatible film	>2.0	>6800	Neg.
LEXAN® MR-4000 (coated sheet)	>2.0	>6800	Neg.

*Strains were applied to 2½"x1" test specimens using 4-point bending jigs. Time at temperature was 1 hour.

Until the discovery that, where the PC surface is uncontaminated, these resins are NOT SUBJECT to craze-cracking (even at outer fiber strain/stress levels up to material yield strength above 2%/6800 psi), it had been thought that stress-cracking occurred naturally--although somewhat variably--in simple air environments. And the phenomenon of "inhibition" exhibited by some coatings was thought to be just that, an inhibition. This insight into the probable mechanism of inhibition of crazing, and the demonstration that PC resins are not subject to stress-cracking unless contaminated by an identifiable contaminant present as a removable or inactivatable separate phase at any given stressed area in a structure has useful implications. It means:

- Where environmental-stress cracking occurs in PC structures there IS a contaminating environment present even if it is not immediately evident and identified. It can generally be identified if we look for it.

- The contaminating environment is present as a superficial phase that can be readily and completely removed before it has initiated damage.

- Decontaminated, as well as initially clean surfaces in vulnerable stress areas can be protected from subsequent environmental contamination by use of a compatible barrier coating, and such barrier can be expected to effectively inhibit stress-crack flaws from initiating and developing.

The "stress" of this part of my discussion is:

- CHERCHEZ L'ENVIRONMENT: Identify it, remove it, or better, avoid it initially, and protect vulnerable stressed areas from subsequent recontamination.

- This is the secret to inhibiting and eliminating environmental-stress crack flaws which are so critical in promoting fracture failures in PC structures.

V. SUMMARY AND CONCLUSIONS

The effects of thermal annealing on yield strength and yield strain properties together with the effect of these property changes on notch sensitivity are reviewed and brought into perspective. For example, even at the significantly higher yield and modulus characteristics which exist at liquid nitrogen temperature (-195°C) these resins remain ductile in the absence of "critical flaws" in the part. Conversely, fracture can occur at room temperature or above if such flaws exist. The importance of environmental-stress interactions on the creation and growth of craze-crack type flaws is emphasized since such extremely sharp flaws are particularly critical. Means of inhibiting these phenomena are discussed. It is demonstrated that the uncontaminated polycarbonate surface is not subject to stress-cracking phenomena in air and thermal environments even under stresses up to the tensile yield strength of the material. Techniques which have been found effective in eliminating and preventing undesirable contamination and stress concentrators are discussed.

BIBLIOGRAPHY

(1) Caird, D. W. "Maximizing LEXAN® Performance" Principles of Thermoforming. Chapter Gordon & Breach (1973).

(2) Andrews, E.H. "Fracture in Polymers" pp 48-54 American Elsevier (1968)

(3) LeGrand, D.G. "Crazing, Yielding & Fracture of Polymers. I. Ductile-Brittle Transition in Polycarbonate". J. Appl. Polymer Sci. 13, 21-29 (1969).

(4) Kambour, R.P. "Role of Crazing in the Mechanism of Fracture of Glassy Polymers" A.C.S. Div. of Coatings & Plastics Applied Polymer Symposia #7, 215, (1968).

SESSION 4

MATERIALS CHARACTERIZATION (PART II)

ENVIRONMENTAL RESISTANCE OF COATED AND LAMINATED POLYCARBONATE TRANSPARENCIES

G. E. Wintermute and R. A. Huyett
Goodyear Aerospace Corporation
Litchfied Park, Arizona

and

S. A. Marolo
Air Force Materials Laboratory
Wright-Patterson Air Force Base, Ohio

BLANK NOT FILMED

ENVIRONMENTAL RESISTANCE OF COATED AND LAMINATED POLYCARBONATE TRANSPARENCIES

by

Glenn E. Wintermute, Goodyear Aerospace Corporation

Richard A. Huyett, Goodyear Aerospace Corporation

Samuel A. Marolo, Air Force Materials Laboratory,
Wright-Patterson AFB, Ohio

ABSTRACT

This paper describes a program conducted to determine and define the environmental resistance characteristics of selected coated and acrylic laminated polycarbonate aircraft windshield materials when exposed to aggressive environments.

All current abrasion-resistant coatings being used or recommended for Air Force high-performance aircraft were evaluated in this program. The coatings were applied to aircraft grade polycarbonate.

The test laminates consisted of an acrylic face sheet bonded to aircraft-grade polycarbonate. Bond layers evaluated included all proprietary and commercially obtainable interlayer materials approved for aircraft transparencies: silicones; polyurethanes; polyvinyl butyral; and ethylene terpolymer.

An initial screening test program was conducted using accelerated aging tests to obtain comparative data for further comprehensive testing of candidate materials. Aging tests utilized the facilities of the Desert Sunshine Exposure Test Laboratory (DSET), (EMMA). Other tests being employed included humidity testing, ultraviolet radiation exposure testing, and Weather-Ometer exposure tests.

Candidates selected from the screening test program were subjected to long-term outdoor exposure in Arizona and Florida. Exposure periods were 3, 6, and 9 months.

A complete test series was performed on the coated and laminated specimens to evaluate physical and mechanical properties.

Degradation of the test specimens caused by the various environments was determined by comparing the physical properties before and after exposure.

A comparative environmental performance data base has resulted which defines the relative merits of coatings and interlayers for use in polycarbonate aircraft windshields.

The work was performed by Goodyear Aerospace Corporation for the Air Force Materials Laboratory, Wright-Patterson AFB, Ohio, on Contract F33615-74-C-5005.

I. INTRODUCTION

1. GENERAL

a. Scope

The performance requirements for the newer military aircraft severely test the performance capabilities of the standard glazing materials such as as-cast acrylic, stretched acrylic, and glass. Glazing materials for advanced high-performance aircraft—F-111, A-10, F-15, B-1—must withstand bird impacts at high velocities and will be subjected to thermal abuse in the 270- to 350-degree Fahrenheit range.

One new plastic material—polycarbonate—was introduced several years ago with a high potential for successful use in high-performance aircraft transparencies. Polycarbonate possesses a unique combination of properties: temperature resistance, toughness, impact resistance, and clarity.

A program sponsored by the United States Air Force Materials Laboratory, Wright-Patterson Air Force Base, Ohio, provided an in-depth evaluation of polycarbonate materials and developed usable design criteria on aircraft quality polycarbonate. The results of the study were reported in Technical Report AFML-TR-72-117, "Design Criteria - Transparent Polycarbonate Plastic Sheet," issued August 1972.

This report confirmed the opinion that polycarbonate does possess unique properties which make it the most promising material currently available for high-performance aircraft transparencies.

b. Polycarbonate Properties

Some of the important properties of polycarbonate were shown by the design criteria study to be:

1. Temperature resistance - Deflection temperatures at 264 psi were 265 to 290 deg F. Thermal aging for six months at +160 deg produced no loss in tensile strength

2. Toughness - Polycarbonate materials have much better toughness properties than any other rigid transparent plastic aircraft material thus far developed

3. Impact resistance - Monolithic polycarbonate can sustain impact energy four to six times that of stretched acrylic. The birdproofing capability of the material is readily apparent. Also, no cracking occurred when 1/4-inch polycarbonate was subjected to the high-velocity impact and penetration of caliber .30 ball ammunition

4. Light transmission and haze - Light transmission was above 80 percent and haze measurements were below 2.0 percent for monolithic polycarbonate materials.

c. Polycarbonate Deficiencies

As shown, the contractual study on transparent polycarbonate plastic sheet did prove polycarbonate to be a sound engineering material capable of being used as transparencies for the new generation of high-performance military aircraft.

At the same time, however, the study also emphasized and documented the deficiencies of polycarbonate that are definite problem areas for aircraft glazing applications. These deficiencies are:

1. Optics - Polycarbonate requires a secondary operation to achieve aircraft quality optical properties

2. Abrasion and solvent resistance - Polycarbonate sheet has poor scratch, mar, and abrasion resistance and is softened or crazed by some fluids commonly found around aircraft

3. Ultraviolet degradation - Polycarbonate sheets exposed on outdoor weathering racks in Arizona have exhibited surface degradation within a six-month period. This surface degradation has a detrimental effect on impact strength.

d. Field Experience

The serious aspect of these deficiencies was discovered in the T-37 program, which was the first large-scale Air Force use of polycarbonate windshields. The abrasion resistance of polycarbonate was sufficiently low that ice crystals associated with some cloud formations abraded the windshield.

Abrasion-resistant surface coatings were applied to protect the polycarbonate. However, exposure to ultraviolet radiation and to high humidity conditions attacked the polycarbonate at the interface and weakened the bond between the coating and the polycarbonate substrate. The loss of adhesion caused the coatings to blister and peel.

An accelerated test program on the T-37 windshield showed that the abrasion coatings available at that time would not retain adhesion when subjected to aggressive environments. It was further shown that polycarbonate windshields which had been exposed to weathering had suffered a severe decrease in bird impact resistance.

e. Analysis

It became readily apparent that to retain its desirable properties, polycarbonate required protection against environments which were abrasive, which caused crazing, or which produced ultraviolet radiation.

It was also apparent from a practical point of view that the protective system itself had to be durable, and, further, that the techniques and materials used in applying the protective film could not initiate attack on the polycarbonate substrate.

The requirements are essentially twofold:

1. Determine systems that protect polycarbonate against aggressive environments without sacrificing desirable properties of optics, toughness, heat resistance, and impact strength. The glazing must be functional

2. The durability of the protective system and the properties of polycarbonate must remain essentially unchanged when exposed to aggressive environments for extended periods of time. The service life of the glazing must be acceptable.

The most obvious answer to the problem is to laminate a thin acrylic sheet to the surface of the polycarbonate. The acrylic is an effective ultraviolet radiation screen and possesses acceptable abrasion- and solvent-resistant properties.

Also, despite their earlier failures, abrasion-resistant surface coatings remained a potential solution to the protective problem. New improved coatings which possess abrasion and moisture resistance and incorporate ultraviolet screening agents had been developed and were available for evaluation.

However, regardless of which protective system is used—acrylic laminate or solution coating—the criteria of "functional and durable" had to be met. A data base on the environmental resistance of interlayer bonded acrylic/polycarbonate laminates and coated polycarbonate was lacking.

2. PROGRAM SCOPE AND OBJECTIVES

The purpose of this program was to conduct a comprehensive evaluation of the environmental resistance characteristics of the best available interlayer bonded laminates and coatings for the protection of polycarbonate. The nine interlayers evaluated included ethylene terpolymer, silicone, polyurethane, and polyvinyl butyral materials. A total of 21 protective coatings were tested.

The data obtained defines the comparative performance of the various laminates and coatings when subjected to a number of natural and accelerated environmental exposures. The data also disclosed any degradation of the structural or optical properties of the polycarbonate attributable to the interlayer or coatings.

II. TECHNICAL APPROACH, INTERLAYFR ENVIRONMENTAL RESISTANCE PROPERTIES TEST DATA

1. GENERAL

The test data were accumulated by subjecting the candidate interlayers to a comprehensive screening test series. Each interlayer was evaluated in laminated form, joining 0.10-inch-thick Plexiglas[a] II acrylic and 0.25-inch-thick SL2000-111 grade Lexan[b] polycarbonate substrates. Some of the materials evaluated in this program are proprietary. Many of the test laminates were prepared by the manufacturers of these proprietary materials for use in this program. The remainder of the interlayers were processed into laminate form by Goodyear Aerospace personnel. Control testing was utilized to establish the properties of the as-fabricated laminates. The control data provided the comparative base by which the effect of the various environmental exposures was judged.

A summary of the environmental test exposure and physical property testing conducted after each type of exposure is presented in Table 1.

2. CONTROL TESTS

The control tests conducted on all interlayer bonded laminates are shown in Table 2. Data obtained from the control testing are presented later in the text in Table 5.

---

[a]TM, Rohm & Haas, Philadelphia, Pa.

[b]TM, General Electric Co., Pittsfield, Mass.

TABLE 1. LAMINATE ENVIRONMENTAL TEST SCHEDULE

Environmental test exposure	Physical property testing after exposure
Weather-Ometer	D, E, G, H, I
Humidity	A, D, E, G, H, I
Thermal cycle	A, D, E, G, H, I
Ultraviolet radiation	D, E, G, H, I
Outdoor weathering, accelerated, EMMA	A, D, E, G, H, I
Outdoor weathering, natural, 45-deg south	
Arizona	A, B, C, D, F, G, H, I
Florida	A, B, C, D, F, G, H, I

Physical property test code:

A - falling plummet

B - low-temperature fracture

C - thermal shock

D - shear

E - shear modulus

F - flatwise tensile

G - light transmission

H - haze

I - visual examination

TABLE 2. LAMINATE CONTROL TESTS

Type of test	Test method
Light transmission	ASTM D1003-61 (1970)
Haze	ASTM D1003-61 (1970)
Falling plummet	GACA CLA-12798A
Falling ball	MIL-P-25374A
Low-temperature fracture	MIL-P-25374A
Thermal shock	MIL-P-25374A
Shear strength	FTMS No. 406, Method 1042
Shear modulus	FTMS No. 406, Method 1042
Flexural strength	FTMS No. 406, Method 1031
Flatwise tensile	MIL-STD-401B
High-temperature stability	MIL-P-25374A

III. TECHNICAL APPROACH, COATING ENVIRONMENTAL RESISTANCE PROPERTIES TEST DATA

1. GENERAL

The test data were obtained by conducting a comprehensive series of screening tests on candidate protective coatings applied to polycarbonate material. All coatings were applied to 0.25-inch-thick material. All polycarbonate used was General Electric Lexan SL2000-111N grade material with the exception of several coating manufacturer supplied test sheets. Some of the coatings evaluated in this program are proprietary. Many of the coated test sheets were prepared by the manufacturers of these proprietary coatings. The remainder of the coatings were processed and applied to the polycarbonate sheets by Goodyear Aerospace personnel. Control testing was utilized to establish the original properties of the coatings and to provide a comparative base by which the effect of the various environmental exposures could be judged.

In addition to the effect of environmental exposures, it was necessary to determine the effect of the various coatings on the polycarbonate physical properties. Therefore, uncoated polycarbonate material was also subjected to the control testing.

A summary of the environmental test exposures and physical property testing conducted after each type of exposure is presented in Table 3.

2. CONTROL TESTS

The control tests conducted on the coated polycarbonate candidates as well as the uncoated polycarbonate reference material are shown in Table 4. Data obtained from the control testing are presented in Table 6.

TABLE 3. COATING ENVIRONMENTAL TEST SCHEDULE

Environmental test exposure	Physical property testing after exposure
Weather-Ometer	H, I, J, K
Humidity	A, B. C, H, I, J, K
Thermal cycle	A, B, C, H, I, J, K
Ultraviolet radiation	H, I, J, K
Outdoor weathering, accelerated, EMMA	A, B, C, H, I, J, K
Outdoor weathering, natural, 45-deg south	
Arizona	A, B, C, D, G, H, I, J, K
Florida	A, B, C, D, G, H, I, J, K

Physical property code:

A - falling plummet

B - abrasion

C - solvent resistance

D - low-temperature fracture

E - tensile

F - flexure

G - bearing

H - light transmission

I - haze

J - visual examination

K - adhesion

TABLE 4. COATING CONTROL TESTS

Type of test	Test method
Light transmission	ASTM D1003-61 (1970)
Haze	ASTM D1003-61 (1970)
Falling plummet	GACA CLA-12798
Adhesion	GACA CLA-1735
Abrasion resistance	GACA CLA-2340
Abrasion resistance	PPG salt blast procedure
Solvent resistance	S.A.E. AMS 3614 (proposed)
Low-temperature fracture	MIL-P-25374A
Tensile strength	FTMS No. 406, Method 1011
Flexural strength	FTMS No. 406, Method 1031
Bearing strength	FTMS No. 406, Method 1051

IV. TEST RESULTS AND ANALYSIS PROCEDURES

1. GENERAL

The quantity of interlayers and coatings evaluated and the many environmental exposure modes yielded a significant quantity of test data. This paper describes the analysis procedure and criteria used and limits the actual data presented to that obtained during control testing and after natural outdoor weathering exposure. The data are included in toto in the contract final technical report.

The analysis of the data generated in this program represented one of the most important aspects of the work effort. Particular care was required during the review of the data to extract the most meaningful findings with regard to the validity of the test methods as well as the relative performance of the candidate interlayers and coatings.

During the course of the data analysis effort, judgments were made with regard to the following considerations:

1. The extent which each interlayer or coating degraded or otherwise altered the structural and optical properties of the transparency materials

2. Which environmental test procedures were the most discriminating for determining interlayer and coating performance

3. What levels of performance as measured by these test procedures were required to perform adequately in the service environment

4. What was the relative comparative performance of the various candidate interlayers and coatings tested in this program.

2. DATA ANALYSIS PROCEDURE

Individual data sheets were used during the testing phase to record all test parameters and results for each interlayer or coating material. These data sheets were reviewed and the results transferred to tables for inclusion in monthly progress reports. These tables were updated as the work progressed and were finalized upon completion of the test phase.

As a part of the analysis effort, graphs were prepared summarizing performance levels. Typical graphs depicting performance of the interlayers and coatings following outdoor weathering exposure are shown in Figures 1 and 2.

3. TEST RESULTS

a. Control Tests

The results of the control tests measuring the as-received performance of the interlayers and coatings are shown in Tables 5 and 6.

b. Environmental Tests

The performance of the interlayers and coatings tested following 9 months of 45-deg south outdoor weathering in Florida and Arizona is shown in Tables 7 and 8. Graphical presentation of the effect of this outdoor weathering on the interlayers and coatings is shown in Figures 1 and 2.

V. SUMMARY

1. GENERAL

The program has provided a comparative environmental performance data base which defines the relative merits of interlayers and coatings for use in polycarbonate aircraft windshields and related applications. This data base provides information to aid the transparency designer in several ways. Selection of the most suitable protective concept, whether acrylic laminated or coated, and specific material selections can be made for specific polycarbonate aircraft windshield designs.

The program also identified deficiencies in certain aspects of even the best interlayers and coatings evaluated. The data are therefore also valuable in directing research and development efforts to correct these deficiencies and improve the state of the art.

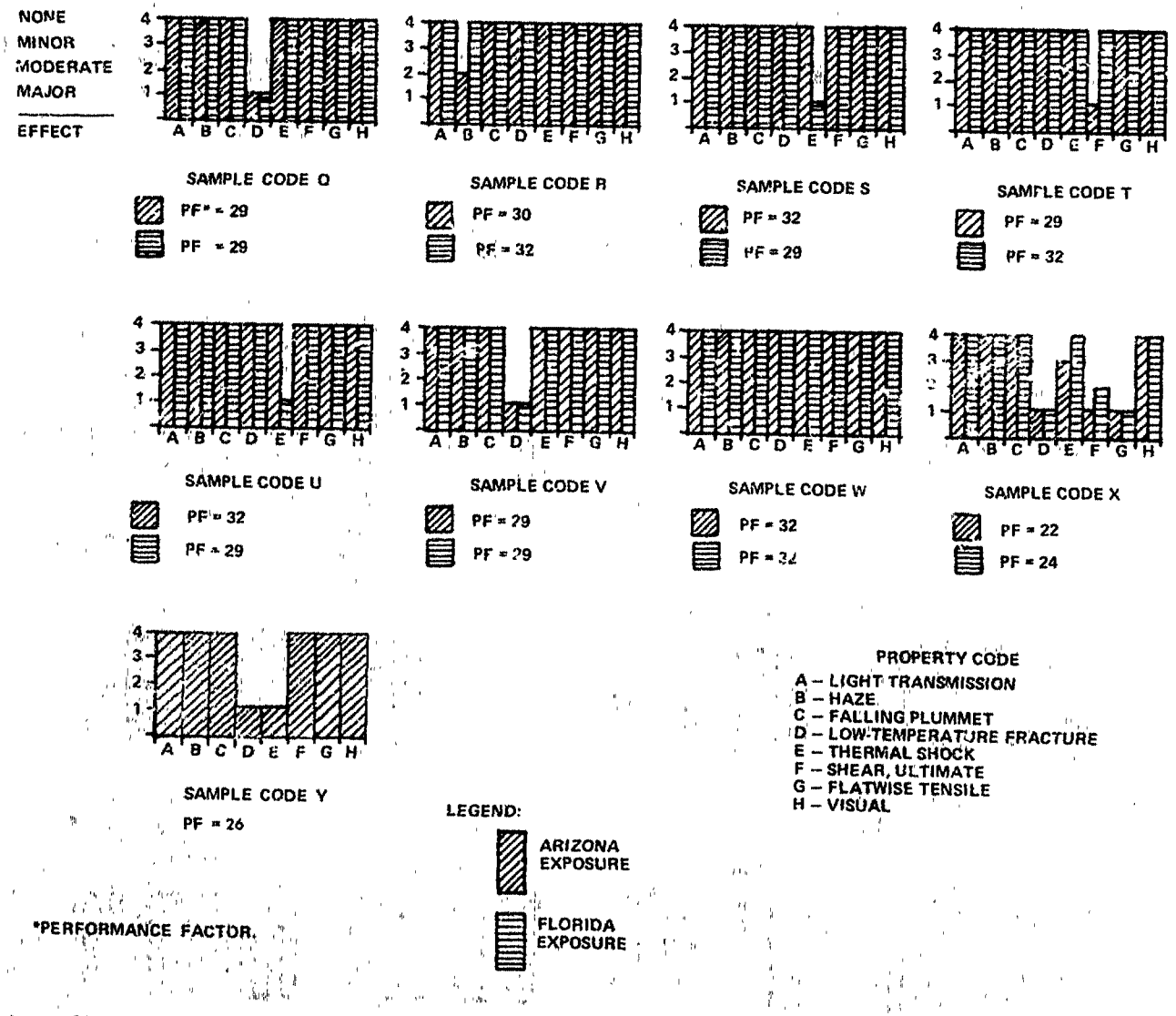


Figure 1. Effect of Outdoor Weathering on Laminated Polycarbonate; 45-Deg South, Nine-Month Exposure

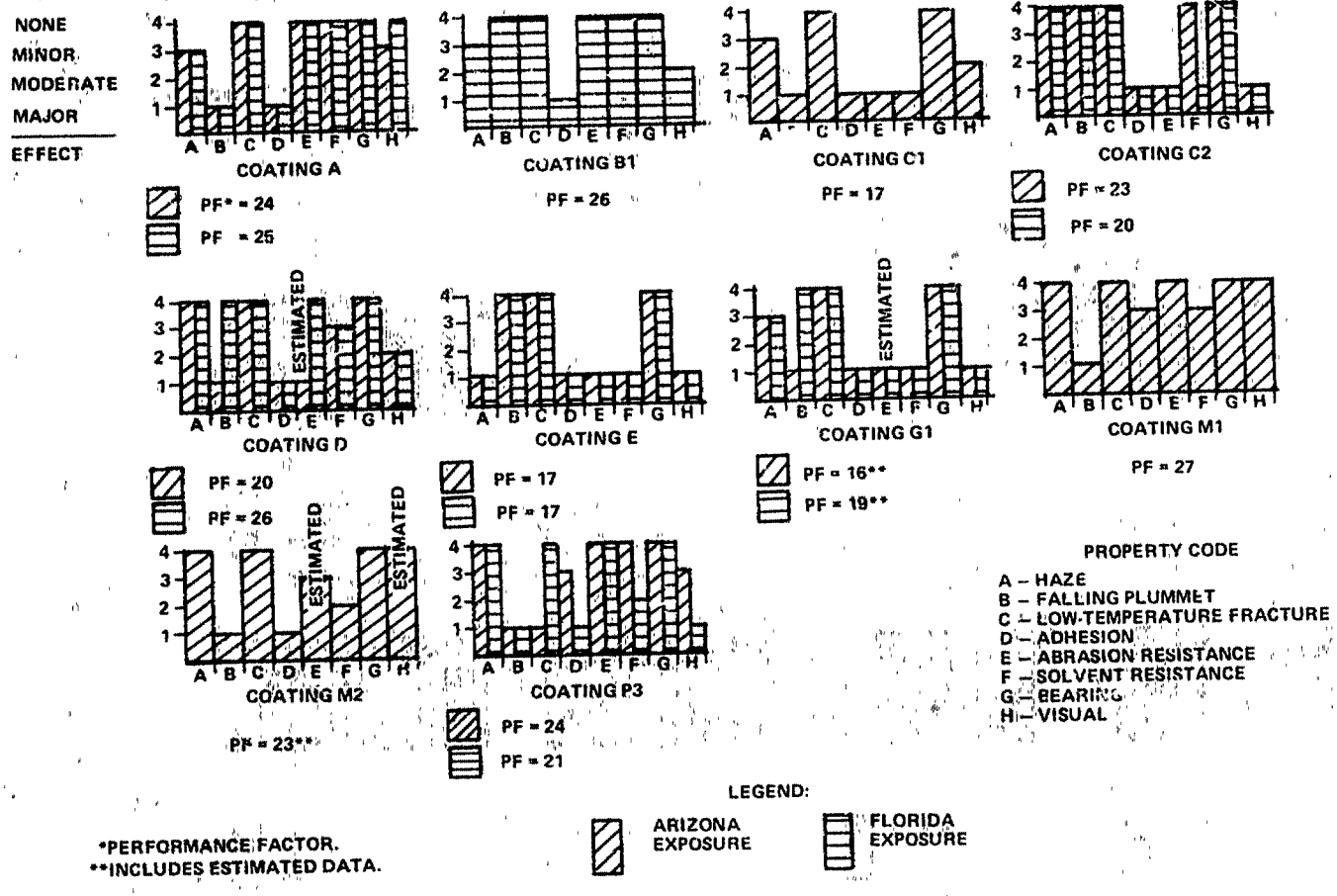


Figure 2. Effect of Outdoor Weathering on Coatings; 45-Deg South, Nine-Month Exposure

TABLE 5. CONTROL TEST DATA, LAMINATED POLYCARBONATE

Sample code	Light transmission (percent)	Haze (percent)	Falling plummet (feet)	Falling ball	Low temperature fracture	Thermal shock	Shear - ultimate (PSI) Test temperature (degrees F)			Shear - modulus (PSI)	Flexure (PSI)	Flatwise tensile (PSI)	High temperature stability
							-65	75	160				
Q	88.5	2.1	16	Pass	Pass	Pass	280	153	97	68	5,200	248	Pass
R	87.9	2.9	16	Pass	Fail	Pass	382	54	81	23	5,590	74	Pass
S	89.0	1.0	18	Pass	Fail	Pass	490	228	26	144	8,800	793	Pass
T	87.6	1.1	20	Pass	Pass	Pass	1,248	1,740	440	634	13,580	1,751	Pass
U	89.5	2.5	18	Pass	Pass	Pass	549	325	102	267	8,870	709	Pass
V	89.2	4.7	14	Pass	Pass	Pass	66	5	18	20	5,420	149	Pass
W	87.5	3.0	14	Pass	Fail	Bubbled	56	317	9	112	12,500	730	Bubbled
X	85.9	1.2	16	Pass	Pass	Bubbled	250	286	25	298	12,246	922	Bubbled
Y	87.6	3.9	16	No test	Pass	Pass	328	236	130	51	6,580	235	Pass

TABLE 6. CONTROL TEST DATA - COATED POLYCARBONATE

Sample code	Light transmission (percent)	Haze (percent)	Falling plummet (feet)	Adhesion (percent) scribed	GACA abrasion (cycles vs. haze percent)	PPG salt blast abrasion (haze percent, 50 cycles)	Solvent resistance*	Low temperature fracture	Tensile ultimate (PSI)	Flexure ultimate (PSI)	Bearing 4-percent deformation (PSI)
A	88.2	1.1	16	100	500-19.0	3.8	Pass	Pass	10,085	17,500	9,485
B1	88.7	1.4	18	100	500- 7.3	8.9	Failed steps 1 and 4	Fail	9,870	17,100	9,120
B2	89.8	0.8	18	100	1,000- 2.0	-	Pass	Pass	10,175	17,730	8,960
B3	88.6	1.0	18	100	500-19.0	-	Failed steps 1 and 4	Pass	9,860	17,250	7,520
C1	91.3	0.5	22	100	1,000- 2.5	-	Pass	Pass	10,023	16,415	8,640
C2	91.0	0.5	20	100	1,000- 3.8	15.4	Pass	Pass	10,000	15,350	8,000
D	88.4	1.3	18	100	500-24.5	20.5	Pass	Pass	10,360	17,960	6,400
E	86.0	1.3	18	100	500-20.7	6.5	Failed steps 1 and 4	Pass	9,630	15,630	10,075
F	88.3	0.6	18	100	500-17.7	23.6	Pass	Pass	9,710	16,540	7,590
G1	91.6	0.6	18	100	1,000- 2.5	15.3	Failed steps 2, 3, and 4	Pass	9,760	17,580	7,680
G2	91.2	0.6	14	100	1,000- 6.8	-	Pass	Fail	9,720	16,040	6,810
H1	89.3	0.6	20	100	500-15.3	5.2	Failed step 1	Fail	9,825	17,760	8,475
H2	89.2	0.6	18	100	500-19.4	-	Failed step 4	Fail	9,950	15,400	8,165
I	85.4	3.0	16	100	1,000- 5.2	0.4	Failed steps 1, 3, and 4	Pass	9,560	15,310	9,520
K	88.7	1.4	20	100	500-16.7	-	Failed step 1	Pass	9,690	16,250	7,682
M1	89.8	1.9	20	100	-	-	-	-	-	-	-
M2	87.9	0.9	16	100	1,000- 2.5	-	Pass	Pass	10,200	16,995	8,000
N	89.5	1.7	20	100	500-73.6	-	Failed steps 2, 3, and 4	Pass	9,900	15,900	6,718
P1	83.6	0.6	14	100	500-32.6	-	Pass	Pass	10,022	16,590	6,560
P2	83.7	0.6	18	100	500-30.0	-	Failed step 4	Pass	9,870	16,220	6,480

*Solvent resistance exposure code:

Step 1. Methyl ethyl ketone; 30 minutes; unstressed.

Step 2. Thirty minutes, dry; 2,000 PSI outer fiber stress following methyl ethyl ketone application of step 1.

Step 3. Ninety percent aliphatic naphtha/10 percent methyl ethyl ketone; 30 minutes; 2,000 PSI outer fiber stress.

Step 4. Ninety-five percent glacial acetic acid/5 percent water; 30 minutes; 2,000 PSI outer fiber stress.

TABLE 6. CONTROL TEST DATA - COATED POLYCARBONATE (CONT)

Sample code	Light transmission (percent)	Haze (percent)	Falling plummet (feet)	Adhesion (percent) scribed	GACA abrasion (cycles vs. haze percent)	PPG salt blast abrasion (haze percent, 50 cycles)	Solvent resistance*	Low temperature fracture	Tensile ultimate (PSI)	Flexure ultimate (PSI)	Bearing 4-percent deformation (PSI)
P3	81.3	1.3	20	100	500-37.9	2.1	Pass	Pass	9,600	15,680	5,850
Uncoated control	88.4	0.7	18	-	10 cycles/ 25 percent	2 cycles/ 40 percent	Failed steps 1, 3, and 4	Pass	10,143	16,555	9,921

*Solvent resistance exposure code:

Step 1. Methyl ethyl ketone; 30 minutes; unstressed

Step 2. Thirty minutes; dry; 2,000 PSI outer fiber stress following methyl ethyl ketone application of step 1.

Step 3. Ninety percent aliphatic naphtha/10 percent methyl ethyl ketone; 30 minutes; 2,000 PSI outer fiber stress.

Step 4. Ninety-five percent glacial acetic acid/5 percent water; 30 minutes; 2,000 PSI outer fiber stress.

TABLE 7. OUTDOOR WEATHERING TEST DATA, LAMINATED POLYCARBONATE, NINE-MONTH EXPOSURE PERIOD

Sample code	Light transmission (percent)	Haze (percent)	Falling plummet (feet)	Low temperature fracture	Thermal shock	Shear - ultimate (PSI)	Flatwise tensile (PSI)	Visual
Q D9*	88.2	2.8	16	Fail	Pass	217	241	Sleek
Q C9*	88.9	3.5	16	Fail	Pass	186	319	Scratches, gouges
R D9	86.2	8.0	14	Fail	Pass	306	280	Slight edge delamination
R C9	88.9	3.5	14	Fail	Pass	197	234	Scratches, gouges
S D9	89.1	1.9	18	Pass	Pass	243	775	Hairlines
S C9	88.9	2.9	16	Pass	Pass	243	619	Scratches, gouges
T D9	88.6	3.0	20	Pass	Pass	468	2,273	Sleek
T C9	89.1	2.2	18	Pass	Pass	2,260	1,669	Scratches, gouges
U D9	89.2	1.0	18	Pass	Pass	373	794	Hairlines - minor scratches
U C9	89.2	3.5	16	Pass	Fail - bubbled	389	638	Scratches, gouges
V D9	89.6	4.8	16	Fail	Pass	56	224	Hairlines
V C9	90.0	8.8	14	Fail	Pass	42	118	Scratches, gouges, pits opposite exposed side
W D9	87.9	3.5	16	Pass	Fail - bubbled	399	839	Sleek
W C9	88.5	3.9	16	Pass	Fail - bubbled	319	713	Scratches, gouges, pits opposite exposed side
X D9	82.3	2.6	14	Fail	Fail - fogging and bubbled	99	392	Minor scratches
X C9	81.8	4.3	16	Fail	Fail - bubbled	199	280	Scratches, gouges, pits opposite exposed side
Y D9	88.8	4.0	16	Fail	Fail - edge delamination	315	266	Hairlines

*Weathering site code:
C9 is Florida exposure; 45 degrees south; nine-month period.
D9 is Arizona exposure; 45 degrees sourth; nine-month period.

TABLE 8. OUTDOOR WEATHERING TEST DATA, COATED POLYCARBONATE, NINE-MONTH EXPOSURE PERIOD

Sample code	Light transmission (percent)	Haze (percent)	Falling plummet (feet)	Adhesion (percent) scribed	Abrasion cycles vs. haze percent	Solvent resistance*	Low temperature fracture	Bearing ultimate (PSI)	Visual
A D9**	87.5	4.9	10 Shattered	10	500-17.6	Pass	Pass	6,795	Minute coating blisters; overall appearance good.
A C9**	88.3	3.5	10 Shattered	0	500-13.4	Pass	Pass	7,040	Coating appearance good; polycarbonate back surface opaque.
B1 C9	89.2	3.0	20	0	1,000-5.2	Failed steps 1 and 4	Pass	8,480	Coating spotty; polycarbonate back surface pitted.
C1 D9	90.8	2.6	18 Shattered	0	No test	Failed steps 1, 3, and 4	Pass	7,520	Exposure side coating removed by protective paper.
C2 D9	91.2	1.0	20	0	No test	Pass	Pass	6,640	Coating on both sides removed by protective paper; polycarbonate appearance good.
C2 C9	91.7	0.8	20	0	No test	Failed steps 1, 3, and 4	Pass	7,120	Coating on both sides removed by protective paper; polycarbonate appears pitted.
D D9	88.4	2.5	16 Shattered	0	No test	Failed step 4 only	Pass	9,600	Coating had minute blisters or pits; coating was removed by protective paper.
D C9	89.0	1.5	18 Shattered	0	500-16.2	Failed step 4 only	Pass	6,560	Coating has small blisters.
E D9	88.6	7.7	16	0	No test	No test	Pass	7,600	Coating gone; polycarbonate hazy, blotchy; minute blisters.

*Solvent resistance exposure code:

Step 1. Methyl ethyl ketone; 30 minutes; unstressed.

Step 2. Thirty minutes; dry; 2,000 PSI outer fiber stress following methyl ethyl ketone application of step 1.

Step 3. Ninety percent aliphatic naphtha/10 percent methyl ethyl ketone; 30 minutes; 2,000 PSI outer fiber stress.

Step 4. Ninety-five percent glacial acetic acid/5 percent water; 30 minutes; 2,000 PSI outer fiber stress.

**Weathering site code:

C9 is Florida exposure; 45 degrees south; nine-month period.

D9 is Arizona exposure; 45 degrees south; nine-month period.

TABLE 8. OUTDOOR WEATHERING TEST DATA, COATED POLYCARBONATE, NINE-MONTH EXPOSURE PERIOD (CONT)

Sample code	Light transmission (percent)	Haze (percent)	Falling plummet (feet)	Adhesion (percent) scribed	Abrasion cycles vs. haze percent	Solvent resistance*	Low temperature fracture	Bearing ultimate (PSI)	Visual
E C9	87.9	14.4	18	0	No test	No test	Pass	6,880	Coating gone; polycarbonate hazy, blotchy; minute blisters. Coating flaking off.
G1 D9	90.3	2.3	16 Shattered	0	No test	No test	No test	No test	Coating flaking off.
G1 C9	89.0	2.0	18	0	No test	No test	Pass	6,640	Coating crazed on both sides; exposure side coating removed by protective paper.
M1 D9	89.9	2.4	18 Shattered	80	1,000-3.8	Failed step 4 only	Pass	6,320	Coating intact; good appearance.
M2 D9	88.0	1.5	12 Shattered	0	No test	Failed steps 3 and 4	Pass	6,000	Coating removed by protective paper.
P3 D9	82.3	1.8	10 Shattered	80	500-16.4	Pass	Failed	6,480	Minute blisters; overall appearance good.
P3 C9	82.0	1.8	10 Shattered	20	500-35.1	Failed steps 3 and 4	Pass	5,920	Coating severely blistered; small speckled spots.

*Solvent resistance exposure code:

Step 1. Methyl ethyl ketone; 30 minutes; unstressed.
Step 2. Thirty minutes; dry; 2,000 PSI outer fiber stress following methyl ethyl ketone application of step 1.
Step 3. Ninety percent aliphatic naphtha/10 percent methyl ethy. ketone; 30 minutes; 2,000 PSI outer fiber stress.
Step 4. Ninety-five percent glacial acetic acid/5 percent water; 30 minutes; 2,000 PSI outer fiber stress.

2. CONCLUSIONS

a. Interlayers

Many of the interlayers evaluated exhibited physical properties and environmental stamina which appear suited for military aircraft windshield usage.

Many of the interlayers tested have physical properties which limit their suitability for high-performance aircraft windshield applications. The test data obtained at elevated temperatures defines some of the deficiencies of the materials for such usage. A few noteworthy examples of serious elevated temperature-induced degradation are as follows.

Interlayer Code X bubbled during the 200 deg F thermal cycle exposure. Both interlayer Codes W and X bubbled during 275 deg F high-temperature stability testing.

The thermal strain accommodation factor calculated from data obtained at 160 deg F was rated poor for all of the interlayers except Codes T and Y which rated fair and good, respectively.

The ultimate shear strength of all of the interlayers was decreased significantly at 160 deg F except for Codes R and V which showed an improvement.

Most of the interlayers tested developed a milky appearance (opacity) during the elevated temperature, high relative humidity exposure. This appearance ranged from edges or corners only in interlayer Codes S, T, U, and W to a more uniform overall opacity in Codes Q, R, V, and Y. These data were obtained on laminates having exposed interlayer edges. Effective protective sealants or other means of isolating the edge of the interlayer from the environment could improve this problem. Moisture permeation through the hygroscopic polycarbonate material may be sufficient to develop opacity in interlayer Codes Q, R, V, or Y laminates having sealed edges. No testing was accomplished on this program which could resolve this question.

It must be remembered that the majority of the interlayers tested are proprietary products of various companies. Most such products are available only as a component of a complete windshield assembly.

b. Coatings

None of the coatings evaluated in this program appear to have sufficient environmental stamina to provide effective protection on polycarbonate aircraft windshield exterior surfaces.

Most of the coatings evaluated would be capable of adding significant protection to the interior surface of a polycarbonate aircraft windshield.

One of the most prevalent deficiencies noted was a loss of adhesion which was caused by high relative humidity, ultraviolet radiation, and outdoor weathering exposures.

Many of the coatings exhibited a loss of physical integrity after high relative humidity and outdoor weathering exposures. This was manifested by various degrees of flaking, blistering, crinkling, and cracking.

The abrasion resistance of the best coatings evaluated provides a significant level of protection for routine cleaning and particle impingement actions.

None of the coatings evaluated were effective in protecting against scratching or marring resulting from contact with sharp objects.

Variability in processing or material composition may significantly alter the environmental performance of a coating. One coating in the program was processed in two distinctly different manufacturing runs in separate facilities. A considerable difference was evident in the physical properties of the coatings from these two runs after environmental exposure. The coatings coded M1 and M2 were identical in composition and processing except for the cure schedule used. Significant differences in physical properties are also observed for these coatings after environmental exposure.

STABILITY OF TRANSPARENT MATERIALS UNDER WORLDWIDE CLIMATIC CONDITIONS

J. M. Kolyer
Rockwell International Corp.
Autonetics Group
Anaheim, California

STABILITY OF TRANSPARENT MATERIALS UNDER WORLDWIDE CLIMATIC CONDITIONS

J. M. Kolyer

Rockwell International Corp.

ABSTRACT

World climates are reviewed in terms of temperature and rainfall. For convenience, these may be classified as arctic (cold), temperate (mild), desert (hot/dry), and tropical (hot/wet). The general effects of these climates on plastics are discussed. Results often are unpredictable, because regional weather data are poorly correlated with the highly-variable "microclimate" prevailing at a material's surface. This involves moisture condensation and hot spots, for example. Microclimatic factors, weathering mechanisms, and failure modes are reviewed. Material failures are arbitrarily defined by the application, and they can vary from impaired light transmission to drastic embrittlement.

Recent years have seen great improvements in both continuous-exposure and intensified-exposure accelerated weathering tests. In the future, improved methods for detecting early signs of degradation coupled with a better understanding of weathering mechanisms should allow useful long-range predictions of outdoor lifetimes by a statistical approach. Work already done along these lines is mentioned, and literature is cited.

Published weathering data are reviewed for several transparent plastics. FEP (fluorinated ethylene propylene) is transparent enough in thin sections for solar cell encapsulation and has superb weather-resistance. Poly (vinyl fluoride) and other fluoropolymers are excellent, as is poly (methyl methacrylate). When stabilized, polycarbonate, cellulose acetate butyrate, and Mylar have good resistance, while transparent polystyrene and styrene-acrylonitrile copolymer are poor. Polysulfone is poor without stabilization but may be greatly improved in the future with ultraviolet absorbers. In fact, reported outdoor lifetimes must be considered lower limits because there is always the possibility of development of purer, inherently more stable polymers as well as improved stabilizers.

I. INTRODUCTION

The weathering of coatings such as paints has been studied for many decades, but weathering tests on plastics have been reported extensively only since World War II. Perhaps the most-investigated are reinforced compositions and polyolefins, neither of which are transparent. This review paper summarizes data on several transparent materials against a background of world regional climates and the erratic "microclimate" peculiar to any precise location. Weathering mechanisms and accelerated tests are reviewed briefly, with a suggestion of future analytical/predictive methods.

II. WORLD CLIMATES

Temperature and rainfall data (as smoothed bar graphs of mean monthly values) are shown for various weather stations in Figure 1 (reference 1). Besides the obvious temperature trends, it is seen that rainfall may continue all year at a low level (e.g., Astrakan) or at a high level (e.g., Singapore), or it may be concentrated in a rainy season (e.g., Timbo). Worldwide conditions are generally simulated within the continental United States (Figure 2, reference 2). For example, note the temperature and rainfall extremes observed (reference 3). Florida has been called "marine, subtropical" and Arizona a "semidesert" (reference 4). Annual insolation (solar energy received at the earth's surface) is less affected by latitude than one might expect, but generally decreases from the equator to the poles (Figure 3, reference 5 and U. S. Weather Bureau reports). For example, on a June day, insolation in langleys (gram-cal/cm^2) was 550 in Alaska and 600 in Miami, Florida (reference 6). Five-year insolation averages are provided by the U. S. Weather Bureau. In general, world climates may be classified for convenience as arctic (cold), temperate (mild), desert (hot/dry), and tropical (hot/wet). However, the usefulness of this simplification is quite limited as will be seen.

III. CLIMATIC VARIATIONS

1. With Season

Among the factors involved in plastics degradation, the most important is the ultraviolet (UV) component of sunlight with wavelength below 400 nanometers (reference 7). This varies from 2.8% of the total solar energy in January to 5.0% in August for Phoenix, Arizona (an important test site) (reference 8). Radiation between 290 and 315 nm. varies even more — by a factor of 3 (reference 5). Similarly, it was found in Stamford, Conn., that UV at 350 nm. was 3 times as intense in September as in January (reference 9). Total solar radiation, which includes about 53% infrared, is less variable (reference 5). Samples exposed south at a 45° angle, the usual test condition, received 12,000 langleys in December compared with 15,600 in April in Miami; respective values for Phoenix are 15,000 and 18,000 langleys (reference 10). There are indications that the ratio of UV

under 400 nm. to total sunlight may be about the same throughout the U.S. on any given day (reference 11). Haze can reduce the UV below 400 nm. by a factor of 5 (reference 9).

Rain can be highly seasonally dependent as we have seen.

Air temperature variations with season are well documented, but the temperature of the exposed material determines degradation rates. A formula for this "sol-air temperature" or S.A.T. (reference 7) is:

$$\text{S.A.T.} = \text{temp. of air} + \frac{(\text{solar absorptivity})(\text{solar radiation})}{(\text{surface conductance})} .$$

Solar absorptivity ranges from 0.2 for white surfaces to 0.9 for black, while surface conductance is proportional to wind velocity. For a black material, when the air is 90 F, the S.A.T. is 120 F for a 5 m.p.h. breeze and 165 F with no breeze. Note that temperatures of 200 F have been measured for insulated roofing materials, while 170 F black bulb temperatures are found on the Nigerian desert (reference 12). By the rule of thumb that reaction rates double for a 10 C rise, an increase of 45 F (from 120 F to 165 F) would accelerate hydrolysis and secondary photochemical reactions sixfold! For branched polyethylene, a 40 C rise in temperature has accelerated photooxidation fourfold (reference 13). The role of air temperature presumably accounts for the greater effect of latitude on degradation than insolation values would suggest (Figure 3). As an example of seasonal variation, weathering conditions in Tennessee are said to be ten times more severe in summer than winter (reference 14).

2. With Year

Year-to-year weather variations are a common observation. The following values are for the relatively-stable climate of Phoenix (reference 10):

Year	Annual Insolation, langleys	Annual Rainfall, inches	Mean Monthly Temp., F Low	High
1962	194,500	4.8	49.8	87.9
1970	197,900	16.8	58.0	82.3

If wetness of the material were an important factor in degradation, it would have been unsatisfactory to take the abnormally wet year of 1970 and extrapolate to longer exposures in Phoenix. In the more-variable climate of Miami, a five-year weather record shows that rainfall in August varied from 3.1 to 13.5 inches, sun-hours ranged from 175 to 339, and the time test-panels were wet varied from 47 to 189 hours (reference 15).

3. With Specific Location

Altitude also affects the amount of ultraviolet energy received. For example, UV at 350 nm. is twice as intense at Mount Wilson, Calif. (elevation 1,789 m.) as at Washington, D. C. (sea level). Above the atmosphere, it is about three times as intense as at sea level (reference 16). An example of the limitations of weather-station data is that a low hill and a valley can vary by 40 F; the hill is warmer until the wind exceeds 10 m.p.h. and then becomes cooler (reference 5). Rainfall can vary between nearly locations, and dew formation is also important. Wetting-through by dew, followed by sunshine exposure, is particularly damaging to paint films (reference 15) and presumably also to plastics that are susceptible to hydrolysis, e.g., cellulose acetate butyrate. Many workers believe that oxygen, released from nearby grass, can accelerate weathering of some materials (reference 17)!

IV. EFFECT OF CLIMATE ON WEATHERING

Because regional weather data do not really describe the "microclimate" experienced by an exposed material, correlations of climate with rate of degradation are erratic. In the relatively simple case of high-density polyethylene, which is degraded by light and heat but not by moisture, the lifetime (to 10% elongation or 2/3 tensile strength retained) was 3 months in Arizona, 6 months in Florida, and 12 months in New Jersey (reference 18), which is easily understood.

Polycarbonate, unli polyethylene, might be hydrolyzed. For UV-stabilized polycarbonate, the loss in elongation after 3 years was 22% in Pennsylvania, 31% in Arizona, and 79% in Florida (reference 19). In this case, Florida exceeded Arizona in severity, presumably because of the moisture factor. Note that South Miami, Florida, has a marine climate, and salt in the air may influence degradation. Also, rain in Miami often comes as brief showers followed by bright sunlight, and the high humidity at night is conducive to dew formation.

Miami is the most severe location in the continental U.S. for the majority of paints (reference 20), and the salt factor is said to accelerate degradation of reinforced polyester surfaces. For the latter, Panama exposure was far less damaging than Miami exposure (reference 21). Acetal, which is subject to hydrolysis, expectedly deteriorated more rapidly in a hot/wet Australian climate than a hot/dry one (reference 22). For cellulose acetate butyrate, the time for the original tensile of 6960 psi to fall to about 2000 psi was over 3 years in northern Canada, 1.5 years in New Jersey, 1.0 year in New Mexico, and 0.8 year in Panama (reference 23). Again, this seems logical. Less easily rationalized is the order for surface degradation and strength loss of cellulose acetate: New York $\gg$ Panama $>$ Alaska $>$ New Mexico or Canada (reference 24). For flexible, filled PVC (poly(vinyl chloride)), the degradation found in

Australia and South Africa exceeded that in Canada, England, Germany, and the U.S.A. in severity. For rigid PVC, Canada's climate was most severe, followed by Germany's, with the other sites ranked together as least severe (reference 25). These results are difficult to explain. Another unexcepted result is that greater loss of gloss in poly(methyl methacrylate) or haze development in poly(vinyl fluoride) occurred in Washington, D. C. than in Miami, Florida (reference 26).

As a final example, the tensile strength of heat-resistant acrylic sheet decreased from 11,200 psi to 5000 psi after 3 years in a temperature climate, to 3900 psi after 3 years in a subarctic climate, to 3600 psi after 2.5 years in a dry/hot climate, and to 2200 psi after 2.5 years in a tropical climate (reference 27). The greater degradation in a subarctic than a temperate climate is unexpected. In conclusion, the gross or regional climate sometimes correlates with degradation rates, but exceptions are too numerous to inspire confidence in "logical" correspondences.

V. THE MICROCLIMATE

A plastic sample is affected only by its "microclimate" — the conditions at its immediate surface. For example, transparent PVC sheet mounted on wooden test racks darkened only where the presence of a wooden member restricted air circulation and produced a higher material temperature (reference 28); note the influence of air movement on the sol-air temperature discussed above. The microclimate varied from one place on the sheet to another and was not described by the regional temperature data. It has been said that "microclimatic variations are carefully avoided in regional weather records" (reference 28).

Figure 4 shows diagrammatically some of the microclimatic factors. Obviously, it is the radiation reaching the sample surface and not the regional insolation which determines degradation. Soot or "chalk" (particles of degraded plastic) may have a protective effect. On the other hand, "acidic soot" (reference 7) or "muck" (reference 17) is known to degrade nylon and might attack other plastics also. Thickness of the sample is another important factor; most degradation may be superficial so that films crumble while heavy sheets survive. Infrared re-radiated from the surroundings (rocks, vegetation, etc.) will raise the temperature of the sample (reference 5). Skylight may contain the same ratio of UV as direct sunlight on a clear day and even more when the total radiation is low and scattered (reference 7). Breezes have an important cooling effect; they can also erode the material surface with windblown particles.

Stress is a vital factor and has been utilized in accelerating polyethylene weathering for test purposes (reference 29). Molded-in stresses have caused rapid failure of cellulose acetate butyrate outdoors (reference 30). Thus, degradation of unrestrained test samples is liable to be decelerated relative to that under actual stressed conditions if cracking and crazing are the failure criteria

(reference 31). For example, the forming process for cast acrylic sheet can introduce stresses which cause cracking/crazing on outdoor exposure (reference 28). The chemical effect of salt has been mentioned, but salts may crystallize due to temperature and humidity changes to produce cracking (reference 32).

Industrial air pollutants discolor cellulose acetate butyrate (reference 33). Atlas Electric Devices Co. supplies a gas exposure cabinet for subjecting samples to polluting gases such as ozone, sulfur dioxides, and nitrogen oxides. Rain rinsing may retard degradation by removing corrosive material or accelerate degradation by washing off protective barriers and leaching stabilizers.

Dew-soaking has been mentioned as a very damaging factor in some cases. Indeed, the frequency of wetting may be as important as total hours of wetness (reference 34). This is another variable not shown in regional weather data. Cyclic swelling and shrinkage caused by successive absorption and evaporation of water can cause internal stresses (reference 35). Besides the obvious importance of the exposure direction, the influence of the exposure angle is considerable and illustrates the criticality of minor variations in microclimatic conditions. For polycarbonate (reference 19), samples placed vertically, such as windows, resist degradation 2-1/2 times longer than samples placed at 45° south. PVC sheet lost elongation at the fastest rates when it was mounted horizontally in Florida (reference 31). This is explained by greater rain-leaching of plasticizer from panels in the horizontal position. On the other hand, enamels degraded faster at a tilt of 85° than at 45° in Florida. In other studies, the Miami latitude angle (26°) gave the same weathering results as the conventional 45° angle (reference 36). In conclusion, it is easy to see why it has been said that "it is impossible to duplicate or accelerate natural weathering" (reference 37).

VI. WEATHERING MECHANISMS AND FAILURE MODES

Mechanisms are summarized in Figure 5. Chain scission by photolysis is one of the most damaging reactions. Poly(methyl methacrylate) degrades in this manner, but apparently without the crosslinking reactions which are typical of other polymers (reference 38). Oxidation of plastics leads to discoloration and/or crosslinking and embrittlement. Polystyrene crosslinks under UV irradiation without air, while in the presence of oxygen, chain scission occurs also. Yellowing takes place under nitrogen as well as oxygen (reference 39). Degradation by hydrolysis is important for polyesters and acetals. Crystallization of some polymers can cause embrittlement. Erosion and biological action are other factors. Degradation theory is rapidly developing but is beyond the scope of this paper (see reference 40).

Some failure modes are listed in Figure 6. These vary with the application. For example, a cellulose acetate butyrate sign

remained in service for 9 years in New York City (reference 14). Presumably, certain mechanical properties deteriorated, but the optical properties were most significant in this application. Gloss, haze, light transmission, and color stability are the principal criteria for rating the weatherability of aerospace transparencies. However, cracking and crazing are also critical because they affect transparency and a crack might lead to catastrophic failure.

VII. ACCELERATED TESTS VS. OUTDOOR EXPOSURE

"The only true indicator of the results of outdoor weathering is actual outdoor exposure" (reference 30). Surely, in outdoor exposure tests the actual factors of weather are at work, but conditions are nonreproducible due to uncontrollable microclimatic variations. Regional weather varies from year to year as we have seen, and it has been said that "every outdoor exposure is an artificial weathering test" (reference 31) and that weather never duplicates itself (reference 36). Another interesting point is that "the weather prevalent immediately on exposure often influences the entire life" of a test sample (reference 29). Certainly, the season must be considered for short-term exposures. In England, polystyrene lost 80% of its elongation in 0.7 month in summer compared with 3.6 months in winter (reference 41).

In contrast, accelerated tests provide reproducible conditions. On the average, Weather-Ometers were found to duplicate Florida weather better than Florida weather duplicates itself (reference 29). Two methods are used in accelerated weathering machines: continuous exposure and intensified exposure. As an example of the former, simulated noon sunshine is maintained in the Xenon-arc Weather-Ometer. This high light intensity persists for at most a few hours a day in nature. As an example of continuous exposure, natural sunlight is concentrated 8 times by mirrors in the EMMA device (reference 38). The appropriateness of these exposures is a disputed subject. It has been suggested that continuous exposure is more reliable than intensified exposure because the latter can cause extraneous reactions (reference 4 and 29). The correlation of Xenon-arc with outdoor data was found to decrease when the radiant energy exceeded a critical level characteristic of individual polymers (reference 29). For some materials, the EMMA test has corresponded well with outdoor exposures in arid climates. With the addition of water-spraying (EMMAQUA), correlations are obtained with wetter climates such as Florida (reference 42). A simplified Weather-Ometer-like device is the QUV Cyclic Ultraviolet Weathering Tester. This simulates sunny days and hot/wet nights (reference 43).

"Exact prediction of the useful lifetime of a given polymer in a specific geographic location is still the dream of both consumers and manufacturers" (reference 7). Statistical treatments have been proposed. Kamal (reference 44) has suggested the Exposure Parameter Technique (also discussed in reference 31). The empirical equation is:

$$\text{extent of degradation} = Ae^{B(\text{time} - C)}$$

where A, B, and C are constants (exposure parameters).

Clark and Slater (reference 45) have developed a statistical reliability function. This Weibull model is a "wear-out" function which has been used to describe fatigue life and failure time for various materials:

$$\text{retention of property} = b_1 e^{-\left(\frac{\text{time} + b_2}{b_3}\right)^{b_4} + b_5}$$

where the b's are parameters, with b_3, b_4 and b_5 being most important. Specifically, b_3 was significantly correlated with time to failure.

Both the above equations gave good correlations, Kamal's having been used to predict outdoor degradation data for polystyrene based on Weather-Ometer tests (reference 31).

VIII. FUTURE TRENDS IN ACCELERATED TESTING

Recent years have seen closer duplication of sunlight and better temperature control. For example, a black panel temperature of 140 F is commonly used in the Xenon-arc Weather-Ometer. In addition, there is more meaningful rain/dew simulation, exposure to aggressive air pollutants such as sulfur trioxide, more sophistication in reporting both weather and plastic test data, and the beginnings of statistical analysis as mentioned.

Key factors such as UV, temperature, moisture, stress, and thickness of section should be studied separately and in combinations to provide an understanding of degradation mechanisms. Then arbitrary microclimates may be studied in the laboratory and eventually computer-simulated to give degradation curves (or equations). Fitting of early degradation data by a sensitive analytical method such as infrared spectroscopy to these curves would allow long-term predictions with a degree of confidence. The important role of anticipatory methods for assessing change has been stressed (reference 31). The key to long-term prediction lies in a better understanding of the degradation mechanisms rather than in closer simulation of ever-changing weather conditions.

IX. INTRODUCTION TO REVIEW OF WEATHERING EXPERIENCE

The weathering of several transparent plastics is reviewed in the next section. Summaries are necessarily brief, and mostly outdoor exposure data are discussed. There are several difficulties in quoting and using data from the weathering literature, which has been called "somewhat confused" (reference 17). For instance, commercial

formulations have changed over the years. Thus, amber polycarbonate samples became embrittled in 3 years in Alaska or Panama (reference 46, published in 1964), whereas later polycarbonate samples showed no significant changes in tensile strength or elongation after 3 years in Panama or other sites (reference 47, published in 1970). Better UV stabilization of the more recent material could explain this. Other difficulties are the qualitative/subjective nature of much data and incompletely defined formulations and test procedures. In addition, microclimatic conditions are not really known. It is only in recent years that the reporting of regional weather data has become more detailed. For example, instead of sun-hours, the langleys of sunlight (total energy) are now given. However, even this is inadequate because the component of importance (UV) varies widely with the season, amount of haze, etc., as described above. A great deal of weathering data is proprietary and not published at all. Finally, because better UV stabilization is always a possibility, the lifetimes reported must be considered lower limits. Also, it has been postulated that impurities in polymers absorb UV and initiate breakdown (reference 40). Purer commercial polymers may be developed in the future without these problems. The following section should be read with these considerations in mind.

In the following discussion, "tensile strength" means ultimate tensile strength and "elongation" means elongation at break. Such values can depend on strain rate and even sample thickness, but the references must be consulted for details. "Florida" means South Miami, Florida (a coastal location). Exposures are conventionally conducted at 45° inclination facing south. Sample thickness is usually about 1/8 inch, except for film materials (Mylar, and fluoropolymers in the present context).

X. RESISTANCE OF TRANSPARENT PLASTICS TO WEATHERING

1. Poly(Methyl Methacrylate)

Poly(methyl methacrylate) ranks only behind polytetrafluoroethylene in demonstrated weather-resistance. In the fast-developing plastics industry, this relatively "old" plastic has been in use long enough to allow impressive case histories. For example, cast acrylic roof lights which had been in use for 30 years in London, England, were free of significant cracking or crazing, were only slightly discolored, and light transmission was "still adequate" (reference 28). Skydomes in Waltham, Massachusetts, were in "perfect condition" after 17 years, as were windows and skylights after 8 years in South Florida (reference 48). Outdoor exposures of poly(methyl Methacrylate) for over more than 20 years have shown "no effect of weathering and no significant loss of physical performance" (reference 33), and 20 years service "can be expected" (reference 17).

However, detailed studies indicate at least minor losses. For Lucite 140 Gr 8 (1/8 inch thickness), 4 years exposure in Florida (650,000 UV langleys) or in Arizona (725,000 UV langleys) caused,

respectively, 8 and 10% loss in tensile strength and 5 and 7% loss in elongation (reference 49); 1 year in Florida caused no significant loss in Izod impact strength or light transmission (reference 19).

Acrylic usually contains a UV-absorber. The yellowing of old samples is blamed at least partly on the stabilizer. However, Tinuvin P, which is the stabilizer now used, does not cause yellowing (reference 50). Unstabilized acrylic lost only 1% light transmission, 27% tensile strength, and 23% gloss, with a slight increase in haze (0.6% to 3.8%) after 6 years in Florida (reference 51). The property losses for Plexiglas G (1/8 inch thickness) after 5 years in Bristol, Pennsylvania, were 15% for tensile strength, 32% for elongation, and 11% for Charpy impact strength, with a haze increase from 1.2 to 3.0% (reference 49 and 52). Performance of 60 mil sheet was excellent; it was colorfast and retained all its elongation after 6 years in Washington, D. C., Miami, or Arizona. Its gloss retention was 72% in Florida, 75% in Arizona, and 87% in Washington, and haze (at 420 or 550 nm.) remained at 9% or less (reference 26). Note that polycarbonate, cellulose acetate butyrate, and poly(vinyl fluoride) all lost gloss much more rapidly.

Effects of various climates on heat-resistant acrylic sheet were mentioned above. These indicate considerable loss in tensile strength, but the elongation deteriorated little in New Jersey, Canada, and New Mexico for 3 years' exposure. Injection-molding grade gave similar results to cast sheet (reference 23 and 17). Lucite 140 NC10 (injection-moldable) had an original transmission of 91.9% and yellowness index of 0.6. These values changed to 92.1 and 1.9 after 5 years in Arizona and to 90.6 and 2.1, respectively, in Florida. After 4 years in Florida, Lucite 147 NC10 changed -7% in tensile strength, -29% in elongation, and +33% in notched Izod impact. Its haze increased from 0.8 to 2.7 in 5 years (reference 53). Yellowing of 1/8 inch thick cast sheet after 2 years in Florida or Arizona was slight (reference 29), and the yellowness index of Lucite (7449l-B) was only 1.6 after 10 years in Arizona, with 91.1% light transmission (reference 53). Acrylic sheet (about 1/10 inch thick) showed good color stability and lost 8% tensile and 15% flexural strength after 5 years in Sapporo, Japan (reference 54). Plexiglas 55 survived 20 years in New Mexico and with high light transmission and only slight yellowing (reference 55). Transparent acrylic coatings have shown good weather-resistance. For example, baked Acryloid B-66 survived 7 years in Pennsylvania and 4 years in Florida (reference 56).

For unstressed MIL Spec P-8184 material (modified acrylic sheet), 50% of the samples exposed at Bristol, Pennsylvania, showed their first crazing in 10 years, while a "half-life" of over 12 years was found for P-5425 (heat-resistant acrylic sheet) (reference 52). However, sheet forming can introduce residual stresses, as noted above. For test purposes, weights are hung on cantilevered bars of material, giving stresses which can cause crazing in short exposure times, though it must be kept in mind that the higher experimental fiber stresses are not normally encountered in service. At 4000 psi fiber stress, cast sheet crazed in 1.5 days at Bristol, Pennsylvania

(reference 52), Plexiglas II crazed in 35 days, and as-cast Plexiglas 55 (crosslinked) crazed in 120 days (reference 57). In other work, at the same stress and location, heat-resistant acrylic crazed in 85 days, heat- and craze-resistant acrylic in 146 days, and modified acrylic had not crazed in 568 days (reference 58). Stretching of acrylic to give bi- or multiaxial orientation increases the craze resistance under weathering (reference 52). For example, modified acrylic sheet (P-8184), after stretching, resisted weathering damage in terms of tensile creep rupture behavior better than as-cast or laminated material (reference 27). With 4000 psi fiber stress in Bristol, Pennsylvania, unstretched Plexiglas 55 took 56 days to craze, while stretched material had not crazed at 378 days. Furthermore, three years' exposure of the stretched sheet caused no significant drop in Charpy impact strength (reference 50). Reference 59 is a detailed report on the effect of stretching.

Aircraft windows present a special case of weathering because cyclic stresses occur and at high altitude UV is more intense (especially the shorter wavelengths). Outside the atmosphere, UV intensity is three times the sea level value. Chain-scission by UV energy eventually ruptures the polymer chains and this is manifested as crazing. Airplane windows of stretched Plexiglas 55 must be replaced because of crazing 60% of the time and because of scratches and other defects 40% of the time (reference 50). At 600 m.p.h., some erosion of the forward edge of protruding windows is observed. The cyclic stress due to altitude changes causes enough crazing in 3 or 4 years to impair visibility. Since this is a surface phenomenon, airline plane windows are resurfaced and returned to service (reference 60).

Acrylic sheet is available with abrasion-resistant coatings. For example, Lucite AR, coated with a crosslinked fluoropolymer, has performed well in weathering tests (reference 61).

2. Polycarbonate

Polycarbonate is inherently rather susceptible to degradation by weathering, but addition of UV absorbers (benzotriazoles or benzophenones) has made it serviceable outdoors. There is little change in mechanical or physical properties after several years in a moderate climate. However, strong sunshine combined with humidity causes superficial yellowing and embrittlement which can lead to fine cracks and ultimately to failure (reference 62). The most harmful UV wavelengths are said to be 295 and 330 nm. (reference 51). It has been postulated that longer wavelengths (over 280 nm.) cause chain scission whereas shorter wavelengths (240-280 nm.) lead to cross-linking (reference 63).

For unstabilized polymer, the elongation fell 80-83% after 6 months under hot/dry or hot/wet Australian conditions. After 4 years the notched Izod impact strength fell about 13% (hot/dry) or 35% (hot/wet) compared to 22% for an unexposed control. A yellow color developed, principally at the surface, and this was accompanied

by a loss of gloss particularly under hot/wet conditions. This yellowing and dulling were the only effects of 2 years in a temperate climate (reference 64).

UV-stabilized material (Lexan 103-112) showed no loss in tensile strength or elongation after 3 years in hot/dry or hot/wet Australian sites (reference 47). This result contrasts strikingly with the afore-mentioned drop of 80-83% in 6 months for unstabilized polymer. Exposures in New Jersey, New Mexico, and Panama gave the same result. This material (Lexan 103-112) after 5 years in Florida showed no loss in tensile yield strength, 41% loss in elongation, 34% increase in notched Izod impact strength, 62% loss of gloss, 6% loss in light transmission, and a haze increase from 3.6 to 29.9%. This loss in elongation was not considered serious since both Izod and falling ball impact strength increased. Yellowing was slight; the yellowness index increased from 5.0 to 9.7 (reference 51). Another UV-stabilized polycarbonate, Merlon M-50, gave similar results. After 3 years in Arizona, the elongation fell 31%, the notched Izod impact strength fell 2%, gloss fell 79%, light transmission fell 6%, and haze (a surface effect) increased from 0.5 to 10% (reference 19). In the temperate climate of Pittsburgh, Pennsylvania, the corresponding values were 22%, 2%, 51%, 3%, and from 0.5 to 12%. Note that, contradicting the trend of the other properties, haze development was slightly greater in Pittsburgh. A relatively high rate of gloss deterioration is shared by poly(vinyl fluoride) and cellulose acetate butyrate, as will be seen.

In another study of UV-stabilized polycarbonate, 6 months' weathering in Arizona caused no change in tensile properties, a decrease in notched Izod (1/8 inch specimens) of about 50%, almost no change in light transmission, slight haze increase, little or no yellowing, and some surface degradation (pits and craters). After a further 6 months' exposure, surface crazing and yellowing were noted. Protective coatings survived 6 months weathering. Long-term annealing incidentally, increased the ductility of polycarbonate to give a no-break result in the notched Izod impact test (reference 63).

In conclusion, the effects of weathering on polycarbonate are concentrated at the surface. Hard, brittle coatings, e.g., Sierracin HC-2 (reference 65), have been evaluated in aircraft transparency applications. More recently, a ductile coating (Sierracote 233) was developed and has been in use on F-15 windshields for 2 years. A thick fusion-cladding of polyurethane (Sierraclad) is currently being tested (reference 66). Laminates with an outer layer of acrylic are another approach to better environmental resistance of polycarbonate.

3. Polystyrene

Polystrene is inherently susceptible to ultraviolet degradation, presumably because of the labile tertiary hydrogen atom and the UV-absorbing phenyl group. The most damaging UV wavelength is 319 nm., and UV light causes crosslinking even under vacuum. Chain scission occurs in the presence of oxygen (reference 39). Ultraviolet

absorbers do offer some protection, seemingly at the expense of the surface layer (reference 39). However, stabilized transparent polystyrene is poor compared to other weather-resistant polymers (reference 33). Opaque polystyrene formulations, in which sunlight is screened by fillers, held up well in New Jersey, Alaska, and Panama for 3 years (reference 32).

Examples of degradation of crystal polystyrene are: 80% loss of original elongation in England in 0.7 months in summer vs. 3.6 months in winter as mentioned above, 70% loss of tensile strength after 1 year in Stamford, Conn. (reference 67), 84% loss of unnotched Izod impact strength after 1 year in Arizona (reference 4). The impact strength of all styrenics including impact polystyrene and ABS drops off rapidly within 6 months outdoors (reference 68). There was 37-79% loss of elongation after 3 years in Dover, New Jersey (reference 32), 52-70% loss of tensile strength after 1 year in Canada, New Jersey, New Mexico, and Panama (reference 23), and 77% loss of tensile and 83% loss of flexural strength in 1/10 inch thick samples after 5 years in Sapporo, Japan (reference 54). In the last case, a weather-resistant grade did about as badly (72 and 82% losses, respectively). Color stability was noted as poor in the Japanese exposure, most of the final color having developed after one year. Window glass transmits enough UV to degrade polystyrene. For example, inside a north window in Midland, Mich., natural polystyrene lost 87% of original notched Izod impact strength after 1 year (reference 4). This is an example of degradation by skylight, mentioned above as a weathering factor.

SAN (styrene-acrylonitrile copolymer) is a rigid, transparent styrenic plastic also severely affected by the weather. Its elongation fell 58% after 1 year in Michigan and 70% in Arizona (reference 4). In another test, unnotched Izod (originally 5.0) fell to 1.3 ft.lb./in. after 1 year in Michigan and 0.7 after 1 year in Arizona (reference 32). After a year of exposure, tensile strength decreased slightly in New Jersey and Canada but fell 63% in New Mexico and 57% in Panama, with yellowing and haze development (reference 23).

4. Cellulose Acetate Butyrate

When properly stabilized, cellulose acetate butyrate has good weather resistance. Clear outdoor formulations may be expected to endure 3-8 years exposure "without objectionable deterioration in either appearance or performance" (reference 30), and a useful life of at least 5 years in the continental U.S. is anticipated (reference 14). The most weather-resistant formulations lost only 5% of original tensile strength after 3.5 years in Arizona and "remain useful" for 5 years or more in Arizona. A sign remained in service in New York City for 9 years although the plastic's useful life in Arizona was only 2 years (reference 14). Heavy industrial air pollution causes discoloration, and molded-in stresses accelerate weathering failure.

In other tests, clear, UV-stabilized material exposed in Florida lost 70% gloss in 4 years (99% in 6 years), 8% light

transmission in 4 years (20% in 6 years), and 5% tensile strength in 4 years. Haze increased from 1.8 to 22.8% in 4 years and to 58.0% in 6 years. Flexural strength increased 14% in 6 years (reference 51). The poor results on early weather-resistant formulations (reference 23, published in 1955) presumably are due to inadequate UV stabilization. For example, tensile strength of an old formulation fell 32% after 2.5 years in New Mexico (reference 23) compared with a 5% loss in 3.5 years in Arizona for a modern formulation. This is an example of published data representing only a lower limit for weather-resistance because improved UV-stabilization changes the picture completely.

5. Weatherable Mylar

Mylar, which is biaxially-oriented poly(ethylene terephthalate) film, has inherently only "medium" weather resistance (reference 13). For example, the elongation of 5 mil sheet fell to 0 after 4 years in Florida or Arizona (reference 26). However, by impregnation with a UV-stabilizer (by HCA-Martin, Inc.) a dramatic improvement is achieved. Sheet of 7 mils thickness is used to cover greenhouses and can withstand 8-10 years outdoor exposure without discoloration or embrittlement (reference 69). A testimonial letter from a user indicates a useful life of at least 9 years in Indiana. This is another example of the great improvement possible by UV stabilization.

6. Polysulfone

The weather-resistance of polysulfone has been described as "poor" (reference 37). After 1 year in Florida, tensile strength decreased 25%, notched Izod impact decreased 62%, light transmission decreased 25%, and gloss decreased 95% (reference 19). However, polycarbonate has been effectively stabilized, and polysulfone is a chemically-related polymer which contains the same bisphenol A moiety. Although polysulfone is not recommended for outdoor use at present, a UV stabilization system is being sought (reference 70). The performance of "weatherable Mylar" suggests optimism.

7. Fluoropolymers

a. FEP (Fluorinated Ethylene-Propylene)

FEP is not glass-clear as are the plastics previously discussed. However, in thin sections its light transmission is high enough to allow the film to be used for encapsulating solar cells. The haze is due to crystallinity (spherulitic structure).

Some reported test results on FEP weathering are: exposure of 2 mil film in Florida for 3 years with no sign of degradation (reference 48), negligible (2-4%) losses in tensile strength and elongation after 3 years in Florida or Michigan (reference 49), and no effect on tensile or elongation after 7 years in Florida (reference 71). Like the chemically-similar PTFE (polytetrafluoroethylene), FEP seems "inert to the effects of weather"

(reference 23). PTFE has been exposed for 30 years in Florida with little change in properties (reference 33). The outstanding weather-resistance of FEP (and other fluoropolymers) has been attributed to its high transparency to UV light (references 71 and 72).

b. PVF (Poly(Vinyl Fluoride))

Although PVF is an analog of the UV-sensitive poly(vinyl chloride) and bears only one fluorine atom for three hydrogen atoms, it has proved itself to be remarkably weather-resistant. After 25 years of exposure it showed "remarkable retention" of appearance and physical properties (reference 73). These tests were conducted with the thin film Tedlar. No significant loss of properties was reported for 20 years in Florida or Arizona (reference 48), and at least 50% of original tensile strength was retained by unsupported Tedlar after 10 years in Florida (reference 74). There was no significant change in "blue film" after 3 years in New Jersey, New Mexico, Panama, or hot/wet or hot/dry Australian sites (reference 47). In another study, the results of exposure of 1 mil film for 6 years were: 5 units (slight) color change in Washington, D. C., 1.5 in Florida, 1.0 in Arizona; 78% retention of elongation in Washington, 69% in Florida, 57% in Arizona; gloss 75-90% gloss reduction at the three sites; haze (420 and 550 nm.) 58 and 50% in Washington, 30 and 24% in Florida, and 34 and 26% in Arizona (reference 26). PVF seems to be gradually degraded and less stable than FEP, but, as plastics go, its weathering performance is excellent.

c. PVF_2 (Poly(Vinylidene Fluoride)

PVF_2 (Kynar) is described as having "excellent" weatherability. Exposure of a thin film to an industrial atmosphere for 8 years caused no loss of tensile or yield strength, the final values being higher than the initial (reference 75). Like Tedlar, Kynar has been used as a surfacing film to protect other materials from the weather. Its excellent weather-resistance might be expected from the fact that it is "fluorinated PVF" and bears only one hydrogen atom per fluorine atom.

d. Aclar (Polychlorotrifluoroethylene)

Aclar 22-C film (Allied Chemical Corp.) after 3000 Weather-Ometer hours (perhaps equivalent to 1-2 years in South Florida) retained 72% of its original tensile strength in the machine direction and 84% in the transverse direction (reference 76). Excellent long-term performance would be expected unless the carbon-chlorine bond proves susceptible to weathering.

e. Newer Fluoropolymers: Tefzel, Halar, PFA

Because of the recent commercial introduction of these plastics, little weathering information is available.

Tefzel, the largely-alternating copolymer of tetrafluoroethylene and ethylene, survived 1 year in Michigan and Florida without effect, and 2000 Weather-Ometer hours exposure did not reduce tensile strength or elongation (reference 77).

Halar, the chlorotrifluoroethylene analog of Tefzel, showed no significant change in tensile strength or elongation when exposed for 40 days as a 5 mil film in New Jersey (reference 49) or as a 2 mil film in Arizona (reference 33).

PFA (perfluoroalkoxy resin) is said to have excellent weatherability (reference 78).

It seems likely that all these materials will prove to have good weather-resistance, although multiple ethylene units (due to imperfect alternation of the monomers) could be weak points in Tefzel and Halar. If so, improvements in polymerization technique might "purify" the polymer and prove previous weathering data merely a lower limit.

REFERENCES

1. E. B. Espenshade, Jr., Editor, Goode's World Atlas, Rand McNally and Co., 1960.

2. H. L. Nelson, Climatic Data for Representative Stations of the World, Univ. of Nebraska Press, Lincoln, 1968.

3. H. Wachter, Meteorology, Collins, 1973.

4. Anon., "Permanence Properties of Plastic Molding Materials," brochure from the Dow Chemical Co., 1968.

5. G. R. Rugger, et al, "Weathering of Glass Reinforced Plastics," Plastics Technical Evaluation Center, Picatinny Arsenal, Dover, N.J., 1966 (AD 630 987).

6. G. D. G. Lof, et al, Solar Energy, 10, 27 (1966).

7. J. E. Clark, in Encyclopedia of Polymer Science and Technology, Volume 4, Pgs. 779-795 (1970)

8. G. A. Zerlant, "Accelerated Outdoor Weathering Employing Natural Sunshine," Proceedings of the Institute of Environmental Sciences, pg. 153-158 (1975).

9. N. Z. Searle and R. C. Hirt, J. Opt. Soc. Am., 55, 1413 (1965).

10. Anon., "Summary of the Weather, 1955-1974," Desert Sunshine Exposure Tests, 1975.

11. R. W. Singleton and P. A. C. Cook, Textile Res. J., 39, 43-49 (1969).

12. Ministry of Aviation, Great Britain, Reports on Plastics in the Tropics - 14. Low Pressure Glass-Fibre Laminates Bonded with Polyester Resins.

13. F. H. Winslow, W. Matreyek, and A. M. Trozzolo, "Polymers under the Weather," SPE Journal, 28, 19-28 (July 1972).

14. Anon., "Weathering of Tenite Butyrate," Technical Report TR-25, Eastman Kodak, 1968.

15. R. M. Burns and W. W. Bradley, Protective Coatings for Metals, 3rd Edition, Reinhold, N.Y., 1967, pgs. 476 and 479.

16. Forsythe, W. E., Measurement of Radiant Energy, McGraw-Hill, N.Y., 1937.

17. J. M. J. Estevez, "Some Thoughts on the Weathering of Plastics," Plastics Institute Transactions, 33, 89-93 (1965).

18. H. M. Quakenbos and H. Samuels, "Practical Problems of Predicting Weathering Performance," Modern Plastics, April 1967, pg. 143.

19. Anon., "Outdoor Weathering of Marlon Polycarbonate," Mobay Chemical Corp., Plastics Dept., brochure, undated.

20. E. G. Trousil, Chairman, "High Altitude Testing of Paint Films," J. of Paint Technology, 45, No. 576, pg. 89-94 (1973).

21. D. V. Rosato and R. T. Schwartz, editors, Environmental Affects on Polymeric Materials, Vol. I, Interscience, 1968, pg. 384.

22. J. Wright, "Outdoor and Accelerated Weathering of Elastomers and Plastics: The Assessment of an Accelerated Weathering Test Chamber," Explosive R&D Establishment, Waltham Abbey, England, 1972 (AD 752 373).

23. R. B. Barrett, "Resistance of Plastics to Outdoor Exposure (a Condensation)," Picatinny Arsenal, Tech. Report 2102, PB 131331, 1955.

24. S. E. Yustein, R. R. Winans, and H. J. Stark, "Three Years' Outdoor Weather Aging of Plastics Under Various Climatological Conditions," ASTM Bulletin Feb. 1954, pgs. 29-39.

25. E. Szabo and R. E. Lally, "World-Wide Weathering of Poly(Vinyl Chloride)," Polymer Engineering and Science, Vol. 15, No. 4, April 1975, pgs. 277-280.

26. W. J. Rossiter, "Outdoor Performance of Plastics. X. Final Update of Weathering Data," National Bureau of Standards, Washington, D. C., NBSIR 73-146, March 1973 (COM-73-10989).

27. Anon., "Plastics for Flight Vehicles, Part II, Transparent Glazing Materials," Military Handbook, MIL-HDBK-17, Approval Date August 14, 1961, Armed Forces Supply Support Center, Washington, 25, D. C.

28. J. W. Simpson and P. J. Horrobin, Editors, The Weathering and Performance of Building Materials, Wiley - Interscience, 1970, pgs. 30, 244, 259.

29. M. R. Kamal, Editor, Applied Polymer Symposia No. 4, Weatherability of Plastic Materials, Interscience, Wiley and Sons, 1967.

30. H. Mark, Editor, Encyclopedia of Polymer Science and Technology, Vol. 3, pg. 386 (1965).

31. M. R. Kamal and R. Saxon, "Recent Developments in the Analysis and Prediction of the Weatherability of Plastics," Applied Polymer Symposia No. 4, 1-28 (1967).

32. J. D. Titus, "The Weatherability of Polystyrenes and Related Copolymers and Terpolymers," Plastics Tech. Evaluation Center, Picatinny Arsenal, Dover, N.J., PLASTEC-R-38, July 1969 (AD 700 091).

33. Anon., "Stabilizers and Coatings Protect Plastics Against Weathering," Materials Engineering, April 1974, pgs. 54-57.

34. R. A. Kinmonth, Jr., "Laboratory Weathering — Correlating Effectiveness," Atlas Sun Spots (publication of Atlas Electric Devices Co.), Vol. 2, Issue 5, Nov. 1973.

35. M. R. Kamal, "Cause and Effect in the Weathering of Plastics," Polymer Engineering and Science, March 1970, Vol. 10, No. 2, pgs. 108-121.

36. R. G. Neuman, ASTM Committee D-20 (V-H), Cincinnati Meeting, Oct. 1965.

37. W. L. Hawkins, Polymer Stabilization, Wiley - Interscience, 1972, pg. 415.

38. R. B. Fox, L. G. Isaacs, and S. Stokes, "Photolytic Degradation of Poly (Methyl Methacrylate)," J. Polymer Science, Part A, 1, 1079-86 (1963).

39. H. Mark, Editor, Encyclopedia of Polymer Science, Vol. 13, pg. 239 (1970).

40. R. D. Deanin, S. A. Orroth, R. W. Eliasen, and T. N. Greer, "Mechanism of Ultraviolet Degradation and Stabilization in Plastics," Polymer Engineering and Science, Vol. 10, No. 4, pp. 228-234 (1970).

41. S. H. Pinner, Editor, Weathering and Degradation of Plastics, Gordon and Breach, Science Publishers, Inc., London, 1968.

42. Anon., brochures provided by Desert Sunshine Exposure Tests, Inc., Box 185, Black Canyon Stage, Phoenix, Arizona 85020.

43. Anon., literature from the Q-Panel Co., 15610 Industrial Parkway, Cleveland, Ohio 44135.

44. M. R. Kamal, Polymer Engineering and Science, 6, 333 (1966).

45. J. E. Clark and J. A. Slater, "Outdoor Performance of Plastics III. Statistical Model for Predicting Weatherability," National Bureau of Standards Report 10 116, Oct. 30, 1969.

46. F. J. H. Blinne and L. E. Day, "Addendum No. 5, Resistance of Plastics to Outdoor Weathering," Picatinny Arsenal, April 1964 (AD 609 405).

47. A. F. Readdy and R. B. Bonk, "Addendum No. 7, Resistance of Plastics to Outdoor Weathering," Picatinny Arsenal, November 1970 (AD 877 236).

48. Anon., "The Score on Weatherability," Modern Plastics, May 1967, pgs. 86-175.

49. Modern Plastics Encyclopedia, 1974-75, pgs. 658-674.

50. H. L. Redfoot, Rohm and Haas Co., private communication, September 1975.

51. Anon., "Weatherability of Lexan Polycarbonate," brochure from the General Electric Co., received 1975.

52. H. L. Redfoot, Report for Serial No. 8653, for Rockwell International by Rohm and Haas Co. Plastics Engineering Laboratory, "Weatherability of Transparent Acrylic Polycarbonate, CAB, and Styrene Plastics," September 26, 1975.

53. Du Pont Co., private communication, October 1975.

54. S. Suzuki, H. Kubota, and O. Nishimura, "Studies on Testing Methods and Weatherability of Plastics," in Mechanical Behavior of Materials, Proceedings of the First International Conference, Kyoto, Japan, August 15-20, 1971, pg. 657 ff., Vol. 3.

55. L. G. Rainhart and W. P. Schimmel, Jr., "Effect of Outdoor Aging on Acrylic Sheet," Sandia Laboratories, SAND 74-0241, September 1974.

56. Anon., "Durability of Clear Acryloid Resin Coatings," TC-21-15, Rohm and Haas Co. Resins Dept., October 1963.

57. C. G. Yundt and E. C. Mboring, "Screening Tests on Transparent Plastics, Long Term Outdoor Flexural," Report DEV-24-2 (Douglas Aircraft Co.), 1957.

58. J. J. Gouza and W. F. Bartoe, "A Method of Studying the Resistance of Plastics to Outdoor Exposure," presented at the annual SPE conference, 1955.

59. J. J. Gouza and D. A. Hurst, "The Investigation of Multiaxially Stretched Acrylic Plastic," WADC Technical Report 54-619, Part 1, Wright Air Development Center, 1954.

60. W. Evans, United Airlines, private communication, September 1975.

61. Du Pont Co., "Lucite AR Abrasion Resistant Sheet, Weather Resistance," data sheet, November 1974.

62. H. Mark, Editor, Encyclopedia of Polymer Science and Technology, Vol. 10, pg. 745 (1969)

63. R. S. Hassard, "Design Criteria — Transparent Polycarbonate Plastic Sheet," prepared by Goodyear Aerospace Corp. for Air Force Materials Laboratory, 1972 (AD 751 551).

64. "The Weathering of Plastics Materials in the Tropics, 1. Polycarbonates," Report by the Procurement Executive, Ministry of Defence, British Plastics Federation Joint Committee on the Behaviour of Plastics Materials under Tropical Conditions, 1973 (AD 777 306).

65. W. A. Miller, "Aircraft Transparency Applications of Polycarbonates," presented at the Optical Transparency Symposium, Royal Aeronautical Society, London, June 9, 1971.

66. D. L. Voss, Sierracin/Sylmar, private communication, October 2, 1975.

67. M. R. Kamal and R. Saxon, "Prediction of Weatherability of Plastics," Modern Plastics, April 1967, pg. 150.

68. Tech. Service Dept., Monsanto Polymers and Petrochemicals Co., private communication, 1975.

69. Letter from the HCA-Martin Co., Martinsville, Va., September 16, 1975.

70. Union Carbide, private communication, August 1975.

71. Anon., "Weatherability Performance," Teflon FEP Bulletin T-6B, E. I. du Pont de Nemours and Co., 1966.

72. F. H. Winslow and W. L. Hawkins, Modern Plastics, 44, 141 (April 1967).

73. H. Mark, Editor, Encyclopedia of Polymer Science and Technology, Volume 14, pg. 616 (1971).

74. Anon., "Weatherability Performance," Tedlar Bulletin TD-6, E. I. du Pont de Nemours and Co., revised May 1974.

75. Anon., "Kynar" brochure from Pennwalt Corporation, 1974.

76. Anon., "Aclar Fluorohalocarbon Film," brochure from Allied Chemical Corporation, undated.

77. Anon., "Du Pont Tefzel Fluoropolymer Design Handbook," 1973.

78. Modern Plastics Enclyclopedia, 1973-4, pg. 44.

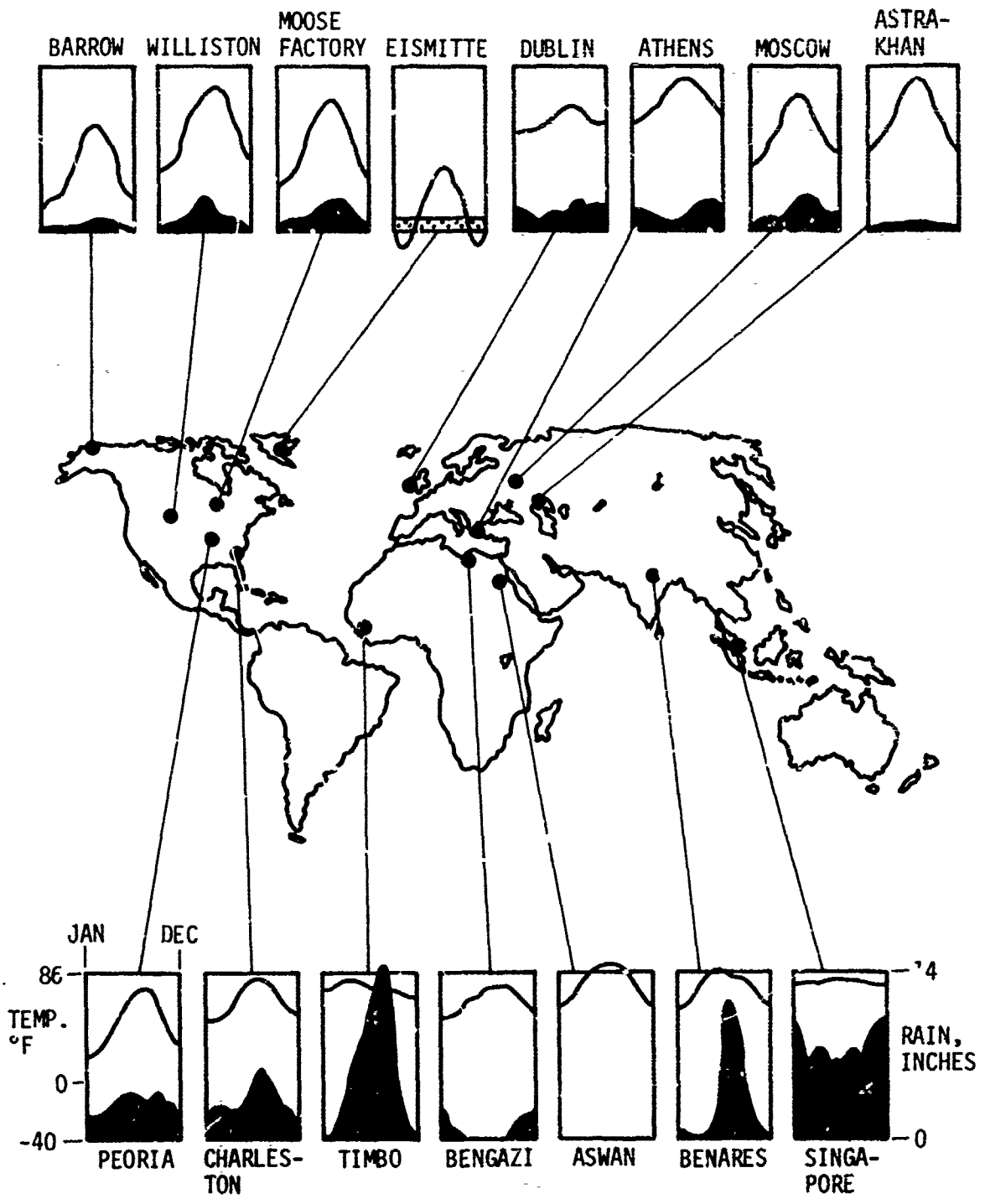

REPRESENTATIVE WORLD CLIMATES
BARROW
WILLISTON
MOOSE FACTORY
EISMITTE
DUBLIN
ATHENS
MOSCOW
ASTRA-KHAN
JAN
DEC
86
TEMP. °F
0
-40
4
RAIN, INCHES
0
PEORIA
CHARLES-TON
TIMBO
BENGAZI
ASWAN
BENARES
SINGA-PORE

Figure 1

REPRESENTATIVE CLIMATES IN U.S.A.

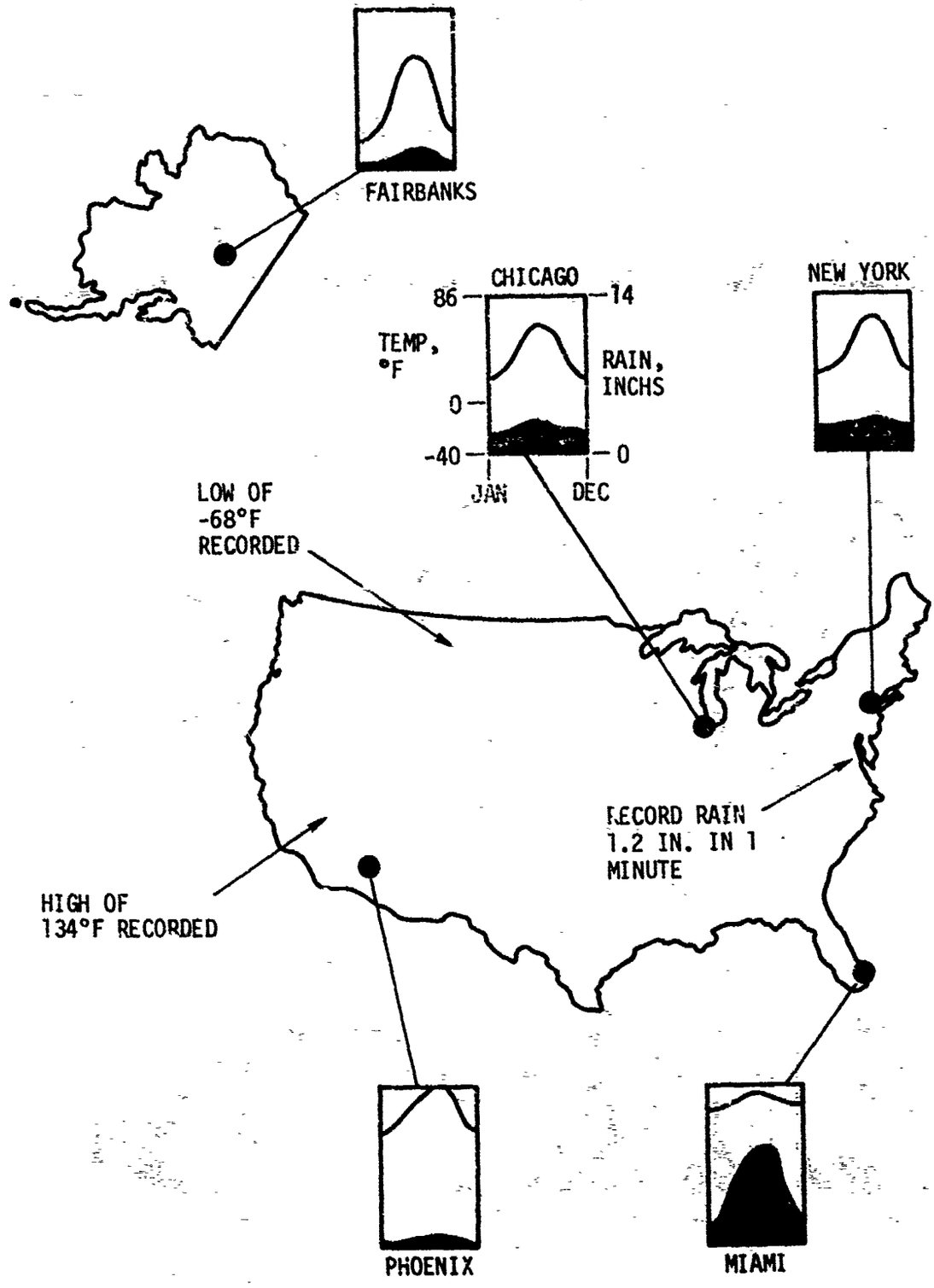


Figure 2

ANNUAL SOLAR RADIATION

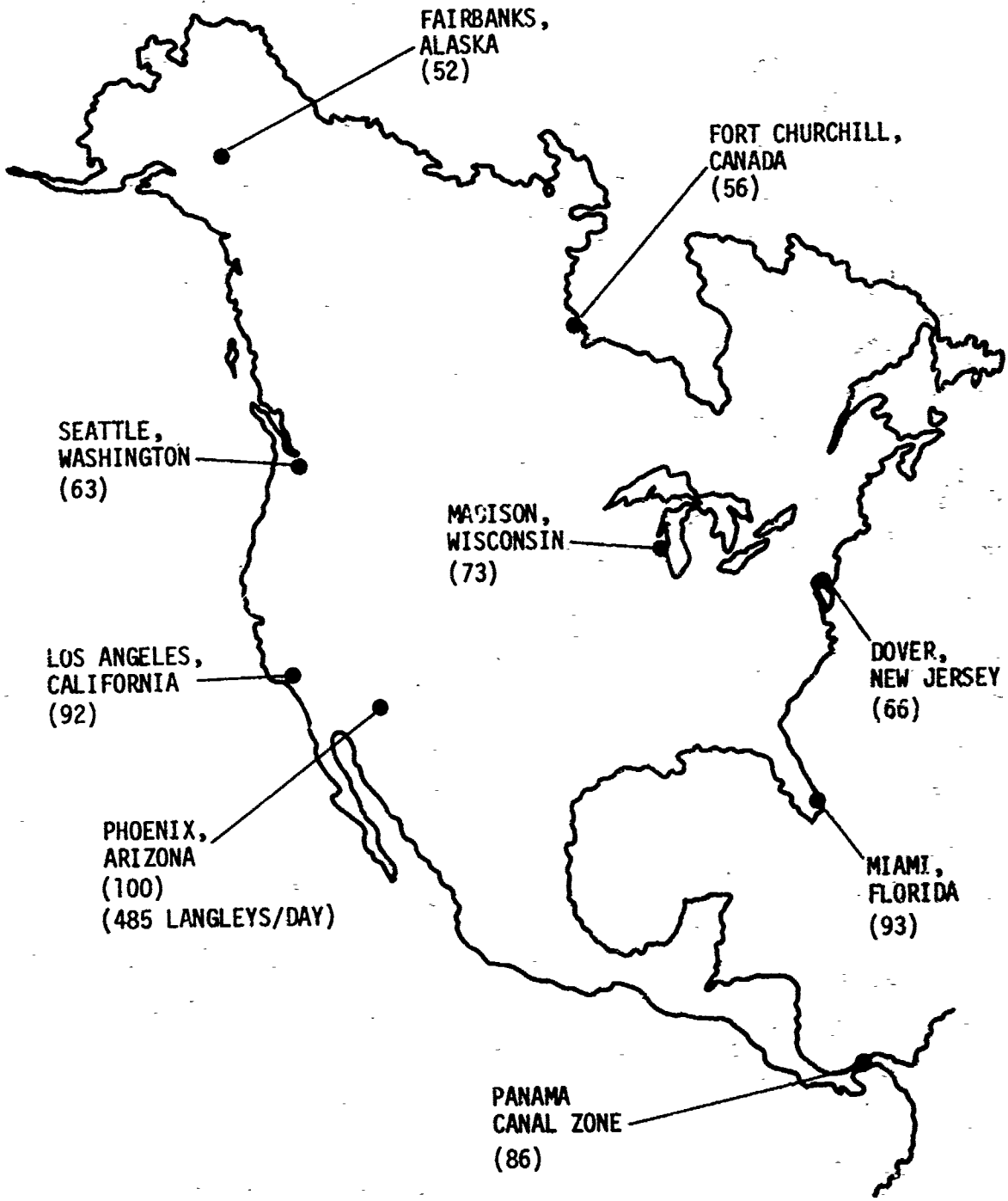


Figure 3

MICROCLIMATE

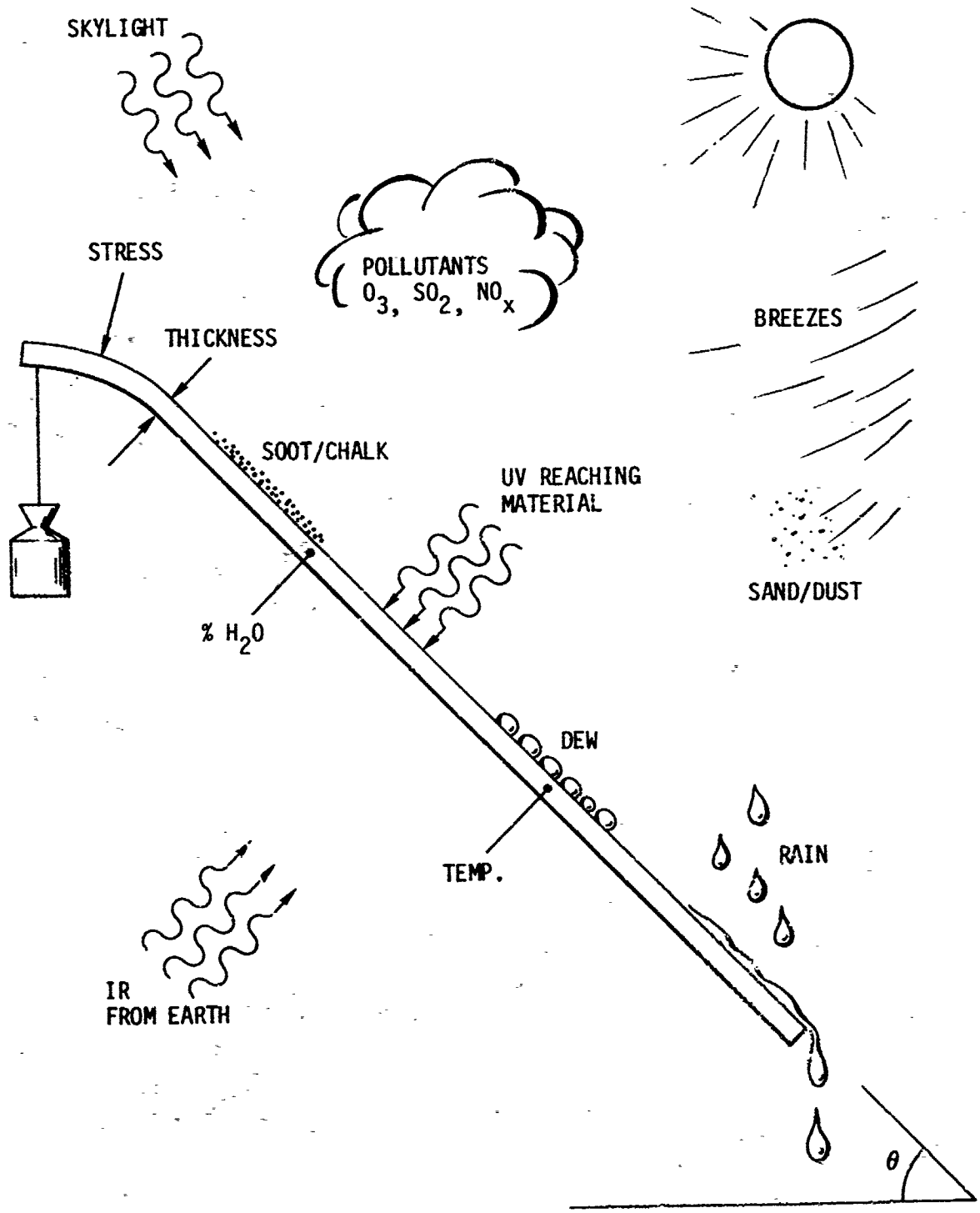
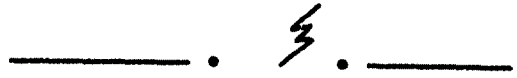


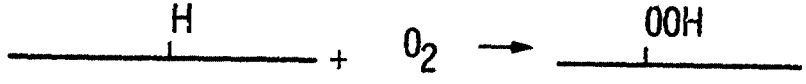
Figure 4

WEATHERING MECHANISMS

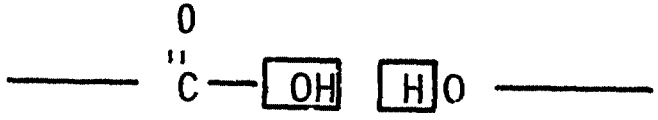
CHAIN SCISSION



OXIDATION



HYDROLYSIS



CROSSLINKING



CRYSTALLIZATION



EROSION



BIOLOGICAL (FUNGI, BACTERIA, ANIMALS)

Figure 5

FAILURE MODES

- EMBRITTLEMENT
- LOW TENSILE (TOTAL DETERIORATION)
- SURFACE EFFECTS
- CRACKING / CRAZING
- HAZE
- COLOR

Figure 6

AT LAST, A MEANINGFUL WINDSHIELD LIFE TEST

J. B. Olson
Sierracin/Sylmar
Sylmar, California

AT LAST, A MEANINGFUL WINDSHIELD LIFE TEST

Jan B. Olson
Chief Engineer
SIERRACIN/SYLMAR

ABSTRACT

Sophisticated aircraft windshields designed to FAR Part 25 requirements, including those of all commercial airliners, are somewhat unique among aircraft components in that they serve two critical functions, and have two different service life considerations as a result. First, being part of the pressurized aircraft structure, they must satisfy all structural safety requirements including fail-safe and fatigue life considerations, plus bird impact resistance, and are thoroughly tested under FAA scrutiny to prove that they do. The actual service life of these windshields, however, is almost always determined by a failure to perform the second function, that being the ability to provide adequate visibility in a variety of environments including icing conditions.

Characteristically, these windshields are laminated and electrically anti-iced, and failure is usually a delamination and/or breakage of the non-structural outer ply or electrical failure in the anti-ice coating or temperature sensor. FAA concern in this area is primarily the safety-of-flight implications of how it fails, but how often it fails is an economic consideration only, and therefore left to the prime contractor to evaluate and control. Life testing, therefore, has been less formal and standardized, and almost without exception has not duplicated "real world" conditions well enough to prevent disappointments when the design enters service.

This paper describes a new windshield life test facility, Sierracin's Windshield Flight Environment Simulator (WFES), which not only more closely duplicates all conditions experienced by a windshield than has ever been possible before on an accelerated basis, but it allows the test to be performed in representative structure, which in many cases has considerable influence on the performance of a windshield. Originally used to evaluate Boeing 747 design improvements, the facility is currently in operation using an entire cab structure from a Lockheed L-1011, which, coupled with the WFES's accurate flight simulation, undoubtedly represents the most realistic windshield test program ever conducted.

Windshield Qualification Testing -- Historically

All aircraft windshields, from the simplest to the most sophisticated, perform two prime functions -- keeping the wind out (and air in, in the case of pressurized aircraft), and providing adequate forward vision. The conditions in which the windshield is expected to perform these functions varies considerably among aircraft types. In the simplest case, that of an unpressurized light aircraft, very little more is required of the windshield than that it perform these two functions in nominal conditions. At the other end of the spectrum is the sophisticated commercial airliner windshield designed to FAR Part 25, which includes structural requirements of fatigue life, fail-safe and bird resistance as well as maintenance of visibility in adverse weather conditions such as severe icing. Conformance to these safety-of-flight requirements must be verified under careful FAA scrutiny, and this is done very formally in the certification process.

Characteristically these more complex windshields are laminated and electrically anti-iced. Equally characteristically, failure is in the form of delamination and/or breakage of the non-structural outer ply, or electrical failure of the anti-ice heater element. Because these failures have no structural implications, FAA's concern is limited to the safety-of-flight considerations of the failure; e.g., if the glass can break, is the break pattern large enough to provide adequate vision or is alternate vision available. In other words, FAA's chief concern in the area of windshield durability and service life is limited to how, not how often a windshield fails.

The issue of how often a windshield fails is primarily an economic consideration, and it is therefore left to the prime contractor to establish requirements and verify that they are met. For this reason, life testing is considerably less formal, less rigorous and less consistent than are the FAA-monitored structural and fail-safe tests. This testing varies considerably among aircraft types and builders, and the only thing reasonably consistent has been that test realism is usually subordinated to economic and equipment limitation considerations. In the past, these accelerated life tests have not been sufficiently realistic of all conditions and hazards encountered by a windshield to prevent disappointment when the design enters service.

A New Concept Needed

Traditionally, the real world of actual service has been the test bed on which windshields have been developed and refined. As windshields become increasingly sophisticated, they become both more expensive and more failure prone, and the economics of service life become more and more significant. At the time, the Boeing 747 windshield was undoubtedly the most novel and most

ambitious windshield concept in recent history, based on its glass-faced plastic (composite) construction, extensive metal subframing, large size and curved shape (see Figure 1). As such, it was the most expensive windshield of its type and the most probable to encounter initial service problems and require considerable design refinement before achieving its service life goal. The usual slow and cumbersome process of evolutionary design improvement based on service experience feedback progressed through the first five years on the 747 windshield. This history is covered in more detail in Reference 1.

While aided by the fact that, due to the inherent reworkability of the design, every failed part was returned to the manufacturer and a failure analysis performed, this process was slow and getting slower as performance improved. As the design approached a level of service life acceptability, there was less receptiveness to the introduction of novel design changes, even on a limited basis for the purpose of in-service evaluation. This, coupled with the excessive design negotiation/fabrication/service evaluation time span, severely hindered further improvement based on this conventional approach.

Not being satisfied with the performance of the design at this stage, Sierracin set about to develop a test facility which would duplicate all of the significant aspects of the real world environment on an accelerated basis. The facility that evolved from that activity is called the Sierracin Windshield Flight Environment Simulator (WFES) which, along with the history of testing to date, is the subject of this paper.

Design Criteria

The service and laboratory experience that had been gained on the 747 windshield, and its subsequent counterpart, the Lockheed L-1011 windshield (see Figure 2), suggested that two of the three aspects of the actual service environment which play key roles in determining the service life of a windshield are, in fact, almost always missing in conventional accelerated life testing. These essential conditions are (1) weathering, and (2) representative temperatures and temperature gradients within and adjacent to the heated area. The third important factor, pressurization deflection, is usually present in conventional testing.

Weathering

Results from actual service exposure, confirmed by weatherometer testing in the laboratory, showed that moisture ingress into the interlayer coupled with ultraviolet (UV) radiation has a significant effect in reducing the laminate integrity. Conventional qualification testing rarely, if ever, acknowledges and imposes these conditions.

Temperature and Temperature Gradients

Conventional accelerated life testing on windshields usually employs a representative outside air temperature (OAT), but does not duplicate the convective heat loss or "cooling rate", Q_c, of high speed flight in dry air. This convective heat loss, Q_c, equals the product of the convective film coefficient, h_c, and the temperature differential between the windshield's outer surface and the adjacent boundary layer, or $Q_c = h_c \Delta T$, $\Delta T = T_s - T_{bl}$.

The worst-case flight simulation condition is the one in which high h_c and low boundary layer temperature (T_{bl} = OAT plus "ram rise") combine to create the highest Q_c, hence the coldest windshield surface temperature. As shown in Figure 3 for the L-1011, this occurs at 30,000 feet with an h_c of 29 BTU/hr ft^2 °F and a cold-day OAT of -80°F.

In conventional testing, a less-than-realistic power density is produced by the anti-ice heater because the heater element, which would be in a full demand mode delivering full power in actual flight, instead is in a control mode with resultant power reduction in conventional low airflow testing. Figure 4 shows that a typical 2000 BTU/hr ft^2 (4 watts/sq. in.) windshield will deliver full power operating at some temperature below the controller set point in a realistic -65°F, h_c = 29 BTU/hr ft^2 °F environment, but will be limited by the controller to deliver only about one watt/square inch in a conventional test with an h_c of about 4 BTU/hr ft^2 °F. Paradoxically, this reduced power and h_c test condition allows the heated area to operate considerably warmer than in actual flight, and, as a result, does not produce appropriately steep thermal gradients across the windshield's cross section. As can be seen on Figure 4, the ΔT (temperature of windshield's outer surface above that of the boundary layer air) is about 145°F, for a comfortable +80°F windshield temperature in a typical -65°F conventional test, versus a ΔT of about 70°F in the more realistic h_c = 29 case, with a near zero Fahrenheit surface temperature. This, of course, means that differential expansion and low-temperature material "hardening" problems in actual flight conditions are not recreated in the heated area in a conventional test -- a glaring omission in light of today's understanding of windshield performance factors.

Another, perhaps more significant aspect of this unrealistically low h_c is that lateral heat transfer in the materials, particularly the outer ply which is usually high conductivity glass, tends to "smear out" the transition from the heated area to the unheated "cold edge". As can be seen in Figure 5, this edge thermal gradient is about twice as steep with a realistic Q_c as in the nearly "still air" conventional test.

Exaggeration of ΔT by lowering the air temperature or raising the heater temperature to unrealistic values in order to achieve a realistic Q_c (remember $Q_c = h_c \Delta T$) is not valid because of the considerable variation of material properties with temperature. In other words, it is necessary to duplicate h_c directly, which means considerably more mass flow of air over the surface than has been typical in conventional testing.

Based on this knowledge, a commitment to produce a specialized test facility for accelerated windshield life testing was made by Sierracin. The design requirements for this facility were as follows:

1. Ability to reproduce the convective film coefficient, h_c, of all flight conditions.
2. Duplication of the boundary layer temperature (OAT plus "ram rise") of all flight conditions.
3. Reproduction of the pressurization deflection and resultant stressing of the windshield.
4. Maintenance of cabin-side temperature.
5. Realistic application of windshield power.
6. Duplication of air flow pattern on windshield surface.
7. To the extent possible, reproduction of the fuselage deflections at the windshield interface.
8. Realistic sequencing of all of these conditions into a representative flight profile on a compressed time scale.
9. Inclusion of the effects of moisture, ultraviolet exposure and rain.
10. Visual and photographic observability of windshields under test.

WFES Facility

These conditions have all been met with the facility called the Windshield Flight Environment Simulator, or WFES. The analytical design and constructional features are covered in considerably more detail in an earlier paper on the subject, Reference 2. Basically, the WFES consists of two side-by-side specialized wind tunnels, independently operated for maximum test flexibility, in which the throat area has, as one wall, the windshield being tested (see Figure 6). The opposite wall is a clear vision port

or transparent shroud about the same size as the test windshield, permitting full observability during test. The "throat" section between these surfaces, along with the intake and exhaust sections and guide vanes if required, are designed to produce airflow patterns representative of flight.

Liquid cooling mediums with higher heat capacities to attain a realistic h_c at low velocities were ruled out as being nonrepresentative in terms of evaluating seal performance, and they hinder visibility. Instead, large centrifugal blowers are used to create high speed air flow and liquid nitrogen, LN_2, is used as the cooling medium supplied from a 20 ton cryogenic storage tank. The orientation of these components in the 747-configured facility is shown schematically in Figure 7 and photographically in Figure 8, while Figure 9 shows the control and monitoring equipment currently installed.

LN_2 was chosen over the more conveniently available CO_2 because of its close match to the properties of air, so that its variable introduction into the air stream for cooling would not appreciably change the h_c. In its original configuration for testing the 747 windshield, a "boiler plate" cockpit structure for mounting and pressurizing the windshield was designed and constructed to create the same structural deflections as measured on actual 747 structure by Boeing.

The determination of air velocity required to attain a realistic convective film coefficient, h_c, was based on the following consideration. From Reference 3 which covers the subject of windshield thermal design in more detail, two commonly used equations for the convective film coefficient of air are:

$$h_c = \frac{.656\ (VP_o)^{.8}}{y^{.2}\ T_{avg}^{.5}} \quad \text{for turbulent flow}$$

and

$$h_c = .13 \left(\frac{VP_o}{y}\right)^{.5} \quad \text{for laminar flow,}$$

where:

- V is velocity in ft/sec
- P_o is atmospheric pressure in inches H_g
- y is distance from stagnation point in ft, and
- T_{avg} is average of surface and boundary layer temperature $\frac{T_s + T_{bl}}{2}$ in °R.

As can be seen in either equation, the product V x P_o is a constant for any h_c desired in test. In creating a representative h_c, we are able to take advantage of the density of sea level air, so that the actual velocity need not be duplicated in order to attain the h_c of high altitude flight. For instance, we duplicate the h_c of high altitude cruise at an airflow velocity about 30% of aircraft speed because the density (reflected in P_o) at sea level is 3.36 times that at 30,000 feet.

The shape of inlet and outlet ducting as well as the tapered spacing between the transparent shroud and the windshield are carefully designed to provide accurate velocity distribution and airflow direction over the face of the windshield. On both the 747 and L-1011 program, wind tunnel data of the type shown on Figure 10 for the L-1011 was available. Tuft studies were conducted as shown in Figure 11, and ducting and guide vanes modified as required to accurately duplicate the airflow pattern and velocity distribution.

Moisture and UV are introduced separate from "flight" cycles, as they require longer soak periods and cannot be accelerated at the same rate as the flight parameters.

WFES Capabilities

As currently configured, the capabilities of the WFES are as follows:

Test Condition

Airspeed over windshield	-- 2-200 knots (230 mph)
Maximum heat transfer coefficient, h_c	-- 35 BTU/hr ft^2 °F (roughly equivalent to 800 mph at 35,000 feet)
Outside air temperature	-- -100°F to +120°F (without heaters)
Cabin pressure differential	- 0-15 psi
Environmental conditions	-- moisture, UV and rain

Present control, instrumentation and recording capability and safety features consist of the following (independent for each "hand" or aircraft except as noted):

Control

- Cockpit-side pressure (not independent for each hand on L-1011)
- Outside air velocity
- Outside air temperature
- Anti-ice heater operation (use of actual controller preferred)
- Cycle times and sequencing

Instrumented and/or Recorded

- Electrical to windshield -- voltage and current
- Anti-ice heater resistance
- Redundant sensor resistance

Cockpit pressure

Outside air velocity

Selected windshield temperatures

Windshield deflection

Pressure cycles

Fail-Safe "Shut-Down" -- initiated by:

Windshield temperature, high limit

Outside air temperature, low limit

Power failure

Blower vibration

There is nearly limitless potential for the addition of features such as high aerodynamic heating for supersonic aircraft, shock or vibration loads, other instrumentation, etc.

Windshield Life Test

In designing a life test profile for the 747, we constructed an idealized typical flight profile as shown in Figure 12. We then selected three cruise boundary layer temperature conditions of -40°F, -60°F and -90°F, the latter being more severe than actual worst-case in assuming a -90°F OAT with no ram rise. The accelerated, but coordinated temperature/cabin pressure differential profiles for these three flight conditions are shown in Figure 13. The hold time at each air temperature was selected to allow attainment of near steady state temperature conditions in the windshield, and is therefore longer at the lower temperatures. Fast temperature recovery during the accelerated "descent" phase is aided by compressive heating from the blowers. The pressure differential was exaggerated to account for creep deflection and, at 10 psi, represents the pressure required in these short cycles to accomplish the same deflection as occurs in an eight hour flight at the normal 8.9 psi operating pressure differential. A total flight cycle is completed in 12, 20 and 30 minutes, respectively, for -40, -60 and -90°F air temperature conditions.

These three flight conditions along with an extreme humidity cycle and a rain/UV cycle were programmed as shown in Figure 14. The weathering cycles, which cannot be accelerated to the same degree, were programmed to take advantage of the longer unmanned overnight and week-end periods. This program allowed the windshield's entire lifetime to be compressed into a six to eight week period.

Eureka!

The major triumph in the life cycle testing of the 747 windshield was the day when a failure, identical in every detail to the predominant service failure mode, was reproduced in test. To that point, we had not been able to duplicate the typical service failure and did not, therefore, have confidence in any laboratory verification of proposed "fixes". With this breakthrough, we now had a tool with which to analyze and correct known deficiencies on the 747 windshield, and did so over a period of about 14 months involving 24 test windshields.

Other Specialized Tests

Several other types of tests or investigations have been conducted using the special capabilities of the WFES. These have included:

1. testing the windshields' resistance to extreme low temperatures as a function of exposure time in actual service (returned, but unfailed windshields)

2. testing windshields' ability to withstand loss of power (as in a controller failure) as a function of air temperature and aging effect (also returned windshields)

3. obtaining thermal data on "cold" edges, transition zones, etc.

4. witnessing relative deflections between frame and windshield in "flight" and observing the performance of existing and proposed weather seal configurations when exposed to this deflection at realistic thermal conditions

5. witnessing faceply shedding characteristics for vision restoration as a function of flight conditions

In most of these tests, the observability of the windshield during tests is as valuable a consideration as the accurate duplication of the actual flight conditions. It gives the designer the opportunity to closely examine relative deflections, component performance or failure sequence of a windshield "in flight" to a degree never before possible.

A recent example of a special use of the facility was in optimizing the design of internal edge heaters. These are thin, nontransparent heater strips slated for incorporation in the interlayer edges of the 747 windshield to reduce the severity of the edge thermal gradients shown in Figure 3. An instrumented prototype part was constructed and run in the WFES with closely spaced thermocouples at right angles to the edge as shown in Figure 15. The edge heater power density was varied until the

optimum temperature condition was achieved, as shown in Figure 16. Note that the edge heaters are not at the same level as the anti-ice element and the insulation caused by an overlapping sealant adds to the difference, so its optimum power density is not the same as the anti-ice coating.

Next, the L-1011

Based on a number of refinements that evolved from, or were verified by WFES testing, the 747 windshield design was upgraded to the point where it would not fail in the WFES in any reasonable time. This did not convince us that we have an invincible windshield, or even that it represents the ultimate stage in this design concept. It simply meant that we have a considerably improved windshield and must await the results of actual service experience to uncover the next life-limiting factor, and revise or recalibrate the WFES and life test to duplicate it.

At that time, Lockheed wanted to use the WFES to improve the performance of the L-1011 windshield. Unlike the 747 design which isolates the windshield from structural loads as has been the practice for earlier all-glass windshields, the L-1011 design deliberately carries those loads through the windshield (compare windshield mounting concepts shown in Figures 1 and 2). The deflection characteristics and imposed loads on the windshield because of its interaction with the surrounding structure are significant, and testing in anything but a realistic structure would be meaningless.

For this reason, it was decided the L-1011 windshield testing would be conducted in a flight-weight cockpit structure which would be interfaced with WFES as shown in Figure 17. An actual L-1011 flight station section was obtained and modified by Lockheed for use as a windshield test bed. Figure 18 shows this structure being positioned in the WFES facility. Figure 19 shows the L-1011 flight station installed in the WFES, making this, to the best of our knowledge, the most realistic accelerated aircraft windshield test program ever attempted.

The WFES, as now configured, contains both 747 and L-1011 windshield test sections. One or both sides of either model can be under test simultaneously, the conversion from one to the other consisting essentially of simply swapping blower-to-test section transition ducts.

WFES Test Summary To Date

Up to this writing, a total of 38 windshields, either 747 or L-1011, have been or are being tested in the WFES. The breakdown of these is as follows:

--	test set-up and calibration	-- 4
--	service life calibration (existing designs)	-- 7
--	service life determination (new and proposed)	-- 5
--	determination of aging effects (parts returned from service)	-- 13
--	special purpose or condition tests	-- 9
	Total	38

To date, more than 23,000 controlled, fully instrumented and closely observed "flight" cycles have been conducted on these windshields over a period of 22 months. During this time, several design refinements have been developed and/or evaluated, some adopted, some pending or in the process of incorporation, some discarded and others "waiting in the wings". Due to the first-in, first-out spares philosophy on the 747, a service feedback time lag exists such that we are just beginning to receive significant service data on changes adopted over a year ago, and it is very encouraging. Extrapolating from these "early returns", a service life increase of from 20-70% is expected with the current 747 windshield over the preceding version.

Currently, the WFES is dedicated to the development and evaluation of more fundamental changes which are potentially capable of providing dramatic service life increases, with a 200-300% improvement being the goal. Foremost among these are a more durable, higher light transmission anti-ice coating, Sierracote® 343B, and a soft, tough cast silicone interlayer designated S-100. A revolutionary moisture seal concept is also under development in the WFES.

Future Plans

Programs conducted to date have been aimed at improving existing designs with deficiencies which escaped detection in conventional development and qualification testing, but which showed up in actual service. It is hoped that in future major windshield programs, especially those which push the state-of-the-art in the many aspects affecting performance (materials, environment, size, shape, structural interaction, etc.), this life testing concept will be used to avoid such expensive experiences as have occurred in the 747 and L-1011 programs. The Rockwell B-1 fits this description in all respects, and should be the next major candidate for this type of testing. In fact, the WFES was configured to accept a B-1 cockpit section as depicted in Figure 20, should the opportunity arise.

Conclusions

The Sierracin Windshield Flight Environment Simulator (WFES) has proven the importance of full simulation of the service and flight environment in life testing aircraft windshields.

It has been used successfully on existing designs to accurately reproduce known service deficiencies, and has provided the means for developing and verifying "fixes". On future designs, the WFES should enable us to avoid, or at least dramatically reduce, the previously unavoidable and expensive process of design refinements based on feedback from actual service. While somewhat expensive in itself due to high LN_2 consumption (approximately eight tons per day), the WFES-type testing will pay for itself many times over by preventing otherwise expensive service problems before a design enters production. Service reliability will be pre-established with greater confidence than ever before. The more complex or novel the design, the more it will benefit from this concept.

REFERENCES:

1. "Design Considerations Affecting Performance of Glass/Plastic Windshields in Airline Service", Jan B. Olson, Sierracin, February 1973

2. "Windshield Flight Environment Simulator", L. G. Campbell, J. W. Marshall, Sierracin, April 1974

3. "Anti-Icing Aspects of Helicopter Windshield Design", Phillip A. Miller, Sierracin, May 1972

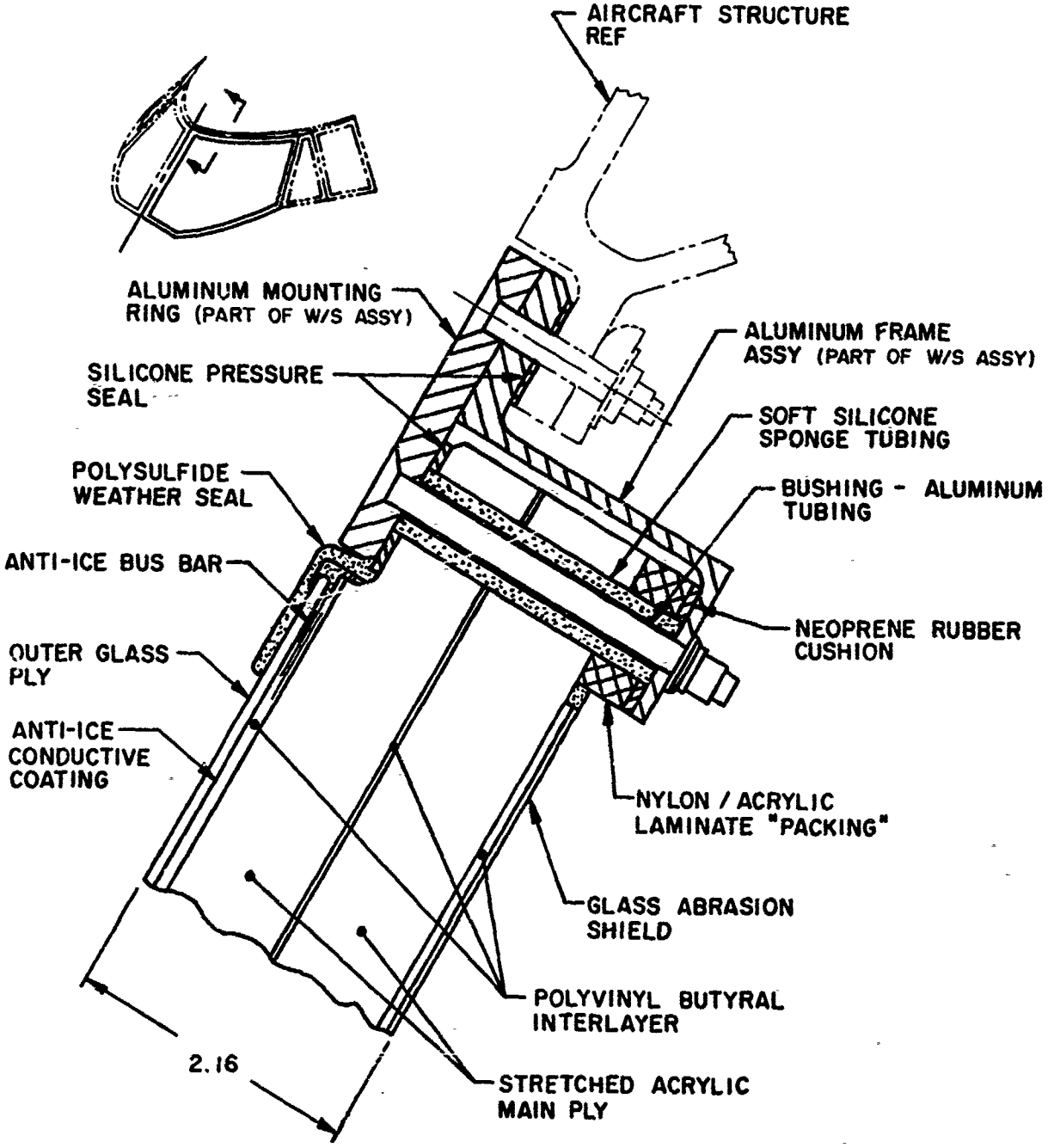


FIGURE 1
747 WINDSHIELD CROSS SECTION
(FULL SIZE)

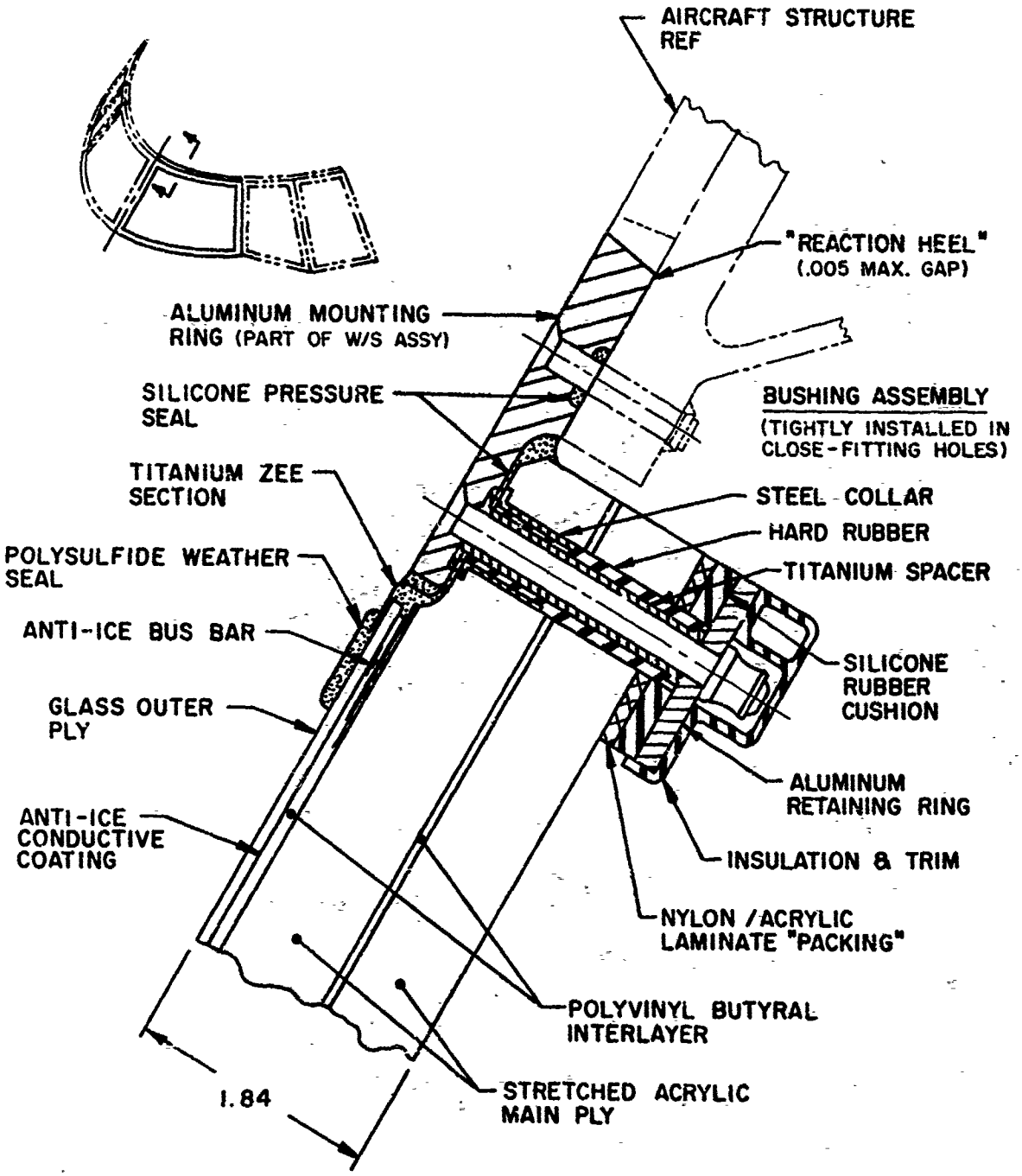


FIGURE 2

L-1011 WINDSHIELD CROSS SECTION
(FULL SIZE)

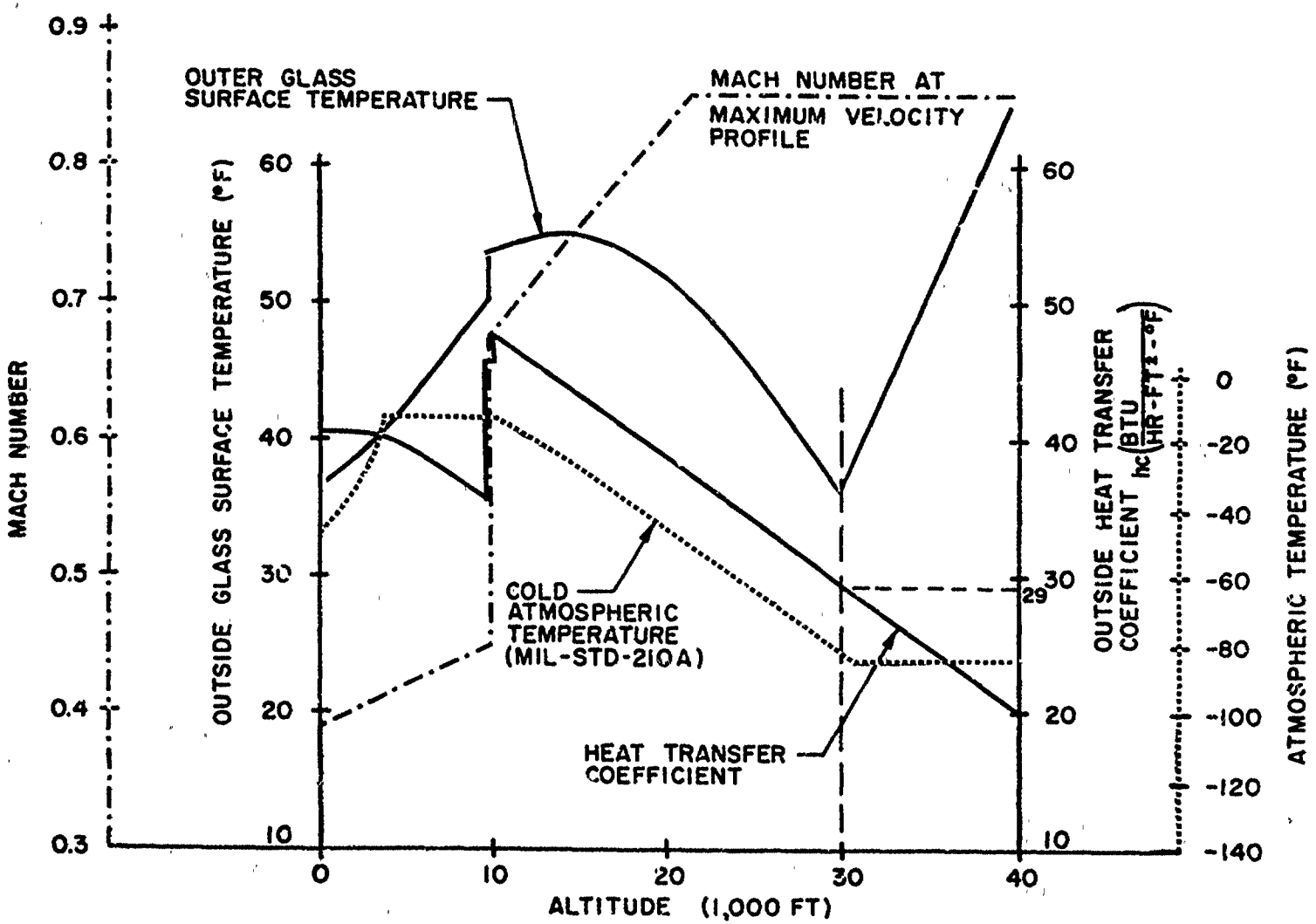
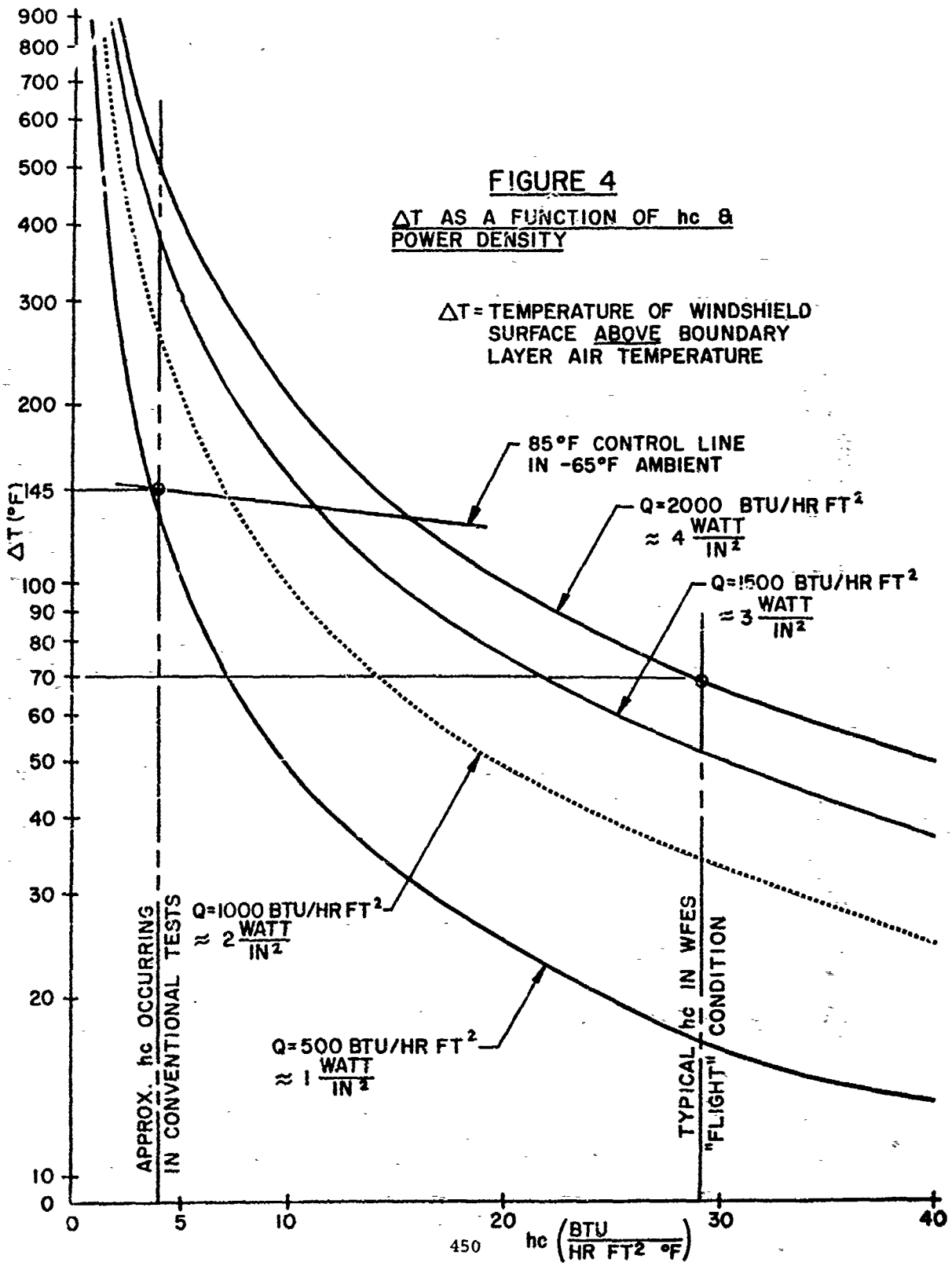


FIGURE 3

TYPICAL L-1011 FLIGHT CONDITIONS


FIGURE 4
ΔT AS A FUNCTION OF hc & POWER DENSITY
ΔT = TEMPERATURE OF WINDSHIELD SURFACE ABOVE BOUNDARY LAYER AIR TEMPERATURE
85°F CONTROL LINE IN -65°F AMBIENT
Q=2000 BTU/HR FT² ≈ 4 WATT/IN²
Q=1500 BTU/HR FT² ≈ 3 WATT/IN²
Q=1000 BTU/HR FT² ≈ 2 WATT/IN²
Q=500 BTU/HR FT² ≈ 1 WATT/IN²
APPROX. hc OCCURRING IN CONVENTIONAL TESTS
TYPICAL hc IN WFES "FLIGHT" CONDITION
ΔT (°F)
hc (BTU/HR FT² °F)
900
800
700
600
500
400
300
200
145
100
90
80
70
60
50
40
30
20
10
0
0
5
10
20
30
40

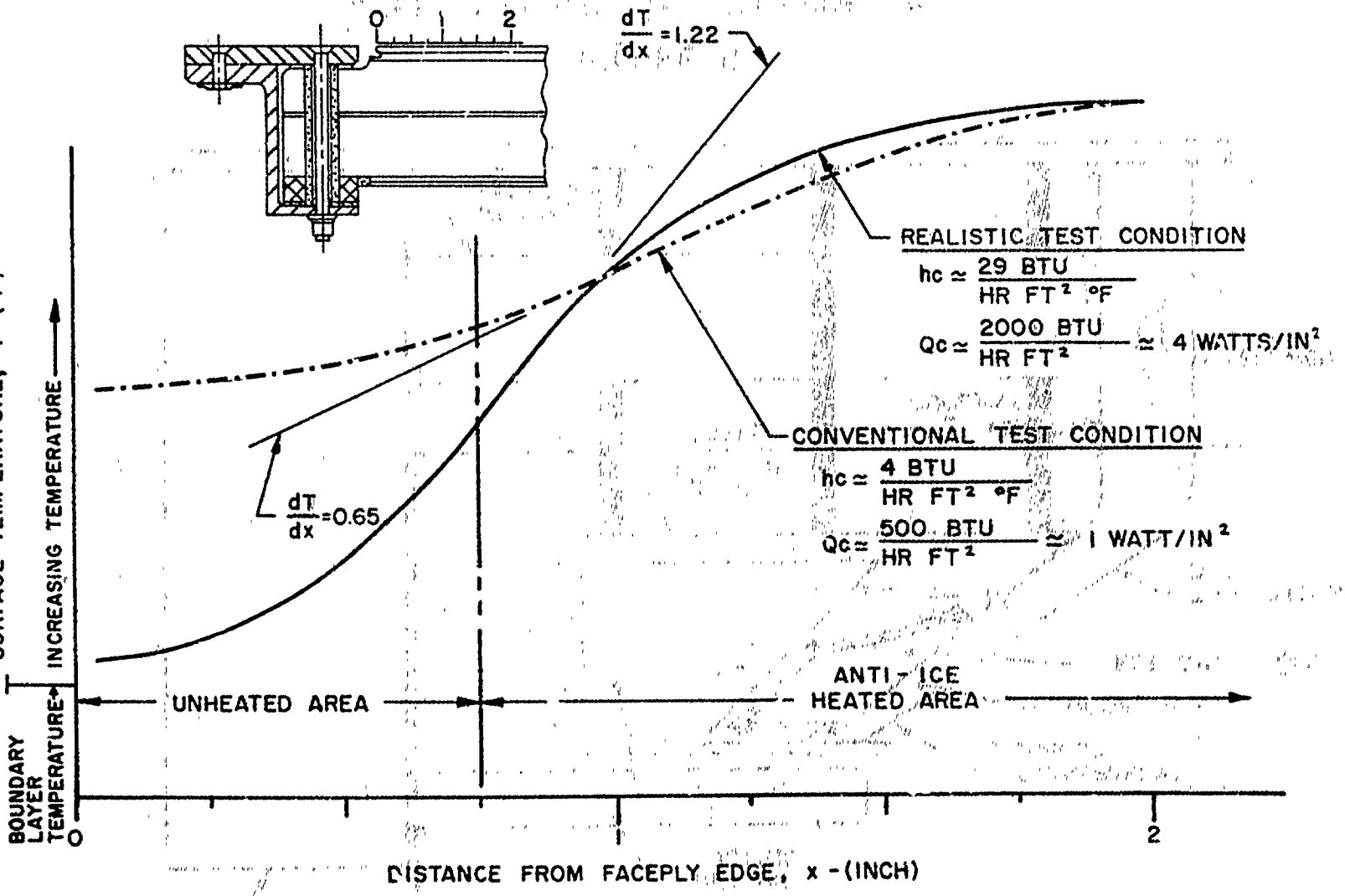


FIGURE 5

TEST CONDITION EFFECT ON EDGE THERMAL GRADIENT

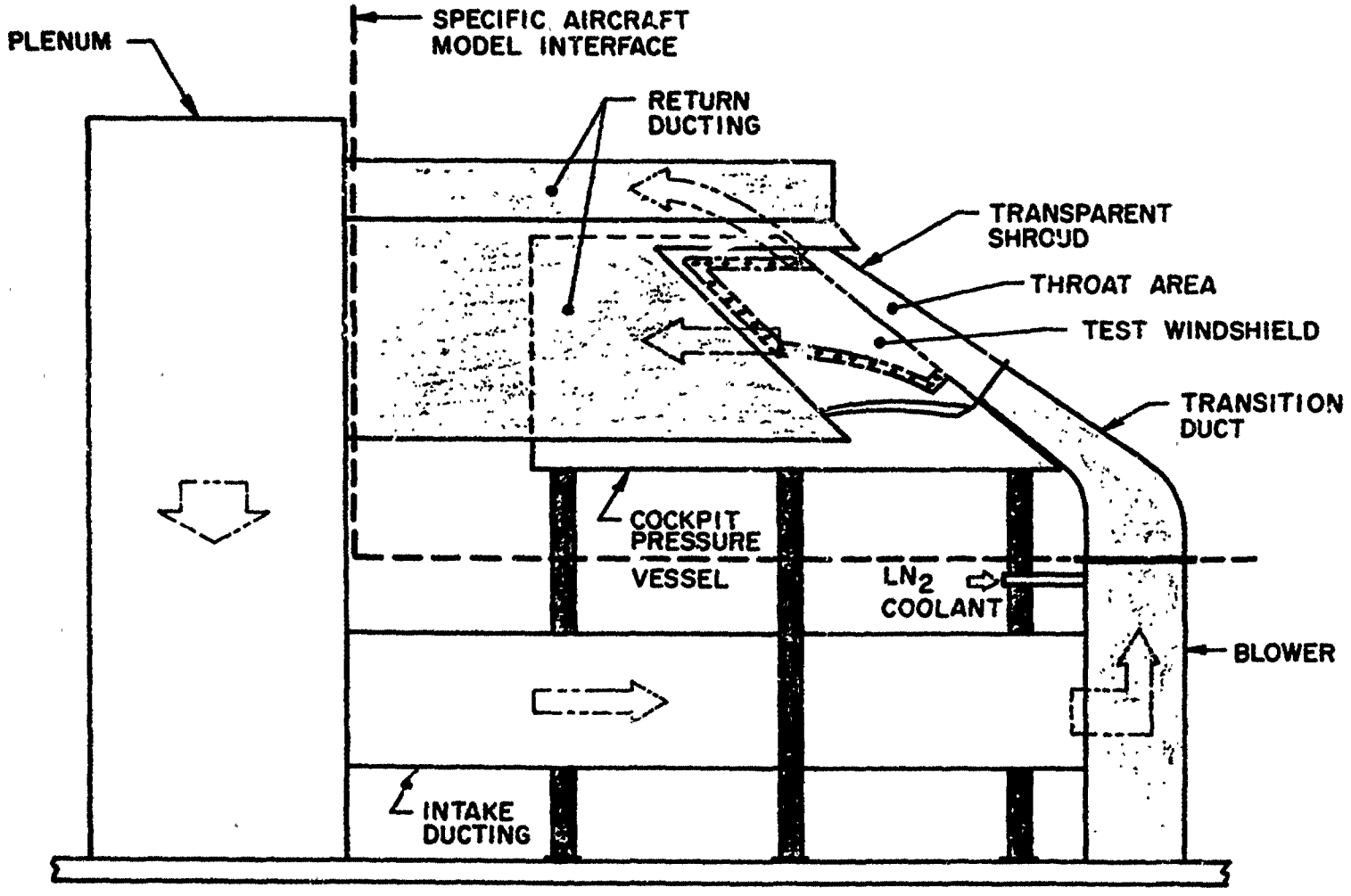


FIGURE 6

WFES SCHEMATIC – 747 CONFIGURATION

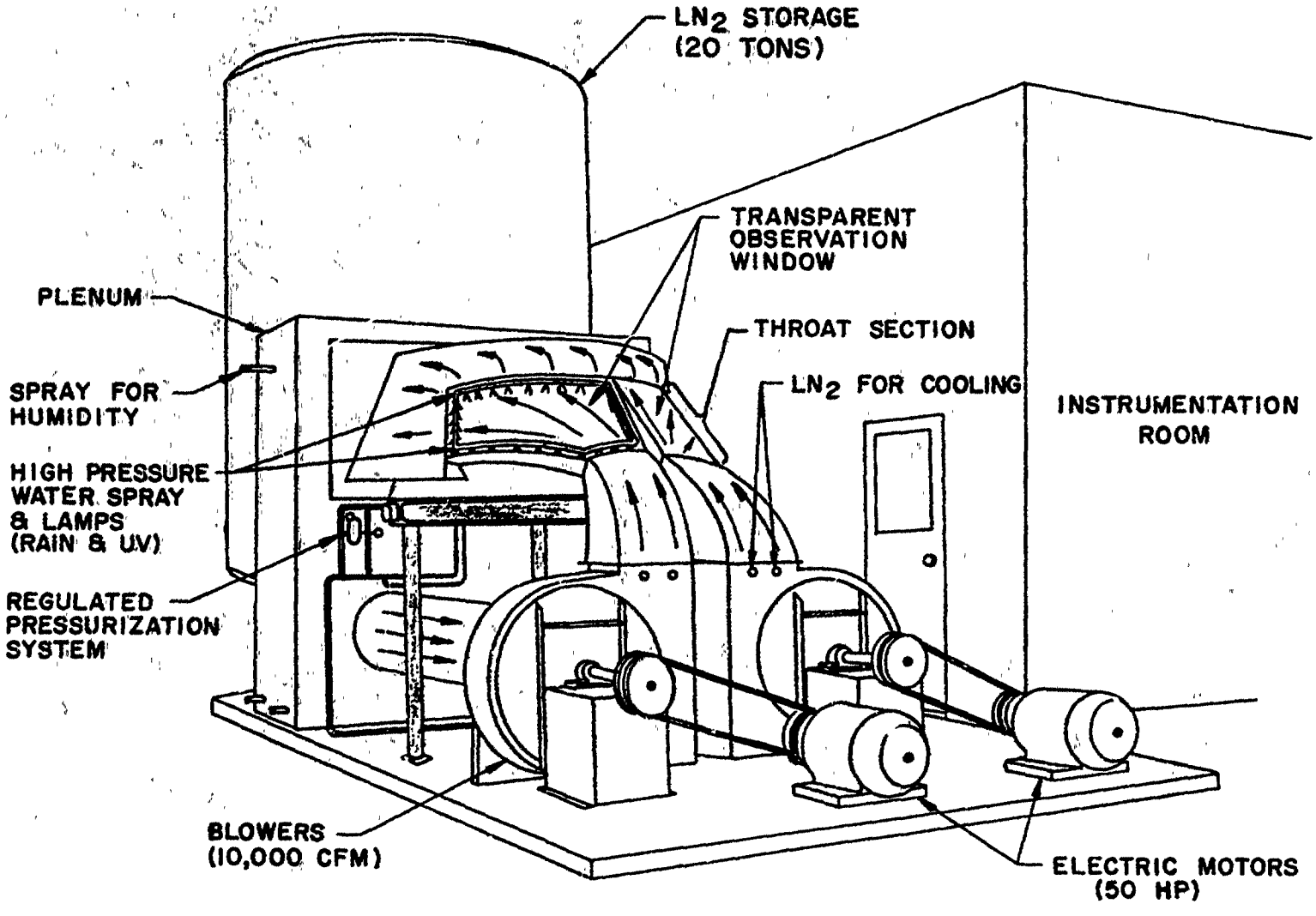


FIGURE 7

SIERRACIN/SYLMAR WINDSHIELD FLIGHT ENVIRONMENT SIMULATOR

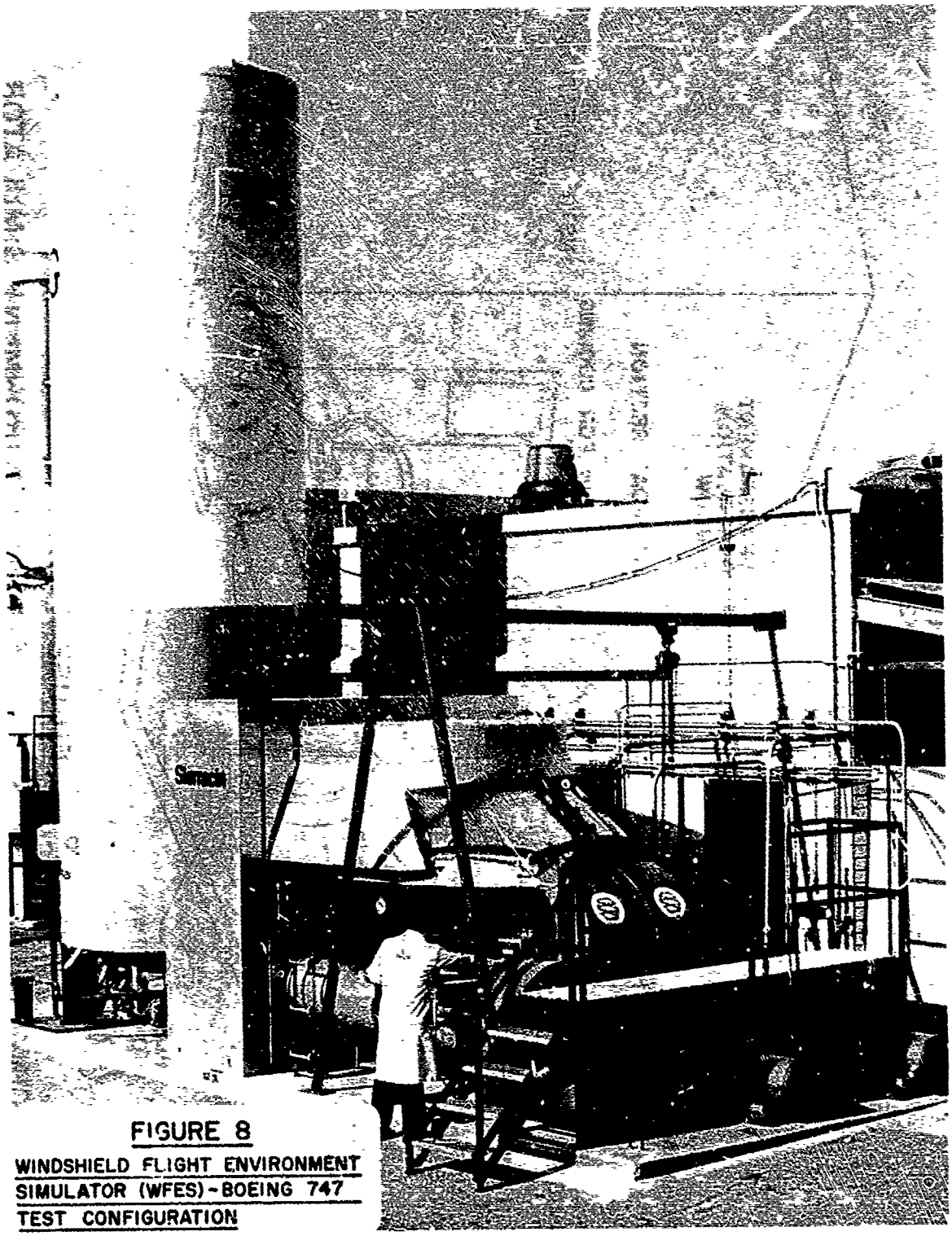


FIGURE 8

WINDSHIELD FLIGHT ENVIRONMENT SIMULATOR (WFES) - BOEING 747 TEST CONFIGURATION

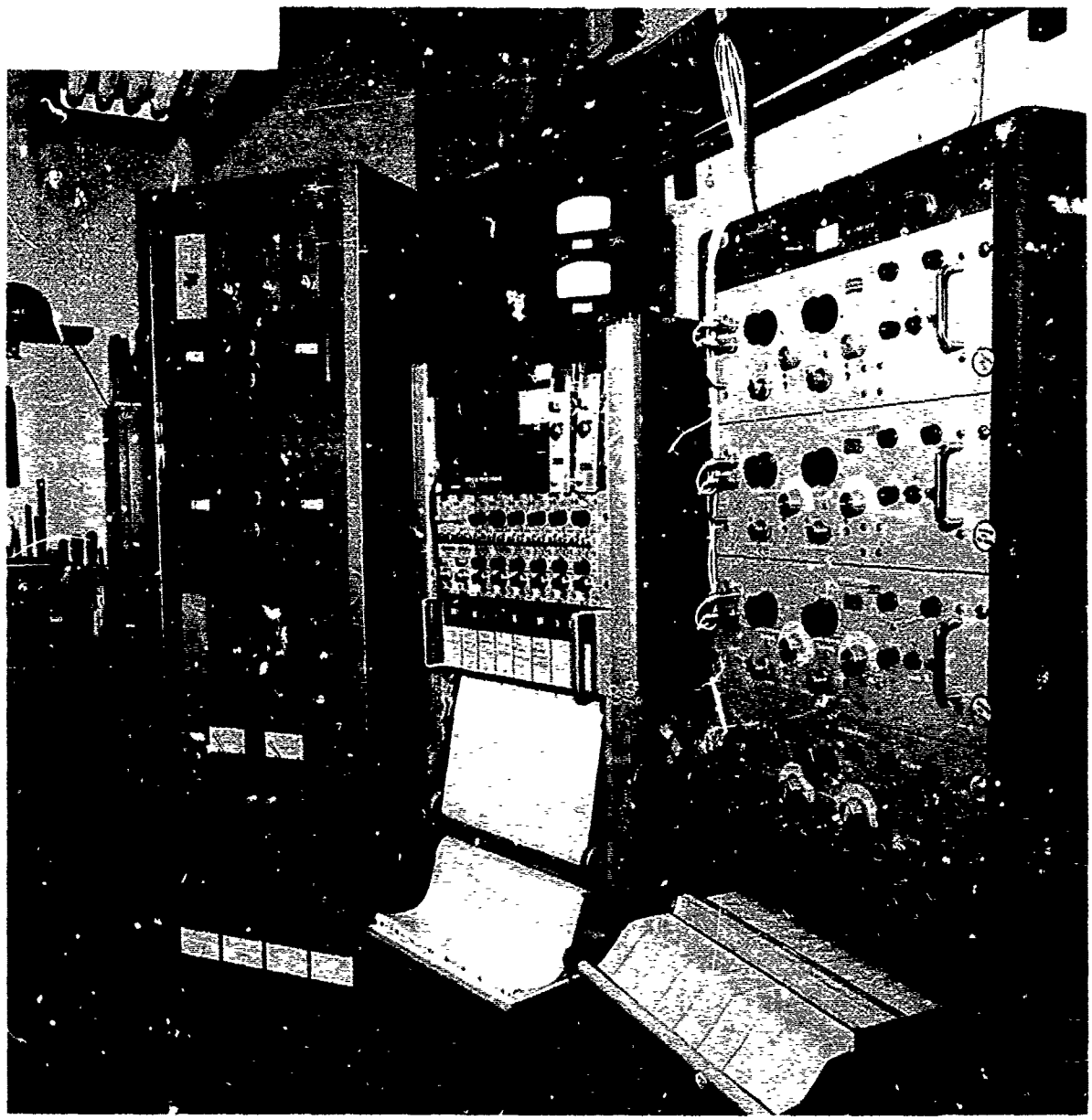


FIGURE 9

WINDSHIELD FLIGHT ENVIRONMENT SIMULATOR (WFES) - CONTROL AND INSTRUMENTATION

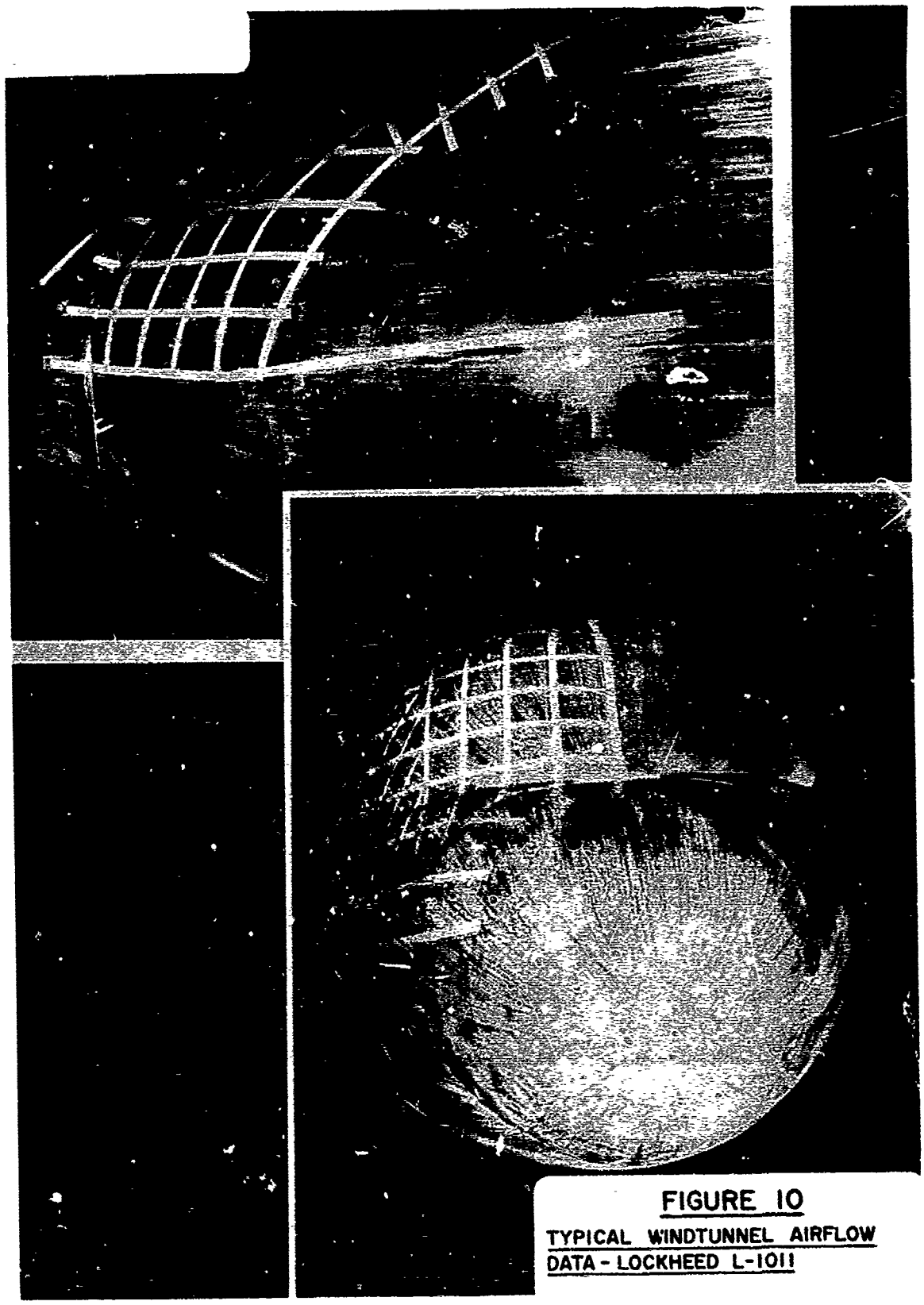


FIGURE 10

TYPICAL WINDTUNNEL AIRFLOW
DATA - LOCKHEED L-1011

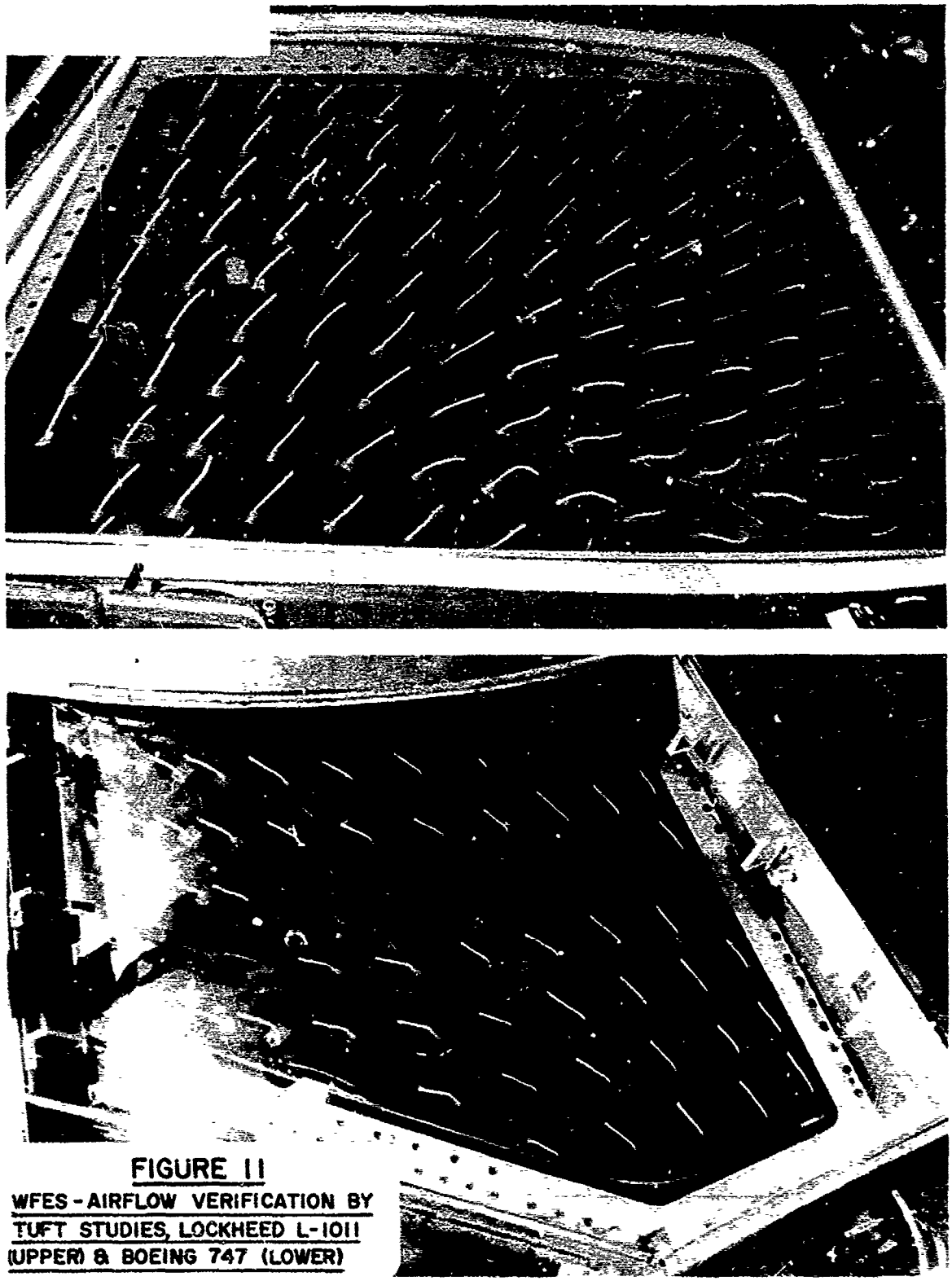


FIGURE 11
WFES - AIRFLOW VERIFICATION BY TUFT STUDIES, LOCKHEED L-1011 (UPPER) & BOEING 747 (LOWER)

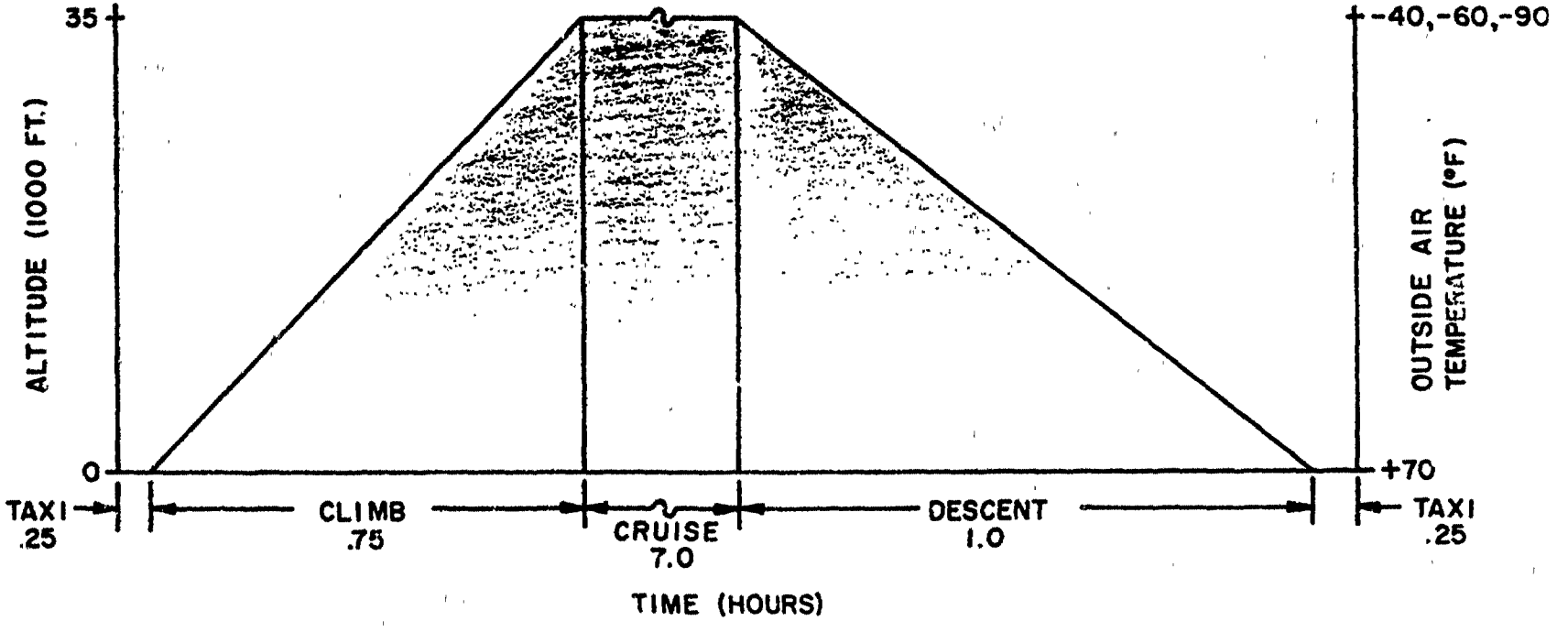


FIGURE 12

IDEALIZED 747 FLIGHT PROFILE

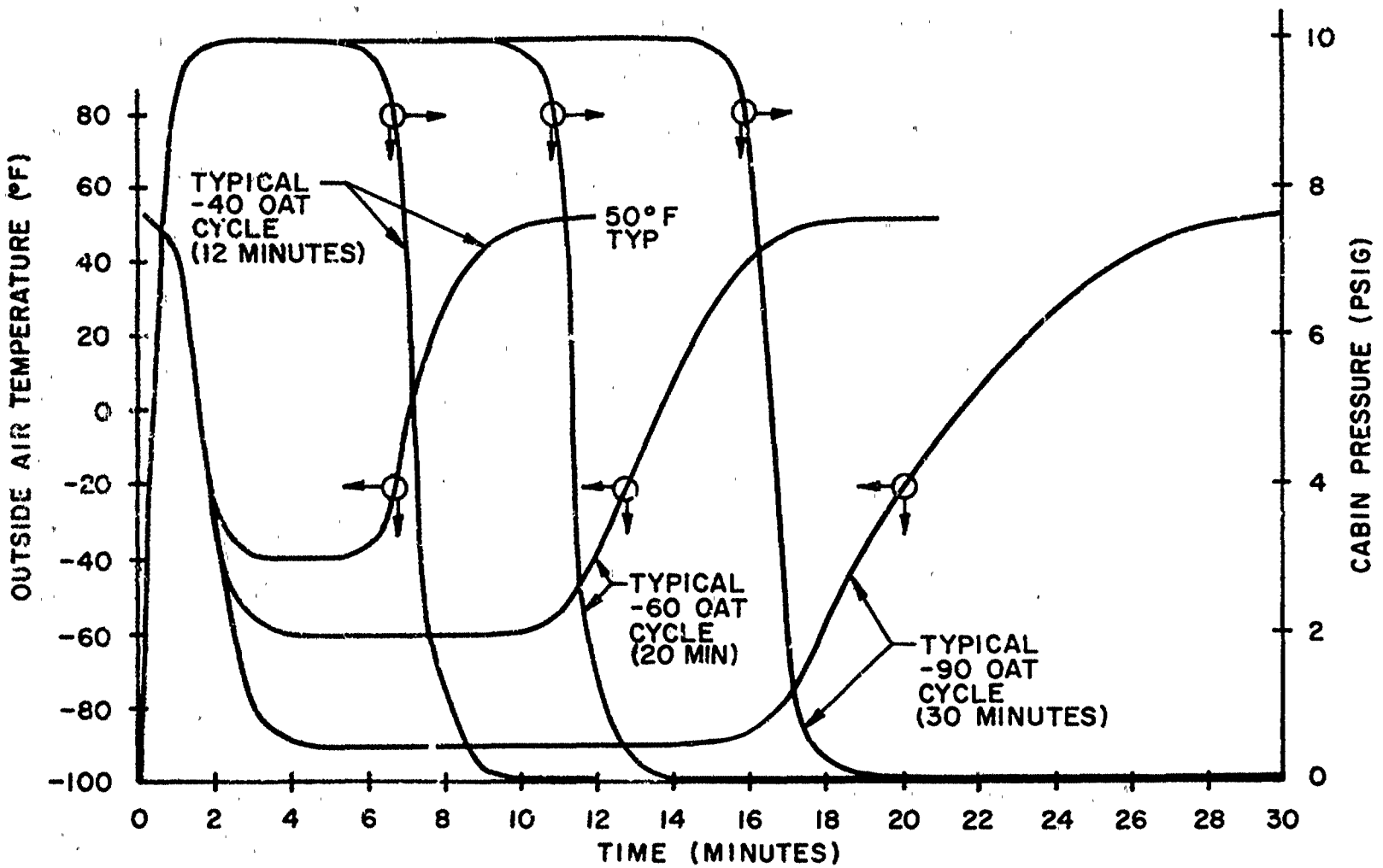
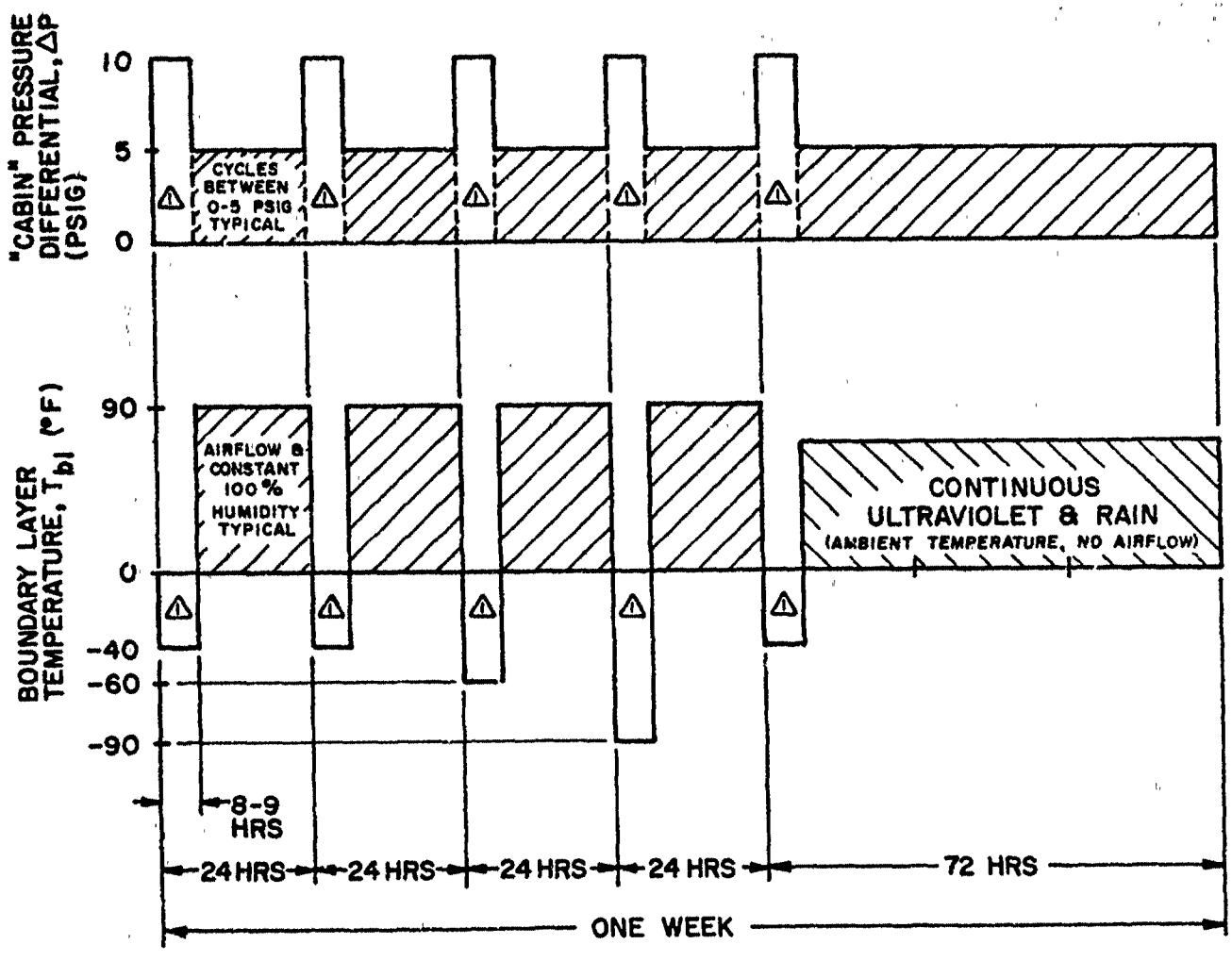


FIGURE 13

TYPICAL COORDINATED TEMPERATURE / PRESSURE TEST PROFILE



⚠ COORDINATED ΔP & T_{bl} "FLIGHT" CYCLES PER FIGURE 13

FIGURE 14

WFES LIFE TEST SEQUENCE - 747 PROGRAM

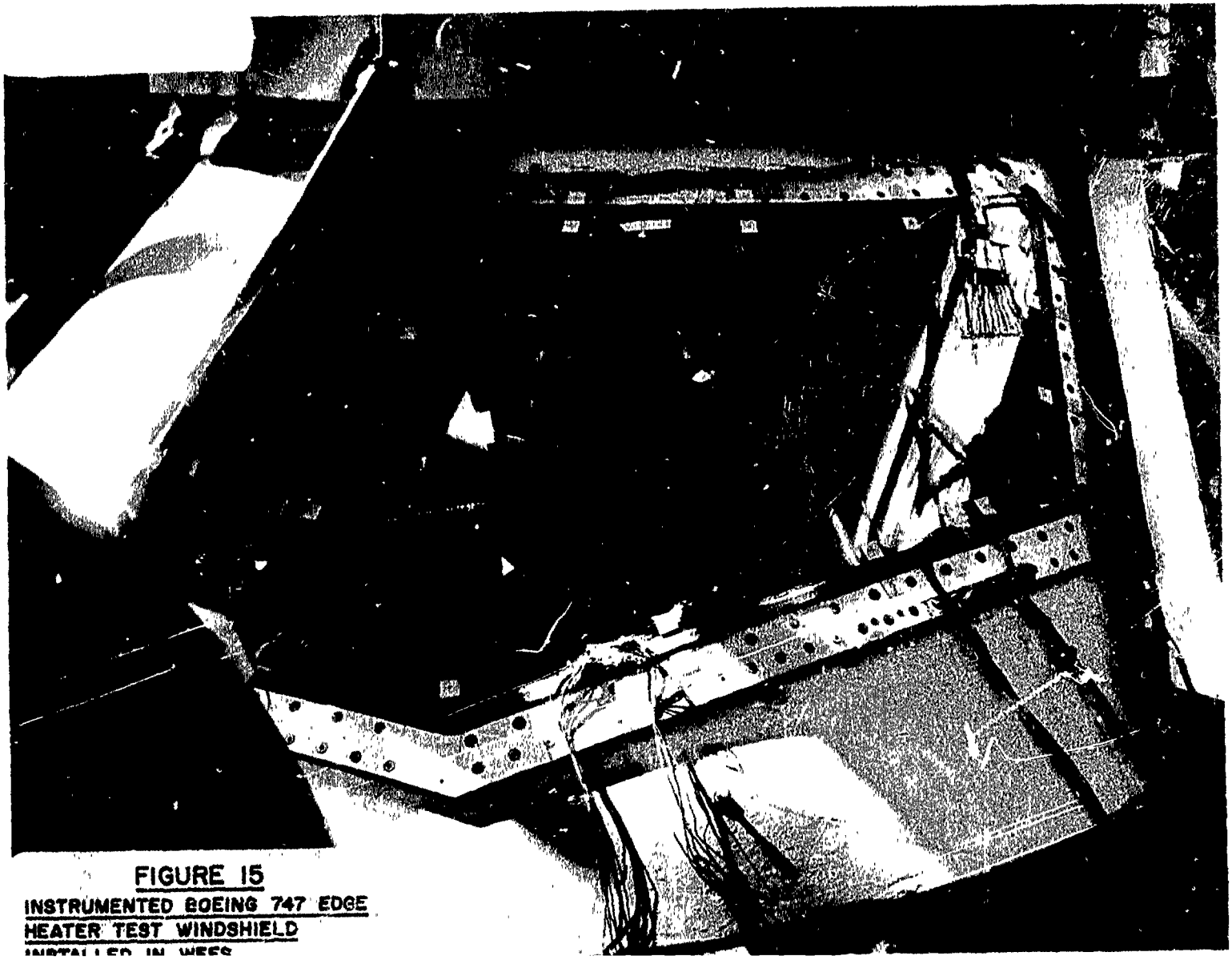


FIGURE 15
INSTRUMENTED BOEING 747 EDGE
HEATER TEST WINDSHIELD
INSTALLED IN WEES

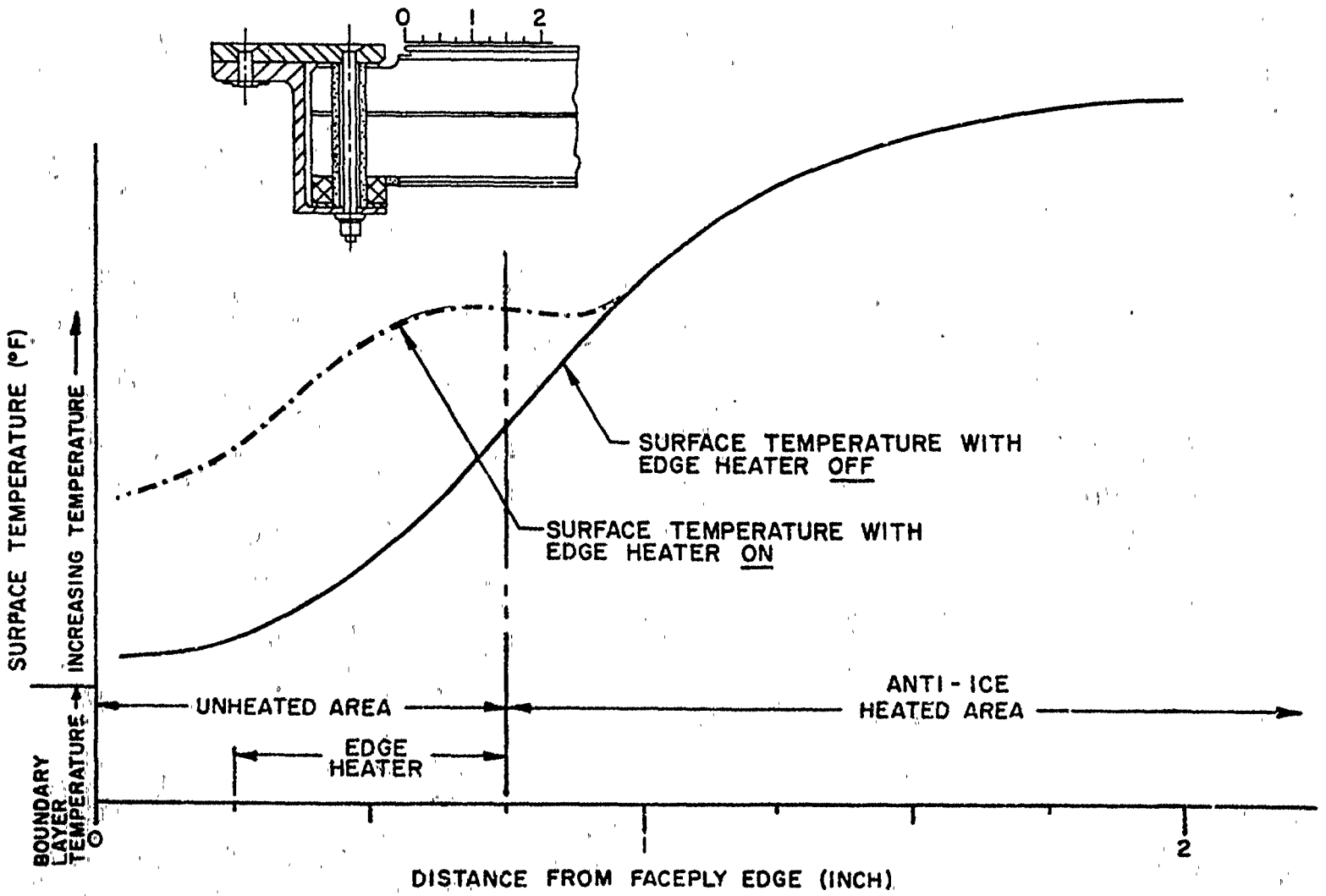


FIGURE 16

EDGE HEATER EFFECT ON EDGE THERMAL GRADIENT

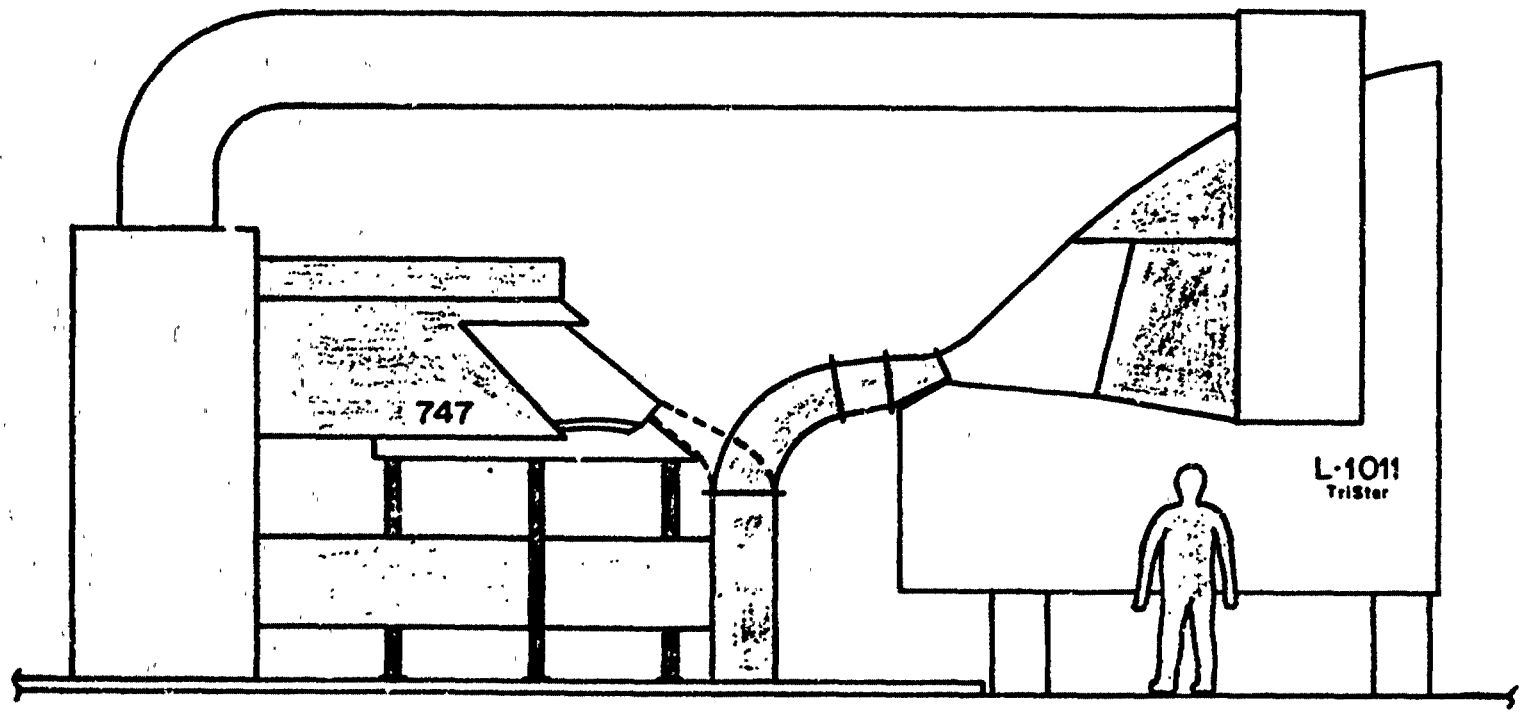


FIGURE 17

PRESENT L-1011/747 WFES FACILITY

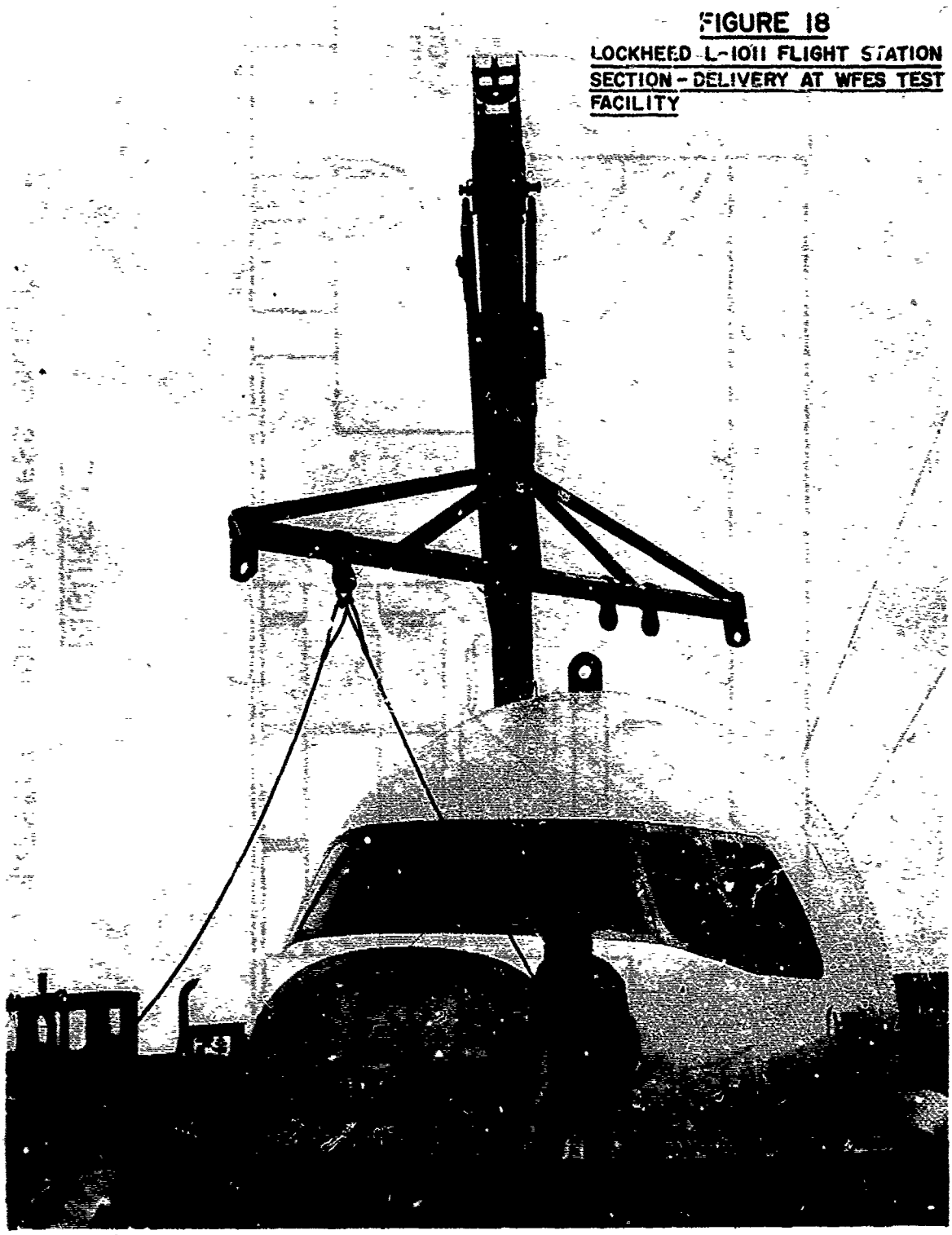


FIGURE 18
LOCKHEED L-1011 FLIGHT STATION SECTION - DELIVERY AT WFES TEST FACILITY

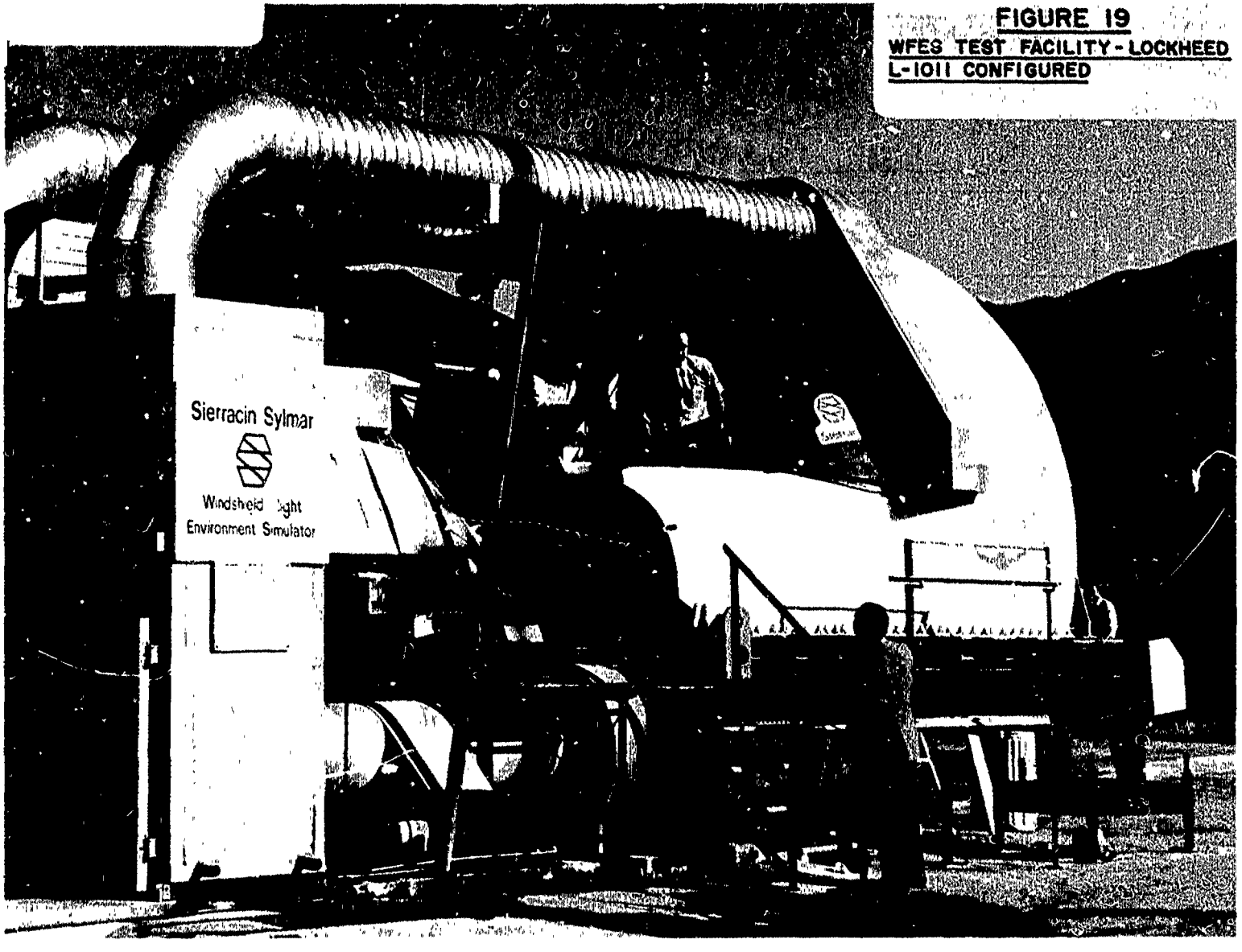


FIGURE 19
WFES TEST FACILITY - LOCKHEED L-1011 CONFIGURED

9971

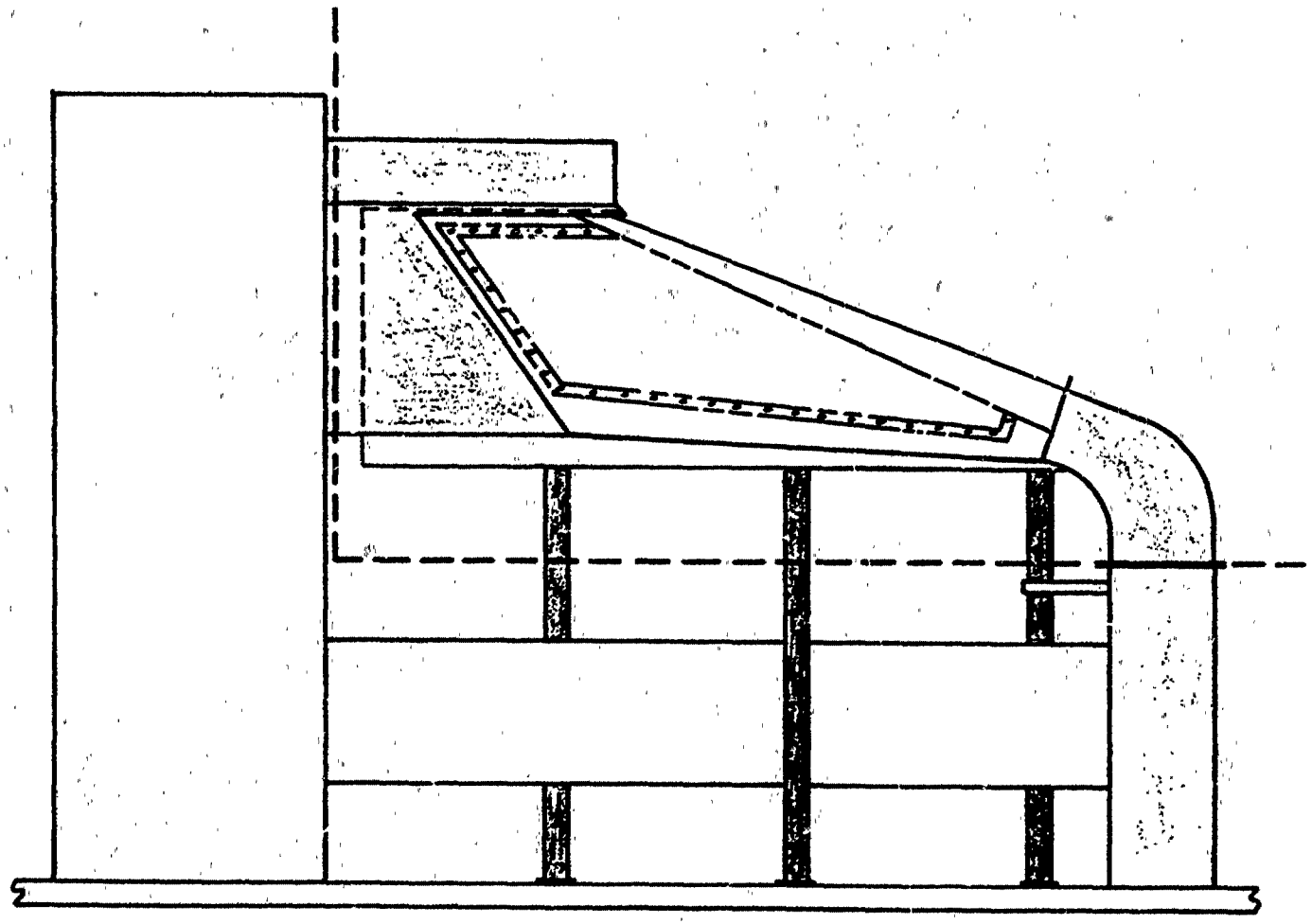


FIGURE 20

WFES SCHEMATIC – B-1 CONFIGURATION PLAN

Copyright 1975, Sierracin® Corporation

The information contained in this document is thought to be reliable, but the Sierracin Corporation expressly disclaims all responsibility for loss or damage caused by or resulting from the use of the information herein contained. The information is given on the express condition that the user assumes all risk.

CURRENT ASPECTS OF OPTICAL REQUIREMENTS FOR AIRCRAFT TRANSPARENCIES

N. S. Corney and W. Shaw
Ministry of Defence
Procurement Executive
London, England

CURRENT ASPECTS OF OPTICAL REQUIREMENTS

FOR AIRCRAFT TRANSPARENCIES

N. S. Corney, W. Shaw

MINISTRY OF DEFENCE (PE)

UNITED KINGDOM

ABSTRACT

A paper given at the 1973 Conference in Las Vegas broadly reviewed the topic of optical requirements for aircraft transparencies, and where possible indicated numerical limits for the parameters involved. Independent support for the views expressed was given in the subsequent paper by Grether AMRL-TR-73-57. The present paper summarises experience gained in the interim period, and outlines critical areas requiring investigation in order that transparency performance may be adequately matched to human demands under extreme conditions.

One area of interest has been in the light transmission of transparencies which are highly raked so that it is necessary to specify the lower acceptable limit acceptable for the task in hand.

The earlier concern in specifying optical resolution has proved to be fully justified, particularly in the situation where binoculars are used for reconnaissance duties.

The adequate definition of tolerances for minor defects such as scratches, bubbles and other foreign matter in terms of optical performance is difficult to formulate and can lead to problems in inspection. Requirements have been prepared and a suitable inspection method developed.

1. INTRODUCTION

A paper[1] given at the 1973 Conference outlined the optical requirements for satisfactory vision through aircraft transparencies and attempted to formulate provisional standards defining minimum acceptable quality. Experience gained since that time has permitted the formulation of firm requirements for military aircraft which, it is believed, will also have an influence in the field of civil aircraft.

The appearance in September 1973 of a paper by Grether[2] summarising much American experience in the field not previously available to the present authors, confirmed most of the ideas presented in the earlier paper and did not produce any conflicting evidence. The collected experience has enabled a comprehensive specification to be prepared covering all aircraft transparencies for the visible spectrum other than those for photographic equipment. The specification is framed in terms of five rather broad categories of transparencies based upon their function and the optical quality required. By defining the desired optical quality at the design stage for a complete transparent panel or selected area thereof, optimum performance may be achieved with economy in manufacture. In order to maintain quality assurance a set of standard methods of test has been prepared which although not exclusive can be recommended for routine inspection purposes.

The broad categories are listed in table 1 and the parameters defining adequate vision such as transmission etc are discussed in the following paragraphs. It will be noted that some revision of the earlier [1] statements has occurred principally in the introduction of a category specifically for reconnaissance and search applications, where there is a special demand for high resolution. It is believed that the method for haze is simpler, and preferable to the older method for measurements on panels. A single test equipment has been introduced for determining resolution, absolute and binocular deviation, and rationalised procedures have been introduced for optical distortion and for specifying and detecting optical defects.

2. LIGHT TRANSMISSION

Provision of the maximum possible light transmission is considered to be essential to vision through a panel under low light level conditions or to enable recognition of targets under conditions of poor contrast. This requirement invariably conflicts with aerodynamic factors such as the demand for highly raked forward facing panels, and structural factors such as need for thick panels to resist bird impact. The forward parts of windscreens in many military aircraft are believed not to afford light transmission consistent with satisfactory vision under all conditions, probably due to undue emphasis having been placed on aerodynamic considerations.

To ensure satisfactory vision, light transmission should be measured along sight lines up to the maximum angle of incidence at the panel to the pilot's (or user's) eye position; a minimum value of 40% transmission at the maximum angle of incidence, and minimum of 60% transmission in the plane of horizontal flight is recommended, for categories I, III, IV and V. Higher values are recommended for reconnaissance and search panels (Category II).

These lower limits of transmission have been recommended taking cognisance of the increasing use of multiple helmet vizors which reduce the amount of light reaching the eye. Obviously the highest demands for transparency of materials and heating films are involved.

The measurement of transmission requires a defined light source with stabilised power supply, and a photometer corrected to have approximately the same spectral response as the human eye. The light source should be combined with an optical system to produce a parallel beam. By measuring the decrease in photocell response when the transparency is inserted

in the beam, the percentage transmission can be evaluated. For thick panels at non-normal incidence provision should be made to accommodate the displacement of the beam, so that the exit beam is fully received by the photometer.

3. HAZE

The existence of haze in transparent panels can be disturbing as the light scattering results in lack of clarity of the image. The effect must be minimised in new panels because deterioration can occur in use particularly with plastics subject to windscreen wiper abrasion or careless cleaning.

It is generally convenient to use the same equipment for determining both light transmission and haze; for the latter an integrating sphere must be used in conjunction with the photometer, an addition which is desirable but not essential for light transmission measurement. For haze measurement two readings of the photometer output are taken:-

a with the transparency in contact with the aperture of the integrating sphere

b with the transparency moved a distance equal to the diameter of the sphere, away from the aperture.

The first reading a is the total transmission, the second b is the transmission less scattered light and the haze is given by $\frac{100\,a-b}{a}\%$.

It will be noted that this method reduces the measurement to two readings as against the four readings required by the American Standard Test Method ASTM D 1003-52, moreover, the method and calculation is simpler. However care has been taken to retain the same geometrical relationship between the size of the aperture, the diameter of the light beam, and the diameter of the sphere. Tests have been carried out to ensure that both methods produce substantially the same results. When examining thick windscreens, the haze or light scatter may occur from either surface or from within the material and therefore the basic measurement of total light transmission is difficult because some light is lost outside the sphere. This loss of light will become insignificant if the sphere is sufficiently large. It is therefore considered that haze measurement cannot accurately be made with a small sphere, a minimum diameter of 500 mm being recommended. The light beam should have a minimum diameter of 50 mm.

For new transparent panels, the haze should not exceed 2.5% of the total visible light transmission measured normal to the transparency.

4. OPTICAL RESOLUTION

In the earlier paper the concept of optical resolution was introduced as a critical feature of aircraft transparencies used in reconnaissance duties. At that time a degradation of the resolution by the transparency below that of the unaided eye was considered unacceptable. However it has now been realised that the use of binoculars is common in aircraft engaged in reconnaissance and search roles. The optical quality of the binoculars will contribute to the advantage gained in their use, but the optical quality of the aircraft transparency itself may well be the controlling factor. To justify the use of binoculars the transparency must be of such a quality that an image finer than that resolved by the unaided eye can be resolved by use of binoculars. In these special circumstances, with binoculars of 7x magnification in common usage, the transparent

panel should be of sufficiently high quality that two lines of 10 seconds thickness and 10 seconds separation may be satisfactorily resolved.

It must be emphasised that only in the special circumstances of a transparent panel used in conjunction with binoculars will the stringent requirements described above need to be invoked and even then it would be expected that only a defined area of the panel need meet these requirements. The application involving use of binoculars has led to a reconsideration of binocular deviation in these circumstances as discussed below, paragraph 6.

For inspection of Category II areas which have this stringent resolution requirement is has been found convenient to set up a suitable target at a distance of 20m from the 7 x 50 binoculars with the transparent panel in the specified use position relevant to the binoculars. The target consists of a double black cross on a white background the angular thickness and separation of the lines being 10 seconds of arc (1mm at 20m). The image of the target is considered resolved if it can be identified as two parallel lines, as seen by one or both eyes, refocussing of the binoculars being allowed. The whole of the vision area is inspected by rotating the transparency panel about the axis of the viewer's eye position to the target.

5. ABSOLUTE DEVIATION

Absolute deviation derives from the departure from parallelism between the two surfaces of a flat panel ("wedge"), or from the curvature itself, as well as local variations in the radius of curvature of a curved panel. For flat panels of Category I, the absolute deviation must be known and variations from this controlled within close tolerances; this control will automatically dictate the visual distortion and double image separation qualities of the panel to be discussed later.

For normal vision panels, absolute deviation is measured at latice points covering the vision area and maximum values of 15 and 25 minutes for category III and IV areas respectively allow satisfactory vision.

The assessment of a transparency for both absolute deviation and binocular deviation can conveniently be made using a single piece of equipment, within which may also be incorporated measurement of resolution. (Fig 1) The use of 150mm diameter optics in both the collimator and telescope of this equipment permits the accommodation of the substantial displacement of the light beam which occurs when testing thick panels. For absolute deviation measurements, the diameter of the telescope aperture is reduced to 12mm by a suitable stop at the front. For binocular deviation two 12mm diameter apertures with centres 64mm apart are used in front of the telescope. For each test a different graticule is required in both the collimator and the telescope, and this can be accomplished by placing all the graticules on a revolving disc so that each can be placed in position as required. If the collimator graticule is provided with suitable double black cross wires, then optical resolution measurement (at least to the 1 minute of arc level) may be incorporated in absolute deviation assessment.

6. BINOCULAR DEVIATION

For normal vision panels a difference in deviation of two parallel rays 64mm apart should not exceed 10 minutes of arc in order to avoid eye fatigue. An interesting point has arisen in connection with transparency areas of Category II used in conjunction with binoculars for reconnaissance. Whereas the angular accommodation of the eyes in a horizontal plane is reasonably large, the safe limit in the vertical plane is limited. The deviation of sight lines is magnified by the use of binoculars and experiment has shown that merging of the two images

in the vertical plane can only be comfortably achieved if the angular deviation is less than 2.5 minutes of arc. It has therefore become necessary to place a limit of 2.5 minutes on binocular deviation in the vertical plane for Category II areas in addition to the 10 minutes in the horizontal plane.

The collimator-telescope apparatus described above may be used for assessing binocular deviation of Category II areas by using a graticule in the collimator in the form of an opaque ellipse of angular vertical dimension 2.5 minutes and horizontal dimension 10 minutes.

7. SECONDARY IMAGE SEPARATION

Specification of this parameter is normally required only in rather special cases for example when thick panels are involved and at high angles of incidence. If the extent of secondary image separation is noticeable or if the contrast between the secondary image and the background is sufficient to be disturbing, then a method of evaluation of the effect is available, and acceptable limits may be defined in the transparency specification.

The collimator and telescope used for deviation measurement is also suitable for the measurement of double image separation. The collimator requires a target having a bright spot of light superimposed on a dimmer background of circles. This may be achieved by using an additional light source in conjunction with a cube beam splitter. This source may be incorporated in the collimator without affecting its uses as described in paragraph 5. The bright spot of light is masked by a black spot on the telescope graticule so that any secondary image is easily seen. The angular measurement of the secondary image may be determined relative to the circles on the collimator graticule.

8. VISUAL DISTORTION

Over the area of a transparent panel local variations of deviation can occur which result in distortion of the image; known straight lines become crooked or curved and the effects are magnified in the case of thick panels. It is common practice to display photographs of grids taken through the panel to demonstrate lack of distortion, and this offers a qualitative estimate of the quality of the transparency. However a numerical assessment can be more conveniently obtained by measurement of an image projected upon a screen.

A suitable procedure has been to project the image of a grid on to a translucent screen which itself carries a grid of lines arranged to coincide exactly with the projected image in the absence of distortion. When a transparency for evaluation is inserted between the projector and the translucent screen, and distortion is displayed, the slope of the lines of the projected image can be measured relative to the grid on the screen. The support for the transparency is arranged to rotate about vertical and horizontal axes, passing through the design eye position.

The slope of the lines is a function of the distance between the projector and transparency relative to the distance between projector and translucent screen, as well as of the absolute deviation of the area of the transparency under examination. In order to compare the qualities of different transparencies it is necessary to standardise these distances. Another problem arises in that while it is tempting to insist that all measurements be made from the user's eye position, certain disadvantages ensue. When using a normal projection system, the lens is so close to the transparency that only a small area thereof can be examined at one time. Substitution of a wide angle lens to cover a greater area demands a very large translucent screen making the assessment more difficult. However by moving the projector away from the transparency (ie from the design eye position), a larger area of the transparency can be

conveniently covered, although increasing the apparent image distortion. Providing the specification makes allowance for this, the measurements are considerably easier to make.

A compromise arrangement is recommended in which the projector to screen distance is 5 m, the transparency being mounted at the installed angle with the design eye position 4 m from the screen. These distances are convenient for a 50 mm x 50 mm slide projector with 150 mm focal length lens.

9. VISIBLE INCLUSIONS, SEEDS, FIBRES AND SCRATCHES

Discussion upon acceptable limits for minor visible defects can be extremely time consuming because of the subjective nature of the subject. In the earlier paper the rather limited basis upon which a specification could be formulated was discussed, and the recommended method of assessing defects can now be described. (Fig 2).

A horizontal matt white screen large enough to accommodate the area to be examined is provided with even illumination from 40 w fluorescent tubes set above the screen and just below the transparency to be examined. The lights are suitably shaded so that the screen is illuminated without direct line of vision between the viewer and these lights. The transparency panel is laid parallel to the screen. Spotlights are provided and are suitably screened so that the viewer can examine the panel with strong oblique illumination. The transparency may be examined against either background and the defects marked and measured using a microscope of 10 x magnification having a graticule graduated in 0.1 mm.

The limits for defect size and distribution are given in Tables 2 and 3.

It is believed to be of interest to append here a method based upon that described by Kirkham [3] for assessing the degradation of optical quality of transparencies by scratches. In this method a laser beam is scanned across the scratch under investigation by means of a vibrating mirror driven by a torque motor. The light beam passes through the transparency and on to a screen of 'Scotchlight' retro-reflecting material. This has the property that it returns the scanning incident beam along its own path. Hence the scanning beam will always be returned back through the optical system and is diverted on to a silicon photodiode detector by means of a cube beam splitter. The advantage of using a retro-reflecting screen is that any non-parallelism in the sample is of no consequence.

If there is a scratch on the transparency under investigation, a certain amount of incident light will be scattered. The scattered light will not return through the optical system and will not therefore reach the photocell. As the light beam scans across a scratch the intensity of the light upon the photodetector is reduced. The attenuation of the beam is directly proportional to the amount of light scattered by the scratch. The information from the photocell can be amplified and displayed on an oscilloscope or xy recorder. As the annoyance factor of any defect is directly related to the light scatter or attenuation of the light this method has advantages over other subjective methods. The creation of suitable standards to calibrate the instrument has still to be solved and effort is being directed towards this solution.

10. RECOMMENDATIONS AND CONCLUSIONS

In the early stages of aircraft design the purpose of each transparency must be clearly defined in terms of the function it has to perform. In addition to the field of view afforded by the transparency, the optical requirements must be specified, with the definition if necessary of specific areas of high optical quality to meet special needs while preserving economy in

manufacture and quality assurance. Compromise will always be necessary between the conflicting demands of aerodynamic and structural considerations with the best vision performance, although vision should not be regarded as a secondary consideration.

A rationalisation of the uses of transparencies has been attempted in the five categories of vision areas presented in Table 1. In the design stage, analysis will be made of each panel to ensure that the quality of each area thereof is pertinent to the function envisaged. Thus a particular windscreen may have a central area of category I quality surrounded by an area of category III to ensure safe and accurate flying with specific weapon aiming quality when needed.

The parameters determining adequate vision have been discussed in the text and the limiting values within each category are collected in Table 3. These values of the parameters except for haze are at sight lines through the pilot's or user's eye position so that the transparency specification may be phrased in terms of its in-flight function.

Practical methods of evaluation of each of these parameters in the quality assurance of transparencies have been outlined. Economy of inspection procedure has been uppermost without, it is believed, sacrifice of accuracy. Alternative methods may become available and could be employed if they offer further economy without loss of quality.

Undoubtedly the most difficult aspect in compiling this specification has been in obtaining sufficient feed-back of operational experience. Only by accummulation of such experience may these considerations be justified and improved.

Copyright © Controller, HMSO London 1975

REFERENCES

1. N S Corney — "Optical requirements for aircraft transparencies" AFML-TR-73-126 (1973) pp 47-67

2. W F Grether — "Optical factors in aircraft windshield design as related to pilot visual performance" AMRL-TR-73-57 (1973)

3. A J Kirkham — "Automatic inspection of optical components for cosmetic defects" The Optician 165 4 (1973)

TABLE 1

Categories of transparencies or areas thereof to be used in specifying optical requirements.

Category	Description
I	Areas of forward facing windscreens of the highest optical quality suitable for weapon aiming.
II	Vision areas of panels used for critical reconnaissance and search purposes i.e. for use with binoculars.
III	Main vision areas of forward facing panels other than those in categories I and II; defined areas of side panels and quarter lights.
IV	Areas of side panels or of other non-forward facing transparencies for all aircraft other than reconnaissance and search, selected areas of canopies.
V	Cabin windows, defined areas of canopies.

TABLE 2

Classification of defects such as inclusions, seeds, hairs and scratches

TYPE A	Diameter in the range 0.2 - 0.5 mm or equivalent area (0.03 - 0.2 mm^2); this includes hairs, fibres or hair scratches of width not exceeding 0.1 mm and equivalent area 0.2 mm^2.
TYPE B	Diameter 0.5 - 1.0 mm or equivalent area (0.2 - 0.8 mm^2) including hairs etc of width not exceeding 0.2 mm and equivalent area 0.8 mm^2.
TYPE C	Diameter 1.0 - 1.5 mm or equivalent area (0.8 - 1.8 mm^2) including hairs etc of width not exceeding 0.2 mm and equivalent area 1.8 mm^2.
	Defects larger than Type C not admissible.

TABLE 3

ACCEPTABLE LIMITS OF THE PARAMETERS ASSOCIATED WITH VISION THROUGH OPTICAL TRANSPARENCIES

PARAMETER	CATEGORY I	CATEGORY II	CATEGORY III	CATEGORY IV	CATEGORY V
In-line visual light transmission In horizontal plane In area of lowest transmission	Not less than 60% Not less than 40%	Not less than 70% Not less than 50%	As Category I	As Category I	As Category I
Haze	Not more than 2.5%	As Category I	As Category I	As Category I	As Category I
Absolute deviation	5 minutes from an agreed value	Not more than 10 minutes	Not more than 15 minutes	Not more than 25 minutes	Not specified
Optical Resolution	Ability to resolve 1 minute lines with 1 minute separation	Ability to resolve 10 seconds lines with 10 seconds separation	As Category I	As Category I	Not specified
Visual Distortion - as assessed by divergence of adjacent grid lines	Requirement covered by other parameters	Not greater than 1 in 25	Not greater than 1 in 20	Not greater than 1 in 10	Not greater than 1 in 5
Binocular Deviation	Not more than 10 minutes	As Category I, also not to exceed 2.5 minutes in vertical direction	As Category I	As Category I	Not specified
Secondary image separation	Not specified - see text.	As Category I	As Category I	Not specified	Not specified
Visible inclusions, seeds,	Allow 1 type A defect only within any circular area of 100 mm radius No type B defects No type C defects	a. Allow 1 type B defect and 4 type A defects within any area of 150 mm radius b. Allow 8 type A defects only within the same area. No type C defects.	As Category II	a. Allow 1 type C defect and 4 type A defects within any area of 150 mm radius b. Allow 2 type B and 8 type A defects in the same area.	As Category IV

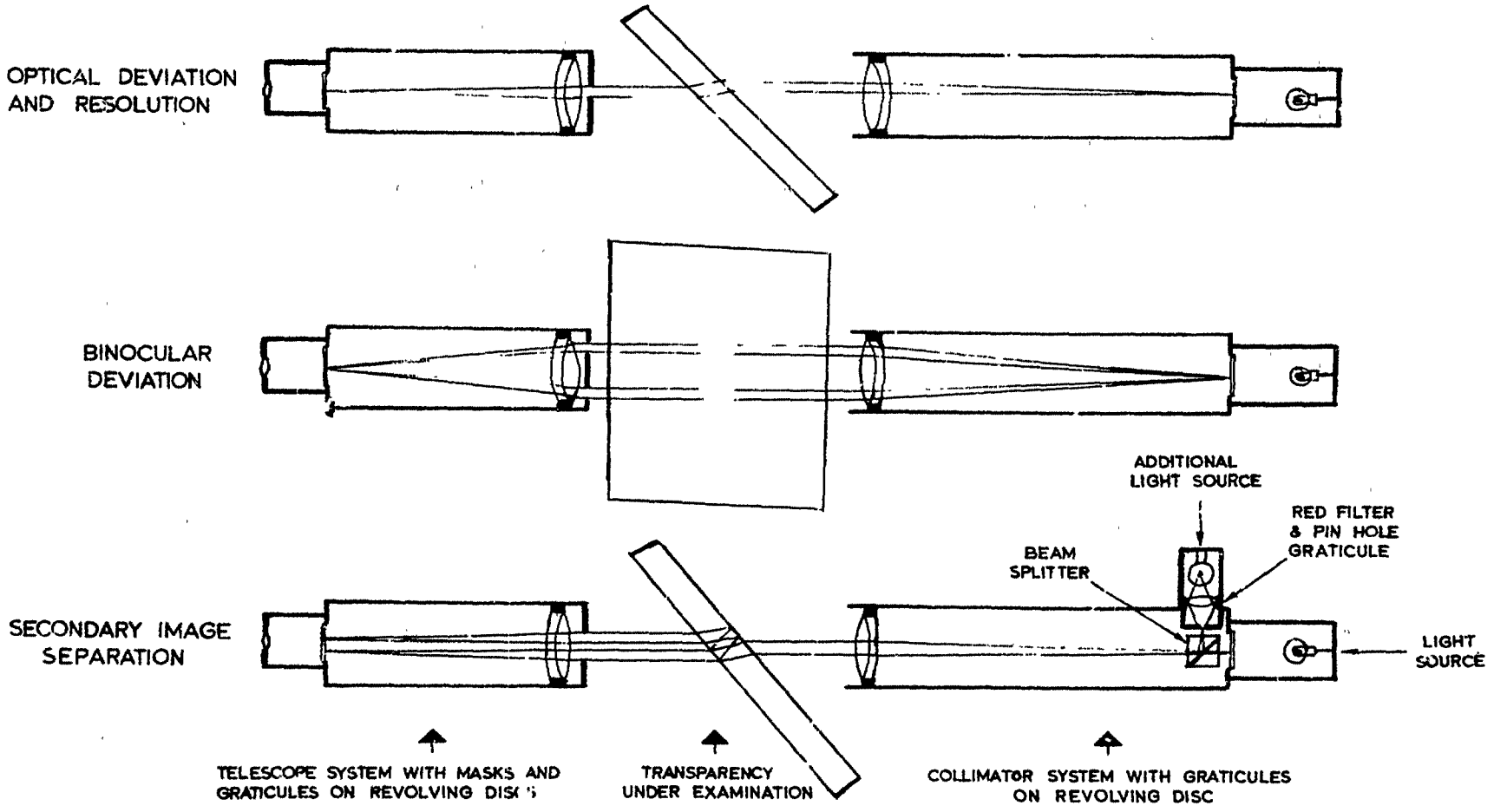


FIG.1 ILLUSTRATION OF FUNCTIONS COMBINED IN MULTI-PURPOSE APPARATUS

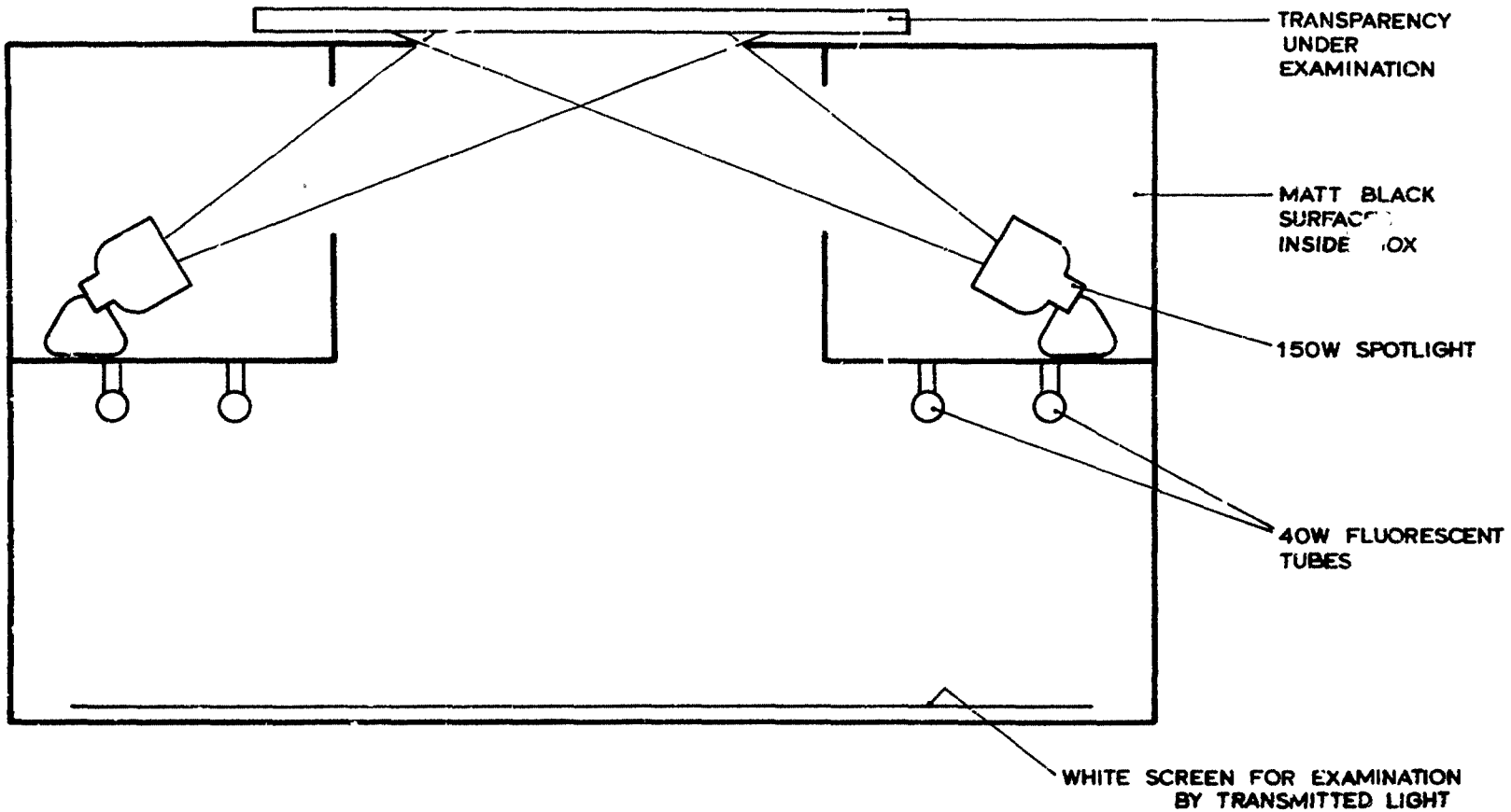


FIG. 2 LIGHT BOX FOR EXAMINATION OF TRANSPARENCIES FOR SCRATCHES ETC.

SESSION 5

MATERIALS AND PROCESSES (PART I)

PROGRESS IN THE DEVELOPMENT OF NEW TRANSPARENT PLASTICS AND INTERLAYER MATERIALS

T. J. Reinhart, Jr. and E. A. Arvay
Air Force Materials Laboratory
Wright-Patterson Air Force Base, Ohio

PROGRESS IN THE DEVELOPMENT OF NEW TRANSPARENT PLASTICS AND INTERLAYER MATERIALS

T. J. REINHART, JR.
AND
E. A. ARVAY

AIR FORCE WRIGHT AERONAUTICAL LABORATORIES (AFSC)
AIR FORCE MATERIALS LABORATORY
WRIGHT-PATTERSON AIR FORCE BASE, OHIO 45433

ABSTRACT

The AFML is following a broad spectrum approach to providing better transparent materials for use in advanced aircraft windshields and canopies. This approach includes the improvement of current materials' performance by various coatings, evaluating existing but not commercially available materials as transparents, and exploratory development programs on plastics and interlayers. The need for greater thermal stability is seen as the most critical near-term, future requirement, while greater environmental resistance represents a more immediate goal. Current programs to be discussed will be limited to the development efforts on five transparent plastics - two for intermediate and three for high temperature uses, and on three thermally stable transparent interlayers. Objectives of and progress on these programs will be described in detail consistent with the state of development of each material.

INTRODUCTION

Transparent plastics and elastomeric interlayer materials are integral, vital components of transparent enclosures for aircraft. The functions performed by each type of material cannot be efficiently accomplished by other materials without invoking a severe penalty in either performance, weight, fabricability or cost. Transparent plastics, primarily acrylics, have in the past provided the optical clarity, impact resistance, environmental protection and structural integrity necessary and with an ease of forming, a low specific gravity, and low cost. Interlayers such as polyvinylbutyral (PVB) have provided the optical clarity, adhesion to glass or plastic, elongation for bird impact and elongation for matching thermal expansions of dissimilar materials. When necessary, these materials are combined with glass plies to form laminated composites with the required properties. While these materials are not without their problems, they have performed in an exemplary manner for many years in aircraft applications.

Requirements for greater field of view, bird impact resistance and increased temperatures in advanced fighter aircraft led designers to the polycarbonate plastics as the primary structural ply in transparencies. This material along with certain temperature resistant interlayers have the stability at elevated temperature to function in the environment of MACH 2 flights. At speeds over MACH 2.5, a durable plastic transparency becomes problematical. Abrasion resistance and bird impact resistance becomes academic in relation to thermal stability in high-speed dashes and cruising at altitudes below fifty thousand feet. Materials for use in this regime must be of prime concern in current and near-future research and development.

The Air Force has addressed the three major problems of aircraft enclosures - bird impact damage, abrasion of surfaces and thermal stability. The Flight Dynamics Laboratory has investigated the problem of bird impacts from every aspect in an attempt to avoid birds and to develop improved transparencies. The Materials Laboratory has done likewise for improved coatings and improved materials. Coatings were seen as the most rapid, low-cost solution to the abrasion problem and the static charge buildup problem, and both were therefore investigated. Research on thermally stable plastics continues in several current programs and in limited efforts on both plastics and interlayers.

Current efforts, involving three separate contracts, are discussed in the following text.

DISCUSSION

High Temperature Plastics

The magnitude of the thermal stability problem can perhaps best be seen in Figure 1, which illustrates the relationship between speed-altitude and temperature. The sector annotated as Current Plastics includes polycarbonate and strengthless, as cast acrylics; as the prime material as outer abrasion resistant plies in transparencies. At a point marking MACH 2.5 and an altitude of 50,000 feet, the indicated temperature is 370°F which represents a surface temperature roughly 10°F above the bubble point of polycarbonate. While it is recognized that such a temperature for a short period of time will not cause catastrophic failure in the plastic, we must consider the possible degradative effects of repeated excursions to these temperatures. Also, to be considered are the possible emergency flights involving longer dash conditions, higher speeds in dashes and such flights at lower altitudes; these conditions are cause for concern. The thermal conductivity and the thicknesses of glass being used as outer plies would offer little thermal protection to underlying structural plies. Under conditions of high temperature and high velocity air flow, as-cast-acrylic surfaces can become unstable due to high shear forces. A glass outer ply would prevent rippling; however, the areal density increases markedly as shown on Figure 2. This and high cost remains the prime disadvantage of glass enclosures.

Our programs for the development of new temperature resistant plastics evolved from the materials properties shown in Figure 3. Here, the current materials are compared in tensile strength at temperature with several experimental materials. We have learned that the polyarylsulfone family of plastics suffer greatly from the exposure to ultraviolet radiation - losing transmittance and gaining haze with exposure time. The phenolphthalein polycarbonate processes with great difficulty and has little impact strength. It is evidence that if these classes of plastics are transparent and retain strength, then others should be available. Also, the two polycarbonates differ markedly in thermal stability and impact strength, a combination of the two could possess a compromise in properties. This philosophy led to two programs, outlined below.

A program to survey materials suppliers for available materials, and to characterize those materials with an indication of good properties reaches completion later this year. Our contractor, Goodyear Aerospace, has identified approximatley sixty materials, acquired and screened twenty and continues to evaluate about ten experimental materials. Figure 4 identifies many of these materials which were not necessarily intended for use as transparents. Elimination from the program should not reflect upon their performance in their intended uses.

Evaluation procedures used in the program are as "standard" and accepted tests as allowed by the nature of this technical area. Briefly, these tests are outlined in Figure 5. Exceptions to either ASTM or FTMS Nr. 406 are given in the 3d column and are contractor's tests. A 6-pound plummet, released from various heights is used as the impact test. A weighted-shoe, 2-cycle-abrasion test replaced the Taber type abrader. Solvent resistance procedures differ only in the solvents used. The screening test should be, therefore, representative and reproducible between evaluators. Thermal stability of materials has been emphasized throughout the program over optical and other properties. Pending completion of all evaluations, the following materials have been found to merit further development. Data presented in the following figures are on unmodified polymers - no antioxidants, no UV stabilizers, etc..

Figure 6 outlines the properties of NR-140 from the DuPont Company. Properties which recommend this material are the heat distortion temperature (479°F), fracture toughness, impact resistance and overall property retention after exposure to adverse environments. The initial optical properties are less than desired; our experience with the polyarylsulfones indicate that much can be done to improve transmittance and haze values. Solvent resistance poses a serious problem.

Figure 7 shows the screening properties of polyethersulfone, PES 720, from the Imperial Chemical Ind.. The heat distortion temperature, tensile strengths and a degree of impact resistance are this materials credentials for possible future work. Again, the initial optical properties are poor and the material needs further development. Moisture resistance of this material will also have to be evaluated.

The third candidate high temperature material is a copolymer of

phenolphthalein and bisphenol-A polycarbonates. This work was initiated in June and has not reached the mechanical property evaluation phase as yet. The contract will, during the course of the program, investigate blends, random and ordered (block) copolymers with variations in inherent viscosities, molecular weights, and end groups. Figure 8 shows the effect of the percentage of bisphenol-A on the glass transition temperature of phenolphthalein - BPA blends. The addition of almost 20 percent BPA which should enhance the impact strength and processing characteristics of copolymers as well as blends and yet, should still provide a high temperature stable material.

At least four materials with lesser thermal stability have been identified as having potential. Two of these are described in the next two figures.

Figure 9 describes a second polyether sulfone PES 200 from Imperial Chemicals. The heat distortion temperature, impact resistance, and tensile strengths recommend this material. Initial opticals are poor; however, the retention of properties under the four environments are encouraging.

Figure 10 shows data on one of Goodyear's 590 materials. This group is a family with HDT of up to 350°F possible. Note the color and opticals of this material. All properties and property retention are reasonable. Impact strength may present a problem.

The materials described in the preceding figures represent the prime candidates for use in windshield and canopies as either protected inner heat-shield type plies or as outer monolithic, self-supporting materials. Research and development is continuing on these and other materials to some degree. Hopefully, these efforts will provide improved materials capable of use individually or in composites with current materials.

Interlayer materials represent an area where considerable improvements could be made in processing ease, control of thickness and thermal stability. Figure 11 presents the tensile properties of representative current materials. The need for a thermally stable material, with properties approaching the target properties line, in a sheet form was identified and programs were initiated for the development of such materials. These include contractual and in-house efforts. Selected for the major contractual program were the family of ethylene terpolymer materials because of their inherent thermal stability and ease of handling. Work has proceeded along two lines - materials with a nominally 3% and 7% hydroxyl content. Material with 3% hydroxyl is discussed in a following paper. The 7% hydroxyl material offers an advantage in greater tensile and tear strengths over the ETP introduced several years ago.

Figure 12 lists properties of the ETP 7 material. The zero tensile strength temperature test was utilized as a fast evaluation test for these materials. A sample is lightly loaded and exposed to increasing temperature at a programmed rate. The temperature at which the sample, after elongation, breaks is the zero tensile strength temperature. The zero tensile strength temperature of the two are about equivalent; however, the tensile impact strength, elongation, tensile strength and the upper working temperature of the 7% material are higher. This material is undergoing addition evaluations.

A silicone interlayer material developed by Dow Corning for applications involving intense heat and fire was only recently introduced and is currently in evaluation. Preliminary tests indicate that while the material shows some exciting properties, additional work on primers and processing are necessary.

The ethylene terpolymers and the silicone interlayers are materials which offer potential for improving the thermal stability and processing characteristics of and for laminated transparencies.

CONCLUSIONS

New and improved transparent plastics and interlayers are needed to provide a greater capability in aircraft transparencies to be exposed to extreme environments. The development of these experimental materials, by Government agencies and industry, must be accelerated in order to provide the necessary margin of safety in advanced aircraft. Candidates discussed are all experimental and will require considerable characterization and evaluation prior to their use in aircraft. The careful, patient testing of materials under a host of conditions is time consuming and costly; however, better materials will result from the research in progress.

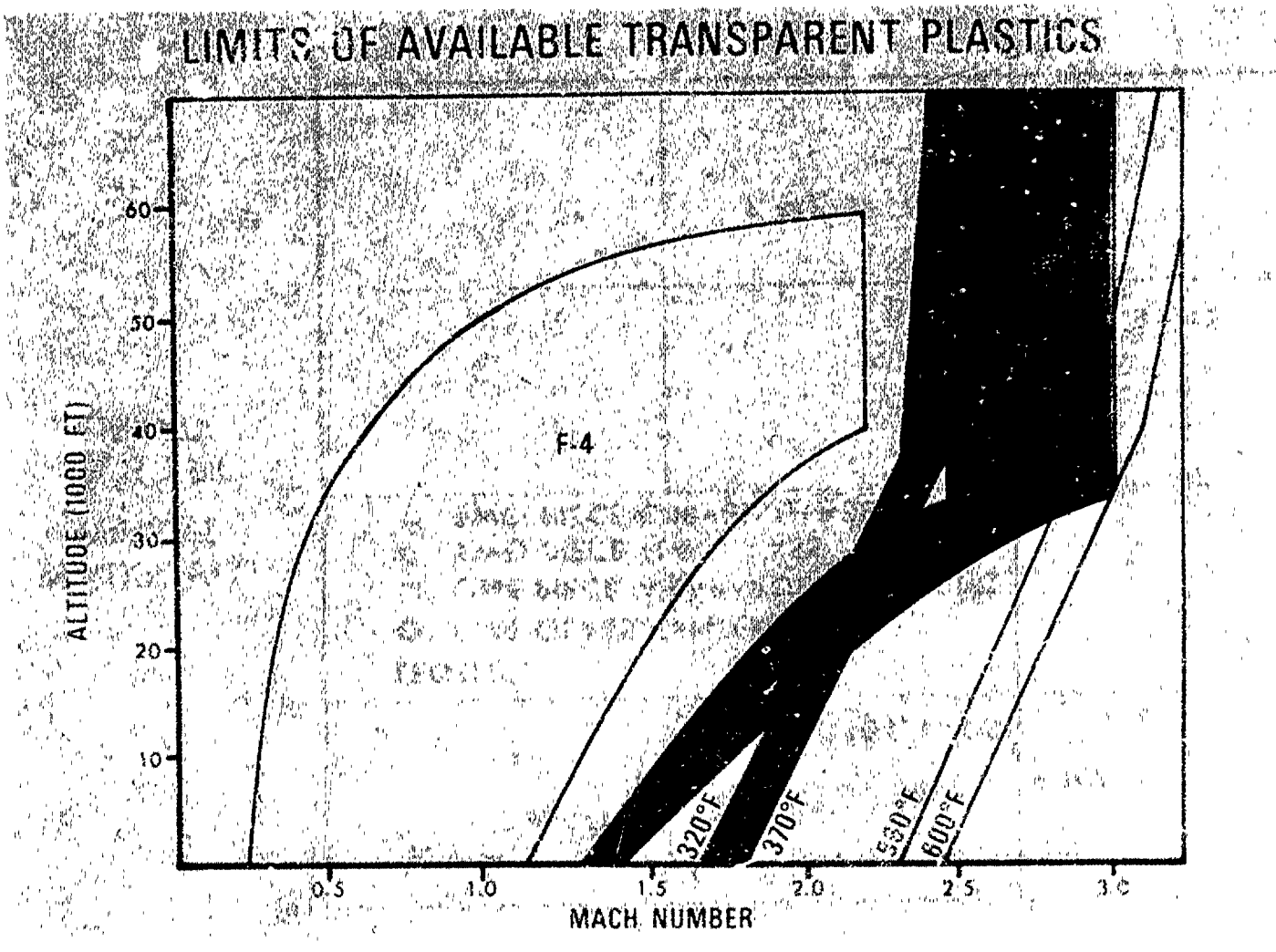

LIMITS OF AVAILABLE TRANSPARENT PLASTICS
ALTITUDE (1000 FT)
60
50
40
30
20
10
F-4
320°F
370°F
530°F
600°F
0.5
1.0
1.5
2.0
2.5
3.0
MACH NUMBER

FIGURE 1

PRESENT WINDSHIELD WEIGHTS

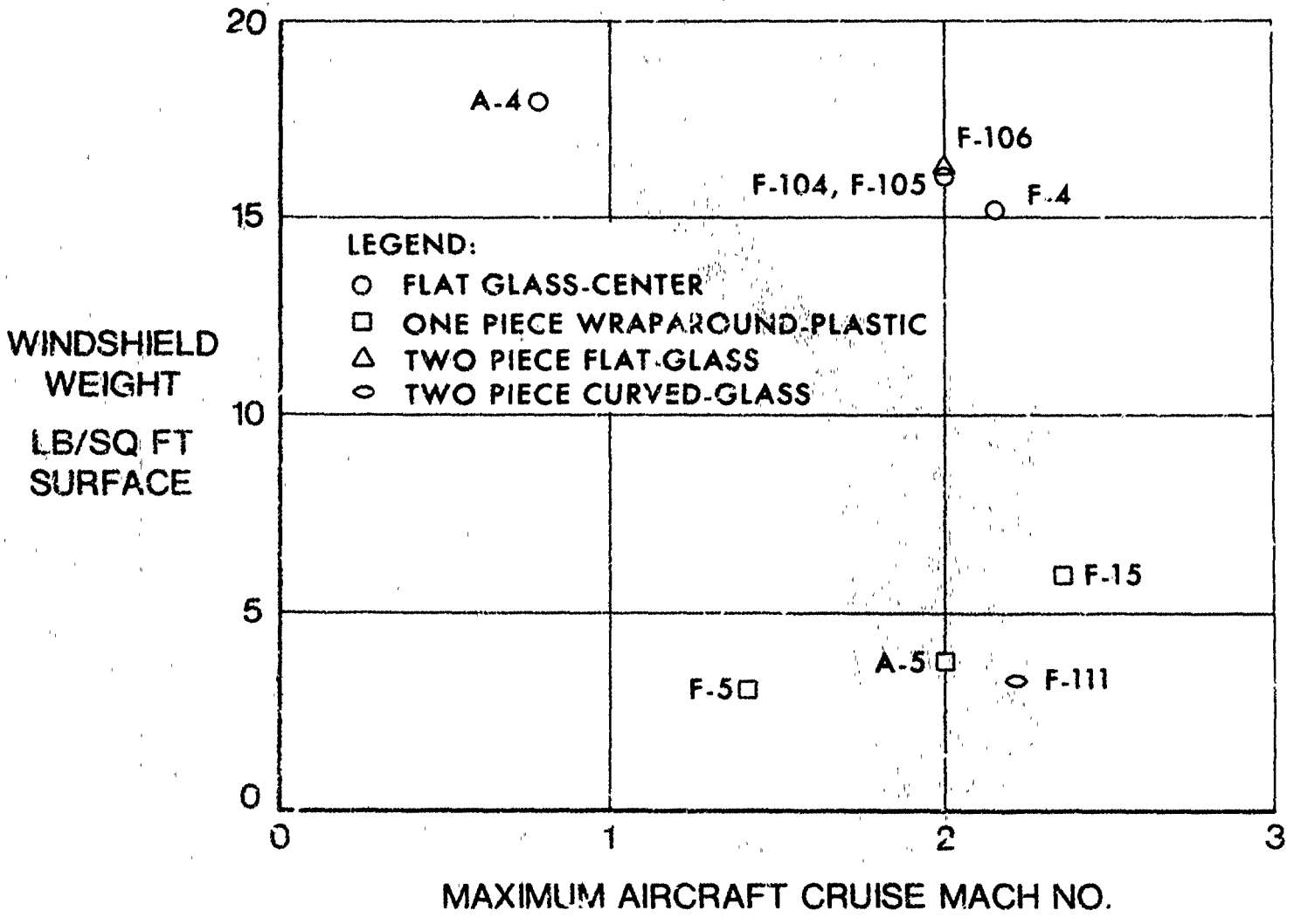


FIGURE 2

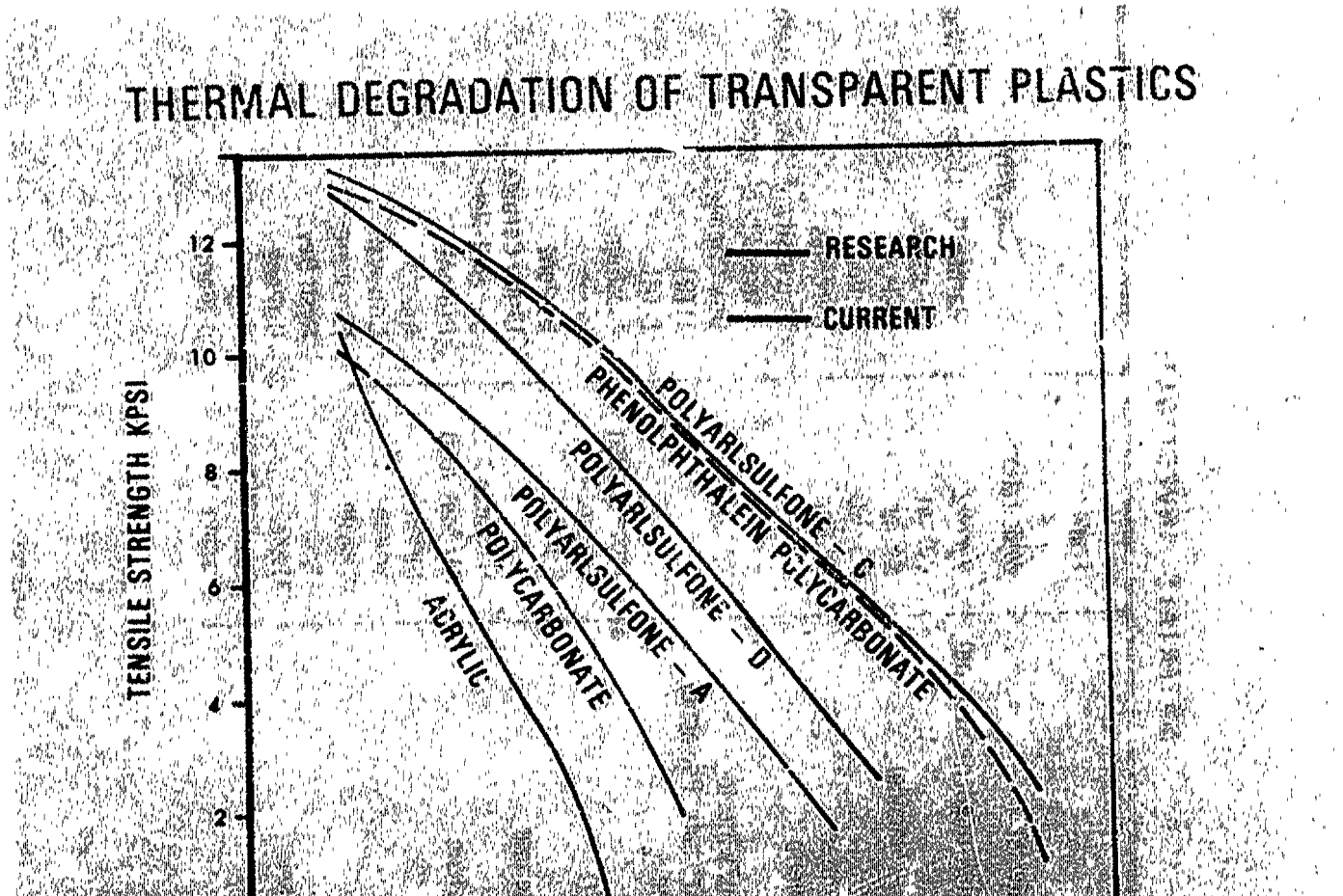

THERMAL DEGRADATION OF TRANSPARENT PLASTICS
TENSILE STRENGTH KPSI
12
10
8
6
4
2
0
100
200
300
400
500
TEMPERATURE °F
RESEARCH
CURRENT
POLYARLSULFONE – C
PHENOLPHTHALEIN POLYCARBONATE
POLYARLSULFONE – D
POLYARLSULFONE – A
POLYCARBONATE
ACRYLIC

FIGURE 3

MATERIALS INVESTIGATED

Material	Trade name or designation	Company
ABS (Acrylonitrile/Butadiene/Styrene)	Cycolac	Marbon Division, Borg-Warner
Acetal	Celcon	Celanese
Armid (Aromatic Polyamide)	Kevlar	DuPont
	KS-105	DuPont
Chlorinated Polyether	Penton	Hercules
Crystalline Polyolefin	-	University of Massachusetts
	-	University of Michigan
Cyclic Sulfonium Zwitterions	XD-8156L	Dow Chemical
Cyclo Aliphatic-Aromatic Polyamide	-	IITRI
Diamide Carbonate	-	IITRI
Epoxy	Isochem Reg	Isochem
Hydrocarbon Resin	Escorez	Exxon
Isomer	Surlyn	DuPont
Modified Polycarbonate	C-4	Union Carbide
Nylon	Trogamid T	Dynamit-Nobel
Oriented Polyethylene	Alathon 7050	DuPont
Polyamide-imide	Torlon	Amoco
Polyaryl Ether	Arylon	Uniroyal
Polybutadiene	Dienite	Firestone
	Hystl	Hystl Dev.
Polyester Elastomerλ	Hytrel	DuPont
Polymide	Code 2080	Upjohn
	Kapton	DuPont

FIGURE 4a

MATERIALS INVESTIGATED (CONT)

Material	Trade name or designation	Company
Polymethyl Pentene	TPX	Mitsui
Polyparabanic Acid	PPA	Exxon
Polyphenylene Oxide	Noryl	General Electric
Polyterephthalate	Tenite PTP	Eastman
Rubber-Plastic	Kraton G	Shell Chemical
	Plex 70	Rohm & Haas
	-	Goodyear Tire & Rubber Co.
Thermoplastic Polyester	Celanex	Celanese
	Ekkcel	Carborundum
	Ekonol	Carborundum
	Valox	General Electric
Triazine	-	Whittaker
Acrylonitrile/Styrene/Acrylic	Luran S	BASF-Wyandotte
Butadiene/Styrene	K-resin	Phillips
Hydrocarbon Resin	Piccodiene	Penn Ind. Chems.
Polyamide	Zytel 63	DuPont
Polyimide	Sablon 424	Solar
Polyphenylene	H-resin	Hercules
Polysulfone	-	Udel-Union Carbide

FIGURE 4b

SCREENING TEST PROGRAM

Type of Test (Properties)	Test Methods		
	ASTM	FTMS No.406	GACA-CLA
Sample Received			
Optical (Original)			
Color (Gardner	D-1544		
Haze	D-1003		
Light Transmission	D-1003		
Physical			
Heat Deflection	D-648	2011	
Specific Gravity		5012	
Mechanical (Original)			
Fracture Toughness (K) (MIL-P025690)(4. 6. 5)			
Hardness (Shore D)	D-2240	1083	
Impact Strength			2326
Tensile (Room Temperature)			
(-40 F)	D-638	1011	
(300 F)	D-638	1011	

FIGURE 5a

SCREENING TEST PROGRAM (CONT)

Type of Test (Properties)	Test Methods		
	ASTM	FTMS No. 406	GACA-CLA
Environmental Exposure (Permanence) Abrasion Effects			2340
Haze	D-1003		
Light Transmission	D-1003	6024	
Ultraviolet Irradiation (1000-Hour Sunlamp Only)			
Color	D-1544		
Haze	D-1003		
Light Transmission	D-1003		
Hardness	D-2240	1083	
Tensile (Room Temperature)	D-638	1011	
Temperature-Humidity (30 Days)			
Color	D-1544		
Haze	D-1003		
Light Transmission	D-1003		
Hardness	D-2240	1083	
Tensile (Room Temperature)	D-638	1011	

FIGURE 5b

SCREENING TEST PROGRAM (CONT)

Type of Test (Properties)	Test Methods		
	ASTM	FTMS No. 406	GACA-CLA
Moisture Absorption	D-570	7031 (24 Hours)	
Haze	D-1003		
Light Transmission	D-1003		
Outdoor Weathering	D-1435 (3-6-9-Mos.)		
Color	D-1544		
Haze	D-1003		
Light Transmission	D-1003		
Hardness	D-2240	1083	
Tensile (Room Temperature	D-638	1011	
Accelerated Weathering	D2565-70	Xenon-Arc Weather-Cmeter (1000 hours)	
Color	D-1544		
Haze	D-1003		
Light Transmission	D-1003		
Hardness	D-2240	1083	
Tensile (Room Temperature)	D-638	1011	

FIGURE 5c

SCREENING TEST PROGRAM (CONT)

Type of Test (Properties	Test Methods ASTM	FTMS No. 406	GACA-CLA
EMMA Exposure/EMMAQUA Esposure (30 Days)			
Color	D-1544		
Haxe	D-1003		
Light Transmission)	D-1003		
Hardness	D-2240	1083	
Tensile (Room Temperature)	D-638	1011	
Thermal Aging	D-794	Maximum 1000 hours 160-270-325° F	
Color	D-1544		
Haze	D-1003		
Light Transmission	D-1003		
Hardness	D-2240	1083	
Tensile (Room Temperature)	D-638	1011	
Thermal Cycling	D-759 (3 cycles) 2-hour per. -40/200 F		
Color	D-1544		
Haze	D-1003		
Light Transmission	D-1003		
Hardness	D-2240	1083	
Solvent Resistance (Stress-Craze)			2339

FIGURE 5d

EXPERIMENTAL TRANSPARENT NR-140 , DuPont

	Original	Abrasion Resistance (2 Cycles)	UV (1000Hr)	Humidity Temp. (120°F/100%)	Moisture Absorption (24 Hr)	Thermal Cycle (-40/200°F)
Heat Dist. Temp (°F)	479					
S.G.	1.43					
Impact Str (ft)	80					
Tensile Str(psi)RT	10,200		7800	9300	7900	9500
-40	9,900					
300	6,700					
Transmittance ?	71.2	68.0	67.7	68.4	67.8	70.1
Haze ?	9.4	28.6	12.6	11.7	17.2	9.5
Color (Gardner)	4	-	6	4	4	4
Hardness (Shore K)	83	-	85	84	83	86
					.08%	

FIGURE 6

EXPERIMENTAL TRASPARENT PES-720 Imperial Chemicals

	Original	Abrasion Restance	UV	Humidity Temp	Moisture Absorptions	Thermal Cycle
Heat Dist. Temp	436					
S.G.	1.38					
Impact S	1.5					
Tensile S RT	14,200		9,100	12,700	14,300	14,500
-40	16,000					
300	9,300					
Transmittance	38.4	39.3	38.4	37.3	37.1	41.7
Haze	12.4	27.5	23.0	14.5	17.0	11.7
Color	12	-	12	12	12	12
Hardness	83	-	86	86	84	87
					0.59	

FIGURE 7

EFFECT OF COMPOSITION ON THE "t_g" OF
PHENOLPHTHALIEN/BPA COPOLYMER BLENDS

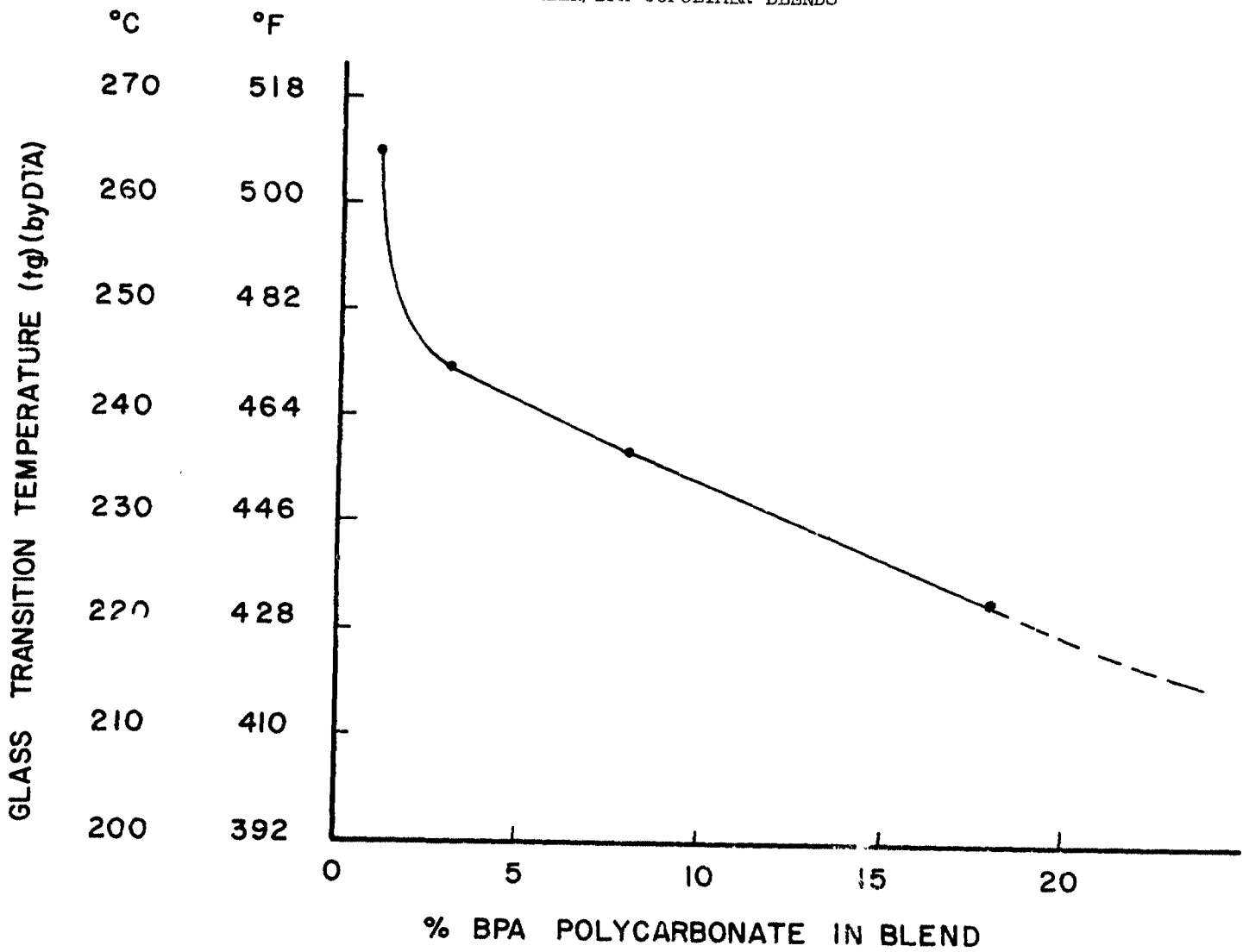


FIGURE 8

EXPERIMENTAL TRANSPARENT PES 200

	Original	Abrasion Resistance	UV 1000 Hrs.	Humidity Temp.	Moisture Absorption	Thermal Cycle
Heat Dist. Temp.	381					
S G	1.43					
Impact S	3.0					
Tensile S RT	12,200		7,100	10,900	11,972	12,300
-40	15,700					
300	7,600					
Transmittance	66.4	55.5	58.1	66.7	63.7	66.2
Haze	11.8	35.7	20.5	14.1	16.8	14.9
Color	4		6	4^+	4^+	4
Hardness	82		86	83	82	83
					0.31	

FIGURE 9

EXPERIMENTAL TRANSPARENT GAC 590

	Original	Abrasion Resist	UV	Humidity Temp.	Moisture Resist.	Thermal Cycle
Heat Dist. Temp.	305					
S G	1.13					
Impact S	0.5					
Tensile S Rt	13,200		13,200	10,000	12,900	10,500
-40	9,300					
300	3,500					
Transmittance	89.5	90.2	90.0	90.2	89.7	89.7
Haze	2.3	6.1	2.0	2.3	4.1	5.9
Color	W/W		1	2	2	2
Hardness	88		87	86	87	87
					0.16	

FIGURE 10

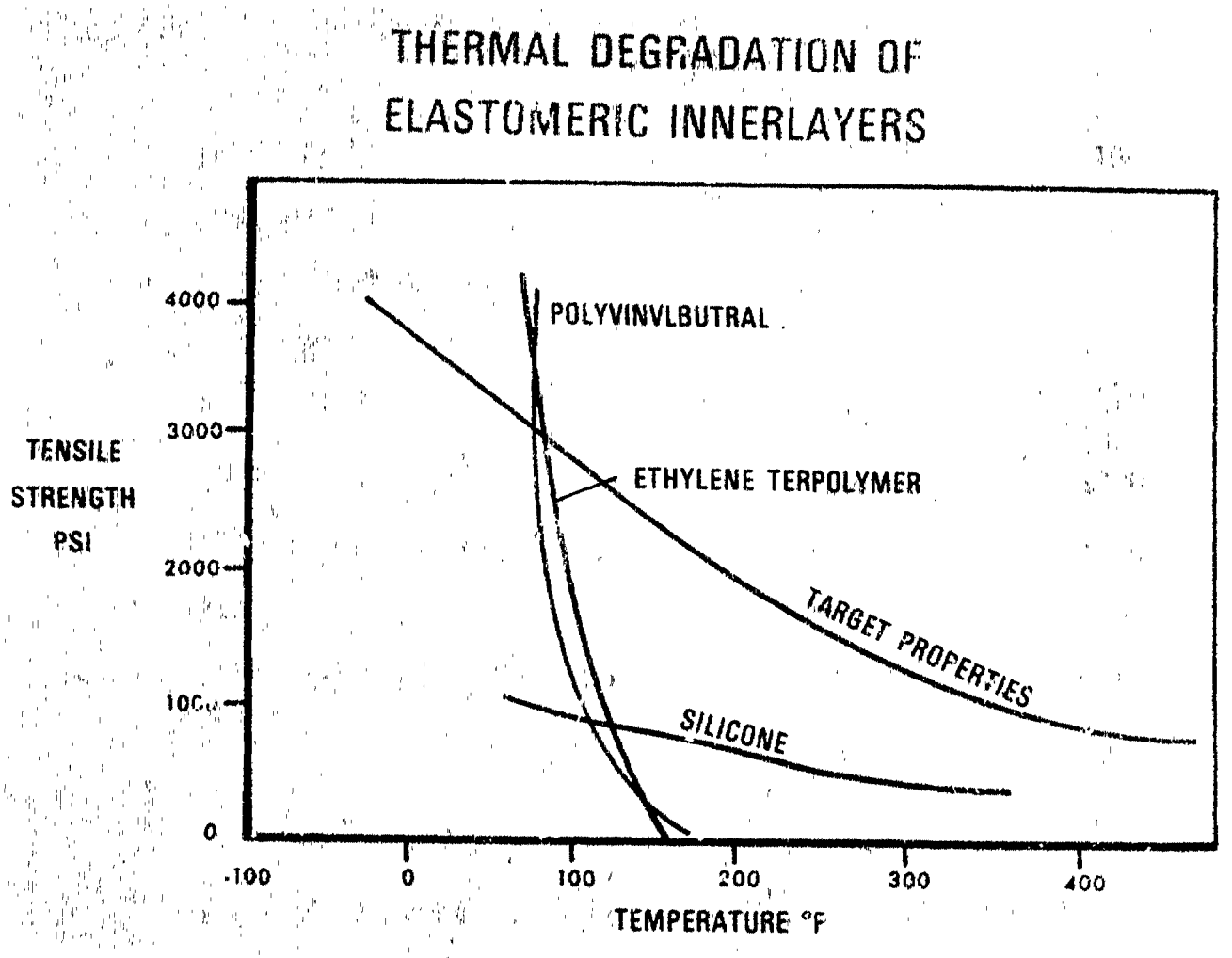

THERMAL DEGRADATION OF
ELASTOMERIC INNERLAYERS
TENSILE
STRENGTH
PSI
4000
3000
2000
1000
0
-100
0
100
200
300
400
TEMPERATURE °F
POLYVINVLBUTRAL
ETHYLENE TERPOLYMER
TARGET PROPERTIES
SILICONE

FIGURE 11

EXPERIMENTAL INTERLAYER ETANOXO 78

	7 8	PVB
Zero Tensile Str. Temp. (^{0}F)	188^{0}	190^{0}
SG	.98	1.08
Impact Str. ft-lb/in^{2}	1530	1250
Tensile Str (psi) Rt	6100	4300
-40^{0} F		7400
150^{0} F		250
200^{0} F		-
Tensile Elongation %	1140	300
Tear Str. lb	415	350
Temp. Limit	275	160^{0} F

FIGURE 12

TOUGH, TRANSPARENT, HEAT- AND FLAME-RESISTANT THERMOPLASTICS VIA SILICONE BLOCK-MODIFIED BISPHENOL FLUORENONE POLYCARBONATE

R. P. Kambour, J. E. Corn, S. Miller
and G. E. Niznik
General Electric Company
Corporate Research and Development
Schenectady, New York

TOUGH, TRANSPARENT, HEAT- AND FLAME-RESISTANT THERMOPLASTICS VIA SILICONE BLOCK-MODIFIED BISPHENOL FLUORENONE POLYCARBONATE

R.P. Kambour, J.E. Corn, S. Miller and G.E. Niznik
General Electric Company
Corporate Research and Development
Synthesis & Characterization Branch
CHEMICAL LABORATORY
Schenectady, New York

ABSTRACT

Bisphenol fluorenone carbonate-dimethylsiloxane block polymers have been synthesized by interfacial condensation of phosgene with various mixtures of BPF-end capped silicone oligomers and free BPF or its monosodium salt. The multisequence block polymers described here contain 7 to 27% silicone consisting of blocks of number average degree of polymerization 10 to 40.

Cast films are clear and colorless. Two glass temperatures are evident in each resin, one at about -100°C for the silicone microdomains and one at temperatures as high as 275°C for the polycarbonate matrix. While BPF polycarbonate is brittle, block polymers with as little as 10% silicone yield by shear deformation before breaking. Ultimate elongations are increased by pre-orientation at silicone contents above 15%.

At temperatures far removed from BPF carbonate domain T_g's both modulus and yield stress decrease with increasing silicone content, independent of block length, in a manner rationalized quantitatively by hard phase-soft phase continuum models. Ultimate tensile elongation, impact toughness and plane strain stress intensity factors increase with silicone content, first through a stress whitening mechanism and at higher silicone contents through shear deformation.

Heat distortion temperatures of 200°C or more are achieved Flame resistance exceeds that of any known non-halogenated resin. The resins are extrudable and injection moldable with only minor changes in color, transparency, and strength properties.

Resins with 15 to 20% silicone can have a balance of properties that makes them attractive as tough, transparent heat- and flame resistant engineering plastics.

I. INTRODUCTION

Current aircraft canopies are limited to use at ambient temperatures less than about 125°C. The basic source of this limitation is the thermomechanical behavior of the sheet material. This behavior reflects primarily the glass temperature of the resin involved--100°C in the case of polymethyl methacrylate and 150°C in the case of the polycarbonate of bisphenol acetone. The use of other higher-temperature resins available on a commercial or developmental basis has been ruled out due to failure in each case to meet one or more of the various requirements involved in addition to heat resistance, e.g. transparency, color, UV resistance, toughness and ease of fabrication. Thus, almost all crystalline plastics have poor clarity. And generally glassy polymers having T_g's higher than that of BPA polycarbonate are too brittle.

This paper deals with the development of a family of transparent thermoplastics having sufficient heat resistance and toughness to meet many advanced canopy applications. In addition the flammability characteristics of these resins suggest their attractiveness for uses where flame resistance and low smoke production are important characteristics.

Technically, the impetus for this work came from the aforesaid knowledge of the brittleness limitations of high temperature glassy plastics and the discovery of the effect on impact toughness of BPA polycarbonate of the introduction of short dimethyl siloxane blocks.(1,2) These multisequence block copolymers contain microdomains of silicone blocks and of polycarbonate blocks. Two T_g's are evident, one for the silicone domains in the neighborhood of -100°C and one for the polycarbonate domains at temperatures somewhat below the T_g of high molecular weight homopolycarbonate.(3) When made properly, these resins are all as clear as BPA polycarbonate itself. Although polydimethyl siloxane and BPA polycarbonate have different refractive indices the small sizes of the silicone blocks result in silicone domains that are much too small (e.g., 40Å) to cause appreciable light scattering. The stiffness and strength of these resins decrease with increasing silicone content; at 25% silicone for example these are reduced by 50% from the corresponding quantities for the homopolymer. While 1/8 in. thick BPA polycarbonate exhibits an abrupt ductile-brittle transition in notched Izod impact toughness at about -10°C the 25% silicone block polymer remains very tough down to -105°C. Thus, the considerably increased low temperature toughness in this resin suggested that silicone block introduction into high T_g resins that are brittle at room temperature might augment their toughness considerably without damaging clarity or heat resistance severely.

The polycarbonate of bisphenol fluorenone (BPF) can be made by rather standard condensation polymerizations.(4) It was initially reported to have an exceptionally high T_g.(4) The lack of aliphatic hydrogens in the homopolymer was expected to confer good thermal and thermo-oxidative stability up to about 420°C where CO_2 evolution begins (vide infra). The similarity of the polymerization chemistry to that for BPA polycarbonate made the formation of the BPF carbonate silicone block polymers appear feasible using chemistry similar to that for the corresponding BPA block polymers.

II. RESIN SYNTHESIS AND ISOLATION

In the last three years we have synthesized high molecular weight BPF polycarbonate and BPF carbonate-silicone block polymers of a range silicone contents.(5,6) Silicone block lengths have ranged from 10 to 30 on a number average basis. The synthesis is an interfacial copolycondensation of phosgene with BPF admixed with a pre-formed siloxane oligomer each end of which is capped with BPF. The reaction is carried out in a mixture of chloroform and aqueous caustic at pH ≈ 9.7. Following neutralization and washing the polymer is precipitated by pouring the chloroform layer into an excess of a nonsolvent. Although 5% of the BPF is converted to BPF carbonate cyclic side products during the reaction this unwanted material is left behind in solution if the proper nonsolvent is used in the precipitation (e.g., acetone).

Intrinsic viscosities of the resins produced have ranged as high as 2.0 dl/g. Values of 0.7 dl/g appear to be sufficient, however, to achieve maximum strengths and elongations. At this viscosity osmotic molecular weights of polymers containing less than 25% silicone are in the range 25,000 to 40,000.

Resin synthesis was scaled up in three stages from 10g to 3 lbs. per run with a 90% yield. The large resin batches were re-dissolved in chloroform after isolation and then steam precipitated; the granular product had a rather uniform particle size (e g., 2mm.) which aids substantially in controlling melt extrusion. Three-lb. runs were routinely made, cleaned up, steam precipitated and dried at the rate of one batch per man week. Films cast from these resins had excellent clarity and barely detectable color by visual inspection.

III. VISCOELASTIC BEHAVIOR

The viscoelastic behavior of the BPF and BPA block polymer families are very similar except for two basic factors: First, the T_g of BPF polycarbonate is 275°C compared to 150°C for the BPA analogue (Fig. 1); second, the elastic modulus of the first is 410,000 psi compared to 340,000 psi for the latter (Fig. 2).

Related differences are seen in the block polymers.

Each homopolymer exhibits a broad β relaxation that is centered at roughly -100°C at 110 H_3 (Fig. 2). Each silicone block polymer exhibits additional relaxation in the same temperature range due to the glass-to-rubber relaxation of the silicone domains. For resins of 15% silicone or more this relaxation is stronger than the polycarbonate β relaxation (Fig. 3).

At elevated temperatures block polymers of the same polycarbonate content differ significantly in terms of the temperatures of their polycarbonate domain α relaxations (Fig. 4). When the two families of resins are compared on the basis of polycarbonate block degree of polymerization it is seen that these upper temperature relaxations differ only because the Tg's of the homopolymers differ (Fig. 5). The reduction in the temperature of this relaxation with decreasing block length is attributed (3) to a block junction concentration effect analogous to the chain end effect seen in the T_g's of homopolymers: the ends of each polycarbonate block appear to possess essentially the same degree of mobility as possessed by the ends of a homopolymer molecule due to the fact that the molecular mobility of the attached silicone moieties is so high.

The upper relaxations of BPA and BPF block polymers of the same weight or volume fraction polycarbonate and the same silicone block length differ by a lesser amount (Fig. 6) because the degrees of polymerization of their respective polycarbonate blocks differ (in turn due to the different bisphenol molecular weights--376 vs. 254).

At intermediate temperatures where the silicone domains are rubbery elastic moduli vary with BPF carbonate content in a way that can be rationalized in terms of hard phase-soft phase continuum models. (7-12) Thus, resins of about 50% BPF carbonate are leathery at room temperature (Fig. 6) while those of about 35% BPF polycarbonate are thermoplastic elastomers. Resins useful as engineering thermoplastics should have moduli of about 250,000 psi or more. This requirement restricts the amount of silicone that can be usefully incorporated in the BPF carbonate plastics to about 22% (vide infra).

IV. ULTIMATE TENSILE PROPERTIES OF CAST FILMS

Thoroughly dried cast films of BPF polycarbonate craze and then fracture in a brittle manner at 11,000-12,000 psi. The material is brittle enough that compression moldings made in unlubricated steel dies fracture during cooling. The homopolymer is ductile in low speed tensile tests only at temperatures above 235°C (Fig. 7). Cast films containing residual chloroform (the casting solvent) fail in a ductile manner. Extrapolation of yield stresses of cast films to zero residual

solvent gives a yield stress of 14,000 psi for the thoroughly dry polymer at 25°C.

Cast films of resins containing from 8-9% to 27% silicone are ductile from room temperature upward, although they break almost immediately upon neck formation. Yield stresses are dependent on temperature in the same way, qualitatively as is that for the homopolycarbonate (Fig. 7). Yield stresses at a given temperature in the range well below the range of polycarbonate domain T_g's, are dependent only the silicone content of the resin essentially. The actual dependence can be rationalized by assuming that the only effect of the silicone domains is to cause stress concentrations on the microscopic level, the polycarbonate domains responding to local stress in a way unchanged from the way the homopolycarbonate responds to stress on a macroscopic level. Thus the reduction in yield stress with silicone incorporation is predictable from the same hard phase-soft phase continuum models that rationalize the dependence of modulus on silicone content. In Fig. 8 yield stresses of various resins obtained at 25 and 75°C are plotted vs. silicone content. The solid lines are generated from the Halpin-Tsai equation for the modulus of a hard continuum phase containing spherical inclusions of negligible modulus. (7,8) The yield stress of the homopolymer at the particular temperature of test is the only experimental parameter used and there are no adjustable parameters in the original equation.

The neck is a zone of shear deformation essentially although some stress whitening is evident therein. Plastic strain in the neck, as determined from post-test measurements of the cross sectional area in the neck, is about 80%--similar to that in BPA polycarbonate. In the BPF block polymers, however, fracture occurs at a total specimen elongation of 9 to 13% or so independent of silicone content or block length. (By contrast the corresponding BPA family sustains specimen elongations above 100%.) The fracture initiates in the middle of the neck generally.

Hot stretching can have a marked effect on subsequent tensile elongation. Thus, films of several resins including the homopolymer were subjected to dead loading for different lengths of time at temperatures slightly above their respective polycarbonate T_g's. At the appointed times the film jigs were removed from the air ovens in order that the films cool quickly while under the stretching loads. The degrees of hot elongation attainable by this procedure increased substantially with silicone content, the homopolycarbonate being completely refractory in this regard while a resin of 25 wt. % silicone was drawn to elongations as high as 45%. In subsequent room temperature tensile tests (Fig. 9) specimens were found to elongate more the greater the degree of hot stretching.

Although the yield stress of the pre-oriented films was somewhat higher the plastic strain in the neck was substantially reduced and the stress whitening and crazing eliminated entirely. Thus, pre-orientation reduces true stress in the neck by increasing cross sectional area and also eliminates potential sites of crack initiatic . One or both of these changes appears responsible for the substantial increases in neck stability, fraction of test section drawn out, and thus total elongation.

On the basis of limited experimentation it appears that both the ability to hot-stretch successfully to a given elongation and the effectiveness of a given degree of hot stretching in increasing ultimate elongation in subsequent room temperature tensile tests increase with silicone content. In Fig. 10 average ultimate elongation is displayed vs. silicone content: the number inside each datum square is the percent hot stretch in the specimens giving that elongation. Only above 15% silicone do the elongations begin to be susceptible to improvement by this process.

V. MODULUS, FRACTURE TOUGHNESS AND NOTCHED IMPACT STRENGTH

Three kinds of toughness measurements have been made using sections of extrudate and injection molded specimens, all 1/8 in. thick. First, standard notched Izod tests have been conducted. Second, the plane strain stress intensity factor K_{Ic} has been determined using single edge notch, half-inch wide specimens. Third, a ball impact puncture test that gives puncture energies has been used (Section VI).

In each K_{Ic} specimen a small cut was sawn into the side and a crack induced at the base of the cut by fatigue flexing. The specimens were then pin-loaded to failure. Because the length a of the crack constituted a significant fraction of the specimen width w the stress intensity factor was calculated as (13)

$$K_{Ic} = \sigma_b \, a^{\frac{1}{2}} \left[7.59 - 32\frac{a}{w} + 117\,\frac{a^2}{w^2}\right] \qquad (1)$$

where σ_b is the breaking stress. Strain energy release rates were also calculated as

$$G_{Ic} = K_{Ic}^{\,2}/E \qquad (2)$$

where E is the elastic modulus. Elastic moduli were measured in 3 point flexure according to ASTM test D790 on the same specimens prior to notching.

Whereas BPF polycarbonate fracture surfaces are clear and smooth, copolymers containing as little as 8 or 9% silicone show stress whitening, presumably due to a cavitation process like crazing. The extent of whitening is greater at 15% than at 10% silicone, but changes little with increasing silicone content thereafter. No evidence of shear deformation was apparent in these specimens. In tensile tests, however, a measure of necking can be seen above 10% silicone; shear deformation increases extensively only above 20% silicone however.

In Fig. 11 several mechanical properties are displayed vs. silicone content. Modulus is reduced to 250,000 psi, the approximate limit for an engineering material by about 20% silicone incorporation. Over the range 10 to 20% silicone K_{Ic}, notched Izod impact energy and ultimate tensile elongation are essentially constant. Nominal tensile elongation is constant in this range and only begins to rise rapidly at silicone contents above 20%.

Two conclusions can be inferred from Fig. 11 and associated failure morphologies. First, a silicone content of 15% appears to be optimum: toughness is as good as that of stretched acrylic and modulus is acceptable at this point, while the increase in silicone content necessary to bring any increase in ductility from that at this silicone level is great enough to reduce modulus below the acceptable level.

Second, there are three failure regimes evident: a) homopolycarbonate is highly brittle, failure occurring in a manner superficially reminiscent of "crystal" polystyrene and the same is probably true of all resins having much less than 7-8% silicone; b) a first regime of toughness exists between about 8 and 20% silicone in which the function of the silicone is simply that of inducing stress whitening, which we infer to be a crazing phenomenon; c) a second regime of toughness begins at 20% silicone more or less (depending on stress configuration) that involves the onset of shear flow in addition to stress whitening.

VI. BALL IMPACT PUNCTURE ENERGIES

These regimes of ductility are also evident in ball impact puncture tests on injection molded square $2\frac{1}{2}$ in. x $2\frac{1}{2}$ in. in area by 1/8 in. thick. The test used consisted of driving a ram at constant rate through a plaque mounted in a holder on a load cell. The best machine was an MTS closed loop hydraulic tester. The ram used was a steel cylinder 2 cm. in diameter with a hemispherical head of the same diameter. The ram was driven at 6000 in./min. through the plaque to a fixed depth (1 in.) below the bottom surface of the plaque each time. The hole edge had a radius of 0.001 in. Force-displacement data were recorded via a Nicollet digital oscilloscope and

integrated appropriately to yield impact puncture energies. Thus, like the Izod test but unlike the Gardner dropping ball test, this procedure gives a failure energy for each specimen tested.

This test was conducted on four block polymers and also specimens of Acrylite polymethyl methacrylate and Lexan® BPA Polycarbonate for reference purposes. Puncture energies (Table 1) ranged from 2.4 ft.-lbs. for PMMA to 126 ft.-lbs. for BPA polycarbonate. The BPF block polymers gave energies from 5 ft.-lbs. at 18% to 26 ft.-lbs. at 23% silicone. These energies varied also with the quality of the molding used. The failures were completely brittle (2-5 ft.-lbs.) to semi-brittle with stress whitening (~ 10 ft.-lbs.) to largely ductile with a little stress whitening (26 ft.-lbs) to completely ductile with no stress whitening (125 ft.-lbs.). Force displacement traces and associated failure morphologies for these four types of failure are shown in Fig. 12.

Impact energy and fracture morphology also varied from specimen to specimen of a given block polymer, depending on molding conditions. Thus, for the resin of 23% silicone a relatively low melt temperature gave 10 ft.-lbs while a higher temperature gave 26 ft.-lbs. The lower temperature conditions appear to result in poor knitting of skin and core of the plaque and delamination of these occurs on impact.

These differences in molding quality reflect the very limited amounts of material available for perfecting molding conditions so far. We expect that larger amounts of resin would enable further optimization of molding conditions and bring about higher impact puncture energies generally.

VII. TEMPERATURE RESISTANCE OF EXTRUDATES AND MOLDINGS

While the modulus, strength and toughness at low temperatures depend primarily on silicone content independent of block length, the heat resistance depends primarily on the softening temperature of the polycarbonate domain. This temperature is in turn dependent on the BPF polycarbonate block length and independent of silicone content.

Yield stress and ultimate elongation of several melt-processed block polymers have been determined vs. temperature to 200°C or above. Yield stress shows the same temperature dependence as for cast films of similar silicone contents and block lengths. For several resins of 15 to 24% silicone, yield stress is 2000 psi or greater at 200°C (Fig. 13). Although the block lengths of these resins are such as to lead to average polycarbonate T_g's of 225 to 250°C yield stress drops rapidly toward zero at roughly 210°C. Ultimate elongation for these block polymers (Fig. 14) rises gradually from room tem-

perature to 150°C; the temperature dependence increases abruptly at that point. This abrupt change in temperature dependence occurs at a temperature coincident with the onset of the polycarbonate domain α relaxation, which has a much greater breadth on the temperature scale (Fig. 4) than does that for the high molecular weight homopolymer (Fig. 1). Part of this great breadth probably arises from the polycarbonate block size distribution; because the synthesis is a polycondensation the block size distribution should be random roughly. If so, it seems likely that a segregation of blocks into domains of differing average block size occurs: viewed in terms of the N^{-1} dependence of T_g (Fig. 5) such a segregation would give rise to a significant dispersion of domain T_g's and thus to the spreading out of the E" vs. T curve. A loss of shear resistance and yield stress for a fraction of the polycarbonate matrix would also be expected at a temperature well below the temperature of the center of the E" peak. The change in the temperature dependence of ductility at 150°C is therefore attributed to the softening of microregions of the polycarbonate matrix having the lowest values of N^{-1}.

These results suggest that changes in synthesis procedures leading to broader block length distributions could bring increased ductility at low temperature with little or no sacrifice of heat resistance.

ASTM heat deflection temperatures at 264 psi have also been determined on several melt processed block polymers of 17 to 24% silicone. Results are summarized in Table 2. Heat deflection temperatures exceed 200°C except for two resins (129B3 and 129B-5) which had been contaminated during steam precipitation with an organic impurity that we believe acted as a plasticizer.

VIII. FLAMMABILITY

Oxygen Index: The Fennimore-Martir limiting oxygen index (ASTM Test No. D2863-70) has been determined on 1/8 in x 1/2 in. x 2-1/2 in. specimens of the homopolycarbonate and four of the block polymers (Table 3). Indices for the block polymers are far higher than those of any other transparent non-halogenated plastic known to us. In this test all of the BPF resins char rapidly and extensively; little smoke is produced and no dripping occurs.

Curiously the indices of the block polymers appear to be higher than that of BPF polycarbonate in spite of the fact that homopolydimethyl siloxane has a much lower oxygen index (Table 3). The mechanism of this synergism (if indeed it is real) is unclear. However, the mechanism very likely involves the extent of char formation and the ability of the char to insulate the underlying resin. Correlation of residues from

thermogravimetric analyses with oxygen index is ambiguous. The difficulty lies in the choice of atmosphere for the TGA run. Thermogravimetric analyses run in air give amounts of black residue at 700°C that appear to increase linearly with silicone content. TGA's run in nitrogen, however, give amounts of residue that decrease gradually with silicone content. Which of these trends is relevant to the oxygen index depends on the oxygen content of the atmosphere at the surface of the OI specimen. Since the burning of organic solids is thought to involve a thermal decomposition and volatilization of the decomposition products the inner part of the oxygen index test flame should constitute a reducing atmosphere. If true, the TGA's run in nitrogen should be more relevant ones and the tempting positive correlation of air-TGA residue with silicone content irrelevant.

Flame-out Time: A test designed to assess the resistance to burning over a flame that arises from another source is as follows. A 1/8" x 1/2" x 2-1/2" bar of plastic is gripped at one end by tongs and held vertically with the lower end in a Bunsen burner flame. After 10 seconds in the flame it is removed and the time for the flame to extinguish is measured. When the flame is extinguished the specimen is immediately returned to the flame for another ten seconds, then removed and the flame-out time again determined. Times are measured with a stop watch. Any tendency to drip is also noted. The test is like--but not identical to- U.L. Bulletin 94.

Flame-out times are 1 to 3 seconds generally for the block polymers but greater than 30 seconds for BPA polycarbonate and polymethyl methacrylate. (Table 3)

IX. MELT PROCESSING

BPF polycarbonate and the silicone block polymers have been compression molded, extruded and injection molded with varying degrees of success. Compression molding, carried out at 320 to 360°C has been least successful, particularly with the block polymers. Because of the low degree of melt shear inherent in compression molding and the high melt viscosities of these resins air bubbles are often entrapped and frequently sections are not well knitted internally.

Extrusion studies have been carried out with a Brabender 3/4 in. diameter extruder to which dies of various geometries have been attached. One pound of BPF polycarbonate was dried at 125°C overnight and then extruded at 350 to 370°C through a ribbon die of cross section 1 in. by 1/16 in. using a 1:1 compression screw. The extrudate was clear and light yellow. Most sections contained tiny bubbles thought to arise from entrapped air.

Several of the block polymers have been extruded. The largest and best extrusions have most recently been made with a bar die of cross section 1/8 in. by 3/4 in. A 2:1 compression screw appeared to help considerably in providing the necessary shearing of the resin and in backing out the air.

Best results were obtained when large amounts of a dried resin (i.e. one pound or more) were available in the form of free-flowing steam precipitated granules. Resins were "starve-fed" to the extruder hopper using controlled-flow rate feeders until steady state extrusion conditions developed. Feed rate could then be raised to a flood condition. Barrel and die temperatures of 335 to 360°C worked well and screw speeds from 10 to 120 RPM were used. In most cases a stream of air was directed at the emerging extrudate to quench it and thereby suppress die swell.

Torque increased with screw speed but wide variations were seen from resin to resin not only in the shape of the torque-speed curve but even in the ease of establishing a steady torque at a given speed. Temperature changes of 10 or 20° seemed to have little effect on torque.

On several occasions a run was stopped and the extruder screw pulled from the barrel. Frequently, a compacted mass of granules was found in the last two or three flights of the compression section of the screw. Each of the flights of the pumping section of the screw would be found mostly empty but a cap of resin more or less well fused would be found covering the screw torpedo.

Finally it was found that the steam precipitated granules (each of which is a weak aggregate of fibrous particles) processed much more easily than the same granules after acetone treatment (which swells the granules; upon drying they shrink and harden considerably).

On the basis of these observations it seems clear that the torque characteristics were primarily determined by the processes going on in the compression section of the screw where resin is softened by the heat generated through internal friction effects rather than by external heat. Modifications in screw design should eventually bring a substantial improvement in the ease and quality of extrusions.

The extrudate varied considerably in quality. When conditions were optimized, however, clear bubble-free sections several yards long were extruded. In 1/8 in. thick sections the extrudates of some resins were golden yellow to straw color. Color intensity in a given run varied noticeably with barrel temperature and screw speed, which controls residence time. Residual color is believed to arise from impurities largely;

with further development extrudate color should be as good as that of commercial BPA polycarbonate sheet. Theoretically, thermal stability and oxidation, resistance of the BPF residue are high compared to the BPA residue, since BPF contains no aliphatic hydrogens.

Injection molding trials were carried out on some of the block polymers using a 45 ton Battenfeld reciprocating screw machine having a shot size of 3/4 oz. The mold used has a rotatable valve at the sprue that allows the runners to one, two or three mold cavities to be open. From these cavities Izod bars, ASTM heat distortion bars and 2 in. x 2 in. plaques, all 1/8 in. thich are obtained respectively. A total of about ten pounds of several resins was available in various forms (chopped extrudate, steam precipitated granules, etc.).

Conditions were optimized quickly enough to be able to fill any two of the three cavities at once (filling all three would have required a greater shot size). With the last of the moldings splay was entirely eliminated and well-knit, golden yellow clear moldings resulted. Barrel temperatures in the range 330 to 345°C, injection pressures of 1300 to 1500 psi and a hold time (residence time of resin in barrel) of 25 seconds gave these results.

X. CONCLUSIONS

This development program has demonstrated the feasibility of converting suitable high temperature brittle resins to melt processable plastics having a sufficiently good balance of stiffness, strength, toughness and heat resistance to qualify as high temperature engineering plastics of high transparency. A comparison of selected properties of one of these block polymers with the properties of BPF polycarbonate and BPA polycarbonate is made in Table 4.

The major improvement over the base resin comes about through effects of the rubbery domains on stress-induced cavitational phenomena in the matrix (i.e., crazing and the craze breakdown). Superficially, this action is similar to that of toughening in resins containing much larger conventional rubber particles, in than stress whitening is involved. Since the silicone domains in these block polymers are smaller than the filaments of the craze in a homopolymer while conventional rubber particles are very much larger than these filaments the details of the stress whitening processes involved are undoubtedly different in the two cases. Whatever the mechanism the toughening action becomes great enough with increasing silicone content to delay fracture to the point that shear deformation can occur extensively.

Finally, it is worth reiterating that the two independent molecular characteristics of the block polymers tend to influence different properties: while polycarbonate block length dominates in the fixing of the softening temperature, composition seems to control all mechanical properties at low temperature rather independently of block length. The looseness of the coupling between these cause and effect relationships brings great flexibility to the design of optimally tailored resins.

ACKNOWLEDGMENTS

This work was carried out under contract to the Naval Air Systems Command, Department of the Navy. We wish to thank S. Kantor for pointing out BPF polycarbonate as an attractive matrix for silicone block incorporation and C.F. Bersch for outlining the deficiencies of existing aircraft canopy materials and defining target properties for a high temperature canopy material. We also gratefully acknowledge early exploratory synthesis work by P.C. Juliano as well as helpful discussions with him during the course of this work. Finally, we thank B.M. Gendron, E.E. Kampf, E.M. Lovgren, G.A. Mellinger, W.V. Olszewski, A.R. Shultz and A.L. Young for help with much of the experimental work.

REFERENCES

1. B.M. Beach, R.P. Kambour and A.R. Shultz, J. Polym. Sci., Letters Ed. 12, 247 (1974).

2. R.P. Kambour, D. Faulkner, E.E. Kampf, S. Miller, G.E. Niznik and A.R. Shultz, Am. Chem. Soc. Organic Coatings and Plastics Preprints., Vol. 34, (2) 346 (Sept. 1974).

3. R.P. Kambour in "Block Polymers", S.L. Aggarwal, Ed., Plenum Press, New York, 1970, p.263.

4. P.W. Morgan, Macromolecules, 3, 536 (1970).

5. R.P. Kambour and G.E. Niznik, "Synthesis and Properties of Bisphenol Fluorenone Polycarbonate and BPF Carbonate-Dimethylsiloxane Block Polymers", Final Report, Contract No. N00019-73-C-0152 for Naval Air Systems Command, Department of the Navy, January 1974.

6. R.P. Kambour, J.E. Corn, S. Miller and G.E. Niznik, "Bisphenol Fluorenone Carbonate-Dimethyl Siloxane Block Polymers: Transparent, Tough, Heat- and Flame-Resistant Thermoplastics", Final Report, Contract No. N00019-74-C-0174 for Naval Air Systems Command, Department of the Navy, July 1975.

7. J.E. Ashton, J.C. Halpin and P.H. Petit, "Primer on Composite Analysis", Ch. 5, Technomic Publ. Co., Stamford, Conn., 1969.

8. J.C. Halpin, J. Composite Materials, 3, 732 (1969).

9. L.E. Nielsen, J. Applied Phys., 41, 4626 (1970).

10. T.B. Lewis and L.E. Nielsen, J. Applied Polym. Sci., 14, 1449 (1970).

11. L.E. Nielsen, Applied Polym. Symp., No. 12, 249 (1969).

12. L.E. Nielsen, "Morphology and the Elastic Modulus of Block Polymers and Polyblends", Report No. MPC-71-144, ARPA Contract No. N00014-67-C-0218 Sept. 1972.

13. J.E. Srawley and W F. Brown, Jr. in Fracture Toughness Testing and its Applications, ASTM Special Technical Publication 381, American Society for Testing and Materials, Philadelphia, Pa., page 190.

14. A.R. Shultz and B.M. Gendron, J. Applied Polymer Sci., 16, 461 (1972).

TABLE 1

Ball Impact Puncture Energies on 1/8" Plaques*

Resin	Injection Shot No.	Ram Speed (in/min)	Plaque Thickness(in)	Energy (ft-lbs)
10053-129B-3 (24% silicone)	23	6000	0.126	6.82
	24	6000	0.128	6.07
10053-132C (24% silicone)	60	6.0	0.125	10.71
	64	6000	0.125	10.86
	73	6000	0.137	26.24
10053-136C (21% silicone)	49	6000	0.124	8.99
	50	6000	0.125	7.96
10053-151 (18% silicone)	4	6000	0.123	4.73
	5	6000	0.122	4.93
PMMA(Acrylite)		6000	0.120	2.38
Lexan BPA Polycarbonate	Extruded Sheet	6000	0.126	125.9

* Ram driven 1.0" below position of lower face of plaque each time at rate listed above.

Punch: 2 cm dia. with hemispherical nose. Hole in support plate: 4 cm. dia.

TABLE 2

Heat Deflection Temperatures of Injection Molded Block Polymers by ASTM D648 at 264 psi

Resin	Wt.% Silicone	Temp (°C)
10053-129B3	24	187
10053-129B5	23	184
10053-132C	24	208
10053-136C	21 ca.	204
10053-151	18	214
10053-152	21	208

TABLE 3

Flammability Characteristics of BPF Polycarbonate,
BPF Carbonate-Dimethyl Siloxane Block Polymers and Some Commercial Resins

Resin	Wt. % Silicone	Limiting Oxygen Index	Burning Characteristics in Oxygen Index Test	(%) Residue (TGA-700°C) (air)	Flame-Out* Times (sec) 1st	2nd
BPF Polycarbonate	0	40	Rapid charring Low smoke No drip	2	-	-
10053-129B	23	48-49	Rapid charring Low smoke No drip	16.5	2	3
10053-132C	24	49.1-50.2	Rapid charring Low smoke No drip	17.0	1	3
10053-136C	21	49.8-50.3	Rapid charring Low smoke No drip	15.5	1	3
10053-151	16	50.3-51.1	Rapid charring Low smoke No drip	10	1	5
BPA Polycarbonate	0	30	Little char; Dripping; smoke	0	>30	
Polymethyl-methacrylate	0	ca.18		0	>30	
Polydimethyl-siloxane(SE-30)	100	ca.22		11	-	-

*Explanation of Test: A single 1/8"x1/2"x2-1/2" bar held vertical in Bunsen burner flame for 10 sec and removed; time for flame to extinguish then measured. Specimen returned immediately to flame for 10 sec. and removed; time for flame to extinguish measured again.

TABLE 4

Properties of Selected Resins

	BPF Polycarbonate	BPFC Block Polymer #1	BPFC Block Polymer #2	BPA Polycarbonate
Silicone Content (Wt.%)	0	18.5	21	0
BPFC Block Degree of Polymerization	10^2	16	14	-
Flex Modulus (psi)	410,000	250,000	245,000	340,000
Tensile Strength (psi)	11,000 b	6,900y	7,400y	9,000y
Nominal Ultimate Elongation (%)	$\leq$ 18	21	24	110
Izod Impact Strength (ft-lbs/in. notch)	0.2*	1.9	2.3	16
K_{Ic} (psi - $in^{\frac{1}{2}}$)	<1000*	1500-3500	2300	1000-3500**
Heat deflection temp (°C) at 264 psi	280*	214	208	135
Temp. for Strength = 1000 psi (°C)	280	216	210	150
Limiting Oxygen Index	40***	50***	50***	30***
Ease of Grinding & Polishing	———	Same	———	———
Extrusion Temp (°C)	370	340	340	260
Injection Molding Temp (°C)	>370	330	335	280

* Estimated value based on other observations
** High value applied only to low crack velocities
*** No flame retardants added
b = brittle
y = yields before fracture

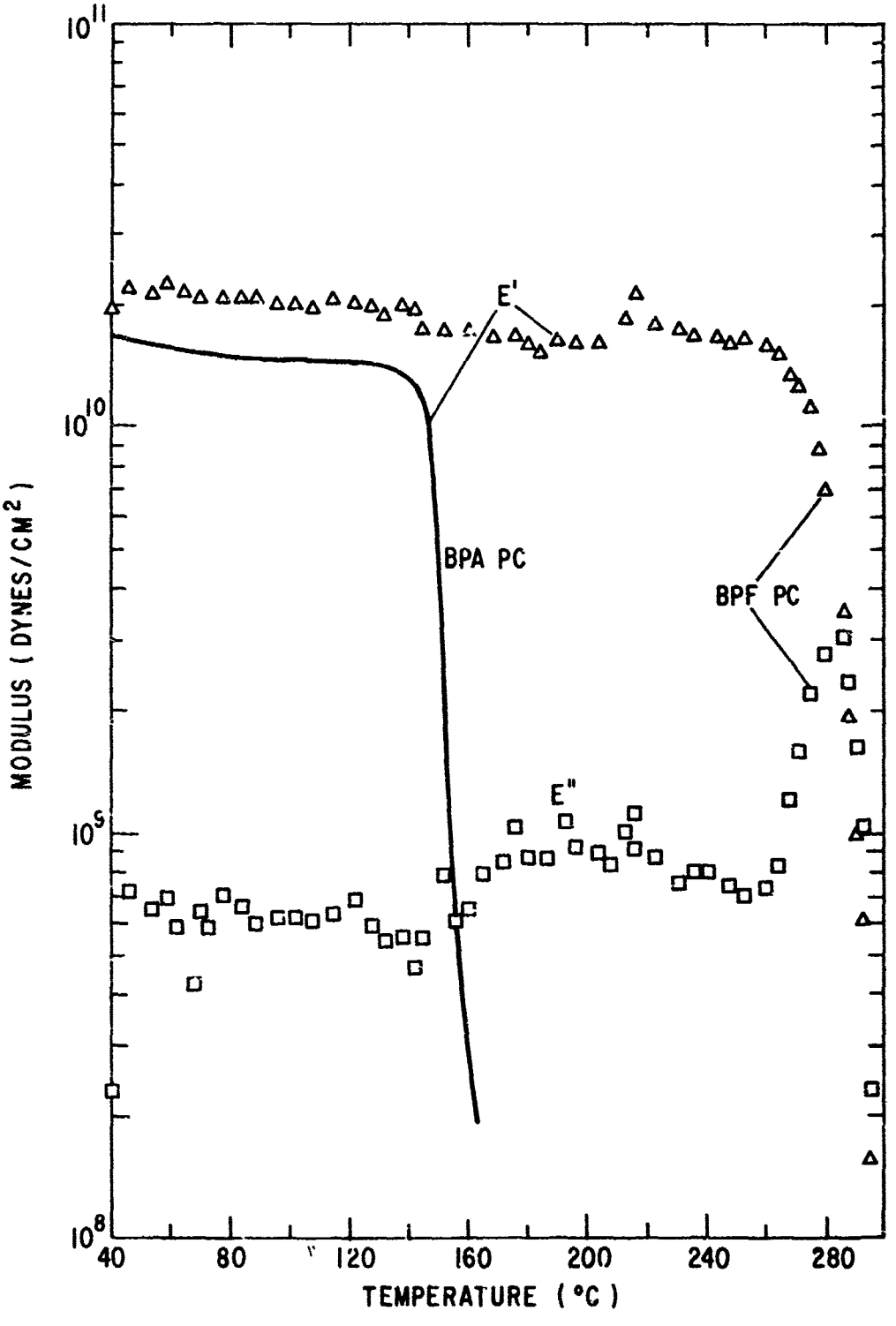


Figure 1. Temperature dependence of dynamic storage (E') and loss (E") moduli at 110 Hz for BPF polycarbonate.

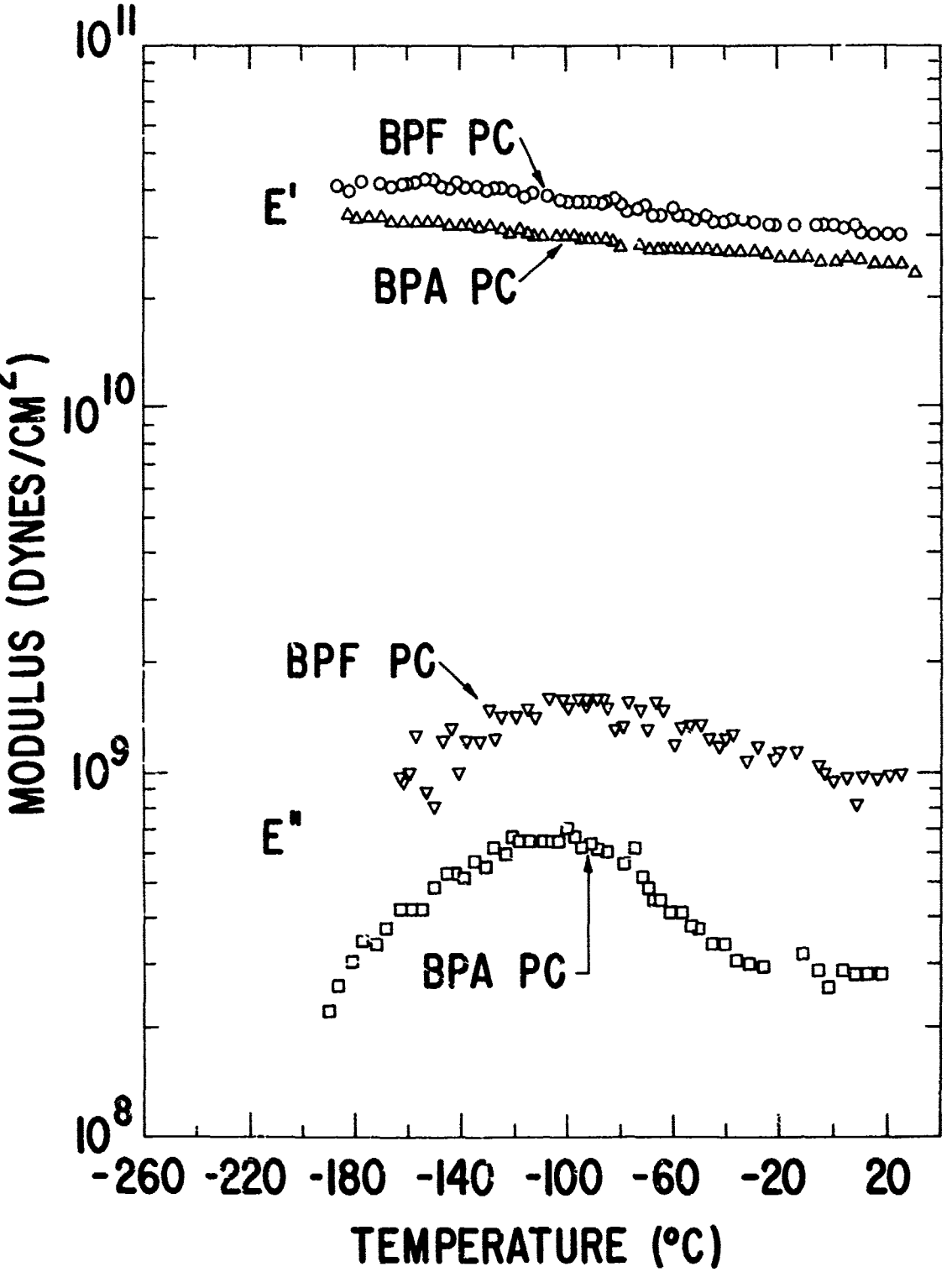


Figure 2. Temperature dependence of E' and E" at 110 Hz for BPA - and BPF polycarbonate.

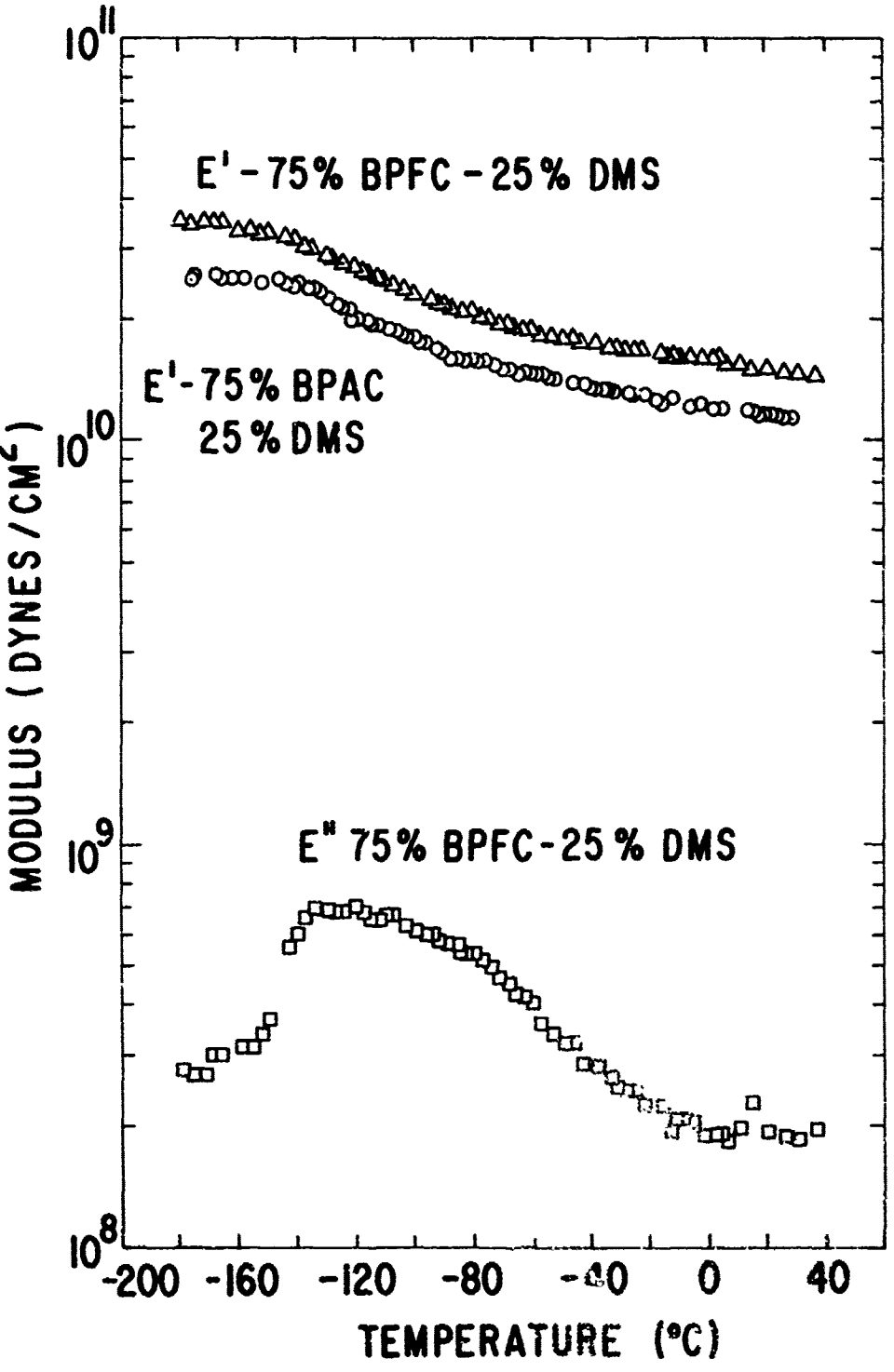


Figure 3. E' and E" at 110 Hz and low temperatures for one BPF carbonate-silicone block polymer. E' for BPA carbonate-silicone block polymer of same Wt. % silicone shown for comparison.

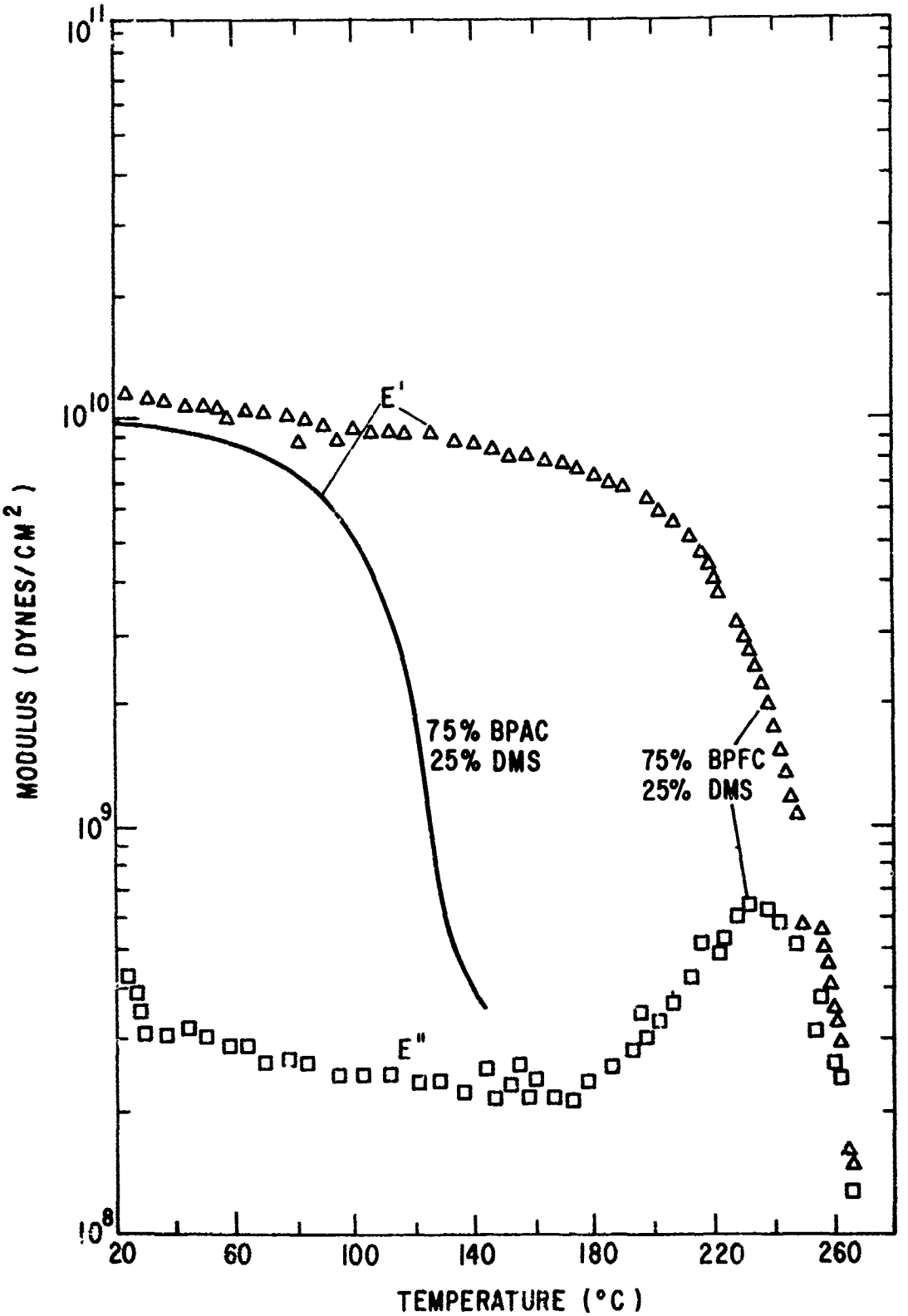


Figure 4. E' and E" at 110 Hz and high temperatures. Same block polymers as in Fig. 3.

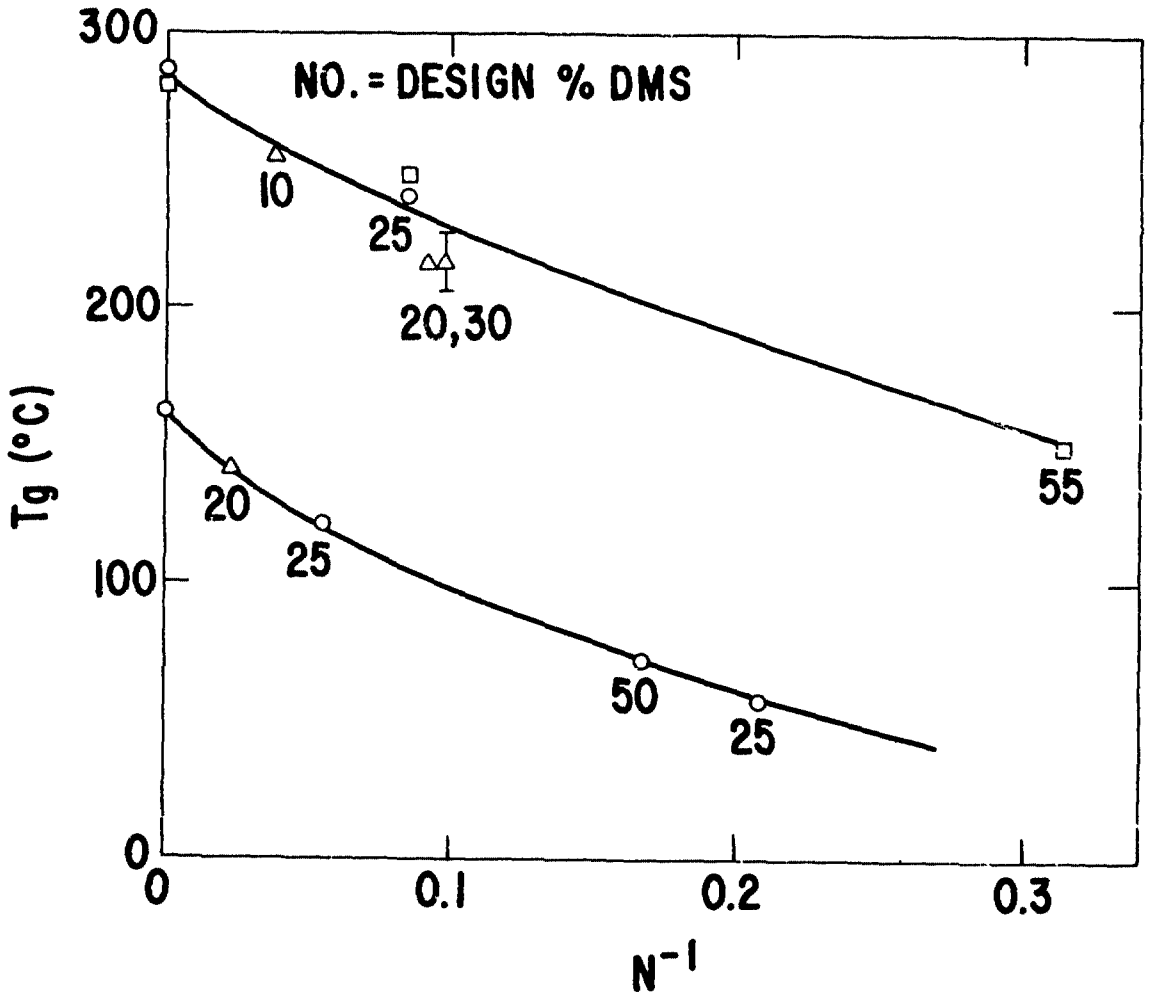


Figure 5. Dependence of polycarbonate domain T_g on reciprocal number average degree of polymerization N^{-1} of polycarbonate block. Upper line: BPFC-silicone family. Lower line: BPAC-silicone family. Circles: dynamic mechanical E" or middle of E' dispersion. Squares: differential scanning calorimetry. Triangles: TOA thermo optical analysis.(14)

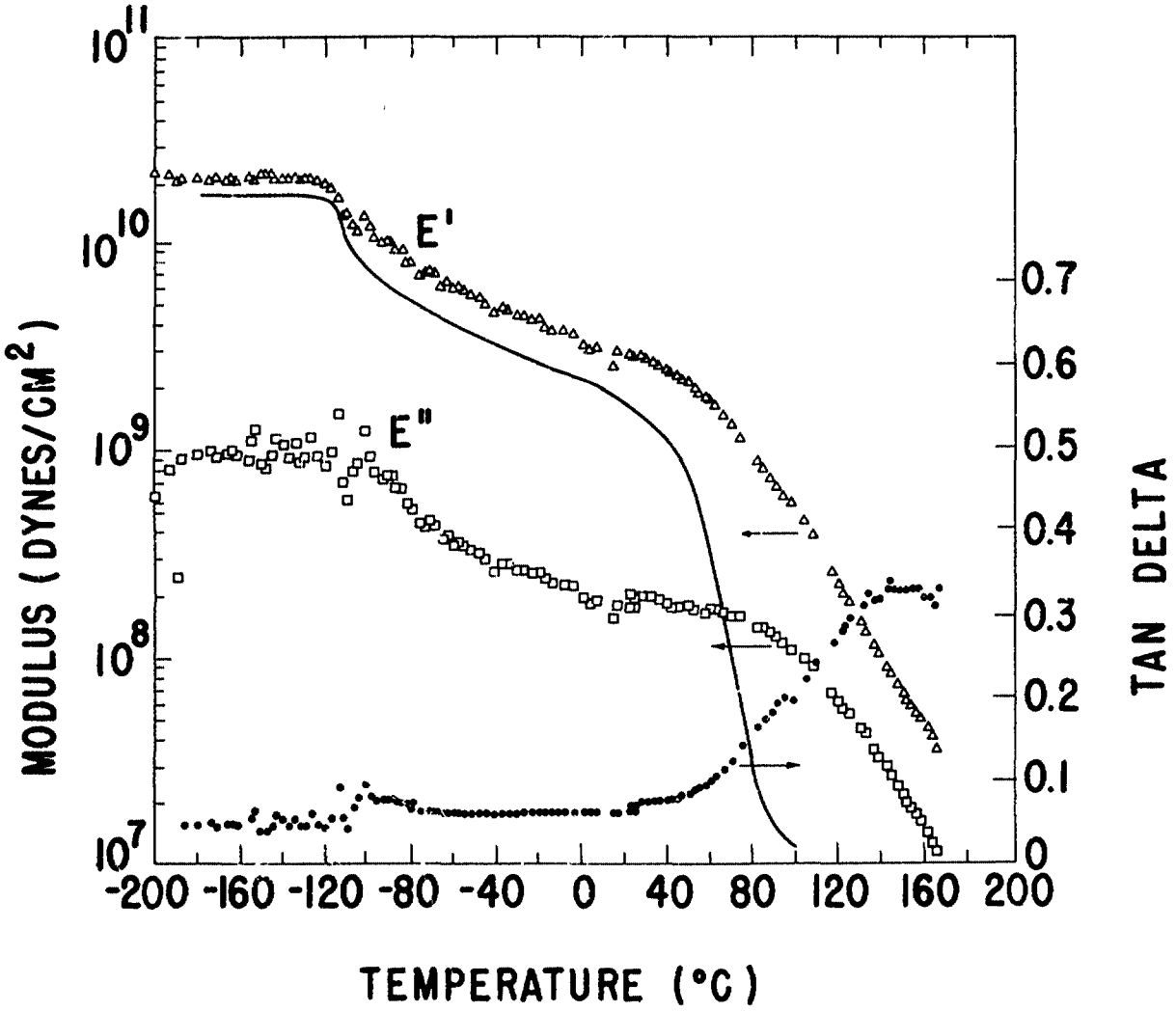


Figure 6. Temperature dependence of E', E" and tan δ for block polymer designed to be: 45% BPF carbonate (3.9 units/block) - 55% silicone (20 units/block). Solid line: Storage modulus of 50% BPA carbonate (6 units/block) - 50% silicone (20 units/block).

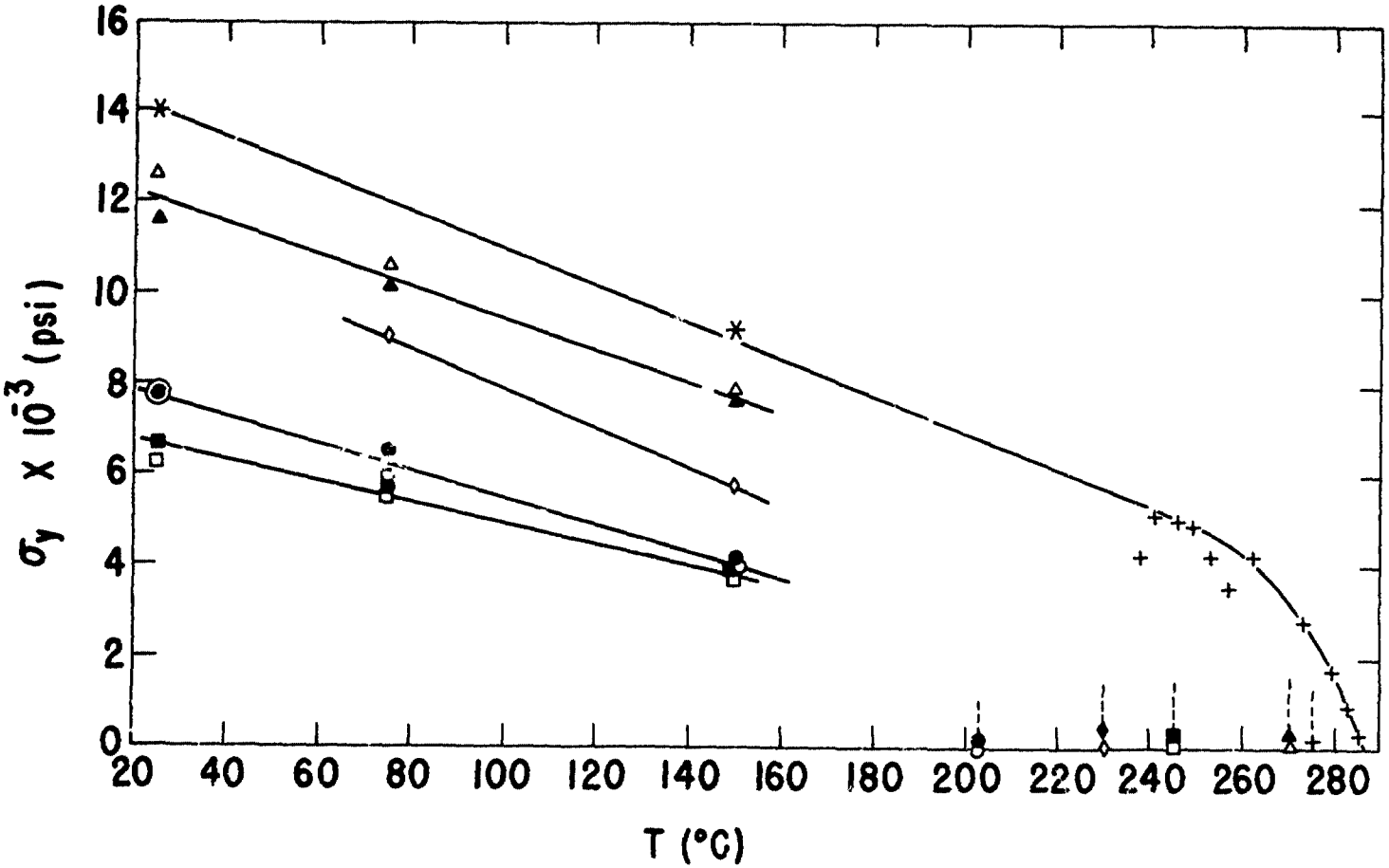


Figure 7. Temperature dependence of yield stress for several resins + BPF polycarbonate molded bars; * BPFPC films (value at 25°C extrapolated from values of films containing residual casting solvent); Circles: 23% silicone, 14.3 unit silicone block length; triangles: 7% silicone, 8 unit silicone block length; diamonds: 16% silicone, 8 unit silicone block length; squares: 27% silicone, 23.5 unit silicone block length. Dashed vertical lines at right indicate corresponding polycarbonate domain T_g's

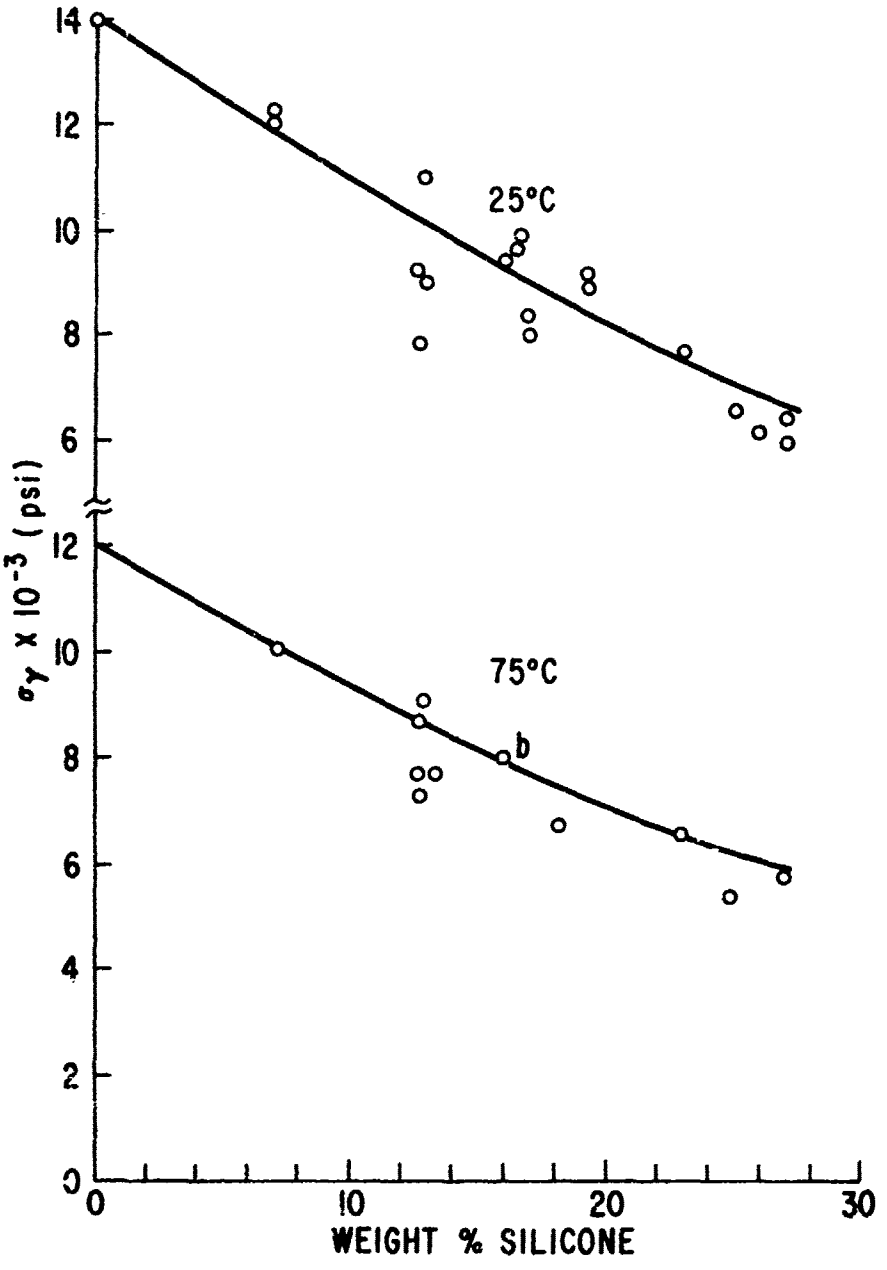


Figure 8. Dependence of yield stress on silicone contents of several BPFC - silicone block polymers at 23°C and at 75°C. Solid lines: predictions based on Halpin-Tsai equation for moduli of two phase composite and experimental yield stresses of homopolycarbonate.

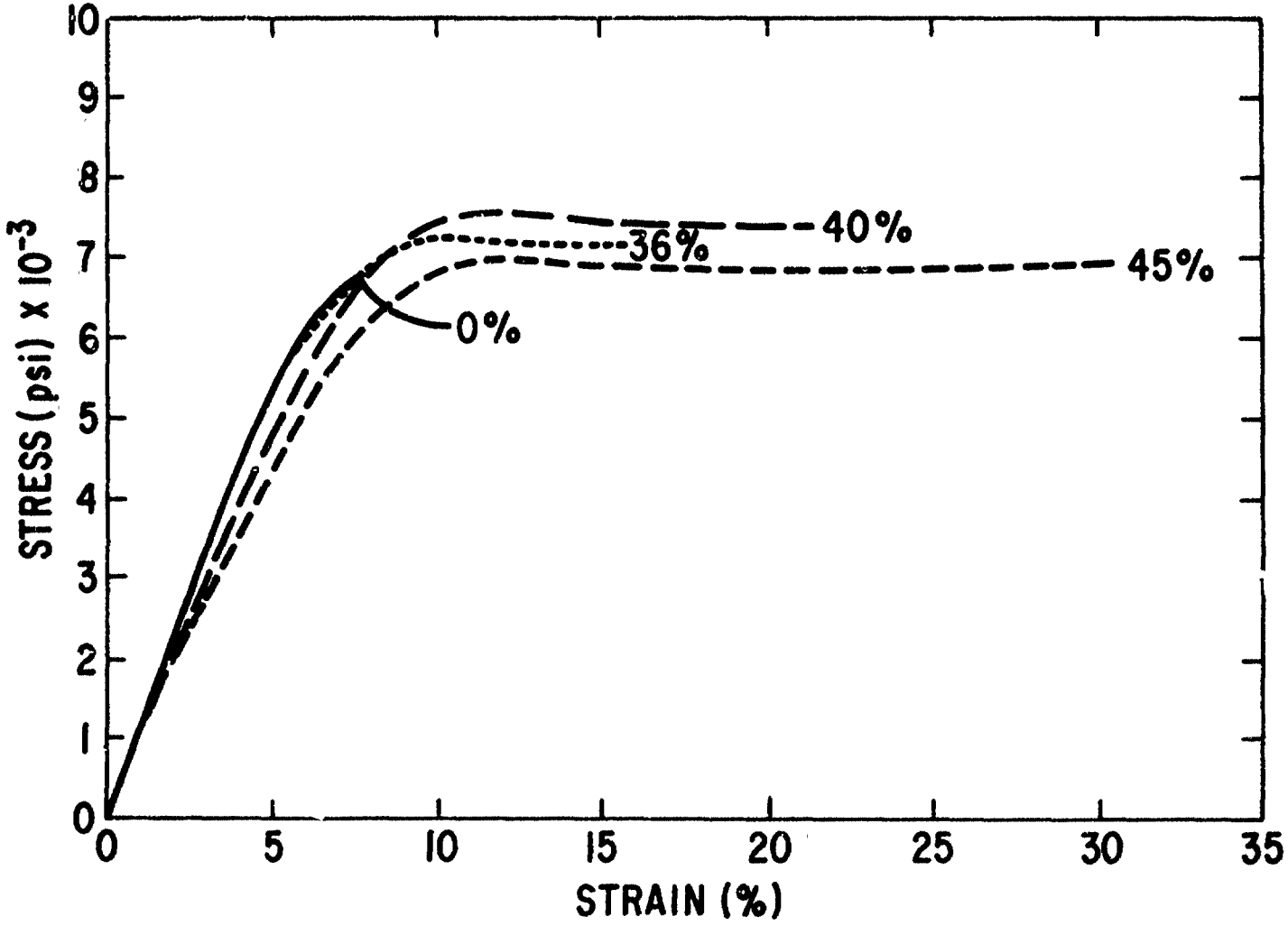


Figure 9. Room temperature stress strain curves for BPFC-silicone block polymer of 25% silicone, 35.8 unit silicone block length.

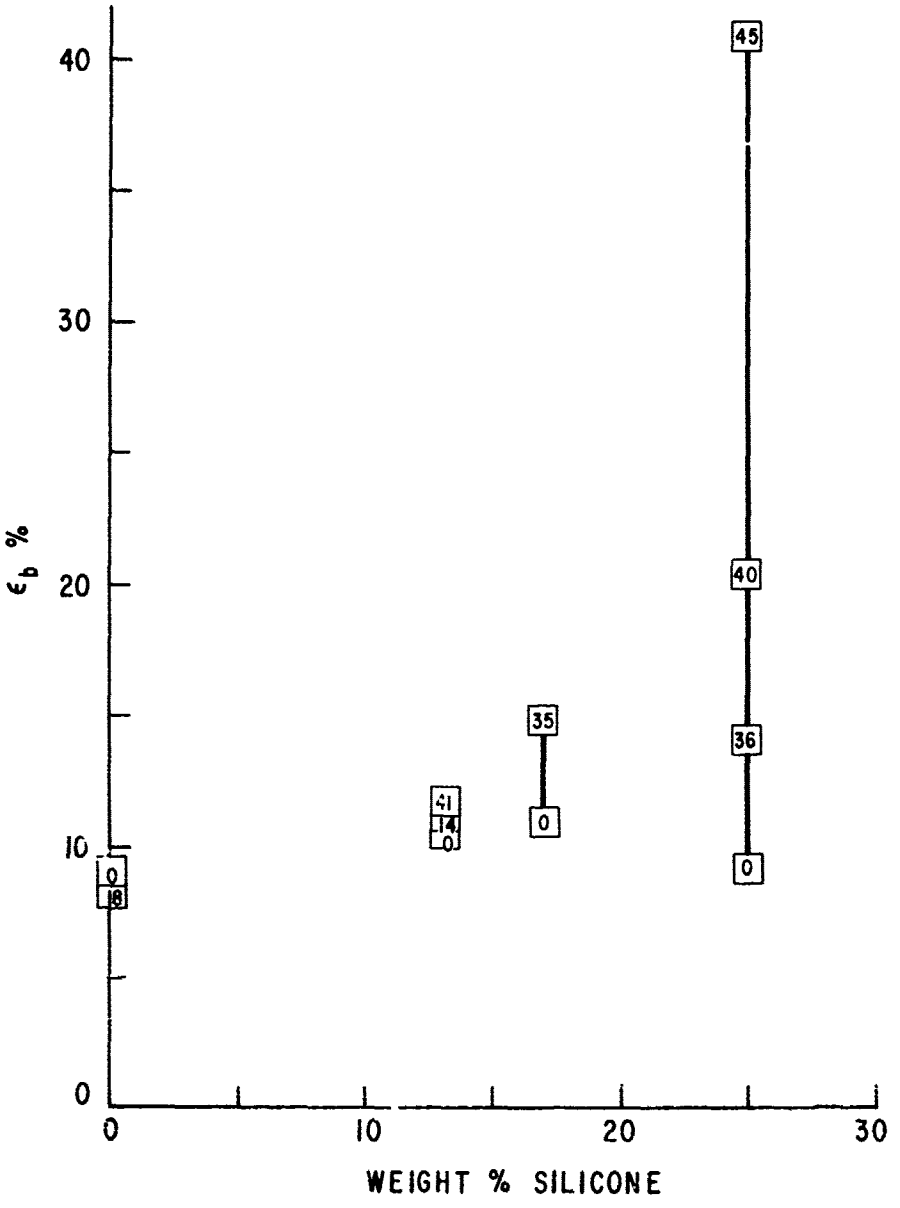


Figure 10. **Ultimate elongation ϵ_b at 23°C vs. silicone content of films hot stretched to the percentages indicated in the data symbols.**

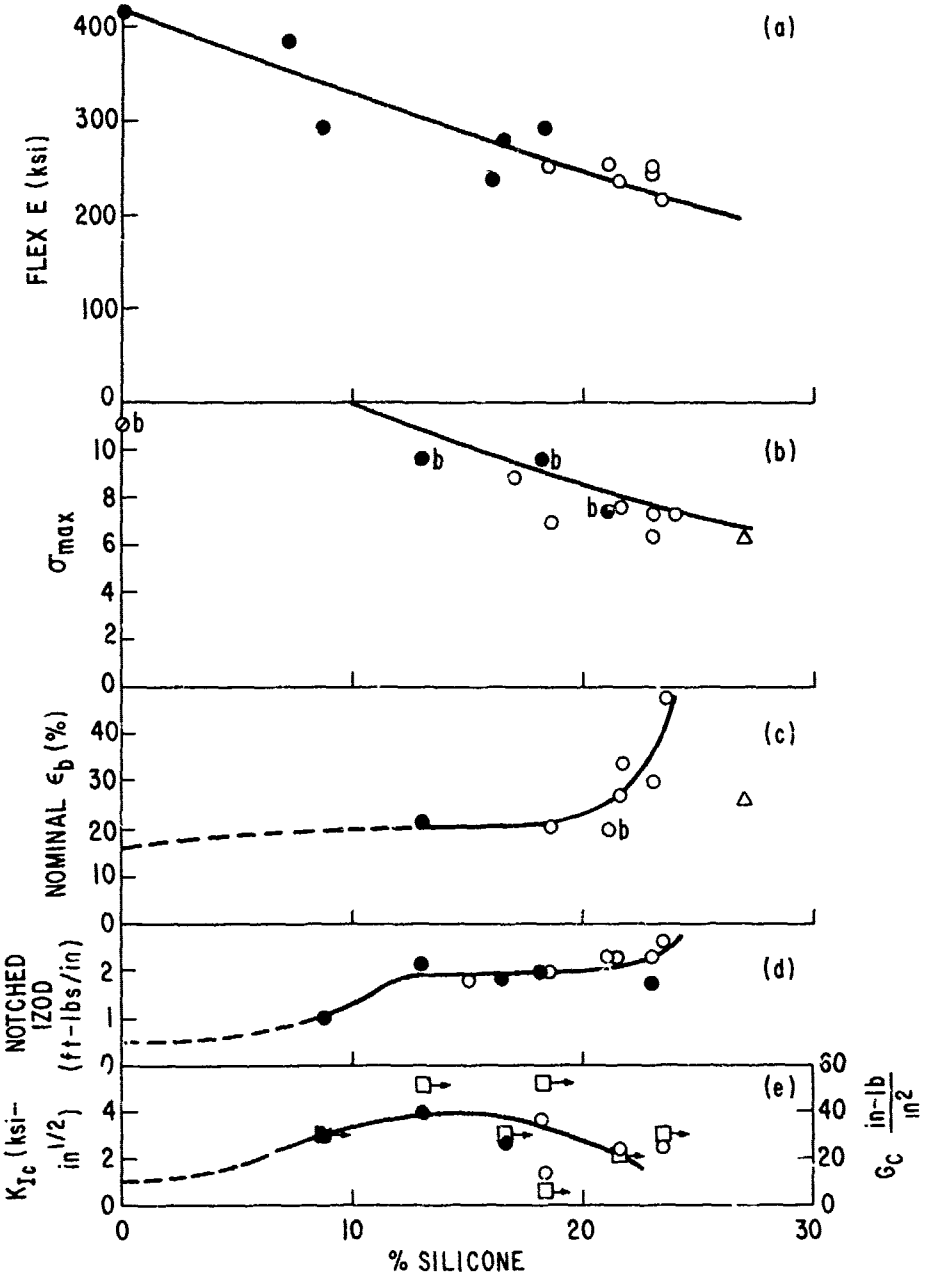


Figure 11. Dependence on silicone content of several room temperature mechanical properties of moldings and extrudates of BPF polycarbonate and its block polymers.
a) Flex modulus. Line: Halpin-Tsai equation
b) Yield stress. Line: Halpin-Tsai equation
c) Nominal ultimate elongation (exceeds gauge elongation by 10 to 15% due to shoulder effects)
d) Notched Izod impact energy
e) Stress intensity factor K_{Ic} and strain energy release rate G_{Ic}

Code: ● - compression molding; o - bar extrudate; Δ - ribbon extrudate with longer gauge section; □→ - G_{Ic} datum corresponding to K_{Ic} value at same silicone content; b - brittle failure

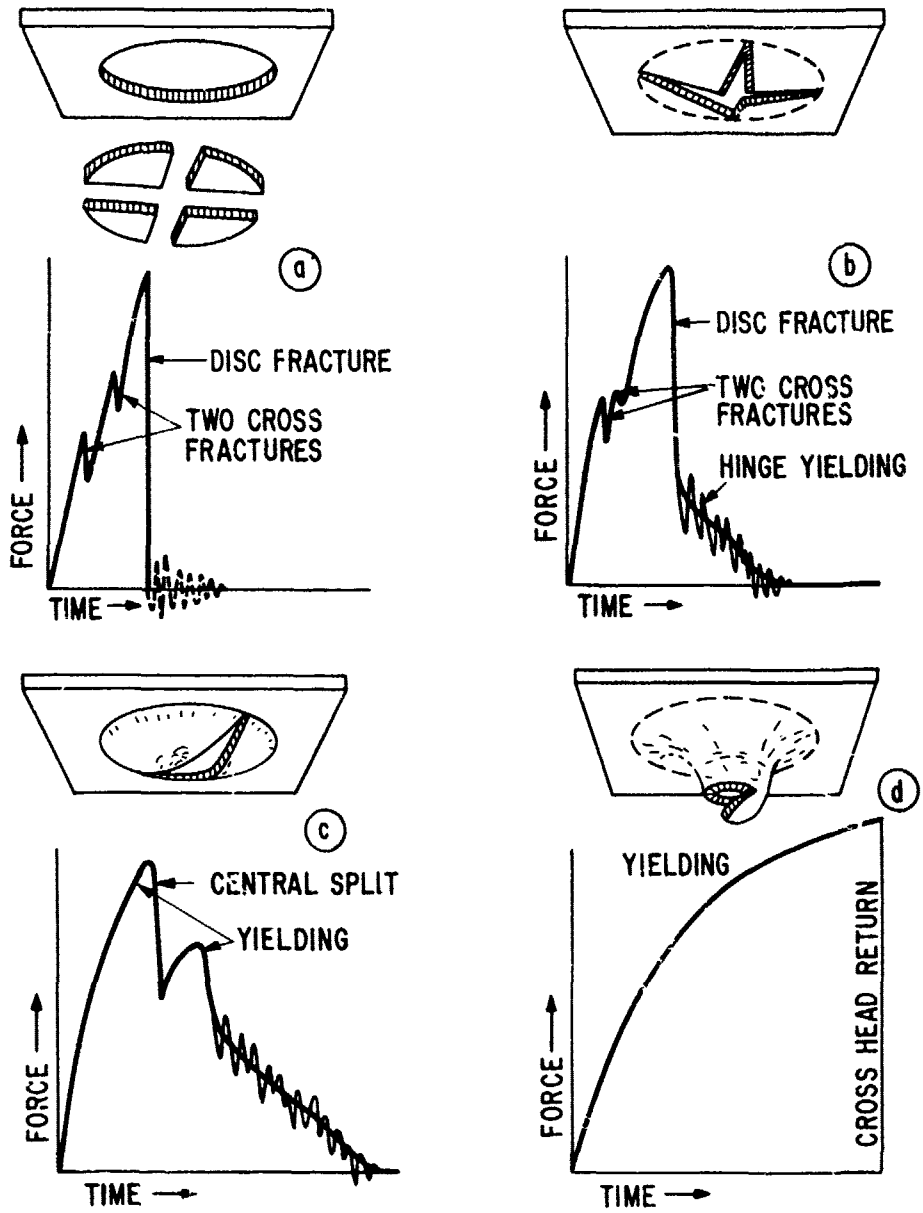


Figure 12. **Ball impact puncture morphologies and associated force-time traces for plastics of varying ductility. a) completely "brittle" fracture into four separate quadrants (ca. 2-5 ft.-lbs.) b) brittle fracture except for lower surface "hinges" that attach quadrants to disc circumference (ca. 10 ft.-lbs.) c) single cross-disc crack with gross shear deformation and some stress whitening (26 ft-lbs.) d) only shear deformation (125 ft.-lbs.). Oscillations at ends of load time trace arise fron ringing of load cell washer.**

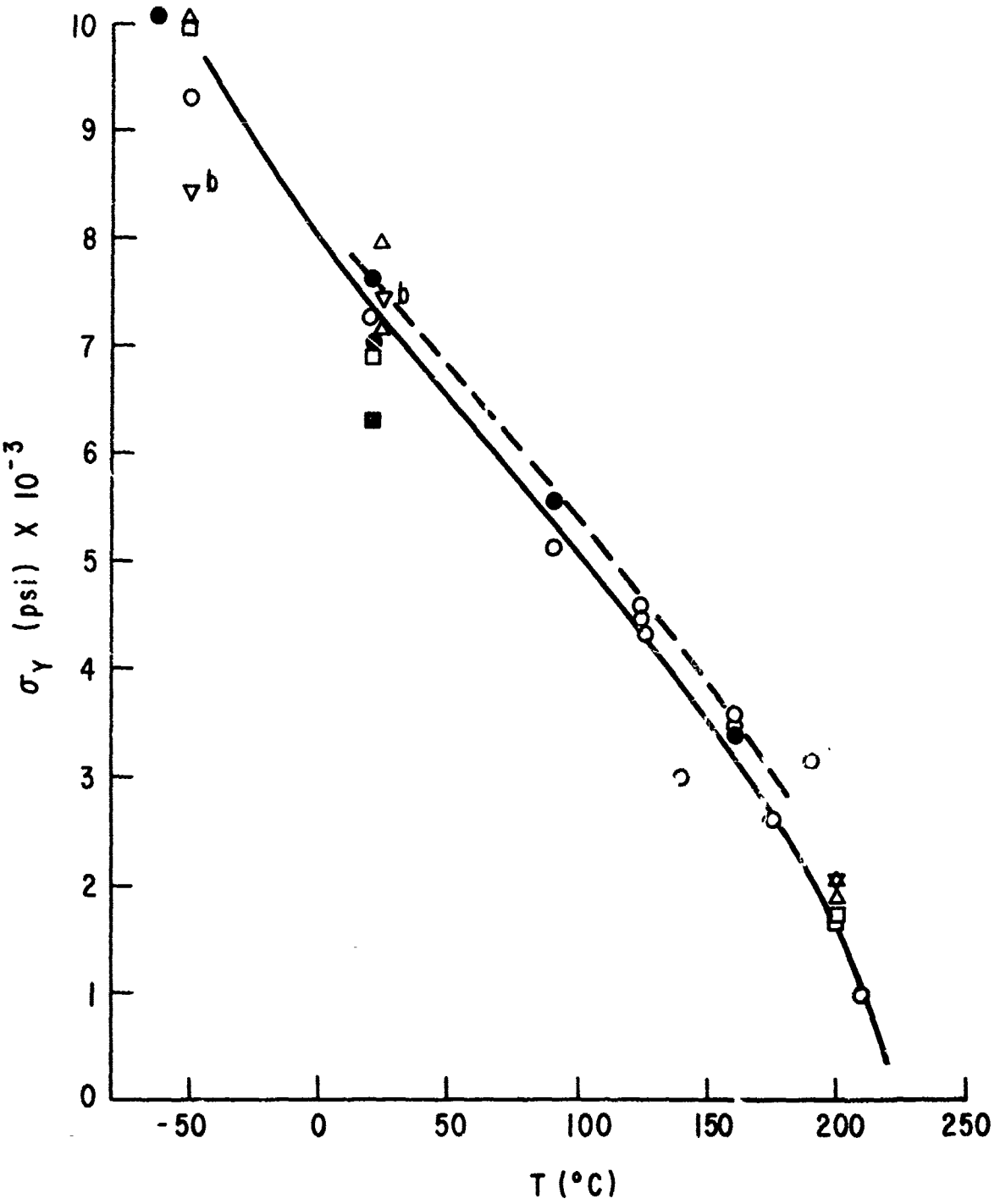


Figure 13. Tensile yield stress vs. temperature for several BPFC - silicone block polymers, all containing silicone blocks of number average degree of polymerization = 18.8

Silicone Contents: ● - 23.0%, ■ - 23.8%, o - 24%, Δ - 21%, □ - 18.5%, ▽ - 21%, b = brittle failure datum.

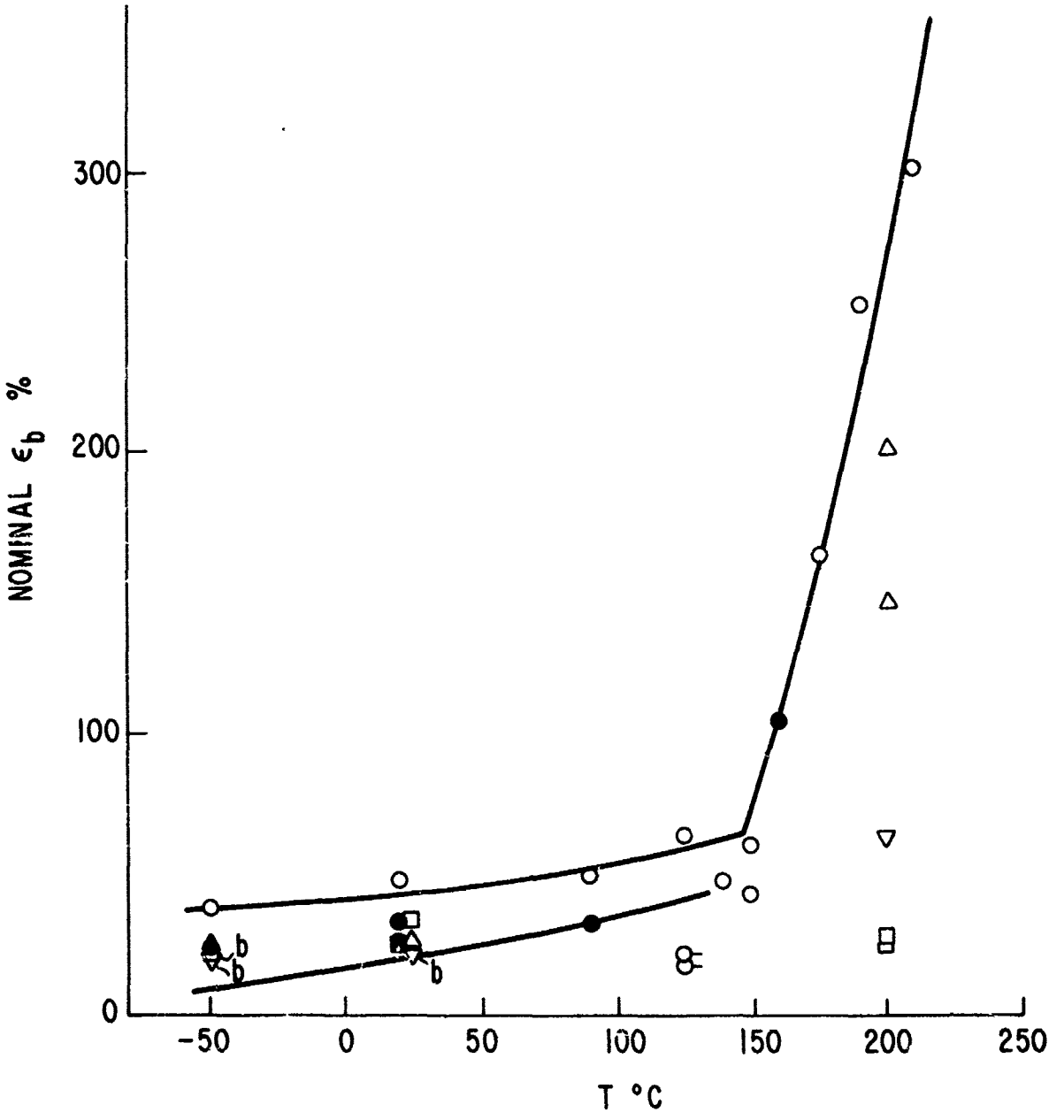


Figure 14. Nominal ultimate elongation vs. temperature for several extruded block polymers. Nominal elongations exceed gauge elongations by 10 to 15%. Code: Same symbols as in Fig. 13; O- indicates sections of extrudate that were compression-flattened.

DESIGN, SYNTHESIS, AND DEVELOPMENT OF NEW TRANSPARENT POLYMERS FOR MILITARY APPLICATIONS

R. Fish, J. Parker, and G. Fohlen
National Aeronautics and Space Administration
Ames Research Center
Moffett Field, California

DESIGN, SYNTHESIS, AND DEVELOPMENT OF NEW TRANSPARENT POLYMERS FOR MILITARY APPLICATIONS

R. Fish, J. Parker, and C. Fohlen

Ames Research Center, NASA
Moffett Field, Calif. 94035

ABSTRACT

NASA's program on transparent polymers for military aircraft canopies has been expanded and now includes a wide range of performance properties not identified previously. The three major areas that are considered are: (1) fire resistance — particularly in relation to carrier deck fires; (2) utility barriers to high energy radiation; and (3) ballistic tolerance. In this paper attention is focused on the role of polycyclic aromatic transparent polymers, in solving these three classes of problems, and on the enunciation of the underlying thermochemical mechanisms we have found useful in the case of the epoxy derivatives. A new material based on a methylolated epoxy system is discussed. Relative to the third problem area, ballistic tolerance, it was noted that monolithic epoxy panels were quite brittle and laminate structures were considered. The results of ballistic tests on these laminates is discussed together with research into the molecular configuration of some polycarbonate structures.

INTRODUCTION

The NASA program on transparent polymers for military applications is an outgrowth of research into the development of fire-resistant materials that would provide increased protection of passengers involved in civilian aircraft fires. The work, jointly sponsored by NASA and the Joint Technical Coordinating Group for Aircraft Survivability (JTCG/AS), has been addressing aircraft cockpit protection against carrier deck fires and crash fires. This paper describes some of the current research and development work as well as the testing in order to permit comparison of the product of this research and development effort with state-of-the-art materials. It is shown that material developed for fire-resistance can, in general, be considered as hardened against other thermal threats as well.

Some related problems and early work were identified in a previous NASA paper presented at the 1973 Conference on Transparent Enclosures; some of the desired performance characteristics for advanced aircraft canopies, taken from reference 1, are shown in Fig. 1. The glass transition temperature (T_g) has been used as a guide in estimating the retention of mechanical strength at elevated temperatures. Polymers that have glass transition temperatures above 260° C have been considered suitable for use in the aerodynamic heating environment. In general, the higher the glass transition temperature the greater the tensile strength one can expect at the service temperatures. Because of its excellent impact resistance, polycarbonate was chosen as the starting point of an investigation into the feasibility of achieving improved thermal performance while retaining good mechanical properties (Ref. 1). None

of the state-of-the-art transparent polymers perform very well when exposed to fuel fire thermal environments.

Parker and Winkler (Ref. 2) have shown that the primary thermochemical anerobic char yield as measured from a thermogravimetric analysis (TGA) bears a direct relationship to the number of multiply bonded aromatic rings present in the initial polymer. Fish and Parker (Ref. 3) have shown that the resistance of a polymer to the intrusion of thermal radiation, as in the case of a JP-4 fuel fire, is critically controlled by aromatic nature of the initial polymer or its primary pyrolysis residue.

Figure 2 shows the effect of aromatic structure on the thermochemical char yield of transparent polymers as well as on some other aromatic polymers. Here, the char yield at 700° C versus the number of moles of multiply-bonded aromatic rings per gram of polymers is plotted. Two polymers reported previously (Ref. 1), epoxyboroxine and phenolphthalein polycarbonate, are plotted with bisphenol-A polycarbonate for reference. This relationship has provided a convenient means of characterizing polymers for selection as transparent composite components.

BACKGROUND

Material Development

In the 1973 conference on transparent aircraft enclosures, we reported (Ref. 1) on the development of a transparency consisting of a laminate of an aromatic polymer made from a cured epoxy material and a polycarbonate. An epoxy resin was chosen as one of the components because its aromatic and cross-linked structure would contribute to the desired thermal stability. The particular epoxy resin system with which most of the work has been done is a purified version of the common diglycidyl ether of bisphenol A (DGEBA) using 5 pph of trimethoxyboroxine (TMB) as a curing agent. This material is known as EX-112. The cure cycle was a three step process: 3 hr at 80° C; 3 hr at 135° C; and finally 2.5-3 hr at 180° C. The cast plates of the partially cured resin could be made to the proper curvature and conformation by carrying out the final curing step on the properly shaped form. Many castings of the resin system have been made with little or no modification and laminated to commercially available bisphenol A polycarbonate plates to form windows for evaluation in aircraft (Ref. 4). The structure of EX-112 is shown at the top of Fig. 3.

It has been possible to cast the epoxy system directly onto the surface of existing polymethyl methacrylate (PMMA) canopies. In this case a lower final cure temperature was necessary because of the low melting-temperature substrate PMMA, but a longer cure time at the lower temperature apparently permitted an adequate cure since little loss in the final thermal or physical properties was observed.

An analytical study of the epoxy-TMB system used has shown that about 2.3% of low molecular weight extractable oligomers (monomer, dimer and trimer), containing unreacted epoxide groups, remain in the cured resin (Ref. 5). These unreacted epoxide groups contributed 17.3% of the exothermic heat evolved at 430° C.

In 1973 (Ref. 1) we reported on the use of diglycidyl ether of bisphenol A as the only epoxy monomer used in the making of the polyether casting. This may indeed remain the preferred material because of its availability, color, cost, ease of use, and adequacy of performance. However, we have since investigated several other epoxide materials that we believed would have even better thermal properties because of their molecular structure. One of these was the "Apogen" (trademark) resins produced by the Metal and Thermit Company, Rahway, New Jersey. These are mono- and di-methylolated derivatives of DGEBA and were disclosed in a Belgian patent issued in 1965 (Ref. 6). The additional reactive methylol groups have the effect of easily forming crosslinkages between the resin molecules leading to a more dense network structure (Ref. 1). These resins were also cured with TMB, but are more difficult to process than the DGEBA/TMB system. These resins are more reactive and viscous. If one warms the resin to reduce the viscosity the increased reactivity due to the higher temperature, together with the additional reactivity due to the substituent, makes the casting process for thick sections quite difficult. However, there are ways of overcoming the difficulties: (1) by the use of reduced concentrations of TMB, (2) by the use of the less reactive tri-isopropoxyboroxine in mixture with the trimethoxyboroxine, or (3) by the use of mixtures of the Apogen resins with DGEBA. Not all of these combinations have been thoroughly investigated — especially as they relate to the thermal properties of the casting.

Using Apogen 101, the predominately monomethylolated derivative of DGEBA, preheated to 60° C to insure complete mixing with 5 pph of TMB, and otherwise proceeding as per the process with DGEBA, produced a clear transparent casting; this epoxide system is known as 4F9. In a thermogravimetric analyzer (TGA), this material exhibited an anaerobic char yield of 45% at 700° C compared to 34% obtained with the EX-112. In the T-3 thermal test the Apogen derived polymer (4F9) also showed improved thermal resistance — even longer time to burn-through and the black porous char that formed was stronger and had a finer, denser structure than that of the EX-112. The structure of 4F9 is shown as Epoxy No. 2 in Fig. 3.

The polyether resins made from the epoxy material are in general too brittle to be considered for use monolithicly in places where the impact of birds and other objects would be a problem. For that reason these castings were laminated to the high impact strength polycarbonate polymers as discussed in the 1973 paper (Ref. 1). The poly-bisphenol A carbonate material has been used in most of the prototype windows. It may be that this material will be the ultimate choice because of its availability, cost, color, and adequacy of performance, even though it lacks the required thermal properties (too low a melting point, glass transition temperature, and char yield).

Previously we chose as a promising candidate for our purposes the polycarbonate made from phenolphthalein, the structure of which is shown at the bottom of Fig. 3. In addition to the added aromatic ring, there is also a lactone ring capable of additional reactivity and crosslinking. The polycarbonate from phenolphthalein had good thermal and physical properties. There were problems, however, in the processing of this polymer. To make plates thick enough to use as windows required extraordinary procedures: molding of solvent plasticized polymer powder and the subsequent removal of the solvent

were extremely tedious tasks that required weeks of heat and vacuum treatment and often resulted in warped plates. High pressure and high temperature "forging" of the dry polymer powder required temperatures too near the decomposition temperature with the result that decomposition and premature cross-linking occurred. The lactone ring present in this material made the polymer somewhat too reactive for processing into window plates.

In a recent study (Ref. 7), other aromatic polycarbonates were made having as bisphenol monomers the structures shown in Fig. 4. All of these monomers have the pivotal carbon atom incorporated within a cyclic aromatic structure. The first compound, the 1,1-bis(hydroxyphenyl)-indan, was made but could only be obtained in a poor yield — 10 to 15%. The one below it in Fig. 4 — the 9,9-bis(4-hydroxyphenyl)-fluorene — was obtained in a considerably better yield of about 60%. There were problems in the synthesis of the other monomer materials and it was not feasible to spend more time in their study. The properties of these homopolymers are shown in Fig. 5.

Sufficient quantity of the indanyl bisphenol was obtained to make several batches of the polycarbonate; as shown in Fig. 6, it had very good physical and thermal properties. The polycarbonate made from the more accessible fluorenyl bisphenol was also made, but there were problems with its solubility in the polymerization mixture. This resulted in inherent viscosities of 0.18 to 0.26 (0.5% in tetrachloroethane) and films made from the material were cloudy and brittle. The addition of catalytic amounts of pyridine increased the inherent viscosity to 0.9; films made of this material were tougher but still somewhat cloudy.

Extensive work with this fluorenyl-bisphenol polycarbonate elsewhere has shown similar problems (Ref. 8). Gel permeation chromatograms were bimodal showing considerable low molecular weight oligomers to be present. Some of these can be removed by extraction with acetone. The thermogram (TGA) of the poly fluorenyl-bisphenol carbonate shows a T_d of 400° C and an anerobic char yield at 800° C of 61%. In air the onset of oxidative weight loss is at 300° C with the T_d again about 400° C and a surprizing char yield in air of 31%. The resulting charred foam had good integrity.

The excellent thermal properties of this fluorenone-bisphenol based polycarbonate, together with the ease of obtaining the monomer makes this an attractive candidate for further development. Because of difficulties in the polymerization of this material alone, however, attempts were made to make copolycarbonates of fluorenyl-bisphenol with both bisphenol A and with phenolphthalein. It was found that these co-polymerizations proceeded more readily.

Figure 7 shows the results of some of this copolymer work. The decomposition temperature and anerobic char yield are given for four copolymers. The anerobic char yields of these copolymers were quite satisfactory and the films of them were clear and tough. A quantity of the monomers has been obtained in order to make the larger amounts of the several copolymers that are necessary to permit further evaluation of the processability, and thermal and mechanical properties of these materials.

LABORATORY TESTS

The tests performed on the materials followed standard ASTM, Mil Spec, or Federal test procedures wherever possible to enable comparison with handbook values of materials not included in the program; however, some tests are not standard types. These include the Ames T-3 test for "crash fire endurance," ne high energy laser penetration tests, and ballistic tolerance tests.

The Ames T-3 thermal test facility is a JP-4 fuel-fired unit where the heat flux and thermal-chemical environment of a crash fire can be duplicated in a controlled manner. The results reported can either be burn-through or temperature-time history of the unexposed surface of materials undergoing test.

Using a high energy CO_2 laser the resistance of the materials was determined by exposing them to known flux rates for precise periods of time.

The ballistic impact tolerance of the materials was determined by observing their behavior in response to the impact of ball and armor piercing ammunition, and to the impact of fragments simulating nearby bursts of high explosive (H.E.) shells.

In the tables of properties the following material abbreviations are used:

1. acrylate, PMA
2. stretched acrylic, SPMA
3. bisphenol A polycarbonate, BPAPC
4. epoxy EX-112, 112
5. epoxy EX-4F9, 4F9
6. phenolphthalein polycarbonate, PHPC
7. polyarylsulfone type A, PASA

Physical Properties

The physical properties measured were tensile strength and modulus, flexural strength and modulus of elasticity, Izod impact strength and hardness. Tests of tensile properties were performed in accordance with ASTM D-638. The samples had a gage length of 2.54 cm and a cross section of 0.6 cm by specimen sheet thickness of approximately 0.6 cm. The tensile strength is the ultimate strength and tensile modulus was determined at 1.5% offset from the straight-line portion of the tensile stress-strain plot. The flexural tests were performed in accordance with ASTM D-790, method I, where the sample rests on two supports with a span of 10 cm, and is centrally loaded at a uniform rate. The modulus of elasticity is determined from the straight-line portion of the stress-strain curve during the maximum loading rate on the outer surface of the specimen.

The Izod impact strength tests, as prescribed by ASTM D-256, were performed on both virgin materials and on weathered materials — the weathered samples having been exposed to 500 hr (250 cycles) of continuous xenon light, with water spray for 18 min of each 2-hr cycle. The 6000-W xenon light with borosilicate filters has a spectrum similar to direct noon summer sunlight at Chicago, Illinois. In the impact test, notched samples were impacted by a weighted pendulum and the bending moment per width of specimen (width of notch) recorded. The hardness tests were performed on a Rockwell hardness tester and are shown both in "M" and "P" scales due to the wide range of hardnesses of the materials tested (ASTM D-1706). (The "M" scale uses a 6.35-mm steel ball penetrator and a major load of 100 kg; the "P" scale uses a major load of 150 kg.) Another indication of the relative hardness of the material is shown by abrading the surface in a cyclic fashion with a standard abrasion material. For these tests, a Taber abrader was equipped with Calibrase CS10F abrasion wheels that were loaded with 1000-gm weights. The milligram weight loss per 1000 Hz is reported along with other physical properties in Table 1. Electrical properties of the dielectric constant and the dissipation factor are also noted in Table 1. These properties were determined by capacitive measurements at audio frequencies.

Optical Properties

Since we are considering transparent materials, their optical properties are of extreme importance. The color ranges from clear, water-white, through pale blue to amber. A more definitive color response may be seen by measuring the transmittance T, reflectance R, and thereby the absorptance A, with a scanning spectrophotometer. This was done for the virgin polymers, for polymers that had been abraded with CS10F wheels and 500-gm weights for 50 Hz, and for polymers that had been weathered for 500 hr of continuous xenon light and periodic water spray. Haze, the ratio of diffused transmittance to total transmittance times 100, is also reported. The index of refraction (n) was determined by ASTM D-542 using the microscope method. Here the apparent thickness is measured optically and the true thickness, mechanically. Therefore, $n = d_{true}/d_{apparent}$, the index of refraction.

These optical properties are shown in Table 2. The T and R values listed are the integrated areas under the spectrophotometric traces from approximately 380 to 1670 nm. Also listed are single-wavelength transmittance values T for approximately 450 nm (blue), 550 nm (yellow), and 650 nm (red). These wavelengths would generally bracket the peak visual efficiency range of the human eye.

Thermochemical Properties

Thermogravimetric analysis (TGA) was used to determine weight loss in terms of temperature when the materials were subjected to a uniform rate of heat rise. Although the materials may be heated in a variety of atmospheric gases, the most useful is dry nitrogen for determining the true thermodynamic char yield (ash residue) of a polymer. The results closely parallel the reaction of a polymer to large pool-fire heating situations. The TGAs of the material systems being reported on are reproduced on a common weight loss vs temperature plot (Fig. 8). From the TGA, the percent char yield at any

temperature, the decomposition temperature, and the rates of thermochemical reactions that occur can be determined. The heat distortion temperature is a measure of the point where a weighted penetrator enters or causes a deflection of the heated specimen.

Two other thermal properties were measured: the coefficient of linear expansion α, determined by the dilatometer method, and the thermal conductivity coefficient k, determined by guarded hot plate method. These and other thermochemical properties are listed in Table 3.

Fire Properties

A number of related tests are used to determine the fire properties of materials. Those reported here are: (1) flammability, in accordance with ASTM 635, in which the polymer is placed in a horizontal position, ignited by a bunsen burner, and note made of the rate of burning and occurrence of any self-extinguishment (SE); (2) limiting oxygen index (LOI) which is determined by placing the material vertically in a preset mixture of nitrogen and oxygen and measuring the concentration of oxygen required to burn the sample once it is ignited; and (3) fire barrier test, T-3, used to determine how long it takes for either burn-through to occur or for the backface temperature to reach a predetermined temperature when the sample is exposed to a fuel fire of 115 kW/m^2 heat flux. These values are presented in Table 4.

The laser-resistant properties are being determined at this time, with some preliminary results presented previously in a paper by Parker et al., at the Las Vegas Symposium on Transparent Aircraft Enclosures (Ref. 1). The epoxy systems, EX-112 and 4F9, and the phenophthalein polycarbonate material all show extremely good resistance to high-energy radiation transmission.

Current laser penetration data are presented in a classified paper by S. R. Riccitiello et al. (Ref. 9). Although reference 9 is classified, certain design data of a nonclassified nature can be presented here. As mentioned previously, one very good tool for use in the development of fire resistant ablative materials is the primary thermochemical char yield. This has been shown in the past (Refs. 2 and 3) to be related to the aromatic equivalance of the polymer, or the basic polymer structure. Although epoxies cannot be related in this way to the basic structure, the thermochemical char yield can be measured; a plot of char yield versus polymer recession rate when the polymer is exposed to high energy CO_2 laser impact is shown in Fig. 9. As can be seen, the polymer recession rate decreases as the char yield of the polymer is increased. It is this behavior that enables one to screen many materials that may be candidate laser barriers. The other materials shown on the plot of Fig. 9 are various formulations that were tried but that are not reported here.

APPLICATION TO MILITARY AIRCRAFT

Depending on the aircraft use, the particular characteristics desired in a new transparent polymer will vary considerably: A prime consideration for carrier-based aircraft might be fire resistance to burn-through; for transport aircraft it might be for crash-fire resistance. Helicopter designers might

want transparent materials that resist abrasion and have ballistic tolerance to shattering and spallation. In advanced fighters, resistance to bird impact, aerodynamic heating tolerance, and resistance to rain erosion might be of prime interest. Obviously, all of these properties may not be acquired in a single monolithic polymer. For instance, the epoxy systems show, due to their increased hardness and higher cross-linking, a definite improvement in fire resistance, abrasion resistance, laser resistance, etc., but these very properties make them more susceptible to impact shattering and ballistic intolerance.

One might trade on a synergistic combination of materials to gain the needed improvement. One combination already being considered is a composite of epoxy on bisphenol A polycarbonate. An outer surface of epoxy would yield fire, laser, and abrasion resistance and the polycarbonate backing, due to its extreme ductility, would provide ballistic and shock resistance with spall retention. In this combination, the interlaminar adhesive used could be significant. Specimens have been fabricated using ethylene terpolymer (ETP), silicones, and others; the ETP interlayer has a disadvantage in that it burns readily but this problem might be overcome by using a silicone interlayer.

Laboratory specimens have been prepared with the epoxy cast directly on acrylate as mentioned earlier. These show a substantial increase in fire resistance with increasing thickness of epoxy (Fig. 10). This might lend itself to a ready retrofit capability for increasing the fire and laser resistance of existing aircraft canopies. However, as the thickness of directly cast epoxy increases, the resistance to thermal shock decreases due to a slight difference in thermal expansion coefficients. Further, the epoxy thus applied cannot be fully cured, as can be the FX-112 system, because the acrylate base cannot withstand the temperatures required. In this regard, another alternative would be to use a laminate of epoxy on acrylic in conjunction with a suitable interlaminar adhesive.

A contractor was selected to construct panels of epoxy cast on acrylics, laminated epoxy 112 (EX-112) and polycarbonate, and a laminated epoxy on acrylate (Ref. 4).

An extension of this contract is providing prototype canopies for the A-4 aircraft of the same basic construction as the laminated panels for large scale fire tests at the Naval Weapons Center, China Lake, California. The A-4 and its canopy section are shown schematically in Fig. 11.

In addition to the sliding canopy section, sets of the forward side panels of the canopy will also be fabricated for use in the tests.

BALLISTIC TOLERANCE TESTS

The Naval Surface Weapons Center was given the task, by the JTCG/AS, to evaluate ballistically the laminated transparent materials developed by Ames Research Center. These tests were conducted primarily to determine the damaged area produced by impacts of caliber .30 APM2 projectiles, caliber .30 ball M2 projectiles, and caliber .22 fragment simulating projectiles (FSP). In addition, estimated protection ballistic limits (PBLs) were obtained for caliber .22 FSP.

Five transparent materials were evaluated:

1. EX-112 cast on acrylic
2. EX-112/30 mil ETP/acrylic
3. EX-112/10 mil ETP/polycarbonate
4. polycarbonate
5. stretched acrylic

The polycarbonate and stretched acrylic served as baseline materials for damaged area comparisons. The caliber .30 AP and ball projectiles were fired at approximately 2350 ft/sec, a velocity that corresponds to a range of 200 yards. The caliber .22 FSP had a striking velocity of about 1100 ft/sec. When damaged areas are compared, the materials performed in the following order of preference (smallest damage with polycarbonate).

1. polycarbonate
2. epoxy/30 mil ETP/acrylic
3. epoxy/10 mil ETP/polycarbonate
4. stretched acrylic
5. epoxy cast on acrylic

There was very little difference between materials (2), (3), and (4). The estimated PBLs for the NASA-Ames materials were equivalent to those of polycarbonate within experimental error. Behind the armor, debris was very low for polycarbonate and epoxy/10 mil ETP/polycarbonate, somewhat higher for the stretched acrylic and epoxy/30 mil ETP/acrylic, and very high for the epoxy cast on acrylic. The epoxy cast on acrylic targets suffered severe delamination against all impacting projectiles.

CONCLUSIONS

It has been shown that aromatic polymers offer extremely good resistance to thermal threats. These aromatic transparent polymers, discussed in terms of their use as canopy materials, provide resistance to fuel fire burn-through and laser resistance, and protection against high-temperature operating environments. Two high-temperature-resistant epoxy systems, EX-112 and 4F9, with reasonable impact properties, and a phenolphthalein polycarbonate having a high glass-transition temperature and impact resistance were developed as a result of this investigation. The results of this study suggest that a good compromise of properties can be obtained from a laminate of the epoxy-boroxine polymer sheet with the bis-phenol A polycarbonate. Epoxy-boroxine laminated to acrylate substrates shows a surprizing resistance to thermal effects and acceptable ballistic tolerance. This may offer a good compromise for retrofit of existing aircraft. Additional efforts to increase the environmental tolerance of these NASA developed transparent materials is currently underway.

REFERENCES

1. Parker, J. A., Fohlen, G. M., and Sawko, P. M.: Development of Transparent Composites and Their Thermal Responses. Conference on Transparent Aircraft Enclosures, Las Vegas, Nevada. Feb. 5-8, 1973.

2. Parker, J. A., and Winkler, E. L.: The Effects of Molecular Structures. NASA TR R-276, Nov. 1967.

3. Fish, R. H., and Parker, J. A.: Relationship of Molecular Structure and Thermochemical Char Yield on Thermal Properties of Foamed Polymers. SAMPE, Los Angeles, Calif., April 1972.

4. Schwartz, Seymour, and Kimmel, Boyce C.: Transparent Laminated and Monolithic Windows. Hughes Aircraft Co., Contract NAS-2-7765, March 1974.

5. Lopata, E. S., and Riccitiello, S. R.: The Influence of the Extent of Polymerization on the Thermal Behavior of an Epoxy-Based Polyether Resin. Applied Polymer Science, 19, 1127-1133 (1975).

6. Schwartzer, G. G.: Belgian Patent 659,074. July 29, 1965.

7. Synthesis and Characterization of Polycarbonates from Geminally Substituted (Cyclic) Methylene Bisphenols. Whittaker Corporation Final Report, NASA Contract NAS-2-8012, May 1975.

8. Kamboar, R. P., and Niznik, G. E.: Synthesis and Properties of Bisphenol Fluorenone Polycarbonate and BPF Carbonate — Dimethylsiloxane Block Polymers. General Electric Co., Final Report, Contract N 000 19-73-C-0152, Jan. 1974.

9. Dyble, T., Riccitiello, S., and Cagliostro, D.: Laser Hardened Transparent Polymers. Proc. of 1975 DOD Laser Effects/Hardening Conf., Ames Research Center, NASA, Moffett Field, Calif., July 8-11, 1975.

TABLE 1. PHYSICAL PROPERTIES

	PMA	SPMA	BAPC	112	4F9	PHPC	PASA
TENSILE STRENGTH, MN/m^2	60.95	77.57	62.60	20.22	16.46	91.7*	89*
TENSILE MODULUS, GN/m^2	1.20	1.13	0.97	0.61	0.60	–	–
FLEXURAL STRENGTH, MN/m^2	108.2	108.2	78.6	49.1	66.9	–	–
MODULUS OF ELASTICITY, GN/m^2	3.0	2.7	1.8	33.9	41.0	–	–
IZOD IMPACT STRENGTH, Nm/m	15.0	15.5	53	10.3	13.4	80*	160*
IZOD IMPACT STRENGTH, Nm/m (WEATHERED)	8.5	11.8	52.3	9.1	9.6		
HARDNESS ROCKWELL "P"	86	91	30	102	114		
HARDNESS ROCKWELL "M"	102	104	72	114	120		110*
TABER ABRASION, mg/KHz	23.1	47.8	9.7	30.3	17.7		
SPECIFIC GRAVITY, g/cc	1.17	1.18	1.2				
DIELECTRIC STRENGTH	4.25	4.25	3.78	4.25	4.73	3.93	4.25
DISSIPATION FACTOR	0.04	0.04	<0.001	0.003	0.004	0.0065	<0.001

*FROM OTHER SOURCES.

TABLE 2. OPTICAL PROPERTIES

		PMA	SPMA	BAPC	112	4F9	PHPC	PASA
COLOR (VISUAL)		WATER WHITE	WATER WHITE	PALE BLUE	VERY PALE YELLOW	PALE YELLOW	PALE YELLOW	AMBER
VIRGIN POLYMER, %	T	84.3	82.1	77.2	84.5	79.6	77.5	53.1
	R	15.9	15.3	18.1	17.1	16.2	20.1	16.0
	HAZE	0.47	1.75	1.28	1.78	1.55	6.60	4.64
ABRADED POLYMER, %	T	84	77	76	80	76	79	57
	R	16	15	17	17	16	19	15
	HAZE	18.2	33.5	14.9	14.4	11.8	18.7	24.5
WEATHERED POLYMER, %	T	81.0	78.5	73.4	74.5	58.4		
	R	14.4	14.2	17.7	14.0	12.1		
	HAZE	0.62	1.97	0.86	6.57	19.42		
% TRANSMITTANCE, 450 nm (BLUE)		89	88	85	85	81	72	33
% TRANSMITTANCE, 550 nm (YELLOW)		93	92	85	90	89	88	60
% TRANSMITTANCE, 650 nm (RED)		93	92	87	89	90	91	74
INDEX OF REFRACTION		..527	1.497	1.616	1.606	1.594	1 613*	

*OTHER SOURCES.

TABLE 3. THERMAL PROPERTIES

	PMA	SPMA	BAPC	112	4F9	PHPC	PASA
% CHAR YIELD AT 700°C	0	0	25	32	39	44*	
MELT TEMP., °C	160-200	160-200	263	NONMELT	NONMELT	295 (SOFTENS)	
DECOMPOSITION TEMP., °C	265	265	460	430	325	425	
HEAT DISTORTION TEMP., °C	105	105	140	112		250*	275
LINEAR EXPANSION x 10^{-5}/°C	6.46	6.39	6.43	6.22	6.47		
THERMAL CONDUCTIVITY, W-cm/cm^2°C	2.32	2.32	1.95	3.50			

*OTHER SOURCES.

TABLE 4. FIRE PROPERTIES

	PMA	SPMA	BAPC	112	4F9	PHPC	PASA
FLAMMABILITY (ASTM 635)							
BURNING RATE mm/sec	0.23	0.49		0.13	0.12		
SELF-EXTINGUISHING?	NO	NO	YES	NO	NO	YES	YES
LIMITING OXYGEN INDEX, % O_2	17.3	15.3	23	20.5	20.8	47	35
FIRE BARRIER TEST (1/2-in THICK)							
TIME TO 150°C, sec				600	360		500
TIME TO BURN THRU, sec	120	120	460	NO BURN THRU	NO BURN THRU	540*	NO BURN THRU

*3/16-in THICK.

(a) RETENTION OF FUNCTIONAL PROPERTIES (MECHANICAL STRENGTH AND TRANSPARENCY) WITH INTERMITTENT SERVICE FROM ~-50°C TO + 260°C

(b) CRASHWORTHY TO 308 METER PER SECOND* IMPACT

(c) RESISTANT TO THE HEAT PENETRATION OF BURNING JET FUEL

(d) PROVIDES THERMAL PROTECTION FROM HIGH ENERGY COHERENT RADIATION

* 600 knots

Figure 1. Desired combination of properties for advanced transparent enclosures.

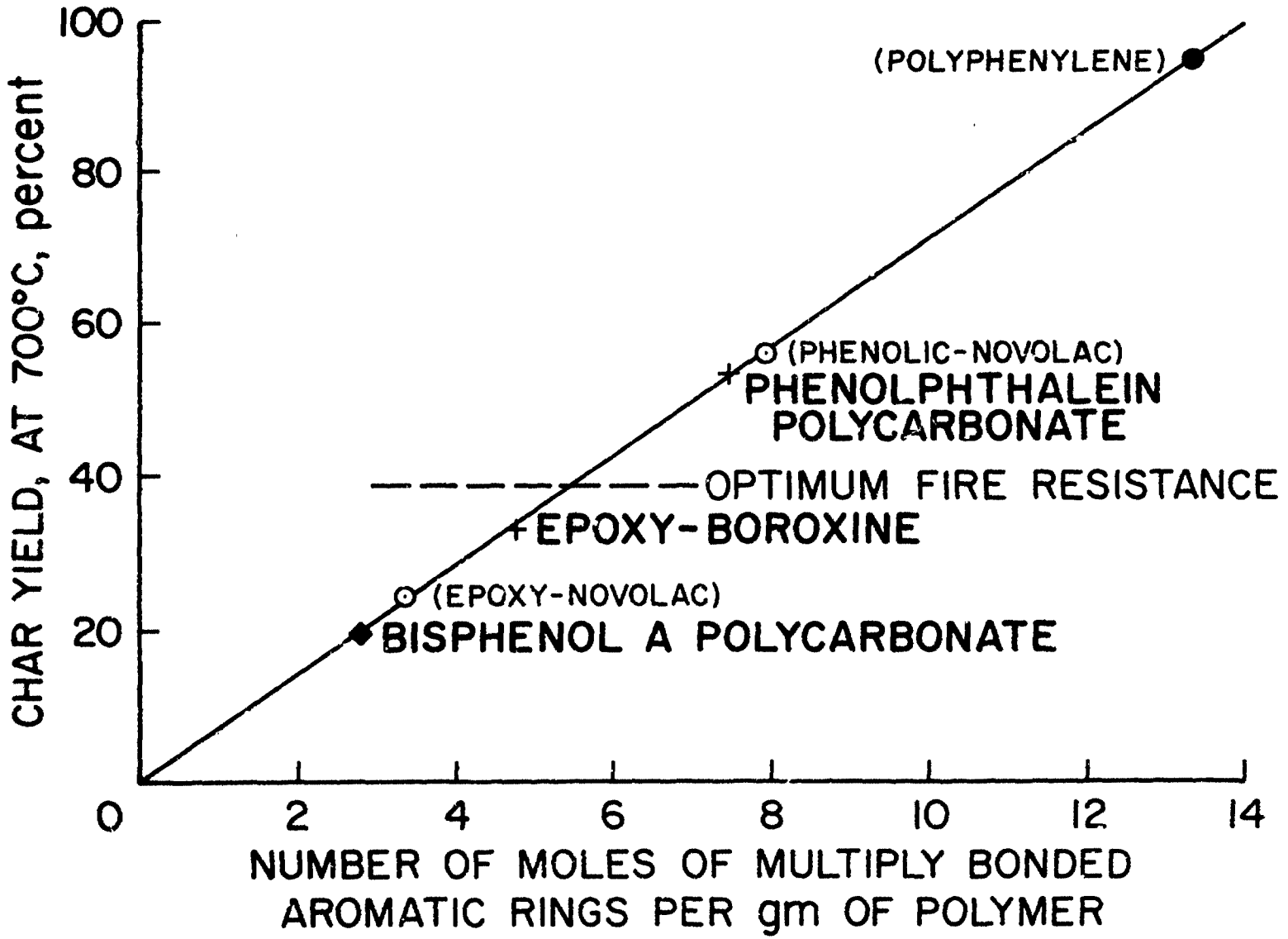
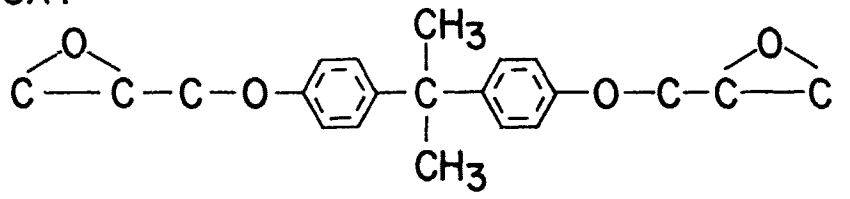


Figure 2. Effect of aromatic structure on thermochemical char yield of transparent polymers.

1. EPOXY

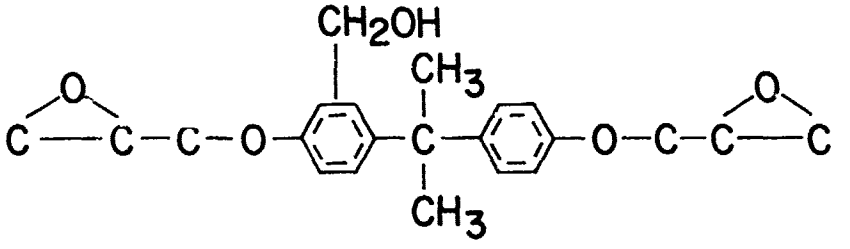


a. CURED WITH TRIMETHOXYBROXINE-YIELD POLYETHER TYPE POLYMER

b CURED WITH HEXAHYDROPHTHALIC ANHYDRIDE YIELD POLYESTER TYPE POLYMER

c CURED WITH DIETHYLENE DIAMINE YIELDS POLYETHER TYPE POLYMER

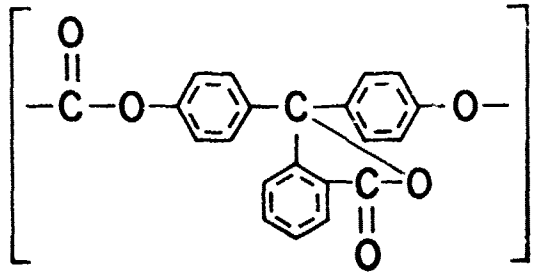
2. EPOXY



80% MONO 20% di

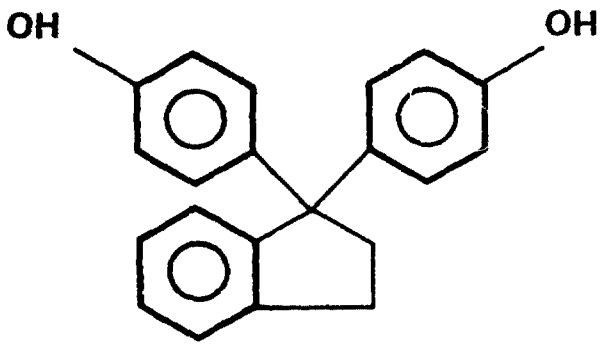
a. CURED WITH TRIMETHOXYBOROXINE-YIELD POLYETHER TYPE POLYMER

3. POLYCARBONATES

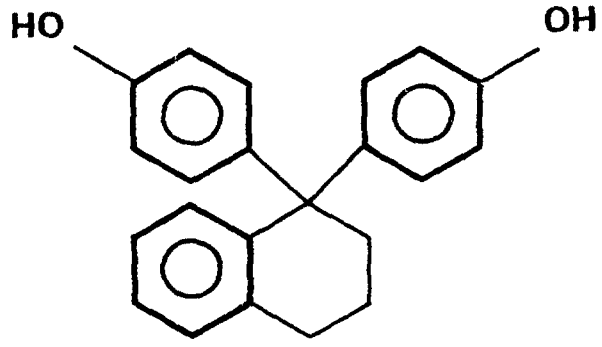


PHENOLPHTHALEIN POLYCARBONATE

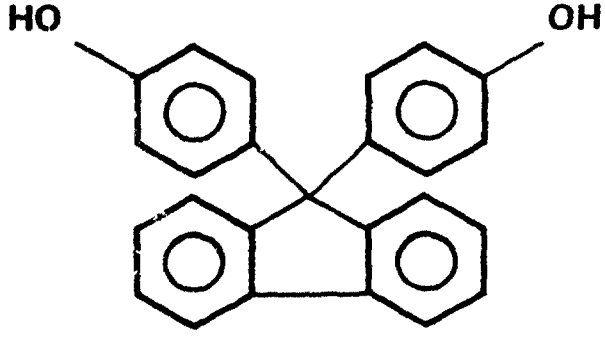
Figure 3. Transparent polymers of interest.



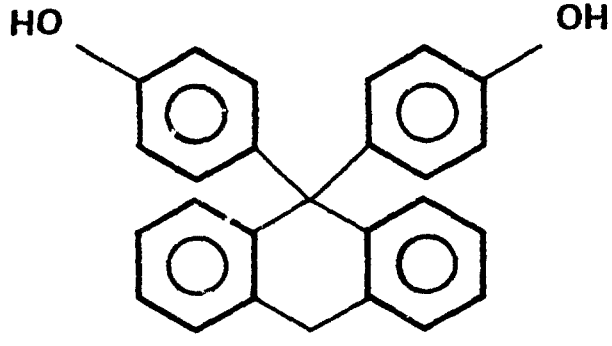
1, 1-BIS (4-HYDROXYPHENYL-INDANE)



1, 1-BIS (4-HYDROXYPHENYL) - 1, 2, 3, 4-TETRAHYDRONAPHTHLENE



9, 9-BIS (4-HYDROXYPHENYL)-FLUORENE



9, 9-BIS (4-HYDROXYPHENYL) - 9, 10-DIHYDROANTHRACENE

Figure 4. Some proposed aromatic bisphenols.

MONOMER	T_g, °C	T_D, °C	$Y_C^{800°}$, %
BISPHENOL A	150	425	20
PHENOLPHTHALEIN	270	400	54
INDANYL - BISPHENOL	216	395	39
FLUORENYL - BISPHENOL	280	400	61

Figure 5. Summary of polycarbonate properties — homopolymers.

THERMAL PROPERTIES			
Tm	Tg	T_D	Y_c^{800}
~292°C	216°C	400°C	39%

PHYSICAL PROPERTIES

TENSILE STRENGTH, psi	10,300 ± 150
TENSILE MODULUS, psi	135,000 ± 7000
ELONGATION, %	5.5 ± 0.5
ULTIMATE ELONGATION, %	14.0 ± 0.5
BARCOL HARDNESS (5 sec)	24 – 26
DENSITY, gm/cc	1.19
IMPACT STRENGTH, IZOD (ft.-lb/in NOTCH)	0.71 ± 0.05

MOLDABLE AT 260°C, 3000 psi PRESSURE.

Figure 6. Poly-bis(hydroxyphenyl)indane carbonate.

WITH BISPHENOL A	T_D, °C	Y_C^{800}, %
50/50	350	43
WITH PHENOLPHTHALEIN		
25/75	380	54
50/50, $[\eta] = 1.20$	370	59
50/50, $[\eta] = 1.60$	380	60
(T_g by TBA = 275°C)		

Figure 7. Copolymers of bis(hydroxyphenyl)fluorene.

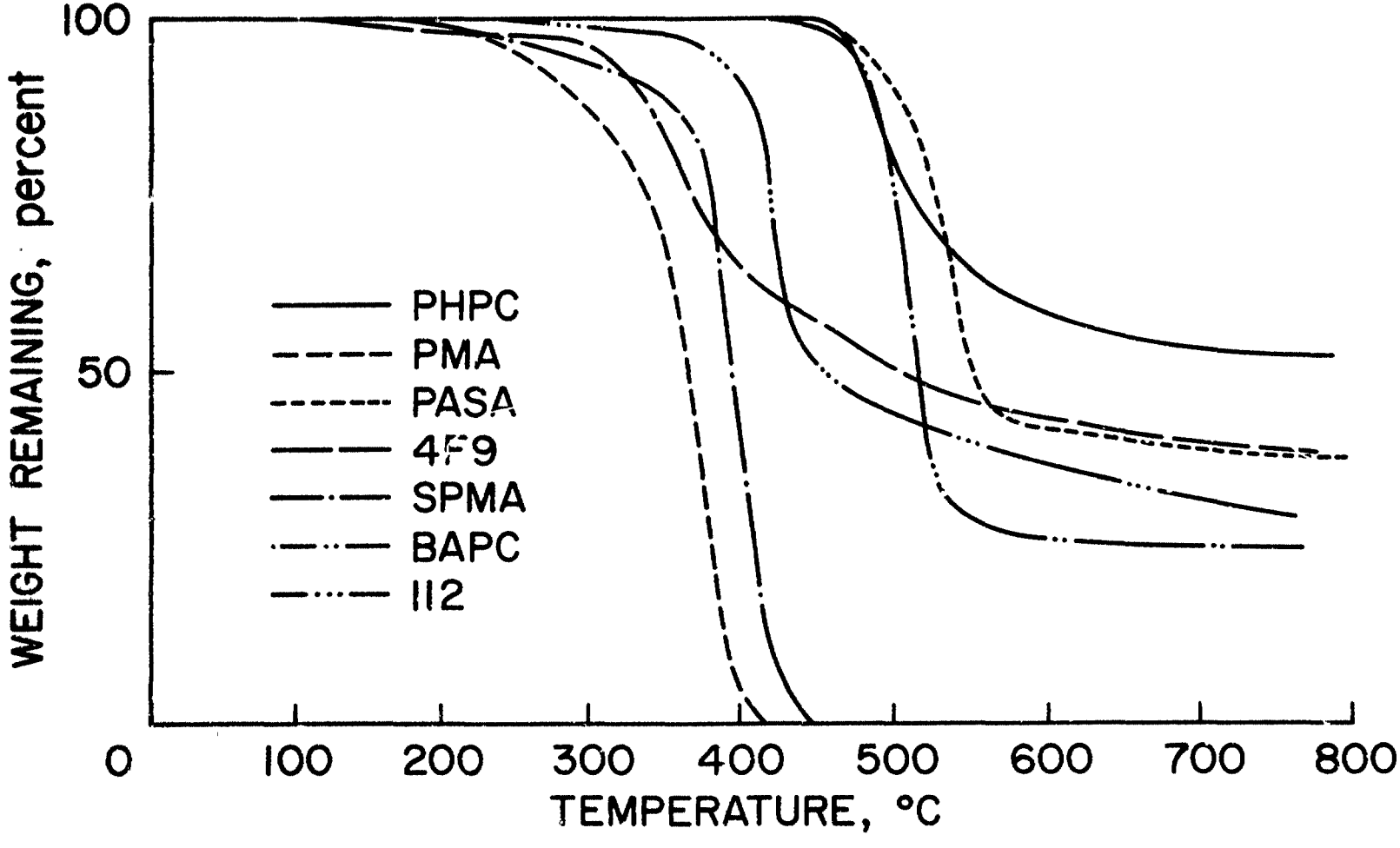


Figure 8. TGAs of transparent polymers.

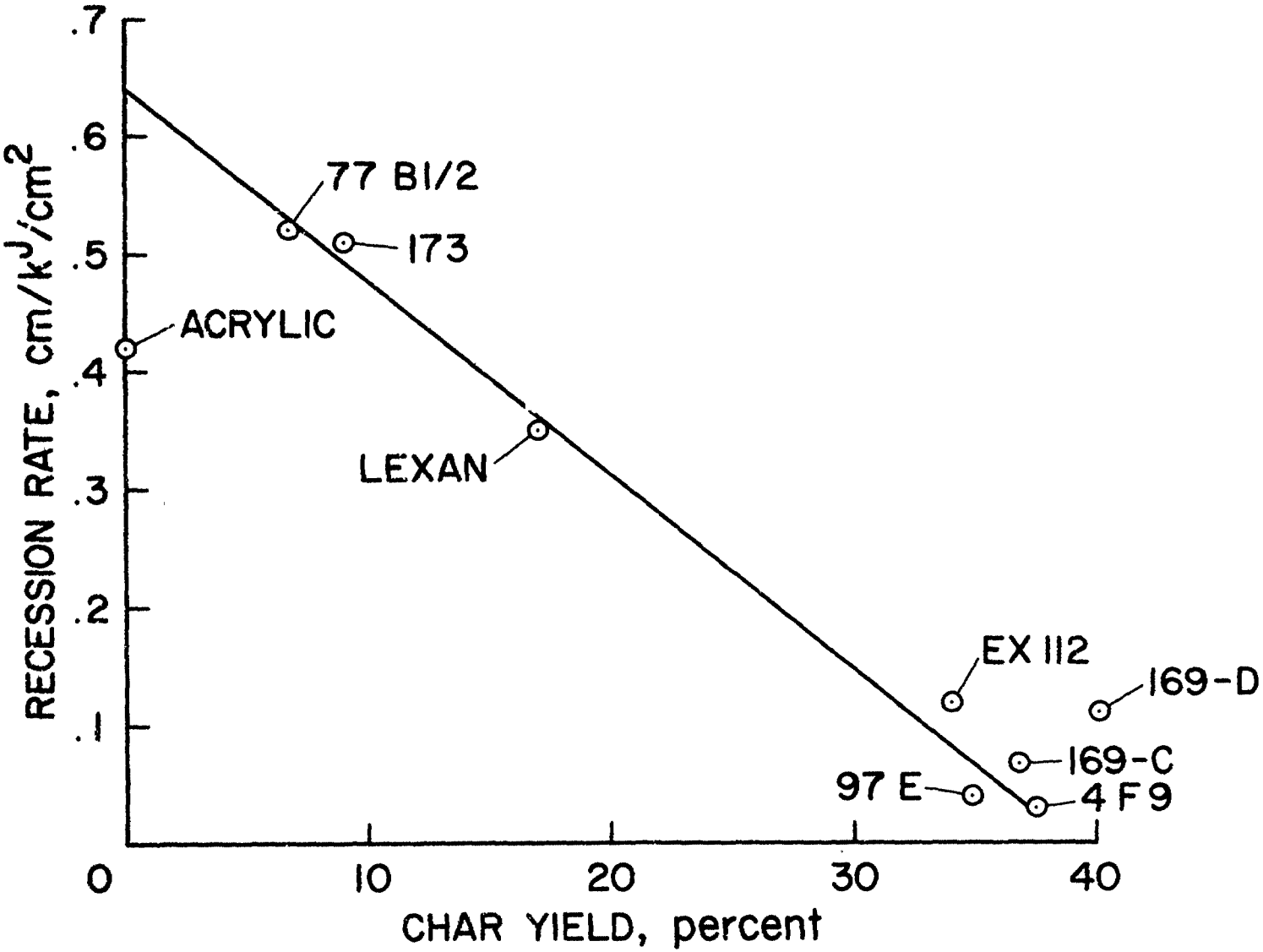


Figure 9. Recession rate versus char yield.

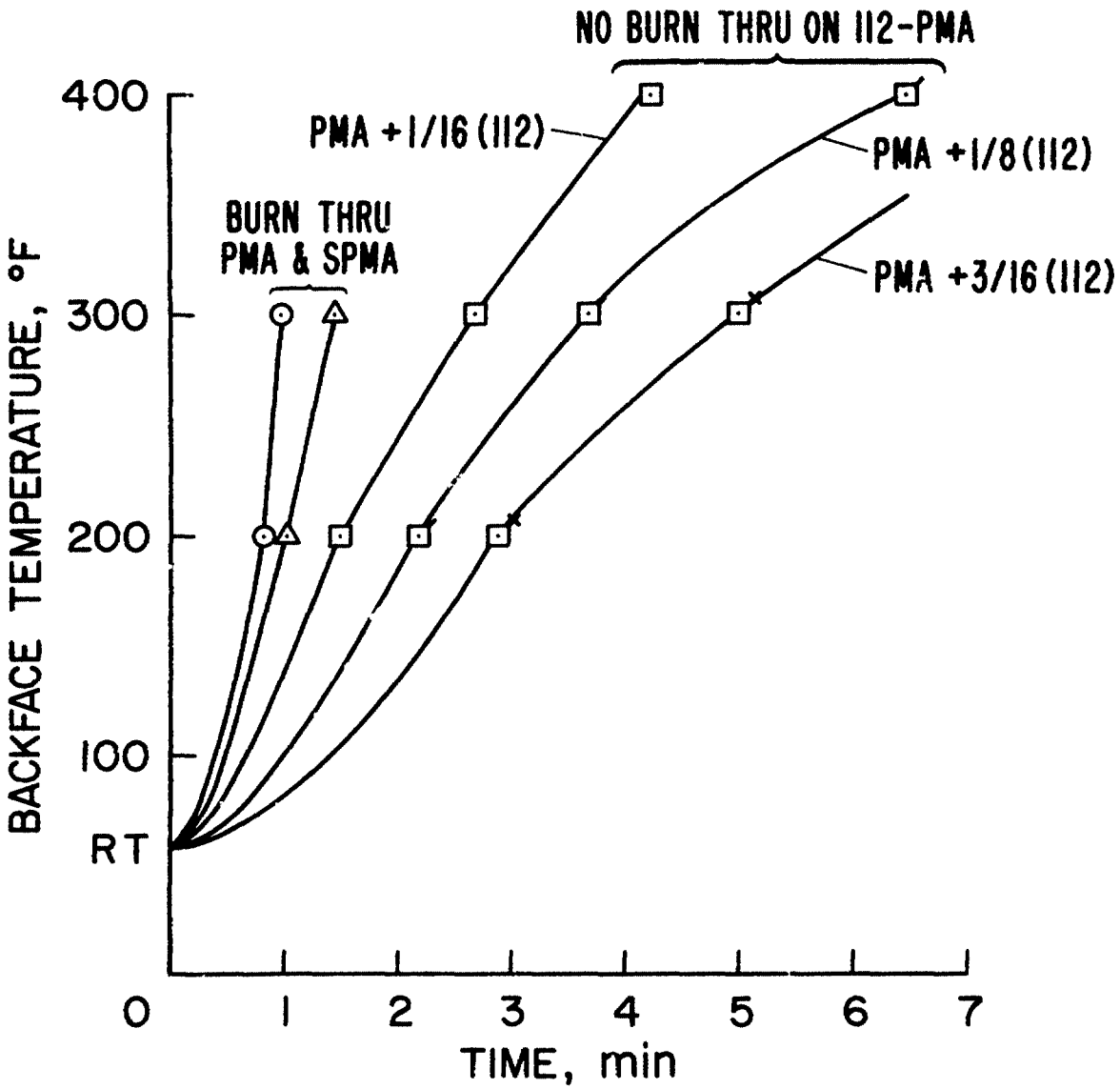


Figure 10. Backface temperature of acrylate-Ex 112 laminates exposed to JP-4 fuel fire.

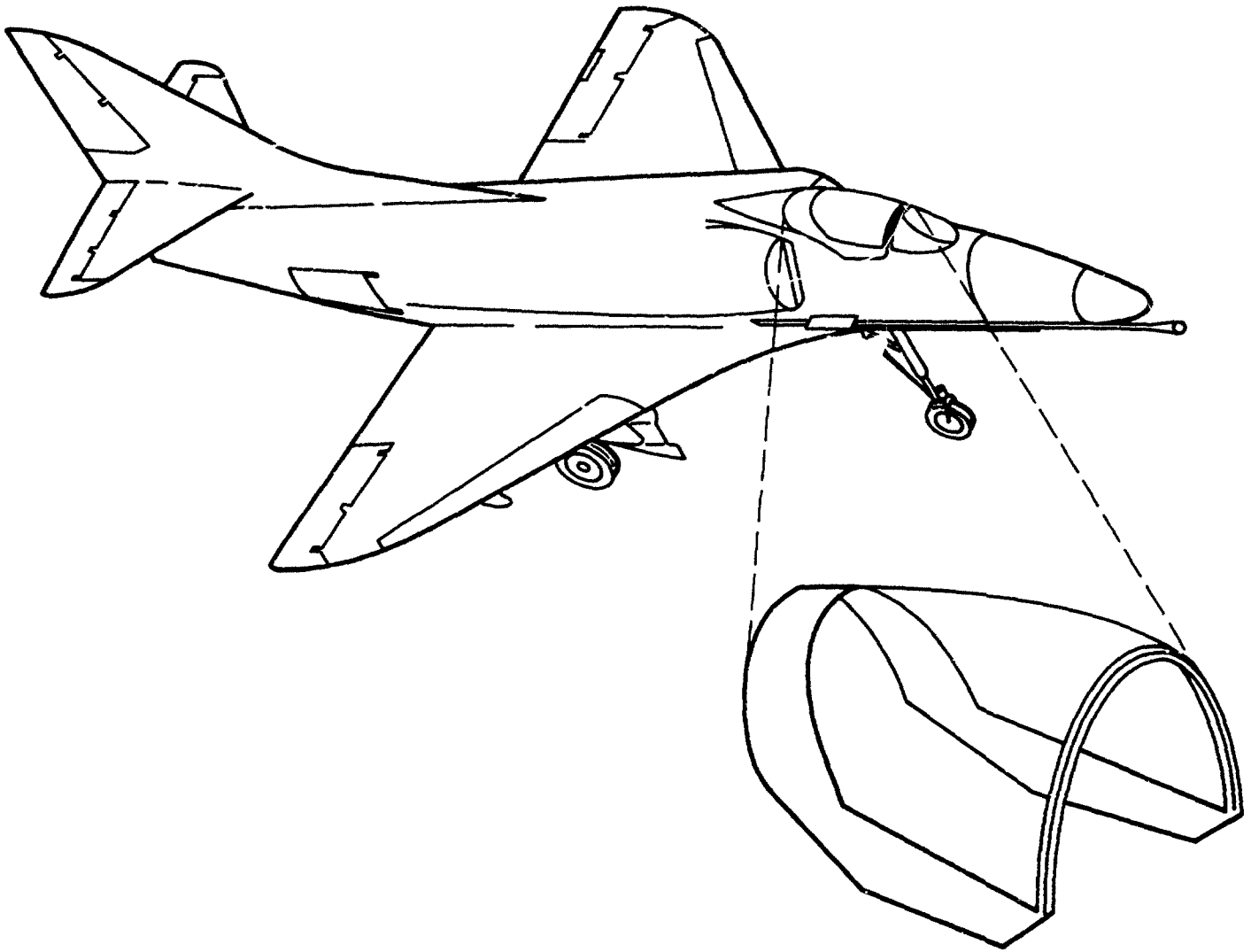


Figure 11. Development of improved transparencies for fabrication of aircraft canopies.

FABRICATION OF FIRE RESISTANT TRANSPARENCIES

S. S. Schwartz
Hughes Aircraft Company
Culver City, California

and

D. Kourtides and R. Fish
National Aeronautics and Space Administration
Ames Research Center
Moffett Field, California

FABRICATION OF FIRE RESISTANT TRANSPARENCIES

S. Schwartz, Hughes Aircraft Company
Culver City, Ca.

D. Kourtides and R. Fish, NASA/Ames Research Center
Moffett Field, Ca.

ABSTRACT

NASA/Ames Research Center in the early 70's, as part of its work on development of fire resistant aircraft materials, produced a transparent epoxy compound with considerably more fire resistance than conventional plastic transparencies. This compound, identified as EX-112, is a combination of Shell Epon 825 resin and Callery Chemical Co. trimethylboroxine as the hardening agent. The EX-112 can be cast into sheets and laminated to another plastic transparency, such as polycarbonate, to result in a tough, fire resistant composite transparency. Alternatively the epoxy can be cast directly onto the other plastic material.

Hughes Aircraft Company was given the task to produce a limited number of typical aircraft transparencies. The techniques which were developed included methods of casting sheets, curving the sheets into the required contours and then laminating the epoxy transparencies to other plastics. Boeing 737 laminated side windows were made, using the epoxy as the outer surface and polycarbonate as the inner surface. Identical sized windows were also made using a single cast monolithic sheet of EX-112.

One foot square laminated samples for ballistics tests were made with polycarbonate and acrylic substrates.

An acrylic A4-D canopy was coated with approximately 1/8 inch of EX-112 using a technique whereby the epoxy was cast directly onto the acrylic.

Tests of the composite transparencies consisted of determination of heat distortion temperature, limiting oxygen index, burning rate, thermal conductivity and the coefficient of thermal expansion.

The results indicated that a substantial improvement in fire resistance could be obtained over state-of-the art acrylic transparencies.

INTRODUCTION

A number of investigations are currently being made to improve plastic aircraft windows and airplane canopies from the standpoint of fire resistance. Such windows are lighter than glass, considerably more shatterproof and could be fabricated of materials which would have high flame resistance, by virtue of char formation on exposure to high heat.

One concept for making plastic windows is to cast a monolithic window using a transparent, char forming, epoxy resin. Another concept is to laminate a very tough, strong transparent polycarbonate sheet with the transparent char forming epoxy sheet, using a compatible interlayer material.

To investigate the feasibility of these two concepts, Hughes Aircraft Company was selected by NASA/Ames Research Center to fabricate a number of windows of each type similar in size and contour to the Boeing 737 outer window (Part No. 65-45791). An epoxy formulation, EX-112, developed by NASA Ames Research Center, was utilized in the fabrication of both types of windows. An ethylene terpolymer (ETP) interlayer developed by Monsanto was used to laminate the epoxy to the polycarbonate. In addition to the 737 type windows, two types of composite ballistic transparencies were made, and an A4-D acrylic canopy was coated with EX-112 material.

The determination of the flame resistance and other thermal characteristics of the various transparencies was done by a series of tests performed by NASA/Ames. These included heat distortion temperature, limiting oxygen index, burning rate, thermal conductivity and coefficient of thermal expansion. The ballistic behavior was determined by the Naval Surface Weapons Center, Dahlgren, Virginia. The projectiles used for testing were 0.30 armor piercing and ball rounds and 0.22 caliber fragment simulating rounds.

II. SUMMARY AND CONCLUSIONS

This paper describes the development of the processing technique used in the fabrication of transparent, heat-resistant aircraft windows of the Boeing 737 configuration. Several types of transparent composite ballistic samples were made, and an A4-D canopy was coated with an epoxy overlay.

Two types of windows were fabricated:

1) monolithic type, one-half inch thick, made from NASA epoxy formulation EX-112 (Epon 825 containing 5 PHR of trimethoxyboroxine), and 2) a laminated type consisting of a quarter-inch thick polycarbonate inner ply bonded to a quarter-inch thick EX-112 ply with an ethylene terpolymer interlayer material.

By the proper choice of processing conditions, the feasibility of fabricating heat-resistant aircraft windows of the above types has been clearly demonstrated. The principal difficulties involved the development of conditions for the casting and curving of the relatively large epoxy sheets required. Completely curing these epoxy sheets in the casting mold was found to be impractical due to curing shrinkage and resultant cracking. Additionally, the curving of the completely cured sheets to the desired radius of curvature was difficult to control. Both problems were solved by partially curing the epoxy in the casting fixture and then completing the cure and curving to the required radius of curvature in a single operation. The laminating operation was accomplished readily in an autoclave which was modified to allow its operation as a vacuum chamber. No difficulty was experienced in the machining of the monolithic or laminated blanks to the final 737 window configuration.

The ballistic samples were made by laminating some with an interlayer, and also by casting the epoxy against the acrylic. The A4-D canopy was coated with EX-112 by casting the epoxy directly onto the acrylic. Both processes could be used in production.

III. DETAILED PROCEDURES

Essentially the fabrication process for production of the 737 windows consisted of six steps:

- Tooling preparation
- Epoxy sheet casting
- Curving and final curing of the epoxy ply
- Polycarbonate curving
- Lamination
- Final Finishing

A. Tooling Preparation

Initial tests were made by casting the epoxy between quarter-inch thick glass plates covered with a sprayed PVA parting film and/or silicone release agent and wax. Only partial success was obtained, since the optical surface was poor, and release was not perfect. Mylar film worked reasonably well as a parting film, except that some "orange peeling" was observed in the epoxy castings, apparently due to curing shrinkage.

Far better results were obtained by the use of half-inch thick aluminum tooling plates covered with stainless steel Ferrotype plates (bonded with American Cyanamide FM 123-2 film adhesive). Fair to good release was obtained by coating the Ferrotype plates with Ram Chemical Co. 87X76 mold release followed by Simoniz or carnauba wax. The fixtures used to make the 737 windows were 18x22 in. The plates were clamped together with spring clamps, or bolts, using a [illegible] Corning DC-4 coated neoprene or silicone gasket and aluminum spacers.

B. Casting

The casting formulation, originally developed by NASA-Ames, Ref. 1, consisted of the following (the amount shown is sufficient to make one 16"x20"x1/4" ply):

Shell Chemical Co. Epon 825	- 1200 gm
Callery Chemical Co. Trimethylboroxine	- 60 gm
Patent Chem. Co. Perox blue dye (.17 gm in 125 gm Epon 828)	- 50 drops

The dye-epoxy mixture is heated to 50±3°C (120±5°F). Then the TMB is added and mixed rapidly and then the mixture immediately vacuum degassed. As soon as the mixture "breaks" in the vacuum chamber it is removed and immediately cast through a paint strainer into the mold which has been preheated to 50±3°C (120±5°F). The temperature is then raised to 71±3°C (160±5°F) as rapidly as possible, and kept at 71°C for two hours.

C. Curving and Final Cure

At the end of the two hour "semi-cure" period the mold is opened, while still hot, and the "rubbery" casting is immediately removed and placed on a Ferrotype covered bend fixture. (The Ferrotype is bonded to a curved aluminum plate and parting agent coated, similar to the casting forms).

The entire assembly is placed in a nylon film bag (Allied Chemical Co. Capran) which has fittings for argon flushing.

A final cure, with slow argon flushing, is as follows:

3 hours at 135±3°C (275±5°F)
4 hours at 168±3°C (335±5°F)

The assembly is then slowly returned to room temperature. The casting is examined, trimmed to 13x17 in. and buffed, if required.

D. Polycarbonate Curving

The curving of the 13x17x1/4 inch polycarbonate panels is done using the same tooling employed for curving and curing of the epoxy plies.

Prior to the curving operation the flat polycarbonate sheets are circulating air oven dried for 24 hours at 130±3°C (265±5°F), or 96 hours at 115±3°C (220±5°F). The latter procedure is used for week-end drying. After drying, the panels are kept, with a desiccant, in sealed polythylene bags, unless they are to be used immediately.

To curve the polycarbonate it is placed on the Ferrotype form and held down with five spring clamps, and 1x18x1/4 in. aluminum bars at each end. One clamp and a small bar are also placed in the middle, at each side. Two #36 wire thermocouples are placed, one at each end of the plastic sheet, one under and one on top of the sheets. Aluminum tape is used to hold the couples. Aluminum foil is placed over the entire assembly to act as a dust shield.

The oven is set to a maximum temperature of 157°±3°C (315± 5°F), and the part temperature is monitored by a recorder. When the plastic reaches 155±3°C (310±5°F), the oven temperature is reduced so the part can be kept at 155°C for 10 minutes, after which the oven is turned off and the doors are opened. The part is allowed to cool to room temperature, before removal from the fixture. During the heating period, the assembly should be checked for buckling, due to differential expansion. If this is found,the clamps should be loosened from one end, the sheet smoothed down and reclamped. A slight over or under bend (1/8 in. max.) is not deletericus.

E. Lamination

Prior to lamination, the epoxy and polycarbonate plies are rinsed with detergent solution and alcohol until a water break-free surface is obtained. The terpolymer is likewise washed with two alcohol rinses. All the components are then dried for a minimum of 4 hours at 50±3°C (120±5°F) in a vacuum oven.

The laminate is then assembled as shown in Fig. 1. The polycarbonate sheet is laid on a Ferrotype, followed by the polyethylene terpolymer. Care should be taken to entrap a minimum number of air bubbles under the ETP. Any visible bubbles should be carefully pricked and smoothed out by hand, to avoid bubbles in the final laminate.

After removal of as many bubbles as possible under the terpolymer, the epoxy ply should be carefully placed, starting at one end, so as to also minimize air entrapment. Three or four fine wire thermocouples are fastened to corners of the laminate using aluminum pressure sensitive tape. The laminate assembly is then wrapped with two layers of Burlington #51789 nylon fabric, followed by four layers of 1/8 in. thick SAE STD. F-6 felt. The entire package is then oven dried for 16 hours minimum at 50±3°C (120±5°F) in a vacuum oven.

After the drying period, the package is installed on a curved fixture covered by a 4 mil Capran vacuum bag. Two sealants were found best for holding the vacuum bag to the fixture. A low temperature sealer (L.T.Fuller-O'Brien 3992) is placed on the outer periphery of the bag, and inside a high temperature sealant, Shnee and Morehead #9156, is used. Two sealants are used since the low temperature resistant,highly tacky material establishes the initial seal and enables the vacuum bag to be drawn down fully, thus also compressing the high temperature resistant seal. On reaching the higher temperatures, the latter material is then responsible for maintenance of a good seal around the bag.

The vacuum bag is checked for maintenance of a satisfactory vacuum, then the entire assembly-laminate package and fixture is placed in the vacuum chamber. Thermocouple and electrical leads are fastened to appropriate lead-throughs in the chamber wall.

Since it is important that the rate of rise of temperature during the laminating operation follow a definite curve, the laminating fixture has its own electrical heating blanket. The rate of temperature increase is controlled from outside the chamber by a large Variac. The heating rate is monitored by means of the three thermocouples on the part, and two others on the laminating fixture.

In order to accurately determine the pressure inside the bag, two vacuum outlets are used, one at each end of the bag, one going to the vacuum pump, and the other to the bag manometer, or pressure gage. A second manometer is installed with one leg connected to the bag and the other to the vacuum chamber interior; thus this manometer will continously indicate the differential pressure between the bag and the vacuum chamber.

Prior to turning on the heat the bag is evacuated to at least 29-1/2 in. Hg. Then the chamber is evacuated until the chamber pressure is approximately 2 in. Hg above the bag. The fixture heater is then turned on and a heating rate of approximately 42°C (75°F) per hour is used. The temperature rise and pressure differential are maintained as shown in Fig. 2, Ref. 2. After one hour at 127°C (260°F) the heat is turned off, the chamber

is allowed to reach full atmospheric pressure, and after cooling to below 40°C (104°F), the vacuum bag pressure is released and the laminate is removed. A final trimming and buffing then completes the window.

Ballistic Samples

Laminated samples were made for ballistic tests by laminating 1/8 inch thick cured EX-112 flat sheets to 1/4 acrylic and polycarbonate sheets, using the ETP interlayer and the same laminating procedure as above.

Another type of ballistic sample was made in which the EX-112 was cast directly onto an acrylic ply. By maintaining the composite transparency in the casting fixture, it was possible to obtain a complete cure in the epoxy. Differential thermal expansion strains were apparently not severe enough to cause any delamination on cooling.

A4-D Canopy Coating

Using the experience gained in the above operations, it was possible to coat an entire A4-D airplane canopy. In order to cast the coating directly onto the acrylic, a special fixture was made which, with the canopy held in an inverted position, was molded to the canopy lines, with an allowance of 1/8 to 1/4 inch. The tool was coated with Garalease prior to casting.

Casting was done with the tool and canopy in an oven at 71°C (160°F). The assembly was held for four hours at 71°C after pouring, after which it was slowly cooled (overnight). The coated canopy was removed the next day. An extra long post-cure (120 hours) up to a maximum temperature of 220°F was used to bring the epoxy up to its final hardness of Barcol 30-35.

IV TESTING

The Boeing 737 windows fabricated from EX-112 were evaluated for fire protection performance using a stretched polymethylmethacrylate 737 window as the control. An oil burner that provided a heat flux of 11.3×10^4 w/m^2 was used to simulate a JP-4 fuel fire. The acrylate window exposed to this environment exhibited the typical melting with combustion; burn-through occured in about 1 minute. The EX-112 prototype exposed to the same environment formed a hard, tough, surface char, which maintained internal protection for this window for about 6 minutes or about six times that of the standard window. Burn-through occured from thermochemical failure due to a small amount of stress.

Other thermophysical and flammability properties are summarized in Table I (Reference 1) and are compared to the acrylic currently used as the other aircraft window. The superior thermal performance of the EX-112 is exhibited by its higher limiting oxygen index, higher heat distortion temperature and longer time to burn-through. Since the major use intended for these transparencies is to provide thermal protection beyond that afforded by current windows and canopies, the most critical test was exposure to the heat flux of a JP-4 fuel proof fire. To simulate this this exposure, the samples were tested in the Ames T-3 thermal test facility. This facility is capable of simulating the typical fluxes encountered in large scale aircraft crash fires. As shown in Table I (Ref. 1) the acrylic transparencies exposed to this environment burn through in approximately 1-1/2 minutes, while the EX-112 epoxy exposed to the same conditions had not burnt through after 16 minutes. Equally as good in this respect is the laminated versions of this material, even when when laminated to acrylic substrates.

In regard to the epoxy systems for military aircraft canopies, the principal test was ballistic tolerance. The monolithic epoxy system is quite brittle and only laminated systems were ballistically tested. Epoxy cast directly on acrylic suffered delamination under ballistic impact as one would expect. However, epoxy laminated with an interlayer adhesive to either acrylic or polycarbonate substrates performed well, and had a ballistic tolerance that in some cases exceeded that of the stretched acrylic panels.

Acknowledgment

The development of the processing methods and fabrication techniques described herein was performed under NASA Contract NAS2-7765.

References

1. J. A. Parker, G.M. Fohlen and P. M. Sawko, Development of Transparent Composites and their Thermal Responses, AFML Conference on Transparent Aircraft Enclosures, AFML-TR-73-126, June 1973.

2. G. L. Ball and I. O. Salyer, Development of a Transparent Adhesive Compatible with Polycarbonate for use in Ballistic Shields, AFML-TR-70-144, June 1970.

FIGURE 1 LAMINATION PACKAGE

HUGHES
HUGHES AIRCRAFT COMPANY

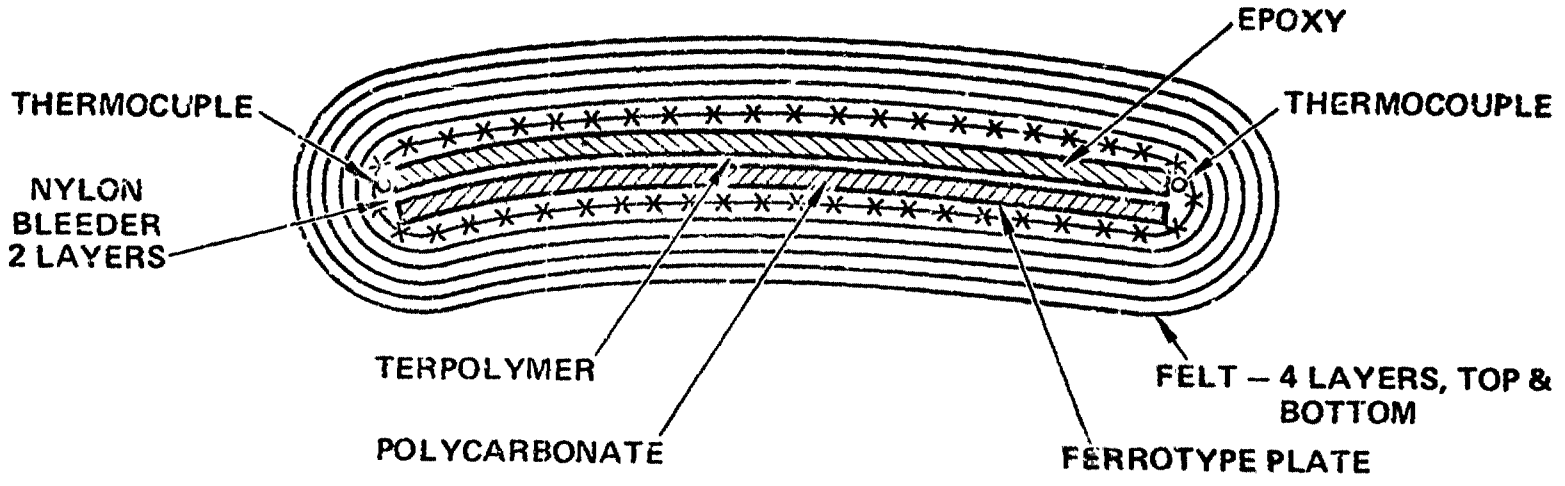


FIGURE 2 LAMINATION CURE AND PRESSURIZATION CURVE

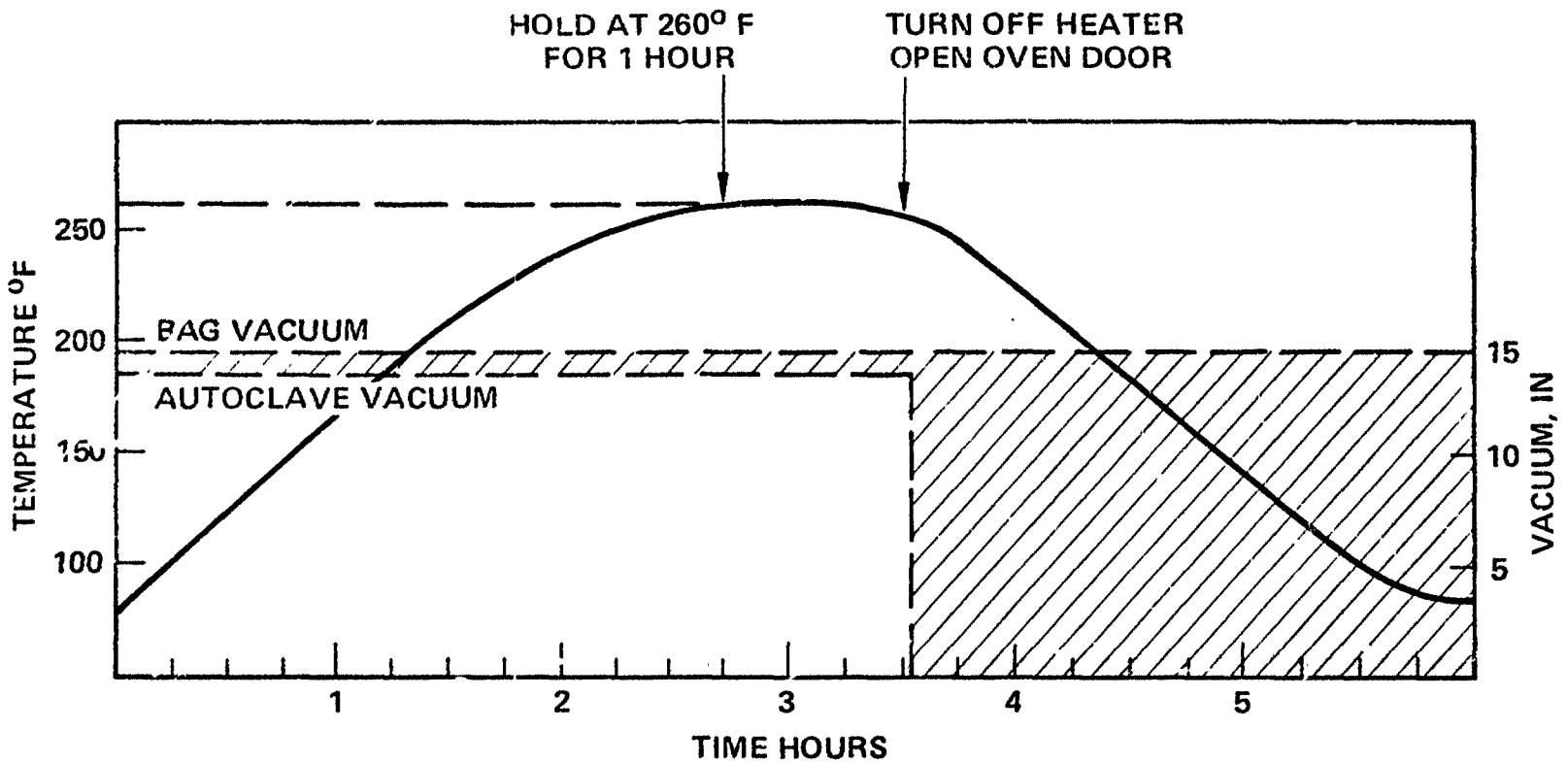


TABLE 1 COMPARISON OF SOME KEY THERMAL PROPERTIES OF ACRYLIC AND EX-112 TRANSPARENCIES (DATA FROM REF. 1)

PROPERTY	ACRYLIC	EX–112
HEAT DISTORTION TEMPERATURE, 1750 KN/M^2, ^oC	106	112
LIMITING OXYGEN VALUE, % 0_2	18	21
THERMAL CONDUCTIVITY, W/CM/CM^2, $^oC \times 10^3$	2.32	3.50
COEFF OF THERMAL EXPANSION, CM PER $^oC \times 10^{-6}$, AT 23^oC	60	42
TIME TO BURN THROUGH, SECONDS, 1.3 CM THICK SAMPLE (AMES T-3 TEST)	100	>1080

THE USE OF LAMINATED ACRYLIC TRANSPARENCIES ON HIGH-PERFORMANCE AIRCRAFT

R. C. Shelton
Swedlow, Inc.
Garden Grove, California

THE USE OF LAMINATED ACRYLIC TRANSPARENCIES ON HIGH-PERFORMANCE AIRCRAFT

R. C. Shelton

SWEDLOW, INC.

ABSTRACT

At the Conference on Transparent Materials for Aerospace Enclosures held in June of 1969, Swedlow, Inc. presented a paper on "Laminated Acrylic Transparencies for High-Performance Aircraft". That paper presented a summary of Swedlow's activity from concept, through sub-scale testing to evaluation as back-up transparencies for the F-111 aircraft.

The use of laminated acrylic transparencies on the F-111 aircraft demonstrated the capability to perform under actual high temperature flight conditions, and provided added confidence in the concept.

After being used as the back-up transparency on the F-111, laminated acrylic was the material selected for use on the F-14 aircraft.

This paper will review some of the previous history of laminated acrylic and will present the improvements in and performance of laminated acrylic composites. In addition, we will examine the service history obtained on current high performance aircraft, (F-14), where laminated acrylic was the original design rather than the back-up.

In general, this paper presents an updating on the "heat shield" concept for aircraft transparencies.

1.0 INTRODUCTION

In 1969, at the Conference on Transparent Materials for Aerospace Enclosures, Swedlow, Inc. presented a paper entitled "Laminated Acrylic Transparencies for High Performance Aircraft" (Reference 1). That paper discussed the use of laminated acrylic from concept to back-up transparencies for the F-111 Aircraft.

This paper will present a review of past history of the heat shield concept, and an examination of the service history of the F-14 transparencies, the first high performance aircraft where laminated acrylic was selected as the baseline design.

2.0 HISTORY

The development of high performance aircraft placed rigorous requirements on the transparent enclosures. High heat resistance, retention of physical properties at high temperatures, excellent optical quality and large viewing areas were a few of the more obvious requirements demanded of the transparent enclosures.

In the past, the requirements for plastic transparent enclosures had been fulfilled through the use of materials such as cast polyester, as-cast acrylic and stretched acrylic; in the monolithic and laminated forms.

Stretched acrylic, meeting the requirements of MIL-P-25690, is considered the best structural plastic material available for transparent enclosures. It has increased resistance to crack propagation ("K" factor), increased resistance to crazing and increased service life over as-cast acrylic. The wide spread use and excellent service history of stretched acrylic has proven it to be the most favorable plastic material for transparent enclosures.

It can be readily shaped to a variety of configurations with excellent optical quality. Evidence of this is the many thousands of stretched acrylic enclosures currently in service.

Inherent in the material is a temperature limitation, (thermal relaxation), at which stretched acrylic begins to revert to its original as-cast condition.

Because the operational temperatures expected of the newer aircraft were considerably higher than the relaxation temperature for stretched acrylic, a means of protecting it from aerodynamic heating was necessary.

Thus, the need for a high temperature resistant, transparent heat shield to protect the structural stretched acrylic.

The cross-section of a typical all plastic composite for high temperature operation is shown in Figure 1. The details have been intentionally omitted because a general configuration cannot be established since performance requirements, temperature profiles, temperature

gradients and structural loading will vary from case to case. Also, such items as radar reflective and electrical conductive coatings may be required for some configuratiors.

The outer heat shield and interlayer thickness is that required to reduce the thermal gradient to a temperature satisfactory for the structural stretched acrylic.

Many materials have been, and continue to be evaluated as heat shield materials, including as cast acrylic, polyester, epoxy, and polycarbonate.

It was determined in earlier testing that as cast acrylic, meeting the requirements of MIL-P-8184, was the best available material for use as a heat shield. It is a proven material, will withstand high temperatures and has excellent optical quality. The manufacturing processes for the production of as cast acrylic enclosures were well established.

The heat shield is laminated to the structural stretched acrylic with a high temperature resistant cast-in-place interlayer.

The successful application of the heat shield concept has been the result of the development of high temperature resistant cast-in-place interlayers. The use of a castable interlayer provides maximum flexibility in fabrication and design possibilities.

Swedlow, Inc. has developed and evaluated many high temperature resistant cast-in-place interlayers, including polyesters, epoxies, acrylics and silicones.

Our most successful interlayer to date has been our high temperature resistant cast-in-place silicone, coded SS-5272Y(HT).

SS-5272Y(HT) interlayer possess properties compatible with known requirements including excellent optical qualities, clarity, adhesion to the transparent face sheets, toughness and performance capabilities across the expected temperature range. This interlayer is a low modulus material that does not become rigid or brittle at depressed temperatures. Figure 2 illustrates the retention of tensile strength and elongation at temperatures from -160°F to +300°F. SS-5272Y(HT) is compatible with vacuum deposited metallic films as required for radar reflective or electrical conductive coatings.

Table 1 presents additional physical properties of the SS-5272Y(HT) cast-in-place interlayer.

3.0 EVALUATION OF THE HEAT SHIELD CONCEPT

To support the heat shield concept, Swedlow conducted a test program to determine the effect of high temperature exposure on laminated composites. Test specimens, both flat and formed to a compound configuration, were fabricated utilizing a 0.250 inch as cast acrylic heat shield, a 0.100 inch cast-in-place interlayer, and a 0.350 inch stretched acrylic structural member. The test specimens incorporated

a high temperature reinforced edge attachment.

The test specimens were instrumented to record the temperatures obtained at the outer surface of the heat shield, the interlayer heat shield interface, the interlayer structural member interface, and the inner surface of the structural member.

The composites were subjected to repeated temperature cycling and steady state conditions, and successfully withstood the test conditions without any noticeable effect.

4.0 APPLICATION OF LAMINATED ACRYLIC FOR HIGH TEMPERATURE OPERATION

4.1 F-111 Aircraft

The first production use of a plastic composite incorporating the heat shield concept was on the F-111 aircraft. Even though the original F-111 transparency design was not plastic, both monolithic and laminated acrylic played a major role in the overall program.

Early in the F-111 program, Swedlow, Inc. supplied monolithic acrylic transparencies fabricated from MIL-P-25690 material to permit the initial flight testing of the F-111 aircraft. The monolithic panels served only as an interim solution since they would not meet the total design objectives.

As a result of this early effort, Swedlow, Inc. designed and fabricated laminated acrylic transparencies for the F-111 aircraft incorporating an outer heat shield of as cast acrylic, a structural member of stretched acrylic, mated together with Swedlow's castable interlayer SS-5272Y(HT).

Because the mounting structure was previously fixed, Swedlow had to design an edge member adaptable to the existing structural framework that would maintain exterior mold line smoothness. The laminated composite was mounted to the aircraft structure through the use of a composite reinforced edge member.

Figure 3 illustrates the edge configuration utilized on the F-111 transparencies.

Considerable sub-scale evaluation and refinement was required to minimize the edge rotation which occurs as a result of the loading condition.

After full-scale testing, Swedlow's laminated design was approved for limited safety-of-flight. This allowed flight testing of the F-111 aircraft to temperature conditions beyond the capability of the monolithic stretched acrylic panels.

With continuing improvements and modifications to the interlayer system including basecoats, primers and curing mechanisms; and subsequent evaluation of full-scale transparencies, safety-of-flight approval was attained.

As a result of the excellent performance of laminated acrylic on the F-111A Program, under adverse mounting conditions, laminated acrylic was selected and specified as the base line material for the F-111B aircraft; the carrier version of the F-111A.

However, prior to the actual production program, the F-111B was cancelled by the Government, and was replaced with the Grumman F-14. (Figure 4)

4.2 F-14 Aircraft

Early in the F-14 design phase, Grumman elected to have the windshield side panels and forward and aft canopies fabricated from laminated acrylic.

The typical cross-section of the laminated acrylic transparencies is shown in Figure 5.

The material thicknesses specified for each of the transparencies are shown in Table 2.

Since the laminated acrylic composite was selected originally as the baseline design the mounting structure was designed accordingly.

A typical installation is shown in Figure 6.

Element specimens were furnished to Grumman for evaluation. Once Grumman satisfied themselves of the adequacy of the laminated acrylic composite from test specimen work, full-size test units were manufactured.

It is not the intent of this paper to present the test program or results obtained by Grumman. However, the results were acceptable and production units were manufactured.

The fabrication of the windshield side panels and canopies required the development of unique (proprietary) manufacturing methods. Where our past experience on the F-111 required the manufacture of cylindrical shapes for the windshield and slight compound shapes for the canopies; the F-14 transparencies are much larger and more complex.

The windshield side panels are approximately four (4) feet long. (See Figure 7)

The forward canopy is approximately six (6) feet long and the aft canopy approximately seven (7) feet long. (See Figures 8 & 9)

To illustrate the amount of transparent area utilized on the F-14, see Figure 10.

To meet the F-14 specification, Swedlow applied ingenuity to our already known cast-in-place laminating tooling and procedures and developed special tools and processes to manufacture the complex shapes, large

sizes and difficult cptics required for the F-14. The production program has been remarkably trouble-free and is primarily due to the development, by Swedlow, of the unique fabrication process for production of F-14 transparencies.

As of October 1975, Swedlow, Inc. has delivered to Grumman more than 300 ship sets of F-14 windshield side panels and forward and aft canopies. Grumman advises us that 175 F-14's have made more than 30,000 flights involving approximately 47,000 flight hours. The maximum flight time on any individual transparency is approximately 650 hours.

This not to say that there have been no problems associated with the laminated acrylic transparencies. Recent reports indicate some crazing has occurred on the outer as cast acrylic heat shield, which is predominantly an edge restraint problem and is being corrected. Any damage that occurs to the outer as-cast acrylic heat shield has no effect on the structural stretched acrylic; basically due to the non hardening nature of the SS-5272Y(HT) castable silicone interlayer.

5.0 EDGE ATTACHMENT

5.1 Materials

The edge attachment materials required for use at elevated temperatures must be capable of performance at the temperatures expected.

Currently used materials, nylon and fiberglas, satisfy the requirements when fabricated using high temperature resin systems.

Figure 11 illustrates the tensile strength of Epoxy Nylon (Swedlow Code X6N-225) and Epoxy Fiberglas (Swedlow Code X6G-298) versus temperature.

These materials have been proven in service - the epoxy nylon on the North American A-5 and the Grumman F-14, and the epoxy fiberglas on the General Dynamics F-111.

5.2 Adhesives

Several adhesives are available for high temperature application. Swedlow's HO-614 modified epoxy has proven satisfactory for use in service as the adhesive on the A-5, the F-111 and the F-14.

6.0 CONCLUSION:

The successful application of laminated acrylics for high temperature operation has been demonstrated. Considering the recent problems encountered by other transparencies, the early decision by Grumman is further strengthened.

The successful use of laminated acrylics has supported our belief in the ultimate success of the concept, when considered in the initial design phases. Improvement of high temperature resistant interlayers

and the evaluation of the new transparent glazings is a continuing effort by Swedlow. It is our aim to lead the way in the development of transparent enclosures for aircraft.

7.0 REFERENCES

1. R. C. Shelton, Swedlow, Inc. "Laminated Acrylic Transparencies For High Performance Aircraft". Paper presented at the Conference on Transparent Materials For Aerospace Enclosures, Dayton, Ohio. June 24 - 26, 1969.

2. S. Z. Fixler, Grumman Aerospace Corporation. "Thermostructural and Material Considerations in the Design of the F-14 Aircraft Transparencies". Paper presented at the AIAA Aircraft Systems and Technology Meeting, Los Angeles, California. August 4 - 7, 1975.

TABLE 1

TYPICAL PROPERTIES

SWEDLOW SS-5272Y(HT)

CAST-IN-PLACE INTERLAYER

PROPERTY	RESULT
Specific Gravity	1.02
Index of Refraction	1.409
Water Absorption (%)	0.028
Shore A Hardness	43
Thermal Conductivity ($BTU/HR/FT^2/^oF/IN$)	0.76
Specific Heat ($BTU/LB/^oF$)	0.345
Coefficient of Thermal Expansion ($IN/IN/^oF$)	$212X10^{-6}$
Light Transmission % (1)	90
Haze % (1)	2

(1) Interlayer evaluated as a composite. 0.188" MIL-P-8184, 0.188" SS-5272Y(HT), 0.250" MIL-P-25690.

TAB E 2

TRANSPARENCY MATERIAL THICKNESSES

TRANSPARENCY	OUTER AS CAST ACRYLIC (MIL-P-8184)	SS-5272Y(HT) CAST-IN-PLACE INTERLAYER	INNER STRUCTURAL STRETCHED ACRYLIC (MIL-P-25690)
WINDSHIELD SIDE PANEL	0.125	0.100	0.300
FORWARD CANOPY	0.100	0.100	0.205
AFT CANOPY	0.100	0.100	0.205

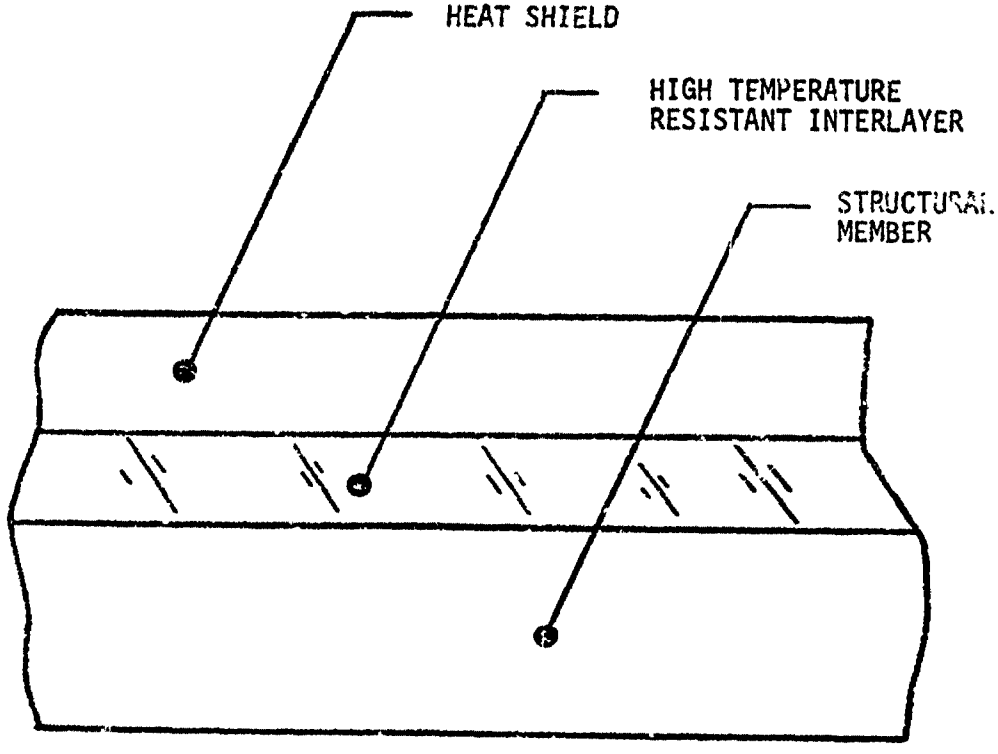


FIGURE 1 - TYPICAL CONSTRUCTION OF AN ALL PLASTIC COMPOSITE FOR HIGH TEMPERATURE OPERATION

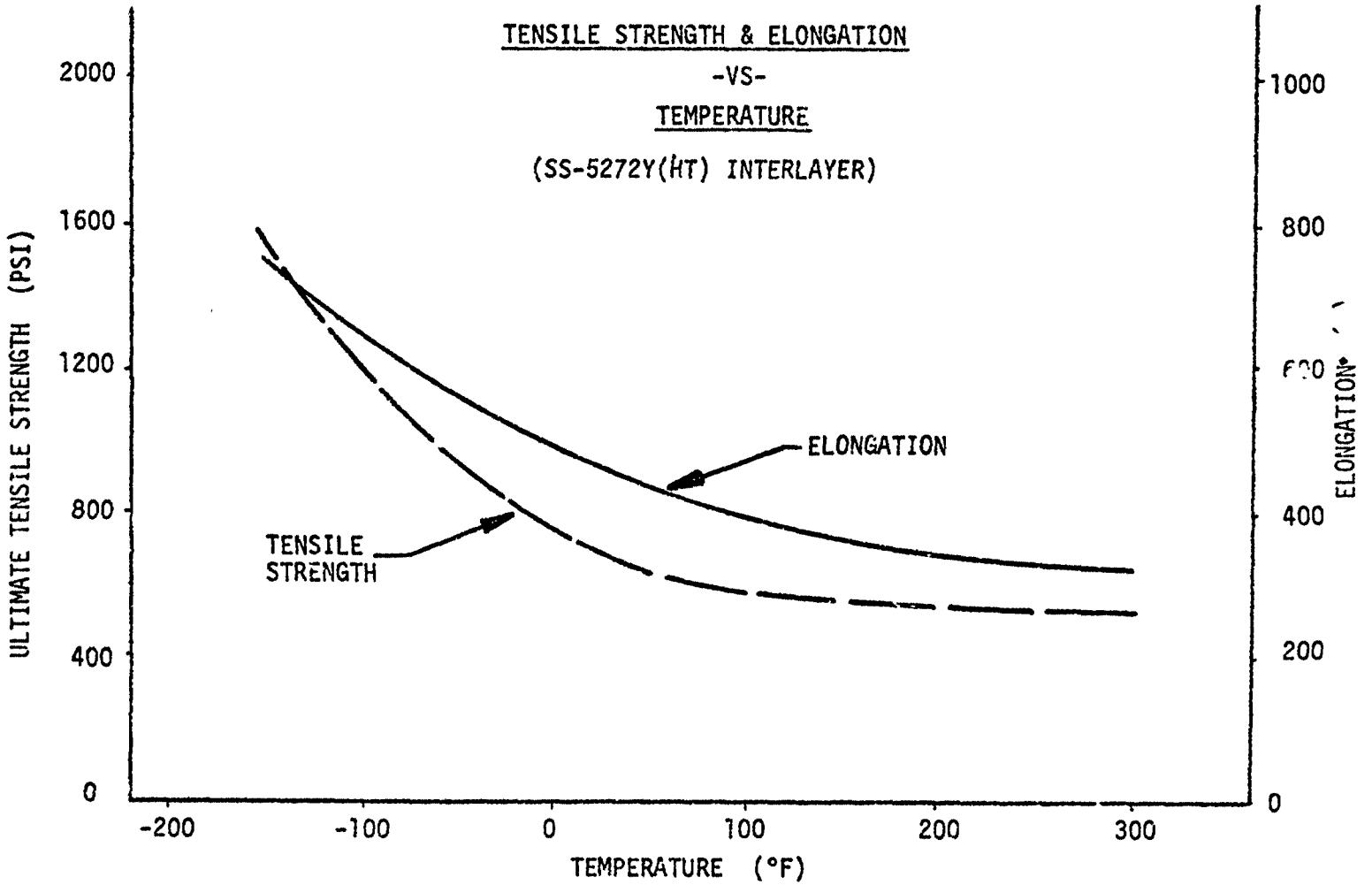


FIGURE 2 - TENSILE STRENGTH AND ELONGATION OF SS-5272Y(HT)

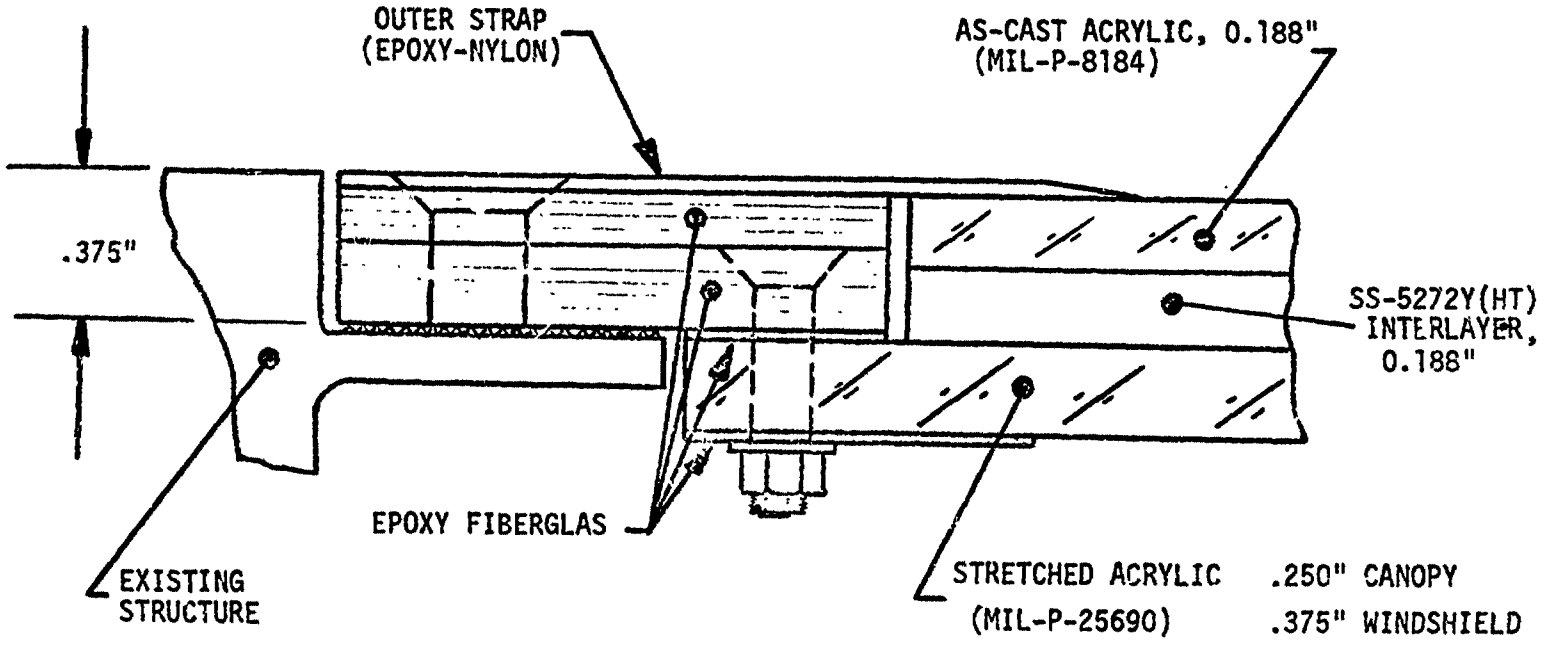


FIGURE 3 - LAMINATED ACRYLIC EDGE DESIGN FOR THE F-111 ENCLOSURE

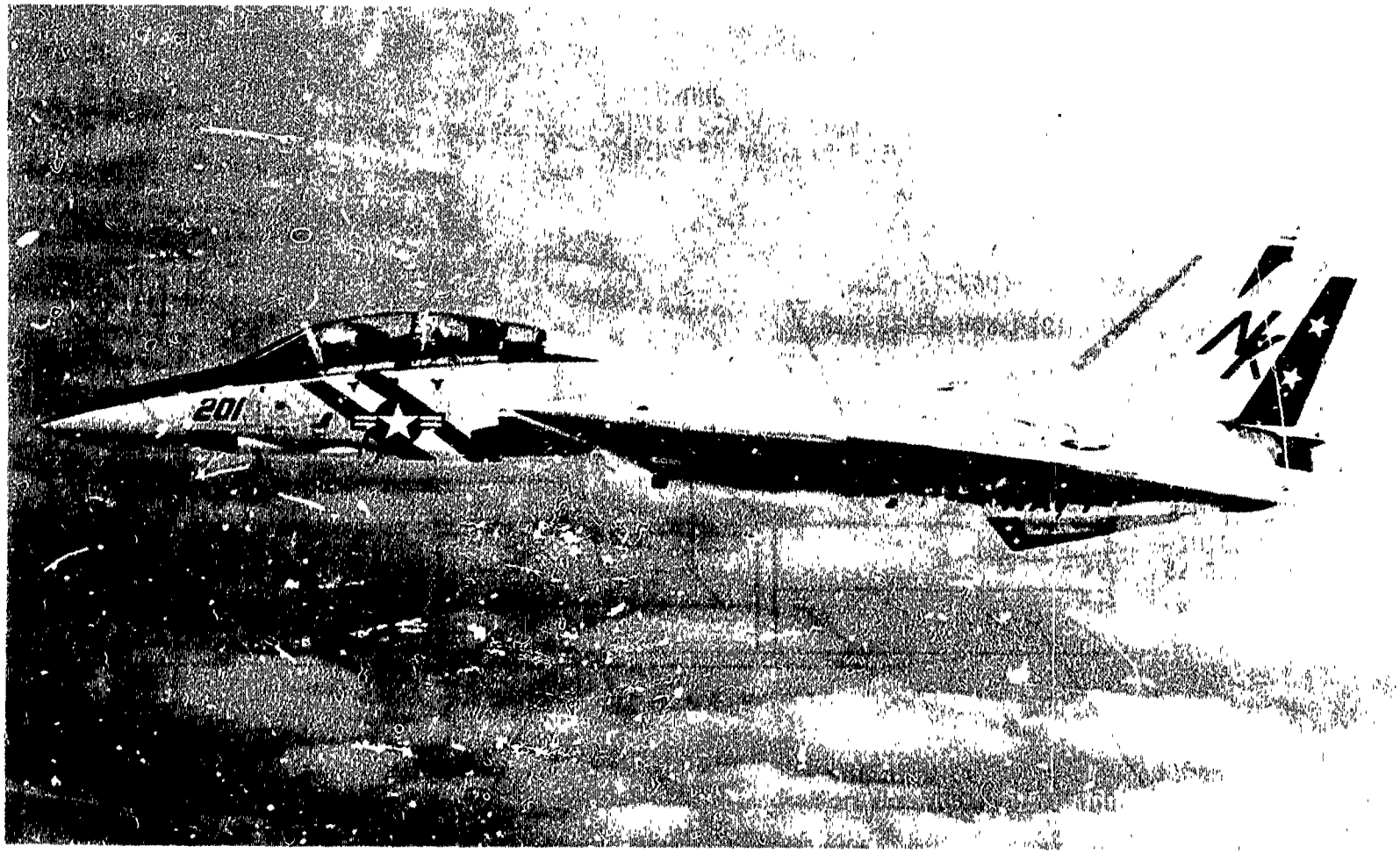


FIGURE 4 - GRUMMAN F-14 "TOMCAT"

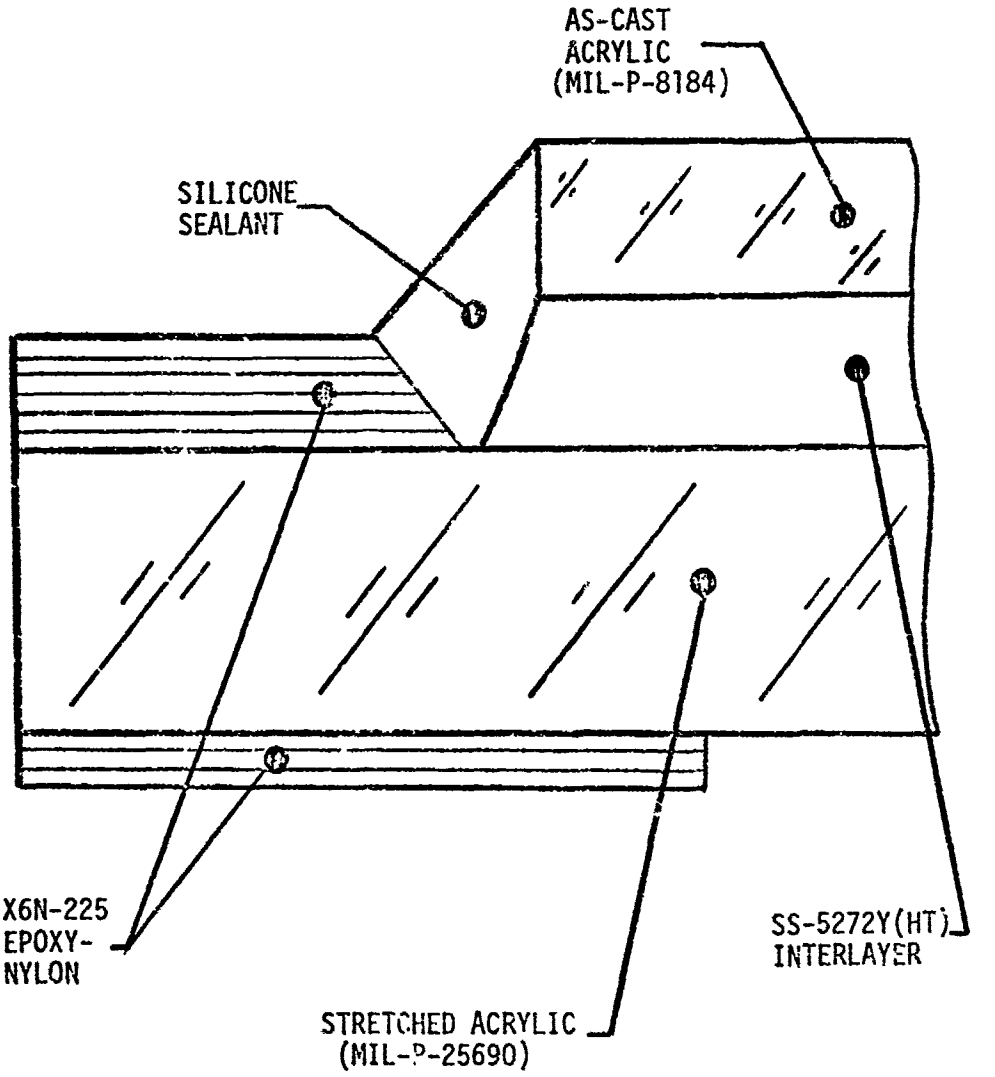


FIGURE 5 - TYPICAL F-14
CROSS-SECTION

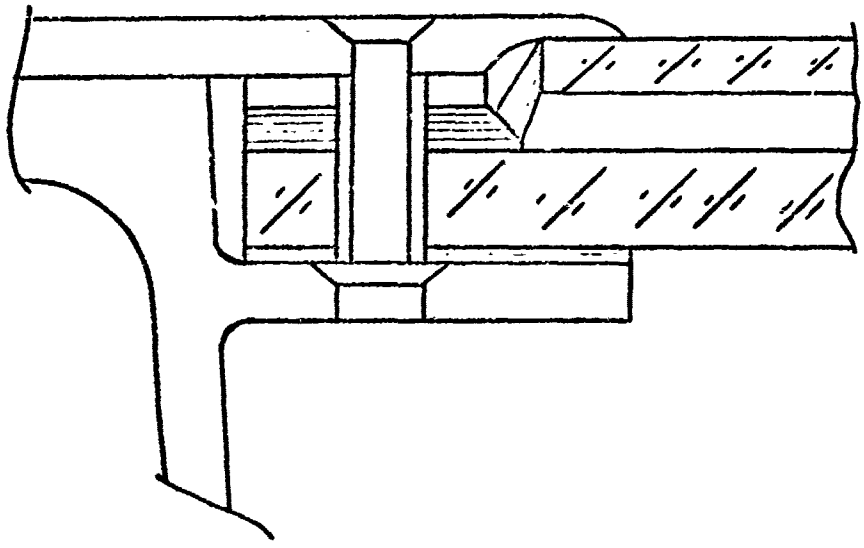


FIGURE 6 - F-14 ENCLOSURE, TYPICAL INSTALLATION



FIGURE 7 - F-14 WINDSHIELD
SIDE PANEL

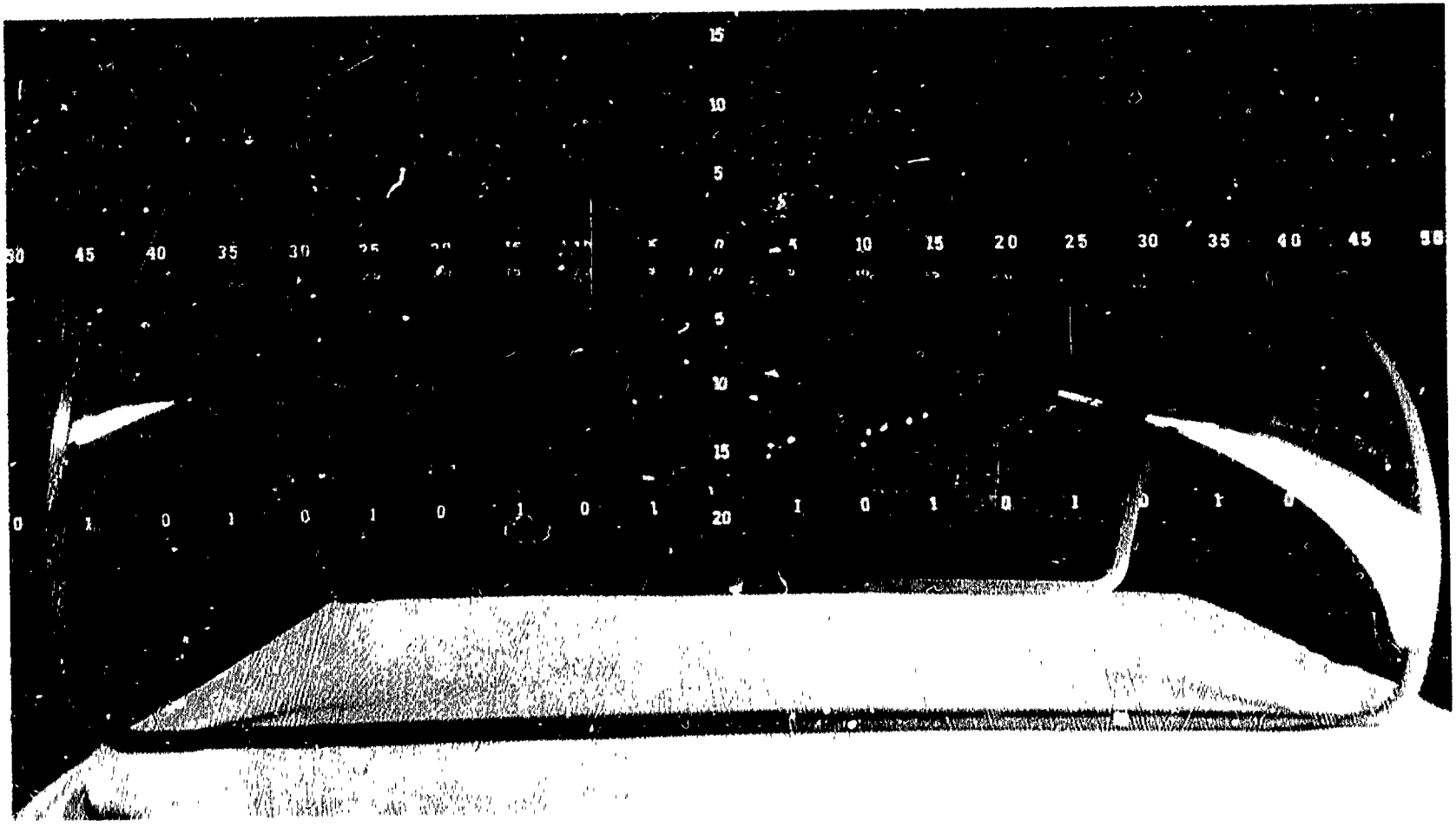


FIGURE 8 - F-14 FORWARD CANOPY

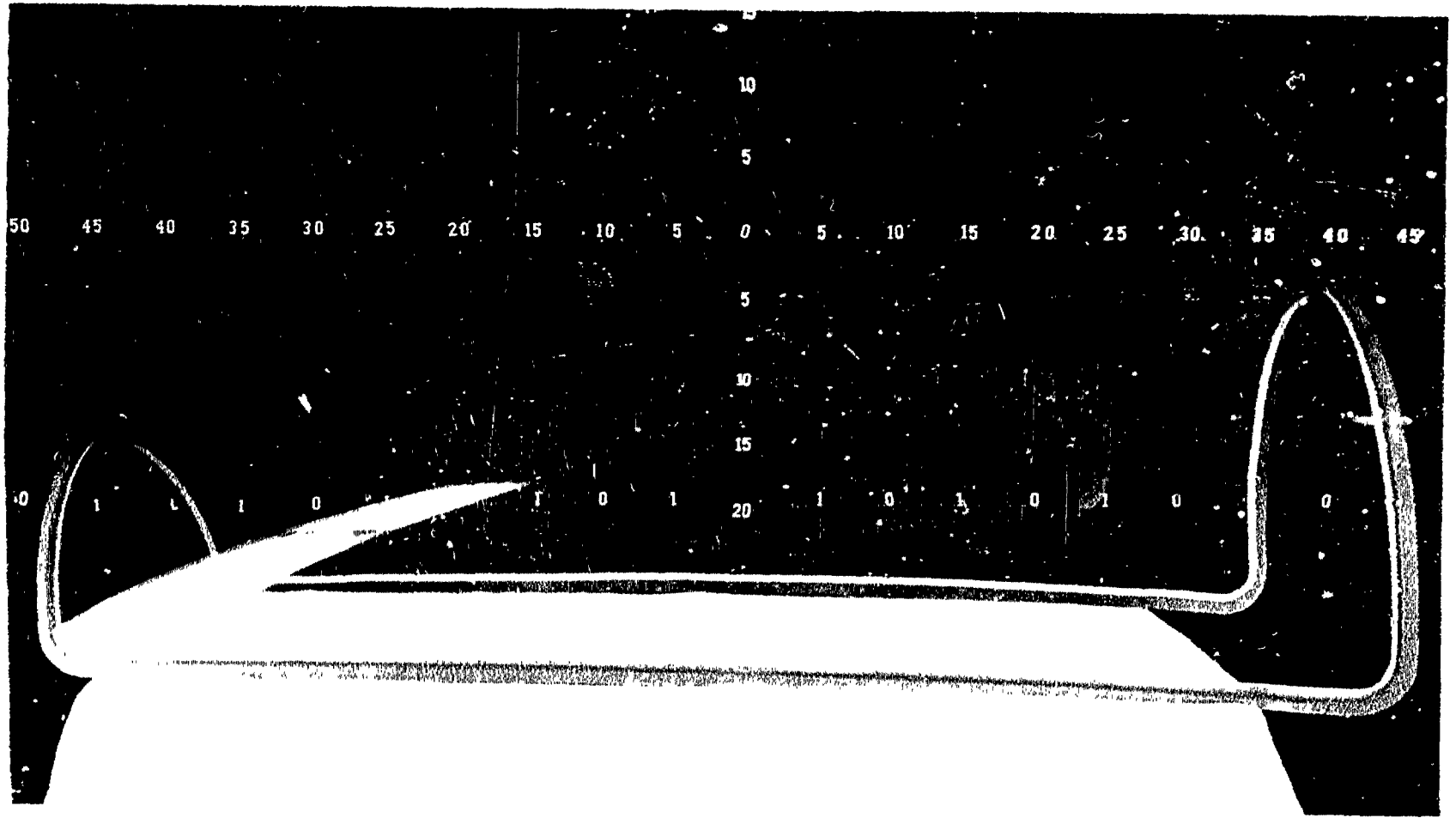


FIGURE 9 - F-14 AFT CANOPY

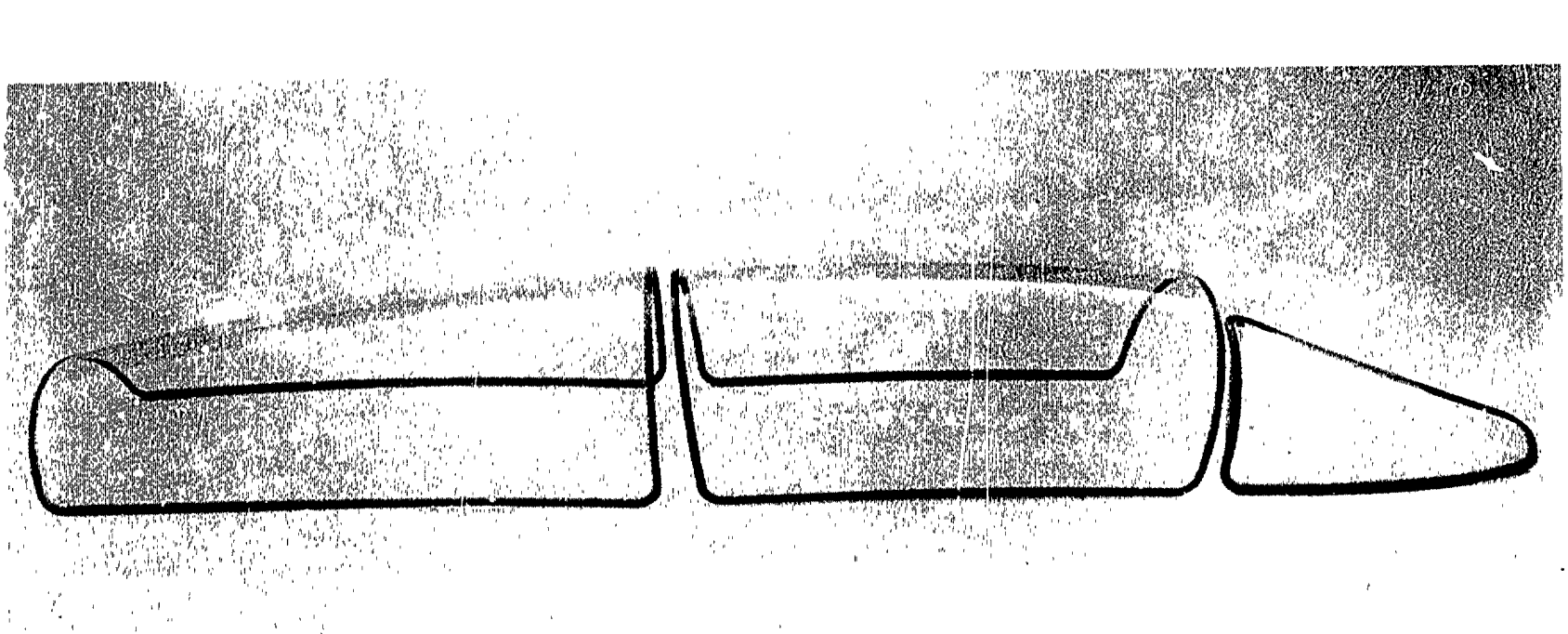


FIGURE 10 - F-14 TRANSPARENCIES

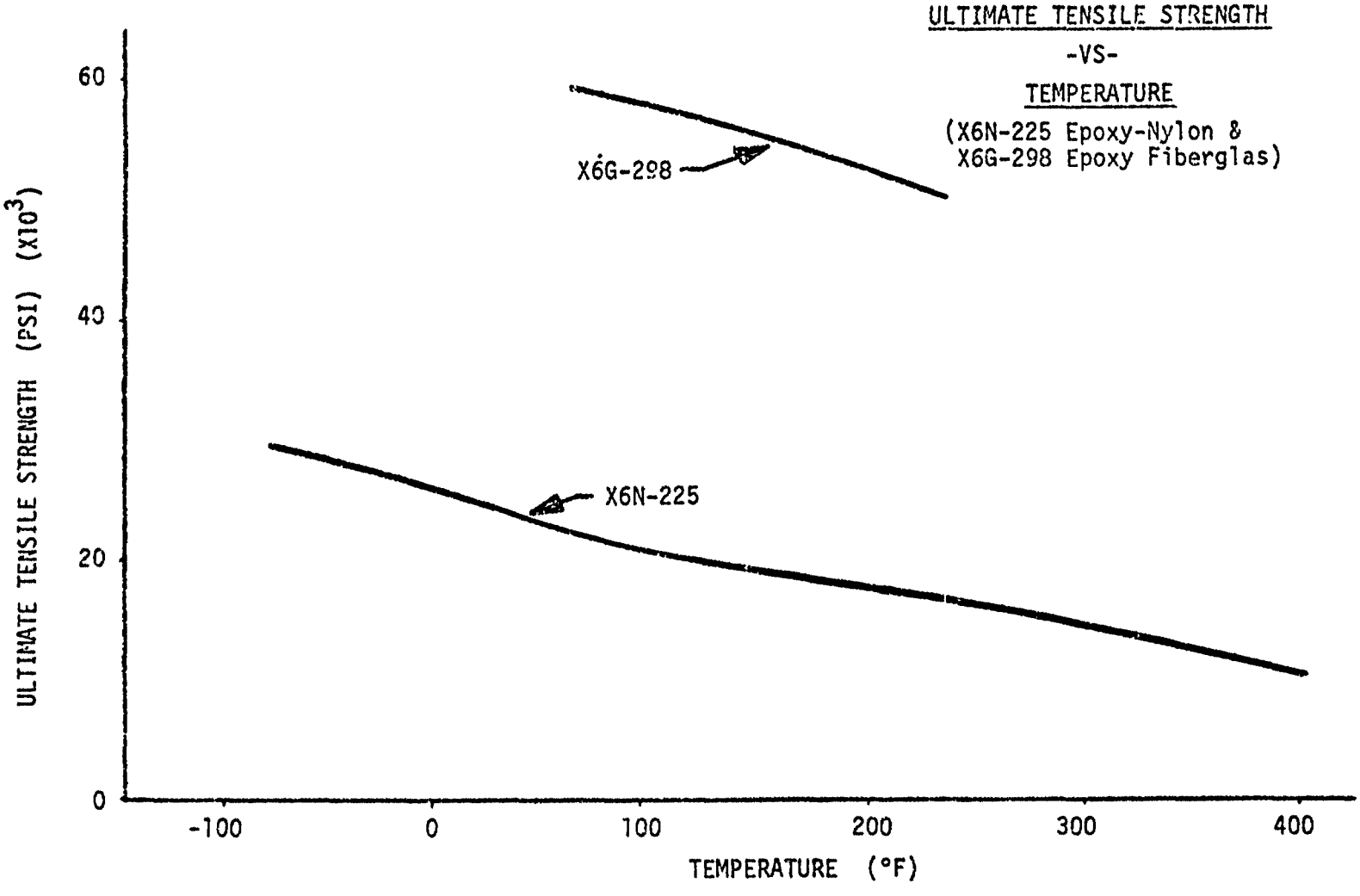


FIGURE 11 - ULTIMATE TENSILE STRENGTH OF EPOXY-NYLON AND EPOXY FIBERGLAS

THE CHALLENGE OF COATING AND ASSEMBLING SPACE SHUTTLE WINDOWS

J. K. Murphy
Optical Coating Laboratory, Inc.
Santa Rosa, California

PRECEDING PAGE BLANK-NOT FILMED

THE CHALLENGE OF COATING AND ASSEMBLING SPACE SHUTTLE WINDOWS

John K. Murphy

Optical Coating Laboratory, Inc.

Abstract

A capability has been developed to coat and assemble the windows and windshields of the Space Shuttle. Some of these spectral coatings function to dramatically reduce the fresnel reflectance of the visible spectrum, while others reflect (out of the system) much of the harmful infrared radiation. One of the substrates used absorbs most of the harmful ultraviolet radiation. The components of the window system and its eye protection capability will be discussed.

The Shuttle window specifications have some rigid requirements which necessitated designing large scale precision tooling that would hold the windows centered in the tooling without scratching them, through a thermal cycle of 200°C.

Slides of the special hardware designed and built to carefully position and hold these large substrates will be shown. Slides of the machine loading and unloading equipment and its function will be viewed. Techniques for assembling the coated substrates into their retainers will be discussed.

Coating uniformity across the 46 inch diameter coating racks will be examined. The design and function of a unique thick window spectrophotometer, designed and fabricated for this program, will be discussed.

This talk will focus on the processing of Space Shuttle windows, the level of cleanliness required, the special equipment utilized, and safety precautions exercised during window handling.

INTRODUCTION

By now, most of us have been exposed to some description of the Space Shuttle concept (Figure 1). The National Aeronautics and Space Administration's Space Shuttle was designed to be a multimission space vehicle. After each landing, the Shuttle is to be refitted and readied for its next space mission.

The objective of this spacecraft is to provide a large reusable cargo carrying work platform, from which a multitude of space experiments can be carried out (Figure 2). The Space Shuttle will have the ability to carry and launch as many as five satellites during one mission. It will have the ability to erect a large space telescope for viewing completely outside the contaminants of the earth's atmosphere. It will also have the ability to pluck a satellite from orbit, repair or replace defective components and reinsert it into an earth orbit.

A multitude of exotic experiments are being considered for various Space Shuttle missions, many others have been proposed. The Space Shuttle is designed to be a reusable workhorse of the sky, to blast-off from earth, achieve an earth orbit, perform its work function, loiter for as much as one month, return through earth's atmosphere and land like an airplane.

This thing that has seemed like a Buck Roger's fantasy is now becoming a reality. The Space Shuttle is really being built and many of us have an active part in its construction.

OCLI is coating and assembling the Space Shuttle windows into retainers. These assembled retainers will be installed in the crew module of the Shuttle.

THE WINDOW SYSTEM

The windows of the Space Shuttle (Figure 4) are rigid transparent structural members of the crew module. Their primary function is to provide pilot visibility for the space craft command function. Their secondary function is to provide viewing ports for the pilot and crew. (Especially the side hatch, overhead, and rear viewing windows).

The windshields are the largest of the Shuttle windows. Their largest dimensions are their 43" diagonals. The exterior windshield is called the thermal window. It is made of fused silica, and ranges from approximately .6" to .7" thick. It is the thermal barrier for the window system. The exterior surface of the thermal windows will see reentry temperatures up to ≈900°F, according to Rockwell calculations (Figure 5). Rockwell has predicted that the interior surfaces of the thermal windshields will rise to approximately 800°F during reentry.

(THE WINDOW SYSTEM Continued)

The thermal windows are assembled into (Figure 6) retainers which will mount to the exterior crew module. These thermal assemblies are not designed to maintain cabin pressure.

The pressure windows are highly tempered aluminosilicate glass approximately .7" thick. The redundant windows are fused silica, and are approximately twice as thick as the pressure windows. These two windows are assembled, after coating, into a pressure retainer assembly. This assembly is required to maintain cabin pressure.

The pressure window is the primary pressure retaining member of this system. Should that pressure window fail, the redundant window is the back up structure. Now we should look at the function of the thermal and pressure assemblies.

COATING FUNCTION

The exterior surface of the thermal window is uncoated. The interior surface of that window is coated with a high efficiency anti-reflection coating (HEA®) (Figure 7). This coating reduces the visible reflectance of the glass surface from approximately 4% to less than 4/10% average.

Both surfaces of the redundant window are HEA coated. Typical average transmittance values of that coated window are approximately 99%.

The exterior surface of the pressure window is coated with a "Red Reflector" coating, which reflects much of the undesired infrared radiation, while transmitting the visible spectrum (Figure 8). The interior window surface is coated with a high efficiency anti-reflection coating. Typical average visible transmittance of the window exceeds 90%. Most of the harmful ultraviolet radiation is removed from the window system by the intrinsic absorption of the aluminosilicate substrate, and the Red Reflector coating.

APPLICATION OF COATINGS

The Space Shuttle production area was designed to be a "clean" area. Most of the process functions require clean room type cleanliness. The window final cleaning and loading process requires a basically clean, lintfree atmosphere. The assembly process requires an even higher degree of cleanliness, i.e., no lint or air born particles, which would settle on the windows during assembly.

(APPLICATION OF COATINGS Continued)

Within the Shuttle area, all incoming air is filtered through 65% pre-filters and then conditioned. The air that "feeds" the clean tents which surround the critical cleaning-loading and assembly processes is filtered through class-100 clean air modules.

The particle count in the cleaning-loading area typically ranges from 50-100. The particle count in the assembly area is typically from 30-50 particles per cubic foot.

To maintain this state of cleanliness, all cabinets, equipment and floors are cleaned regularly, and the plastic walls of the clean tents are wiped down with an anti-static agent. Cleaning and loading personnel wear tightly (Figure 9) woven jumpsuits and hard hats to reduce additional contamination in the cleaning-loading area.

Assembly personnel wear the full clean room suits, e.g., class-100 coveralls, booties, hoods, beard covers, face masks and gloves (Figure 10).

The Space Shuttle windows are received from Corning Glass Works in massive boxes designed to withstand just about every type of poorhandling conceivable (Figure 11). Each box holds from one to three polished windows. As windows are needed, the boxes are moved with a floor crane and placed in a horizontal position. The side is removed and the windows are unpacked (Figure 12).

The windows are shipped with a protective tape over the polished surfaces. This tape is removed, and the windows are cleaned for receiving and incoming inspections (Figure 13).

Receiving inspection is basically an examination for shipping damage while incoming inspection is a thorough surface and subsurface inspection. The incoming inspection is performed in a "black" room (Figure 14). In addition to the general surface quality inspection, the windows are measured for transmittance prior to coating on an OCLI designed and fabricated thick window spectrophotometer (Figure 15).

After the windows have been accepted, they are cleaned for coating.

(APPLICATION OF COATINGS Continued)

The appropriate tooling is then selected, cleaned, and outgassed to prepare for substrate loading (Figure 16).

Special loading equipment was designed and fabricated at OCLI to handle the large windows without damage. The fused silica windows have a scratch depth specification that is very tight. No scratch shall be greater than .0006" deep. Therefore, window handling methods require that window movement be deliberate, limited, and cautious. The holding devices must provide firm, positive support, yet generate no scratches.

Neoprene covered blocks were fabricated somewhat smaller than the windows, but in the configuration of the window (Figure 17). These blocks are used to support the Shuttle windows during inspection and cleaning. The loading operation utilizes an adjustable table (x, y, z, θ) in conjunction with a modified stacker. The adjustable table is basically a machinist's table with an x, y, θ set of ways mounted on it. On top of the ways a Neoprene covered block is mounted. This block is covered with lens tissue before the window is placed on it. Prior to the window being placed on the block, a modified motorized hydraulic stacker which holds (Figure 18) the coating tooling, is placed below the level of the ways. The coating tooling is raised slowly around the window. The window is positioned very accurately using the x, y, θ action of the ways. The stacker lifting speed can be reduced to an almost imperceptable rate for this operation. When the window is positioned completely within the tooling, it is lifted above the x, y table a few inches.

A Teflon-coated jig lip is positioned over the window, lowered, and bolted to the tooling (Figure 19). The flip clamp tooling is then tightened up so the window is firmly and securely held against the Teflon-coated jig lip. A modified floor crane is positioned over the tooling and the tooling is transferred to trunnion plates on that crane and bolted in place. The crane and tooling are then pulled a few feet away from the stacker.

At this point, the tooling is inverted (rotated) so the jig lip is on the bottom. The coating chamber door (Figure 21) is opened and the tooling is raised to the backing plate and bolted in place.

In its present configuration, the 100 inch diameter coating chamber can hold two 43" diagonal windows, or three 41" diagonal windows. Almost all the rotary motion system is made of stainless steel. It was designed to safely hold 500 pounds per planetary spindle. The present window-holding tooling combinations are well within that limit.

(APPLICATION OF COATINGS Continued)

When the chamber door is closed, the chamber is roughed-out and pumped down to base vacuum. The chamber is then brought slowly up to coating temperature (Figure 22). The coating is deposited, and the chamber is slowly brought back to room temperature and atmospheric pressure.

After coating, the windows and holding tooling combinations are removed from the coating chamber in the same manner (reverse order) in which they were put in. The coated windows are wrapped and put back into the storage boxes. The coating chamber is then readied for the next coating run (Figure 23).

Spectral variation across the coating racks ranges from approximately one percent to three percent. This means the film thickness may vary from one percent to three percent of nominal across the full diameter of the coating rack (Figure 24).

ASSEMBLY OF WINDOWS

The coated windows are accumulated and are assembled into Rockwell furnished retainers at OCLI. These retainers are made from aluminum and stainless steel.

Assembly is a slow, tedious process, requiring patience, skill, and coordination. The assembly team trained for this task using a mock-up retainer and windows. After several training sessions, a very definitive assembly procedure was written.

The windows are unpacked, recleaned, and prepared for assembly. The basic assembly process is very similar to the loading operation, but the alignment tolerances are infinitely closer. An aluminum frame which holds the retainer is bolted to the trunnions of the stacker (Figure 25). This subassembly is lowered around an adjustable table. A Neoprene covered block is mounted on top of the table ways and centered within the retainer aperture. The Neoprene block is covered with lens tissue and the appropriate window is placed on the lens tissue.

With four people observing and guiding, the retainer is slowly raised around the window (Figure 26). The window edges are protected by the use of at least six thin Teflon shims. During this operation, the window is often repositioned to maximize the window to retainer clearance on all sides. When the window is resting completely within the retainer the stacker is raised so that the window is one to two inches above the Neoprene pad.

(APPLICATION OF COATINGS Continued)

In the case of the thermal retainers, the retainer which has just been raised around the window is the inner retainer (Figure 6). The next operation is the installation of the outer retainer.

All retainer O-rings are Viton, with the exception of the thermal barrier, which is made of braided glass fibers, backed by a silicone-rubber compression strip. These O-rings and thermal barrier must be placed in the outer retainer and must remain in place during installation. When both retainers are securely positioned together, the fasteners must be installed and torqued to a nominal 25 inch-pounds.

At this point, the thermal retainer assemblies are reviewed for workmanship, viewed in the beauty-aesthetic test, recleaned if necessary, and packaged for shipment.

The pressure assemblies are somewhat more difficult to assemble since three retainer sections fit together to hold the two windows.

Contamination cannot be tolerated in the cavity between the windows. Extra care is taken to remove all dust and keep contamination from the inner surfaces of the windows during assembly.

TESTING

When a pressure assembly is complete, it is tested for its ability to hold a vacuum for a defined period of time (Figure 28). The allowable leak rate is $\leq$ 0.1 standard cubic inches/lineal foot of seal per minute (scim). Typical pressure rise time specification from 10μ to 200μ is 60 seconds. The assembled retainers may then be tested for spectral conformance on a special thick-window spectrophotometer designed and built at OCLI. This spectrophotometer is designed to measure transmittance through combinations of windows up to three inches thick at incidence angles up to 45° (Figure 29). The spectrophotometer measures average transmittance in approximately 50 nanometer segments across the visible region. The detector position is controlled by a unique cam and linkage system which continually aligns the detector with the source, regardless of the Shuttle window angle (Figure 30). This source construction compensates for the parallax effect of the thick windows and maintains optical equivalence of the system. If the assembly is within the allowable leak rate, and it is spectrally acceptable, it is inspected for workmanship, viewed in the beauty-aesthetic test, recleaned if necessary, and packaged for shipment.

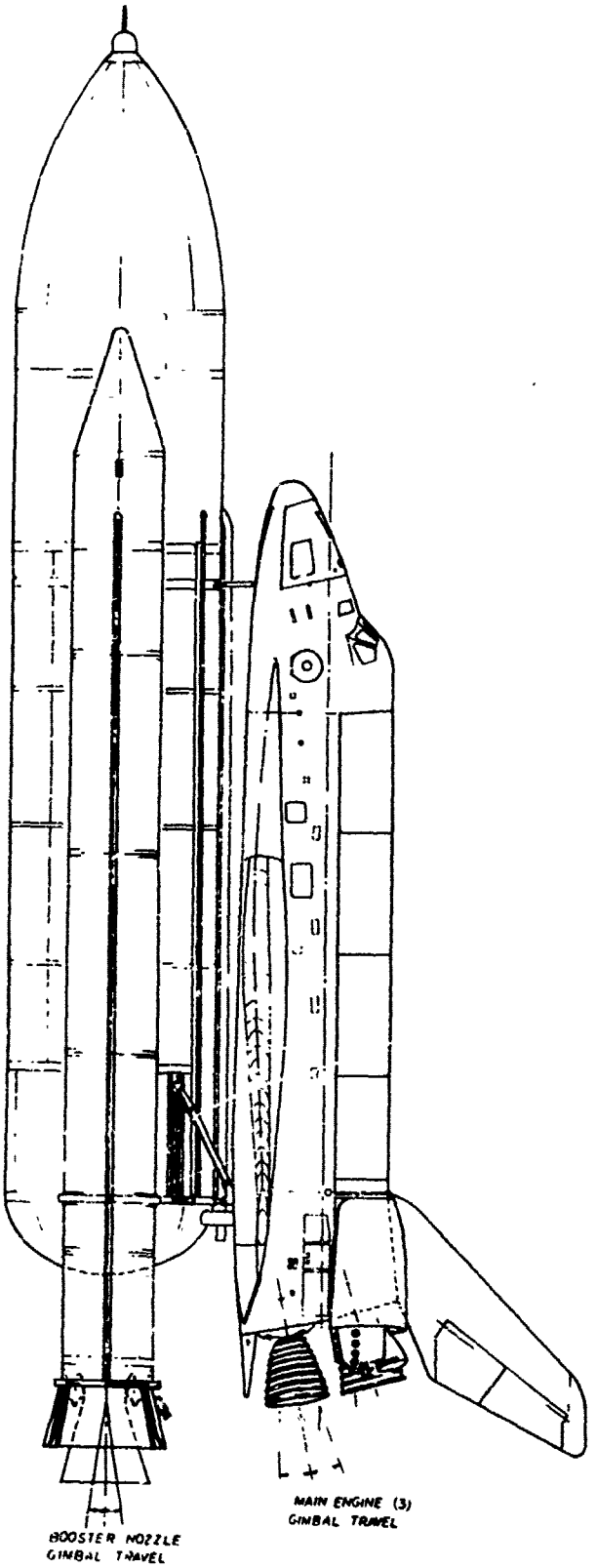


Figure 1. Side View - Shuttle

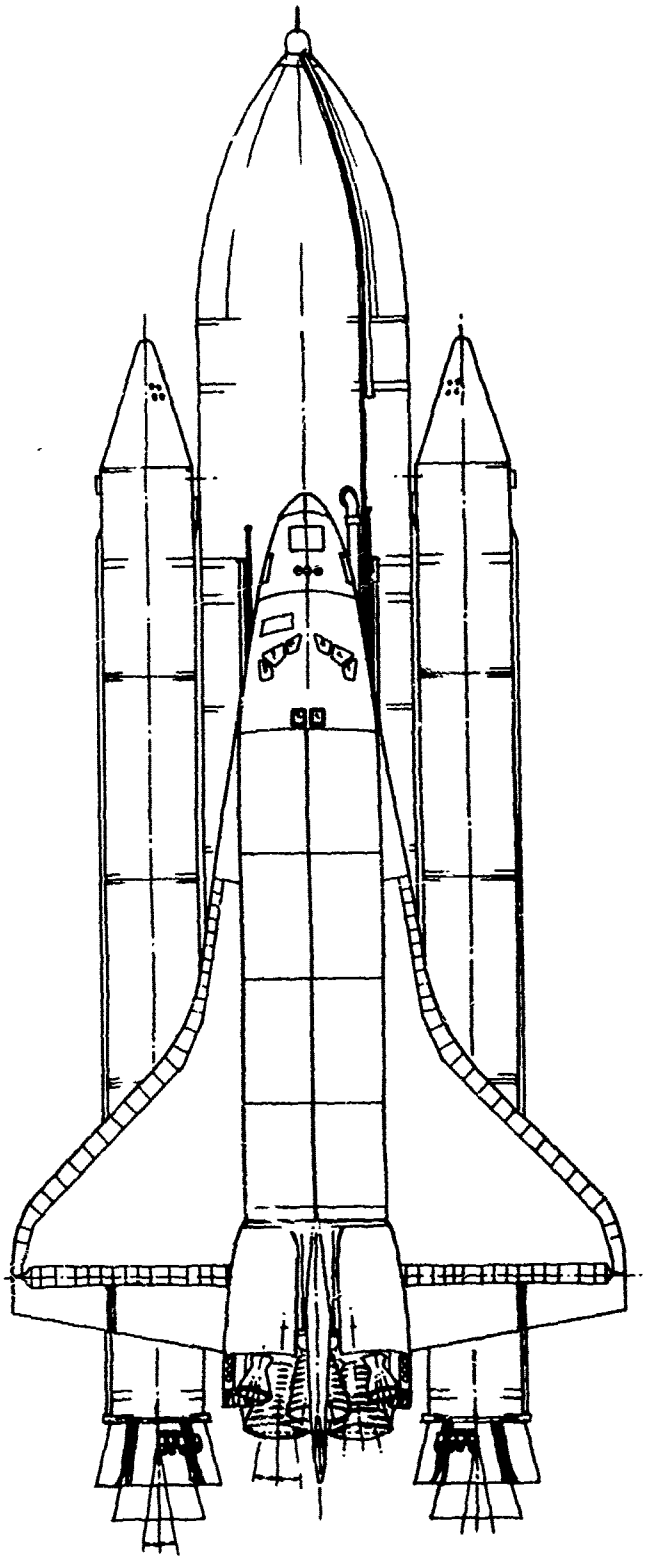


Figure 2. Top View - Shuttle

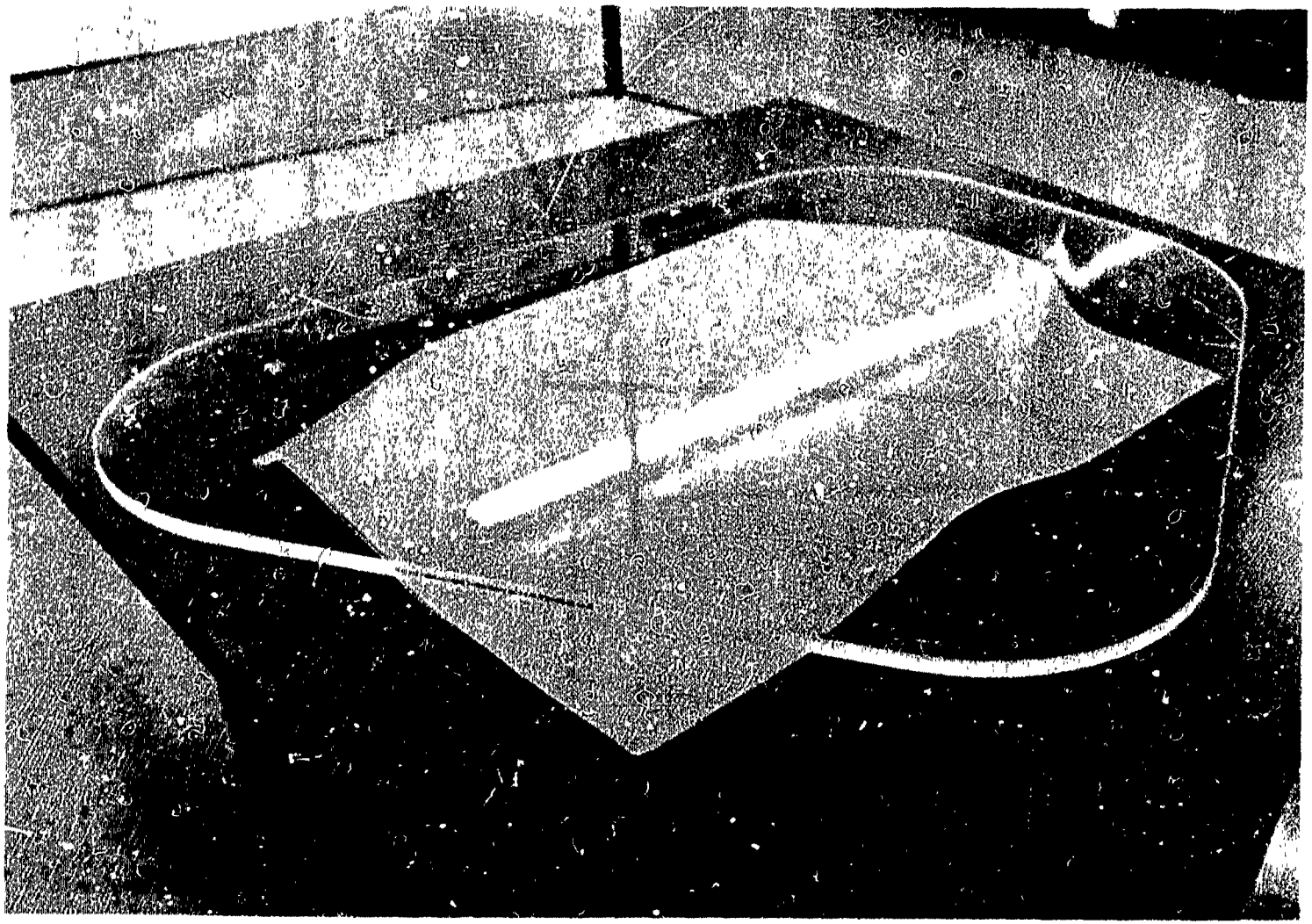
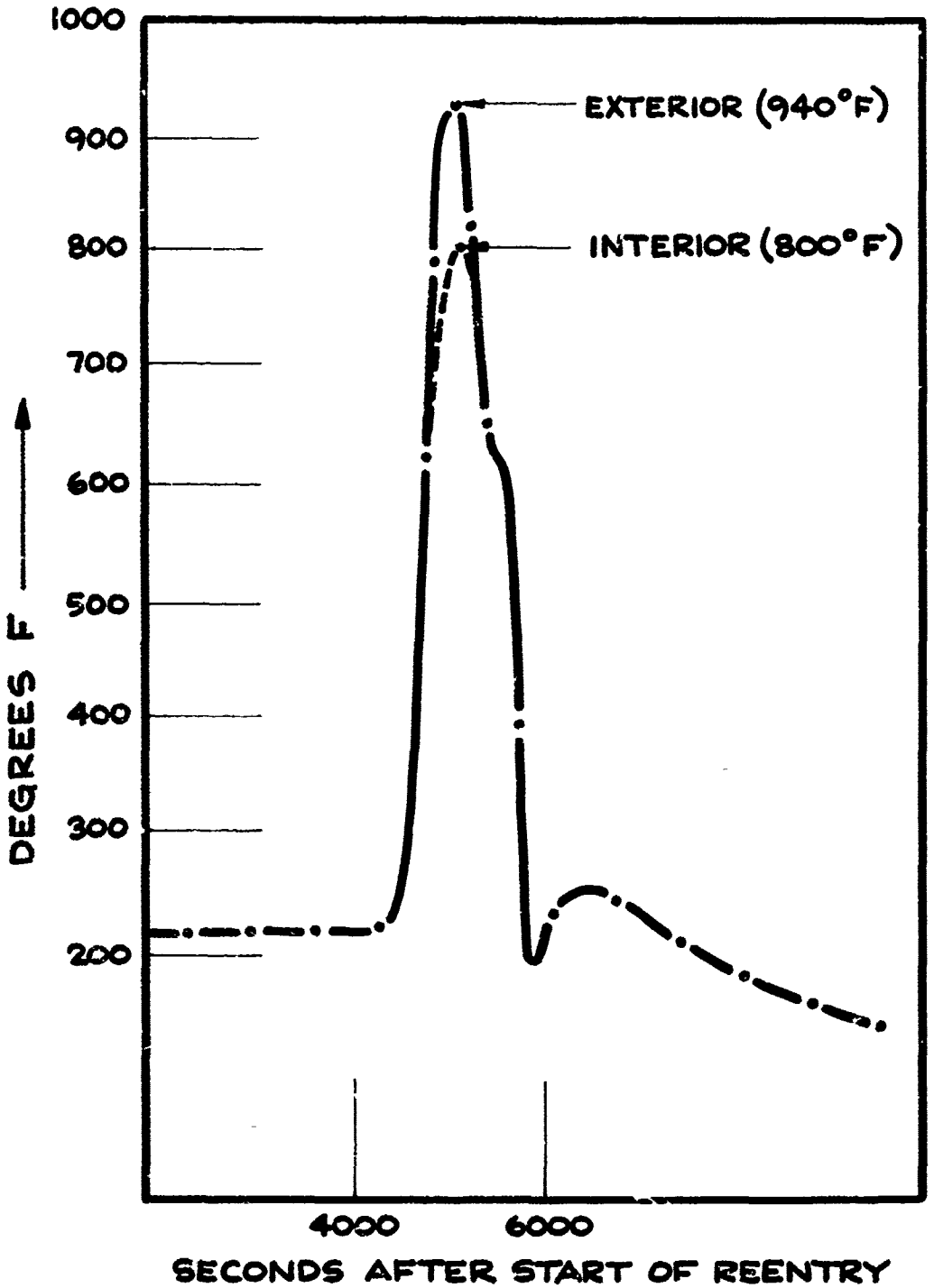


Figure 4. Thermal Window



SIMULATED TEMPERATURE RISE OF THERMAL WINDSHIELD PANES

Figure 5. Simulated Temperature Rise of Thermal Windshield Panes

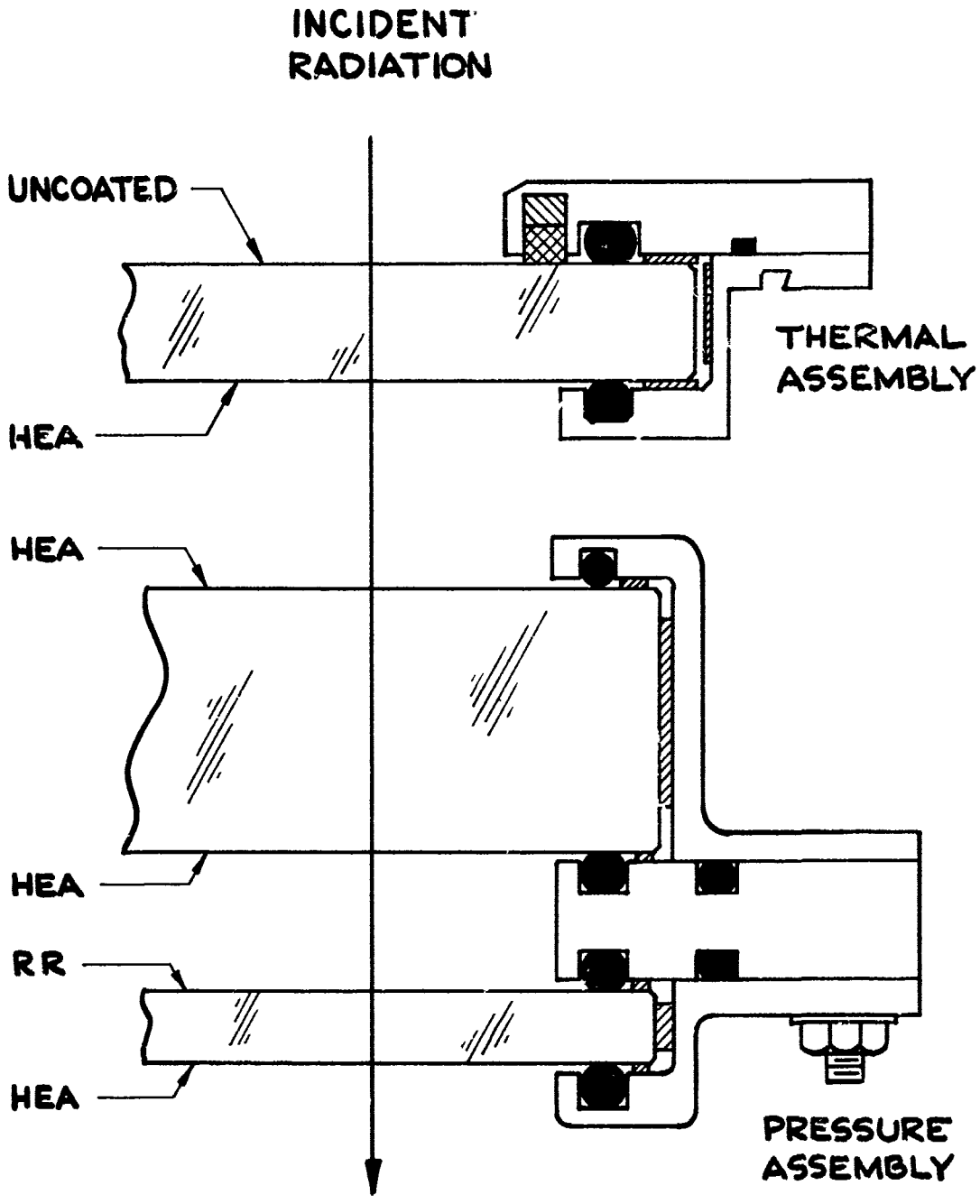
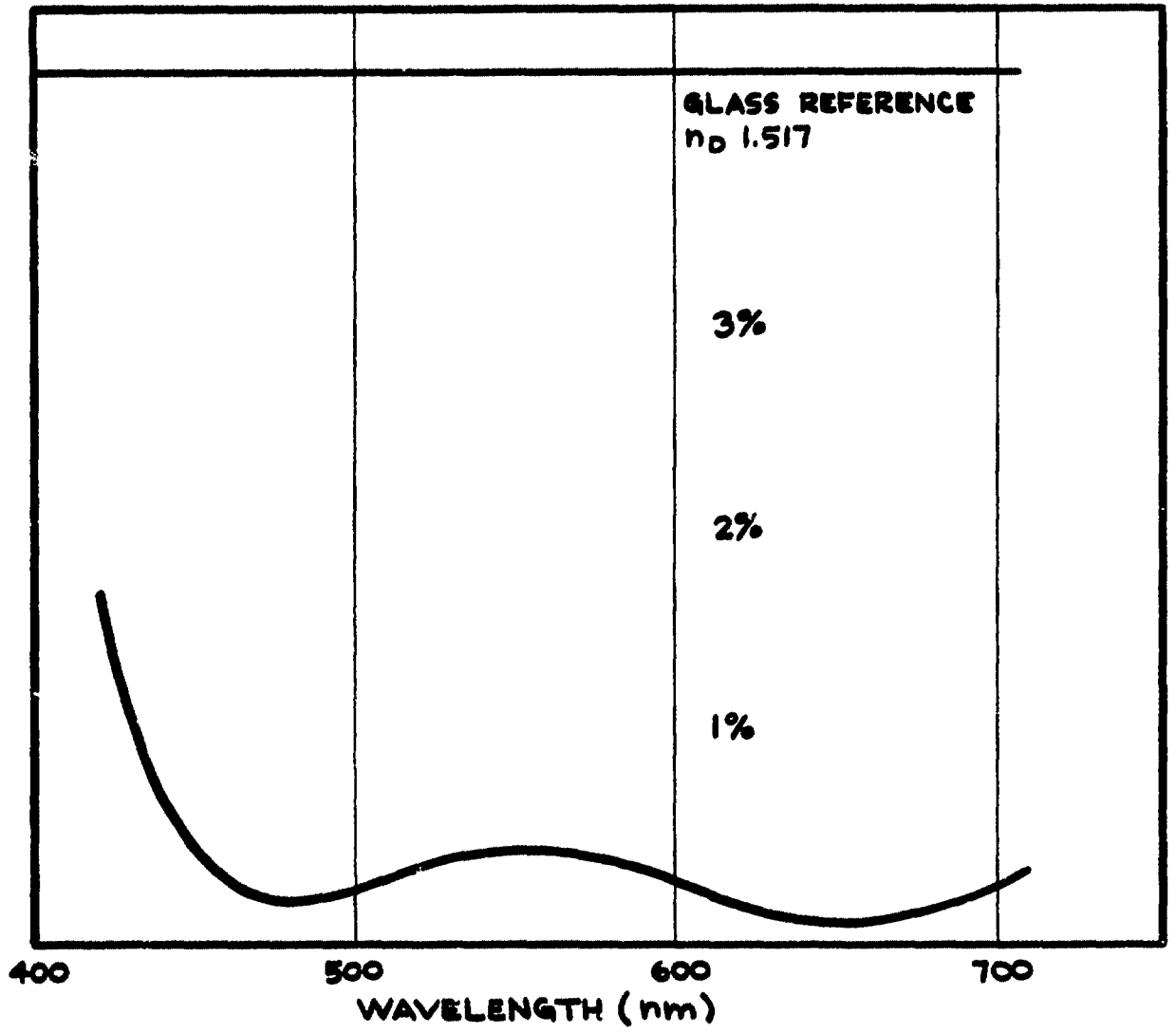


Figure 6. Window System



REFLECTANCE OF HEA® COATED FUSED SILICA $\theta = 30°$

Figure 7. Plot of HEA

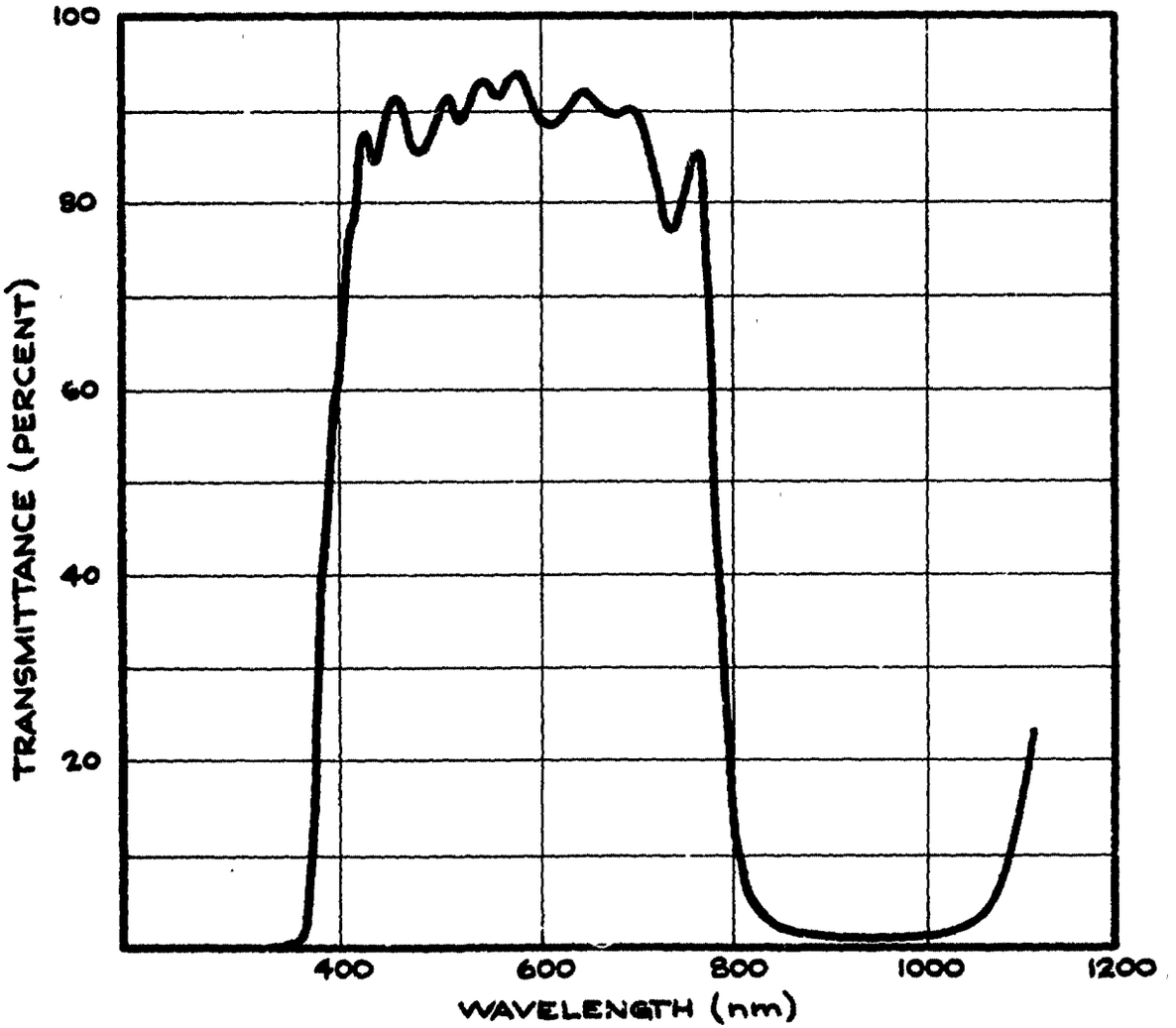


Figure 8. RR Coating Plot

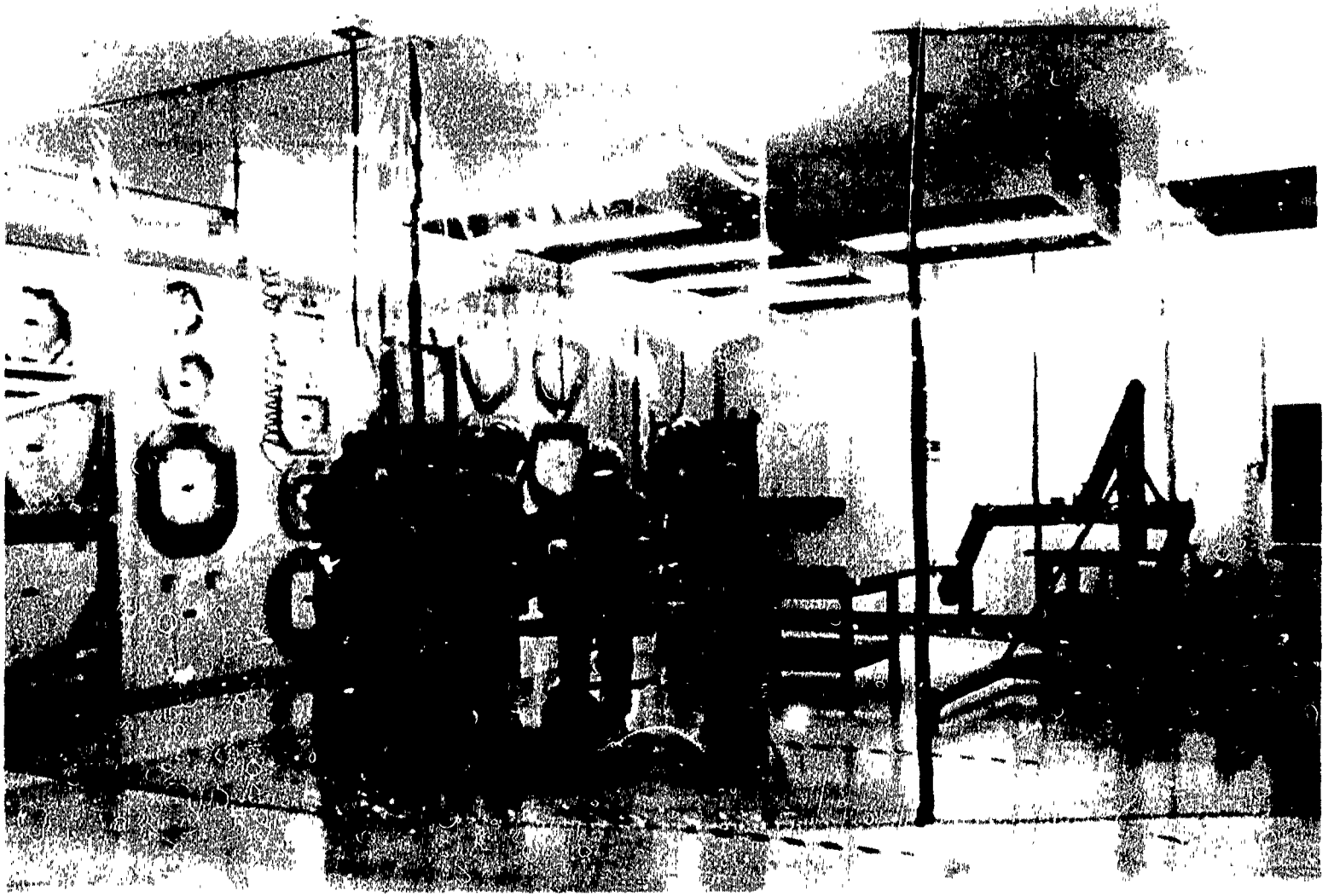


Figure 9. Cleaning and Loading Clothing



Figure 10. Assembly Clothing

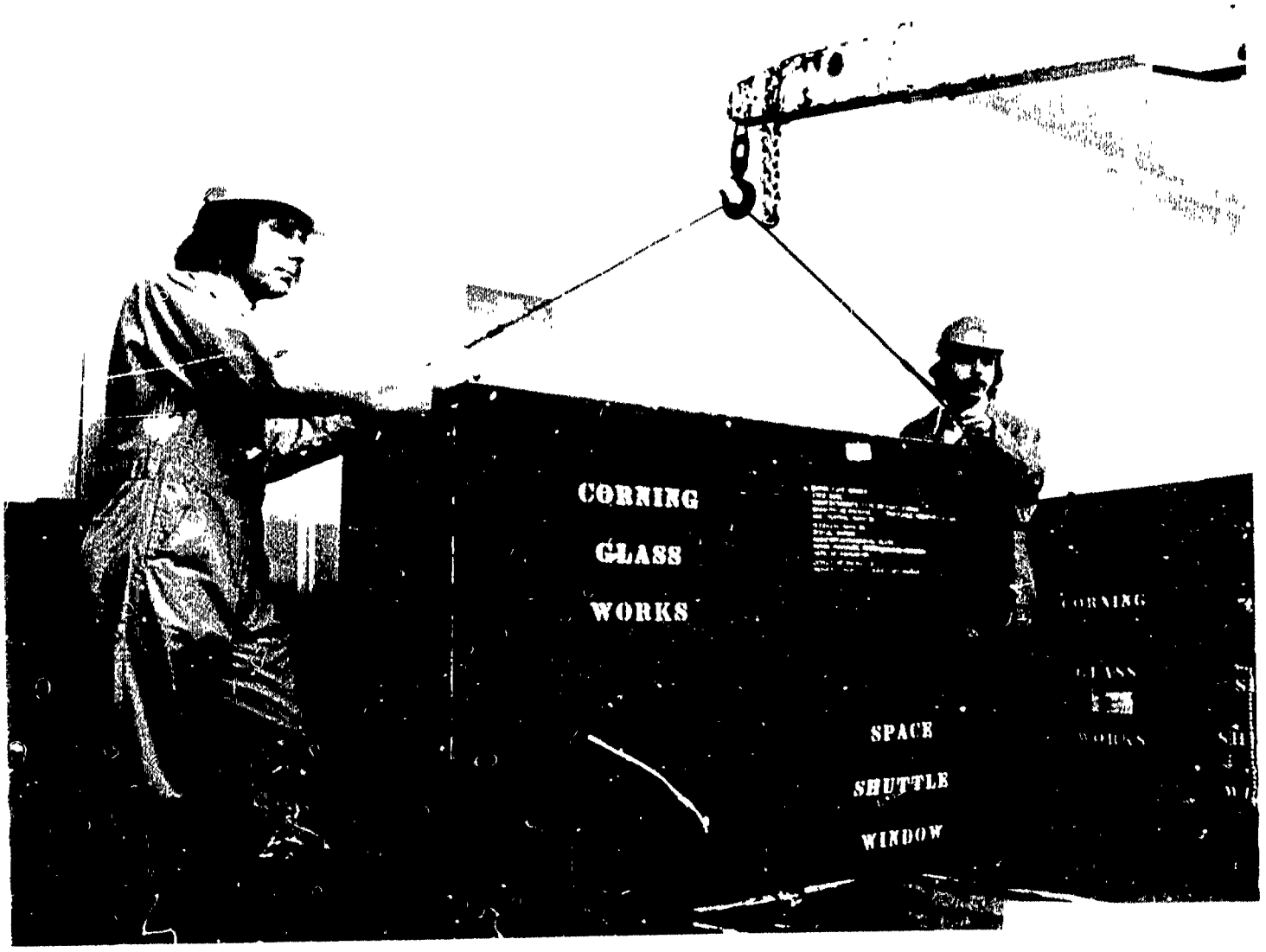


Figure 11. Shipping Containers



Figure 12. Unpacking



Figure 13. Window Cleaning

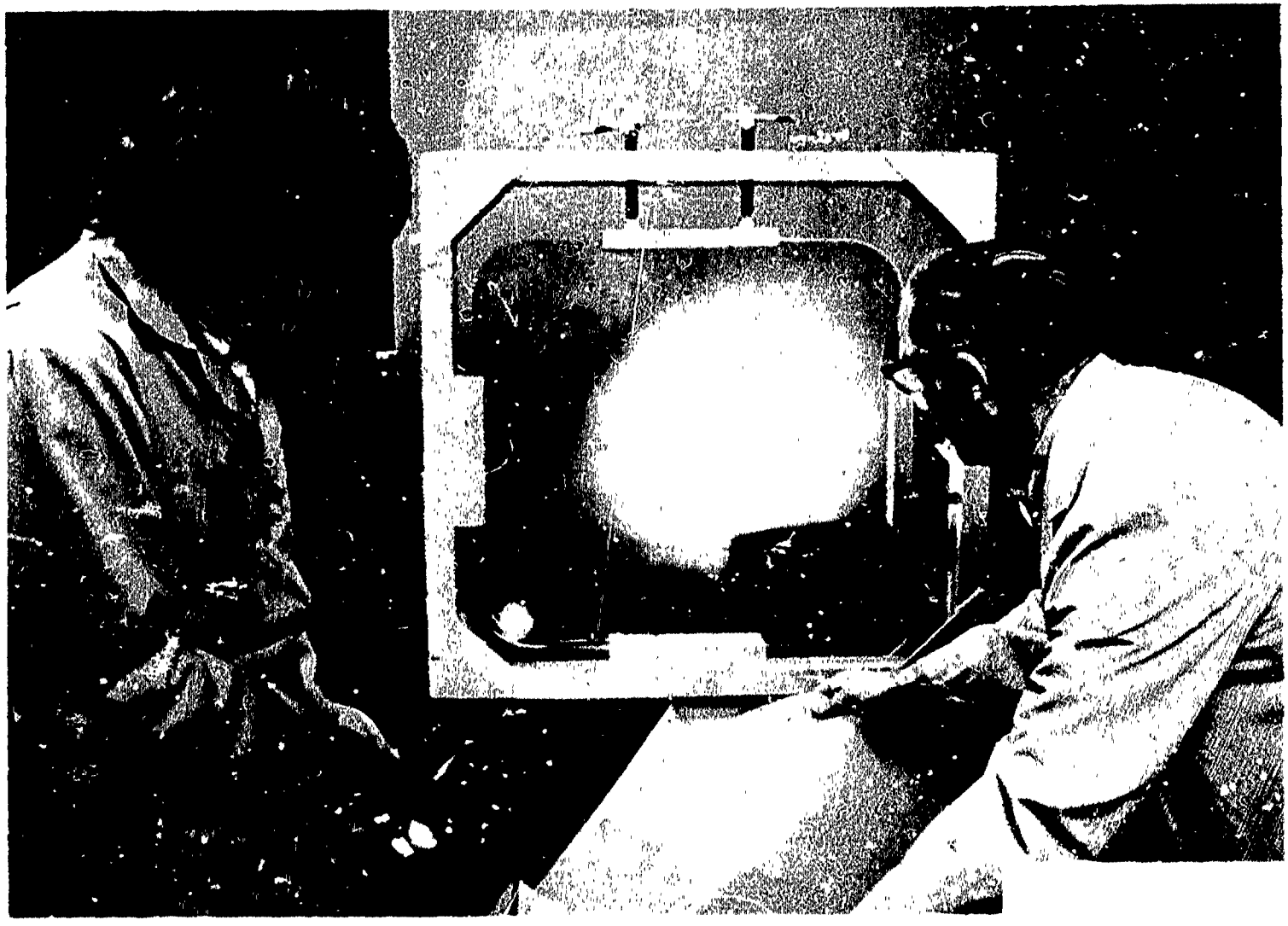


Figure 14. Incoming Inspection

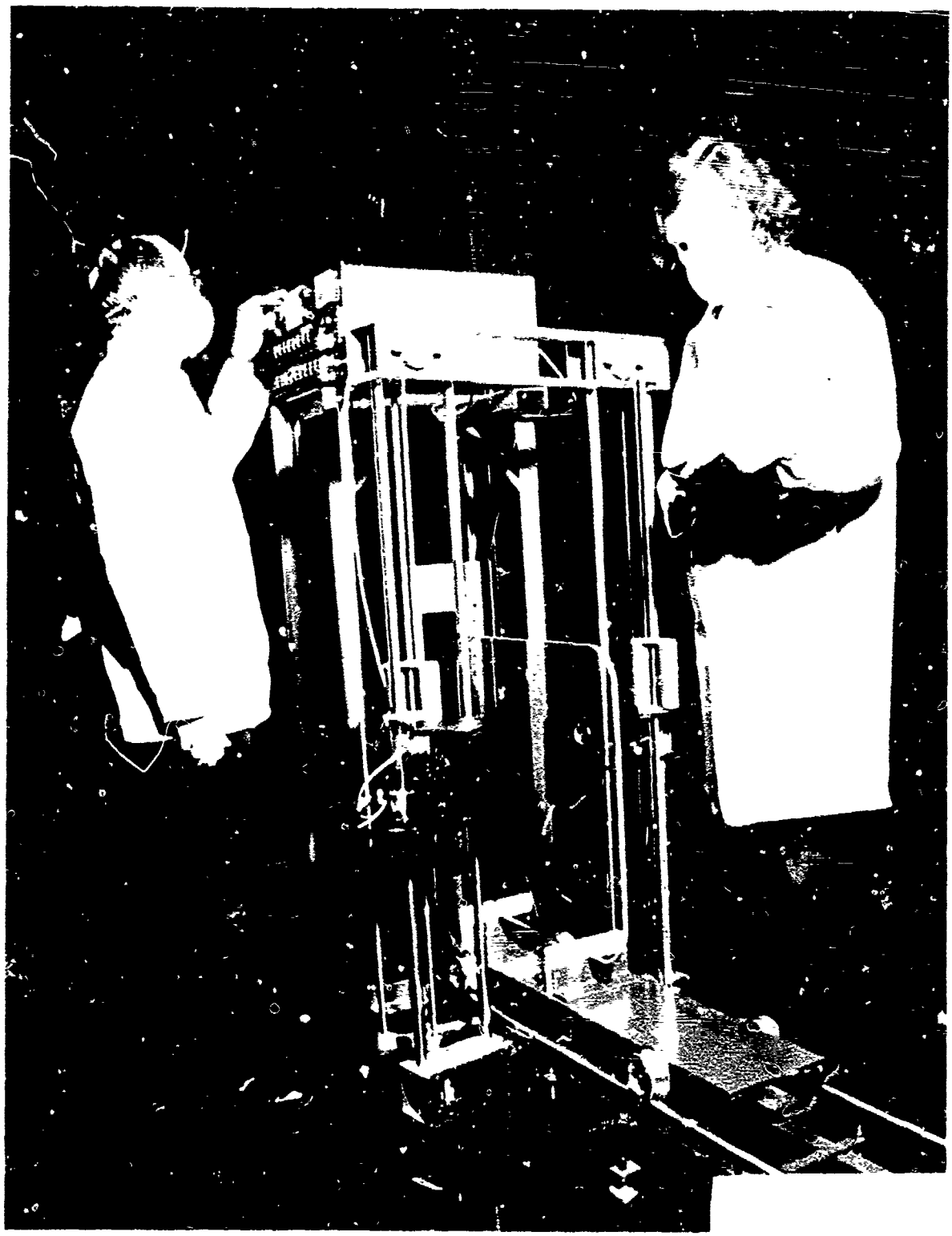


Figure 15. Spectrophotometer

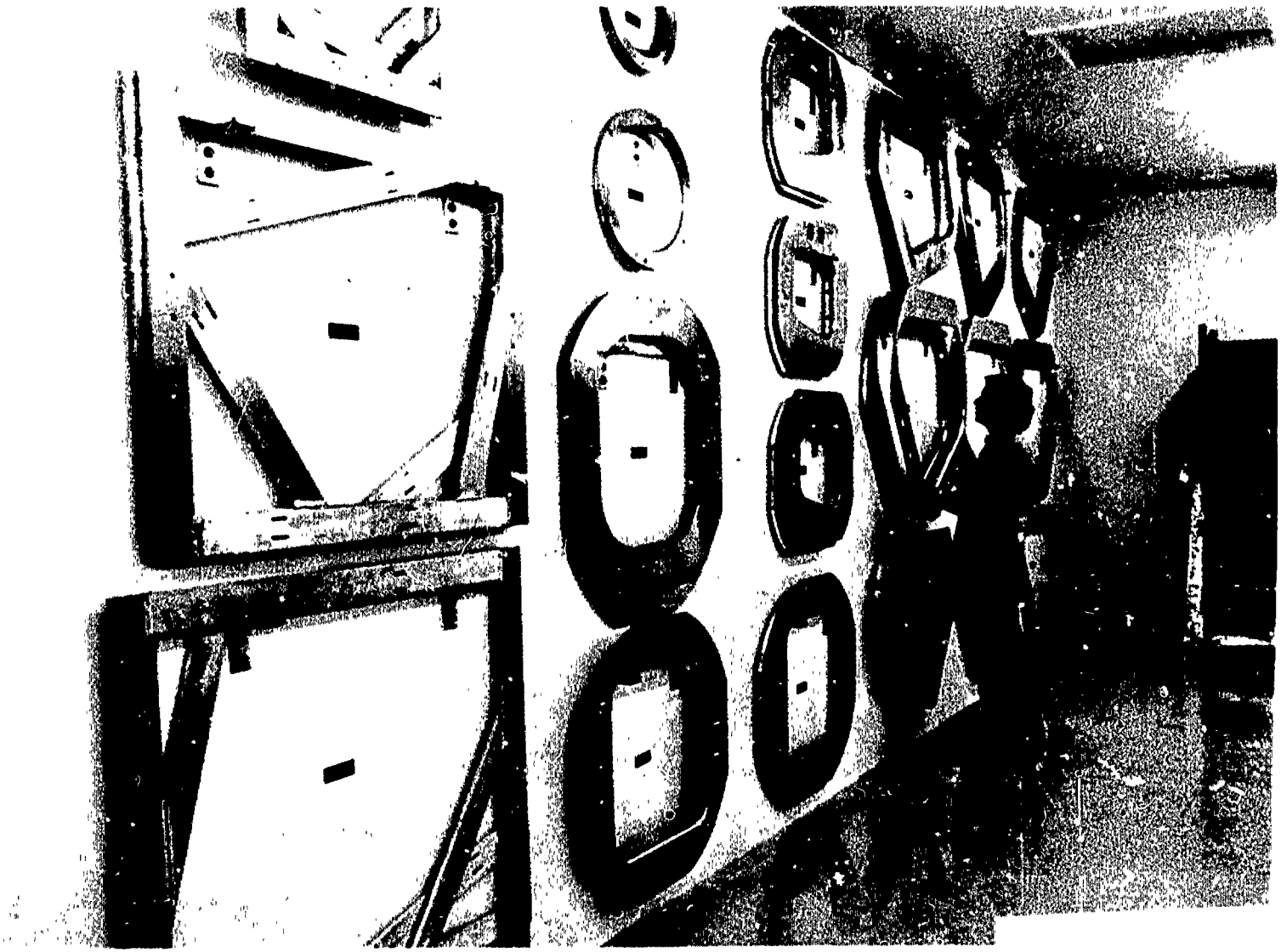


Figure 16. Tooling

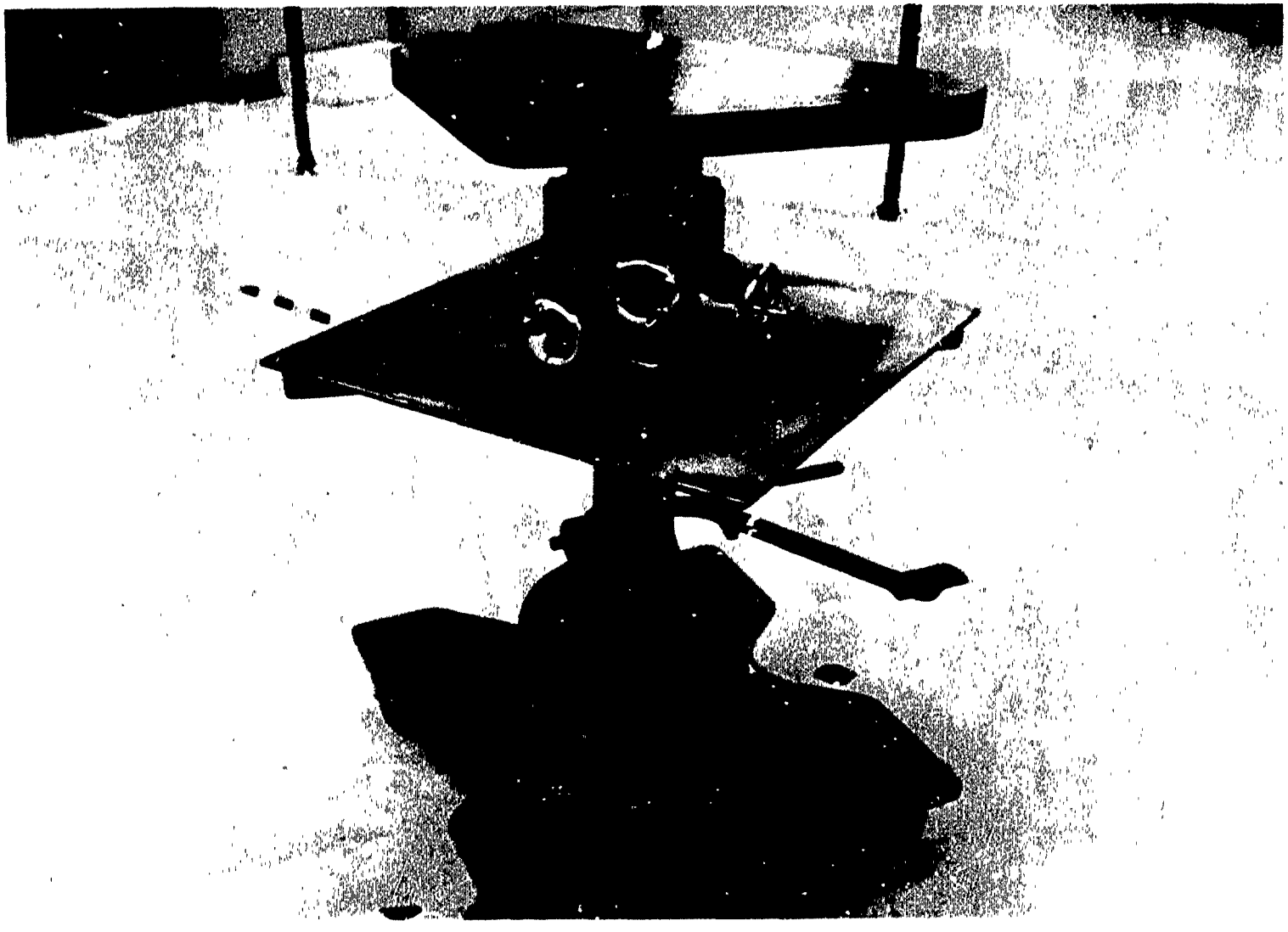


Figure 17. Machinist's Table with Pad

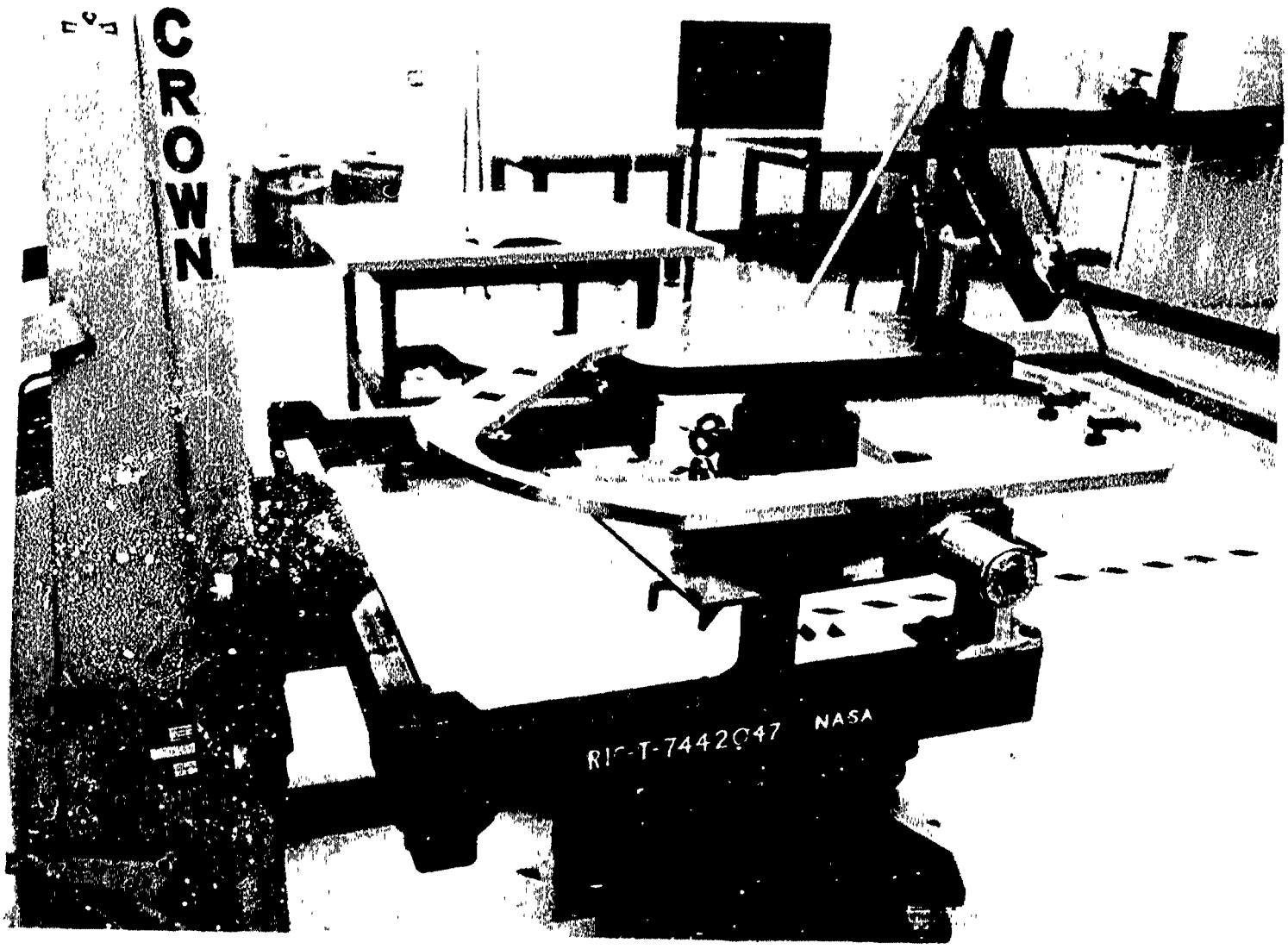
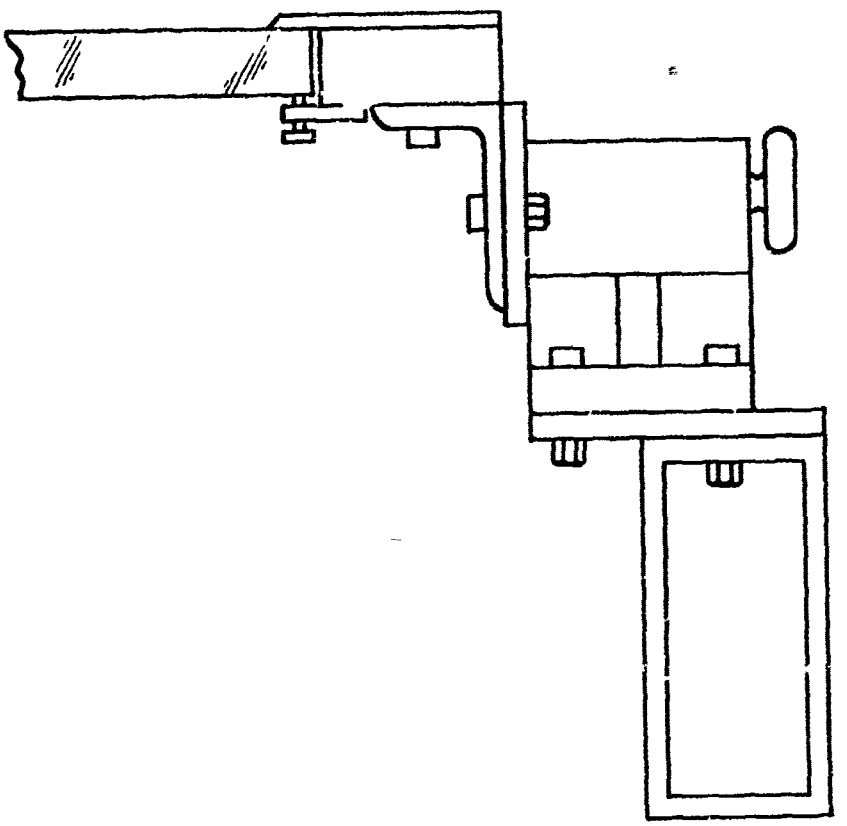


Figure 18. Stacker and Table



LOADING

Figure 19. Loading

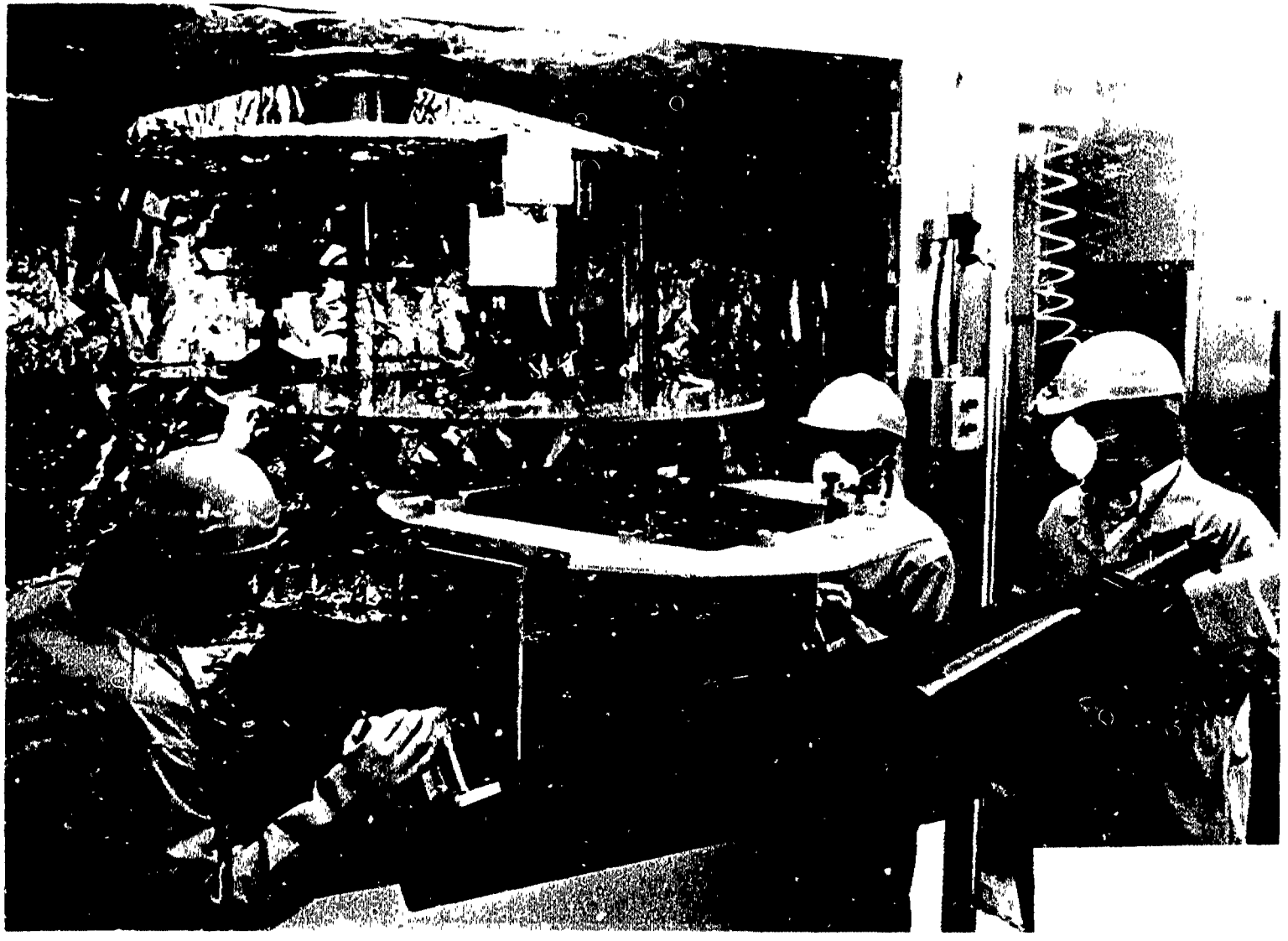


Figure 21. Rotated Tooling

Figure 22. Coating



Figure 23. Coating Chamber

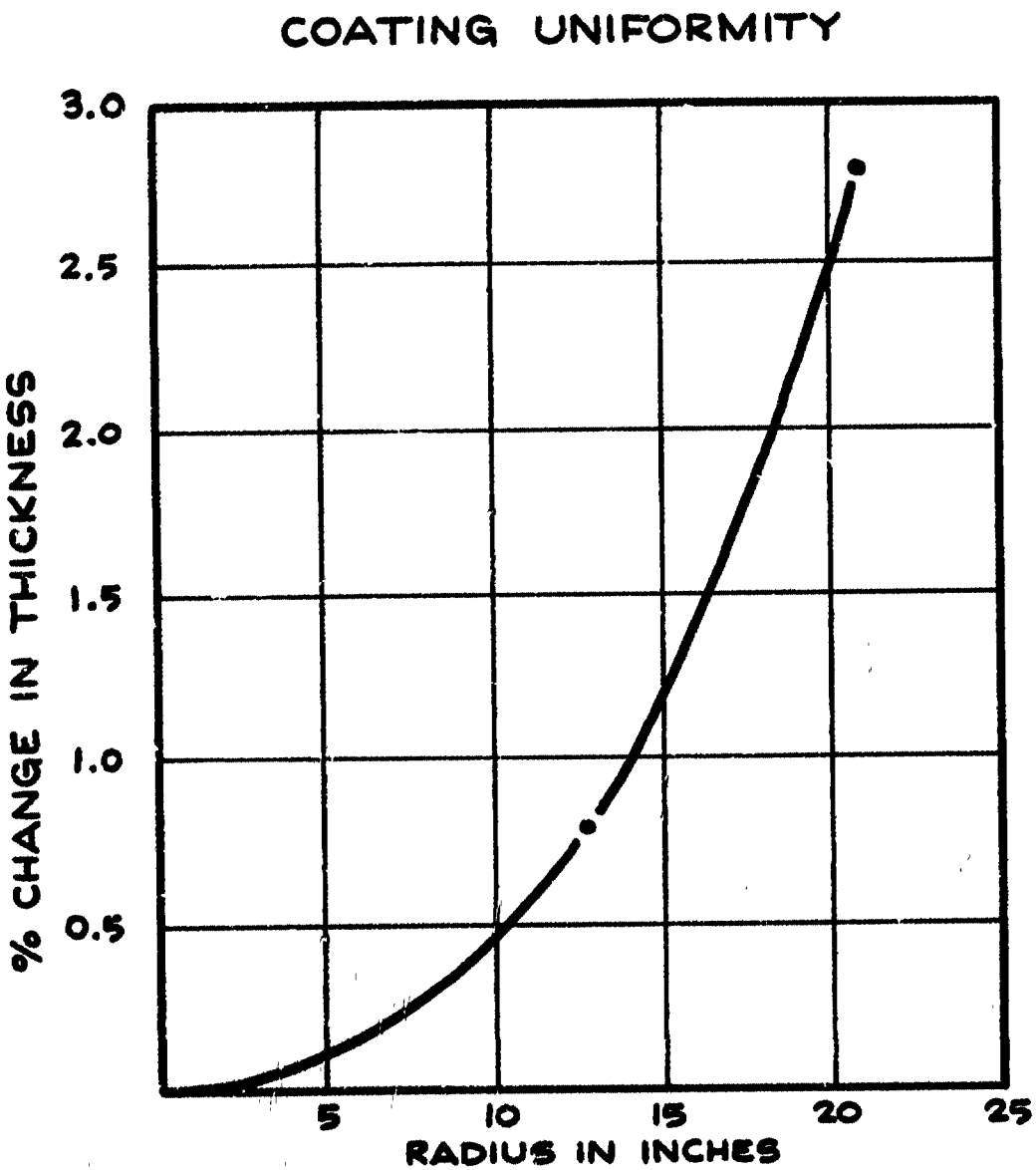
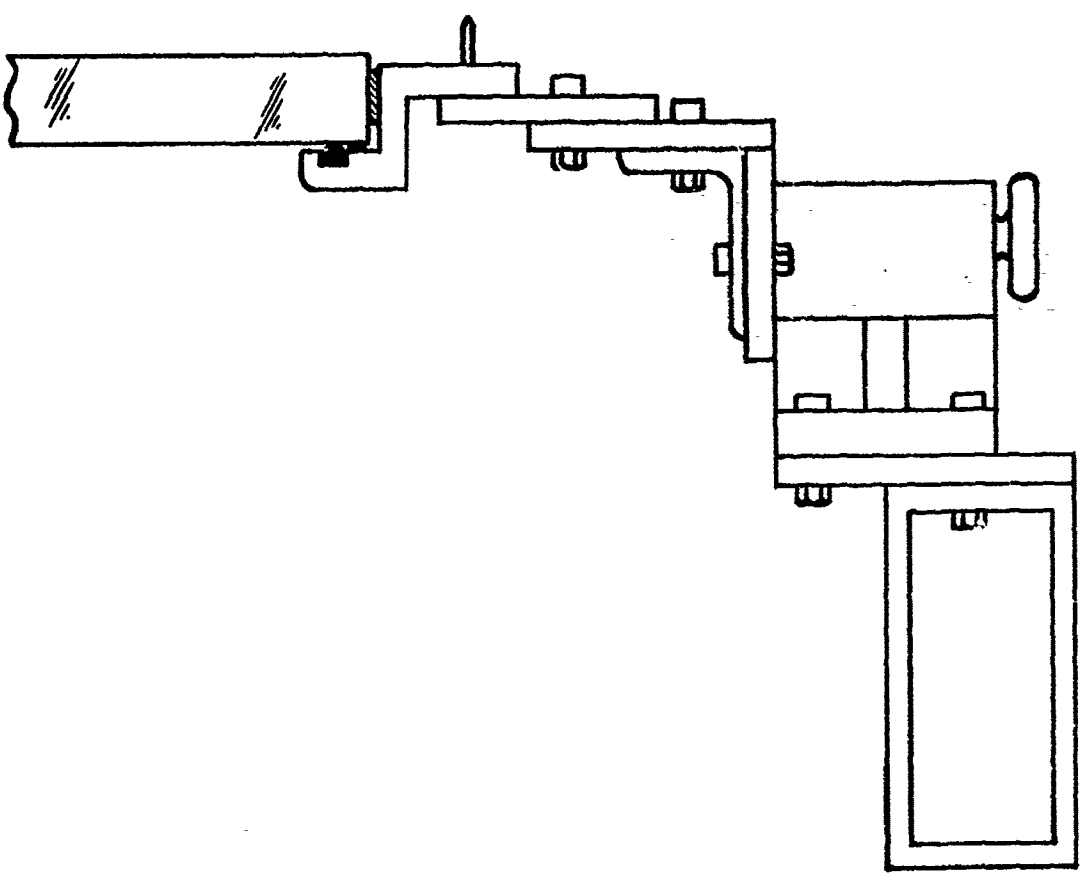


Figure 24. Coating Uniformity



ASSEMBLY

Figure 25. Assembly

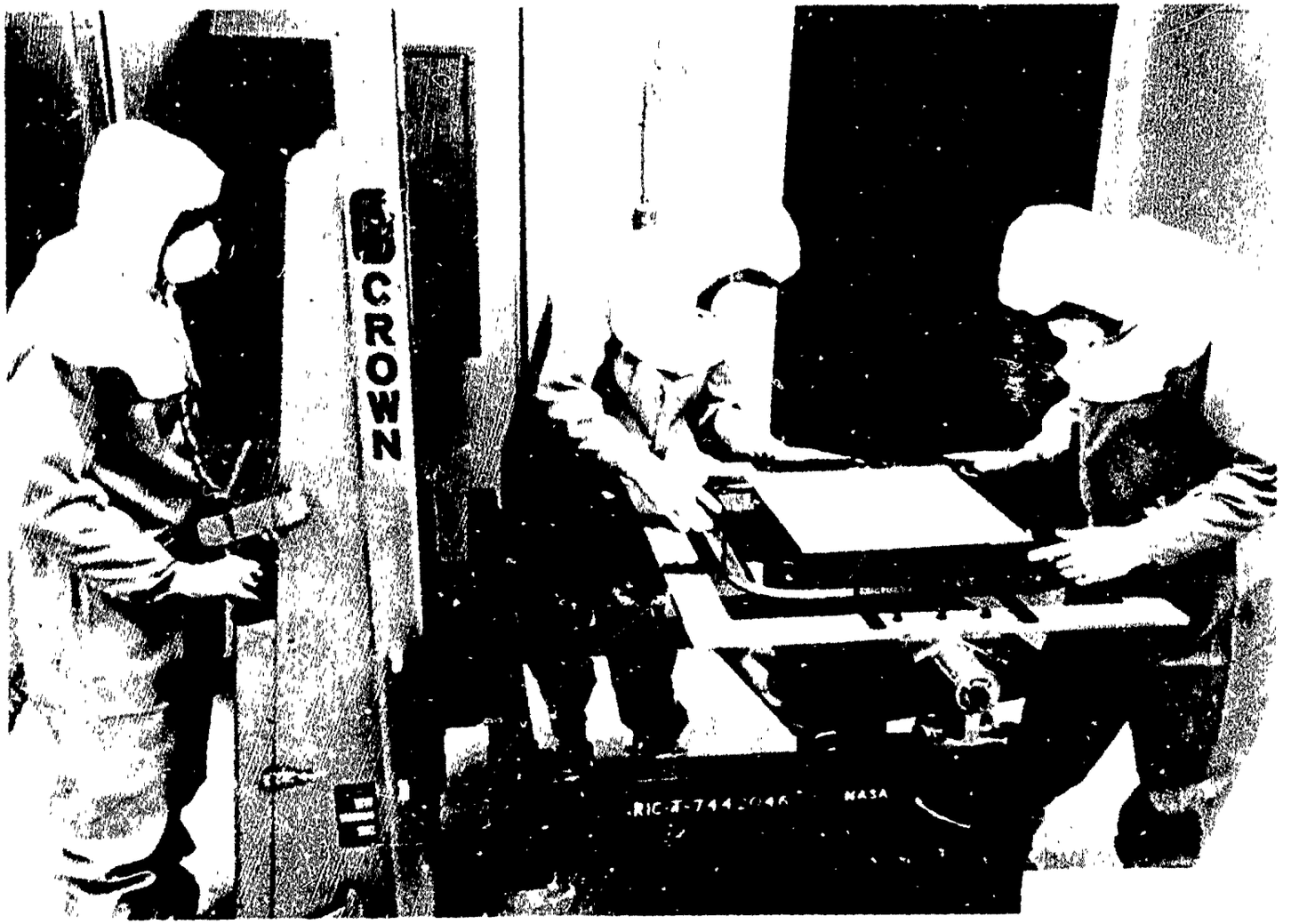


Figure 26. Assembly Operation

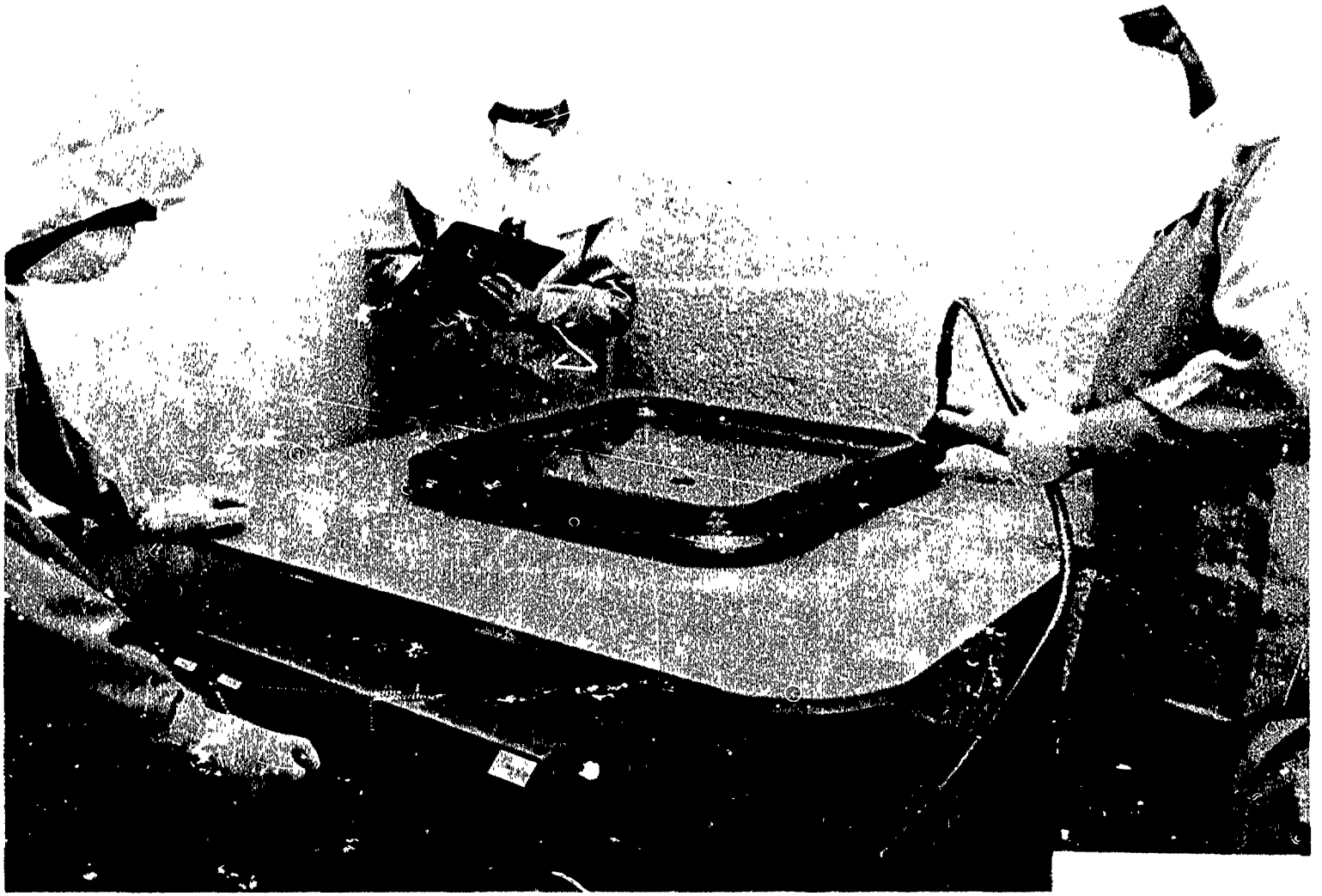


Figure 28. Leak Test

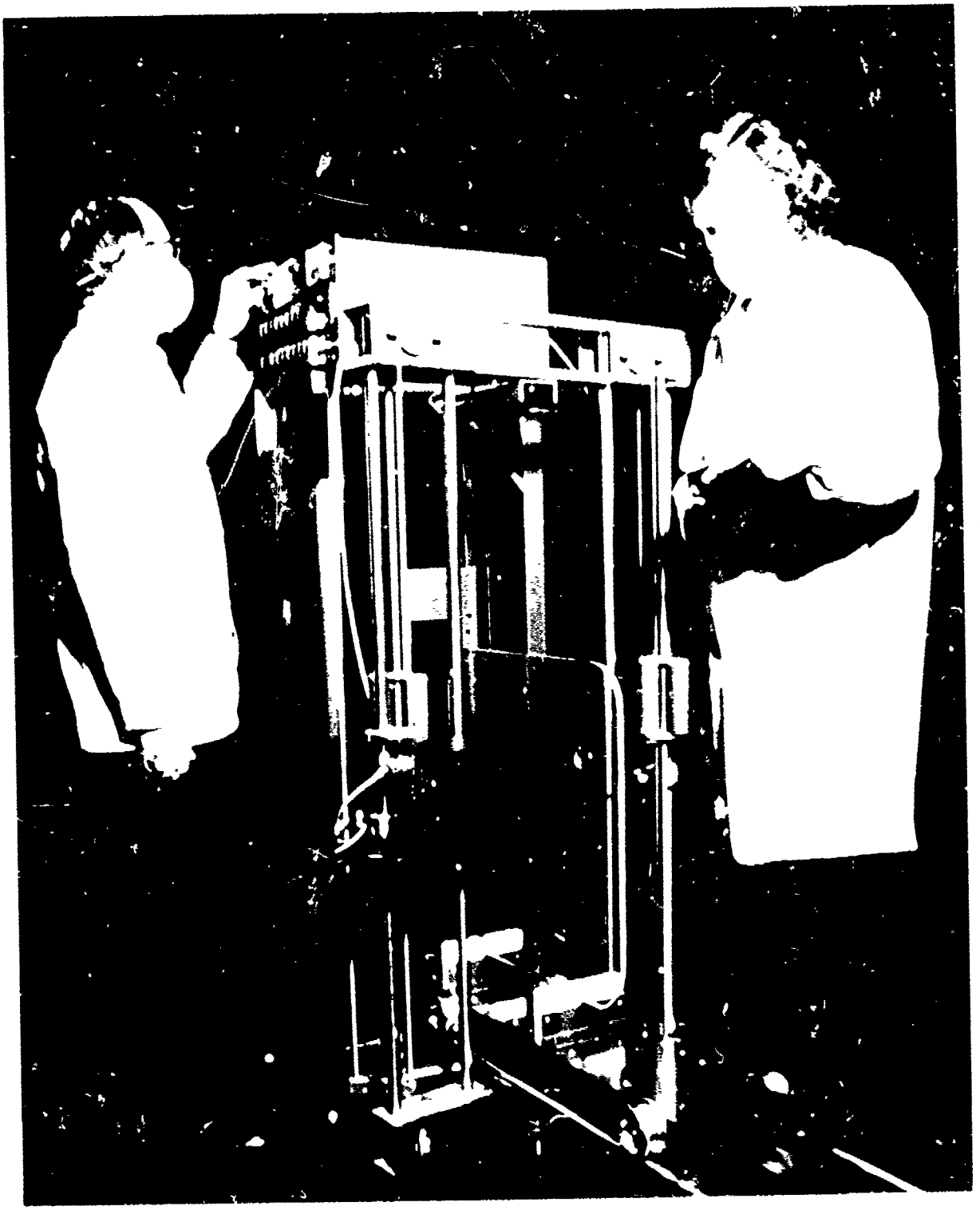


Figure 29. Spectrophotometer

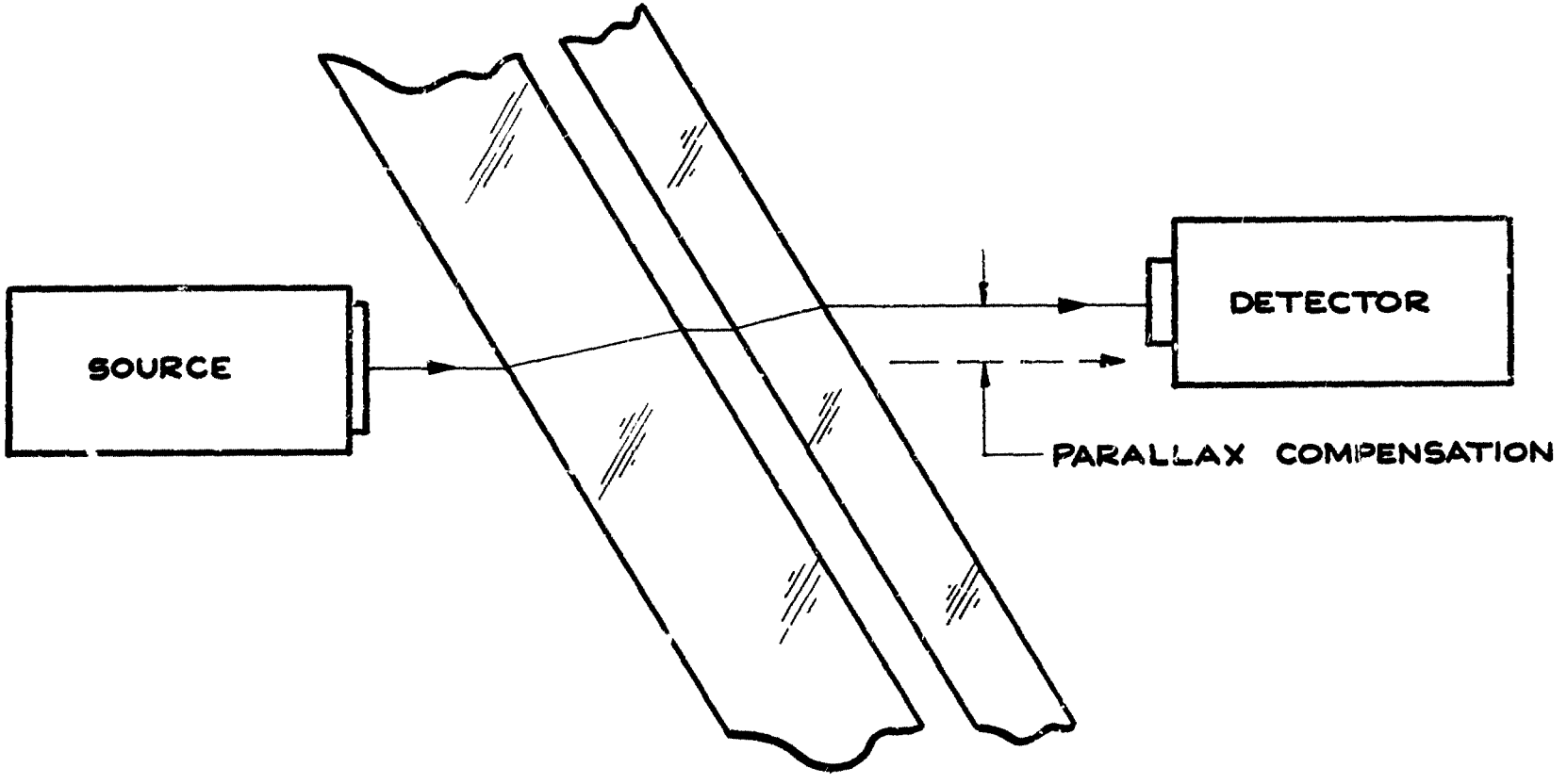


Figure 30. Parallax Compensation

SESSION 6

MATERIALS AND PROCESSES (PART II)

AN ELASTOMERIC, THERMOPLASTIC, POLYCARBONATE-COMPATIBLE AIRCRAFT INTERLAYER USEFUL FROM -65 TO 350°F

G. L. Ball III, D. W. Werkmeister, and I. O. Salyer
Monsanto Research Corporation
Dayton Laboratory
Dayton, Ohio

PRECEDING PAGE BLANK-NOT FILMED

AN ELASTOMERIC, THERMOPLASTIC, POLYCARBONATE-COMPATIBLE AIRCRAFT INTERLAYER USEFUL FROM -65 TO 350°F

AUTHORS

George L. Ball III, Dennis W. Werkmeister and I. O. Salyer

MONSANTO RESEARCH CORPORATION
DAYTON LABORATORY
Dayton, Ohio 45407

ABSTRACT

An ethylene terpolymer that is thermally stable to 550°F and compatible with glass, polycarbonate, and other transparent plastics, was shown earlier to be useful as an aircraft glazing interlayer from -65°F to +165°F. Recent Air Force-funded research provided the basis for extending its useful upper temperature to +350°F. This improvement, reflected primarily in improved form stability, was achieved while retaining its otherwise excellent aircraft glazing interlayer physical characteristics and thermoplastic laminating processability. The added form stability was introduced through limited crosslinking accomplished in a manufacturing process discrete from laminating. Three alternative crosslinking systems, two chemical and one electron bombardment, were provided.

INTRODUCTION

Aircraft windscreen temperatures of up to 350°F are anticipated for high performance military aircraft. These windscreens must resist bird impacts, which makes it desirable to use bonded plies of glass and polycarbonate (or other plastics). Effective utilization of these materials requires an interlayer that is compatible with both the glass and polycarbonate and that will be elastomeric over a wide temperature range to accommodate a variety of thermal expansion conditions. It is also desirable, from a windscreen fabricator's point of view, that the material be capable of being processed by thermoplastic laminating techniques.

A family of ethylene terpolymer adhesives (ETA) exist that have been defined as aircraft interlayers useful in the temperature range from -65 to +165°F (Ref. 1,2,3,4). These ethylene terpolymers lack any measurable strength above 125°F but have inherent thermal stability well into the range of 550°F. Mechanical performance could be improved above 120°F simply

by limited crosslinking, without affecting the desired thermoprocessing character. This thermal form stability enhancement was demonstrated earlier (Ref. 1) where the useful temperature was raised to +165°F by controlled crosslinking.

The objective of an ongoing effort (Ref. 5) is to incorporate useful mechanical performance into the ethylene terpolymer at temperatures up to +350°F without impairing its otherwise excellent aircraft glazing interlayer characteristics. This was to be done, if possible, while retaining thermoplastic processability.

Enhancement of these elevated temperature mechanical properties was to be approached through (a) crosslinking, (b) grafting, or (c) polyblending of the basic ethylene terpolymer. Controlled crosslinking, using fractional stoichiometric quantities of crosslinking agents, was expected to provide the most practical approach.

The nature of the product developed was to be illustrated through detailed mechanical characterization from -65 to +350°F, the preparation and characterization of laminates, and a demonstration of applicable processes for laminating.

SUMMARY

An ethylene terpolymer aircraft glazing interlayer, designated ETAXXX032, was developed that has reasonable strength to 350°F while retaining excellent high elongation down to -65°F. This high temperature performance was achieved while retaining the low temperature thermoplastic laminating formability at 250°F required for polycarbonate. This improved mechanical performance to 350°F introduced no changes in the basic (550°F) thermal stability of the ethylene terpolymer. Its properties are summarized in Table 1 and Figure 1.

The most significant improvement in properties occurred between +165°F and 350°F, where no measurable performance had existed before. Tensile and tear strengths were increased slightly between -65°F and +165°F, while both tensile impact and tensile elongation were decreased slightly between -65°F and room temperature. Ultimate elongations, however, of up to 220% were retained at -65°F.

Laminates of glass/polycarbonate were shown to survive repeated thermal cycling between -65°F and 300°F. Failures occurred only in the polycarbonate, which softened at this higher temperature. Glass/glass laminates containing the ETAXXX032 survived this thermal cycling and also thermal soaking at 350°F.

Table 1.

ENGINEERING DATA
ON ETHYLENE TERPOLYMER ADHESIVE XXX032

Property	Value
Temperature at Modulus of	
45,000 psi, °F	-27
675 psi, °F	+17
Stiffiex Range, °F	44
Resistance to heat, °F	450
Zero Tensile Strength, °F	380
Zero Tensile Elongation, %	100
Liminate Utility Temperature Range	
Glass-Glass, °F	-65 to + 350
Glass-Polycarbonate, °F	-65 to + 270
Polycarbonate-Polycarbonate, °F	-65 to + 270
Tensile (Room Temperature)	
Strength, psi	4300
Elongation, %	1400
Impact (Tensile) Strength, ft lb/in.^{2}	580
Tear Strength, lb/in. thickness	350
Color (Laminate)	
Transmission at 550 m_μ, %	90
Haze (Adhesive)	
at 550 m_μ, % 0.02 in. thickness	1.0
0.032 in. thickness	1.7
Laminating Conditions	
Temperature, °F	250
Pressure, psi	30

1719

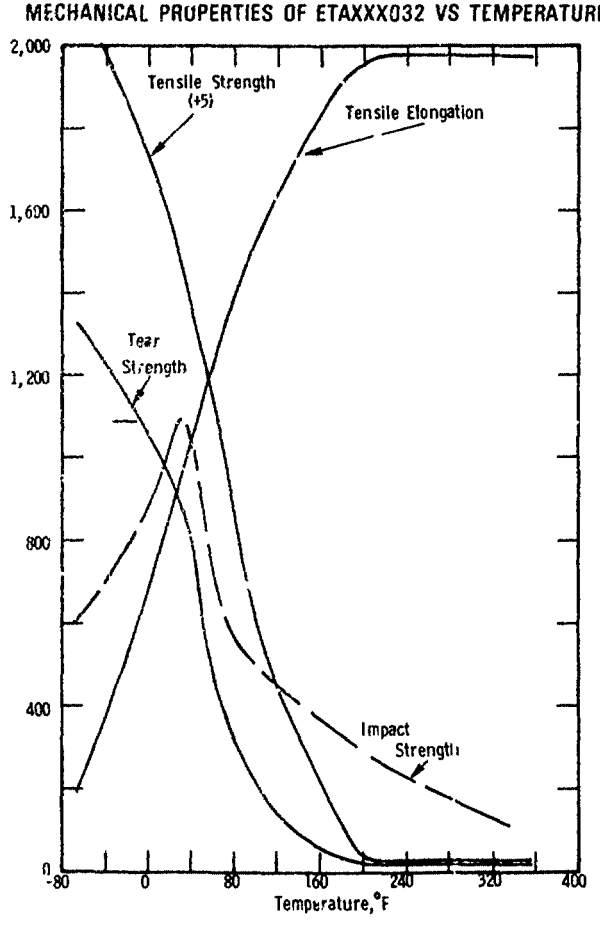


Figure 1. Summarized Mechanical Properties of ETAXXX032 Versus Temperature (Tensile Strength, psi; Elongation, %, Impact Strength, ft-lb/in.^{2} and Tear Strength, lb/in. thickness).

The improved thermal form stability to 350°F was achieved through a "controlled limited crosslinking" of the basic ethylene terpolymer system (containing 3.2% hydroxyl). It was shown that this improved form stability could be provided by any one of three crosslinking systems. This crosslinking could be conducted during or after formation of the ethylene terpolymer in sheet form. The crosslinking would be taken to completion, therefore the interlayer sheet would be completely stable with time.

DISCUSSION

Thermal Characteristics

For any material to function mechanically up to 350°F, it must exhibit thermal stability up to and beyond that temperature. The thermal stability of the ethylene terpolymer adhesive (ETA) is illustrated in Figure 2 by thermogravimetric analysis (TGA) curves up to 1000°F. These curves show that no appreciable weight loss occurs at temperatures below 550°F.

The thermogravimetric analysis was conducted in an inert atmosphere (helium). This atmosphere was necessary to prevent oxidation at the higher temperatures. Interlayers usually are contained between plies of other material that exclude air. These data are thus valid for this type of configuration. A similar TGA curve would be expected if air were present, but generation of color (due to oxidation) would be expected in the region of 300°F.

The mechanical performance over a similar temperature range is well illustrated in graphs of creep as a function of temperature. The temperature at which failure occurs under a 3 psi test load is referred to as the zero tensile strength (ZTS) temperature. Figure 3 shows the ZTS temperatures of the unmodified ETA (119°F) and of a modified ETA (ETA 138200) developed earlier (178°F; Ref. 1,4). The ETA 138200 was reported to be useful as an interlayer up to 165°F and processable for laminating at 250°F. This adequate mechanical performance as an interlayer and processability would be anticipated from the illustrated ZTS characteristics.

The two additional curves in Figure 3 illustrate the performance of the newly developed material referred to as ETAXXX032 (two variations) to 350°F. These curves show that these materials would have some, albeit minimal, useful mechanical properties at 350°F. However, it is not entirely obvious that this material is processable at 250°F, as will be discussed later. These data illustrate a point that must be considered to resolve what may seem to be a contradiction in properties versus processability. Although the ETAXXX032 has a limited degree of thermoplasticity

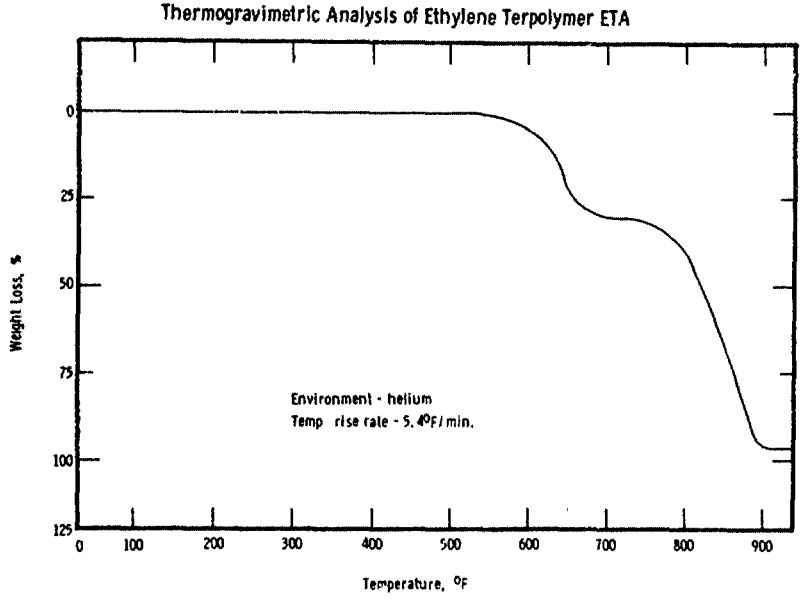


Figure 2. Thermogravimetric Analysis of All Ethylene Terpolymers in Inert Atmosphere

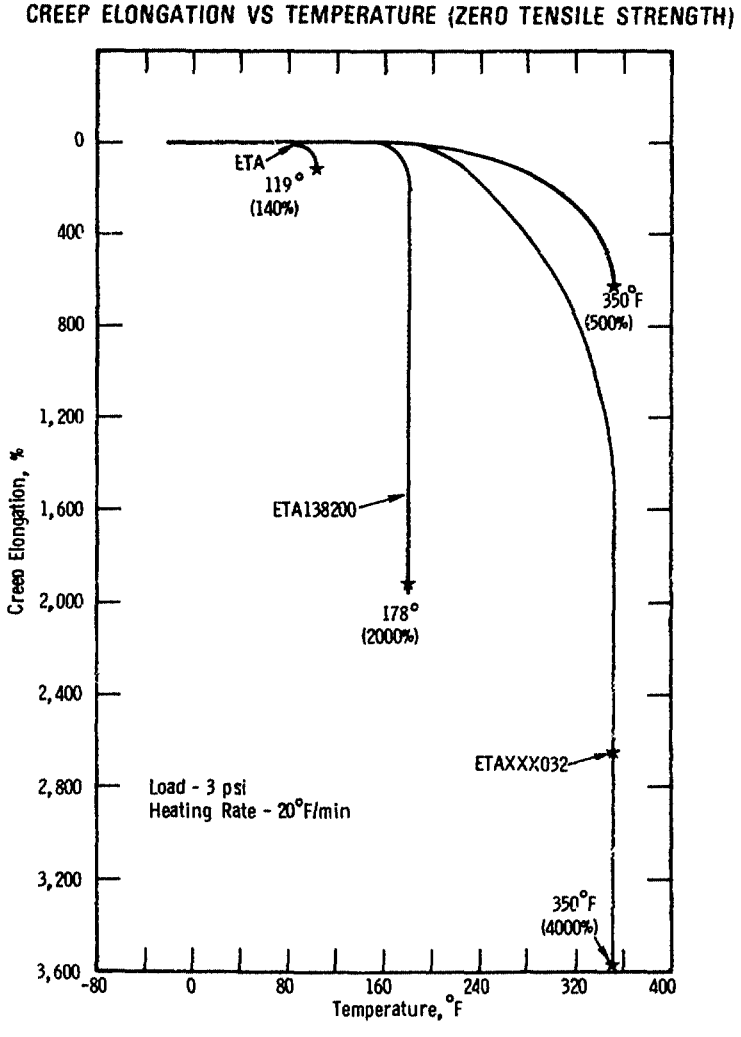


Figure 3. Creep Elongation Versus Temperature for Various Ethylene Terpolymer Compositions

at 250°F, which provides sufficient flow for laminating of plies, it is not a thermoplastic in the usual forming sense, nor does it contain thermally reversible chemical bonds such as those available in some urethanes.

One last mention of the creep elongation data must be made to answer the question, "Why not just increase the zero tensile strength temperature to well above 350°F and thus be assured of good mechanical performance in that temperature range?" The answer is that either processing temperatures much greater than 250°F or higher pressures would be required. The system would then not be compatible with polycarbonate, the material with which it was intended to be used. This does not discount the future possibility that zero tensile strength temperatures could be further increased and higher performance materials be made available for use with plastics capable of processing at higher temperatures.

Physical Characteristics

The physical performance of the high temperature ethylene terpolymer adhesive (ETAXXX032) is best illustrated by tensile strength, tensile elongation, tensile impact, and tear strength data. These physical characteristics as a function of temperature from -65°F up to +350°F are summarized graphically in Figure 1. The same data are also shown in Tables 2 through 5 and Figures 4 through 7, where comparison is made to the earlier developed ETA 138200 adhesives, that had been determined to be usable to 165°F. Data on a more familiar thermoplastic material, PVB-3GH (Ref. 1), are also included for reference. PVB-3GH, not being crosslinked, would not be expected to perform at the higher temperatures.

The physical characteristics of the ETAXXX032 illustrated in Tables 2 through 5 and Figures 4 through 7 merit discussion, especially compared with the characteristics of ETA 138200. Any differences between these two reflect improvements or degradation in properties, accountable to the high temperature modification. During the development of a higher temperature material, degrading effects were to be minimized. Beneficial effects other than improvement in the mechanical properties above 165°F were considered an added bonus.

In all cases (tensile, impact and tear) increases in mechanical performance above 165°F were achieved. The magnitude of these properties, while low, were deemed adequate for an aircraft windscreen interlayer application. This is because the primary function of the interlayer is to bond the actual load-bearing materials, glass and polycarbonate (or other plastic) together and transmit loads to them.

Table 2

TENSILE STRENGTH OF ETHYLENE TERPOLYMERS AS A FUNCTION OF TEMPERATURE

	STRENGTH, psi						
Temperature, °F	-65	-40	+32	+74	+165	+200	+350
ETA138200	8,200	8,800	6,000	3,600	20	0	0
ETAXXX032	10,500	10,000	7,000	4,300	-	24	2
PVB-3GH	8,900	7,400	5,600	4,300	195	-	-
ETANOX078	12,000	8,700	9,000	8,000	-	0	0

Table 3

TENSILE ELONGATION OF ETHYLENE TERPOLYMERS AS A FUNCTION OF TEMPERATURE

	ELONGATION, %						
Temperature, °F	-65	-40	+32	+74	+165	+200	+350
ETA138200	460	570	1,400	1,200	600	0	0
ETAXXX032	220	360	900	1,400	-	>2,000	>2,000
PVB-3GH	10	210	420	320	1,100	-	-
ETANOX078	300	270	780	1,100	-	0	0

Table 4

TENSILE IMPACT STRENGTH OF ETHYLENE TERPOLYMERS AS A FUNCTION OF TEMPERATURE

	IMPACT STRENGTH, ft lb/in.^{2}						
Temperature, °F	-65	-40	+32	+74	+165	+200	+350
ETA138200	360	890	1,100	1,100	135	0	0
ETAXXX032	600	670	1,100	580	-	300	120
PVB-3GH	100	220	1,510	1,290	410	-	-
ETANOX078	600	520	1,480	1,500	-	0	0

Table 5

TEAR STRENGTH OF ETHYLENE TERPOLYMERS AS A FUNCTION OF TEMPERATURE

	TEAR STRENGTH, lb/in.						
Temperature, °F	-65	-40	+32	+74	+165	+200	+350
ETA138200	1,100	1,000	410	180	5	0	0
ETAXXX032	1,300	1,150	780	350	-	10	3
PVB-3GH	1,800	1,300	790	340	23	-	-
ETANOX078	1,520	1,450	800	260	-	0	0

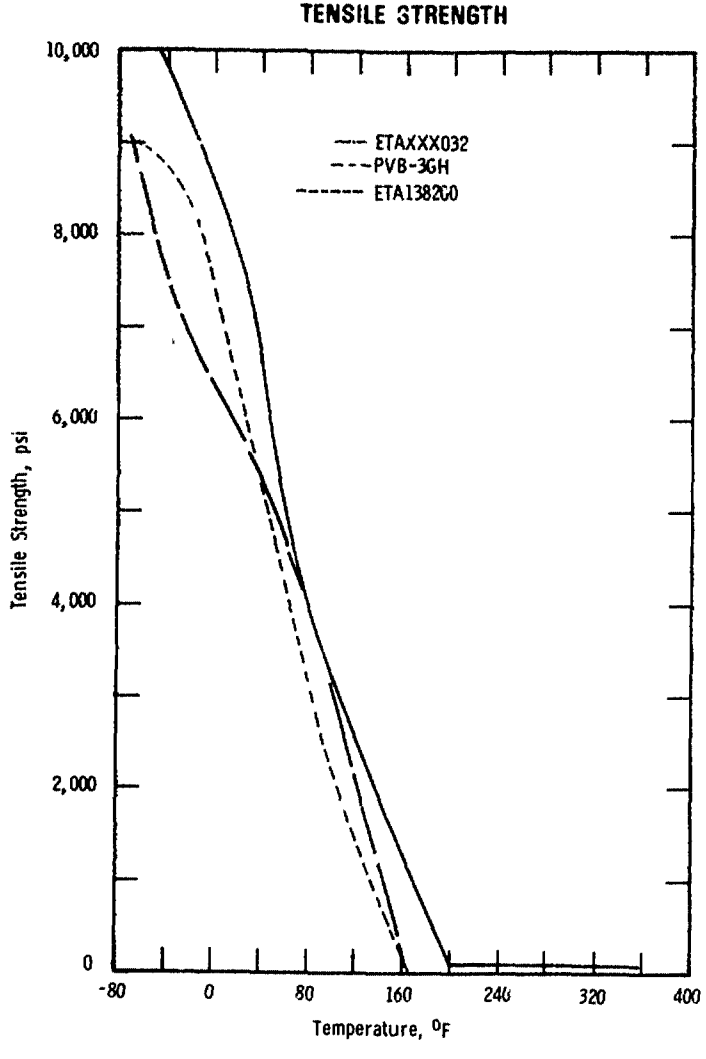


Figure 4. Tensile Strength of the Ethylene Terpolymers and PVB-3CH from -65 to +350°F

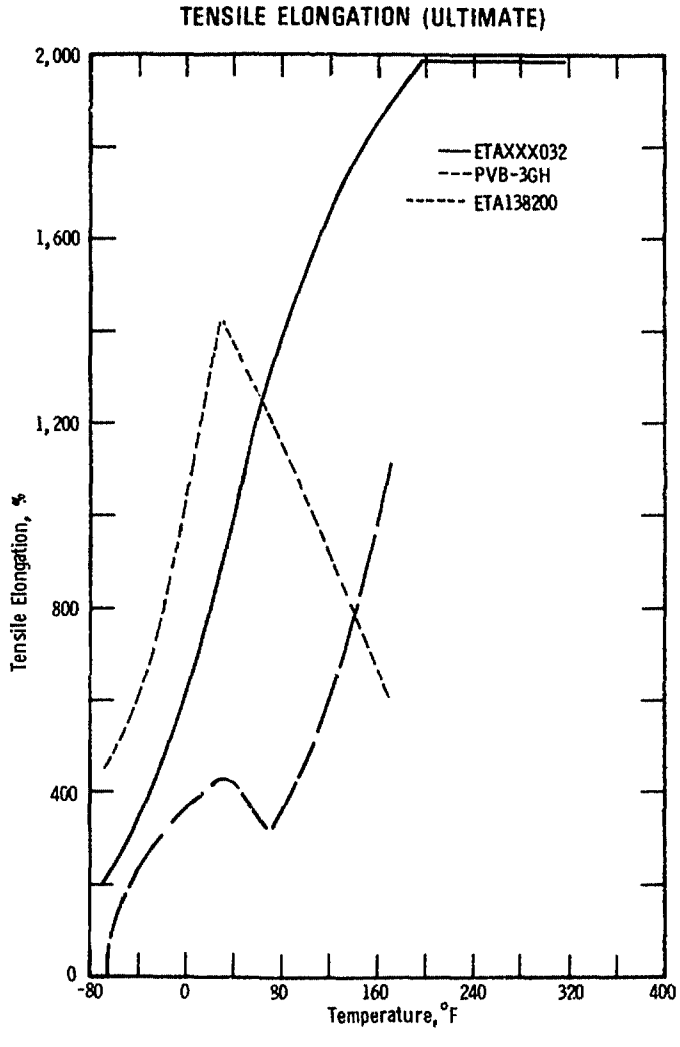


Figure 5. Ultimate Tensile Elongation of the Ethylene Terpolymers and PVB-3GH from -65 to +350°F

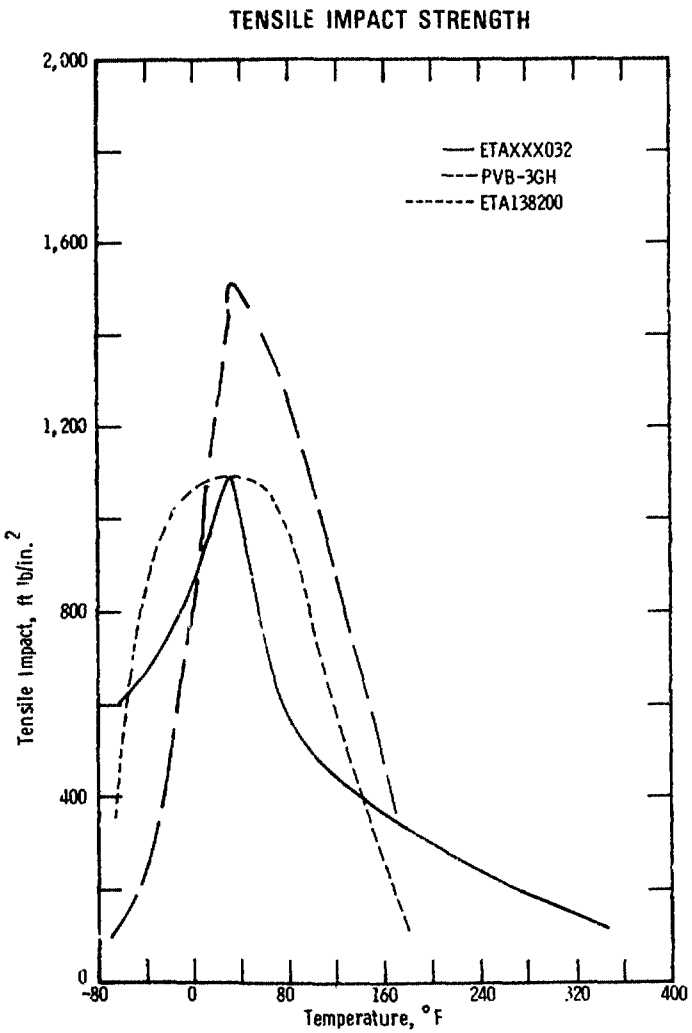


Figure 6. Tensile Impact Strength of the Ethylene Terpolymers and PVB-3GH from -65 to +350°F

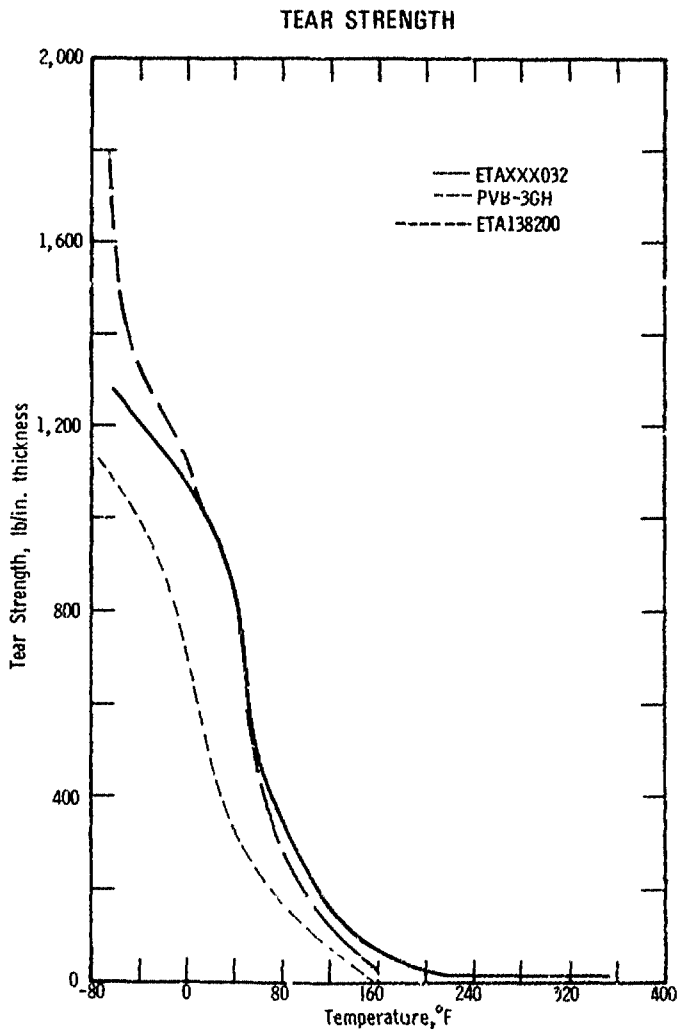


Figure 7. Tear Strength of the Ethylene Terpolymers and PVB-3GH from -65 to +350°F

The biggest difference in properties between the two materials occurred between room temperature and -65°F. Increases in tensile and tear strength, illustrated in Figures 4 and 7, were achieved. Over the same temperature range, decreases in tensile elongation and tensile impact were exhibited. While some decreases in tensile elongation were anticipated due to the modification, the low temperature elongations were still quite substantial, being as high as 220% at -65°F. In both materials, the elongation at yield was about 10% of the ultimate elongation.

The physical integrity and functioning of the ETAXXX032 was further illustrated through the thermal cycling of glass/polycarbonate, glass/glass, and polycarbonate/acrylic laminates containing the ETAXXX032. 5 inch x 5 inch three ply laminates were prepared using 1/4-inch plies of glass, polycarbonate, or acrylic and 0.030 inch of interlayer. These laminates were repeatedly thermal cycled between -65 and +165°F with occasional excursions to 350°F (for glass/glass), or 300°F (for laminates containing polycarbonate).

Repeated thermal cycling of the ETA bonded laminates resulted in no visible failures of any sort to the ethylene terpolymer adhesive, or to its bond with any of the laminate plies. The only degradation of properties noted was due to softening of the polycarbonate during excursions to 300°F.

The shear strength of the ethylene terpolymer adhesive at 350°F was demonstrated by heating the 5 in. x 5 in. laminates to 350°F with one of the plies clamped in a vertical position. A shear force consisting of the weight of the other 1/4 inch thick glass ply (0.02 psi) was then exerted on the adhesive. Upon heating, a slight deflection of the free plies of glass was noted and could be related to the expected change in modulus. No further creep following 48 hour exposure to this temperature was found. Similar experiments were conducted with a glass/polycarbonate laminate to temperatures of 300°F. In this case, the clamp caused compression and bending of the polycarbonate ply, but still no sliding or separation of the glass ply resulted.

Included in the tables are data on an ethylene terpolymer referred to as ETANOX078 from -65°F up to room temperature. This information is shown for completeness in describing the ethylene terpolymers that have been made in pilot quantities for the U.S. Air Force and U.S. Army and that thus may become available to aircraft windscreen manufacturers operating under a government contract. This is the case for both the ETA 138200, discussed above, and the material designated ETANOX078 recently produced for the Air Force (Ref. 6). The ETANOX078 aircraft interlayer was selected to be used in an acrylic/polycarbonate windscreen at temperatures between -40 and +180°F.

The ETANOX078 represents a change in the basic ethylene terpolymer system rather than a modification of existing terpolymer. The exact nature of the change can not be discussed. It demonstrates that the ethylene terpolymer can be tailored to provide a variety of improved performance especially with respect to tensile strength, tensile impact, and tear at lower temperatures. Low temperature elongation is sacrified. The tensile elongation data shown in Table 3 for the ETANOX078 are slightly misleading since this elongation is ultimate, rather than elastic. At -65°F the elastic portion of the elongation would be no more than 10% of ultimate (30% elongation). Accordingly, this material is not recommended for use in glass/polycarbonate laminates or those with plies of widely differing thermal expansion coefficients. The ETANOX078 would be amenable to the modifications which produced improved high temperature properties in the ETAXXX032.

Processing

The ETAXXX032 is a thermoplastic sheet that can be plied up with plates of most any material and bonded together with moderate temperature and low pressure. It has been specifically tailored to be usable with polycarbonate, where laminating temperatures of less than 250°F are desirable.

The fabrication cycle used in our laboratory for the preparation of laminates is shown in Figure 8. Whereas this cycle is known to work, it is expected that much shorter times can be used if heat transfer were better than that provided in the air-type autoclave used.

The laminating cycle consists simply of heating the entire composite to 250°F, applying a pressure of 30 psi (ΔP = 45 psi) and cooling the part down. This low pressure cycle should be especially attractive for minimizing residual strains. This laminating cycle is also almost identical to that previously described for the ETA 138200 material (Ref. 1) except that the pressure has been doubled.

Materials that can take temperatures greater than 250°F can be laminated at higher temperatures. This is recommended for glass/glass laminates. Laminating temperatures greater than 300°F, however, are of little increased value.

The laminating cycle shown in Figure 8 illustrates the application of a vacuum to a bagged laminate during processing. This is desirable to minimize the possibility of any entrapped vapors. It is probably not necessary, if routine aircraft windscreen pre-drying procedures are used.

LAMINATING CYCLE FOR ETA

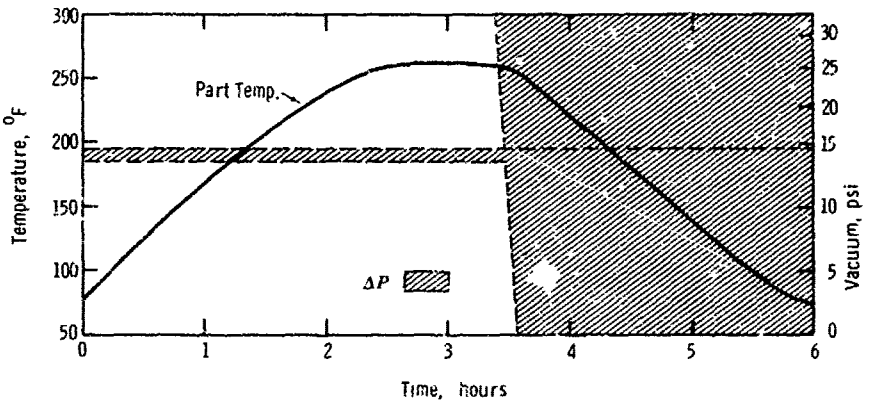


Figure 8. Typical Laminating Cycle for the Ethylene Terpolymer, ETAXXX032

Table 6

EFFECT OF CROSSLINKING ON IMPACT STENGTH

	Impact Strength, ft. lb / in.^{2}					
Temperature, °F	-65	-40	+32	+74	+200	+350
Crosslinker						
none -	660	850	1,150	530	0	0
Chemical 1	380	600	1,100	610	180	90
Chemical 2	960	850	1,390	650	310	140

The High Temperature Modification

The nature of the high temperature modification was illustrated in Figure 2, Creep Elongation Vs. Temperature, with respect to the physical result achieved. Chemically what is being done is limited crosslinking and/or chain extension. The crosslinking is introduced either by addition of chemical crosslinking agents and thermal initiation, or through generation of free radicals by electron bombardment. Since only fractional stoichiometric amounts of crosslinker were used, the products retained some thermoplasticity rather than becoming intractable. The ethylene terpolymer adhesive has pendant hydroxyl groups. It can be crosslinked either through these groups or through other segments in its structure.

Development of the ethylene terpolymer to achieve the high temperature properties involved (a) defining crosslinking agents that would be effective in partial stoichiometric amounts, and (b) defining a suitable process to achieve the desired improvement in mechanical properties at elevated temperatures without causing intractability. Two crosslinking agent were found to be useful

Crosslinking (limited) of the ETA with either of the two agents was achieved by (a) compounding the ingredients together on a cold mill roll, (b) compression molding and curing under pressure, followed by (c) post-curing.

Some minor difference in the physical characteristics between the two systems resulted. These are reflected in Figure 3 and Table 6. The two creep elongation curves that reach 350°F resulted from these chemical additives. The lower elongation (500%) result is for one; the higher (4000%) is for the second type cured product.

The tensile strength, tensile elongation, and tear strength were indistinguishable for the two compositions. However, the one (the Chem II-) cured system appeared best with respect to impact strength, as shown in Table 6.

Exploration of Electron beam crosslinking has been completed. Conditions are being determined. This technique is highly attractive, since no addition of material to the ETA is required.

REFERENCES

1. G. L. Ball III et al., "Engineering Data on Ethylene Terpolymer as an Adhesive for Polycarbonate Composite Aircraft Transparencies," Technical Report AFML-TR-72-109, July 1972.

2. G. L. Ball III et al., "A Thermoplastic Transparent Adhesive for Bonding Polycarbonate to Glass," Report No. AMMRC CR71-10, July 1971.

3. G. L. Ball III et al., "Development of a Transparent Adhesive Compatible with Polycarbonate for Use in Ballistic Shields," Technical Report AFML-TR-70-144, June 1970.

4. First Conference on Aerospace Transparent Materials and Enclosures, Las Vegas, Spring 1974.

5. Air Force Contract F33615-75-C-5090, "Heat Resistant Transparent Interlayers".

6. Air Force Contract F33615-75-C-0078, "Ethylene Terpolymer Interlayer Material".

HEAT RESISTANT SHEET INTERLAYER

J. E. Mahaffey
PPG Industries, Inc.
Harmarville, Pennsylvania

HEAT RESISTANT SHEET INTERLAYER

J. E. Mahaffey
PPG INDUSTRIES, INC.

Abstract

A need has existed for an improved film type interlayer to satisfy the increased functional requirements for the transparent enclosures of high performance aircraft. Approximately three years ago, PPG Industries completed the basic research for a heat resistant proprietary sheet elastomer identified as 112 interlayer. The material is characterized by excellent physical properties over a wide temperature range, flexibility at low temperature, good adhesion to glass and transparent plastic substrates, and excellent processing characteristics.

Comprehensive testing and evaluation of this interlayer has been performed by PPG Industries over the past three years including development programs for full scale prototype and production windshields. The results of these programs have been very encouraging and the interlayer is currently being used on several types of aircraft transparent enclosures for both military and commercial aircraft. The purpose of this paper is to present pertinent data generated on 112 interlayer in these programs and to review the performance of this material in actual service to date.

The mechanical and physical property data presented includes tensile stress-strain characteristics as a function of temperature, shear strength, adhesion to glass, coated glass, and plastic substrates, optical qualtiy, and physical properties. The resistance of 112 interlayer to the various environments associated with aircraft transparencies is also presented which includes humidity, ultraviolet light, thermal stability, temperature cycling, and cold chip resistance. The interlayer is currently used in the transparencies of approximately 15 different types of aircraft ranging from the F-111 improved windshield and canopy to the DC-10 and 747 wide bodied jets. These applications consist of one ply of 112 interlayer in combination with PVB interlayer and all 112 interlayer composites. The performance of 112 interlayer in these applications, which in some cases involve several thousand flight hours, is reviewed.

INTRODUCTION

Polyvinyl butyral has been used successfully as an interlayer in laminated aircraft transparencies for many years and is still used in a large number of aircraft glazing applications. While PVB has a remarkable performance record, certain properties of this material have limited the service life of many aircraft windshields. The relatively severe environments associated with the high performance aircraft of today have actually precluded the use of PVB in many applications.

PPG Industries has recognized the need for an improved interlayer for aircraft transparent enclosures and has been engaged in a continuing research and development program in this area. Several years ago, the basic research was completed on a new film type organic polymer designated 112. This interlayer is characterized by excellent physical properties over a wide temperature range, flexibility at low temperature, excellent adhesion to glass and transparent plastic substrates, and ideal processing characteristics.

Comprehensive testing and evaluation of this interlayer has been conducted by the Aircraft and Specialty Products Division for the past three years including development programs for utilizing this material in aircraft transparencies. The results of this development effort have been very encouraging and the interlayer is currently being used successfully on several types of production and prototype windshields. Mechanical and physical properties have been provided to prime contractors and governmental agencies who are using or contemplating the use of 112 in aircraft transparencies. The purpose of this paper is to present all pertinent data generated on this interlayer during the last three years and review performance of the material in aircraft transparency applications up to the present time.

MATERIAL PROPERTIES

Mechanical and physical property data are important to the design engineer in designing aircraft transparencies and to determine if an interlayer will perform satisfactorily in a specific application. The properties of 112 interlayer presented in this paper are those properties most frequently requested by the design, stress, or materials engineers. Polyvinyl butyral data are presented in some cases for comparison purposes to illustrate the primary differences between these two materials.

Tensile Stress-Strain

Tensile stress-strain property as a function of temperature is an important characteristic of interlayer materials. This property provides an indication of the ability of the interlayer to accommodate the relative movement between the structural plies of a laminated composite without cohesive failure. The tensile stress-strain characteristics of 112 interlayer are presented in

Figure 1 which illustrates the flexibility of the material over a wide temperature range in combination with good tensile strength. By comparison, the stress-strain curve for 3GH vinyl at 70°F is practically identical to 112 interlayer at -30°F. Figure 2 compares the elongation of 112 interlayer to 3GH vinyl. Note that the ultimate elongation of 112 interlayer at -65°F is close to 200% compared to 20% for vinyl. Elongation at elevated temperature is in excess of 550%, the limitation of the test equipment used.

Adhesion

The adhesion of an interlayer to the various transparent structural materials used in aircraft transparent enclosures is just as important as the properties of the interlayer itself. Interlayer delamination has probably been the most common mode of failure in laminated aircraft transparencies. Table I illustrates the excellent adhesion of 112 interlayer to glass, coated glass, acrylic, and polycarbonate substrates. The test procedure is the NASA 90° peel strength test using a wire screen reinforcement in the interlayer to preclude excessive interlayer elongation during the peel test. The data includes adhesion levels after humidity exposure which is considered the most adverse environment for interlayer adhesion. Note that in most cases, the failure mode was failure of the wire screen reinforcement. The NESA® and NESATRON® coatings are PPG electrically conductive coatings for electrically heated windshields.

Shear Strength

Compressive shear strength of interlayer materials laminated to various substrates is another property which is indicative of interlayer performance in aircraft transparencies. Figure 3 compares the shear strength of 112 interlayer to 3GH vinyl laminated to glass. The same order of magnitude of shear strength is obtained with coated glass and plastic substrates. These data show that shear strength of 112 interlayer at 250°F is approximately the same as vinyl interlayer at 150°F which is another indication of the improved temperature resistance of 112 interlayer.

Cold Chip Resistance

Cold chipping has been a continuing problem in glass-PVB interlayer laminated transparencies because of the brittle nature of PVB at low temperature. This problem is essentially eliminated when 112 interlayer is substituted for PVB. Cold chip resistance tests have been conducted on bilayers of both 112 interlayer and PVB interlayer laminated to one ply of glass. The test panels were subjected to cyclic low temperature exposure from 0°F to -100°F. The temperature required to produce cold chipping in the PVB laminates was 0°F compared to -90°F for 112 interlayer. Similar tests have been conducted on composites consisting of two plies of glass with the same results.

Thermal Stability

Thermal stability tests have been performed on 112 interlayer by exposing laminated test panels consisting of glass face sheets and 3/8" 112 to temperatures of 300°F for 48 hours. There was no bubbling, discoloration, or

interlayer flow after this exposure. By comparison, aircraft vinyl will develop bubbles in three to four hours at 250°F.

Optical Quality

Light transmission and haze data for 112 interlayer are presented in Table II. Light transmission loss per 0.1" thickness varies between 2.0 and 2.5% immediately after lamination. It has been determined that exposure of a laminated composite using 112 interlayer to solar radiation for several days reduces the light straw color of 112 interlayer with a corresponding increase in light transmission. These data show that the optical quality of 112 interlayer after exposure to solar radiation is comparable to vinyl.

Tests have also been conducted to determine the effect of weatherometer exposure on the mechanical properties of 112 interlayer in a laminated composite. The tensile stress-strain curves are practically identical to virgin material through 300% elongation. A reduction in stress of approximately 25% is experienced at 400% elongation. This is not considered significant, particularly in view of the fact that interlayers rarely will be subjected to this magnitude of strain.

ENVIRONMENTAL RESISTANCE

Various types of environmental conditioning tests have been performed on 112 interlayer laminated to glass and plastic substrates. Humidity is one of the worst environments for many materials and one that has been used extensively in the development and evaluation of 112 interlayer. All peel strength adhesion reported earlier employed the MIL-STD-810 humidity exposure for ten days with insignificant reduction in adhesion. This exposure has been continued up to 30 days on 112 interlayer laminated to stretched acrylic with resulting peel strengths in excess of 100 lbs per inch.

Subscale composites employing 112 interlayer have been subjected to severe temperature and humidity cycling tests. The test panels consisted of 112 interlayer and vinyl interlayer and all 112 interlayer composites with coated and uncoated glass face sheets. The test panels were subjected to the cyclic thermal shock, heat aging, and humidity exposure listed in Table III. After completion of this sequence of tests, there was no delamination, cold chipping discoloration or other evidence of degradation in 112 interlayer composites. In contrast, cold chipping and delamination were incurred in composites with vinyl interlayer adjacent to the glass.

Subscale composites of several types of cross-section designs employing 112 interlayer have been subjected to natural weathering in Florida and Pennsylvania. The cross-sections of these test panels are representative of production and prototype windshields being fabricated by PPG, including all-glass, all-plastic, and glass-plastic composites. These panels have been exposed for nine months at the present time with no evidence of delamination or composite degradation. The test panels are scheduled for a minimum of two years exposure.

Structural integrity and/or cyclic environmental qualification tests have been conducted on full-scale aircraft windshields employing 112 interlayer. These tests included simulated severe mission profile thermal tests, cyclic pressurization loading, thermal shock tests, cyclic humidity tests, and bird impact tests. Typical full-scale aircraft transparencies which have been tested are the F-111 plastic windshield and canopy, and the F-15 laminated plastic windshield. In each case, the 112 interlayer has performed extremely well and all of these windshields have met the qualification test requirements.

SERVICE PERFORMANCE

Simulated environmental and structural integrity tests on subscale and full-scale aircraft transparencies provide a reasonable indication of interlayer performance and reliability in service. The ultimate criteria, however, for determining interlayer capabilities is performance in actual service. Since 112 interlayer is relatively new, extended service performance data are not available compared to other interlayers such as vinyl. It has been in use, however, on several types of aircraft windshields for time periods in excess of one year and for flight times in excess of 3000 hours.

Figure 4 illustrates the two basic methods of utilizing 112 interlayer in aircraft windshields employed at the present time. The first is a substitution of a ply of 112 interlayer for a ply of PVB adjacent to the glass-interlayer interface in glass windshields. This approach is normally used in windshields originally designed and qualification tested with all-PVB interlayer. The use of one ply of 112 adjacent to the glass provides the advantages of the improved adhesion and cold chip resistance characteristics of 112 interlayer without complete requalification tests.

The second approach is the use of multiple sheets of 112 interlayer only in the composite. This approach is normally used in new windshield designs where initial qualification tests can be performed using the 112 interlayer and this is the design approach recommended. The single sheet of 112 in combination with PVB is also used in windshields which use relatively thick interlayers since the light transmission of 112 is slightly less than PVB.

The 112 interlayer is currently in use on approximately 15 different aircraft windshield designs including commercial, military, and general aviation aircraft. Prototype or production windshields employing 112 interlayer are currently flying on such aircraft as the DC-10, 747, DC-8, DC-9, BAC-111, F-111, S-3A and several others. Other transparencies using this material are scheduled to go into production in the near future. At the present time, there have been no reported instances of interlayer delamination, cold chipping, discoloration or other problem areas associated with the interlayer.

SUMMARY

Comprehensive evaluation of 112 interlayer performed over the past several years and service experience to date have demonstrated this interlayer satisfies the demanding functional requirements of aircraft transparencies including the high performance aircraft of today. 112 interlayer is currently being recommended for use in practically all new aircraft transparency designs contracted for and a change to 112 in existing designs where feasible.

1199

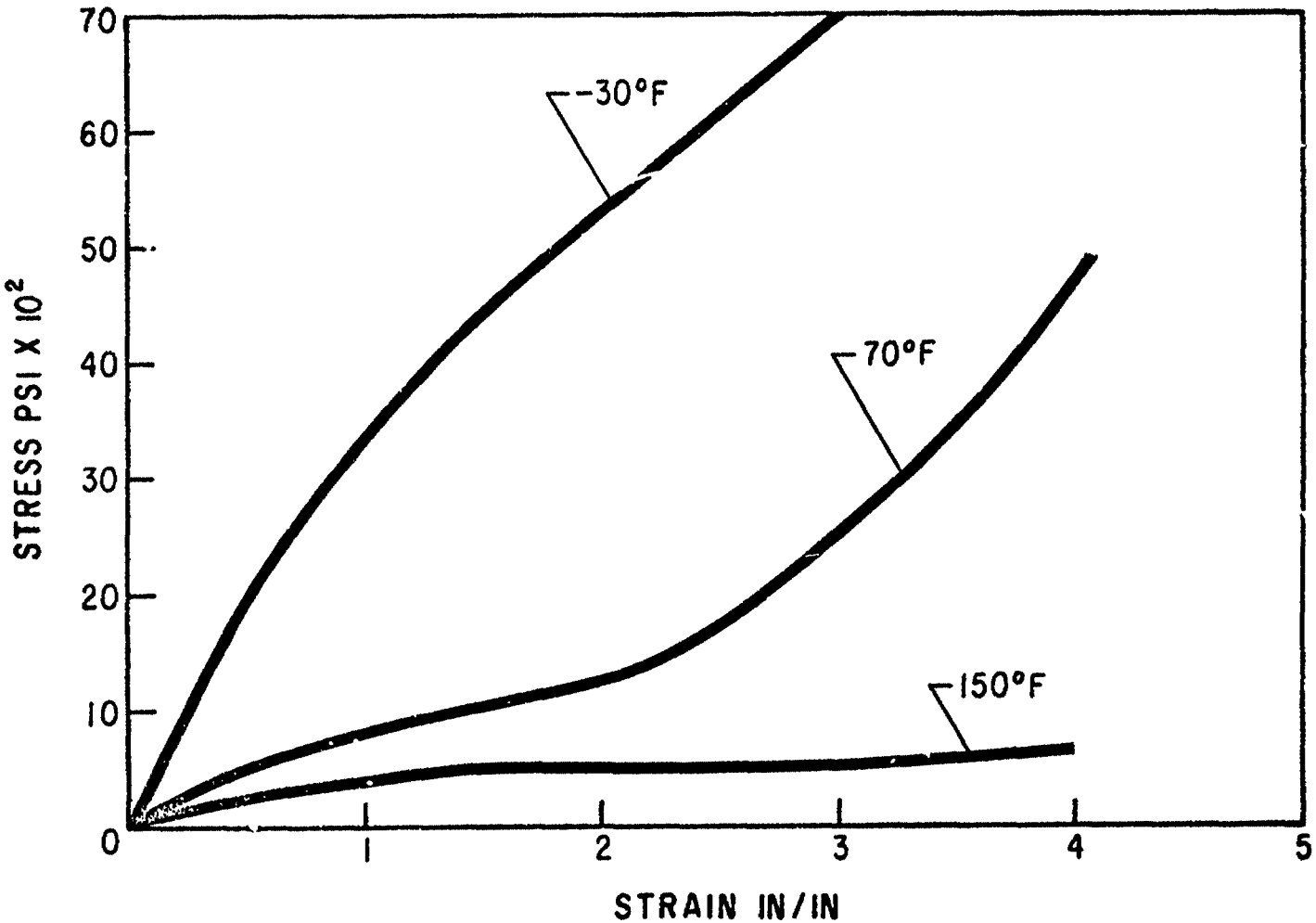


FIGURE I. TENSILE STRESS-STRAIN CHARACTERISTICS OF 112 INTERLAYER.

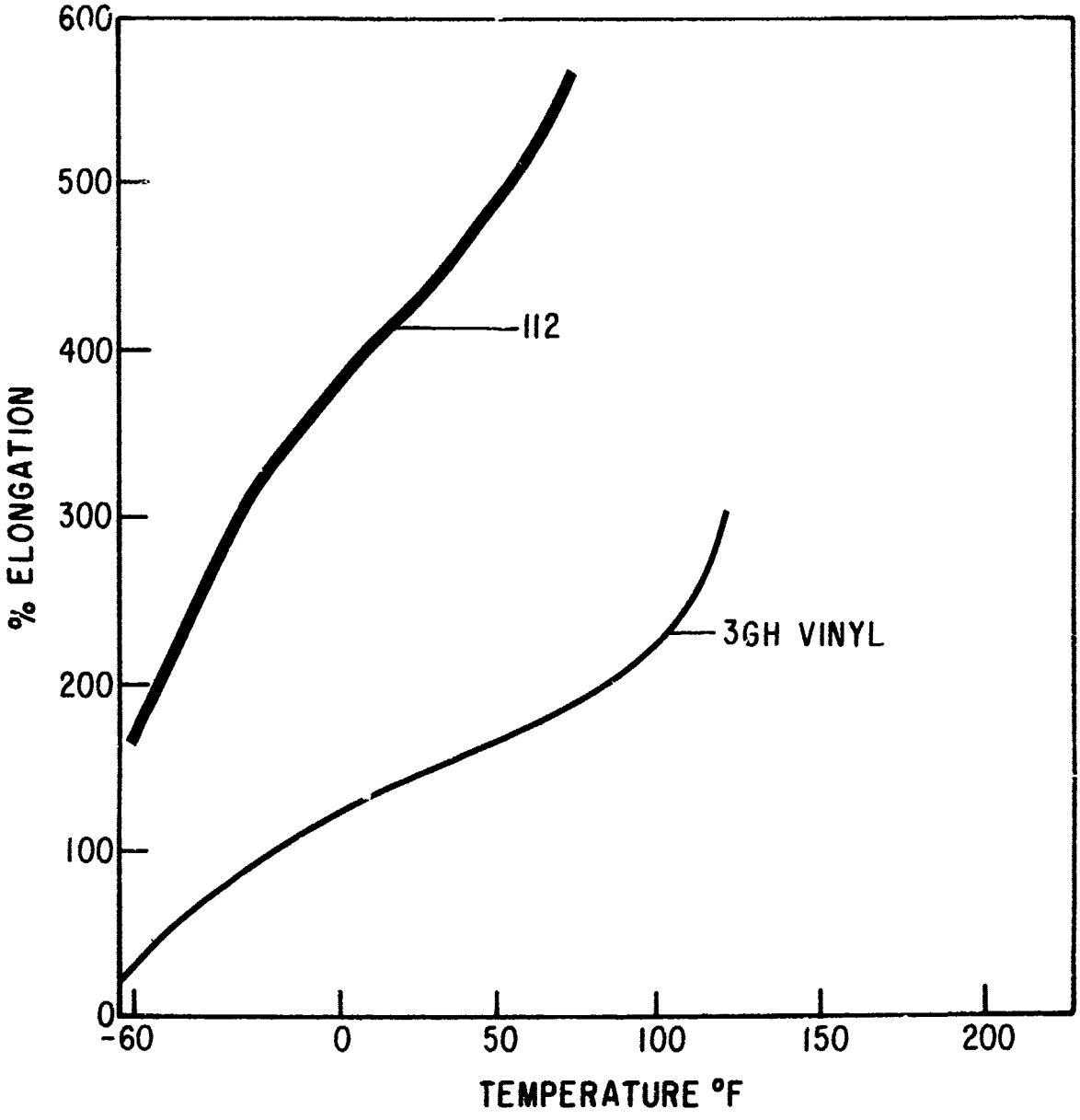


FIGURE 2. ELONGATION OF INTERLAYER MATERIALS

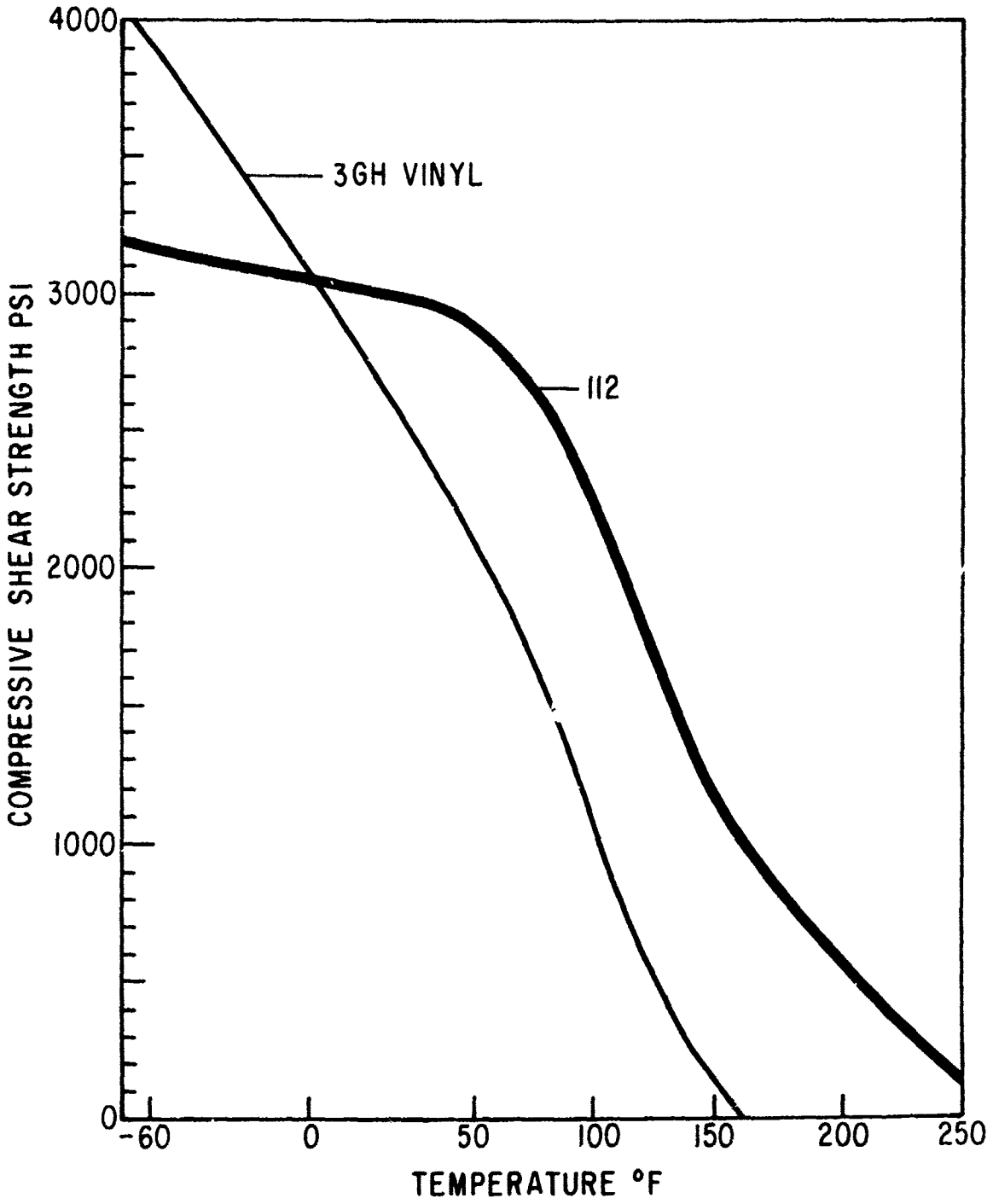
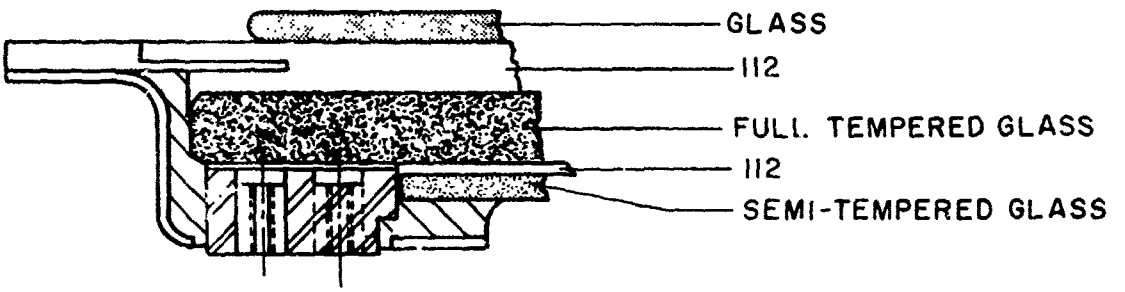


FIGURE 3. COMPRESSIVE SHEAR STRENGTH OF 3GH VINYL, AND 112 INTERLAYERS TO CHEMICALLY TEMPERED GLASS

112 INTERLAYER ONLY



112 IN CONJUNCTION WITH 3GH VINYL

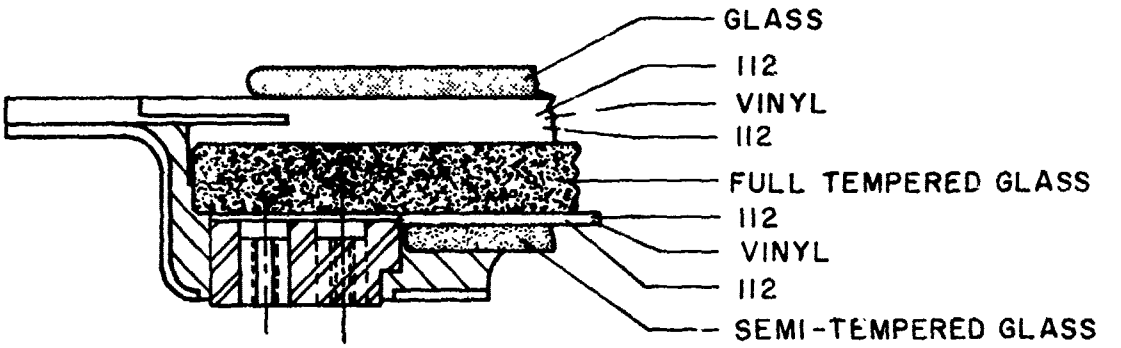


FIGURE 4. TYPICAL APPLICATIONS FOR 112 INTERLAYER

TABLE I

112 INTERLAYER ADHESION TO TRANSPARENT SUBSTRATES

	PEEL STRENGTH (LBS/INCH)	
SUBSTRATE	UNCONDITIONED	AFTER HUMIDITY*
POLYCARBONATE	> 200	> 200
CAST ACRYLIC	> 200	> 200
STRETCHED ACRYLIC	> 200	140 - 200
GLASS	> 200	> 200
GLASS - NESATRON®	> 200	115 - 200
GLASS - NESA®	> 200	100 - 200

*MIL-STD 810 CYCLIC HUMIDITY, 10 DAYS

> DENOTES WIRE MESH FAILURE

TABLE II

LIGHT TRANSMISSION AND HAZE DATA

MATERIAL IDENTIFICATION	% TRANSMISSION LOSS PER 0.1" THICKNESS	% HAZE GAIN PER 0.1" THICKNESS
112 INTERLAYER (UNEXPOSED)	2.0 TO 2.5	0.6
112 INTERLAYER (AFTER UV EXPOSURE)	1.5 TO 2.0	0.6
AIRCRAFT VINYL	1.5	0.5

TABLE III

ENVIRONMENTAL CYCLING TESTS

TEST SEQUENCE	TYPE TEST	TEST CONDITIONS	TEST DURATION
1	THERMAL SHOCK	-65°F COLD SOAK AND APPLY 7 WATTS PER SQ IN POWER	20 CYCLES
2	HEAT AGING	200°F	4 HOURS
3	THERMAL SHOCK	SAME AS 1	2 CYCLES
4	HUMIDITY EXPOSURE	120°F AND 95% R.H.	7 DAYS
5	THERMAL SHOCK	SAME AS 1	2 CYCLES
6	HUMIDITY EXPOSURE	SAME AS 4	7 DAYS
7	THERMAL SHOCK	SAME AS 1	2 CYCLES
8	HEAT AGING	200°F	100 HOURS
9	THERMAL SHOCK	SAME AS 1	2 CYCLES
10	ULTRAVIOLET	WEATHEROMETER	100 HOURS

ADVANCED ADHESIVES FOR TRANSPARENT ARMOR

R. E. Sacher and J. R. Plumer
Army Materials and Mechanics Research Center
Watertown, Massachusetts

Advanced Adhesives for Transparent Armor

By

Robert E. Sacher and John R. Plumer

Army Materials and Mechanics Research Center, Watertown, MA

Abstract

Four film interlayers were fabricated in four different cross-sectional composite configurations and evaluated for adhesion, optical, ballistic properties and thermal stability. Each interlayer was laminated into three-ply composites having face plies of acrylic (Plex-55), Chemcor glass, (Code 0401 and Code 0313) and Pyrex glass (Code 7740). The opposing face of each composite was polycarbonate Lexan. Upon evaluation, two of the systems were within limits generally accepted for transparent composites for vehicles.

Advanced Adhesives for Transparent Armor

By

Robert E. Sacher and John R. Plumer

Army Materials and Mechanics Research Center, Watertown, MA

Introduction

The Army has an urgent need for a clear adhesive system for use in transparent armor applications. A monolithic sheet acrylic is the primary helicopter glazing, and is currently utilized as configurations in helicopter windows in the UH-1, AH-1, CH-47, etc. Presently these windows require periodic replacement, primarily due to abrasion or breakage. Replacement rate for more than 7,000 aircraft averaged about 1 window per aircraft during 1971. Repair is often not possible and the replacement cost is about $300.00 per window, excluding replacement labor, for a total cost of about 2.1 million dollars.

Except for CH-47 windshield of laminated glass, and a recently approved UH-1 laminated glass windshield, all helicopter glazing are of acrylic plastic. Of course, glass (or acrylic) designs do not address the problem of spallation as no polycarbonate is included in the configuration. This material is quite soft and is abraded by windshield wipers and soil debris made airborne by the rotary wing airflow. The CH-47 windshields have adequate abrasion resistance; but they spall under small partical impact. Spallation also occurs with acrylics, the glass spallation being more dangerous than the acrylic. Polycarbonate plastics, while more spall resistant than acrylics, are softer and abrade more rapidly, therefore they are impractical to use as a monolithic replacement for windshield glazings. No other commercially available material could be utilized as a replacement glazing.

To address both spallation and abrasion problems of the current acrylic windshields a laminate configuration may be used. This system incorporates an outer ply of glass, for optimal abrasion resistance, and adhesive interlayer, and an inner ply of polycarbonate, for spall resistance. It is the task of this program to evaluate less expensive film adhesive systems for suitability as an aircraft glazing interlayer.

Most commercially available transparent film adhesives are generally brittle or incompatible with polycarbonate (an exception is a PPG 112 sheet adhesive) Ref. 1. It has been demonstrated that brittle adhesives severely degrade the ballistic properties of polycarbonate, the usual backup component of transparent armor composites. Most of the adhesives with effective ballistic behavior have poor optical properties or cause crazing on the adhered polycarbonate surface and thus reduce the overall ballistic and optical quality

of the laminate transparent armor. It has been recognized that the processing techniques required for fabrication generally results in somewhat higher unit costs when the cast-in-place (C-I-P) techniques are utilized.

Recent advances have been made in producing film adhesives in limited quantities. Initial screening tests conducted to date have been very promising since these adhesives do not adversely affect transparency or spalling characteristics, and in addition are more easily processable than cast-in-place adhesives; industry estimates indicate a potential 10%-15% reduction in fabrication costs of transparent armor systems using such adhesives.

This program procured four different experimental transparent film adhesives from four producers (Monsanto, ethylene terpolymer; Dupont, polyurethane; General Electric, silicone polycarbonate; and Union Carbide, ethylene-acrylic acid). Tests samples were fabricated in three layers (glass/adhesives/polycarbonate), after the bonding processes had been defined for each of the adhesives the samples were evaluated for ballistic optical, environmental, and thermal shock behavior. On the basis of this evaluation, the optimal laminated configuration will be evaluated in actual windshield configurations and under expected environmental conditions. The results of this work will also have application in other transparent items such as gasmasks, visors, jeep windshields and tank vision blocks.

Experimental

The four experimental interlayers were incorporated into four different cross-sectional configurations. Each interlayer type was laminated into three-ply composites having face plies of acrylic (Plex-55); Chemcor glass, Code 0401 and Code 0313; and Pyrex glass, Code 7740. The opposing face of each composite was Lexan polycarbonate. Figure 1 shows the composition of the 4 laminated constructions. Each configuration was fabricated in 12" x 12" size samples and all but the Pyrex/polycarbonate configuration were fabricated in 2' x 3' size samples.

All the laminates with the exception of the GE laminates (silicone adhesive) were processed by Swedlow, Incoprorated. GE provided completed laminates. Types A, B, and D were all autoclave-laminated with minor variation in time and temperature cycles. With the exception of the Type D interlayer, little trouble was encountered in laminating these materials.

Test laminates were selected at random from each interlayer configuration. Light transmission, haze, and optical deviation were measured on each test laminate. The laminates were photographed in front of a grid board and then subjected to a thermal exposure of 6 hours at -54±5°C, and 3 hours at 72 ± 2.2°C extremes. After thermal testing, the parts were visually examined for bubbles, haze, delamination or other signs of deterioration. Light transmission, haze and optical deviation were again measured, and the test laminates were rephotographed at the grid board. Tables I through VI, inclusive, give the results of the Test Program.

The impact performance was evaluated by ballistic testing. Ballistic testing was conducted with (1) caliber 22, 17 grain fragment simulating projectiles FSP; (2) caliber 30 FSP; and (3) caliber 30 M2 ball projectiles. Velocities were accurately recorded by a chronograph.

Results

A. Processing and Optical Properties

Type A Interlayer, Monsanto Ethylene Terpolymer

This interlayer processed with a minimum of difficulty in the four configurations. One minor problem encountered was a tendency to form fine bubbles during lamination which later enlarged during thermal exposure. Modification of the lamination cycle should remedy this problem. The acrylic/polycarbonate laminates, (construction Type 2.1.1) were more prone to have bubbles than the glass faced laminates, this was attributed to low thermal conductivity of the substrate.

Warpage was a problem with Type A interlayer laminates. This condition can be expected when laminating asymmetric composites at elevated temperatures.

Light transmission, haze and optical deviation, both before and after thermal testing, were within the limits generally accepted for transparent composites for vehicles. These requirements are a 70% minimum light transmission, a 4% maximum transmitted haze, and a grid line slope maximum of 1 in 12.

Type B Interlayer, DuPont Soft Polyurethane

Of the three interlayers laminated by Swedlow, Type B was the easiest and most trouble-free to process. Some small bubbles did appear during thermal testing but were confined for the most part to the acrylic/polycarbonate laminates. Light transmission, haze, and optical deviation measurements were very good (less than 2% change) both before and after thermal testing. Warpage of Type B interlayer laminates was similar, in extent, to the warpage of the Type A interlayer laminates.

Clarity of Type B laminates was excellent; except for the poor performance of the 2.1.4 (Pyrex) laminates, this interlayer fared well in all tests.

Type C Interlayer, G.E. Silicone/Polycarbonate Block Polymer

Since this interlayer was not laminated by Swedlow, but by GE its processing characteristics are unknown. The limited number of laminates tested by Swedlow restricts the amount of data generated. However, the Type C interlayer laminates that were tested displayed good clarity in light transmission and lack of haze, acceptable optical characteristics and resistance to physical breakdown during thermal testing.

Warpage of the Type C interlayer laminates does not appear as severe as in Types A and B.

Type D Interlayer, Union Carbide Ethylene/Acrylic Acid

The most difficult of the interlayers to process, Type D, was unsatisfactory in its performance. All the Type D interlayer laminates produced are characterized by degrees of haze varying from 4% to 35%. In addition, severe warpage, bubbles and delamination from Lexan surfaces were typical of laminates made with the Type D interlayer.

Photographs of laminate 2.1.3 D-2 after thermal testing shows the hard, brittle nature of the Type D interlayer. On the other hand, at laminating temperature, 250°F, the liquefying of the interlayer was such as to cause the inadvertent bonding of substrate, bleeder material and glass laminating cauls, resulting in the loss of several laminates.

A lack of cold-flow in this interlayer apparently creates enormous stresses in glass-faced laminates. In one case, a 2.1.4D laminate exploded, almost violently, while sitting at room temperature.

Of particular note was the failure of all Pyrex (Code 7740) laminates (construction 2.1.4) to survive the cold cycle. Breakage of the pyrex during autoclaving also resulted in considerable loss of laminates.

B. Ballistic Testing

Ballistic V_{50} data for these configurations (2.1.1, 2.1.2, 2.1.3, and 2.1.4) permitted a comparative evaluation to be made between the mechanical properties i.e., ballistic response of the four adhesives utilized in this study. It also allows a comparison to be made of this data with results of other adhesive systems previously tested, (Ref 1.)

Adhesiveness of the candidate interlayers is not directly measured by ballistic testing. Previous studies (Ref 2.) have shown that only adhesiveness of the interlayer sufficient to hold the transparent laminate intact upon projectile impact is required. Adhesive properties of the film interlayers also affect such properties of the laminate as thermal shock, and thermalcycle survivability by allowing expansion of dissimilar materials (glass/plastic). Thermalcycle testing is reported elsewhere in the paper. Ballistic test results for the film adhesive interlayers are shown in Table V. Data for other transparent adhesives tested in prior AMMRC programs are shown in Table VI for comparison.

Observations and Conclusions

I Ballistic impact testing (V_{50}) with 22 FSP (Table V) demonstrates that two adhesives (Type A and Type B) offer up to a 10% higher ballistic impact

response over adhesive Types C and D when tested in configuration 2.1.1. Configurations 2.1.2 and 2.1.3 demonstrated no appreciable differences in impact response (V_{50}) between adhesive Types A, B, and D, (no C sample was available for testing in configurations 2.1.2 and 2.1.3). Similarly, (V_{50}) data for 30 caliber (FSP) and 30 caliber ball impact testing showed no appreciable differences in the performance of adhesive Types A, B, and D when tested in configuration 2.1.4. No sample was available on the Type C adhesive in this configuration.

II Considering commercial tolerances in component materials, it may be concluded (data, Table V) that none of the adhesives (A, B, C, and D) tested, offered a relative improvement in ballistic limit (V_{50}) sufficient to indicate significantly superior mechanical properties to be present among the four adhesives.

III Prior ballistic testing (Table VI) with Plexiglass/Lexan (2.1.1) transparent materials has shown a V_{50} range of 1580 to 1645 feet per second. This represents a 45% improvement over either material alone and 200 feet per second increase over this laminate without an interlayer (Ref 3.). Ballistic date (Table V) for this configuration (2.1.1) shows a similar V_{50} range of 1477 to 1639 feet per second.

IV Ballistic impact testing of configurations 2.1.4 using 30 caliber FSP and 30 caliber ball projectiles show less than 10% improvement in V_{50} over laminates of similar construction developed in previous transparent armor programs, Table VI.

V The V_{50} data for adhesive types A, B, C, and D shows that these materials (when incorporated into configurations 2.1.1 and 2.1.4) perform within the ballistic limits reported in previous work (Table VI), i.e., it may be concluded that these materials offer state of the art performance as interlayers in ballistic test samples.

In summery, three adhesive systems have been chosen for further evaluation. This includes fabrication of prototype helicopter windshields followed by flight and runway storage testing.

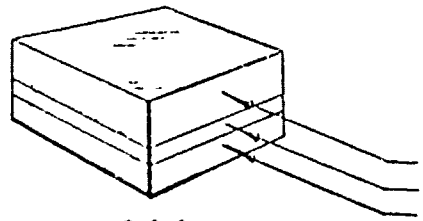
References

1. AMMRC TR 73-36 "Effect of Adhesive on the Impact Resistance of Laminated Plastic for Windshield Applications" J. L. Illinger and R. W. Lewis August 1973.

2. "Proceedings, Army Science Conference" June 1974.

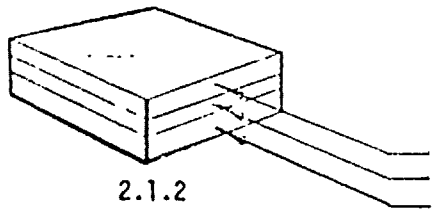
INTERLAYER

Type 'A' = .010"
Type 'B' = .030"
Type 'C' = .010"
Type 'D' = .010"



.250" Plex 55
(1.)
.125" Lexan *

2.1.1



.085" Chemcor Code 0401
(2.)
.125" Lexan

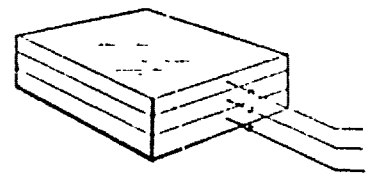
2.1.2

(2) INTERLAYER

Type 'A' = .030"
Type 'B' = .030"
Type 'C' = .030"
Type 'D' = .030"

(3) INTERLAYER

Type 'A' = .030"
Type 'B' = .030"
Type 'C' = .030"
Type 'D' = .030"

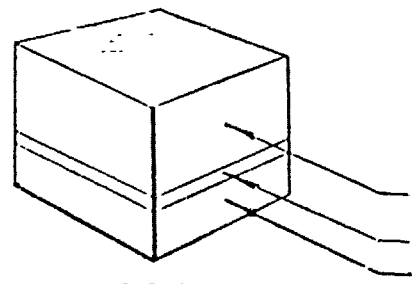


Code 0313
.050" Chemcor
(3.)
.125" Lexan

2.1.3

INTERLAYER

Type 'A' = .040"
Type 'B' = .060"
Type 'C' = .060"
Type 'D' = .060"



.500" Pyrex Glass
Code 7740
(4.)
.250" Lexan

2.1.4

LEGEND:

Type 'A' Monsanto Terpolymer
Type 'B' Du Pont Soft Polyurethane
Type 'C' G.E. Silicone/Polycarbonate
Type 'D' U.C. Ethylene/Acrylic Acid

*Lexan - General Electric Trademark for Polycarbonate Sheet

Figure 1

TABLE I

INTERLAYER TYPE 'A', MONSANTO TERPOLYMER

Construction	Size	Before Thermal Testing (1) L.T. %	Haze %	(2) Dev.	Condition	(3) After Thermal Testing L.T. %	Haze %	Dev.	Condition
2.1.1A	24" x 36"	86.7	1.9	0-4	Fine bubbles, Slt. warp	87.0	2.2	0-3	Bubbles, heat cycle
2.1.1A #3	24" x 36"	87.1	1.7	0-4	Fine bubbles, Slt. warp	87.3	1.9	1-3	Bubbles, heat cycle
2.1.1A #7	24" x 36"	86.4	1.8	0-3	Fine bubbles, Slt. warp	86.7	3.4	1-2	Bubbles, heat cycle
2.1.2A #1	24" x 36"	84.0	2.8	0-4	Clear, Slt. warp	85.0	3.6	1-5	Clear, Slt. warp
2.1.2A #2	24" x 36"	84.3	2.3	0-3	Clear, Slt. warp	85.1	3.3	0-4	Clear, Slt. warp
2.1.2A-1	12" x 12"	86.4	2.1	0-4	Clear, Slt. warp	86.3	2.0	0-4	Clear, Slt. warp
2.1.2A-2	12" x 12"	86.2	1.9	0-6	Clear, Slt. warp	86.4	1.7	0-7	Clear, Slt. warp
2.1.2A-3	12" x 12"	86.3	1.6	0-2½	Clear, Slt. warp	86.5	1.7	0-2	Clear, Slt. warp
2.1.3A #6	24" x 36"	84.0	2.0	0-3	Clear, Slt. warp	-	-	-	Glass failed,cold cycle
2.1.3A #13	24" x 36"	83.6	1.9	0-4	Clear, Slt. warp	85.1	3.6	0-4	Clear, Slt. warp
2.1.3A-1	12" x 12"	85.6	1.7	0-3	Clear, Slt. warp	85.8	1.8	0-3	Clear, Slt. warp
2.1.3A-2	12" x 12"	85.4	2.5	0-4	Clear, Slt. warp	85.6	2.6	0-4	Clear, Slt. warp
2.1.4A #10	24" x 36"	81.2	2.9	0-3	Clear	-	-	-	Glass failed,cold cycle
2.1.4A #12	24" x 36"	81.4	3.6	0-3	Clear	-	-	-	Glass failed,cold cycle

Laminates Tested in Group II

NOTES:
(1) Light transmission and haze measured on Gardner large surface area hazementer.
(2) Deviation values are in minutes - of-arc obtained per MIL-G-25871-A.
(3) All test laminates subjected to thermal test procedure outlined in Para. 5.28 USA Standard Z26.1-1966 (6 hrs. @ -54 ± 5°C/3 hrs. @ +72 ± 2.2°C)

TABLE II

INTERLAYER TYPE 'B', DuPONT POLYURETHANE

		Before Thermal Testing				(3) After Thermal Testing			
Construction	Size	(1) L.T. %	Haze %	(2) Dev.	Condition	L.T. %	Haze %	Dev.	Condition
2.1.1B	24" x 36"	86.8	2.1	0-9	Edge fractures	86.8	2.3	0-4	Sm Bubbles, heat cycle
2.1.1B #4	24" x 36"	86.6	1.6	0-3	Clear, Slt. warp	87.4	4.1	0-4	Sm Bubbles, heat cycle
2.1.1B #5	24" X 36"	87.2	1.1	0-5	Clear, Slt. warp	87.6	1.5	0-5	Clear, Slt. warp
2.1.2B	12" x 12"	86.9	1.7	0-2	Clear, Slt. warp	86.9	0.8	0-2	Clear, Slt. warp
2.1.2B #1	12" x 12"	87.0	0.9	0-1	Clear, Slt. warp	86.5	4.0	0-2	Clear, Slt. warp
2.1.2B #2	12" x 12"	86.8	0.3	0-3	Clear, Slt. warp	86.7	1.7	0-1	Clear, Slt. warp
2.1.3B #5	12" x 12"	86.6	0.8	0-2	Clear, Slt. warp	86.5	3.0	0-4	Clear, Slt. warp
2.1.3B #6	12" x 12"	86.2	0.8	0-2	Clear, Slt. warp	85.8	2.9	0-1	Clear, Slt. warp
2.1.4B #8	24" x 36"	83.3	1.8	0-8	Clear	-	-	-	Glass failed,cold cycle
2.1.4B #11	24" x 36"	83.5	0.8	1-7	Clear	-	-	-	Glass failed,cold cycle

Laminates Tested in Group II

NOTES:
(1) Light transmission and haze measured on Gardner large surface area hazemeter.
(2) Deviation values are in minutes - of-arc obtained per MIL-G-25871-A.
(3) All test laminates subjected to thermal test procedure outlined in Para. 5.28 USA Standard 226.1-1966 (6 hrs. @ -54 ± 5°C/3 hrs. @ +72 ± 2.2°C)

TABLE III

INTERLAYER, TYPE 'C', G. E. FABRICATED

Construction	Size	Before Thermal Testing (1) L.T. %	Haze %	(2) Dev.	Condition	(3) After Thermal Testing L.T. %	Haze %	Dev.	Condition
2.1.1-C #14	24" x 36"	87.6	1.1	0-2	Clear	87.2	1.9	0-2	Clear
2.1.1-C #15	24" x 36"	87.5	1.1	0-4	Clear	8..2	3.0	0-4	Clear
2.1.2-C # 3	12" x 12"	86.8	1.5	0-1	Clear	87.0	3.8	0-3	Clear
2.1.2-C # 4	12" x 12"	86.6	1.8	1-2	Clear	86.5	2.7	0-3	Clear

NOTES:

(1) Light transmission and haze measured on Gardner large surface area hazemeter.

(2) Deviation values are in minutes - of-arc obtained per MIL-G-25871-A.

(3) All test laminates subjected to thermal test procedure outlined in Para. 5.28 USA Standard Z26.1-1966 (6 hrs @ -54 ± 5°C/3 hrs. @ +72 ± 2.2°C)

TABLE IV

INTERLAYER, TYPE 'D', ETHYLENE/ACRYLIC ACID COPOLYMER

		Before Thermal Testing				(3) After Thermal Testing			
Construction	Size	(1) L.T. %	Haze %	(2) Dev.	Condition	L.T. %	Haze %	Dev.	Condition
2.1.1D #16	24" x 36"	78.7	6.3	0-2	Haze, warp	83.5	10.5	0-2	Haze, warp
2.1.1D #17	24" x 36"	83.9	9.0	0-3	Haze, warp	84.0	8.9	1-3	Haze, warp
2.1.2D # 7	12" x 12"	73.5	10.5	0-4	De-Lams	74.4	12.7	0-5	Bubbles, heat cycle
2.1.2D # 8	12" x 12"	79.6	4.1	0-4	De-Lams	81.6	7.4	0-6	De-Lam, cold cycle
2.1.3D-1	12" x 12"	77.2	27.9	0-3	Haze, bubbles, warp	77.3	22.1	0-4	De-Lam, cold cycle
2.1.3D-2	12" x 12"	76.7	18.2	0-4	Haze, bubbles, warp	-	-	-	Glass failure,coldcycle
2.1.4D # 9	24" x 36"	55.4	35.5	0-4	Haze, warp, de-lams	-	-	-	Glass failure,coldcycle
2.1.4D	24" x 36"	-	-	-		-	-	-	Unfit to test

Laminates Tested In Group II

NOTES:

(1) Light transmission and haze measured on Gardner large surface area hazemeter.
(2) Deviation values are in minutes - of-arc obtained per MIL-G-25871-A.
(3) All test laminates subjected to thermal test procedure outlined in Para. 5.28 USA Standard Z26.1-1966 (6 hrs. @ -54 ± 5°C/3 hrs. @ +72 ± 2.2°C)

TABLE V

BALLISTIC DATA COMPARING FILM ADHESIVES

CONFIGRUATION -	ADHESIVE	Areal Density (oz/sq ft)	Velocity (fps) 17gn FSP 0° Obliquity V_{50}	High Partial	Low Complete	Ballistic Test
2.1.1	A Ethylene Terpolymer	1077gm	1575 8 rounds	1554	1594	139-75
	B Polyurethane	1055	1639 11 rounds	1631	1650	W-63-75
	C Silicone/ Polycarbonate	1050	1541 6 rounds	1531	1315	142-75
	D Ethylene/ Acrylic Acid	1098	1477 12 rounds	1435	1525	968-74
2.1.2	A	932gm	1178 5 rounds	1137	1222	974-74
	B	930	1189 6 rounds	1165	1195	976-74
	C No sample	--	--	--	--	--
	D	930	1150 6 rounds	1188	1145	973-74
2.1.3	A	725	973 6 rounds	926	1018	977-74
	B	725	1001 6 rounds	1011	1011	975-74
	C No sample	--	--	--	--	--
	D	725	1010 5 rounds	989	1031	972-74

TABLE V

30 Cal FSP 0° Obliquity

2.1.4	A	7.25 lbs	3767 6 rounds	3674	3860	978-74
	B	"	--	4329	--	980-74
	C No sample	--	--	--	--	--
	D	"	3801 6 rounds	3800	3815	981-74

30 Cal Ball 0° Obliquity

2.1.4	A	7.375 lbs	2636 8 rounds	2658	2627	W-123-75
	B	7.51 lbs	2602 8 rounds	2570	2634	W-122-75
	C No sample	--	--	--	--	--
	D	--	--	--	--	--

TABLE VI

(U). BALLISTIC BEHAVIOR OF ¼" PLEX 55/ADHESIVE/1/8" LEXAN LAMINATES AGAINST THE .22 CALIBER FSP AT 0° OBLIQUITY AND ROOM TEMPERATURE

Adhesive*	V_{50} B.L. (fsp)	Areal Density (oz/ft)	High Partial (fps)	Low Complete (fps)	Ballistic Test No.
Unbonded (12" x 12" panel)	1400	38.5	1421	1414	W-499-70
Thermal Bond (12" x 12" panel)	-	36.9	1096	1104	HSP-39-71
0.010" Epon 828	-	39.5	-	1291	-
0.010" Polyvinyl-butyral	-	39.0	-	1100	HSP-53-71
0.010" Polyurethane	1585	38.7	1624	1578	HSP-59 and 61-72
0.010" General Electric	1630	38.5	1645	1634	HSP-51 to 53-72
0.060" Goodyear CIP**	1026	36.3	1055	965	191-72

* Test panel size: 6 in. x 6 in. unless otherwise noted
8-round V_{50} B.L.
Chemical composition is 1.261 methylene diisocyanate:0.2 butanediol: 1 polyethylene/polypropylene glycol
** 1/16" thick Lexan in lieu of 1/8"

30 Cal FSP at 0° Obliquity and Room Temperature

1/2" Soda-limeglass 0.09 PPG-112 Interlayer 1/8" PC 9030-112	3735	7.6 lbs	664-74
1/2" Polished Plate .04 CIP (F-3X-15)GYAC .250 PC 9030	2301	7.58 lbs	GYAC Test***

*** Goodyear Aerospace Corporation
Litchfield Park, Arizona

THIN FILM COATINGS ON PLASTIC SUBSTRATES

J. D. Rancourt
Optical Coating Laboratory, Inc.
Santa Rosa, California

THIN FILM COATINGS ON PLASTIC SUBSTRATES

Dr. James Rancourt

Optical Coating Laboratory, Inc.

Abstract

This paper is an up to date summary of what Optical Coating Laboratory, Inc., considers to be the state-of-the-art in vacuum deposited optical thin film coatings on plastic substrates. The aerospace applications and problems relevant to their fabrication and use are considered. The applications include antireflection coatings, transparent conductors, and abrasion resistance enhancement.

Some of the problems encountered in the coating of substrates are intrinsic to the nature of the coatings, such as the changes in the spectral response of the reflectance as a function of the angle of incidence. This is a problem in the design of some recent cockpit configurations, where the pilot looks out through a panel at a very high angle of incidence. In such situations, it is difficult to design a coating which will work well as an antireflection coating. Other difficulties discussed are associated with the coating of plastic substrates and include: the prominence of scratches and blemishes; cleaning of the substrate before coating; limited coating hardness due to coating temperature constraints; the adhesion of the coating to the substrate; and finally, the problems of coating large and complex geometries.

Large panels of both acrylic and of polycarbonate materials have been successfully coated for aerospace uses such as helicopter canopies and implosion shields for large surface area cathode ray tubes.

Future improvements are likely to come in the areas of substrate preparation processes, abrasion resistance enhancement of the coatings, and the adhesion of the coatings to the substrate.

I. Introduction

Optical coatings have been successfully put on glass substrates for years. These coatings are used to control the transmission and the reflection of light at various wavelengths. A common use of such coatings is to reduce the reflectance from a surface; then, extraneous ambient light will not interfere with vision through the surface or window.

Glass, as a substrate material, has a relatively fixed overall composition. Some small percentages of extra ingredients are added to the basic silica component to give it some desired property, but these do not affect the surface characteristics very significantly.

Plastics, on the other hand, are relatively pure organic compounds, but they come in a wide variety of chemcial compositions; over 40 chemically different types can be counted in a recent edition of the Plastics Encyclopedia. The molecules which make up plastics are generally interlinked and the chemical bonds at the surface can and do vary significantly from one type of plastic to another. Furthermore, the methods of processing and finishing the plastic surfaces greatly influence these bonds. These difficulties of characterizing the surface of a plastic substrate are the source of numerous difficulties observed when depositing coating plastics.

When coating a plastic surface with thin films, one hopes to get a spectral performance which approaches that which is obtained with a similar coating on glass. In addition, the coating is usually expected to enhance the ability of the surface to resist abrasion.

In this talk, I would like to introduce you to optical thin films and give examples of their use on plastic substrates. We will look at the various measurements which can be made to quantify the durability of a coating. Following a review of some of the successful coatings that have been applied to plastics, we will point out some of the problem areas and the pitfalls one should avoid, or else be prepared to resolve.

II. Optical Thin Films

The kind of thin films we are discussing here are discrete, solid, and homogeneous; they generally have a thickness which is less than a wavelength of light, i.e., a physical thickness in the range of 50 to 100 nanometers, or one to two microinches. Depending on the application, several of these films might be deposited on top of each other (i.e., layered) in order to achieve

a particular optical effect. The design of the stack of films is accomplished by following some general rules, working from standard designs, and finally, using a computer to optimize the result.

The films are deposited sometimes by either a D.C. or a radio frequency sputtering process, or, more commonly, by evaporating the coating material in a high vacuum and allowing the vapors to condense upon the substrate.

A large variety of different inorganic materials are used for coating purposes, with magnesium fluoride probably being the best known. The size of the vacuum chambers can vary from small 18 inch bell jars used in research labs to large automated continuous coaters. In the last paper this morning, we saw a large batch coater in which the Space Shuttle windows are presently being coated by OCLI. Figure 1 shows a large automated continuous coating machine at OCLI which has been in operation for several years.

The optical phenomena that makes these films useful is the interference which occurs between light waves reflected from each interface of the film structure, as shown in Figure 2. As an example, and without going into any mathematics, when the sum of all of the light reflected backwards from the stack is zero, we get no reflection from this combination of film and substrate. Since the individual films can be made transparent, there is no absorption of light. Since energy must be conserved, all of the incident light is transmitted into the substrate, i.e., $T \sim 100\%$. Thus we have not only eliminated the undesired reflected light, but have converted it to something useful. This is the basis for most thin film antireflection coatings applied to optical surfaces. An uncoated single glass surface will reflect about 4% of the light incident upon it; a pane of glass will reflect approximately 8% due to the fact that there are two surfaces. A good antireflection coating will reduce this total reflection to an average of less than 1/2% across the visible spectrum, and the transmission through the pane increases to 99% or better. We can also make the summation of the waves different from zero for various wavelengths. Then, certain colors can be transmitted through while others are reflected by the filter. Many applications exist for such filters; examples are long wave pass or short wave pass filters, heat transmitters or reflectors, and bandpass filters.

In some instances coatings compete with entirely different technologies. For example, another way of eliminating the specular reflectance from a surface is to etch it very lightly. This works by scattering away in all directions light which would otherwise be specularly reflected. This might be fine and cost effective in some instances, such as in a pane in a picture frame. It has no place in a precision optical system, on lighting wedges used in aircraft instrument lighting, or on cockpit canopies. In the former case, the scattered light reduces the resolution of the image formed by the optical system, while in the latter case, a frosted canopy would make outside vision difficult when bright sunlight falls upon it. In these cases, only the thin film approach can be used.

III. Use of Thin Film Coatings on Plastic Substrates

Now that we have reviewed what thin films are and how they work optically, I'd like to point out some of the applications that they have in various areas which could be of interest to you.

We have already mentioned their use as reflection-reducers on optical surfaces. A related application is in filters called contrast enhancement filters. In this case, it is desired to reduce not only the reflected light but also to prevent ambient light from being reflected from a surface behind the filter. Such filters are useful when placed over a CRT or other self-illuminated display which might be used in high ambient light conditions. When one looks at such a combination, the main source of the observed light it from the display itself with the surrounding area relatively dark, thus the name, contrast enhancement.

Beamsplitters can be coated on a flat plate; when this plate is put in an inclined position in the line of sight of a pilot, it can serve as the combining element for a head-up display.

Transparent conductive coatings placed on the implosion shield in front of a CRT screen can serve as radio frequency interference filters. In this case, the coating is not strictly an optical coating, though for such an application, it must be transparent.

Lighting wedges are becoming more popular as a means of illuminating aircraft instruments, thus eliminating the outdated floodlight method. There are four surfaces in the typical wedge lighting system used in modern cockpits as shown in Figure 3. One of the wedges is the one which actually illuminates the instrument face by allowing light to leak out uniformly along its length. Light leaks out the other side as well. The second wedge serves to compensate the prismatic distortion introduced by the first wedge. We have a total of four surfaces, all of which could give rise to multiple ghost images unless they were anti-reflection coated. This coating does not interfere with the lighting properties of the wedge; as a matter of fact, since they reduce unwanted reflections, it is easier to see through the wedges, so a lower light intensity level may be used for the illumination.

A non-optical use for thin films is for the enhancement of the abrasion resistance of a plastic substrate. Note that I said enhance. Since the coatings are rather thin, any deflection of the substrate could cause the film to break. This is akin to armor plating a marshmallow; without a good structure to build upon, it is difficult to construct a good protective layer. Thus, we should say that we can improve the abrasion resistance of a coated plastic part over its uncoated counterpart. It takes a very thick and tough layer of some protective coating to protect completely a soft substrate from all abrasion tests to which it can be subjected.

Another area which is going to come of age very shortly is the holographic beamsplitter used in some of the recent announcements of head up displays. Since these devices use photographic emulsions, they will most likely require some sort of protection against scratching and water damage. A coating can offer a great deal of protection for such substrates by improving their abrasion and humidity resistance.

Up to now, we have been discussing general areas where thin film optical coatings might be used in a cockpit.

We will now review some projects which might be of interest to the aviation community which actually involved the coating of plastic substrates.

(USE OF THIN FILM COATINGS ON PLASTIC SUBSTRATES Continued)

OCLI is coating about 1,200-22 inch diameter substrates on both sides with a high efficiency antireflection coating for FAA. These panels are used for implosion protection in front of large CRT's and are made of green Lexan polycarbonate plastic with a polymer abrasion resisting surface finish on them. The coating reduces the reflection of ambient light and light from the adjacent consoles in the enroute air traffic control center, and also the multiple ghost images which can occur within the 3/8 inch thick plastic panels. The coated parts pass the 50 rub cheesecloth test, and they are not affected by 24 hours' exposure to humidity testing. Figure 4 shows the effect the coating has on the visibility through the part. It shows a sample part which has been coated in quadrants. One area has no coating, two areas are coated on alternate sides only, and the fourth quadrant has a coating on both sides. Figure 5 shows the entire part; the one on the left is coated on both sides, while the one on the right is an uncoated part. The bare substrate has a single surface reflectance of approximately 4 to 5%, while the coated surface has a reflectance about an order of magnitude less.

Another effort involved the evaporation of an antireflecting coating on helicopter canopies to reduce the reflected glare, thereby decreasing the range at which the helicopter might be spotted due to sunlight reflected from the canopy. Figures 6 and 7 show the large size and complex shape of the parts involved. In these photographs, the canopies are not coated. The coating effort was quite successful, even on large parts such as these. A second benefit of such coatings is the reduction of the intensity of the light reflected by the canopy into the cockpit. For example, the firing of missiles creates a large amount of light; at night, the direct glare can be worsened by reflections from the canopy. An antireflection coating would reduce this reflected glare and make vision recovery more rapid. Reflections of sources of light inside the cockpit would also be minimized.

Recent developments in helicopter design have tended towards the use of flat panels for the cockpit enclosure. While this can make the coating geometry simpler, a problem arises from the fact that it is quite difficult to design an acceptable antireflection coating for use at high angles of incidence.

(USE OF THIN FILM COATINGS ON PLASTIC SUBSTRATES Continued)

An in-cockpit use of coatings on plastic substrates is shown in Figure 8. The beamsplitter in this head-up display, which is manufactured by Sundstrand for use in 737's and Tridents, and also in DC-10's and 747's, is made of plastic. It is a thick part with curved surfaces.

The front surface has a coating which reflects about 30% of the light from a display device into the field of vision of the pilot.

The back surface has an antireflection coating to prevent ghose images caused by multiple reflections taking place within the unit.

In 1964, plastic windows were under consideration for the Apollo spacecraft. Coatings which transmitted in the visible portion of the spectrum and which reflected infrared energy were successfully coated on them. Eventually the decision was made to go with glass windows, and OCLI coated these with similar designs.

One final item which I will mention here is a 5" by 12" acrylic plastic panel which was placed in front of a CRT. One side of the sheet had a transparent conductive gold RFI shielding layer, while the other side had a High Efficiency Antireflecting (HEA®) coating. This allowed the user a good view of the display while minimizing electromagnetic interference.

IV. Testing of Thin Films

Of course, the optical performance of coatings, be they coated on glass or plastic substrates, is measured with standard recording photometers or spectrophotometers. Not so well known are the standards used to measure the environmental characteristics of these coatings, so we will touch upon that for a moment.

The adhesion of a thin film to its substrate is measured with binary test of the go/nogo type known as "the Scotch Tape test". In this test, a standard cellulose adhesive tape is pressed against the film and then slowly pulled off. There should be no evidence of film removal from the substrate where the tape had been stuck. This test is specified by MIL-M-13508C.

The abrasion resistance of a coating is tested with a standardized rubber eraser or with a ball of cheesecloth. These tests are standardized as MIL specs, MIL-M-13508C for the cheesecloth rub, and MIL-C-675A for the eraser rub. In the case of the latter test, two to 2 1/2 pounds of force are applied to the eraser and 20 strokes over a given area are made. After this test, there should be no evidence of any damage to the film when the rubbed area is viewed with the unaided eye. This is a very severe test of a coating, especially when appropriate edge lighting conditions are used to examine the tested part. A more lenient test replaces the eraser with a dry cheesecloth pad and a force of about one pound but uses 50 rubs instead of the 20. The eraser characteristics are specified by the Frankford Arsenal, as are the cheesecloth and the adhesive tape.

Standardized tests are also available for evaluating the ability of the coating to withstand exposure to the elements. In particular, there are standard specs for 24 and 48 hours of exposure to salt fog, 24 and 72 hours of exposure to humidity, and 240 hours' (10 days') exposure to an environment of cycled temperature and humidity. Other tests include only temperature cycling and solubility. These standard specifications should be used when specifying thin film coatings, since they are well known and used in the industry. These tests are typically binary and so give no indication as to how close the part came to passing or failing.

V. Glass vs. Plastic Substrates

The thin film industry started by applying solid films to glass lenses to reduce the reflectance at the surfaces. Glass is generally a good substrate material since it is hard, durable, and tolerates temperature levels usually required for coating a durable thin film layer. Plastic, on the other hand, is relatively soft and cannot be raised to as high a temperature as glass during the coating process. Furthermore, it exhibits a higher coefficient of expansion which can lead to crazing of the coating. The adhesion of the coating to the plastic substrate is inferior to that obtained with glass.

These differences all combine to limit the number of possible choices of coating designs and materials one may use on plastics.

(GLASS VS. PLASTIC SUBSTRATES Continued)

Another distinction between glass and plastics is in the area of costs. Glass substrates are generally more expensive than plastic ones since glass surfaces are often polished one at a time, or at most a few at a time. On the other hand, plastic lenses can be manufactured at very high rates, which makes them relatively inexpensive in large quantities. Thin film coatings cost approximately the same, whether they are deposited onto glass or plastics. Thus, the relative cost of film and substrate are radically different, so that in some instances where the thin film coating might be a small percentage of the cost of an item made of glass, it is a significant fraction of the cost of a plastic part, often costing several times as much as the substrate.

As mentioned previously in the introduction, there are many different chemical compounds which make up the class of materials called "plastics", and each of these has its own peculiar surface chemistry. A single coating design for a specific plastic can therefore not be expected to perform as well on some other kind. According to Murphy's law, it won't.

Complicating matters is the fact that the method of preparation of the plastic plays a crucial role. With glass, one commonly encounters only two basic surface types these days: polished and float. With plastics, the number of methods of preparation is huge; some methods that immediately come to mind are injection molded, cast, stretched, stamped, machined, and polished. Each of these gives the surface a different character that shows up as coating difficulties which manifest themselves as problems such as staining of the substrate, and adhesion and crazing of the coating. Thus, each type of plastic and method of fabricating it into a substrate must be taken into consideration.

VI. Discussion: Problems Associated with Coating Plastic Substrates

I would now like to touch briefly upon other problems one encounters when he is trying to coat plastic substrates. First, we should look at the optical aspect of the situation. An antireflection coating applied to a substrate of either glass or plastic can reduce the average reflectance to 1/2% or less. Any defect on the surface, whether it is due to cleaning, a scratch, or what have you, will be much more apparent to the eye

after coating than before. The reason for this is two-fold: 1) The eye is especially sensitive to small changes in color and brightness when such a change takes place over a small distance, thus small defects appear very prominent. 2) A scratch or other defect might not be noticeable when compared to the uncoated surface whose reflectance is 4% (or 8% for two surfaces). Once coated, the scratch's scattered light intensity is not significantly changed, while the overall reflectance of the surface has been reduced significantly, thus making the scratch appear more prominent.

This problem with scratches and other blemishes is more serious for plastic substrates for several reasons. With glass substrates, the surfaces are generally polished smooth, so the surface quality is often better to start with. Next, since plastics are softer than glass, they are more easily scratched during handling. Finally, since the coating parameters are more restricted when coating plastics substrates than when coating glass, it is not always possible to ensure the same durability of the coating on plastics as on glass, which makes the coating more succeptible to scratching in use in the field.

Since plastics used for optical purposes are generally attacked by the common organic solvents used to clean glass, and since abrasives cannot be used for fear of scratching the soft plastic surfaces, the cleaning procedure takes on a new perspective. A common technique used when coating glass is to clean it with a high voltage glow discharge after the substrate has been loaded into the vacuum chamber. A thorough cleaning with a glow discharge is not always possible with plastic substrates because the energetic ions and electrons in the plasma cause subsurface damage to the plastic. When the tape test is made, it is found that the coating and the surface layer of the plastic come off together. The coating has stuck to the outer surface, but the outer surface hasn't stuck to the bulk material.

From the foregoing, it is apparent that the cleaning step is critical to being able to coat plastic substrates satisfactorily.

(DISCUSSION: PROBLEMS ASSOCIATED WITH COATING PLASTIC SUBSTRATES Continued)

Some plastics are available with a polymer coating which enhances their abrasion resistance, and these are considerably easier to handle and coat. Examples of these are the MR-4000 process used by GE on its polycarbonate sheets, and Abcite used by Dupont on acrylics.

As previously mentioned, there can be a problem in placing a hard coating on an otherwise soft substrate. The substrate may yield when the environmental tests are performed; this stresses the film, causing it to break up.

Plastics are easy to mold into complex shapes, and this can lead to coating difficulties. The preferred geometry for coating a substrate is at or near normal angle of incidence of the coating material. A complex shape can make it impossible to coat the entire surface at the optimum angle, thus leading to the necessity to make compromises and trade-offs among durability, uniformity, and spectral performance.

VII. Solutions

Solutions to the problems outlined above must certainly exist. It is a matter of knowing that there is enough interest in coatings to warrant a search for them. The areas in which studies should be undertaken are cleaning, abrasion enhancement, and adhesion improvement.

The first step taken in a cleaning study would be to identify the types of contaminants which are found on the surface of a plastic substrate. Then, a technique which does not harm the substrate would be found to remove these. A concurrent effort would be made to find a way of keeping the surface clean after it had progressed through the cleaning process. One of the problems, static electricity, should also be overcome, since it can cause dust and other contaminants to be attracted to the surface after it has been thoroughly cleaned.

Several means have been suggested for coating hard materials, such as glass and fused silica, onto plastic substrates. To date, none of these has yet achieved the hardness of the coated material in its bulk state. More should be done to see what can be done to improve the abrasion resistance of these substrates. It might be possible to combine the technology of putting on polymer coatings with thin film technology to achieve a result which is better than what the state-of-the-art is today.

(SOLUTIONS Continued)

In parallel with the cleaning study, we would be aware that the surface also holds the key to the adhesion of the film to the substrate. Thus it could be possible to learn how to bond the films more tightly to the substrate. Some chemical treatment could open up surface bonds which would bind the film more tightly to the substrate. These studies might lead to some way of evaporating the coating at a lower temperature and yet retain the adhesive properties of one evaporated at a higher temperature. Also included here would be studies directed at improving the sticking coefficient of the coating material at large deposition angles.

Novel coating designs would be investigated to see if they offer the potential of producing a hard surface. Included among these might be replication studies. In this case, the coating would first be evaporated onto a mandrel. If necessary to improve the durability of the coating, this could be done at high temperatures since there would be no heat sensitive plastic in the chamber. Then, the coating could be trnasferred to the softer and less temperature resistant substrate.

VIII. Conclusion

We have seen that thin films can be successfully coated onto plastic substrates.

Compared to glass substrates, plastics and their methods of fabrication come in an almost infinite number of combinations, and this is the source of some of the difficulties in coating them. A second important point is that careful handling of plastic parts is necessary to prevent accidental damage.

It certainly appears that there is a future for coatings on plastic substrates. It would seem that the way to make progress is to attack only a small number of problems at a time, and with a specific goal in mind. We should not try to find a single coating which will be a cure for all problems with coatings on plastic substrates. We would like to work closely with the user on his application in order to work out a plan to solve specific problems.

NOTE:

MR-4000 and Lexan are registered trademarks of the General Electric Company.

HEA is a registered trademark of OCLI.

Abcite is a registered trademark of the Dupont Corporation.

LIST OF FIGURES

1. Large automated continuous coater at OCLI

2. Thin film on substrate

3. Lighting wedge geometry

4. Quadrant-coated FAA part

5. FAA parts - one coated, one uncoated

6. Cobra helicopter (AH-1G)

7. Observation helicopter (OH-58)

8. Sundstrand head-up-display

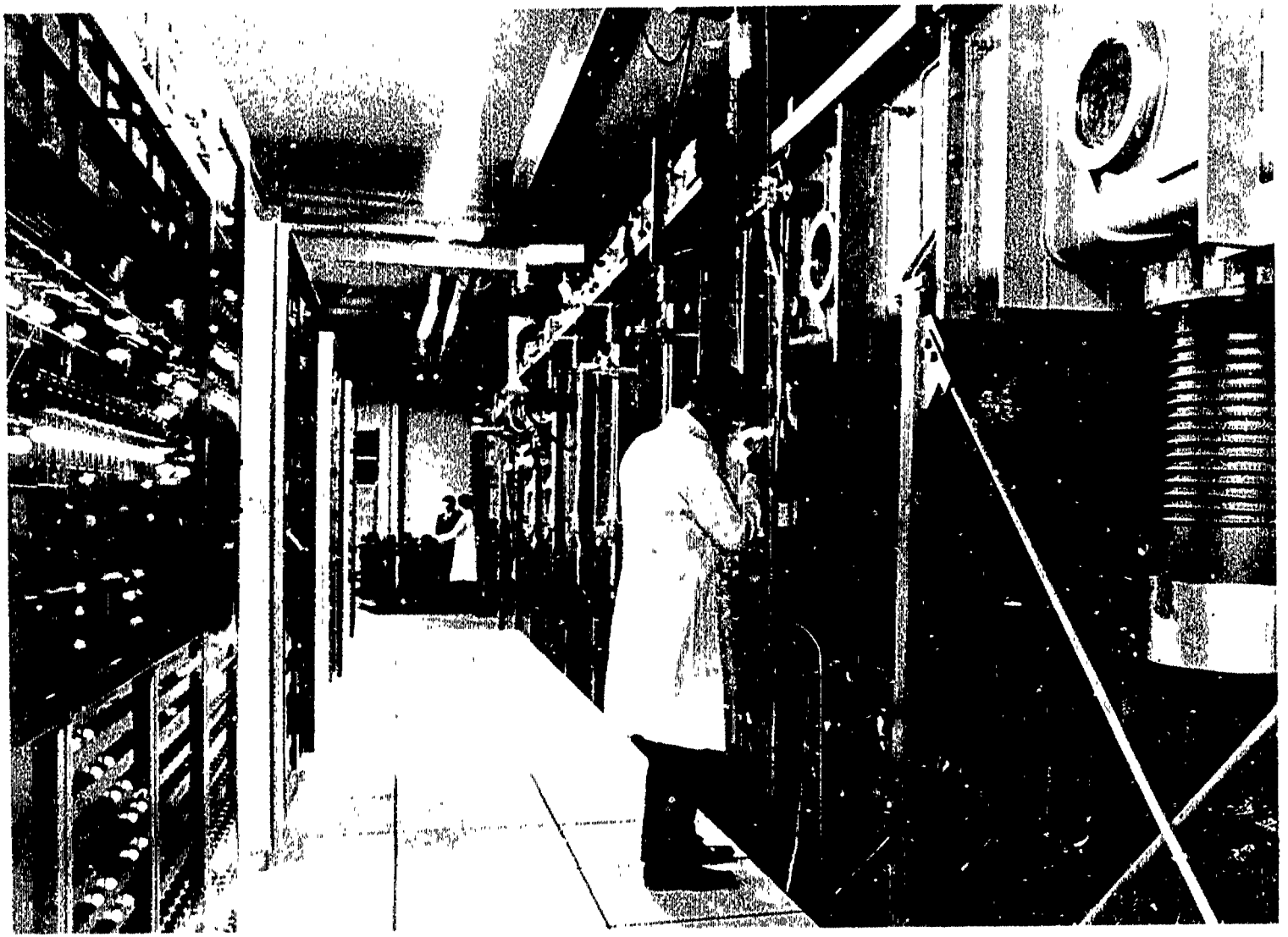


Figure 1. Large Automated Continuous Coater at OCLI

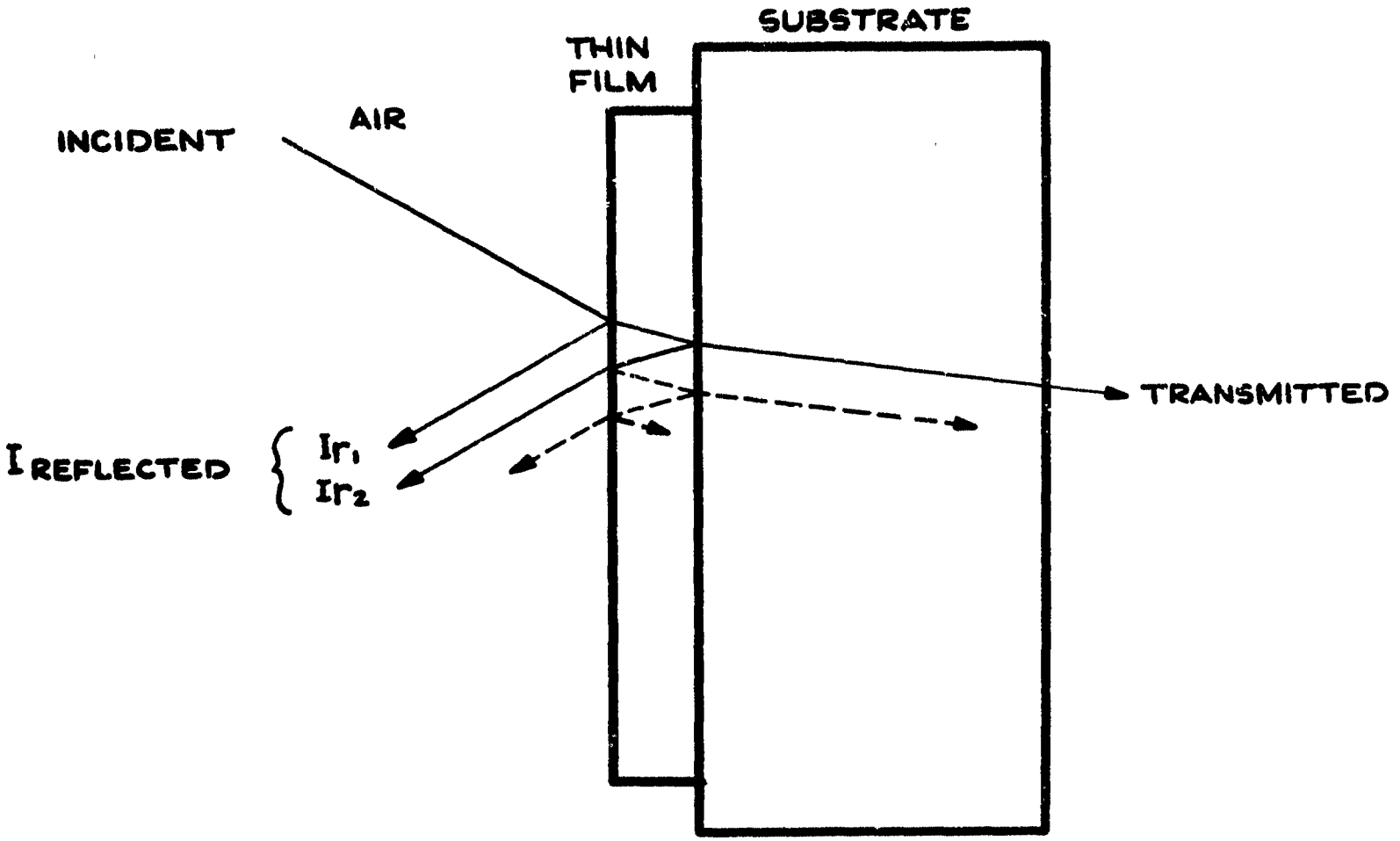


Figure 2. Thin Film on Substrate

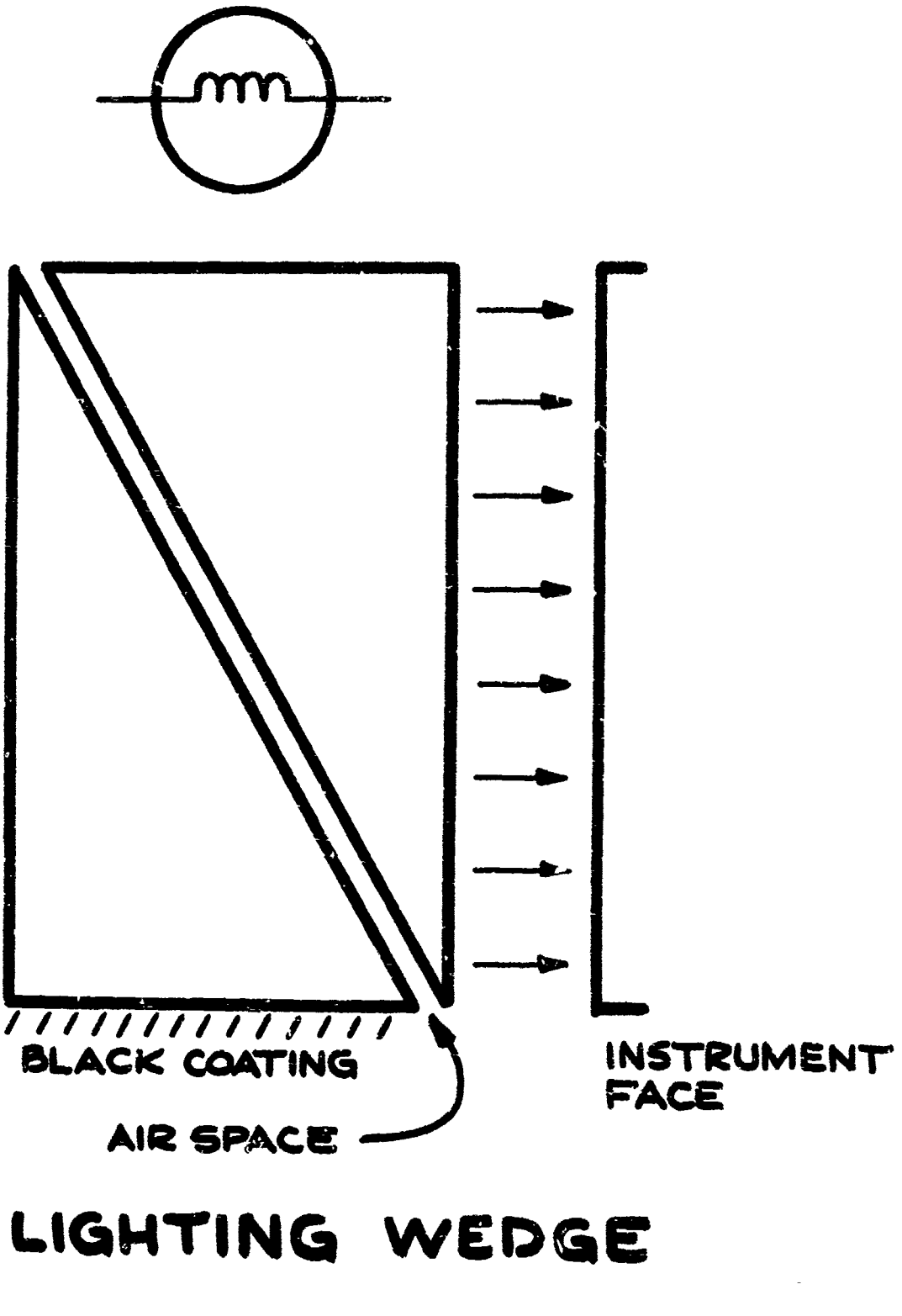


Figure 3. Lighting Wedge Geometry



Figure 4. Quadrant-Coated FAA Part



Figure 5. FAA Parts - One Coated, One Uncoated



Figure 6. Cobra Helicopter (AH-1G)

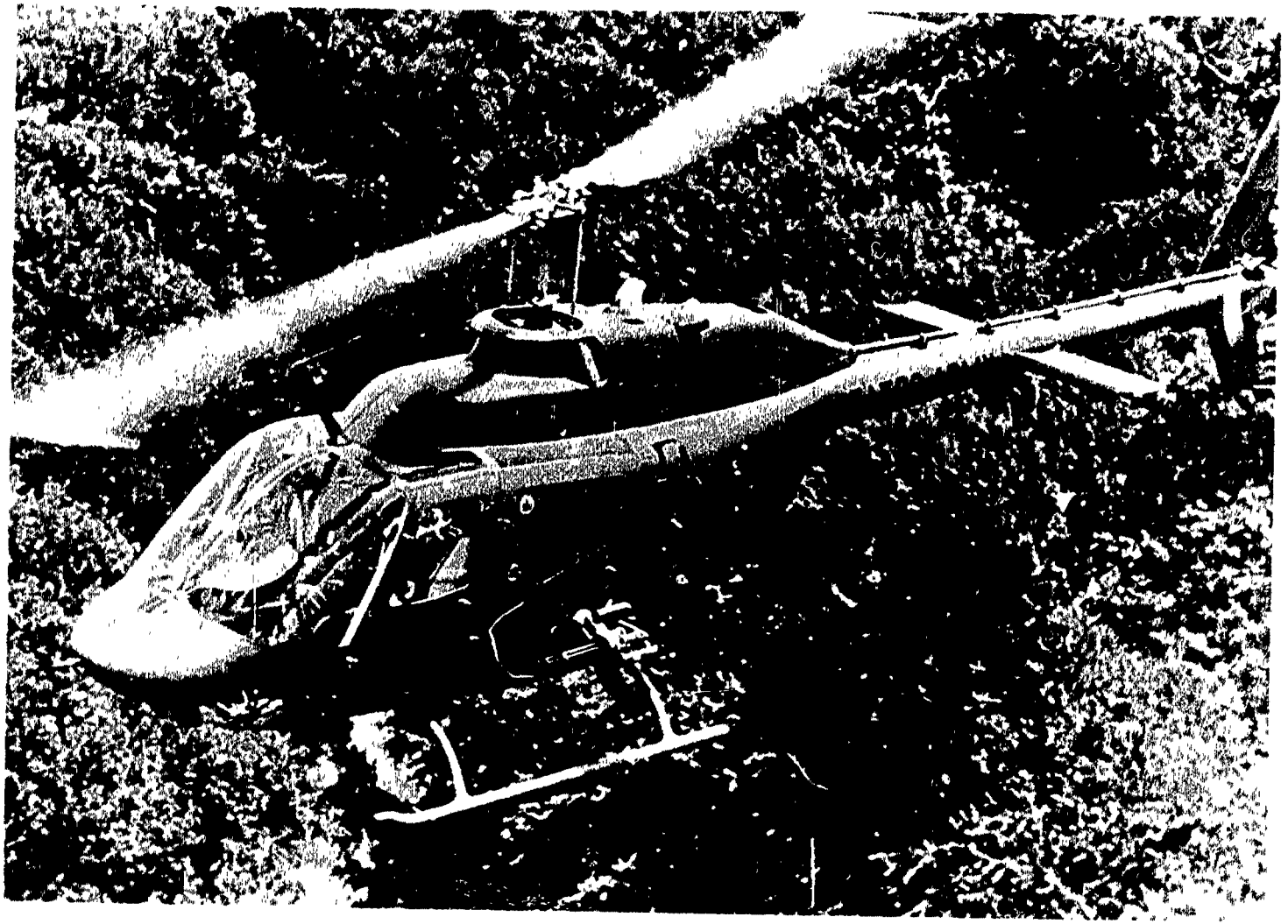


Figure 7. Observation Helicopter (OH-58)

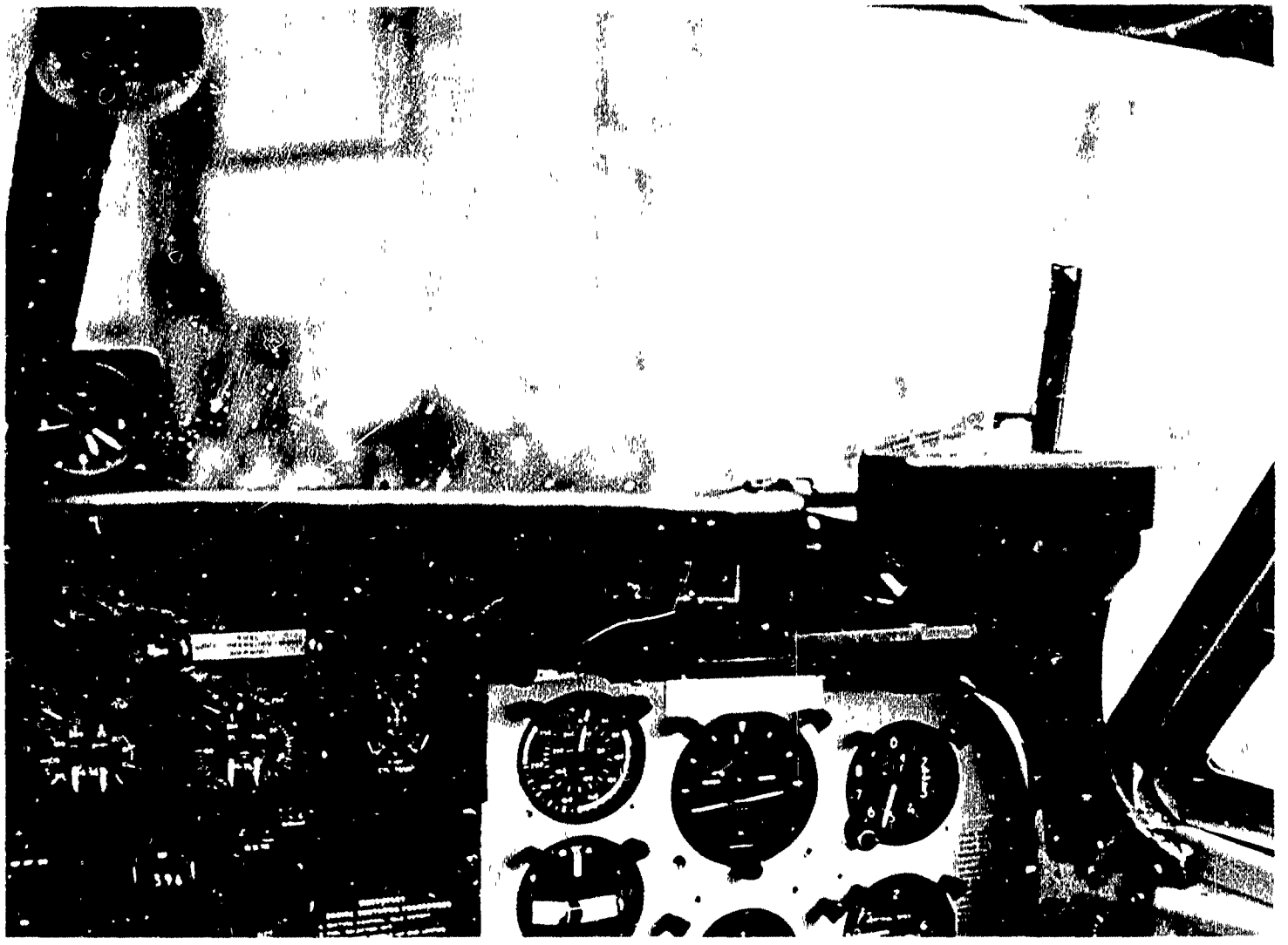


Figure 8. Sundstrand Head-Up-Display

POLYCARBONATE PROTECTION

D. L. Voss
Sierracin/Sylmar
Sylmar, California

POLYCARBONATE PROTECTION

D. L. Voss
Manager
Material & Process Development

SIERRACIN/SYLMAR

ABSTRACT

Although polycarbonate has been commercially available for many years, it has only recently been refined to a level of optical quality that permits its use in critical aircraft transparencies. Windshields and canopies for the F-15, YF-16 fighters and bird-proof windshields for T-37 and A-37 aircraft were the first major aircraft applications of this high temperature, impact resistant thermoplastic. Extensive service use has revealed only one significant problem area, namely surface protection.

The simplest and lightest method of protection is to use a thin protective coating of a hard transparent polymer. Such coatings must have good abrasion, erosion and solvent resistance; they must be firmly adhered to the surface; they must not adversely affect the exceptional impact strength of polycarbonate; and above all, must be able to withstand the rigors of both flight and weather. Shortcomings of current protective coatings in service environments will be discussed.

Use of a non-structural layer of acrylic applied by fusion cladding directly to the surface of polycarbonate, as well as laminating glass or acrylic to polycarbonate with a flexible interlayer will also be reviewed. Applications of those various constructions to polycarbonate windshields and canopies of F-15, YF-16, T-37 and A-37, and B-1 aircraft will be described.

Finally, the promising new concept of direct fusion cladding of a tough polyurethane layer onto the surface of polycarbonate will be explained in considerable detail. Various screening tests, including high-speed rain erosion, ice crystal abrasion, gunfire and severe impact have shown that this new construction, called SIERRACLAD™, can greatly extend the utility of polycarbonate in transparencies for high performance aircraft.

INTRODUCTION

Polycarbonate has several distinct advantages for aircraft windshields and canopies, including high strength/weight ratio at elevated temperatures, outstanding impact strength, toughness, and formability into deep compound contours. On the other hand, polycarbonate is vulnerable to surface damage by abrasion, erosion, weather, and chemical solvents. Therefore, to fully realize its outstanding potential, polycarbonate must be given some form of surface protection. This can be provided in a number of ways, such as applying a thin protective coating, laminating-on a protective layer of glass or another plastic, or by direct cladding with another plastic. A thin protective coating permits the use of a monolithic design, with negligible weight penalty. To date, however, no coating is available that can meet all these rigorous requirements, particularly for protection of exterior surfaces of forward facing windshields of high speed aircraft. Each of the other solutions has its own set of advantages and problems or constraints, which will be explored later in this paper. First, a brief review of the basic properties of polycarbonate itself will be presented.

DISCUSSION

I. PROPERTIES OF POLYCARBONATE

Polycarbonate has a number of advantages that make it the optimum choice for the transparencies of high performance aircraft, where substantial aerodynamic heating, bird impact, or gunfire must be considered, and for which deeply contoured shapes are needed for maximum visibility and low drag.

A. Strength

Figure 1 compares the ultimate tensile strength of polycarbonate with as-cast and stretched acrylic, (Reference 1). At temperatures in the range 70 to 90°F, stretched acrylic is the stronger of the three materials, but polycarbonate's superior strength at higher temperatures is shown clearly. Also note that stretched acrylic starts to lose its toughness (K-factor) at temperatures much above 200°F and above 220°F it loses its shape (i.e., it begins to relax to its pre-stretched size). At 260°F, as-cast acrylic has a strength of only 750 psi. A practical upper limit for the operating temperature of polycarbonate is the onset of internal bubbling. This occurs at about 350°F for brief exposures, and 315°F for long-term heating.

Published data (Reference 2), in Figure 2 shows the extremely high tensile elongation of polycarbonate (greater than 100% in the temperature range of 0°F to above 250°F), which accounts for its extraordinary impact strength described below.

B. Impact

The extremely high impact strength of polycarbonate is probably its most publicized feature, (Reference 3). No other structural transparency material can match the 16 ft. lbs. per inch of notch achieved by 0.125 inch polycarbonate in Izod testing. This represents at least a five fold strength increase over stretched acrylic, which has a corresponding impact strength of 3 ft. lbs. per inch, and which, itself, is at least three times stronger than any other available aircraft transparency material.

C. Weathering

Report AFML-TR-72-117 (Reference 4), shows the effect of exposure to Arizona weather of unstressed, flat panels of polycarbonate. In less than one year, pitting and crazing had severely impaired visibility through the test panels. Other outdoor weathering tests conducted by General Electric, show a similar degrading influence of the natural environment. Data presented in Figure 2, shows that haze has increased to 14.4% in only one year, and increases rapidly with time. It is extremely important to note that this weather degradation is limited to the immediate surface, and therefore has little effect on tensile strength, ultimate elongation and impact strength. However, the optical effect is objectionable in aircraft transparencies.

D. Abrasion

All currently available transparent plastics are prone to marring and scratching to varying degrees. Taber abrasion data presented in Figure 3 shows that polycarbonate is inferior to the other commonly used aircraft transparency plastics in this respect. This is, of course, the primary reason for using the various surface protection schemes that are the subject of this paper. In the Taber test, abrasion damage is assessed by measuring haze. The lower the haze, the more abrasion resistant the material.

II. SURFACE PROTECTION

During the past five years, several methods of polycarbonate surface protection, listed below, have been evaluated by Sierracin and used on production parts for the Cessna A/T-37 Attack/

Trainer, McDonnell Douglas F-15 and TF-15 Advanced Tactical Fighter, General Dynamics YF-16 Light Weight Fighter, and Rockwell International B-1 Strategic Bomber. Those methods are:

Diffusion cladding with acrylic

Thin (0.5 mil) protective coatings

Acrylic facings laminated on with a flexible interlayer

Glass facings laminated on with a flexible interlayer

A brief chronology of the noted aircraft transparencies with emphasis on the particular method of protection employed follows.

A. Cessna A/T-37 Attack/Trainer Windshields

The initial bird-proof windshields of the T-37 Trainer which replaced the earlier acrylic non-bird-proof designs were bare monolithic polycarbonate. However, when these windshields were flown through clouds at high altitudes, they became hazy or translucent almost immediately, due to ice crystal abrasion. Acrylic-fusion cladding, (Reference 5), which McDonnell Douglas was then developing for their F-15 (and which will be discussed later in this paper) was tested at Cessna as a possible solution to the T-37 ice abrasion problem. However, the T-37 clad windshield failed the bird impact test, due to the embrittling effect that direct acrylic cladding has on polycarbonate. Next, several hardcoats were tried in service on the original monolithic polycarbonate windshields. These brittle, glass-like coatings provided a hard abrasion resistant surface but they peeled off after rather brief service, for reasons to be detailed later. Brittle hard coatings were also tried on polycarbonate canopies of the F-111 with similar results.

Accordingly, exterior coatings were abandoned for the T-37. At that time, Sierracin suggested that the large inventory of T-37 polycarbonate windshields could be upgraded by retrofitting them with the laminated-on acrylic faceply, using a process Sierracin had developed in 1972 for possible future use on F-15 windshields. This was tried, and after extensive laboratory qualification tests and bird impact tests, the laminated construction was adopted and is now in service on T-37's and A-37's. Two sheet interlayers (poly-vinyl butyral and ethylene terpolymer) and a cast-in-place silicone interlayer (Sierracin's S-100™) have been used successfully to bond the acrylic faceplies to the polycarbonate structural ply. The three constructions have passed all qualification tests, though only the PVB version has been produced in quantity to date. Figures 4 and 8 show the aircraft and the laminated windshield respectively.

B. McDonnell Douglas F-15/TF-15 Windshields and Canopies

Figure 5 shows the aircraft and Figure 9 the initial design of the F-15 windshield which was acrylic-diffusion-clad polycarbonate. It successfully met bird test requirements, but static tests performed by McDonnell Douglas and also high speed flight testing resulted in cracking of the acrylic outer layer. (More recently, experimental F-111 windshields incorporating acrylic-diffusion-clad polycarbonate outer plies, have shown similar tendencies in flight tests). Accordingly, in 1973 the F-15 windshield was changed to monolithic polycarbonate, .90 inches thick, using the thin protective coating already in service on F-15 canopies to protect both the exterior and interior surfaces.

Early F-15 canopies had been protected with a brittle, hard Sierracin coating similar to those evaluated by other suppliers on unsuccessful T-37 windshields. By the time the decision was made to use coated windshields on the F-15, a ductile coating more compatible with the large thermal expansion of the F-15 canopy had been developed and adopted, (Reference 6 presents a detailed discussion of protective coatings). This was Sierracote 230®. Shortly thereafter, an improved version of this coating, Sierracote 233® with superior weathering performance, was adopted on all F-15 transparencies. However, on the exterior surfaces, the weather resistance of Sierracote 233 still left something to be desired. Extensive laboratory tests have shown that S-233, like all other protective coatings evaluated gradually loses adhesion from the effects of ultraviolet radiation. Later, as more F-15 aircraft were flown in weather less gentle than that which prevailed during early flights at Edwards Air Force Base, it was found that rain erosion and ice crystal abrasion (remember the T-37) were quite effective in damaging or removing these coatings.

To overcome these inherent weaknesses of thin protective coatings, McDonnell Douglas has recently evaluated several acrylic laminated polycarbonate windshields fabricated with "crack-stopping" high temperature interlayers. Rapid thermal changes occurring in these screening tests caused unacceptably high "locked-in" stresses in the acrylic faceply which can cause early crazing and delamination. This concept, therefore, has recently been abandoned for F-15 windshields.

In October 1975, monolithic stretched acrylic was selected as the material for all F-15 transparencies until a completely satisfactory high temperature construction can be developed and put into production. It appears, therefore, that the ultimate solution has not yet been reached.

C. General Dynamics YF-16 Windshield/Canopy

One of two YF-16 light weight fighters is shown in Figure 6 and the deeply-contoured one-piece windshield/canopy is well illustrated by Figure 10. Sierracin formed ten parts from 0.38 inch monolithic polycarbonate, with Sierracote 233 protective coating on both surfaces. Optical quality was excellent and compared with F-15 experience, effects of rain erosion and/or ice crystal abrasion has been minimal. Nevertheless, rain erosion has gradually damaged the outer coating in the front-facing area, starting at the lower edge. Clearly, a substantial improvement will be needed for the production aircraft.

D. Rockwell B-1 Windshields

Figure 7 shows the B-1 supersonic bomber, and Figure 11 shows a set of Sierracin B-1 production windshields, (Reference 7). Electrical anti-icing and static drain requirements dictated a glass faceply for these large, curved, laminated polycarbonate windshields. Corning Chemcor™ thin chemically strengthened glass is used (.050 inch thick). Figure 12 shows the cross-section. Note that the interior surface is protected by Sierracote 233 coating.

The glass faced construction of the B-1 windshield provides excellent rain erosion and abrasion resistance for the polycarbonate structural plies. This construction tends to be costly and it is presently limited to simple contours, but it provides an effective means of protecting polycarbonate for certain applications, particularly where the glass is required or highly desirable for reasons other than polycarbonate protection, as is the case with the B-1 windshield.

III. EVALUATION OF EXISTING SURFACE PROTECTION

Before describing the advanced polyurethane-clad polycarbonate (Sierraclad) now under development at Sierracin, it is important to present certain explanations and test data relating to the various protection arrangements already discussed, so as to provide a basis for evaluating the results of extensive testing of Sierraclad, which appears in the next section of this paper.

A. Acrylic-Diffusion Cladding

The "embrittling" effect of diffusion-clad acrylic upon the polycarbonate has already been mentioned. It results from the fact that as-cast acrylic is itself brittle, and when it is

intimately bonded to polycarbonate, a crack which begins in the acrylic tends to propagate unimpeded into the polycarbonate causing the latter to fail in a brittle manner, thus effectively negating its normally outstanding toughness. Using the Sierracin Dart Impact Tester shown in Figure 13, the coupons seen in Figure 14 were impacted. Note the brittle fracture of the thick diffusion-clad sample (0.75" polycarbonate clad with 0.060" and 0.187" acrylic), at an impact which did not fail a much thinner piece (0.32") of plain polycarbonate. As will be reported later, all Sierraclad constructions are evaluated in this same impact test.

B. Protective Coatings

Mention has been made of the weather degradation that has been evidenced by all thin protective coatings used to date. The exterior surface of aircraft canopies and windshields encounter many environmental extremes in service, such as rapid and large temperature changes, solar irradiation, high humidity, and combinations thereof. Sierracin, therefore, tests all potential protective materials in accelerated weathering tests which attempt to duplicate these environments as closely as possible within a reasonable time span. Weatherometer testing is perhaps the most indicative of actual service conditions, as it combines heat, humidity, UV exposure and temperature cycling in FTMS 406, Method 6024 as follows:

One 24-hour cycle consists of:

2 hours fog, followed by

2 hours UV radiation and hot air (130°F), followed by

2 hours fog, followed by

18 hours UV radiation and hot air

By comparing data obtained on other development programs, with natural weathering tests at Sierracin, we consider ten days of these accelerated weathering cycles to be roughly the equivalent of one year outdoor exposure in Southern California. This test was of immeasurable help in optimizing the weathering properties of the basic Sierracote 233, as well as in establishing the most effective type and concentration of UV absorbers in the final formulation. Our tests have shown that any additional UV absorber degrades other properties of the coating and adds nothing to its capacity for enduring weather exposure. This weathering effect takes the form of a progressive loss of adhesion, apparently due to UV, reacting with the surface of the polycarbonate and photo-oxidizing it. This would appear to be an intrinsic shortcoming of thin coatings for protecting the exterior of a polycarbonate canopy or windshield.

Frequent monitoring of naturally weathered parts, as well as those on flight test F-15 aircraft at Edwards Air Force Base, suggests that the durability of the exterior coating is of the order of eighteen months to two years. On the other hand, Sierracote 233 and similar coatings should fare much better on interior surfaces due both to the obvious physical protection from the rigors of weather, and the fact that polycarbonate effectively blocks out UV. Evaluation of all parts that have S-233 protection on cockpit surfaces proves the point, as no loss of adhesion or deterioration of the coating has been observed.

Comparatively brief doses of high speed rain erosion or ice crystal abrasion can damage or remove protective coatings on forward facing polycarbonate, as shown by T-37, F-111, F-15 and YF-16 experience. No doubt the known degradation of coating adhesion from weathering contributes to this tendency. We have not yet completed rain erosion and ice crystal abrasion tests of pre-weathered coatings, but we strongly advise that weathering be included in all future evaluations of this type.

C. Acrylic Laminating

As mentioned earlier, laminating an acrylic faceply onto the front surface of T-37 polycarbonate windshields has been a successful solution to the earlier ice crystal abrasion problem. To date, Sierracin has produced more than 200 T-37 and A-37 windshields of this design, using PVB interlayers and some of them have been flying since early 1973. In addition, five experimental versions using Ethylene Terpolymer interlayer have entered flight evaluation. More recently, a third variant, using Sierracin's S-100 cast silicone interlayer has been qualified. All three constructions have passed bird tests at 250 knots. Thus, for subsonic applications, acrylic/polycarbonate laminated windshields are successful.

When this construction was tested by McDonnell-Douglas for possible use in windshields for their supersonic F-15, simulated aerodynamic heating produced varying degrees of delamination and also was shown to produce permanent tensile stresses in the as-cast acrylic faceply, sufficient to indicate early crazing and eventually cracking in service. The fast-moving F-15 program simply could not endure the rain erosion/ice crystal abrasion problem for long enough to await solutions to these problems encountered with the laminated construction, or to develop alternate solutions. Therefore, in late 1975 the decision was made to produce monolithic stretched acrylic windshields and canopies for F-15 aircraft, as an interim measure until a construction can be developed which will meet the full temperature/performance envelope of F-15 aircraft, while providing satisfactory resistance to erosion and abrasion.

IV. POLYURETHANE FUSION CLAD ONTO POLYCARBONATE

In early 1975, several related breakthroughs in Sierracin's continuing research resulted in a promising new concept for protecting polycarbonate from abrasion, ultraviolet, moisture, high speed rain erosion, ice-crystal abrasion, and chemical attack, while preserving the outstanding formability and impact resistance inherent in the polycarbonate. This new construction, which will hereafter be referred to by its trademark "SIERRA-CLAD", consists of a thin (.03 to .05 inch) polyurethane cladding attached to one or both surfaces of polycarbonate sheet, by direct fusion bonding. There is, of course, no reason why significantly thicker or thinner clad sheets could not be used. This polyurethane cladding, in fact a family of materials with a broad range of properties, was custom-formulated by Sierracin chemists to meet the specific needs of this application. This cladding, compared to conventional thin coatings or films, provides vastly improved protection to the polycarbonate surface from the damaging ultraviolet radiation in sunlight. Figure 15 compares UV transmission in different spectral regions.

The remainder of this paper will describe the extensive testing completed to date in the development of this new product, and will compare its performance with that of other transparent materials and protective coatings described earlier. These tests include accelerated weathering, humidity, dart impact, full-scale bird impact, gunfire, thermal stability, forming, high-speed rain erosion, simulated ice-crystal and dust abrasion, chemical attack, and light transmission and haze measurements. The data reported herein, relates to three of the several Sierracin polyurethane formulations evaluated to date; namely, "Clad-4", "Clad-5", and Clad-8".

A. Accelerated Humidity Exposure

Some polyester-based urethanes have suffered "reversion" (i.e., hydrolytic breakdown) under prolonged humidity. For this reason, only the stable polyether-based urethanes have been used in this program. Excellent hydrolytic stability has been demonstrated by exposure to 30 days at 200°F and 98 to 100% RH; the Shore D hardness dropping only 3 points for some formulations (Clad-8), and zero for others (Clad-4 and 5). This aggressive test, designed to determine the potential reversion resistance of urethanes, was established jointly by the U.S. Navy and McDonnell Douglas. Each formulation successfully met the test requirements (maximum drop in hardness of 3 points), without the use of any stabilizing additive.

B. Accelerated UV Exposure

Clad-8 formulation (highest impact strength of those evaluated), was exposed to high intensity UV for ten days. No degradation or color change was observed. This contrasts with a typical aromatic polyester formulation which bubbled and yellowed under the same test conditions, an area masked from UV for comparison remained unchanged. This emphasizes the UV stability of Sierracin polyether urethanes compared to conventional polyester urethanes.

C. Accelerated Weathering Exposure

Weathering of three of the more promising urethane formulations (Clad 4, 5 and 8) in the standard FTMS 406 test, revealed negligible or no effect after ten days. Continuing the exposure to thirty days revealed some tendency to haze and softening of the surface when solvents were applied. Clad-8 was particularly susceptible, Clad-4 exhibited only slight effect and Clad-5 was unchanged. Accordingly, UV stabilizers and other additives have been investigated with excellent results to date.

Additional tests are in progress using even more severe test conditions; namely, continuous high humidity of 98% to 100% RH, and continuous UV at a constant temperature of 200°F. Results to date have shown very good performance with the appropriate additives, although this phase of the investigation is by no means complete. This modified test appears to be at least five times as severe as the standard FTMS 406.

D. Impact Tests

Dart impact test data in Figure 16, of monolithic urethane clad materials, demonstrates the versatility of this family of urethanes, and compares them to as-cast and stretched acrylics. Note that Clad-8 and Clad-4 monolithic sheets are far more impact resistant than even stretched acrylic. As we have seen, three A-37 windshields protected on both sides with the Clad-8 formulation successfully "bounced" a 4-lb bird at 250 knots. These Sierraclad parts did not crack or spall and visibility after impact was preserved. Figure 17 shows one of these Sierraclad windshields after bird impact. The rectangle marked on the windshield corresponds to the area of impact of the bird and clearly demonstrates the excellent retention of visibility. Figure 18 shows the cross-section.

E. Ballistic Tests

Gunfire performance of the Sierraclad construction was compared to as-cast, stretched acrylic and also monolithic poly-

carbonate. 30-06 ammunition was fired from 30 yards at specimens mounted at an angle of thirty degrees. Extensive shattering and damage occurred to stretched acrylic causing severe impairment of the field of vision; there was severe cracking of as-cast acrylic. No delamination, spalling or cracking occurred with Sierraclad. Damage was highly localized and identical to that obtained with bare polycarbonate; in both cases excellent visibility prevailed. Figure 19 shows typical results of these ballistic tests.

F. Thermal Stability

Monolithic sheets of three urethane formulations, (designated Clad-4, 5 and 8 respectively) were exposed to temperatures ranging from 70° to 300°F for one hour. Hardness measurements were taken and compared with as-cast acrylic (MIL-P-8184) and polycarbonate. Figure 20 presents the data and shows the rubber-like and varied hardness of each urethane. Accordingly, a severe thermal gradient test was run on a formed part (48" x 10") to determine if the Clad-8 formulation could withstand extreme temperatures (above 300°F) and rapid temperature changes, without visual deterioration. A test beam (A-37 cross-section) was formed to a typical fighter windshield radius and strapped to a wooden support as shown in Figure 21. Using electric heating blankets and then rapid carbon dioxide cooling, the beam was subjected to three cycles of the most severe aspect of the F-15 windshield test program, including the Mach 2.5 thermal profile shown in Figure 22. No delamination, bond deterioration or visible degradation of the urethane cladding occurred. As we have mentioned earlier, there were high stresses locked into the acrylic faceply of laminated polycarbonate after exposure to Mach 2 temperatures, which can result in early crazing when subsequently weathered. Similar stresses are no doubt generated in the urethane cladding, but these materials suffer no crazing or other undesirable effects at those stress levels or at significantly higher stress, as is shown by test results which appear later in this paper.

G. Formability

To be formable, a material such as Sierraclad must be able to stretch considerably at forming temperatures. The tensile elongation data shown in Figure 23 indicates good formability for these materials. A simple but practical demonstration of formability are the small domes shown in Figure 24, fabricated from flat Sierraclad sheets.

H. Abrasion and Erosion Resistance

Sierraclad has good erosion and abrasion properties as a result of the inherent toughness of the urethane polymeric

structure. Urethanes are, in fact, widely used for abrasion and erosion protection of other materials, in a variety of industrial equipment. Specific abrasion and erosion tests of Sierraclad are presented below.

Taber Abrasion

Figure 3 compares the results obtained on Sierraclad 4 and 8 and other transparent plastics subjected to the standard Taber test. Polycarbonate without any surface protection developed extreme haze (over 50%). Stretched acrylic, widely used on fighter aircraft, showed haze of over 35%. The Sierraclad formulations tested were superior to both stretched and as-cast acrylic as well as bare and coated polycarbonate developing haze of 12% for the Clad-4 formulation and 18% for Clad-8.

Rain Erosion

Results of simulated high-speed rain erosion testing at the Air Force Materials Laboratory, Dayton, Ohio, are presented in Figures 26, 27 and 28. The materials used in this investigation were evaluated in 1 in./hr. simulated rainfall, using rain droplets of 1.5 and 2.0 mm diameter. The specimens are attached to the leading edges of a horizontally mounted propeller blade which rotates at high rpm. This test does not exactly predict the amount of erosion that will occur in service during the same time interval. However, it has been shown quite useful in rating materials in the relative order of their probable service durability. Only the data from a 30° angle of impingement is presented because this approximates the bluntest windshield angle of most fighter aircraft.

Exposure time has been plotted vs percent haze rather than the more traditional light transmission, as increase in haze more accurately correlated with vision impairment. (A small loss in light transmission will have negligible effect on a pilot's ability to fly an airplane, but direct sun or lights at night viewed through a hazy windshield can be hazardous). Figure 25 shows the appearance of various degrees of haze for reference.

Figure 26 presents the data obtained at 345 mph, which is the speed specified for survival of the exterior coating on the windshield/canopy of the YF-16. At this speed, Sierracote 233 protective coating was largely eroded away after 30 minutes, while all the other materials tested were still in satisfactory condition when the test was terminated at 3 hours. (As-cast acrylic was stopped arbitrarily after one hour; however, this test indicates that it probably would have been in good condition after 3 hours). Especially noteworthy is the exceptional performance of Sierraclad-4 which showed no measurable change after 3 hours of rain erosion.

Increasing the velocity to 500 mph readily demonstrates in Figure 27 the limitations of current thin protective coatings. S-233 was removed in 5 minutes, which is typical of all coatings tested to date from various manufacturers. Much like polycarbonate, the more ductile urethanes absorb the impact of rain at high speed with very little or only moderate increase in haze, while the more brittle acrylic suffers a seven-fold increase of haze in 3 hours.

Increasing the velocity further to 600 mph results in the rapid development of high haze for all materials tested. After 30 minutes exposure, the following data, shown in Figure 28, was obtained:

	Haze	Rating	Light Transmission	Rating
Polycarbonate	14.4%	1	85.0%	3
As-cast Acrylic	18.8%	2	89.6%	1
Sierraclad-4	21.4%	3	86.0%	2
Sierraclad-8	26.4%	4	79.4%	4

Note that haze of all materials tested is too high for safe vision after this test. It is important also to note that the standard method of measuring the effects of rain erosion tests--light transmission, would have indicated that all four of these materials were still quite safe (i.e., 79.4% light transmission is entirely adequate for an aircraft windshield). Also, light transmission indicates different relative performance than the more meaningful haze readings adopted at Sierracin. For example, light transmission rates polycarbonate as Number 3, whereas haze shows it survived with the best residual vision and, therefore, is rated Number 1. Also, acrylic suffered only a very small change in light transmission (3.4% from an original 93% to 89.6%), but it is certainly not flyable with a high haze of 18.8%. Transmission simply does not measure the sort of damage that occurs from rain erosion, which is why Sierracin adopted haze as its criterion.

Ice and Dust Erosion

In addition to the rain erosion testing, the abrasive effects of flight through high altitude clouds (ice crystals) were simulated at Sierracin by the equipment shown in Figure 29. Common salt closely resembles the hardness of ice on the MOH scale. This hardness is generally referred to as the scratch hardness and is defined as the ability of a material of one hardness level to scratch a material of a lower hardness level. Accordingly, salt entrained in an air stream striking a coupon at near-sonic velocity at 25°F was used to indicate the effect of ice crystal abrasion. As in rain erosion testing, an impingement angle of 30°

was used and haze was also measured to compare the effect of different materials. Rain erosion testing, however, is continuous in that a constant rainfall rate is used, but the salt test is not continuous and consists of a number of separate and discrete blasts. After viewing numerous samples with haze ranging from 1 to 30% haze, we chose 10% haze as representing the upper limit that could be tolerated from a safety of flight standpoint. On this basis, we have used the number of cycles (one second each) of salt blast to produce 10% haze for comparison of the various materials. Figure 25 shows the effect of various degrees of haze on visibility. Figure 30 shows that at 25°F, uncoated polycarbonate reaches 10% haze after only one cycle, whereas, as-cast (MIL-P-8184) acrylic withstood 32 cycles before 10% haze occurred, and stretched acrylic reached this limit after 24 cycles. Clad-4 is superior to stretched acrylic, while Clad-8 was not quite as good as the as-cast acrylic. Under these test conditions, Sierracote 233 provides little protection to polycarbonate. Data should be compared to that obtained with stretched acrylic as it provides a familiar standard of performance in this test and is widely used. Inasmuch as we know of no complaints of ice-crystal abrasion with this material, which has been used as an aircraft transparency for many years, it is shown as "acceptable performance".

Data is presented in Figure 31 for tests performed at 75°F but ice crystal impact at this temperature is probably not realistic. At 75°F, Clad-4 is superior to stretched acrylic, whereas Clad-8 is inferior, although this level of resistance might still be satisfactory in service.

Windshields are also subject to abrasion by airborne dust, especially at supersonic speeds. Therefore, this same salt blast test was run at elevated temperatures. The upper limit of the YF-16 thermal profile, 275°F, was selected as the next test temperature, as shown in Figure 32. Clad-4 was superior to all other materials; after 40 cycles it still showed less than 10% haze. Clad-8 (12 cycles) was almost as good as MIL-P-8184 acrylic (15 cycles) and bare polycarbonate was poorest (2 cycles). Stretched acrylic could not be tested under these conditions, as severe shrinkage (relaxation) occurs above 25°F.

The upper design limit for the F-15 windshield at Mach 2.5 is 345°F, so this temperature was selected for tests reported in Figure 33. Polycarbonate was poorest and Clad-4 was best in performance. The less heat-resistant Clad-8 was clearly out of its element at 345°F, showing performance no better than bare polycarbonate. Again, stretched acrylic could not be tested at this temperature. S-233 coated polycarbonate was included in these tests, but it must be realized that any protection it provides will be of short duration under these conditions.

I. Craze Tests

Bare polycarbonate is known to be attacked by various solvents at zero and moderate stress levels, (Reference 8). Thin protective coatings can and do offer excellent solvent protection to polycarbonate, but service experience and the tests described above have shown that weather, rain erosion, ice and dust abrasion can make this protection temporary.

Tests were performed on the three polyurethane cladding formulations described herein, at stresses up to 5,000 psi, using such aggressive solvents as; toluene, ethyl acetate, acetone, lacquer thinner, methylene chloride. No craze or degradation was observed, confirming the known chemical stability of these materials.

IV. SUMMARY

The multiplicity of designs in which polycarbonate has been used in windshields and canopies of a number of aircraft has, as we have seen, necessitated a considerable amount of work in the field of surface protection. Sierracin's extensive research in this area has shown that there is no easy answer to the problems described and that there exists a great need for durable and simple methods to protect polycarbonate surfaces in aircraft applications.

Intensive laboratory testing of the new SIERRACLAD concept has shown it to be a very promising potential solution to some or most of the problems described in this paper. However, this testing is by no means complete at this time, and in any case, there is no substitute for "real-world" flight service in proving any new material or design concept.

The accomplishments to date are summarized below:

(1) Formulation of transparent thin sheets of urethanes which when fusion bonded directly to polycarbonate provide a high degree of surface protection without affecting impact strength.

Specifically, urethane cladding provides protection against:

Rain Erosion
Ice Crystal Abrasion
Abrasion
Ultraviolet Solar Radiation
Chemical Solvents
High Temperature Bubbling

(2) Fabrication and successful bird testing of three Sierraclad A-37 windshields.

Future development will include:

(1) Effect of weathering on impact, abrasion, erosion, etc.

(2) Long-term natural weathering

(3) Correlation of chemistry, elongation and formability

(4) Impact studies related to formulation and thickness

(5) Process optimization and upscale

(6) Formability of simple and compound curved Sierraclad transparencies

(7) Repairing and polishing

We eagerly invite your assistance in making Sierraclad a service-proved product, available to the aircraft industry at large.

REFERENCES:

(1) "Polycarbonate for Advanced Aircraft Transparencies", by David L. Voss; presented at the Air Force Materials Symposium, Transparent Materials, Dayton, Ohio; 24 June 1969.

(2) Anon.; "Lexan Polycarbonate Performance Data"; General Electric Company

(3) "Aircraft Transparency Applications of Polycarbonate", by William A. Miller; presented at the Optical Transparency Symposium, Royal Aeronautical Society, London England; 9 June 1971.

(4) "Design Criteria Transparent Polycarbonate Plastic Sheet", Technical Report AFML-TR-72-117; August 1972; by Richard S. Hassard; Goodyear Aerospace Corp., Litchfield Park, Arizona.

(5) U.S. Patent 3,810,815, "Transparent Laminate"

(6) "Protective Coatings", by David L. Voss; presented at the Conference of Transparent Enclosures, Las Vegas, Nevada; 5 - 8 February, 1973

(7) "Polycarbonate Aircraft Transparencies", by William A. Miller; presented at the 6th National Sampe Technical Conference, Dayton, Ohio; 8 - 10 October, 1974.

(8) "Plastics For Aerospace Vehicles - Part II, Transparent Glazing Materials": MIL-HDBK-17A; January 1973

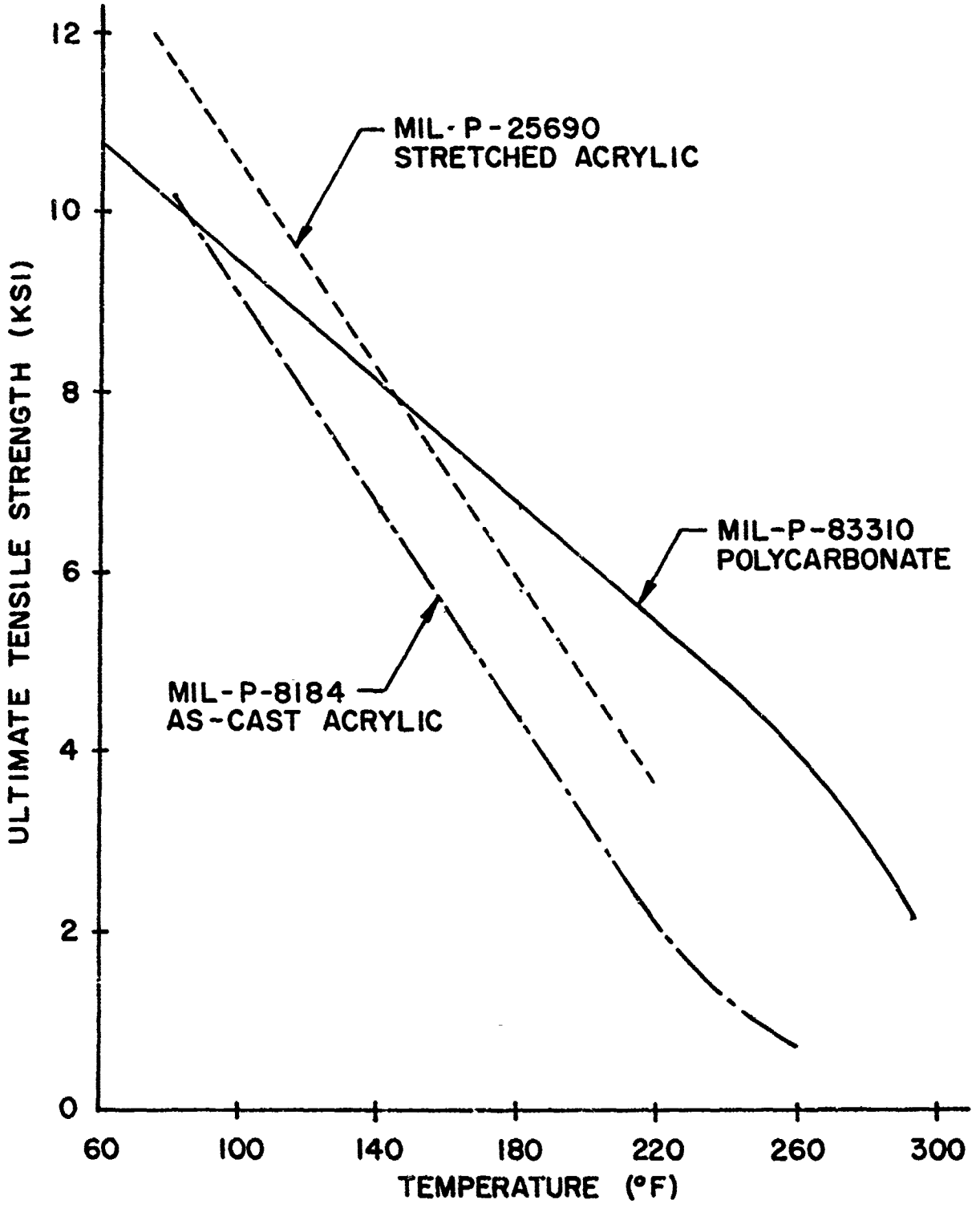


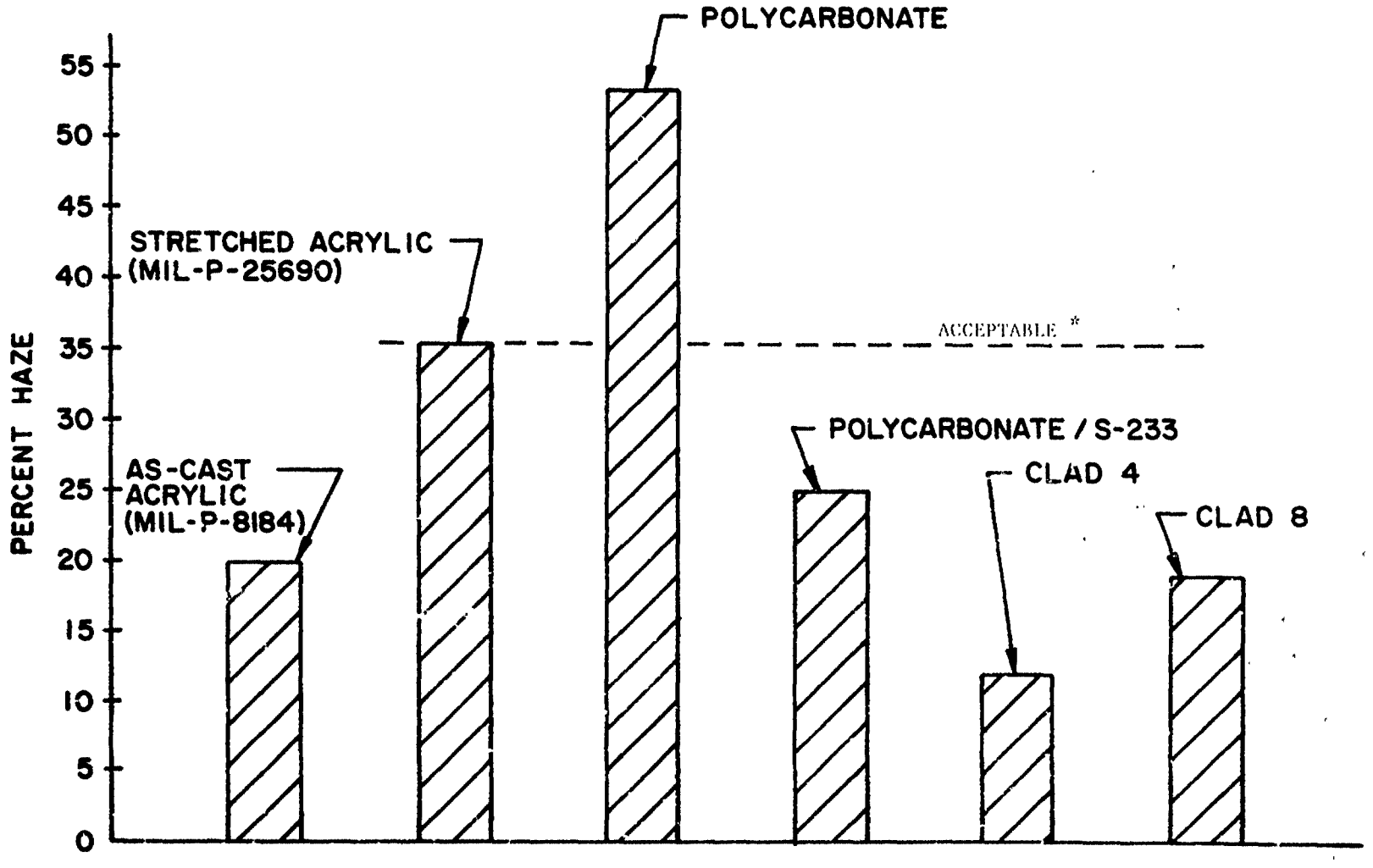
Figure 1. Ultimate Tensile Strength vs Temperature

MATERIAL: LEXAN POLYCABONATE 103-112 RESIN

PROPERTY	NATURAL OUTDOOR WEATHERING - MONTHS							
	0	6	12	18	24	36	48	60
HAZE, %	3.6	3.7	14.4	12.2	17.0	21.2	28.3	29.9
LIGHT TRANSMISSION %	83.3	83.6	82.1	82.2	81.8	81.4	80.4	78.7
TENSILE STRENGTH, PSI								
ULTIMATE	10840	10160	8710	9100	9200	8930	8720	7980
ULTIMATE ELONGATION	118	114	93	92	100	94	95	70
IZOD IMPACT STRENGTH,								
FT-LBS/IN 1/8" THICKNESS	12.0	14.8	--	13.5	16.2	11.0	15.5	16.1

(DATA FROM GENERAL ELECTRIC)

Figure 2. Outdoor Weathering Effects on Polycarbonate



* Stretched acrylic provides satisfactory performance in service and is, therefore, used as a standard for comparison.

Figure 3. Taber Abrasion



Figure 4. CESSNA A/T-37 Attack Trainers

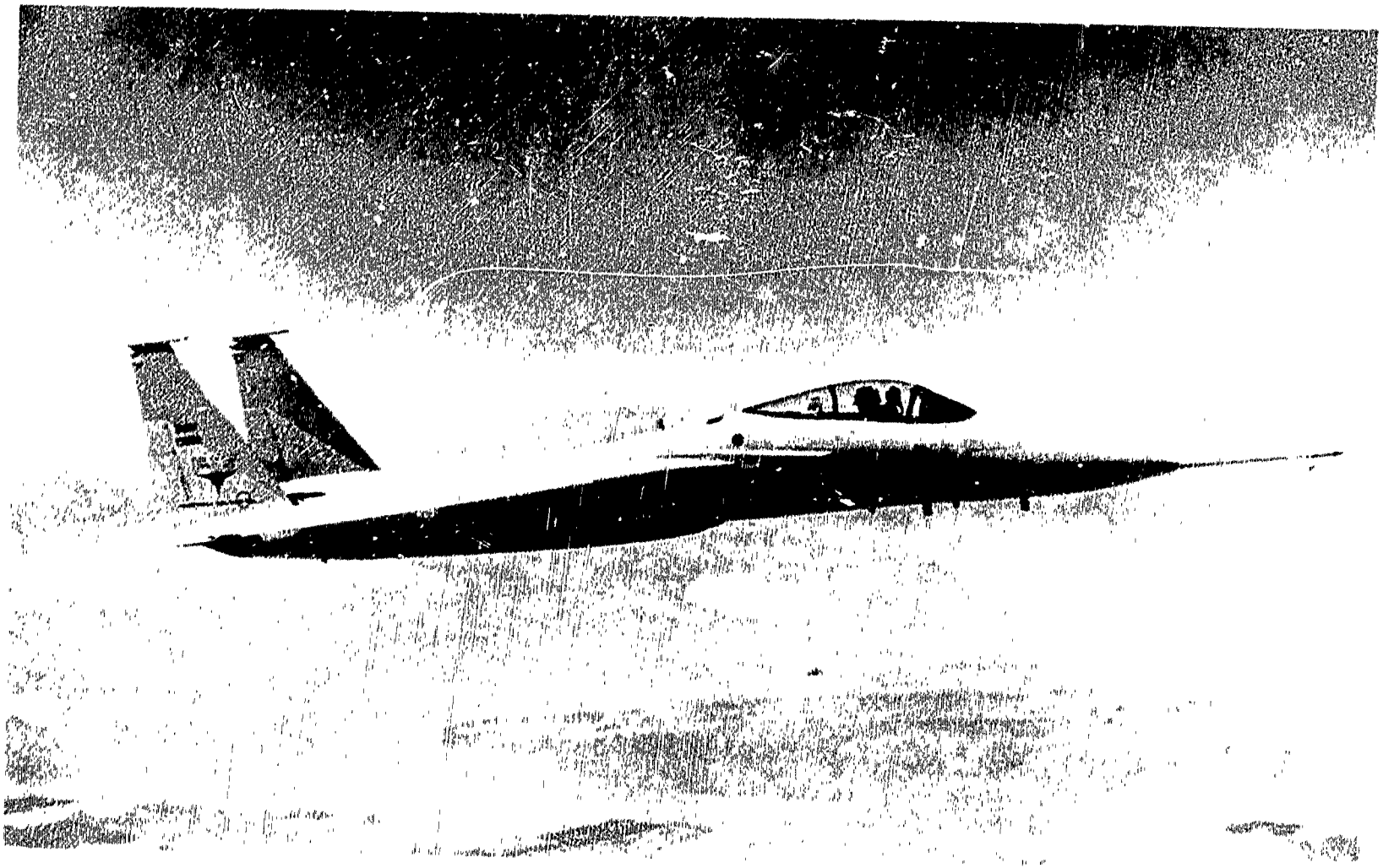


Figure 5. McDonnell Douglas F-15 Eagle



Figure 6. General Dynamics Lightweight Fighter YF-16

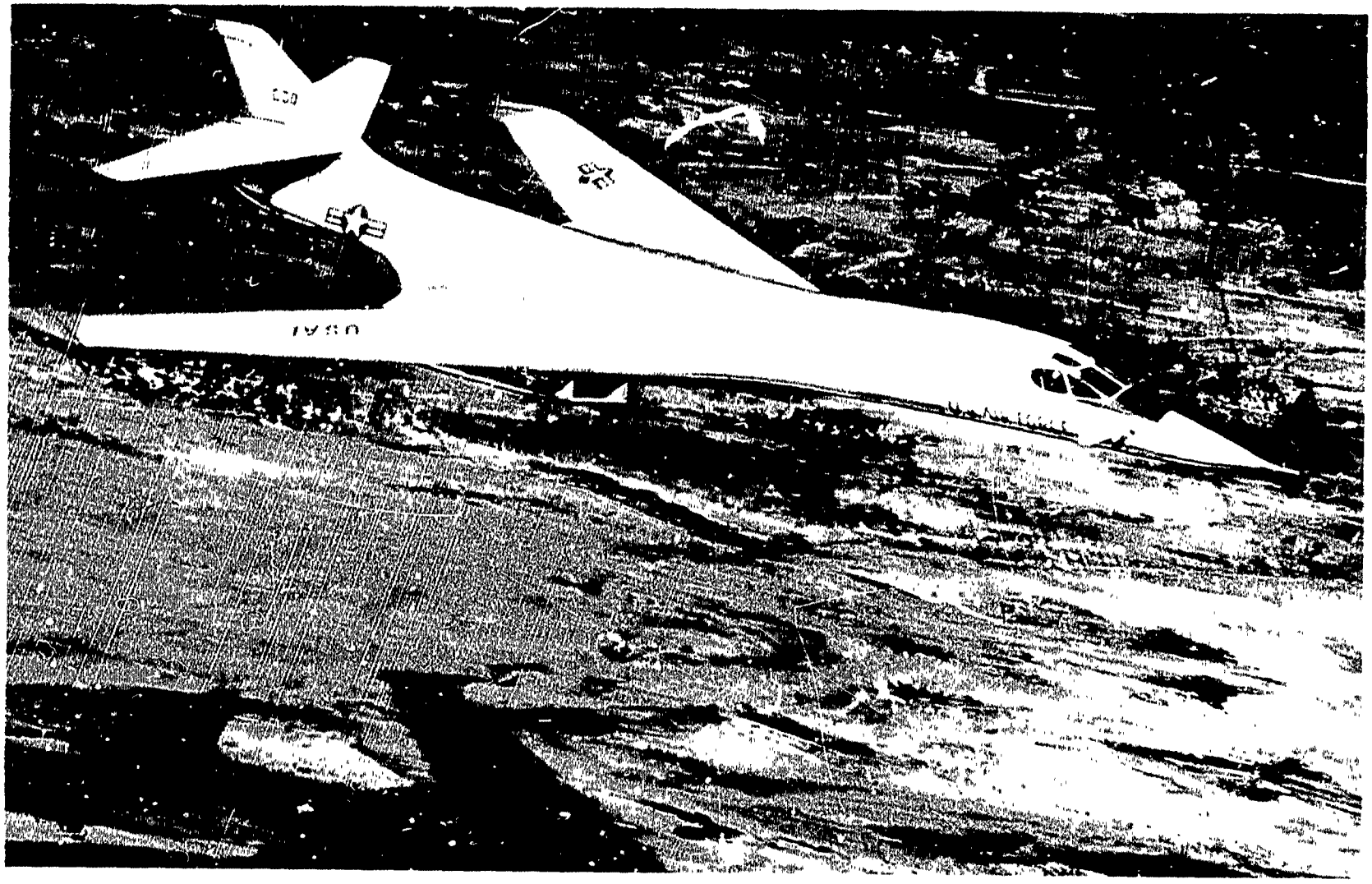


Figure 7. Rockwell International B-1 Strategic Bomber



Figure 8. A/37 Windshield Acrylic-Polycarbonate Laminate Construction

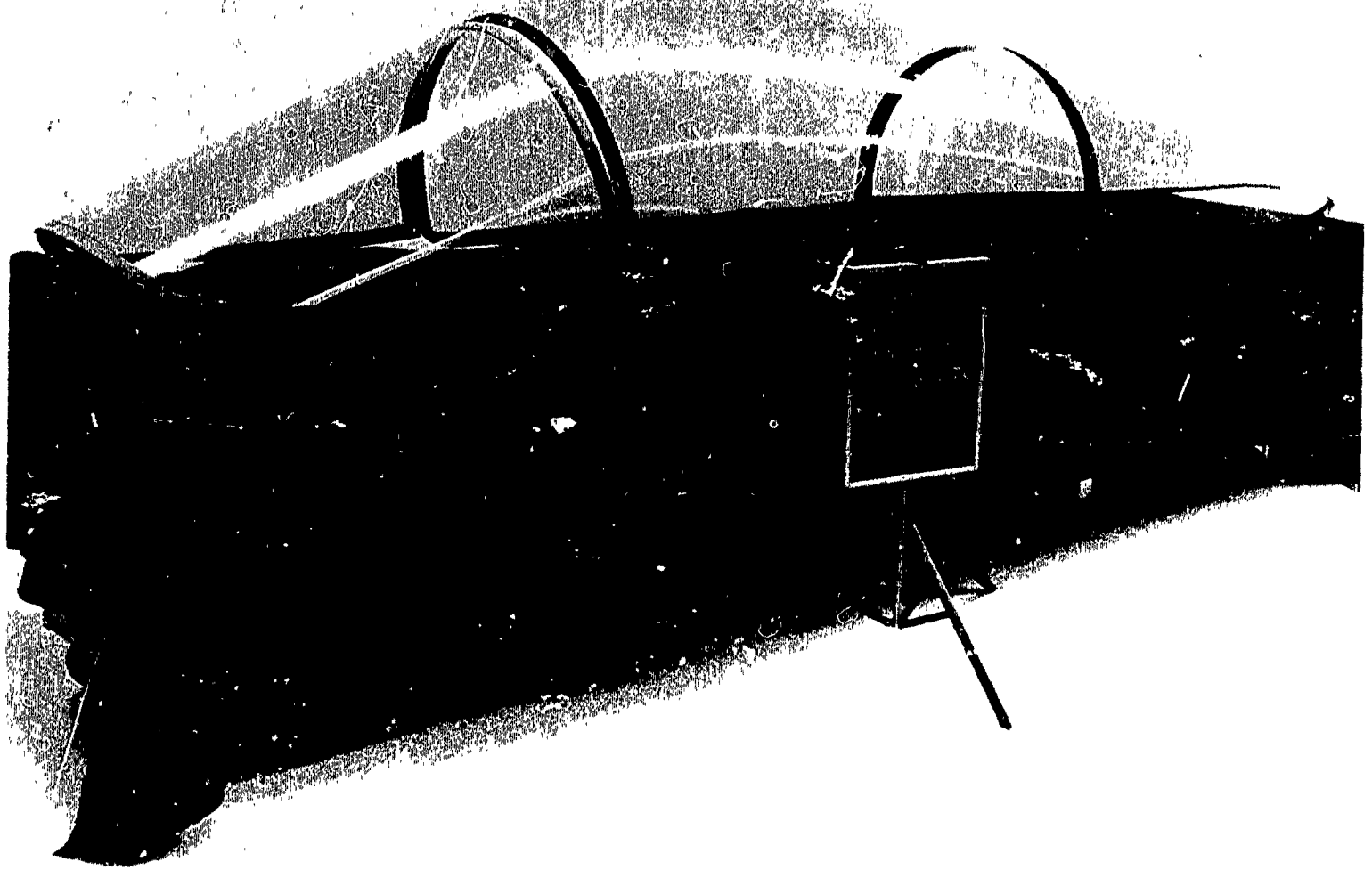


Figure 9. F-15 Polycarbonate Windshield Foward and Aft Canopies



Figure 10. YF-16 Single Piece Polycarbonate Windshield/Canopy



Figure 11. B-1 Bomber Windshields Glass-Polycarbonate Composite Construction

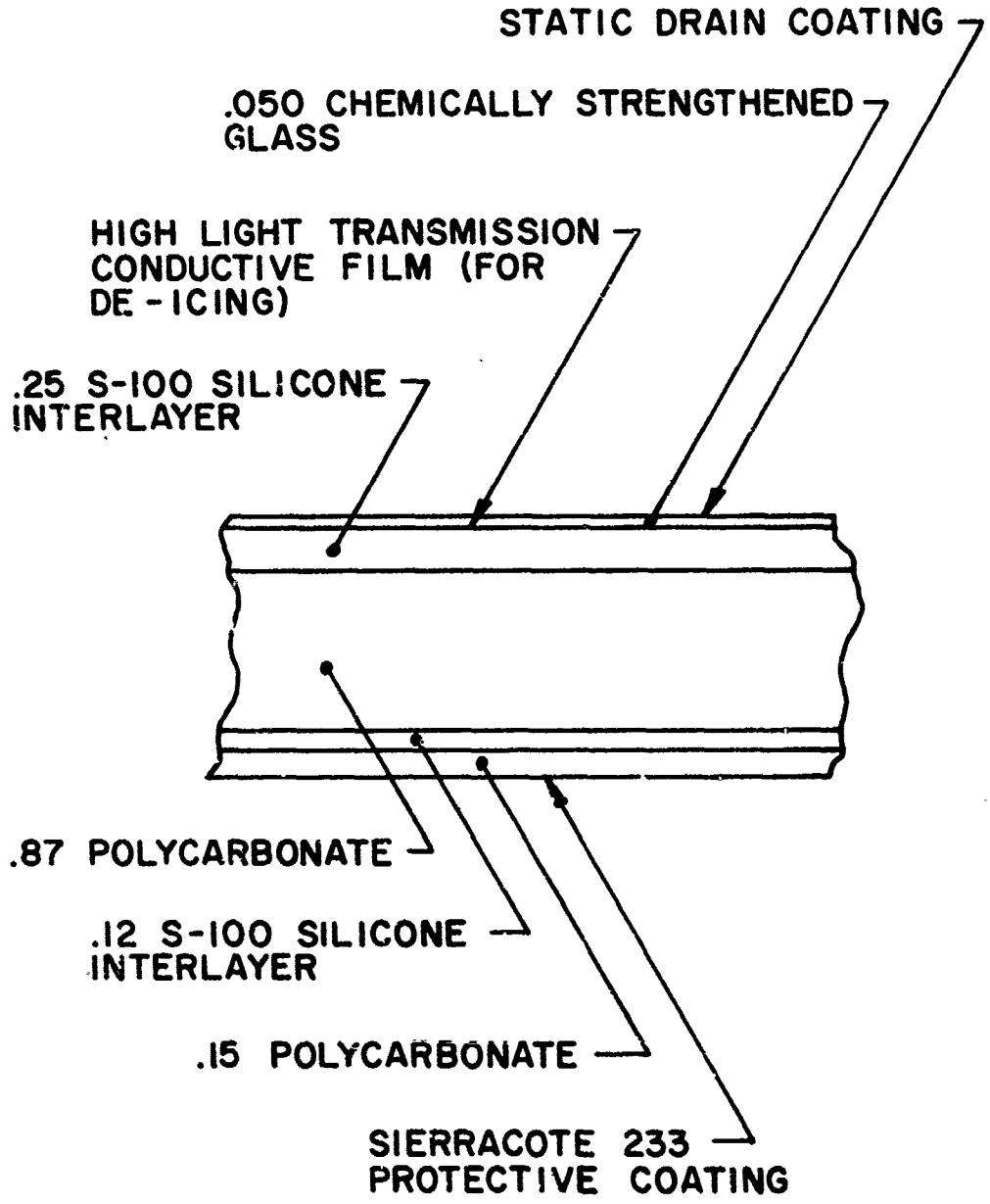


Figure 12. B-1 Windshield Cross Section

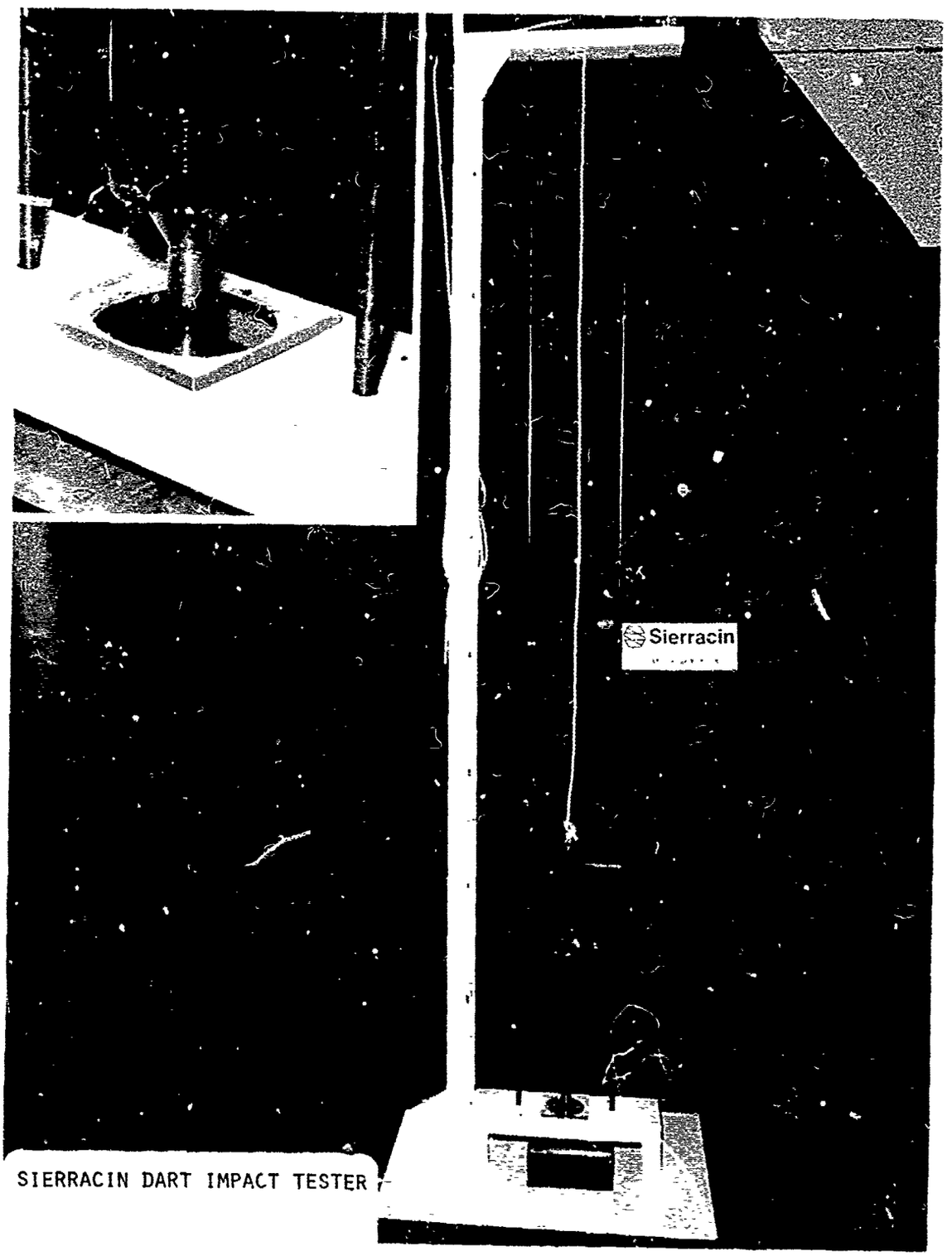


Figure 13. 1-Inch Diameter Dart Capable of Up to 330 Ft-Lbs

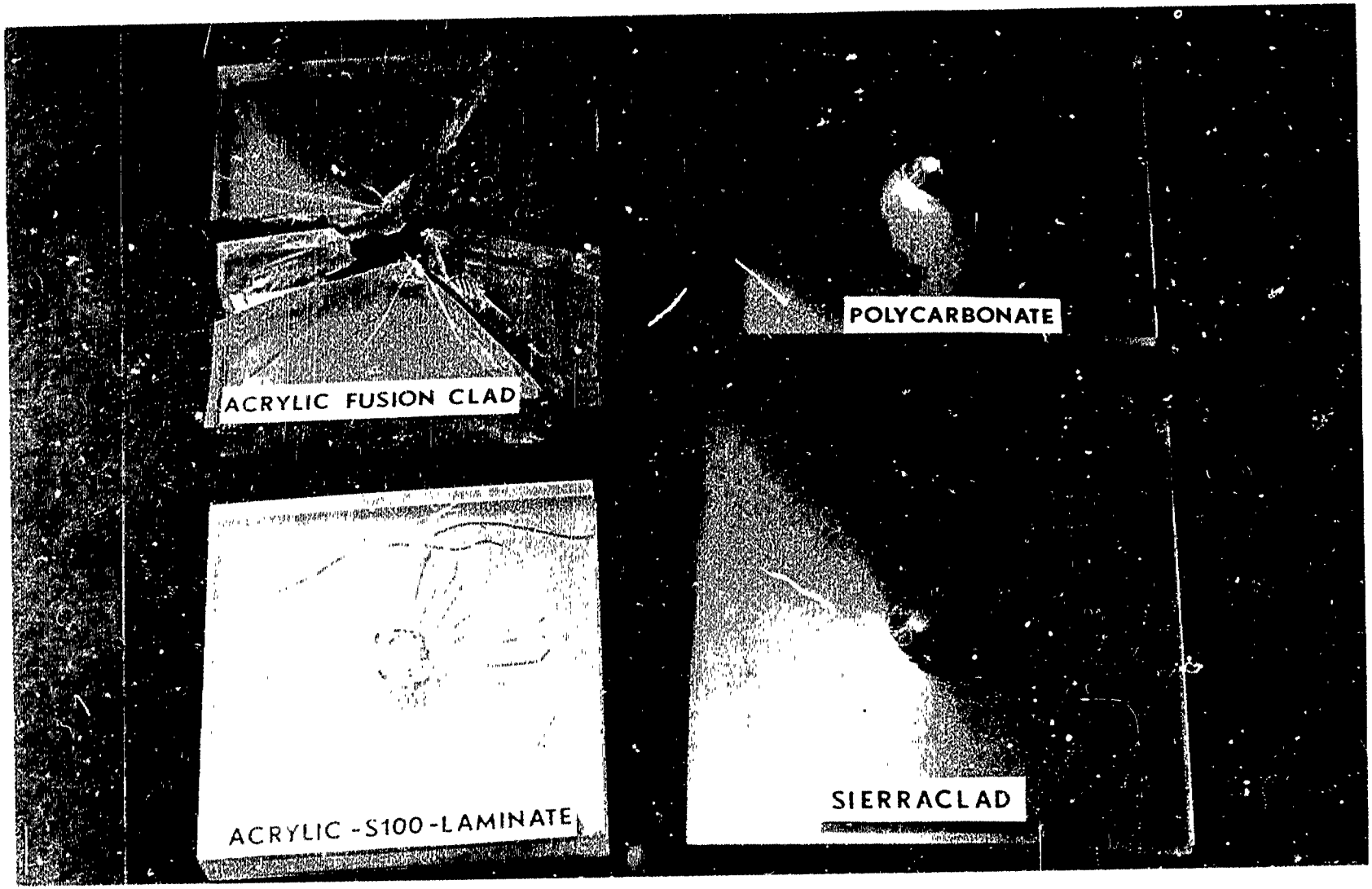


Figure 14. Dart Impact Tests

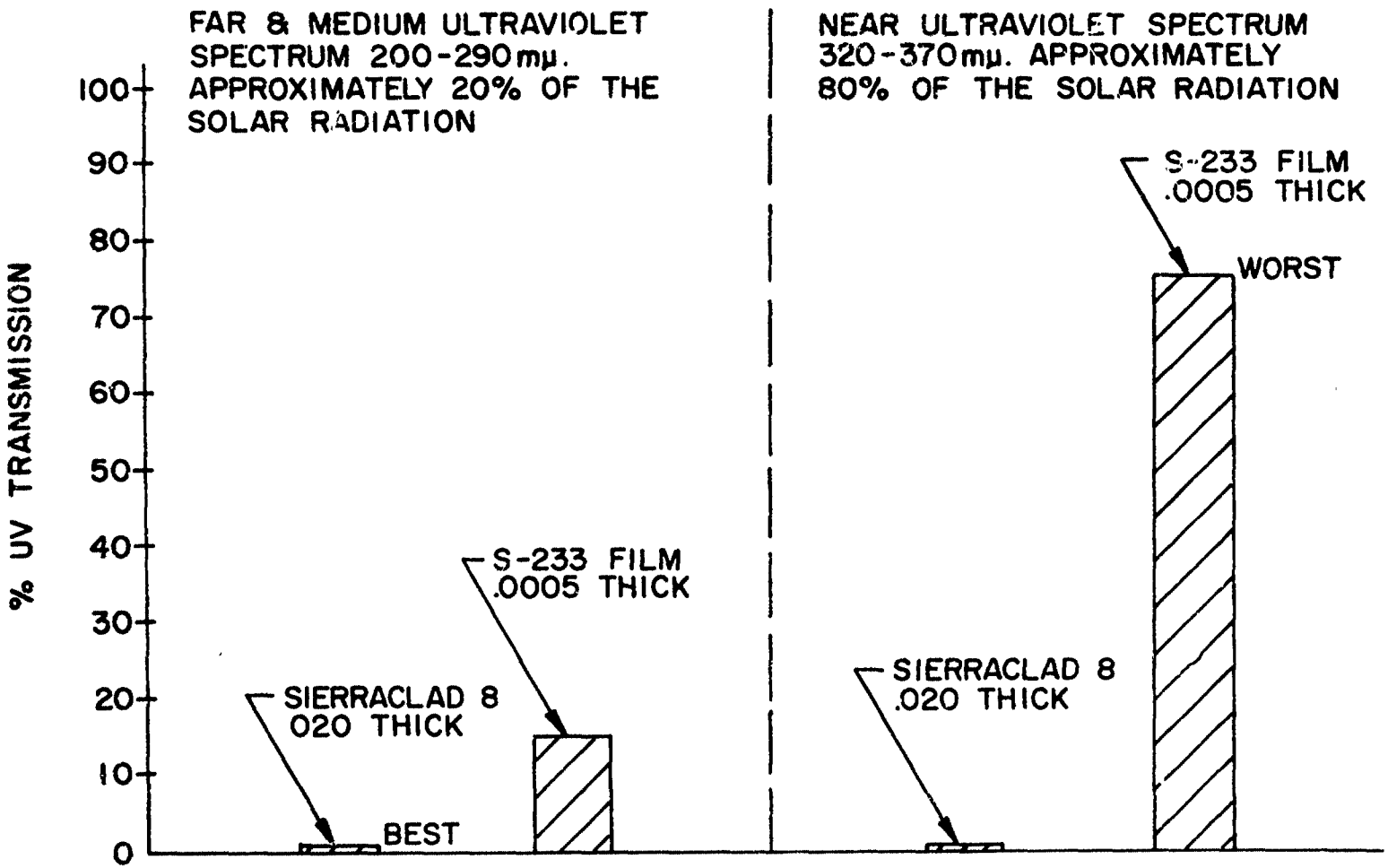


Figure 15. UV Transmission

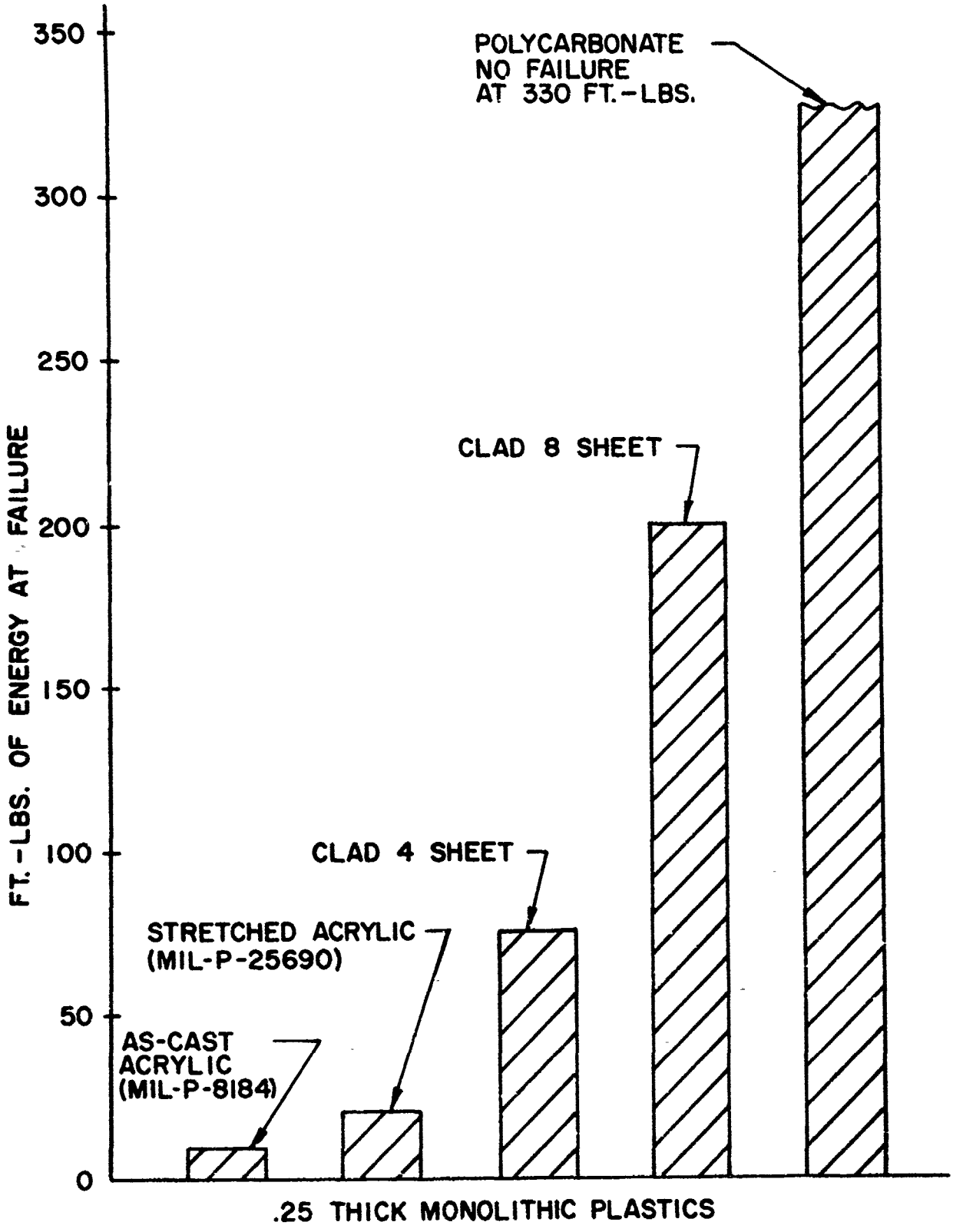


Figure 16. Falling Dart Impact Strength - 75°F



Figure 17. After Bird Impact

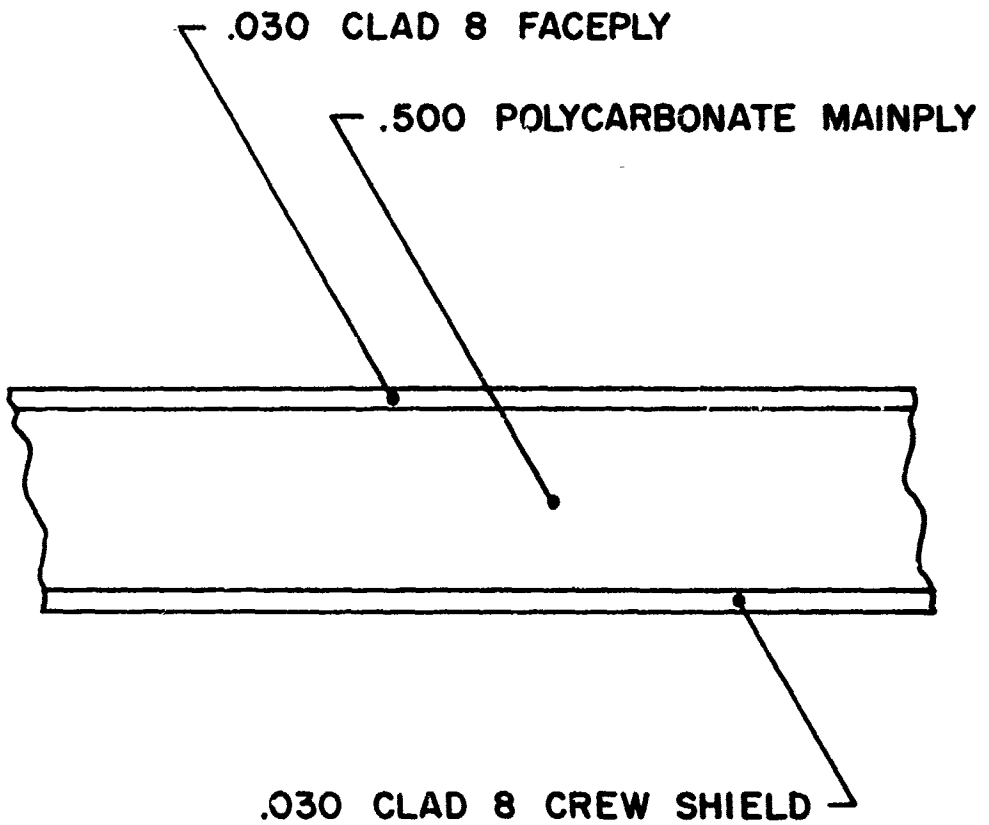


Figure 18. A-37 Sierraclad Construction

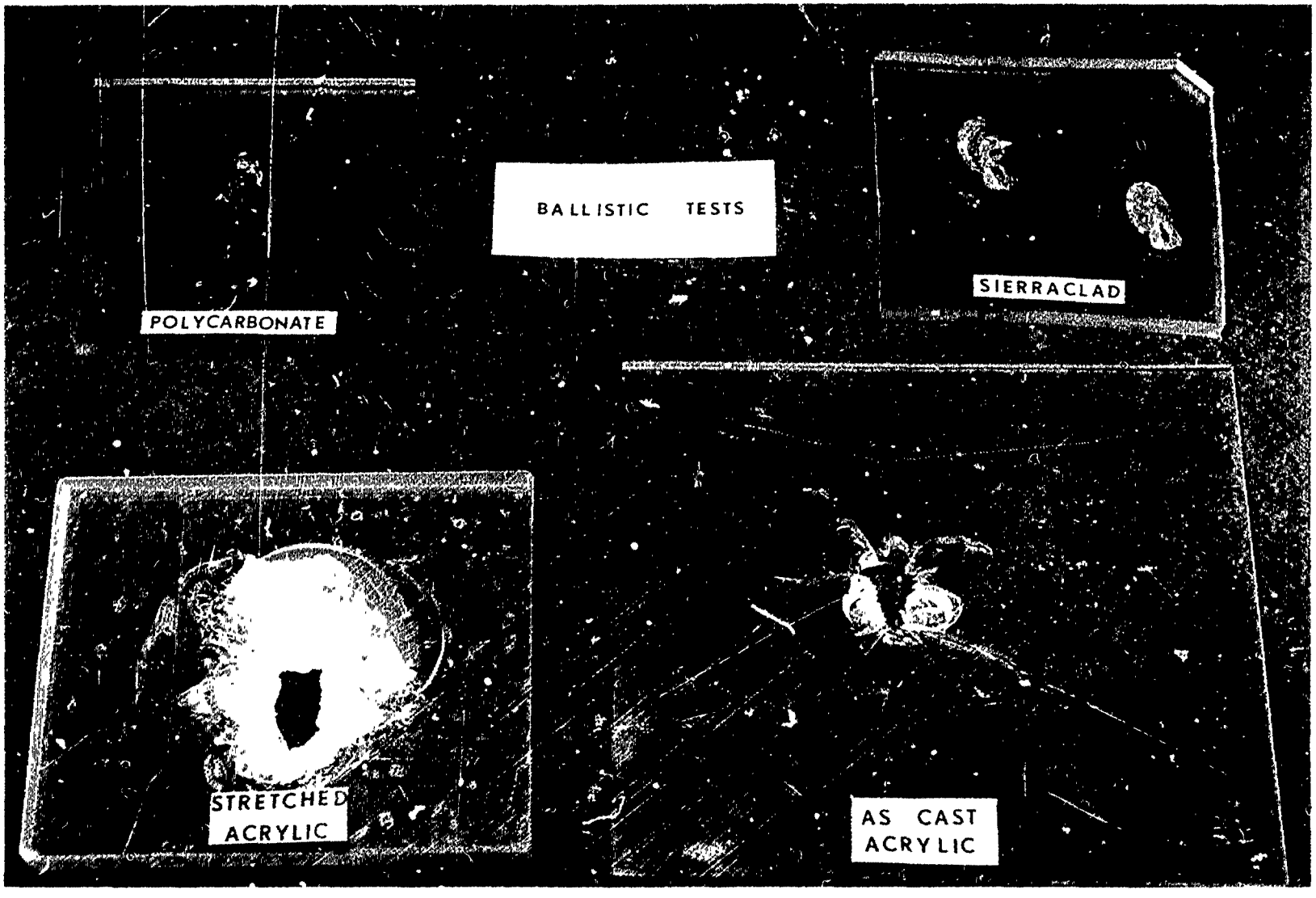


Figure 19. 30-06 Ammunition Fired; 30 Yards at 30° Angle

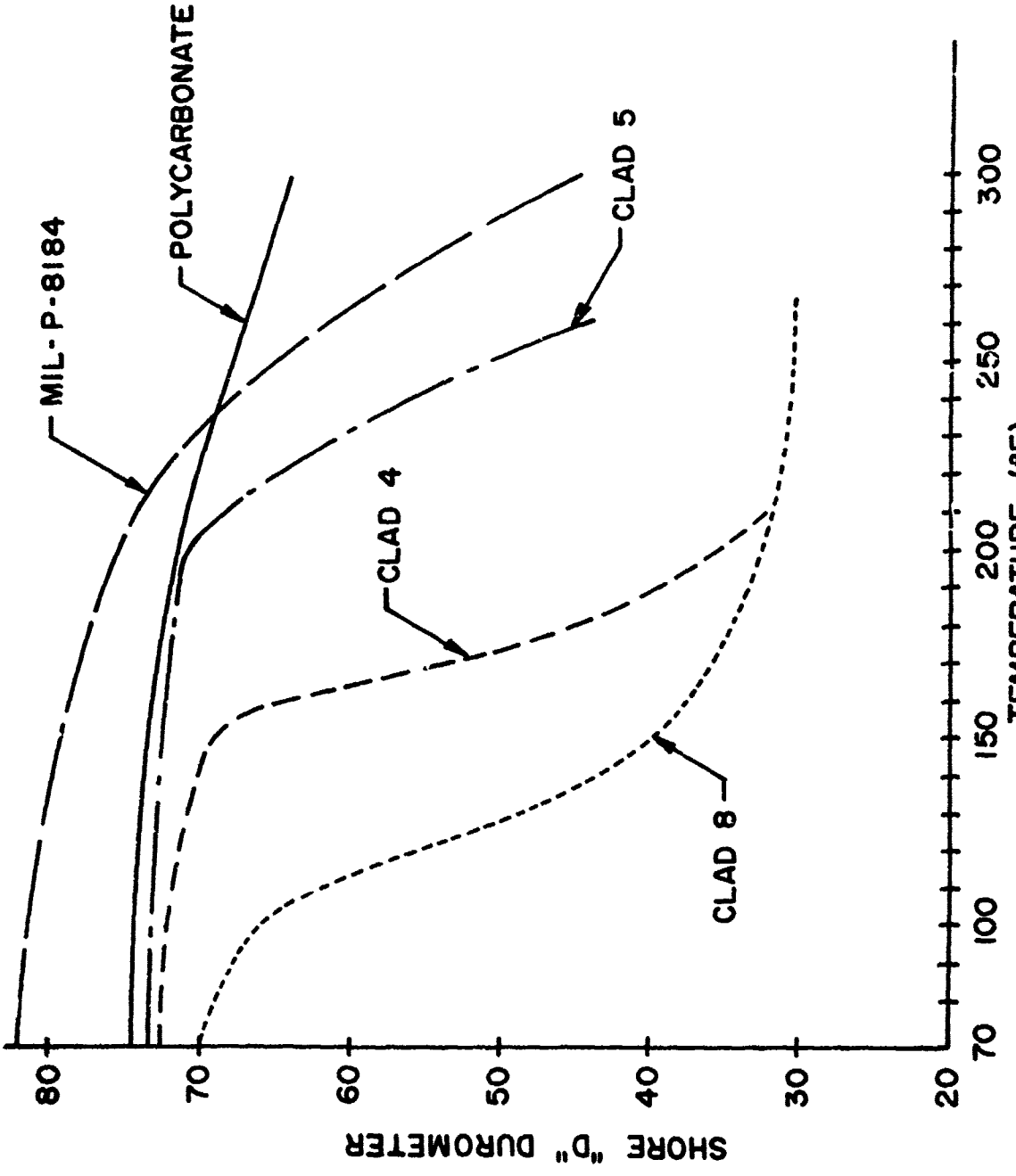


Figure 20. Hardness vs Temperature Monolithic Plastics

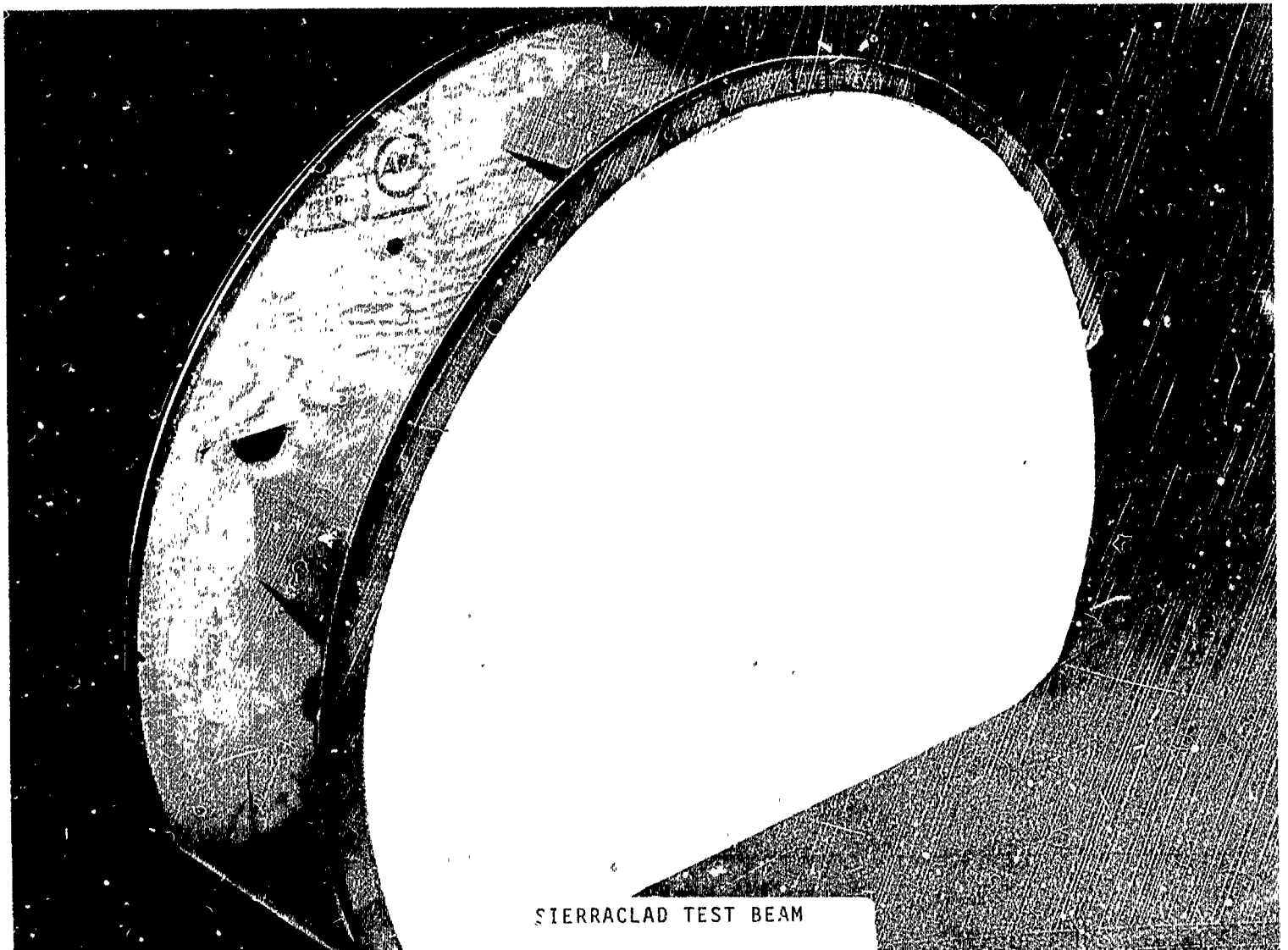


Figure 21. Typical Fighter Windshield Radius for Thermal Cycling

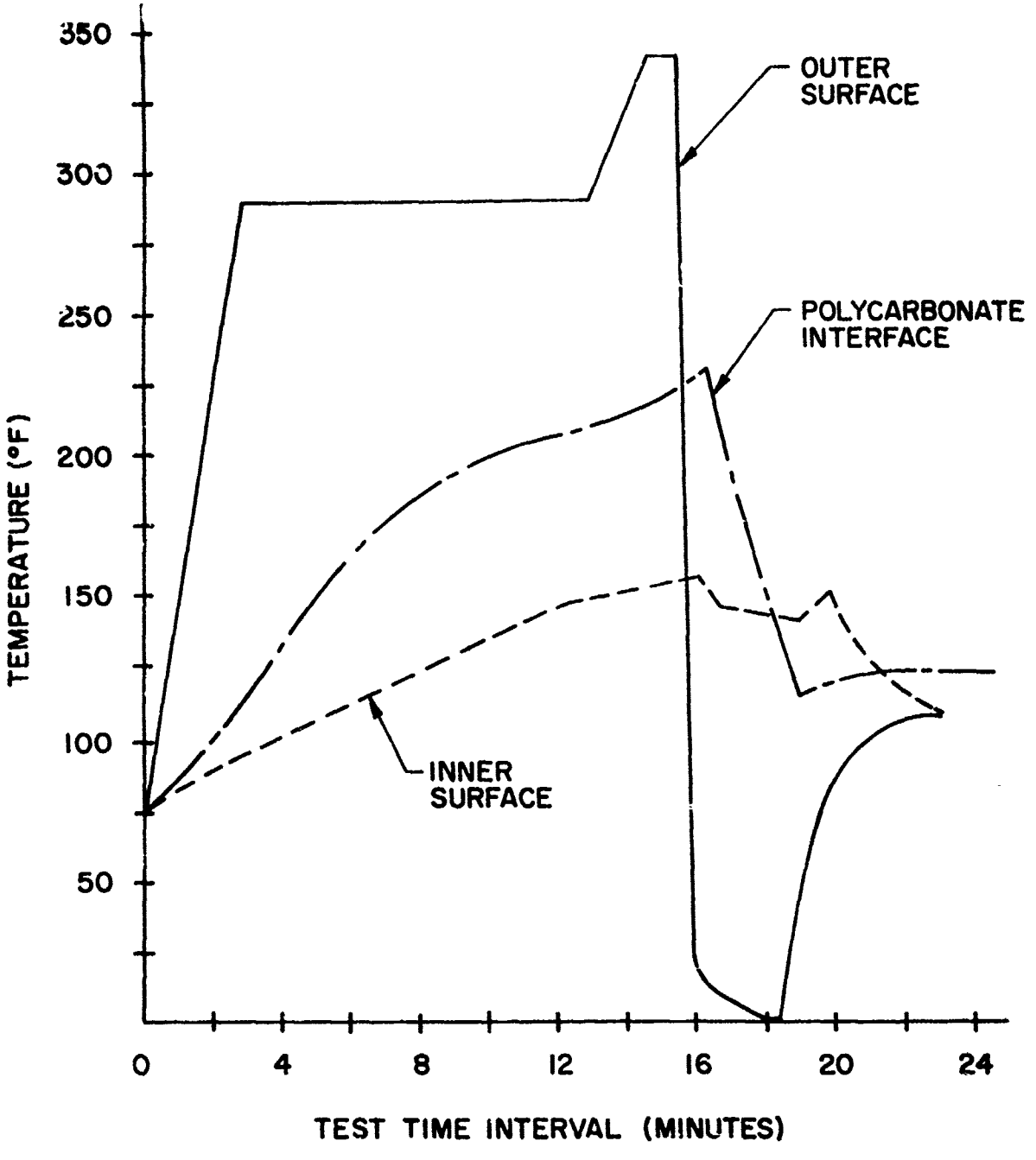


Figure 22. Thermal Profile

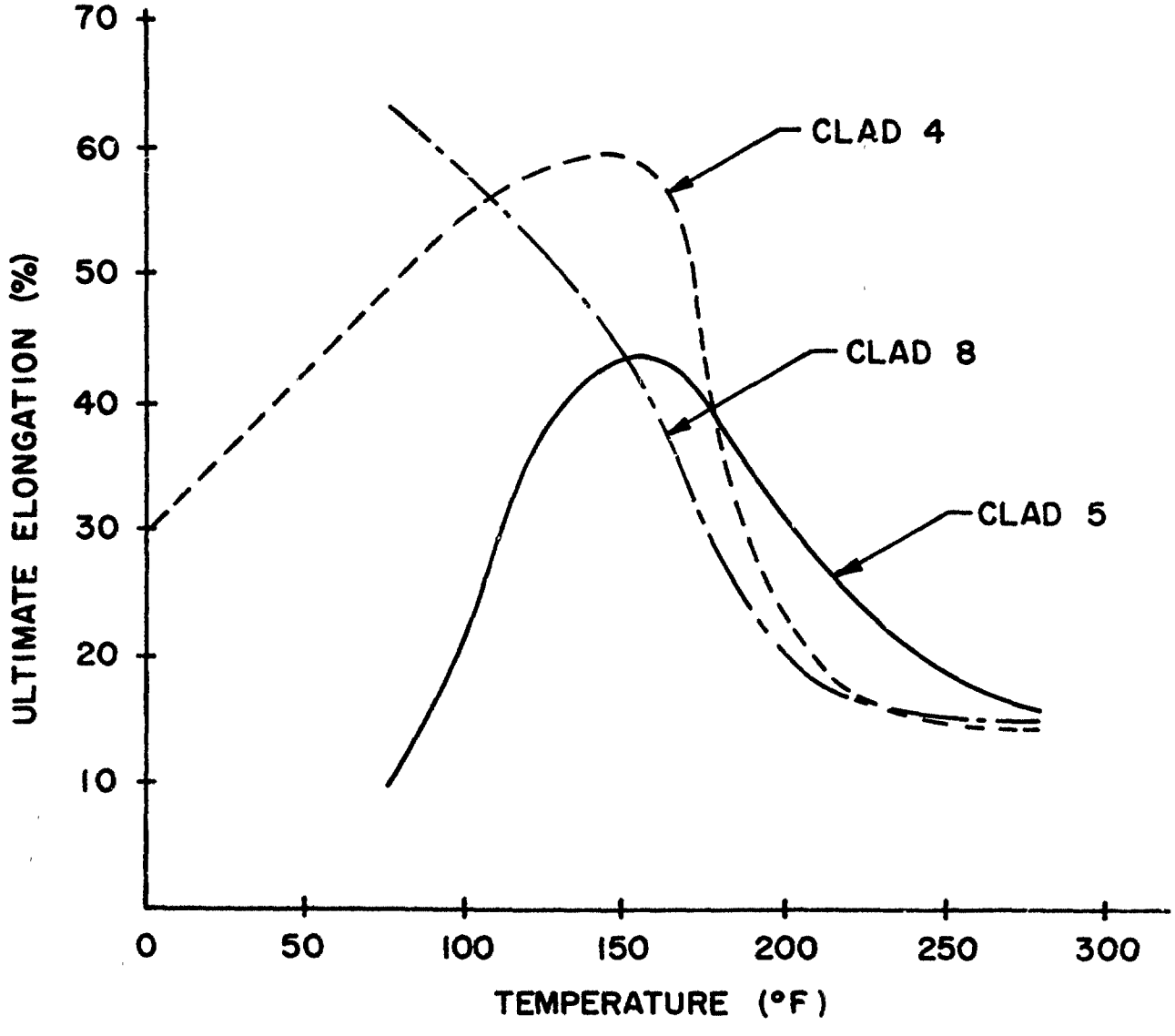


Figure 23. Ultimate Elongation vs Temperature of Monolithic Urethanes



Figure 24. Sierraclad Formability Single and Double Clad Domes

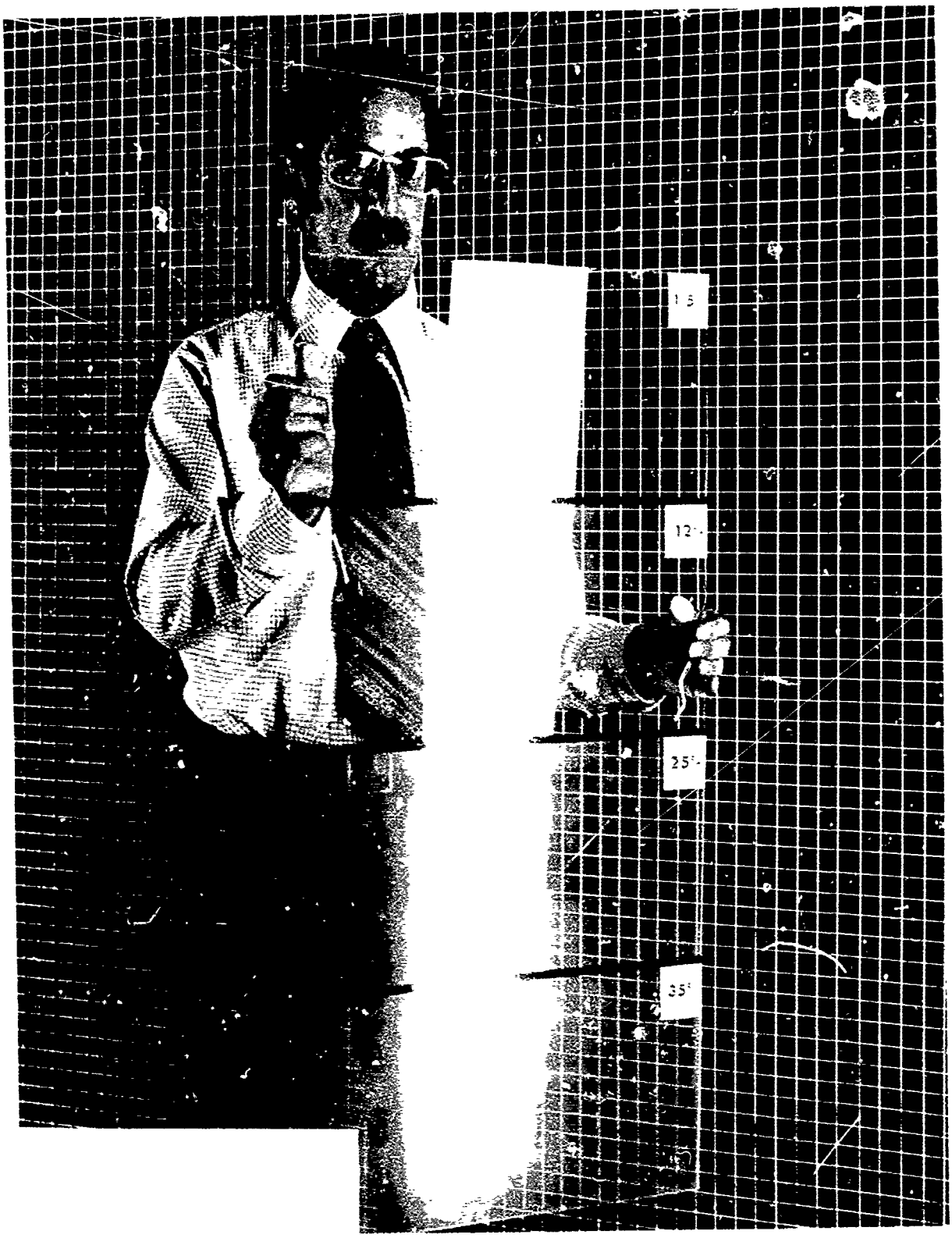


Figure 25. Effect of Haze on Visibility

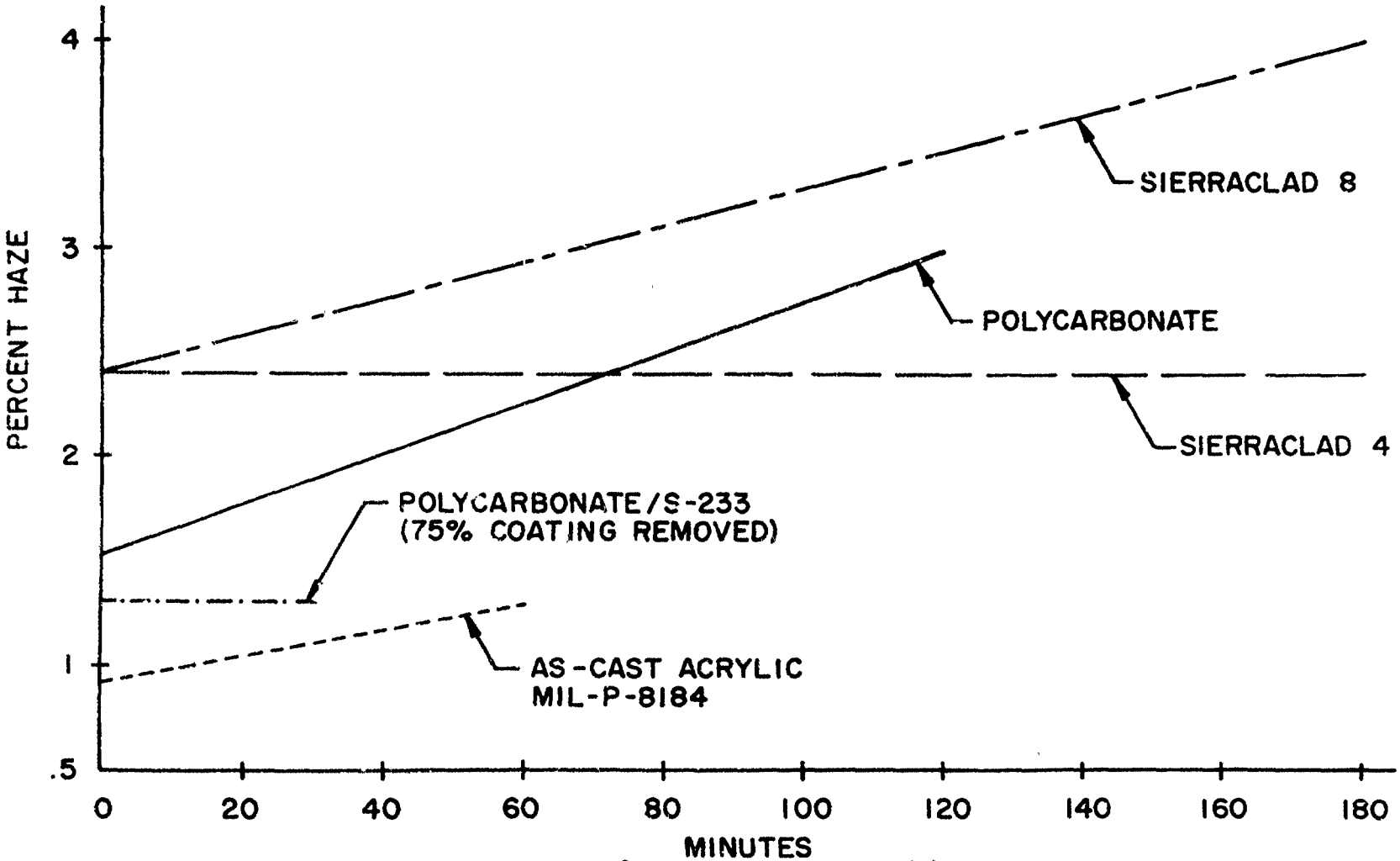


Figure 26. Rain Erosion, 30° Impingement Angle, 345 MPH

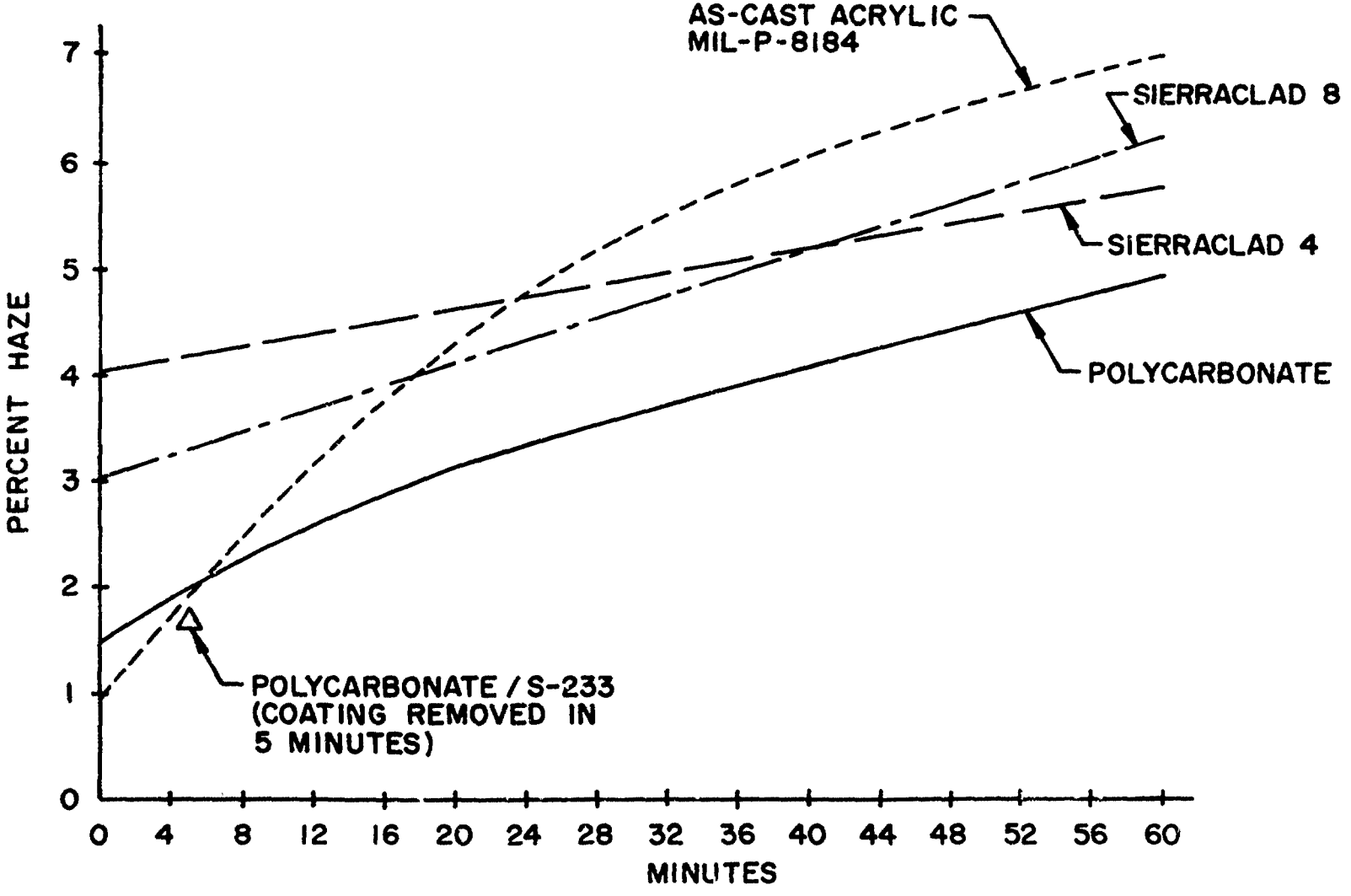


Figure 27. Rain Erosion, 30° Impingement Angle, 500 MPH

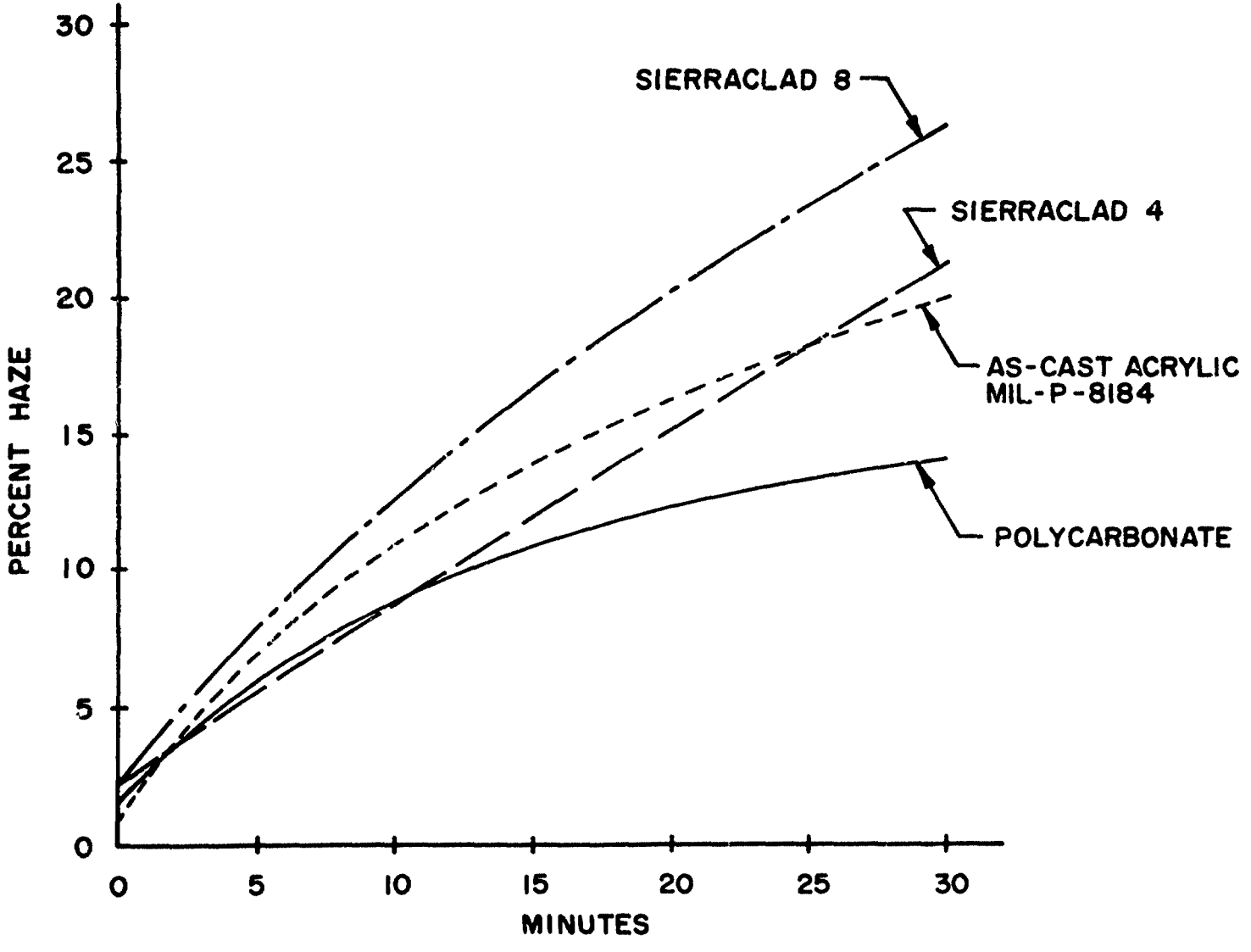


Figure 28. Rain Erosion, 30° Impingement Angle, 600 MPH

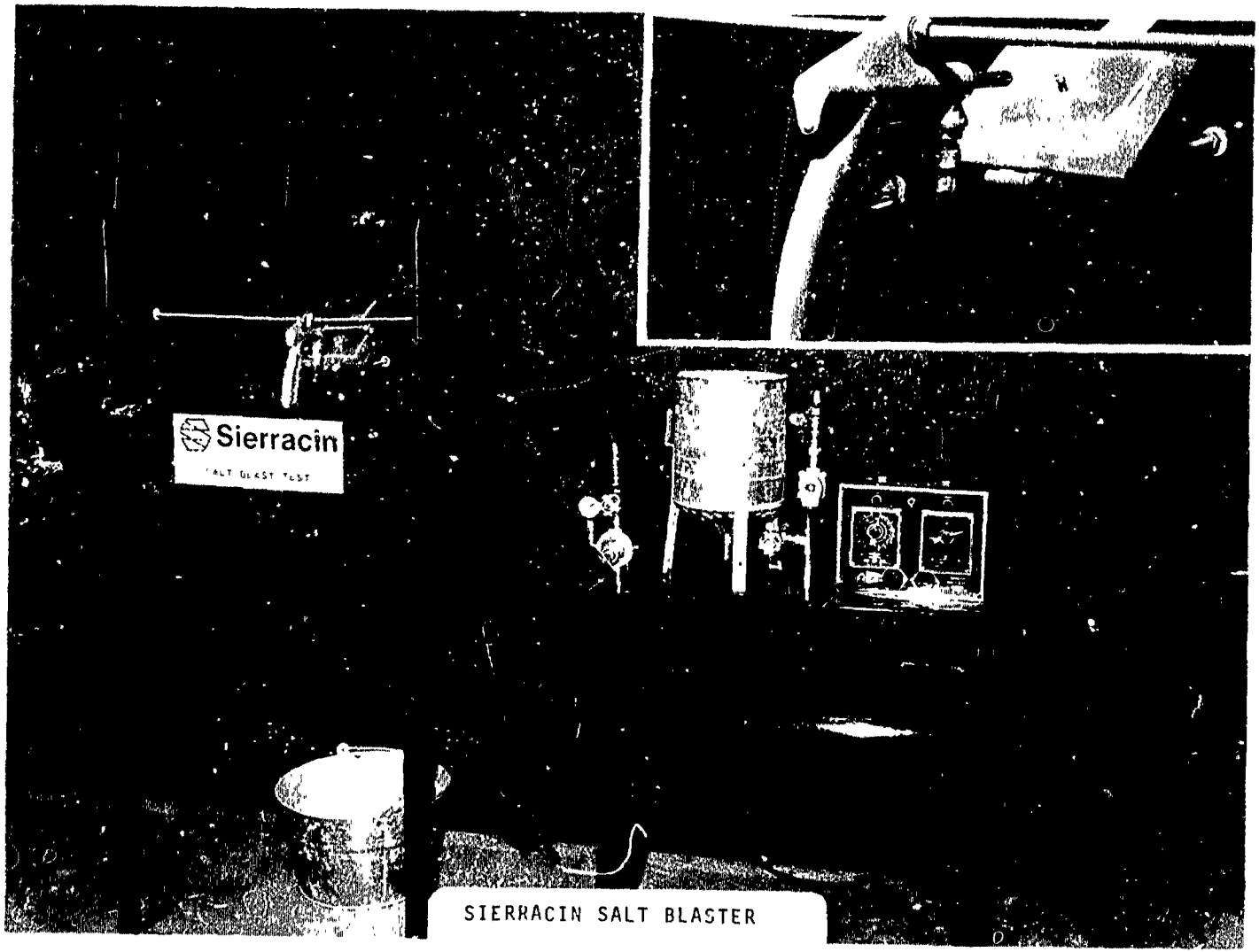
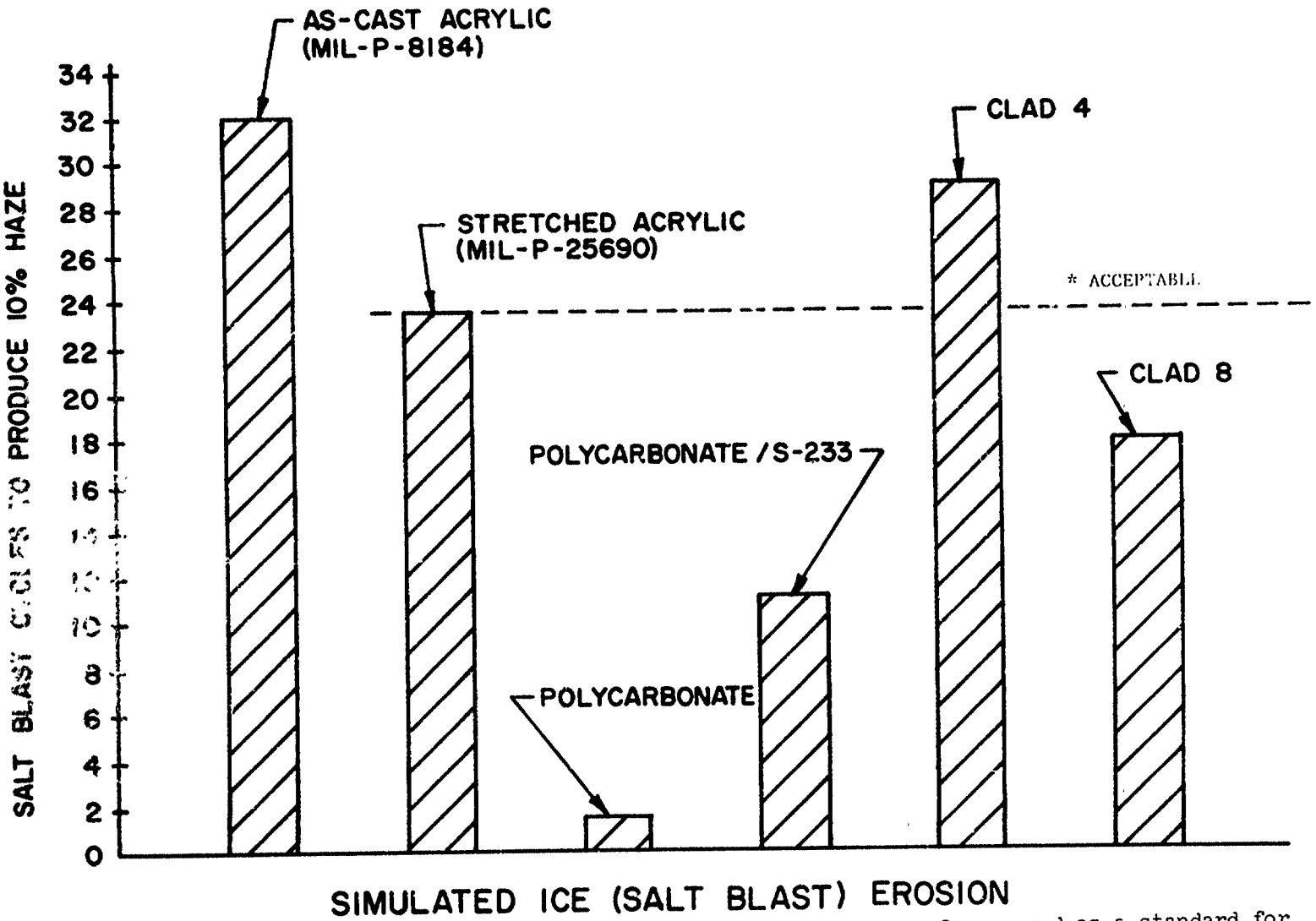
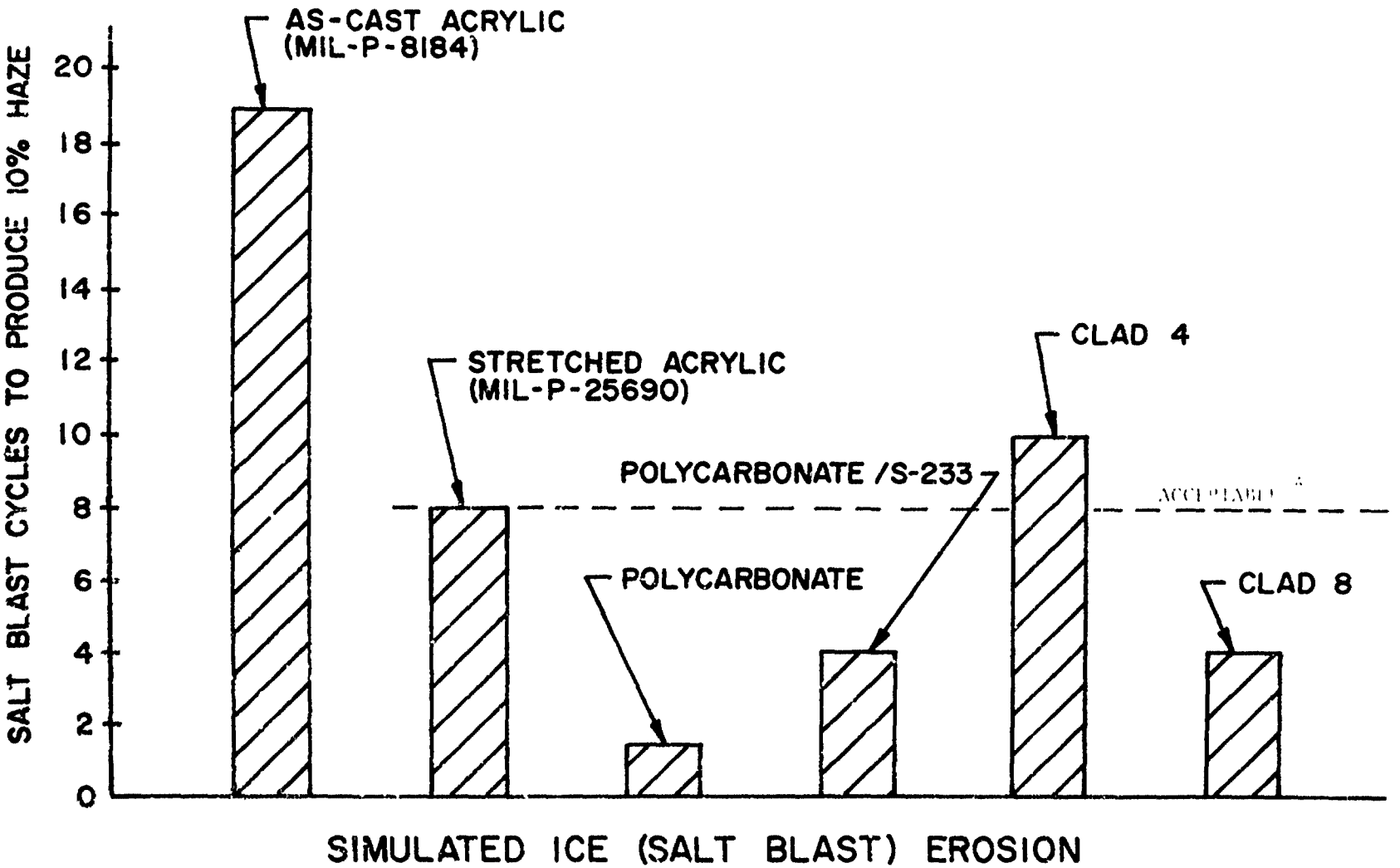


Figure 29. Simulates Ice and Dust Erosion of Plastics



* Stretched acrylic provides satisfactory performance in service and is, therefore, used as a standard for comparison.

Figure 30. 30° Impingement Angle, 25°F Test Temperature



*Stretched acrylic provides satisfactory performance in service and is, therefore, used as a standard for comparison.

Figure 31. 30° Impingement Angle, 75°F Test Temperature

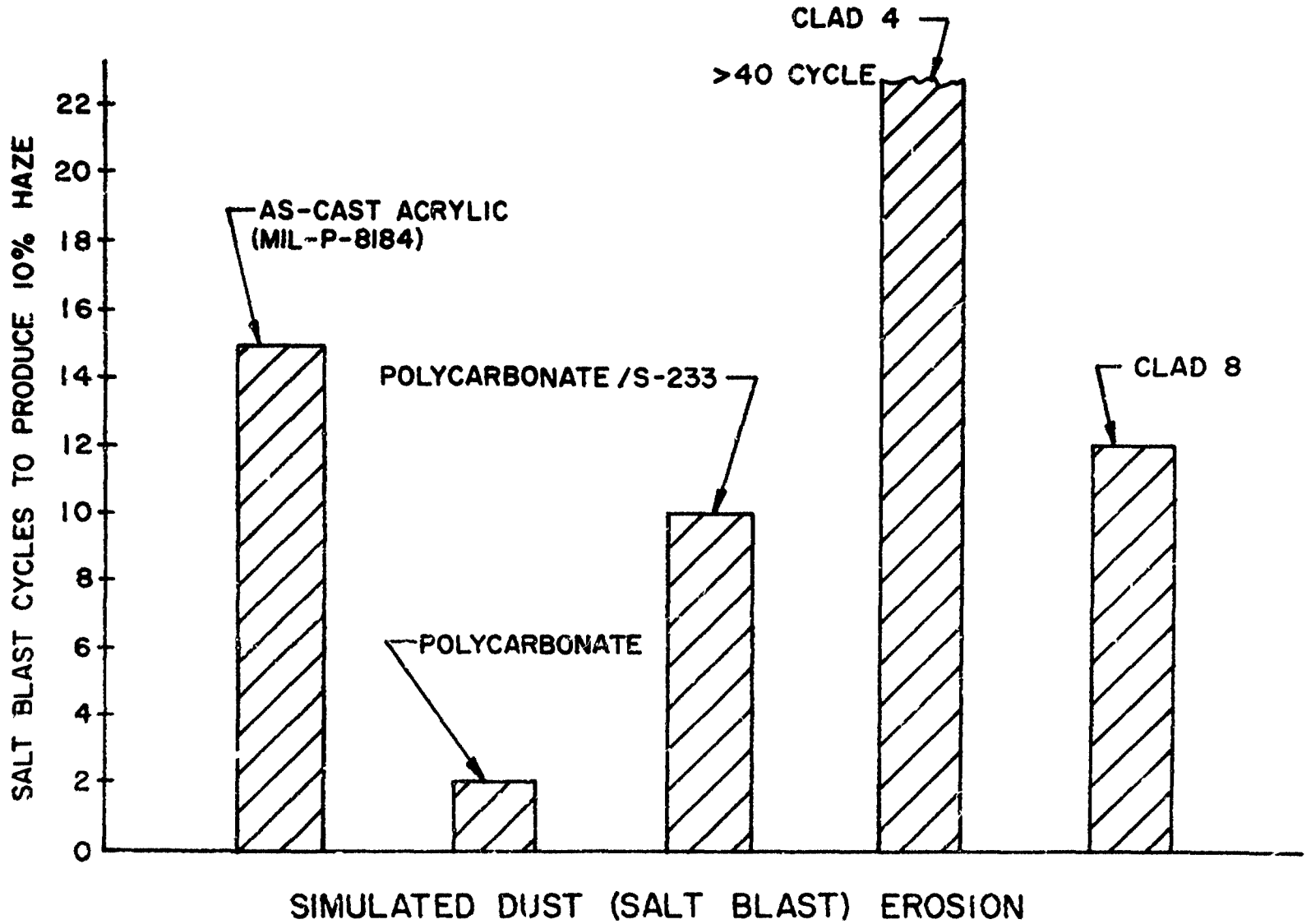


Figure 32. 30° Impingement Angle, 275°F Test Temperature

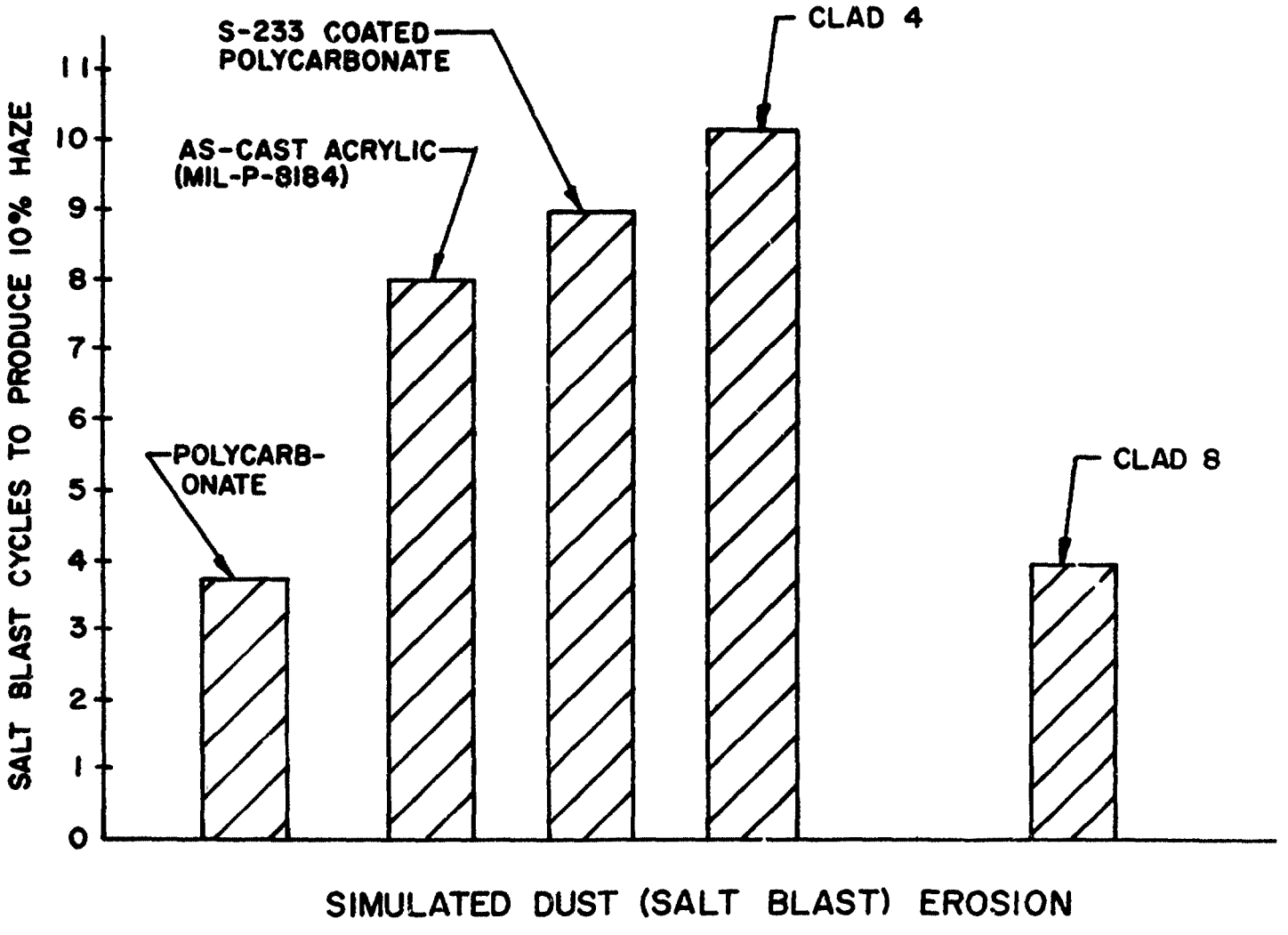


Figure 33. 30° Impingement Angle, 345°F Test Temperature

Copyright 1975, Sierracin® Corporation

The information contained in this document is thought to be reliable, but the Sierracin Corporation expressly disclaims all responsibility for loss or damage caused by or resulting from the use of the information herein contained. The information is given on the express condition that the user assumes all risk.

SESSION 7

BIRD IMPACT RESISTANCE

BIRDSTRIKES AND THE UNITED STATES AIR FORCE

Major A. T. Driscoll
Air Force Inspection and Safety Center
Directorate of Aerospace Safety
Norton Air Force Base, California

PRECEDING PAGE BLANK-NOT FILMED

BIRDSTRIKES AND THE UNITED STATES AIR FORCE

MAJOR ALFRED T. DRISCOLL

AIR FORCE INSPECTION AND SAFETY CENTER
DIRECTORATE OF AEROSPACE SAFETY
NORTON AIR FORCE BASE, CALIFORNIA

ABSTRACT

This paper provides an overview of USAF birdstrike statistics. Trends since 1966 are reviewed. Birdstrikes occurring since 1972 are discussed in more detail. The reporting system used to collect birdstrike reports in the USAF is addressed. Birdstrikes to windshields and canopies occurring since 1973 are detailed. This paper does not discuss programs designed to reduce the birdstrike hazard.

INTRODUCTION

The United States Air Force (USAF) has been collecting birdstrike data as part of the aircraft mishap reporting system for over 20 years. However, only during the last 10 years has the data been arranged and stored in a manner which allows easy access. The more recent the data, the better the data. It's important to remember that birdstrikes are reported only because they meet the criteria for reporting USAF aircraft mishaps.

To generate a report and become a statistic, the birdstrike must result in an aircraft accident or incident as defined by Air Force directive. The next logical question is, "What's an accident or incident?" There are three kinds of accidents; major, minor, and those involving only personnel injury or death. The major and minor accidents are determined by the manhours required to return the aircraft to service. For example, if over 800 manhours are required to repair the aircraft, the mishap is classified as a major accident. If between 150 and 800 manhours are required, the mishap is classified as a minor accident. Naturally, if the aircraft is destroyed, the mishap is a major accident. The manhour figures vary from one kind of aircraft to the next. If a pilot is injured or killed, the mishap is called an accident, regardless of the manhours required to fix the aircraft.

Birdstrikes are classified as incidents when:

a. The aircraft is damaged requiring repair prior to next flight and the manhours expended are less than those needed to put it in the accident category, or

b. The birdstrike constitutes a "significant hazard to the crew or aircraft."

This last criterion is pretty subjective and, in part, accounts for some of the peaks and valleys in birdstrike curves and reflects levels of concern throughout the Air Force.

Now that you understand how and why birdstrikes are reported in the USAF, we can look at the birdstrike statistics for the last 10 years.

DISCUSSION

Figure 1 shows the number of birdstrike incidents and accidents which have been reported in the last 10 years.

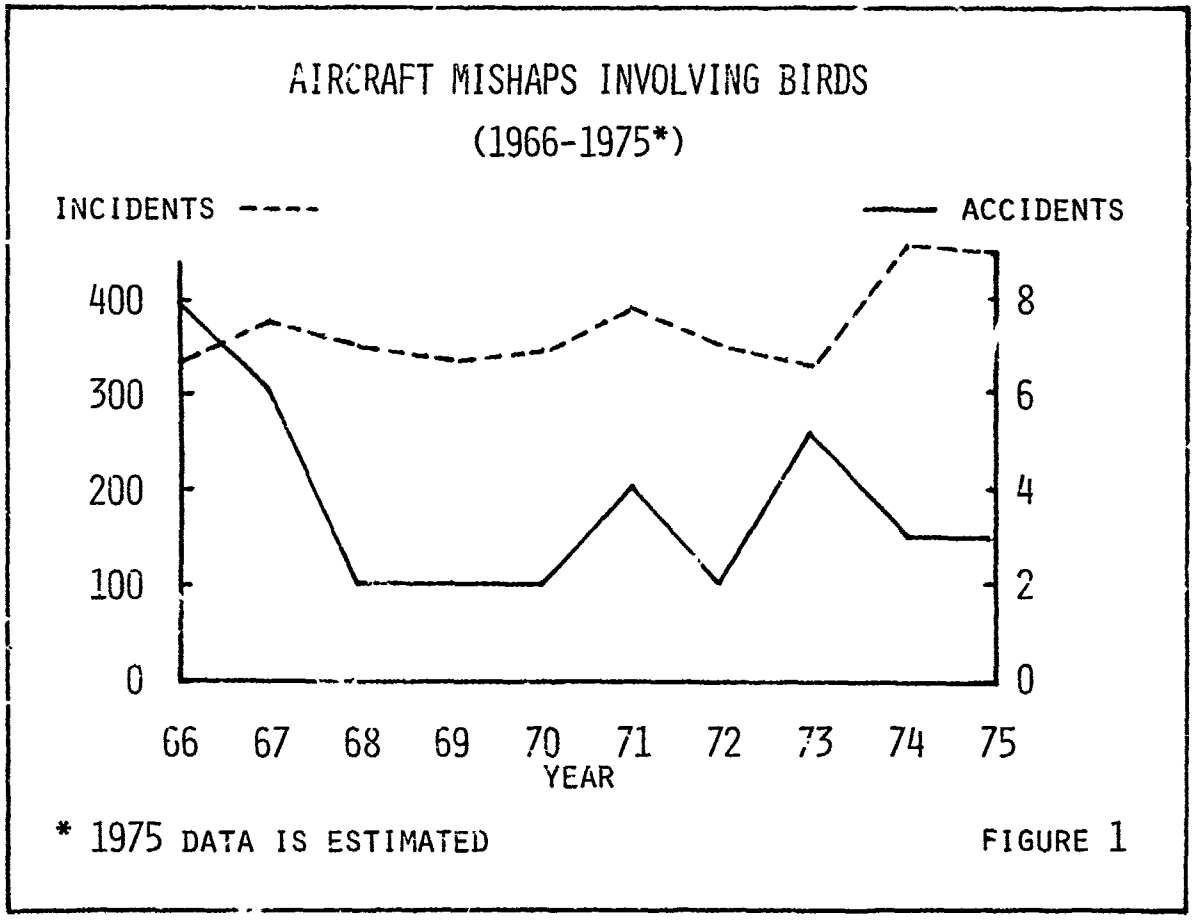


FIGURE 1

You'll note that until 1974 between 300 and 400 birdstrikes were reported each year. During 1974, 464 were reported. This year we'll probably exceed 450. As stated in the Introduction, these birdstrikes met the criteria for aircraft incidents or accidents. To determine total numbers of birdstrikes occurring, we asked our flying units to

report all birdstrikes, regardless of damage, during the period 1 January through 31 December 1971. Over 1,000 birdstrikes were reported during that year, but only 390 met the accident/incident criteria. If this 1 year sample holds true for other years, then for every birdstrike reported, two to three additional strikes actually occur.

The solid line represents aircraft accidents of all three types. Since 1966 we've never had less than two birdstrike accidents a year, and since 1969 we've averaged three a year. These accidents resulted in the loss of 14 aircraft and 7 pilots during the past 10 years. Birdstrikes were strongly suspected in several other accidents involving aircrew fatalities and destroyed aircraft.

Figure 2 depicts dollar losses since 1970. Over $60 million have been lost due to damaged or destroyed aircraft during the past 5 years.

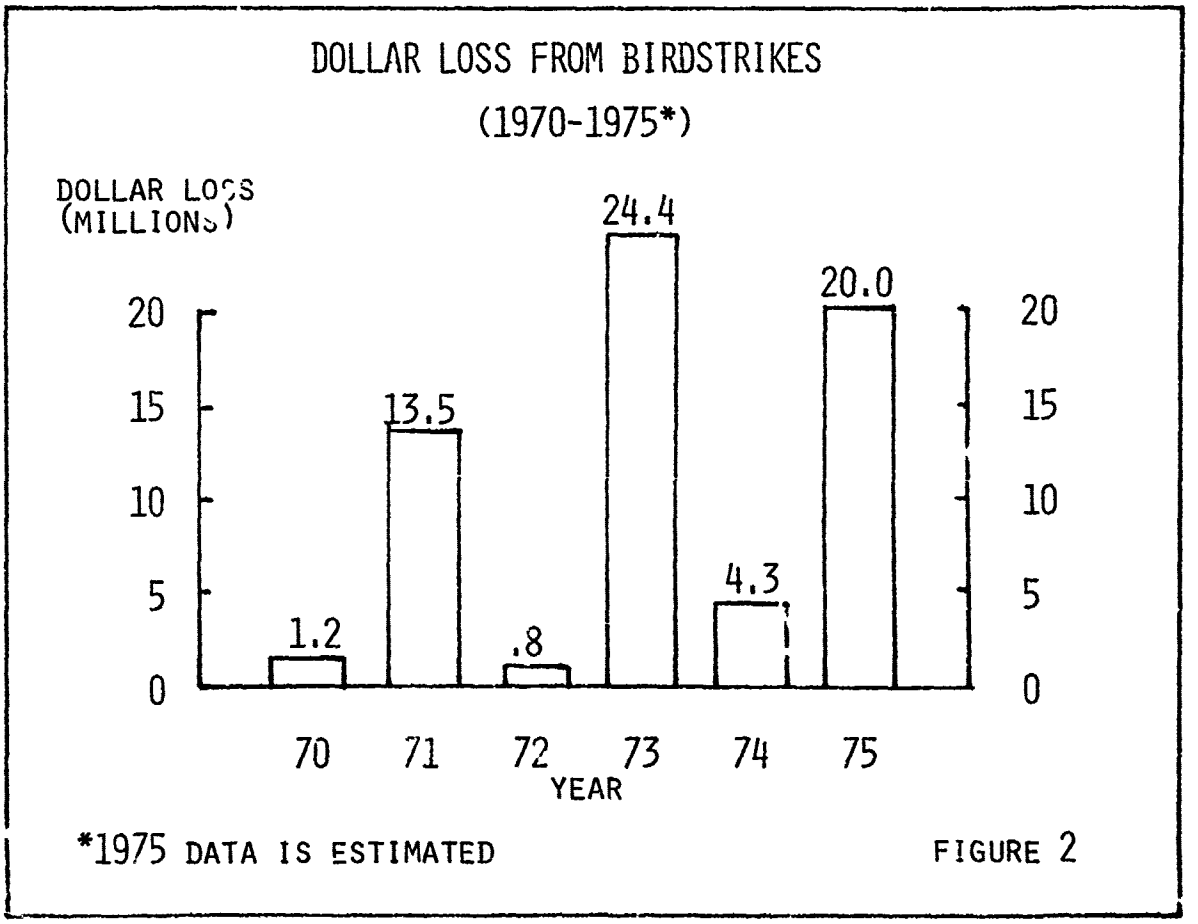
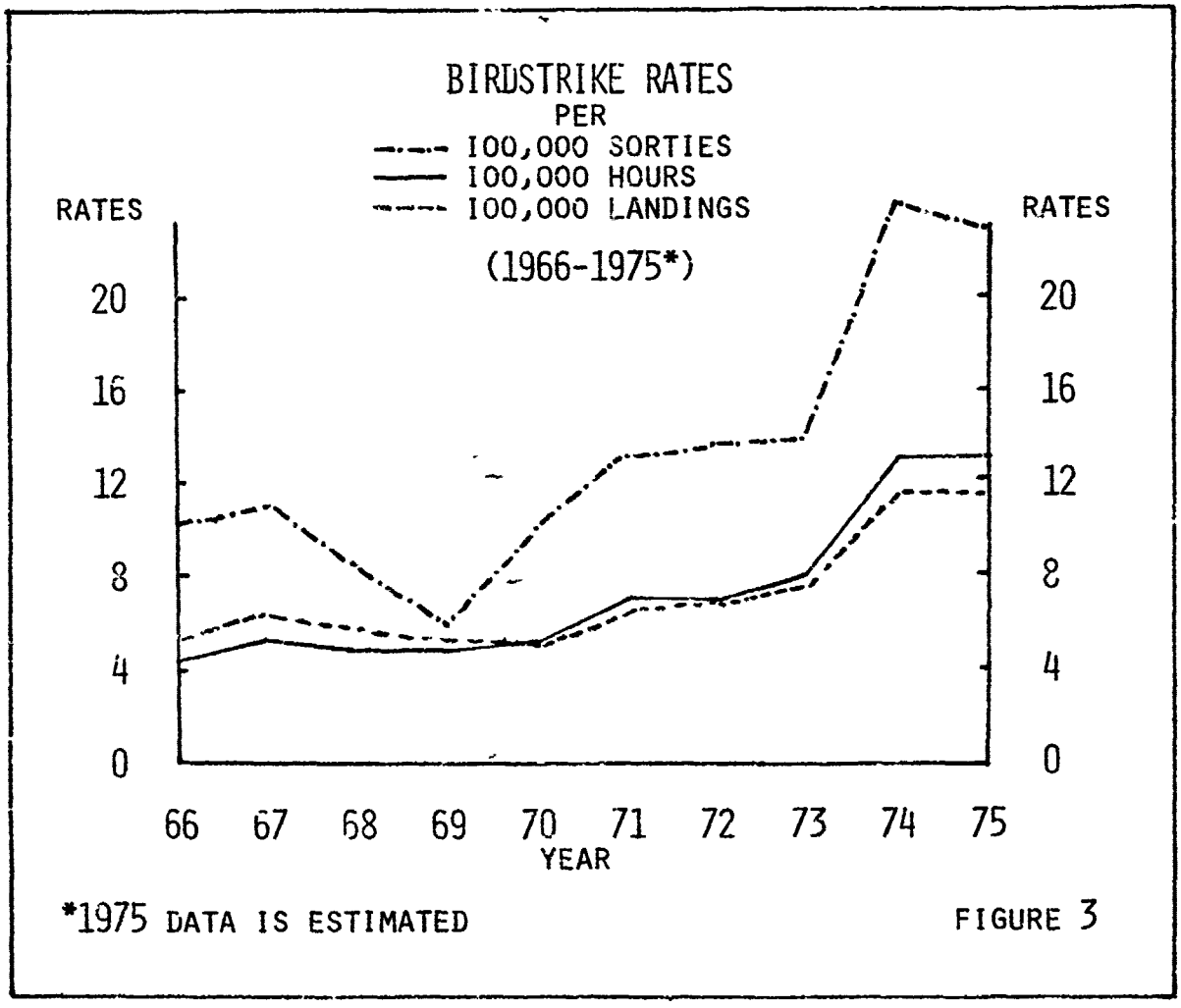


FIGURE 2

Over $50 million involved the cost of destroyed aircraft. The cost to repair damaged aircraft usually runs around $1 million per year.

Absolute numbers of birdstrikes per year don't really define the problem. Reductions in flying time and changes in training requirements tend to confuse the issue. In order to determine trends, birdstrike rates were developed based on 100,000 sorties, hours and landings as shown in Figure 3.



*1975 DATA IS ESTIMATED

FIGURE 3

Since 1969 there has been a steady increase in rate regardless of which yardstick you use. All three rates have at least doubled during the last 6 years. The rapid increase in strikes per sortie may reflect the fact that we are spending more time in the bird hazardous environment. For example, shooting more landings per sortie. One thing is clear; if the current trend continues, we can expect one damaging birdstrike every 5,000 sorties.

The monthly average number of birdstrikes throughout the year is shown in Figure 4.

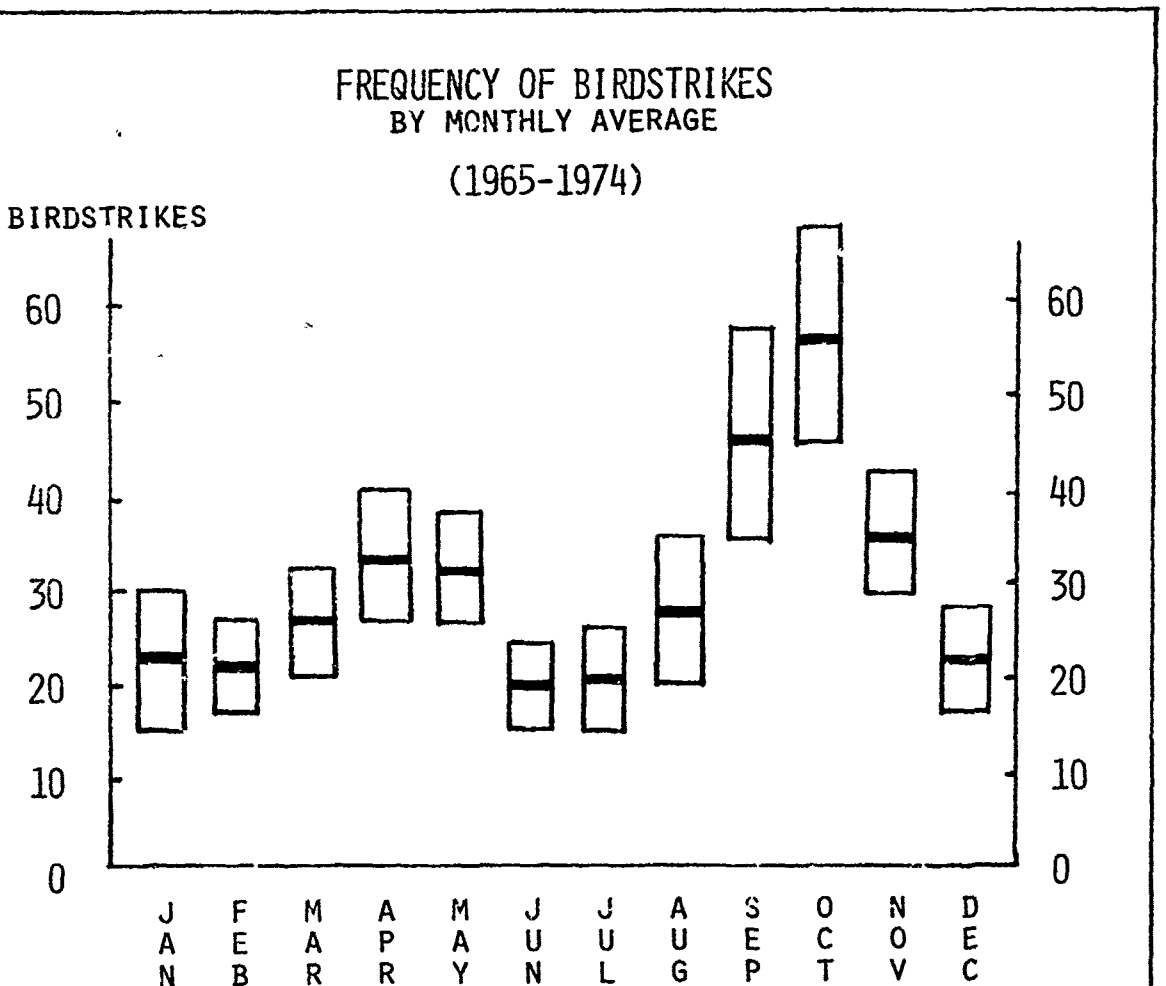
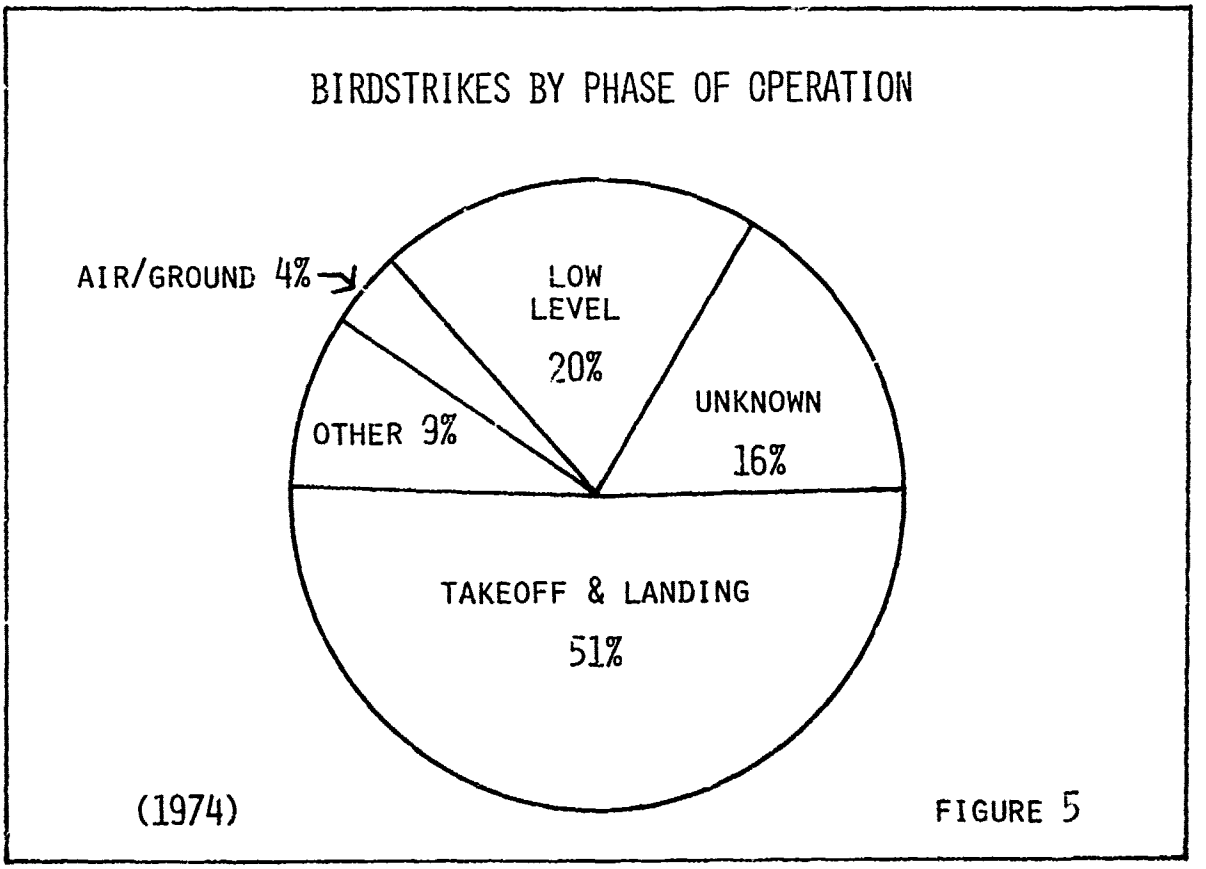


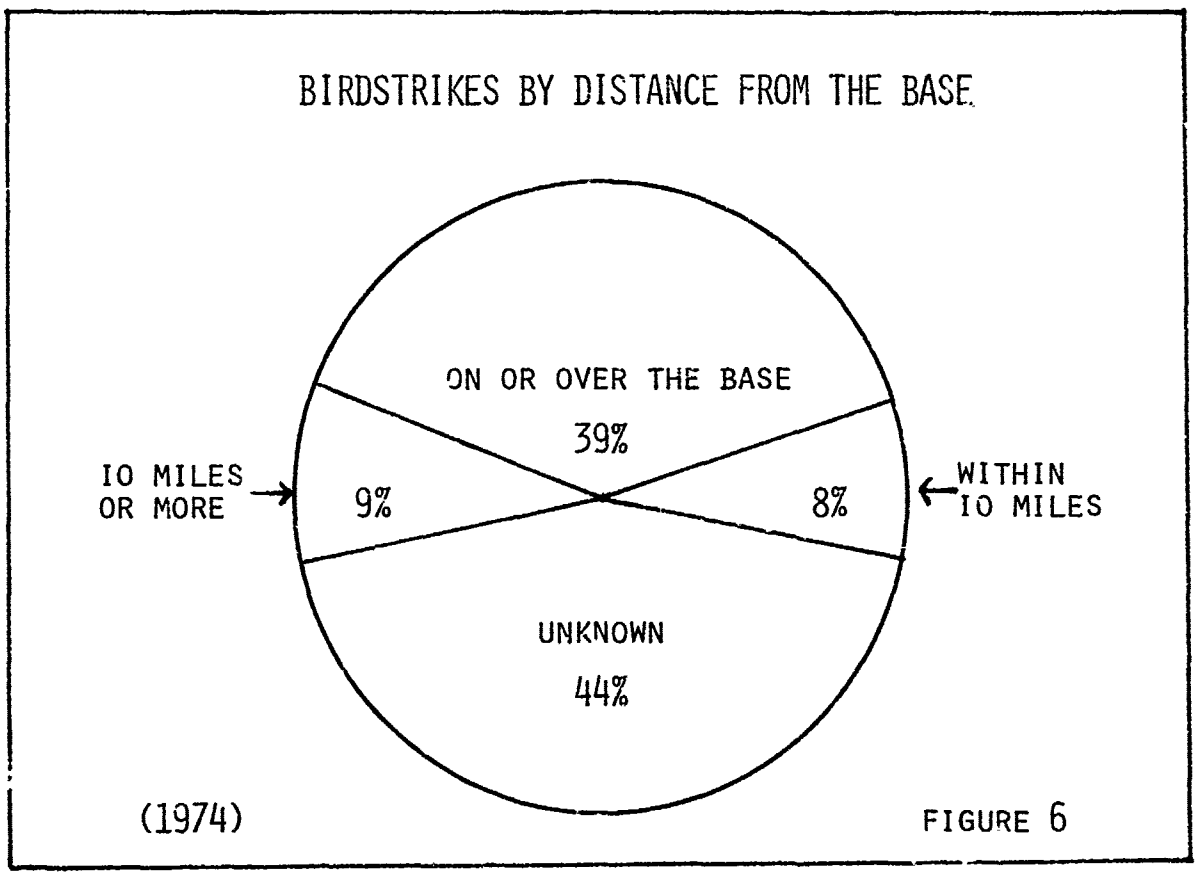
FIGURE 4

The effects of the spring and fall migration are clearly evident from the chart. The United States is a crossroads for millions of birds which travel from the northern portions of Canada and the United States to the southern portions of the United States and points south. The spring migration is reflected by the increased monthly averages in April and May. June and July are quiet months. During these 2 months, most of the large flocks of waterfowl and shore birds are far to the north. Resident birds of the US are nesting and not moving around much. By August the fall migration has started. The number of birds is increased 2 to 4 times over the spring migration by all the young birds which have recently left the nest. As many as half of these young birds will not survive to return north in the spring. December and January are relatively quiet months; however, large flocks of waterfowl winter in the southern parts of the US where our training bases are located.

We'll now look at the 1974 birdstrikes in more detail. Except for the overall high number of birdstrikes reported, 1974 was a typical year. Figure 5 gives a breakdown as to where our aircraft are running into birds.



As in the past, roughly 50 percent of the birdstrikes occur during takeoff or landing. Twenty percent occur during low level flight and constitute a serious safety hazard because of the high speeds and low altitudes involved. Figure 6 divides birdstrikes by distance from the base.



You'll note the large percentage which occur close to the air base. The unknown category accounts for all the unknowns shown in Figure 5 plus most of the low level birdstrikes in which the exact distance to the nearest base is also unknown. It also includes some incidents in which the narrative stated only, for example, that the birdstrike occurred during the initial climbout and did not give the exact distance from the base.

Figures 7 and 8 show birdstrikes by type of aircraft.

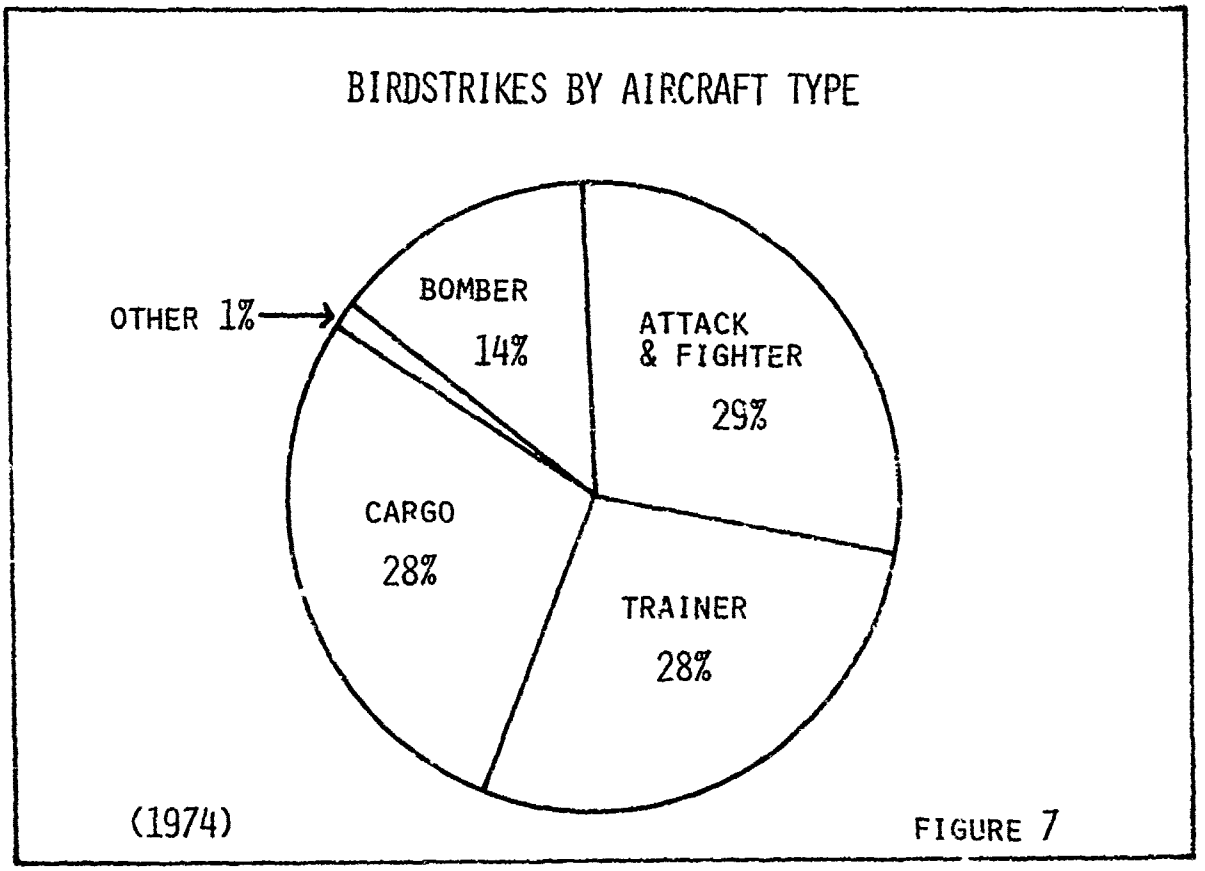


FIGURE 7

The strikes are divided rather evenly between fighter, trainer, and cargo aircraft, with bomber aircraft receiving half as many strikes as the other three. However, Figure 7 does not reflect the usage and relative abundance of these aircraft.

Figure 8 plots birdstrikes against aircraft flying time by type. The high number of birdstrikes per flying hour for bomber aircraft is readily apparent. Low level flying and the large size of the B-52 aircraft may be responsible for this high rate. Low-level flying also affects the fighter rate while most of the trainer birdstrikes occur during takecff and landing.

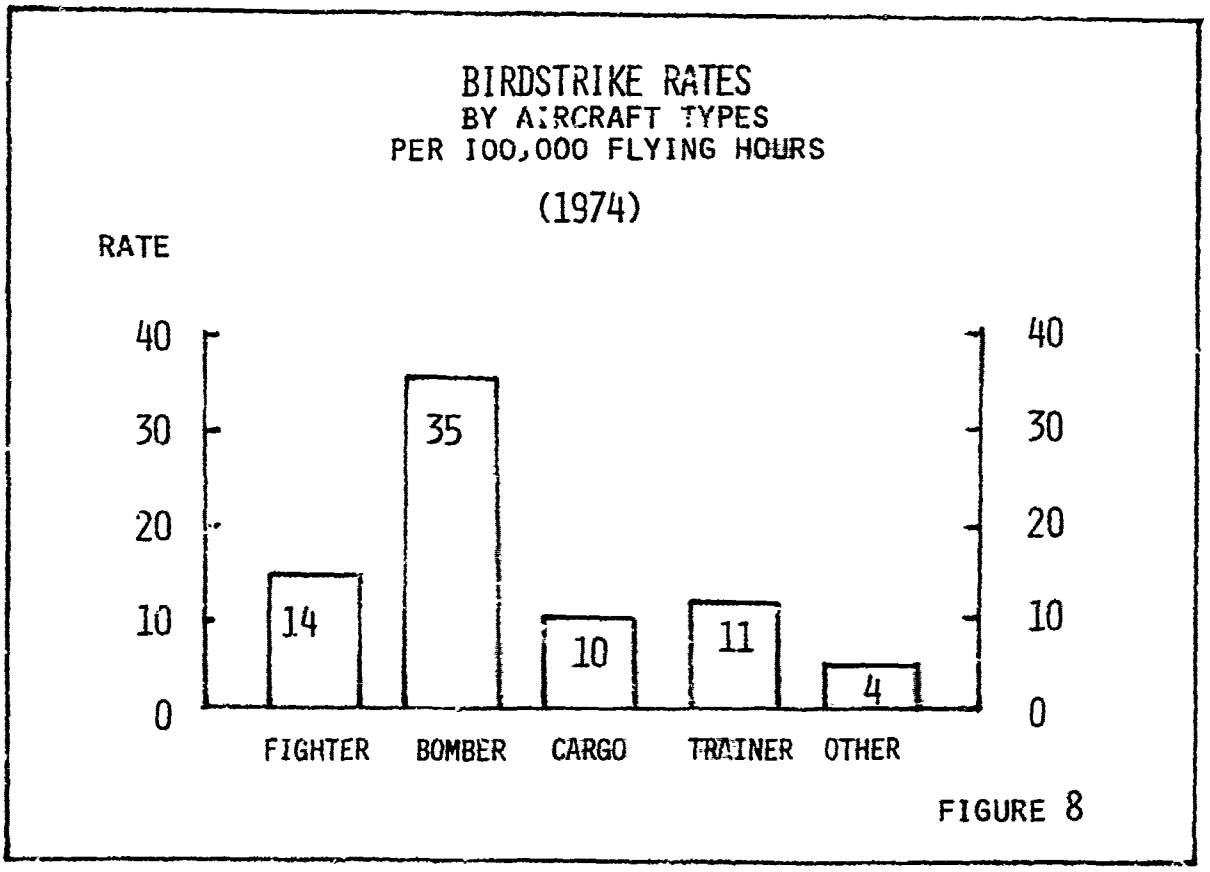


FIGURE 8

The majority of birdstrikes occur below 3,000 feet as shown in Figure 9.

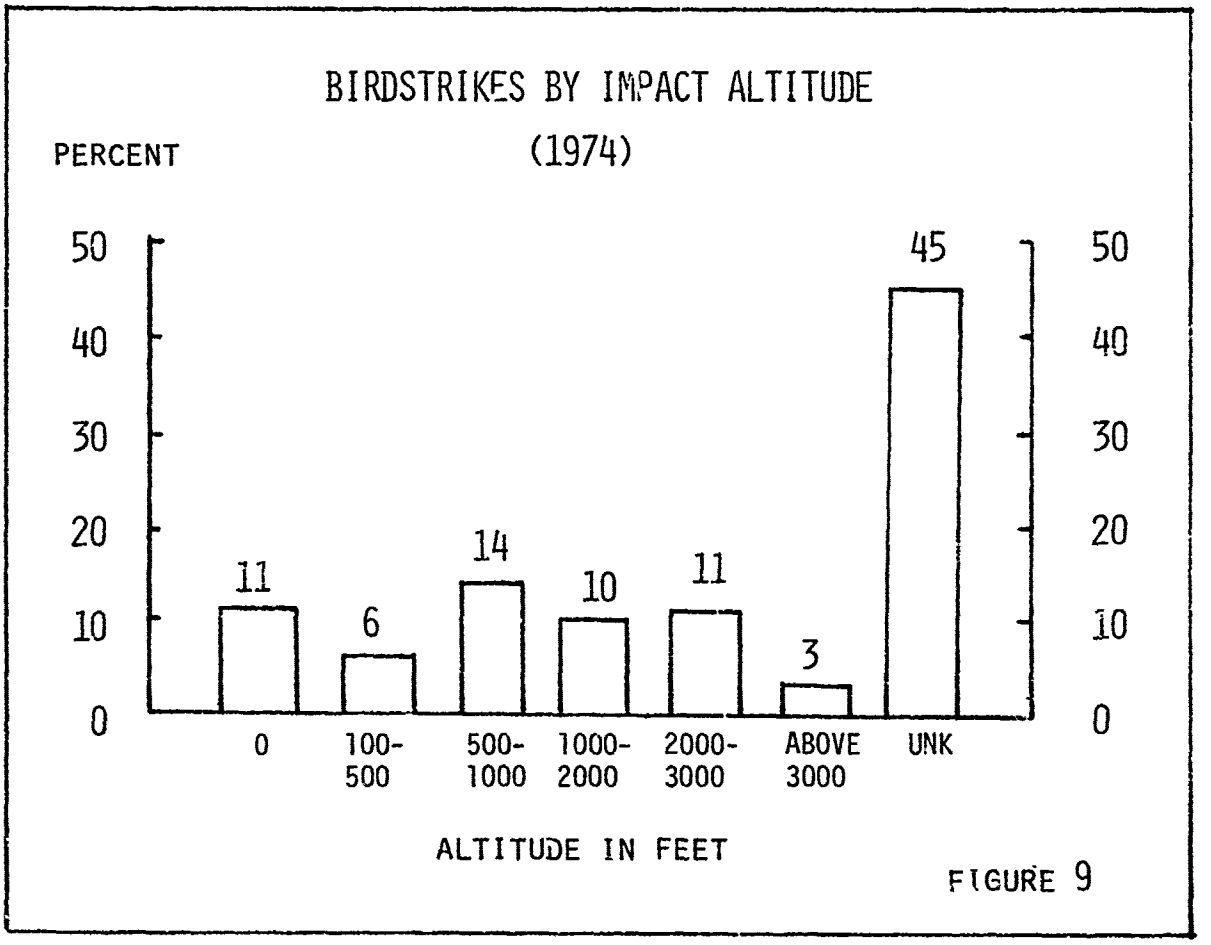
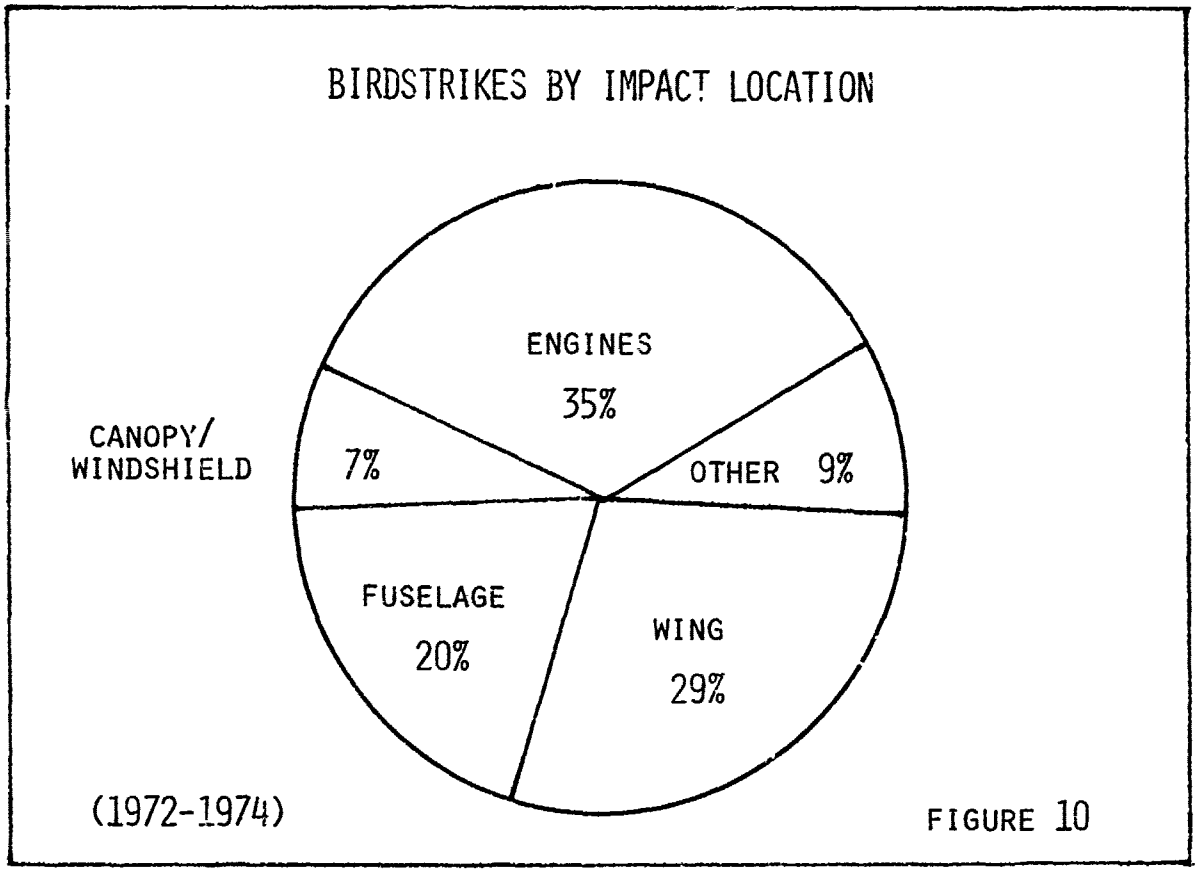


FIGURE 9

The high percentage of unknowns include those birdstrikes which were found after the flight had been completed and those birdstrikes for which the crew failed to report the altitude.

Figure 10 shows areas of the aircraft hit by birds, and is fairly representative of previous years.



Remember, if a bird hit a part of the aircraft and there was no damage, probably no report would be submitted. As usual, engine birdstrikes lead the pack. When a bird hits the engine, it usually does damage and gets the pilot's immediate attention. The "other" category includes such items as drop tanks, landing gear, landing lights, pylons, and munitions. Canopies and windshields accounted for 7 percent of the birdstrikes reported during this period. Although the percentage is small, the effects of these birdstrikes are not. Out of the 10 accidents caused by birds during these 3 years,

three involved windshield or canopy failures. Three of the four accidents occurring in 1974 and 1975 involved windshield/canopy failures. Out of the 1,130 birdstrikes reported between 1 January 1973 and 30 September 1975, 56 involved strikes in the windshield and 13 involved strikes in the canopy area. Windshield failures were reported 14 times and canopy failures were reported seven times. Impact speeds ranged from 480 knots to as low as 160 knots. Bird sizes involved in these failures ranged from a 2-ounce white-throated swift to a turkey vulture of 3 or 4 pounds. In the majority of cases, the species and weight of the bird were undetermined.

Detailed studies by aircraft type, windshield design, and birdstrikes of known weight and velocity might yield useful data concerning structural design parameters.

RADAR ORNITHOLOGY AND BIRD/AIRCRAFT COLLISIONS

S. A. Gauthreaux, Jr.
Department of Zoology
Clemson University
Clemson, South Carolina

RADAR ORNITHOLOGY AND BIRD/AIRCRAFT COLLISIONS

Sidney A. Gauthreaux, Jr.
Department of Zoology
Clemson University
Clemson, South Carolina 29631

ABSTRACT

As the cost of aircraft continues to rise and new aircraft specifications call for faster speeds and lower flying, the problems that birds aloft pose to these new aircraft will more than likely be considerable. One means of planning for the problem involves engineering, making transparent materials and enclosures stronger and aircraft engines more bird resistant. However, with every bird/aircraft collision we find that engineering cannot do the job alone; biologists can and are helping to improve flight safety. Although a number of biological approaches are being used to work on the problem, radar ornithology is one approach that is proving to be successful.

The use of radar to detect and monitor weather phenomena and radar's vital role in the detection and control of aircraft are well known, but relatively few radar technicians and operators realize the importance of radar for the detection and monitoring of hazardous bird concentrations aloft. In this report the application of radar to detect and study the movements of birds will be emphasized. The need for such an undertaking is clear when one realizes that many radar operators and technicians cannot recognize bird echoes on radar, and more importantly, new developments in radar technology are in part devoted to eliminating the "clutter" produced by bird targets.

Just as there is a need for exact weather information to meet the requirements of air safety, there is an increasing need for similar information on bird concentrations and movements in the atmosphere. This information can be obtained from radar units now operated by the National Weather Service and the Federal Aviation Agency. This report emphasizes: 1) the recognition of bird targets on radar, 2) the estimation of numbers of birds aloft based on radar displays, and 3) the measurement of bird altitudes using radar. This information should greatly benefit aviation interests, both civilian and military, by reducing the number of bird/aircraft collisions and improving flight safety through early detection and warning of dangerous concentrations of birds in the atmosphere.

INTRODUCTION

With regard to the biological aspects of the bird/aircraft collision problem, investigations of approaches to remedy the problem have followed three major lines: 1) ecological alterations within the airdrome to render the airport environment less attractive to birds, 2) scaring devices to eliminate birds from the airfield and anti-collision devices on the aircraft to make birds avoid the aircraft while in flight, and 3) radar and direct visual detection of hazardous concentrations of birds and warning pilots of potential danger. Although these three approaches continue to receive great attention as possible solutions to the bird/aircraft problem (ref. 1), the radar approach will be emphasized in this paper.

The use of radar to detect and monitor weather pheromena and radar's vital role in the detection and control of aircraft are well known, but relatively few radar technicians and operators realize the importance of radar for studies of bird, bat, and insect movements in the atmosphere (refs. 2-8). In this report the application of radar to detect and study the movements of birds will be emphasized. The need for such an undertaking is apparent when one examines the figures showing that damages in the millions of dollars are being sustained each year by civilian and military aviation because of bird/aircraft collisions.

Just as there is a need for exact weather information to meet the requirements of air safety, there is a mounting need for similar information on bird concentrations and movements in the atmosphere. This information can be obtained from radar units now operated by the United States National Weather Service and the Federal Aviation Administration. Such information should aid radar operators in recognizing the various types of echoes from birds displayed on weather and air-traffic control radars, in estimating the numbers of birds passing over the radar stations and in gathering information on the altitude of the birds aloft. The radar approach will greatly benefit aviation interests, both civilian and military, by reducing the number of bird/aircraft collisions and improving flight safety.

PATTERNS OF BIRD/AIRCRAFT COLLISIONS

Bird/aircraft collisions can occur during three rather distinct phases of the operation of an aircraft. Bird impact often occurs during the initial phase of takeoff when the aircraft has not cleared the runway. The collision results because birds are feeding close to and flying back and forth across the active runway or because birds are actually sitting on the runway. As the aircraft approaches, the birds sitting on the runway or feeding nearby are startled and take off. Many may be directly in the flight path of the aircraft and may be hit. The second phase of aircraft operation that is particularly vulnerable to bird impact is during the period when the aircraft has cleared the runway and is climbing to its cruising altitude or when the aircraft is descending in a landing approach. It is during this phase that the aircraft is passing through an altitudinal zone where bird activity aloft is most common. Most birds in migration

and birds flying to and from a roost or feeding area usually fly below 3,000 ft, and particularly during the day they are in sizeable flocks. The third phase of aircraft operation subject to bird collisions, the en route phase, occurs when the aircraft is at its cruising altitude. In general, unless the aircraft is flying below 3,000 ft, this phase should sustain the least amount of bird collisions, because far fewer birds are flying at these higher altitudes. However, it is important to point out that the larger birds fly at higher altitudes with faster airspeeds. Consequently, even though the probability of a bird impact is reduced at higher altitudes, when it does occur it is likely to be quite serious because of the larger sizes of the birds involved. Moreover, the larger species regularly fly in flocks during daylight and darkness and, as mentioned previously, at faster airspeeds.

RADAR SYSTEMS

Fortunately, radar systems are currently available that can be used to detect and monitor the movement of birds at the airport, within 60 miles of the airport, and along air routes. A number of radar studies are underway that will eventually provide excellent data on the use of various radar systems to detect and monitor bird activity during all phases of aircraft operation.

Because a majority (67%) of bird/aircraft collisions involving civil airlines and a quarter to a half of the bird impacts involving military aircraft occur at or very near the airport (refs. 9-11), radar systems that can detect and monitor bird activity on the airfield and within 10 miles of the airfield are highly desireable if a surveillance and warning capability is to be developed to avoid bird/aircraft collisions during the beginning and end of a flight. "Close-in-seeing" radars have been used to investigate the feasibility of using this equipment at airports to detect and monitor the presence and movements of birds in the airport environment. Schaefer (ref. 12) has provided a detailed feasibility study and concluded that a high resolution X-band (3-cm wave length) radar with an antenna at a height of 20-30 m would meet the requirements for a radar which would display an airfield map showing the presence and magnitude of bird groups on the runway and shorter vegetation in all weathers except in heavy rain. He found that a commercial marine radar, with only one major modification, can meet the requirements, at a cost of approximately $5,000. Schaefer concluded that the use of airport bird detection equipment (ABDE) radar with direct visual surveillance when possible should greatly reduce bird impacts.

Flock (ref. 13) evaluated the utility of a ship-board navigation radar (GEC-AEI No. 654) for warning of bird hazards at airfields. He found the 654 radar to be useful without modification, but recommended improvements to the radar system to allow bird detection at greater distances. The Federal Aviation Administration has recently installed new airport surface detection (ASD) radars at airports having heavy traffic. Although no bird detection capability studies have been conducted with this unit, it might well prove to be effective in monitoring the movement

of birds on the airfield. Similarly, I am currently using a ship-board navigation radar of 3-cm wave length, the LN-66, to study echo characteristics of birds displayed on the plan position indicator (PPI) at short ranges (less than two miles). This study is necessary because it is essential that an air-traffic controller be able to recognize and discriminate echoes on the PPI produced by birds.

Two types of surveillance radar are being used for intensive studies of bird movements at intermediate ranges from about two nautical miles to approximately 40 nautical miles from the radar location. One type, the airport surveillance radar (ASR-4, -5, and -7), is operated by the FAA at nearly 152 airports in the United States. The military uses the same equipment under the designation of the FPN-47 radar. The other type, the weather surveillance radar (WSR-57M), is operated by the National Weather Service at nearly 55 locations in the United States. These radar can readily detect birds, and this capability has been thoroughly investigated for the ASR series by Flock (ref. 14), Richardson (ref. 15), and Gauthreaux (ref. 16-18) and for the WSR-57 by Gauthreaux (refs. 8, 16-18) The major characteristics of the two types of radar systems are summarized in Table 1.

ASR-4 RADARS

Although the ASR-4 is only one type of radar in the ASR series, it is the radar that has been used most often in studies of bird migrations. The military calls the ASR-4 the FPN-47. Most of my comments in this paper will refer to the ASR-4, but they also can apply to the rest of the radars in the ASR series. The ASR-4 has three important characteristics which the WSR-57 lacks. Firstly, the short pulse length (0.833 μsec), the pulse repetition frequency (1200 per second), and the 425-kw peak power output give the ASR-4 good resolution of close-in targets. Bird targets within a mile of the transmitter are clearly displayed on the PPI when it is adjusted to the 11.1 km (6 nm) range. Secondly, the radar is equipped with MTI circuits that eliminate ground clutter so that only moving targets are displayed. Thirdly, the radar completes a sweep in 4 seconds. This fast sweep rate does not permit a given echo to fade completely before the next echo is painted on the PPI. This results in each moving target having a tail much like the tail of a shooting star. The tails are made up of progressively fainter echoes from previous sweeps of the radar beam. Slower moving targets, like birds, have rather continuous, short tails, whereas faster targets, like aircraft, show longer, broken tails. The presence of tails on the echoes gives immediate information on the direction of target movement.

The disadvantages of the ASR-4 for migration studies are bothersome but certainly do not overshadow the radar's beneficial characteristics. The most serious limitations are the lack of a range-height indicator and the extreme vertical dimensions of the beam. Without accurate altitudinal information, flight controllers would have to vector aircraft around dangerous concentrations of birds even though their altitudes may be widely separated. An additional shortcoming of the ASR series is the absence of

Table 1

CHARACTERISTICS OF WEATHER AND AIRPORT SURVEILLANCE RADARS USED FOR BIRD STUDIES

Radar	WSR-57M	ASR-4, 5, 6, 7*
band (wavelength)	S(10.35 to 11.10 cm)	S(10.35 to 11.0 cm)
frequency	2700 to 2900 MHz	2700 to 2900 MHz
peak power	500 kw	425 kw
pulse length and PRF	0.5 μsec - 658 pps 4.0 μsec - 164 pps	0.833 μsec - 1040 pps 1170 pps 1200 pps
polarization	linear	linear and circular
antenna type	paraboloid	slotted dish
diameter	3.7 m (12 ft)	2.7 m (9 ft) high 5.2 m (17 ft) wide
gain	38.6 dB	34 dB
min. detect. sig.	-110 dBm	-109 dBm (no MTI) -107 dBm (with MTI)
beam type	conical	fan (vertical)
width	2°	1.5° horizontal 5.0° vertical Csc^2 to 30°
range, kilometers (nautical miles)	46.25, 92.5, 231.25, 462.5 (25, 50, 125, 250)	11.1, 18.5, 37, 55.5, 111 (6, 10, 20, 30, 60)
ranging accuracy	±0.5%	±1.0%
type of sweep	automatic and manual in horizontal and vertical either direction. Max 4 rpm; normal 3 rpm	automatic PPI, 15 rpm
presentation (scopes)	PPI off center, PPI, RHI, R, A	PPI off center, PPI
special circuits	STC, isoecho, VIP (some)	MTI, STC, CSS-1, CSS-2, PRF staggering, FTC

*The characteristics are those for ASR-4, but some are also found in the other radars in the series.

a stepped attenuator that can be used to measure the intensity of echoes from birds. Such a measure reflects the number of birds aloft or the number of birds in a given flock (ref. 18).

WSR-57 RADARS

The WSR-57 is a 10-cm (S-band) weather radar that is normally operated with a pulse length of 4.0 μsec. The shorter pulse (0.5 μsec) has a greater resolution, but because of the pulse repetition frequency and peak power (500 kw) there is a loss of sensitivity. The WSR-57 can detect birds on short pulse only when they are highly concentrated in the air. Although long pulse does not afford good resolution, even very meager movements of birds are readily detected. The WSR-57 has three major advantages for its use in studies of bird migration. Firstly, the radar has a relatively narrow, conical beam (2.0°) which permits the extraction of altitudinal information directly from the PPI provided the antenna is tilted to 2° to 3°. Secondly, the radar has a range-height indicator (RHI) that permits quick determination of the altitudinal distribution of birds automatically or manually. Thirdly, the radar, because it is a weather radar, has a stepped attenuator (3 db increments) that is normally used to measure the intensity of shower activity within 231.25 km (125 nm) of the station. The latter feature also permits the measurement of the density of birds aloft in much the same manner as radar meteorologists measure the density and size of rain drops in weather cells. The radar does, however, possess some shortcomings. Because of its recovery time, targets within 9.25 km (5 nm) are distorted and difficult to detect. The WSR-57 radar does not have a moving target indicator (MTI), and ground clutter often obscures bird movements taking place within 9.25 to 18.5 km (5 to 10 nm) of the transmitter site. The ground clutter problem is particularly bothersome in hilly or mountainous areas or at locations where the radar has been placed on top of a tall building in a large city. Side lobing is a major cause of extensive ground clutter when the radar is elevated high above the surrounding terrain, and at such locations it is not unusual for ground clutter to extend outward in most directions for 46.25 km (25 nm). The sweep rate of 20 seconds on the WSR-57 does not permit an observer to look at the PPI and see movement because the old echo from a target has completely disappeared before the next echo is painted. Fortunately, the airport surveillance radars complement the WSR-57 network.

In retrospect, the ASR-4 and WSR-57 systems truly complement each other. Those characteristics that are not present in one system can be found in the other. If a radar network is to be established to detect and monitor the movements of hazardous bird concentrations throughout the United States, both the National Weather Service and FAA radars should be integral parts of that network.

ARSR-2 RADARS

The air route surveillance radar (ARSR-2) network consists of 89 radars operated by the FAA throughout the United States. This radar is currently being used in several studies of bird migration in the United States and Canada. The radar has a wave length of 23 cm, a peak power of approximately 5,000 kw, a pulse repetition frequency of 360 Hz, and a pulse length of 2 μsec. The antenna is a cosecant^2 reflector type (7 x 14 m) with an antenna gain of 34 db. The dimensions of the primary beam are 3.75° in the vertical and 1.2° in the horizontal. The radar has a range of 200 nautical miles and is equipped with a number of specialized circuits, including MTI, staggered PRF, point target, and distributed target attenuation. The radar can be operated with circular or linear polarization and has a minimum detectable signal of -110 dbm. The ARSR-2 has detected bird echoes out to 75 nautical miles. Because of its power and sensitivity the radar is ideal for study of bird movements at greater ranges. A serious limitation of the ARSR-2 is its inability to measure the altitude of bird movements because of the large vertical beam width.

BIRD ECHOES ON SURVEILLANCE RADARS

Bird echoes have a characteristic appearance on the PPI's of most radars. On the LN-66 ship-board radar the echoes are usually distinct and appear as discrete dots when individually flying birds are detected. When flocks of birds are detected the echoes on radar show the shape of the flock and individual bird echoes are nearly impossible to delimit (Figure 1A). Because this radar does not have MTI, ground reflections are particularly noticeable. Figure 1B is a photograph of the PPI of the WSR-57 at New Orleans, Louisiana, when no bird movement is underway. Figure 2A shows the change in the PPI display when a heavy daytime bird migration of flocked songbirds is underway. Each dot on the average represents approximately 20 birds flying in a tight flock. Figure 2B shows the change in the PPI display when the migration is still underway after dark. Notice that the bird echoes (the fine sugar-like dots) are now concentrated closer to center reflecting a lowering of the altitude of migration at night. The birds are now flying individually in the night sky.

Because of the short pulse length, MTI, and short range, the echoes from individual birds displayed on the PPI of the ASR-4 radar are quite distinct. Figure 3A shows echoes from migrating birds flying individually at night. A close examination of the photograph reveals that the bird echoes have faint "tails." These are produced by fading echoes previously registered. Thus the tails instantly indicate movement and can be used to tell the flight directions of the birds. On the ARSR-2 bird echoes appear as dots (Figure 3B). The darkened band through the bird display results from the cancellation of birds flying perpendicular to the sweep of the beam. This is a result of the MTI circuit eliminating targets at the point where they show minimal radial velocity. Because of the power of this radar, bird echoes can be recorded over extensive geographical areas.

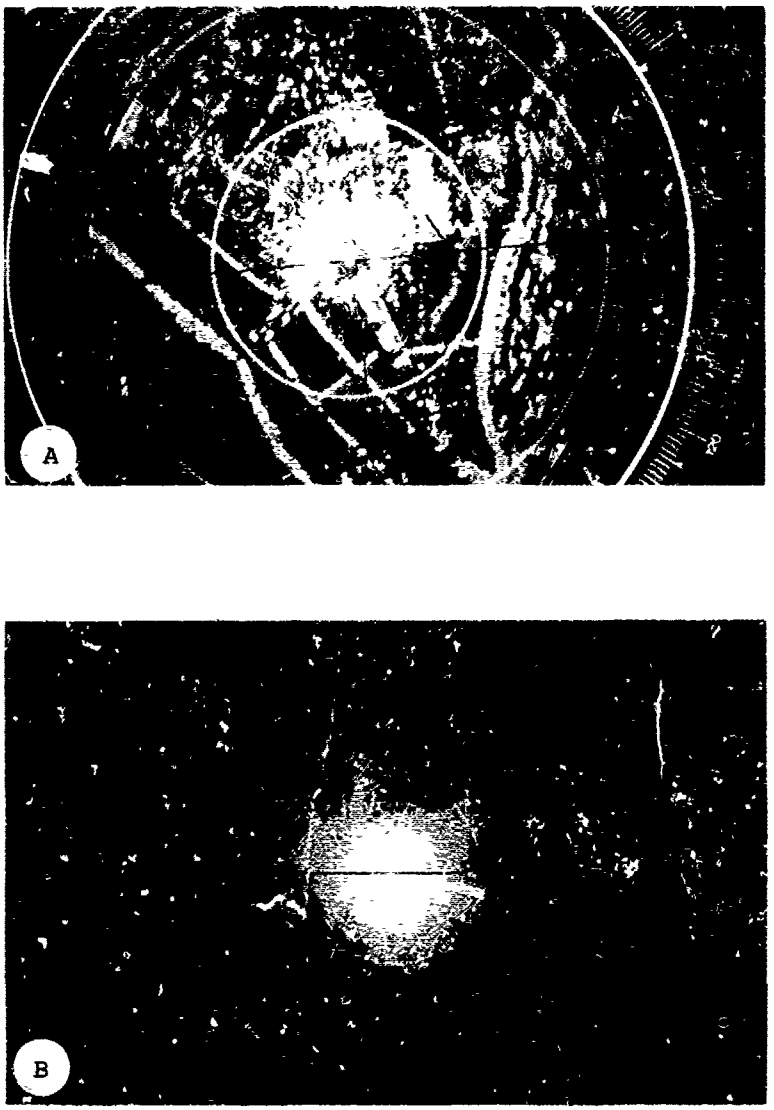


Figure 1. Photographs of PPI of the LN-66 radar (A) and WSR-57 radar (B). (A) Flocks of blackbirds (arrow) on the LN-66 radar; exposed for two sweeps of antenna; 12 February 1972, at Bosque de Apache National Wildlife Refuge, New Mexico; range marks 0.25 nm. (B) No bird movement on the WSR-57 radar; 10 May 1967, at New Orleans, Louisiana; 22:11 CST; 2.5° antenna elevation.

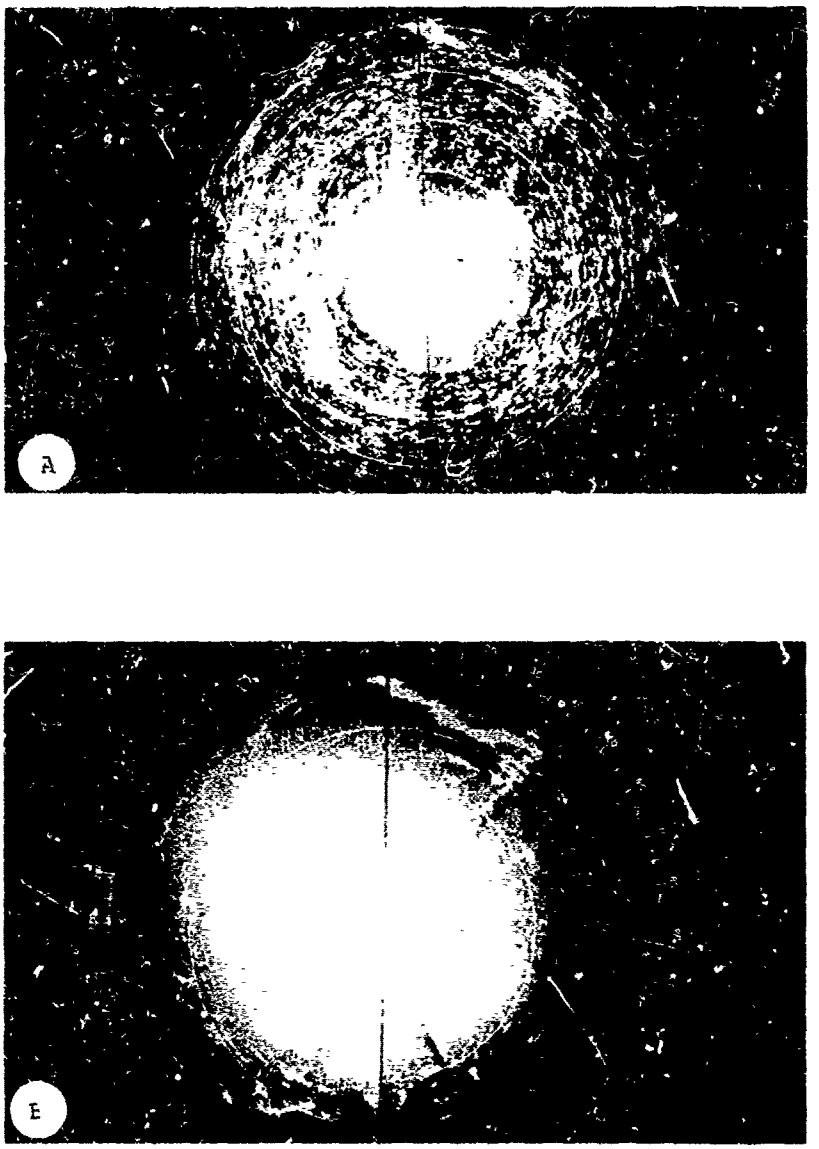


Figure 2. PPI of the WSR-57 radar at New Orleans, Louisiana, on 25 nm range. (A) 22 April 1967; 16:54 CST; 3.0° antenna elevation; daytime migration. (B) 22 April 1967; 20:17 CST; 2 5° antenna elevation; nocturnal migration.

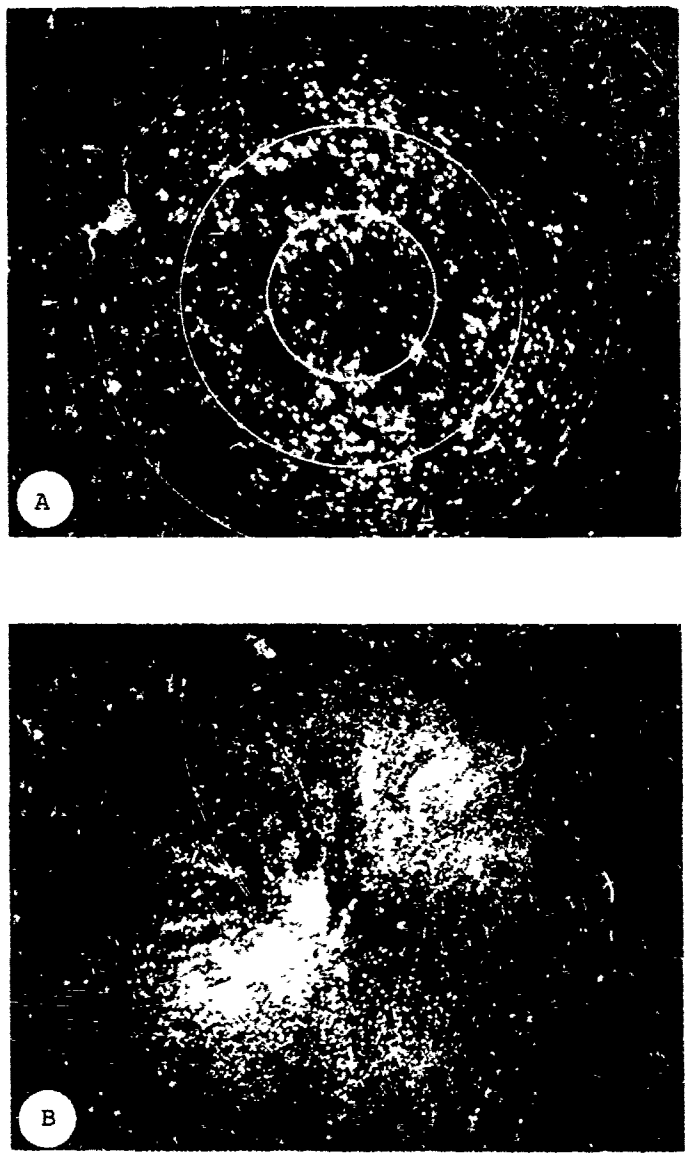


Figure 3. Photographs of PPI of the ASR-4 radar (A) and ARSR-2 radar (B). (A) Bird echoes on the PPI of the ASR-4 at Greenville Municipal Airport, South Carolina; 24 March 1973; 22:17 EST; 6 nm range; MTI on; STC and CSS off; IF gain high. (B) Bird echoes on the PPI of the ARSR-2 at Phoenix, Arizona; 27 September 1973; 22:00 MST; MTI on; point target attenuation; 50 nm range; 1 revolution.

DISCUSSION AND CONCLUSIONS

One of the greatest problems facing those who wish to use radar in preventing bird/aircraft collision is the continued modification of radar units to eliminate echoes from clutter, particularly birds. Most air traffic control radars now have circuits that can dramatically reduce the number of birds displayed on the radar screen. These circuits attenuate the return signals so that only large targets (aircraft) remain. This I believe to be necessary for flight controllers to direct air traffic, but it is imperative that the information on bird echoes be easily displayed with the flip of a switch. If this is not the case, then very valuable information on potentially hazardous concentrations of birds will not be available to the radar operator, and he will not be able to warn the pilot of the danger. Even the WSR-57 weather radar has been modified to display "processed" data on the PPI. The processing largely eliminates the bird echoes that would otherwise be displayed.

Existing types of ground-based surveillance radar can be used quite effectively to detect and monitor bird movements during most phases of an aircraft's operation, but each type suffers some shortcomings. The wedge beam radars with MTI give distinct bird echoes without confusing ground clutter, but these units cannot provide very useful information on the altitude of the bird flights. The WSR-57 gives valuable data on the altitude of bird movements because of its pencil-shaped beam, but the pulse length is too long to display distinct echoes from individual birds. Thus the ideal radar for detecting birds would be a combination of the ASR-4 and WSR-57 radars, one having a pencil beam, high power, MTI, stepped attenuation to measure the size and quantity of birds aloft, and a short pulse length to provide good information on spacing of the birds.

ACKNOWLEDGMENTS

I wish to thank Robert C. Beason for the use of his radar photographs in Figures 1A and 3B and Anne L. Harshman for her help with the preparation of the manuscript. This paper was written while I was supported by a grant from the Air Force Office of Scientific Research, AFOSR-73-2534.

LITERATURE CITED

1. Gauthreaux, S. A., Jr. (ed.). 1974. Proceedings: A Conference on the Biological Aspects of the Bird/Aircraft Collision Problem. Clemson University, Clemson, South Carolina, February 1974. 535 pp.

2. Crawford, A. B. 1949. Radar reflections in the lower atmosphere. Proc. Inst. Radio Eng., 37: 404-405.

3. Geotis, S. G. 1964. On sea breeze "angels." Proc. Eleventh Weather Radar Conf., Boston: Amer. Meteor. Soc. pp. 6-9.

4. LaGrone, A. H., A. P. Deam, and G. B. Walker. 1964. Angels, insects, and weather. Radio Science J. Res., Nat. Bur. Standards, Washington, D. C., 68D: 895-901.

5. Deam, A. P. and A. H. LaGrone. 1965. Quantitative observations of dot angel echoes at two frequencies. Radio Science, 1: 537-543.

6. Eastwood, E. 1967. Radar Ornithology. London: Methuen. 278 pp.

7. Williams, T. C. and J. M. Williams. 1969. An investigation of the collisions of bats and birds with high performance aircraft. Technical Report, 69-1021, AFOSR. 41 pp.

8. Gauthreaux, S. A., Jr. 1970. Weather radar quantification of bird migration. BioScience, 20: 17-20.

9. Thorpe, J. 1975. Bird strikes during 1973 to European registered civil aircraft. Proceedings, Tenth Meeting Bird Strike Committee Europe, Stockholm, April 1975. (N/Ref: BSCE/10 WP/5A). 35 pp.

10. Salter, A. 1975. Military aircraft bird strike analysis, 1973. Proceedings, Tenth Meeting Bird Strike Committee Europe, Stockholm, April 1975. (N/Ref: BSCE/10 WP/5B). 40 pp.

11. USAF Bird Strikes Summary, 1 Jan 1973 - 31 Dec 1973. Directorate of Aerospace Safety, Air Force Inspection and Safety Center, Norton AFB, California, 1973. 22 pp.

12. Schaefer, G. W. 1969. An airport bird detection radar for reducing bird hazards to aircraft. Proceedings, World Conference on Bird Hazards to Aircraft, sponsored by the National Research Council of Canada through the Associate Committee on Bird Hazards to Aircraft, Kingston, Ontario, September 1969. 32 pp.

13. Flock, Warren L. 1972. Flight safety aspects of precision radar near air bases in bird-aircraft collision avoidance. Technical Report, AFWL-TR-72-25, Air Force Weapons Laboratory. 57 pp.

14. Flock, W. L. 1968. Monitoring bird movements by radar. IEEE Spectrum, 5: 62-66.

15. Richardson, W. J. 1972. Temporal variations in the ability of individual radars in detecting birds. Field Note No. 61, Associate Committee on Bird Hazards to Aircraft, National Research Council, Ottawa, Canada. 70 pp.

16. Gauthreaux, S. A., Jr. 1973. Quantification of bird echoes on airport surveillance radars. Proceedings, Conference on Transparent Aircraft Enclosures, Las Vegas, Nevada. (AFML-TR-73-126, Wright-Patterson AFB, Ohio). pp. 515-529.

17. Gauthreaux, S. A., Jr. 1974. The detection, quantification, and monitoring of bird movements aloft with airport surveillance radar (ASR). Proceedings, Conference on Biological Aspects of the Bird/ Aircraft Collision Problem, Clemson, South Carolina. pp. 289-304.

18. Gauthreaux, S. A., Jr. 1975. Radar ornithology: Bird echoes on weather and airport surveillance radars. Clemson University, Clemson, South Carolina. 47 pp.

BIRD IMPACT FORCES IN AIRCRAFT WINDSHIELD DESIGN

R. L. Peterson
Air Force Flight Dynamics Laboratory
Wright-Patterson Air Force Base, Ohio

and

J. P. Barber
University of Dayton
Research Institute
Dayton, Ohio

BIRD IMPACT FORCES IN AIRCRAFT WINDSHIELD DESIGN

by

Richard L. Peterson

Air Force Flight Dynamics Laboratory
Wright-Patterson AFB, Ohio

and

Dr. John P. Barber

University of Dayton Research Institute
Dayton, Ohio

ABSTRACT

In order to design transparent aircraft windshield and canopy panels which can withstand the impact of birds, and at the same time meet other equally important operational requirements, it is necessary to define the forces generated during the birdstrike event. It is important to define the total force in order to understand the far field structural response; and the local pressure and pressure distribution in order to understand local structural response. The total force as a function of time was measured by impacting birds onto a large diameter Hopkinson bar. The local pressures and pressure distribution during the bird impact were measured by flush mounting piezo-electric pressure transducers in a heavy rigid flat plate and impacting the plate/transducer assembly. The forces and pressures are a function of the relative impact velocity and angle, the weight and average density of the bird and the stiffness of the impacted structure. In order to define the temporal and spatial distribution of the bird impact forces, the AFFDL has initiated a substantial parametric bird/plate impact test program. These tests are being conducted at AFML/UDRI and the AEDC and cover a velocity range from 30 m/s to 350 m/s, impact angles from 15° to 90° to trajectory and bird weights from 0.05 kg to 3.6 kg. The results at the 90° test angle indicate that: (1) birds behave essentially as a fluid during impact; (2) birds do not bounce at impact - the impulse is equal to the initial impact momentum; (3) the high frequency component of pressure superimposed on the base pressure-time pulse is caused by breakup of the bird flesh and inhomogeneities in the bird; and (4) the duration of loading is approximately equal to the 'squash up' time.

SECTION 1

INTRODUCTION

Bird impacts on aircraft windshields and canopies may produce damage or catastrophic failure which can result in mission abortion, loss of the aircraft and/or loss of crewmembers. Aircraft birdstrikes have greatly increased over the last 20 years principally because of increased speeds in jet engine aircraft and the advent of low altitude high speed penetration missions. The engines and the windshields and canopies have proven to be the most vulnerable portions of an aircraft.

Since 1966, the U.S. Air Force has lost at least eleven aircraft worth over 61 million dollars due to bird impacts on transparent enclosures. These include the loss of a T-37B with one fatality, three T-38s with two fatalities, two F-100s with one fatality, and five F-111s with, fortunately. no fatalities. In addition to the $61 million loss in airframes, and the incalculable loss due to fatalities, an estimated $20 million has been spent in repair costs during the period 1966 through 1972. Further, the role of bird impacts in aircraft losses in Southeast Asia is not fully known.

In order to utilize analytical windshield design techniques and computer programs in the windshield design process, it is necessary to first adequately understand how a windshield is loaded by a bird during the birdstrike event. This involves determining the local pressure and pressure distribution (both temporal and spatial) in order to understand local structural response; and the total force in order to understand the far field structural response.

The AFFDL is currently conducting several R&D programs at AEDC and the AFML/UDRI which will define local pressure and total force on a flat rigid plate for various bird weights and velocities, and for various angles of impact.

SECTION 2

EXPERIMENTAL TECHNIQUES

Bird/plate impact experiments are conducted using birds (chickens) ranging in size from 0.05 kg to 3.6 kg. The AEDC facility is used for bird weights above 0.25 kg. The birds must be launched intact at velocities from 30 m/s to 350 m/s. Some of the pertinent launcher design considerations and constraints are:

a. Birds must be prevented from breaking up during launch by use of appropriate saboting and/or bagging techniques.

b. Acceleration must be kept sufficiently low to prevent destruction of the bird.

c. The bird must separate freely from the sabot.

d. The sabot must be stopped in the launch tube or diverted from the bird trajectory to prevent the sabot from impacting the target.

e. Acceleration must be removed from the bird for a sufficient period of time to permit the bird to 'relax' before impact.

2.1 AFML/UDRI Facility Description

2.1.1 The Range - The AFML/UDRI range[1] consists of an 8.90 cm bore x 4.27 m long powder driven gun, a blast tank and a target tank as shown in Figure 2.1. Each end of the gun tube is threaded to accept a breech block at the breech end and a sabot stopper at the muzzle end. Four longitudinal slits, 46 cm long, were machined in the gun tube to vent the powder gas and permit the sabot to begin deceleration before striking the sabot stopper.

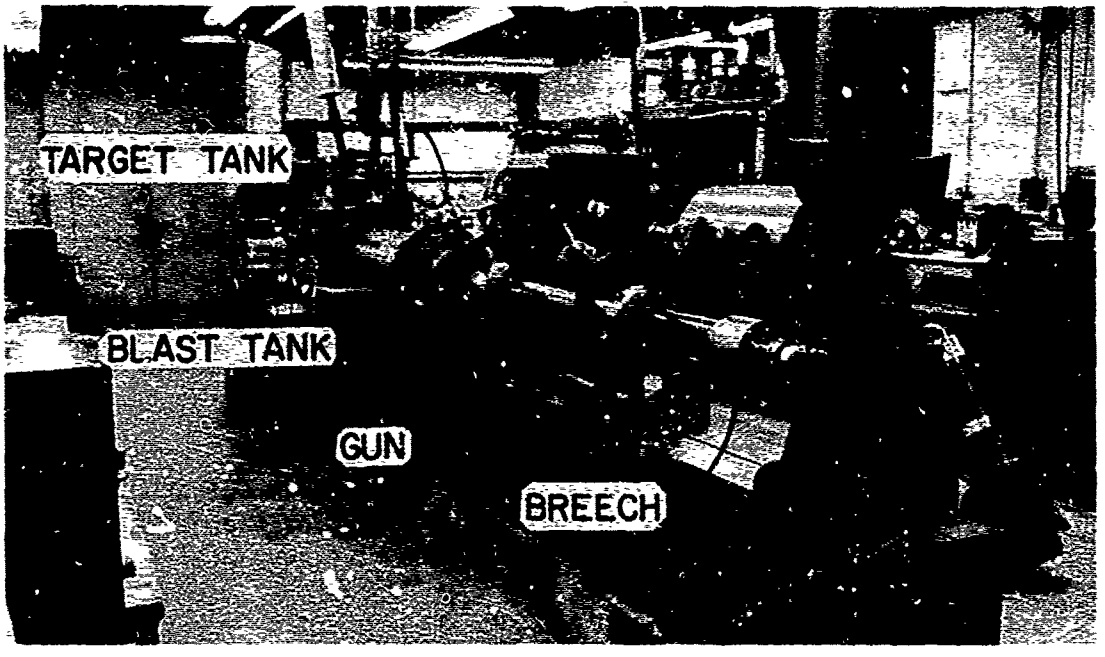


Figure 2.1 Overall View of AFML/UDRI Bird Range Facility

The breech block incorporates a soft launch buffer technique which generates a low but constant acceleration pressure behind the projectile until the pressure is relieved by the longitudinal slits at the muzzle. The buffer system consists of a chamber in the breech block into which the powder gas expands. The output port of the chamber is necked down to restrict gas flow into the gun.

During a test, the range is evacuated to an air pressure of 5 torr to assure repeatable bird orientation at impact. The sabot is fabricated from high density polyethylene. A 1.27 cm thick hard rubber ring attached to the sabot stopper plate acts as a pad for the sabot wall to strike. A conical steel spreader ring with an interior diameter of 0.65 cm greater than the diameter of the sabot pocket is attached to the stopper plate as shown in Figure 2.2. The spreader ring cuts into the wall of the sabot

forcing most of the wall to spread outward and into the stopper plate. Only the outer portion of the sabot wall is deformed and the pocket remains intact. The pocket in the sabot is sized to accommodate birds weighing 0.05 kg to 0.15 kg. Satisfactory sabot separation is achieved and there are no secondary impacts of sabot material on the target surface. The bird releases without any apparent damage or disruption to its attitude or flight path as evidenced by the x-radiographs and photographs.

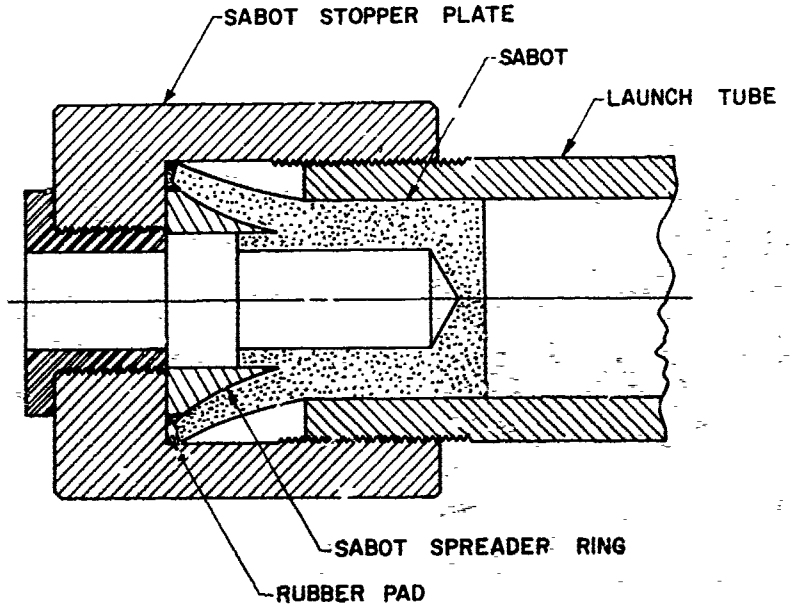


Figure 2.2 Sabot Stopper

2.1.2 Velocity Measurement System - Velocity is calculated from the time of flight as the bird passes through two pairs of laser light beams. The time interval is measured with a digital time interval counter. Two laser beams are aligned at each station to form a triangular plane perpendicular to the projectile trajectory with the beams converging at the element of a photomultiplier tube. Because the beams are independent, they must both be interrupted simultaneously to produce a signal of sufficient amplitude to overcome the bias on a built-in pulse amplifier and generate a signal. The use of two lasers at each velocity station is necessary to assure that the velocity of the main body of the bird is measured and not the velocity of loose feather or debris. Photographs and x-radiographs verify the reliability of this trigger system. The accuracy of the velocity measurement system is $\pm 1\%$.

2.1.3 Photograph and x-radiography - Each bird launched is x-rayed and photographed immediately prior to impact to verify that it was properly oriented and intact. In addition, high speed cinematography of the bird during impact is obtained on selected shots to aid in the description and understanding of the bird breakup. The x-ray and light sources are triggered from the output of the first interrupted laser beam velocity measuring station.

All birds are launched tail leading and impact the plate in that orientation. From the x-radiographs, no breaking or crushing of bones during launch for muzzle velocities of up to 350 m/s is observed.

A xenon flash tube light source and 10 cm x 12.5 cm camera are used to obtain photographs of the bird prior to impact to verify the x-radiographic results. Typical photographs are shown in Figure 2.3.

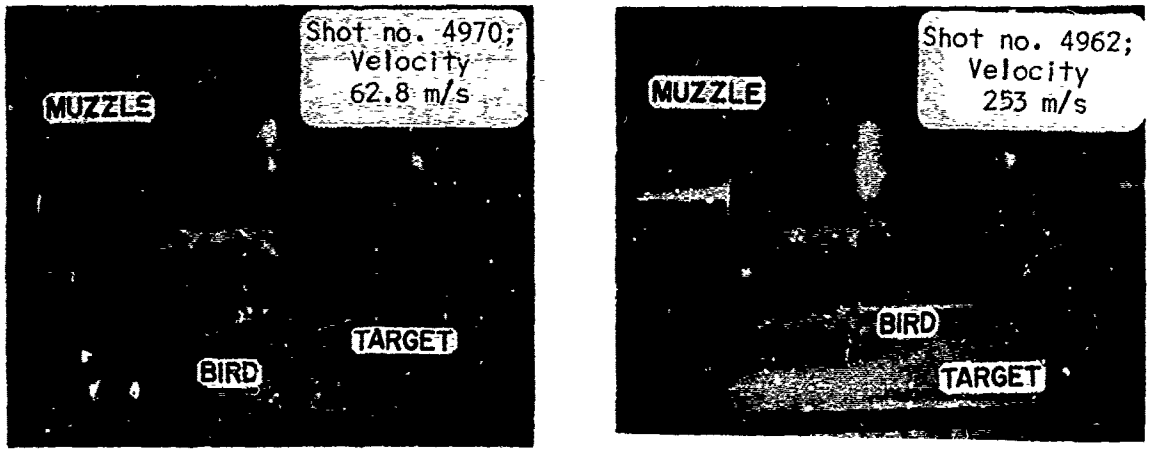


Figure 2.3 Photographs of Launched Birds

A full framing 16 mm Fastax camera at a framing rate of 7500 frames per second is used to record the impact process in order to observe bird breakup and debris distribution during and after impact.

2.1.4 Hopkinson Bar Study - Hopkinson bars have been used over the last 50 years for measuring force-time histories of impulsive events. The basic concept on which a Hopkinson bar operates is that a force rapidly applied to the end of a homogeneous bar of elastic material will generate a stress wave that propagates along the bar at constant (near sonic) velocity. The stress wave can be detected at any point along the bar by placing a strain gage on the bar surface and monitoring the output. The strain-time history is related to the instantaneous force, F, applied to the end of the bar through the Youngs modulus, E, of the bar material and the cross-sectional area of the bar, A, as $F = \varepsilon EA$, where ε is the measured strain as a function of time.

This principal is applied to determine the force-time history of a bird striking a rigid plate as follows. The birds are launched against the end of a long aluminum bar on which strain gages are mounted 10 diameters down the bar from the impacted end. The resulting strain pulse in the bar is recorded and related to the stress pulse. The bar must be long enough to

assure that the entire stress pulse from the impact is recorded before a reflected wave from the far end of the bar can propagate back to the strain gage. A 3.66 m long, 7.62 cm diameter rod of 7075 T6 aluminum was chosen. The 7.62 cm diameter is the minimum which would permit the lateral expansion of the bird upon impact without allowing material to flow around the rod and continue down-range. Two strain gages are mounted on opposite sides of the bar 76.2 cm (10 rod diameters) from the impact end as shown in Figure 2.4. The two gages are connected in series to a strain gage bridge such that the signal from each gage is added to double the sensitivity of the system. Rod bending (which occurs if the impact is slightly off center) produces compression in one gage and tension in the other; the signals then subtract and the bending signal is rejected.

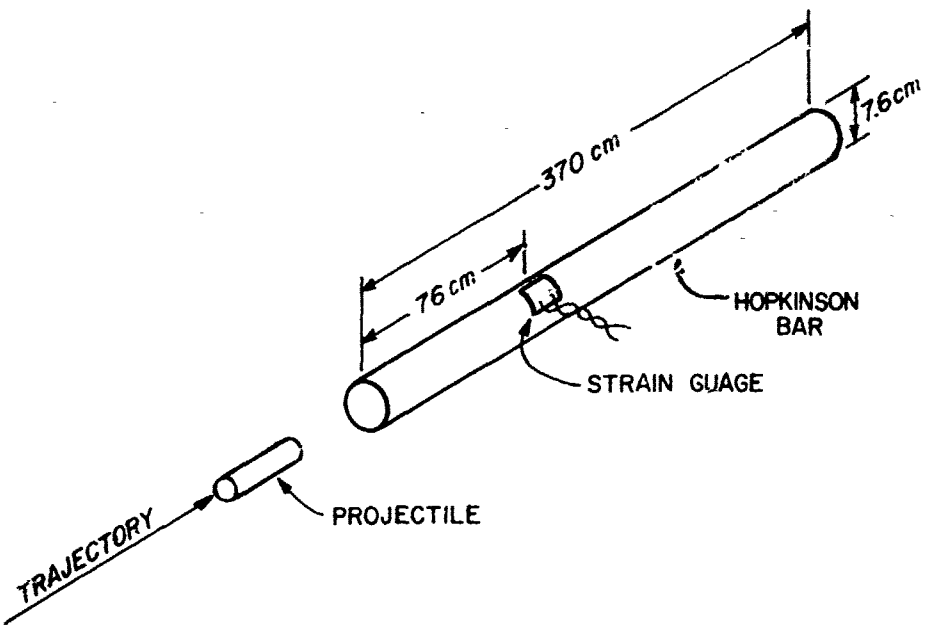


Figure 2.4 A Hopkinson Bar As Configured To Measure Impact Forces

Considerable thought was given to techniques for mounting the bar in the ballistic range. Rigid longitudinal restraint of the bar introduces error signals into the data while insufficient restraint of the bar permits the bar to recoil and move down the range. The solution chosen is to connect the front end of the bar to the ballistic range with a rubber boot which allows almost total freedom of motion while permitting the range to be evacuated. The bar is supported along its length on teflon rings which provide good lateral support and virtually no longitudinal constraint. The rear end of the bar is butted against a rigid constraint to prevent cross motion. A photograph of the Hopkinson bar mounted on the range is shown in Figure 2.5.

Strain data is recorded by observing the output of a standard strain gage bridge with an oscilloscope and photographing the resultant trace. A cine camera is also used to view the impact of birds striking the end of the rod. The films show clearly that the birds are totally stopped by the rod

(no material flows around the rod and continues in its original direction). In addition, it is observed that 'bounce' is negligible and the bird material flows radially away from the impact point along the end surface of the rod.

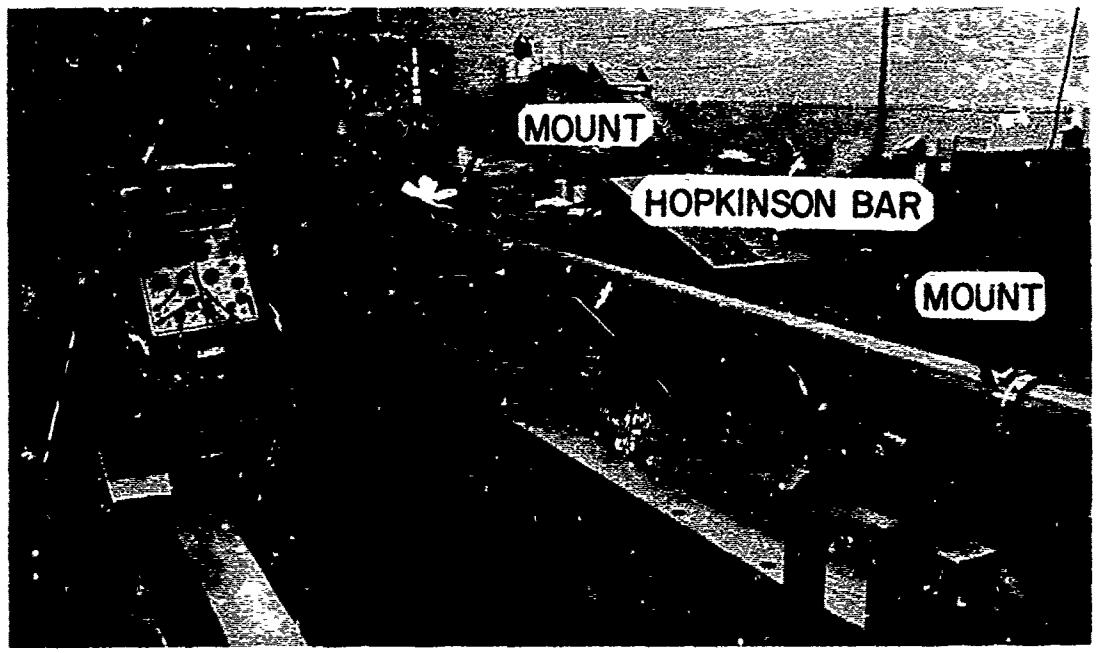


Figure 2.5 A Photograph Of The Hopkinson Bar Mounted On The AFML/UDRI Range

2.1.5 Pressure Measurement - Piezo-electric quartz pressure transducers which employ a compact impedance converter physically located in the coaxial line close to the crystal are used to sense local pressure in these experiments. Since these transducers are not designed for impact testing, considerable experimentation and calibration was necessary to verify their operation. A calibration method for the transducers was developed to verify the applicability of the manufacturer's calibration data to the unidirectional loads anticipated. A device was fabricated to enable unidirectional axial loads, similar to the bird/plate impact loads, to be applied to the transducer and measurements were taken to determine the response of the transducers. It is concluded that the transducers will provide reliable, accurate pressure data over the range of pressures and frequencies expected.

The target, a 15.25 cm diameter 5.10 cm thick steel disk, is mounted on the tank wall approximately 36 cm from the gun muzzle as shown in Figure 2.6. The transducers are flush mounted at 1.27 cm radial intervals in the steel target disk. The disk is supported by a 10.16 cm diameter, 1.27 cm wall tube, which is welded to a 3.81 cm thick flange. This design provides a rigid target support while permitting ease of access to the transducers.

A series of bird (chicks) impact experiments against the instrumented target were conducted over a velocity range of 30 m/s to 300 m/s. Bird weights range from 0.05 kg to 0.15 kg. The target was positioned at 25°, 45°, and 90° to the bird trajectory during the test program. The pressure-time pulse was recorded using oscilloscopes. The pressure pulse was filtered to 10 kHz to eliminate the majority of the high frequency signal. The results are reported in Section 3.

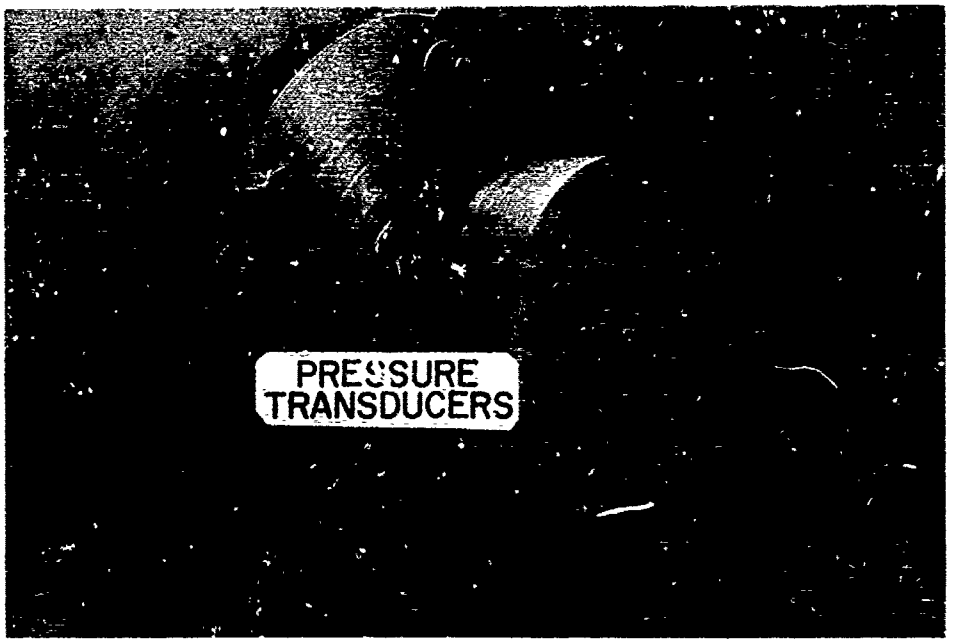


Figure 2.6 A Photograph Of The AFML/UDRI Pressure Plate Showing The Pressure Transducers Flush Mounted On The Impact Surface.

2.2 AEDC Facility Description

2.2.1 The Range - The AEDC bird launcher[2] is an air operated gun consisting of a driver, launch tube, breech section and sabot stripper tube as shown in Figures 2.7 and 2.8. The launcher consists of a 9.45 m long driver having a 20.3 cm diameter bore with a volume of 0.329 m^3, and a two-piece launch tube 18.3 m long having a 17.8 cm diameter bore with a volume of 0.448 m^3. The bird and its sabot are loaded between the driver and the launch tube immediately forward of a double diaphragm section. The bird is launched by charging the driver with air to the desired pressure while simultaneously charging the volume between the two diaphragms to some intermediate pressure. The volume between the diaphragms is then vented whereupon the diaphragms are overpressured and rupture, propelling the sabot containing the bird down the launch tube. The diaphragms are made of Mylar and vary in thickness from 0.13 cm to 0.36 cm depending upon the desired burst pressure.

The test area consists of a 6.9 m by 9.7 m covered concrete pad (reference Figure 2.8) upon which are set steel H-beams used for mounting targets. The area is equipped with a high pressure water hose with which bird debris is washed into a container located underneath the floor near the back edge of the pad. The target is located 7.6 m from the stripper muzzle. The accuracy of the launcher in striking the designated target point with the projectile is $\pm$ 2.5 cm. The birds used are chickens, and they are packaged in a nylon bag before insertion into the sabot in order to prevent aerodynamic breakup during flight to the target. Balsa wood sabots are used because of their light weight, low cost, relatively high strength, ease of manufacture, and simplicity of removal from the stripper after the shot. The density of the balsa wood varies and the denser high strength material is used for higher speed shots.

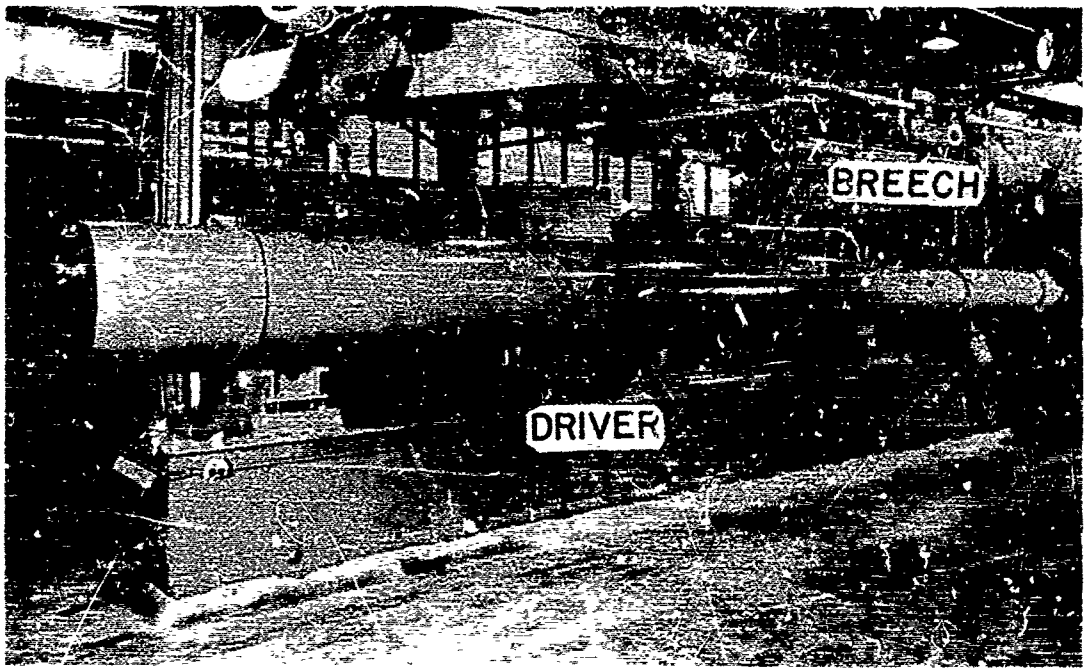


Figure 2.7 AEDC Bird Impact Launcher

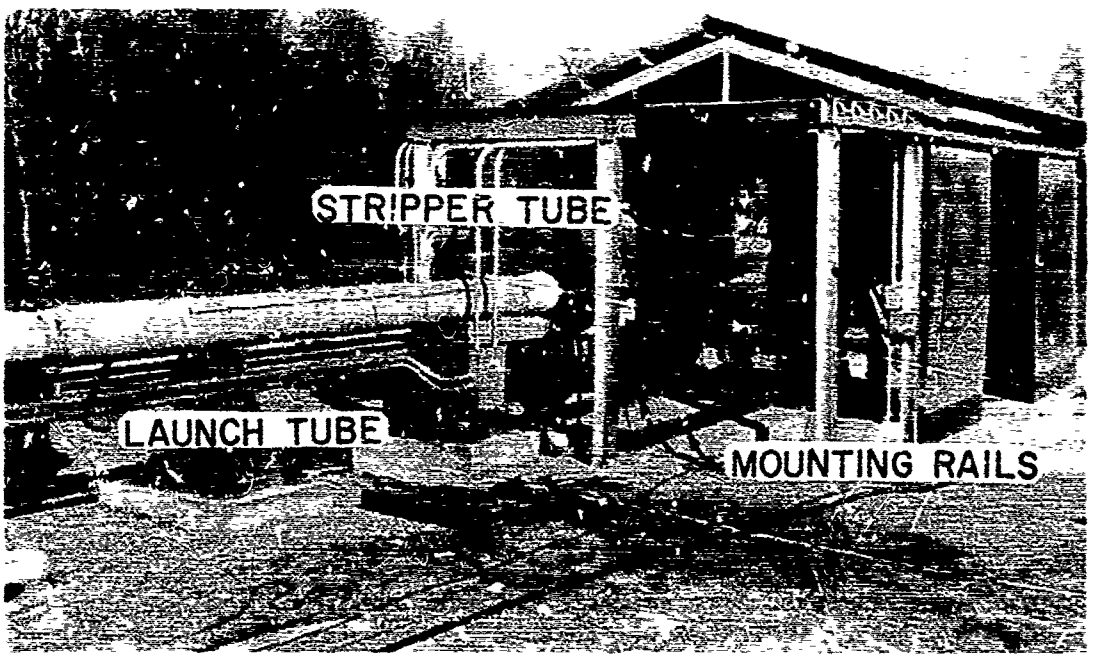


Figure 2.8 AEDC Bird Impact Facility Test Area

The sabot is prevented from striking the target by a tapered stripper tube attached to the muzzle of the launch tube. The stripper tube as shown in Figure 2.9 consists of a 0.61 m long vent section to allow escape of the driving gas, followed by a 3.05 m length of pipe with a taper machined in the bore. The taper reduces from the 17.8 cm launch tube bore diameter down to approximately 13.3 cm diameter at the muzzle. The sabot is removed from the stripper after the shot by driving it back into the vent section, then splitting it into pieces small enough to be removed between the vent section guide rails.

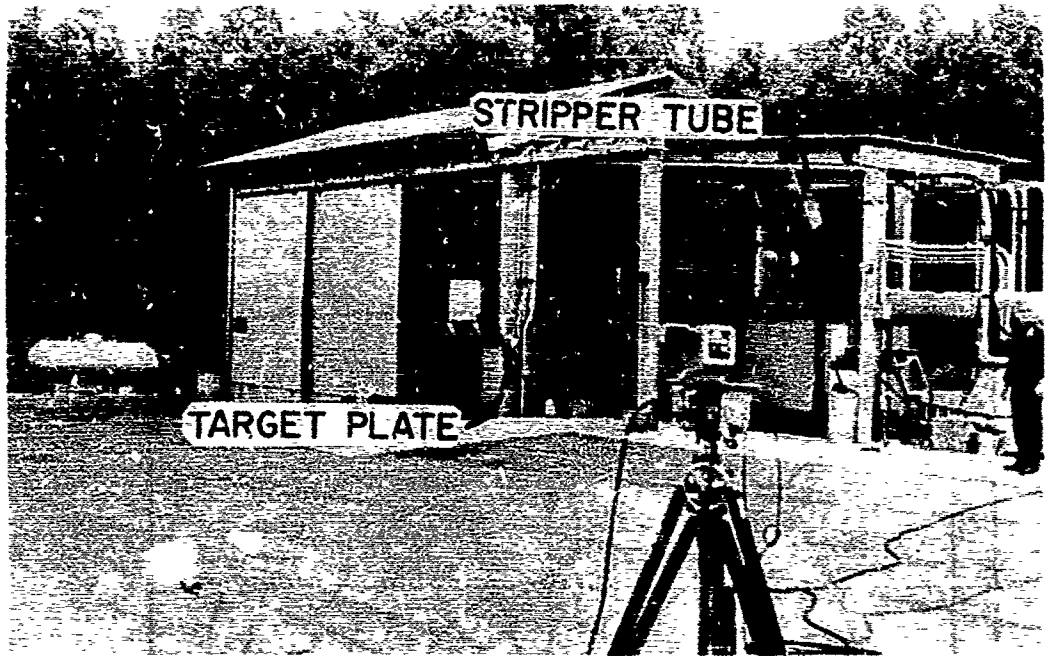


Figure 2.9 AEDC Target Plate At 90°

2.2.1 Test Instrumentation - Test instrumentation includes a projectile velocity measuring system, piezo-electric pressure transducer/recording system and general still and cine picture coverage of the impact event.

The primary system for measuring projectile velocity consists of two x-ray stations located a known distance apart along the flight path between the launcher muzzle and the target. The x-ray pulsers are triggered by breaking a 24 gauge copper wire in an electrical break-wire system. The time between firing of the pulsers is recorded with a digital chronograph and, using this time together with the distance measured between images of the projectile on the x-ray film (after corrections for point source parallax), velocity is determined. The velocity measuring system is mounted on an instrumentation dolly with the first station located approximately 1.07 m from the muzzle of the stripper tube. The distance between the two x-ray stations is 2.13 m. The accuracy of this velocity measuring technique is better than $\pm$ 1%.

2.2.2 Pressure Measurement - Piezo-electric quartz pressure transducers which employ a compact impedance converter in the coaxial line close to the crystal are used to sense impact pressure. FM magnetic tape recorders are used to record the pressure data.

The target, a 76 cm x 76 cm steel plate, 10 cm thick, is mounted on the birdstrike fixture approximately 7.62 m from the gun muzzle (reference Figure 2.9). The target plate can accommodate up to 29 pressure transducers positioned as shown in Figure 2.10.

2.2.3 Test Program - A series of full size bird (chicken) impact experiments against the instrumented target are scheduled over a velocity range of 90 m/s to 350 m/s. Bird weights range from 0.9 kg to 3.6 kg. The target is positioned at 15°, 30°, 45°, 60°, 75° and 90° to the impact trajectory during the test program. The pressure-time pulses are recorded on FM magnetic tape for data reduction at a later date. Oscillograph traces from the FM system are obtained for quick check reference. Selected high speed cine and still coverage are also accomplished.

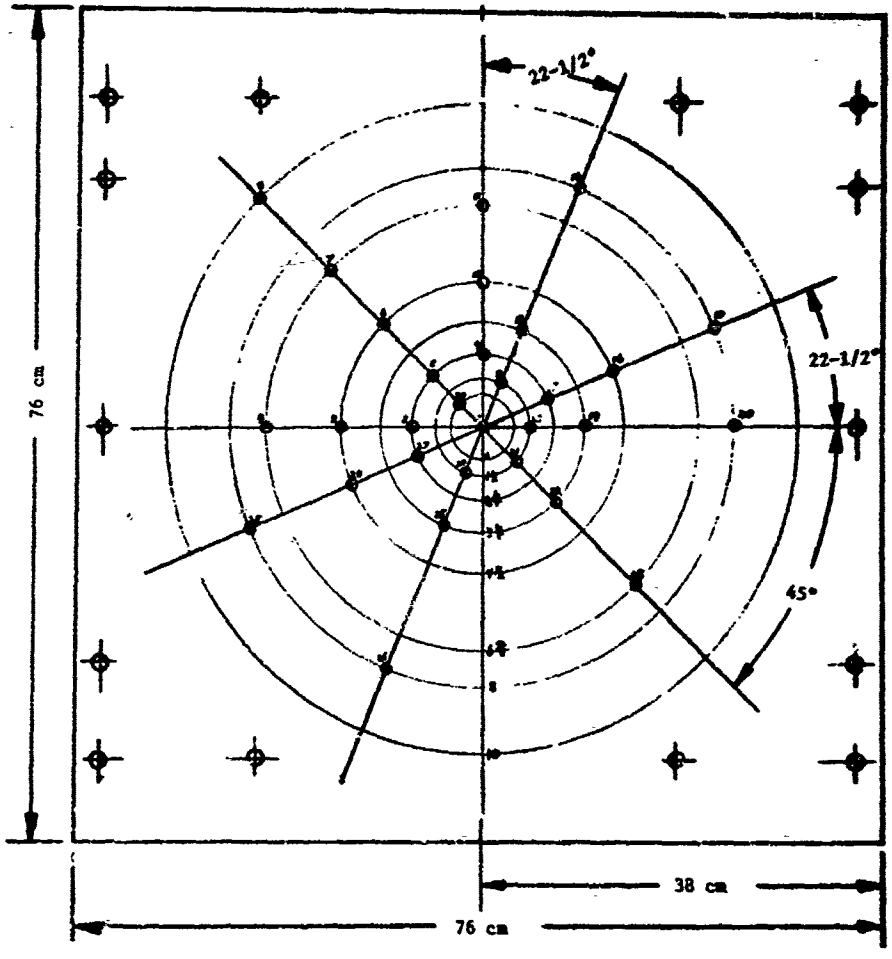


Figure 2.10 Location Of Pressure Transducers In AEDC Target Plate

SECTION 3

EXPERIMENTAL RESULTS

This section reports and discusses the results obtained to date. The AFML/UDRI and AEDC results are reported separately and a comparison is made at the end of this section.

3.1 AFML/UDRI Results

3.1.1 Hopkinson Bar Results - A series of bird impact tests on the Hopkinson bar were conducted. The bird masses were in the range from 0.05 kg to 0.15 kg. Impact velocities ranged from about 30 m/s to almost 300 m/s.

The force-time record for a typical bird impact is shown in Figure 3.1. The force rises rapidly to a maximum and then falls linearly for some time followed by an exponential drop to zero. The total duration of the impact is closely approximated by the time required for the bird to travel its own length at the impact velocity.

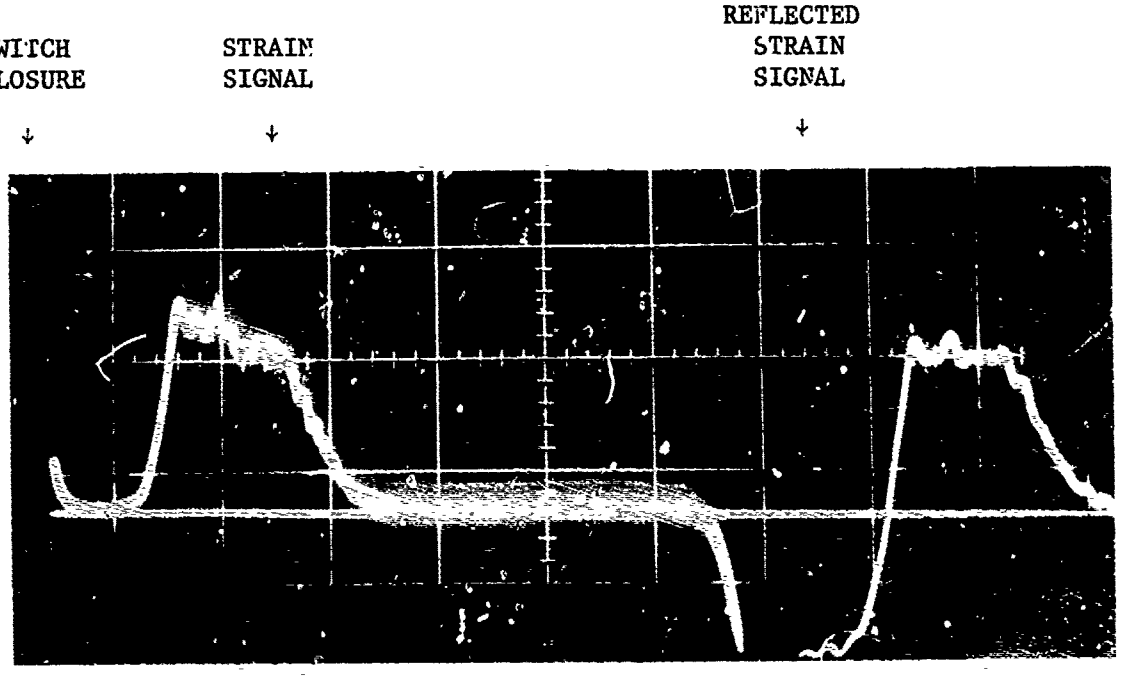


Figure 3.1 An Oscillograph Of The Strain Gage Output On A Hopkinson Bar During A Bird Impact.

The area under the force-time curve is simply the impulse imparted to the target during the impact. If the bird does not bounce, the impulse should be exactly equal to the initial bird momentum. The force-time records from the Hopkinson bar were integrated to yield impulse and the measured impulse as a function of impact momentum is displayed in Figure 3.2. There is no evidence of bird bounce (and resultant systematic impulse augmentation) and the entire momentum of the bird is converted to impulse.

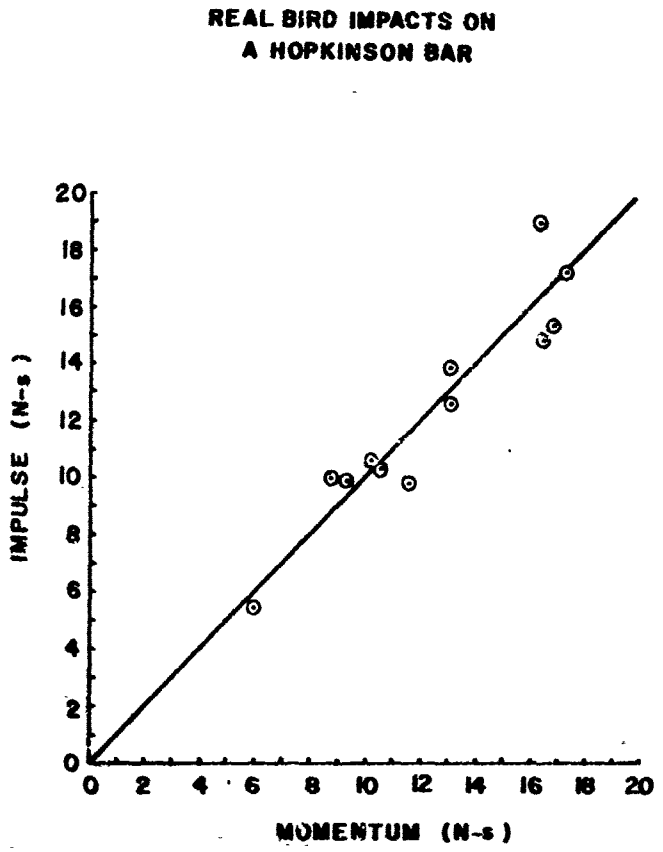


Figure 3.2 Impulse Versus Impact Momentum For Birds Impacted On A Hopkinson Bar

If the bird does not decelerate during impact (i.e., the impact is supersonic) then the duration of the force-time pulse should be equal to the time it takes for the bird to 'squash up'. The 'squash up' time is given by the length of the bird divided by the impact velocity. The measured results are shown in Figure 3.3. Within the experimental accuracy the results indicate that the duration is equal to or slightly greater than the 'squash up' time. The bird therefore decelerates very little, if any during the impact.

The impulse imparted to the target is given by the initial momentum, $P = mv$, of the bird where m is the bird mass and v is the impact velocity. The time, t, over which this impulse is imparted is the 'squash up' time, $t = \ell/v$, where ℓ is the length of the bird. The average force, F_{avg}, is therefore given by

$$F_{avg} = P/t = mv^2/\ell. \qquad (3.1)$$

The peak force is higher than the average force by some factor. If the basic 'shape' of the force-time pulse remains constant, independent of bird mass

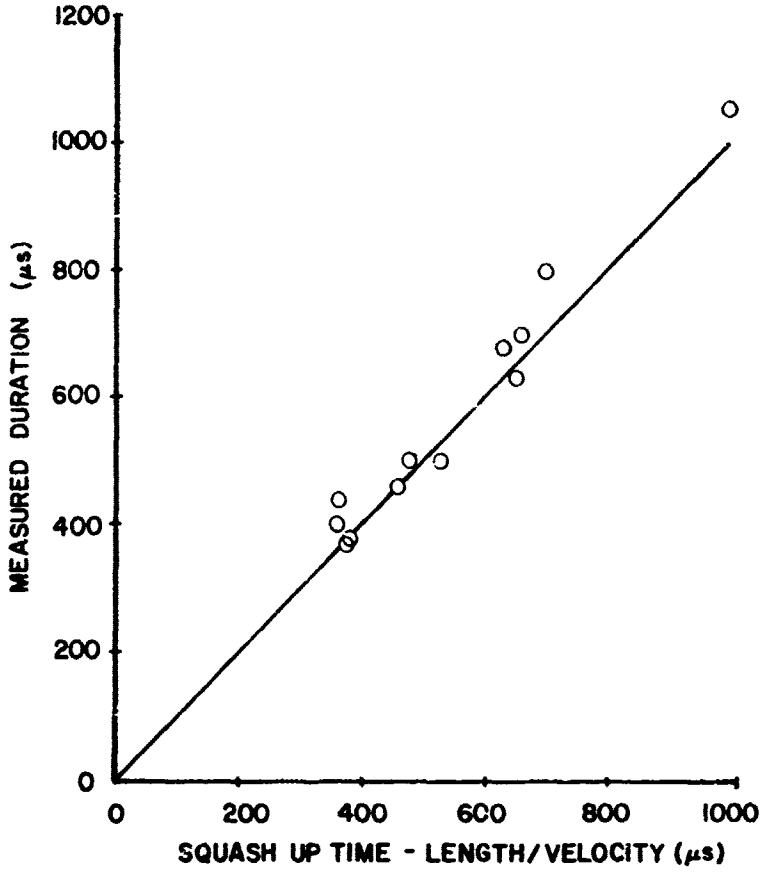


Figure 3.3 Force Time Pulse Duration Versus Calculated 'Squash Up' Time For Bird Impacts On A Hopkinson Bar

and velocity, then that factor should remain constant. This may be formalized by introducing a nondimensional force

$$\bar{F} = F/F_{avg} . \qquad (3.2)$$

The peak force was measured in the Hopkinson bar records and the results in terms of the nondimensional peak force, $\bar{F}_{peak}$, are shown in Figure 3.4. From Figure 3.4 it is apparent that although there is considerable scatter, particularly at low velocity, the nondimensional peak force is approximately 2. It is noteworthy that the nondimensional peak force would be exactly 2 if the force-time curve was 'triangular.' A large number of curves have been examined, and they are roughly 'triangular.' The force rises linearly to a peak force of twice the average and falls linearly to zero.

3.1.2 Pressure Plate Results -- More than 100 impact tests were conducted on the pressure plate at AFML/UDRI to determine the manner in which a bird loads a plate during impact. The output from the pressure transducers were recorded with oscilloscopes. Typical pressure-time records at the center-of-impact are shown in Figure 3.5. Pressures of 100 MN/m^2 and pressure durations of the order of hundreds of microseconds are typical. The recorded pressure time

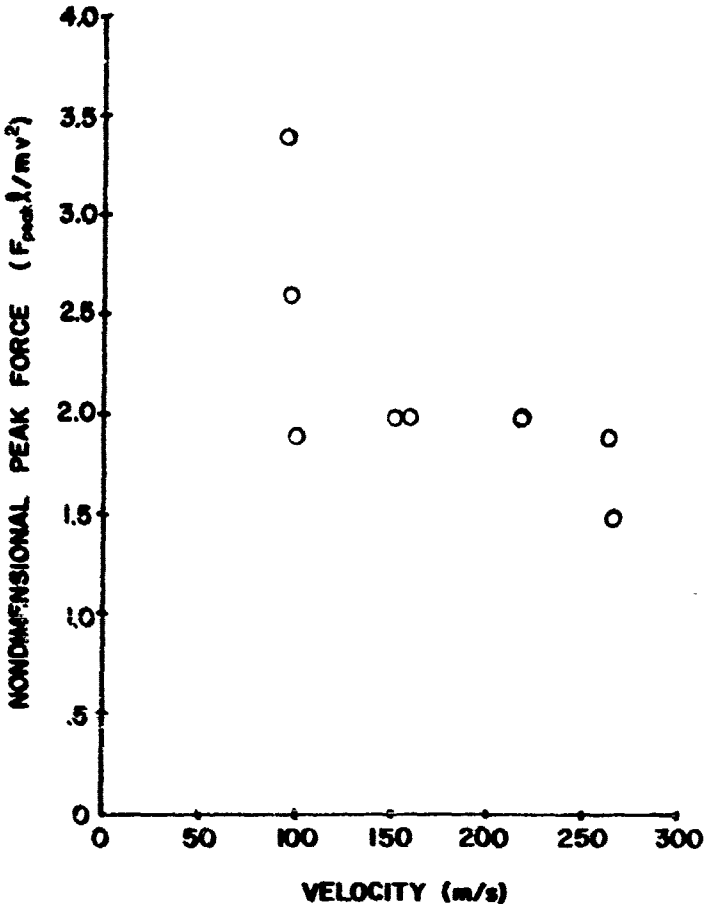
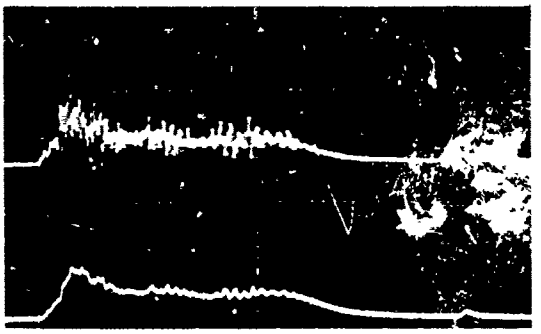
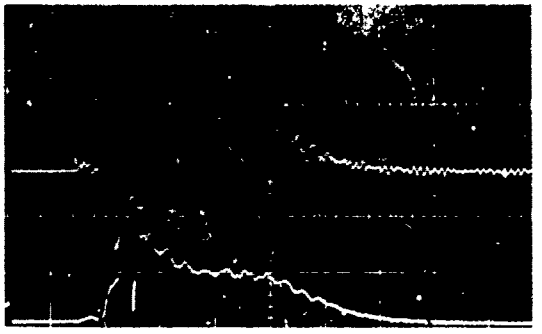


Figure 3.4 Nondimensional Peak Force Versus Velocity For Bird Impacts On A Hopkinson Bar

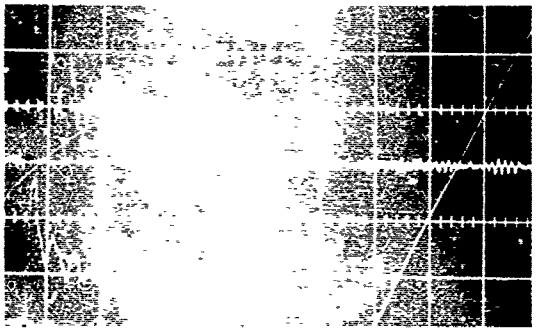
pulse can be described as a relatively low frequency 'base' pressure pulse on which is superimposed a high frequency pressure variation as illustrated in Figure 3.6. The base pressure profile remains similar from shot to shot, although amplitude and duration vary with velocity and bird size. The high frequency component varies in frequency and amplitude from shot to shot and appears to have little repeatable structure. Acceleration measurements on the impact plate verified the ability of the acceleration compensation mechanism in the pressure transducers to adequately reject high amplitude, high frequency shock accelerations. A number of impact tests conducted using 'RTV' (GE RTV-560) rubber cylinders generated accelerations similar to those produced by birds, but the 'RTV' pressure data lacked the high frequency content as indicated in Figure 3.7. The high frequency pressure component of real bird impacts must therefore be regarded as a particular and real characteristic of bird impact and not just instrumentation noise. Further tests were conducted with boneless beef and the results are shown in Figure 3.7. The similarity in the high frequency content of beef and birds indicates that the high frequencies are related to the fracturing of flesh. Other tests on RTV-560 with large inhomogeneities introduced (voids, plastic rods, etc) indicate that inhomogeneities contribute a small portion of the noise.



Shot no. 5404; velocity 109 m/s;
horizontal scale 200 μs/cm; vertical scale 12.3 $MN/m^2/cm$;
upper trace unfiltered; lower trace filtered



Shot no. 5399; velocity 199 m/s;
horizontal scale 100 μs/cm; vertical scale 24.5 $MN/m^2/cm$;
upper trace unfiltered; lower trace filtered



Shot no. 5396; velocity 279 m/s;
horizontal scale 100 μs/cm; vertical scale 49.0 $MN/m^2/cm$;
upper trace unfiltered; lower trace filtered

Figure 3.5 Centerline Pressure Transducer Outputs For AFML/UDRI Target Disk

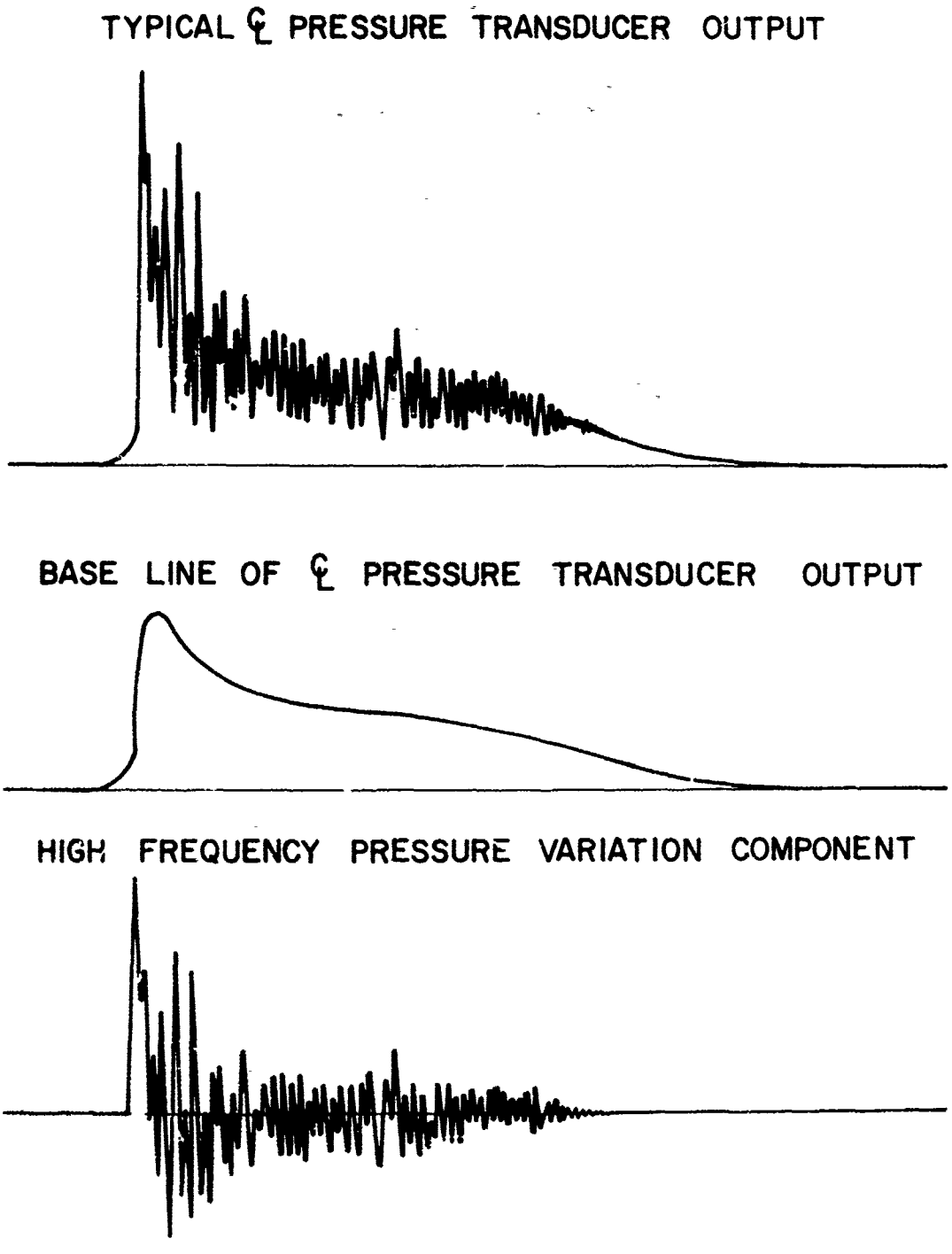
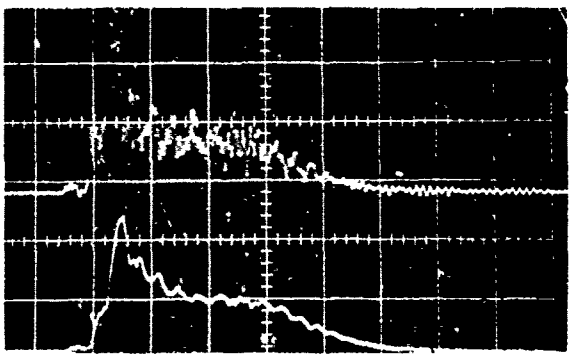
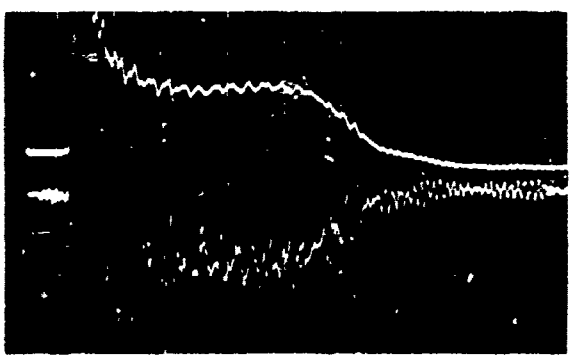


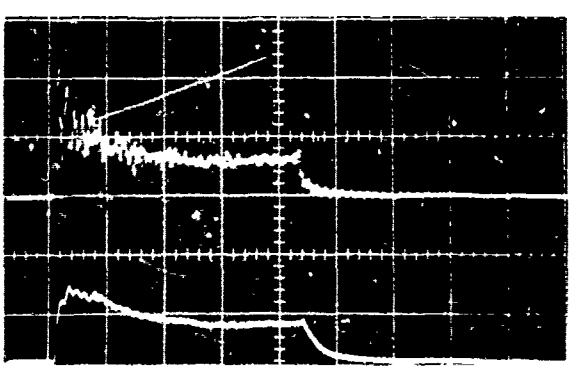
Figure 3.6 Typical Components Of Impact Pressure For Bird Impacts



Bird impact; shot no. 5399; velocity 199 m/s;
horizontal scale 100 μs/cm; vertical scale 24.5 MN/m^2/cm;
upper trace unfiltered; lower trace filtered



Beef impact; shot no. 5306; velocity 174 m/s;
horizontal scale 100 μs/cm; vertical scale 11.9 MN/m^2/cm;
upper trace filtered; lower trace unfiltered



RTV-560 impact; shot no. 5369; velocity 192 m/s;
horizontal scale 100 μs/cm; vertical scale 23.9 MN/m^2/cm;
upper trace unfiltered; lower trace filtered

Figure 3.7 Pressure Transducer Output For Bird and 'RTV'-560 And Boneless Beef Impacts

If the bird is regarded as a homogeneous fluid-like material characterized by some density and the physical dimensions of the bird, then the flow of the bird material on the rigid plate generates the pressure observed. When the bird initially impacts the plate, a plane stress wave propagates into the bird. The pressure at the center-of-impact rises rapidly to the uniaxial impact stress (the Hugoniot). The edge of the bird is a free surface and a release wave propagates radially in towards the center causing the pressure to decay. 'Steady' radial flow is established and the center-of-impact pressure remains steady at $1/2\ \rho v^2$. The end of the bird reaches the plate and the pressure then falls to zero. There is a marked similarity between the filtered bird pressure trace and the RTV (homogeneous) pressure trace shown in Figure 3.7. The 'steady state' pressure generated is close to that which might be expected from a fluid of specific gravity somewhat less than one. Local density variations and/or large local material differences (for example bones) in the bird in addition to flesh breakup contribute to the high frequency pressure variations. Most of the high frequency signal is above 10 kHz in frequency.

The response and mode of failure of a particular component such as an aircraft windshield during impact depends on the shape and material of the windshield. For example, a thick windshield would not respond or deform grossly to the high frequency pressure variations of the impact load. The high frequency variation of the pressure would, therefore, be incapable of failing the windshield in flexure. However, delamination or spalling may occur. For a typical windshield configuration with a thickness of the order of 3 cm and a sound speed of 2 mm/μs (lexan), the double transit time across the material is approximately 30 μs. The material cannot deform appreciably for frequencies above 10-20 kHz. It was, therefore, decided to filter the pressure data above 10 kHz and record the filtered pressure (base pressure). As shown in Figure 3.7, filtering removes most of the high frequency component and the base or low frequency pressure remains. Present considerations center on gross deformation of windshield materials and further analysis is restricted to the filtered base pressure data. It must be noted that if other failure mechanisms are considered (e.g., delamination) or different components (e.g., fan blades), then the high frequency variations may be important loading mechanisms and any analysis must recognize this.

The following parameters are identified and extracted from the filtered or base pressure-time data:

a. Steady state pressure - the 'steady' pressure to which the pressure falls after the initial high peak.

b. Pressure duration - measured by extending the maximum slopes of the rise and fall of pressure to the zero pressure baseline.

c. Impulse intensity - the area under the pressure-time curve obtained by numerically integrating digitized data.

The 'steady state' pressure is indicative of the magnitude of the load imposed on the target during impact and, as the pressure-time curves have a similar shape from shot to shot, provides a convenient parameter for characterizing the pressure data. The 'steady state' pressure generated at the center-of-impact was measured for a number of shots and is plotted in Figure 3.8 as a function of impact velocity. The following observations are made:

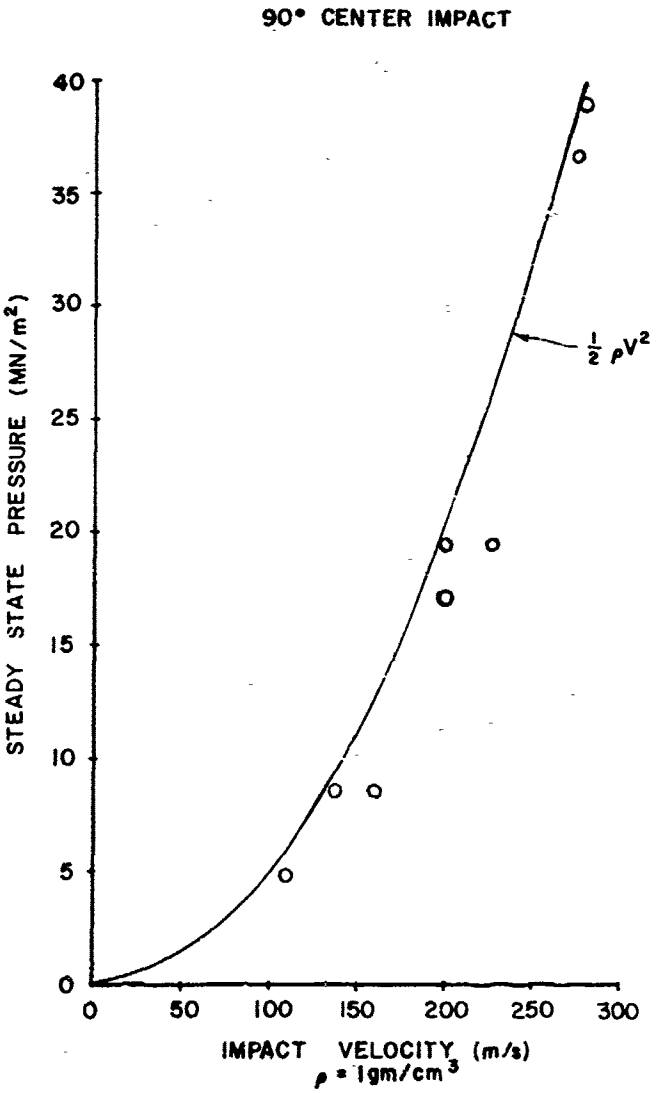


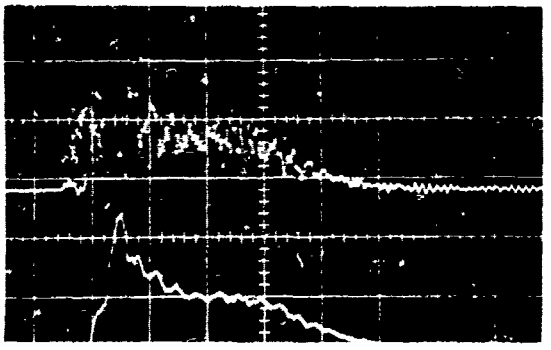
Figure 3.8 Steady State Pressure Vs Impact Velocity For Birds Impacted On A Rigid Plate At 90°

a. The 'steady state' pressure appears to be independent of bird size over the range of birds tested (0.05 kg to 0.10 kg). This supports the fluid impact model of a bird in which the pressure depends only on density and velocity and not on the size of the bird.

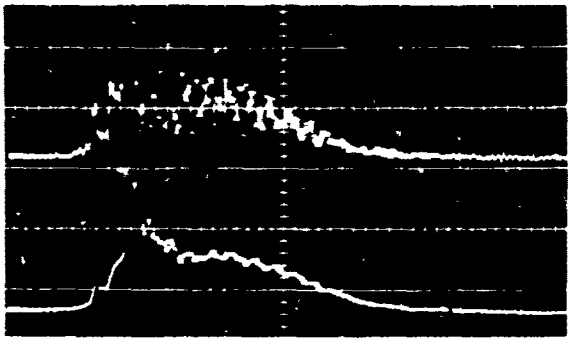
b. The 'steady state' pressure is, within experimental uncertainty (largely in bird density), equal to $1/2\ \rho v^2$, as expected in incompressible fluid flow.

c. There is considerable scatter in the data and this is attributed to non-repeatability of bird structure, orientation at impact and center-of-impact all of which are beyond experimental control.

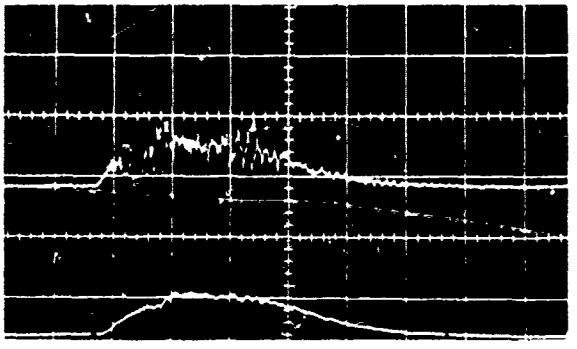
Pressure is measured and recorded off axis at three radii, 1.27 cm, 2.54 cm, and 3.81 cm; examples are displayed in Figure 3.9. This data is filtered and reduced in a similar manner to the centerline data as reported above. 'Steady state' pressures are shown plotted as a function of velocity in Figures 3.10 and 3.11.



Shot no. 5399; velocity 199 m/s; center transducer;
horizontal scale 100 μs/cm; vertical scale 24.5 MN/m^2/cm;
upper trace unfiltered; lower trace filtered



Shot no. 5399; velocity 199 m/s; transducer 12.7 mm off center;
horizontal scale 100 μs/cm; vertical scale 24.0 MN/m^2/cm;
upper trace unfiltered; lower trace filtered



Shot no. 5399; velocity 199 m/s; transducer 25.4 mm off center;
horizontal scale 100 μs/cm; vertical scale 23.9 MN/m^2/cm;
upper trace unfiltered; lower trace filtered

Figure 3.9 Off Axis Pressure Transducer Outputs For AFML/UDRI Target Disk

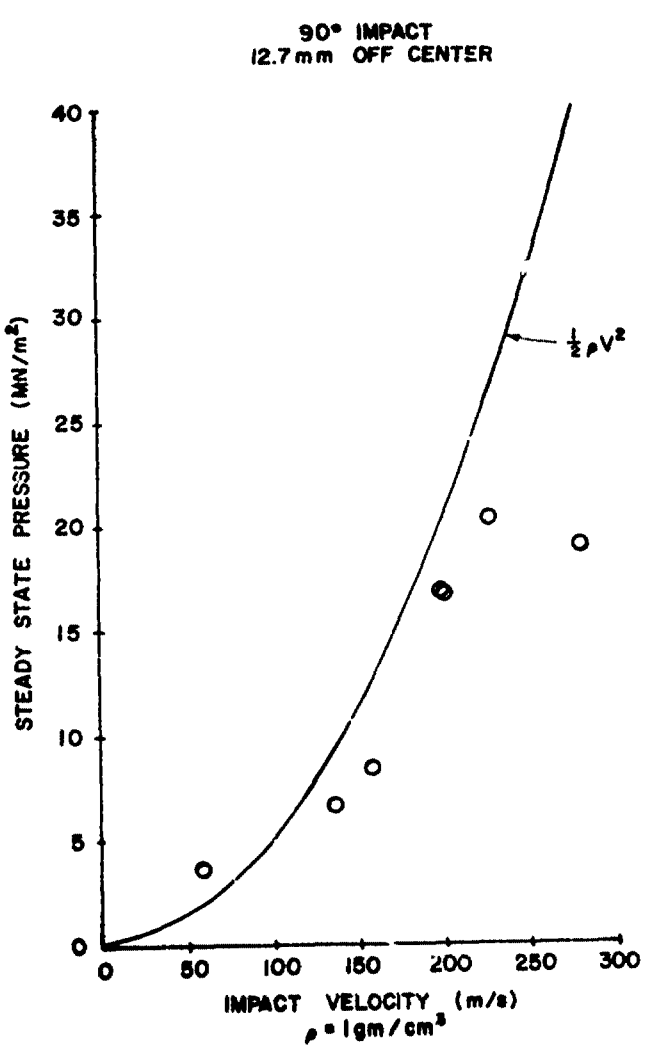


Figure 3.10 Steady State Pressure Vs Impact Velocity At 12.7 MM From The Center Of Impact For Birds Impacting A Rigid Plate At 90°

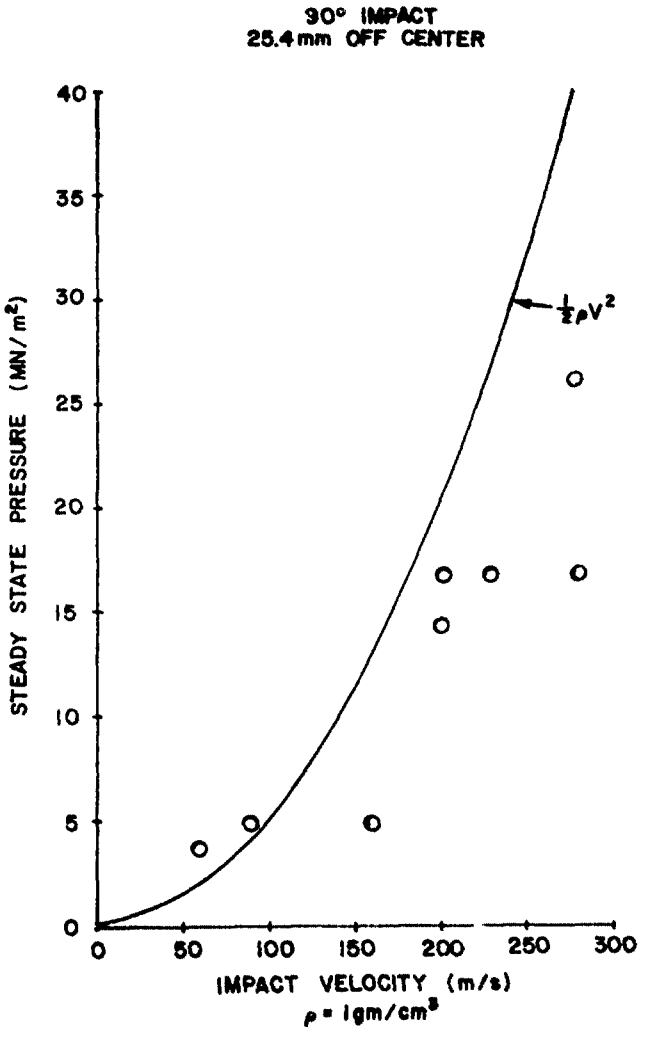


Figure 3.11 Steady State Pressure Vs Impact Velocity At 25.4 MM From The Center Of Impact For Birds Impacting A Rigid Plate At 90°

At 3.81 cm the 'steady state' pressure is essentially zero. From the data the following observations are made:

a. The form of the pressure-time response is the same as the center-of-impact data; that is, it consists of a base pressure on which is superimposed a high frequency component. The high frequency components are filtered out for purposes as explained previously.

b. 'Steady state' pressures are dependent on the impact velocity squared in a similar manner to the center-of-impact data and consistent with a fluid bird model.

c. Pressure falls with increasing radial distance from the center-of-impact, as shown in Figure 3.12.

d. Scatter in the data is comparable to that of the center-of-impact data and is similarly attributed to uncontrolled variations in bird structure, orientation and location of impact.

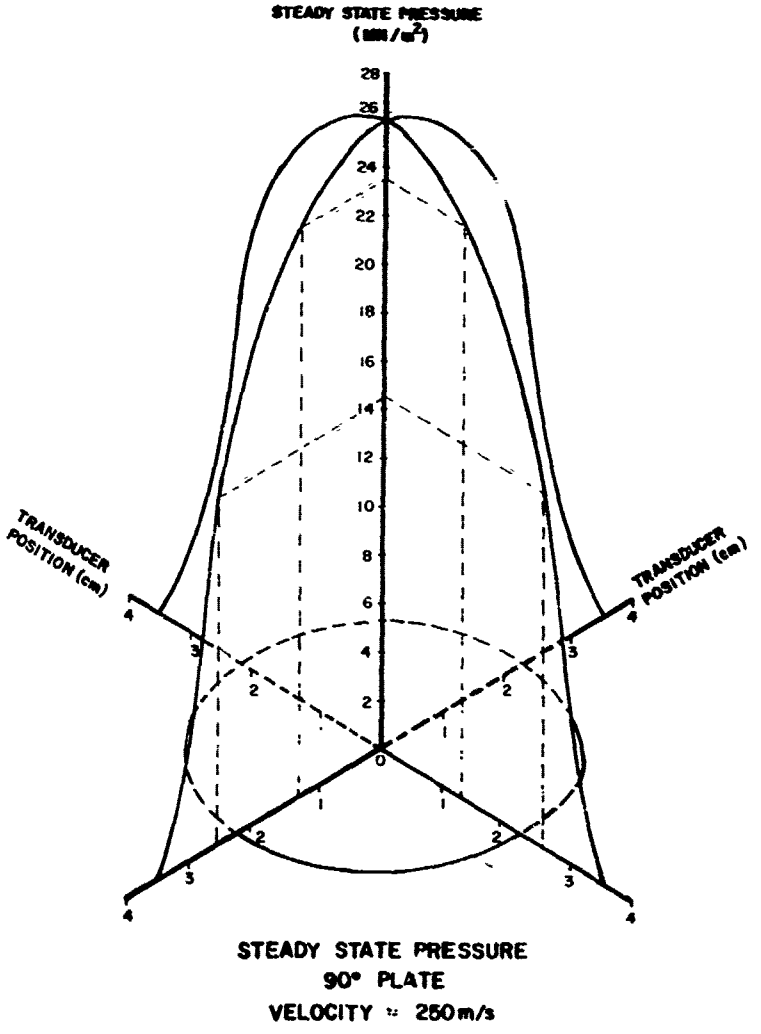


Figure 3.12 The Radial Distribution Of Pressure For A Bird Impact On A Rigid Plate At 90°

'Steady state' pressure versus impact velocity at the center-of-impact for targets at angles of 45° and 25° are shown in Figures 3.13 and 3.14. The impact area of a bird in oblique impacts is an ellipse and pressure measurements were made at various positions along the principal axes of the impact elipse. Curves similar to those shown in Figures 3.13 and 3.14 were generated at 12.7 mm intervals along the principal axes. From these curves the spatial distribution of 'steady state' pressure is determined as shown in Figures 3.15 and 3.16.

From Figure 3.15 it is apparent that the maximum 'steady state' pressure occurs 'upstream' on the acute side of the impact. The pressure distribution is highly 'peaked' and the maximum 'steady state' pressure is very close to the bird 'stagnation' pressure, $(1/2\ \rho v^2)$ as shown in Figure 3.17.

Figure 3.16 indicates that at 25°, the maximum 'steady state' pressure is not nearly as high as for the 45° impacts and the distribution of pressure is more uniform (not so highly 'peaked'). The maximum 'steady state' pressure occurs above the center-of-impact on the acute side of the impact. The maximum 'steady state' pressure varies closely with the normal component of the impact velocity and is described reasonably well by $1/2\rho(v \sin \theta)^2$as shown in Figure 3.18.

These results are consistent with the fluid model of a bird. At 90° the bird material flows out in all directions as shown in Figure 3.19 and at the 'stagnation' point, the steady pressure equal to $1/2\ \rho v^2$ appears. As the angle of impact obliquity decreases the bird material still flows out in all directions as shown for the 45° impact in Figure 3.19. Again a 'stagnation' point appears and a steady pressure equal to $1/2\ \rho v^2$ is measured. When the obliquity falls below a certain 'critical' angle the bird material no longer flows 'upstream' as shown for the 25° impact in Figure 3.19. A 'stagnation' point no longer appears and the maximum 'steady state' pressure is related to the normal component of the impact velocity by $1/2\ \rho(v \sin 25°)^2$. The critical angle depends on the properties of the bird material. No 'upstream' jetting occurs when the deflected bird material travels supersonically and a shock wave forms in the bird material at the impact point. For birds the critical impact angle is apparently between 45° and 25°.

Impulse intensity for 90° impacts has been investigated. Impulse intensity is defined as the integral of pressure with respect to time and indicates the transfer of momentum to a local area in the target plate. Figures 3.20, 3.21 and 3.22 show impulse intensity as a function of impact velocity. The radial distribution of the impulse intensity is shown in Figure 3.23. From these curves it is apparent that impulse intensity increases with velocity and falls roughly sinusoidally from the center-of-impact to the nominal edge of impact.

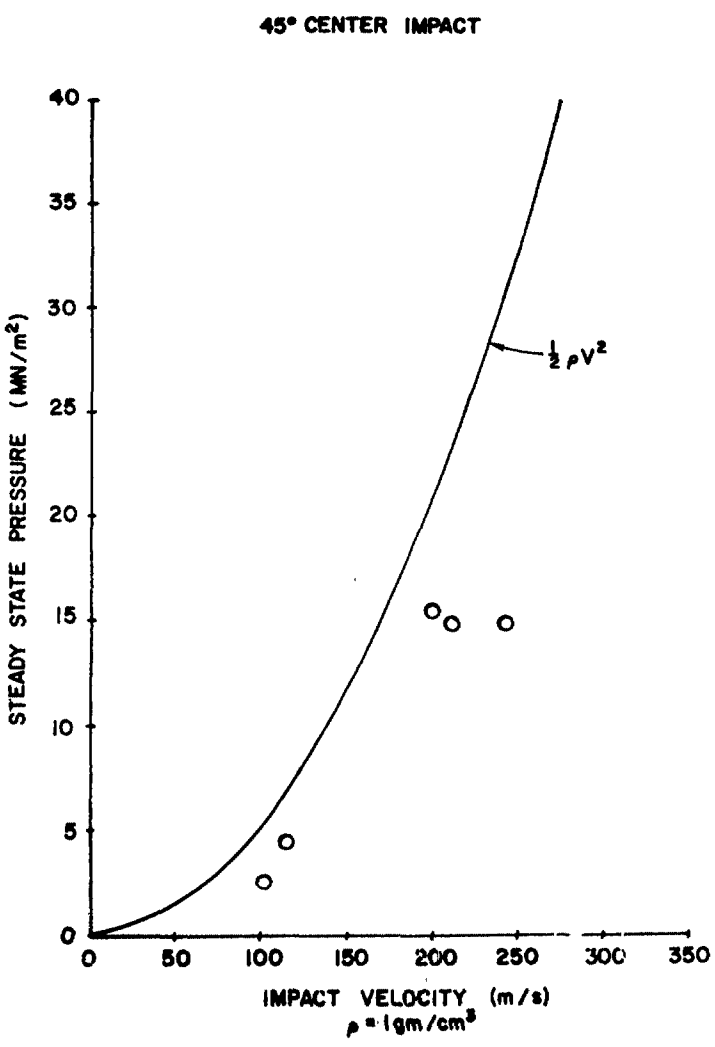


Figure 3.13 Steady State Pressure Versus Impact Velocity For 45° Center Impact Location

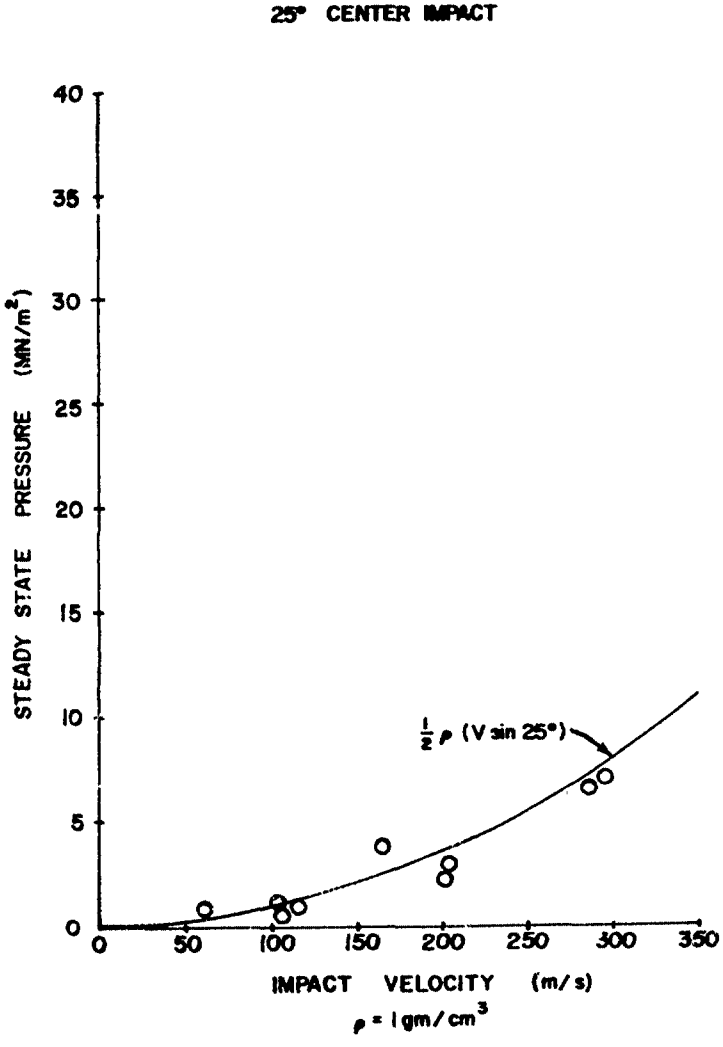


Figure 3.14 Steady State Pressure Versus Impact Velocity For 25° Center Impact Location

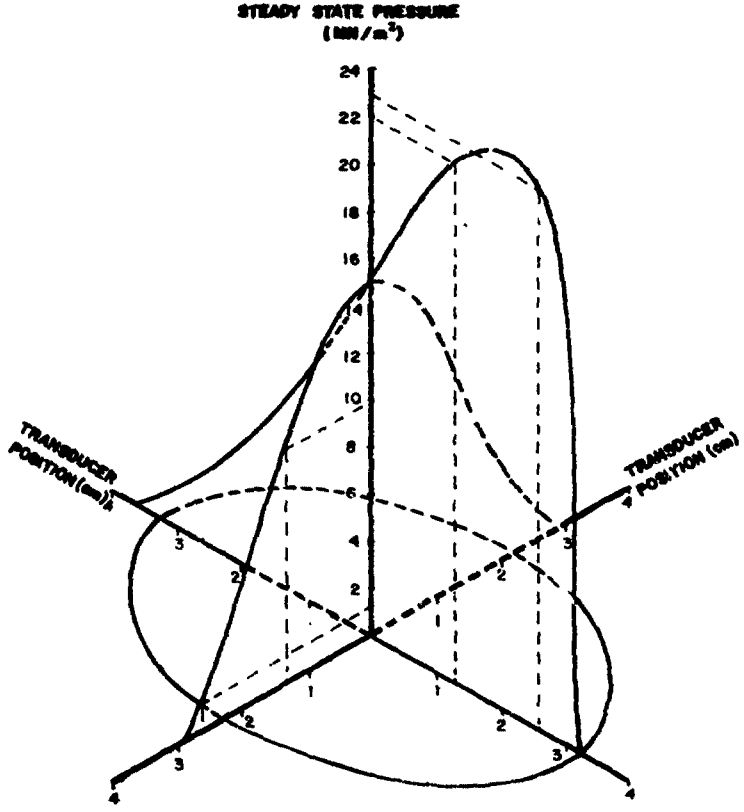


Figure 3.15 Steady State Pressure Distribution Plot For A 45° Target

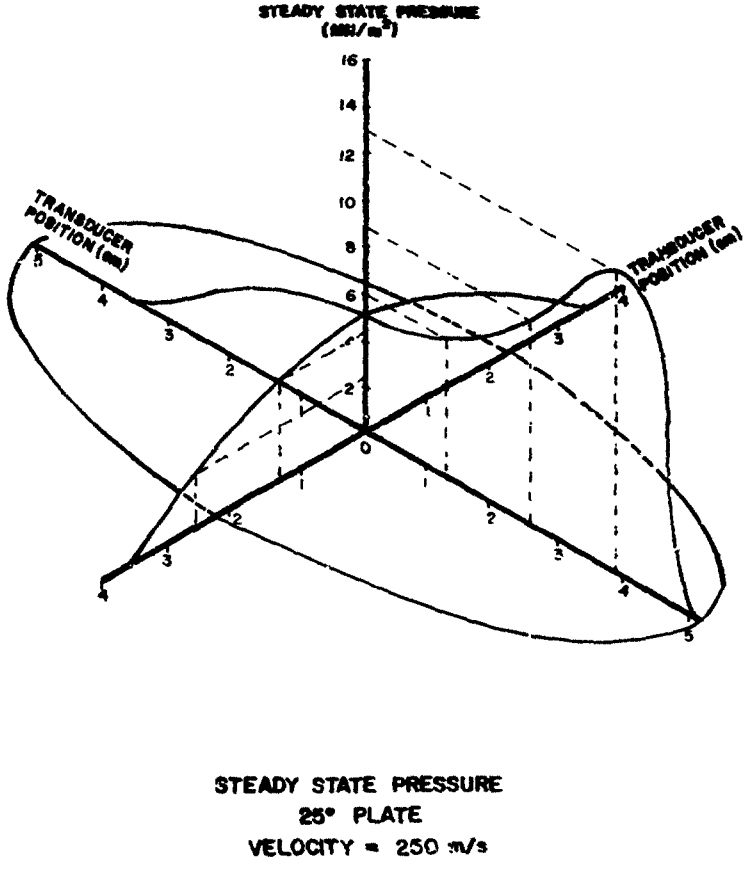


Figure 3.16 Steady State Pressure Distribution Plot For A 25° Target

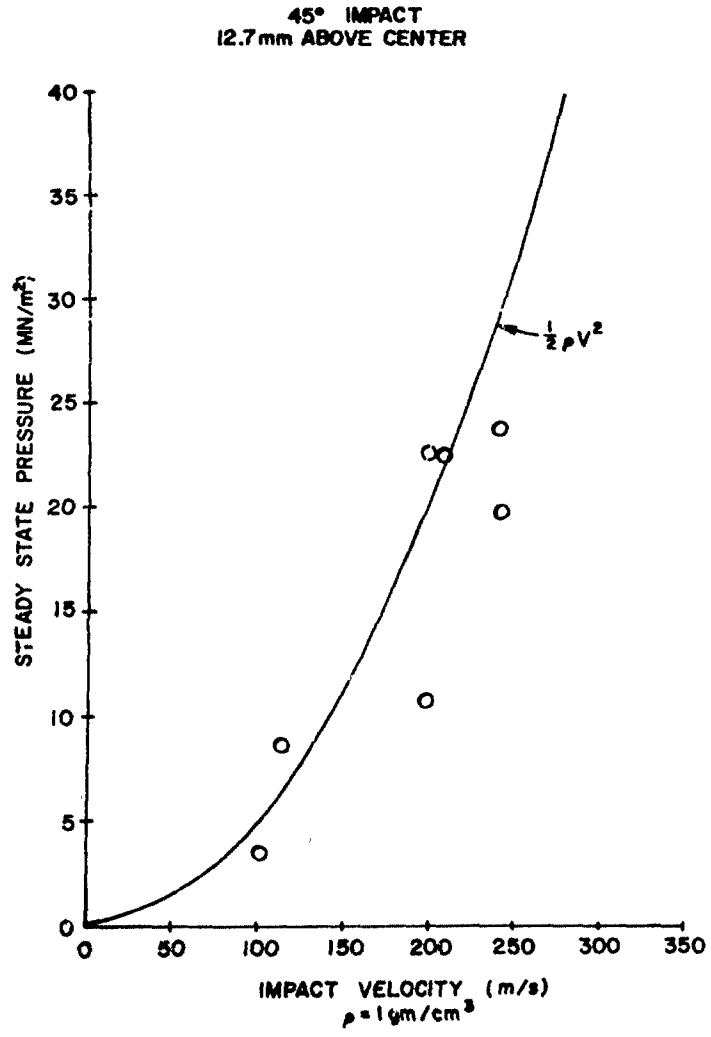


Figure 3.17 Steady State Pressure Vs Impact Velocity At 12.7 MM Above The Center-Of-Impact For Birds Impacting A Rigid Plate At 45°

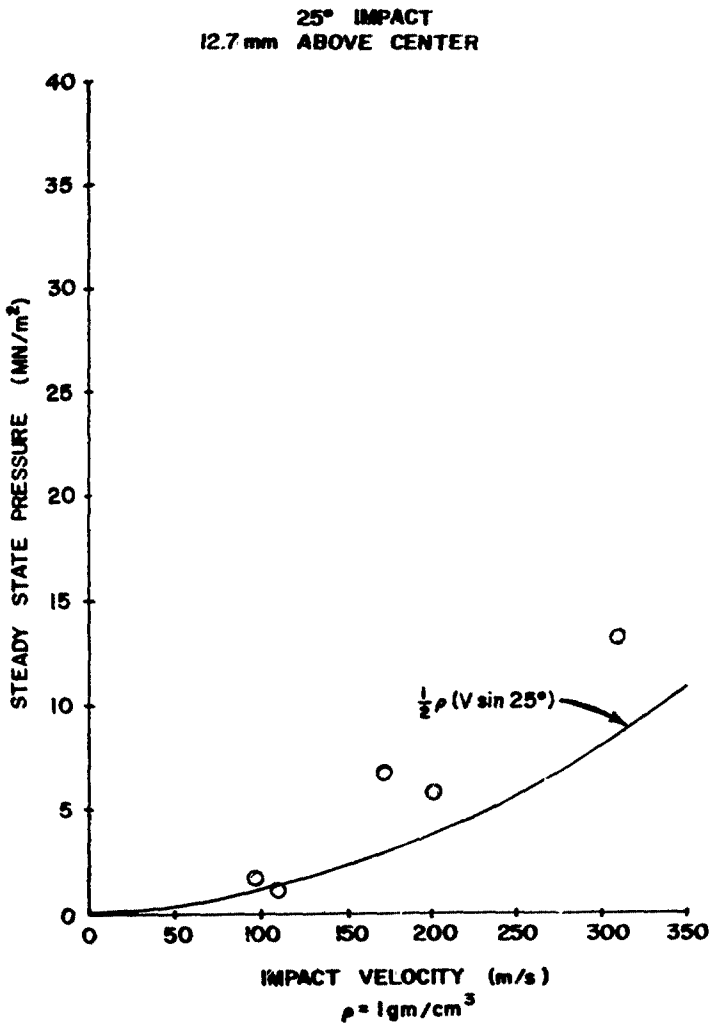


Figure 3.18 Steady State Pressure Vs Impact Velocity At 12.7 MM Above The Center-Of-Impact For Birds Impacting A Rigid Plate At 25°

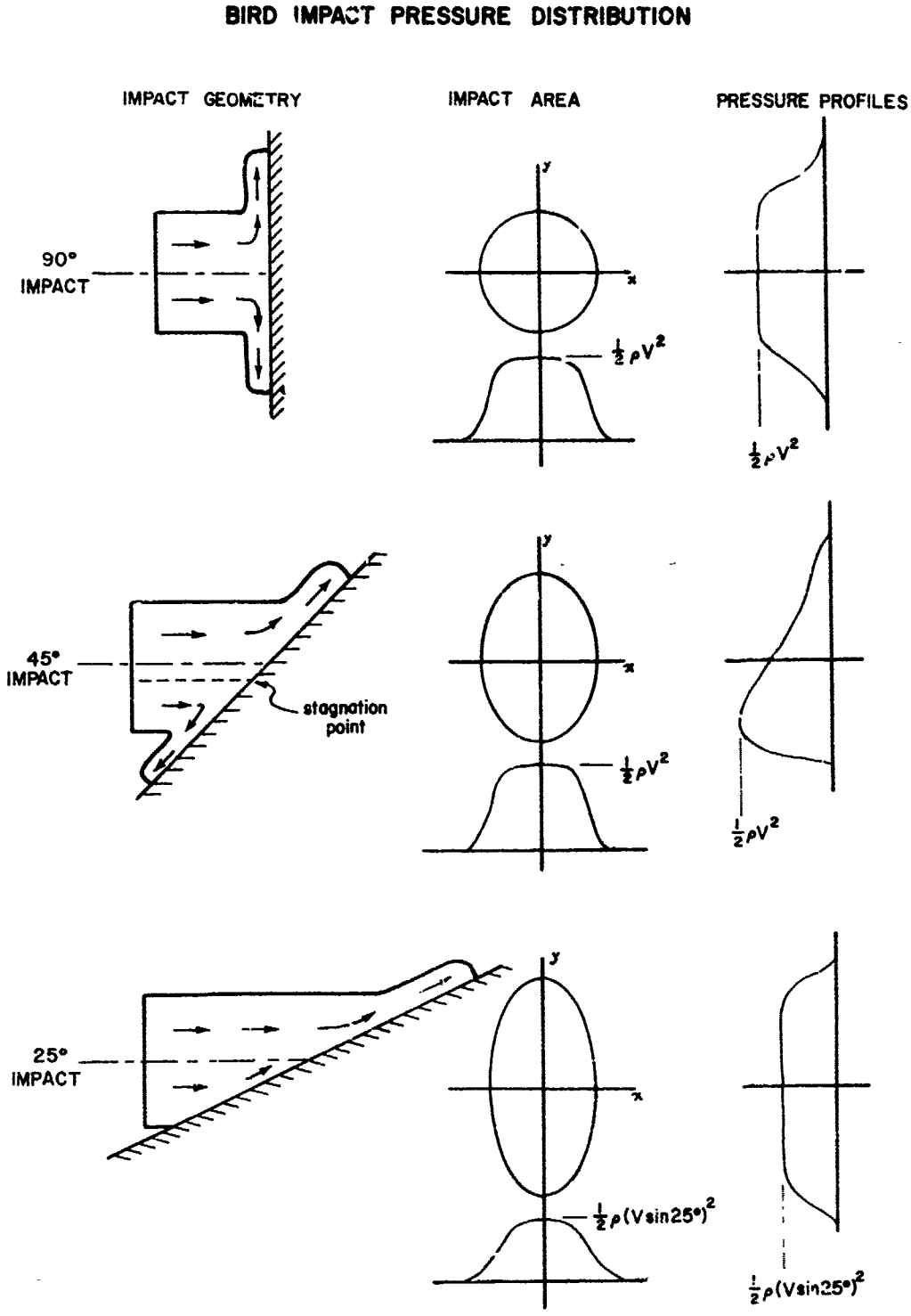


Figure 3.19 Bird Material Impact Geometry, Impact Area And Pressure Profiles At 90°, 45° And 25° Impacts

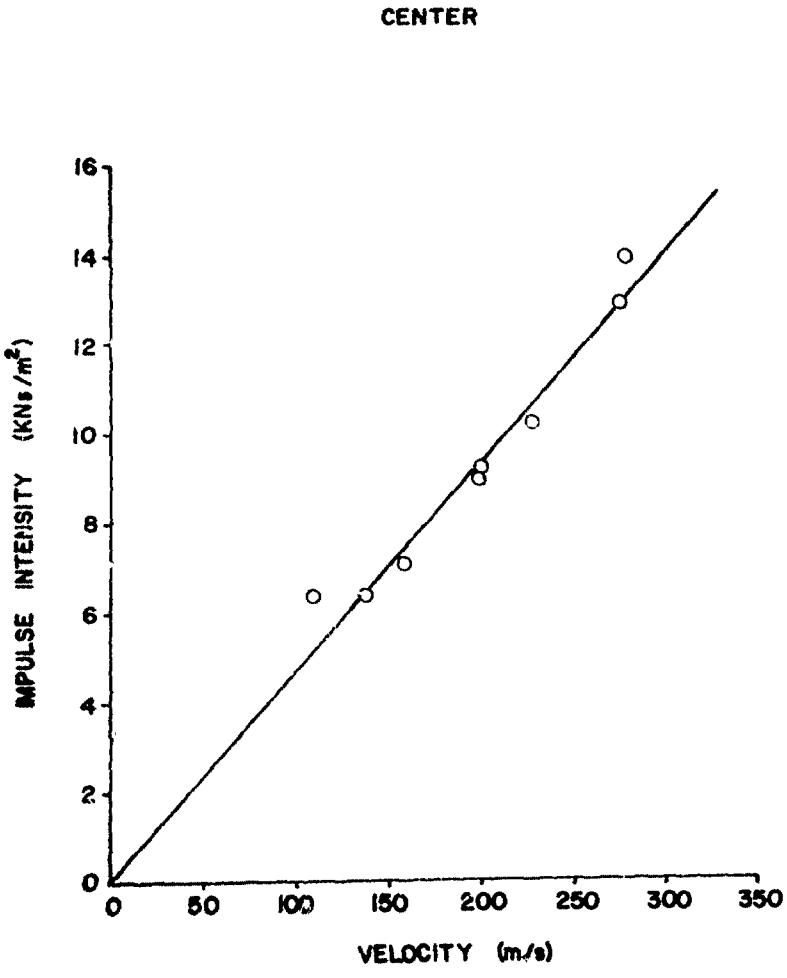


Figure 3.20 Impulse Intensity (∫Pdt) Versus Impact Velocity At Center-Of-Impact For 90° Impact

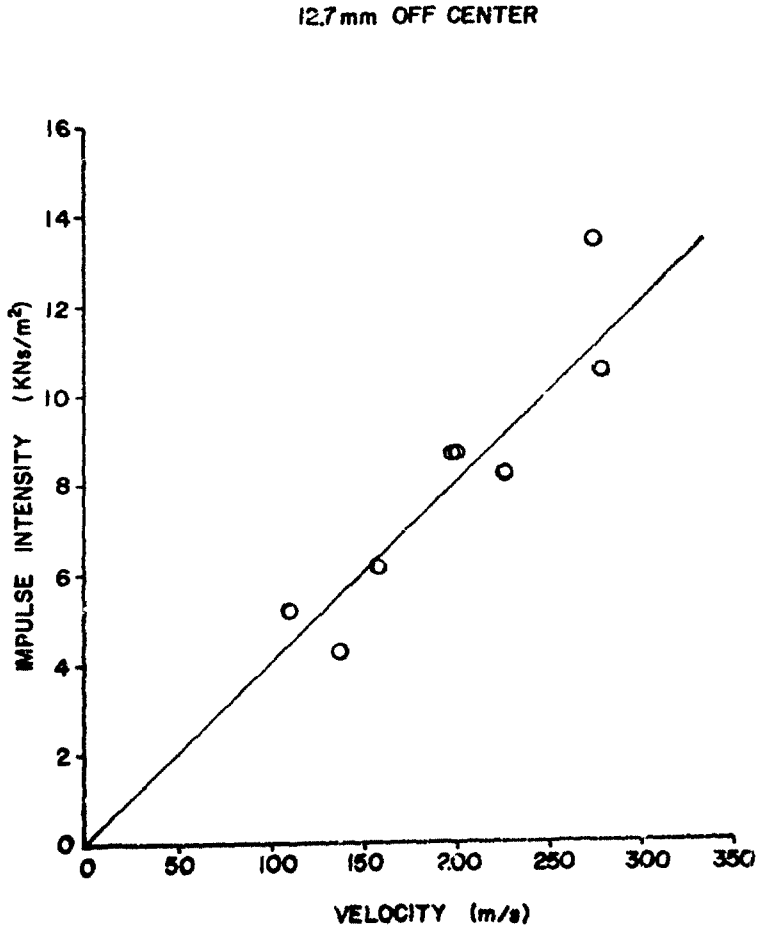


Figure 3.21 Impulse Intensity (∫Pdt) Versus Impact Velocity 12.7 MM From Center-Of-Impact For 90° Target

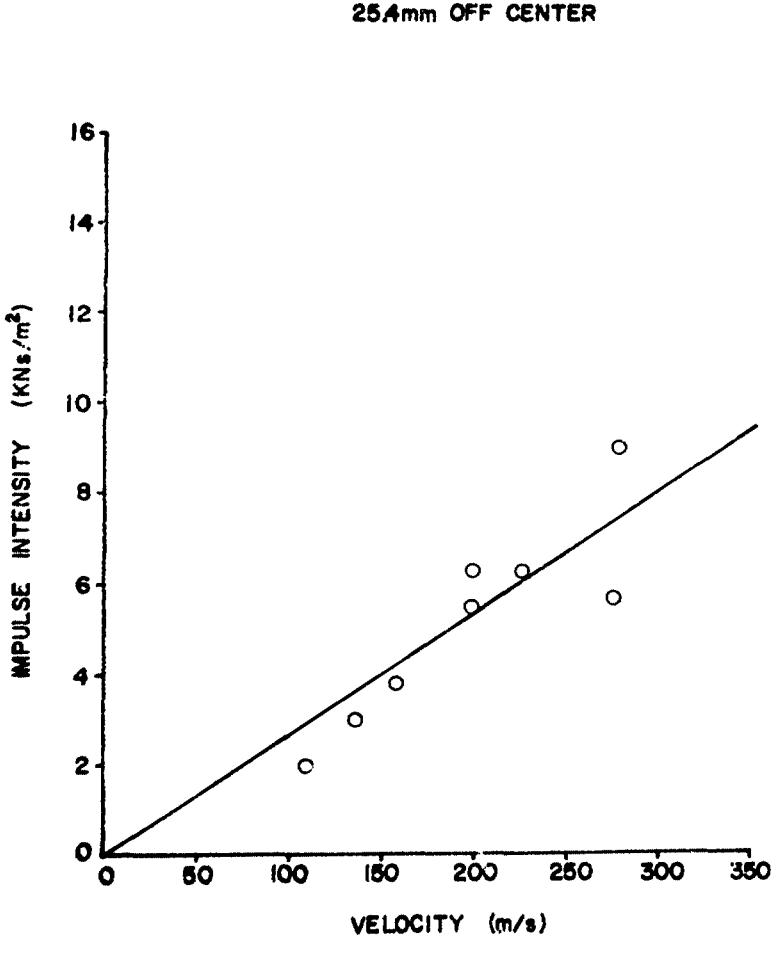


Figure 3.22 Impulse Intensity (/Pdt) Versus Impact Velocity 25.4 MM From Center-Of-Impact For 90° Target

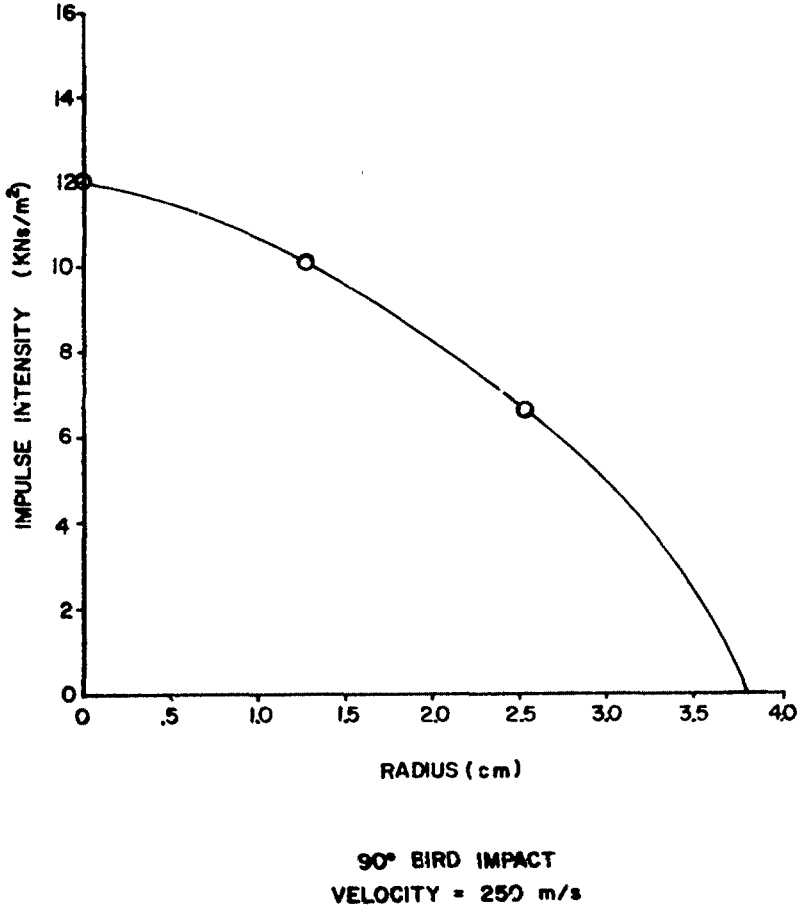


Figure 3.23 The Radial Distribution Of Impulse Intensity For Birds Impacting A Rigid Target At 90° At 250 M/S

3.2 AEDC Results - A total of 66 impact tests (21 data shots) at the 90° target angle have been conducted. The nominal test velocities are 91 m/s and 152 m/s and the nominal projectile weights are 0.9 kg, 1.8 kg, 2.7 kg and 3.6 kg. The output from the pressure transducers with appropriate in-line amplifiers and couplers are recorded on FM magnetic tape. Pressure versus time records for test number BP-43 at pressure transducer locations P-1, 2, 5, 9, 12, 13, 15, 18, 19, 21, 22, 24, 25, 27 and 30 (reference Figure 2.10) are shown in Figures 3.24 through 3.27. The test velocity and projectile weight for BP-43 were 91 m/s and 1.9 kg, respectively. Maximum peak pressure of 113 MN/m^2 occurs at location P-30, and the average pressure equals 5.5 MN/m^2.

On the AEDC data a 'steady state' pressure is difficult to identify as the pulse durations are relatively long and the pressure appears to fall steadily during the impact. At this time, insufficient data has been analyzed to determine if this is a real size scaling effect. Instead of 'steady state' pressures, average pressures, defined as the impulse intensity divided by the duration, are determined.

The total impulse imparted to the target is calculated by multiplying the impulse intensity by the effective area monitored by each transducer and adding the results for all the transducers together.

3.2.1 Comparison of AFML/UDRI and AEDC results - The average pressure as determined from the AEDC tests is plotted together with the 'steady state' pressure from AFML/UDRI results for the center-of-impact at 90° in Figure 3.28. If the initial pressure spike does not contain a significant portion of the impulse intensity (this appears to be true in the AEDC data) the two sets of data should agree as demonstrated in Figure 3.28. The data now covers a range of bird masses from 0.05 kg to 3.60 kg, over a factor of 70, and the magnitude of the pressures generated at impact are, as expected, independent of bird size.

The impulse imparted to the target as a function of impact momentum is shown in Figure 3.29. As expected, the impulse is equal to the impact momentum within the measurement uncertainty. Again, the AFML/UDRI and AEDC data agree and indicate negligible bird bounce.

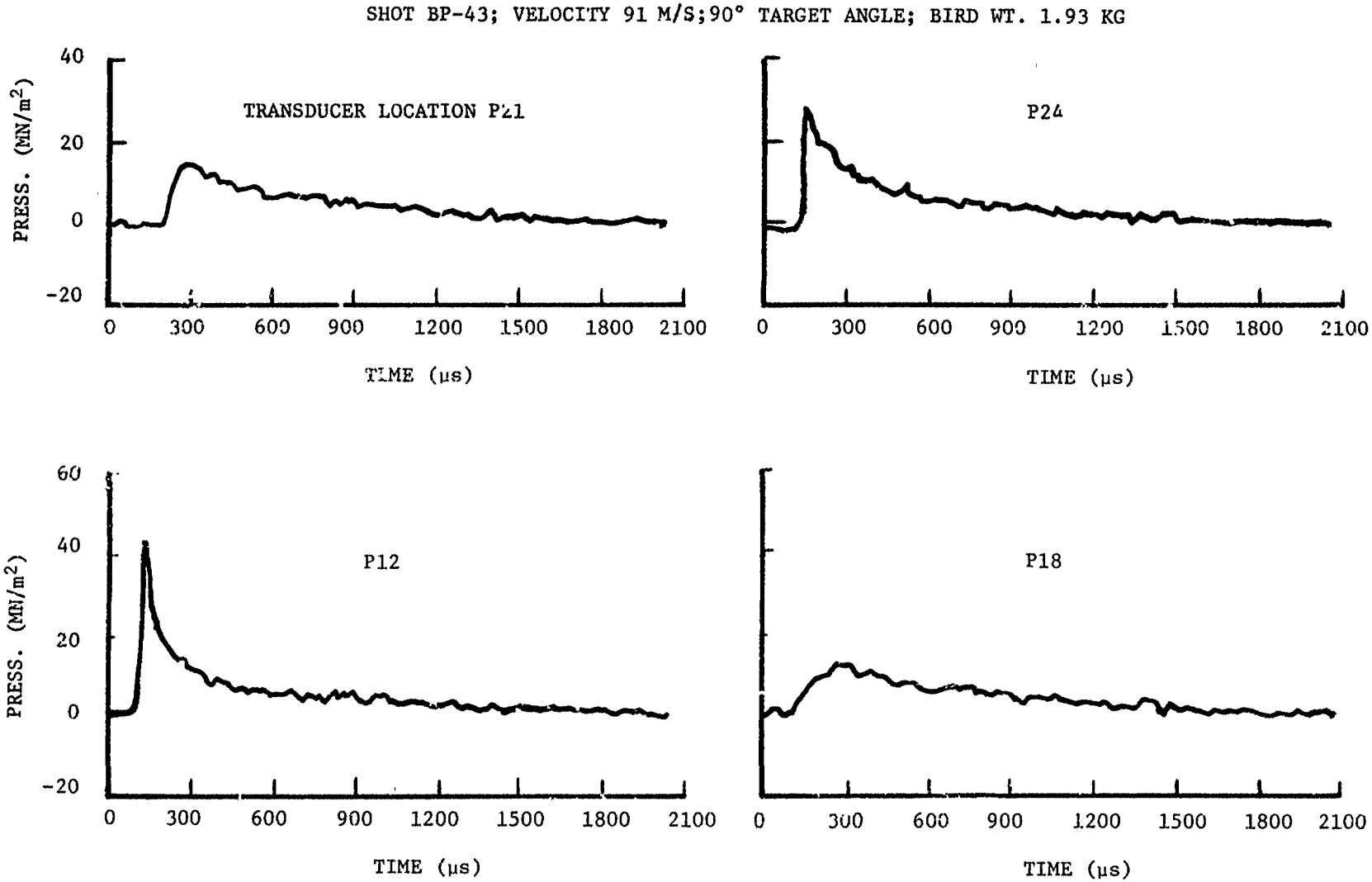


Figure 3.24 Pressure As A Function Of Time For Transducer Locations P12, P18, P21, & P24

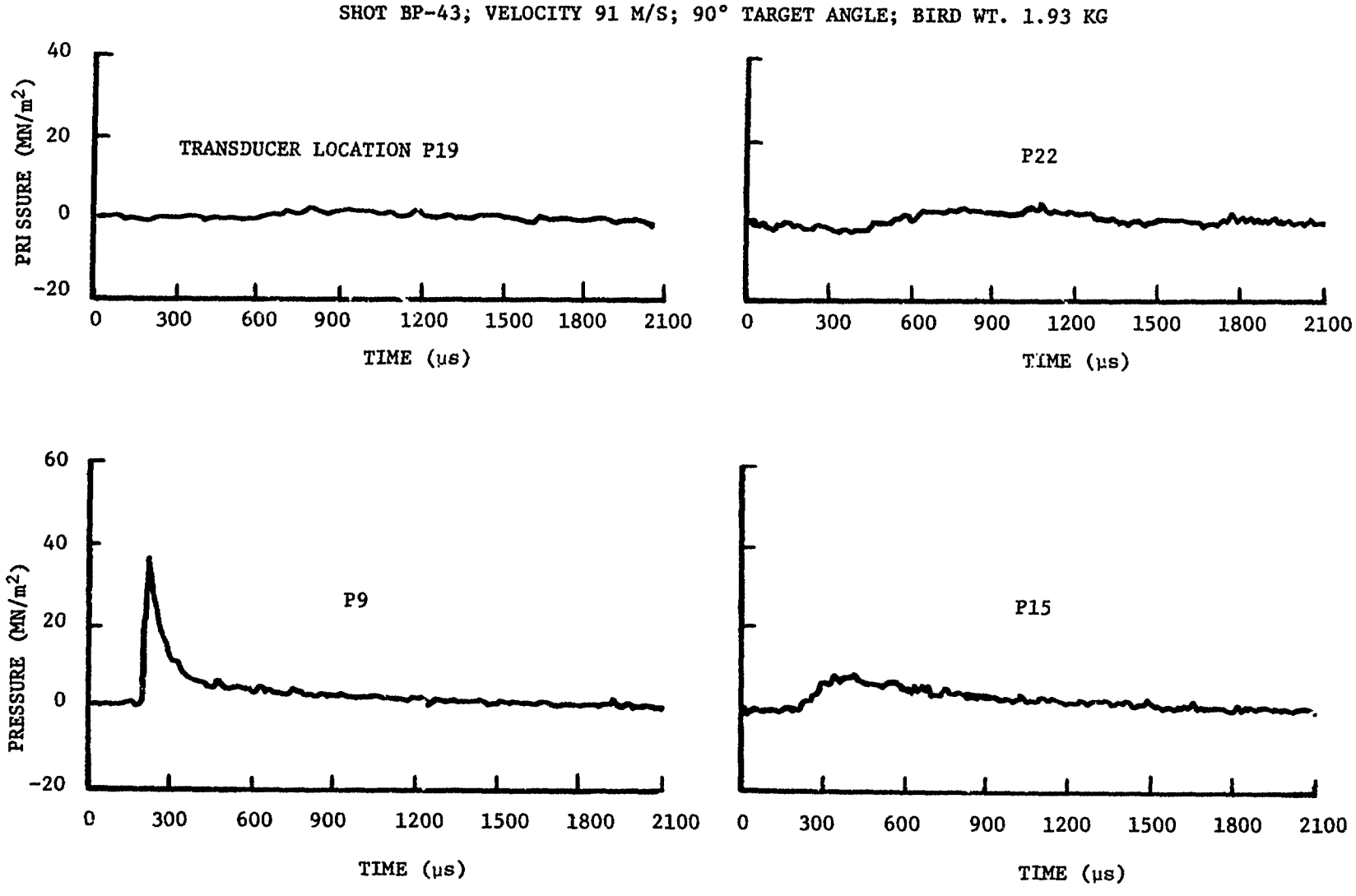


Figure 3.25 Pressure As A Function Of Time For Transducer Locations P9, P15, P19, & P22

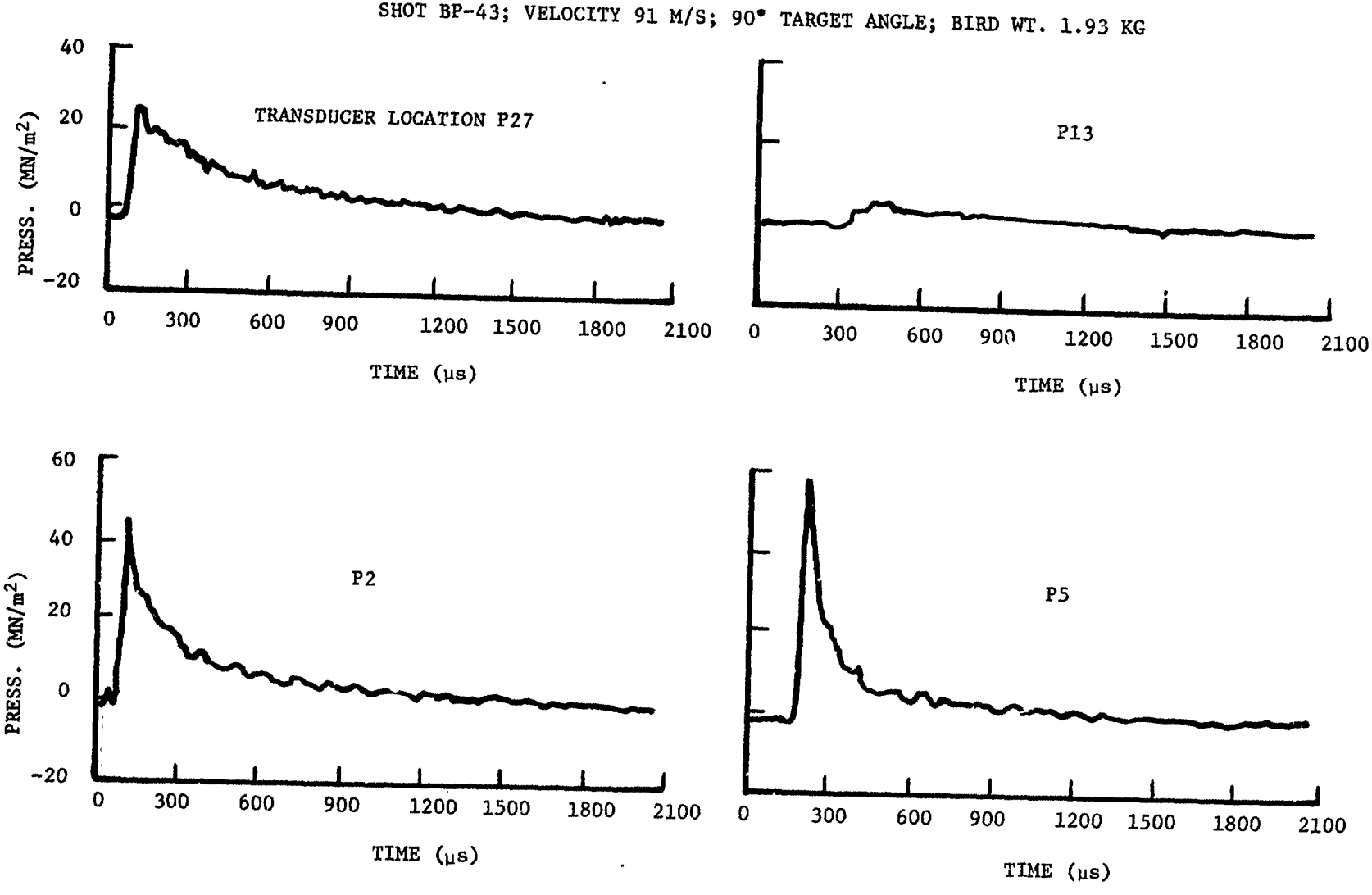


Figure 3.26 Pressure As A Function Of Time For Transducer Locations P2, P5, P13, & P27

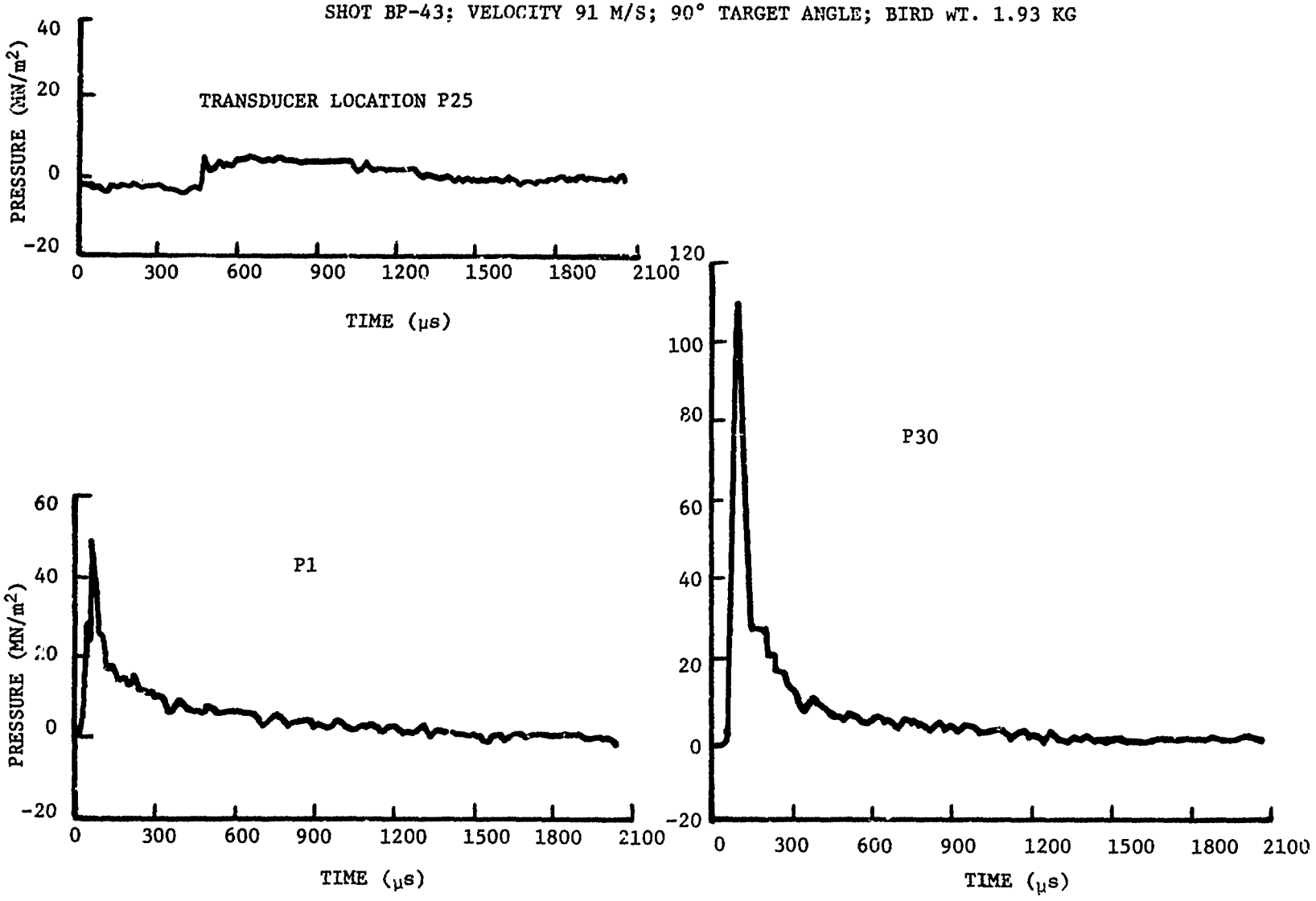


Figure 3.27 Pressure As A Function Of Time For Transducer Locations P1, P25 & P30

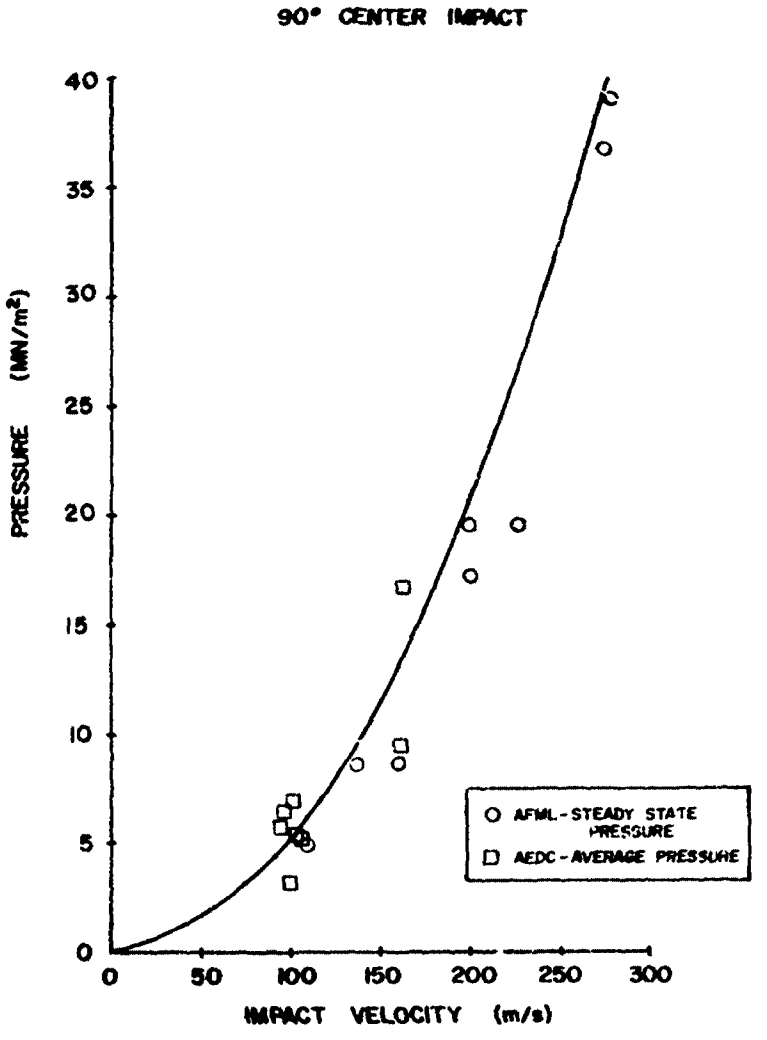


Figure 3.28 Comparison Of AFML/UDRI And AEDC Pressure Vs Impact Velocity For The 90° Center-Of-Impact

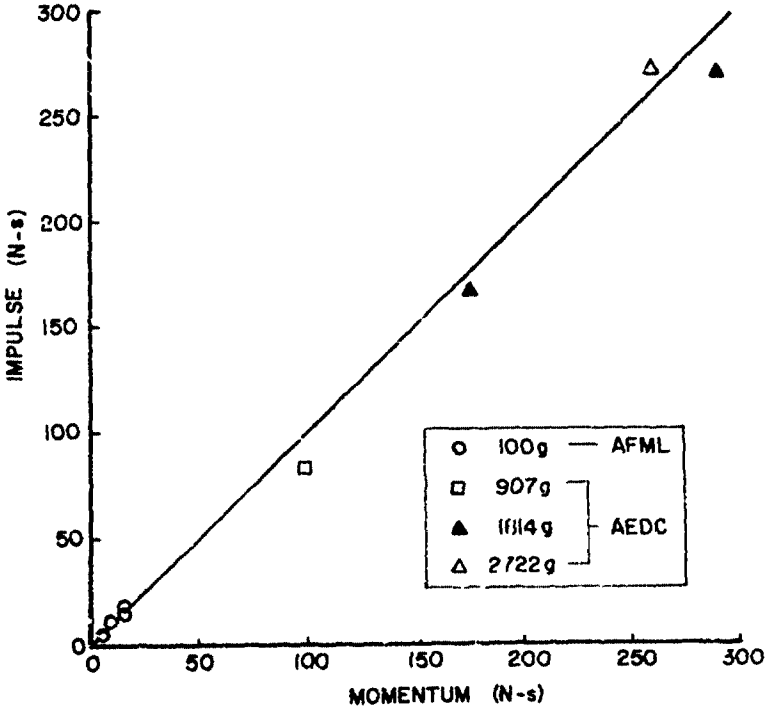


Figure 3.29 Comparison Of AFML/UDRI And AEDC Impulse Vs Momentum

SECTION 4

CONCLUSIONS

From the experimental data collected and analyzed to date a number of important conclusions may be drawn.

4.1 Hopkinson Bar Results - From the Hopkinson bar measurements it is seen, for a rigid plate impact, birds display negligible bounce. That is, the impulse imparted to the target is equal to the impact momentum.

The duration of the total force-time pulse is closely approximated by the 'squash up' time (the length of the bird divided by the impact velocity). Therefore the average force exerted during the impact is given by the momentum divided by the 'squash up' time. The measured peak force is shown to be very nearly twice the average, and the force-time pulse is approximately 'triangular.'

Integration of the AEDC pressure measurements to yield total force versus time yields similar results, but insufficient data has been collected and reduced to completely verify this behavior for very large birds.

4.2 Pressure Plate Results - The pressure plate measurements indicate clearly that birds behave as a fluid during impact. The impact process may be described as the non-steady flow of a finite cylinder of matter on the plate surface.

At the instant of impact, a plane shock wave propagates into the bird. This plane shock wave generates very high initial pressures approximately equal to the uniaxial strain or Hugoniot pressure. Rarefaction waves rapidly travel in from the edges of the bird and attenuate the pressures at the center of impact. The pressure decays to the steady flow 'stagnation' value given by the density times the velocity squared divided by two, where the apparent density of the bird is somewhat less than 1 g/cm^3.

As the obliquity of impact is decreased a critical angle is reached at which bird material no longer flows out in every direction. The maximum 'steady state' pressure then falls to reflect only the normal component of impact velocity. For example at 45°, which is apparently above the critical angle, the maximum 'steady state' pressure is the full 'stagnation' pressure (the same as for a 90° impact). At 25°, which is below the critical angle, the maximum 'steady state' pressure falls to $(\text{Sin } 25°)^2$ of the 'stagnation' pressure.

The 'steady state' pressure is independent of bird size.

The pressure is exerted over approximately the nominal impact area of the bird. The pressure is highest at the center-of-impact (or slightly 'upstream' for oblique impacts) and falls off gradually towards the edges of the bird.

There is a considerable high frequency component in the bird pressure pulse. This high frequency variation is attributed largely to the breakup of the flesh with contributions from inhomogeneities in the bird.

4.3 Future Work - The analysis of oblique impact pressure data is not yet complete and this work is continuing. No large bird data from AEDC is available as yet on oblique impacts and this data will be obtained.

Oblique impact Hopkinson bar tests will be conducted at AFML/UDRI to address the question of total force variations with impact obliquity.

The measurements reported herein and the additional work noted above are limited by the rigid plate technique. Real aircraft components subjected to birdstrike are not rigid, the effects of target compliance must be addressed. An investigation of the coupling between bird impact loading and target response will be undertaken in the near future.

REFERENCES

[1]Barber, John P., Taylor, Henry R., and Wilbeck, James S., "Characterization of Bird Impacts On A Rigid Plate: Part I," Air Force Flight Dynamics Laboratory Report No. AFFDL-TR-75-5, January 1975.

[2]Sanders, E. J., "The AEDC Bird Impact Test Facility," Air Force Materials Laboratory Report No. AFML-TR-73-126, PP 493 through 514, June 1973.

BIRD STRIKE CAPABILITIES OF AIRCRAFT TRANSPARENCY MATERIALS

A. O. Ingelse and G. E. Wintermute
Goodyear Aerospace Corporation
Litchfield Park, Arizona

BIRD STRIKE CAPABILITIES OF AIRCRAFT TRANSPARENCY MATERIALS

by

A.O. Ingelse and G.E. Wintermute

Goodyear Aerospace Corporation

ABSTRACT

This paper presents a summary of a program performed by Goodyear Aerospace under contract with the Air Force Materials Laboratory, W-PAFB, Ohio, to obtain meaningful materials response data on the bird strike capabilities of selected transparency materials. A test program was established to test a wide variety of materials and composite constructions including acrylics, polycarbonate, acrylic-clad polycarbonate, and glass-plastic or all-plastic laminates. The basic test specimen was a rectangular 30-in. × 40-in. flat panel, but comparative testing was also performed on flat panels both larger and smaller than this, on rectangular planform curved panels with 20-in. or 40-in. curvature radii, and on single-piece, cone wedge section windshields. Test parameters varied were material thickness, temperature, impact angle, bird weight, impact locations, and interlayer type and thickness. A total of 380 individual panels were tested using 932 bird impacts at velocities from 70 to 640 knots. A variety of data plots are presented which depict the effects of parameter changes on the bird penetration velocities for the panel configurations tested. Empirical expressions developed by previous investigators for predicting penetration velocities are discussed briefly and compared with each other and with the test results from this program.

The information developed by this program provides a substantial data base for use by the transparency designer in comparing the bird impact performance of various transparency materials and types of construction. The test results were shown to provide reliable information for predicting the performance of design windshield configurations for new high-performance aircraft.

I. INTRODUCTION

As evidenced by other papers presented at this conference, the Air Force has long recognized the flight safety hazards associated with bird impacts on aircraft transparencies. Both the Air Force and industry have been responsive to the changing requirements being imposed on the transparency because of increased maximum speeds and changes in typical mission profiles. However, almost no valid design information has been available to aid the transparency designer in the use of newly developed materials and processes to develop bird-resistant transparencies. Because of this, the Air Force Materials Laboratory contracted with Goodyear Aerospace Corporation to conduct a program to obtain engineering data on the bird strike capabilities of selected transparent materials and composite constructions.

This paper describes the test program and summarizes some of the most important test results.

II. DISCUSSION

To help establish a comprehensive test plan, it was considered important to obtain as much background data as possible relating to bird impact. A worldwide data survey of industry and government agencies was conducted. The reports and data obtained from this survey were cataloged and reviewed to aid in establishing standard specimen configurations and support fixture requirements and in defining the important test parameters and their test ranges.

From the literature review, it was soon apparent that no standardized panel size had been established throughout the industry. Since the current trend is toward larger windshield areas, a basic flat panel size of 30 in. × 40 in. was selected. This panel is somewhat larger than the sizes used by most previous investigators. The rectangular configuration assured that, for center impacts, the forces radiating from the impact point would not all reach the panel edges at the same time. This shape was felt to provide a better simulation of an actual windshield than a square panel would.

It was originally planned to utilize a 2-in.-wide fiberglass-reinforced laminate 0.060 in. thick, to be bonded to both faces of the panel around its periphery. These laminates were to reinforce the holes and to prevent direct contact of the transparency and the holding frame. However, early comparative testing showed

that the panels with the reinforced edges failed at the same or lower velocities than equivalent panels without the reinforcements. This was true for both stretched acrylic and polycarbonate panels. Additional testing, including changes in the adhesive, continued to show the same results; therefore, it was decided that the best approach would be to delete the bonded reinforcement. However, predrilled loose edge bands two inches wide were placed around the edges of the panels to avoid direct contact of the transparencies and the metal support frames.

Because this program was primarily intended to determine the pure materials response to bird impact, the attachment fastener and support frame effects were supposed to be eliminated to the maximum extent possible. One-half-inch-diameter bolts at two-inch spacing were used for the attachments. Nine-sixteenths-inch-diameter holes were used in the test specimens except for those panels subjected to high or low temperature, where 5/8-in.-diameter holes were used to allow for the differences in expansion rates of the steel fixture and the plastic test specimen.

A standard 4-inch-steel channel with a weight of approximately 14 lb/ft was used for the support frame. Figure 1 shows the typical attachment to the support frame.

Although most of the test specimens were the flat panel configuration just described, other sizes and shapes were also fabricated and tested to determine the effects panel size and shape on penetration velocity. Other specimen configurations were 40-in. × 40-in., 20-in. × 40-in., and 45-in. × 60-in. flat panels; 30-in. × 40-in. panels with 20-in. or 40-in. radii of curvature; 45-in. × 60-in. panels with a 40-in. radius of curvature; and single-piece, cone wedge section windshields of the general type used on F-5 and F-15 aircraft.

A wide variety of panel configurations was tested, beginning with monolithic polycarbonate and stretched acrylic. Laminates used polycarbonate and stretched acrylic structural plies and varying thickness interlayers of urethane, silicone, ethylene terpolymer (ETP), or PVB. All-plastic and glass/plastic laminates were tested, as well as a few acrylic-clad polycarbonate flat panels.

In addition to the variety of panel constructions, sizes, and shapes, other test parameter variations were panel temperature, thickness, bird impact angle, impact velocity, impact point, attachment bolt diameter and spacing, support flexibility, bird weight, and material processing variations.

A special bird impact test facility was designed and fabricated to permit efficient completion of the required testing. The basic element of the facility is a compressed air gun consisting of a 60-ft-long, 6-in.-diameter launch tube with a 30-ft^3 pressure tank assembly. Mylar diaphragms in a removable holder assembly are mounted over the opening between the pressure tank and the launch tube. The release of the tank pressure to accomplish a launch is initiated by cutting the diaphragms with a cutter actuated by an air cylinder.

For the projectile package, the bird is placed in a thin plastic bag which is then placed feet first into a cylindrical cardboard carton. This assembly is then wrapped with several strips of tape to prevent breakup of the package prior to target impact. The complete package is then placed in a six-inch-diameter thin aluminum can which acts as a sabot. This sabot is caught by a stripper device attached to the exit end of the launch tube so that only the projectile package impacts the target.

The chickens used for these tests were frozen immediately after killing and were thawed prior to use. The total weight of the projectile package was controlled to within plus or minus one ounce of the desired weight, normally four pounds. Some tests were made using one-, two-, or three-pound birds to check the effect of variations in bird weight.

A break-wire system in conjunction with electronic counters is used for velocity measurement. Two independent systems are used for redundancy.

For environmental conditioning of the test panels, a hinged hood assembly was designed to cover the panel and support fixtures. Cooled or warmed air was circulated in the hood until the panel temperature was stabilized at the desired level. Then the hood was hinged back and the gun fired, generally within about a 30-second interval. In addition to temperature monitoring of the panels, high-speed motion picture coverage was used to record the bird impacts on selected tests. An overall view of the bird gun facility is shown in Figure 2.

Because many tests were to be conducted in a relatively short time, one concession was made in the test setup to minimize cleanup problems. The test panel support fixtures were designed to hold the test panels in an inverted position so that the bird debris was deflected down to the floor. This arrangement tended to concentrate the debris in a smaller area and simplified the cleanup.

The test procedure as originally planned was to impact one panel at each data point at successively higher impact velocities until penetration or severe damage occurred. Then a second panel was to be impacted at a velocity just below the panel penetration velocity, as estimated from the prior series of tests, to serve as a confirmation of the test results. This procedure was followed early in the program with good results. However, as the program developed, the desirability of adding tests to evaluate additional test parameters, in addition to the tendency to test more costly panel configurations, made it desirable to delete the second verification test at each data point. Consequently, the data base for each test point is very small, being limited to one or two test specimens for most points. In the majority of cases, this practice was satisfactory, and smooth and consistent data plots could be developed. In a few cases, however, the test results appeared inconsistent, and extra tests were needed to resolve the discrepancies.

A question which frequently arises is, "What effect do repeated impacts have on the actual penetration velocity of a windscreen?" Although no specific tests were conducted to positively answer this question, it is the authors' opinion that the detrimental effects of repeated impacts are minor so long as no damage is visible. Some tests were experienced in which a specimen withstood a single impact at a higher velocity than an identical panel subjected to multiple impacts, but there were also tests in which a panel with one impact failed at a lower velocity than a panel with repeated impacts. For most materials and constructions, the inherent panel-to-panel variations are such that the width of the penetration velocity zone is enough to mask possible adverse effects from repeated impacts.

The temperature of the test panel was found to be an important parameter for both polycarbonate and stretched acrylic. In general, the penetration velocity is maximum near room temperature and less at both elevated and low temperatures for flat panels. Depending upon the material, its thickness, and the bird impact angle, reductions in penetration velocity can range to 40 percent at -40 deg F and to over 50 percent at 140 deg F. Curved panels tend to show less degradation in the penetration velocity at elevated temperatures.

Figure 3 shows typical temperature effects curves for two thicknesses of polycarbonate and stretched acrylic flat panels.

Another factor which can significantly influence the performance of polycarbonate is its processing state. Fusion-bonding or press-polishing processes used to

improve the optical quality of the material can cause a substantial reduction in the penetration velocity. The amount of the reduction varies depending upon the temperature, impact angle, material thickness, and panel construction. Figure 4 shows a typical comparison for monolithic 0.50-in. material at a 45-deg bird impact angle.

The effects of total panel thickness on penetration velocity for polycarbonate flat panels are shown in Figure 5. Monolithic and laminated panels are included in this figure, and the results are seen to group quite well along a straight line.

A separate test series designed to evaluate the effects of three interlayer types and thicknesses was also conducted. These results, with an expanded velocity scale, are shown in Figure 6. In the thinner interlayer thicknesses, the silicone interlayer provided a slightly higher penetration velocity for these tests at the 45-deg bird impact angle.

Comparison of the test results for similar panel constructions at varying bird impact angles revealed an interesting phenomenon. This can be observed by referring to the curves for the 0.50-in. as-extruded or fusion-bonded polycarbonate in Figure 7. Contrary to what might be expected, the penetration velocity for these 0.50-in. panels takes a substantial dip at the 20-deg bird impact angle. This same phenomenon was experienced for the 0.50-in. stretched acrylic flat panels at the 20-deg angle. Extra tests at the same angle gave the same results. Examination of the panels after testing, plus evaluation of the test films, indicated that severe pocketing of the panel at the rear frame member, combined with the rigid frame and attachment fasteners, contributed to these results. Later tests on similar panels with smaller-diameter (and therefore more flexible) fasteners resulted in higher penetration velocities at the 20-deg angle. Use of these smaller-diameter fasteners in combination with a more flexible support frame would probably have resulted in further increases in the penetration velocity.

Figure 8 presents a family of curves to show the effect of material thickness on penetration velocity for monolithic polycarbonate at varying bird impact angles. Again, the low penetration velocity for the 0.50-in. material at the 20-deg angle is apparent.

The effects of panel size and shape are shown in Figure 9. Although tests are limited, the trend toward increased penetration velocities for increases in panel

area is evident. This appears true for center impacts both for flat and curved panels with a 40-in. curvature radius. The data also shows that for polycarbonate, panels with a smaller radius of curvature have a higher penetration velocity.

All prior results are based upon center impacts on flat or curved rectangular planform panels. Some testing was also performed to determine the effects of edge and corner impacts on polycarbonate. Results for both the 0.50-in. and 1.0-in. monolithic polycarbonate were similar except that the changes in penetration velocity were greater for the 1.0-in. material. The impacts at the center edge of the panels resulted in slightly lower penetration velocities than center impacts, while the impacts in the front corners were about eight percent higher. The aft corner impacts gave the lowest penetration velocities. Figure 10 illustrates the effect of impact location for 0.50-in. polycarbonate.

The effects of varying bird weights on the penetration velocity of monolithic polycarbonate are shown in Figure 11. Previous investigators have suggested that, for varying bird weights, the kinetic energy to cause similar damage will remain constant. For polycarbonate flat panels, this relationship appears approximately correct only when the results for three- and four-pound birds are being compared.

Presented here has been a brief summary of some of the results obtained from a study program during which a total of 380 panels were subjected to 932 impacts. It has been found that a wide variety of parameters influences the penetration velocity of a transparency. Size, shape, temperature, angle, material processing variables, and support and edge attachment methods all have influences, each of which can vary as a function of changes in other parameters. While empirically developed analytical expressions have been formulated (see Figure 12) which provide prediction capability for certain limited transparency materials and test parameters, a long road lies ahead before the capability to handle all parameters exists. No claim is made that all the problems faced by the transparency designer have been answered. However, the emphasis on tests of newer materials and construction concepts has provided a substantial data base from which it is possible to determine their relative performance and efficiency through use of comparisons such as that shown in Figure 13.

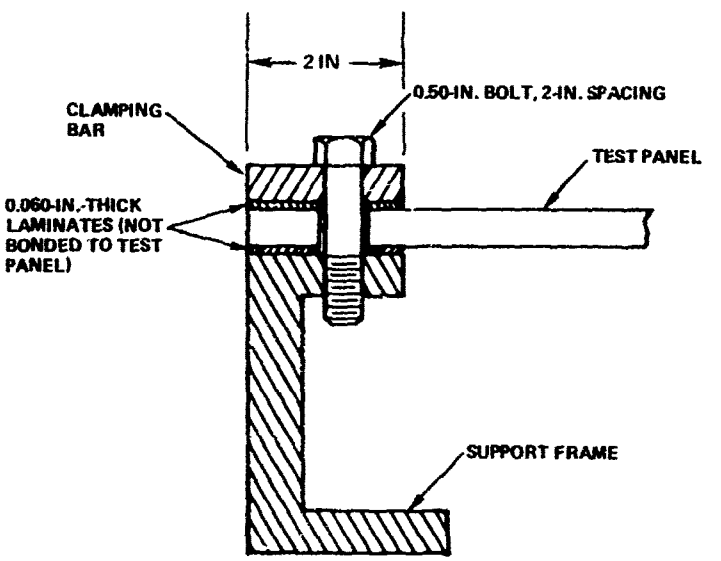


Figure 1 - Test Panel Attachment to Support Frame

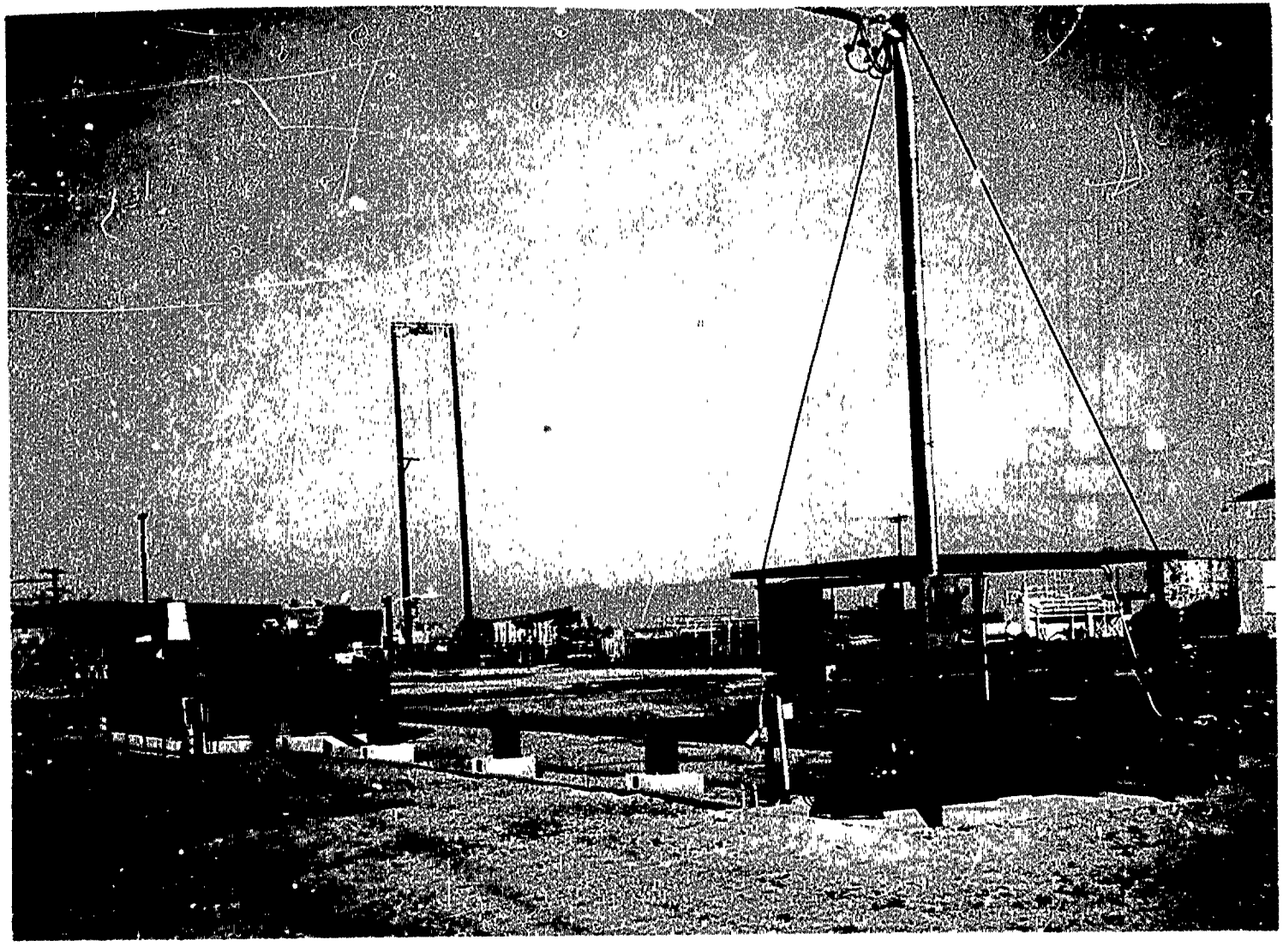


Figure 2. Bird Gun Facility

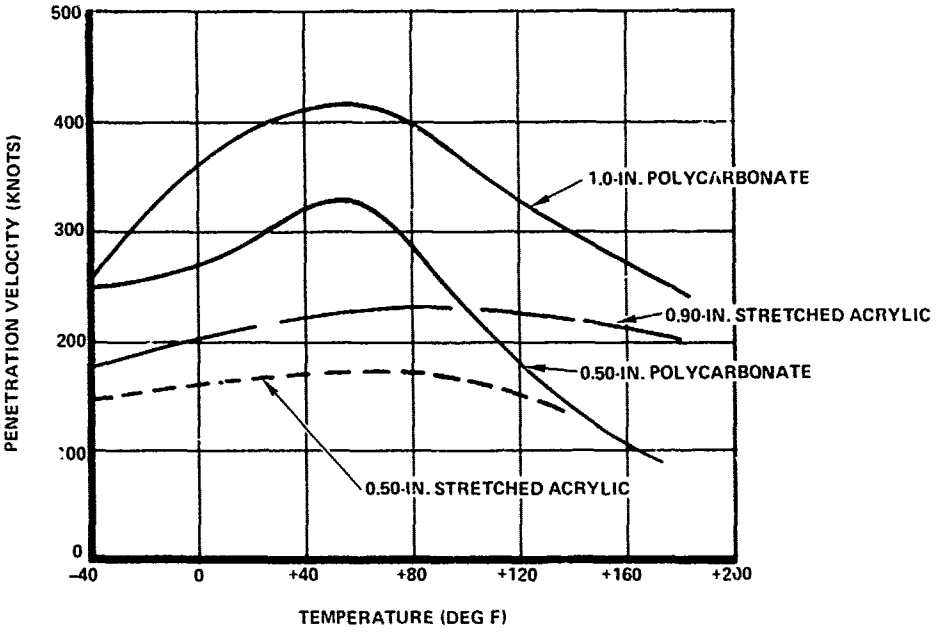


Figure 3 - Effect of Temperature on Penetration Velocity for Monolithic Materials at 45-Deg Bird Impact Angle

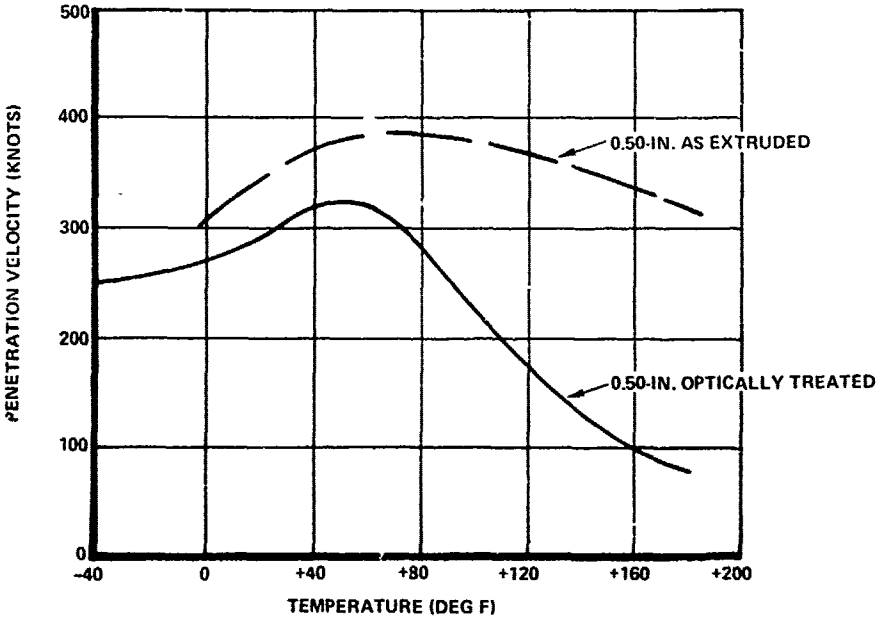
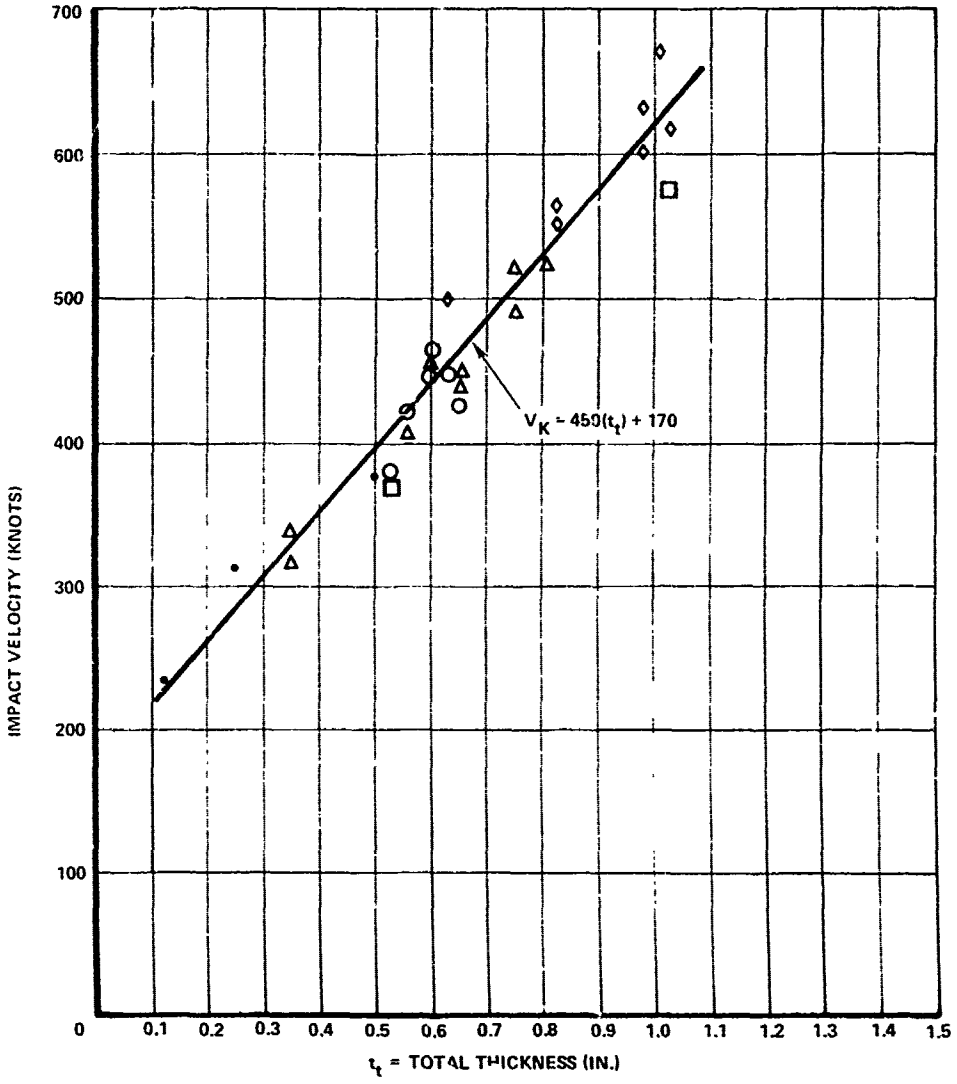


Figure 4 - Effect of Temperature on Penetration Velocity for Optically Treated and As-Extruded Polycarbonate



NOTES:
1. CENTER IMPACTS.
2. ROOM TEMPERATURE.
3. 4-LB BIRDS.
4. AS-EXTRUDED POLYCARBONATE.

LEGEND:
- • MONOLITHIC
- △ BALANCED LAMINATE – CIP URETHANE INTERLAYER
- ○ BALANCED LAMINATE – CIP SILICONE INTERLAYER
- □ BALANCED LAMINATE – ETP SHEET INTERLAYER
- ◇ MULTIPLE INTERLAYER LAMINATE

Figure 5 - Effect of Total Thickness on Penetration Velocity of Polycarbonate Flat Panels at 45-Deg Bird Impact Angle

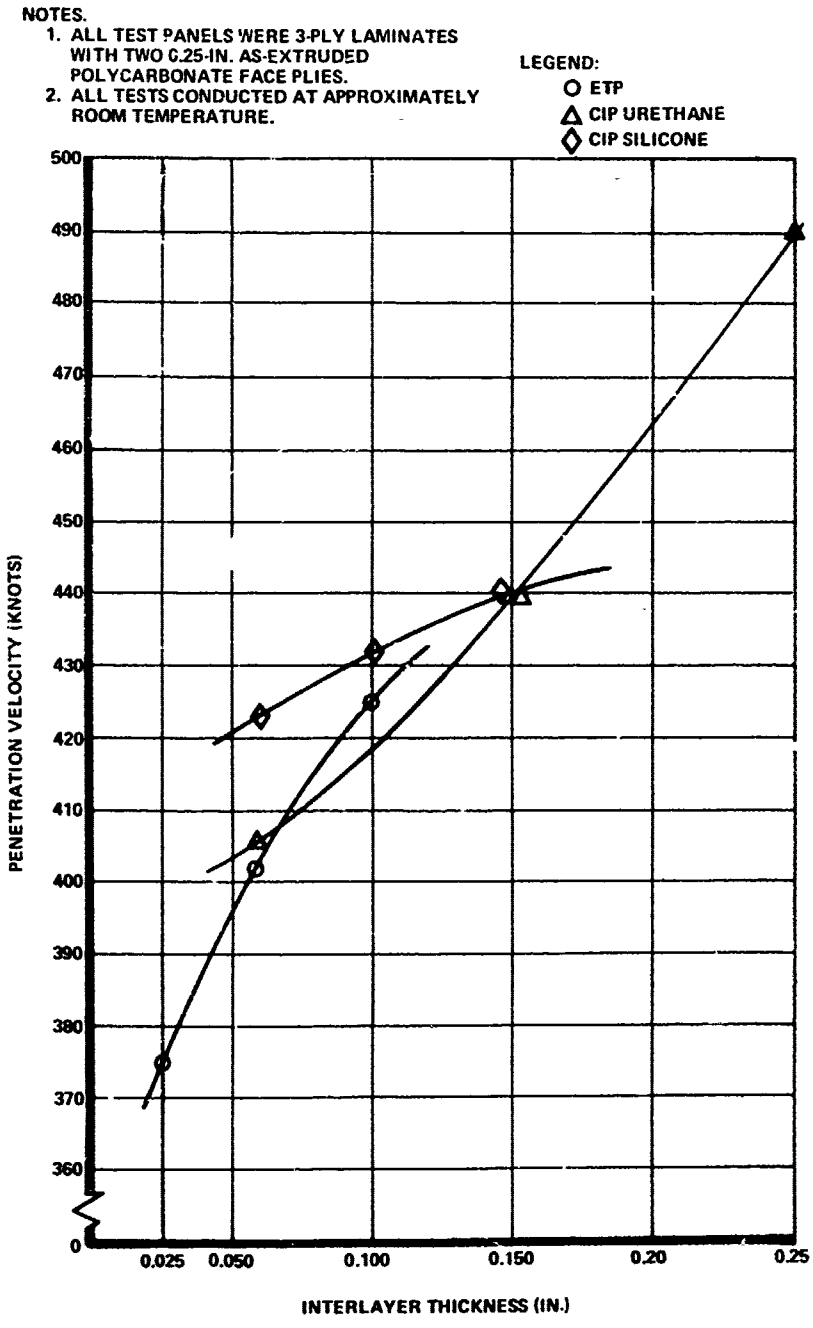
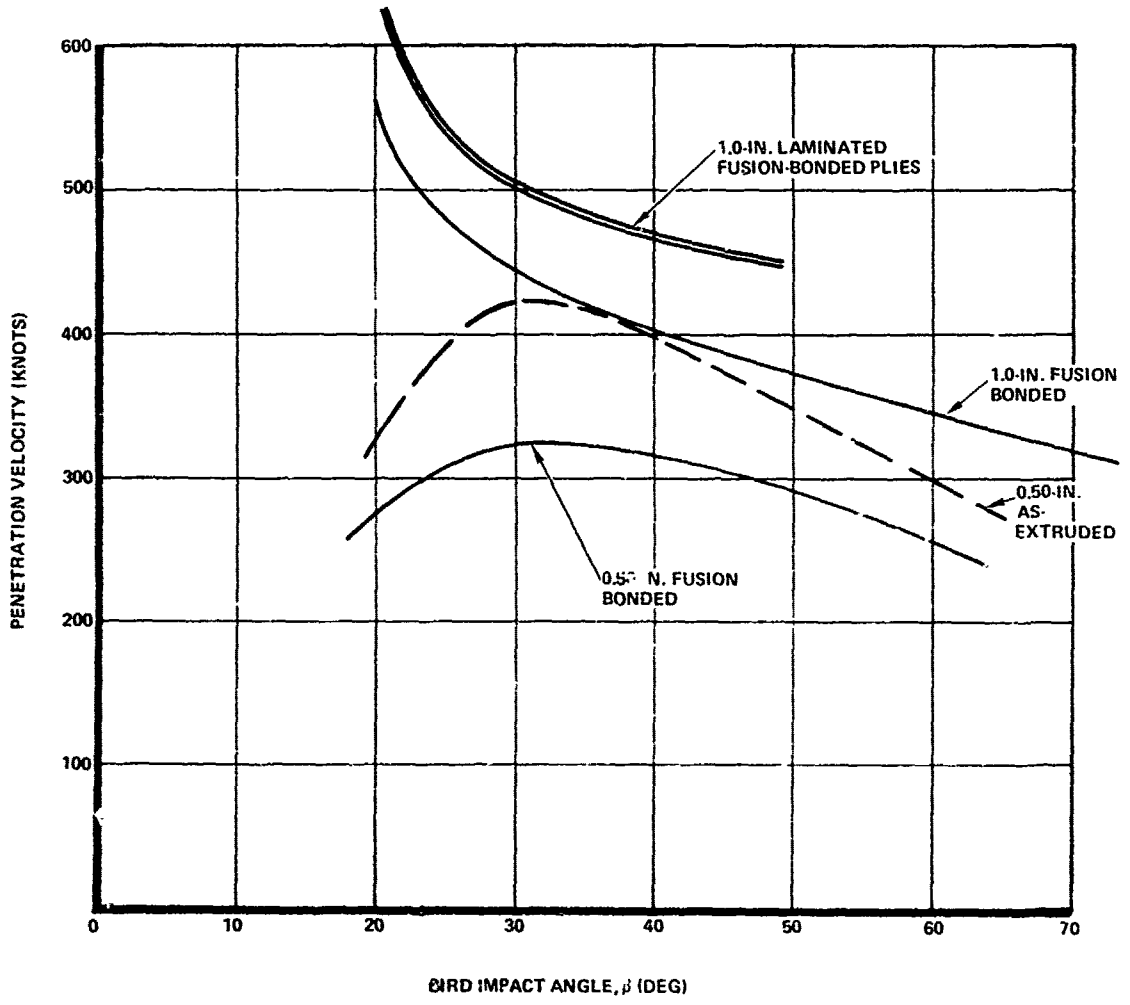


Figure 6 - Effect of Interlayer Type and Thickness on Penetration Velocity at 45-Deg Bird Impact Angle



NOTES:
1. CENTER IMPACT.
2. ROOM TEMPERATURE.

Figure 7 - Effect of Bird Impact Angle on Penetration Velocity of Polycarbonate Flat Panels

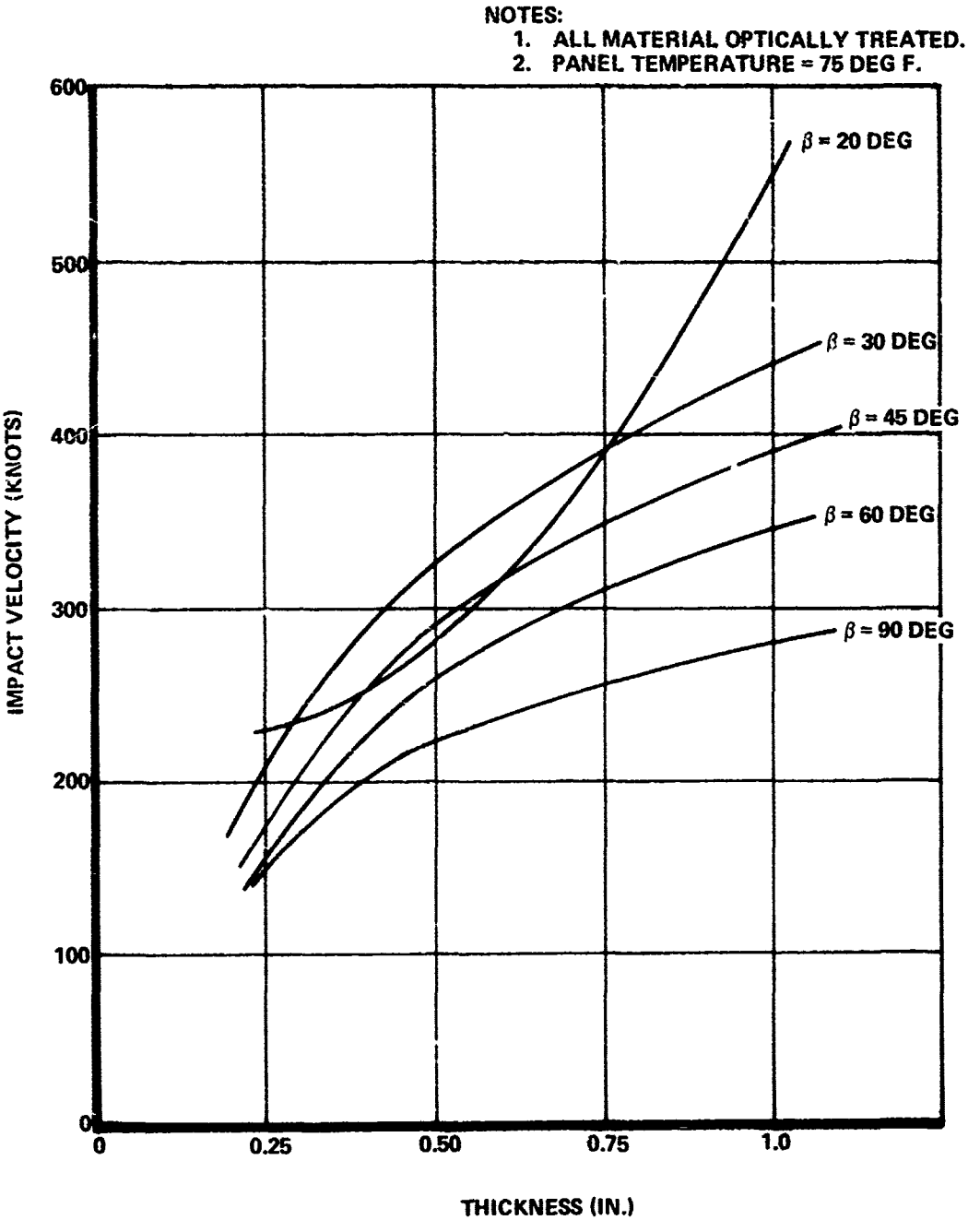


Figure 8 - Effect of Material Thickness on Penetration Velocity for Monolithic Polycarbonate at Varying Bird Impact Angles

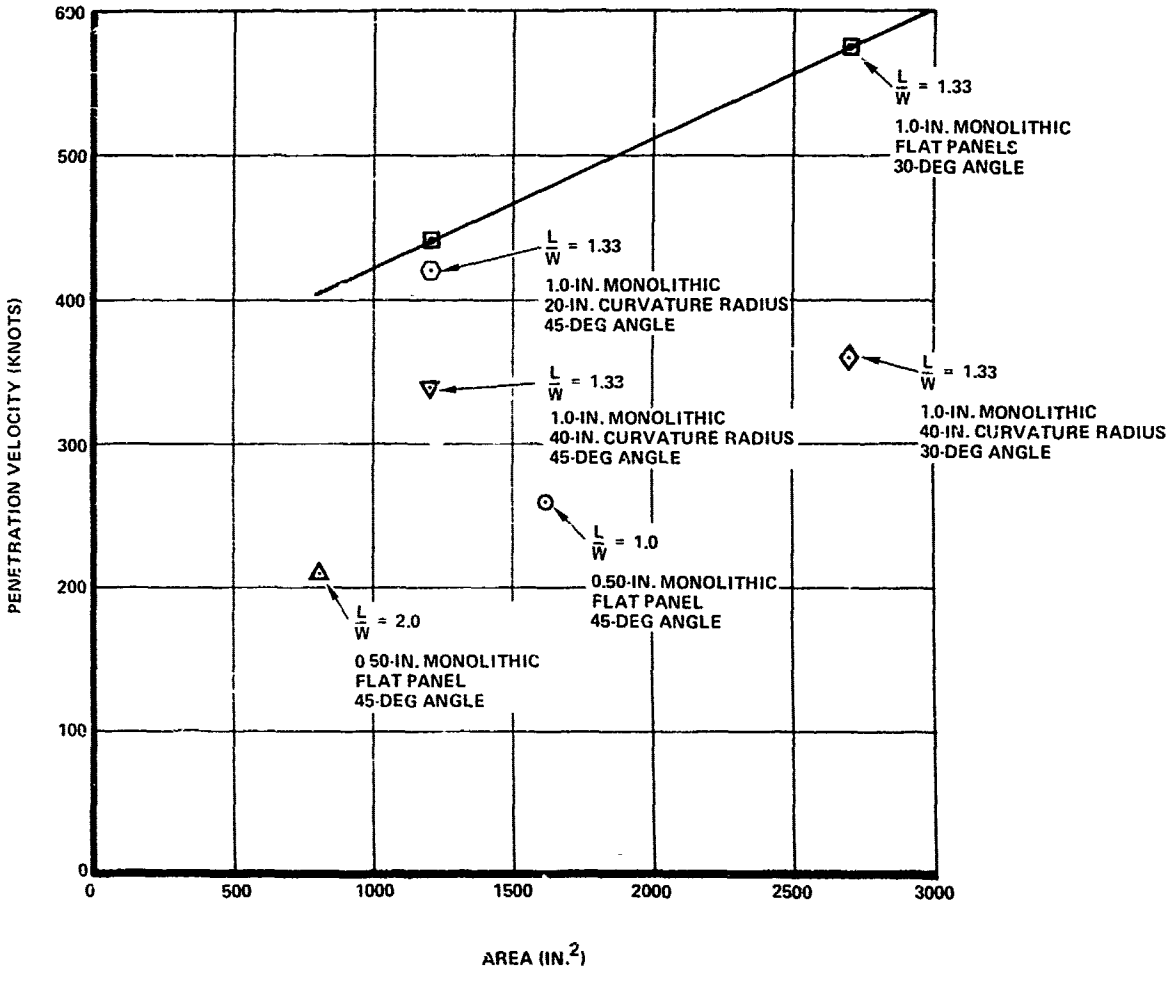


Figure 9 - Effect of Panel Size and Shape on Penetration Velocity for Polycarbonate

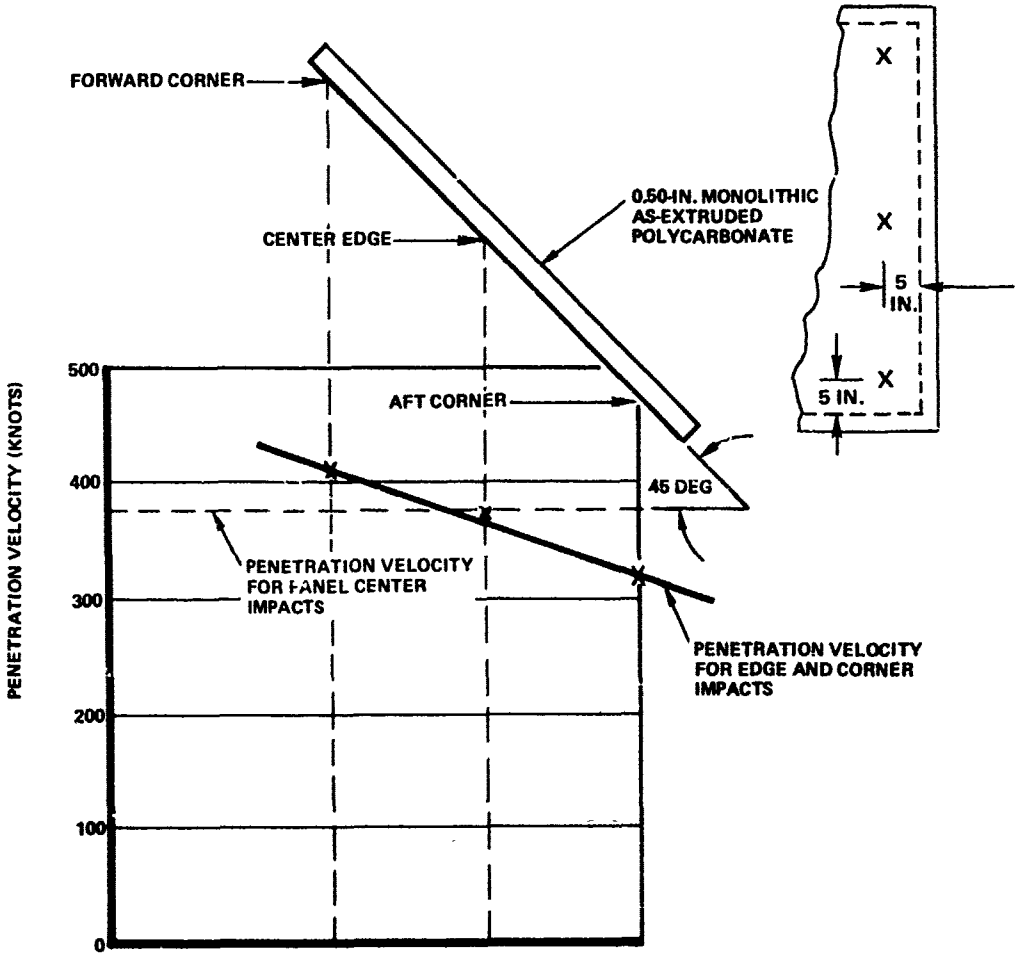


Figure 10 - Effect of Impact Location on Penetration Velocity for 0.50-In. Monolithic As-Extruded Polycarbonate

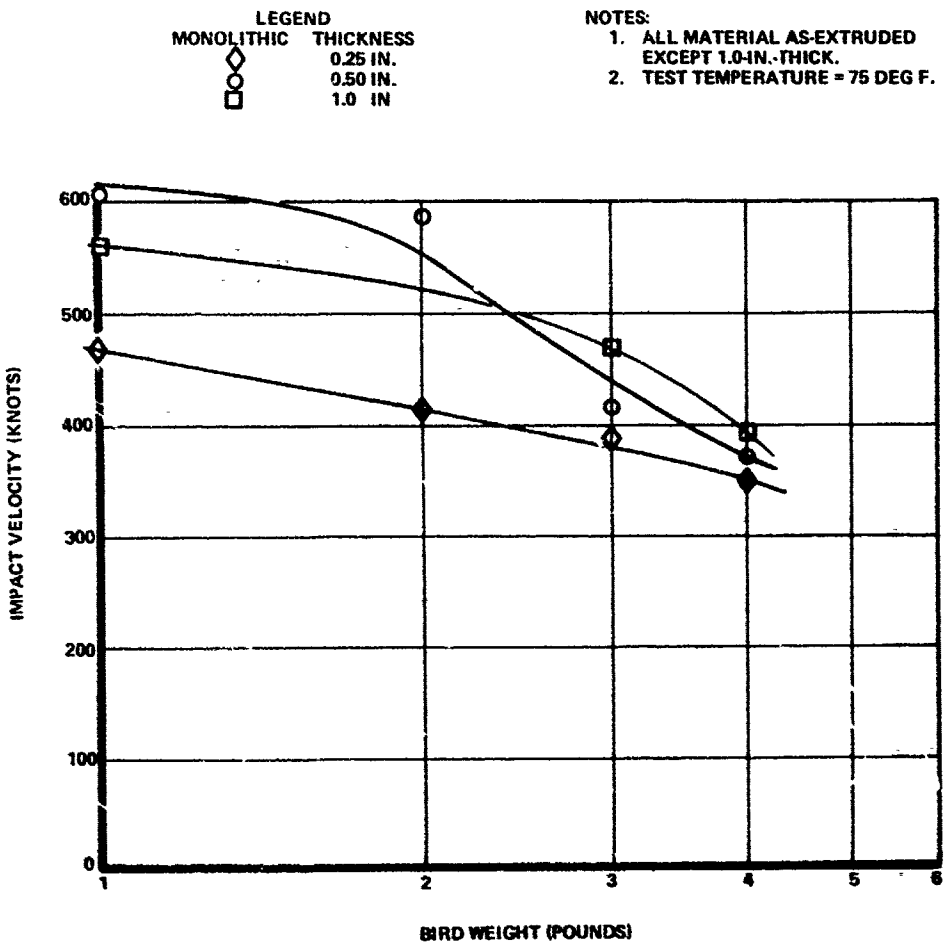


Figure 11 – Polycarbonate Penetration Velocity versus Bird Weight at 45-Deg Bird Impact Angle

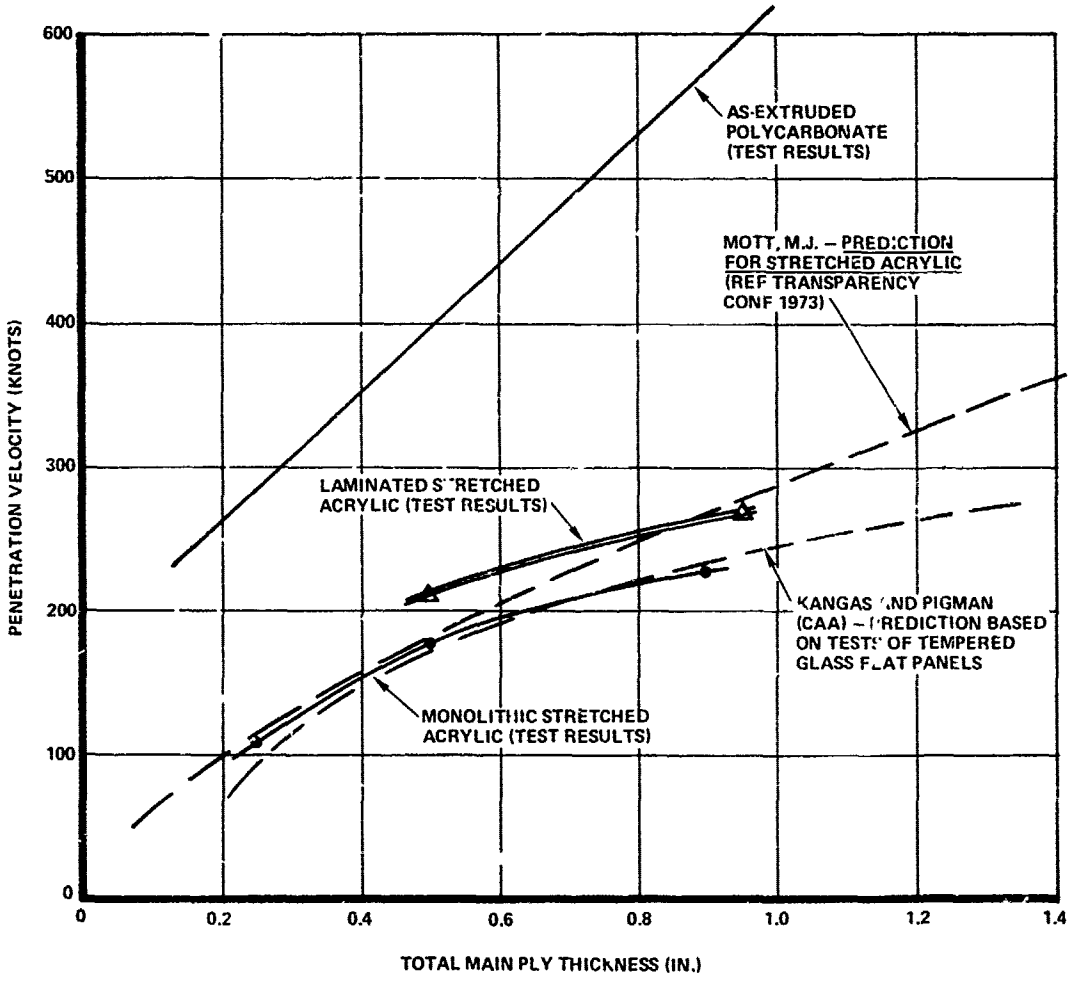


Figure 12 - Comparison of Test Results with Analytical Predictions for 4-Lb Bird Impacts at 45-Deg Angle

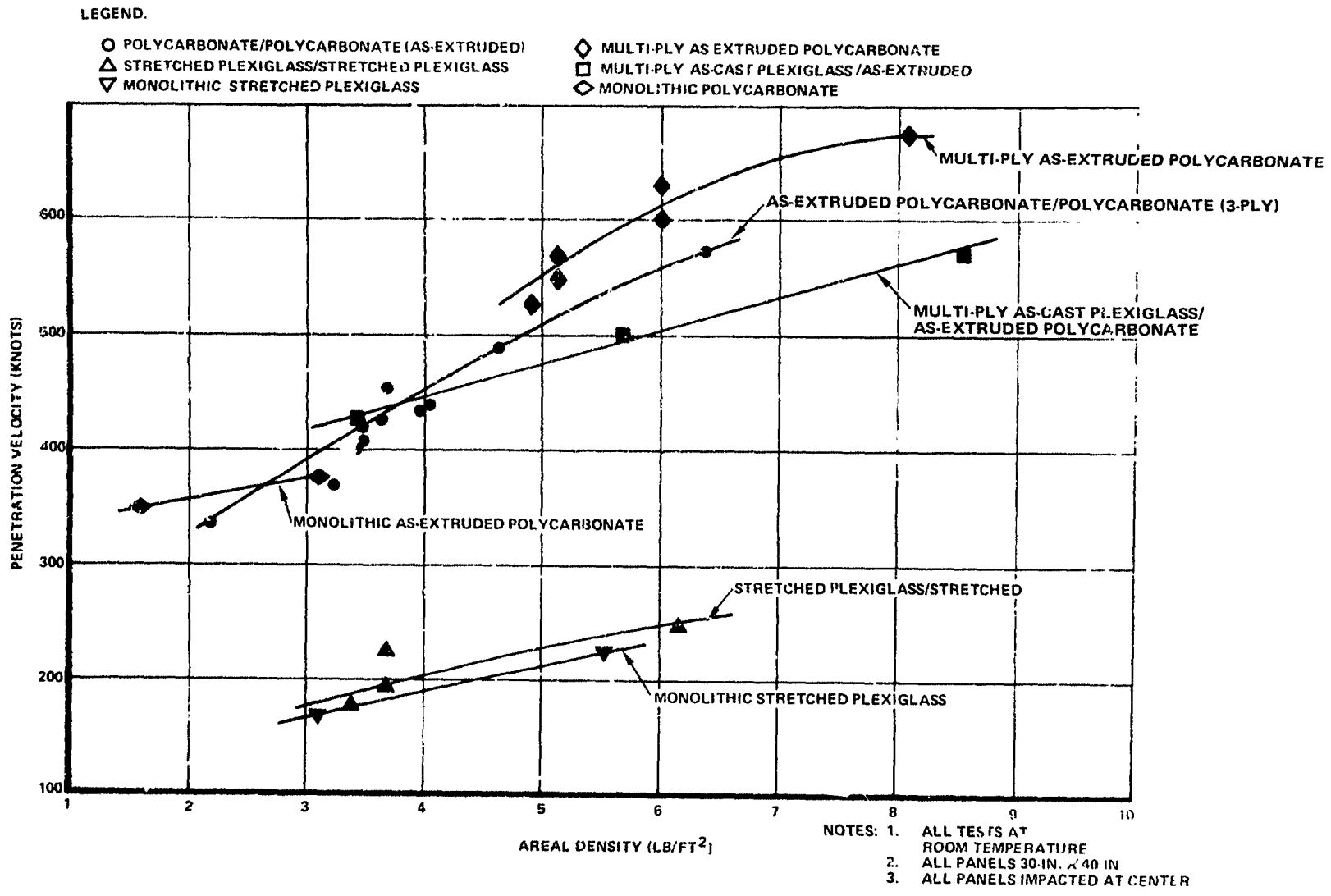


Figure 13 - Penetration Velocity versus Areal Density of Flat Laminated and Monolithic Panels at 45-Deg Bird Impact Angle

BIRD IMPACT TEST PROGRAM FOR WINDSHIELDS OF SMALL, LIGHT AIRCRAFT

J. B. R. Heath and A. J. Bosik
National Aeronautical Establishment
National Research Council
Ottawa, Ontario, Canada

Bird Impact Test Program for Windshields of Small, Light Aircraft

J.B.R. Heath and A.J. Bosik
National Research Council
Ottawa, Ontario, Canada

Abstract

An experimental program has been carried out to generate design information on the bird impact resistance of windshield materials for small, light aircraft. In this program, the penetration velocities of monolithic panels of as-cast acrylic, stretched acrylic and polycarbonate were determined for 2 ft. × 2ft. flat panels in thicknesses from 0.093 to 0.375 inches and with one, two and four pound bird weights. The panels were restrained by either bolting through or clamping the edges to a rigid frame. Although the bulk of the program was carried out under normal room temperature conditions and with an impact angle of 45°, a selected thickness of each material was also tested with a two pound bird weight at temperatures of -40°F and 110°F and the impact angle was varied 45 ± 20°.

Bird Impact Test Program for Windshields of Small, Light Aircraft

Introduction

In a survey conducted on 19 light aircraft, it was found that 80% had windshields of as-cast acrylic 0.125 inches or less in thickness and a number of these aircraft operate with unheated windshields in a low temperature environment. Because there are no bird strike requirements in North America for the light aircraft category windshields, data for windshield glazing to withstand bird impacts are lacking and the adequacy of the existing windshield designs are questionable. The present program was therefore established to study the impact resistance of aircraft transparency materials in order to generate information that would lead to superior windshield designs without incurring penalties of weight, loss of optical properties and the necessity of operating in a limited temperature environment. The category of aircraft which served as a guide for this program is a low speed, unpressurized and unsophisticated aircraft with a maximum cruise speed of 250 mph as reported by the Associate Committee on Aerospace Structures and Materials in reference 1. Although there are a number of factors to be considered when choosing a suitable aircraft windshield material, this study was concerned with the bird impact aspect only.

Test Program

In order to accomplish the basic objective of generating bird impact design data for light aircraft windshields, the test program outlined in Table 1 was drawn up. This program comprised the determination of the penetration velocities of flat monolithic panels of as-cast acrylic, stretched acrylic and polycarbonate materials mounted in a highly rigid support frame. Real chicken carcasses were used and all of the tests were centre panel impacts.

In the primary phases of the program, penetration velocities of the three materials were determined for room temperature conditions by impacting the panels mounted at 45° with one, two and four pound birds. The acrylic panels were tested using two methods to restrain the edges, bolting and clamping. The polycarbonate panels were tested with a bolted edge condition only. Panel thicknesses of 1/8, 1/4 and 3/8 inches of the acrylics and 3/32 1/8, 1/4 and 3/8 inches of the polycarbonate were used.

In subsequent phases of the program, a limited study was carried out to determine the effect on the penetration velocity of varying the impact angle and of varying the panel temperature. For these tests, the penetration velocities of 1/8 inch thick panels were determined by impacting with two pound birds. The impact angle was varied 25° and 65°, and the panel temperature was varied -40°F and +120°F.

The specifications of the materials used in the program and the variation in thickness encountered are given in Appendix A.

Definitions

The following definitions were applied for this program.

Penetration - bird impact must result in definite hole or opening in panel.

Penetration Velocity - $V_p = \frac{V_a + V_b}{2}$

where V_a = minimum velocity with penetration
V_b = maximum velocity less than V_a without penetration

Birds - all birds are real chicken carcasses of 1, 2 or 4 pound body weight.

Impact Angle - angle measured between vertical angle of windshield panel and bird's flight path.

Edge Restraint - refers to type of fastening - bolted or clamped rather than stiffness of support frame.

Test Method

The program was conducted at the NRC/NAE Flight Impact Simulator Facility in which the 10 inch bore compressed air powered gun, shown in Figure 1, was used to propell the birds to the stationary panels.

The birds were real chicken carcasses, previously frozen then thawed to room temperature prior to packaging in polyethylene bags for usage. The nominal one, two and four pound chicken carcasses were selected or adjusted so that the respective weights of the packaged projectiles were 1 lb. $^{+\ 2}_{-\ 0}$ oz., 2 lb. $^{+\ 2}_{-\ 0}$ oz. and 4 lb. $^{+\ 4}_{-\ 0}$ oz. The weight adjustments, when necessary, were accomplished by either trimming portions of the extremities of the carcasses or by adding jell (98% water and 2% sodium carboxymethylcellulose by weight) into the packages. The amount of weight adjustment was limited to about 10% of the final projectile weight. The method of adapting the gun sabot for the three nominal bird weights is shown in Figure 2.

The velocity of a projected bird package was timed just prior to impact with the two, independently operating optical-electronic timing systems of the facility shown in Figure 3. A recorded impact velocity was determined by averaging the mean of the velocities obtained from the two systems. The accuracy of these systems is considered to be within 0.5%.

A typical test panel, mounted in the structural steel support frame for an impact, is shown in Figure 4. The panels had outside dimensions of 2 ft. × 2 ft. and the methods of attaching the panel edges to the support frame are shown in Figure 5. The bolted edges utilized 1/4 inch diameter bolts on one inch centers and torqued to 40 in. lbs. The clamped edges utilized 1/4 inch diameter bolts on two inch centers and torqued to 100 in. lbs. The support frame, shown in Figure 6, was first aligned to the gun for a central panel impact and then secured at its base to tie-down points on floor of the test site. Spacers were placed under the 4 × 4 × 1/4 inch members supporting the panel mounting plate in order to alter the impact angle from 45° to 25° or 65°.

An enclosure constructed of styrofoam insulation, shown in Figure 7, was erected around a mounted test panel for a low or elevated temperature test. The panel was soaked to the desired temperature by introducing either cooled or heated air into the enclosure with ducts going to each side of the panel as shown in Figure 8. Grid-type copper-constantan thermocouples were used to monitor the panel center and corner temperatures as well as the temperature of the panel mounting plate during the panel conditioning. Typical panel cooling and heating curves are given in Figures 9 and 10. A panel was impacted after the center of the panel reached a temperature of -40 ±5° F for the low temperature tests and +120 ±5°F for the elevated temperature tests.

Results

The precision to which the penetration velocities were obtained are shown with the plotted results and are indicated beside the tabulated results. Although only two impacts were theoretically required to obtain a result for a specific condition, in general three to five impacts were performed to obtain a penetration velocity.

(1) Room Temperature, 45° Impact Angle

The penetration velocities for the panels impacted at 45°, under room temperature conditions, are given in Figures 11 to 15. The results generally indicate a non-linear increase in penetration velocity for an increase in panel thickness or decrease in bird weight. For the same material thickness, the average increase in penetration velocity obtained with one and two pound birds compared with the four pound bird results were as follows:

Material	One Pound Bird	Two Pound Bird
As Cast, bolted	54%	28%
As-Cast, clamped	38%	23%
Stretched, bolted	51%	6%
Stretched, clamped	70%	33%
Polycarbonate	76%	19%

The disproportionate increase of the stretched acrylic, bolted case is noteworthy.

Figures 16 and 17 compare the three materials for one panel thickness and one bird weight in each case. In each of the two comparisons, the superior impact resistance ability of the polycarbonate panels over the acrylic panels is clearly displayed. These comparisons also indicate the improvement of the acrylic panels when clamped at the edges rather than bolted at the edges. Overall, the clamped as-cast acrylic panels had an increase in penetration velocity of 13% to 42% with an average increase of 27%. The increases for the stretched acrylic panels were even more pronounced with these ranging from 18% to 97% and an average of 64%.

Within the limits of the material thicknesses tested, the results indicate that of the three materials tested, only the polycarbonate material would be suitable for a windshield that would be required to withstand a four pound bird strike at 250 mph. One or two pound bird strikes could, however, be withstood at 250 mph with a stretched acrylic windshield clamped at the edges.

(2) Variation of Impact Angle

The results obtained from varying the impact angle ±20° from 45° for 1/8 inch thick panels and using two pound birds are given in Table 2. The results show an increase in penetration velocity for the as-cast acrylic panels and for the bolted edges stretched acrylic panels when the impact angle was reduced from 45° to 25°. The reduction of the impact angle in the case of the clamped edges stretched acrylic panels and the polycarbonate panels produced a slight decrease in penetration velocity. The penetration velocity was reduced in all cases when the impact angle was increased from 45° to 65°.

(3) Variation of Panel Temperature

The effects on the penetration velocity of cooling the panel temperature or elevating it from a room temperature condition is given in Table 3. Although slight variations of the penetration velocities occurred, the results indicate no significant changes in the penetration velocities due to the change in panel temperatures from room temperature conditions.

(4) Fracture Patterns

The unique fracture patterns of the three different materials tested in this program were of practical significance in determining their penetration velocities.

For the acrylic panels, the penetration of a panel with a velocity near its penetration velocity was apparent with almost the complete panel being fractured into large panel fragments.

If a penetration occurred at a velocity considerably above the penetration velocity of a panel, the area fractured was less, approaching the projected area of the projectile and the panel fragments were reduced in size. These comparisons of typical panels are shown in Figures 18 and 19. An acrylic panel impacted at a velocity below its penetration velocity in general displayed no visible damage. At an impact angle of 25°, the fracture of a panel was concentrated near the top of the panel, Figure 20, as would be expected because of the load distribution for this configuration. The fracture patterns of the acrylic panels with a 65° impact angle were similar to those with a 45° impact angle. The fracture patterns of the low and elevated temperature test panels were similar to the fracture patterns of the room temperature tested panels.

At room and elevated temperatures, a penetrated polycarbonate panel exibited large deformations at the impact point and a fracture along the bolt holes at the top edge of the panel, which propagated along each side of the panel as is shown in Figure 21. In general, a short propagation length along the sides indicated that the impact velocity was near the penetration velocity. Exceptions to this fracture pattern were cited in two cases, in each of which the fracture occurred at the point of impact. The first of these was in a panel whose impact angle was 65°, shown in Figure 22, and the second, shown in Figure 23, was in a panel, impacted at 45°, in which the fracture appeared to initiate from an imperfection created by a chemical contaminant. At -40°F, the polycarbonate panels fractured in a pattern more typical of as-cast acrylic panels, displaying a brittle rather than ductile failure, as shown in Figure 24. The elevated panel temperature fractures were similar to the room temperature ones.

Conclusions

(1) The results indicate that the polycarbonate panels have a superior impact resistance to bird impacts over the acrylic panels and that the stretched acrylic panels are an improvement over the as-cast acrylic panels.

(2) For the same material thickness, the average increase in penetration velocity, compared to the penetration velocity of a four pound bird, ranged from 38% to 76% with a one pound bird and 6% to 33% with a two pound bird.

(3) By changing the panel edge restraints from bolted to clamped, the room temperature results indicated an average increase in penetration velocity of 27% for the as-cast acrylic panels and 64% for the stretched acrylic panels. Continuous rather than spot edge fastening should therefore be utilized in order that the optimum usage of acrylic windshields is achieved.

(4) The penetration velocity was reduced in all cases when the impact angle was increased from 45° to 65° but the results were inconsistent when the impact angle was reduced from 45° to 25° indicating that the effect of impact angle on penetration velocity may also be material and installation dependent.

(5) The low and elevated temperature results indicated no significant changes in the penetration velocities compared with the room temperature results.

(6) Because in general, the polycarbonate panel fractures appeared to initiate at the bolt holes, higher penetration velocities could be expected for these panels if they were restrained continuously at the edges and future work should be conducted to confirm this.

(7) The results obtained give a good comparison of the three materials tested and should be considered conservative because the panels were mounted on a highly rigid support frame. The present results would achieve further usefulness if they were complemented with studies determining the effects on penetration velocity of adding flexibility to the support structure and the effects of changing panel size.

References

1. Report ACASM-TN-1, Associate Committee on Aerospace Structures and Materials, National Research Council of Canada, 1971.

TABLE 1

TEST PROGRAM

Material	Thickness (in.)	Edge Restraint	Impact Angle (°)	Bird Wt. (lb.)	Temperature Condition
A.C.Acrylic	1/8,1/4 & 3/8	Bolted	45	1, 2 & 4	Ambient Room
A.C.Acrylic	1/8,1/4 & 3/8	Clamped	45	1, 2 & 4	Ambient Room
Str.Acrylic	1/8,1/4 & 3/8	Bolted	45	1, 2 & 4	Ambient Room
Str.Acrylic	1/8,1/4 & 3/8	Clamped	45	1, 2 & 4	Ambient Room
Polycarbonate	3/32,1/8,1/4 & 3/8	Bolted	45	1, 2 & 4	Ambient Room
A.C.Acrylic	1/8	Bolted	25 & 65	2	Ambient Room
A.C.Acrylic	1/8	Clamped	25 & 65	2	Ambient Room
Str.Acrylic	1/8	Bolted	25 & 65	2	Ambient Room
Str.Acrylic	1/8	Clamped	25 & 65	2	Ambient Room
Polycarbonate	1/8	Bolted	25 & 65	2	Ambient Room
A.C.Acrylic	1/8	Bolted	45	2	-40°F & 120°F
A.C.Acrylic	1/8	Clamped	45	2	-40°F & 120°F
Str.Acrylic	1/8	Bolted	45	2	-40°F & 120°F
Str.Acrylic	1/8	Clamped	45	2	-40°F & 120°F
Polycarbonate	1/8	Bolted	45	2	-40°F & 120°F

TABLE 2

VARIATION OF PANEL IMPACT ANGLE

(2 POUND BIRD, 1/8 THICK PANEL, ROOM TEMPERATURE)

Material	Edge Restraint	Penetration Velocity (MPH)		
		25°	45°	65°
A.C.Acrylic	Bolted	127 $\pm$3	87 $\pm$3	83 $\pm$1
A.C.Acrylic	Clamped	122 $\pm$7	116 $\pm$4	90 $\pm$5
Str.Acrylic	Bolted	150 $\pm$6	99 $\pm$3	80 $\pm$4
Str.Acrylic	Clamped	147 $\pm$8	165 $\pm$4	142 $\pm$7
Polycarbonate	Bolted	243 $\pm$7	265 $\pm$12	251 $\pm$2

TABLE 3

VARIATION OF PANEL TEMPERATURE

(2 POUND BIRD, 45°, 1/8 THICK PANEL)

Material	Edge Restraint	Penetration Velocity (MPH)		
		-40°F	Room Temp.	+120°F
A.C.Acrylic	Bolted	101 ±3	87 ±3	87 ±3
A.C.Acrylic	Clamped	123 ±5	116 ±4	112 ±4
Str.Acrylic	Bolted	106 ±3	99 ±3	109 ±5
Str.Acrylic	Clamped	146 ±5	165 ±4	149 ±6
Polycarbonate	Bolted	260 ±5	265 ±12	251 ±13

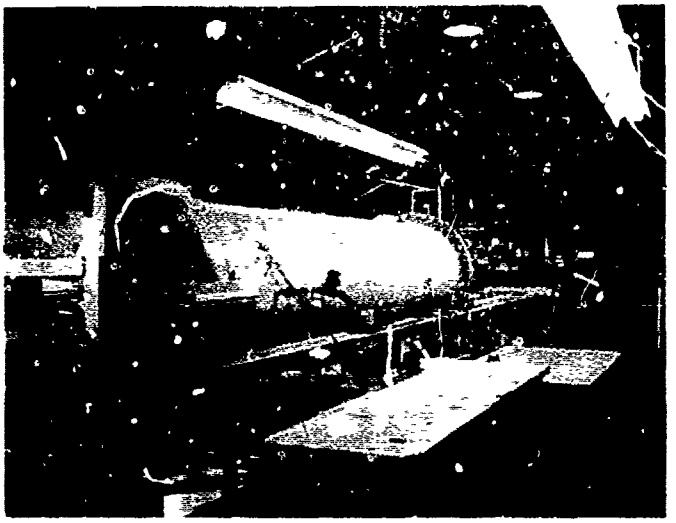


FIG. 1 NRC/NAE FLIGHT IMPACT SIMULATOR

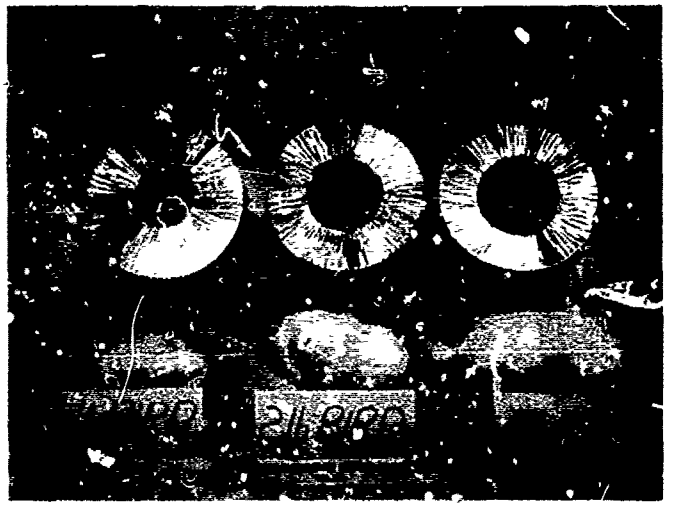


FIG. 2 GUN SABOTS FOR DIFFERENT BIRD WEIGHTS

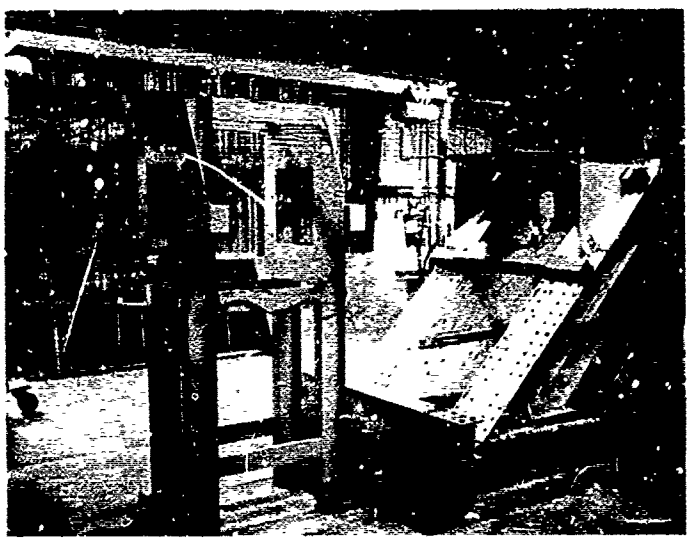


FIG. 3 VELOCITY TIMING SYSTEMS

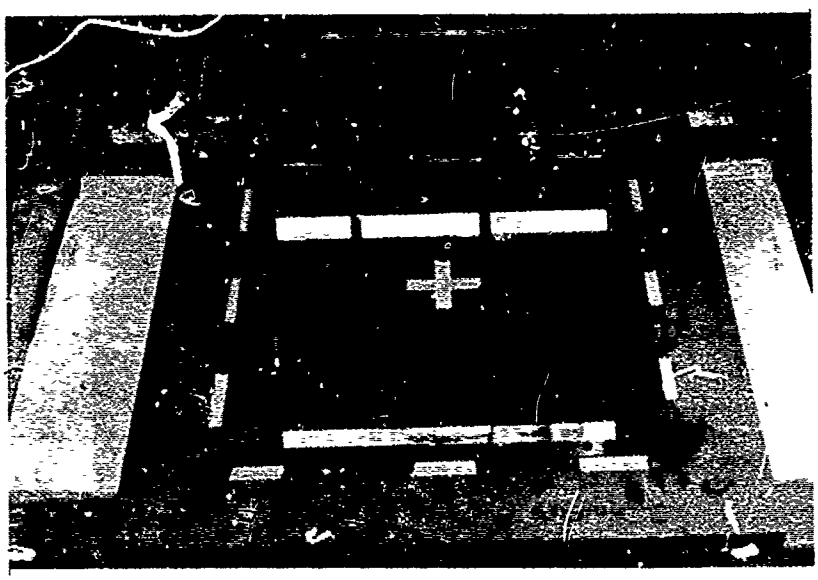
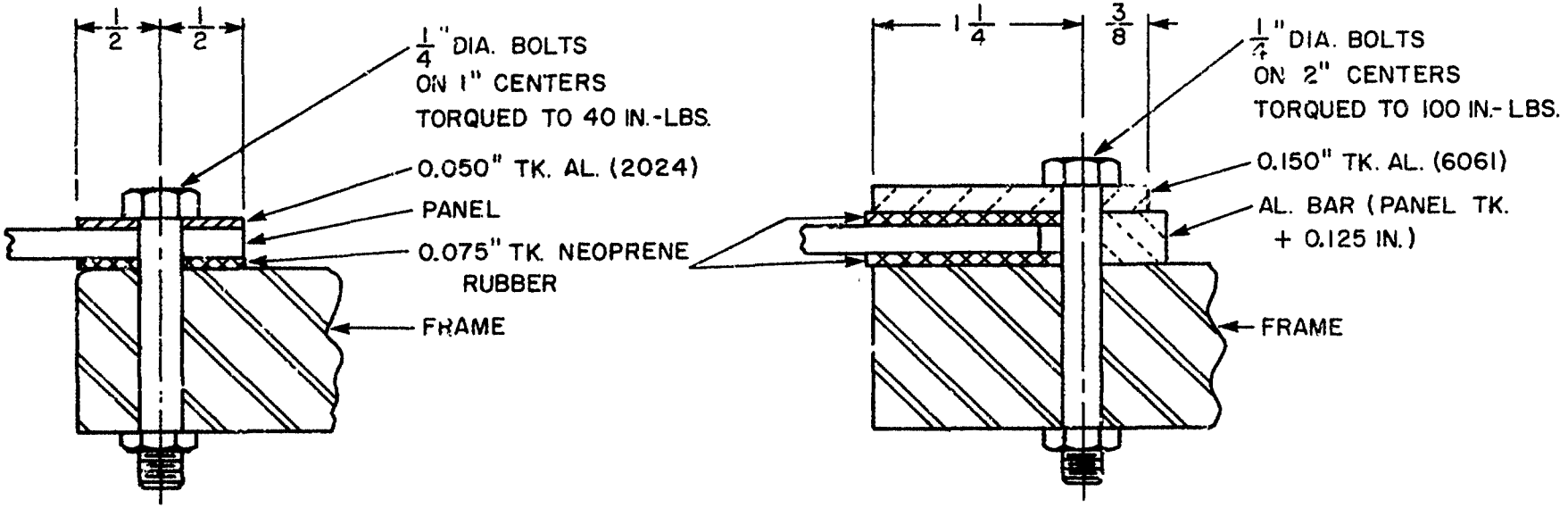


FIG. 4 TYPICAL TEST PANEL MOUNTED FOR AN IMPACT



BOLTED EDGE

CLAMPED EDGE

PANEL EDGE RESTRAINTS

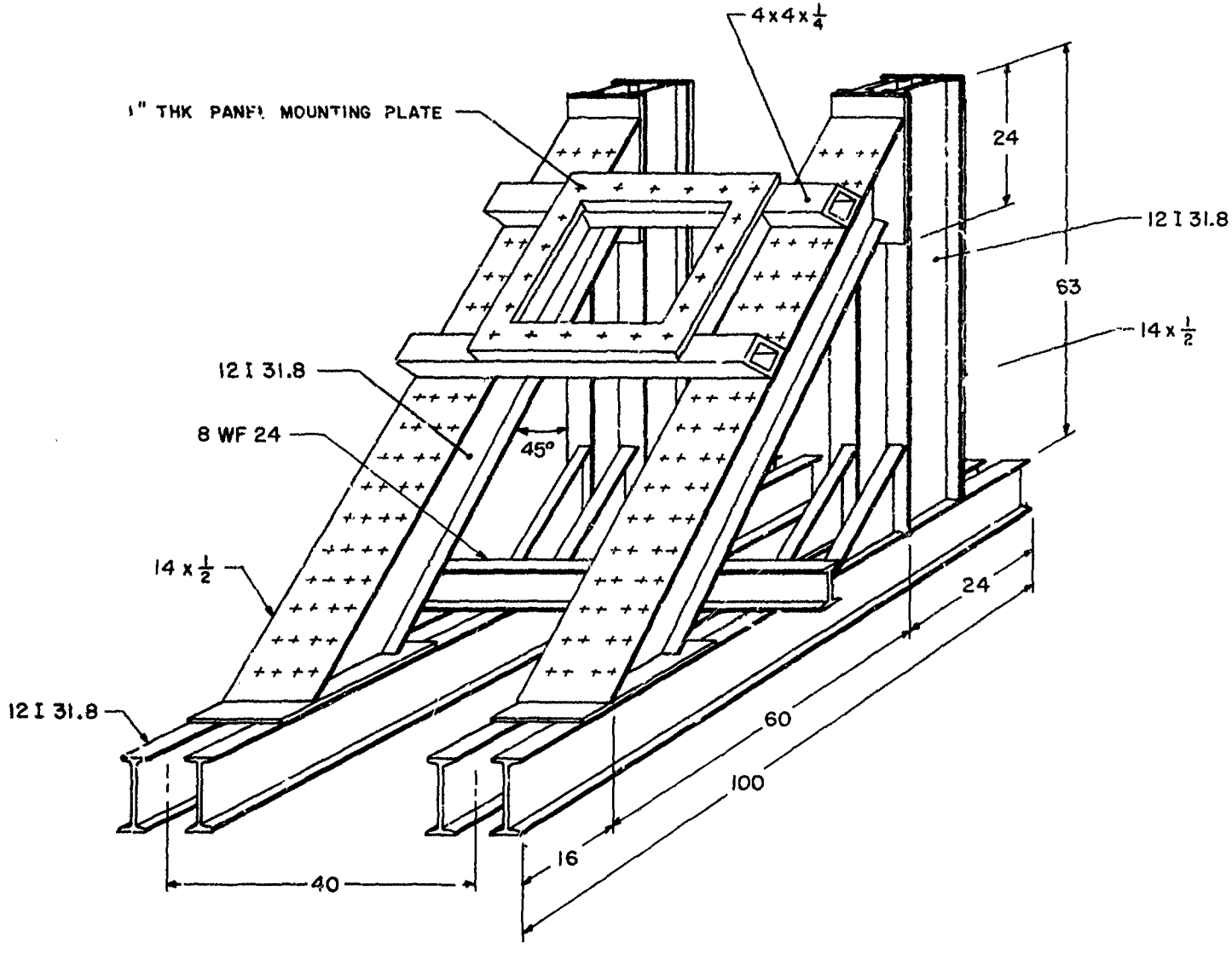


FIG 6 NAE/NRC TEST PANEL SUPPORT FRAME

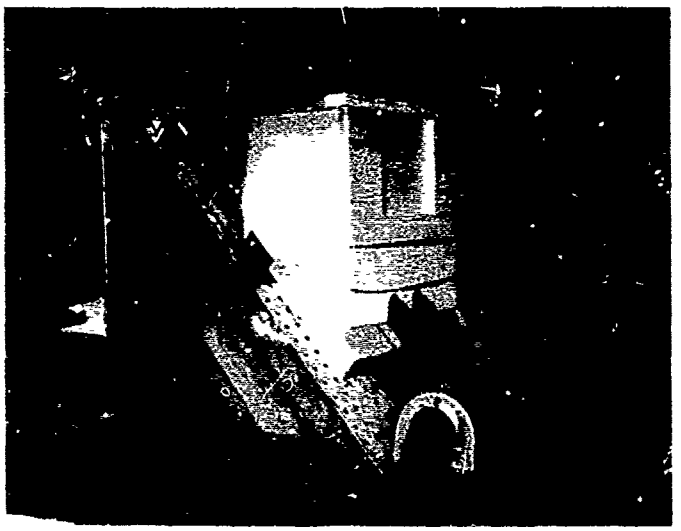


FIG. 7 INSULATED ENCLOSURE FOR LOW OR HIGH TEMPERATURE TESTS

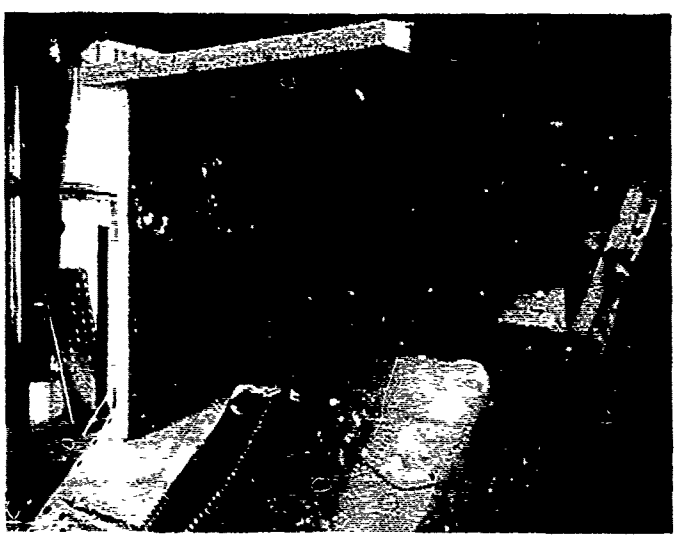


FIG. 8 AIR DUCTS USED FOR COOLING OR HEATING PANEL

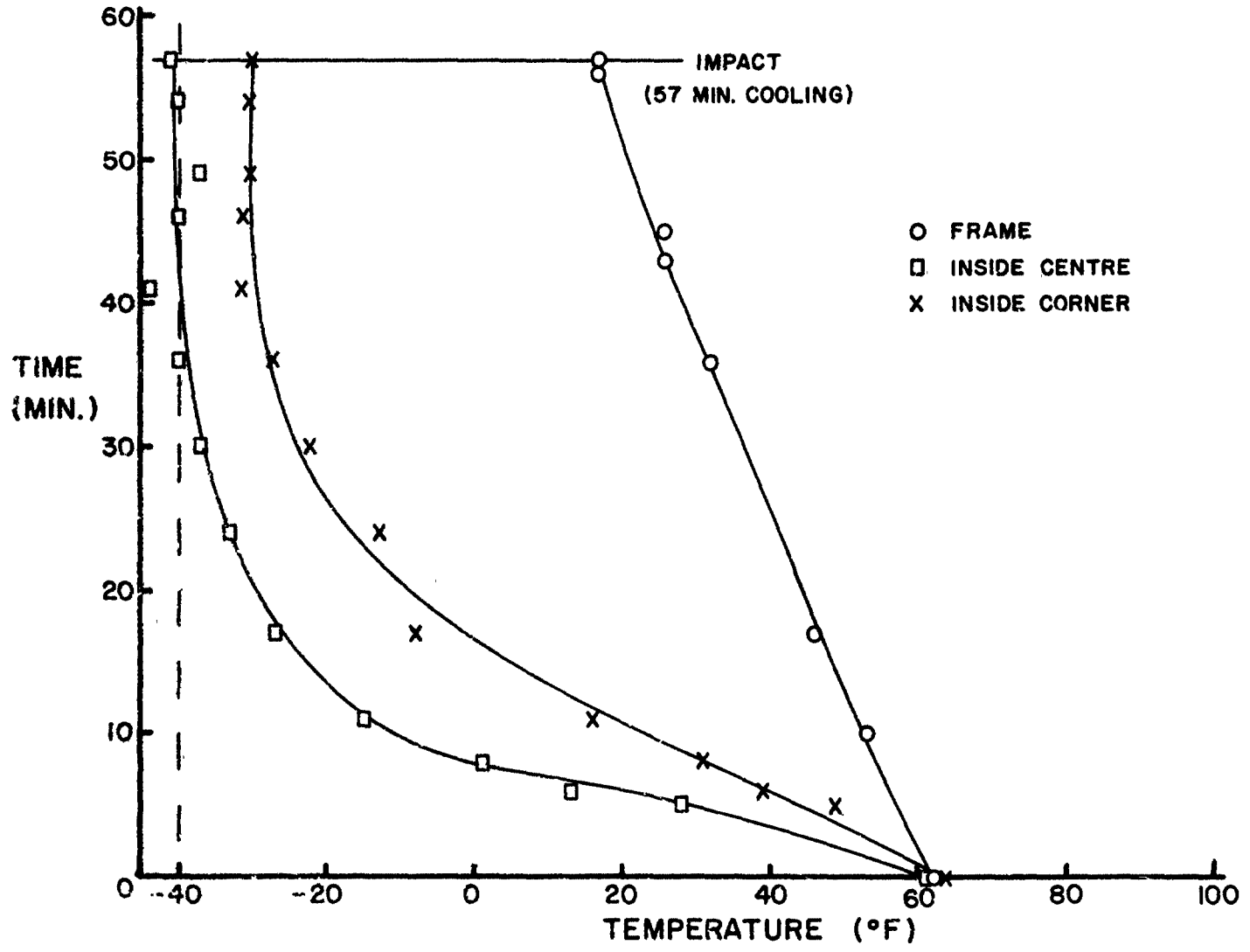


FIG. 9 TYPICAL PANEL COOLING CURVE (-40°F TEST CONDITION)

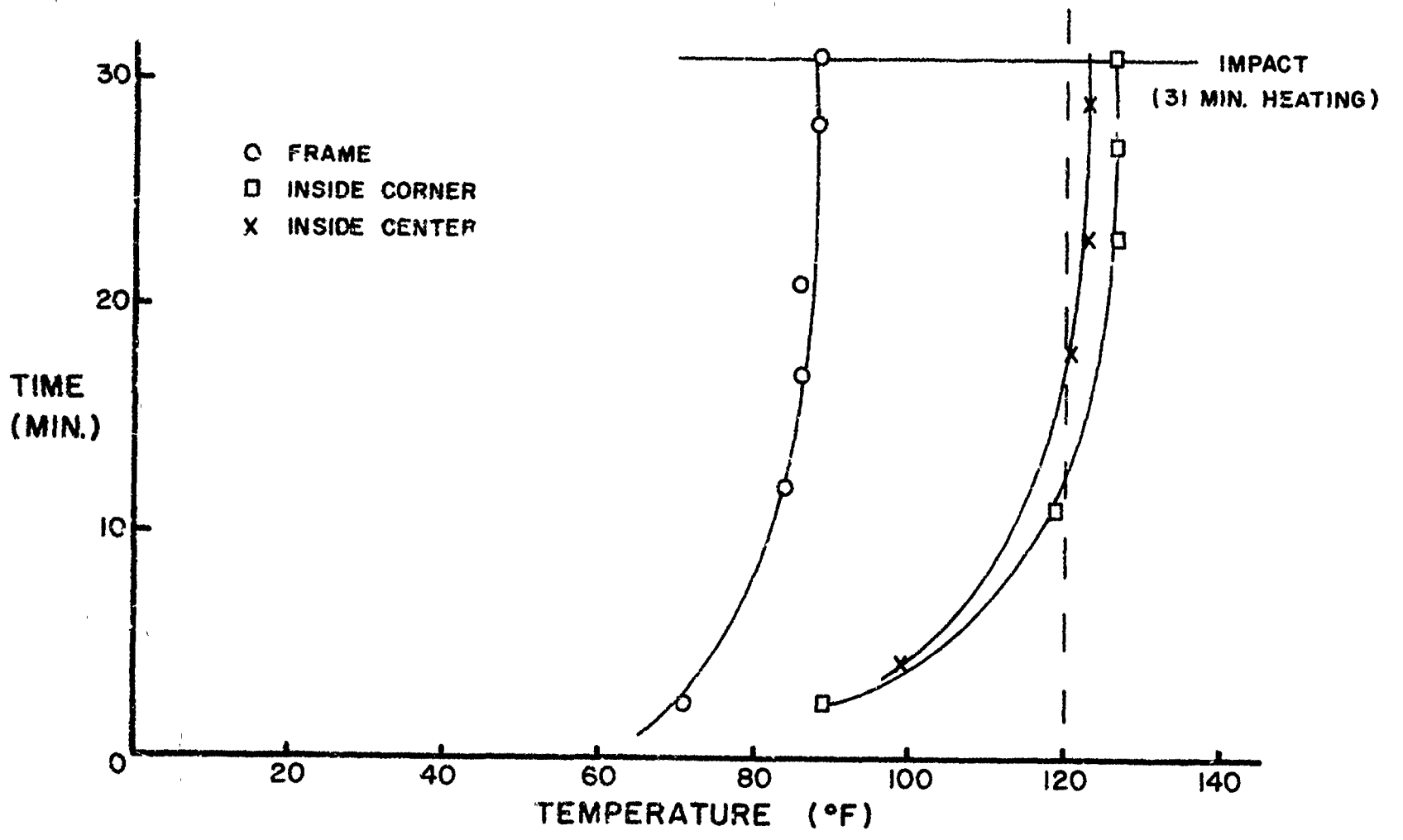


FIG. 10 TYPICAL PANEL HEATING CURVE (+120 °F TEST CONDITION)

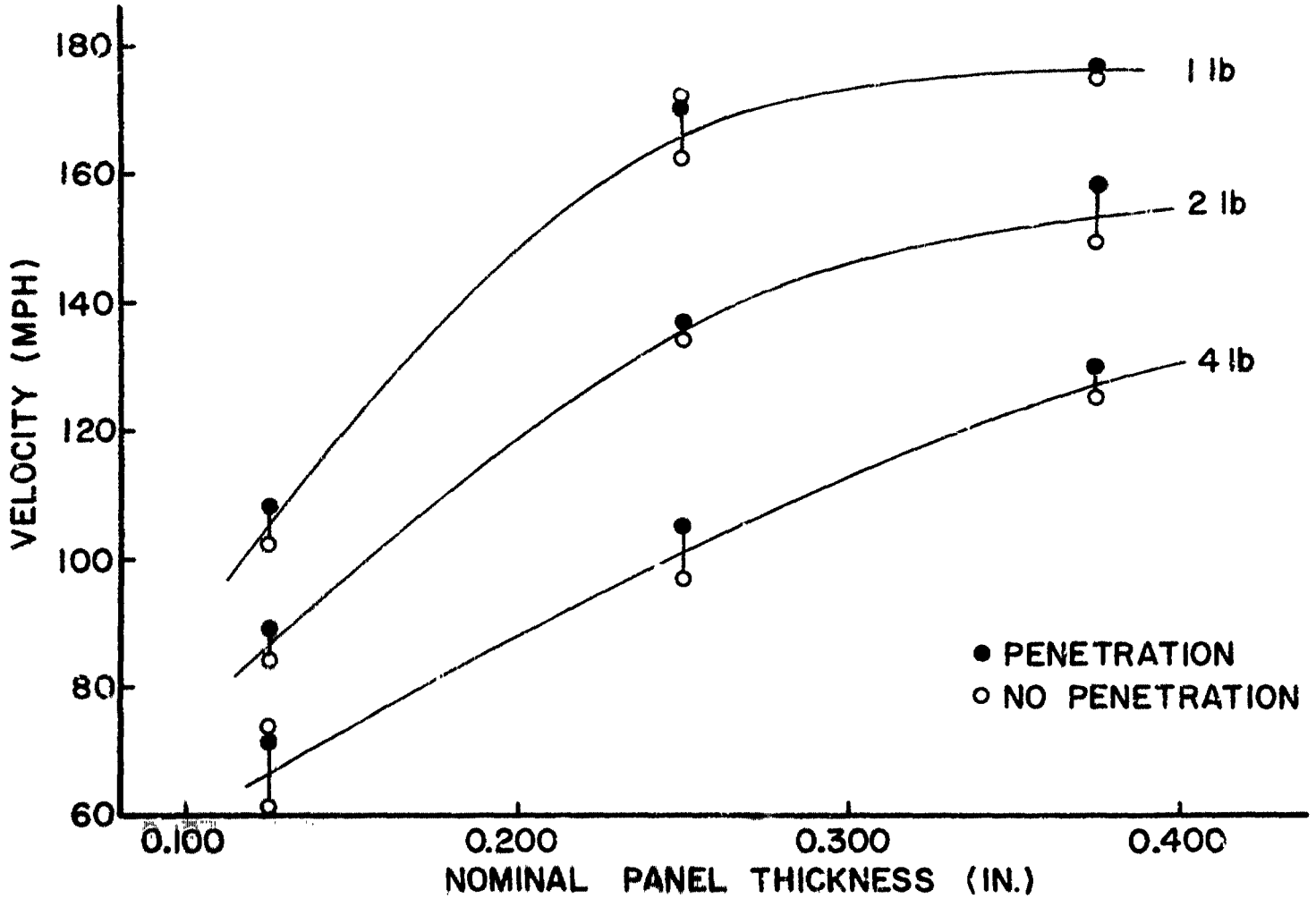


FIG. 11

AS-CAST ACRYLIC

(1, 2 & 4 POUND BIRDS, 45°, BOLTED EDGES)

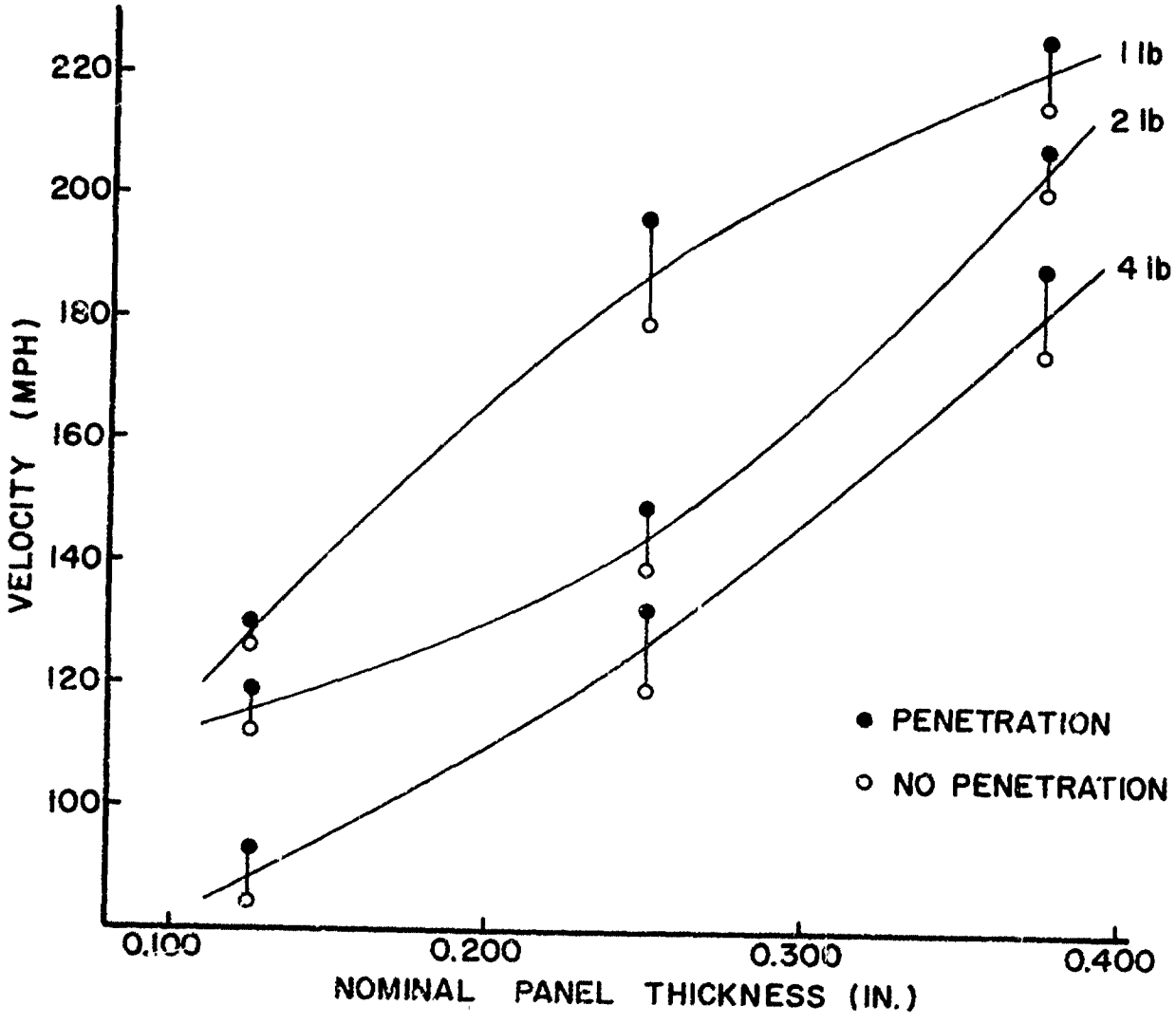


FIG. 12

AS-CAST ACRYLIC
(1, 2 & 4 POUND BIRDS, 45°, CLAMPED EDGES)

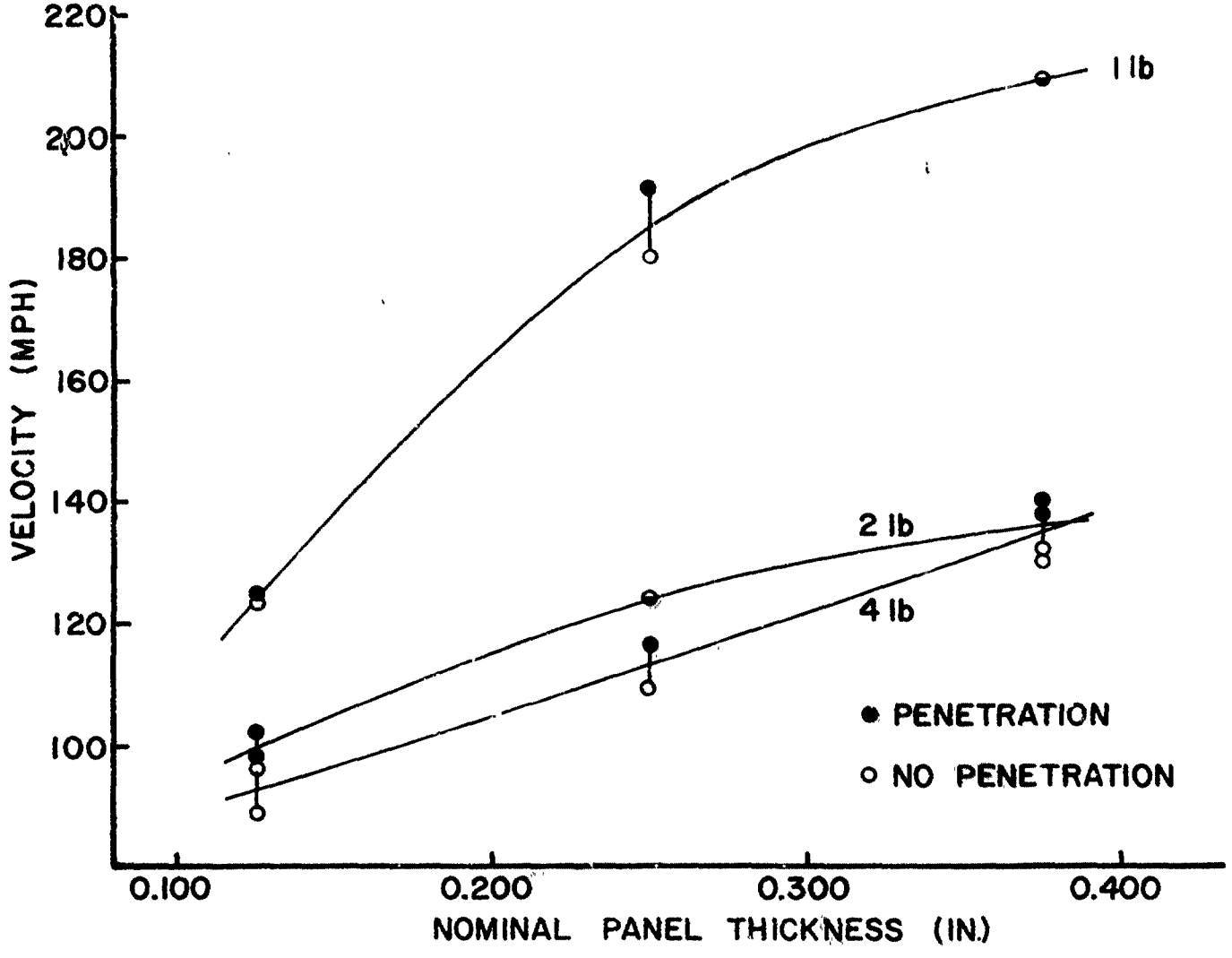


FIG. 13

STRETCHED ACRYLIC
(1, 2 & 4 POUND BIRDS, 45°, BOLTED EDGES)

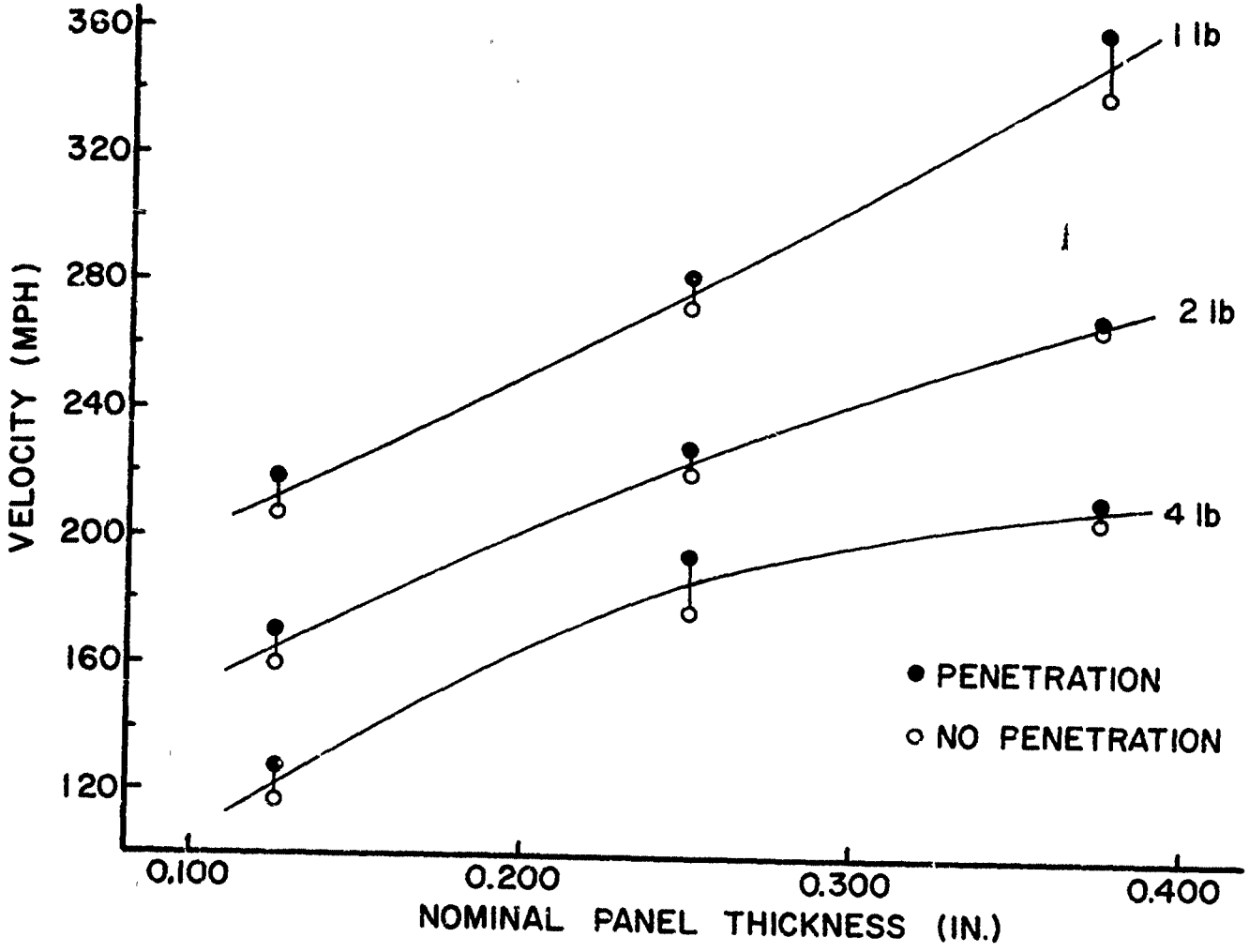


FIG. 14

STRETCHED ACRYLIC

(1, 2 & 4 POUND BIRDS, 45°, CLAMPED EDGES)

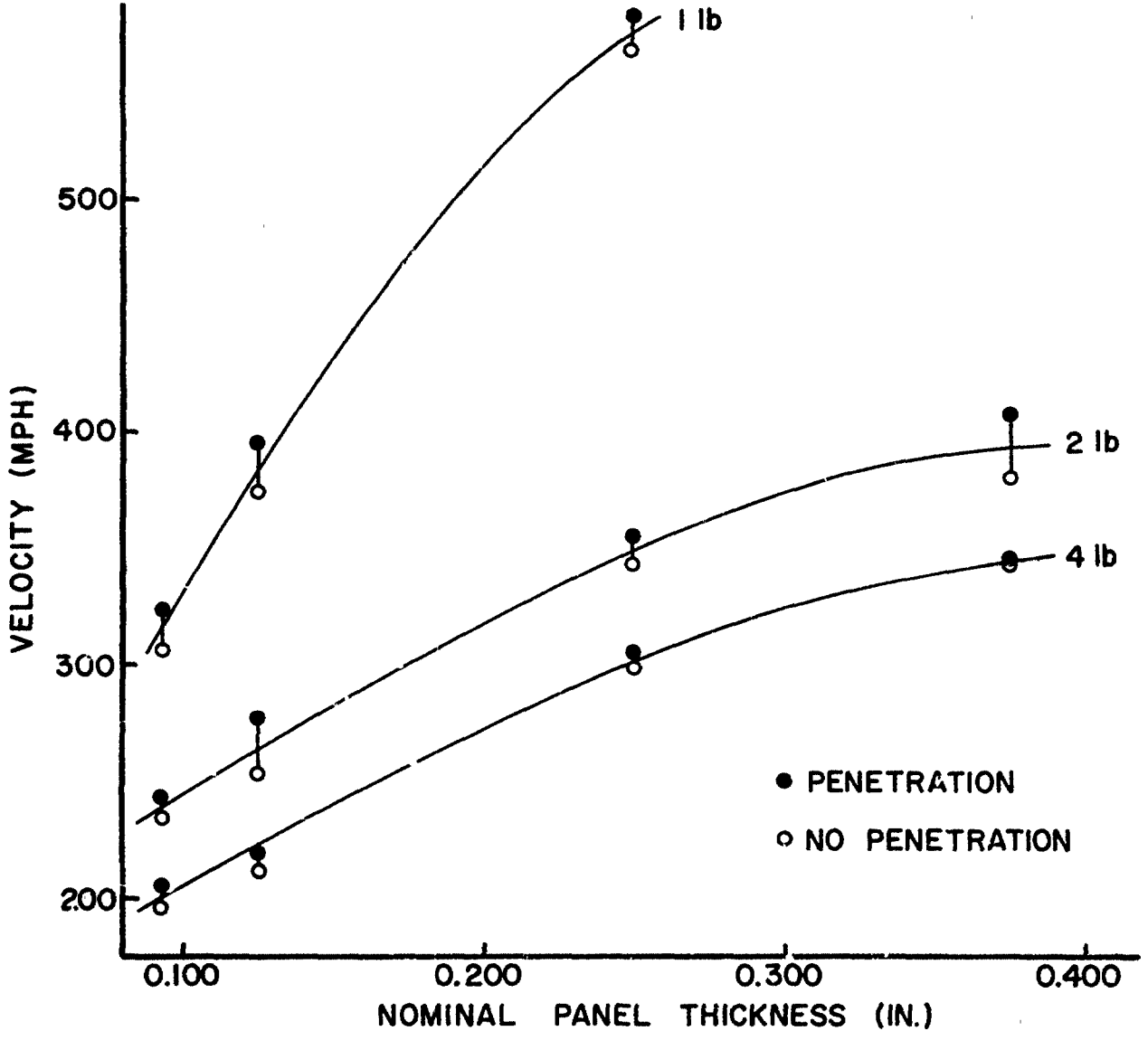


FIG. 15

POLYCARBONATE

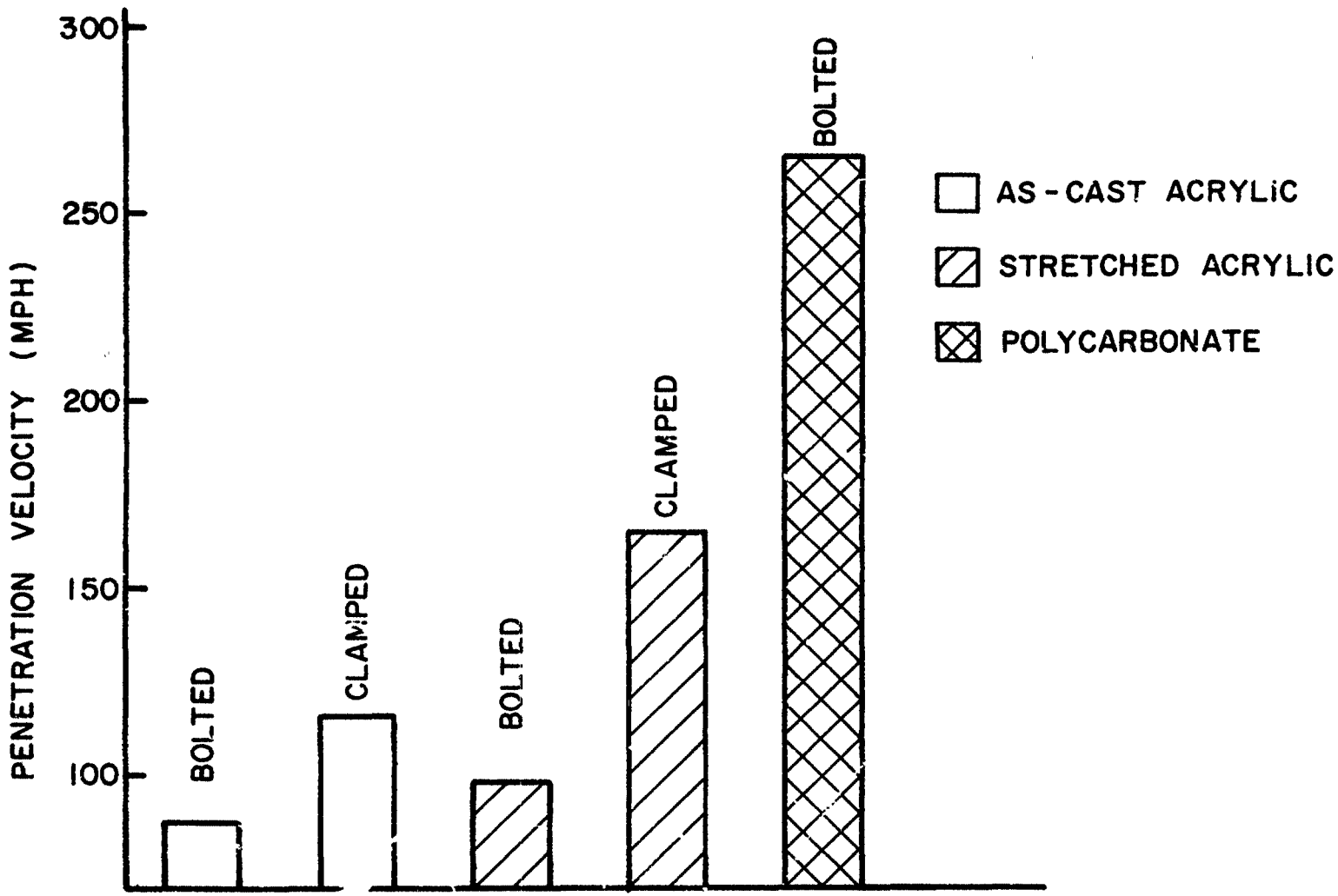


FIG. 16 COMPARISON OF MATERIALS AND EDGE CONDITIONS

(0.125 THICK, 45°, 2 POUND BIRD)

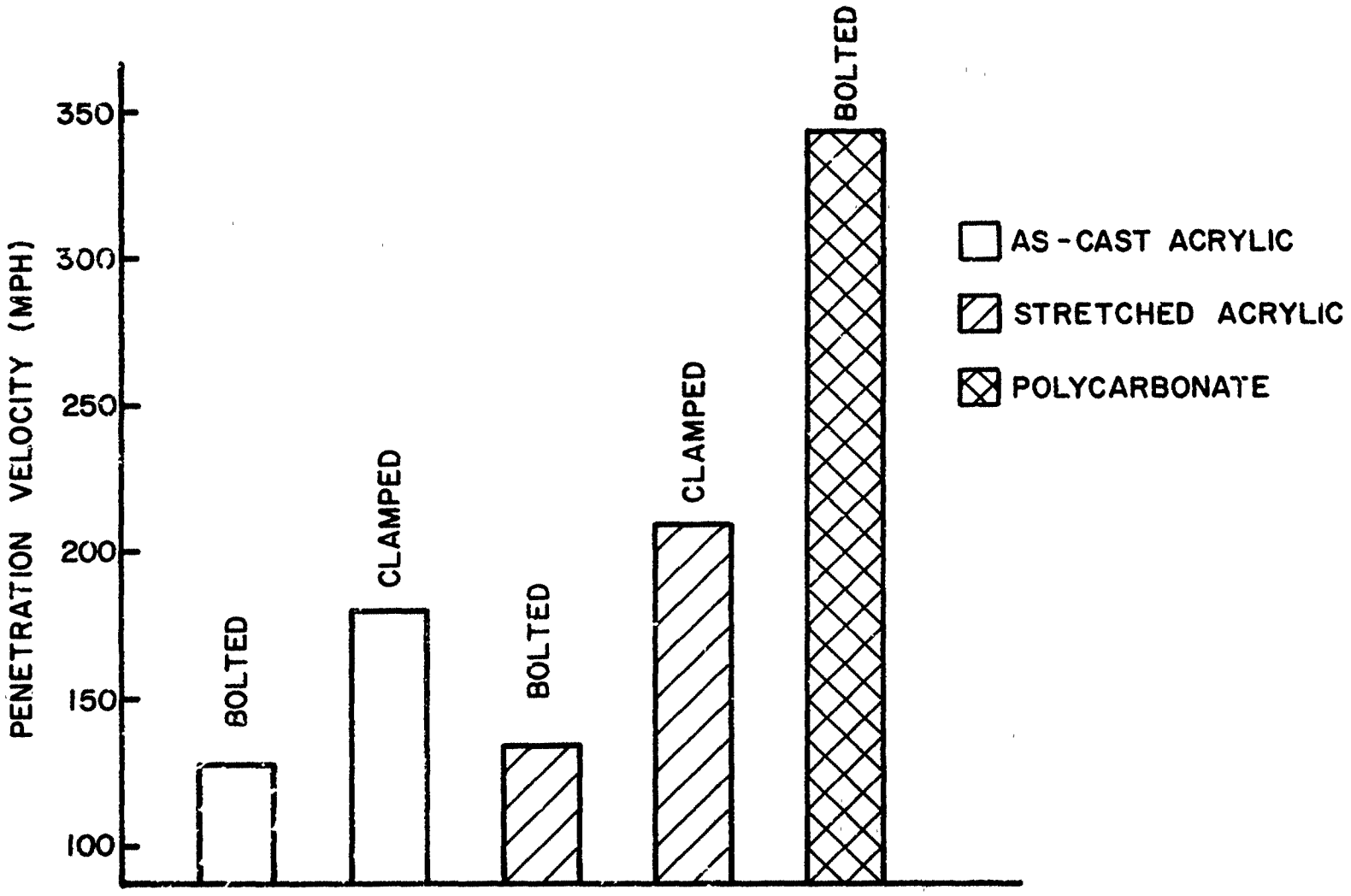
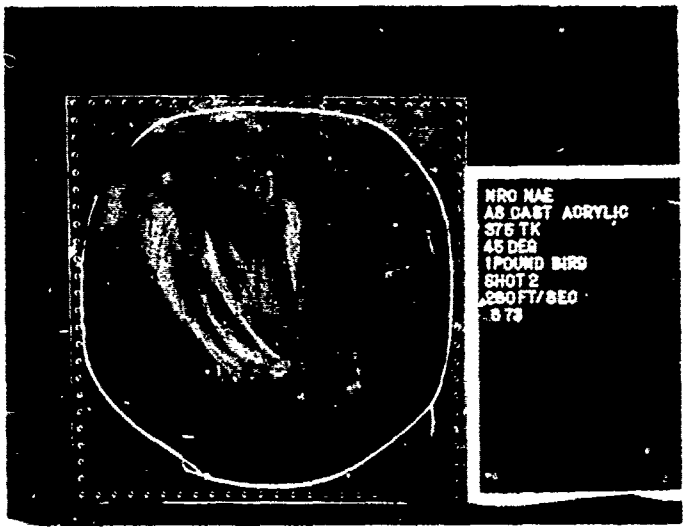


FIG. 17 COMPARISON OF MATERIALS AND EDGE CONDITIONS
(0.375 THICK, 45°, 4 POUND BIRD)

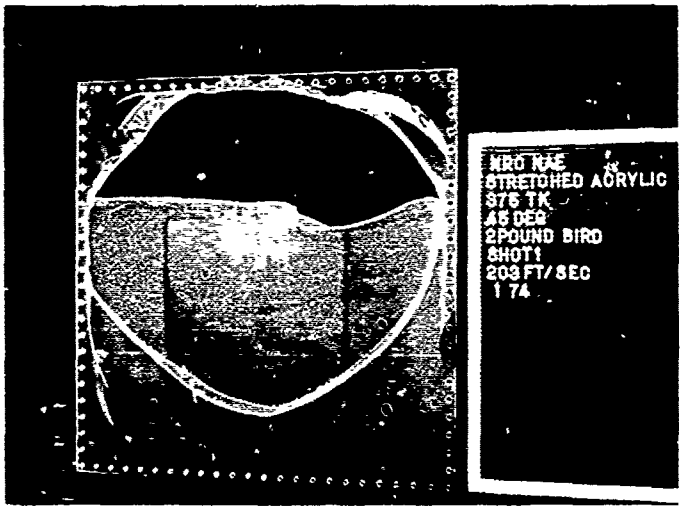


(a) IMPACT VELOCITY NEAR PENETRATION VELOCITY (45°)

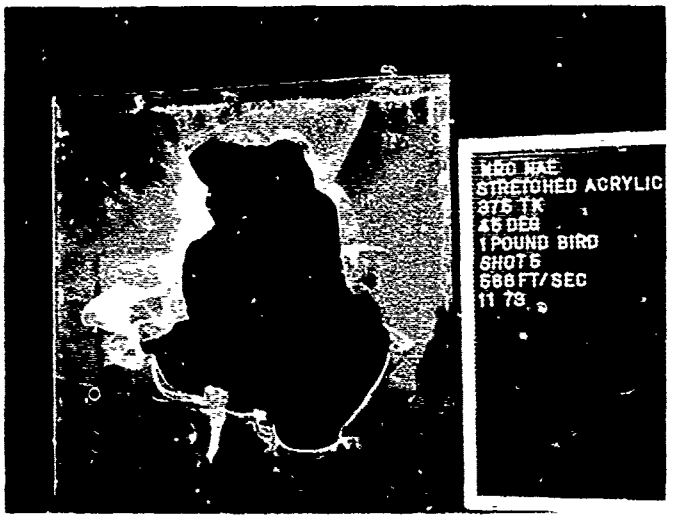


(b) IMPACT VELOCITY CONSIDERABLY HIGHER THAN PENETRATION VELOCITY (45°)

FIG. 18 TYPICAL AS-CAST ACRYLIC PANEL FRACTURE

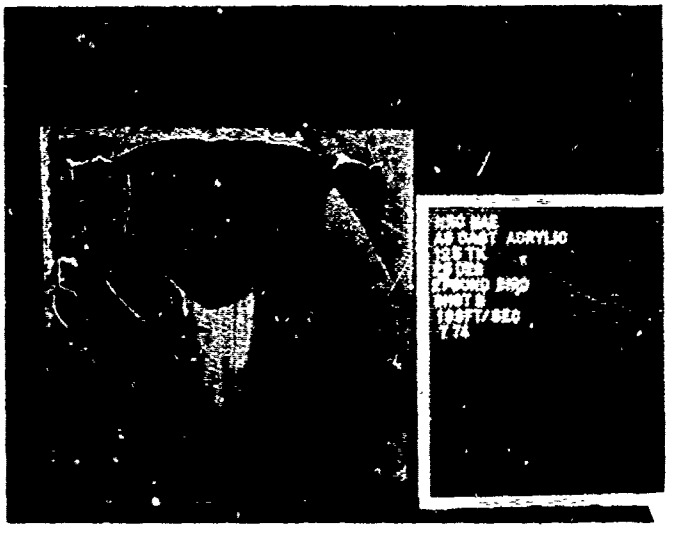


(a) IMPACT VELOCITY NEAR PENETRATION VELOCITY (45°)

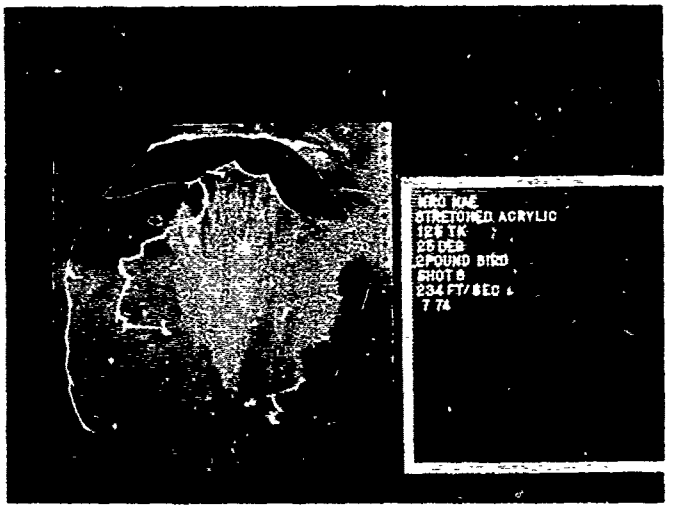


(b) IMPACT VELOCITY CONSIDERABLY HIGHER THAN PENETRATION VELOCITY (45°)

FIG. 19 TYPICAL STRETCHED ACRYLIC PANEL FRACTURE



(a) AS-CAST ACRYLIC



(b) STRETCHED ACRYLIC

FIG. 20 TYPICAL ACRYLIC PANEL FRACTURE, WITH 25° IMPACT ANGLE

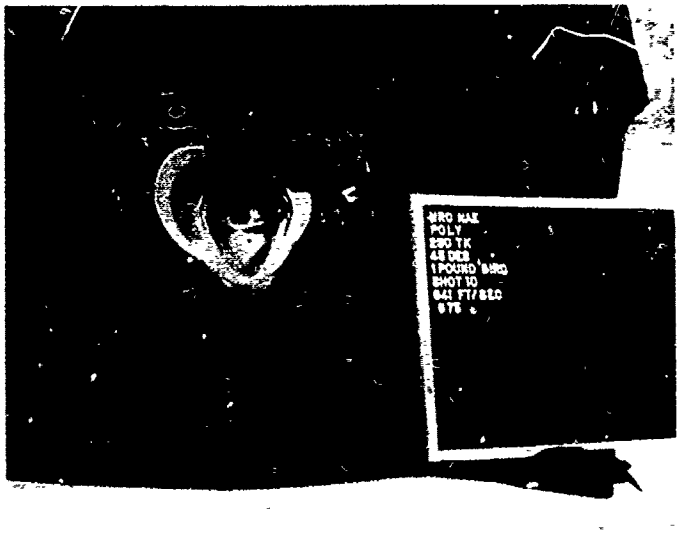


FIG. 21 TYPICAL POLYCARBONATE PANEL FRACTURE

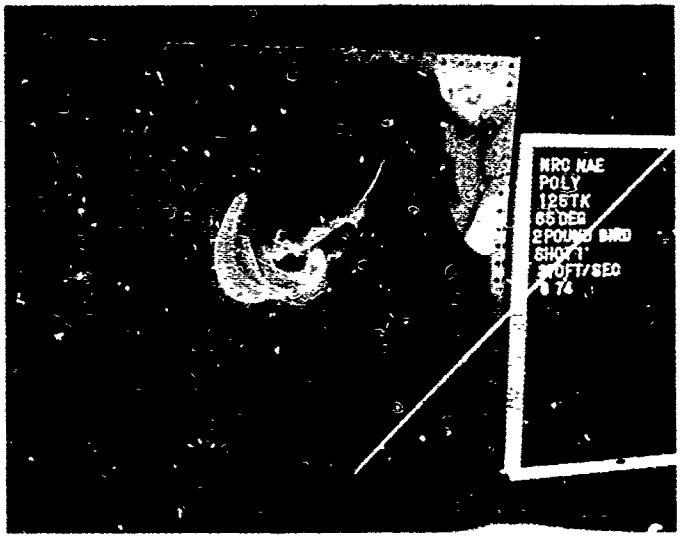


FIG. 22 POLYCARBONATE PANEL FRACTURE WITH 65° IMPACT ANGLE



FIG. 23 POLYCARBONATE PANEL FRACTURE INDUCED BY IMPERFECTION

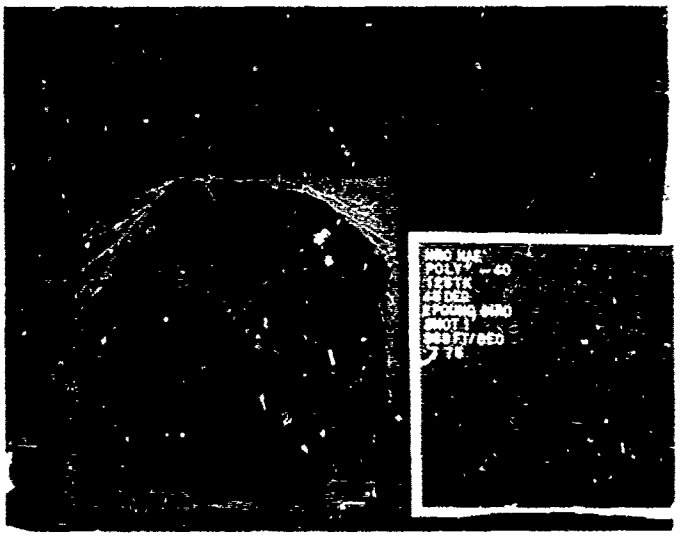


FIG. 24 FRACTURED POLYCARBONATE PANEL AT -40 °F

APPENDIX A

MATERIAL SPECIFICATIONS

Materials

The three types of materials used for windshield glazing that were studied are:

(a) As-cast Acrylic

This material is most frequently used for glazing in small light aircraft. In military aircraft the material is procured to the requirements of MIL-P-8184A Amendment 2, "Plastic sheet, Acrylic, Modified", a comparison of the physical properties of the commercial grade as given in Modern Plastics Encyclopedia 1971-72, to the MIL specification type indicate no basic differences other than a somewhat improved value for heat distortion temperature and superior craze resistance properties that should not significantly affect impact resistance; on this basis the commercial grade was used for the program.

(b) Stretched Acrylic

The material used for the program was procured to the requirements of MIL-P-25690A Amendment 2 "Plastic, sheets, and Parts, Modified Acrylic Base, Monolithic, Crack Propagation Resistant"; the optical requirements were waived.

(c) Polycarbonate

FAA imposes more stringent flammability requirements and higher heat deflection temperatures than the conventional commercial grade of polycarbonate sheet for aircraft applications but the physical electrical and chemical properties are essentially the same.* Commercial grade was procured for the program.

The trade names of the materials procured for the program and the manufacturer quoted mechanical properties are given in Table A-1. The thickness of each panel tested was measured at each corner. The maximum thickness variations encountered are given in Table A-2.

---

*Ballard, J. Polycarbonate Film and sheet, Modern Plastics Encyclopedia p.194, Vol 48/No 10A 1971-72.

Table A-1 MECHANICAL PROPERTIES

Mechanical Properties	ASTM Method	Units	Perspex	Acrylite	Plexiglas	Stretched Acrylic	Lexan
Tensile Strength	D638	P.S.I.	12,000 Av	10,000 Av	10,500 Max	11,000	9,500 Av
Elongation		%		4.2 Av	4.9 Max		110 Av
Modulus		P.S.I.	475,000 Av	400,000 Av	450,000	450,000	320,000 Av
Flexural Strength	D790	P.S.I.	20,000 Av	16,500 Av	16,000 Max	16,000	13,500 Av
Modulus		P.S.I.	420,000 Av	475,000 Av	450,000		340,000 Av
Compressive Strength	D695	P.S.I.		18,000 Av	18,000 Max	16,000	12,500 Av
Modulus		P.S.I.	440,000 Av	430,000 Av	450,000		345,000 Av
Shear Strength	D732	P.S.I.	11,000 Av	9,000 Av	9,000	11,000	
Impact Strength Izod Milled Notch	D256	Ft. lbs. / in. Notch	0.32 Av	0.4 Av	0.4	0.6	16.0
Rockwell Hardness	P+H P-20		M-90 Av	M-94 Av	M-93	M-97	M-70

Table A-2 MATERIAL THICKNESS VARIATIONS ENCOUNTERED

Material	Nominal Thickness (in.)	Thickness Extremes (in.)		Max. Variation in Panel (in.)
		Min.	Max.	
As-Cast Acrylic	0.125	0.087	0.145	0.031
As-Cast Acrylic	0.250	0.229	0.261	0.031
As-Cast Acrylic	0.375	0.351	0.394	0.037
Stretched Acrylic	0.125	0.110	0.145	0.013
Stretched Acrylic	0.250	0.243	0.283	0.023
Stretched Acrylic	0.375	0.351	0.418	0.038
Polycarbonate	0.093	0.089	0.101	0.011
Polycarbonate	0.125	0.118	0.132	0.009
Polycarbonate	0.250	0.242	0.264	0.008
Polycarbonate	0.375	0.367	0.379	0.009

BIRD RESISTANT TRANSPARENCIES IN HIGH PERFORMANCE AIRCRAFT - AN UPDATE

H. E. Littell, Jr.
PPG Industries, Inc.
Creighton, Pennsylvania

PRECEDING PAGE BLANK-NOT FILMED

BIRD RESISTANT TRANSPARENCIES IN HIGH PERFORMANCE AIRCRAFT - AN UPDATE

H. E. Littell, Jr.

PPG Industries, Inc.

Abstract

The Air Force Flight Dynamics Laboratory has sponsored a detailed program to develop and test aircraft transparencies to protect against impacts by 4-lb birds at speeds above 500 knots. This paper discusses the program and presents general conclusions.

The Improved Windshield Protection Development Program consisted of three tasks to evaluate basic materials and designs, test optimized configurations and manufacture prototype transparencies. Altnough the important goals related to bird impact, a significant part of each task was directed toward maintaining acceptable thermal, structural and optical performance to insure satisfactory service performance.

The purpose of the first task was to obtain supporting data for recommending full-size test panel configurations. It included a laboratory materials capability study which placed emphasis on new sheet interlayers such as Monsanto Ethylene Terpolymer and PPG 112. Promising materials were included in flat polycarbonate-based bird impact test panels for preliminary center impact screening of variables such as facing ply materials, effect of coatings and polycarbonate ply thickness. Inputs from this activity and edge reinforcement developments were incorporated in other sample bird impacts and bench-scale thermal-pressure tests. As a result of the Task I work, designs with two plies of thin polycarbonate and either plastic or glass facing plies were chosen for testing in full-size transparency configurations.

During the second task, bird impacts on the full-size windshields added the effects of geometry, impact location and mounting structure. A penetration resistance "map" was generated to locate the worst impact point. Shots at this location against windshields in both test frames and actual airframes emphasized the interrelationship of windshield and support structure. Airframe mounting modifications were proposed, carried out and tested in conjunction with different transparency cross-sections. Parallel thermal-pressure tests were used to recommend facing ply materials for the combined windshield-structure system that was selected for prototype production.

Twenty-four laminated plastic prototype windshields and canopies were made during Task III. These were delivered to the Air Force for optical, impact and structural qualification tests. Since Task III, an additional group of forty improved bird resistant transparencies has been placed in service around the world. These panels are now undergoing flight service evaluation.

INTRODUCTION

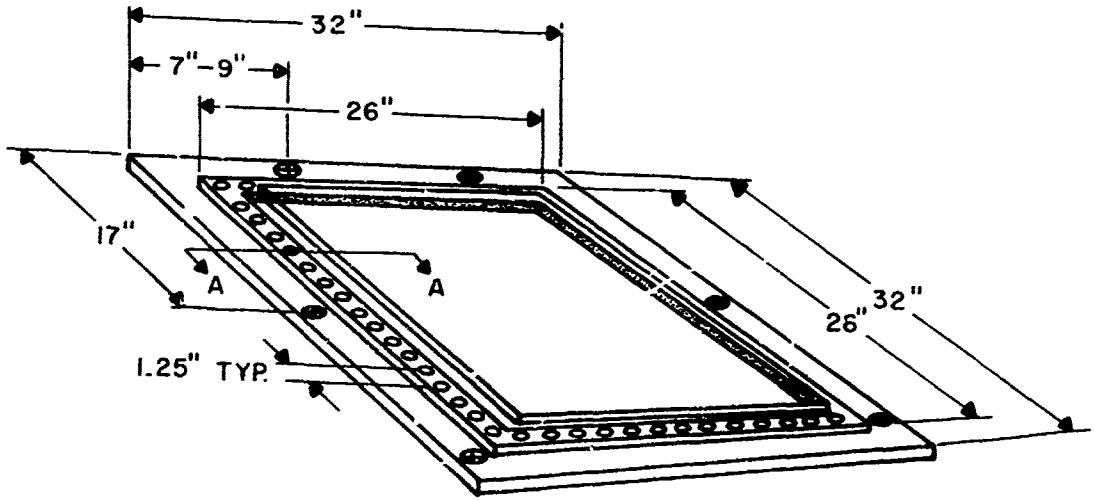
A paper titled "Composite Bird Resistant Aircraft Transparencies" (Reference 1) was presented at the 1971 Conference on Transparent Aircraft Enclosures. It described some initial efforts to develop efficient windshields capable of protecting against impacts by 4 lb birds at speeds above 500 kt. Since that time, the Air Force Flight Dynamics Laboratory has sponsored a detailed program to evaluate materials and designs, test optimized configurations and manufacture prototype transparencies. Although important goals related to bird impact existed, and will be discussed in detail here, a significant part of the Improved Windshield Protection Development Program (Reference 2) was directed toward maintaining satisfactory thermal, structural and optical performance of proposed new designs.

TASK I

The purpose of the first phase of the program was to obtain data for use in recommending full-size test panel configurations. This was achieved primarily by testing in areas critical to performance; namely, material properties, impact resistance, edgemember design and thermal effects. Since other results, including those reported in the 1973 paper, had indicated that the most promising designs would be laminated polycarbonate-based composites, much of the laboratory material capability study centered on new sheet interlayers such as Monsanto ethylene terpolymer and PPG 112. Some of the results for 112, using PVB as a standard, are reported elsewhere (Reference 3).

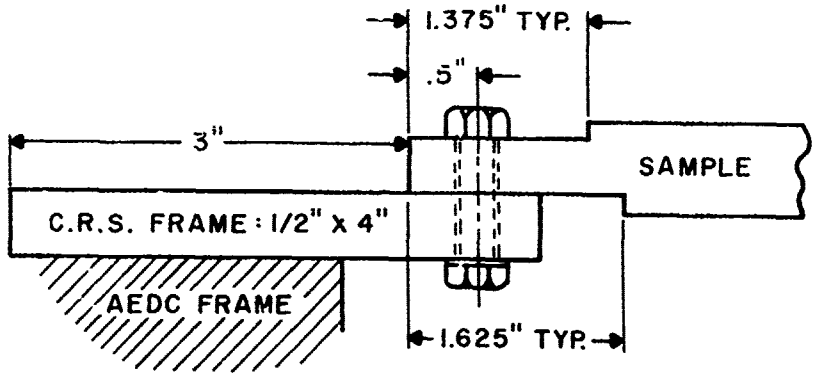
Promising candidate materials were included in a series of preliminary bird impact tests. These were conducted at Arnold Engineering Development Center (AEDC) (Reference 4), and were center, room temperature impacts using 4 lb birds. A schematic of a typical flat, 26" x 26" panel and edge mounting section appears in Figure 1. Figure 2 is an overall view of the target with panels mounted at 22° from the line of flight of the bird.

Preliminary windshield constructions ranged from those based on relatively thick monolithic polycarbonate (PC) to laminates of various PC ply thicknesses. Surface protection was provided via a "hard" coating, or protective plies of glass, as-cast acrylic or stretched acrylic. Specific cross-sections were picked to show effects of thickness, composition and arrangement of structural or facing plies in panels of equivalent overall thickness. As listed in Table I, four basic thickness groups were selected. The first consisted of monolithic .750" PC. The second series, seen in Figure 3, compared monolithic .625" PC, laminated .250" PC and laminated .125" PC components. The third group, shown also in Figure 4, compared thicker designs with monolithic .688" and .750" PC to laminated combinations of .125" and .188" PC. Finally, monolithic and laminated PC components were compared, but, as Figure 5 shows, a floating .125" PC ply was placed between the outboard facing ply and the first extended PC mounting ply.



NOTE:

⊕ = FINAL CLAMP LOCATIONS



SECTION A-A

FIGURE 1. TASK I BIRD IMPACT SAMPLE AND MOUNTING FRAME

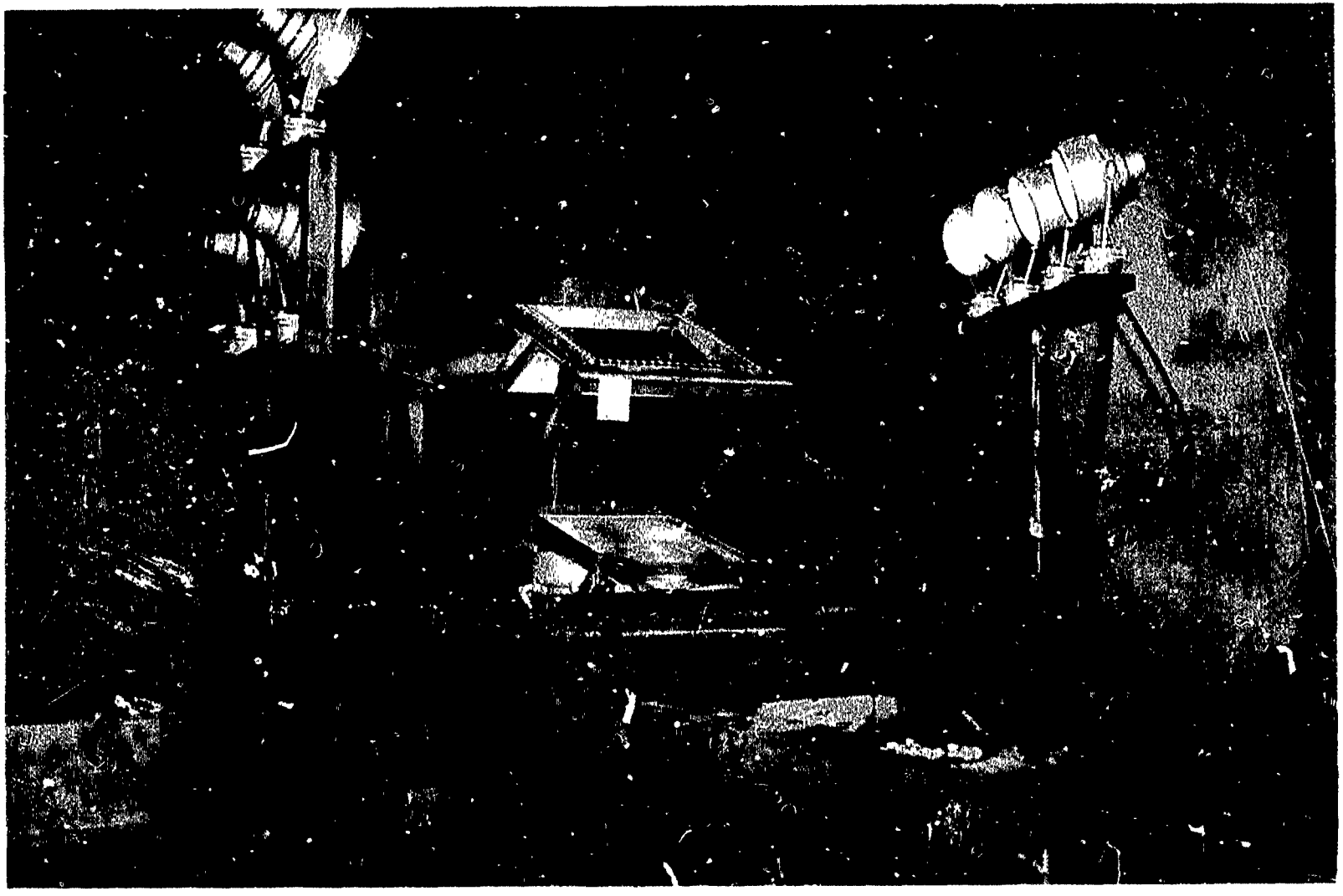
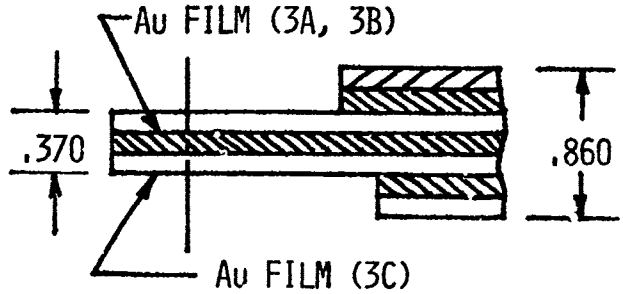


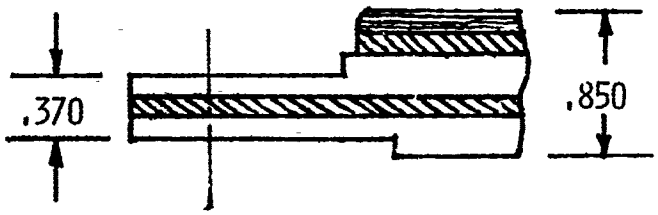
Figure 2. Preliminary Task 1 Flat Panel Bird Impact Target Area

TABLE I - PRELIMINARY BIRD IMPACT TEST SPECIMENS

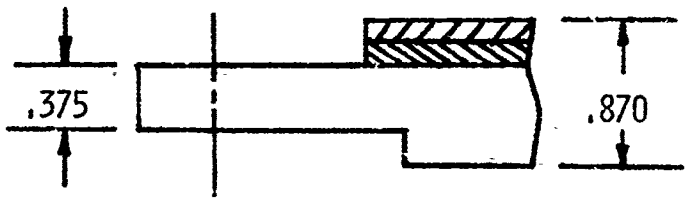
GROUP	SAMPLE	CONSTRUCTION (IMPACT-FACING SURFACE LISTED FIRST)
1	1A	.750" PC
	2A	.750" PC (coated both sides with OI 650)
		* * * * * * * * * * *
2	3A,3B	.125" Acrylic - .120" 112 - .125" PC (15 ohms/sq gold film) - .120" 112 - .125" PC - .120" 112 - .125" PC
	3C	.125" Acrylic - .120" 112 - .125" PC - .120" 112 - .125" PC (15 ohms/sq gold film) - .120" 112 - .125" PC
	4A,4B	Same as Code 3, without 15 ohms/sq gold coating
	8A	.110" Glass - .120" 112 - .250" PC - .120" 112 - .250" PC
	5A,5B	.125" Acrylic - .120" 112 - .625" PC
		* * * * * * * * * * *
3	6A	.125" Acrylic - .090" 112 - .750" PC
	7A	.125" Acrylic - .120" 112 - .188" PC - .090" 112 - .188" PC - .120" 112 - .125" PC
	13A	.060" Acrylic/.093" PC - .120" 112 - .125" PC - .090" 112 - .188" PC - .120" 112 - .125" PC
	14A	.060" Acrylic/.093" PC - .120" 112 - .688" PC
		* * * * * * * * * * *
4	9A	.110" Glass - .120" 112 - .125" PC - .120" 112 - .125" PC - .120" 112 - .125" PC - .120" 112 - .060" Acrylic
	10A	Same as Code 9 but with 15 ohms/sq gold film on glass
	11A	.110" Glass - .120" 112 - .625" PC - .120" 112 - .060" Acrylic
	12A	.110" Glass - .120" 112 - .125" PC - .120" 112 - .125" PC .120" 112 - .125" PC - .120" 112 - .125" Stretched Acrylic



3A	FAILED	447 KT	PUNCHED THRU TOP (FRAME)
3B	OK	525	NO SHEARING OR PC DAMAGE
3C	FAILED	538	SHEARED TOP EDGE
4A	OK	510 KT	NO PC DAMAGE
4B	FAILED	504	1ST SHOT - CUT BY FRAME

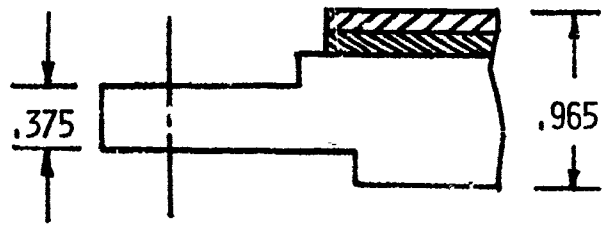


8A	FAILED	497 KT	SHEARED AT TOP, CRACKED EDGES

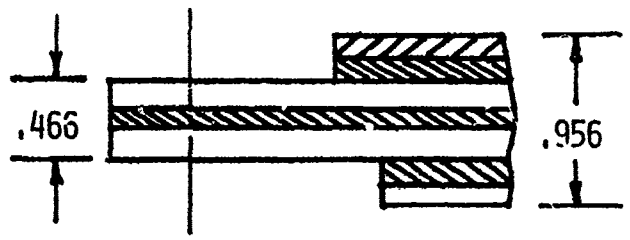


5A	FAILED	483 KT	BLEW OUT CENTER
5B	FAILED	447	" " "

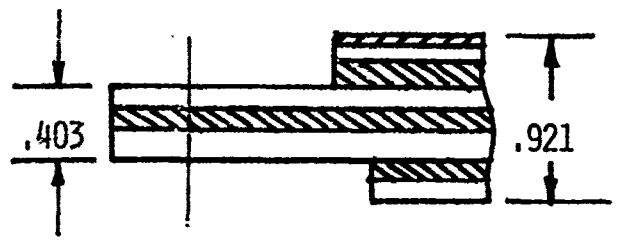
FIGURE 3 . SUMMARY OF TASK I PRELIMINARY BIRD IMPACTS (GROUP 2)



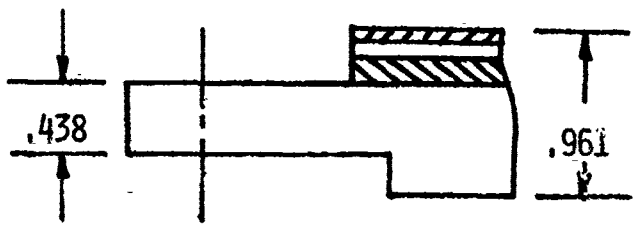
6A FAILED 511 KT BLEW OUT CENTER



7A OK 507 KT NO PC DAMAGE

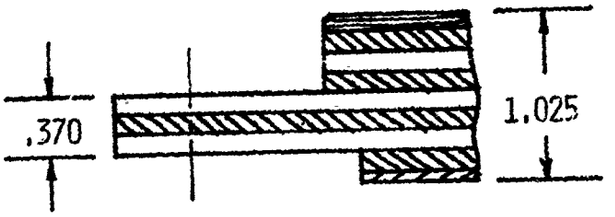


13A OK 499 KT NO SERIOUS DAMAGE

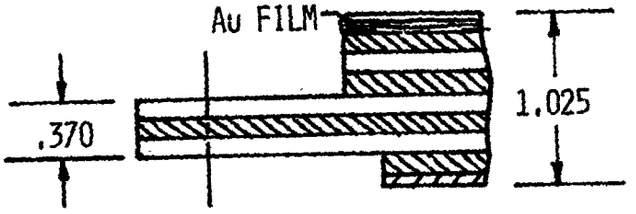


14A FAILED 478 KT BLEW OUT CENTER

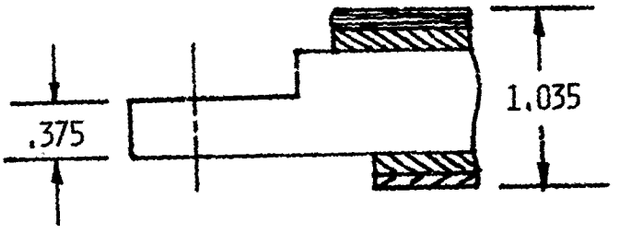
FIGURE 4 . SUMMARY OF TASK I PRELIMINARY BIRD IMPACTS (GROUP 3)



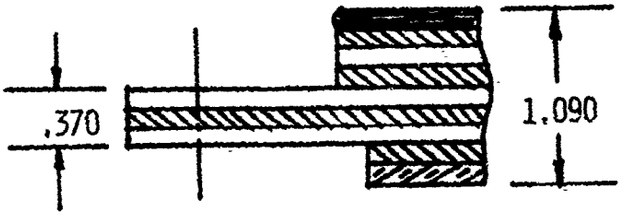
9A OK 517 KT PC CRACK AT TOP (CRAZING) PLEX OK



10A OK 491 KT PC CRACK AT TOP, GOLD FILM OK, PLEX OK



11A FAILED 509 KT BLEW OUT CENTER



12A OK 512 KT PC CRACK AT TOP, DANGEROUS S/A SPALL

FIGURE 5. SUMMARY OF TASK I PRELIMINARY BIRD IMPACTS (GROUP 4)

Several basic conclusions were drawn from the results obtained for the four groups which influenced the selection of optimized Task I test panel constructions and are of general interest in designing for high energy bird impacts.

1. Even with center impacts, the panel support system can influence results. In initial shots, clamp restraint and sharp frame corners caused unexpected failures along the aft edge. In subsequent tests, support structure edges were rounded to minimize shearing.

2. In general, the liklihood of brittle failure was proportional to PC structural ply thickness. The Group 1 monolithic panels were destroyed by impacts even 44 kt below the 500 kt requirement. Likewise in the other groups, the panels with relatively thick monolithic PC plies exhibited catastrophic failures while equivalent panels with thin plies prevented penetration. Group 2 provided perhaps the best comparison of ply thickness effects. One sample with .625" monolithic PC was blown apart at 447 kt while the panel with two .250" PC plies was sheared or cracked around the periphery at 497 kt. The design with two .125" PC plies, however, sustained hits up to 525 kt and was not penetrated until 538 kt.

3. The other thickness effect was demonstrated by Group 4 in Figure 5. The stiff outboard section of glass and an extra PC ply did not improve the penetration resistance over thinner designs. In fact, PC cracking indicated that the opposite was true.

4. As far as bird impact resistance was concerned, there was little difference between glass, acrylic or fused acrylic/PC outboard. The final choice of a facing ply was then possible on the basis of other criteria, such as abrasion and thermal resistance, expansion mismatch, residual visibility, etc.

5. Cast acrylic can be used as an inboard abrasion ply with no serious spalling or degradation of penetration resistance assuming a suitable interlayer bond is provided. Stretched acrylic, on the other hand, was unacceptable. Large, sharp spall pieces were ejected at speeds up to 269 ft/sec during deflection of samples which used stretched acrylic as an inboard floating ply.

6. A two PC ply edge section with thicknesses of .125" and .188" provided the best penetration resistance for the center impacts at the required 500 kt.

Edge attachment development in the first phase also included a material evaluation followed by a design optimization effort. A goal of 870 lb/lineal inch ultimate tensile at 260°F was established during bench-scale thermal/pressure tests as a rigorous interpretation of requirements for the demonstration windshield which is loaded in hoop tension. The material screening phase indicated that the required structural performance can be gained from the PC structural plies using impregnated nylon (epoxy-Nomex) for bolt hole reinforcement bonded to the PC with RTV 630 silicone. Also, an outboard retainer for the windshield mounting was recommended to enhance clamping to the frame structure without the use of tapered bushings.

Figure 6 shows two reinforcement geometries tested in the preliminary edge attachment development and the tensile load values achieved. The lower four cross-sections indicate the constructions and edgemembers used in the final tensile and bird impact test series. The final tensile results showed that ultimate tensile values were higher with increasing reinforcement and that straps were preferable to inserts. Yield values, however, were generally irrespective of reinforcement. Addition of facing plies did not add significantly to the tensile strength of the laminates.

The second series of flat bird impact panels incorporated the candidate reinforcement system on the .125" PC - .188" PC load bearing plies selected from initial bird shots. Schematic edge sections in Figure 6 show that glass-glass, glass-acrylic, and acrylic-PC facing ply combinations were evaluated. Again, the eleven center shots were room temperature impacts ranging from 486 kt to 533 kt. Additional general conclusions were drawn from this group which are applicable to high performance bird resistant windshield design.

1. Although there was no major difference in bird impact resistance between edge attachment types, the reinforcement did transfer sufficient load to cause mounting bolt failure and pullout from the rigid frame.

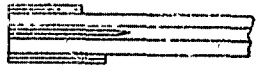
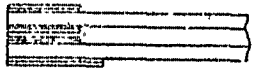
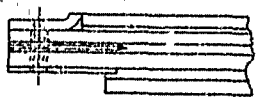
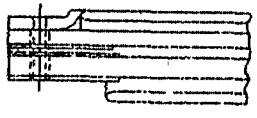
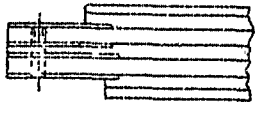
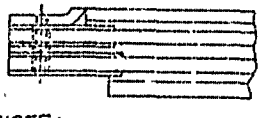
2. Aft edge retainer geometry should include a taper on the leading edge. In tests, this prevented concentration of hydrodynamic pressure under the peeling retainer and shearing of the extended plies.

3. Failure of chemically strengthened glass plies during impact deflection resulted in complete loss of visibility. In addition, spall particles were ejected at average speeds from 296 to 315 ft/sec and embedded in styrcfoam placed up to 40" below the target point.

4. Although a floating inner ply of .125" PC had performed acceptably, the use of a .188" floating ply inboard appeared to make the center section too stiff, which resulted in edge shearing. Panels of this type were penetrated at speeds as low as 486 kt, while those with either .060" acrylic or .085" chemically strengthened glass inboard were not penetrated at up to 510 kt.

In designing for high speed bird impact resistance, then, the most efficient design would be laminates of PC, 3/16" thick or less. The PC should be bonded with an interlayer which maintains its elastomeric properties over a wide temperature range. The reinforced edge of the PC core section should be bolted to the airframe to transfer the impact loads. The impact-absorbing section should be physically isolated by facing plies on the inboard and outboard surfaces. Facing plies such as glass, fused acrylic-PC or acrylic should be chosen according to the specific requirements of the aircraft. Important characteristics of the materials are shown in Table II.

In selecting facing plies for full-size windshield testing, plastic facing plies were chosen to minimize weight and spall and to maximize residual visibility. Thermal/pressure tests indicated that a fused acrylic-PC ply would provide necessary insulation for the outermost interlayer. Thin (.060") cast acrylic was chosen for the inboard ply.

SIPD IMPACT CONFIGURATION PANEL REF.		TEMPERATURE 200°F YIELD LB./IN.	200°F ULT. LB./IN.	260°F YIELD LB./IN.	260°F ULT. LB./IN	COMPONENTS PLY ARRANGEMENT AND REINFORCEMENT
		1205 (1810 (-65°F)	1745 2080)	885	1175	
		1350	1850	1060	1280	
9030-17		1190	1400	890	1000	ACRYLIC-[PC CORE]-PC AND RETAINER-INSERT-STRAP
9030-21		1250	1500	1080	1280	GLASS-[PC CORE]-GLASS AND RETAINER-STRAPS
9030-19		1250	1670	1060	1280	GLASS-[PC CORE]-ACRYLIC AND STRAPS
9030-18		1230	1740	1070	1310	ACRYLIC-[PC CORE]- PC AND RETAINER-STRAPS

NOTE: REINFORCEMENT: ALL STRAPS .020" EPOXY NOMEX BONDED WITH RTV 630 SILICONE ADHESIVE.
EDGE LOAD GOAL =870 LBS. / LINEAL INCH.

FIGURE 6. EDGE REINFORCEMENTS

TABLE II - COMPARISON OF FACING PLY CHARACTERISTICS

Abrasion Resistance:	Glass - Excellent; Acrylic - Poor
Chemical Resistance:	" " " "
Thermal Expansion:	Glass - 1/10 PC; Acrylic $\cong$ PC
Thermal Conductivity:	Glass $\cong$ 5X Acrylic
Weight:	Specific Gravity Glass $\cong$ 2X Acrylic
Spall:	Glass - Considerable; Acrylic - Negligible
Residual Visibility:	Glass - Negligible; Acrylic - Acceptable

TASK II

The second phase of the Improved Windshield Protection Development Program concerned testing of windshields for a specific application. However, conclusions of general interest were drawn and will be discussed briefly.

The primary design selected for bird impact testing of windshields is shown in Figure 7. As before, all tests were conducted at room temperature using 4 lb birds fired from the AEDC uncher. Initially, panels were mounted in a rigid test frame shown in Figure 8. The goal of this series was to establish a map of penetration resistance. During the tests summarized, additional observations were made.

1. During impacts in the 500 kt range, the inboard acrylic cracked but was held by the interlayer. Near the goal of Mach 1.2, impacts led to large localized deflections which caused minor spalling of several small pieces of the acrylic from the bulged area.

   Even with the extreme local bulging from high speed impacts, there was no crack propagation from the inboard acrylic through the innermost 112 interlayer.

2. As shown in Figure 9, the primary windshield construction provided different protection levels ranging from the goal of Mach 1.2 for impacts near the center to below the 500 kt requirement in the aft beam corner, which was established as the worst location.

3. Shearing of the PC structural plies was related to the proximity of impact location to a restraining edge or edges.

4. High speed motion pictures showed that there was negligible deflection of the frame in the aft arch-beam corner.

Since frame edge effects were not representative of dynamics of the actual installation, eight aft arch shots were conducted on windshield and arch reinforcement combinations in an airframe module. Windshield constructions were proposed to minimize the shearing of the inboard PC ply which caused tensile failure of the outer PC ply. Arch reinforcement iterations were accomplished by McDonnell Douglas Corporation to match the rotational and flexural stiffness of the transparency.

The program of aft beam corner impacts on the interrelated mounting structure-windshield led to the following, more specific conclusions.

1. An outer fused ply of .060" as-cast acrylic and .188" PC, dictated by thermal requirements, would not adversely affect bird resistance.

2. Even modified designs with two extended PC plies were not capable of sustaining aft beam corner impacts without penetration. All demonstrated a mode of failure with shearing of the innermost extended ply which caused tensile failure of the other ply.

PRIMARY DESIGN

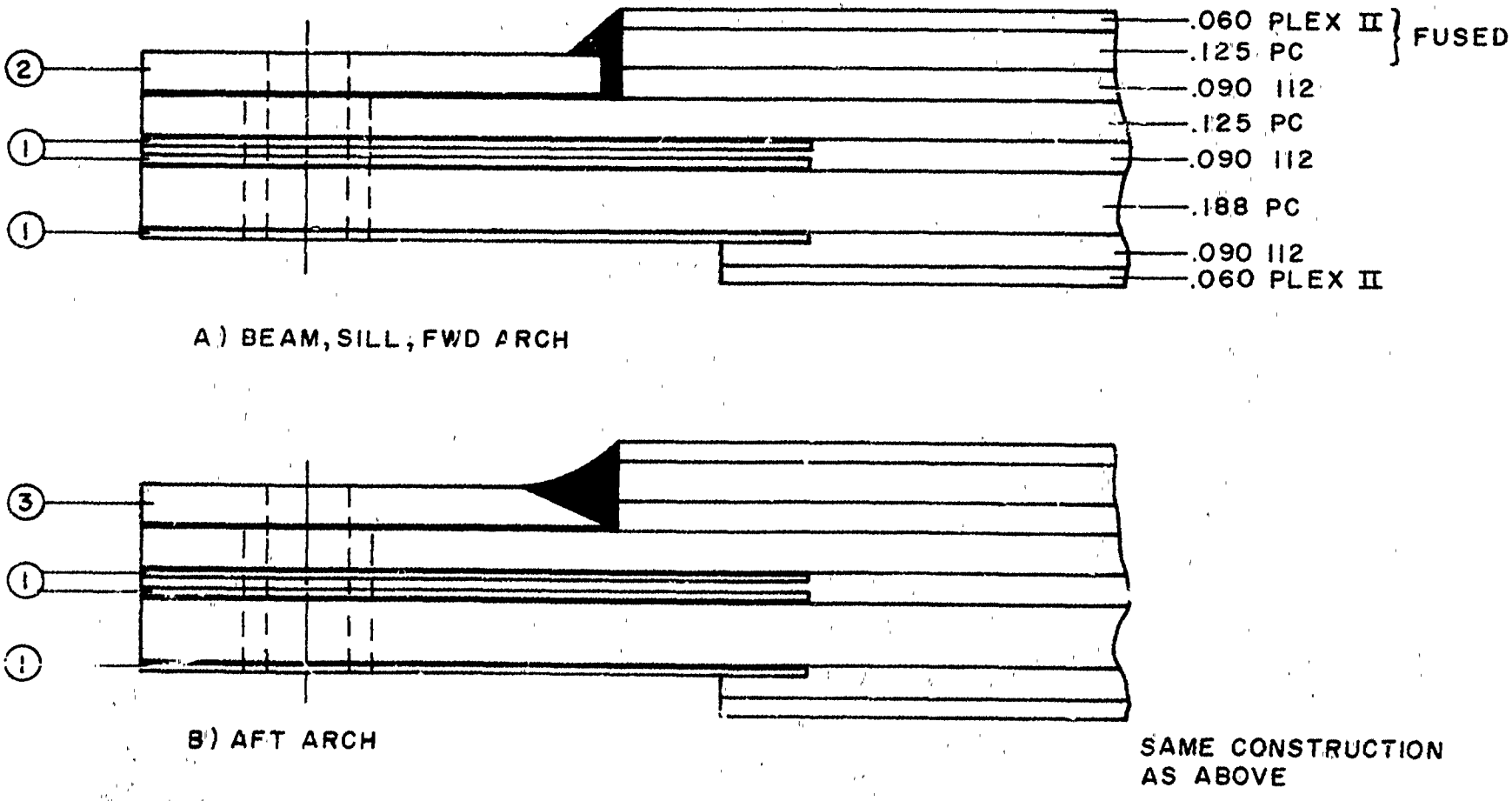


FIGURE 7. PRELIMINARY TASK II WINDSHIELD

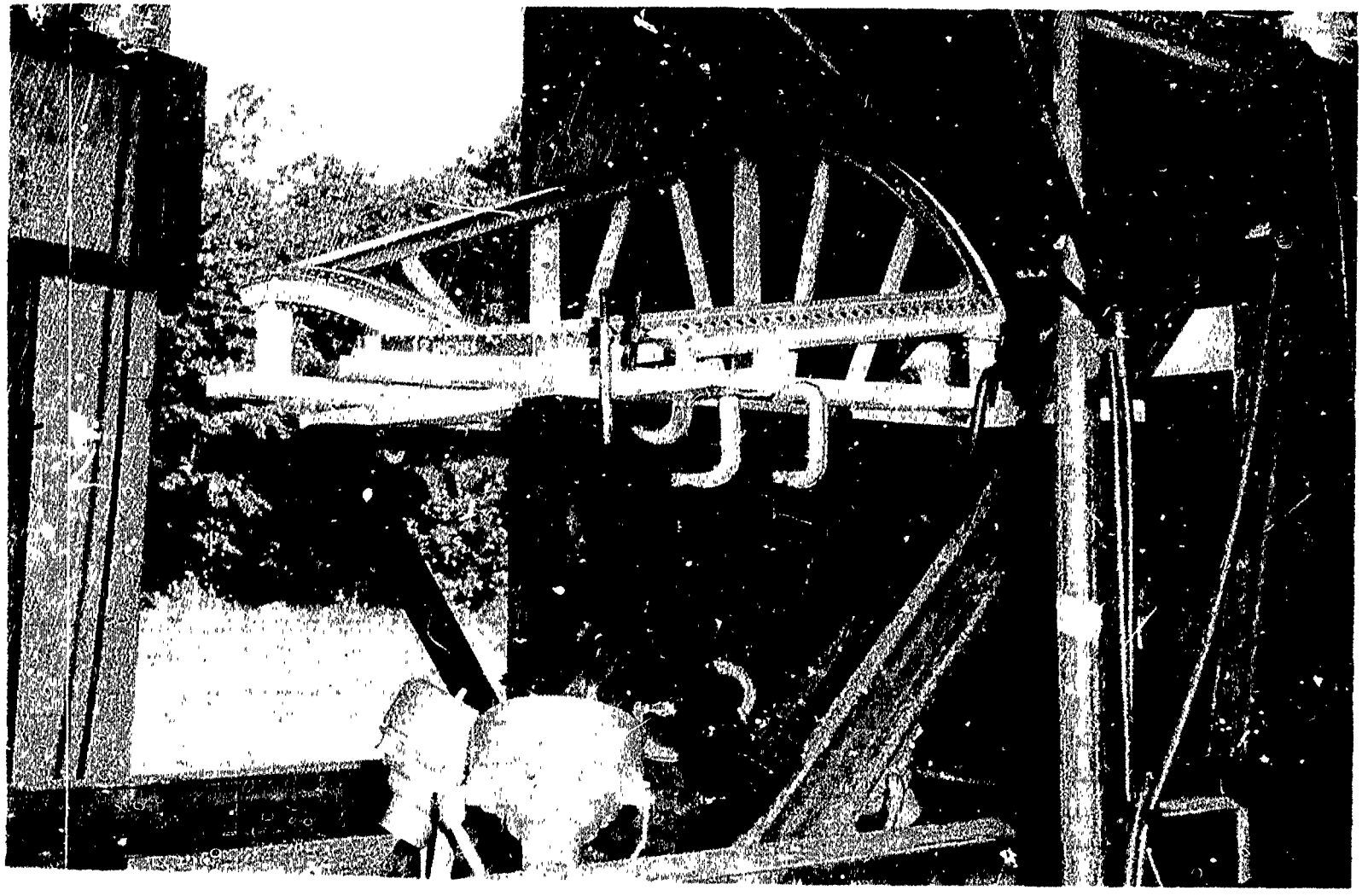
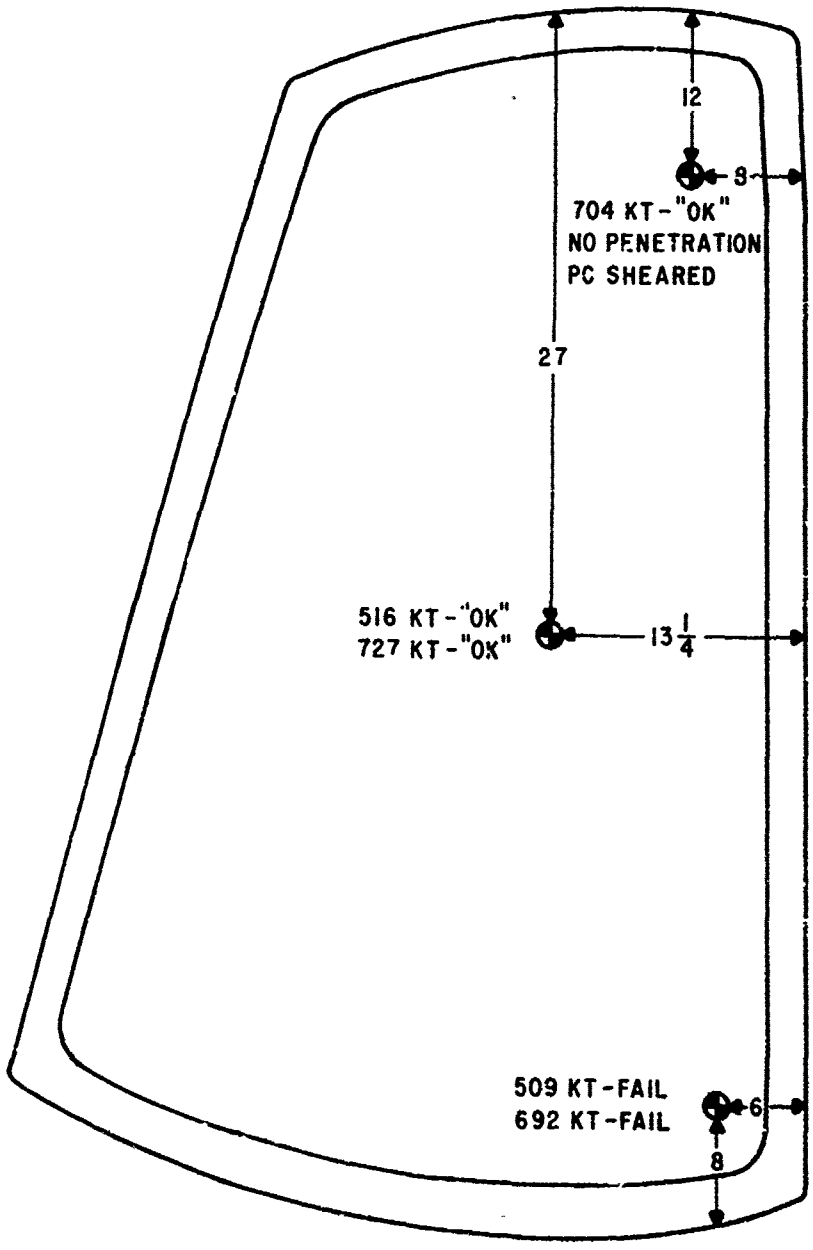


Figure 8. Task II Bird Impact Test Windshield in Rigid Frame



NOTE:

SEE FIGURE 7. FOR CONSTRUCTION DETAILS.

FIGURE 9. WINDSHIELD BIRD IMPACTS IN FRAME.

3. Panels with three extended PC plies did meet the 500 kt requirement in the aft beam corner.

4. A titanium or stainless steel support strip between the windshield and mounting surface tended to reduce edge shearing.

5. Edge shearing was also reduced by grinding the top corner of the mounting surfaces in the module to increase the bending radius.

6. Windshield arch reinforcement was as critical to bird impact resistance as design of the windshield itself. An optimized level of stiffness was necessary between limits which caused either transparency or arch failure.

7. Optimization of system to meet specific requirements (aft beam corner impacts) required actual hardware rather than test frames.

The resulting windshield-arch system which was recommended for prototype production is shown in Figure 10. The windshield differs in several respects from the preliminary windshield cross-section. The most obvious is the extended section of three plies of .125' PC. A fused outboard ply of .060" acrylic plus .188" PC was chosen as the result of static thermal/pressure tests and Air Force wind tunnel experiments.

The aft arch section in Figure 10 shows the tapered retainer with a second taper used on the aft arch only to prevent "tunneling" of bird tissue. The retainer and each of the .020" epoxy/Nomex straps were bonded with .010" RTV 630 silicone. One additional edge attachment item was the .025" titanium support strip adhered superficially to the innermost strap to provide bending support during impact deflection.

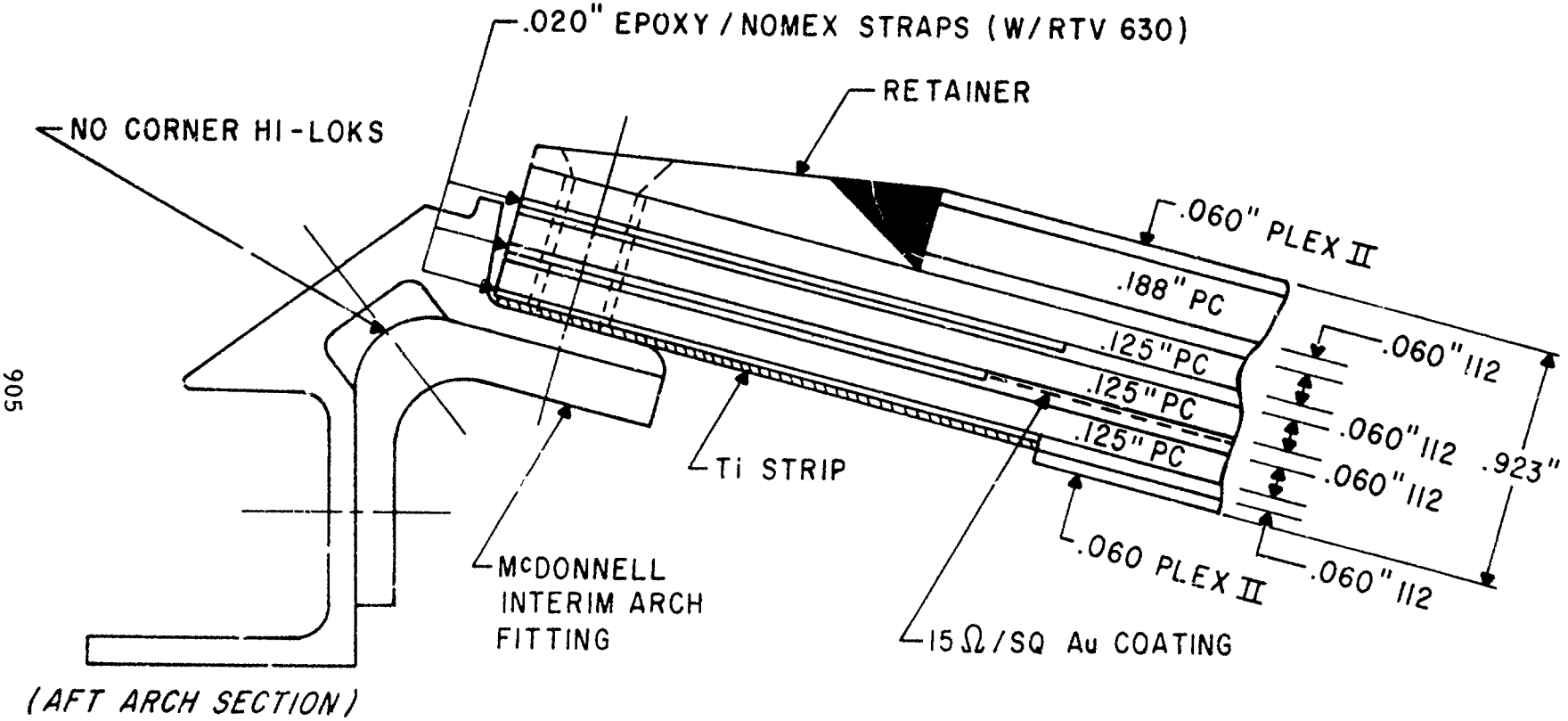
TASK III

The final effort in the program included fabrication of prototype hardware. Eighteen laminated plastic windshields of the recommended design and six similar canopies were delivered to the Air Force for optical, structural and impact qualification.

FOLLOW-ON

Testing of the new bird resistant transparencies has continued. Since the Improved Windshield Protection Development Program and subsequent qualification tests, an additional group of panels was produced. At present, forty improved bird resistant transparencies (twenty canopies and twenty windshields) are now undergoing flight service evaluation at five bases around the world.

RECOMMENDED WINDSHIELD



905

FIGURE 10. RECOMMENDED WINDSHIELD

References

1. H. Edward Littell, Jr., "Composite Bird Resistant Aircraft Transparencies," Conference on Transparent Aircraft Enclosures, AFML-TR-73-126, June 1973.

2. H. Edward Littell, Jr., Improved Windshield and Canopy Protection Development Program, Air Force Flight Dynamics Laboratory, Technical Report AFFDL-TR-74-75, June 1974.

3. J. E. Mahaffey, "Heat Resistant Sheet Interlayer," Conference on Aerospace Transparent Materials and Enclosures, November 1975.

4. E. J. Sanders, "The AEDC Bird Impact Test Facility," Conference on Transparent Aircraft Enclosures, June 1973.

☆ U. S. GOVERNMENT PRINTING OFFICE: 1976 — 657-630/947